15232

NATIONAL LIBRARY
OTTAWA

CANADA

BIBLIOTHÈQUE NATIONALE
OTTAWA

NAME OF AUTHOR... DELWYN G. FREDLUND

TITLE OF THESIS... Volume Change Behavior of Unsaturated Soils

UNIVERSITY... of Alberta, Edmonton

DEGREE FOR WHICH THESIS WAS PRESENTED... Ph.D.

YEAR THIS DEGREE GRANTED... 1973

Permission is hereby granted to THE NATIONAL LIBRARY OF CANADA to microfilm this thesis and to lend or sell copies of the film.

The author reserves other publication rights, and neither the thesis nor extensive extracts from it may be printed or otherwise reproduced without the author's written permission.

(Signed) Delwyn G. Fredlund

PERMANENT ADDRESS:

1714 East Heights

Saskatoon, Saskatchewan

DATED March 13 1973

NL-91 (10-68)

THE UNIVERSITY OF ALBERTA

VOLUME CHANGE BEHAVIOR OF UNSATURATED SOILS

BY

© DELWYN G. FREDLUND

A THESIS

SUBMITTED TO THE FACULTY OF GRADUATE STUDIES AND RESEARCH

IN PARTIAL FULFILMENT OF THE REQUIREMENTS FOR THE

DEGREE OF DOCTOR OF PHILOSOPHY

DEPARTMENT OF CIVIL ENGINEERING

EDMONTON, ALBERTA

SPRING, 1973

THE UNIVERSITY OF ALBERTA

FACULTY OF GRADUATE STUDIES AND RESEARCH

The undersigned certify that they have read, and recommend to the Faculty of Graduate Studies and Research for acceptance, a thesis entitled "VOLUME CHANGE BEHAVIOR OF UNSATURATED SOILS" submitted by Delwyn G. Fredlund in partial fulfilment of the requirements for the degree of Doctor of Philosophy.

.....
N.R. Morgenstern
Supervisor

.....

.....

.....

.....

.....
E.L. Matyas
External Examiner

Date October 27, 1972

ABSTRACT

This dissertation deals with the prediction of volume changes in unsaturated soils. First, the theoretical density and compressibility relationships of air-water mixtures are developed. Throughout the testing program, experimental evidence was obtained which confirms the compressibility equation.

Four pieces of apparatus were developed to test unsaturated soils. Two employed modified Anteus oedometers for one-dimensional conditions. The other two allowed isotropic volume change testing conditions in modified triaxial cells. The diffusion of air through the water in the high air entry disc was an important design consideration. A new diffused air volume indicator was built to measure and correct the water volume change for the diffused air volume change.

The unsaturated soil is considered as a four phase system; two solid phases that come to equilibrium under the application of stresses (i.e., soil particles and contractile skin) and two fluid phases that flow under the application of stresses (i.e., air and water).

Each phase is considered as a continuum with an independent force equilibrium equation. Two independent stress state tensors are extracted from the equilibrium equations. The stress state variables are verified experimentally by means of null tests, for soils with varying degrees of saturation. They are verified to within 1 part of volume change per 10,000 parts of volume.

Independent displacement fields are written for each phase of an unsaturated soil. Unifying the deformations is the continuity requirement that states that the sum of the volumetric deformations of each phase is equal to the volumetric deformation of the overall element.

A constitutive relationship for the soil structure and the contractile skin is developed. These two equations link the stress and deformation state variables and allow the evaluation of all volume-weight soil properties. The uniqueness of the proposed constitutive relationship was proven for small deviations from a stress point. The experimental results show a correlation coefficient for the predicted versus measured volume changes which is in excess of the critical correlation coefficient for a 1 percent level of significance.

Hysteresis destroys the uniqueness of the constitutive surfaces and is the result of a reversal in the direction of deformation of either the soil structure or the contractile skin.

A one-dimensional volume change analysis for an unsaturated soil is presented. All volume-weight soil property changes, in response to stress changes, can be predicted provided the constitutive equation soil parameters are known.

A one-dimensional theory of consolidation is derived on the basis of the continuity requirement. It consists of two partial differential equations that must be solved simultaneously. The initial pore air and pore water pressures, as a result of a change in total pressure, are also predictable by solving two simultaneous equations. No attempt has been made to solve or experimentally verify these equations.

ACKNOWLEDGEMENTS

The experimental investigation associated with this dissertation was conducted in the Soil Mechanics Laboratory, Department of Civil Engineering, University of Alberta, under the supervision of Dr. N.R. Morgenstern. The author wishes to express his sincere gratitude to Dr. Morgenstern for his guidance and enthusiasm throughout the research program. The openness of his office at all times for consultation does not pass unremembered.

Many aspects of this dissertation were discussed with members of the civil engineering staff. In particular, the author thanks Dr. D.W. Murray who spent time assisting and checking many of the theoretical aspects. The discussions with Dr. Z. Eisenstein and Dr. N. Rajaratnam were appreciated as were the discussions with my colleagues.

The author received excellent cooperation from Mr. A. Muir during the many hours of equipment development. This integral part does not go unrecognized. The assistance of Mr. O. Wood was also appreciated.

The undisturbed Regina Clay soil samples were obtained from testholes drilled by the Division of Building Research, National Research Council (Saskatoon) and the Saskatchewan Department of Highways (Regina). The piezometers were contributed by the National Research Council and recorded by their personnel. These contributions were much appreciated. The author expresses his thanks to Mr. J.J.

Hamilton for his interest in this research project.

I am grateful to the Canadian Good Roads Association for providing financial assistance in the form of a scholarship during the first year and to the University of Alberta for a Dissertation Fellowship awarded for the second year. I also wish to thank the University of Saskatchewan for granting me two years of educational leave.

The completion of this research work has been greatly facilitated through the constant cooperation and encouragement from my wife JoAnne.

I greatly appreciate the magnificant job of typing performed by Miss Helen Wozniuk and the excellent drafting of the plates performed by Mr. A. Kozlow.

In particular, I am most thankful to my Maker who gives purpose to the completion of another task. Providing I qualify to the title of a "good man", let me quote Solomon's words, "---teach a good man, and he will learn more.--- the reverence and fear of God are basic to all wisdom. Knowing God results in every other kind of wisdom. "I, Wisdom, will make the hours of your day more profitable and the years of your life more fruitful"."

Proverbs 9:9,10,11

TABLE OF CONTENTS

		Page
Title Page		i
Approval Sheet		ii
Abstract		iii
Acknowledgements		v
Table of Contents		vii
List of Tables		xiii
List of Figures		xvii
List of Plates		xxviii
CHAPTER I	INTRODUCTION	1
	1.1 General	1
	1.2 The Nature of Unsaturated Soil	2
	1.3 Development of the Surface Tension Concept	3
	1.4 Conditions at the Air-Water Interphase	6
	1.5 Physical Properties of the Contractile Skin	7
	1.6 Volume-Weight Relationships	9
	1.7 Context of Terminology	13
	1.8 Scope of the Thesis	15
CHAPTER II	MISCIBLE AND IMMISCIBLE MIXTURES OF AIR AND WATER	19
	2.1 Introduction	19

TABLE OF CONTENTS (continued)

		Page
CHAPTER II	continued	
	2.2 Density of Air-Water Mixture	21
	2.3 Compressibility of Air-Water Mixtures for Various Temperatures and Pressures	39
	2.4 Solubility of Air in Water	54
	2.5 Density and Compressibility of a Combined Miscible and Immiscible Air-Water Mixture	85
	2.6 Compressibility of Air-Water Mixtures When the Air Pressure is Not Equal to the Water Pressure	96
CHAPTER III	EQUIPMENT FOR TESTING UNSATURATED SOILS	103
	3.1 General	103
	3.2 Basic Design Considerations	104
	3.3 Literature Review of Equipment Development	109
	3.4 Equipment Development	119
	3.5 Preparation of Equipment	161
	3.6 Tests Procedures and Data Reduction	166
CHAPTER IV	STRESS STATE VARIABLES	168
	4.1 General	168
	4.2 Effective Stress Concept for Saturated Soils	168
	4.3 Literature Review on Stress Variables Controlling Unsaturated Soil Behavior	175

TABLE OF CONTENTS (continued)

		Page
CHAPTER IV	continued	
	4.4 Stress Analysis of a Continuum	183
	4.5 The Element of a Multiphase System	189
	4.6 Theoretical Approach to Multiphase Systems	193
	4.7 Fluid-Solid Multiphase	202
	4.8 Air-Water Multiphase	211
	4.9 Unsaturated Soil Case	224
	4.10 Limiting Stress State Conditions in Unsaturated Soils	235
	4.11 Comparison of the Derived Stress State Variables with Previously Proposed Effective Stress Equations	238
	4.12 Experimental Evidence in Support of the Proposed Stress State Variables	244
	4.13 Proposed Experimental Verification of Stress State Variables	253
	4.14 Discussion of Null Tests	258
CHAPTER V	DEFORMATION ANALYSIS OF MULTIPHASE STYSTEMS	270
	5.1 General	270
	5.2 Deformation Analysis Literature Review	271
	5.3 Multiphase Element for the Deformation Analysis	274

TABLE OF CONTENTS (continued)

		Page
CHAPTER V	continued	
	5.4 Theoretical Deformation Analysis of Multiphase Systems	276
	5.5 Fluid-Solid Multiphase	282
	5.6 Air-Water Multiphase	284
	5.7 Unsaturated Soil Case	292
	5.8 Other Volume-Weight Relationships	295
CHAPTER VI	CONSTITUTIVE RELATIONSHIPS FOR UNSATURATED SOILS	297
	6.1 General	297
	6.2 Constitutive Relationship Review	297
	6.3 Approach to Constitutive Relationships for Multiphase Systems	307
	6.4 Constitutive Relationships for the Water-Solid and Air-Water Multiphases	308
	6.5 Soil Structure Constitutive Relationship for an Unsaturated Soil	309
	6.6 Contractile Skin Constitutive Relationship for an Unsaturated Soil	312
	6.7 Water Phase Constitutive Relationship for an Unsaturated Soil	315
	6.8 Graphical Presentation of Constitutive Relationships	316
	6.9 Sign Convention for Compressibility Modulii	318

TABLE OF CONTENTS (continued)

		Page
CHAPTER VI	continued	
	6.10 Observed Directions of Volumetric Deformation	322
	6.11 Procedure to Experimentally Verify the Uniqueness of the Constitutive Surface at a Point	337
	6.12 Presentation of Uniqueness Test Data	346
	6.13 Analysis of the Uniqueness Test Data	352
	6.14 Theoretical Exploration of the Constitutive Surface for Larger Stress Changes and Reversals of Stresses	405
	6.15 Presentation and Discussion of Data on Hysteresis	412
	6.16 Typical Constitutive Surfaces for Regina Clay	421
CHAPTER VII	TRANSIENT FLOW ANALYSIS	429
	7.1 General	429
	7.2 Literature Review on Transient Flow	430
	7.3 Flow Laws	433
	7.4 Diffusivity Concept Applied to Flow in Unsaturated Soils	438
	7.5 Continuity	441

TABLE OF CONTENTS (continued).

		Page
CHAPTER VII	continued	
	7.6 Transformation Between the Referential and Spatial Descriptions of Motion	442
	7.7 Continuity with Respect to a One Phase, Spatial and Referential System	445
	7.8 Continuity with Respect to Multiphase Systems	448
	7.9 Categorization of Processes	454
	7.10 Theory of Consolidation for Unsaturated Soils	455
	7.11 Pore Pressure Boundary Conditions for the Consolidation Theories	459
CHAPTER VIII	CONCLUSIONS AND SUGGESTIONS FOR FUTURE RESEARCH	464
	8.1 Conclusions	464
	8.2 Suggestions for Future Research	473
LIST OF REFERENCES		476
APPENDIX A	SOIL AND TEST PROGRAM	A1
APPENDIX B	CALIBRATIONS AND CHECKS TO ENSURE PROPER FUNCTIONING OF THE EQUIPMENT	B1
APPENDIX C	ANALYSIS OF THE NULL TESTS	C1
APPENDIX D	DATA REDUCTION	D1
APPENDIX E	PORE PRESSURE RESPONSE TESTS ON HIGH AIR ENTRY DISCS	E1
APPENDIX F	VOLUME CHANGE DATA ON UNSATURATED SOILS	F1

LIST OF TABLES

Table		Page
II.1	Composition of Dry Air	20
II.2	Specific Volume of Dry Air and Saturated Water Vapor	30
II.3	Solubility of Air in Water (Dorsey, 1940)	56
II.4	Diffusivity of Certain Gases in Water	68
II.5	Measured Values of the Coefficient of Diffusion Through Different Materials (From Barden and Sides, 1967)	69
III.1	Summary of Proven Test Equipment (Unsaturated Soil Testing)	111
III.2	Fluctuations in Output Pressure from Pressure Regulators Compared with Changed in Barometric Pressure	125
IV.1	Data from the Bishop and Donald's Triaxial Experiment on Braehead Silt	250
IV.2	Independent Stress State Variables Showing Monotonic Behavior (From Bishop and Donald's Data 1961)	252
IV.3	Possible Tests to Prove and Disprove Independent Stress State Variables	257
IV.4	Null Test Program	259
VI.1	Sign of the Soil Structure Modulii	321

LIST OF TABLES (continued)

Table		Page
VI.2	Sign of the Contractile Skin (Air Phase) Modulii	321
VI.3	Sign of the Water Phase Modulii	322
VI.4	Experimental Data on the Directions of Deformation for Various Stress Component Changes	323
VI.5	Volume-Changes Corresponding to Stress Component Changes for Tests to Evaluate Uniqueness of the Constitutive Surface at a Point	348
VI.6	Sign Designations for Stress State Variable Changes	352
VI.7	Summary of Compressibilities with Respect to Soil Structure, Air and Water Phases	353
VI.8	Comparison of Predicted and Measured Volume Changes (uniqueness at a Point)	360
VI.9	Summary of Regression Analysis Using Linear Constitutive Surfaces	369
VI.10	Comparison of Predicted and Measured Volume Changes (Uniqueness at a Point) Correction Applied for Non Linear Constitutive Surface	385
VI.11	Summary of Regression Analysis Using a Non-Linear Constitutive Surface	386
VI.12	Comparison of Prediction and Measured Soil Structure Volume Changes for a Change in Air Pressure	389
VI.13	Summary of Regression Analysis Using a Non-Linear Constitutive Surface and Applying a Correction for Hysteresis	390

LIST OF TABLES (continued)

Table		Page
VI.14	Comparison of Predicted and Measured Volume Changes (Uniqueness at a Point) Corrections Applied for Hysteresis	391
VI.15	Comparison of Predicted and Measured Water Volume Changes for Sample #15A (5000 minutes) (Water Volume = Excess Water Volume + Soil Structure Deformation)	398
VI.16	Summary of Regression Analysis for the Water Phase Constitutive Surface Assuming Various Rates of Water Loss (Sample #15A, 5000 min)	399
VI.17	Comparison of Predicted and Measured Water Volume Changes for Sample #16 (15000 minutes) (Compressibilities Corrected for Hysteresis)	400
VI.18	Comparison of Predicted and Measured Water Volume Changes for Sample #21 (Equilibrium Conditions) (Compressibilities Corrected for Hysteresis)	403
VI.19	Stress Changes that Produce a Constant Direction of Deformation of the Soil Structure	408
VI.20	Stress Changes that Produce Uni-Directional Deformation of the Contractile Skin	409
VI.21	Directions of Deformation When Air Pressure is Constant	411

LIST OF TABLES (continued)

Table		Page
VI.22	Summary of Tests to Show the Effect of Hysteresis	413
VII.1	Typical k_a/k_w Ratios	434

LIST OF FIGURES

Figure		Page
1.1	Conditions at an Air-Water Surface (After Defay et al, 1966; Derjaguin, 1965)	5
1.2	Element of an Unsaturated Soil	10
1.3	Volume-Weight Relationships for an Unsaturated Soil	11
1.4	Deformation Analysis of Unsaturated Soil	16
2.1	Psychrometric Chart for Air-Water at One Atmosphere (From Spalding and Cole, 1958)	32
2.2	Density of Pure Water	33
2.3	Density of Pure Water at Various Temperatures and Pressures	34
2.4	Effect of Dissolved Air on the Density of Water	36
2.5	Isothermal Compressibility of Air-Free Water	42
2.6	Isothermal Compressibility of Air-Saturated and Salt Water	43
2.7	Effect of Pressure on Isothermal Compressibility (At 20°C)	44
2.8	Theoretical Compressibility of Air-Saturated Water	45
2.9	Compressibility of an Immiscible Air-Water Mixture	50
2.10	Compressibility Versus Pressure of an Immiscible Air-Water Mixture	51

LIST OF FIGURES (continued)

Figure		Page
2.11	Volume Change in the Compartment of Oedometer No. 177 During Loading and Unloading	52
2.12	Volume Change in the Compartment of Oedometer No. 179 During Loading and Unloading	53
2.13	Measured Compressibilities in the Compartment of Oedometer No. 177 and No. 179	55
2.14	Piston and Porous Stone Analogy	58
2.15	Element to Derive the Theory of Air Diffusion Through Water	63
2.16	Independent Measurement of Air and Water Diffusing Through Water, Rubber Membrane and Ceramic Disc	70
2.17	Air Released From Water Flowing Through Ceramic Disc (Dec. 3/71)	71
2.18	Air Released from Water Flowing Through Ceramic Disc (Dec. 6/71)	73
2.19	Diffusion of Air Through Saturated Ceramic Disc (Apparatus #179)	74
2.20	Steady State Diffusion of Air Through Saturated Ceramic Disc (Apparatus #179)	75
2.21	Diffusion Test No. 1 on Saturated Ceramic Disc	77
2.22	Diffusion Test No. 2 on Saturated Ceramic Disc	78
2.23	Accumulated Air Diffusion During Test #1 (U_a = 80 psi and U_w = 0.9 psi)	79

LIST OF FIGURES (continued)

Figure		Page
2.24	Accumulated Air Diffusion During Test #1 (U_a = 80 psi and U_w = 5 psi)	80
2.25	Accumulated Air Diffusion During Test #1 (U_a = 103 psi and U_w = 4.8 psi)	81
2.26	Accumulated Air Diffusion During Test #2 (U_a = 51.5 psi and U_w = 5.8 psi)	82
2.27	Accumulated Air Diffusion During Test #2 (U_a = 30.4 psi and U_w = 5.7 psi)	83
2.28	Diffusivity Values Measured on the Ceramic Discs in the Anteus Oedometer and Published Values from Other Sources	84
2.29	Components of Compressibility of Miscible and Immiscible Air-Water Mixtures	93
2.30	Compressibility of Combined Miscible and Immiscible Air-Water Mixtures	94
2.31	Effect of Solubility of Air in Water on the Compressibility	95
2.32	Pore Air and Pore Water Responses to a Change in Total Pressure in a Closed System	101
3.1	Layout of the Modified Anteus Consolidometer	124
3.2	Base Plate Design for Modified Anteus Consolidometer	129
3.3	Wrench for Tightening and Loosening the Base Plate	132

LIST OF FIGURES (continued)

Figure		Page
3.4	Layout of Plumbing for Modified Anteus Consolidometers	134
3.5	Modifications of - and Operation of Water Volume Change Indicator	137
3.6	Diffused Air Volume Indicator	139
3.7	Layout of Entire Modified Anteus Oedometer	141
3.8	Modified Triaxial Cell No. 1	144
3.9	Mercury Container for Filling and Emptying the Triaxial Cell	146
3.10	Base Plate for Triaxial Cell No. 1	147
3.11	Layout of Plumbing for Triaxial Apparatus No. 1	149
3.12	Layout of Entire Triaxial Apparatus No. 1	152
3.13	Modified Triaxial Cell No. 2	154
3.14	Layout of Plumbing for Triaxial Apparatus No. 2	156
3.15	Modified Lateral Displacement Indicator	159
3.16	Layout of Entire Triaxial Apparatus No. 2	160
3.17	Pore Water Pressure Response on Anteus Oedometer #179 (Oct. 30, 1971)	164
4.1	Three-Dimensional Stress Components at a Point in Space	187
4.2	Equilibrium Stress Fields Across an Element	188
4.3	Equilibrium Across a Water-Solid Multiphase	203
4.4	Stress Equilibrium of a Water Saturated Particulate System	208

LIST OF FIGURES (continued)

Figure		Page
4.5	Fictitious Air-Water Multiphase Element	214
4.6	Equilibrium in an Air-Water Multiphase	216
4.7	Simplified Representation of the Self-Compensating Air-Water Multiphase	220
4.8	Equilibrium of the Fluid Phases of an Unsaturated Soil Element	225
4.9	Equilibrium of the Contractile Skin and Soil Structure for an Unsaturated Soil Element	230
4.10	Stress in the Soil Structure at a Point	233
4.11	Comparison of Tests Performed at Limiting Stress State Variable Conditions	237
4.12	Force Equilibrium to Describe Schiffman's Analysis	242
4.13	A Set of Curves Demonstrating the Dependence of Porosity on Total Stress and on Pore Water Stress, in the Case of Kaolin (After Tiller, 1953)	245
4.14	Typical e - log P Curves from "Consolidation Testing with Backpressure" by J. Lowe III, P.F. Zaccheo & H. Feldman (1964)	246
4.15	Determination of Capillary Pressure by Translation of the Origin (Hilf, 1956)	247
4.16	Effect of Equal Increase in Cell Pressure and Pore Pressure on the Volume of a Sandy Clay (After J. Lowe III and T.C. Johnson, 1960)	248

LIST OF FIGURES (continued)

Figure		Page
4.17	Drained Test on Partly Saturated Loose Silt in Which σ_3, U_a and U_w are varied so as to Keep (σ_3-U_a) and (U_a-U_w) Constant (From Bishop and Donald, 1961)	251
4.18	Null Tests (N-19) and (N-20) on Sample No. 6	262
4.19	Null Tests (N-35) and (N-36) on Sample No. 31	264
4.20	Null Tests (N-37) and (N-38) on Sample No. 31	265
4.21	Null Tests (N-39) and (N-40) on Sample No. 31	266
4.22	Null Test (N-37) on Sample No. 31 (Expanded Scale)	267
4.23	Means and Standard Deviations For Total and Water Volume Changes from all Null Tests on Sample No. 31	268
5.1	Translation and Deformation of a Two-Dimensional Element of a One Phase Solid	277
5.2	Translation and Deformation of a Two-Dimensional Element in a Two Phase System	280
5.3	Translation and Deformation of an Element from a Soap Bubble	287
5.4	Dimensions and Displacements for an Element of the Bubble Along the Z-Axis	289
5.5	Translation and Deformation of a Two-Dimensional Element of Unsaturated Soil	293
6.1	Graphical Representation of Constitutive Surfaces for an Unsaturated Soil	317

LIST OF FIGURES (continued)

Figure		Page
6.2	Features of the Constitutive Surface	319
6.3	Volumetric Deformations for a Change in Total Pressure	326
6.4	Volumetric Deformations for a Change in Air Pressure	327
6.5	Volumetric Deformations for a Change in Water Pressure	328
6.6	Summary of Directions of Volumetric Deformations for a Change in Total Pressure	329
6.7	Soil Structure and Water Phase Volume Changes Test (C-30)	331
6.8	Summary of Directions of Volumetric Deformations for a Change in Air Pressure	332
6.9	Soil Structure and Water Phase Volume Changes Test (C-31)	333
6.10	Soil Structure and Water Phase Volume Changes Test (D-10)	335
6.11	Summary of Directions of Volumetric Deformations for a Change in Water Pressure	336
6.12	Soil Structure and Water Phase Volume Changes Test (D-14)	338
6.13	Soil Structure and Water Phase Volume Changes Test (D-7)	339

LIST OF FIGURES (continued)

Figure		Page
6.14	Ideal Tests to Prove Uniqueness of the Constitutive Surface at a Point for the Soil Structure and the Contractile Skin	341
6.15	Minimum Test Requirements to Prove Uniqueness of the Constitutive Surface at a Point	343
6.16	Stress Path Adhered to for the Soil Structure During the Uniqueness Tests at a Point	344
6.17	Deformation of the Soil Structure for Sample #15A	347
6.18	Theoretical Critical Correlation Coefficient	367
6.19	Comparison of Predicted and Measured Soil Structure Deformation for Sample #15A	370
6.20	Comparison of Predicted and Measured Soil Structure Volumetric Deformations on Sample #16	371
6.21	Comparison of Predicted and Measured Soil Structure Volumetric Deformation for Sample #17	373
6.22	Comparison of Predicted and Measured Soil Structure Volumetric Deformation for Sample #21 (at 2000 minutes)	374
6.23	Comparison of Predicted and Measured Soil Structure Volumetric Deformation for Sample #21 (Equilibrium Conditions)	375
6.24	Comparison of Predicted and Measured Water Phase Volume Changes for Sample #15A	376

LIST OF FIGURES (continued)

Figure		Page
6.25	Comparison of Predicted and Measured Water Phase Volume Changes for Sample #16	378
6.26	Comparison of Predicted and Measured Water Phase Volume Changes for Sample #17	379
6.27	Comparison of Predicted and Measured Water Phase Volume Changes for Sample #21 (At 2000 minutes)	380
6.28	Comparison of Predicted and Measured Water Phase Volume Changes for Sample #21 (Equilibrium Conditions)	381
6.29	Comparison of Predicted and Measured Overall Volume Changes for Sample #16 (Compressibilities Corrected for Non Linearity)	384
6.30	Soil Structure Volumetric Deformations Associated with Air Pressure Changes	388
6.31	Comparison of Predicted and Measured Overall Volumetric Deformations for Sample #16 (Hysteresis Correction Applied)	392
6.32	Comparison of Predicted and Measured Overall Volumetric Deformations for Sample #21 (Hysteresis Correction Applied)	394
6.33	Water Volumetric Deformation Versus Time for Sample #15A	395
6.34	Comparison of Predicted and Measured Water Phase Volume Changes for Sample #15A (Water Volumes Computed Using Excess Water Expelled)	397

LIST OF FIGURES (continued)

Figures		Page
6.35	Comparison of Predicted and Measured Water Phase Volume Changes for Sample #16 (Hysteresis Correction Applied)	401
6.36	Comparison of Predicted and Measured Water Volume Changes for Sample #21 with the Hysteresis Correction Applied)	404
6.37	Incorporation of Hysteresis into Constitutive Surface by Inconsistent Directional Change of Stress State Variables	407
6.38	Hysteresis Resulting from Reversing the Total and Air Pressure Components	414
6.39	Hysteresis Resulting from Reversing the Water Pressure Component	416
6.40	Soil Structure Versus Stress State Variables for Regina Clay	422
6.41	Overall Volumetric Deformation Versus Stress State Variables for Regina Clay (One-Dimensional Oedometer)	424
6.42	Overall Volumetric Deformation Versus Stress State Variables for Regina Clay (Isotropic Loading)	425
6.43	Void Ratio Versus Stress State Variables for Regina Clay	426
6.44	Degree of Saturation Versus Stress State Variables for Regina Clay	428

LIST OF FIGURES (continued)

Figure		Page
7.1	Piston and Spring Analogy for the Generation of Pore Pressures	460

LIST OF PLATES

Plate		Page
3.1	General Laboratory Set-Up	120
3.2	Layout of Modified Anteus Oedometer	122
3.3	Layout of Triaxial Apparatus No. 1	142
3.4a	Layout of Triaxial Apparatus No. 2	153
3.4b	Pivot on Lateral Displacement Indicator	153
3.5	Triaxial Apparatus Base No. 2 with Soil Sample	158

CHAPTER I

INTRODUCTION

1.1 General

The discipline of soil mechanics came into prominence in the 1930's primarily as a result of Terzaghi's convincing evidence to support the effective stress concept. The concept indicated that for a saturated soil, the difference between the total stress and the pore water stress formed an independent stress variable which controlled the deformation and strength characteristics of a soil. This concept has proven to be the key in formulating and analyzing soil mechanics problems. Consequently, soil mechanics has been primarily concerned with the volume change and strength behavior of saturated soils.

Practicing engineers soon became aware that many of the problems they encounter involved unsaturated soils. The construction of earth-fill dams, highways and airport runways all make use of remolded soils that are unsaturated. Also, large portions of the land surface of the earth are subjected to desiccating influences that leave the upper portion of the profile cracked and unsaturated. Light structures placed on these natural soil profiles generally suffer distress due to subsequent expansion of the desiccated soil.

The success of the effective stress concept in describing the behavior of saturated soils has led research workers into a search for a similar statement for unsaturated soils. During the last two decades,

there have been numerous equations proposed in the literature; however, none have proven completely successful in practice. Research into the volume change behavior of unsaturated soils appears to have developed on two independent fronts. First, there were those interested in describing behavior in terms of changes in total stress applied to the soil (i.e. constant volume and free swell tests) and second, those using changes in the pore fluid pressures (i.e. soil suction tests).

1.2 The Nature of Unsaturated Soil

The variation in terminology associated with unsaturated soils requires explicit definition of all terms and variables. Even the term unsaturated soil must be carefully defined.

A soil mass consists of a particulate assemblage of solids; the voids being filled with one or more, compressible or incompressible fluids. Classical soil mechanics has primarily considered the case in which the voids are filled with water (i.e. the saturated soil case). However, the general case involves pores that contain varying portions of gas (i.e. the unsaturated soil case). Although the terms partially and partly are often used to describe this case, the author prefers the term unsaturated. On a macroscopic scale, the inclusion of the smallest amount of free gas renders the system unsaturated.

The unsaturated soil case considered in this thesis involves voids that are filled with varying portions of air (with or without water vapor) and water (with or without dissolved air). In other words, the air phase consists of a miscible mixture of gases plus

water vapor while the water is a miscible mixture of pure water and dissolved air. The air phase is immiscible with the water phase.

Generally an unsaturated soil is considered to be a three-phase system. Lambe and Whitman (1969) state that a soil contains "three distinct phases: solid (mineral particles), gas and liquid (usually water)". Before proceedings, let us consider the definition of the word phase. Sisler, VanderWerf and Davidson (1953) state that "many mixtures are heterogeneous, consisting of two or more physically distinct portions, differing in properties and composition and separated from each other by definite bounding surfaces". This definition appears consistent throughout the fields of chemistry and physics (Gove, 1967 and The International Dictionary of Physics and Electronics, 1961).

Let us apply the above definition of a phase and consider the possibility of an unsaturated soil containing a fourth phase. The fourth phase would be the air-water interface commonly referred to as the "contractile skin" in the surface chemistry literature (Matyevic, 1969).

1.3 Development of the Surface Tension Concept

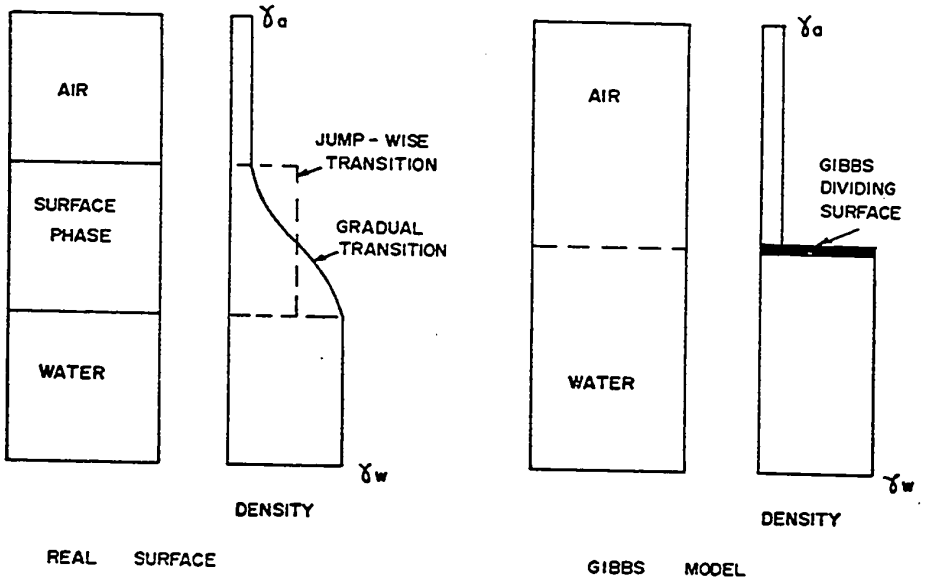
The surface tension concept is not new; in fact, many of the mathematical relationships and quantitative observations concerning surface phenomena were documented prior to the 1900's (Padday, 1969). Leonardo da Vinci (in the 15th century) and Sir Isaac Newton (in the

17th century) observed the rise of a liquid in a fine bore capillary tube. In the 17th century, Hawksbee and Segner performed experiments that allowed them to formulate the first theory of capillarity. "Surface tension" came to denote the supposed presence of a contractile skin at the surface of a liquid.

In 1805, Young stated that the mechanical properties of a two-fluid surface may be related to those of a hypothetical stretched membrane.

The work of Laplace and Young proposed that the radius of curvature of a two-fluid interface was a consequence of two radii of curvature and their equation connected the surface tension and the radius of curvature with the differential pressure.

The concept of surface tension was well established by the turn of the century when Gibbs set out his thermodynamic treatment of the problem. In 1906, Gibbs introduced the concept of "dividing surfaces" where each phase remains homogeneous up to an infinitely thin separating boundary. The properties of the boundary are a combination of the physical properties of the two bulk phases and of the real interface layer. The dividing surface concept is also applied to surface energy, surface entropy and surface free energy. The Gibbs model is an attempt to simplify the real interphase (or phase) that exists between two fluids (Figure 1.1). However, the simplification has caused much confusion and has been shown to have limitations in many analyses. Goodrich (1969) states that Gibbs introduces "certain



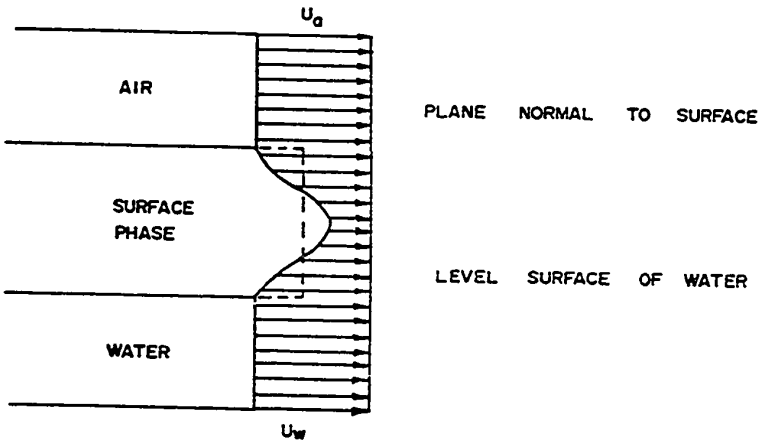


FIGURE 1.1 CONDITIONS AT AN AIR - WATER SURFACE (AFTER DEFAY ET AL , 1966 ; DERJAGUIN , 1965)

dividing surfaces into the theory which have bedeviled the student ever since. These mathematical surfaces were used as synthetic phase boundaries in an attempt to compare the actual interfacial region with fictitious systems in which the transition from one phase to the next was absolutely discontinuous. Experience has shown that this method, already mathematically inelegant, is also a source of endless confusion".

1.4 Conditions at the Air-Water Interphase

Davies and Rideal (1963) commence their book entitled Interfacial Phenomena with the following statement.

"The boundary between two homogeneous phases is not to be regarded as a simple geometrical plane, upon either side of which extends the homogeneous phases, but rather as a lamina or film of a characteristic thickness: the material in this surface phase shows properties differing from those of the materials in the contiguous homogeneous phases. It is with the properties of matter in the surface layer that we are here concerned. Just as in bulk, the matter of the surface phase may exist in the solid, liquid, and gaseous states: i.e. there are various types of interfacial phase". They go on to observe "that a liquid behaves as if it were surrounded by an elastic skin with a tendency to contract". It is for this reason that a drop tends to a spherical shape when uninfluenced by external forces and that any liquid surface area will tend to decrease spontaneously.

The free surface of a liquid behaves as though it is in a

state of tension. However, it has not been possible to directly measure the tensile stress and therefore its existence has been disputed (Adam, 1938). Several simple experiments noted by Padday (1969) lend credence to the existence of a boundary phase.

"(1) The hydrostatic pressure below a curved surface is different than that below a flat surface.

(2) The liquid assumes a shape of minimum area when there is no influence of gravity.

(3) The vapor pressure of a liquid with a curved surface is different than that of a flat surface.

(4) A thin film of liquid stretched on a wire frame pulls in and thereby tends to distort the wire frame".

The existence of the contractile skin can also be explained in terms of the work done to create new surface or in terms of the change in Helmholtz free energy associated with the formation of area.

According to Defay et al (1966) the contractile skin has a pressure deficit that manifests itself macroscopically as a tension. The magnitude of the integral of the tension across the contractile skin is known as the surface tension.

1.5 Physical Properties of the Contractile Skin

Considering the contractile skin as a separate independent phase must be justified on the basis that it has different physical properties than the bulk of either phase in contact with it. The most striking and significant evidence is associated with the tensile pull

observed in only the surface layer of a liquid (Bikerman, 1958). However, research on other physical properties also indicates the independent nature of the surface layer.

Derjaguin (1965) reported that the viscosity of the surface layer is very sensitive to change from the bulk of the liquid. Surface layers 10^{-6} cm thick have viscosities three times greater than that of the bulk liquid. The change in viscosity is believed to be an indication of a structural change. Birefringence data indicates that the surface layer has a structure similar to that of ice. The polar nature of water results in strongly orientated molecules in the surface layer (Padday, 1969). The surface water molecules are therefore attracted on one side and allowed to relax on the other side. The density of the surface layer is slightly reduced due to this structural change.

Metsik (1964) showed an increase in the heat conductance as the surface layer thickness decreased.

There is also evidence to indicate that the transitions from the liquid to the gas phase are not transitional as previously felt but rather are jumpwise or distinct. Derjaguin (1965) states, "The absence of a pronounced drop in these peculiarities in water layers as the distance from the interface increases up to a certain thickness, gives grounds for assuming that the specific structure of water in boundary layers is uniform and changes abruptly, at a certain small distance from the interface, into the normal structure of the bulk liquid phase". "Theoretically, it is natural to assume a jumpwise change as

this is observed in liquid crystals. Thus, there are grounds to speak of boundary phases separated from the bulk liquid by a sharp interface but differing from conventional phases in that their thickness is definite under given conditions and they depend on the nature of the substratum". Throughout this thesis the "contractile skin" is considered as an independent fourth phase in an unsaturated soil.

An element of an unsaturated soil can therefore be visualized as a composite mixture with two phases that come to equilibrium under applied stresses and two phases that flow under applied stresses. In other words, two phases can be treated as solids (i.e. the soil structure and the contractile skin) whereas two phases can be treated as fluids (i.e. the air and water). Figure 1.2 depicts the type of element under consideration.

1.6 Volume-Weight Relationships

The thickness of the contractile skin is believed to be in the order of only a few molecular layers. Figure 1.3a shows a rigorous diagrammetric subdivision of an unsaturated soil. The thinness of the contractile skin make its physical subdivision unfeasible and unnecessary from the standpoint of volume-weight relationships. No significant error is incorporated if the contractile skin is considered as part of the water phase (Figure 1.3b). In this way, the four phase system reverts to a three phase system with respect to the volume-weight relationships.

The definitions and terminology of the volume-weight relation-

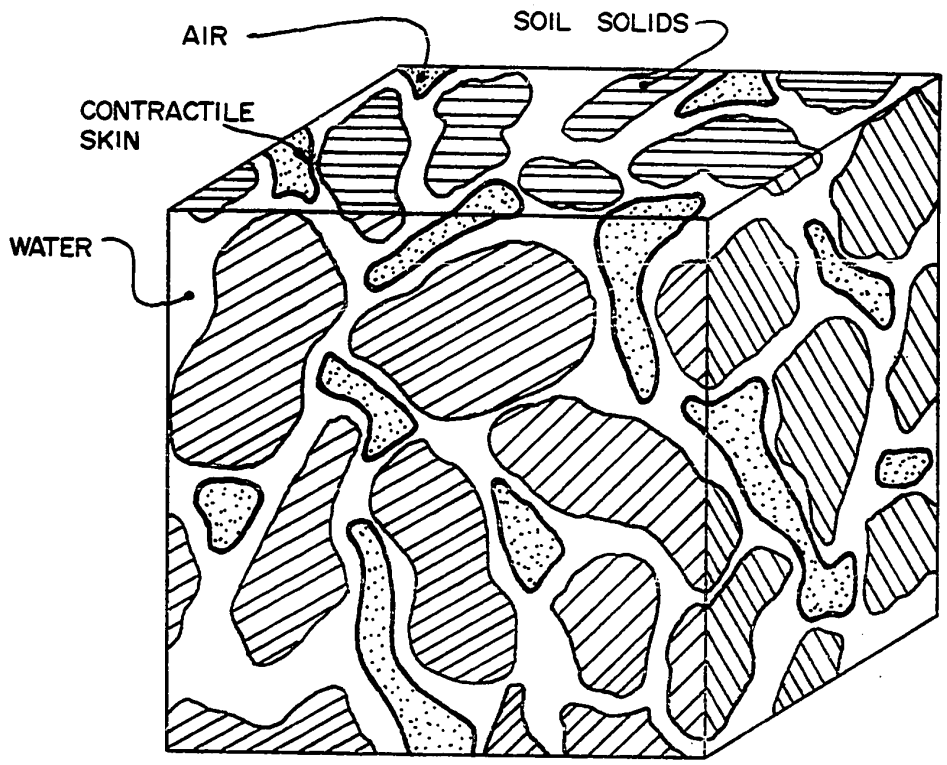


FIGURE 1.2 ELEMENT OF AN UNSATURATED SOIL

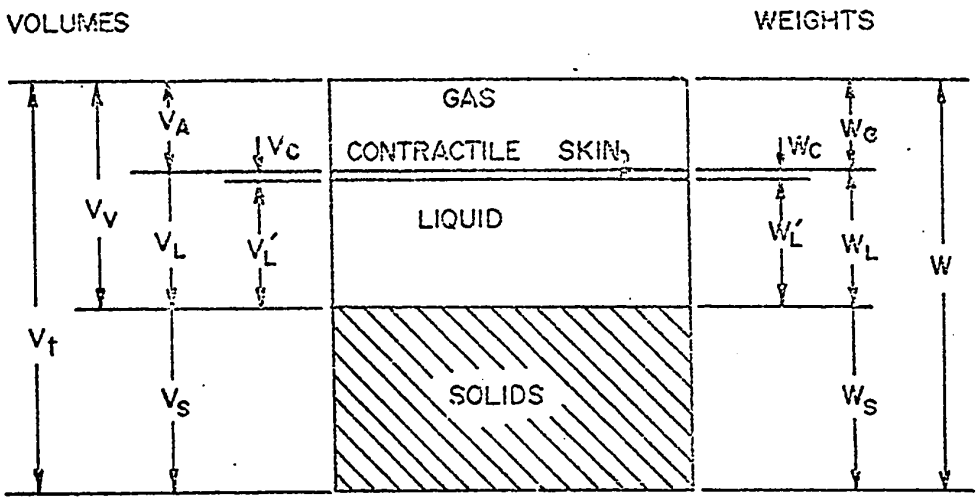


FIGURE I (a) RIGOROUS FOUR PHASE UNSATURATED SOIL SYSTEM

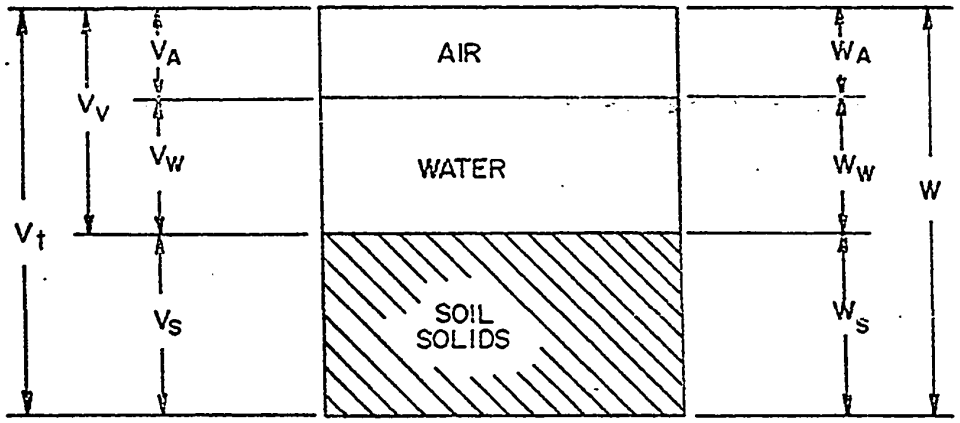


FIGURE I (b) MODIFIED TO A THREE - PHASE SYSTEM

FIGURE 1.3 VOLUME - WEIGHT RELATIONSHIPS FOR AN UNSATURATED SOIL

ships used in this thesis are summarized below. The volume relationships are:

$$\text{Porosity } (n) = \frac{\text{volume of voids}}{\text{total volume}} = \frac{V_v}{V_t} * 100$$

$$\text{Air Porosity } (n_a) = \frac{\text{volume of air}}{\text{total volume}} = \frac{V_a}{V_t} * 100$$

$$\text{Water Porosity } (n_w) = \frac{\text{volume of water}}{\text{total volume}} = \frac{V_w}{V_t} * 100$$

$$\text{Void Ratio } (e) = \frac{\text{volume of voids}}{\text{volume of solids}} = \frac{V_v}{V_s}$$

$$\text{Degree of Saturation } (S) = \frac{\text{volume of water}}{\text{volume of voids}} = \frac{V_w}{V_v} * 100$$

The only weight relationship used is the water content.

$$w = \frac{\text{weight of water}}{\text{weight of solids}} = \frac{W_w}{W_s} * 100$$

The unit weight equations combine the volume and weight relationships. The total unit weight, γ_t, the dry unit weight, γ_d, and the bouyant unit weight, γ_b, are defined in the conventional manner.

The terms "air porosity" and "water porosity" are included in the definitions since they provide a convenient means of expressing the portion of each phase with respect to a common perceptible base. The terms "percent air" and "percent water" are used in a synonymous

manner. The water porosity (n_w) is equivalently written as ($S \cdot n$) or $w \cdot G/(1+e)$. Similarly, the air porosity (n_a) can be written $(1-S) \cdot n$ or $w \cdot G(1-S)/[(1+e) \cdot S]$.

In Chapter IV, a change in volumetric deformation of any phase is equivalent to a change in porosity with respect to that phase. It should be noted that this does not mean that volumetric deformation is equivalent to phase porosity.

1.7 Context of Terminology

The study of the behavior of unsaturated soils embraces numerous areas of science. One of the results has been a lack of consistency with respect to the terminology associated with unsaturated soil behavior. The author attempts to regain some consistency by embracing terminology from continuum mechanics.

An unsaturated soil is a collection of matter which we wish to study and can be referred to as a multiphase system. The complete characterization of the system is referred to as the state of the system. The pertinent aspects of the description of the state of an unsaturated soil are:

(i) the stress field - The stress fields for each phase of an unsaturated soil are described by the equilibrium equations. These are presented in Chapter IV.

(ii) the deviation from the undeformed state - This is the "deformation field" and is discussed with respect to each phase in Chapter V.

In this thesis, only the stresses and deformations are considered as state variables. The selection of independent state variables for a particular problem is very important. However, the state variables for a problem are somewhat arbitrary (Fung, 1965). For example, more than one type of deformation state variable can be used to describe the deformations for a particular problem. Likewise, more than one set of stress state variables may be possible. However, a particular set of stress state variables should have definite advantages over other possibilities. The main factor to consider is the applicability of the state variables, in measurable quantities, to a wide variety of problems.

When a state variable is expressed as a single-valued function of other state variables, it is referred to as a constitutive equation. For example, a constitutive equation can be used to link the stress and deformation state variables. If for the unsaturated soil system, the values of the state variables are independent of time, the system is in equilibrium. If the state variables vary with time, the unsaturated soil system is undergoing a process.

The author has been reluctant to introduce new terminology; however, in the early stages of this study it became obvious that the existing terminology created serious handicaps. The handicaps are primarily related to the thinking associated with the effective stress principle. Chapter IV deals with the problem in detail. The concept of state variables gives rise to a more general and all encompassing description.

1.8 Scope of the Thesis

The behavior of unsaturated soils is approached from a relatively fundamental but phenomenological standpoint. Within the entire spectrum of soil problems of interest, there are two main categories. These are the volume change behavior and the shear strength of unsaturated soils. Both areas involve four similar steps in their solution (Figure 1.4). These are:

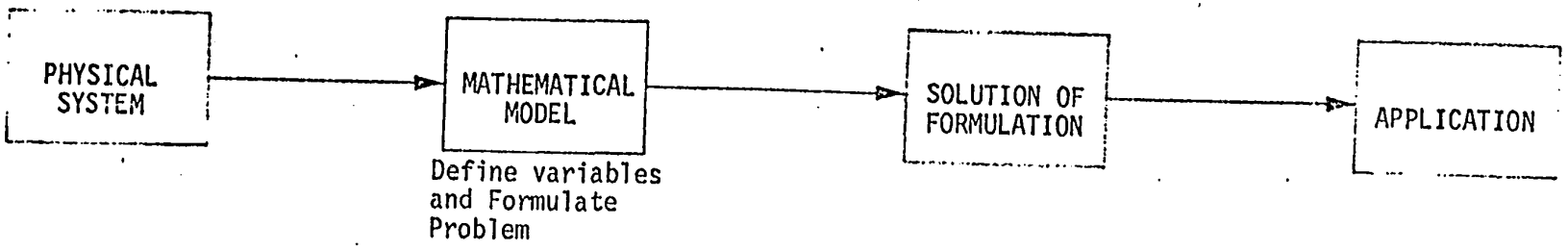
(i) the description of the physical system

(ii) the defining of the variables involved and the formulation of the problem. This is the establishment of the mathematical model.

(iii) the solution of the mathematical formulation. The partial differential equations are generally most readily solved by a finite difference method.

(iv) the application of the mathematical model to the field situation. The end result is a prediction that can be used to increase the reliability and improve the economics of the engineering design.

The complete analysis of the volume change problem with respect to the above four steps is beyond the scope of this thesis. Basically, the scope of this thesis involves the study of volume change behavior in the light of the first two steps (i.e. physical system and the mathematical model). Chapter II deals with the behavior of miscible and immiscible air-water mixtures without respect to the



OBJECT

To describe the DEFORMATION and behavior of every element of an unsaturated soil mass.

DEFORMATION THEORY

Establish the STRESS EQUILIBRIUM.
Extract the STRESS STATE VARIABLES from the equilibrium equations.
Define DEFORMATIONS OF ALL PHASES.
Employ suitable CONSTITUTIVE RELATIONSHIPS.
Impose BOUNDARY CONDITIONS
FORMULATE Problem with the assistance of other Physical Theories.

- Finite Element
- Classical (Closed Form) Solutions
- Finite Difference Solution of Partial Differential Equations

DEFORMATION PROBLEMS

Prediction of the VALUES for the Initial and Final STRESS STATE VARIABLES Insitu.
Laboratory or Insitu Evaluation of CONSTITUTIVE RELATIONSHIPS PARAMETERS
APPLICATION of DEFORMATION THEORY
Compare computed Displacements with ALLOWABLE DISPLACEMENTS

FIGURE 1.4 DEFORMATION ANALYSIS OF UNSATURATED SOIL

soil solids. A clear understanding of this area is required both in the design of the laboratory equipment and in later formulations. The two main properties analysed are density and compressibility.

Each controversial aspect of the mathematical formulation should be verified experimentally. Chapter III reviews existing and attempted laboratory designs and presents the details of the laboratory equipment designed as part of this thesis. Three associated appendices deal with,

(i) the required checks to ensure the proper functioning of the equipment (Appendix B)

(ii) the test procedures (Internal Report SM:12) and

(iii) the data reduction (Appendix D).

The remainder of the thesis presents the mathematical formulation and its experimental verification. Chapter IV presents the formulation of stress equilibrium equations for multiphase systems and the extraction of the stress state variables. This is the most fundamental aspect of the thesis and is verified by an extensive laboratory program (Appendix C).

The mapping of the deformations of a multiphase system are outlined in Chapter V. Now both the stress state variables and the deformation state variables are presented. They are joined by means of the constitutive relationships for the soil structure and the contractile skin (Chapter VI). The uniqueness of both surfaces are experimentally examined. Chapter VI ends with the formulation of a

volume change analysis for one-dimensional problems.

Chapter VII incorporates an additional dimension, time, into the analysis. This is the study of transient flow or in particular, the theory of consolidation. The analysis is restricted to the one-dimensional case. The initial pore fluid boundary conditions required at the commencement of the consolidation analysis, are derived theoretically. No attempt is made to experimentally verify the transient flow equations or even solve them.

CHAPTER II

MISCIBLE AND IMMISCIBLE MIXTURES OF AIR AND WATER

2.1 Introduction

Air and water interact both in the form of a miscible and immiscible mixture. Air is essentially a homogeneous mixture of several different molecules (Table II.1) and interacts with water in relation to the molecules making up air. However, for most practical cases, dry air can be considered as an ideal gas with a molecular mass of 28.97.

When air is mixed with water, it is largely immiscible except for approximately two percent (by volume) that dissolves to form a miscible, dilute solution. Since there is no chemical interaction between the water and air, the resulting miscible solution is a simple mixture. The immiscible air-water mixture remains separate with air overlying the water unless some foreign substance creates capillaries which hold the air within the bulk of the water.

Of primary interest from an engineering standpoint is the density and compressibility of miscible and immiscible mixtures of air and water. An understanding of air diffusion into water is needed to analyse the physical behavior of air-water mixtures.

TABLE II.1

COMPOSITION OF DRY AIR*

	Percentage By Volume	Density (gms/cc)	Specific Volume (cc/gm)	Molecular Weight
Nitrogen (N_2)	78.08	0.00125055	799.65	28.016
Oxygen (O_2)	20.95	0.00142904	699.77	32.000
Argon (Ar)	0.934	0.0017837	560.63	39.944
Carbon Dioxide (CO_2)	0.030	0.0019769	505.84	44.010
Neon (Ne)	1.82×10^{-3}	0.00090035	1110.7	20.183
Helium (He)	5.24×10^{-4}	0.00017847	5603.2	4.003
Krypton (Kr)	1.14×10^{-4}	0.003708	269.69	83.800
Hydrogen (H_2)	$\approx 5. \times 10^{-5}$	0.00008988	11,125.	2.016
Xenon (Xe)	8.7×10^{-6}	0.005851	170.91	131.300
Ozone (O_3)	$1. \times 10^{-6}$ to $1. \times 10^{-5}$	0.002144	466.42	48.000
Air	100.0	0.0012929	773.455	28.966

*Under Standard Conditions (1 atm. and 0°C)

2.2 Density of Air-Water Mixtures

From a theoretical standpoint, the analysis of air-water mixtures can be separated into four categories; namely,

(i) air (dry and moist),

(ii) pure water (air-free)

(iii) miscible air-water mixtures and

(iv) immiscible air-water mixtures.

Each category should be considered with respect to temperature and pressure in order to completely describe its state.

2.2.1 Density of Air

Air is referred to as "dry air" when its humidity is zero. "Moist Air" is a mixture of "dry air" and "water vapor". The equations of state for the "dry air" and the "moist air" are derived separately.

The density of a gas depends on three variables: the pressure, the temperature and the kind of gas (Shortley and Williams, 1955). Correspondingly, there are three experimental laws which give the dependence of density on these three variables:

1. Boyle's Law: If the temperature of a given kind of gas is held constant, its density is proportional to the absolute pressure.

2. Charles' Law: If the pressure on a given kind of gas is held constant, its density is inversely proportional to its absolute temperature.

3. Avagadro's Law: At the same temperature and pressure, different kinds of gases have densities proportional to their molecular masses.

The above three laws are combined to form the general Gas Law for a perfect (or ideal) gas.

$$P \cdot V = W \cdot R \cdot T \qquad 2.1$$

where P = absolute pressure (gm/cm^2)

V = volume (cc)

W = weight (gm)

R = Universal Molar Gas Constant (84,780 cm/°K)

T = absolute temperature (°K)

The Gas Law is often written in terms of specific volume.

$$P \cdot v = R \cdot T \qquad 2.2$$

where $v = V/W$. The specific volume is the inverse of the density.

(i) Dry Air

Air is a mixture of gases, and the general Gas Law is written as a summation (Matveev, 1967)

$$\sum_{i=1}^{n} p_i \cdot v_i = T \sum_{i=1}^{n} R_i \qquad 2.3$$

where p_i = partial pressure of each gas

v_i = specific volume

R_i = specific gas constant for each gas and

n = number of gases in the mixture.

Dalton's Law of Partial Pressures: If a mixture of gases is put into a container, the total pressure exerted on the container is the sum of the pressures that each gas would exert if it alone occupied the container.

Therefore, the behavior of a particular gas of a mixture of gases is independent of the other gases and the total pressure exerted is the sum of the partial pressures.

$$P = \sum_{i=1}^{n} p_i \qquad 2.4$$

Let us consider one gram of dry air, m, and let v be its specific volume (773.46 cc/gm). Then the volume occupied by the i-th gas, v_i, is inversely proportional to the weight of gas, m_i.

$$\frac{v_i}{v} = \frac{m}{m_i} \quad \text{or} \quad m_i = \frac{v \cdot m}{v_i} \qquad 2.5$$

This can also be written in terms of density (gms/cc) since $v = 1/\gamma_a$ or $v_i = 1/\gamma_{ai}$. The specific gas constant is related to the molar gas constant.

$$R_i = R/\mu_i \qquad 2.6$$

where μ_i is the molecular weight of the i-th gas (unitless).

Substituting equation 2.5 into equation 2.3 and summarizing, we obtain

$$v \cdot m \sum_{i=1}^{n} \frac{p_i}{m_i} = T \sum_{i=1}^{n} R_i \quad \text{or}$$

$$v \cdot \sum_{i=1}^{n} p_i = \frac{T}{m} \cdot \sum_{i=1}^{n} m_i \cdot R_i \qquad 2.7$$

Let the specific gas constant for dry air be $R_d = \frac{1}{m} \cdot \sum_{i=1}^{n} m_i \cdot R_i$ and reconsider equation 2.4

$$P \cdot v = R_d \cdot T \qquad 2.8$$

This is the equation of state for dry air. The specific gas constant for dry air is computed with the aid of equation 2.6

$$R_d = \frac{R}{m} \cdot \sum_{i=1}^{n} \frac{m_i}{\mu_i} \quad \text{or}$$

$$R_d = \frac{R}{m} \cdot \left[\left(\frac{m_1}{\mu_1}\right)_{N_2} + \left(\frac{m_2}{\mu_2}\right)_{O_2} + \left(\frac{m_3}{\mu_3}\right)_{Ar} + \left(\frac{m_4}{\mu_4}\right)_{CO_2} \right] \qquad 2.9$$

For nitrogen, N_2 ,

$$m_1 = \frac{v \cdot m}{v_1}$$

where v = specific volume of air reserved for nitrogen and

v_1 = the specific volume of nitrogen.

In other words,

v = (specific volume of air) x (percentage nitrogen by volume)

v = (773.45) x 78.08/100. = 603.91

Therefore,

$$m_1 = \frac{603.91 \times 1.}{799.65} = 0.7552$$

Similarly for m_2, m_3 and m_4

$$R_d = 84{,}780 \left[\left(\frac{0.7552}{28.016}\right) + \left(\frac{0.2315}{32.00}\right) + \left(\frac{0.0128}{39.944}\right) + \left(\frac{0.0005}{44.00}\right) \right]$$

$$R_d = 2927. \text{ cm/°K}$$

The density of dry air (gm/cc) for various absolute temperatures and absolute pressures is,

$$\gamma_a = \frac{1}{2{,}927.} \cdot \frac{P}{T} \qquad 2.10$$

(ii) Moist Air

Moist air behaves as a mixture of dry air and water vapor. Since the critical temperature of water vapor is high, it may condense and sublimate under atmospheric conditions. For condensation of water vapor to begin, it must reach a state of saturation; that is, the partial pressure, p_e, must attain the saturation pressure, p_E. Although water vapor does not behave as a perfect gas, its physical properties have been established experimentally.

The equation of state of saturated and unsaturated water vapor can be approximated as,

$$p_e \cdot v_e = R_e \cdot T \qquad 2.11$$

where p_e = partial pressure of the water vapor

v_e = specific volume and

R_e = specific constant of water vapor.

$$R_e = \frac{R}{\mu_e} = \frac{84,780}{18.02} = 4705 \text{ cm/°K}$$

where μ_e = molecular weight of water vapor.

Consider one gram of moist air, m, that contains, s, grams of water vapor and therefore (1-s) grams of dry air. The specific volume of the water vapor is v_e, the dry air is v_d and the moist air is v.

$$\frac{v_e}{v} = \frac{m}{s} \quad \text{or} \quad v_e = \frac{m}{s} \cdot v \qquad 2.12$$

and

$$\frac{v_d}{v} = \frac{m}{(1-s)} \quad \text{or} \quad v_d = \frac{m}{(1-s)} \cdot v \qquad 2.13$$

Let p be the total pressure of the moist air. Then $(p-p_e)$ is the partial pressure of the dry air. The equation of state for the dry fraction of the moist air is

$$(p-p_e) \cdot v_d = R_d \cdot T \qquad 2.14$$

The relationship between the gas constants for dry and moist air is

$$\frac{R_e}{R_d} = \frac{\mu_d}{\mu_e} = \frac{28.97}{18.02} \quad \text{or} \quad R_e = 1.608 \cdot R_d \qquad 2.15$$

Substituting 2.12, 2.13 and 2.15 into equations 2.11 and 2.14 we obtain

$$p_e \cdot \frac{m}{s} \cdot v = 1.608\ R_d \cdot T \quad \text{or} \quad p_e \cdot v = 1.608 \cdot R_d \cdot s \cdot T \qquad 2.16$$

$$(p-p_e)\ \frac{m \cdot v}{(1-s)} = R_d \cdot T \quad \text{or} \quad (p-p_e) \cdot v = R_d \cdot (1-s) \cdot T \qquad 2.17$$

Adding 2.16 and 2.17 we obtain the equation of state of moist air

$$p \cdot v = R_d(1+0.608 \cdot s) \cdot T \qquad 2.18$$

Let the specific gas constant for moist air be

$$R_m = R_d(1+0.608 \cdot s)$$

Then equation 2.18 takes the form

$$p \cdot v = R_m \cdot T \qquad 2.19$$

In terms of density, the equation is

$$\gamma_a = \frac{1}{R_m} \cdot \frac{P}{T} \qquad 2.20$$

Providing the temperature and pressure remain constant, the density of moist air is always lower than that of dry air. Physically this is due to the fact that moist air contains water vapor (lighter than dry air) which displaces some of the dry air.

Civil engineers, in general, are more familiar with the term relative humidity, ϕ, as a measure of the moisture in the air, than the weight of water vapor, s, in one gram of moist air. Relative humidity can be defined as the partial pressure of the water vapor in a mixture to the saturation pressure of the water vapor at the same temperature (Spalding and Cole, 1958).

$$\phi = \frac{p}{p_E} = \frac{R_e \cdot T/v}{R_e \cdot T/v_E} = \frac{v_E}{v} \qquad 2.21$$

The specific volume of moist air was expressed previously in terms of the grams of moisture, s , (equation 2.12) and the specific volume of dry air is

$$v_d = \frac{v}{1-s} \quad \text{or} \quad v = v_d(1-s) \qquad 2.22$$

Now, the relative humidity can be expressed as

$$\phi = \frac{v_E}{v_d(1-s)} \qquad 2.23$$

Substituting in the Gas Law we obtain

$$\phi = \frac{\frac{28.97}{18.02} \cdot \frac{R_d \cdot T}{p_E}}{\frac{R_d \cdot T}{(p-p_e)} \cdot (1-s)} = \frac{1.608(p-p_e)}{p_E \cdot (1-s)} \qquad 2.24$$

Rearranging and solving for the weight of water, s, in terms of relative humidity and pressure, we obtain

$$s = \frac{p_E \cdot \phi - 1.608(p-p_e)}{p_E \cdot \phi} = \frac{1.0 - 1.608(p-p_e)}{p_E \cdot \phi} \qquad 2.25$$

where $p - p_e = R_d \cdot T/v_d$ and

$$p_E = R_e \cdot T/v_E$$

Thus, there is no direct correspondence between relative humidity and the weight of water in the air, since it also depends on the partial pressure of the dry air and the saturated air.

The partial pressures of the dry air can be computed from the Gas Law by knowing the specific volume at the temperature under consideration. The specific volumes of the air and saturated vapor can be obtained from Physics and Chemistry Tables (Shankland, 1962) (Table II.2).

TABLE II.2

SPECIFIC VOLUME OF DRY AIR AND SATURATED WATER VAPOR

Temperature °C	Specific Volume (cc/gm)	
	Dry Air	Saturated Vapor
0	773.46	206,300.
4		157,200.
10	801.92	106,300.
15	815.66	77,900.
20	829.88	57,800.
25	843.88	43,400.
30	858.37	32,950.
35		25,250

Psychrometric charts present the amount of water in air at various temperatures and relative humidities. Spalding and Cole (1958) plot the weight of water per unit weight of dry air versus temperature. However, the chart can be read as the weight of water per unit weight of moist air, s, without significant error (Figure 2.1).

2.2.2 Density of Pure Water

Water under the pressure of its saturated vapor is called pure, saturated water; that under a lower pressure is called dilated water. In all cases, the water is free of dissolved air. Pure water is considered essentially a homogeneous substance the world over except for variations produced by isotopes of hydrogen and oxygen.

The density of pure water is determined experimentally and published in Physics and Chemistry Handbooks. Figure 2.2 shows the change in density of pure, saturated water with a variation in temperature. Relative density or the specific gravity of water is obtained by dividing each value by the density of water at 4°C. The effect of a variation in pressure on the density of pure water is shown in Figure 2.3. Under pressures normally encountered in civil engineering, the variation in density with temperature is more significant than its variation with pressure.

2.2.3 Density of Miscible Air-Water Mixtures

When air dissolves in water it forms a miscible mixture. The question of interest regards the effect of dissolved air on the density of water. From a theoretical standpoint, the solution of

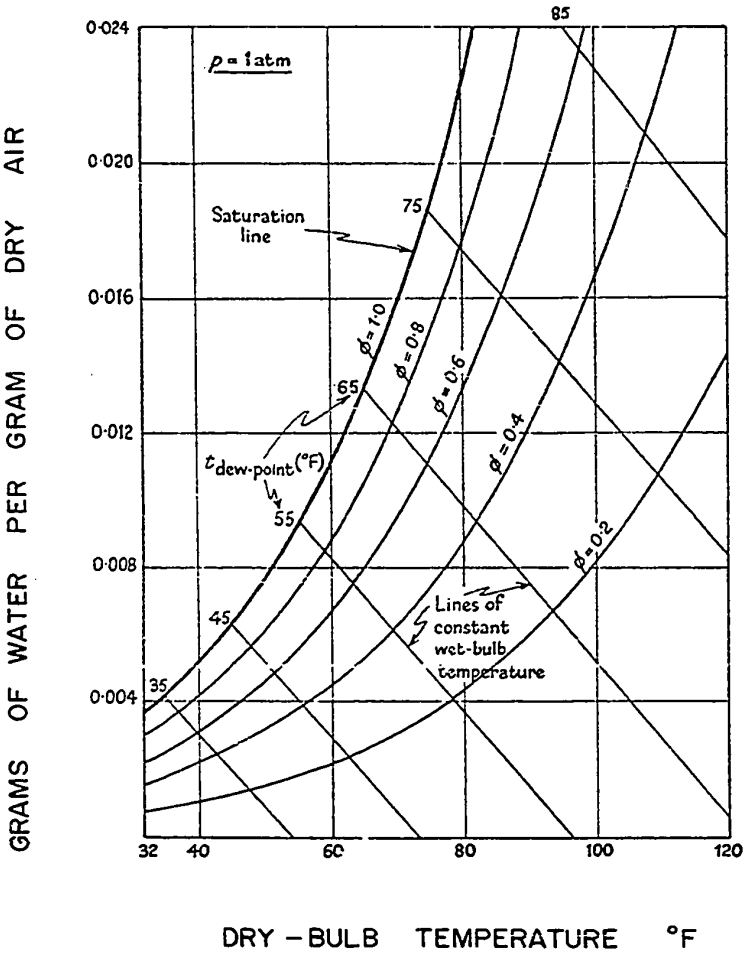


FIGURE 2.1 PSYCHROMETRIC CHART FOR AIR - WATER AT ONE ATMOSPHERE (FROM SPALDING AND COLE , 1958)

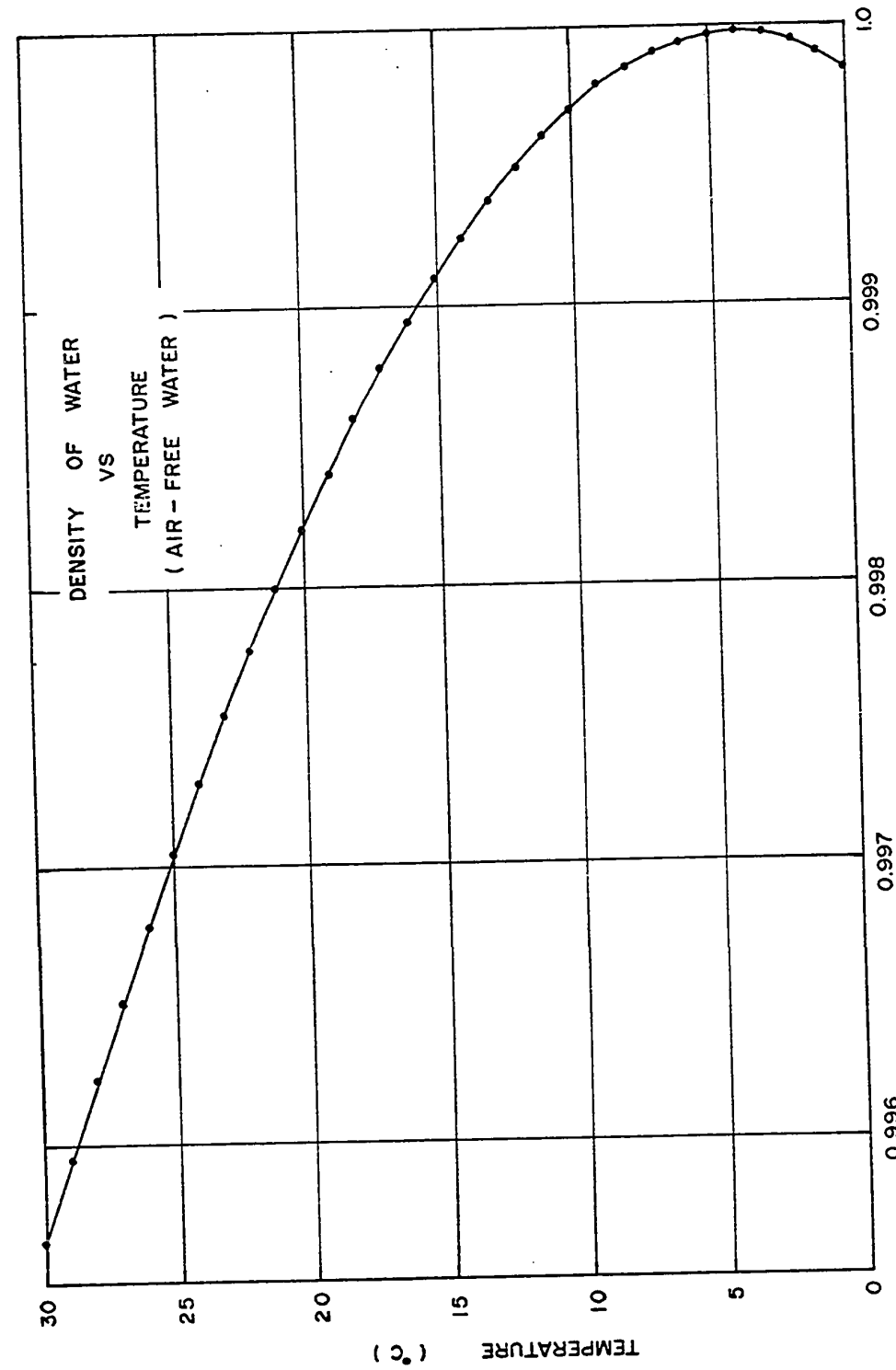


FIGURE 2.2 DENSITY OF PURE WATER

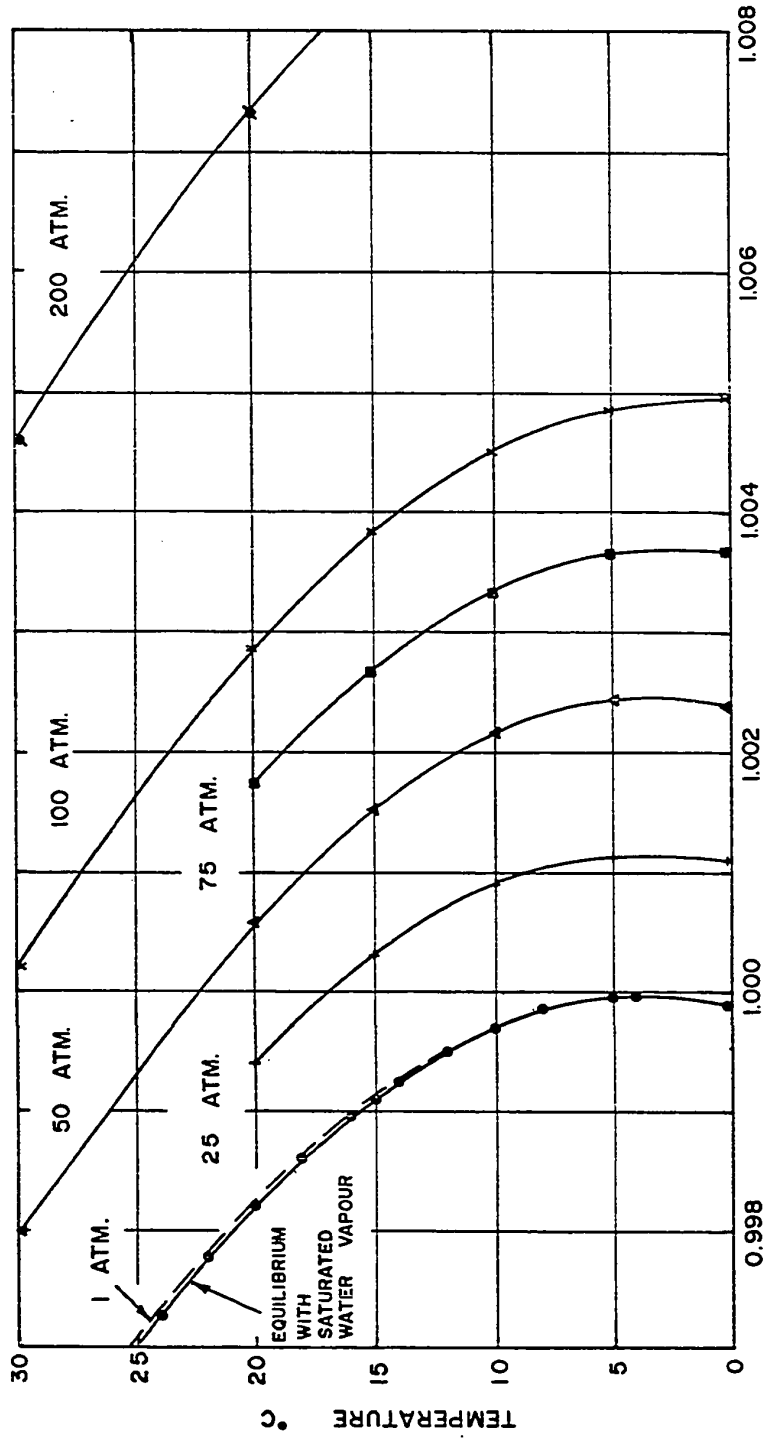


FIGURE 2.3 DENSITY OF PURE WATER AT VARIOUS TEMPERATURES AND PRESSURES

air in water can be considered comparable to the solution of any non-polar molecule in water (Rodebush and Buswell, 1958). There is a lack of attraction between the water molecules and the molecules of air. The water molecules form a "cage" around the gas molecules and when the gas molecules reach a certain concentration, the "cages" unite to form a cubic lattice.

Marek (Dorsey, 1940) showed that the density of air-free water was greater than that of water exposed to air for 1 to 3 days at the same temperature and a pressure of 1 atmosphere (Figure 2.4). The work of Frivold and Chappius (Dorsey, 1940) also verifies that dissolved air slightly decreases the density of water at temperatures below 21°C. It should be noted that the change is extremely small and would not be discernable if plotted on Figure 2.2. At a temperature of 21°C dissolved air has no measurable effect on density.

Due to the insignificant effect of dissolved air on density, it can be surmised that pressure variations will not be significantly different than for pure water. This is further verified when the compressibility of pure and air-saturated water is considered.

2.2.4 Density of Immiscible Air-Water Mixtures

The density of immiscible air-water mixtures can be evaluated by a direct proportioning of the air and water fractions.

Let the volume of water be, V_w, and the volume of air be V_a. Consider a cubic element that has impervious sides. All sides are fixed with the exception of the top which is in the form of a sealed, frictionless piston. By proportioning the components, the

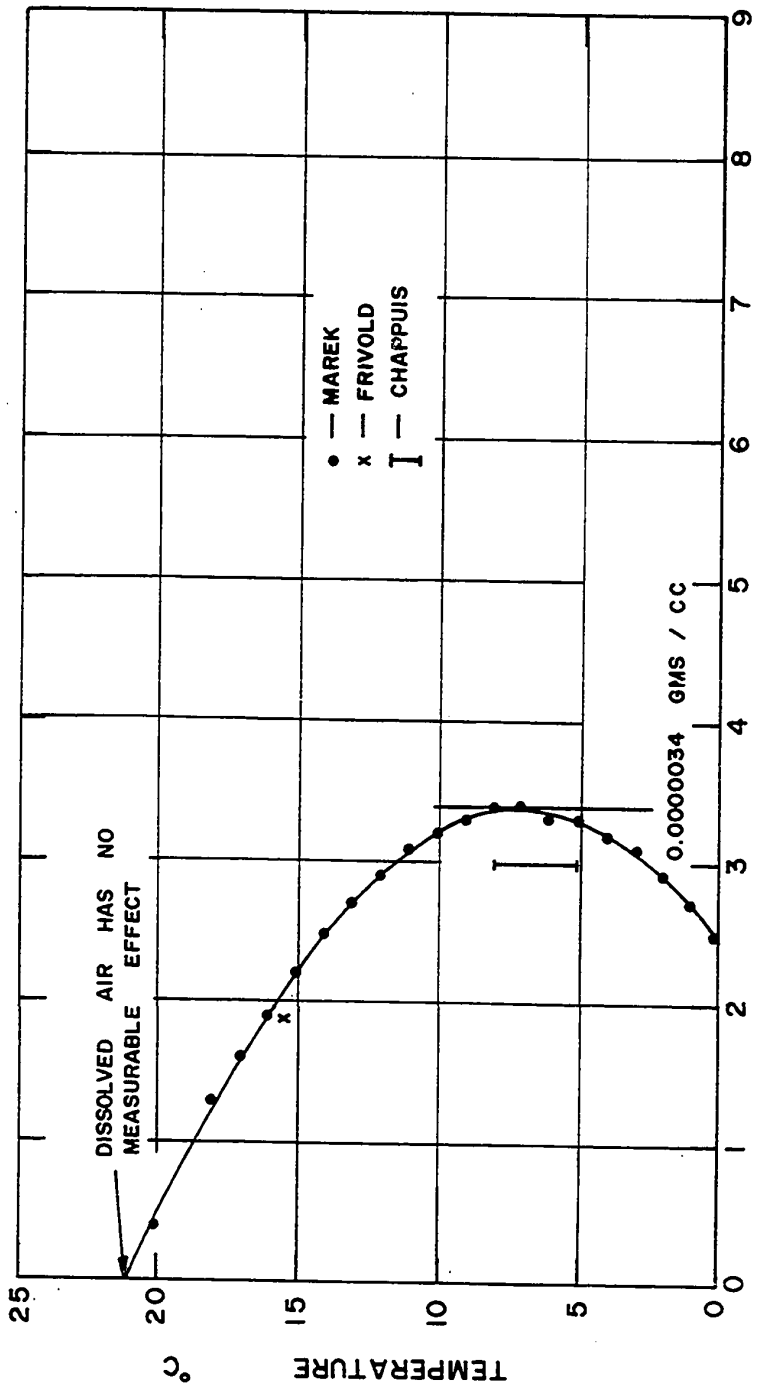


FIGURE 2.4 EFFECT OF DISSOLVED AIR ON THE DENSITY OF WATER

density of the mixture can be written,

$$\gamma_m \cdot V_T = \gamma_w \cdot V_w + \gamma_a \cdot V_a \qquad 2.26$$

where γ_m = density of the immiscible air-water mixture

V_T = total volume of air and water

γ_w = density of water

Rearranging gives

$$\gamma_m = \frac{\gamma_w \cdot V_w + \gamma_a \cdot V_a}{V_a + V_w} \qquad 2.27$$

The weight of air term, $\gamma_a \cdot V_a$, is small and insignificant relative to the other terms in the equation. The volume of water and air can also be written as a percentage of the total volume and the equation becomes,

$$\gamma_m = S \cdot \gamma_w$$

where S = the volume of water divided by the total volume (degree of saturation)

The pressure in the air and water are always equal. The pressure in both phases can be changed by moving the piston. The density of the mixture changes primarily as a result of a change in volume of air.

According to Boyle's Law the volume of air under any pressure is

$$V_a = V_{ai} \cdot u_{ai}/u_a \qquad 2.28$$

where V_{ai} = initial volume of air

u_{ai} = initial air pressure

u_a = air pressure under consideration.

The density of the air at any pressure according to the general Gas Law is

$$\gamma_a = \frac{u_a}{R \cdot T} \qquad 2.29$$

Substituting into equation 2.27 gives

$$\gamma_m = \frac{\gamma_w \cdot V_w + \frac{u_a}{R \cdot T} \cdot \frac{u_{ai} \cdot V_{ai}}{u_a}}{\frac{u_{ai} \cdot V_{ai}}{u_a} + V_w} \qquad 2.30$$

Written in terms of the initial degree of saturation and omitting the weight of air term,

$$\gamma_m = \frac{\gamma_w \cdot S}{\frac{u_{ai}}{u_a}(1-S)+S} \qquad 2.31$$

2.3 Compressibility of Air-Water Mixtures for Various Temperatures and Pressures

Isothermal compressibility is also considered under four categories i.e. air (dry and moist), pure water, miscible air-water mixtures and immiscible air-water mixtures. The air is considered theoretically as an ideal gas while the water is considered experimentally.

2.3.1 Compressibility of Air

Isothermal compressibility of a gas is defined as

$$\beta = -\frac{1}{v}\left(\frac{\partial v}{\partial u}\right)_t \qquad 2.32$$

where v = specific volume at temperature, t, and pressure, u

∂v = change in specific volume for a change in pressure, ∂u

Due to the nature of a gas, the compressibility, β, is not a constant but rather, more closely approximates a second order relationship with pressure. Therefore, it must be evaluated for every pressure under consideration.

(i) Dry Air

The specific volume of dry air under conditions of any pressure and temperature is computed from the gas law

$$v = \frac{R_d \cdot T}{u_a} \qquad 2.33$$

where $R_d = 2927.\ cm/°K$

u_a = absolute pressure (gm/cm^2)

Differentiating the gas law with respect to pressure, we obtain

$$\frac{\partial v}{\partial u_a} = - \frac{R_d \cdot T}{u_a^2} \qquad 2.34$$

Substituting equations 2.33 and 2.34 into equation 2.32, the isothermal compressibility of dry air is inversely proportional to the absolute air pressure.

$$\beta_a = + \frac{u_a}{R_d \cdot T} \frac{R_d \cdot T}{u_a^2} = \frac{1}{u_a} \qquad 2.35$$

(ii) Moist Air

The compressibility of moist air is computed in a similar manner to that for dry air. The compressibility is again inversely proportional to the absolute air pressure.

2.3.2 Compressibility of Pure Water

The isothermal compressibility of pure water has been measured by numerous research workers (Dorsey, 1940). The various techniques of testing and the different ways of presenting the data make it difficult to be assured of proper comparisons. In this presentation, only data showing the compressibility of water at 1 atmos-

phere or upon loading from 1 atmosphere to a higher pressure, are presented (Figure 2.5). The results show considerable scatter.

2.3.3 Compressibility of Miscible Air-Water Mixtures

Few tests are available on the effect of dissolved air upon compressibility. Figure 2.6 shows results analysed by Tait (Dorsey, 1940). The results are very similar to those presented for air-free water. Also presented for comparison are compressibility measurements on sea water.

Considering a temperature of 20°C, a comparison of the compressibilities of air-free water, air-saturated water and sea water can be made (Figure 2.7). Obviously, the results are not as conclusive as would be desirable. In fact, it is not possible to conclusively say that dissolved air makes water more compressible. However, the previous density results would lead us to believe that dissolved air should cause a slight increase in compressibility.

The experimental results definitely show that dissolved air is not as compressible as free air. If the dissolved air were as compressible as a gas, the compressibility of the air-water mixture would be several orders of magnitude greater under atmospheric conditions (Figure 2.8). It would appear that dissolved air fits within the water structure, producing an insignificant change in the compressibility from that of pure water.

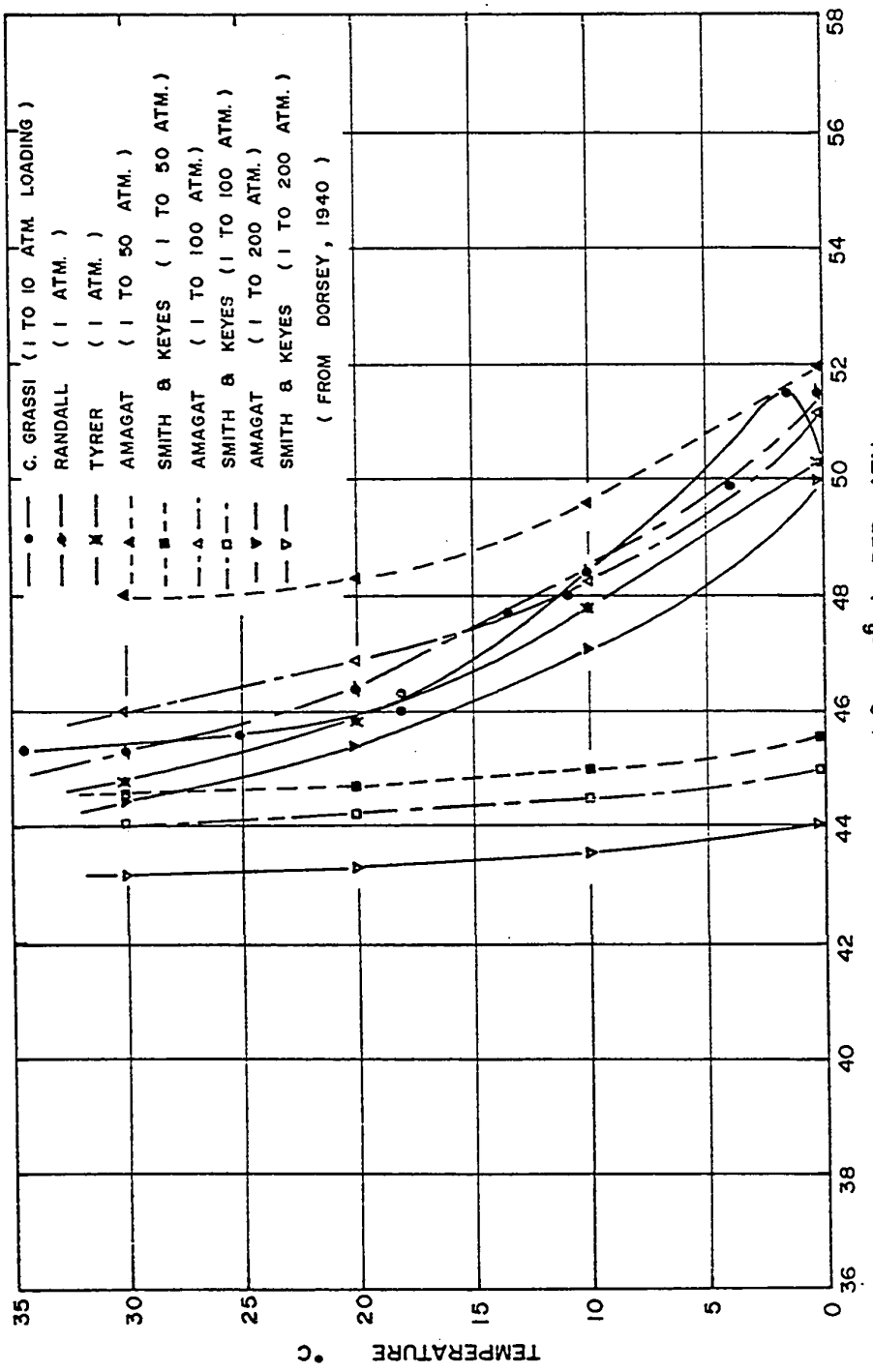


FIGURE 2.5 ISOTHERMAL COMPRESSIBILITY OF AIR - FREE WATER

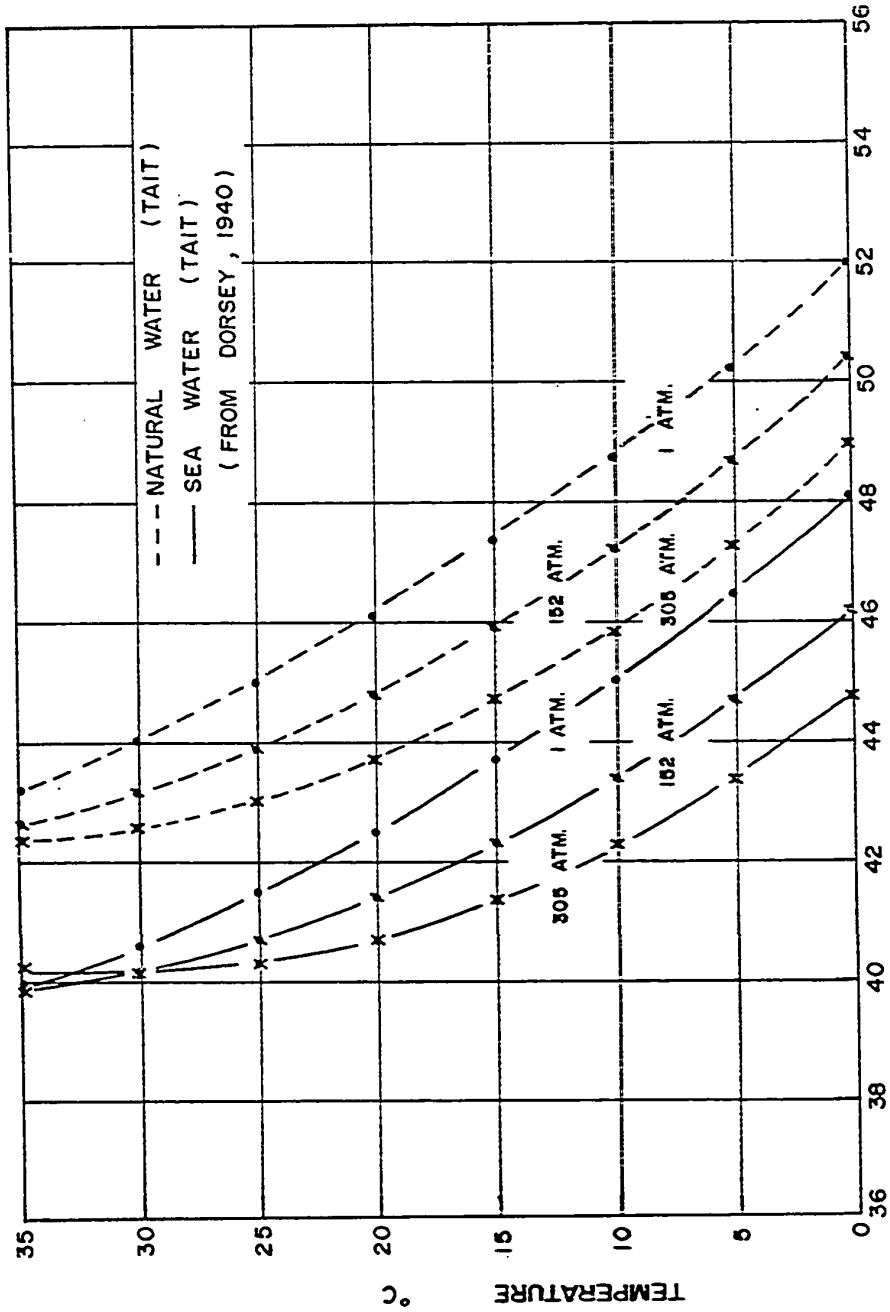


FIGURE 2.6 ISOTHERMAL COMPRESSIBILITY OF AIR - SATURATED AND SALT WATER

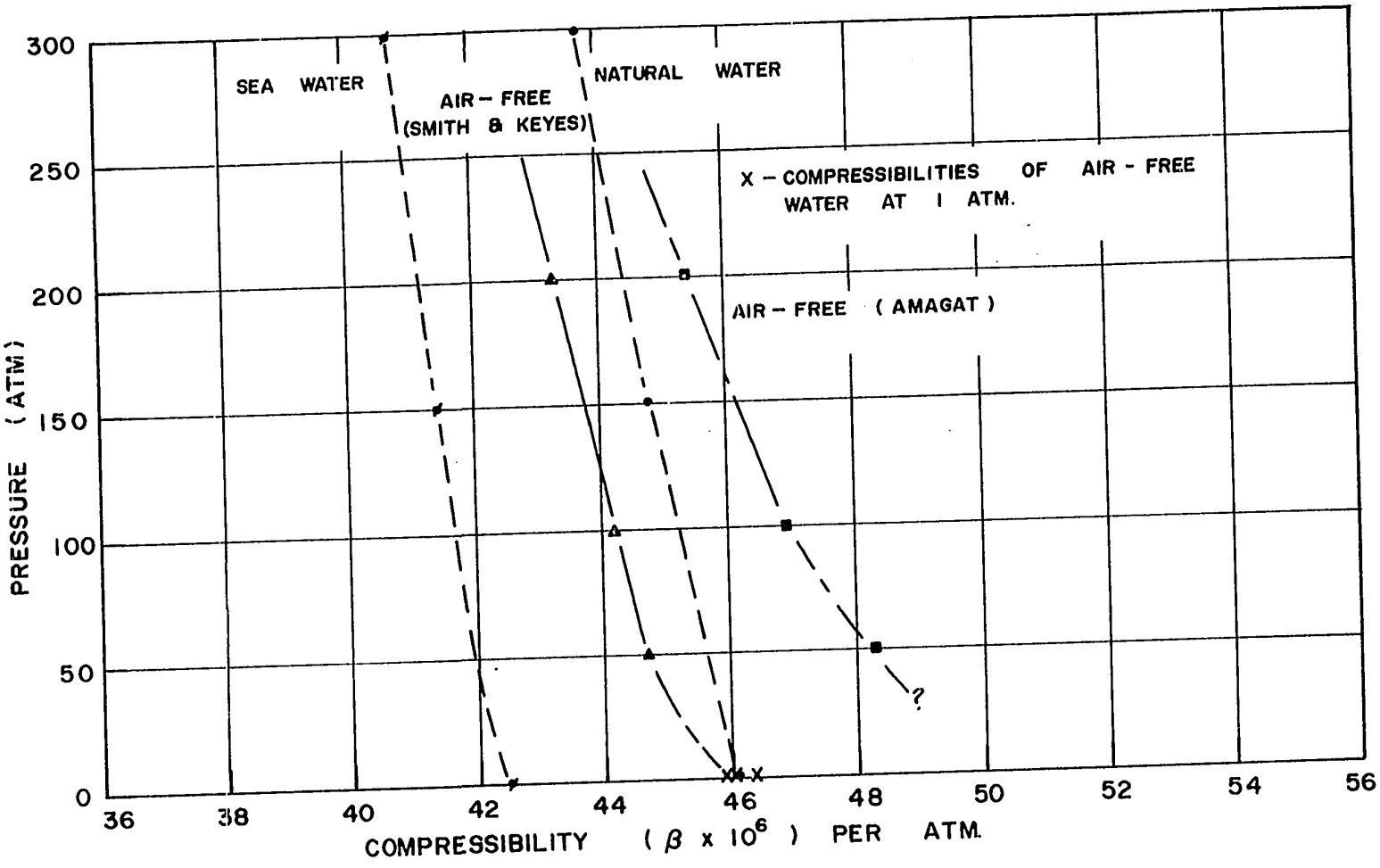


FIGURE 2.7 EFFECT OF PRESSURE ON ISOTHERMAL COMPRESSIBILITY (AT 20 °C)

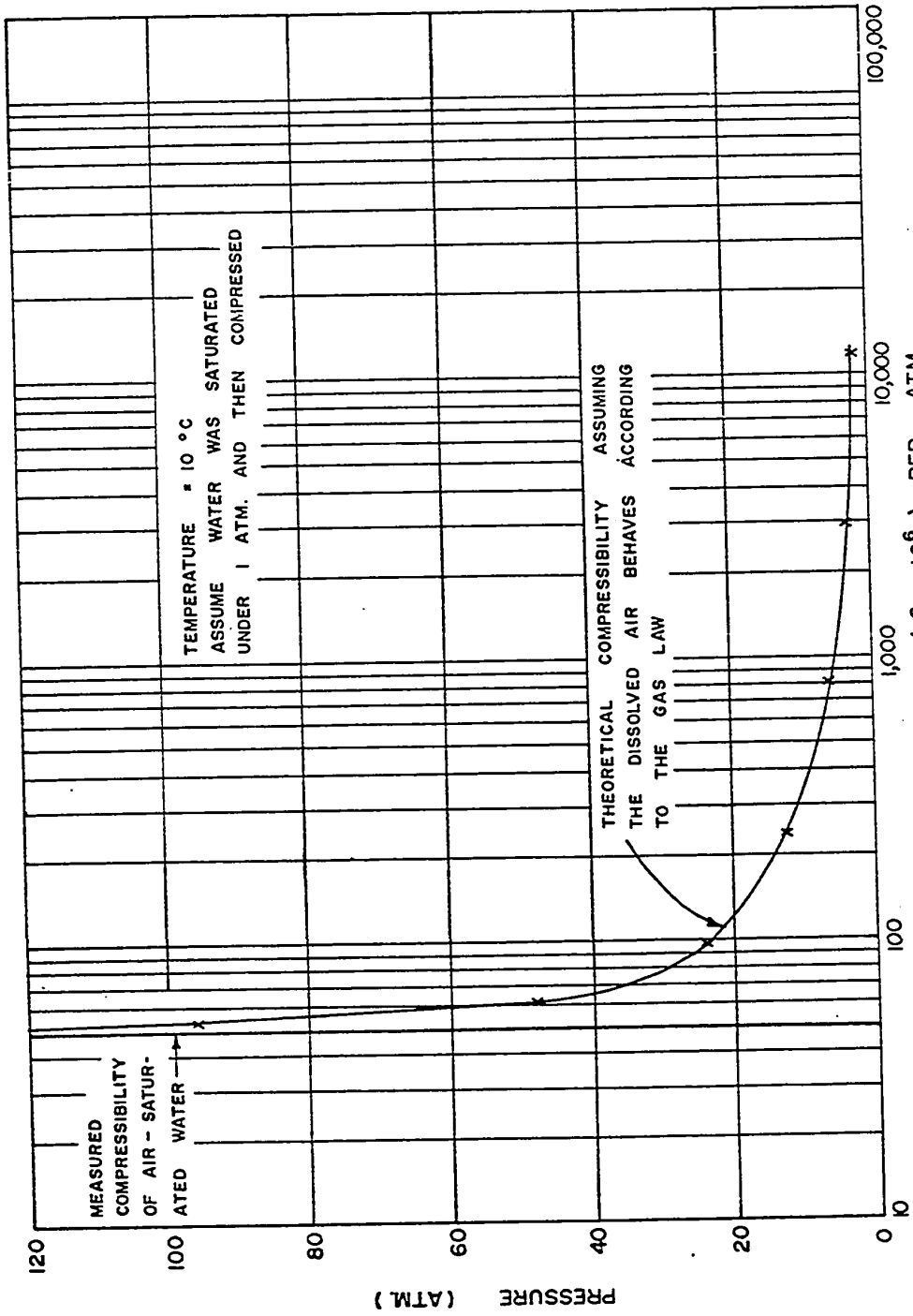


FIGURE 2.8 THEORETICAL COMPRESSIBILITY OF AIR - SATURATED WATER

2.3.4 Immiscible Air-Water Mixtures

Consider a piston and cylinder container of volume, V, partly filled with water, V_w while the remaining portion is air, V_a. The air and water are initially at equilibrium under specified temperature and pressure conditions. Since the surface of the water is horizontal, there will be no surface tension effects (i.e. radius of curvature tends to infinity) and the air and water pressures are equal.

In actuality, the interaction of an air-water mixture is a dynamic system since a change in temperature or pressure causes air to go in or come out of solution. The compressibility of air-water mixtures has been analysed by numerous research workers (Bishop and Eldin, 1950; Skempton and Bishop, 1954; Koning, 1963; Schuurman, 1966). Koning considered the air water mixture as a static system while the other researchers assumed an interaction between the air and water in accordance with Henry's Law of Solubility. The dynamic system is a combination of the miscible and immiscible systems and is considered after a discussion on solubility and solutions.

The compressibility of an immiscible air-water mixture can be computed by a direct proportioning of the air and water. The compressibility of the water portion is

$$\beta_w = - \frac{1}{V_w} \cdot \frac{dV_w}{du_w} \qquad 2.36$$

and the air portion is

$$\beta_a = -\frac{1}{V_a} \cdot \frac{dV_a}{du_a} = \frac{w_a}{V_a} \cdot \frac{R \cdot T}{u_a^2} \qquad 2.37$$

where u_w = pressure in the water phase

u_a = pressure in the air phase

The compressibility of the mixture of air and water is

$$\beta_m = -\frac{1}{V} \cdot \frac{dV}{dp} \qquad 2.38$$

Here, $V = V_a + V_w$ and $u_a = u_w = p$. Now,

$$\beta_m = -\frac{1}{V_a + V_w} \cdot \left[\frac{dV_w}{du_w} + \frac{dV_a}{du_a}\right] \qquad 2.39$$

Substituting 2.36 and 2.37 into equation 2.39

$$\beta_m = \frac{1}{V_a + V_w} \cdot [\beta_w \cdot V_w + \beta_a \cdot V_a] \qquad 2.40$$

where β_w is essentially a constant and

$$\beta_a = \frac{W_a}{V_a} \cdot \frac{R\ T}{u_a^2}$$

In cases where the air content forms a significant portion of the pore space, the compressibility of the pore water can be ignored. This then recovers the form of equation given by Bishop and Eldin (1950),

Skempton and Bishop (1954) and Schuurman (1966). That is,

$$\beta_m = - \frac{1}{V_a+V_w} \cdot \frac{dV_a}{du_a} \qquad 2.41$$

When considering the effect of small quantities of air on the compressibility of the air-water mixture, both the compressibility of the air and water must be considered. Therefore,

$$\beta_m = \frac{1}{V_a+V_w} \cdot \left[\beta_w \cdot V_w + \frac{W_a \cdot R \cdot T}{u_a^2} \right] \qquad 2.42$$

The weight of air is written in terms of a volume by means of the gas law

$$W_a = \frac{V_a u_a}{R \cdot T} \qquad 2.43$$

Substituting 2.43 into 2.42 gives

$$\beta_m = \frac{1}{V_a+V_w} \cdot \left[\beta_w \cdot V_w + \frac{V_a}{u_a} \right] \qquad 2.44$$

Rewritten in terms of the degree of saturation, the equation is,

$$\beta_m = \beta_w \cdot S + \frac{(1-S)}{u_a} \qquad 2.45$$

Figure 2.9 shows the effect of varying the percentage of air on the compressibility. The amplified influence of even a slight amount of air is clearly shown.

Suppose we performed an experiment with a cylinder that contained prescribed portions of air and water. As the sealed, frictionless piston is forced downward, the volume of air decreases substantially. The air and water pressures increase by an equal amount. At any new pressure, the portion of air has changed. In order to follow this type of process, it is desirable to plot the logarithm of compressibility versus the pore air and pore water pressure (Figure 2.10). The graph contains a series of curves that are dependent upon the initial percentage of air. The initial air pressure is taken as atmospheric on the plot presented.

During the laboratory testing program, it was possible to examine the validity of the above equation. The pressure in the base plate compartment of the oedometers (Chapter III) could be altered while the volume change was monitored accurately. No water escaped through the high air entry discs since the air pressure in the chamber was always higher than the compartment pressure. The high air entry disc could not deflect since an aluminum block with a high total stress was placed on it.

The volume changes monitored during the loading and unloading cycles performed on Oedometer No. 177 are shown in Figure 2.11. Similar results for Oedometer No. 179 are shown in Figure 2.12. The volume change data are then converted to compressibility values and

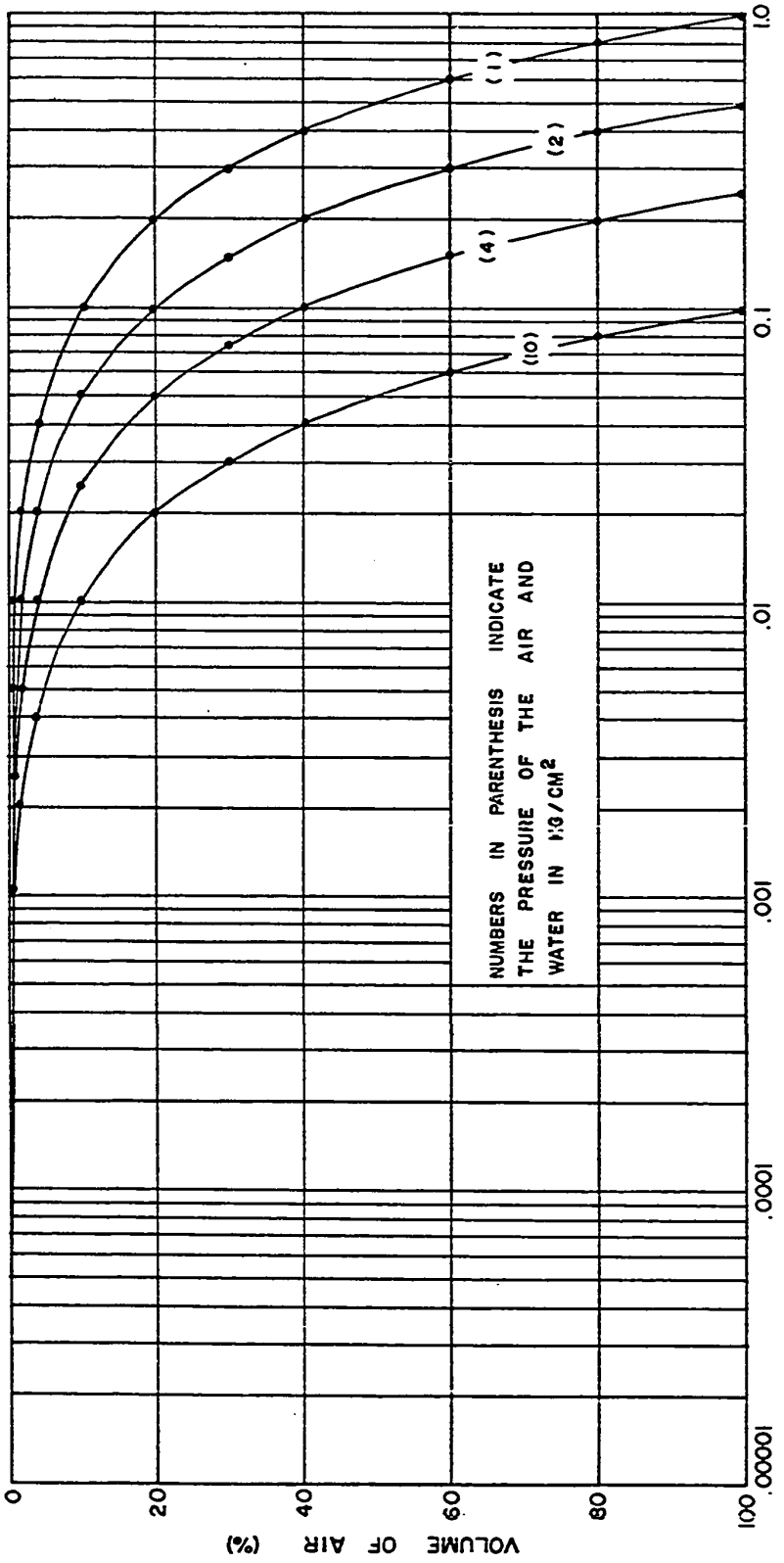


FIGURE 2.9 COMPRESSIBILITY OF AN IMMISCIBLE AIR - WATER MIXTURE

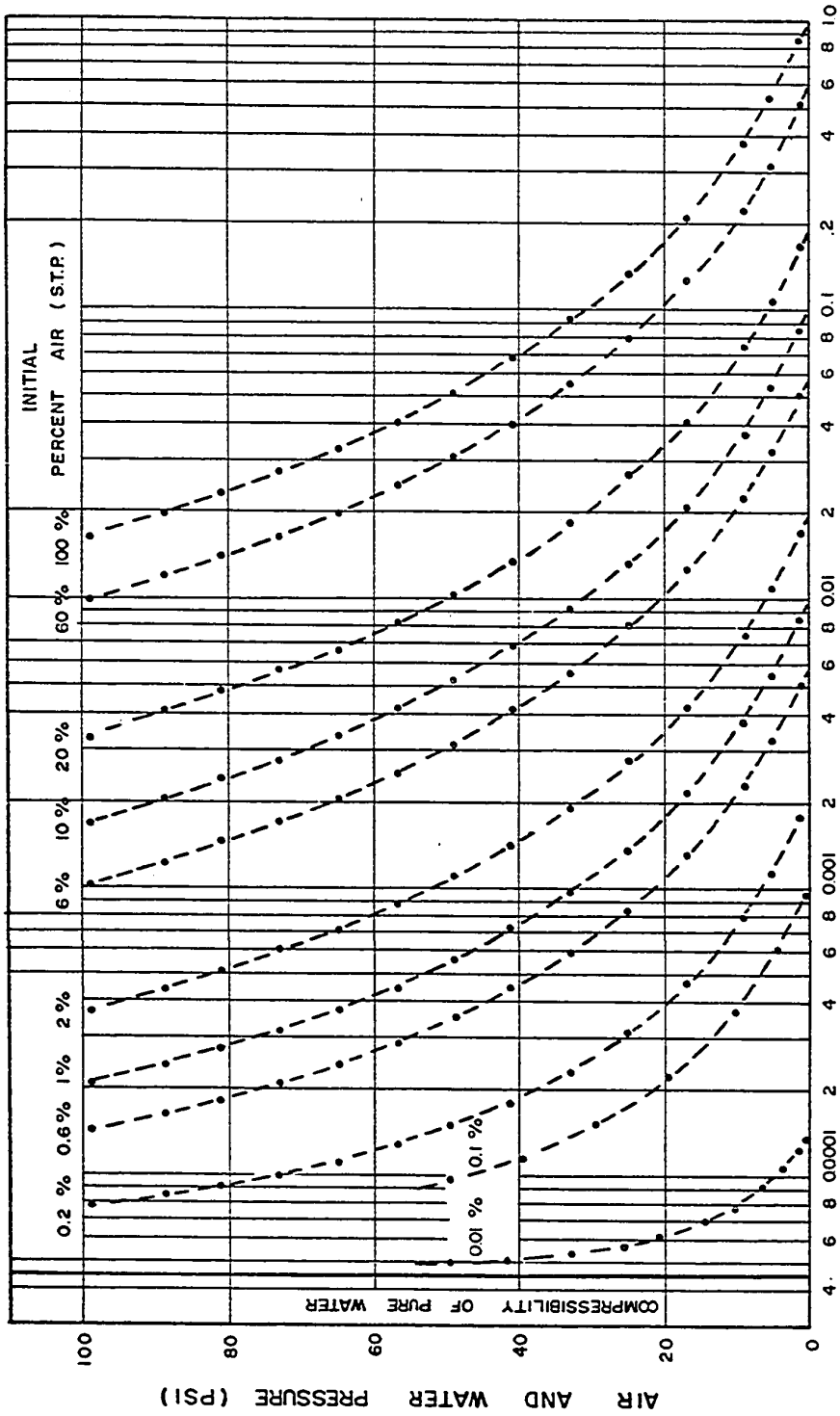


FIGURE 2.10 COMPRESSIBILITY VERSUS PRESSURE OF AN IMMISCIBLE AIR - WATER MIXTURE

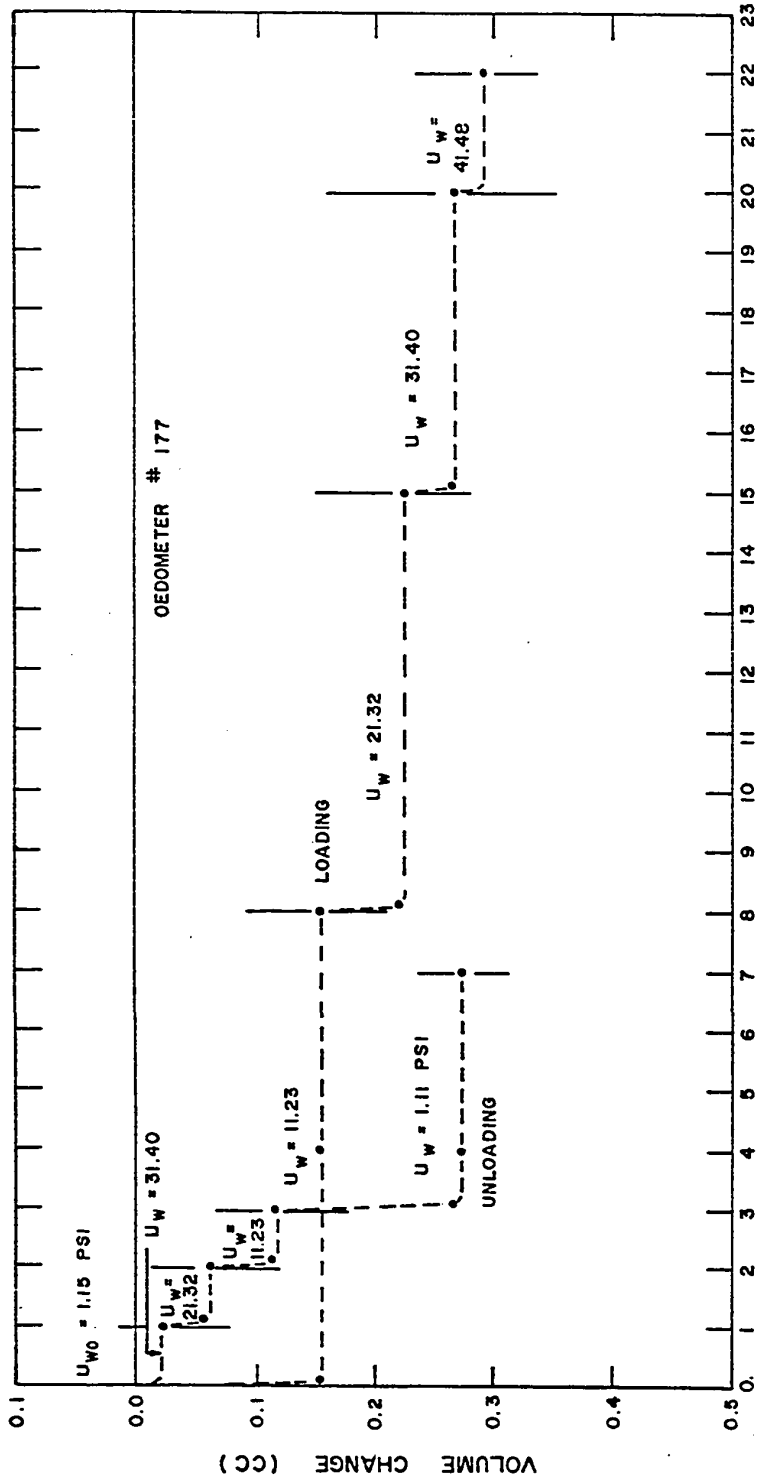


FIGURE 2.11 VOLUME CHANGE IN THE COMPARTMENT OF OEDOMETER NO. 177 DURING LOADING AND UNLOADING

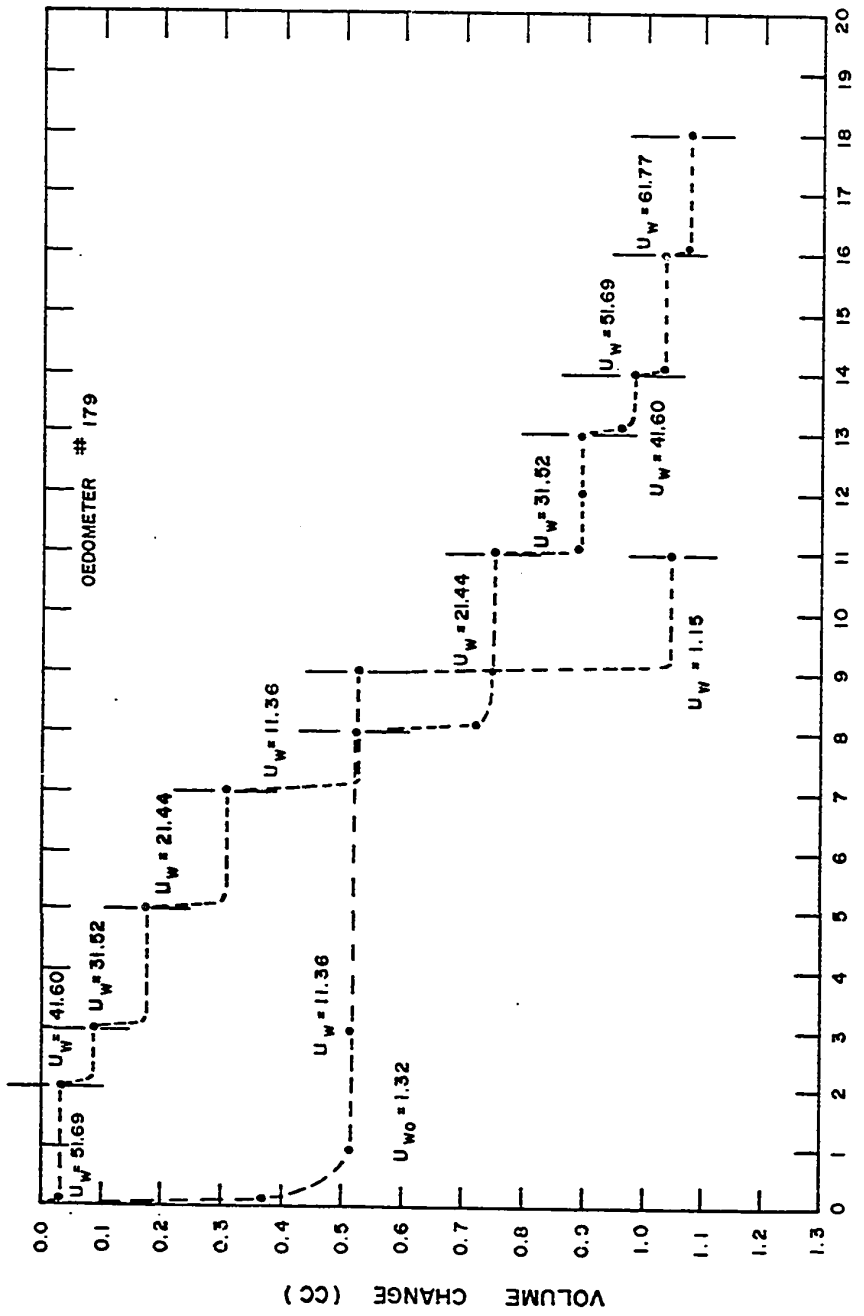


FIGURE 2.12 VOLUME CHANGE IN THE COMPARTMENT OF OEDOMETER NO. 179 DURING LOADING AND UNLOADING

plotted versus the chamber pressure (Figure 2.13). The results are in good agreement with the theory. The significant effect on compressibility of even a small percentage of air is well demonstrated by the results. Other tests with further verification of the theory are presented in Appendix E.

2.4 Solubility of Air in Water

Air dissolves in water in accordance with Henry's Law since there is no chemical interaction between the air and the water.

Henry's Law: The weight of gas dissolved in a fixed quantity of a liquid, at constant temperature, is directly proportional to the pressure of the gas above the solution (Sisler, Vander Werf and Davidson, 1953).

However, there must be some known starting point for applying Henry's Law. The starting point commonly used is the coefficient of solubility. This coefficient is the amount of air dissolved in water (under one atmosphere of pressure) when the water is saturated with air (Table II.3).

If the weights of dissolved air were extracted from the water and compressed at the same pressure as acting on the water, the volume they would occupy can be computed by the gas law. The values are tabulated in the last column of Table II.3.

Each gas composing air, dissolves in water in accordance with its coefficient of solubility, H_i. The coefficient of solubility of nitrogen is almost twice that of oxygen. However, air contains

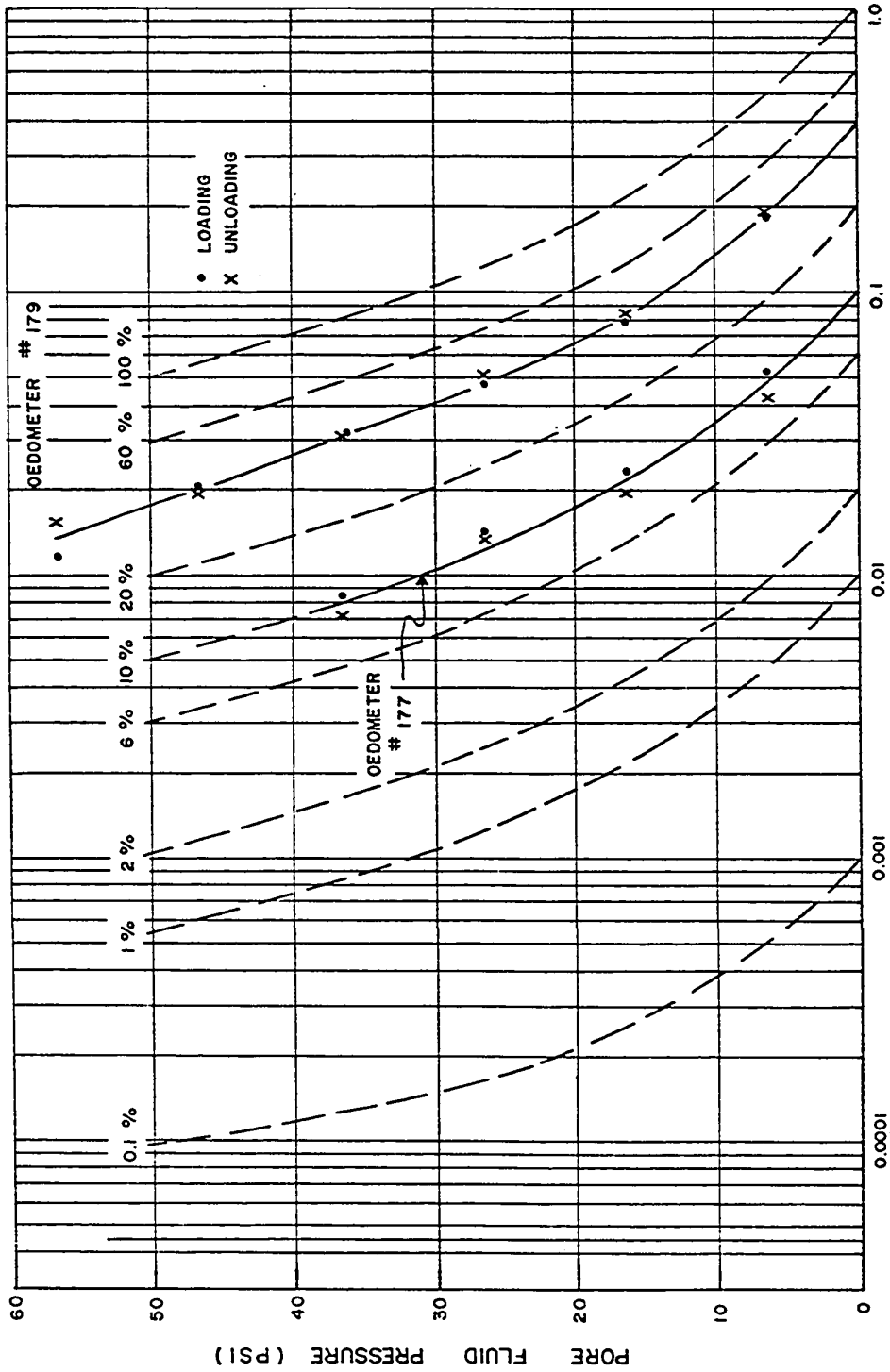


FIGURE 2.13 MEASURED COMPRESSIBILITIES IN THE COMPARTMENT OF OEDOMETER NO. 177 AND NO. 179

TABLE II.3

SOLUBILITY OF AIR IN WATER (Dorsey, 1940)

Temperature	Weight of Gas Per Wt. of Water (H)*			Volume of Air Per Volume of Water (h)
	Oxygen	Nitrogen Argon, etc.	Air (H_a)	
0	14.56×10^{-6}	23.87×10^{-6}	38.43×10^{-6}	0.02918
4	13.06×10^{-6}	21.59×10^{-6}	34.65×10^{-6}	0.02632
10	11.25×10^{-6}	18.82×10^{-6}	30.07×10^{-6}	0.02284
15	10.07×10^{-6}	17.00×10^{-6}	27.07×10^{-6}	0.02055
20	9.11×10^{-6}	15.51×10^{-6}	24.62×10^{-6}	0.01868
25	8.28×10^{-6}	14.24×10^{-6}	22.52×10^{-6}	0.01708
30	7.55×10^{-6}	13.10×10^{-6}	20.65×10^{-6}	0.01564

*At Standard Atmospheric Pressure

almost four times as much nitrogen as oxygen. Therefore, in a closed system, the water tends to be oxygen rich and the air above the water is deficient in oxygen. This effect is insignificant and air can be considered to dissolve as an ideal gas.

$$w_{do} = V_w \cdot \gamma_w \cdot \Sigma H_i = V_w \cdot \gamma_w \cdot H_a \qquad 2.46$$

where w_{do} = weight of air dissolved in water at a pressure, u_{ao}, of one atmosphere

γ_w = density of water (gm/cc)

H_i = coefficient of solubility of each gas that forms the air

H_a = sum of all the coefficients of solubility of the gases composing the air.

2.4.1 Piston and Porous Stone Analogy

The experimental data on the density of water indicates that air dissolves in water by fitting within the water structure, causing essentially no disruption. To further understand this mechanism, consider a piston and cylinder arrangement with a porous stone (having a porosity of approximately two percent) at the base of the cylinder (Figure 2.14). The porous stone is to simulate the behavior of the water.

Also, let us suppose there is an imaginary valve at the contact between the free air and the porous stone. In this way, the movement of air into the stone can be controlled. The air in the

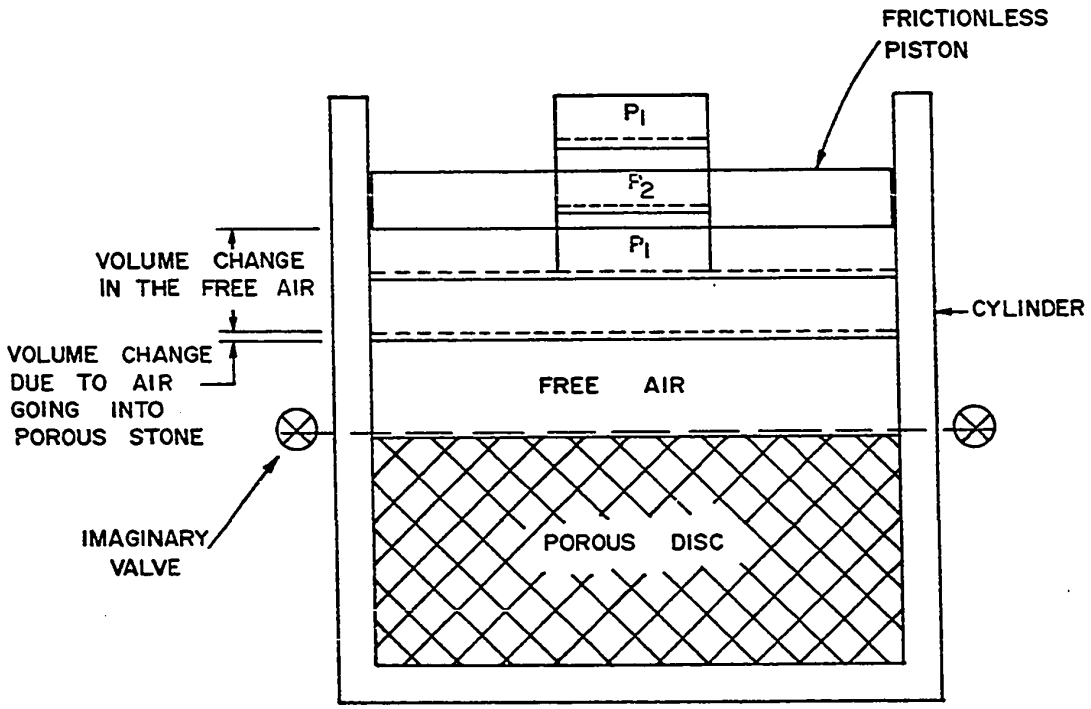


FIGURE 2.14 PISTON AND POROUS STONE ANALOGY

porous stone simulates the air dissolved in water.

Under the initial pressure conditions, u_{ao}, the volume of free air is V_{ao} and the dissolved air is V_d. Suppose the imaginary valve between the free air and the porous stone is closed and the pressure on the piston is increased to u_a. Boyle's Law can be applied to the free air and the new volume computed.

$$u_{ao} \cdot V_{ao} = V_a \cdot u_a \quad \text{or} \quad V_a = \frac{u_{ao}}{u_a} \cdot V_{ao} \qquad 2.47$$

If the imaginary valve is now opened, some air passes into the porous stone, resulting in a further volume decrease. According to Henry's Law, the total weight of air to pass into the porous stone is directly proportional to the applied pressure.

$$\frac{w_{do}}{w_d} = \frac{u_{ao}}{u_a} \quad \text{or} \quad w_d = w_{do} \cdot \frac{u_a}{u_{ao}} \qquad 2.48$$

where w_{do} = the weight of gas dissolved at a pressure, u_{ao}, and

w_d = weight of gas that would be dissolved under the new pressure, u_a.

The weight of free air that passes into the porous stone is the difference between the initial and final weights i.e. $dw_d = w_d - w_{do}$. The volume represented by this weight change (under pressure conditions, u_a) can be computed from the gas law.

$$\Delta V_d = \frac{dw_d \cdot R \cdot T}{u_a} \qquad 2.49$$

This additional volume change must be added to the previous volume change in order to obtain the total volume change of the free air. Or, put in another way,

$$V_a' = V_a - \Delta V_d \qquad 2.50$$

where V_a' = final volume of free air after the dissolving process is complete.

It should be noted that although the weight of gas dissolved is proportional to the pressure, the volume occupied by a gas is also inversely proportional to the pressure (i.e. Gas Law). In other words, the volume of a gas decreases with increasing pressure, just as rapidly as the solubility increases. Therefore, the volume of gas dissolved in a given volume of liquid is independent of pressure. This can be proven as follows:

Applying the gas law to the dissolved air portion,

$$u_{ao} \cdot V_{do} = w_{do} \cdot R \cdot T \quad \text{and} \qquad 2.51$$

$$u_a \cdot V_d = w_d \cdot R \cdot T \qquad 2.52$$

In addition, Henry's Law states that

$$\frac{w_{do}}{w_d} = \frac{u_{ao}}{u_a} \qquad 2.53$$

From equation 2.52

$$V_{do} = w_{do} \cdot R_d \cdot T / u_{ao} \qquad 2.54$$

Substituting equation 2.53 into equation 2.52 gives

$$V_d = \frac{w_d \cdot R_d \cdot T}{u_a} = \left(\frac{u_a \cdot w_{do}}{u_{ao}}\right)\left(\frac{R_d \cdot T}{u_{ao}}\right) \quad \text{or}$$

$$V_d = \frac{w_{do} \cdot R_d \cdot T}{u_{ao}} \qquad 2.55$$

Therefore $V_{do} = V_d$

Since the volume of dissolved air remains a constant, it is also possible to combine the free and dissolved air, and apply Boyle's Law to the entire volume. To separate the air into its dissolved and free phases at any point, the volume of dissolved air can be subtracted from the total volume of air. This is the procedure used by Hilf (1956) and Bishop (1957).

As additional load is applied to the piston, the free air is compressed and a small portion goes into the porous stone. Eventually, all the air is driven into the porous stone.

At this point, no further load can be applied to the air phase since additional load is transmitted directly to the porous disc. Therefore, once the air is driven into solution (the porous disc), the air-water mixture behaves as a fluid with a compressibility essentially equal to that of pure water (porous disc).

2.4.2 Theory of Rate of Diffusion

Air does not dissolve instantaneously in water but rather it involves a slow transient process referred to as diffusion. Diffusion is a mass transfer which occurs on an individual molecular basis. The driving force is a concentration gradient. The mechanism involves a transfer of the molecules composing air, into the vacancies or "holes" in the water (Tuwiner,1962).

Let us consider a cylinder (Figure 2.15) with a regulated air pressure above the water. After the air in the water is in complete equilibrium with the air above the water, let us increase the air pressure in the cylinder. Remove an element from the water at any elapsed time (Figure 2.15).

The element can be viewed on a microscopic scale, as a two-phase, air-water system. Laboratory testing shows that the water behaves as though it has a rigid water structure with air channels and cavities. A basic requirement of the two-phase system is that the deformation of each phase must be equal and opposite at all times (Chapter V). Therefore,

$$\frac{\partial e^w}{\partial t} = \frac{\partial e^d}{\partial t} \qquad 2.56$$

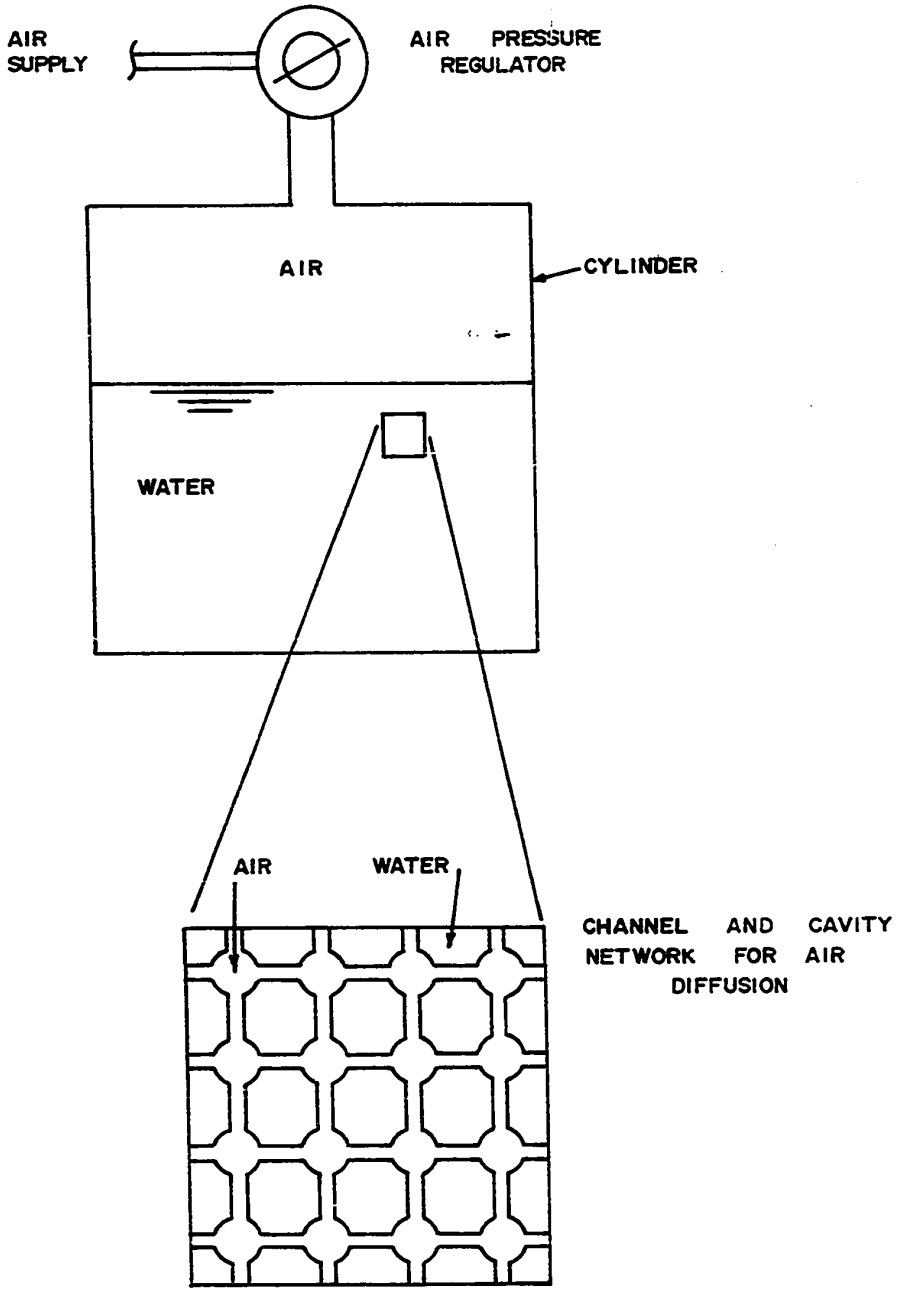


FIGURE 2.15 ELEMENT TO DERIVE THE THEORY OF AIR DIFFUSION THROUGH WATER

where e^w = deformation of the pure water

e^d = deformation of the dissolved air

t = time

As mentioned, laboratory research has shown that the deformation of the pure water phase is essentially zero. That is,

$$\frac{\partial e^w}{\partial t} = 0$$

Then,

$$\frac{\partial e^d}{\partial t} = 0$$

To establish the continuity requirements, only the air phase need be considered. Since only one phase is involved, the conservation of mass for a spatial element can be written directly (Chapter VII).

$$\frac{\partial(n_d \cdot \gamma_a)}{\partial t} = \frac{\partial(\gamma_a \cdot v_x{}^a)}{\partial x} + \frac{\partial(\gamma_a \cdot v_y{}^a)}{\partial y} + \frac{\partial(\gamma_a \cdot v_z{}^a)}{\partial z} \qquad 2.57$$

where n_d = percentage of the elemental volume that is dissolved air

v^a = velocity of the dissolved air

Reducing the problem to one dimension and expanding gives,

$$n_d \cdot \frac{\partial \gamma_a}{\partial t} + \gamma_a \cdot \frac{\partial n_d}{\partial t} = \gamma_a \cdot \frac{\partial v_y{}^a}{\partial y} + v_y{}^a \cdot \frac{\partial \gamma_a}{\partial y} \qquad 2.58$$

The basic requirement previously stipulated means that the second term of equation 2.58 (i.e. $\gamma_a \cdot \partial n_d/\partial t$) is zero. The velocity term on the right-hand side can be written in terms of concentration gradients by means of Fick's first law (Tuwiner, 1962).

$$v_y^a = - D \cdot \frac{1}{\gamma_a} \cdot \frac{\partial \gamma_a}{\partial y} \qquad 2.59$$

where D = diffusivity (cm^2/sec)

Substituting into equation 2.58 gives

$$\frac{n_d}{\gamma_a} \cdot \frac{\partial \gamma_a}{\partial t} = - D \cdot \frac{1}{\gamma_a} \cdot \frac{\partial^2 \gamma_a}{\partial y^2} - D \cdot \frac{1}{\gamma_a^2} \cdot \left(\frac{\partial \gamma_a}{\partial y}\right)^2 \qquad 2.60$$

Recognizing that the second order term in equation 2.60 is negligible, it becomes the conventional one-dimensional diffusion equation.

$$n_d \cdot \frac{\partial \gamma_a}{\partial t} = - D \cdot \frac{\partial^2 \gamma_a}{\partial y^2} \qquad 2.61$$

The porosity with respect to dissolved air can be written as the volumetric coefficient of solubility (i.e., $n_d = h$). Also, the density of the air can be written in terms of air pressures by means of the Gas law (i.e., $\gamma_a = u_a/(R \cdot T)$). Thus, the diffusion equation often takes varying forms in the literature.

The boundary conditions can be written either in terms of

densities or pressures. In terms of densities, for a one-dimensional problem, they are:

$$t = 0 \quad \text{and} \quad 0 \leq y < H \qquad \gamma_a = \gamma_{ao}$$

$$0 \leq t \leq \infty \quad \text{and} \quad y = 0 \qquad \frac{\partial \gamma_a}{\partial y} = 0$$

$$0 \leq t \leq \infty \quad \text{and} \quad y = H \qquad \gamma_a = \gamma_{af}$$

$$t = \infty \quad \text{and} \quad 0 \leq y \leq H \qquad \gamma_a = \gamma_{af}$$

The initial equilibrium air density in the water is designated as γ_{ao} while the new applied air density at the surface is designated as γ_{af}.

For a three-dimensional problem, the governing partial differential equation is,

$$h \cdot \frac{\partial \gamma_a}{\partial t} = - D \cdot \left[\frac{\partial^2 \gamma_a}{\partial x^2} + \frac{\partial^2 \gamma_a}{\partial y^2} + \frac{\partial^2 \gamma_a}{\partial z^2} \right] \qquad 2.62$$

Attempting to apply equation 2.62 to an unsaturated soil results in extreme complexity with respect to boundary conditions. Each element of the soil must be first analysed as a three-dimensional problem in itself. The boundary conditions for each element involve a detailed description of the configuration of the contractile skin. Obviously, this approach is unnecessarily demanding and impractical.

Although a complete investigation of this problem is outside the scope of this thesis, the author suggests that the contractile

skin be viewed from a more macroscopic standpoint with average properties prescribed to each element. Then a "macroscopic diffusivity" value can be defined and used in the analysis in place of the "absolute diffusivity" value. The "macroscopic diffusivity" would need to be measured for each soil under consideration, similar to any constitutive relationship parameter. This approach has more appeal when we realize that the "absolute diffusivity" value of air through water is not very absolute with respect to the water in soils.

2.4.3 Measurement of Diffusivity

Normally the computation of the rate of diffusion of air in water assumes that the water in the soil has the same properties as that of water external to the soil. In many cases where diffusion is of interest, equilibrium is assumed to be reached within minutes or even seconds. The first research workers to strongly dispute this reasoning were Sides and Barden (1967). They conclude that the higher viscosity of the adsorbed water is the prime cause for a reduced diffusivity for water in soils (Barden and Sides (1967)).

The gases composing air, diffuse individually in normal water. Kohn (1965) reports the following values.

TABLE II.4

DIFFUSIVITY OF CERTAIN GASES IN WATER

Gas	Temperature °C	Diffusivity (cm^2/sec)
CO_2	20	1.7×10^{-5}
N_2	22	2.0×10^{-5}
H_2	21	5.2×10^{-5}
O_2	25	2.92×10^{-5}

The diffusivity value generally given for air is 2.0×10^{-5} cm^2 per sec (International Critical Tables). Few attempts have been made to measure the diffusion of air through the water in soils (Poulos, 1964). Barden and Sides (1967) placed soil samples over a rubber seal and monitored the movement of air through the soil (Table II.5).

During the testing program for this thesis, the diffusion of air through the water had a pronounced effect upon the test results. The effects of air diffusion were not fully appreciated at the commencement of testing. The results of tests are presented which demonstrate the effect of diffusing air. Figure 2.16 shows the independent monitoring of air and water through 2.51 cm of water plus a rubber membrane and a ceramic disc. Even after four days it appears that steady state diffusion has not been established.

Figure 2.17 presents the rate of accumulation of air below

TABLE II.5

MEASURED VALUES OF THE COEFFICIENT OF DIFFUSION THROUGH DIFFERENT MATERIALS

(From Barden and Sides, 1967)

Material	Water Content %	Diffusion Coefficient cm^2/sec
Free water	--	2.2×10^{-5}
Natural rubber	--	1.1×10^{-6}
Kaolin consolidated at 60 psi orientated parallel to flow	49	4.5×10^{-6}
Kaolin consolidated at 60 psi orientated perpendicular to flow	49	3.2×10^{-6}
Kaolin consolidated at 70 psi	47	3.0×10^{-6}
Kaolin consolidated at 5 psi	75	6.2×10^{-6}
Derwent clay (illite) consolidated at 5 psi	53	4.7×10^{-6}
Jackson's and 4% bentonite at 5 psi	39	$<1.0 \times 10^{-7}$
Compacted Westwater clay	16	1.0×10^{-7}
Saturated ceramic	49	1.6×10^{-6}
Saturated coarse stone	21	2.5×10^{-5}

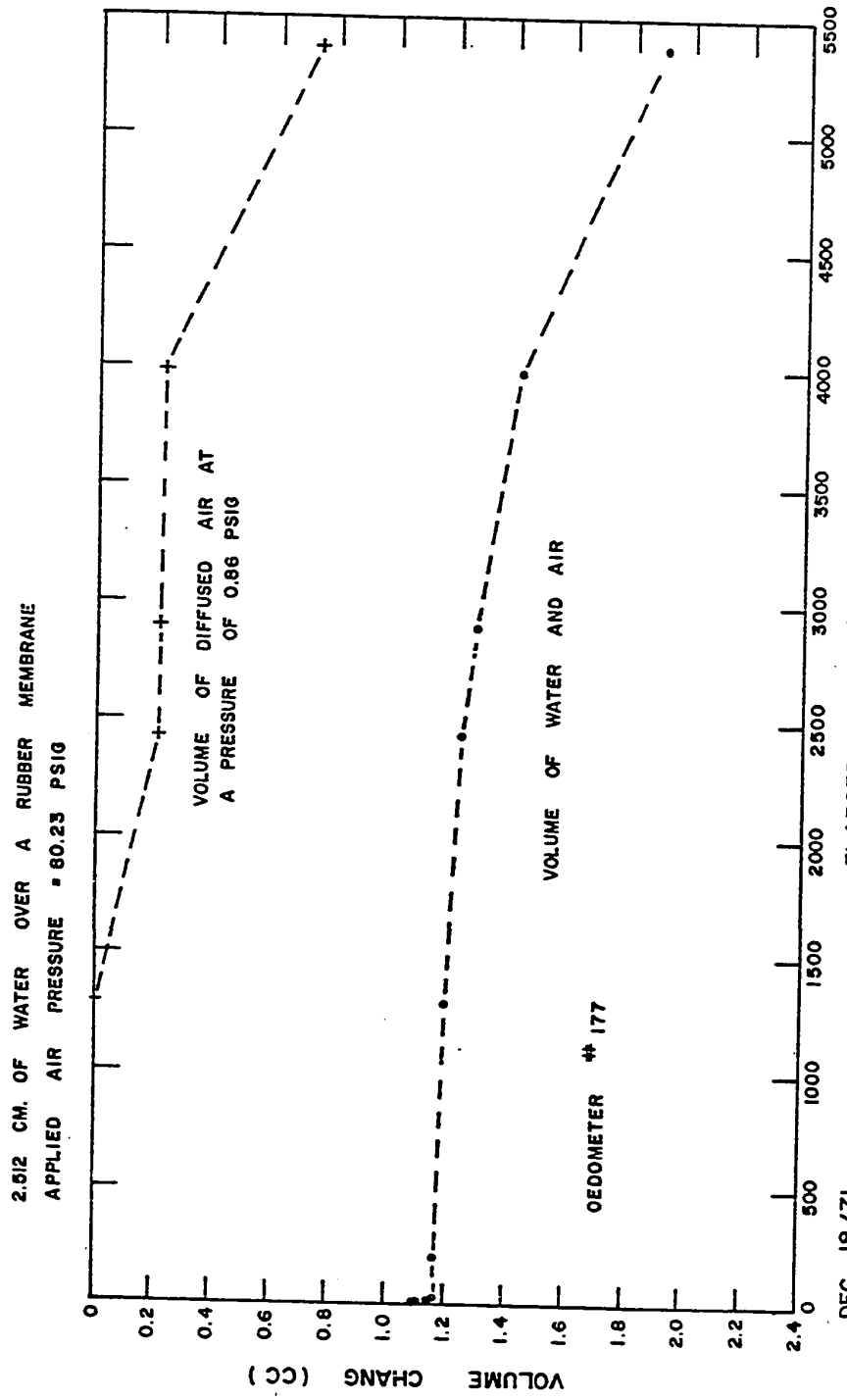


FIGURE 2.16 INDEPENDENT MEASUREMENT OF AIR AND WATER DIFFUSING THROUGH WATER, RUBBER MEMBRANE AND CERAMIC DISC

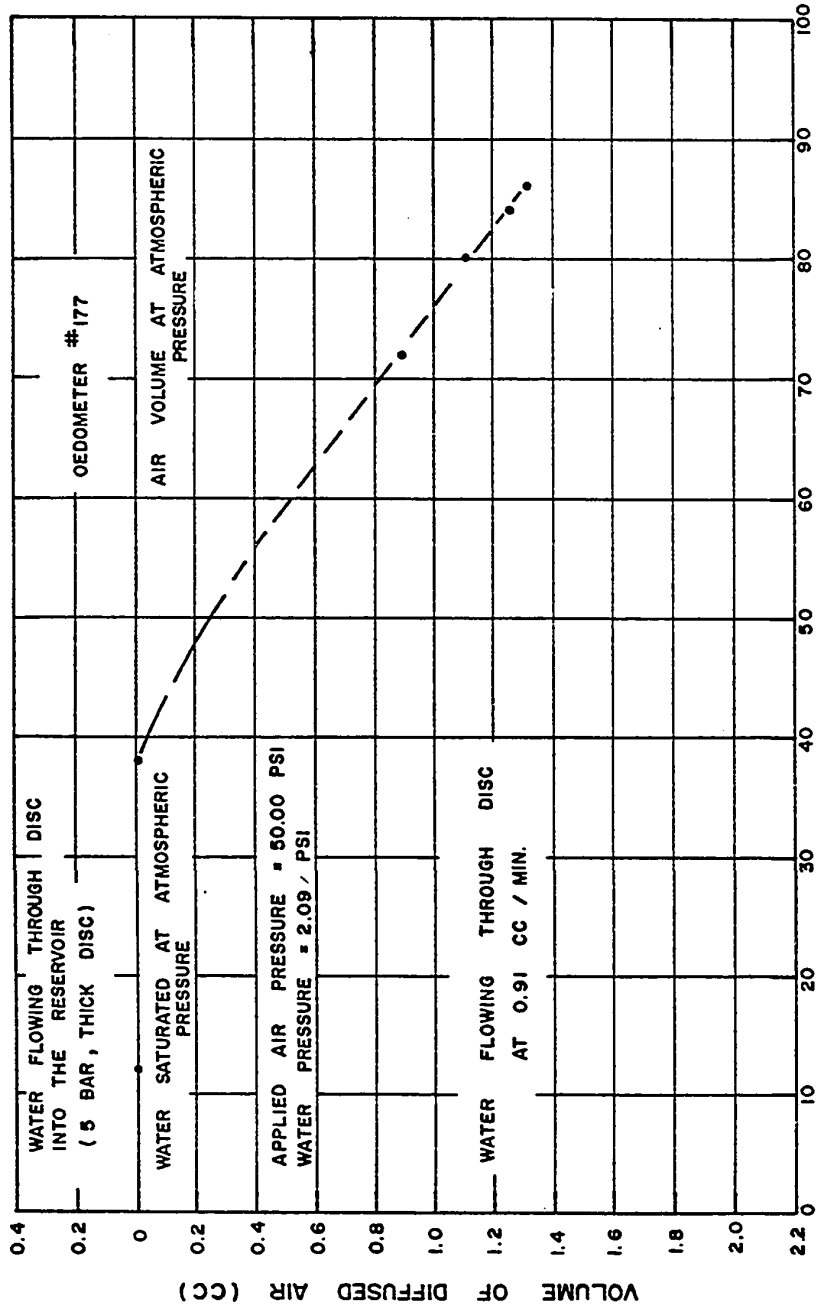


FIGURE 2.17 AIR RELEASED FROM WATER FLOWING THROUGH CERAMIC DISC (DEC. 3/71)

a high air entry disc as water was passed through the disc. The disc has an air entry value of approximately 75 psi and the air pressure applied to the water in the chamber was 50 psi. Initially, the water was saturated with air under atmospheric conditions. The results show that for the first 40 minutes practically no air was released below the high air entry disc. Then more air is released as the water passing through the high air entry disc becomes saturated with air at a pressure of 50 psi. Upon a reduction in pressure below the disc, the air is again released. Another test, (Figure 2.18) shows similar results. The change in water pressure below the ceramic disc at 320 minutes demonstrates the necessity of accurately measuring the pressure of the air-water mixture. The monitored air accumulations shown in Figures 2.17 and 2.18 correspond to an air saturation of approximately 30 percent.

Figure 2.19 shows the measured diffusion of air through a ceramic disc with a high air entry value of approximately 225 psi. The ceramic disc was saturated but had no water above it. Both the water volume change indicator and the diffused air volume indicator record essentially the same amount of volume change. In this case, steady state diffusion conditions should be established rapidly. Figure 2.20 shows the data from the previous figure plotted versus an arithmetic time scale. The plots are straight lines indicating steady state diffusion.

Two additional, long term diffusion tests were performed at several different applied pressures. Both tests were performed

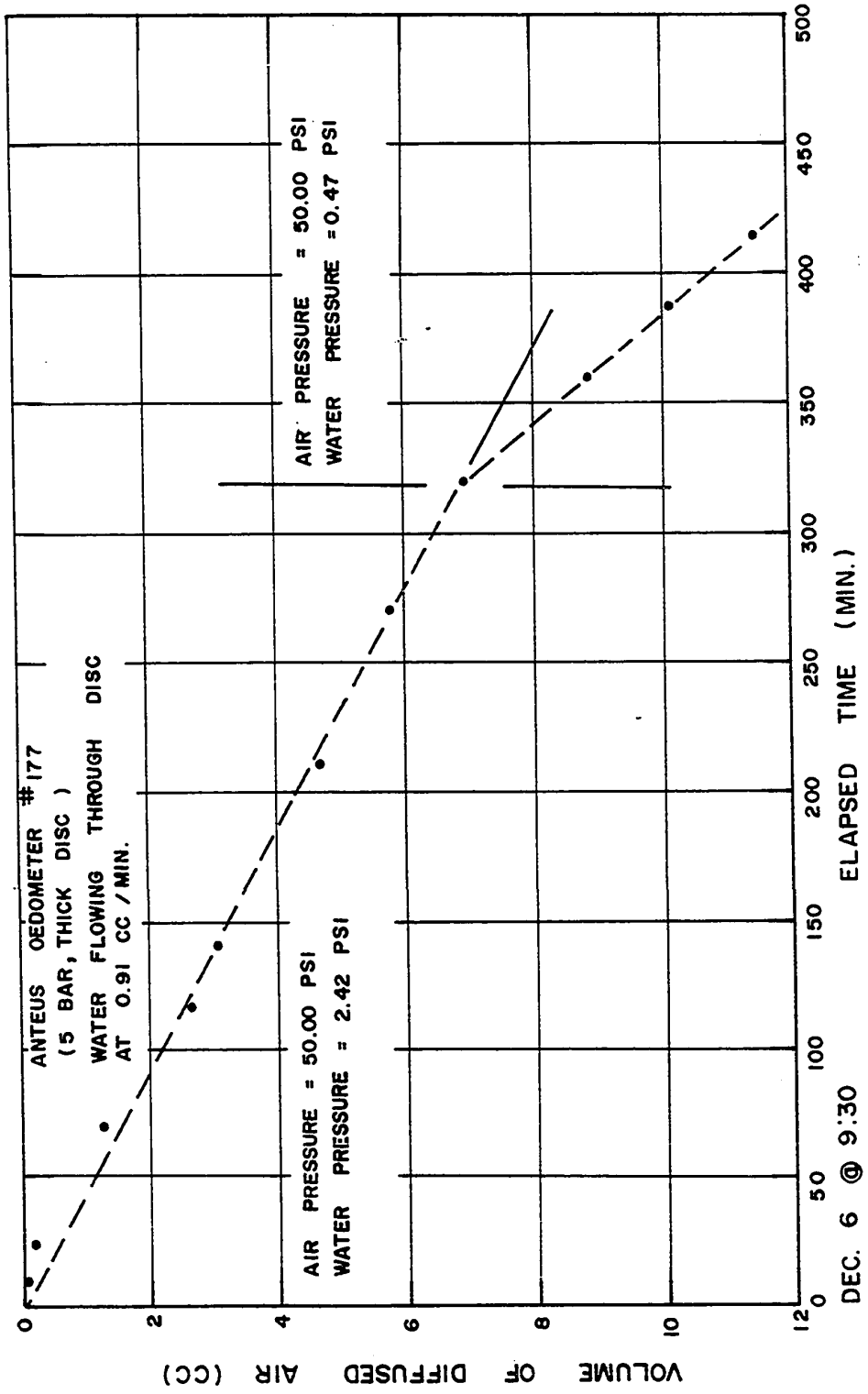
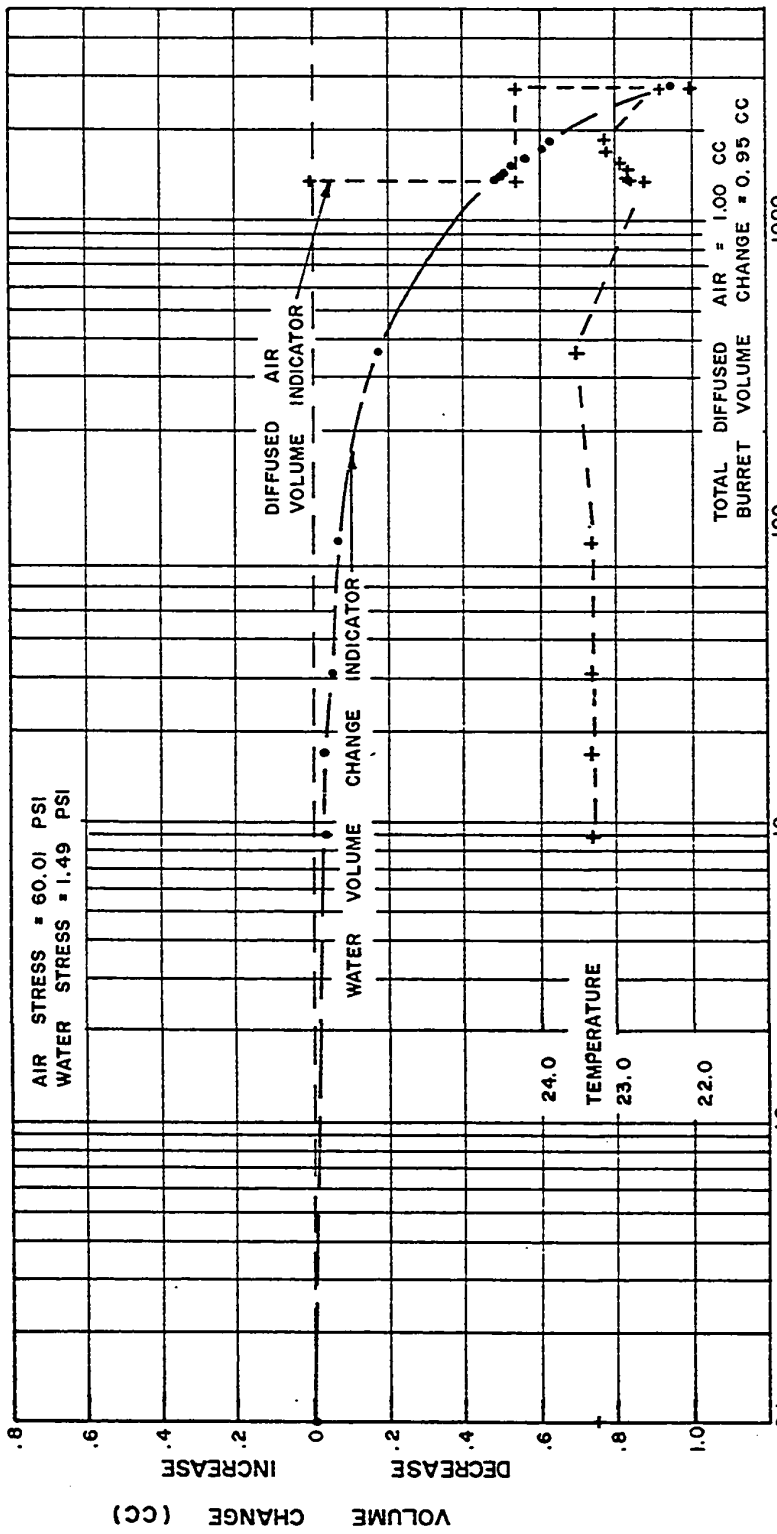


FIGURE 2.18 AIR RELEASED FROM WATER FLOWING THROUGH CERAMIC DISC (DEC. 6/71)



OCT. 21 @ 10:35

FIGURE 2.19 DIFFUSION OF AIR THROUGH SATURATED CERAMIC DISC (APPARATUS #179)

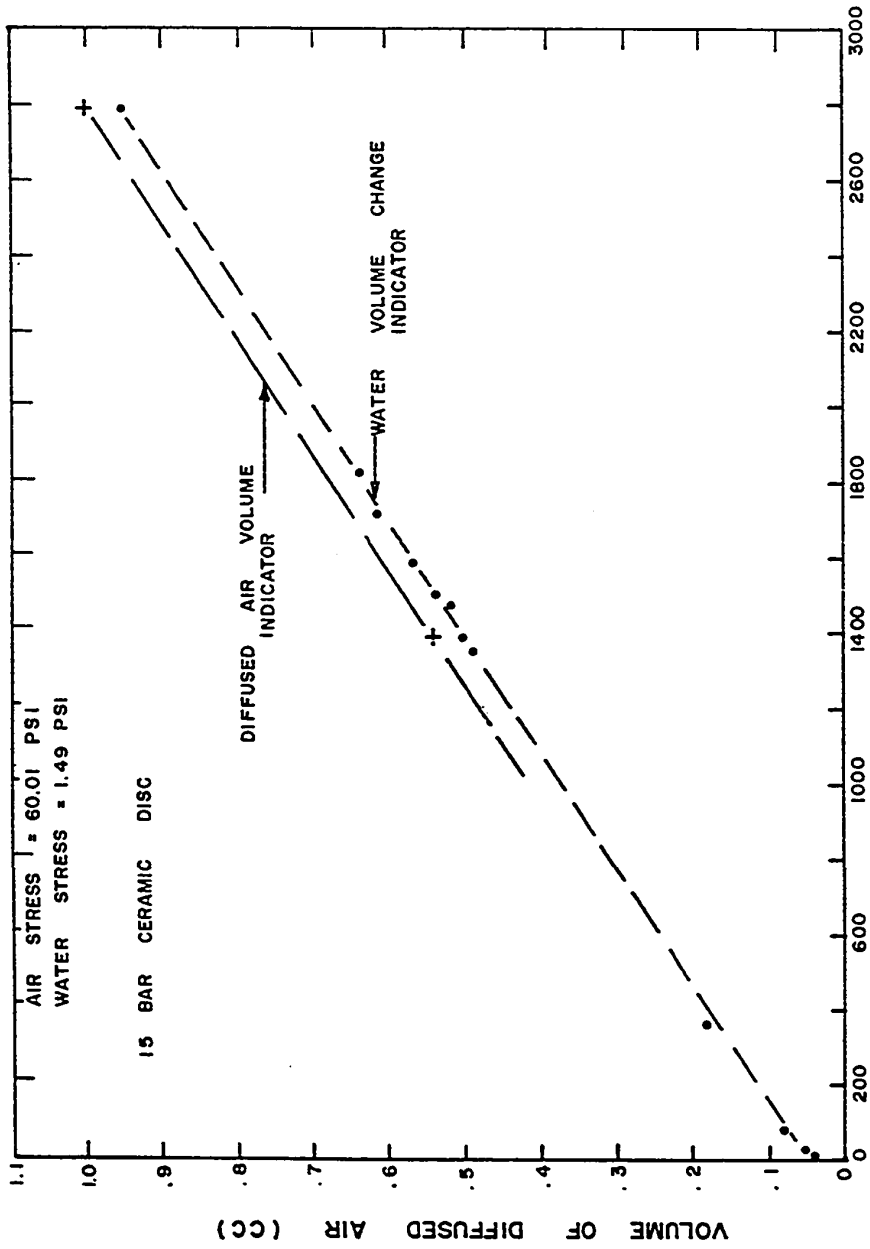


FIGURE 2.20 STEADY STATE DIFFUSION OF AIR THROUGH SATURATED CERAMIC DISC (APPARATUS #179)

on ceramic discs with an air entry value of 225 psi. The plots of net volume change versus time, for diffusion tests number 1 and 2 are presented in Figures 2.21 and 2.22, respectively. The accumulated air volumes measured by the water volume change indicator and the diffused air volume indicator are shown on Figures 2.23 to 2.27, for the various pressure ranges. The diffused air volumes recorded by the two systems are similar with the exception of those shown in Figure 2.27. This test showed excessive quantities of air being released. The accumulated air volume plots were used to compute the diffusivity of air with respect to the water in the ceramic disc. Typical calculations are shown in Appendix B.

The computed diffusivity values are plotted versus the applied pressure head in Figure 2.28. Also shown are some of the results from Barden and Sides' tests (1967). The average diffusivity value when the pressure head was between 70 and 100 psi, was 2×10^{-6} cm^2/sec. These diffusivity values are corrected for the porosity of the ceramic disc. This diffusivity value is one order of magnitude less than that for pure water. When the pressure head was between 20 and 45 psi, the average diffusivity was 2.8×10^{-6} cm^2/sec. Barden and Sides obtained a value of 1.6×10^{-6} cm^2/sec for their high air entry discs.

The manufacturers of the ceramic discs suggest a diffusivity value of 7.2×10^{-6} cm^2/sec. The author inquired of the manufacturer, as to the composition and method of preparation of the ceramic discs

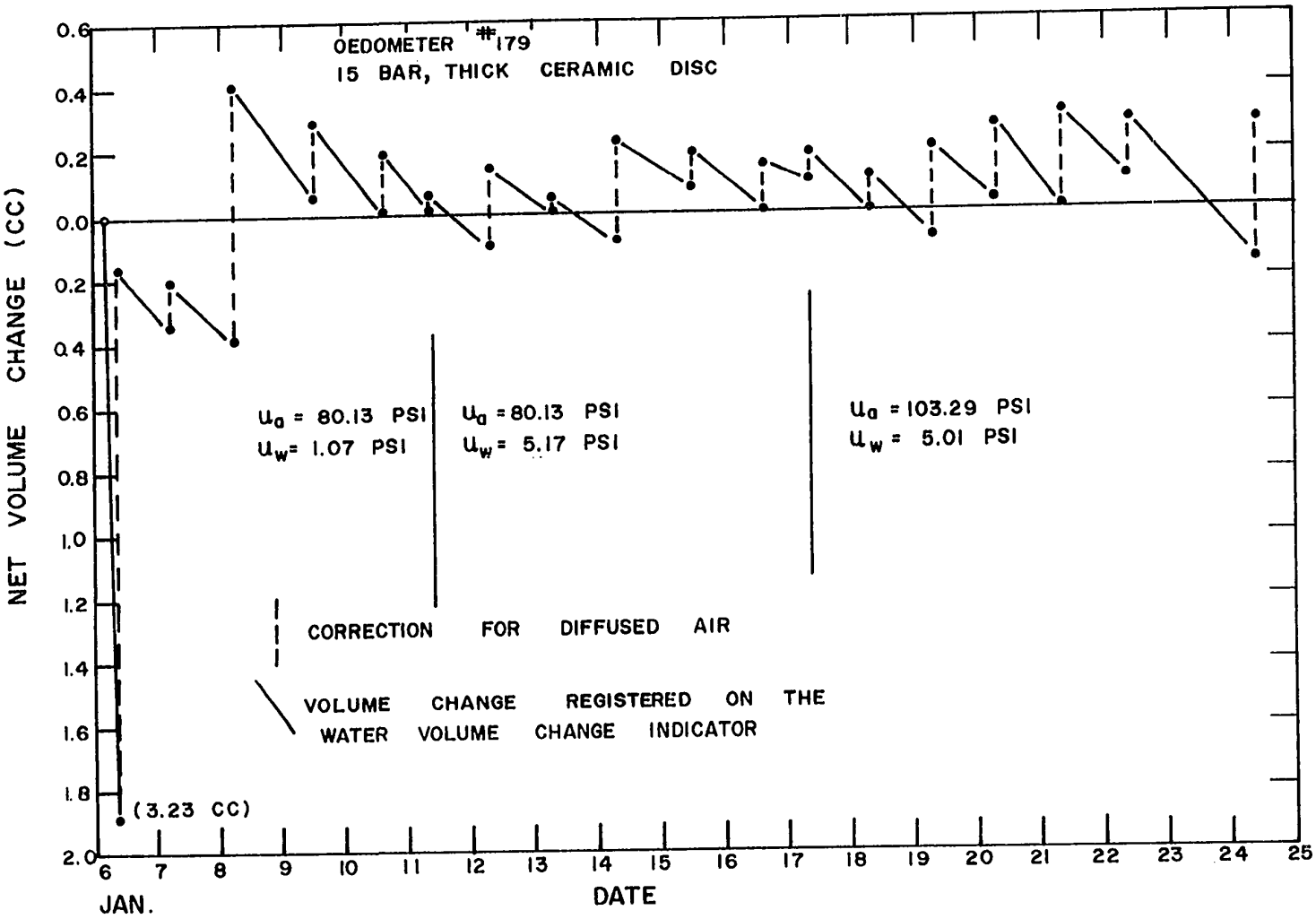


FIGURE 2.21 DIFFUSION TEST NO. 1 ON SATURATED CERAMIC DISC

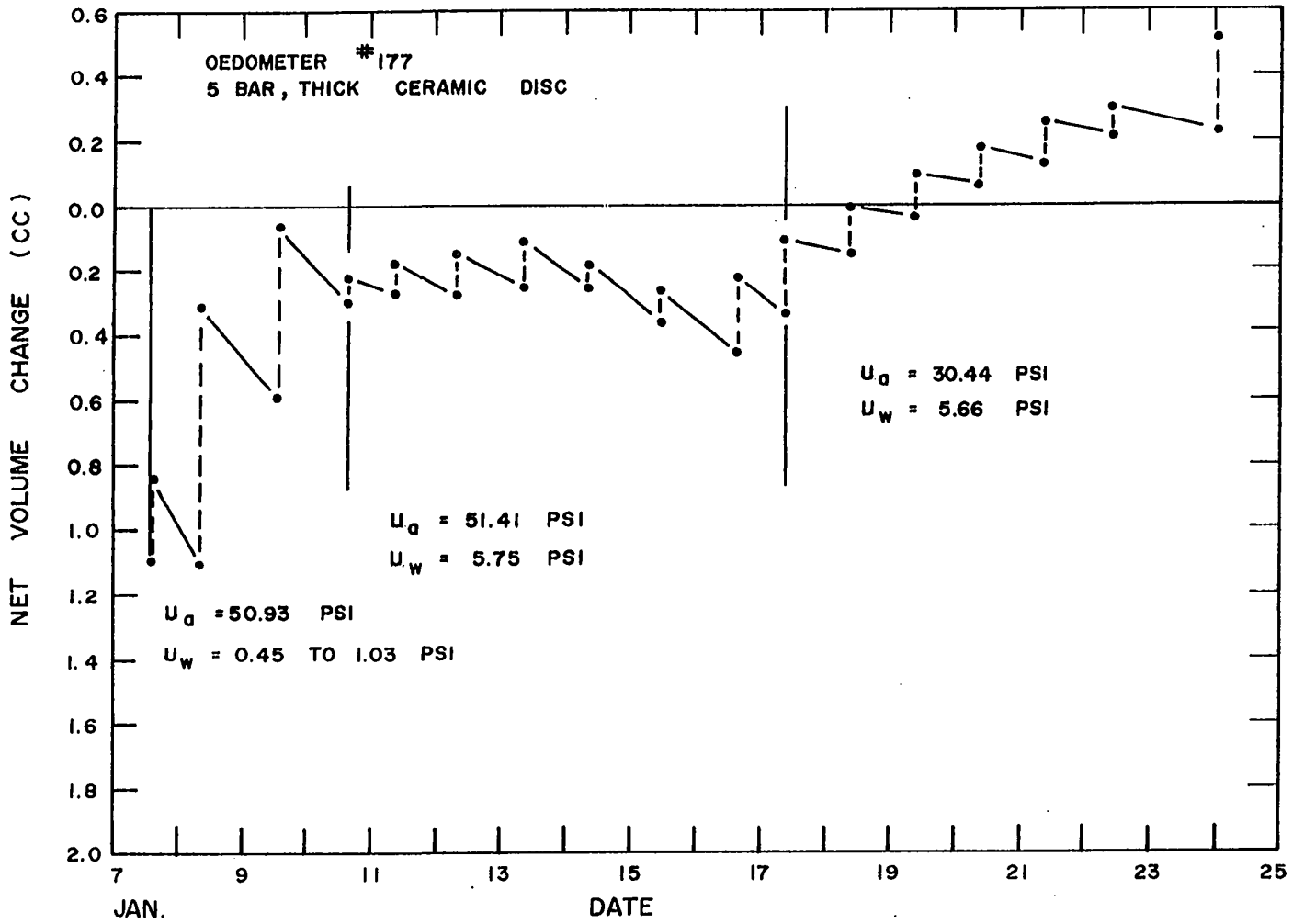


FIGURE 2.22 DIFFUSION TEST NO. 2 ON SATURATED CERAMIC DISC

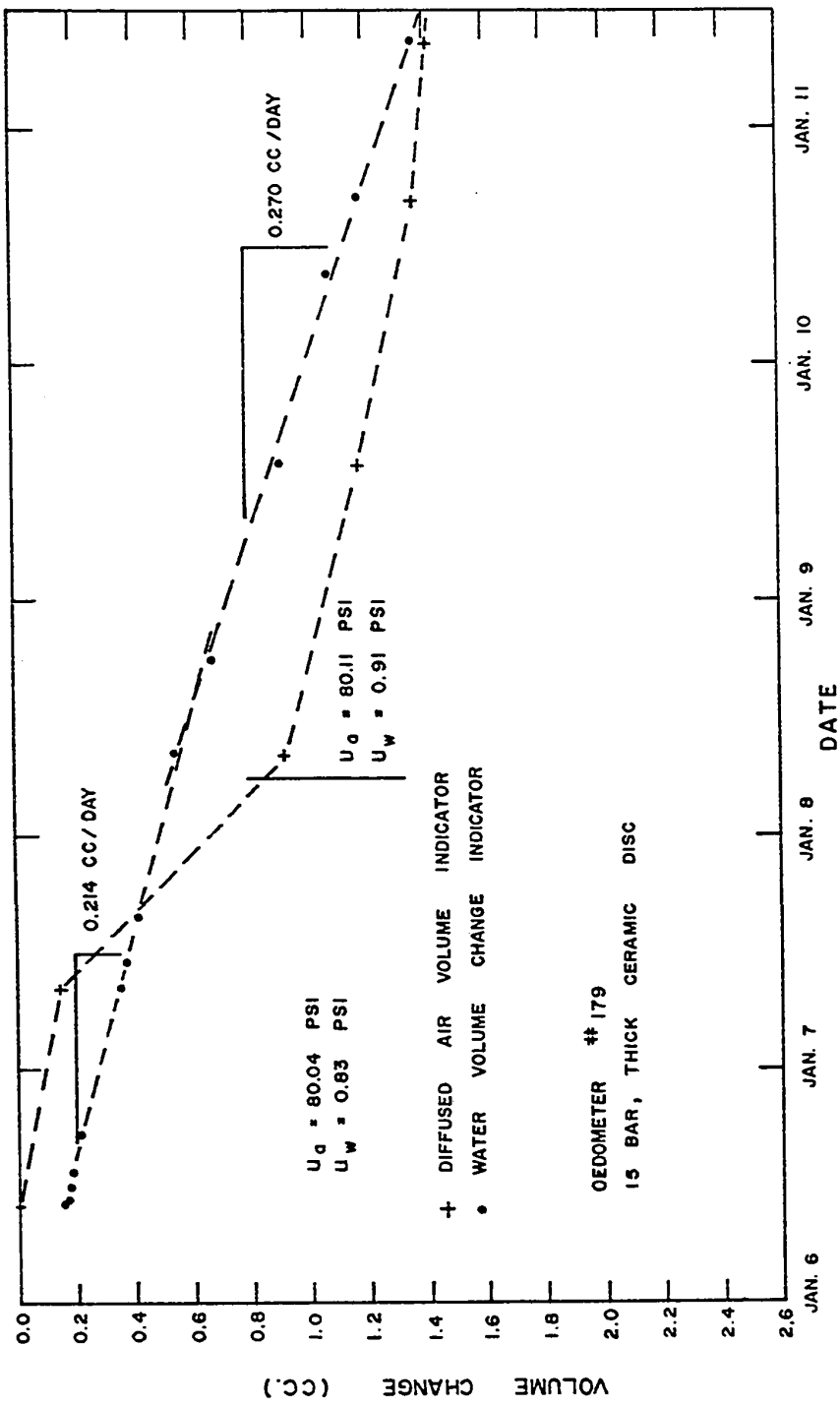


FIGURE 2.23 ACCUMMULATED AIR DIFFUSION DURING TEST #1
(U_a = 80 PSI AND U_w = 0.9 PSI)

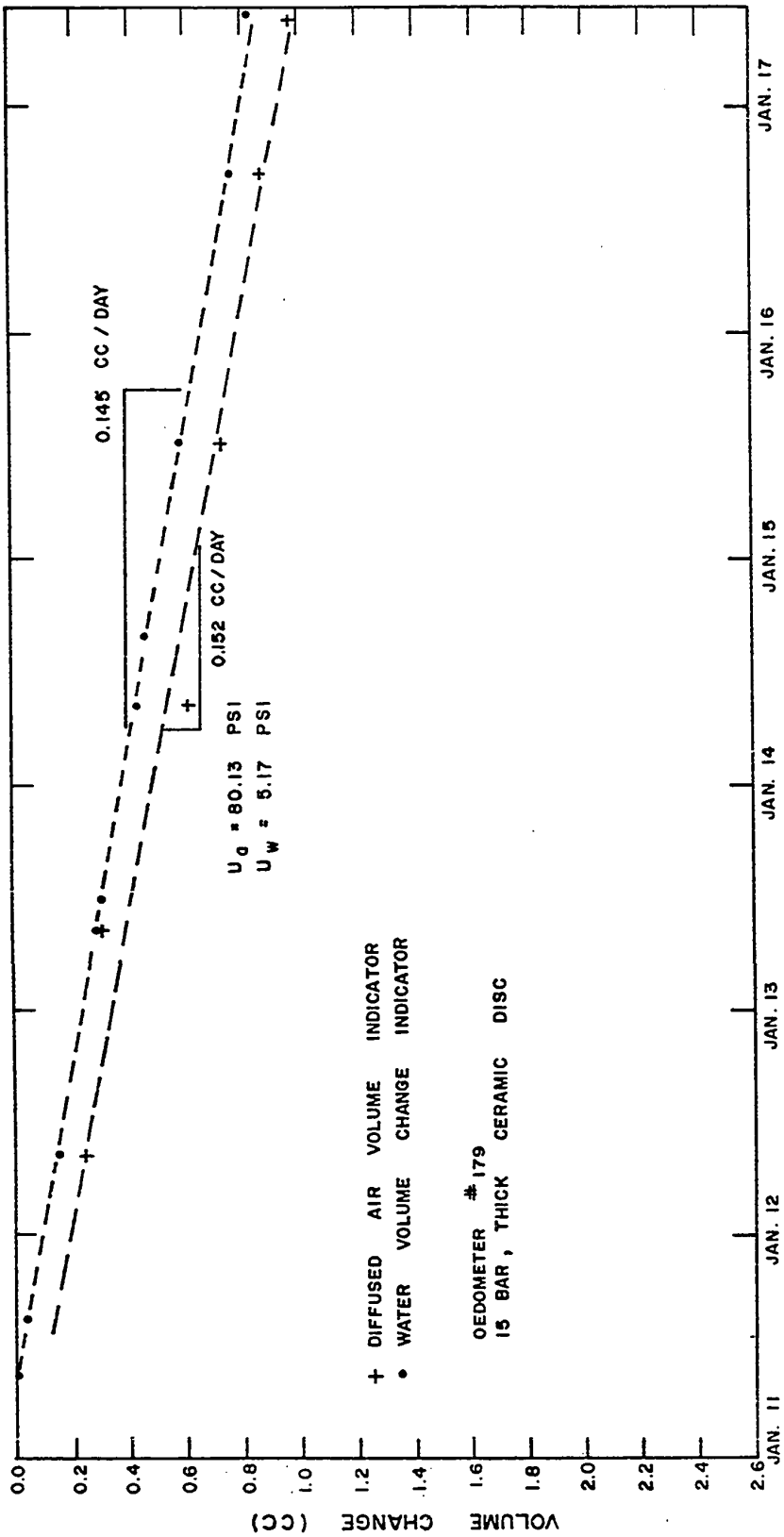


FIGURE 2.24 ACCUMMULATED AIR DIFFUSION DURING TEST # 1
(U_a = 80 PSI AND U_w = 5 PSI)

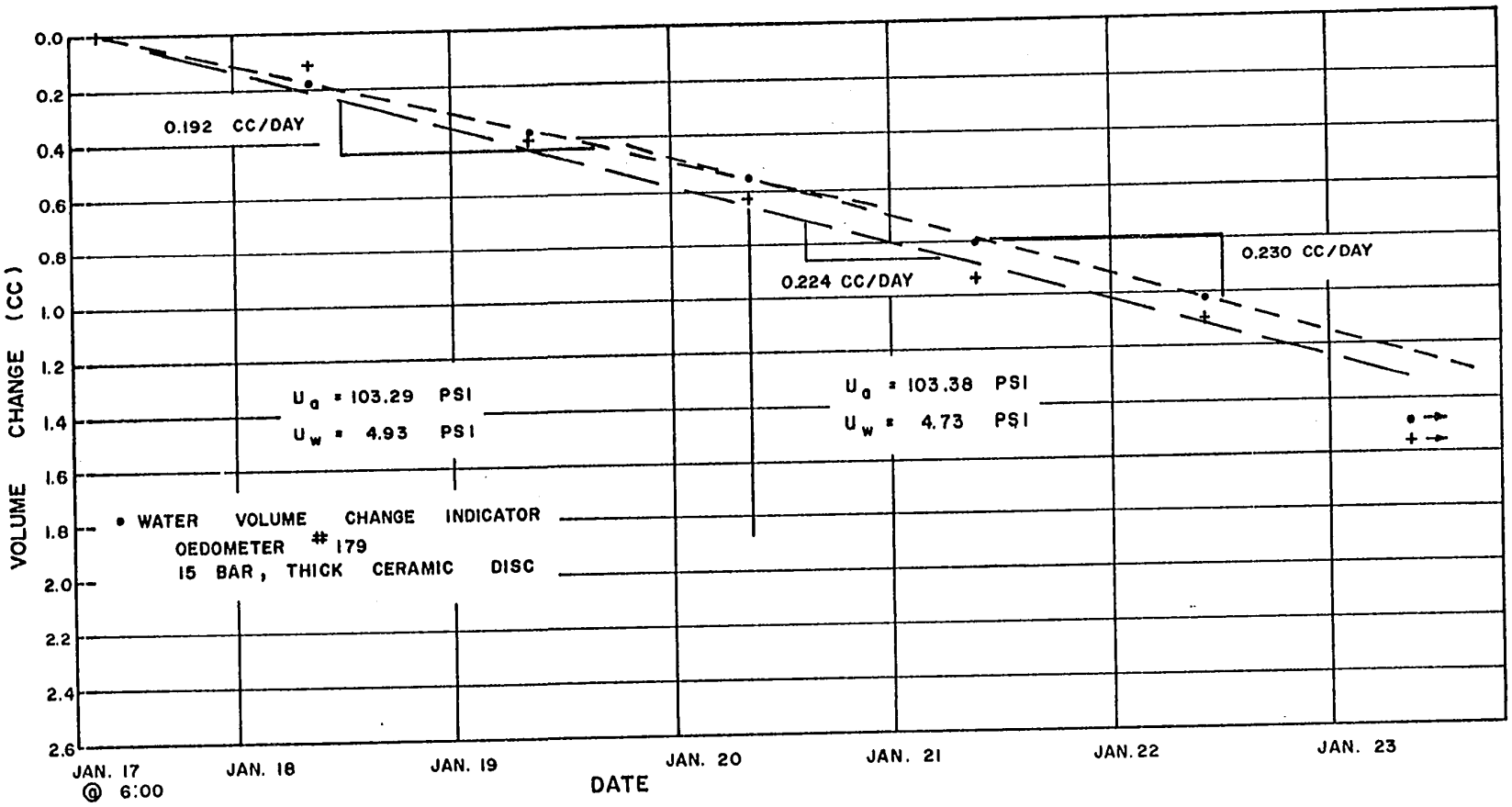


FIGURE 2.25 ACCUMMULATED AIR DIFFUSION DURING TEST # 1
(U_a = 103 PSI AND U_w = 4.8 PSI)

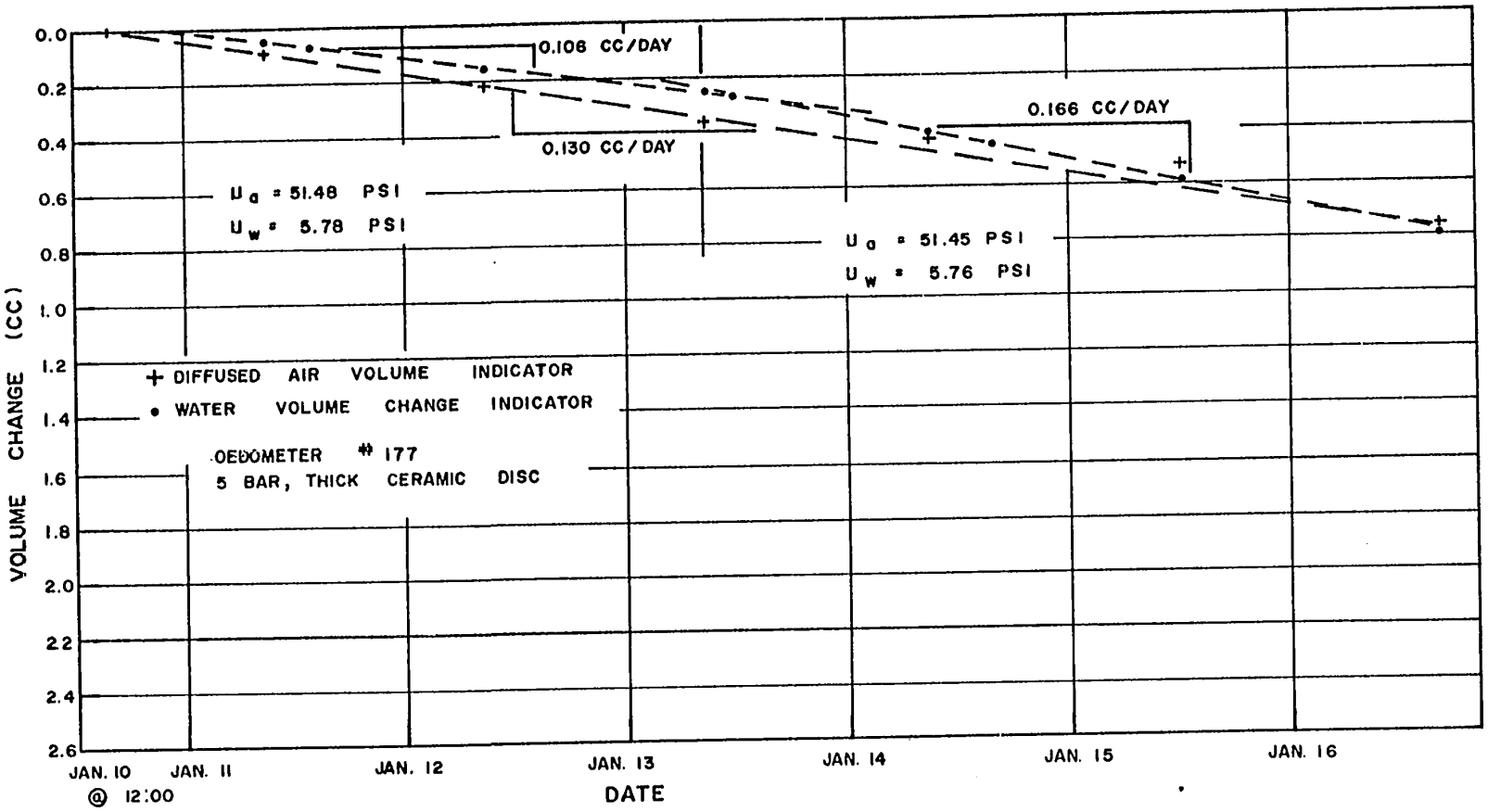


FIGURE 2.26 ACCUMMULATED AIR DIFFUSION DURING TEST # 2
(U_a = 51.5 PSI AND U_w = 5.8 PSI)

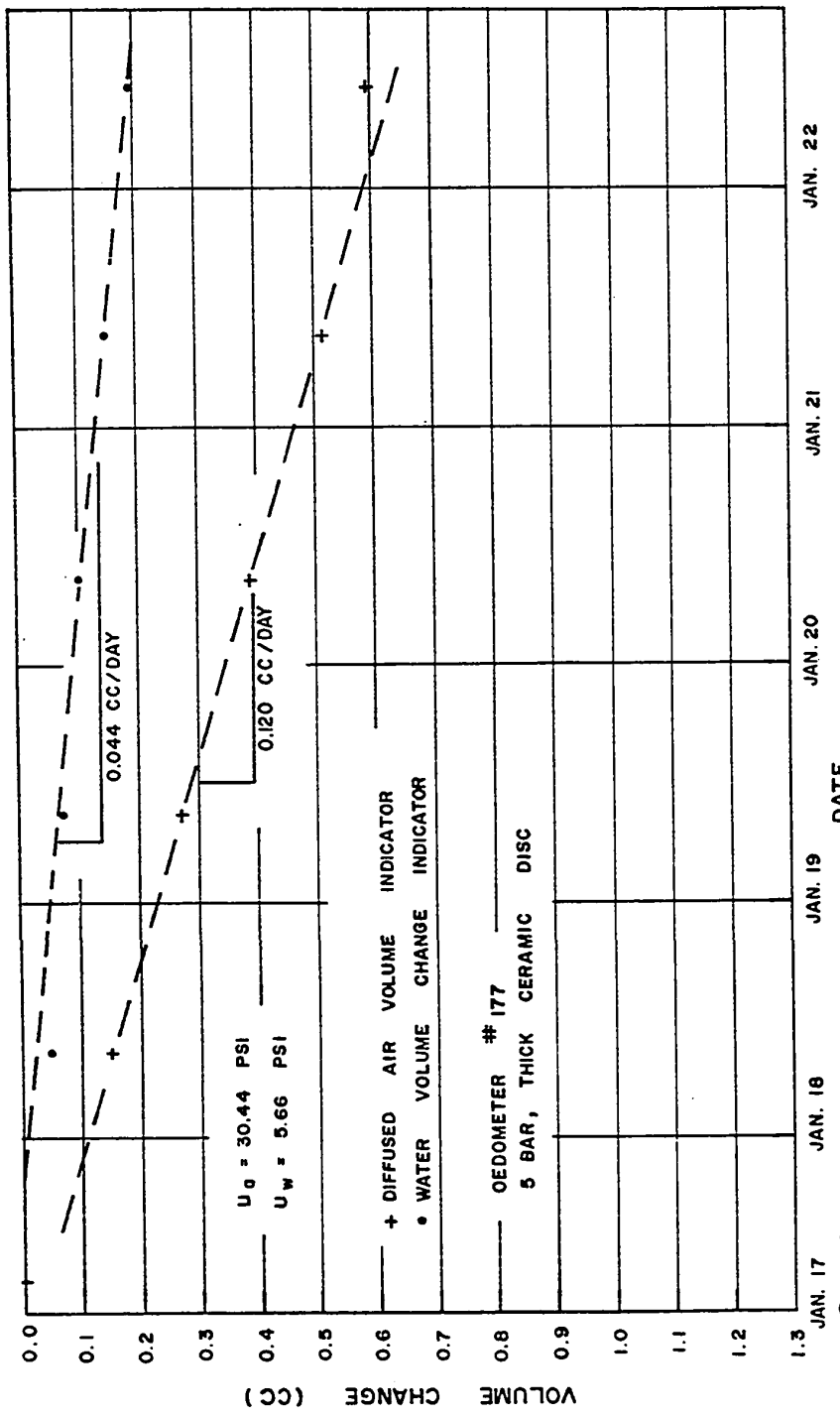


FIGURE 2.27 ACCUMMULATED AIR DIFFUSION DURING TEST #2
(U_g = 30.4 PSI AND U_w = 5.7 PSI)

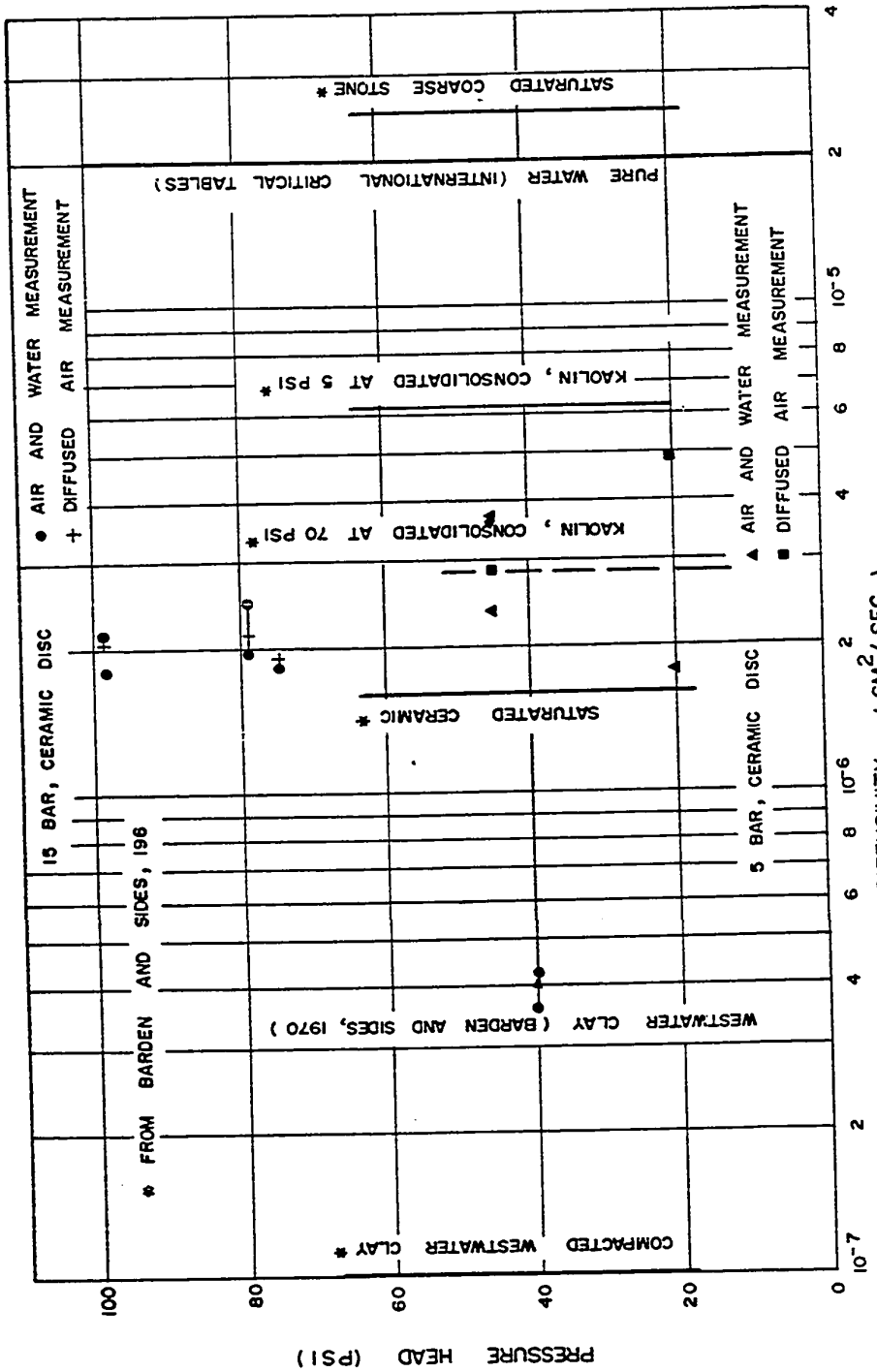


FIGURE 2.28 DIFFUSIVITY VALUES MEASURED ON THE CERAMIC DISCS IN THE ANTEUS OEDOMETER AND PUBLISHED VALUES FROM OTHER SOURCES

but was informed that this information was of a "proprietary nature" and could not be disclosed. Two ceramic discs were ground to a fine powder and tested using the x-ray diffraction technique. The results indicate the presence of quartz. There was no evidence of any clay minerals.

The author is not completely certain as to the interpretation that should be given to the data. If the ceramic discs are essentially an inert material, than it does not seem reasonable to attribute the decreased diffusivity to the change in water viscosity. There does appear to be a slight decrease in diffusivity with an increasing suction; however, the significance of this trend needs further verification in the low suction range. Also, it is understandable that the porosity correction is not sufficient to correct for the increased tortuosity in the ceramic disc.

The results indicate that the diffusivity value of normal water forms an upper limit. However, there is further research required to ascertain the significance of all factors that affect the diffusivity of air through the water in a soil.

2.5 Density and Compressibility of a Combined Miscible and Immiscible Air-Water Mixture

Changing the pressure on an enclosed air-water mixture involves the transient process of the solution of air in water. Generally, it is advantageous to make one of two simplifying assumptions. First, it could be assumed that there is insufficient time for any diffusion.

Then the problem reverts to the immiscible case. Second, it could be assumed that there is sufficient time for complete diffusion. This is the case considered in this section. The assumption is also made that the air pressure is equal to the water pressure.

Referring to the piston and porous disc analogy, it is possible to assume that the imaginary valve is initially closed during the pressure change and then opened to allow air to go into solution. This rigorous analysis is conducted in two steps and strictly employs the physical laws involved. It is also possible to envisage the free and dissolved air as a total air volume that responds simultaneously to a change in air pressure. This is referred to as the simplified formulation.

The density formulation considers the free and dissolved air as one volume. The compressibility formulation considers both the rigorous and the simplified formulations.

2.5.1 Density of a Combined Miscible and Immiscible Air-Water Mixture

Let us consider an element similar to that described in section 2.2.4 for the density of an immiscible air-water mixture. Applying the conservation of mass to the contents of the element gives,

$$\gamma_m \cdot V_T = \gamma_w \cdot V_w + \gamma_a \cdot V_a' \qquad 2.63$$

where V_a' = free air volume.

Under these initial conditions the density is written

$$\gamma_m = \frac{\gamma_w \cdot V_w + \gamma_a \cdot V_a'}{V_w + V_a'} \qquad 2.64$$

Now suppose the pressure on the piston of the element is increased. Let us assume that the volume of water remains constant and the total mass of air remains constant. The density of the air in terms of any pressure is

$$\gamma_a = \frac{u_a}{R \cdot T} \qquad 2.65$$

Boyles law is applied to the free and dissolved air

$$dV_a = dV_a' + dV_d = - \frac{(V_{ai}' + V_{di})}{u_a} \cdot du_a \qquad 2.66$$

where V_{ai}' = initial volume of free air

V_{di} = initial volume of dissolved air

The new volume of free air corresponding to a pressure, u_a, is

$$V_a' = V_{ai}' - (V_{ai}' + V_{di})(1 - \frac{u_{ai}}{u_a}) \qquad 2.67$$

Simplifying and substituting into equation 2.64 gives

$$\gamma_m = \frac{\gamma_w \cdot V_w + \frac{u_a}{R \cdot T} [(V_{ai}' + V_d) \cdot \frac{u_{ai}}{u_a}]}{V_w + V_{ai}'} \qquad 2.68$$

Written in terms of the degree of saturation, S, and the coefficient of solubility, h,

$$\gamma_m = \frac{\gamma_w \cdot S}{S + (1-S)\cdot\frac{u_{ai}}{u_a} + S\cdot h\cdot\frac{u_{ai}}{u_a}} \qquad 2.69$$

The above equation assumes there is sufficient time for the complete solution of air under the new pressure.

2.5.2 Rigorous Finite Difference Formulation of the Compressibility of a Combined Miscible and Immiscible Air-Water Mixture (Imaginary Valve Initially Closed)

The general compressibility definition was given in section 2.3.4. Written as a finite difference equation,

$$\beta_m = -\frac{1}{V_w+V_a'}\left[\frac{V_{wi}-V_{wj}}{u_{wi}-u_{wj}} + \frac{V'_{ai}-V'_{ai}}{u_{ai}-u_{aj}}\right] \qquad 2.70$$

where V_{wi} = volume of water corresponding to a pressure, u_{wi}

V_{wj} = volume of water corresponding to a pressure, u_{wj}

V'_{ai} = volume of air corresponding to a pressure, u_{ai}

V'_{aj} = volume of air corresponding to a pressure, u_{aj}

The compressibility of water is a constant and the first term in the brackets can be written,

$$\frac{V_{wi}-V_{wj}}{u_{wi}-u_{wj}} = -\beta_w\cdot V_w \qquad 2.71$$

The imaginary valve at the air-water interface is initially closed and the volume change is in accordance with Boyles law. This first volume change step is written,

$$\left[\frac{V'_{ai}-V'_{aj}}{u_{ai}-u_{aj}}\right]_1 = \left[\frac{V'_{ai}-\frac{u_{ai}}{u_{aj}}\cdot V'_{ai}}{u_{ai}-u_{aj}}\right] = -\frac{V'_{ai}}{u_{aj}} \qquad 2.72$$

Now the imaginary valve is opened and a portion of the free air moves into the water. This is the second step, and is computed from Henry's law and the Gas law. Henry's law states,

$$w_{dj} = w_{di} \cdot \frac{u_{aj}}{u_{ai}} \qquad 2.73$$

where w_{dj} = weight of gas dissolved at a pressure, u_{aj}

w_{di} = weight of gas dissolved at a pressure, u_{ai}

The weight of gas dissolved at point, i, is computed by applying Henry's law between the known solubilities under atmospheric conditions and point, i.

$$w_{di} = w_{do} \cdot \frac{u_{ai}}{u_{ao}} \qquad 2.74$$

where w_{do} = weight of air dissolved under atmospheric conditions, u_{ao} .

The weight of air dissolved under atmospheric conditions is

written in terms of Henry's coefficient of solubility.

$$w_{do} = H_a \cdot V_w \cdot \gamma_w \qquad 2.75$$

Combining equations 2.75 and 2.74 gives

$$w_{dj} = H_a \cdot V_w \cdot \gamma_w \cdot \frac{u_{aj}}{u_{ao}} \qquad 2.76$$

The volume of air corresponding to any pressure and weight is computed from the Gas law. The volume of free air dissolved at point, i, referenced to a pressure, u_{aj}, is

$$V_{di} = w_{di} \cdot \frac{R \cdot T}{u_{aj}} = w_{do} \cdot \frac{u_{ai}}{u_{ao}} \cdot \frac{R \cdot T}{u_{aj}} \qquad 2.77$$

Similarly at point, j,

$$V_{dj} = w_{dj} \cdot \frac{R \cdot T}{u_{aj}} \qquad 2.78$$

Combining equations 2.78, 2.77 and 2.75 gives us Step 2 of the compressibility of the free air

$$\left[\frac{V'_{ai} - V'_{aj}}{u_{ai} - u_{aj}}\right]_2 = - \frac{H_a \cdot V_w \cdot \gamma_w \cdot R \cdot T}{u_{ao} \cdot u_{aj}} \qquad 2.79$$

The volume of dissolved air is a constant.

$$V_d = H_a \cdot V_w \cdot \gamma_w \cdot R \cdot T / u_{ao} \qquad 2.80$$

Therefore, the overall compressibility equation is written,

$$\beta_m = - \frac{1}{V_w + V'_{ai}} \left[(\beta_w \cdot V_w) + \left(\frac{V'_{ai}}{u_{aj}} \right) + \left[\frac{V_d}{u_{aj}} \right] \right] \qquad 2.81$$

Written in terms of the initial degree of saturation, S, and the coefficient of solubility, h,

$$\beta_m = S \cdot \beta_w + \frac{(1-S)}{u_{aj}} + \frac{S \cdot h}{u_{aj}} \qquad 2.82$$

2.5.3 Simplified Direct Differentiation Formulation

The compressibility equation can be formulated in a few steps if we know how to combine the free and dissolved air volumes. The basic compressibility equation is,

$$\beta_m = - \frac{1}{V'_a + V_w} \left[\frac{dV_w}{du_w} + \frac{dV'_a}{du_a} \right] \qquad 2.83$$

The compressibility can be envisaged as related to the change in the total air volume. This gives somewhat of a false concept of the problem since the compressibility is actually related to the free air volume.

$$\frac{dV_a'}{du_a} = (V'_{ai} + V_d)/u_a \qquad 2.84$$

The compressibility equation is directly written as

$$\beta_m = - \frac{1}{V_a' + V_w} \left[\beta_w \cdot V_w + \frac{V'_{ai}}{u_a} + \frac{V_d}{u_a} \right] \quad \text{or}$$

$$\beta_m = S \cdot \beta_w + \frac{(1-S)}{u_a} + \frac{S \cdot h}{u_a} \qquad 2.85$$

Figure 2.29 shows the components of the compressibility of an air-water mixture at a temperature of 20°C and an air pressure of 2 kg/cm^2. The compressibility due to the solution of air in water is approximately two orders of magnitude greater than the compressibility due to the water. Figure 2.30 shows the change in compressibility as the air pressure is changed. Most noteworthy is the substantial reduction in compressibility as the air pressure is reduced.

Figure 2.31 shows the effect of the dissolved air component on the compressibility. The effect (at any percentage of air) of the solution of air is the same on a logarithmic scale, regardless of the air pressure. The overall compressibility of the mixture does not have a smooth transition back to that of pure water. Rather, there is a discontinuity at the point where the free air is zero. At this point, there is no air to be driven into solution and the last term must be dropped. Thus, the compressibility abruptly decreases to that of pure water.

The dramatically increased compressibility of the pore fluid due to the presence of a small amount of air, is of significance in

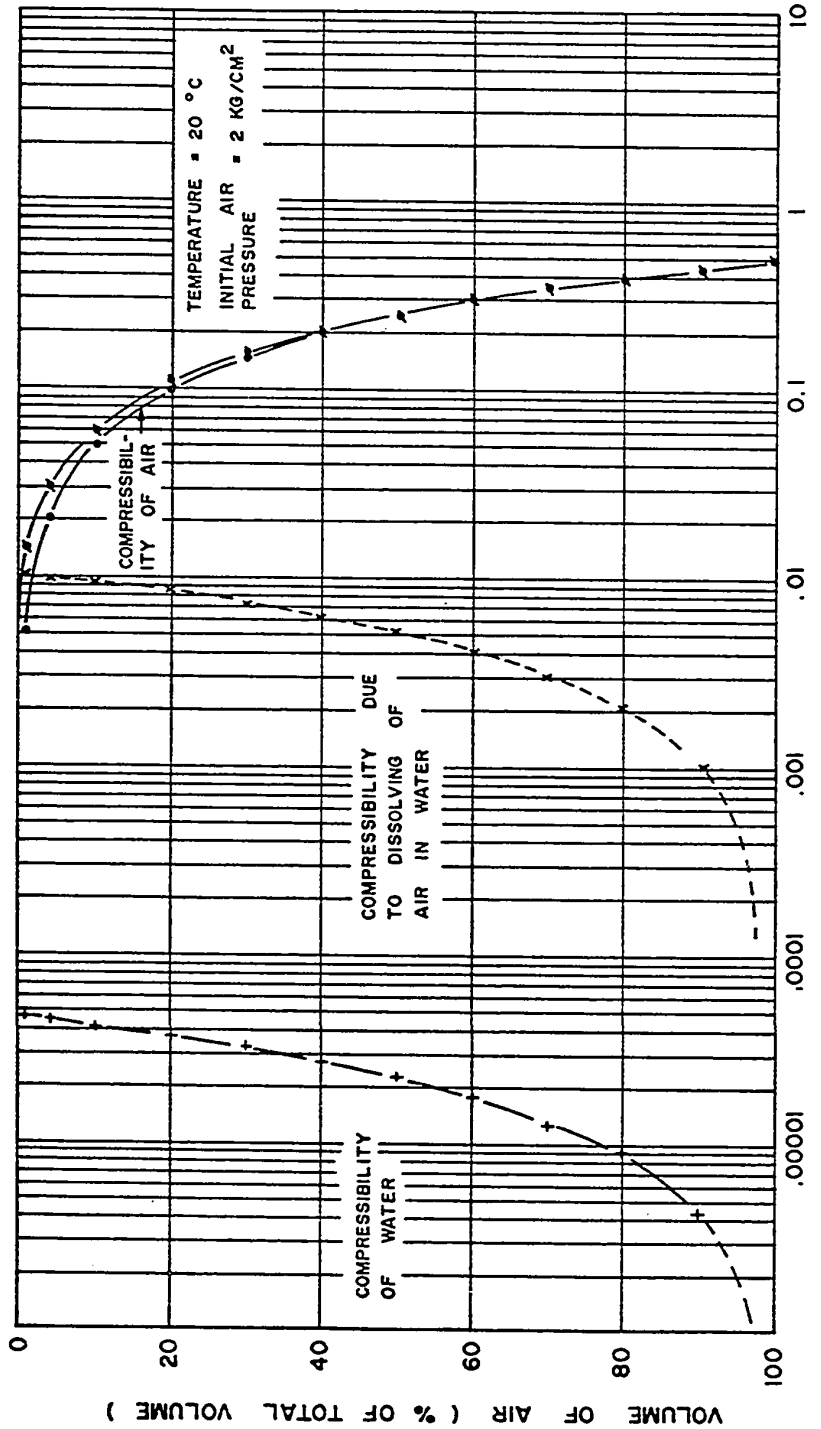


FIGURE 2.29 COMPONENTS OF COMPRESSIBILITY OF MISCIBLE AND IMMISCIBLE AIR – WATER MIXTURES

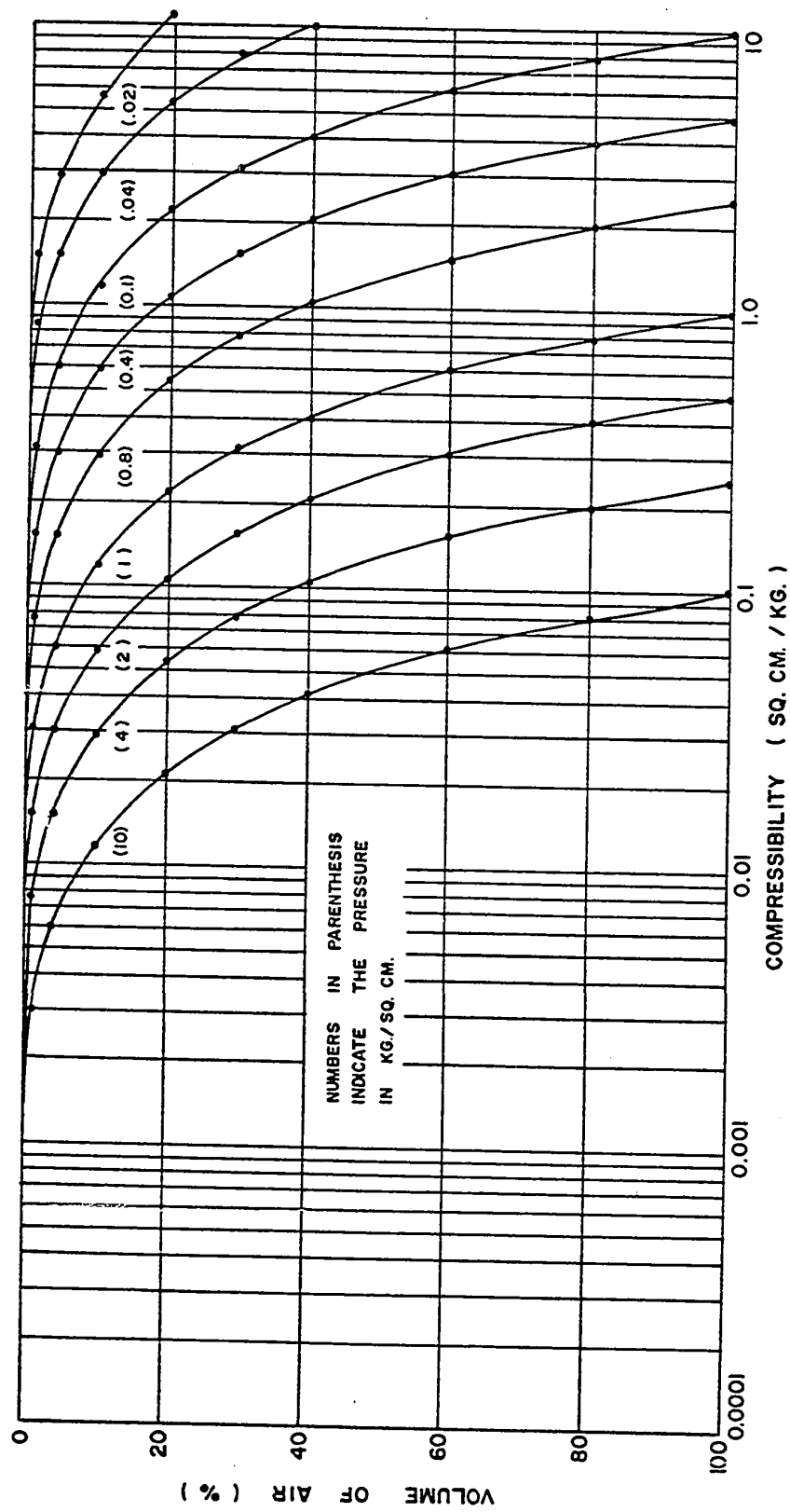


FIGURE 2.30 COMPRESSIBILITY OF COMBINED MISCIBLE AND IMMISCIBLE AIR – WATER MIXTURES

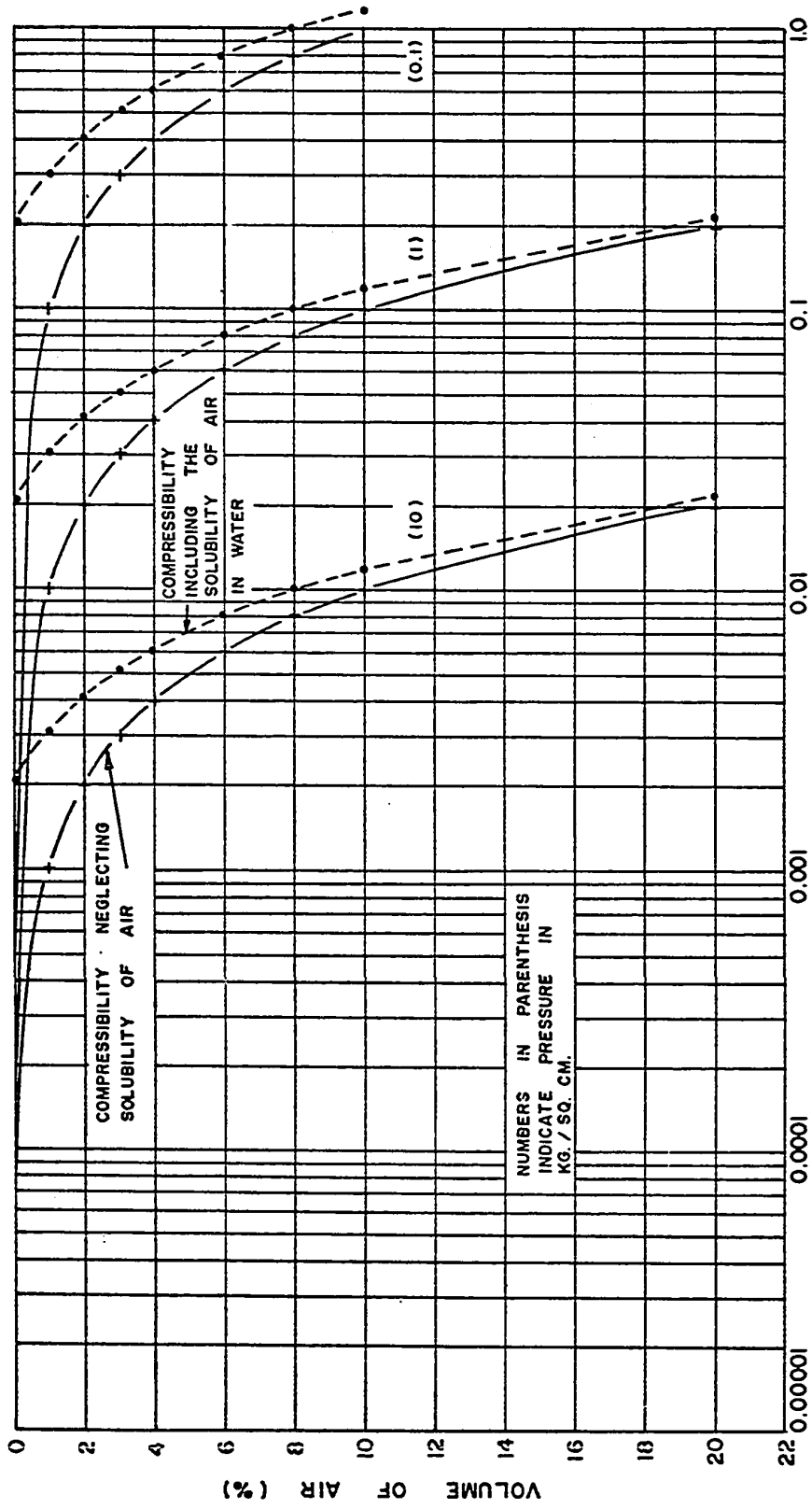


FIGURE 2.31 EFFECT OF SOLUBILITY OF AIR IN WATER ON THE COMPRESSIBILITY

the analysis of various problems. For example, Skempton's B parameter depends on the compressibility of the pore fluid.

$$B = \frac{1}{1 + \frac{nC^f}{C^s}} \qquad 2.86$$

where C^f = bulk compressibility of the pore fluid

C^s = bulk compressibility of the soil structure.

If the soil is completely saturated, the compressibility of the pore fluid is that of pure water (i.e. 4.6×10^{-5} cm^2/kg). The B parameter therefore approaches one for essentially all soils (Skempton, 1954). Figure 2.31 shows that the inclusion of even one percent air at a pressure of one atmosphere, results in a pore fluid compressibility of 3.0×10^{-2} cm^2/kg or an increase of almost three orders of magnitude. This compressibility approaches that of the soil structure and has a significant effect upon the B parameter.

2.6 Compressibility of Air-Water Mixtures When the Air Pressure is Not Equal to the Water Pressure

In the previous analysis the air and water pressures were equal and the compressibility was defined with respect to both pressures. Now let us consider the effect of differing air and water pressures. This case is actually fictitious since the air and water pressures cannot differ apart from the inclusion of a solid medium. Theoretically, the compressibility of the mixture is defined,

$$\beta_m = -\frac{1}{V} \cdot \frac{dV}{dp} = -\frac{1}{V_w+V_a'} \cdot \left[\frac{dV_w}{dp} + \frac{dV_a'}{dp}\right] \qquad 2.87$$

where p = the reference pressure for defining compressibility .

The compressibility of each phase with respect to its pressure can be defined. Applying the chain rule of differentiation,

$$\frac{dV_w}{dp} = \frac{dV_w}{du_w} \cdot \frac{du_w}{dp} \qquad 2.88$$

and

$$\frac{dV_a'}{dp} = \frac{dV_a'}{du_a} \cdot \frac{du_a}{dp} \qquad 2.89$$

Substituting into equation 2.87

$$\beta_m = -\frac{1}{V_w+V_a'} \left|\frac{dV_w}{du_w} \cdot \frac{du_w}{dp} + \frac{dV_a'}{du_a} \cdot \frac{du_a}{dp}\right| \qquad 2.90$$

In order to solve for compressibility, it is necessary to know the relationship of the air and water pressures to the reference pressure, p. Since the reference pressure is not established by any known physics, it can be arbitrarily chosen as either the air or water pressure. Suppose we let the reference pressure equal the water pressure.

$$\beta_m = - \frac{1}{V_w + V_a'} \left[\frac{dV_w}{du_a} + \frac{dV_a'}{du_a} \cdot \frac{du_a}{du_w} \right] \qquad 2.91$$

Regardless of the chosen reference pressure, it is necessary to have a relationship between the air and water pressure. The physics of the capillary model relates the air and water pressures to the surface tension constant and the radius of curvature.

$$u_a - u_w = \frac{2 \cdot T_s}{r} \qquad 2.92$$

where T_s = surface tension

r = radius of curvature of the air-water interface.

If the equation is differentiated with respect to the water pressure,

$$\frac{du_a}{du_w} = 2 \cdot T_s \cdot \frac{d(r^{-1})}{du_w} + 1 \qquad 2.93$$

This physics merely incorporates another unknown variable, r, and does not assist in solving the problem. In addition, the capillary model is pertinent only when a solid phase is in the presence of the air and water. The comprehension of this fact is imperative to the study of the case under consideration. Its omission from the research literature has created considerable confusion (Hilf, 1956; Schuurman, 1966). The reasoning of Schuurman leads him to the conclusion that the air in the minute bubbles must reach extremely high pressures just

prior to collapsing and disappearing. This is absurd and contrary to observed behavior. The author questions the validity of Schuurman's complex compressibility equation.

When the air exists as a bubble in water, the physics controlling the air pressure is Boyle's law. The contractile skin responds to the applied water pressure. This means that for the case under consideration, the air and water pressures are always equal and also their changes are equal.

$$\frac{du_a}{du_w} = 1 \qquad 2.94$$

When the air-water mixture is in the presence of a solid phase, the relationship between the change in the air pressure and the water pressure is a constitutive relationship that must be evaluated for each case. Let us incorporate a new pore pressure parameter that applies to a stress point. It can either be defined as

$$B_{aw} = du_a/du_w \qquad 2.95$$

or

$$B_{wa} = du_w/du_a \qquad 2.96$$

The new parameter can be measured in an unsaturated soil by changing one stress component and measuring the response of the other component. The equipment later described in this thesis

(Chapter III) allows the measurement of the pore water pressure in response to an applied air pressure change. Substituting the new pore pressure parameter into the compressibility equation gives,

$$\beta_m = - \frac{1}{V_w + V_a'} \left[\frac{dV_w}{du_w} + \frac{dV_a'}{du_a} \cdot B_{aw} \right] \qquad 2.97$$

Using a derivation similar to that used in the section on combined miscible and immiscible air-water mixtures, the compressibility equation is,

$$\beta_m = S \cdot \beta_w + B_{aw} \cdot \frac{(1-S)}{u_a} + B_{aw} \cdot \frac{S\ h}{u_a} \qquad 2.98$$

The new pore pressure parameter can also be written as the ratio of the B_a and B_w pore pressure parameters proposed by Bishop and Henkel (1962).

$$B_{aw} = \frac{B_a}{B_w} \qquad 2.99$$

The B_a and B_w parameters are related to the compressibility of an unsaturated soil in Chapter VII. If the compressibilities of the soil structure and the contractile skin are known with respect to the stress state variables, the B_{aw} parameter can be computed.

The above model of the relationship between air and water pressures is in agreement with published data (Bishop, and Henkel, 1962) Figure 2.32 subdivides the air-water mixture in an enclosed soil into

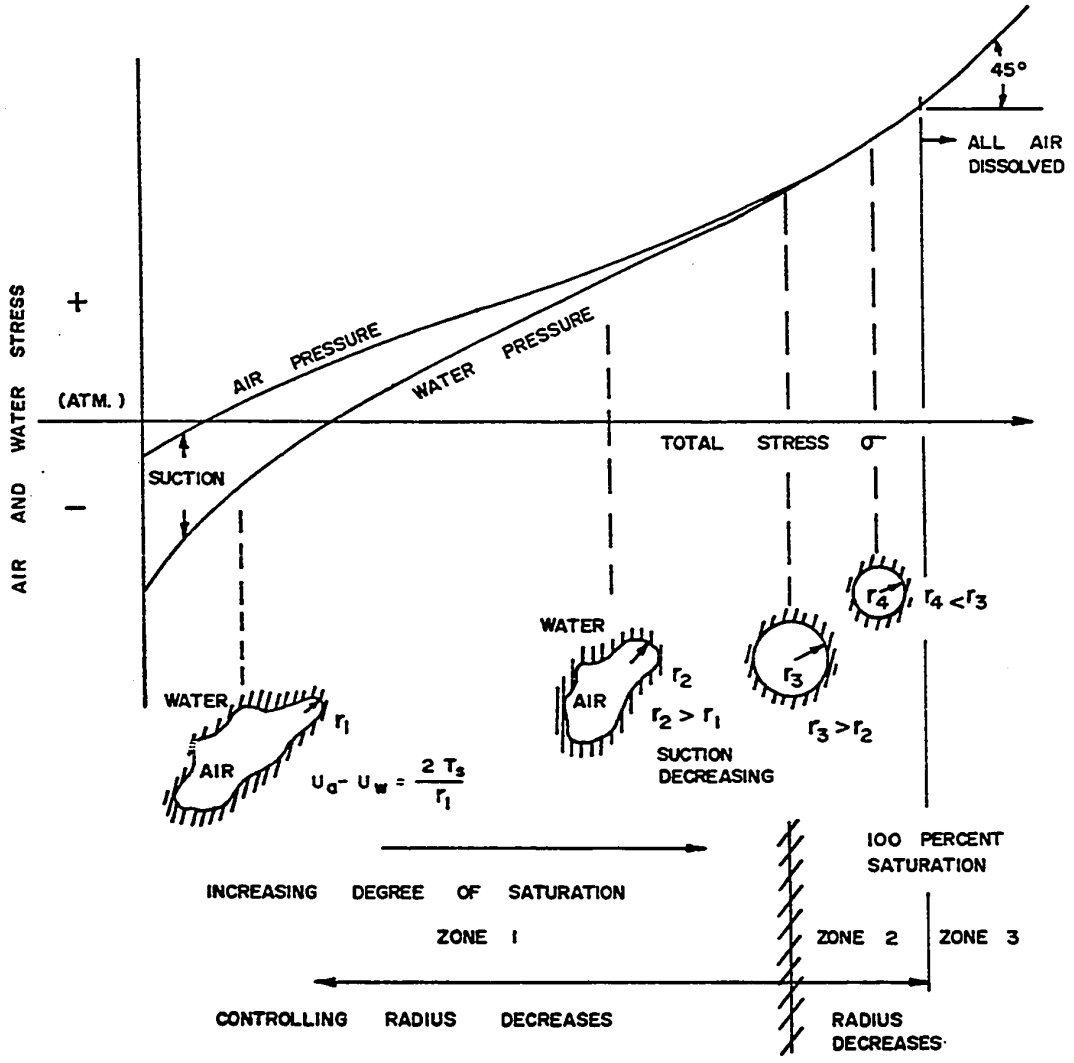


FIGURE 2.32 PORE AIR AND PORE WATER RESPONSES TO A CHANGE IN TOTAL PRESSURE IN A CLOSED SYSTEM

three zones. In zone one the water pressure increases more rapidly than the air pressure. The ratio of their slopes gives the B_{aw} pore pressure parameter. In zone two, the change in the air pressure is equal to the change in water pressure. The pore fluid merely acts as a compressible medium. In zone three, all the air is dissolved and the change in total pressure reflects a direct response in the water pressure.

CHAPTER III

EQUIPMENT FOR TESTING UNSATURATED SOILS

3.1 General

Commercially available soil testing equipment is not sufficiently sophisticated for the complete evaluation of unsaturated soil behavior. However, numerous research workers have developed apparatus that have met with encouraging degrees of success and some have been extended in this thesis.

Four pieces of equipment were used in the examination of volume change behavior of unsaturated soils. Two employed modified Anteus oedometers* for one-dimensional conditions. The other two pieces of equipment allowed isotropic volume change testing conditions in modified, four-inch diameter, Wykeham Farrance triaxial cells.

The significance of air diffusion through the water in the high air entry disc was obvious after the first few tests. Therefore, it was necessary to develop a practical and accurate device for measuring the volume of diffused air. Due to the small volume changes of the overall sample and the water phase, and the lengthy duration of the tests, special care was necessary to protect against erroneous measurements. A series of calibration tests were devised that ensure the

---

*The Anteus oedometers are manufactured by Testlab Corporation in United States.

proper operation of the equipment.

The need for a detailed analysis of the data, along with the ability for rapid re-evaluation, led to the development of computer programs to reduce the data collected from each piece of equipment.

3.2 Basic Design Considerations

The study of the volume change behavior of any material involves the measurement of force and displacement. As described in Chapter I, an unsaturated soil can be envisaged as a combination of two fluids (i.e., water and air) and two solids (i.e., soil particles and contractile skin). Our aim is to be able to describe the flow of the fluids and the deformation of the solids.

The modes of testing an unsaturated soil can be termed as "drained" with respect to each of the fluid phases. In the undrained mode, there is no mass flow of air or water into or out of the sample. When the fluid phases are operated as a drained system, the air and water move into or out of the sample against a controlled constant pressure system. The terms undrained and drained must be linked with the phase under consideration since it is possible for a test to be drained with respect to the air phase and undrained with respect to the water phase. The concepts of a drained and undrained system affect the design of both the pressure and displacement aspects of the laboratory equipment.

Let us first consider the pressures that must be either controlled or measured when testing unsaturated soils. The flow laws for fluids inform us that the pressures heads are required to describe

their behavior. In an unsaturated soil this means that the water and air pressures must be measured independently. To describe the deformation of the soil structure and contractile skin, it would appear that additional stresses must be measured. The only additional stresses that have been successfully measured are the total stresses applied in various directions. Using these three stress components (i.e. total, air and water) an attempt is made to theoretically formulate and experimentally verify stress state variables that uniquely describe the behavior of the soil structure and the contractile skin.

3.2.1 Separation and Measurement or Control of the Air and Water Pressures

Since both air and water are fluids, some means must be found to separately measure them. Porous discs with various pore sizes are commonly used for this purpose (Bishop and Henkel, 1962).

A porous disc with small pores (i.e., high air entry disc) allows the slow passage of water but resists air flow. As long as the difference between the air and water pressure does not exceed the air entry value of the porous disc, there is a continuous column of water from the sample to the pressure transducer below the porous disc and the pressure measured is that of the water phase. Although the fine porous discs do not leak air, dissolved air diffuses through the water in the disc and collects at the base of the disc in the form of free air bubbles. The net result is a gradual increase in the measured water pressure until it approaches the air pressure.

For long term, undrained tests this is a major problem that has not been solved (Bishop, 1969).

The pore water in an unsaturated soil can exist in a highly negative state relative to atmospheric pressure conditions. However, it is impossible to directly measure absolute pressures less than one atmosphere below atmospheric conditions since the water cavitates. Hilf (1956) employed an axis translation technique whereby the air pressure surrounding the sample is elevated by an amount such that the water pressure becomes positive relative to atmospheric pressure. The axis translation technique is acceptable since the equilibrium of the air-water menisci are solely dependent upon the difference between the air and water pressure, regardless of the absolute pressure values.

Olson and Langfelder (1965) experimentally verified the axis-translation technique. They obtained a 1:1.018 ratio between the air and water pressures during translation. The slight discrepancy is likely associated with occluded air in the soil. The full significance of their results is indicated in Chapter IV.

A porous disc with relatively large pores will readily allow the passage of air and thereby form a continuous column of air between the air in the sample and the air measuring system. In an undrained system, the air pressure can be measured using a transducer. The volume of air in the pressure measuring system must be kept to a minimum due to the compressible nature of air. Thin coarse porous discs or glass fibre cloth have proven to be a satisfactory air reservoir

at the end of the sample.

3.2.2 Independent Displacement Measurements in an Unsaturated Soil

The displacement measurements associated with a four phase unsaturated soil system are as follows:

(i) Soil Structure

The vertical and horizontal displacement measurements on the sample allow the computation of the total volume change.

(ii) Contractile Skin

The displacement of the contractile skin cannot be directly measured.

(iii) Water Phase

The water volume inflow or outflow can be monitored.

(iv) Air Phase

The air volume inflow or outflow can be monitored.

Continuity of the soil sample assures that the change in volume of the soil structure is equal to the sum of the changes in the air, water and contractile skin volumes.

$$\Delta V = \Delta V_a + \Delta V_w + \Delta V_c \qquad 3.1$$

where ΔV = change in volume of the soil structure or the overall sample

ΔV_a = change in volume of the air phase

ΔV_w = change in volume of the water phase

ΔV_c = change in volume of the contractile skin.

Let us assume for the present that the change in volume of the contractile skin is negligible due to its thinness. This is dealt with in detail in Chapter V. The continuity requirement becomes,

$$\Delta V = \Delta V_a + \Delta V_w \qquad 3.2$$

One of the volume change measurements is redundant since it can be computed by means of equation 3.2. Generally a complete understanding of the soil structure deformation is desired and therefore the volume change measurements on the overall sample should not be omitted. In addition, either the air or water volume change should be measured.

The measurement of volume change in the air phase is difficult due to its pronounced dependence on temperature and pressure. It is therefore more reasonable to independently measure the water volume change and compute the air volume. The measurement of water volume change is not without its difficulties since air diffuses through the water in the high air entry disc and collects below the disc as free air. Its volume is recorded on the water volume change measuring system as a change in water volume. Some system must therefore be devised to measure the diffused air and subtract it from the recorded water volume change.

In summary, the general basic requirements of equipment for testing unsaturated soils is as follows:

(i) Pressure Requirements

The total, air and water pressures must be either measured in an undrained system or controlled in a drained system. The most versatile equipment would incorporate the ability to either measure or control all pressures.

(ii) Deformation Requirement

The volume change of the overall sample should be measured along with either the air or water phase volume change. The fluid phase volumes must be separable and one must be accurately measured over long periods of time.

3.3 Literature Review of Equipment Development

The testing of unsaturated soils for engineering purposes took on a new perspective as a result of Hilf's work in 1956. Prior to that time, engineers had paid little attention to the difference between the air and water pressures in the pore fluid and their relationship to total stress.

Conventional volume change testing can be broadly subdivided into one of two categories. The first category involves applying total pressures to a sample and monitoring the volume change of the sample. The second category involves applying various differential fluid pressures and monitoring the water volume change. The former approach has been basically that of the engineer whereas the latter has been that of the soil scientist. The different methods of attack appear to be related to the fact that engineers are primarily concerned

with volume change and shear strength whereas soil scientists are more interested in the movement of water through the soil.

While studying the shear strength behavior of unsaturated soils, Bishop and Donald (1961) showed that it was necessary to either control or measure three independent stresses (total, water and air) and measure the volume change of the entire sample plus one of the fluid phases. Later testing appears to have been a regression since subsequent workers have not measured all the basic requirements for understanding volume change behavior. Although Matyas and Radhakrisna (1968) measured both air and water volume change, they ignored the volume of diffused air. Since it was not measured, their water volume changes are likely in error.

Table 3.1 summarizes the major research projects involving the development of equipment for testing unsaturated soils. The basic limitations of each apparatus are readily evident. The general shortcoming is their neglect or inability to accurately measure one of the fluid phase volume changes. For example, it is not sufficient to simply measure water volume change without correcting for the volume of diffused air. Although there are shortcomings with each apparatus, there are also some interesting design techniques that are worthy of review.

TABLE III.1

SUMMARY OF PROVEN TEST EQUIPMENT (UNSATURATED SOIL TESTING)

Reference	One-Dimensional	Three-Dimensional	Controlled* or Measured Stresses			Displacements or Volume Changes			Monitored Diffused Air	Remarks
			Total	Water	Air	Total** Volume	Water	Air		
Conventional Consolidometer	✓		✓	X	X	✓	X	X	X	
Conventional Suction Apparatus		✓	X	X	✓	X	✓	X	X	Pressure plate device
Hilf (1956)		✓	✓	✓	X	✓	X	X	X	Modified concrete air meter
Bishop & Donald (1961)		✓	✓	✓	✓	✓	✓	X	✓	Used for strength testing
M.I.T. (1963)	✓	✓	✓	✓	✓	✓	✓	X	✓	
Dunn (1964)		✓	✓	✓	✓	✓	X	X	X	No test results reported
Matyas & Radhakrishna (1968)	✓	✓	✓	✓	✓	✓	✓	✓	X	Essentially same as Bishop & Donald (1961)
Barden, Madedor & Sides (1969)	✓		✓	✓	✓	✓	✓	X	X	Modified Rowe & Barden consolidometer
Aitchison (1969)	✓		✓	X	✓	✓	X	X	X	Modified conventional consolidometer
Escario (1969)	✓		✓	X	✓	✓	X	X	X	Capable of high suctions
Pufahl (1970)	✓		✓	X	✓	✓	X	X	X	Modified anteus consolidometer
Compton (1970)	✓		✓	✓	✓	✓	✓	X	X	Modified Bishop consolidometer
Neves (1971)		✓	✓	✓	✓	✓	X	X	X	National laboratory of Civil Engineering, Lisbon, Portugal

*The stress can be manipulated to various levels and held constant.

**For one-dimensional testing, total volume decreases for suction increase, cannot be measured.

3.3.1 Hilf (1956)

Hilf used a modified concrete air meter to measure the change in volume and the induced pore water pressure in compacted samples that were subjected to a change in total pressure. A high air-entry porous tip was inserted in the sample and the nulling of a mercury slug in a fine bore capillary tube was used to measure the pore water pressure. The entire specimen was dipped in natural rubber latex to protect it from the surrounding water. Changes in volume of the overall sample were registered in the capillary tube at the top of the concrete air meter.

Later research at the United States Bureau of Reclamation has extended Hilf's testing system to the triaxial cell to accommodate shear strength testing (Gibbs, 1963; Gibbs and Coffey, 1969). Their most recent equipment (1969) measures the total volume change of the sample by measuring the change in volume of the water surrounding the sample. The triaxial cell is single-walled. Vertical and lateral displacements cannot be measured independently. The air pressure is measured or the air volume change is monitored at the base of the sample. The water is similarly controlled at the top of the sample. There is no system for measuring diffused air or even flushing it from the upper cap. Although the equipment appears to have most of the basic requirements for testing unsaturated soils, the reliability of the system leaves much to be desired.

3.3.2 Bishop and Donald (1961)

Conventional triaxial cells (for 1/2 inch diameter and 4 inch diameter samples) were modified as follows for performing shear strength tests on unsaturated soils. A high air entry (i.e. up to 76 psi) ceramic disc was installed in the bottom pedestal. A bubble pump was built to remove and measure the amount of diffused air that collected below the high air entry disc. The water volume change in the sample was measured using a double-walled burret system (i.e. a Bishop paraffin-water volume change indicator) that could be back pressured. The triaxial cell contained a second (inner) lucite cell. Mercury was placed between the inner lucite and the sample. In this way, cell pressure changes do not cause an expansion of the inner lucite sleeve. Therefore, accurate measurements of the vertical and lateral displacement of the sample can be made using a cathetometer. The mercury around the sample also prevented the diffusion of air from the sample. Further details are given in "The Measurement of Soil Properties in the Triaxial Test" by Bishop and Henkel (1962).

3.3.3 M.I.T. (1963)

The equipment developed at M.I.T. was used to evaluate the shear strength and volume change characteristics of unsaturated soils. The four main modifications to conventional equipment involved the:

(i) measurement of negative pore water pressures

(ii) application of a controlled air pressure

(iii) measurement of the volume of water drained from the sample

(iv) control of the volume during saturation and the measurement of volume changes during shear.

For shear strength testing, a reinforced triaxial cell (for 4-inch diameter samples) was used. A 60 psi air-entry ceramic disc was installed in the base plate and a coarse porous disc was placed above the sample. The air pressure was controlled but the air pressure response could not be measured. The water volume change was measured using a burret on a constant volume circulating pump similar to that described by Bishop and Donald (1961). The air bubble pump was fabricated from glassware and could not be back pressured.

Changes in the sample volume were measured by monitoring the cell fluid expelled or taken in. This procedure has limitations since several factors are involved in the measured volume change. These are:

(i) changes in the sample volume

(ii) changes in the volume of air entrapped in the cell, with changing pressure and temperature

(iii) changes of cell volume with changing pressure

(iv) movement of the piston during shear

(v) leakage from the cell.

The technique used to measure the total volume change and the inability to back pressure the water volume change indicator are the main limitations of the equipment.

The one-dimensional compression devices were designed with

some differing features to those used on the triaxial apparatus. The high air-entry discs were installed at the top and bottom of the specimen and the water volume changes were monitored from both discs. The total load on the sample was measured on a stud force transducer at the base of the sample. The total volume change was monitored by measuring the displacement of the loading piston.

3.3.4 Dunn (1964)

A conventional triaxial cell was modified to allow the independent measurement of the total volume change and the air and water pressures. The total volume change was monitored using a procedure developed by Frederick (1962). The method involves enclosing the sample in a lucite cell which itself is housed inside the conventional cell. Water fills the space both inside and outside this inner cell. The line from the inside of the inner cell goes through a Bishop paraffin-water volume change indicator. Calibration tests showed 2 ± 0.5 cc compression in the inner cell water for a pressure change from zero to eighty psi.

No attempt was made to remove and measure the volume of diffused air. Also, there was no means of monitoring the air or water volume changes.

The diffusion of air from the sample by way of the rubber membrane, was prevented by using two sheets of slotted aluminum foil, stuck together with silicone grease. The double aluminum sheets were wrapped around the outside of a rubber membrane placed on the sample.

Another rubber membrane was placed on the outside of the slotted aluminum foil.

3.3.5 Matyas and Radhakrishna (1968)

The equipment was developed by Radhakrishna (1967) and is similar in many respects to Bishop and Donald's (1961) apparatus. A lateral strain indicator could be placed on the sample in order to perform Ko tests. The volume changes of the overall sample, the air phase and the water phase were measured independently. Air volume change measurements were performed only during the constant water content tests. It was measured using a two-limb water manometer between the sample and the air source. There was no attempt to measure the volume of air that diffused through the high air entry disc in the base plate.

3.3.6 Barden, Madedor and Sides (1969)

Their apparatus is a modified form of the Rowe and Barden consolidation cell (1966). The samples tested were six inches in diameter and one inch thick. The water and air pressures were independently controlled at the top and bottom of the sample. The movement of water in or out of the sample was measured by observing the movement of a mercury slug in a horizontal glass tube. Diffused air was periodically flushed out of the base but its volume was not measured.

3.3.7 Aitchison (1969)

Aitchison modified the conventional one-dimensional consolidometer by enclosing the sample in a chamber. The air pressure in the

chamber was regulated to produce the desired suction values. This setup is inadequate for a complete understanding of volume change behavior.

3.3.8 Escario, V (1969)

The apparatus used by Escario was constructed to withstand high pressures. By placing a cellophane membrane over the lower porous disc, suctions greater than 64 kg/cm^2 were measured. A coarse porous disc was used on the top of the sample.

When an unsaturated soil sample is placed on a high air entry disc, there is a tendency for the uptake of water by the soil. This reduces the initial suction of the soil by an amount dependent upon the time required to assemble the equipment and apply the pressures. To overcome this difficulty, Escario lowers the base plate during assembly, thereby leaving a separation between the membrane and the lower water reservoir. At the moment the test is commenced, the base (with reservoir) is raised to come in contact with the membrane.

The equipment does not measure the change in volume of the fluid phases or allow the control of the pressure on the water phase.

3.3.9 Pufahl (1969)

Pufahl modified the Anteus oedometer by installing a high air entry disc in the base. The oedometer was originally designed to allow the water phase of a soil sample to be back pressured during testing. Pufahl regulated the air pressure in the sample by means of the back pressure regulator.

The main deficiency of the apparatus is related to the lack of a means to measure the fluid phase volume changes.

3.3.10 Compton (1970)

The Bishop consolidometer manufactured by Wykeham Farrance was modified for testing unsaturated soils. A high air-entry disc (i.e. 75 psi) was installed in the base. The pore water pressure was manitored using a manual Bishop null indicator. The change in water volume could also be measured; however, no attempt was made to account for diffused air.

3.3.11 Neves (1971)

The equipment is a modified triaxial cell adapted for the measurement of pore water pressure and total volume change during the shear strength evaluation of unsaturated soils. The axis translation technique is used with the air pressure applied at the base of the sample. A transducer is installed below the base with a fine bore polyethylene tubing, cemented in epoxy, connecting the high air entry disc to the pressure transducer. The lateral deformation is monitored by measuring the displacement of a steel wire wrapped around the specimen. The steel wire rested on pieces of aluminum foil placed on the specimen. The displacement is registered on a dial gauge placed inside the triaxial cell.

The equipment does not have any facility for measuring water volume change or volume of diffused air. Also, the water pressure cannot be controlled or regulated.

3.4 Equipment Development

Four apparatus were developed as part of this thesis, to measure or control the variables required to describe volume change behavior in unsaturated soils. Two apparatus investigated one-dimensional (Ko) loading and the other two were designed to study three dimensional (isotropic volume change. The two one-dimensional testing apparatus are essentially the same whereas the triaxial cells are basically two different designs. Plate 3.1 shows a general layout of all four apparatus. Each apparatus is considered under the following headings:

1. Constant Pressure System
2. Design of the Cell
3. Base Plate Design
4. Layout of Plumbing
5. Measurement of Total, Air and Water Pressures
6. Measurement of Total Volume Change
7. Measurement of Water Volume Change
8. Measurement of Diffused Air Volume Change

On all four apparatus, the total volume change of the sample was measured along with a measurement of the water expelled or taken in and the volume of diffused air. No attempt was made to measure the air expelled from or taken into the sample.

In all cases, the pore water pressure can be either measured in an undrained system or controlled in a drained system. The air stress is always controlled. This procedure was selected for two main

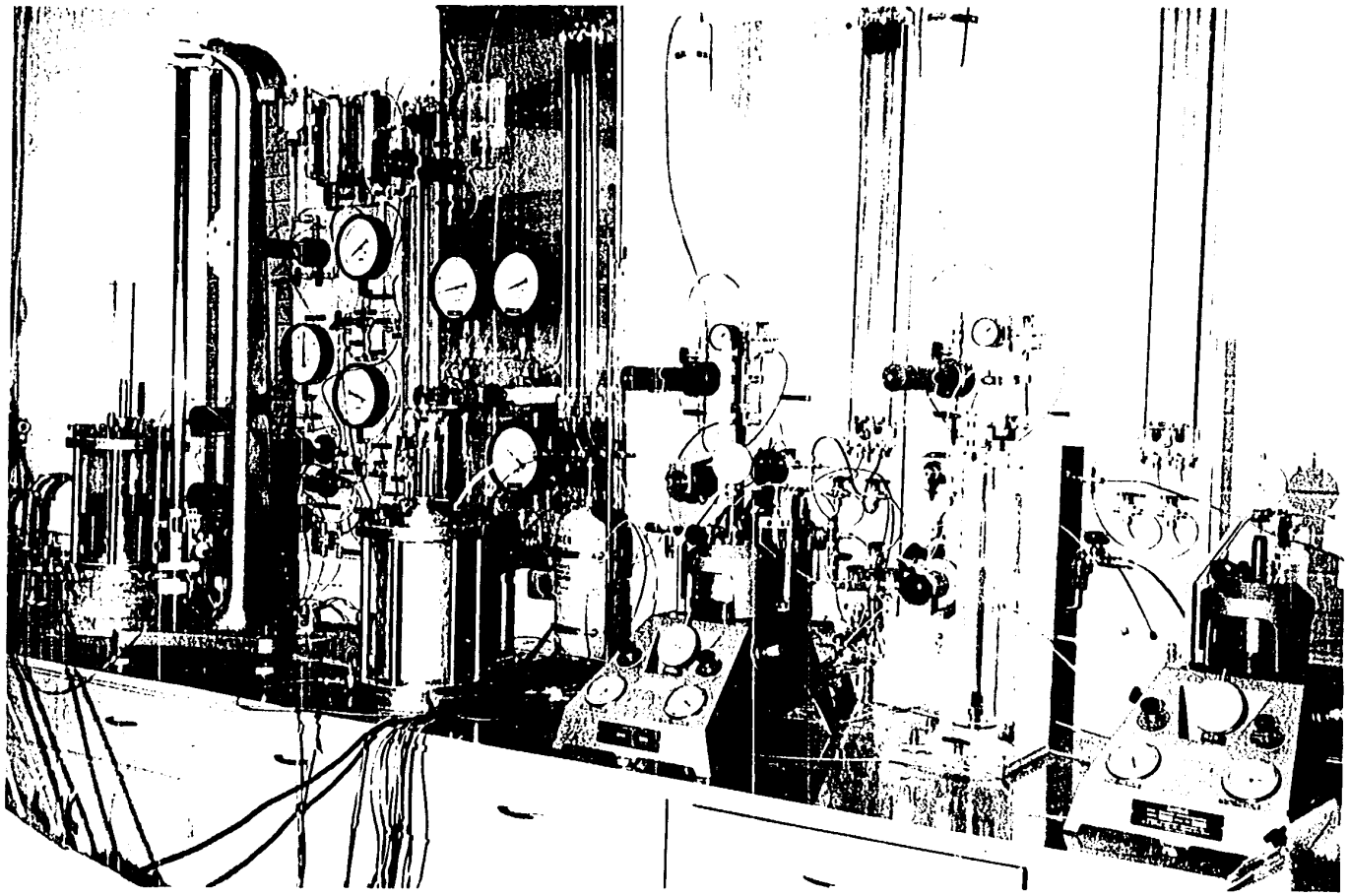


PLATE 3.1 GENERAL LABORATORY SET – UP

reasons. First, the air pressure is difficult to measure due to its susceptibility to pressure and temperature changes. Secondly, the air operates as an open system in nature (i.e. open to atmospheric conditions).

3.4.1 One-Dimensional (Ko) Apparatus

The Anteus oedometer was selected as the basic apparatus for modification due to its versatile design. Plate 3.2 shows the layout of the modified Anteus oedometer. The chamber (normally filled with water for back pressuring the water phase of soils) was filled with air to regulate the air pressure in the soil sample. The water pressure was either measured or else the water pressure was controlled while the water volume change was monitored at the base of the sample. The design of the base plate has fine tolerances and is installed in very cramped quarters. The water volume change indicator and the diffused air volume change indicator are connected to the base plate. Due to the large number of connections, valves and seals, there are numerous sources of leakage. For precise water volume change measurements, there must be assurance that these are virtually eliminated.

1. Constant Pressure System

The pressures were maintained constant by means of Anteus precision air pressure regulators. The manufacturers maintain that the accuracy of the regulator is better than $\pm$ 0.01 psi. However, variations may be significantly larger due to variations in atmospheric pressure. (The regulator operates as a differential pressure regulator

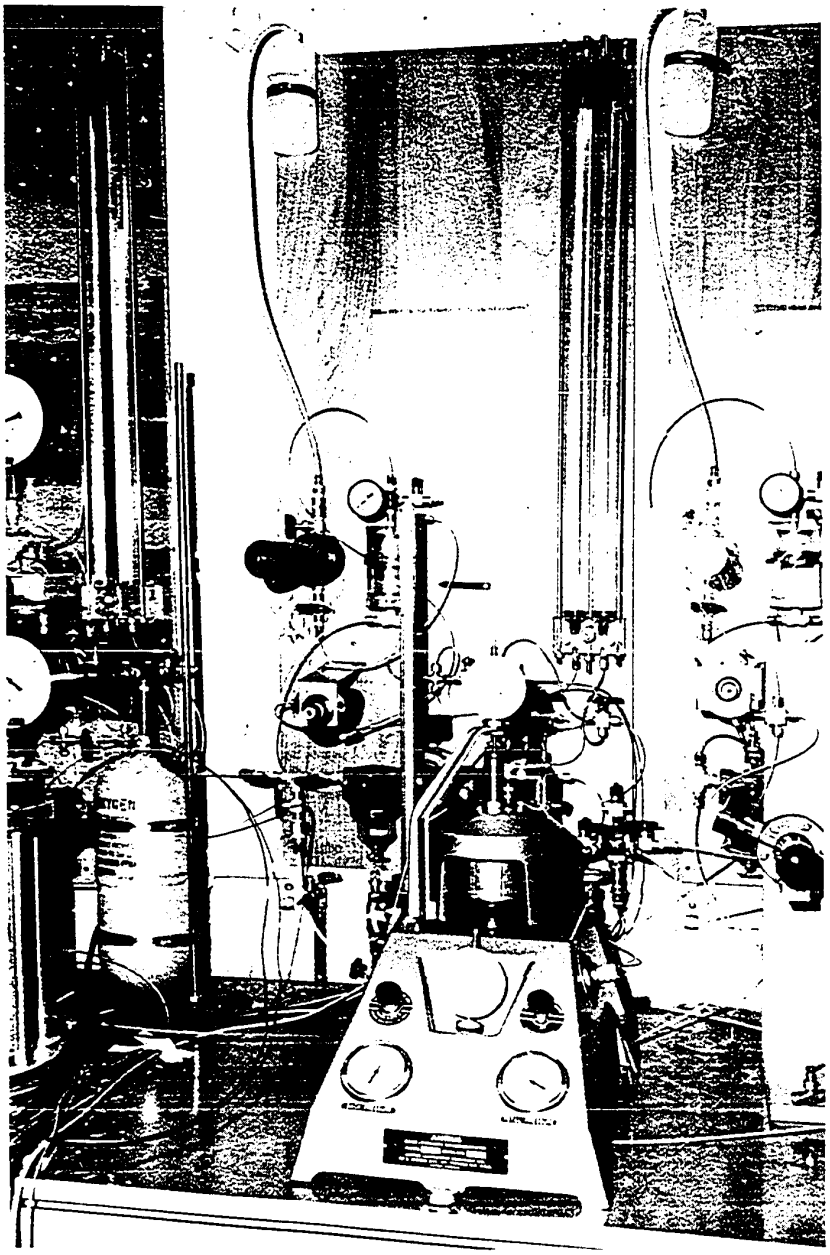


PLATE 3.2 LAYOUT OF MODIFIED ANTEUS OEDOMETER

with respect to atmospheric pressure).

The transducers used to measure the pressure could only record to the nearest 0.04 of a psi. By comparing the behavior of several regulators it was possible to isolate the pressure output fluctuations that were due to regulator inaccuracy. As far as could be detected, there is essentially no fluctuation in pressure output to the apparatus due to inaccuracies in the regulators. Department of Transport records for the City of Edmonton indicate daily barometric pressure fluctuations of approximately $\pm$ 0.09 psi. The deviations during each month, from the monthly mean are $\pm$ 0.23 psi and the deviations of the monthly mean from the yearly mean are $\pm$ 0.13 psi. In the laboratory, each pressure change is applied for approximately one week and deviations of $\pm$ 0.20 psi are to be anticipated (Table 3.2). The same type of regulator was used to control all pressures, (i.e. total, water and air) and therefore the atmospheric pressure fluctuations have a cancelling effect. In other words, the difference between any two pressures was maintained essentially constant.

For the first few tests performed on the modified Anteus consolidometer, the water pressure was held constant by means of self compensating mercury pots. The system was then converted to air pressure regulator control and found to be more satisfactory.

2. Design of the Cell

Pertinent parts of the modified Anteus oedometer are labelled on Figure 3.1*. The total pressure is applied to the top of the sample

---

*Further details on the equipment can be found in literature available from Testlab Corporation, 216N. Clinton St., Chicago, Illinois and in a paper by Lowe III, Zaccheo and Feldman (1964).

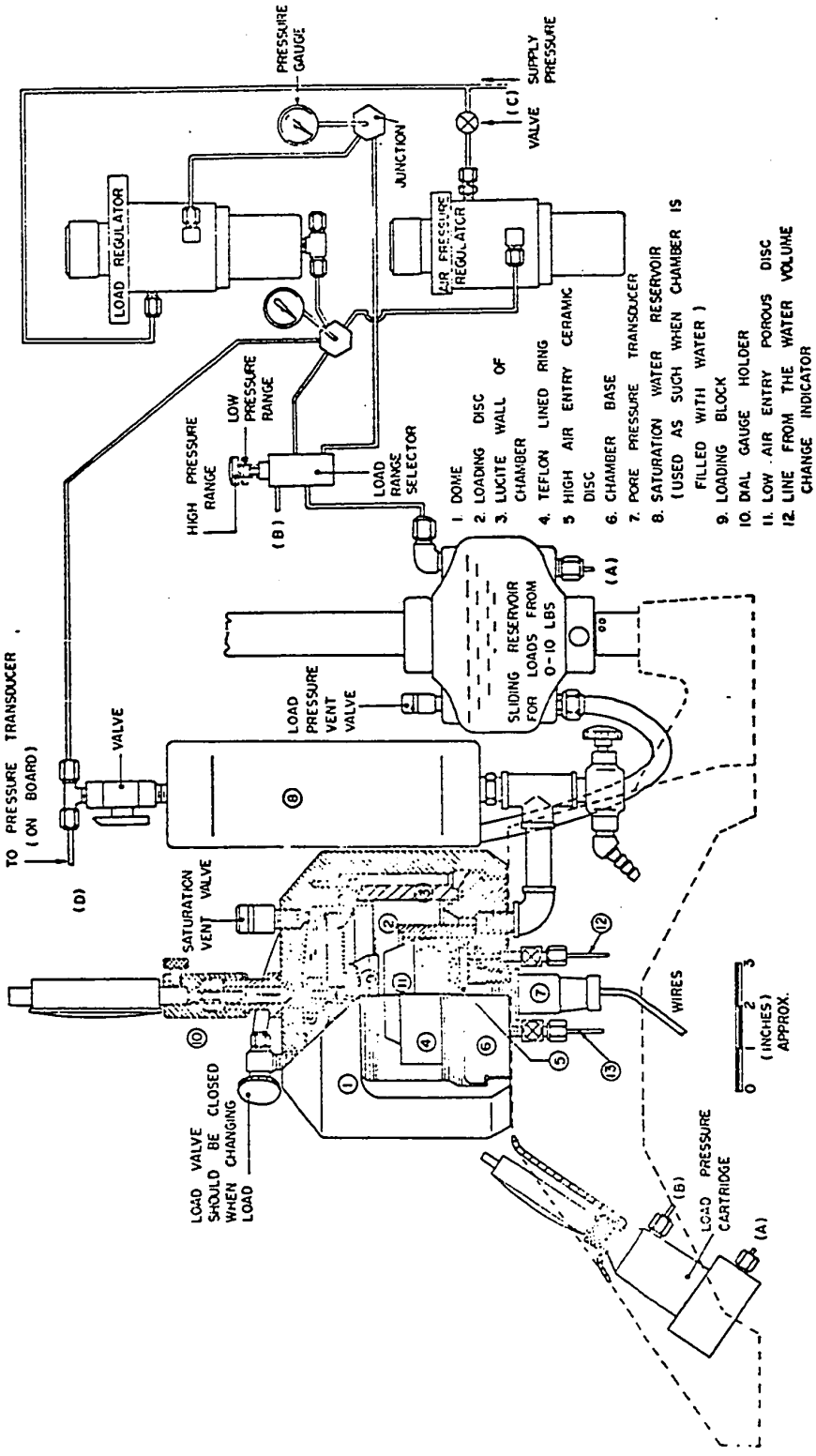


FIGURE 3.1 LAYOUT OF THE MODIFIED ANTEUS CONSOLIDOMETER

TABLE III.2

FLUCTUATIONS IN OUTPUT PRESSURE FROM PRESSURE REGULATORS COMPARED WITH CHANGES IN BAROMETRIC PRESSURE

Aneroid Barometer		Anteus Regulator		Moore Regulator	
Pressure (psi)	Change (psi)	Pressure (psi)	Change (psi)	Pressure (psi)	Change (psi)
13.43*	0.00	52.42	0.00	31.00	0.00
13.44	+0.01	52.44	+0.02	31.02	+0.02
13.38	-0.05	52.44	+0.02	31.00	0.00
13.41	-0.02	52.42	0.00	31.00	0.00
13.49					
13.32	-0.11	52.26	-0.16		
13.10	-0.33			30.60	-0.40
13.27	-0.16			30.74	-0.26
13.38	-0.05			30.84	-0.16
13.52	+0.09			30.95	-0.05

*One reading was taken each day starting at Feb. 10, 1972.

Accuracy of Reading on each system

Aneroid Barometer = $\pm$ 0.003 psi

Anteus Regulator = $\pm$ 0.04 psi

Moore Regulator = $\pm$ 0.04 psi

through a loading disc separated from the chamber by a rolling rubber diaphram.

The air pressure enters the chamber via the saturation water reservoir. An additional valve was placed at the top of the saturation water reservoir in order to isolate the chamber while making air pressure changes. The manufacturer's design only allowed the back pressure to be set at the start of the test (having the load range selector in the low pressure range) and no changes were permitted throughout the test. The equipment is designed such that the back pressure is registered on the load pressure cartridge when the load range selector is in the low range. When the load range selector is in the high range, the total pressure is registered on the load pressure cartridge. This arrangement is unsatisfactory for independently regulating the air pressure while testing unsaturated soils. Two alternate methods of operation were found to function satisfactorily.

(i) Close the load valve on the cell and the valve at the top of the water saturation reservoir. Slowly push the load range selector back to the high pressure range. Opening the load valve on the cell and the valve on the top of the water saturation reservoir simultaneously will increase the air pressure in the chamber but leave the net loading applied by the cap the same as before. The large volume of air involved in the water saturation reservoir and the chamber caused a slight delay in the equilization time for the air pressure.

(ii) An additional line (D) from the top of the water saturation reservoir was connected to the pressure transducer on the "board" pressure transducer without using the load range selector. In other words, the air pressure regulator could be adjusted to any pressure (in about 3 seconds) without manipulating any valves. This alternate was found to be the most satisfactory procedure.

The major modification to the equipment involved the new base plate design. To maintain a maximum of rigidity in the cell, it was desirable that the enlarged hole in the chamber base be kept to a minimum. This meant that the flushing and water volume change ports had to be taken from the base plate through the chamber base by means of aligned holes, sealed off with O-rings.

The advised order of making the ports is:

(i) Drill the holes (i.e. two) in the chamber base, diametrically opposite each other.

(ii) Machine the stainless steel base plate without drilling the ports.

(iii) Screw the base plate into the chamber plate, as snug as necessary to ensure a seal between them.

(iv) Mark and drill the ports in the base plate.

(v) Machine the O-ring recesses and the flushing groove.

(vi) Install the high air entry ceramic disc.

Two circle seal valves are then tapped into the chamber base (i.e. 12 and 13). The fine tolerances may require the following

order of assemblage.

(i) Install valve 13 to the desired location. Ensure that the valve can be opened and closed without interference with the transducer or the frame of the oedometer.

(ii) Insert the transducer and torque it to the desired value.

(iii) Valve 12 will likely need to be disassembled for installation. First tighten the casing of the valve. This may require a slight turning of the base plate with the specially designed torque wrench (Figure 3.3). The valve core can be inserted, assuring that it is free to be opened and closed.

(iv) The entire chamber can be attached to the frame.

Although the fine tolerances make the base difficult to assemble, the minimal sized chamber below the ceramic disc is advantageous for the proper functioning of the base plate.

3. Base Plate Design

The base plate for a 1/4 inch thick ceramic disc, was machined from stainless steel as shown in Figure 3.2. Originally, attempts were made to use 1/8 inch thick ceramic discs. The base plates were machined from aluminum and were 1/8 inch thinner than shown. Difficulties were encountered with cracking of the thin stones which discouraged their use. However, the thicker ceramic discs limited the height of the soil specimen that could be used in the chamber. To overcome this difficulty, a thinner upper coarse porous disc was used along with a higher ring.

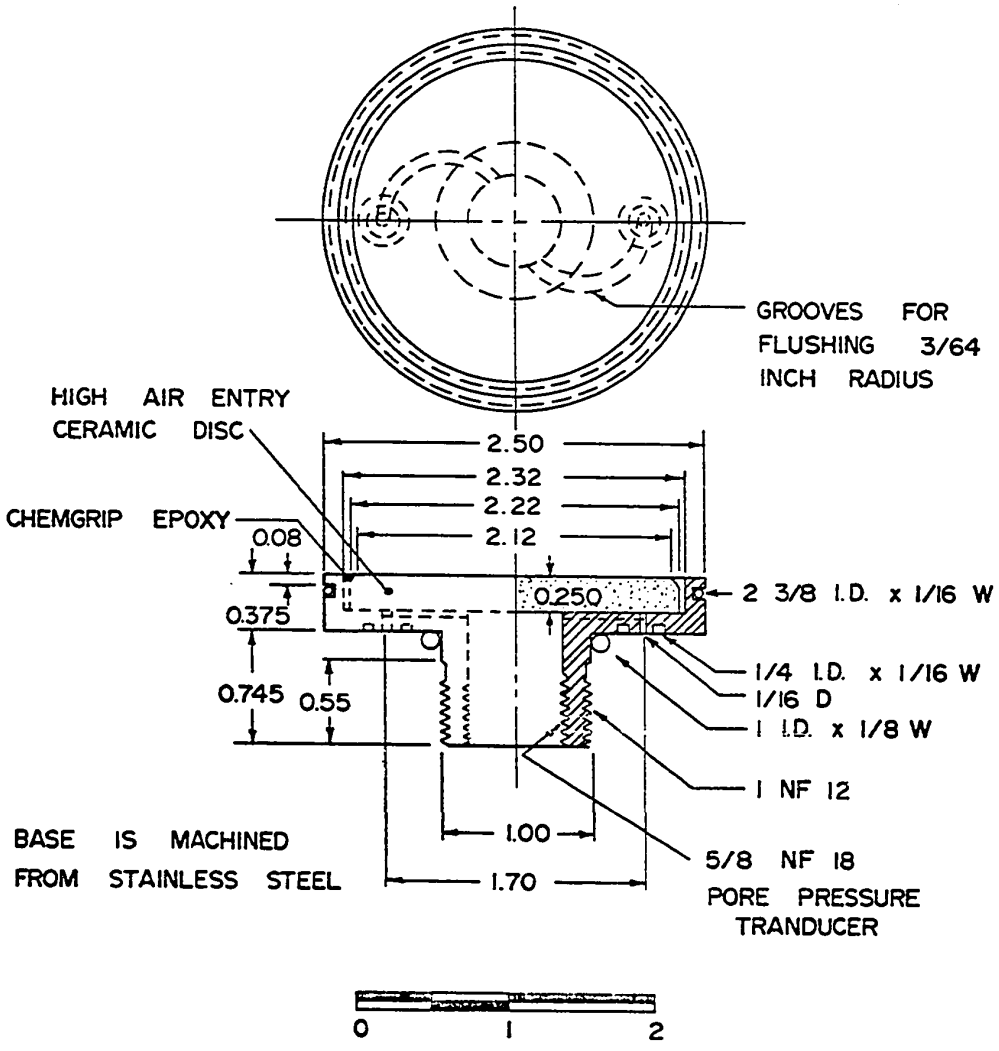


FIGURE 3.2 BASE PLATE DESIGN FOR MODIFIED ANTEUS CONSOLIDOMETER

One of the main design considerations for the base plate is the size of the bore throughout the system. During the flushing of air, the velocity of the fluid should be kept as constant as possible. Large cavities cause a reduction in water velocity and air bubbles become lodged in these zones. On the other hand, highly restricted zones cause a high flow velocity, resulting in cavitation and a mixing of the air and water into a foam.

The constant cross-sectional area requirement also pertains to the tubing leading to the diffused air volume indicator. The original design of the diffused air volume indicator had an enlarged tube leading into the indicator and bubbles of air were constantly becoming lodged in this zone. They could be removed by increasing the pressure gradient, however, it is desirable to keep the pressure differential across the base to a minimum.

The O-ring seals between the base plate and the chamber base must be given an inner shoulder support since they must provide a seal against the higher air pressure that exists outside the port.

The O-ring that seals against the teflon-coated ring can be removed (if desired) for most testing of unsaturated soils. In this way the ring operates as a floating ring. Since most testing involves the swelling mode, water is taken up from the fine ceramic disc and has no desire to leak between the ring and the base plate.

The high air entry ceramic disc was sealed in place using Chemgrip epoxy. Several other types of epoxy were tested, however,

the Chemgrip epoxy appeared to be the most satisfactory. The disc and base plate should not be boiled in order to saturated the disc since their is the danger of a fine crack opening between the glue and the fine porous disc. The different thermal properties of the materials involved causes the serious distress to the ceramic disc. However, this problem was overcome using another method for saturating the ceramic disc (Section 3.5).

If the total pressure is removed from the top of the ceramic disc while a water pressure exists below the disc, the upward bending moment can crack the ceramic disc. It would be desirable to have a safety valve to prevent the water pressure from exceeding the total stress, however, this becomes rather difficult and cumbersome to install. Experience showed that an excess uplift pressure greater than 10 psi on a 1/8 inch thick ceramic disc (2-1/2 inch diameter) could produce fine cracks in the disc. The cracks may not be visible to the naked eye but are evident from an air entry test. One quarter inch thick discs can withstand higher pressures but should be checked by an air entry test whenever they are subjected to an excess water stress greater than 10 psi.

The base plate must be screwed into the chamber base prior to installing the pore pressure transducer in the base plate. A special wrench (Figure 3.3) was designed to hold the top of the base plate while torquing the transducer. It is also used to tighten and loosen the base plate from the chamber base. The wrench enables the turning of the base plate without distress to the ceramic disc.

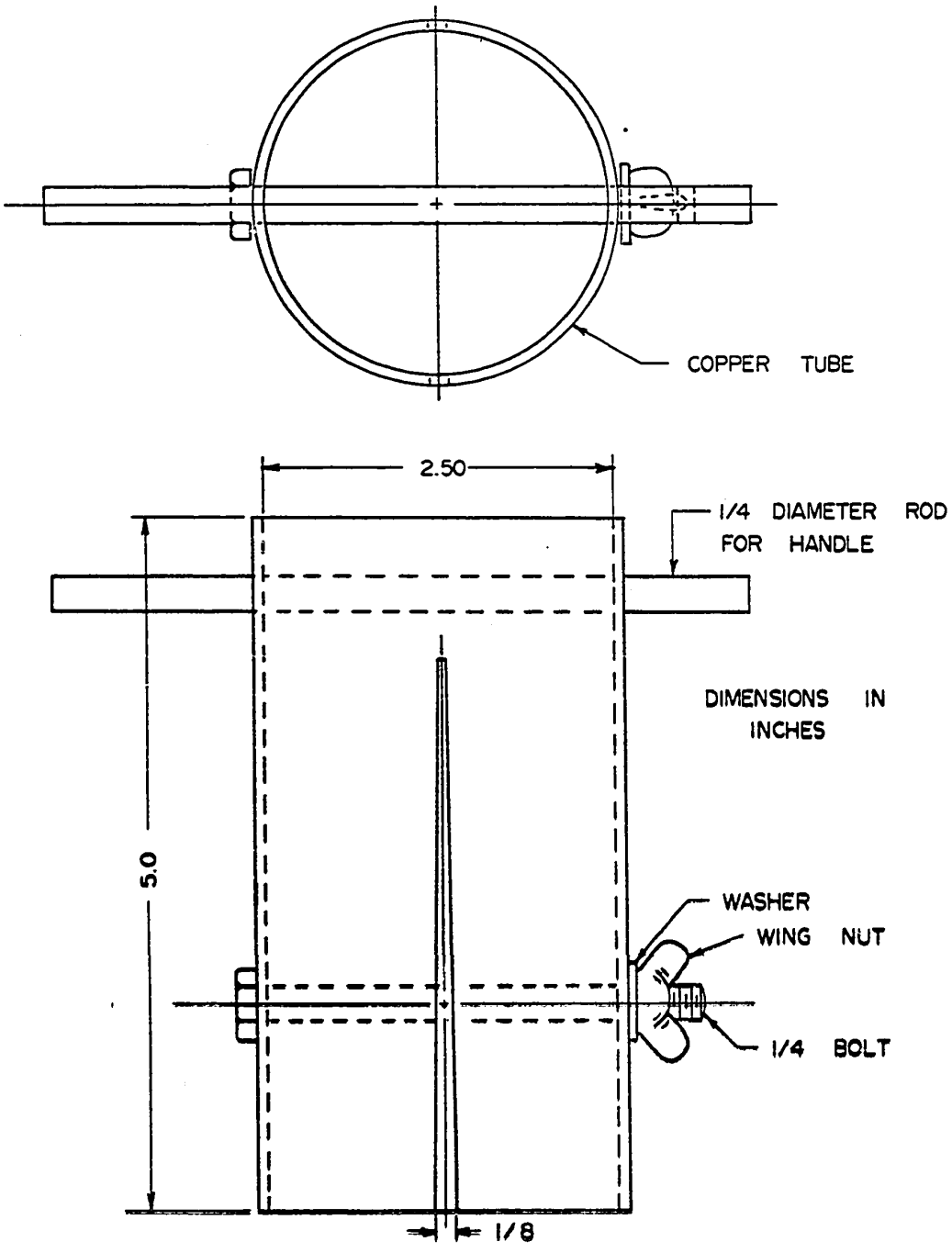


FIGURE 3.3 WRENCH FOR TIGHTENING AND LOOSENING THE BASE PLATE

4. Layout of the Plumbing

Most of the plumbing associated with each modified Anteus oedometer is shown on Figure 3.1. Additional plumbing was placed on a sheet of plywood installed back of each oedometer (Figure 3.4). The plumbing is primarily to accommodate the water volume change indicator. Also included are the switching valves required to measure the pressures (i.e. water, air and diffused air lines).

The pressure regulator on the "board" is the same as those used on the oedometer. The small pressure gauge gives a quick visual indication of the water pressure. The water pressure measured on the "board" transducer must have added to it the difference in elevation head between the water reservoir and the soil sample.

5. Measurement of Pressures

The total differential pressure is recorded on the load pressure cartridge. The air pressure is either recorded on the load pressure cartridge or the transducer on the "board". (The latter is the preferred method). All the pressure transducers used were manufactured by Dynisco. Their range is from 0 to 100 psi and the pressures are recorded to within 0.04 psi.

The water pressure is measured using the transducer on the "board" (when operated as a drained system) or by using the transducer on the base of the oedometer (when operated as an undrained system). Generally the water pressure is manipulated as follows:

(i) In order to increase the water pressure, the water line to the cell 12 is closed and the pressure regulator is increased by the desired amount (registered on the

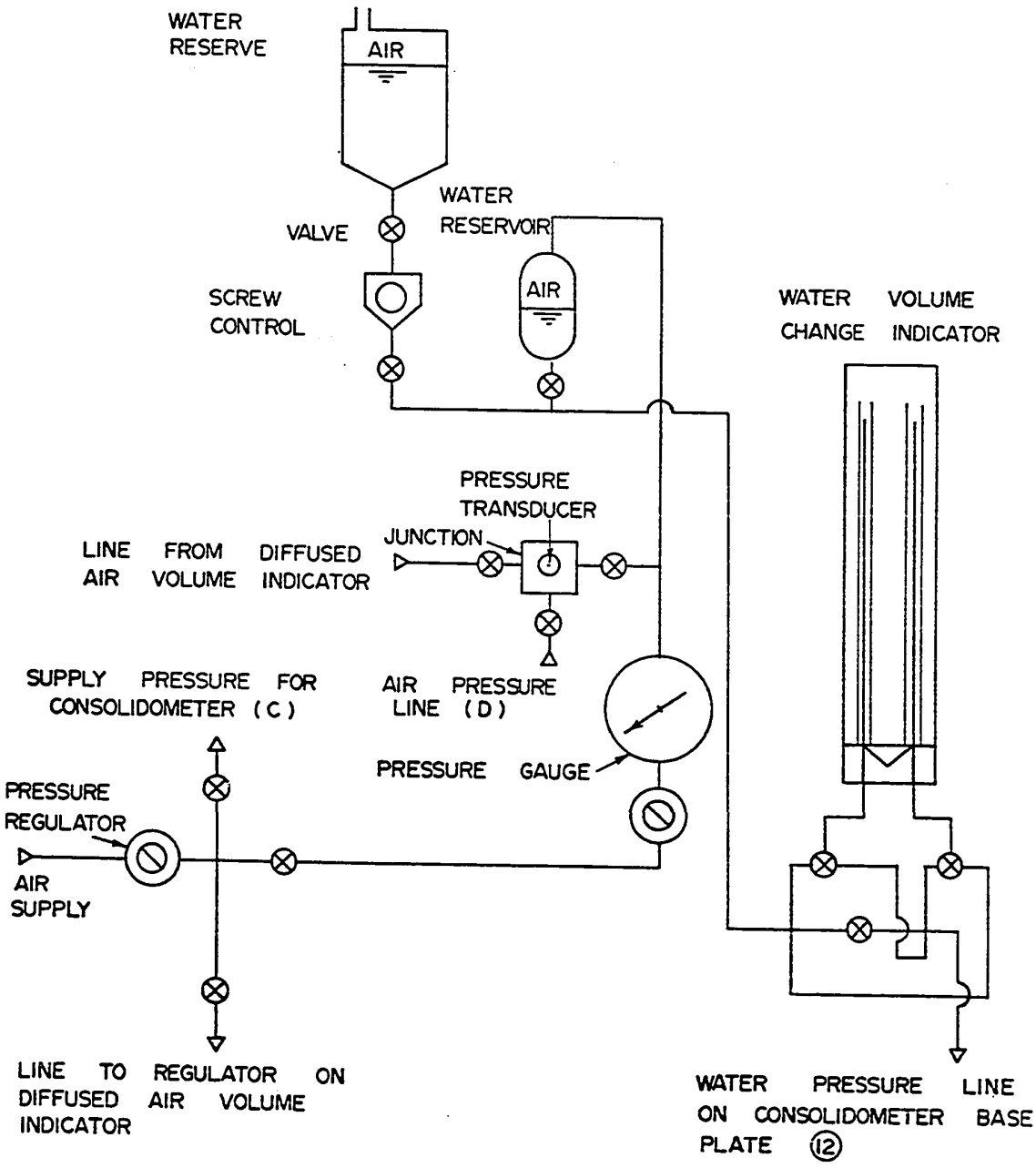


FIGURE 3.4 LAYOUT OF PLUMBING FOR MODIFIED ANTEUS CONSOLIDOMETERS

transducer on the board). This water pressure is applied instantaneously by opening valve 12 .

(ii) If the air and/or total pressure are increased and the pore water reaction is desired, valves 12 and 13 are left closed and the transducer at the base measures the pore water pressure.

Two pressure transducers are required for each apparatus due to these different modes of operation.

6. Measurement of Total Volume Change

The total volume change in the Anteus oedometer is equal to the vertical volume change as recorded by the dial gauge at the top of the cell. This testing technique is satisfactory for saturated soils; however, it has a limitation for unsaturated soils. The behavior of unsaturated soils is affected by suction (u_a-u_w) which behaves as an isotropic stress tensor. Therefore, there is always a tendency for three-dimensional volume change when the suction is changed. As long as suction is decreasing, swelling generally occurs and since swelling in the horizontal direction is prohibited, only the vertical volume change needs to be measured. When the suction is increased, there is generally a shrinkage in the horizontal directions, with the sample pulling away from the sides of the ring. Once this occurs, the total volume of the sample cannot be computed. This is an obvious limitation when attempting to follow certain stress paths; however, the equipment was primarily meant for testing swelling behavior.

7. Measurement of Water Volume Change

The conventional double tube, double acting volume change indicator manufactured by Wykeham Farrance (Figure 3.5) was used to measure the water going into or coming out of the soil sample. The burrets had a full travel of the water-kerosene interface equal to 5 cc. Volume changes were recorded to within 0.005 cc.

After several long term tests it was found that the valves on the volume change indicator allowed a slow leakage of water. Complete details are presented in Appendix B. Due to the long times associated with testing, leakage had to be essentially eliminated. The valves were replaced with two, 3-way Whitey valves and one, 2-way Whitey valve. Swedge-lock fittings on polyethylene tubing were used for the plumbing. The frequent use of the valves warranted the use of a small arrow indicating the direction of the 3-way valves. A small lucite filler was placed at the base of the burret to prevent them from popping-up when tightening down the rubber sleeve around the base of the burret.

Volume change due to the compressibility of the indicator and the fluid in it, could be essentially eliminated by always reading the burret opposite the direction that the three-way valves were pointing. When this procedure was not adhered to, errors in the order of 0.1 cc were often noticed during the duration of one day.

The volume change indicator actually measures the change in water volume plus the volume of diffused air. Since diffused air always moves from the sample through the ceramic disc, its volume can

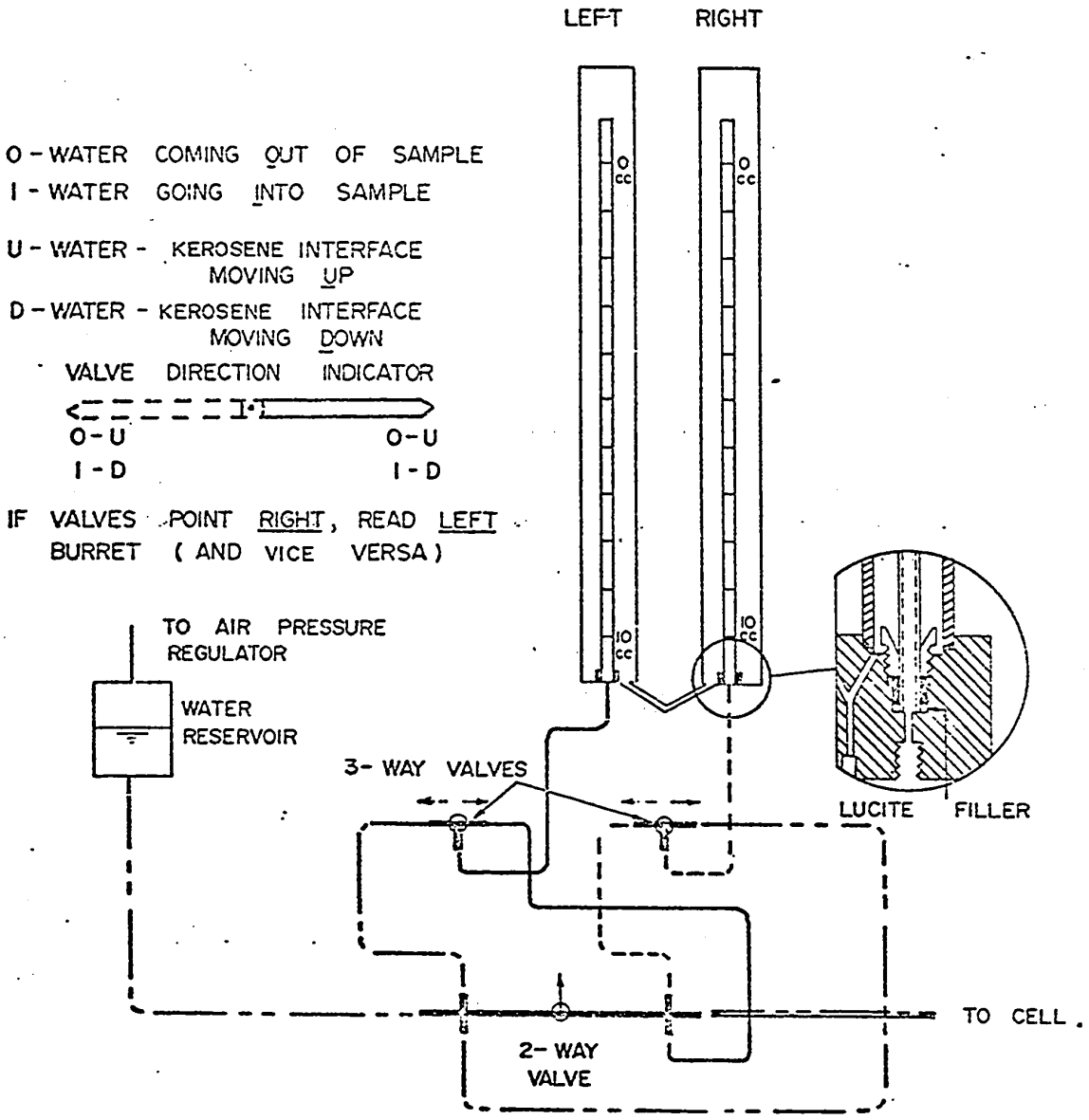


FIGURE 3.5 MODIFICATIONS OF - AND OPERATION OF WATER VOLUME CHANGE INDICATOR

be measured separately and subtracted from the total water volume change. (See Appendix D for sample calculations).

8. Measurement of Diffused Air Volume

A standard (10 cc) graduated burret was inverted and encased in a lucite cylinder to collect air that diffused through the ceramic disc (Figure 3.6). The valve at the end of the burret was removed). Two rolling O-rings were placed around the top of the burret to form a seal with the lucite.

By momentarily creating a water gradient of 1 to 10 psi across the base, the air bubbles are flushed out and measured by displacing the water in the burret. The pressure inside the lucite cylinder can be controlled by an air pressure regulator, at a value that maintains the desired gradient across the base plate. For example, if the water pressure is set at 30 psi, the lucite cylinder would be pressurized to approximately 25 psi. The volume of diffused air is recorded in either of two ways:

(i) The initial burret reading is taken after the diffused air indicator chamber is pressurized to 25 psi. The base plate is flushed out and the final burret reading and pressure in the chamber are recorded.

(ii) The initial burret reading is taken when the diffused air indicator chamber is at atmospheric pressure. The chamber is then pressurized and the air flushed from the base plate. The chamber is depressurized and the final burret reading is recorded.

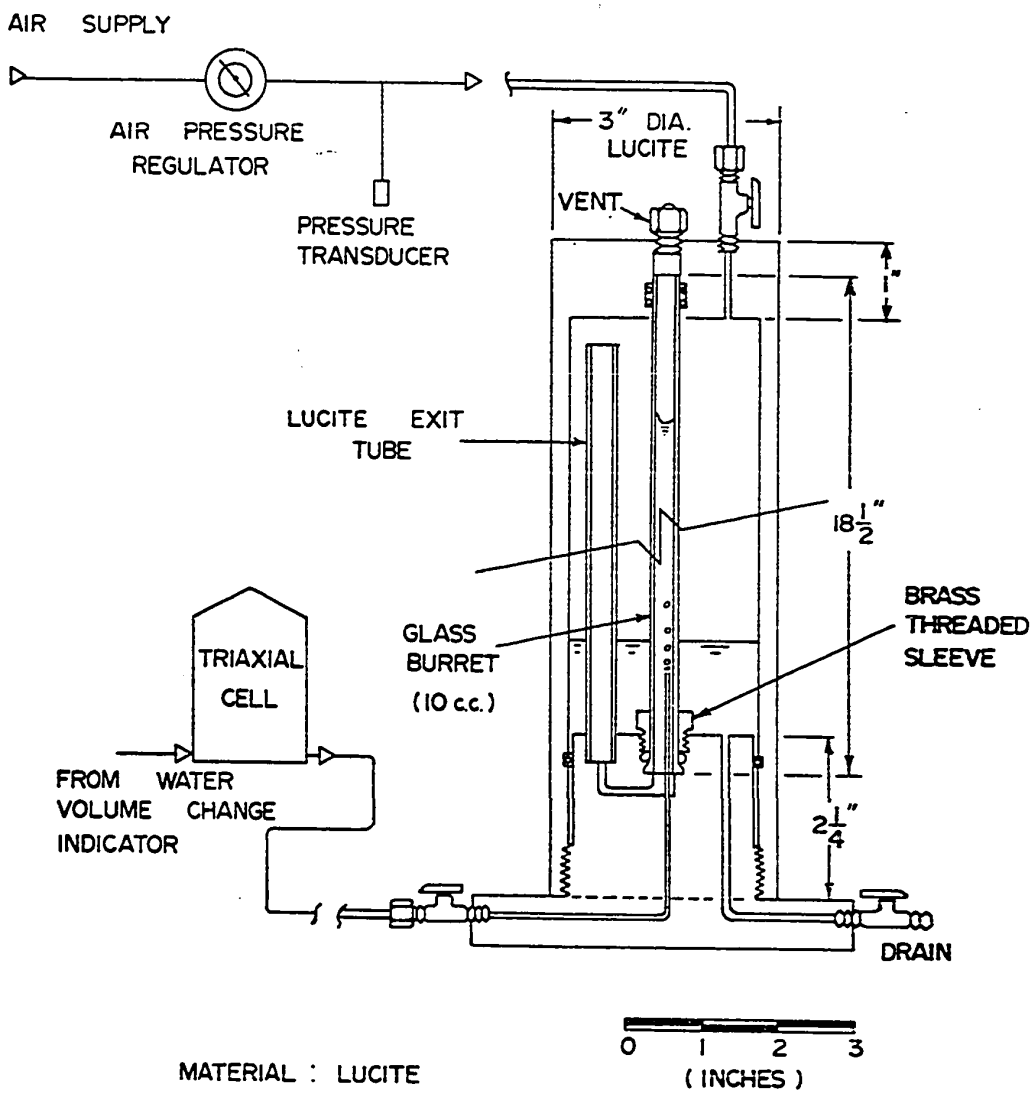


FIGURE 3.6 DIFFUSED AIR VOLUME INDICATOR

In either of the above cases, the volume occupied by the diffused air at the base of the ceramic disc is computed by applying Boyles law to the measured volume of diffused air. The test procedure is detailed in Internal Note SM:12 (Fredlund, 1972) and sample calculations are shown in Appendix D.

When the burret in the diffused air volume indicator becomes empty of water, the vent at the top is opened and the burret is filled. Initially there was some difficulty in getting the air bubbles to freely move up in the burret. This was overcome by filling the burret with the commercial cleaner called "FANTASTIK". Due to its low surface tension the air bubbles readily move up the burret.

The entire layout of the assembled modified Anteus apparatus is shown in Figure 3.7.

3.4.2 Triaxial Apparatus No. 1

In the first triaxial apparatus, isotropic volume change behavior was observed using a modified Wykeham Farrance triaxial cell. The design is similar to that of Bishop and Donald (1961). The main difference involves the method of measuring the volume of diffused air. Plate 3.3 shows the layout of Triaxial Apparatus No. 1.

1. Constant Pressure System

All pressures (i.e. total, air and water) were maintained constant by means of precise air pressure regulators. The cell and water pressures were maintained with the precision regulators from Anteus Corporation and the air pressure was maintained with a precise

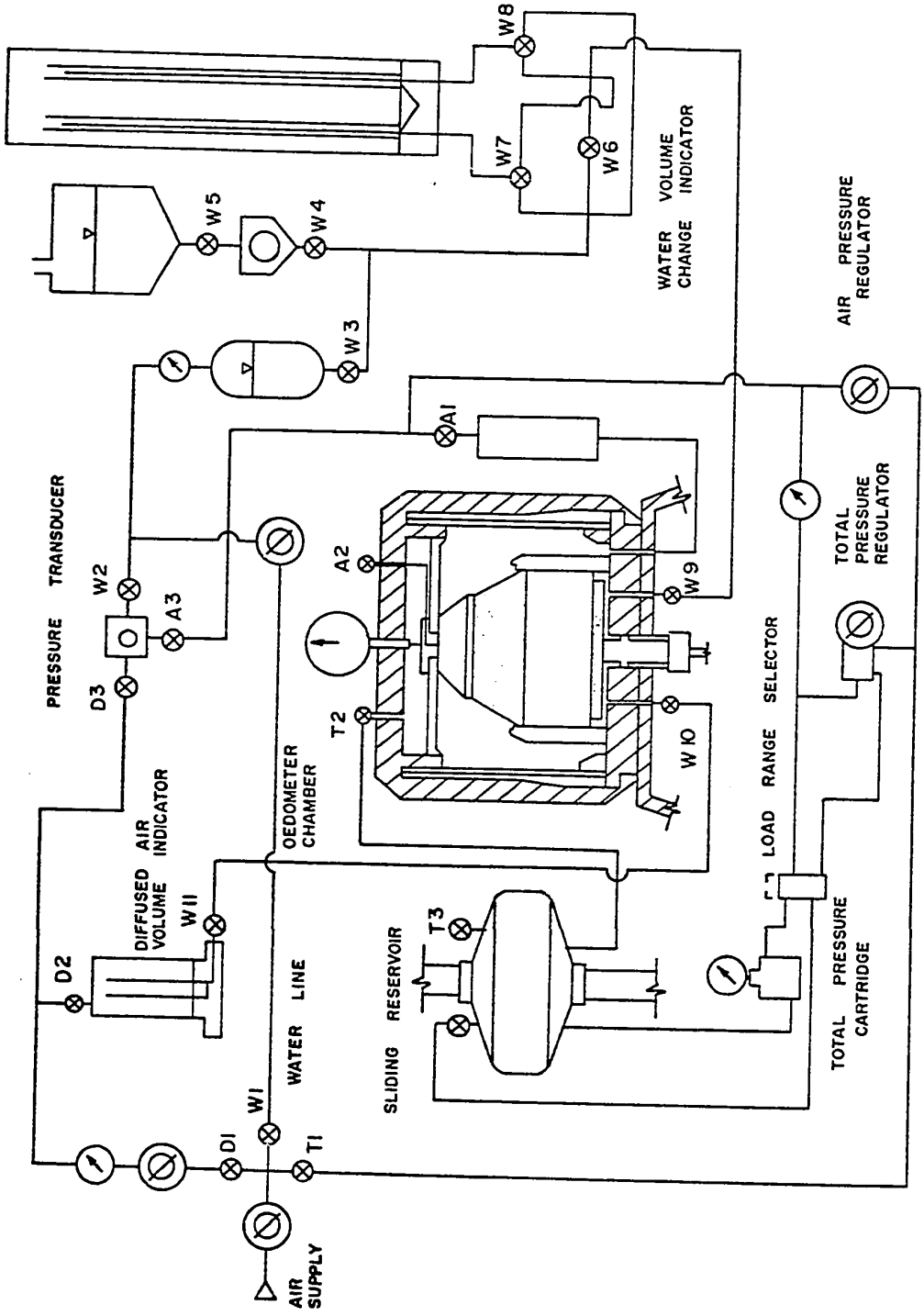


FIGURE 3.7 LAYOUT OF ENTIRE MODIFIED ANTEUS OEDOMETER

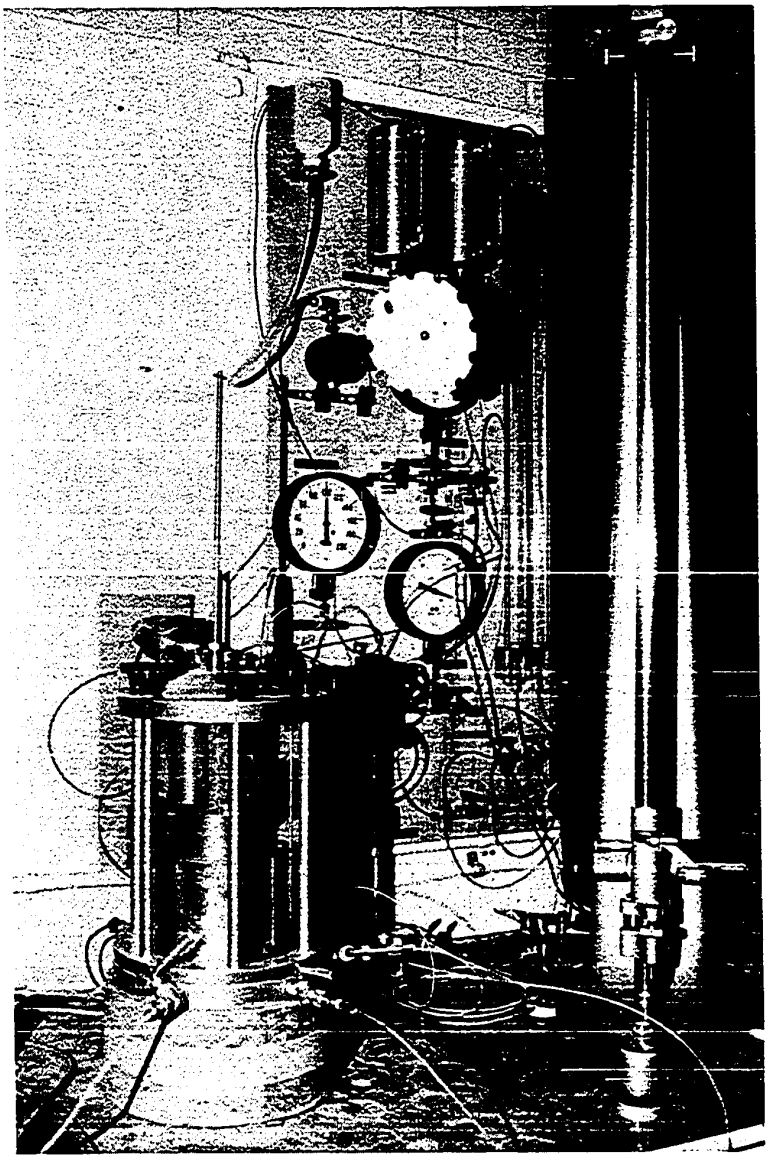


PLATE 3.3 LAYOUT OF TRIAXIAL APPARATUS NO. 1

Moore regulator.* All regulators were of the 0 to 100 psi range.

The regulator from Moore Instrument Co. is referred to as the Model (40-100) Nullmatic pressure regulator. It operates on a null balance principle that holds the output pressure within $\pm$ 0.09 psi, even for a wide range of input (supply) pressures. The Moore regulators are less expensive and were found to be easier to set at a constant pressure, than the Anteus regulators.

The first few triaxial tests were performed with the total and water pressures controlled by constant pressure mercury pots. These were changed to air pressure regulators and found to be more functional and just as accurate.

2. Design of the cell

An additional inner lucite cylinder was installed in the triaxial cell to lend stability for measuring the total volume change of the sample (Figure 3.8). An O-ring seal was provided at the bottom (on the side) of the cylinder as well as an O-ring cushion at the top. Mercury occupied the zone between the inner lucite cylinder and the soil sample. Fluctuations in the elevation of the mercury level allow for the independent measurement of the lateral and vertical displacements.

A four inch diameter stainless steel loading cap was placed on the soil sample. The air pressure was led from the base to the cap through a 1/8 inch stainless steel tube and connected to the top cap with a section of polyethylene tubing. A 1/8 inch thick, coarse, corundum stone acts as a low air entry disc below the top cap. The

---

*Obtained from Moore Instrument Co., Rexdale, Ontario.

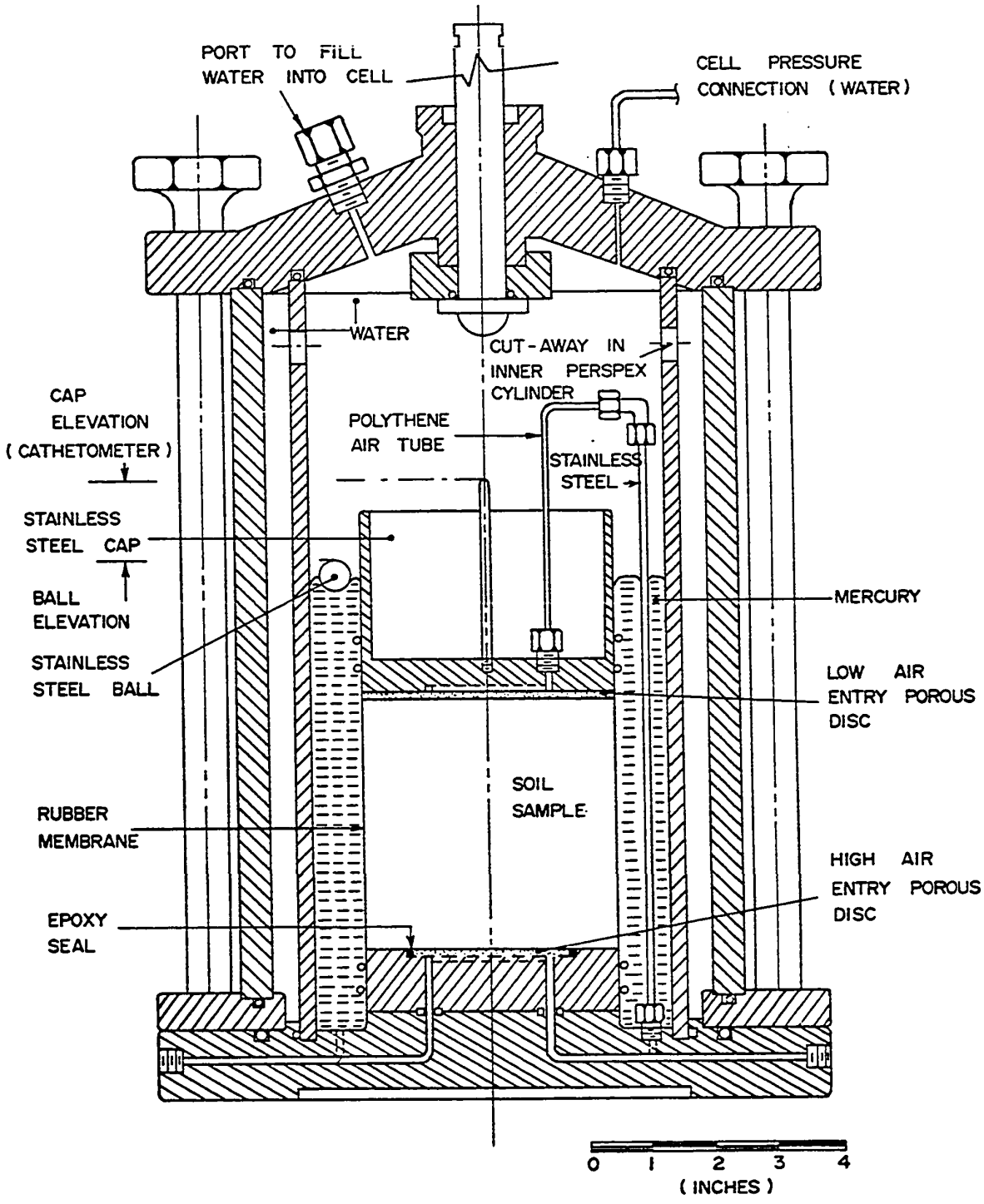


FIGURE 3.8 MODIFIED TRIAXIAL CELL NO. 1

The cell pressure was applied through a connection at the top of the cell.

Water fills the portion of the triaxial cell above the mercury. Since the cell was used only for isotropic loadings, the loading piston was allowed to rise to the top and form a seal (O-ring) against leakage. No oil was used in the cells.

The problems associated with handling large quantities of mercury for filling the cell were largely overcome by keeping the mercury in an enclosed container that was attached to the cell (Figure 3.9). By having the container in a position higher than the triaxial cell, mercury flowed from the container into the cell. To remove the mercury, the container was placed below the level of the triaxial cell and the valves were opened. In this way, much of the danger associated with handling mercury was eliminated. Also, the taking down and setting up of the sample was performed under an exhaust hood to remove mercury vapors.

3. Base Plate Design

Figure 3.10 shows the top view of the base plate. The base was modified to accept a 1/8 inch thick, 2-1/2 inch diameter, high entry disc. (Most tests were performed with a 15 bar disc). The success of the thin stone appears related, in part, to the rigid metal base and the good seating of the disc on the metal base. Circle Seal valves were substituted for the Klinger type valves whenever slow leaks were observed. A brass block was mounted directly on the side of the base to house a pore pressure transducer.

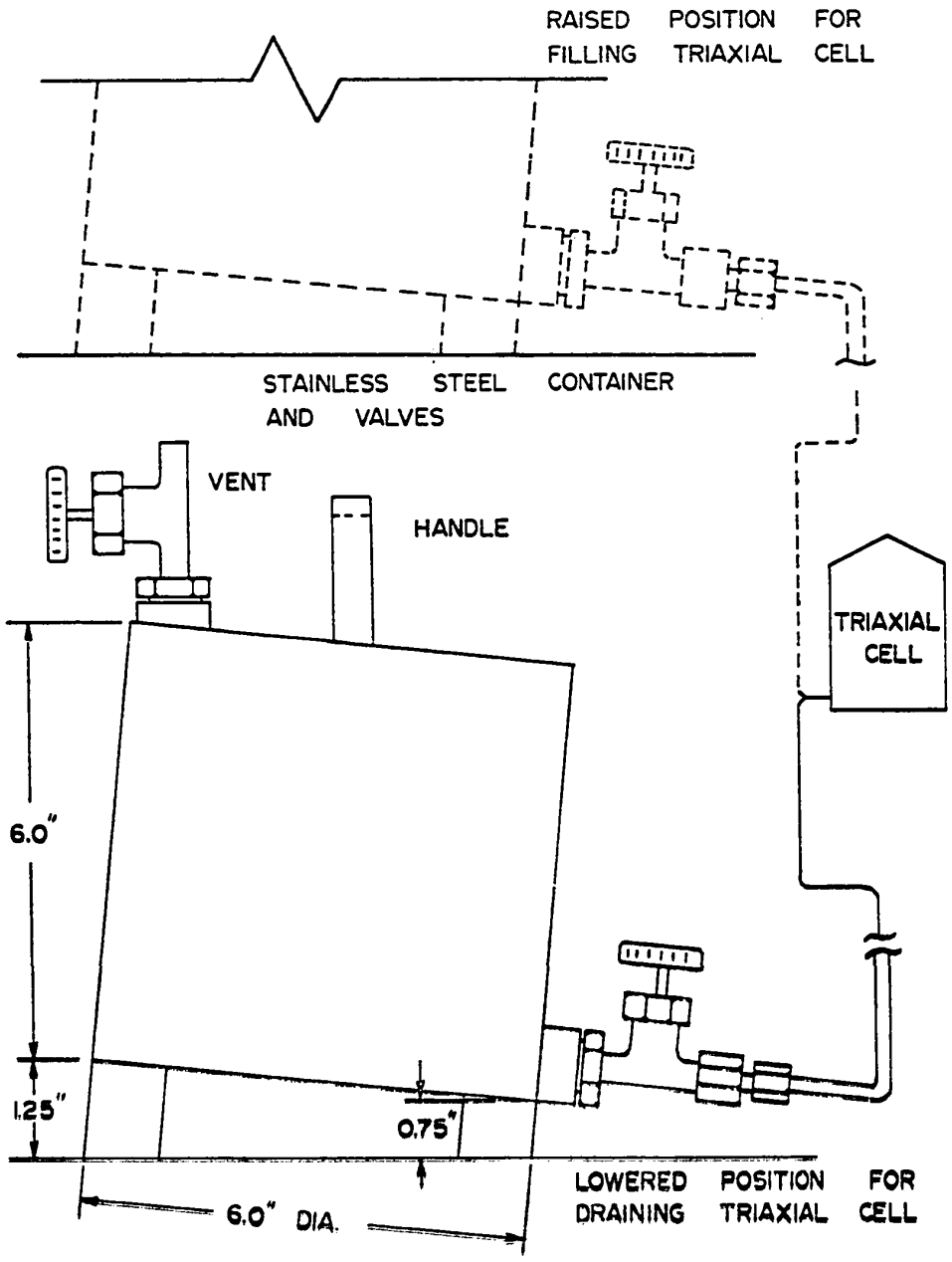


FIGURE 3.9 MERCURY CONTAINER FOR FILLING AND EMPTYING THE TRIAXIAL CELL

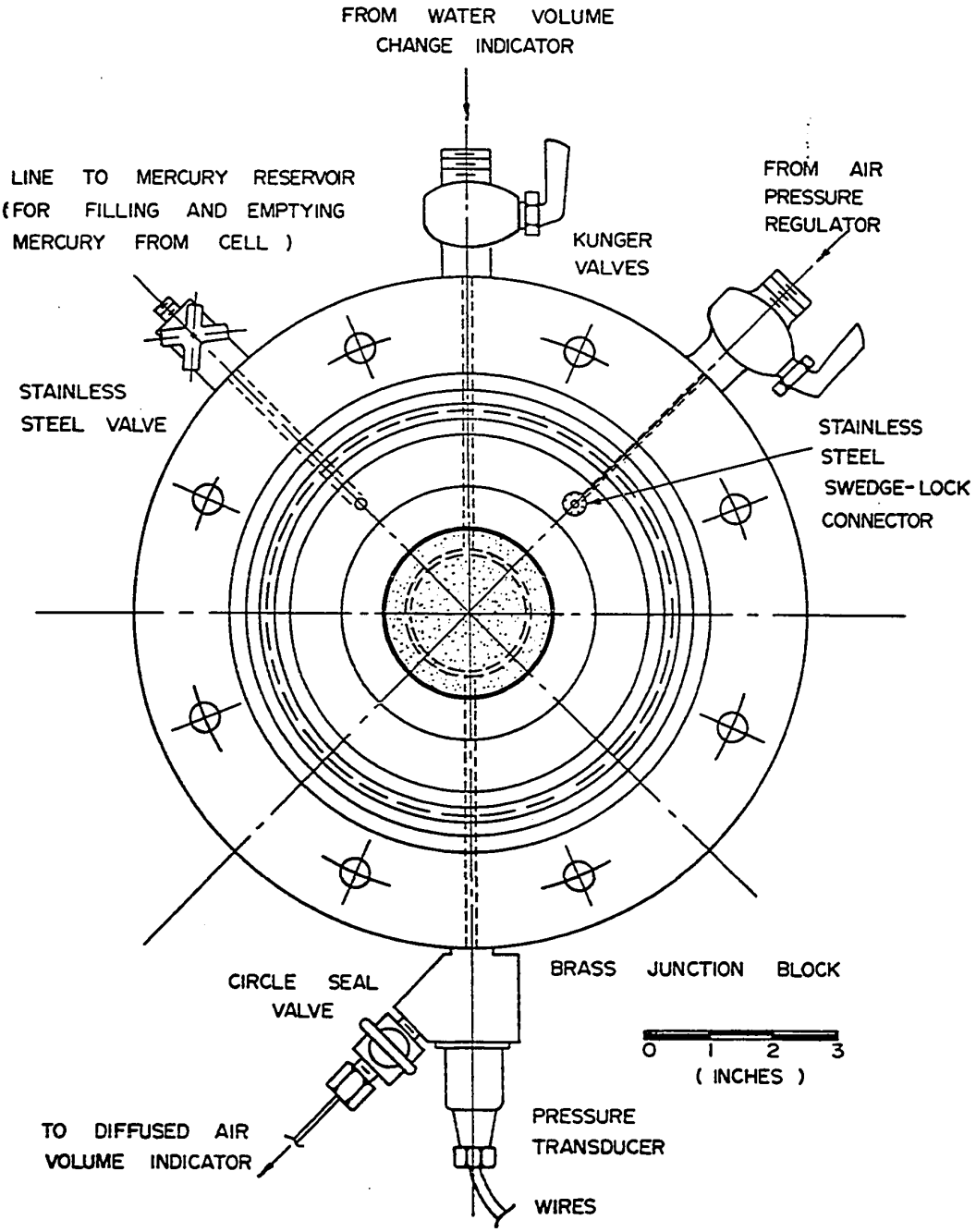


FIGURE 3.10 BASE PLATE FOR TRIAXIAL CELL NO. 1

The conventional cell pressure inlet was used to fill the inner part of the cell with mercury. The Klinger valve on this line was replaced with a stainless steel valve to prevent corrosion and leakage.

4. Layout of the Plumbing

A board of plumbing is required to support the operation of the triaxial cell (Figure 3.11). The total and water pressures are controlled through an air-water reservoir and the air pressure is regulated directly to the sample. The transducer switching junction allows for the measurement of these three pressures plus the pressure applied to the diffused air volume indicator.

5. Measurement of Pressures

The water pressure under undrained conditions is measured using the transducer mounted on the base of the cell. The total and water pressures, measured by the transducer on the board, are corrected for the elevation difference between the sample and the water reservoir. The range of both transducers is 0 to 100 psi and the digital voltmeter reads the pressure to within 0.04 psi.

6. Measurement of Total Volume Change

The total volume change of the soil sample is measured by recording changes in the elevation of the mercury level and the sample cap, by means of a cathetometer. A reference point near the base of the cell is used to correct for minute changes in the elevation of the cell or cathetometer.

The cathetometer is a model M-912 manufactured by Gaertner

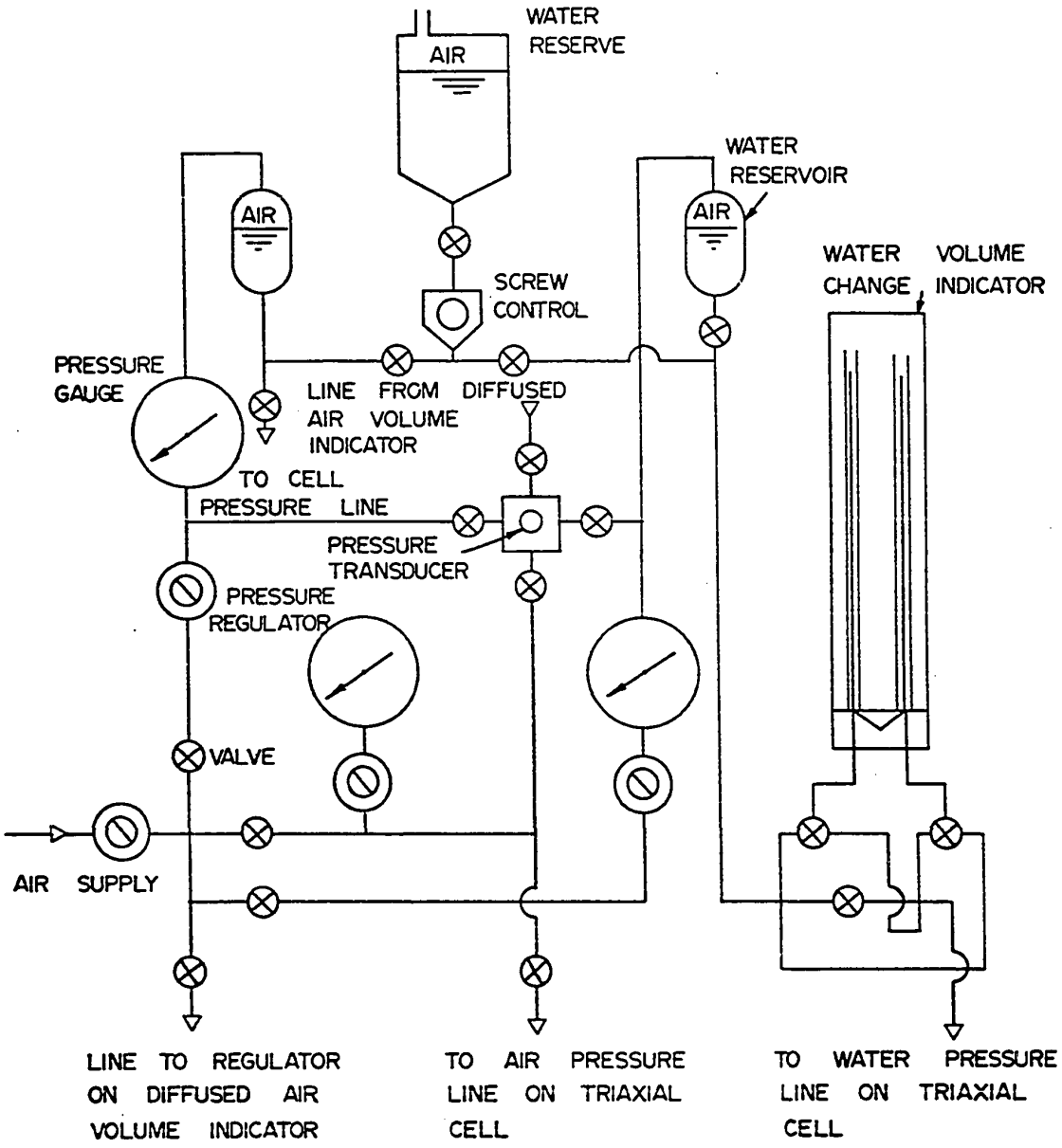


FIGURE 3.11 LAYOUT OF PLUMBING FOR TRIAXIAL APPARATUS NO. 1

Scientific Corporation, Chicago. The cathetometer consists of a telescope and carriage assembly mounted on a precise meter bar. The vernier permits readings to the 1/1000 of a centimeter. An auxilary magnifying lens allows the readings to be taken at a distance of 30 to 60 cm from the object under observation. The reproducibility of the readings is estimated to be within $\pm$ 0.001 cm. The factor for converting the vertical displacements of the ball to a volume change is 87.409 cc per vertical cm. Therefore, the volume change is reproducible to within approximately $\pm$ 0.09 cc. The vertical displacement of the cap has a conversion factor of 80.951 cc per vertical cm and a reproducibility of approximately $\pm$ 0.08 cc.

The temperature in the room was relatively constant, varying at most by $\pm$ 2°F. These fluctuations had an insignificant affect on the volume change readings.

Appendix D contains example calculations of the separation of vertical volume change and lateral volume change.

7. Measurement of Water Volume Change

The water leaving and entering the sample was measured on a double tube, double acting volume change indicator with a stroke capacity of 10 cubic centimeters. Whitey valves are used for shutting off and changing the direction of flow in the indicator. The water volume changes are recorded to the nearest 1/100 of a cubic centimeter.

Once again, the diffused air volume must be subtracted from the total water volume change.

8. Measurement of Diffused Air Volume Change

The diffused air volume was generally measured once a day by flushing water through the base plate and recovering the air bubbles in a 10 cc burret.

Figure 3.12 shows the entire Triaxial Apparatus No. 1 assemblage.

3.4.3 Triaxial Apparatus No. 2

A second triaxial cell accommodating 4-inch diameter samples was designed with the aim of overcoming some of the limitations inherent in the first triaxial design. First, it was highly desirable to avoid the use of mercury around the sample. If air pressures are being measured the mercury essentially eliminates the diffusion of air from the sample and allows for reasonable measurements. However, since the air phase is operated as a drained system, there is no reason why air cannot be allowed to diffuse through the membrane. The second major limitation of the previous equipment was the cumbersome means of measuring the total volume change (i.e. cathetometer). A more appealing system would incorporate linear voltage displacement transducers (i.e. LVDT's) connected to the data acquisition system. A general layout of the Triaxial Apparatus No. 2 is shown on Plate 3.4.

1. Constant Pressure System

The total, air and water pressures were maintained constant using Nullmatic Moore regulators.

2. Design of the Cell

Figure 3.13 shows a cross-section of Triaxial Cell No. 2.

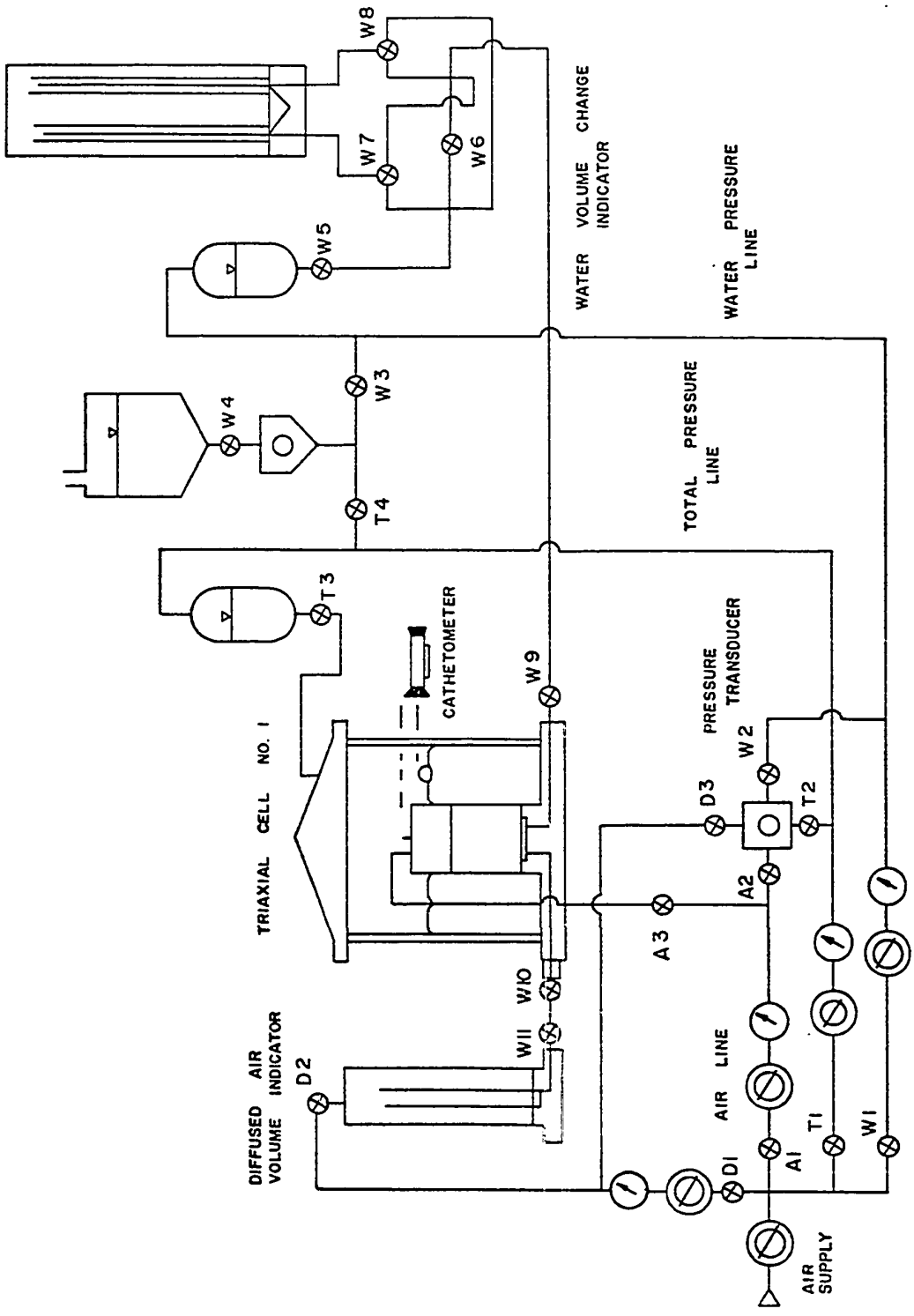


FIGURE 3.12 LAYOUT OF ENTIRE TRIAXIAL APPARATUS NO. 1

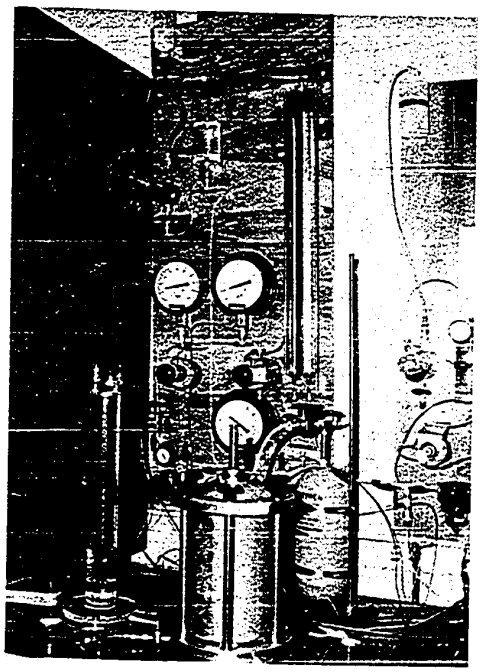


PLATE 3.4 a LAYOUT OF TRIAXIAL APPARATUS NO. 2

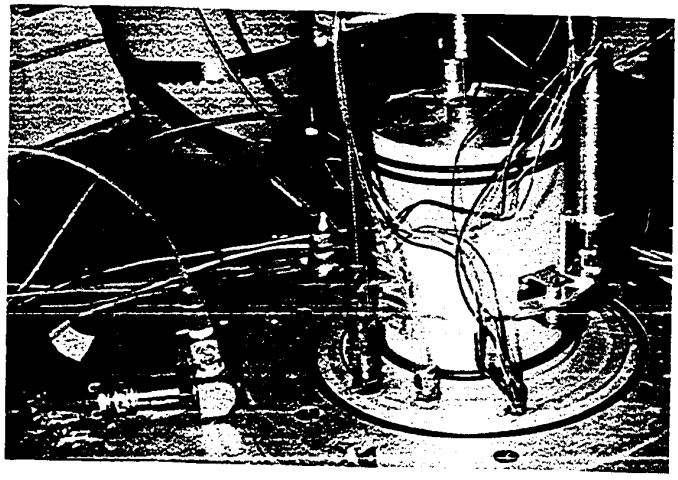


PLATE 3.4 b PIVOT ON LATERAL DISPLACEMENT INDICATOR

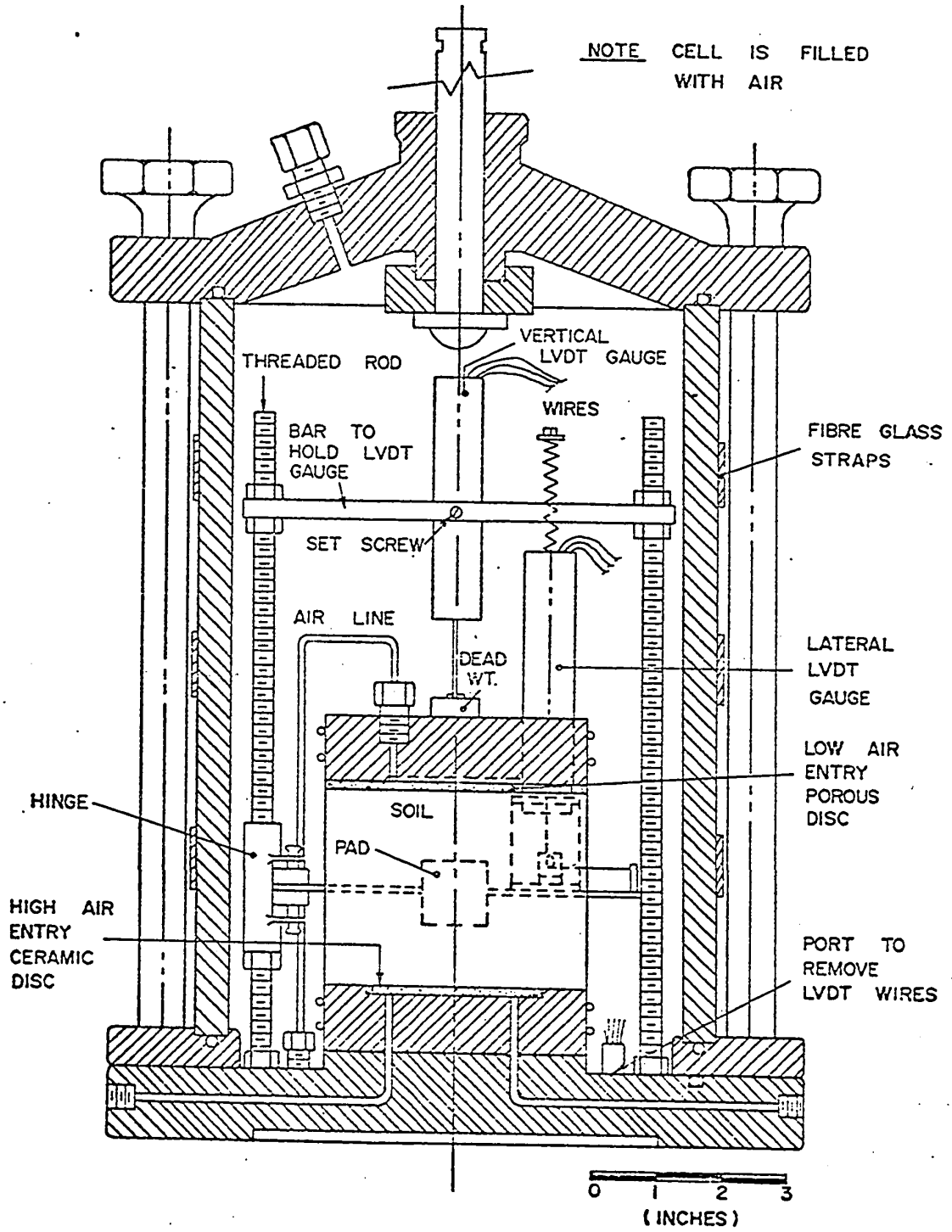


FIGURE. 3.13 MODIFIED TRIAXIAL CELL NO. 2

The lucite cylinder was reinforced with fibre glass stripes for added safety. This precaution is necessary since the cell is filled with compressed air.

Two threaded, 3/8 inch diameter rods are attached to the base and act as supports for the lateral and vertical displacement indicators. The wires from the LVDT gauges are taken through a port drilled in the base. An epoxy was used to seal around the wires to prevent air leakage.

The cell was designed in such a way that the soil sample could be completely assembled prior to attaching the upper part of the cell.

3. Base Plate Design

The base plate is essentially the same as for Triaxial Apparatus No. 1. The only differences involve the port for the LVDT wires, the cell pressure base port and the threaded LVDT support rods.

4. Layout of Plumbing

Only one air-water reservoir was required on the board since the cell pressure was a regulated air pressure (Figure 3.14). The remainder of the plumbing allows for the independent regulation and measurement of the total, air and water pressures.

5. Measurement of Pressures

The system of measuring the pressures is the same as that presented for Triaxial Apparatus No. 1.

6. Measurement of Total Volume Change

The LVDT with the plunger resting on the upper cap measures

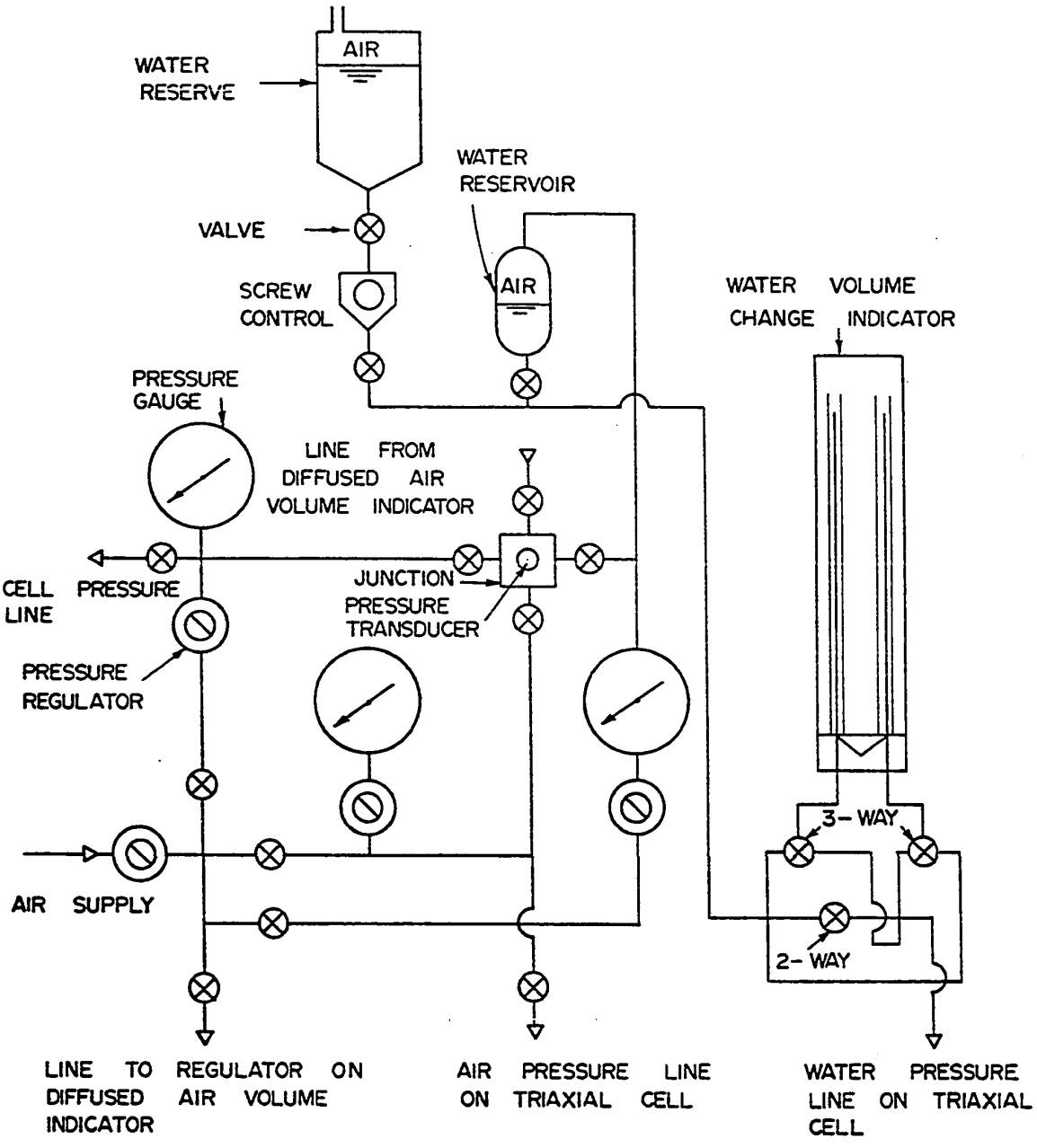


FIGURE 3.14 LAYOUT OF PLUMBING FOR TRIAXIAL APPARATUS NO. 2

the vertical displacement of the sample (Plate 3.5). The lateral displacement is measured by using an LVDT attached to a modified Ko lateral displacement indicator (Figure 3.15). The lateral displacement indicator is particularly satisfactory for relatively small amounts of lateral compression. For large amounts of compression, the LVDT interferes with the loading cap. However, most of our testing was associated with the swelling mode where this interference is not a problem. Large vertical displacements could tend to produce some distortion or twisting of the lateral indicator.

A special spring of proper stiffness was made to retract the plunger on the lateral LVDT. Fine nylon thread was first used from the plunger to the fastener on the opposite aluminum ring. Later, extremely fine piano wire was substituted for the nylon thread when it was discovered that the thread was susceptible to changes in relative humidity. A small aluminum bracket attached to the ring held the LVDT in place.

7. Measurement of Water Volume Change

The water volume change was measured in the same manner as described for Triaxial Apparatus No. 1.

8. Measurement of Diffused Air Volume

The measurement of the diffused air volume was the same as that described for Triaxial Apparatus No. 1.

Figure 3.16 shows the entire assembled layout of Triaxial Apparatus No. 2.

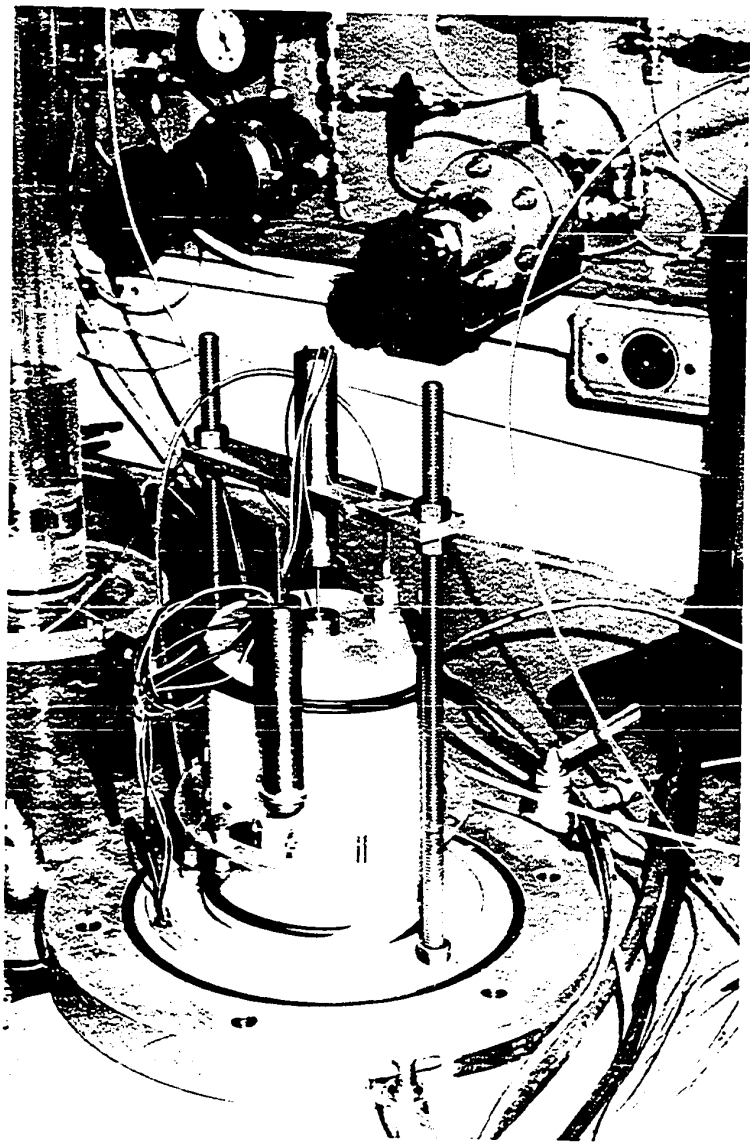


PLATE 3.5 TRIAXIAL APPARATUS BASE NO. 2 WITH SOIL SAMPLE

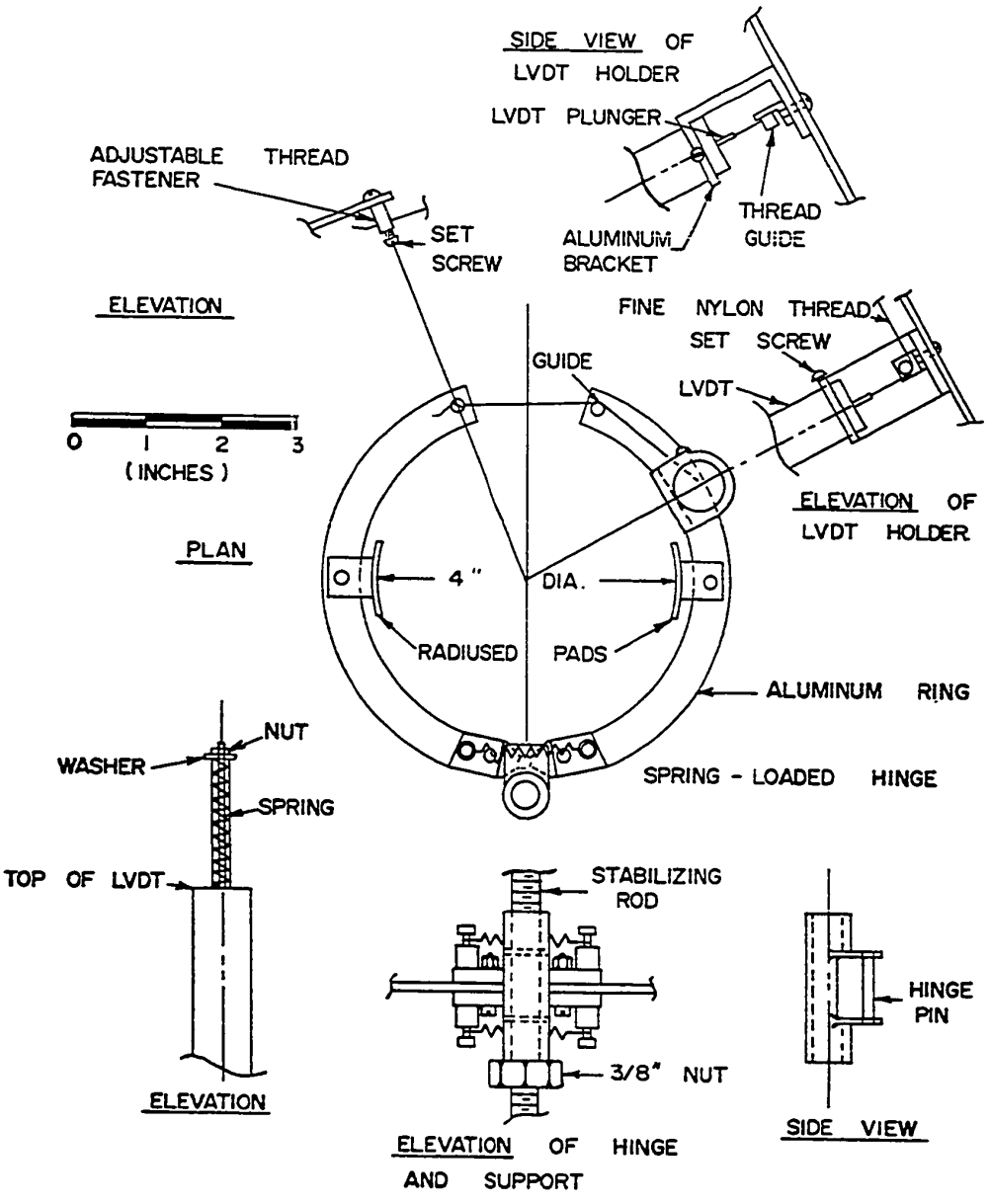


FIGURE 3.15 MODIFIED LATERAL DISPLACEMENT INDICATOR

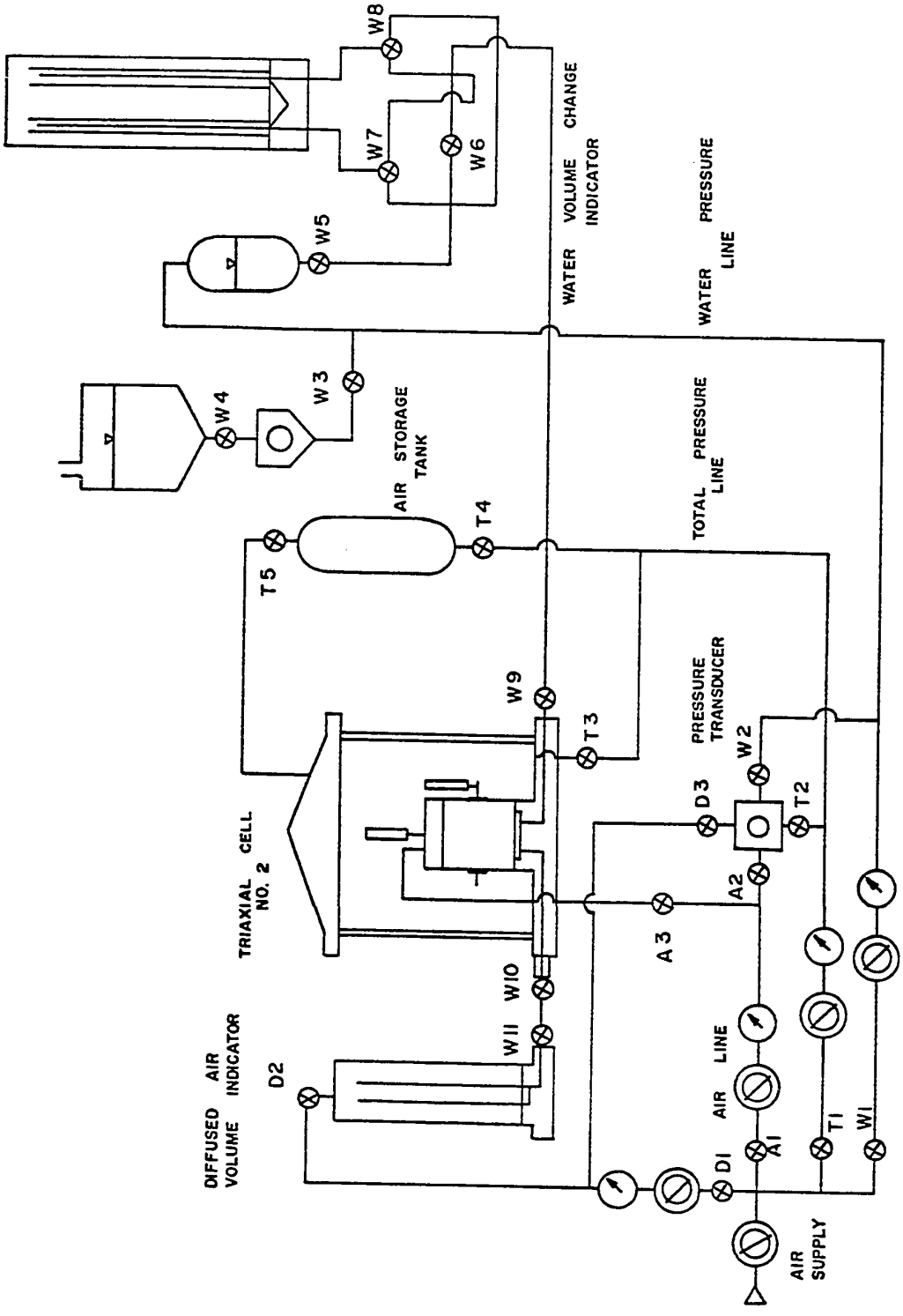


FIGURE 3.16 LAYOUT OF ENTIRE TRIAXIAL APPARATUS NO. 2

3.5 Preparation of Equipment

The text of the thesis contains a general outline of the types of soil tests that can be performed and the procedures that should be used to ensure that the equipment is functioning properly. The comments, in general, apply to all four pieces of equipment.

(a) Saturation of the High Air Entry Disc

The high air entry discs are saturated by first passing water through them and then by driving the air into solution. Once the discs have been saturated, they appear to remain saturated as long as they are kept in contact with moisture. However, a special effort must be taken to initially saturate new porous discs.

The procedure for ensure saturation is as follows: the consolidation ring is placed around the base plate and filled with about 1/2 inch of distilled, deaired water. The chamber (or cell) is put in place and the water is subjected to an air pressure of approximately 80 psi. Water is allowed to flow through the porous disc for approximately one hour.

The air collected below the porous disc is then flushed out and both valves on the base plate are closed. The water in and below the porous disc takes on a pressure equal to the applied air pressure. The pressure is applied for approximately one hour, during which time the air in the porous disc dissolves in the water. The valves at the base are again opened for approximately 10 minutes to allow the water in disc to seep through the disc. The air bubbles are flushed from below the porous disc and the chamber air pressure is reapplied. The

above procedure is repeated about six times after which the porous disc should be saturated. This procedure is similar to that used by Bishop and Henkel (1962).

The base plate must not be boiled in water since the differing thermal properties of the materials composing the base plate can result in a fine crack around the circumference of the high air entry disc. The disc was found to perform satisfactorily without the boiling technique.

(b) Permeability Test

The permeability of the porous disc can be measured during the saturation process by registering the deaired water seeping through the disc on the water volume change indicator. The coefficient of permeability is used to evaluate the compliance of the pore pressure measuring system. The results will also generally reveal the presence of cracks in the porous disc.

Although several porous discs have similar air entry values, their permeabilities may differ considerably. However, if the permeability of a particular disc is measured at one time, it should have a similar magnitude at a later date.

(c) Pore Pressure Response Test

With the water still above the high air entry disc (subjected to a pressure approximately 80 psi), both valves on the base plate are closed. The data acquisition system is allowed to continuously scan the transducer on the base plate, thereby recording the development of pressure. The time required for 100% response depends upon the permeability of the porous disc, the compressibility of the air-water

mixture in the compartment and the volume change of the compartment below the porous disc. Figure 3.17 shows a typical response curve. The theory associated with the response test is derived in detail in Appendix E. The test gives an indication of the time required for pore pressure equilization.

(d) System Leaks

Leaks in the water volume change measuring portion of the system must be essentially eliminated. This requires a lengthy investigation but can be achieved by taking the following steps.

(i) First, be assured that the water volume change indicator itself does not have leaks. The three way valves must be checked in both directions, always reading the burret opposite the direction the valves point.

To check the water volume change indicators, a back pressure of approximately 50 psi is placed on the water volume change indicator and readings are taken every few hours for about 2 days. Then the valves are reversed and the check repeated. Volume changes should not be more than a few hundredths of a cubic centimeter in two days. Continuous volume change in one direction is indicative of a slow leak.

(ii) The right and left Circle Seal valves on the base plate can be checked for leaks by connecting the water volume change indicator line to each valve. The back pressure on the volume change indicator should be low (approxi-

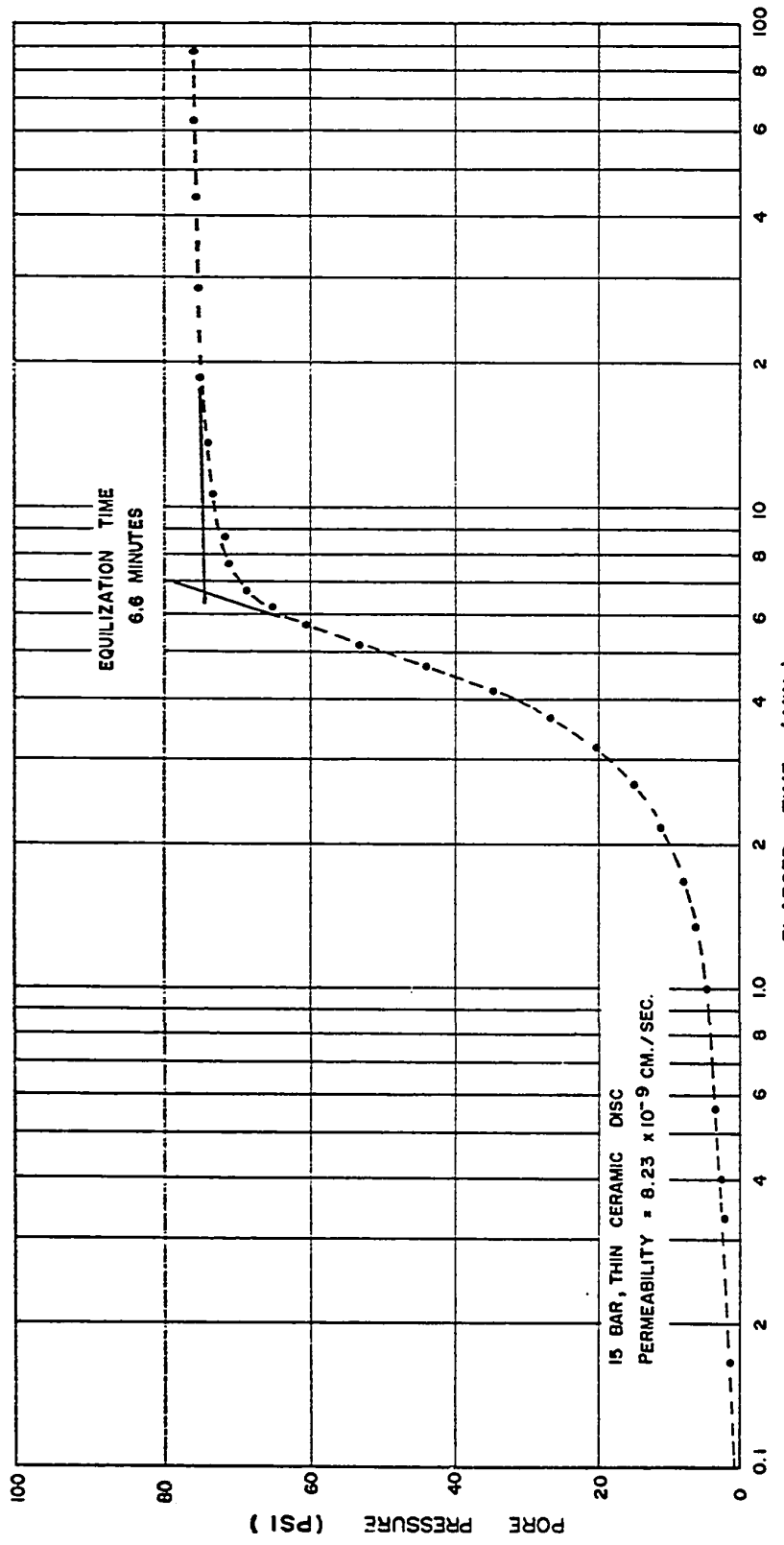


FIGURE 3.17 PORE WATER PRESSURE RESPONSE ON ANTEUS OEDOMETER # 179 (OCT. 30, 1971)

mately 10 psi) while the water pressure below the high air entry disc should be maintained high (i.e. approximately 80 psi) by applying an air pressure to the water above the porous disc. Any leakage through the closed valves is registered on the water volume change indicator. Each valve should be checked for at least one day.

(e) Air Entry Value Check

Almost all the water is removed from the top of the high air entry disc and the air pressure is allowed to act directly on the disc. Various pressure increments are applied and allowed to remain for at least two hours. It is not necessary to check on the actual air entry value of the disc. Rather, the test should assure that the disc can withstand air pressures greater than those that will be used during a test. For example, several of the discs with an air entry value of 225 psi (15 bar) were checked in 20 psi increments up to 100 psi. (The equipment is designed to measure suctions up to 110 psi).

The highest pressure applied to the porous disc should remain for at least one day. The water volume change indicator should show a slow movement of diffused air out of the base plate. However, if the base is periodically flushed and the diffused air measured, its volume should be essentially equal to that registered on the water volume change indicator.

A rapid increase in the amount of air collecting below the base means that either there is a leak in the high air entry disc or a leak past the O-rings sealing off the base plate. However, a properly

designed O-ring seal rarely allows leakage.

Continuous close checks must be kept on the entire water volume change portion of the apparatus. Slow leaks over the long duration of a test can essentially invalidate the results. The proposed checks are not meant to be performed only when the equipment is built but rather, any suspicious test results should be sufficient cause to launch a thorough investigation. The entire checking of the equipment may require 1-1/2 weeks. Improvements in the design of the base plate and water volume change portion of the equipment should reduce the necessity of excessive checking.

3.6 Tests Procedures and Data Reduction

A general outline of the test procedures is given in the body of the thesis while the details of operating the equipment are presented in Internal Note SM:12 (Fredlund, 1972). The methods of performing the calculations and evaluating the compressibilities of the system are outlined in Appendices D and B, respectively.

The test procedures can be subdivided into two broad categories. The first category involves pressure component changes with the fluid phases of the soil responding in a drained mode. In the second category, pressure component changes are applied while one or more of the fluid phases of the sample respond in an undrained mode.

(a) Drained Processes

In general, any one or more pressure components (i.e. total, air or water pressure) can be changed and the volumetric changes monitored.

For example, the total pressure can be increased while the total volume and water volume changes are measured. The air volume at any time, is computed.

The three basic combinations involve the increase or decrease in either the total, air or water pressures. In each case, the change in total volume and water volume are measured. The processes of most practical interest are those involving a change in the total or pore water pressures since the air pressure is generally a constant in nature.

(b) Undrained Processes (Reaction Tests)

In general, one or more of the pressure components can be changed, and one or more of the fluid phases operated in an undrained mode. The total volume changes can be monitored. For example, the total pressure can be increased while the air pressure is kept constant and the reaction of the water phase is measured. On the equipment used in this thesis, the pore water reaction could be measured for a change in the total and/or air pressures.

The test procedures are not standaridized but rather, are flexible and subject to change. For this reason, a general type of data sheet was designed. Any possible drained or undrained process previously mentioned, can be performed while the data is recorded on the same data sheet. The data is later keypunched and then reduced on the computer. A complete documentation of the computer program is given in Appendix D.

CHAPTER IV

STRESS STATE VARIABLES

4.1 General

The analysis of the behavior of multiphase systems cannot proceed without first establishing the state variables. The effective stress statement of Terzaghi (1936) provided the stress state variable necessary to describe the behavior of the soil structure of a saturated soil. Once the stress state variables of a multiphase system are known, the analysis proceeds within the context of continuum mechanics.

Continuing research has endeavored to establish an effective stress for unsaturated soils. Chapter IV commences with a review of the research literature. It first considers the assertions of the effective stress statement for saturated soils. Then the literature on unsaturated soil behavior is reviewed with respect to the thought progression in this area. After the literature review, a theoretical method is proposed for establishing the stress state variables in a multiphase system. It is presented in detail since it is the key to understanding unsaturated soil behavior. The results of the theoretical analysis are then experimentally verified.

4.2 Effective Stress Concept for Saturated Soils

In 1936, Terzaghi stated the effective stress concept as follows:

"The stresses in any point of a section through a mass of soil can be computed from the total principal stresses σ_1, σ_2, σ_3 which act in this point. If the voids of the soil are filled with water under a stress u, the total principal stresses consist of two parts. One part, u, acts in the water and in the solid in every direction with equal intensity. It is called the neutral (or the porewater pressure). The balance $\sigma_1' = \sigma_1 - u$, $\sigma_2' = \sigma_2 - u$ and $\sigma_3' = \sigma_3 - u$ represents an excess over the neutral stress u and it has its seat exclusively in the solid phase of the soil.

This fraction of the total principal stresses will be called the effective principal stresses..... A change in the neutral stress u produces practically no volume change and has practically no influence on the stress conditions for failure..... Porous materials (such as sand, clay and concrete) react to a change of u as if they were incompressible and as if their internal friction were equal to zero. All the measurable effects of a change of stress, such as compression, distortion and a change of shearing resistance are exclusively due to changes in the effective stresses σ_1', σ_2', and σ_3'. Hence every investigation of the stability of a saturated body of soil requires the knowledge of both the total and the neutral stresses."

Terzaghi's statement asserts that all mechanical aspects of a saturated soil are governed by the difference between the total and pore water pressures. From a physical standpoint it refers to the equilibrium of the soil structure of a saturated soil but says nothing of a constitutive nature. Terzaghi's statement on effective

stress is consistent with the definition of a stress state variable as used in continuum mechanics. The validity of the effective stress variable for saturated soil behavior, has been verified experimentally (Rendulic, 1936; Bishop and Eldin, 1950; Laughton, 1955).

Bishop and Eldin (1950) suggested treating the mechanisms of volume change and shear strength separately with respect to effective stress. They suggest that the volume change of a soil in compression is independent of the contact area between soil particles but that the shear strength will depend upon the contact area. Skempton (1961) reinforced Bishop and Eldin's statements, indicating that two different expressions were required to predict the behavior of saturated porous materials with respect to shear strength and volume change. For shear strength

$$\sigma' = \sigma - \left(1 - \frac{a \cdot \tan\psi}{\tan\phi}\right) \cdot u_w \qquad 4.1$$

where σ' = effective stress

σ = total stress

a = area of contact

ψ = angle of intrinsic friction

ϕ' = angle of shearing resistance

u_w = pore water pressure

For volume change,

$$\sigma' = \sigma - (1 - \frac{C^p}{C^s}) \cdot u_w \qquad 4.2$$

where C^p = compressibility of the soil particles

C^s = compressibility of the soil structure

The equation is theoretically justified by equating the forces across a statistical plane passing between particle contacts. Skempton (1960) presents excellent experimental data to substantiate the form of the effective stress equation for compressibility. Nur and Byerlee (1971) performed compressibility tests on rocks over a wide range of pressures and conclude that Skempton's equation "is exact and can be considered a fundamental law for strain in elastic systems...".

Let us, however, more closely examine the mode of testing and the type of analysis performed by Skempton (1960) and Nur and Byerlee (1971) to justify their conclusions. They conducted the experimental verification of their effective stress equation by employing a constitutive equation. In this way, their stress state variable is extracted from a constitutive equation. The general form of their constitutive equation is,

$$\frac{\Delta V}{V} = C^s \cdot \Delta\sigma' \qquad 4.3$$

where C^s = bulk compressibility of the soil structure

$\Delta\sigma'$ = change in effective stress

The form of this equation is such that it assumes that only one stress state variable controls volume change and that the volume change is due to the compressibility of the soil structure. However, a study of the continuity requirement shows that when the particles are compressible, there are two sources of volume change in a particulate system (Chapter V). These are the volume change due to the rolling and sliding of the particles (reflected as a volume change of the soil structure) and the compression of the particles (reflected as a volume change of the soil particles). Therefore, the continuity requirement must be written,

$$\frac{\Delta V}{V} = \frac{\Delta V^s}{V} + \frac{\Delta V^p}{V} \qquad 4.4$$

where ΔV^s = change in volume of the soil structure

ΔV^p = change in volume of the soil particles

Let us assume that the compression of the soil structure is controlled by the difference between the total and water pressures (i.e. $\sigma - u_w$) and that the compression of the soil particles is controlled by the all around pressure (i.e. u_w). Writing the continuity requirement as a constitutive equation gives,

$$\frac{\Delta V}{V} = C^s \cdot (\Delta\sigma - \Delta u_w) + C^p \cdot \Delta u_w \qquad 4.5$$

The equation indicates that there are two independent stress

state variables involved in the behavior of a compressible particulate medium (i.e. $(\sigma-u_w)$ and u_w). Dividing the above equation by the compressibility of the soil structure reveals an equation of Skempton's form. The author agrees with the constitutive equation; however, it does not follow that one effective stress state variable can be extracted from the constitutive equation. The character of Skempton's equation is different from that proposed by Terzaghi. Since the effective stress equation now incorporates soil properties, it must be viewed as a constitutive relationship. The same criticism can be levied against Skempton's proposed effective stress equation controlling strength behavior.

In 1962, Jennings and Burland gave their interpretation of effective stress in the "form of two propositions.

(i) All measurable effects of a change of stress, such as compression, distortion and a change of shearing resistance of a soil are exclusively due to changes in effective stress.

(ii) The effective stress, σ', is defined as the excess of the total applied stress over the pore pressure, u."

These propositions are completely consistent with Terzaghi's presentation and allow the effective stress to be viewed as a stress state variable.

Bishop and Blight (1963) reviewed Skempton's treatment of volume change and shear strength and gave their statement of effective stress. "..... the effective stress is, by definition, that function of total stress and pore pressure which controls the mechanical effects

of a change in stress, such as volume change and a change in shear strength. The principle of effective stress is the assertion that such a function exists, with determinant factors under a given set of conditions." They conclude that the principle of effective stress can be applied to saturated soils, only if account is taken of the effective stress path. Their definition has a subtle difference from Terzaghi's original statement. The incorporation of the word, "function" in two places significantly changes the interpretation of effective stress. In the first case of its usage, the word "functions" indicates that there can be the incorporation of soil parameters. This makes the effective stress statement a constitutive relationship. In the second case of its usage, the word "function" is associated with the interpretation of the word "principle" which they relate to defining volume change and shear strength. However, if the effective stress variable is associated with the equilibrium of the soil element, then it has no relationship with stress paths.

Matyas and Radhakrishna (1968) in their elaboration on effective stress state,

"(i) the changes in volume and shear strength of a soil element caused by a change in its stress state are entirely due to the change in effective stresses, in other words, shear strength and void ratio are unique functions of effective stresses,

(ii) the effective stress which is responsible for the mechanical effects in a soil element is uniquely determined by the total stress and pore pressure."

In their first statement, the first and the last parts of their statement need not be consistent. In other words, a change in effective stress can be the cause of a change in volume or shear strength but it need not necessarily be linked by a "unique function". The words "unique function" refer to a constitutive relationship.

The research literature appears to reveal a progressive deviation from Terzaghi's original concept of effective stress. Originally Terzaghi proposed that the difference between the total and pore pressure was a stress variable that governed all deviations from equilibrium conditions.

4.3 Literature Review on Stress Variables Controlling Unsaturated Soil Behavior

The Roads Research Laboratory under the direction of Croney, Coleman et al was probably the first group to recognize the importance of soil moisture deficiencies in relation to road and air field design. Croney (1952) defined soil suction as the reduction of the water pressure below atmospheric in an unloaded sample in the laboratory. The suction was modified by an alpha (α) factor to take into account the effect of external loading.

Alternatives or modifications to Terzaghi's effective stress equation for saturated soils were apparently not suggested prior to 1955. Bishop (1959) delivered a lecture in Oslo, Norway in 1955 in which he introduced what he termed a "tentative" effective stress expression for unsaturated soils.

$$\sigma' = \sigma - u_a + \chi(u_a - u_w) \qquad 4.6$$

where u_a = pore air pressure

u_w = pore water pressure

χ = a parameter having values between zero and one.

The lecture was published in 1959 in a Norwegian journal, but it was not until 1960 that the information was available in English or American publications (Bishop et al, 1960; Bishop, 1960).

The concept of effective stress for saturated soils was tested in the range of negative pore water pressures by Donald (1956). In 1956, Hilf published his studies on the pore fluid state of stress in compacted soils. During his research work he developed the "axis-translation technique" to measure suction values greater than one atmosphere. The technique involves elevating the atmospheric (or surrounding) air pressure in order that the water pressure can be measured as a positive value.

Croney, Coleman and Black (1958) summarized their findings at the Road Research Laboratory and presented another modified effective stress equation.

$$\sigma' = \sigma - \beta' \cdot u_w \qquad 4.7$$

where β' = the holding or bonding factor which is a measure of the number of bonds under tension effective in contributing to the shear strength of the soil.

In 1960, Bishop, Alpan, Blight and Donald restated Bishop's equation and attempted to prove its validity by comparing the results of triaxial tests performed on saturated and unsaturated samples. Aitchison (1960) proposed another modified effective stress equation

$$\sigma' = \sigma + \psi p'' \qquad 4.5$$

where p'' = pore water pressure deficiency

ψ = parameter with values of zero to one

Jennings also proposed a new effective stress equation in 1960.

$$\sigma' = \sigma + \beta p'' \qquad 4.6$$

where p'' = pore water pressure

β = a statistical factor of the same type as the contact area and it is proposed that it should be measured experimentally in each case

The gaseous phase was assumed to be at atmospheric pressure. Jennings' proposed effective stress equation was the fourth such equation. However, all the equations are equivalent when the pore air pressure is atmospheric. Under these conditions, $\chi = \beta' = \psi = \beta$. The conference on Pore Pressures and Suction in 1960 provided a meeting place for the comparison of the various proposed effective stress equations for un-

saturated soils. There appeared, in general, to be good agreement on the acceptability of Bishop's form of the effective stress equation. All research workers operated on the premise that only one stress variable was necessary to describe the behavior of unsaturated soils. All the proposed equations attempted to modify Terzaghi's effective stress equation in such a way as to encompass unsaturated soils. The effective stress concept was thought of as an independent physical law rather than a stress variable associated with the equilibrium of the soil structure.

In 1961, Bishop and Donald published the results of a strength test on an unsaturated silt sample in which the total, air and water pressures were independently controlled. All pressures (i.e. σ_3, u_a and u_w) were varied in such a way that all differences remained constant. The stress-strain curve was not altered during these changes and therefore, the effective stress was assumed to remain constant. Skempton (1961) states that these results "experimentally verified" Bishop's effective stress equation for unsaturated soils.

Jennings and Burland (1962) were apparently the first research workers to seriously question the validity of Bishop's equation. They felt that Bishop's equation did not uniquely define the relationship between void ratio and effective stress for most soils below a critical degree of saturation. For silts and sands, the critical degree of saturation was estimated at 20 percent and as high as 85 to 90 percent for clays. Jennings and Burland (1962) as well as Coleman (1962) state that the first step in the analysis of triaxial tests on

unsaturated soils is to reduce the stresses with the pore air pressure as the base. The axial stress is therefore σ_1-u_a, the lateral stress is σ_3-u_a and the pore water stress becomes u_w-u_a. Coleman goes on to use these relative pressures as independent stress variables describing volumetric deformation.

In 1963, Bishop and Blight re-evaluated the effective stress equation for unsaturated soils. They noted that variations in the suction term caused problems because it did not result in a direct change in effective stress. This was attributed to the fact that the surface tension in the pore water acted over only a part of the surface area of the soil particles. They noted that the paths of each of the two components (i.e. $(\sigma-u_a)$ and (u_a-u_w)) must be considered in stress-volume change predictions. They felt that shear strength was less sensitive to the stress path.

Blight (1965) pointed out that the χ parameter was dependent on the type of process to which the soil was subjected and observed the collapse phenomenon as constituting a limitation to the effective stress principle. Burland (1965) further questioned Bishop's effective stress equation. He separated the forces on the soil particle in terms of internally applied water stresses and externally applied loads. The water stress always acts isotropically whereas the externally applied loads produce shear. He explained the collapse phenomenon in terms of shear due to a decrease in the normal stress (i.e. suction).

The Review Panel for the soil mechanics symposium, "Moisture Equilibria and Moisture Changes in Soils" (Aitchison, 1965), adopted

the subdivision of soil suction and the definitions quoted by the International Society of Soil Science. The definitions state that total suction is equal to the sum of the matric and osmotic suction. These are defined as follows:

1. Matric suction is the negative gauge pressure relative to the external gas pressure on the soil water, to which a solution identical in composition with the soil water must be subjected in order to be in equilibrium through a porous permeable wall with the soil water.

2. The osmotic suction is the negative gauge pressure to which a pool of pure water must be subjected in order to be in equilibrium through a semi-permeable (i.e. permeable to water molecules only) membrane with a pool containing a solution identical in composition with the soil water.

The acceptance of these definitions is not completely consistent with the views expressed on matric suction at the Pore Pressure and Suction in Soils Conference in 1961. At the 1961 conference it was agreed that the air pressure was an internal pore air pressure. However, the 1965 definition states that the matric suction is the water pressure relative to the "external" air pressure. This subtle difference significantly changes the interpretation of matric suction. For example, let us consider a saturated soil subjected to a high external air pressure in a pressure plate apparatus. The pore water is at atmospheric pressure conditions and drains until equilibrium is reached. According to the 1961 definition, the matric suction does not exist since there is no internal air pressure. Rather, the

soil has a negative water pressure. According to the 1965 definitions, the matric suction is the difference between the external positive air pressure and the atmospheric water pressure. Throughout this thesis, the author adopts the thinking associated with the definitions presented in 1961. Therefore, as a soil approaches 100 percent saturation the difference between the internal air and water pressures approaches zero. The reason for adopting the 1961 definition becomes more obvious when we examine the types of volume change caused by a change in each stress component.

Richards (1966) felt that solute suction played an important role in the physical behavior of unsaturated soils and postulated a further effective stress equation.

$$\sigma' = \sigma - u_a + \chi_m(h_m+u_a) + \chi_s(h_s+u_a) \qquad 4.10$$

where χ_m = effective stress parameter for matric suction

h_m = matric suction

χ_s = effective stress parameter for solute suction

h_s = solute suction

He does not present data to substantiate the equation.

In 1967 Aitchison expressed serious misgivings with regard to the separate rigorous evaluation of the χ parameter and soil suction. He pointed out the complexity of χ was such that a specific value may only relate to a single combination of (σ) and (u_a-u_w) and a particular

stress path. His thinking appears to mark a new direction in the consideration of unsaturated soils. A direct quote of his reasoning states "Its individuality (i.e. χ) in relation to the other components of the equation mean one thing only - that the effective stress law is no longer valid as a law, but is merely a statement of principles. In practice, this involves a second conclusion - that each parameter of effective stress (σ) and (u_a-u_w), must be treated separately and made to follow the correct stress path if the correct value of χ (which may not be known) is to function within a statement as in ($\sigma' = \sigma - u_a + \chi(u_a-u_w)$). Or, to put the point another way: because of the complexity of the χ term we may be forced to accept the fact that we can only achieve a proper value of effective stress in the soil if we allow a unique stress path for each of the terms (σ) and (u_a-u_w); having achieved it by this means, we in fact no longer need to attempt to quantify the χ term. Thus the complexity of the χ term ceases to signify as soon as we uncouple the two parameters in unsaturated soils." In 1969 Aitchison presented constitutive relationships data consistent with the above concepts. The tests were performed on a conventional but modified oedometer that allowed the control of the air (chamber) pressure.

Matyas and Radhakrishna (1968) introduced the concept of "state parameters" to express functional relationships between stress and deformation. Volume change behavior is displayed as a three-dimensional surface with respect to the state parameters (σ-u_a) and (u_a-u_w). The movement of a "state point" along a "state path" produces

a "state surface". They noted there were non-unique aspects of the state surface related to stress history. They recommended the use of an incremental strain theory for the analysis of problems due to the complexity of the surface.

Barden, Madedor and Sides (1969) advocated the separate control of the components $(\sigma-u_a)$ and (u_a-u_w) when predicting volume change in unsaturated soils. They used a modified Rowe consolidometer to obtain constitutive relationship data.

In review of these investigations in the area of soil mechanics, it appears that the stress state variables used for analysis have been justified either on the basis of intuition or on the basis of observed monotonic deformation behaviors. No experimentation has been produced to directly justify the use of a particular stress tensor prior to becoming involved with the physical or constitutive properties of the soil. In fact, the mixing of soil properties with stress state variables does not appear consistent with the method of attack used in continuum mechanics. The two most worthwhile contributions toward establishing satisfactory stress state variables appear to be the work of Hilf (1956) and, Bishop and Donald (1961). These are discussed later in more detail.

4.4 Stress Analysis of a Continuum

The analysis of stress basically involves defining the stresses at a point (i.e. stress tensor) and the equilibrium of stress from one point to another. The equilibrium of the stress field is based on

Newton's force equilibrium equation. In this thesis, force equilibrium is assumed to be the most fundamental physical statement available. The analysis strictly applies to any continuum. In continuum mechanics, the equilibrium equations are commonly referred to as Euler's law. The definition of the body and surface stresses at a point are defined as the Euler-Cauchy stress principle (Truesdell, 1966a).

Let us first consider the definition of a continuum and its inherent assumptions. Fung (1969) states that "a continuum material is a material for which the density of mass, momentum and energy exist in the mathematical sense". The material is pictured as being without gaps or empty spaces and its behavior obeys the classical laws of mechanics and thermodynamics which relate to the properties at a point.

All matter is structured on an elementary particle system and taken to a small enough scale, no matter is strictly continuous. The size of the "holes" varies from a solid to a liquid to a gas. Let the mass of an element of variable size be M_n and the corresponding volume be V_n. If we continuously decrease the size of the element, the ratio of M_n/V_n should tend to a definite limit providing the volume contains a large number of particles. In a mathematical sense, we have defined a continuum. This abstraction applied to a large collection of material particles sets the stage for the description of these particles in space and time.

The analysis of a particulate system could be considered on an interparticle (i.e. fine structure) basis; however, then particle physics or statistical mechanics must be employed. The limited degree

of success in their application in civil engineering discourages their consideration. Intuitively it appears advantageous to investigate particulate system behavior from a macroscopic, phenomenological standpoint. The macroscopic approach can generally be verified experimentally (Frederick and Chang, 1965).

Discontinuities constitute the greatest limitation to the consideration of a material as a continuum. However, even in these cases it generally produces the most practical analysis. Often the discontinuities merely dictate the size of element we must consider. For example, a particulate system is viewed as a system filled with discontinuities if the element under consideration is very small. On the other hand, if the element under consideration contains many particles, the particulate system can be viewed as a continuum.

It is the concept of a continuous medium that permits us to define the stresses at a point (Malvern, 1969). Considering an element of area on an imaginary, rigid internal plane of a continuum, the assumption is made that as the element of area tends to zero, the ratio of the force divided by the area tends to a definite limit. The limiting vector

$$T^{\nu} = \frac{dF}{ds} \qquad 4.11$$

is called the stress vector or traction. Advancing this concept from one to three perpendicular surfaces merging at a point, results in three stress vectors (i.e. $T_x^{\nu}, T_y^{\nu}, T_z^{\nu}$). Resolving the stress vectors

into components perpendicular and parallel to the surface gives nine stress vectors or the stress tensor at a point (Figure 4.1). The stress tensor,

$$\begin{bmatrix} \sigma_x & \tau_{yx} & \tau_{zx} \\ \tau_{xy} & \sigma_y & \tau_{zy} \\ \tau_{xz} & \tau_{yz} & \sigma_z \end{bmatrix}$$

applies to any continuous medium, regardless of its physical properties (i.e. elastic or plastic, viscous or non viscous liquids). In its general form, it is independent of the nature of the continuum. Some materials, however, have properties such that certain components tend to zero. Solids have all nine components whereas in non viscous fluids, the shear components vanish. The non viscous fluids have an isotropic stress tensor which is equally applicable for incompressible and compressible states.

The stresses in a continuum vary from point to point in a stressed body. Considered on an elemental basis, (extending between stress points) we can relate the space derivatives of the various components of stress. The equilibrium of the space derivatives is governed by Newton's laws of statics and dynamics (Figure 4.2). Summing the forces in the x-direction gives

$$\left[\sigma_x + \frac{\partial \sigma_x}{\partial x}\, dx\right]dydz - \sigma_x dydz + \left[\tau_{yx} + \frac{\partial \tau_{yx}}{\partial y}\, dy\right] dxdz$$

$$- \tau_{yx} dxdz + \left[\tau_{zx} + \frac{\partial \tau_{zx}}{\partial z}\, dz\right] dxdy + F_x dxdydz = 0 \qquad 4.12$$

where F_x = body force in x-direction

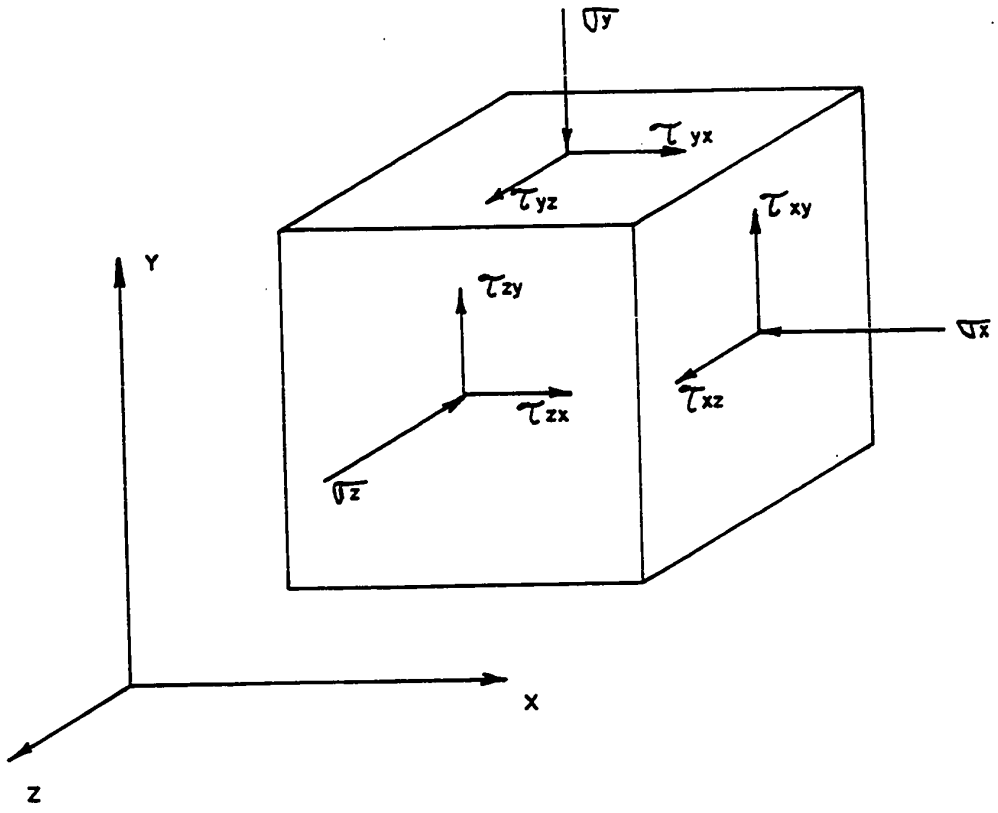


FIGURE 4.1 THREE – DIMENSIONAL STRESS COMPONENTS AT A POINT IN SPACE

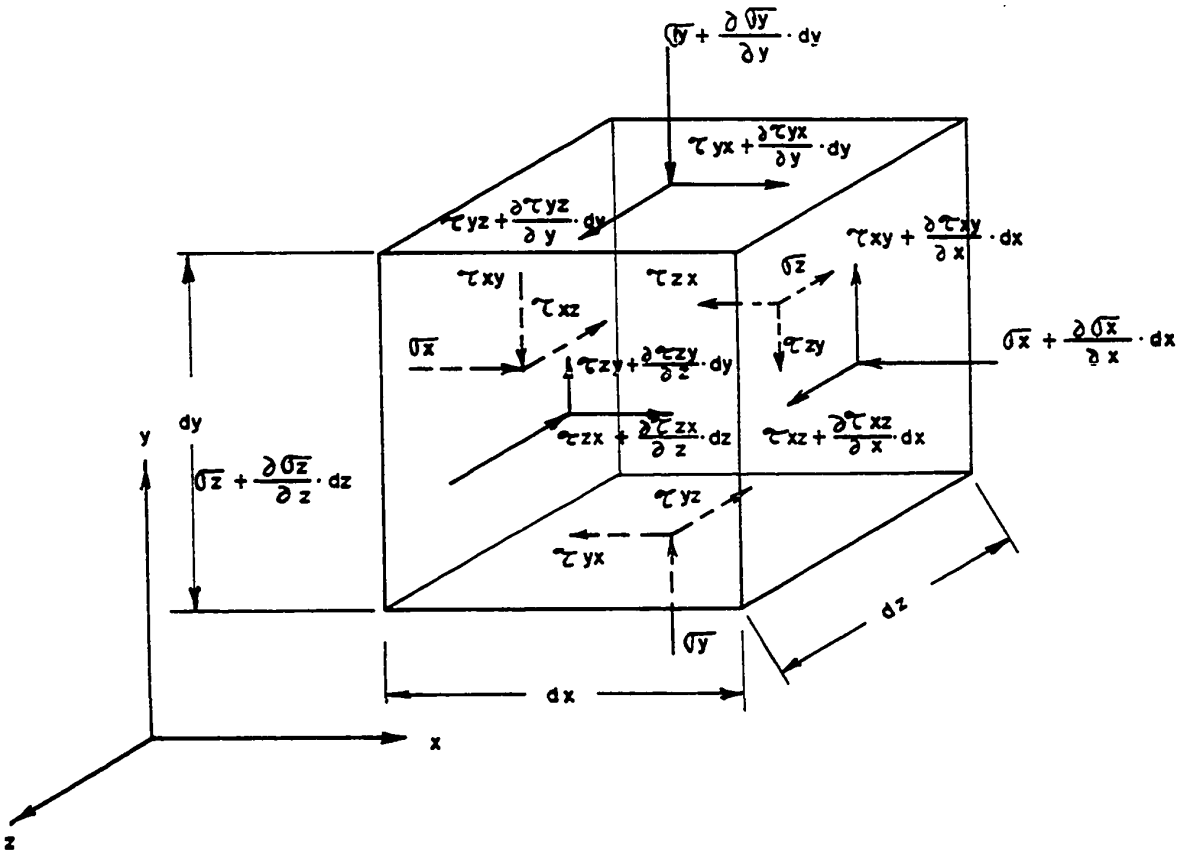


FIGURE 4.2 EQUILIBRIUM STRESS FIELDS ACROSS AN ELEMENT

The right hand side of the equation is zero if the element is not undergoing acceleration. Reducing the above equation gives

$$\frac{\partial \sigma_x}{\partial x} + \frac{\partial \tau_{yx}}{\partial y} + \frac{\partial \tau_{zx}}{\partial z} + F_x = 0 \qquad 4.13$$

The equilibrium equation for the y and z directions can be written by cyclic permutation of the coordinates. The differential equations of equilibrium apply to any material that qualifies as a continuum. The equations assume that the stress components and their first derivatives are continuous. It should also be noted that the equilibrium equations are linear.

4.5 The Element of a Multiphase System

In the field of soil mechanics, the choice of a proper element of soil has deviated from that of classical continuum mechanics. The element should be a cube, completely enclosed by imaginary, rigid boundaries or diaphrams (Fung, 1969). Biot (1955) and Hubbert and Rubey (1959) recognized the importance of the imaginary form of the element when considering the equilibrium of a multiphase system. However, most research workers in the area of soil mechanics (Scott, 1963; Harr, 1966; and Wu, 1966) consider statical equilibrium across a wavey cross-section or plane passed through the soil mass. The area of contact between the particles becomes small and they imply that this is necessary to justify the use of the effective stress equation. Lambe and Whitman (1969) state, "One imagines a "wavey"

plane which is warped just enough so that it passes through mineral matter only at points of contact between particles". "The summation of all the contact areas will be a very small portion of the total area of the plane, certainly less than one percent."

When analysing a multiphase system in accordance with continuum mechanics, it is sometimes necessary to compare the porosity of the mass with respect to volume, and the porosity with respect to the area of a plane. Using the conventional soil mechanics designation for the surface passing through a soil always gives area porosity approaching 100 percent. On the other hand, the volume porosity may be only a fraction of this value.

Consider the area porosity on an imaginary, unbiased plane through a soil mass.

$$n_a = \frac{A_p}{A} \qquad 4.14$$

where A_p = portion of the plane passing through solids

A = the area of the plane

The area of the plane is large compared with the particle size. If the soil is homogeneous, the surface area porosity is constant from a statistical standpoint. Integrating the imaginary plane in the normal direction gives the volumetric porosity

$$n_v = \frac{\int A_p \cdot dz}{\int A \cdot dz} = \frac{A_p \cdot z}{A \cdot z} = n_a \qquad 4.15$$

The volumetric porosity is therefore equal to the area porosity. Likewise, the line porosity is equal to the area porosity. In the Russian literature, (Faizullaev, 1969) this concept is referred to as the "theorem of the equality of volume and surface porosities in a homogeneously porous medium". This concept is later shown to be of importance in taking into account the volume and surface forces when deriving the equations of motion.

The concept of a wavey plane through the soil particle contacts has also been assumed for unsaturated soils (Lambe and Whitman, 1969). Skempton (1960) and, Bishop and Blight (1963) use statics across a wavey plane to justify Bishop's effective stress equation for unsaturated soils.

The use of a wavey plane through a soil mass constitutes a special type of free body diagram. It is a free body diagram for which the spatial variations go to zero. For example, if the stress at the base of an element is σ_y, then the stress at the top of the element is generally written as $\sigma_y + \partial\sigma_y/\partial y \cdot dy$. If the element reduces to a plane, dy, goes to zero and we can no longer write an equilibrium equation that incorporates variations in space.

The common effective stress formulations are based on placing equivalent force systems on opposite sides of a plane. This is actually an "equivalence" formulation. In continuum mechanics, an equivalence equation takes one stress distribution system and substitutes another equivalent stress distribution in its place (Truesdell, 1966b). For example, in a concrete beam, a triangular stress distribution may be

substituted for a highly complicated stress distribution. This equivalency technique is justified as Saint-Venant's principle in the theory of elasticity (Chou and Pagano, 1967).

The wavey plane formulation is inconsistent with the equilibrium considerations in continuum mechanics and unnecessary for defining stress state variables for a multiphase system. It is the author's conviction that the wavey plane concept leads to misconceptions.

Before leaving the discussion on a multiphase element, let us define the density terms associated with such an element. The concept of a "reduced" unit weight for each phase is introduced in order to consider each phase as a continuum. Let us designate the porosity of each phase of an N-phase system as n_n. Consider a fluid with a specific or true unit weight, γ_n, flowing through a porous medium. The "reduced" unit weight is defined as the uniform distribution of the true mass over the whole volume, assuming the absence of the porous medium.

$$\rho_n = n_n \cdot \gamma_n \qquad 4.16$$

where ρ_n = reduced unit weight of the n-th phase.

In the case of water flowing through a soil we can write,

$$\rho_w = n_w \cdot \gamma_w \qquad \text{and}$$

$$\rho_s = n_s \cdot \gamma_s \qquad 4.17$$

where ρ_w = reduced unit weight of water

ρ_s = reduced unit weight of solids

n_w = porosity with respect to the water phase

n_s = porosity with respect to the solids

γ_w = true unit weight of water

γ_s = true unit weight of the soil solids

By definition, the sum of the porosity terms always equals one.

$$n_1 + n_2 + n_3 + \ldots\ldots + n_N = 1 \qquad 4.18$$

By virtue of the relationship between reduced and true unit weights, we can write,

$$\frac{\gamma_1}{\rho_1} + \frac{\gamma_2}{\rho_2} + \frac{\gamma_3}{\rho_3} + \ldots\ldots + \frac{\gamma_N}{\rho_N} = 1 \qquad 4.19$$

4.6 Theoretical Approach to Multiphase Systems

The continuum theory of mixtures has developed into a complex, mathematical formulation. Truesdell and Toupin (1960) developed a dynamical theory of flow relative to each other in a two or more phase continua. They postulate equations of mass, momentum, moment of momentum and energy balance for each constituent. However, Green and Naghdi (1965) show that they have a number of conceptual difficulties in the thermodynamic aspects. They then re-formulate the problem in terms of an energy equation and an entropy inequality and "systematically

apply invariance conditions arising from consideration of superimposed rigid body motions of the whole continuum." In this thesis we are primarily interested in the force equilibrium as presented in continuum mechanics.

In the area of fluid multiphase behavior, the mixture of two or more fluids is either considered as a single-phase, Newtonian or ideal fluid with averaged parameters or as individual fluids with individual properties (Streeter, 1961 and Faizullaev, 1969). The individual phase concept is a newer approach which takes into consideration the relative phase velocities. Each phase is considered as a continuum. Due to the assemblage of an unsaturated soil, the individual, continuous phase approach is appealing.

Scott (1969) mentions that much of the research work in continuum mechanics has not found its way into the soil mechanics literature. Schiffman (1970) references the above continuum mechanics literature in his evaluation of the stress components of a porous medium. In the case of an unsaturated soil, his analysis derives one stress state variable controlling behavior. It is of the form of Bishop's effective stress equation and is based on statical equilibrium across a plane passed through a soil mass.

The approach adopted in this thesis for the equilibrium of a multiphase system is consistent with that used by Green and Naghdi (1965), Truesdell (1966a) and Faizullaev (1969). Basically, the approach assumes that the stress fields of a multiphase system are coincident and that the stress field of one phase can be superimposed upon

the stress field of another phase. As long as the equilibrium equations contain only linear operations, the principle of superposition is applicable. The principle of superposition is generally considered in terms of displacements; however, it is equally true of stresses as demonstrated by Westergaard (1952).

Let us now derive a general theory of equilibrium for multiphase systems. Consider the force systems acting on an element of volume, dx, dy and dz. The sum of the surface forces on the n-th phase acting, for example, on the dy dz plane, is

$$\frac{\partial(\bar{p}_{nx}\ dy\ dz)\cdot dx}{\partial x} \qquad 4.20$$

where $\bar{p}_{nx}$ = the resultant stress vector associated with the n-th phase, acting over the entire area, dydz (i.e. the area is perpendicular to the x-axis).

In the y and z directions, respectively,

$$\frac{\partial(\bar{p}_{ny}\ dxdz)\cdot dy}{\partial y} \quad \text{and}$$

$$\frac{\partial(\bar{p}_{nz}\ dxdy)\cdot dz}{\partial z} \qquad 4.21$$

In addition to the surface tractions associated with each phase, there are interaction forces. In the case of fluids, the interaction forces acting on the n-th phase by the remaining phases has two

components. First, there is the drag forces associated with the relative velocities of the mediums.

$$F_n' = \sum_{j=1}^{N} K_{jn} (\overline{V}_j - \overline{V}_n) \qquad 4.22$$

where $\overline{V}_n$ = velocity vector of the n-th phase

$\overline{V}_j$ = velocity vector of the j-th phase

K_{jn} = interaction coefficient of the n-th and the j-th phases.

Second, there are forces associated with the cross-section variability of the tube through which flow is occurring. This is sometimes referred to as the diffusor effect. The projection of this force onto the coordinate axes gives

$$p\ dydz \cdot \frac{\partial n_n}{\partial x} \cdot dx$$

$$p\ dxdz \cdot \frac{\partial n_n}{\partial y} \cdot dy \qquad \text{and}$$

$$p\ dxdy \cdot \frac{\partial n_n}{\partial z} \cdot dz \qquad 4.23$$

where p = the fluid pressure acting within the element

n_n = the porosity of the n-th phase .

Defined on the basis of the total volume of the element, the diffusor effect forces are,

$$F''_{nx} = p \cdot \frac{\partial n_n}{\partial x}$$

$$F''_{ny} = p \cdot \frac{\partial n_n}{\partial y} \qquad \text{and}$$

$$F''_{nz} = p \cdot \frac{\partial n_n}{\partial z} \qquad 4.24$$

In the event of an interaction between two solid phases, a further drag or friction force could be added to the body forces already described. There is also a gravity body force which corresponds to the reduced unit weight in the y-direction. In general, the gravity body force is written,

$$F'''_n = f_n \cdot \rho_n \qquad 4.25$$

where f_n = unit gravity body force with components, x_n, y_n and z_n.

When the gravity body force is projected onto the coordinate axes, its components are,

$$F'''_{nx} = x_n \cdot \rho_n$$

$$F'''_{ny} = y_n \cdot \rho_n \qquad \text{and}$$

$$F'''_{nz} = z_n \cdot \rho_n \qquad 4.26$$

The general equation of motion for the n-th phase of the medium is now written

$$\frac{\partial \bar{p}_{nx}}{\partial x} + \frac{\partial \bar{p}_{ny}}{\partial y} + \frac{\partial \bar{p}_{nz}}{\partial z} + F_n' + F_n'' + F_n''' = M_n \cdot \frac{d\bar{v}_n}{dt} \qquad 4.27$$

where M_n = mass of the n-th phase

$\frac{d\bar{v}_n}{dt}$ = acceleration of the n-th phase.

When the general motion equation is resolved onto the coordinate axes, we obtain,

$$\frac{\partial p_{nxx}}{\partial x} + \frac{\partial p_{nyx}}{\partial y} + \frac{\partial p_{nzx}}{\partial z} + \sum_{j=1}^{N} K_{jn}(u_j - u_n) + p \cdot \frac{n_n}{x} + x_n \cdot \rho_n = M_n \frac{du_n}{dt} \qquad 4.28$$

$$\frac{\partial p_{nxy}}{\partial x} + \frac{\partial p_{nyy}}{\partial y} + \frac{\partial p_{nzy}}{\partial z} + \sum_{j=1}^{N} K_{jn}(v_j - v_n) + p \cdot \frac{\partial n_n}{\partial y} + y_n \cdot \rho_n = M_n \cdot \frac{dv_n}{dt} \qquad 4.29$$

$$\frac{\partial p_{nxz}}{\partial x} + \frac{\partial p_{nyz}}{\partial y} + \frac{\partial p_{nzz}}{\partial z} + \sum_{j=1}^{N} K_{jn}(w_j - w_n) + p \cdot \frac{\partial n_n}{\partial z} + z_n \cdot \rho_n = M_n \frac{dw_n}{dt} \qquad 4.30$$

where u_n = x component of the velocity, $\bar{V}_n$

v_n = y component of the velocity, $\overline{V}_n$

w_n = z component of the velocity, $\overline{V}_n$

The above equations are general and can be applied to any multiphase system. The surface tractions associated with each phase are presently written in a "reduced" form. They can be modified and written in terms of "true" stresses by applying a porosity correction. For a non viscous fluid, the shear components drop out and the normal components are written,

$$p_{nxx} = n_n \cdot p$$

$$p_{nyy} = n_n \cdot p$$

$$p_{nzz} = n_n \cdot p \qquad 4.31$$

Since we are presently only interested in the equations of equilibrium (as opposed to the equations of motion), the right-hand side of the equation is equal to zero. Also, we are not interested in the velocity distribution of the fluid within each element and therefore the diffusor effect term can be omitted (i.e. F_n'' drops out).

The equilibrium equation in the x-direction, for a non viscous fluid reduces to,

$$n_n \cdot \frac{\partial p}{\partial x} + \sum_{j=1}^{N} K_{jn}(u_j - u_n) + x_n \cdot \rho_n = 0 \qquad 4.32$$

The equations are similar in the y and z directions. Let us divide the above equation by the phase porosity.

$$\frac{\partial p}{\partial x} + \sum_{i=1}^{N} \frac{K_{jn}}{n_n} (u_j - u_n) + \frac{x_n \cdot \rho_n}{n_n} = 0 \qquad 4.33$$

The gravity body term reduces to the true unit weight of the phase (i.e. γ_n).

The above equations demonstrate that the equilibrium of each phase can be written either in terms of their "true" or "reduced" stress fields; however, in each case, the drag and body forces must be modified respectively.

The equilibrium equations can be written for each phase of a multiphase system. The number of independent equilibrium equations is always equal to the number of dimensions under consideration times the number of phases involved (i.e. 3*N). It is possible to also write equilibrium equations for the overall element. However, the equations are independent only when a set of equations for one of the other phases is omitted. In the x-direction, the overall equilibrium equation is,

$$\frac{\partial p_{xx}}{\partial x} + \frac{\partial p_{yx}}{\partial y} + \frac{\partial p_{zx}}{\partial z} + \sum_{n=1}^{N} \frac{F_n'}{n_n} + \sum_{n=1}^{N} x_n \cdot \gamma_n = 0 \qquad 4.34$$

Normally we assume that the sum of the internal drag forces of a multiphase system is zero when considering the total stress system on the entire element. However, we must keep in mind that we have a

special form of the total stress equilibrium equation where the stresses in each phase are the real stresses and not the "reduced" stresses. That is, the equilibrium equations for each phase are divided by the porosity of that particular phase. Let us first consider the original form of the equilibrium equations for a multiphase fluid, neglecting the gravity body force.

$$n_n \cdot \frac{\partial u_n}{\partial x} - F_n = 0 \qquad 4.35$$

This equation applies for each phase and we know that the sum of the drag forces is zero.

$$\sum_{n=1}^{N} F_n = 0 \qquad 4.36$$

The form of the equilibrium equation we are using is,

$$\frac{\partial u_n}{\partial x} - \frac{F_n}{n_n} = 0 \qquad 4.37$$

The pertinent question is; Is the sum of the drag forces divided by their porosities equal to zero?

$$\sum_{n=1}^{N} \frac{F_n}{n_n} \stackrel{?}{=} 0 \qquad 4.38$$

The answer is no. The only way it can be zero is if every

F_n is zero. Therefore, the total stress equilibrium equation must contain a drag force component.

4.7 Fluid-Solid Multiphase

In 1936, Terzaghi proposed the concept that the difference between the total stress and the pore water stress (i.e. effective stress) formed a stress variable that controlled the behavior of a saturated soil. He produced no theoretical explanation for its justification but experimentally demonstrated its application. This concept of effective stress has remained the unifying force in the scientific development of soil mechanics.

Bishop and Eldin (1950) used the superposition of two equivalent force systems on a plane through the contacts of a granular medium to justify the effective stress equation. They show that the area of contact does not come into play. Their concept of the superposition of two force systems is similar to the line of reasoning associated with the superposition of stress fields used in this thesis.

Hubbert and Rubey (1959) attempted to prove the uniqueness of the difference between the total and pore water pressures by means of the application of Archimedes Principle. Their analysis shows that the fluid stress field is continuous throughout the soil particles (i.e. as though they were not present) by integrating around the particles. This is a long, involved way of proving that the water phase stress field is continuous.

Let us consider an element of soil with all voids filled with water (Figure 4.3). The equilibrium equation in the y-direction

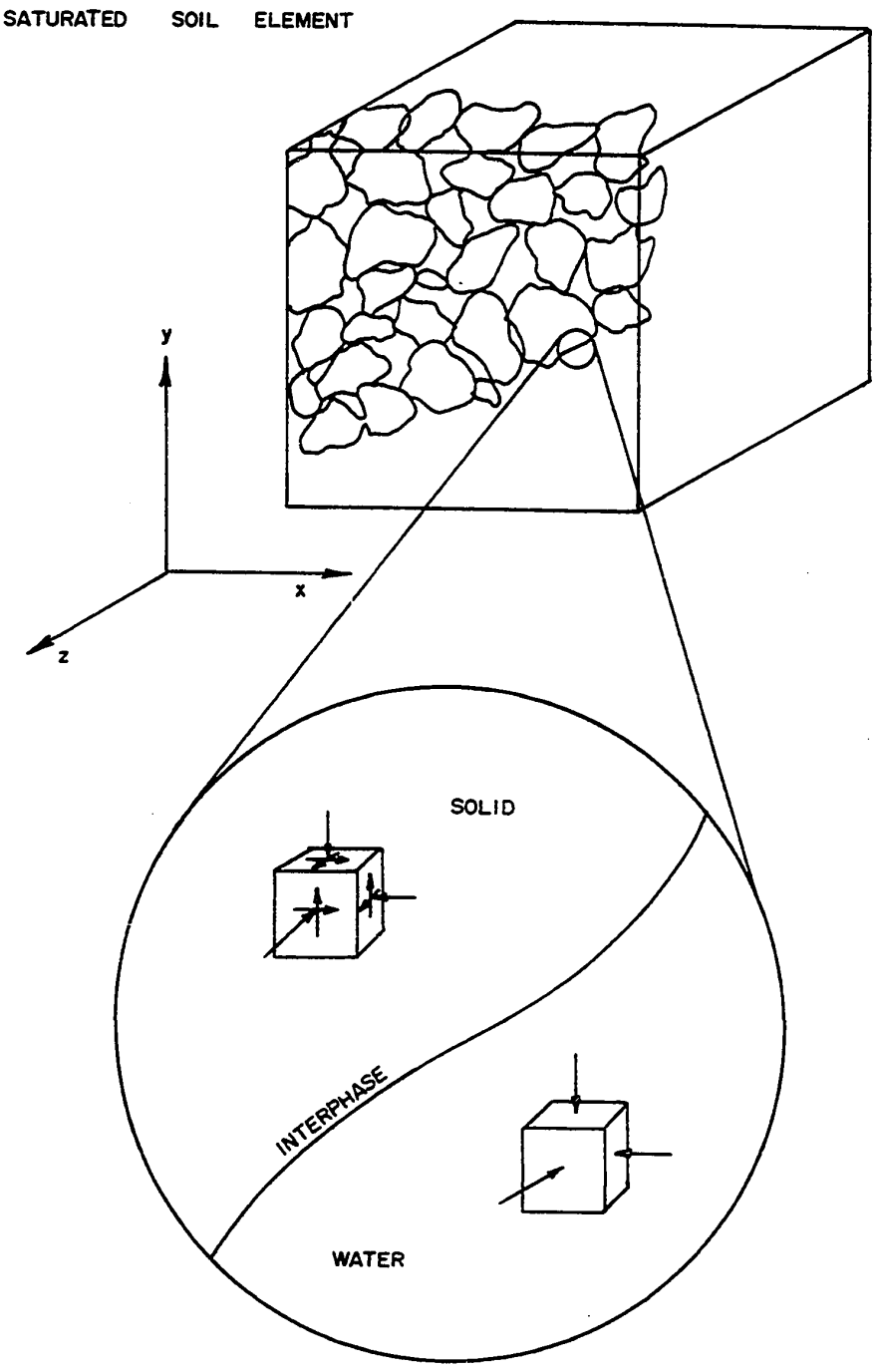


FIGURE 4.3 EQUILIBRIUM ACROSS A WATER - SOLID MULTIPHASE

for the solid phase is,

$$\left[\frac{\partial \tau^p_{xy}}{\partial x} + \frac{\partial \sigma^p_y}{\partial y} + \frac{\partial \tau^p_{zy}}{\partial z} + \frac{F^p_y}{n_s} \right] dxdydz = 0 \qquad 4.39$$

where σ^p_y = normal particle stress in the y-direction

τ^p_{xy} = shear particles stress on the x-plane in the y-direction

τ^p_{zy} = shear particle stress on the z-plane in the y-direction

F^p_y = body forces in the y-direction

n_s = particle porosity or percentage of the element composed of solids (i.e. $(1-n_w)$) .

There are two types of body forces acting in the y-direction. First, the gravity body force or the reduced unit weight of the solids, ρ_s. When this value is divided by the particle porosity, it reverts to the true unit weight, γ_s. Second, there is the drag force of the water on the particles, F_{iy}. This is the seepage force and is defined by the water phase equilibrium equation. Including the defined body forces, the soil solids equilibrium equation is,

$$\frac{\partial \tau^p_{xy}}{\partial x} + \frac{\partial \sigma^p_y}{\partial y} + \frac{\partial \tau^p_{zy}}{\partial z} + \gamma_s + \frac{F_{iy}}{n_s} = 0 \qquad 4.40$$

For the water phase, the equilibrium equation in the y-direction is,

$$\left[\frac{\partial u_w}{\partial y} + \frac{F_y^w}{n_w} \right] dxdydz = 0 \qquad 4.41$$

where F_y^w = body forces in the y-direction associated with the water phase.

Again the body force consists of two components. The gravity body force is the reduced unit weight, ρ_w, which reverts to the true unit weight, γ_w, when divided by the water porosity. There is also a seepage force or a reverse of the previously defined drag force ($- F_{iy}$). Substituting these into the water phase equilibrium equation gives,

$$\frac{\partial u_w}{\partial y} + \gamma_w - \frac{F_{iy}}{n_w} = 0 \qquad 4.42$$

The fluid phase equilibrium equation assumes, as do the equations for all phases, that the stress field is continuous throughout the element. Let us further consider whether this assumption is reasonable. The pressure acting on part of a particle is designated as T^ν with Cartesian components T_x^ν, T_y^ν and T_z^ν. The components of the water phase surface traction on the soil particles can be written,

$$T_x^\nu = u_w \cdot \nu_x \qquad 4.43$$

where ν_x = direction cosine for the x-axis.

Equilibrium requires that sum of the forces acting on a body must vanish when integrated around the body.

$$\int_A \int T_x^{\nu} \cdot dA = \int_A \int u_w \cdot \nu_x \cdot dA \qquad 4.44$$

Similar reasoning is applied for the y and z-directions. Gauss' theorem allows the transformation to a volume integral.

$$\int_A \int u_w \cdot \nu_x \cdot dA = \int_V \frac{\partial u_w}{\partial x} \cdot dV \qquad 4.45$$

The partial derivative of the water pressure with respect to each axis forms continuous potential functions (i.e., $F_x = \partial u_w/\partial x$, $F_y = \partial u_w/\partial_y$ and $F_y = \partial u_w/\partial z$). Therefore, the water pressure fields are continuous throughout the element and act as though the particles were not present. This is referred to as the assumption of coincident stress fields.

Our main interest in the equilibrium equations is the determination of reasonable stress state variables to use when describing the behavior of the soil structure. The equilibrium equations for the soil structure show that the stresses in the particles can be used to describe the behavior of the solids. However, the question arises as to what these stresses are in terms of measurable quantities, and in particular the normal stress? Obviously the soil solids equilibrium equation does not immediately reveal usable stress state variables.

As previously mentioned, it is possible to write a third equilibrium equation in terms of the overall stress field. This is possible due to the linear nature of the equilibrium equations for each phase.

$$\frac{\partial \tau_{xy}}{\partial x} + \frac{\partial \sigma_y}{\partial y} + \frac{\partial \tau_{zy}}{\partial z} + F' + \gamma = 0 \qquad 4.46$$

where $F' = \frac{F_{iy}}{n_s} - \frac{F_{iy}}{n_w}$

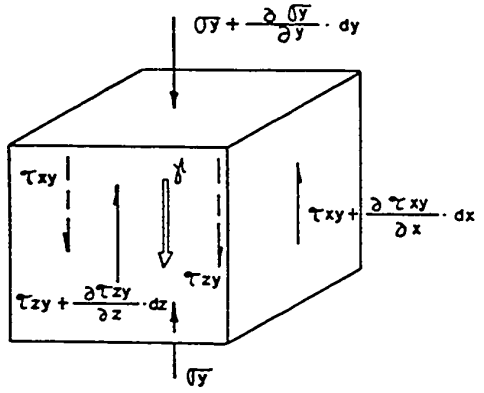
$\gamma = \gamma_w + \gamma_s$

σ_y = total stress in the y-direction

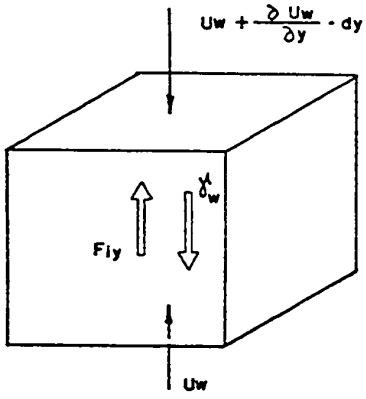
τ_{xy} = shear stress on the x-plane in the y-direction

τ_{zy} = shear stress on the z-plane in the y-direction

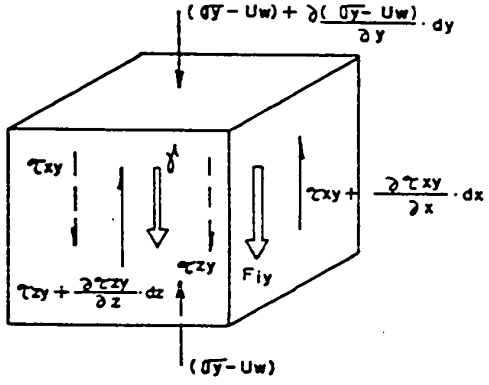
We now have three equilibrium equations; however, only two are independent. Also, only two of the normal stresses are measurable (i.e. σ and u_w). With this in mind it is reasonable to choose the total and water equilibrium equations as the independent equations. Then the equilibrium equation for the soil structure can be written in terms of the total and water equilibrium equations. Since the sum of the phase equilibrium equations is equal to the total equilibrium equation, the equation for the soil structure can be written as the difference between the total and the water equilibrium equations (Figure 4.4). In the x-direction, the soil solids equilibrium equation is,



TOTAL STRESS EQUILIBRIUM OF AN ELEMENT OF SATURATED SOIL



PRESSURE EQUILIBRIUM OF THE WATER PHASE



STRESS EQUILIBRIUM OF THE SOIL STRUCTURE

FIGURE 4.4 STRESS EQUILIBRIUM OF A WATER SATURATED PARTICULATE SYSTEM

$$\frac{\partial(\sigma_x - u_w)}{\partial x} + \frac{\partial \tau_{yx}}{\partial y} + \frac{\partial \tau_{zx}}{\partial z} + \frac{F'_{sx}}{n_s} = 0 \qquad 4.47$$

In the y-direction,

$$\frac{\partial \tau_{xy}}{\partial x} + \frac{\partial(\sigma_y - u_w)}{\partial y} + \frac{\partial \tau_{zy}}{\partial z} + \gamma_s + \frac{F'_{sy}}{n_s} = 0 \qquad 4.48$$

and in the z-direction,

$$\frac{\partial \tau_{xz}}{\partial x} + \frac{\partial \tau_{yz}}{\partial y} + \frac{\partial(\sigma_z - u_w)}{\partial z} + \frac{F'_{sz}}{n_s} = 0 \qquad 4.49$$

Now the stress components of the soil structure equilibrium equation are written in terms of measurable quantities. It is obvious from the equilibrium equations that a change in any one of the differentiated stress components can change the equilibrium of the soil structure. Thus it is logical to use these variables to describe the stress state of the soil structure.

The stress state variables for the soil structure are therefore extracted from the above equilibrium equations. They form the stress tensor,

$$\begin{bmatrix} \sigma_x - u_w & \tau_{yx} & \tau_{zx} \\ \tau_{xy} & \sigma_y - u_w & \tau_{zy} \\ \tau_{xz} & \tau_{yz} & \sigma_z - u_w \end{bmatrix}$$

The normal stress components are equivalent to the conventionally defined effective stress. In other words, the so-called effective stress law is actually a stress state variable which forms a part of the stress tensor required to describe the state of stress in the soil structure of a saturated soil.

The above analysis can also be conducted when the pore fluid is of a compressible nature such as air. The equilibrium equation in the y-direction for the soil structure is,

$$\frac{\partial \tau_{xy}}{\partial x} + \frac{\partial (\sigma_y - u_a)}{\partial y} + \frac{\partial \tau_{zy}}{\partial z} + \frac{F_{ay}}{(1-n_a)} + \gamma_s = 0 \qquad 4.50$$

where F_{ay} = drag force of the air with respect to the solids

n_a = air porosity

The resulting stress tensor controlling soil structure behavior is,

$$\begin{bmatrix} \sigma_x - u_a & \tau_{yx} & \tau_{zx} \\ \tau_{xy} & \sigma_y - u_a & \tau_{zy} \\ \tau_{xz} & \tau_{yz} & \sigma_z - u_a \end{bmatrix}$$

An important observation is the fact that the compressibility of the air does not appear in the stress tensor. This is contrary to the thinking associated with the modified stress variables suggested by Skempton (1961).

The equilibrium analysis can also be conducted for a reverse type of model to that of the saturated soil case just analysed. In other words, let us assume that the water portion of the element is solid and vice versa. This tends to approach a case similar to that of many rock materials. Proceeding with an analysis similar to that of the saturated soil case yields the stress tensor,

$$\begin{bmatrix} \sigma_x - u_w & \tau_{yx} & \tau_{zx} \\ \tau_{xy} & \sigma_y - u_w & \tau_{zy} \\ \tau_{xz} & \tau_{yz} & \sigma_z - u_w \end{bmatrix}$$

Therefore, the same stress tensor applies regardless of the porosity of the material. The only stipulation is that the water is continuous in order that it can form a continuous stress field.

4.8 Air-Water Multiphase

In Chapter I, evidence was presented to support the existence of an independent phase between the air and water phases. The physical properties of this phase were shown to differ from those of the air or water. The properties of this layer allows it to be treated as a thin membrane that responds to the interaction of the air and water phases. The element under consideration is composed of a liquid phase, an air phase and a contractile skin phase, and should be referred to as a three phase system.

Goodrich (1969) considers a moderately curved air-water interphase and shows that an axi-symmetric stress tensor can be used to represent the interphase between air and water phases.

$$\begin{bmatrix} P_T & 0 & 0 \\ 0 & P_T & 0 \\ 0 & 0 & P_N \end{bmatrix}$$

where P_T = tangential stress on the element and

P_N = stress normal to the contractile skin.

In order for the above tensor to apply to a membrane in any direction, it must be set up in a natural coordinate system. The z-axis is always normal to the contractile skin. However, this becomes difficult to compare with, and transform back to the Cartesian coordinate system.

Goodrich considers equilibrium across the contractile skin and relates the stress tensor to the air and water pressures.

$$u_a - u_w = 2 \int (P_T - P_N) \frac{1}{r} \, dr \qquad 4.51$$

where r = radius of curvature of the contractile skin.

Since the contractile skin is very thin, the radius changes only slightly over its thickness. Therefore it is justifiable to re-

move the radius from beneath the integral sign and write the remaining integral as the surface tension. The relationship reverts to the Kelvin-Laplace formula for the mechanical equilibrium across a spherical interface

$$u_a - u_w = \frac{2 \cdot T_s}{r} \qquad 4.52$$

In a three dimensional analysis, there are two principal radii of curvature (i.e. r_1 and r_2). Therefore,

$$u_a - u_w = 2 \cdot T_s \left(\frac{1}{r_1} + \frac{1}{r_2}\right) \qquad 4.53$$

The contractile skin acts as an intermediary phase between the air and water phases and its equilibrium for a general case can be established within the context of continuum mechanics.

Let us consider a fictitious element of water with air channels throughout it that are at a higher pressure than the water (Figure 4.5). The element is not realistic since the air phase would not assume the above configuration and remain stable in the absence of a solid phase. Bubbles of air in the water might appear to be a more realistic model; however, then the air phase is discontinuous and cannot have a continuous stress field. In addition, the air bubbles are not stable in the water in the absence of a solid. The case of occluded air bubbles in water does however, demonstrate the fact that even if the air and water pressures differ, there is no net shear

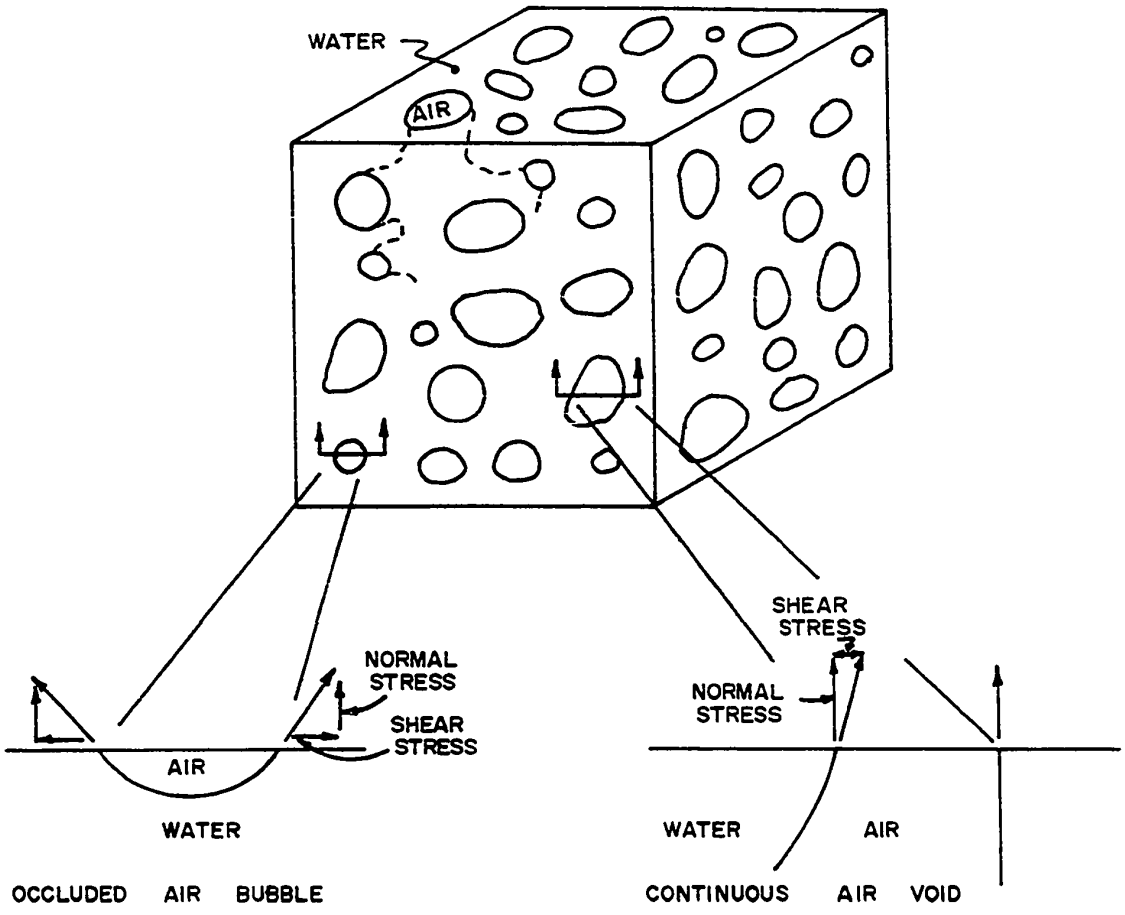


FIGURE 4.5 FICTITIOUS AIR – WATER MULTIPHASE ELEMENT

component on the surface of the element. The components parallel to the surface of the element always concel.

Reconsidering the original air-channel element, it is obvious that the surface of the element can have a net shear component. In a sense it is not a shear component since the contractile skin cannot withstand shear. Rather, it is a net force in the direction parallel to the element surface which arises from the resolution of the surface tension forces that are parallel to the contractile skin.

A highly magnified portion of the air-water element (Figure 4.6) demonstrates the stress fields involved. Let us assume that the air and water stress fields act in opposite directions. In this way it is possible to visualize a case where the two fields tend to counterbalance each other and form a somewhat more stable element. (Even if this assumption was not made, the final sign convention in the analysis would compensate for the directions of the stress fields). The equilibrium equation in the y-direction for the air phase is,

$$- \frac{\partial u_a}{\partial y} + \frac{F_{ay}}{n_a} + \gamma_a = 0 \qquad 4.54$$

where F_{ay} = interaction or drag force of the air with respect to the contractile skin.

The relationship between the pressure gradient and the contractile skin drag force should more correctly be thought of as an interaction force. Since the viscosity of the air is considered negligible, it is the pressure gradient normal to the contractile

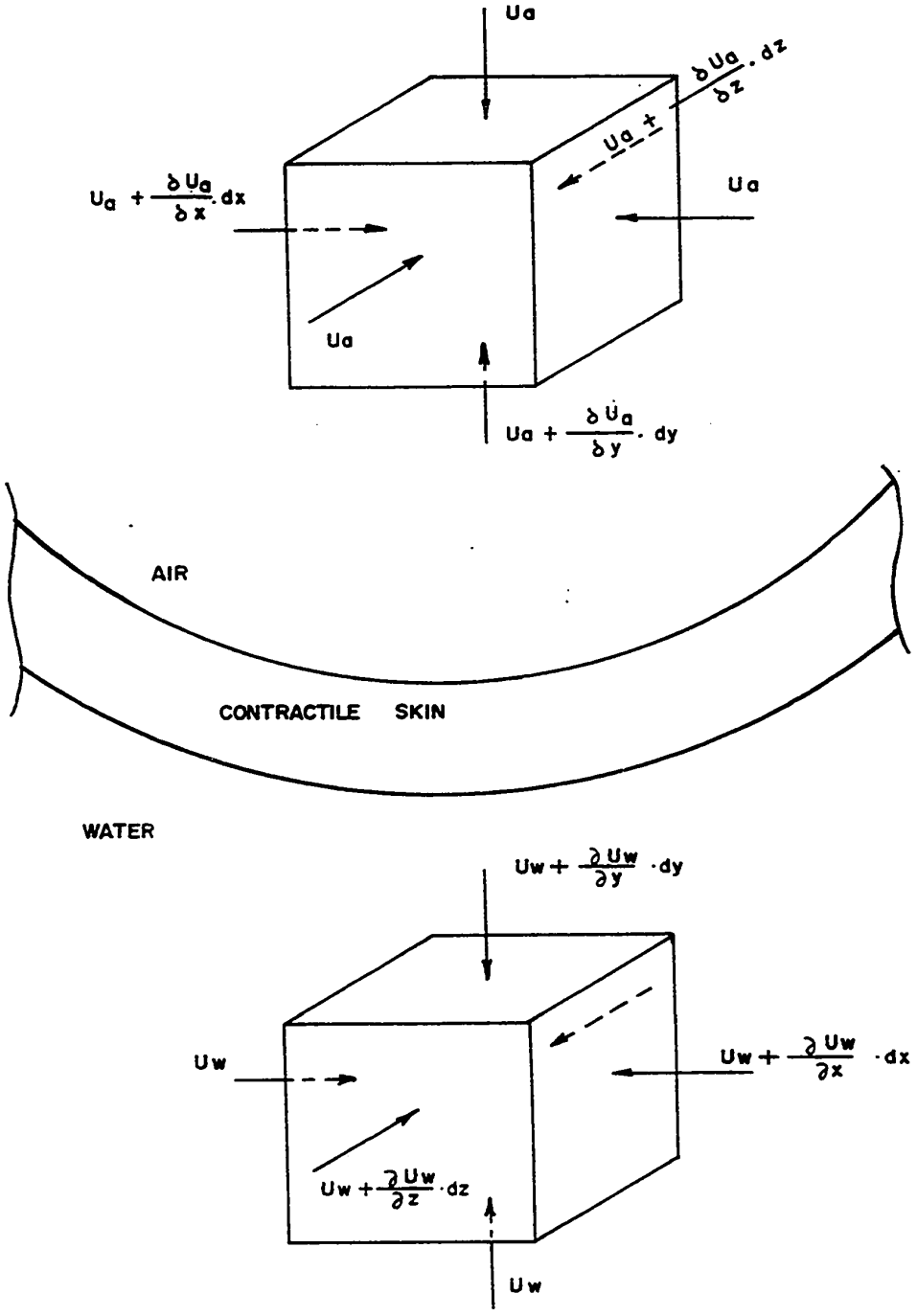


FIGURE 4.6 EQUILIBRIUM IN AN AIR – WATER MULTIPHASE

skin that produces the counteracting force. The same argument holds for the water phase.

The equilibrium equation in the y-direction for the water phase is,

$$\frac{\partial u_w}{\partial y} - \frac{F_{wy}}{n_w} + \gamma_w = 0 \qquad 4.55$$

where F_{wy} = interaction or drag force of the water with respect to the contractile skin.

The equilibrium equation in the y-direction for the contractile skin is,

$$\frac{\partial \tau^c_{xy}}{\partial x} + \frac{\partial \sigma^c_y}{\partial y} + \frac{\partial \tau_{zy}}{\partial z} + \frac{F_{wy}}{n_c} - \frac{F_{ay}}{n_c} + \gamma_w = 0 \qquad 4.56$$

where σ^c_y = normal component of the stress in the contractile skin

τ^c_{xy} and τ^c_{zy} = shear components parallel to the surface of the element

n_c = porosity with respect to the contractile skin.

Upon closer examination we see that the contractile skin stresses are components of the real stresses in the contractile skin (i.e. T_s). The normal stress, for example, is a function of a factor which accounts for the geometry of the contractile skin with respect to the surface of the element.

$$\sigma_y^c = f(\cos\bar{\zeta}_y) \qquad 4.57$$

where $\bar{\zeta}_y$ = the average angle between the normal to the surface of the element and the resultant of the contractile skin force.

If the geometry of the air-water network were known, the angle, $\bar{\zeta}_y$, could be obtained by intergrating around all the portions of the element. The angle, $\bar{\zeta}_y$, is actually a function of the orientation of the element with respect to the air-channel network. Thus, the normal contractile skin stress can be written,

$$\sigma_y^c = \frac{T_s}{t} \cdot \cos\bar{\zeta}_y \qquad 4.58$$

where t = thickness of the contractile skin.

The shear components can also be written in terms of the surface tension by knowing the angles between them and the resultant on the respective faces of the element. Let these angles be designated as $\bar{\zeta}_{xy}$ and $\bar{\zeta}_{zy}$ with respect to the y-direction. Then

$$\tau_{xy}^c = \frac{T_s}{t} \cdot \cos\bar{\zeta}_{xy}$$

$$\tau_{zy}^c = \frac{T_s}{t} \cdot \cos\bar{\zeta}_{zy} \qquad 4.59$$

Presently we have written three independent equations for the three-phase air-water multiphase. Only the air and water pressures can be measured and therefore the stresses associated with the contractile skin remain unknown. Since the stress fields of each phase are linear, it is possible to write an overall equilibrium equation for the combined element.

$$\frac{\partial \tau_{xy}}{\partial x} + \frac{\partial \sigma_y}{\partial y} + \frac{\partial \tau_{zy}}{\partial z} + F' + \gamma = 0 \qquad 4.60$$

where $$F' = -\frac{F_{ay}}{n_a} - \frac{F_{wy}}{n_w} + \frac{F_{wy}}{n_c} + \frac{F_{ay}}{n_c}$$

$$\gamma = +\gamma_w + \gamma_w + \gamma_a$$

The pertinent question that arises is, What is the physical meaning of the total stress field?

Actually the total stress field has no meaning when there are no external stresses applied to the system. The air-water multiphase does not have any external forces applied and therefore all the phase stress fields associated with the system cancel out. In other words we have a self-equilibrating system. Figure 4.7 shows a simplified representation of the element in order to demonstrate the meaning of a self equilibrating system. Each stress field produces a resultant force on each phase. These are represented as F_A, F_C and F_W for the air, contractile skin and water phases, respectively. The

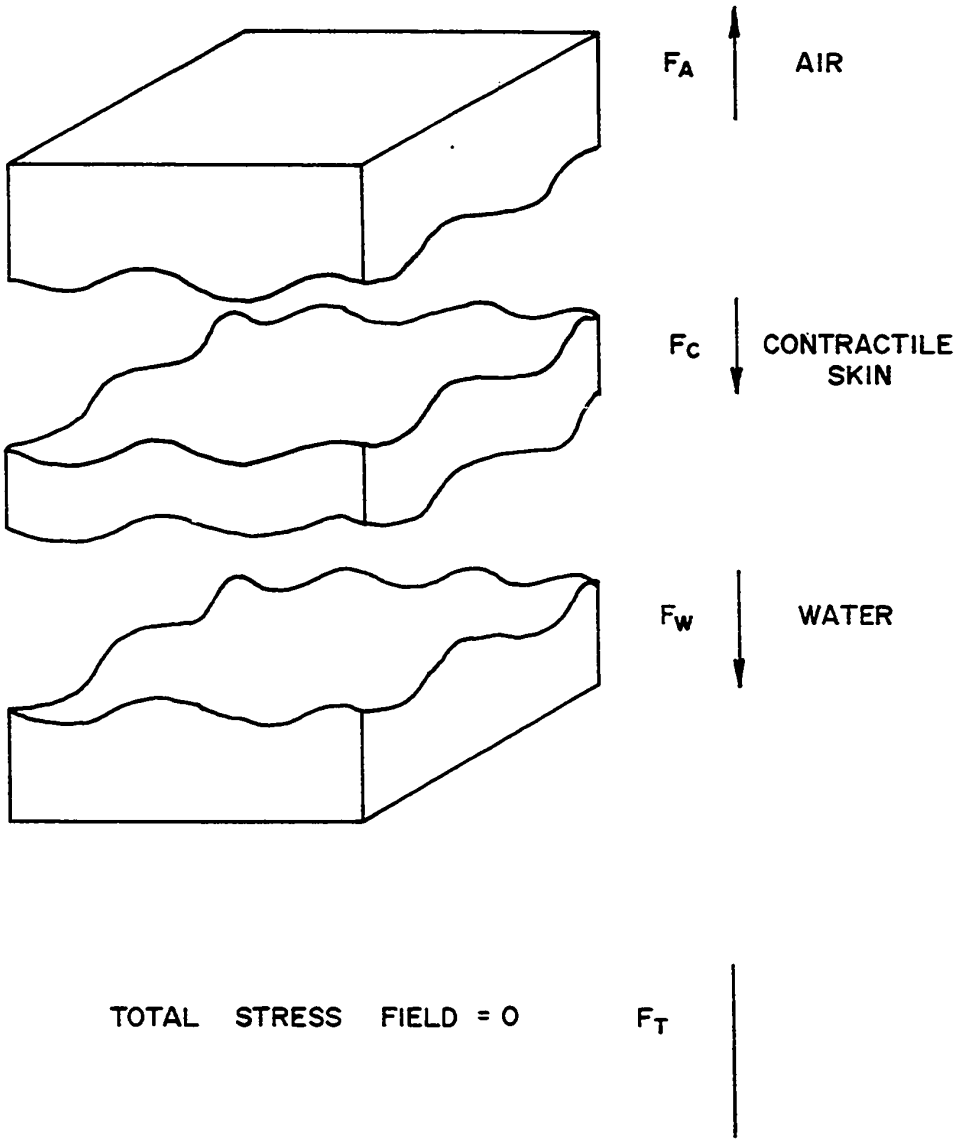


FIGURE 4.7 SIMPLIFIED REPRESENTATION OF THE SELF - COMPENSATING AIR - WATER MULTIPHASE

total stress field results in a resultant force, F_T which is equal to zero.

Referring to the air phase equilibrium equation, F_A can be written as,

$$F_A = -\frac{\partial u_a}{\partial y} = -\frac{F_{ay}}{n_a} - \gamma_a \qquad 4.61$$

On the contractile skin,

$$F_C = \frac{\partial \tau^c_{xy}}{\partial x} + \frac{\partial \sigma^c_y}{\partial y} + \frac{\partial \tau^c_{zy}}{\partial z} = -\frac{F_{wy}}{n_c} + \frac{F_{ay}}{n_c} - \gamma_w \qquad 4.62$$

and on the water phase,

$$F_W = \frac{\partial u_w}{\partial y} = \frac{F_{wy}}{n_w} - \gamma_w \qquad 4.63$$

For the total stress field,

$$F_T = \frac{\partial \tau_{xy}}{\partial x} + \frac{\partial \sigma_y}{\partial y} + \frac{\partial \tau_{zy}}{\partial z} = 0$$

$$= -\frac{F_{ay}}{n_a} - \gamma_a - \frac{F_{wy}}{n_c} + \frac{F_{ay}}{n_c} - \gamma_w + \frac{F_{wy}}{n_w} - \gamma_w \qquad 4.64$$

Only three of the above equations are independent. Let us choose the air, water and total equations as the independent equations and write the equilibrium of the contractile skin in terms of these equations.

Since,

$$F_T = F_A + F_C + F_W \qquad 4.65$$

then

$$F_C = F_T - F_A - F_W \qquad 4.66$$

Substituting into this equation gives,

$$\frac{\partial(u_a - u_w)}{\partial y} + \frac{F_{wy}}{n_c} - \frac{F_{ay}}{n_c} + \gamma_w = 0 \qquad 4.67$$

This is a new equilibrium equation for the contractile skin written in terms of the air and water pressures. The suction component (u_a-u_w) becomes the stress state variable for the contractile skin.

An abbreviated manner in which to view the above analysis is as follows. First, orientate the element such that the normal stress on the contractile skin becomes a principal stress. Since the total normal stress is equal to the sum of the components we can write,

$$\sigma = - u_a + u_w + \sigma^c \qquad 4.68$$

For the self-equilibrating system, the total stress is zero. Therefore,

$$\sigma^c = u_a - u_w \qquad 4.69$$

In the x-direction, the equilibrium equation is,

$$\frac{\partial(u_a-u_w)}{\partial x} + \frac{F_{wx}}{n_c} - \frac{F_{ax}}{n_c} = 0 \qquad 4.70$$

and in the z-direction, it is

$$\frac{\partial(u_a-u_w)}{\partial z} + \frac{F_{wz}}{n_c} - \frac{F_{az}}{n_c} = 0 \qquad 4.71$$

When the stress state variables for the contractile skin are extracted from the equilibrium equations, they form an isotropic stress tensor.

$$\begin{bmatrix} (u_a-u_w) & 0 & 0 \\ 0 & (u_a-u_w) & 0 \\ 0 & 0 & (u_a-u_w) \end{bmatrix}$$

The stress tensor shows that the matric suction can be used to describe the behavior of the contractile skin.

4.9 Unsaturated Soil Case

An unsaturated soil element can be treated as a combination of the water-solid and the air-water multiphase systems. It is possible to write a linear independent equilibrium equation for each of the four phases. Therefore, the overall system also has a linear stress field. In terms of total stresses, the equilibrium equations in the x, y and z-directions are,

$$\left[\frac{\partial \sigma_x}{\partial x} + \frac{\partial \tau_{yx}}{\partial y} + \frac{\partial \tau_{zx}}{\partial z} + F'_x\right] dxdydz = 0 \qquad 4.72$$

$$\left[\frac{\partial \tau_{xy}}{\partial x} + \frac{\partial \sigma_y}{\partial y} + \frac{\partial \tau_{zy}}{\partial z} + \gamma + F'_y\right] dxdydz = 0 \qquad 4.73$$

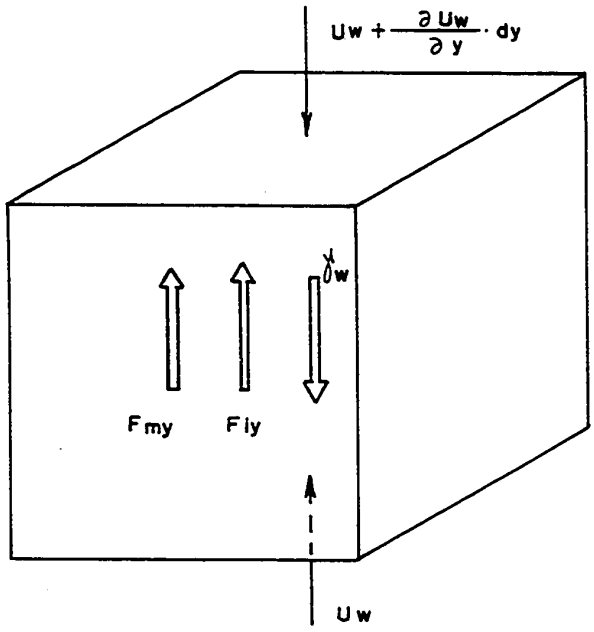
$$\left[\frac{\partial \tau_{xz}}{\partial x} + \frac{\partial \tau_{yz}}{\partial y} + \frac{\partial \sigma_z}{\partial z} + F'_z\right] dxdydz = 0 \qquad 4.74$$

where

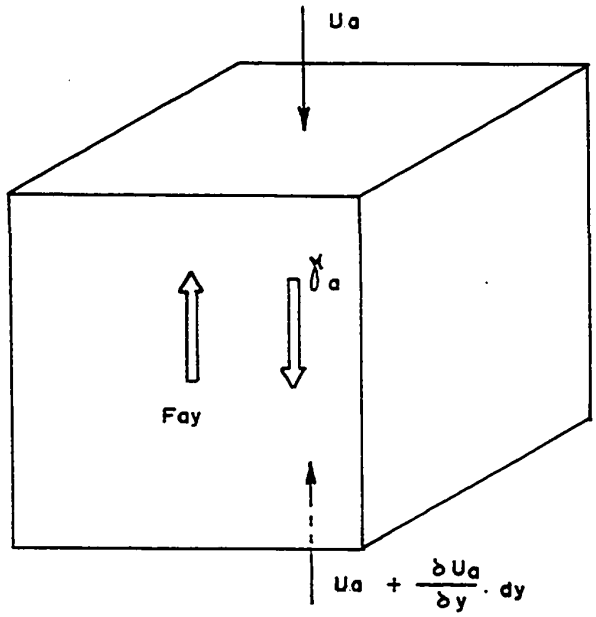
$$\gamma = \sum_{n=1}^{N} \gamma_n$$

$$F' = \sum_{n=1}^{N} \frac{F'_n}{n_n}$$

Figure 4.8a shows the forces associated with the water phase. Assuming that the contractile skin behaves as a stationary membrane, there is an interaction force between the water and the contractile skin. Let the interaction force be represented by a body force designated as F_w. There is also an interaction force between the water and the soil particles, F_i. The equilibrium in the x-direction is



4.8 a EQUILIBRIUM OF THE PORE WATER PHASE



4.8 b EQUILIBRIUM OF THE PORE AIR PHASE

FIGURE 4.8 EQUILIBRIUM OF THE FLUID PHASES OF AN UNSATURATED SOIL ELEMENT

$$\left[\frac{\partial u_w}{\partial x} - \frac{F_{wx}}{n_w} - \frac{F_{ix}}{n_w} \right] dxdydz = 0 \qquad 4.75$$

In the y-direction,

$$\left[\frac{\partial u_w}{\partial y} + \gamma_w - \frac{F_{wy}}{n_w} - \frac{F_{iy}}{n_w} \right] dxdydz = 0 \qquad 4.76$$

In the z-direction,

$$\left[\frac{\partial u_w}{\partial z} - \frac{F_{wz}}{n_w} - \frac{F_{iz}}{n_w} \right] dxdydz = 0 \qquad 4.77$$

Figure 4.8b shows the forces associated with the air phase. Let the interaction force between the air and the contractile skin be designated by the body force, F_a. Summing in the x-direction gives,

$$\left[- \frac{\partial u_a}{\partial x} + \frac{F_{ax}}{n_a} \right] dxdydz = 0 \qquad 4.78$$

In the y-direction,

$$\left[- \frac{\partial u_a}{\partial y} + \gamma_a + \frac{F_{ay}}{n_a} \right] dxdydz = 0 \qquad 4.79$$

and in the z-direction,

$$\left[- \frac{\partial u_a}{\partial y} + \frac{F_{ay}}{n_a} \right] dxdydz = 0 \qquad 4.80$$

Next the contractile skin is considered as an independent phase. Three body forces interact with the contractile skin. The contractile skin interacts with the soil particles producing an interaction force, F_c. The drag of the water and air on the contractile skin are F_w and F_a, respectively. Summing the forces in the x-direction gives,

$$\left[\frac{\partial \sigma_x^c}{\partial x} + \frac{\partial \tau_{yx}^c}{\partial y} + \frac{\partial \tau_{zx}^c}{\partial z} + \frac{F_{wx}}{n_c} - \frac{F_{ax}}{n_c} + \frac{F_{cx}}{n_c} \right] dxdydz = 0 \qquad 4.81$$

In the y-direction,

$$\left[\frac{\partial \tau_{xy}^c}{\partial x} + \frac{\partial \sigma_y^c}{\partial y} + \frac{\partial \tau_{zy}^c}{\partial z} + \gamma_w + \frac{F_{wy}}{n_c} - \frac{F_{ay}}{n_c} + \frac{F_{cy}}{n_c} \right] dxdydz = 0 \qquad 4.82$$

and in the z-direction,

$$\left[\frac{\partial \tau_{xz}^c}{\partial x} + \frac{\partial \tau_{yz}^c}{\partial y} + \frac{\partial \sigma_z^c}{\partial z} + \frac{F_{wz}}{n_c} - \frac{F_{az}}{n_c} + \frac{F_{cz}}{n_c} \right] dxdydz = 0 \qquad 4.83$$

Similarly, equilibrium equations can be written for the soil solids. Once again there is an interaction force, F_c, between the contractile skin and the soil structure. In addition, there is an interaction force of the water on the soil structure, F_i. In the x-direction, the equilibrium equation is,

$$\left[\frac{\partial \sigma_x^p}{\partial x} + \frac{\partial \tau_{yx}^p}{\partial y} + \frac{\partial \tau_{zx}^p}{\partial z} + \frac{F_{ix}}{n_s} - \frac{F_{cx}}{n_s} \right] dxdydz = 0 \qquad 4.84$$

In the y-direction,

$$\left[\frac{\partial \tau^{p}_{xy}}{\partial x} + \frac{\partial \sigma^{p}_{y}}{\partial y} + \frac{\partial \tau^{p}_{zy}}{\partial z} + \gamma_s + \frac{F_{iy}}{n_s} - \frac{F_{cy}}{n_s} \right] dxdydz = 0 \qquad 4.85$$

and in the z-direction,

$$\left[\frac{\partial \tau^{p}_{xz}}{\partial x} + \frac{\partial \tau^{p}_{yz}}{\partial y} + \frac{\partial \sigma^{p}_{z}}{\partial z} + \frac{F_{iz}}{n_s} - \frac{F_{cz}}{n_s} \right] dxdydz = 0 \qquad 4.86$$

We have now written five equilibrium equations for the four phase system and therefore one of the equations is redundant. If we omit the equilibrium equation for the soil structure, its equilibrium can be written in terms of the difference between the total stress field and the stress fields of the remaining phases. The resulting equilibrium equation for the soil structure contains the stress variables for the contractile skin. Likewise, if the contractile skin equilibrium equation is written in terms of the total stress field and the stress fields for the remaining phases, it contains the particle stress field which is also an unknown. Thus, there is an inter-relationship between the soil structure and the contractile skin equilibrium equations.

The above difficulty is readily resolved by uncoupling the unsaturated soil problem into a water-solid multiphase and an air-water multiphase. When this is done, the only difference between the present equations and previously developed equations is the interaction force between the soil structure and the contractile skin. Consider first the soil structure equilibrium equation.

$$\left[\frac{\partial \tau^{p}_{xy}}{\partial x} + \frac{\partial \sigma^{p}_{y}}{\partial y} + \frac{\partial \tau^{p}_{zy}}{\partial z} + \gamma_s + \frac{F_{iy}}{n_s} \right] - \frac{F_{cy}}{n_s} = 0 \qquad 4.87$$

By uncoupling the multiphase system and reconsidering the previous water-solid analysis, the equilibrium equation can be written (Figure 4.9)

$$\left[\frac{\partial \tau_{xy}}{\partial x} + \frac{\partial (\sigma_y - u_w)}{\partial y} + \frac{\partial \tau_{zy}}{\partial z} + \gamma_s + \frac{F_{sy}}{n_s}\right] - \frac{F_{cy}}{n_s} = 0 \qquad 4.88$$

Similarly, the contractile skin equilibrium equation can be re-written for the uncoupled multiphase system.

$$\left[\frac{\partial (u_a - u_w)}{\partial y} + \frac{F_{wy}}{n_c} - \frac{F_{ay}}{n_c} + \gamma_w \right] + \frac{F_{cy}}{n_c} = 0 \qquad 4.89$$

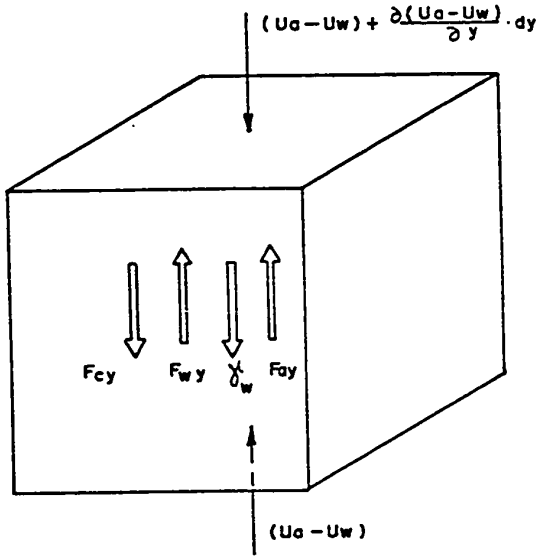
Solving for F_{cy} and substituting into the soil structure equilibrium equation gives,

$$\frac{\partial \tau_{xy}}{\partial x} + \frac{\partial (\sigma_y - u_w)}{\partial y} + \frac{\partial \tau_{zy}}{\partial z} + \gamma_s + \frac{F_{sy}}{n_s}$$

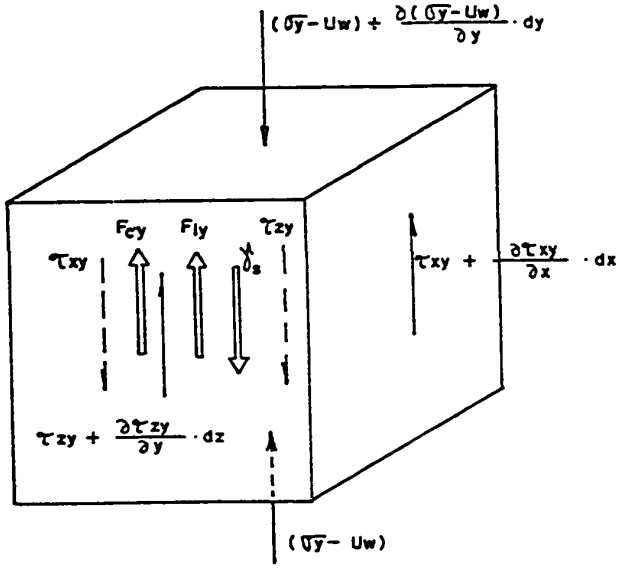
$$- \frac{n_c}{n_s} \left[\frac{\partial (u_a - u_w)}{\partial y} + \frac{F_{wy}}{n_c} - \frac{F_{ay}}{n_c} + \gamma_w \right] = 0 \qquad 4.90$$

This equilibrium equation applies for both the soil structure and the contractile skin. The equation is simplified by lumping the body forces.

$$\frac{\partial \tau_{xy}}{\partial x} + \frac{\partial (\sigma_y - u_w)}{\partial y} + \frac{\partial \tau_{zy}}{\partial z} + \frac{n_c}{n_s} \cdot \frac{\partial (u_a - u_w)}{\partial y} + F' + \gamma = 0 \qquad 4.91$$



4.9 a EQUILIBRIUM OF THE CONTRACTILE SKIN



4.9 b EQUILIBRIUM OF THE SOIL STRUCTURE

FIGURE 4.9 EQUILIBRIUM OF THE CONTRACTILE SKIN AND SOIL STRUCTURE FOR AN UNSATURATED SOIL ELEMENT

where $$F' = \frac{F_{sy}}{n_s} - \frac{F_{wy}}{n_s} + \frac{F_{ay}}{n_s}$$

$$\gamma = \gamma_s - \frac{n_c}{n_s} \cdot \gamma_w$$

The equilibrium equation in the x-direction is,

$$\frac{\partial(\sigma_x - u_w)}{\partial x} + \frac{\partial \tau_{yx}}{\partial y} + \frac{\partial \tau_{zx}}{\partial z} - \frac{n_c}{n_s} \cdot \frac{\partial(u_a - u_w)}{\partial x} + F' = 0 \qquad 4.92$$

In the z-direction, the equilibrium equation is,

$$\frac{\partial \tau_{xz}}{\partial x} + \frac{\partial \tau_{yz}}{\partial y} + \frac{\partial(\sigma_z - u_w)}{\partial z} - \frac{n_c}{n_s} \cdot \frac{\partial(u_a - u_w)}{\partial z} + F' = 0 \qquad 4.93$$

An examination of the equations reveals that two normal stress state variables are involves in describing the equilibrium of both the soil structure and the contractile skin. They are linked with the assistance of the ratio of the contractile skin and soil solids porosities; however, this is an unknown which does not warrant attempts at its assessment. The inclusion of the porosity ratio is also not in keeping with the usage of stress state variables in continuum mechanics. Extracting the stress state variables for both the contractile skin and the soil structure from the equilibrium equations gives,

$$\begin{bmatrix} \sigma_x - u_w & \tau_{yx} & \tau_{zx} \\ \tau_{xy} & \sigma_y - u_w & \tau_{zy} \\ \tau_{xz} & \tau_{yz} & \sigma_z - u_w \end{bmatrix}$$

and
$$\begin{bmatrix} u_a-u_w & 0 & 0 \\ 0 & u_a-u_w & 0 \\ 0 & 0 & u_a-u_w \end{bmatrix}$$

The above stress tensors (Figure 4.10) contain only quantities that can be measured. Therefore they can readily be used in the constitutive relationship for mapping the deformation of the soil structure and the contractile skin.

The stress state variables associated with the fluids can be used to describe their flow. Re-examination of the equilibrium equations for the air and water phases confirms that one isotropic stress tensor controls equilibrium. For the water phase the stress tensor is

$$\begin{bmatrix} u_w & 0 & 0 \\ 0 & u_w & 0 \\ 0 & 0 & u_w \end{bmatrix}$$

and for the air phase, the stress tensor is,

$$\begin{bmatrix} u_a & 0 & 0 \\ 0 & u_a & 0 \\ 0 & 0 & u_a \end{bmatrix}$$

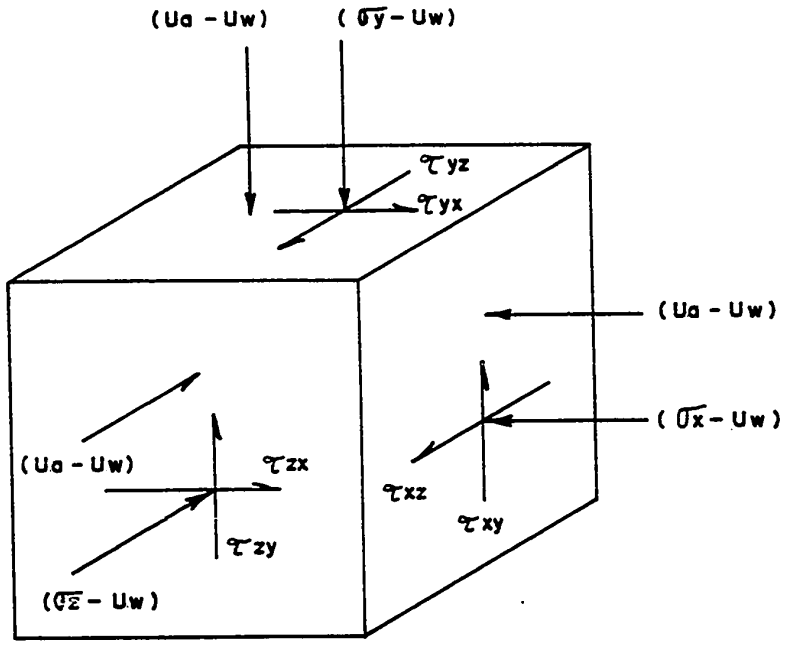


FIGURE 4.10 STRESSES IN THE SOIL STRUCTURE AT A POINT

The above analysis has considered the equilibrium equations by using the water phase as a datum. The physical assemblage of an unsaturated soil system indicates that this is a logical choice. However, when considering the equilibrium of stress fields, the air phase could also be used as a datum. Physically, this can be visualized by considering that the net load transferred to the soil structure is the difference between the total and air pressures. The soil structure and the contractile skin then have the following stress tensors.

$$\begin{bmatrix} \sigma_x - u_a & \tau_{yx} & \tau_{zx} \\ \tau_{xy} & \sigma_y - u_a & \tau_{zy} \\ \tau_{xz} & \tau_{yz} & \sigma_z - u_a \end{bmatrix}$$

and

$$\begin{bmatrix} u_a - u_w & 0 & 0 \\ 0 & u_a - u_w & 0 \\ 0 & 0 & u_a - u_w \end{bmatrix}$$

There is no apparent reason why the total stress could not be used as a reference. The stress tensors for the soil structure and contractile skin equilibrium equations are then,

$$\begin{bmatrix} \sigma_x - u_a & \tau^{\circ}_{yx} & \tau^{\circ}_{zx} \\ \tau^{\circ}_{xy} & \sigma_y - u_a & \tau^{\circ}_{zy} \\ \tau^{\circ}_{xz} & \tau^{\circ}_{yz} & \sigma_z - u_a \end{bmatrix}$$

and

$$\begin{bmatrix} \sigma_x - u_w & \tau'_{yx} & \tau'_{zx} \\ \tau'_{xy} & \sigma_y - u_w & \tau'_{zy} \\ \tau'_{xz} & \tau'_{yz} & \sigma_z - u_w \end{bmatrix}$$

In each of the above cases, the equilibrium equations are different but consistent with the force equilibrium of the element. Thus it appears that any two of the three possible stress tensors can be used for the analysis of the volume change problem.

4.10 Limiting Stress State Conditions in Unsaturated Soils

In order to ensure stable equilibrium at all times, certain restrictions must be observed. For example, we know that a saturated soil mass becomes unstable when the effective stress reaches zero. At this point the soil "quicks" and a further increase in water pressure results in a "geyser". For a stable, saturated soil mass the limiting condition or restriction dictates that the water pressure must be less than the total stress (i.e. $\sigma > u_w$).

For the unsaturated soils there is also a hierarchy with respect to the stress components. For example, if the air pressure is

momentarily increased in excess of the total stress, an "explosion" of the sample can occur. Also, if the water pressure is increased in excess of the air pressure, the soil continually increases in degree of saturation (approaching 100 percent) and steady state seepage takes place through the sample. The sample has reverted to a two-phase system. If the water pressure is equal to the total pressure, the sample again becomes completely unstable.

The hierarchy of the stress components in an unsaturated soil is $\sigma > u_a > u_w$. This corresponds to the following limiting conditions, $\sigma = u_a$ and/or $u_a = u_w$. At the limiting conditions, one of the stress state variables vanishes.

Back pressure oedometer tests and pressure plate suction tests are examples of tests performed under limiting conditions. (See the example calculations in Figure 4.11). Consider the oedometer test performed, with a back pressure on an initially unsaturated soil. With time, the degree of saturation tends to 100 percent. The suction becomes zero. Since one stress state variable is zero, the behavior of the sample can be described in terms of one of the other stress state variables. The limiting condition (i.e., $u_a = u_w$) ensures a smooth transition from the unsaturated case to the saturated case.

The sample in the pressure plate suction device can be visualized as being surrounded by a rubber membrane. The pressure applied to the exterior of the rubber membrane (i.e., total stress) is equal to the interior air pressure. Therefore, the difference between the total stress and the air pressure is zero and one stress

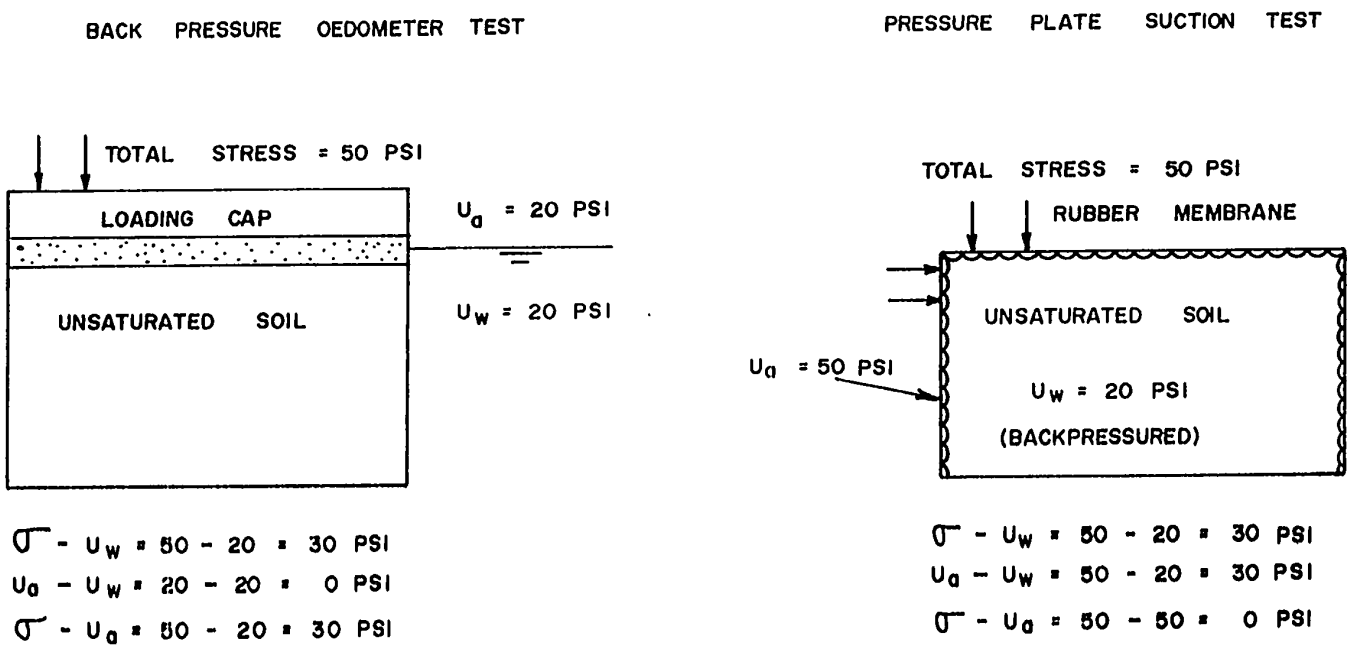


FIGURE 4.11 COMPARISON OF TESTS PERFORMED AT LIMITING STRESS STATE VARIABLE CONDITIONS

state variable $(\sigma-u_a)$ drops out. One of the other two stress state variables can be used to describe behavior. The most logical stress state variable to use is (u_a-u_w). However, since the soil is saturated, it is more correct to consider the air pressure as a total stress. Actually, the contractile skin forms a perfect substitute for the rubber membrane.

Considered in the above sense, the back pressure oedometer and pressure plate oedometer and pressure plate suction tests are limiting tests or special cases of the more general case where $\sigma > u_a > u_a$.

4.11 Comparison of the Derived Stress State Variables With Previously Proposed Effective Stress Equations

The force equilibrium approach to the theoretical justification of the stress state variables for describing soil behavior is basically different than that used by other research workers. Their search was for one effective stress equation and was based on the consideration of a plane passed through the soil. The approach used in this thesis involves the extraction of independent stress state variables from equilibrium equations. The analysis of the unsaturated soil system is conducted within the context of continuum mechanics.

Bishop's effective stress equation has been the most widely accepted equation used in the analysis of unsaturated soils. The author does not completely agree with its formulation or its application, and will attempt to show why it has experienced only a limited

degree of success.

Let us reconsider the equilibrium equation for the soil structure and the contractile skin.

$$\frac{\partial \tau_{xy}}{\partial x} + \frac{\partial (\sigma_y - u_w)}{\partial y} + \frac{\partial \tau_{zy}}{\partial z} + \frac{n_c}{n_s} \cdot \frac{\partial (u_a - u_w)}{\partial y} + F' + \gamma = 0 \qquad 4.94$$

Although the equilibrium equation is written in terms of $(\sigma - u_w)$ and $(u_a - u_w)$, it could also be derived in terms of the $(\sigma - u_a)$ and $(u_a - u_w)$ stress state variables. The body forces change but the equation maintains the same form.

$$\frac{\partial \tau_{xy}}{\partial x} + \frac{\partial (\sigma_y - u_a)}{\partial y} + \frac{\partial \tau_{zy}}{\partial z} + (1 - \frac{n_c}{n_s}) \cdot \frac{\partial (u_a - u_w)}{\partial y} + F' + \gamma = 0 \qquad 4.95$$

For the case of an isotropically loaded soil, the shear stresses disappear. Let us also neglect the body forces. The equilibrium equation reduces to

$$\frac{\partial (\sigma_y - u_a)}{\partial y} + (1 - \frac{n_c}{n_s}) \cdot \frac{\partial (u_a - u_w)}{\partial y} = 0 \qquad 4.96$$

Since both terms of the equation are differentiated with respect to the same value, we can combine the terms within one bracket provided we recognize that $(1 - n_c/n_s)$ is a constant.

$$\frac{\partial}{\partial y} \left[\sigma - u_a + (1 - \frac{n_c}{n_s}) \cdot (u_a - u_w) \right] = 0 \qquad 4.97$$

Only the integrand needs to be satisfied. The integrand is similar to Bishop's equation if we set $\chi = (1 - n_c/n_s)$. The equations can be written for each coordinate and χ is a constant provided the soil is isotropic and homogeneous. (Recall that we previously also assumed isotropic loading conditions). Reverting to the general case with shear stresses, the apparent stress tensor has the form,

$$\begin{bmatrix} \sigma_x - u_a + \chi_x \cdot (u_a - u_w) & \tau_{yx} & \tau_{zx} \\ \tau_{xy} & \sigma_y - u_a + \chi_y \cdot (u_a - u_w) & \tau_{zy} \\ \tau_{xz} & \tau_{yz} & \sigma_z - u_a + \chi_z \cdot (u_a - u_w) \end{bmatrix}$$

The author is quick to emphasize however, that he does not agree with using a stress tensor which has the independent stress state variables coupled. First, it is outside the context of continuum mechanics to involve soil properties with stress state variables. Second, it is unnecessary to incorporate a linking factor that in no way facilitates the solution of problems. Problems are as readily analysed in terms of two stress state variables and in addition it is unncessary to evaluate the linking factor.

In 1970, Schiffman presented a report in which he theoretically derived Bishop's equation for unsaturated soils. He first considers an unbiased plane passing through an elementary volume. However, later in the report he sets the same porosity term to zero since "the actual grain to grain contact is small as compared to the total unit".

Thus, he uses this inconsistency to advantage when he wants the porosity term to be <u>one</u> in the effective stress equation.

Schiffman states that he is "considering a three-dimensional geometry". He writes an "equivalence" statement in terms of the stresses acting on a plane through a multiphase element. Writing the equation in a tensor form makes it appear as though it is a three-dimensional analysis.

The total forces in the y-direction for an unsaturated soil element are written as,

$$F_y = F_y^p + F_y^w + F_y^a \qquad 4.98$$

where F^p = force on the solid phase

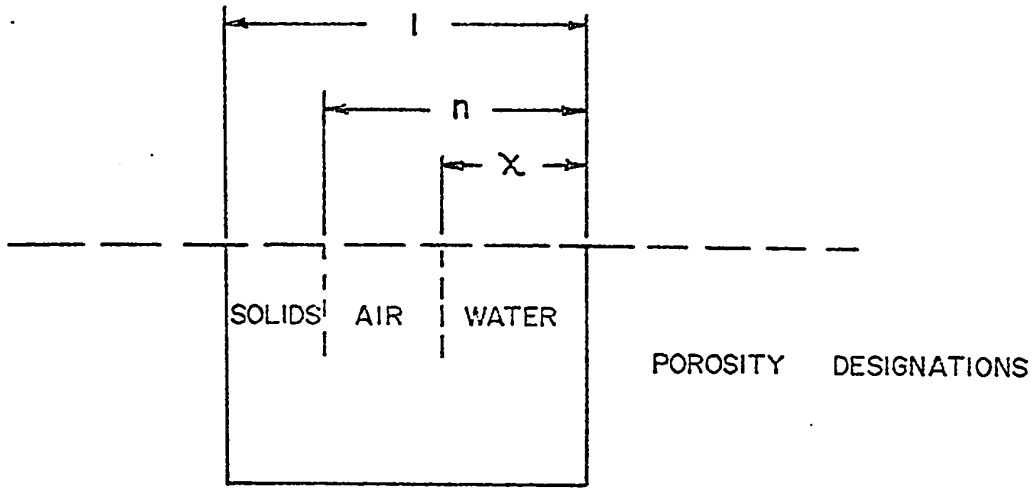
F^w = force on the water phase

and F^a = force on the air phase.

The terminology used in this discussion is similar to that used in Schiffman's report, however, engineering notation is used. Figure 4.12 shows an element with the variation of each force field. The total area of the surface of the element is unity and the volume of voids is n. The portion of the plane passing through the water is χ. On the base of the element, the force on the solids is,

$$(1-n)\ \sigma^p\ dxdz \qquad 4.99$$

The force is $\chi \cdot u_w \cdot dxdy$ on the water and $(n-\chi) \cdot u_a \cdot dxdz$



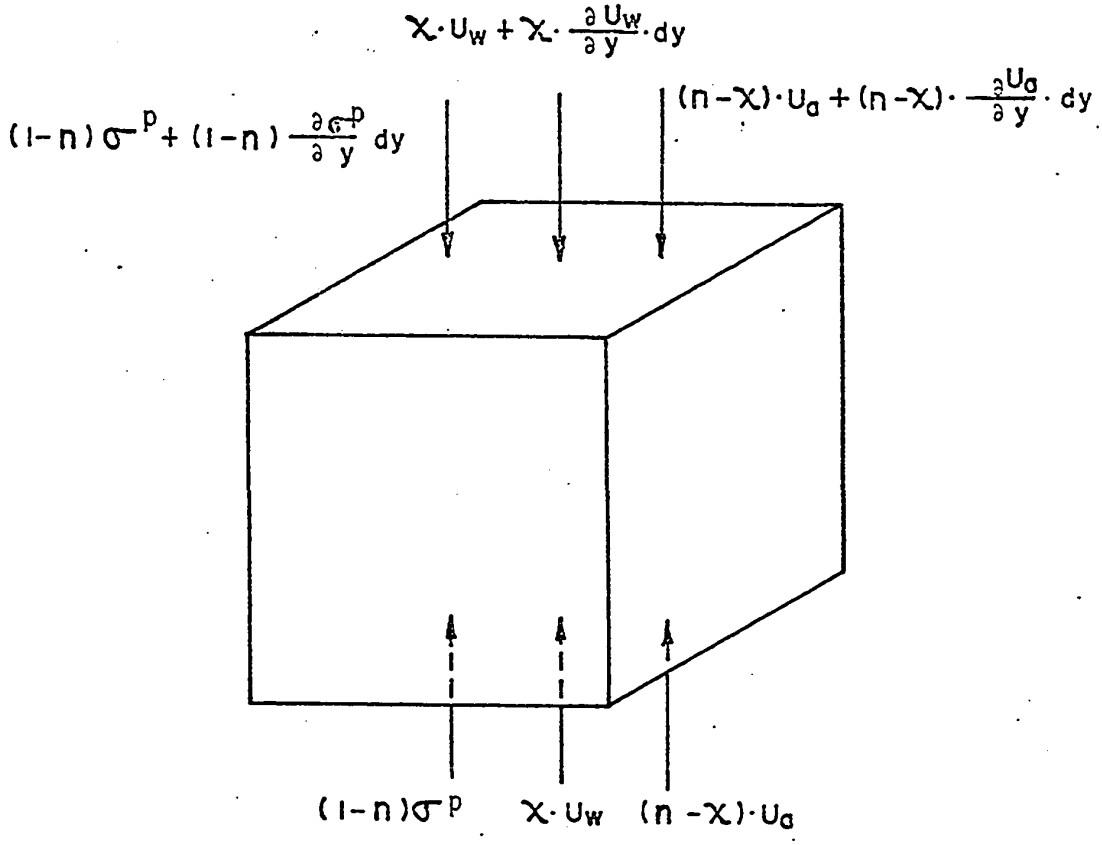


FIGURE 4.12 FORCE EQUILIBRIUM TO DESCRIBE SCHIFFMAN'S ANALYSIS

on the air phase.

At this point, the author departs from Schiffman's presentation and considers the force equilibrium of the element in Figure 4.12. Assuming that each force field is continuous, the forces at the top can be written in terms of the forces at the base plus the rate of change of the forces times the thickness of the element. Summing the forces in the y-direction gives

$$\left[(1-n)\frac{\partial \sigma^p}{\partial y} + \chi \cdot \frac{\partial u_w}{\partial y} + (n-\chi)\frac{\partial u_a}{\partial y}\right] dxdydz = 0 \qquad 4.100$$

Only the integrand needs to be satisfied

$$\frac{\partial}{\partial y}\left[(1-n)\,\sigma^p + \chi \cdot u_w + (n-\chi) \cdot u_a\right] = 0 \qquad 4.101$$

The portion in the bracket is similar to Schiffman's equation.

$$\sigma = \bar{\sigma} + \chi \cdot u_w + (n-\chi) \cdot u_a \qquad 4.102$$

where $\bar{\sigma}$ = solids stress averaged over the element

σ = total stress.

The average solids stress is made synonomous with the effective stress and the porosity is set equal to one. Then the equation reverts to Bishop's form. However, when the porosity goes to one, the stress in the solids becomes discontinuous.

4.12 Experimental Evidence in Support of the Proposed Stress State Variables

To the author's knowledge, no direct tests have been performed to prove the stress state variables that satisfy equilibrium at a state point. The verification of the stress state variable for saturated soils has been arrived at by intuition and observing constitutive and shear strength behavior. Tiller (1953) produced a family of compression curves for kaolin tested at various total and pore water pressures (Figure 4.13) He was demonstrating the dependence of porosity on total and pore water stress; however, all curves coincide when porosity is plotted against the difference between the total and pore water stress. In 1955, Laughton showed that the area of contact between the particles did not affect the stress state variable for a saturated soil (lead shot). Lowe III, Zaccheo and Feldman (1964) performed two one-dimensional consolidation tests on a natural, saturated, organic silt; one with zero back pressure and the other with a water back pressure of 4.32 tons per square foot (Figure 4.14). The two tests show essentially identical results when plotted versus effective stress. Bishop, Webb, and Skinner (1965) performed strength tests on lead shot, sand and calcite using total stresses as high as 5000 psi. However, the pore water pressure was always increased in order to keep the effective stress at 50 psi. The strengths were unaffected by the change in total stress.

In testing unsaturated soils, Hilf (1956) proposed the axis translation technique to measure soil suctions less than one atmos-

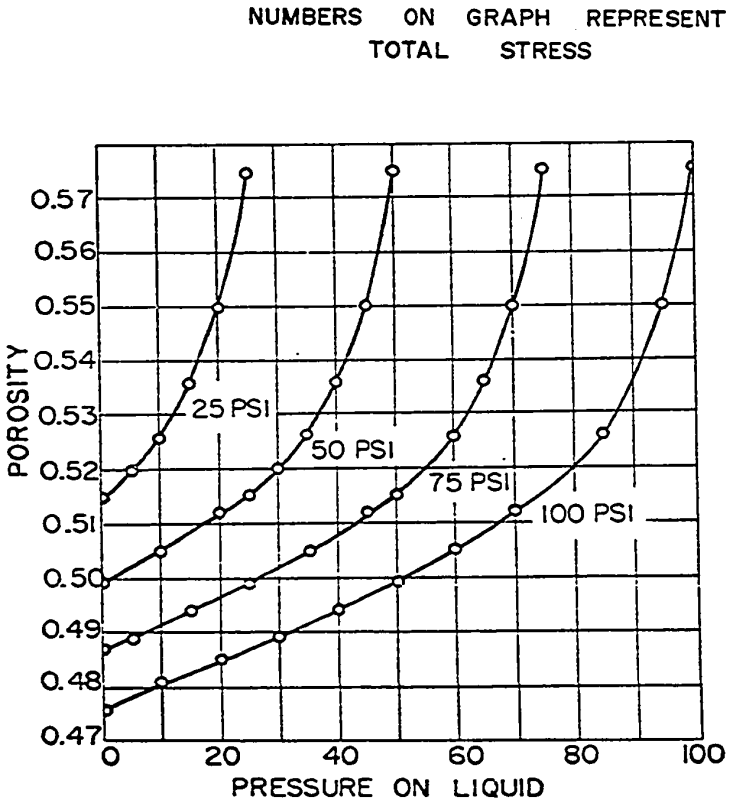
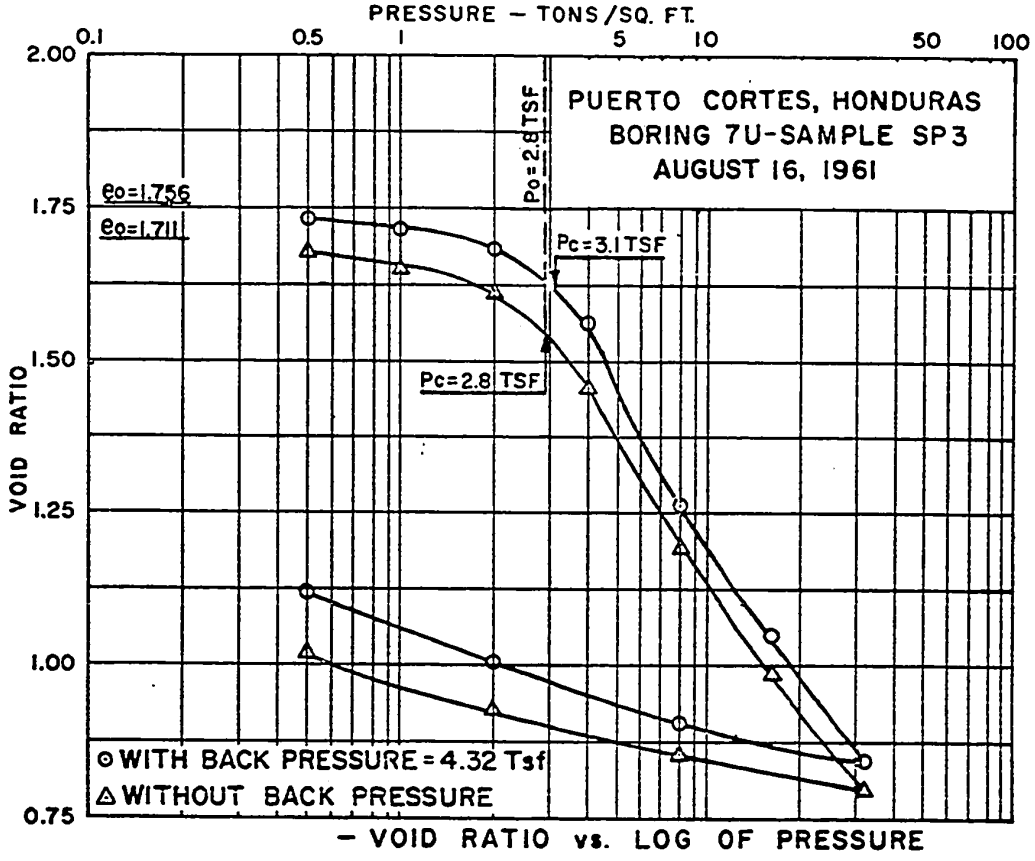


FIGURE 4.13 A SET OF CURVES DEMONSTRATING THE DEPENDENCE OF POROSITY ON TOTAL STRESS AND ON PORE WATER STRESS, IN THE CASE OF KAOLIN (AFTER TILLER, 1953)



TEST DATA			
CLASSIFICATION: GRAY ORGANIC SILT (OH)			
LL: 81	PI: 37	Gs : 2.75	
		WITH BP	WITHOUT BP
DRY UNIT WEIGHT-lbs/ft.^{3}		62.3	63.3
INITIAL WATER CONTENT-%		64.3	62.0
FINAL WATER CONTENT-%		41.9	39.8
INITIAL VOID RATIO		1.756	1.711
FINAL VOID RATIO		1.120	1.020
INITIAL DEGREE OF SATURATION %		100	99.7
FINAL DEGREE OF SATURATION %		100	100

FIGURE 4.14 TYPICAL e – LOG P CURVES
FROM "CONSOLIDATION TESTING WITH BACKPRESSURE"
BY J. LOWE III, P. F. ZACCHEO & H. FELDMAN (1964)

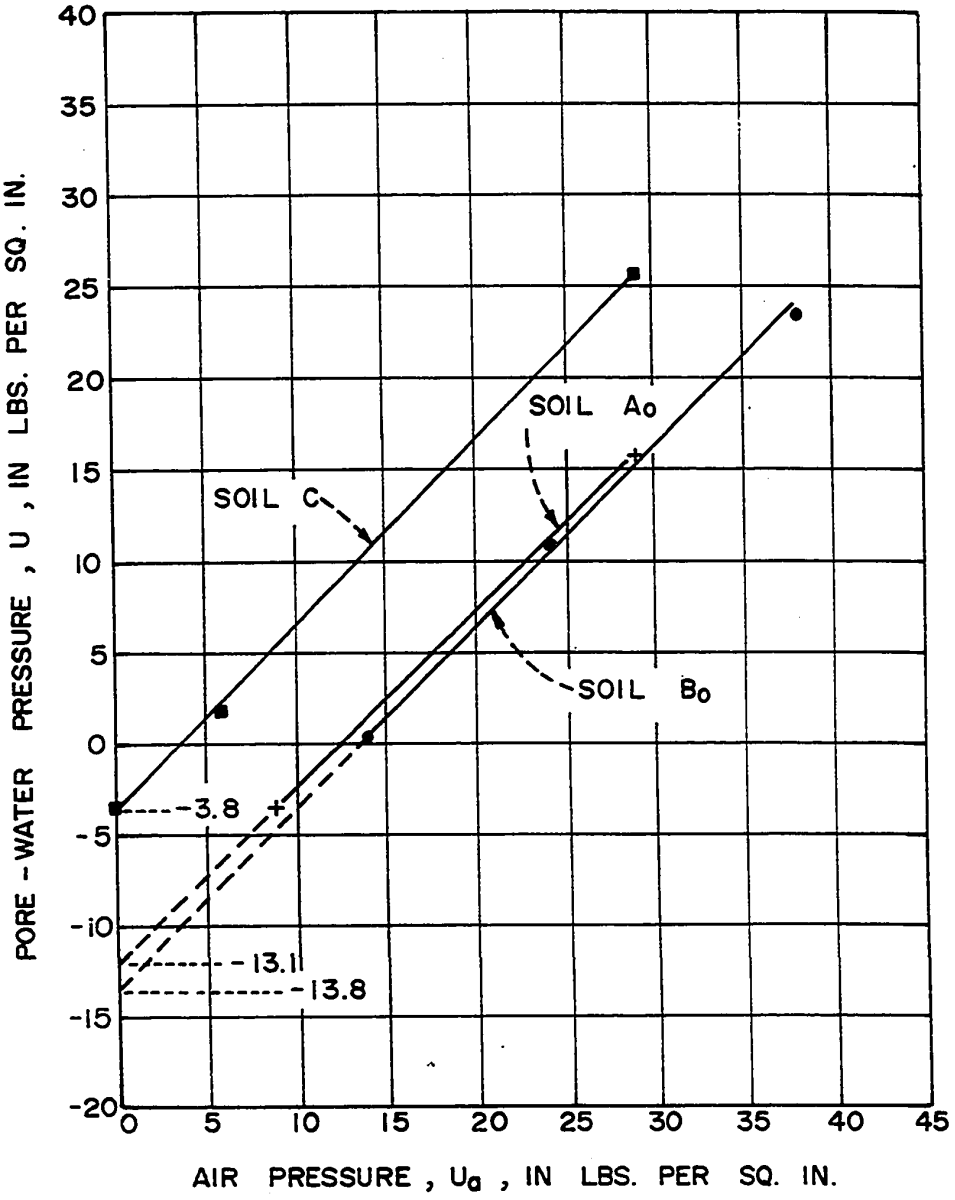


FIGURE 4.15 DETERMINATION OF CAPILLARY PRESSURE BY TRANSLATION OF THE ORIGIN (HILF, 1956)

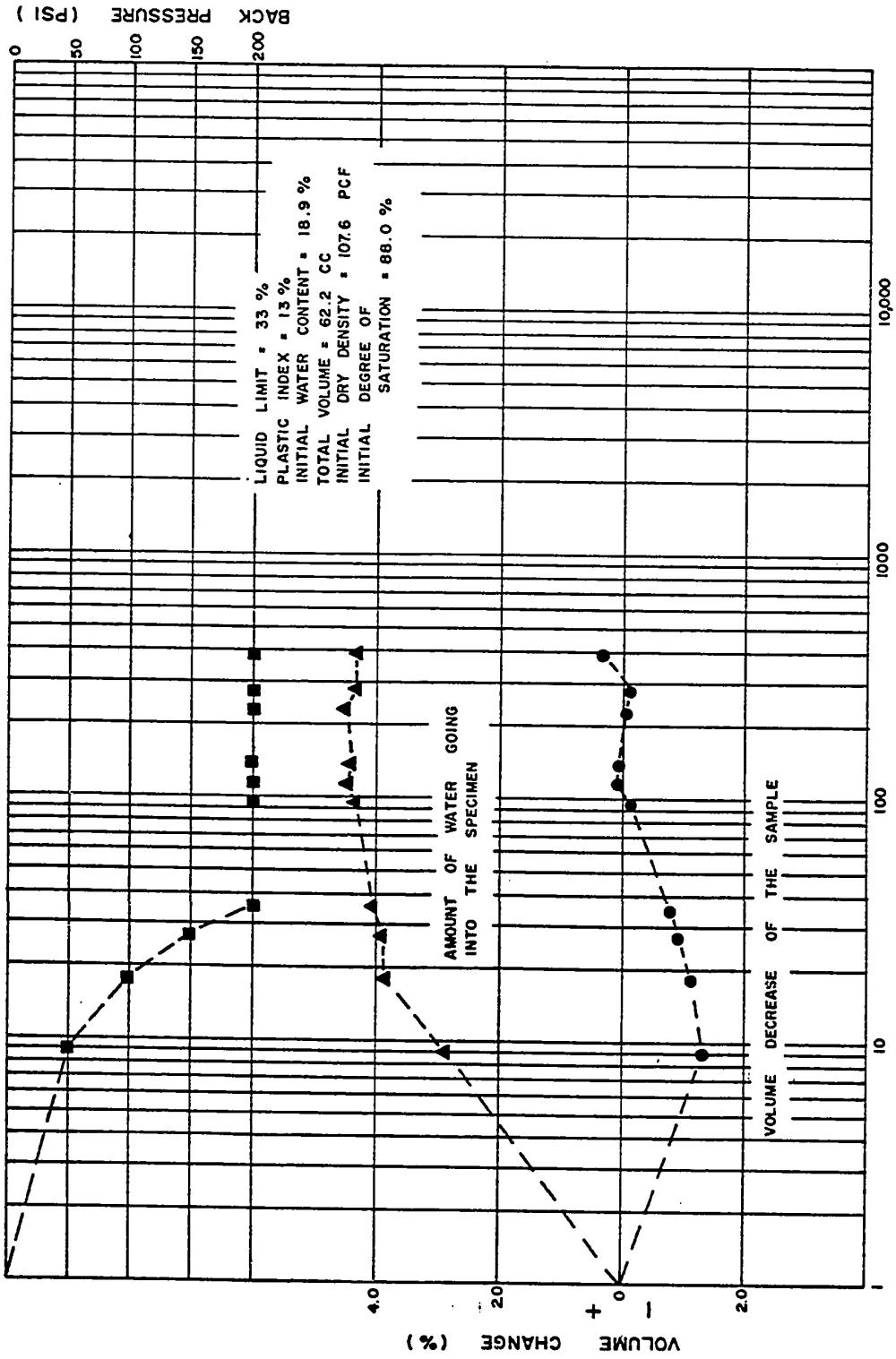


FIGURE 4.16 EFFECT OF EQUAL INCREASE IN CELL PRESSURE AND PORE PRESSURE ON THE VOLUME OF A SANDY CLAY (AFTER J. LOWE III AND T. C. JOHNSON, 1960)

phere. He performed null type pressure plate tests with various applied air pressures (Figure 4.15). The measured pore water pressure reaction was always essentially the same as the applied air pressure change. In other words, the suction remained constant. In retrospect, this technique is a special type of null test for unsaturated soils. It is a null test for the case when the applied air pressure is equal to the total pressure. Actually, Hilf was changing the total, air and water pressures by the same amount. The fact that the translation technique was successful infers that no volume change must have taken place in the total volume of the sample. However, measurements are not available to verify this point.

In 1960, Lowe and Johnson presented the results of a back pressure test on a sandy clay with an initial degree of saturation of 88 percent (Figure 4.16). They measured the total and water volume changes as the back pressure and cell pressure were increased. Water moved into the sample but the total volume of the sample first decreased and then tended toward its original volume. Although the test was performed to show the effect of back pressuring, the technique is similar to that proposed in this thesis for proving the validity of the stress state variables.

In 1961, Bishop and Donald presented the results of a special triaxial test performed on an unsaturated Braehead silt. Skempton (1961) stated that the Bishop and Donald experiment verified Bishop's effective stress equation. This experiment is the only known attempt to explicitly define the stress state variables controlling the behavior

of an unsaturated soil. The results are reproduced in Figure 4.17 and the pressure changes are summarized in Table IV.1.

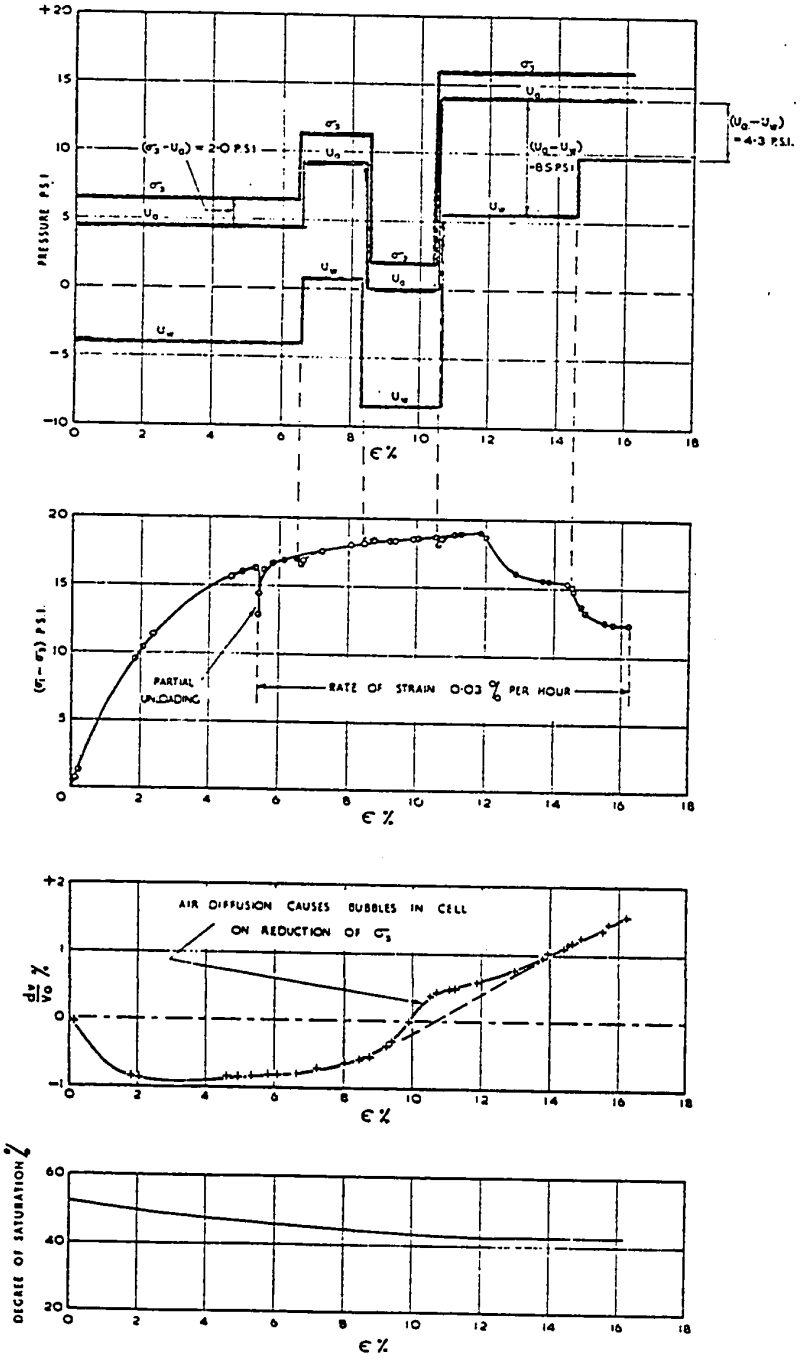
TABLE IV.1

DATA FROM THE BISHOP AND DONALD'S TRIAXIAL EXPERIMENT ON BRAEHEAD SILT

Portion of Stress-Strain Curve *	Confining Pressure σ_3(psi)	Air Pressure u_a(psi)	Water Pressure u_w (psi)	Change in Each Pressure (psi)
1	6.5	4.5	- 4.0	0.0
2	11.2	9.2	+ 0.7	+ 4.7
3	2.0	0.0	- 8.5	- 9.2
4	16.0	14.0	+ 5.5	+14.0
5	16.0	14.0	+ 9.7	

*Portions 1,2,3 and 4 produced monotonic behavior.

The results show that when the total (confining), air and water pressures are changed by equal amounts, the stress-strain relationship remains monotonic. The pressure changes satisfy Bishop's form of an effective stress equation; however, other forms and combinations of pressures are also satisfied. Table IV.2 applies Bishop and Donald's data to three possible combinations of stress state variables. The results infer that all three combinations form possible stress state variables to describe the strength behavior of the soil.



$e_f = 0.86$ $S = 43\ \%$ $LL = 29$ $PL = 23$

FIGURE 4.17 DRAINED TEST ON PARTLY SATURATED LOOSE SILT IN WHICH $\overline{\sigma_3}$, U_a AND U_w ARE VARIED SO AS TO KEEP $(\overline{\sigma_3} - U_a)$ AND $(U_a - U_w)$ CONSTANT (FROM BISHOP AND DONALD, 1961)

TABLE IV.2

INDEPENDENT STRESS STATE VARIABLES SHOWING MONOTONIC BEHAVIOR

(From Bishop and Donald's Data 1961)

Portion of Stress-Strain Curve		Combination 1		Combination 2		Combination 3	
		σ_3-u_a	u_a-u_w	σ_3-u_w	u_a-u_w	σ_3-u_a	σ_3-u_w
Monotonic Behavior	1	6.5- 4.5=2.0	4.5-(-4.0)=8.5	6.5-(-4.0)=10.5	8.5	2.0	10.5
	2	11.2- 9.2=2.0	9.2-(+0.7)=8.5	11.2-(+0.7)=10.5	8.5	2.0	10.5
	3	2.0- 0 =2.0	0 -(-8.5)=8.5	2.0-(-8.5)=10.5	8.5	2.0	10.5
	4	16.0-14.0=2.0	14.0-(+5.5)=8.5	16.0-(+5.5)=10.5	8.5	2.0	10.5
	5	16.0-14.0=2.0	14.0-(+9.7)=4.3	16.0-(+9.7)=6.3	4.3	2.0	6.3

No total volume change was evident at the points where the pressures were changed. However, the data is not sufficiently accurate and complete to verify this with any assurance. For example, even when the pressures were not changed in an equal manner (portion 5), no overall volume change was noted. In addition, only the total volume change readings are presented and there is no record of changes in air or water volume. The Bishop and Donald experiment is most significant from the standpoint of stress state variables; however, it does not specifically consider stress equilibrium at a point under accurately controlled conditions.

4.13 Proposed Experimental Verification of Stress State Variables

Independent stress state variables have been proposed for multiphase systems, based on a consideration of equilibrium stress fields. Now it is desirable to develop an experimental technique to verify the stress state variables at a point.

The author proposes the following definition and proof of independent stress state variables:

> A suitable set of independent stress state variables are those that produce no distortion or volume change of an element when the individual components of the stress state variables are modified but the stress state variable itself is kept constant. Thus the stress state variable for each phase should produce equilibrium in that phase when a stress point in space is considered.
>
> Any proposed tensor can be considered with respect to the

following question. How can the individual components of the state variables be altered without changing the overall stress tensor? The alteration of any one stress state variable should destroy the equilibrium of the system. Consider the stress tensor for a saturated soil

$$\begin{bmatrix} \sigma_x - u_w & \tau_{yx} & \tau_{zx} \\ \tau_{xy} & \sigma_y - u_w & \tau_{zy} \\ \tau_{xy} & \tau_{yz} & \sigma_y - u_w \end{bmatrix}$$

An increase in the total stress in the x-direction accompanied by an equal increase in the water stress should not affect the upper left stress state variable. However, it is impossible to increase the water pressure in only one direction and therefore all the diagonal stress state variables are affected. The problem is overcome by increasing the total stress in all directions. Thus, a test involving an increase in all normal stresses and an equal increase in the water stress, should prove or disprove the validity of the stress tensor. This test is somewhat analogous to the conventional B parameter test where the pore water pressure is measured as an undrained system. A more direct approach for the problem at hand is to operate all phases as an open or drained system and monitor tendencies for volume change. Therefore, the test required to verify $(\sigma - u_w)$ as the stress state variable for a saturated soil can be stated as follows:

$\Delta\sigma_x = \Delta\sigma_y = \Delta\sigma_z = \Delta u_w$; if the change in the soil structure is zero, the proposed stress state variables are verified.

Since the shear stress components have only one variable, it is impossible to alter them and remain at the same point in space.

In the case of an unsaturated soil, there are two stress tensors proposed for both the soil structure and the contractile skin (i.e.)

$$\begin{bmatrix} \sigma_x - u_w & \tau_{yx} & \tau_{zx} \\ \tau_{xy} & \sigma_y - u_w & \tau_{zy} \\ \tau_{xz} & \tau_{yz} & \sigma_z - u_w \end{bmatrix}$$

and

$$\begin{bmatrix} u_a - u_w & 0 & 0 \\ 0 & u_a - u_w & 0 \\ 0 & 0 & u_a - u_w \end{bmatrix}$$

To test the first tensor, all the total stresses can be increased or decreased by an equal amount along with an equal increase or decrease in the water pressure. However, the change in the water pressure disturbs the equilibrium of the second tensor. To maintain the second tensor in equilibrium, the air pressure must also be increased or decreased by an amount equal to the water and total pressures. This test should satisfy the equilibrium of both the soil structure and the contractile skin. In other words, if all phases are operated as a drained system, there should be no tendency for

volume change of the overall sample and no change in the degree of saturation. The test can be stated:

> $\Delta\sigma = \Delta u_w = \Delta u_a$; If $\Delta V = 0$, equilibrium of the soil structure is maintained. If $\Delta S = 0$, equilibrium of the contractile skin is maintained.

These tests are termed NULL tests since the desired result of the changes in pressure is to not produce a process in the phase or phases under consideration. Thus, an attempt is being made to measure "no volume change" or a continuing equilibrium state. It is difficult to measure zero volume change over an extended period of time. Therefore, scientific judgement and discretion must be used in analysing the test results.

Positive results (i.e. no volume change) from the above null test would also place approval on the use of other combinations of the stress tensors.

$$\begin{vmatrix} \sigma_x - u_a & \tau_{yx} & \tau_{zx} \\ \tau_{xy} & \sigma_y - u_a & \tau_{zy} \\ \tau_{xz} & \tau_{yz} & \sigma_z - u_a \end{vmatrix} \text{ and } \begin{vmatrix} u_a - u_w & 0 & 0 \\ 0 & u_a - u_w & 0 \\ 0 & 0 & u_a - u_w \end{vmatrix}$$

or

$$\begin{bmatrix} \sigma_x - u_a & \tau_{yx}^{\circ} & \tau_{zx}^{\circ} \\ \tau_{xy}^{\circ} & \sigma_y - u_a & \tau_{zy}^{\circ} \\ \tau_{xy}^{\circ} & \tau_{yz}^{\circ} & \sigma_z - u_a \end{bmatrix} \text{ and } \begin{bmatrix} \sigma_x - u_w & \tau_{yx}' & \tau_{zx}' \\ \tau_{xy}' & \sigma_y - u_w & \tau_{zy}' \\ \tau_{xy}' & \tau_{zy}' & \sigma_z - u_w \end{bmatrix}$$

Other tests can be envisaged to prove that other combinations of the phase variables do not form unique stress state variables (Table IV.3). These tests should produce a change in the overall volume and/or a change in the degree of saturation.

TABLE IV.3

POSSIBLE TESTS TO PROVE AND DISPROVE

INDEPENDENT STRESS STATE VARIABLES

Independent Stress State Variable Combination		Test to prove or disprove uniqueness
σ-ua	u_a-u_w	$\Delta\sigma=\Delta u_w=\Delta u_a$
$\sigma-u_w$	u_a-u_w	$\Delta\sigma=\Delta u_w-\Delta u_a$
$\sigma-u_a$	u_a-u_w	$\Delta\sigma=\Delta u_w=\Delta u_a$
σ	u_a-u_w	$\Delta u_w=\Delta u_a$
u_a	$\sigma-u_w$	$\Delta\sigma=\Delta u_w$
u_w	$\sigma-u_a$	$\Delta\sigma=\Delta u_a$
$\sigma+u_a-u_w$		$\Delta\sigma+\Delta u_a+\Delta u_w=0$
$\sigma+u_a-u_w$	u_a	$\Delta\sigma=\Delta u_w$
$\sigma+u_a-u_w$	u_w	$\Delta\sigma=\Delta u_a$

*The test verifies the stress state variables if there is no volume change or change in degree of saturation.

4.14 Discussion of Null Tests

The null test results are an important aspect of this thesis since they either prove or disprove the validity of the proposed stress state variables. The stress state variables form the basis for the analysis of the volume change problem. A detailed analysis of the null tests is presented in Appendix C while only a summary is given here.

The key question considered during the analysis was; Does any process or volume change occur as a result of the changes in pressures? If some volume change is measured, an attempt is made to ascertain its cause. Some of the main factors considered with respect to possible volume changes are:

(i) test procedure

(ii) air diffusion through the water

(iii) water loss from the sample

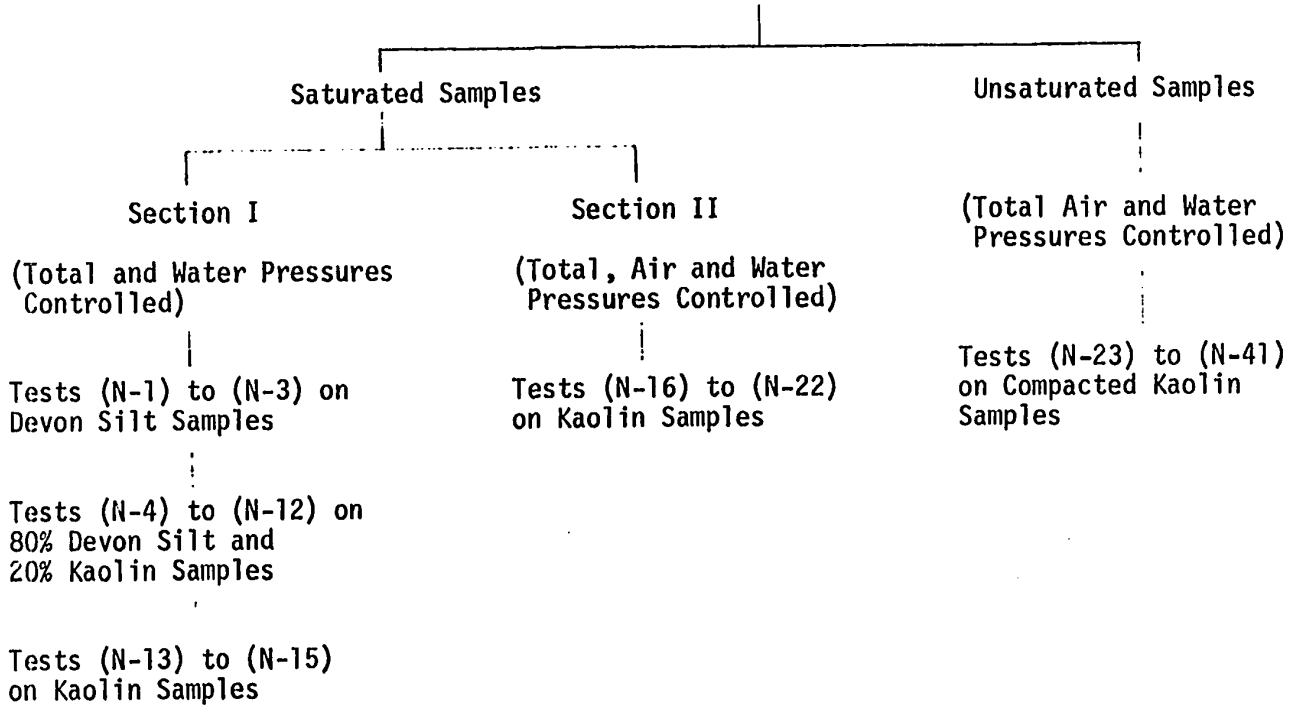
(iv) secondary consolidation.

In the null test program a series of tests were first performed on saturated samples and then a series was performed on unsaturated samples. All volume-weight relationships and pressure changes are presented in Appendix C. A summary of the test program is shown in Table IV.4.

The first fifteen tests on the saturated samples involved changing the total and water pressures and monitoring the water and overall sample volume changes. The tests on the saturated samples

TABLE IV.4

NULL TEST PROGRAM



(Section I) served to assess the reliability of the test procedure and equipment for a known case. The first few tests showed that small amounts of entrapped air in the sample resulted in significant total and water phase volume changes. After the testing technique and the means of removing entrapped air were improved, the results were more satisfactory. The last set of null tests indicated a total volume change of approximately 1.8 percent of that estimated for a corresponding effective stress increase. The corresponding water volume change was approximately 0.4 percent. These volume changes do not reflect any limitation in the effective stress variable for a saturated soil but rather indicate testing technique limitations. The immediate total volume changes are related primarily to entrapped air and measuring system compliance. Long term volume changes are related to slight amounts of secondary compression of the soil structure and compression of the pore fluid. The results are sufficiently accurate to verify the stress state variables for engineering purposes.

In the tests performed for Section II, the top of the saturated samples were subjected to an air pressure. The total and water volume changes were monitored on all tests. With regard to the testing technique, there was some difficulty in applying all three pressures simultaneously. In the one-dimensional oedometer, the air pressure took a few seconds to build up. As a result, the sample underwent a slight immediate compression. A second problem was the diffusion of air through the water phase of the sample. This was reflected as water leaving the sample. However, the overall volume of the sample

remained essentially constant. Figure 4.18 shows typical results. On the more carefully controlled tests, the total volume change over a period of several days was less than 0.1 percent for a 10 psi pressure increase on a soft, saturated soil. This is approximately 2 percent of that anticipated for a corresponding change in effective stress.

A total of nineteen null tests were performed on unsaturated samples. Even the first few tests performed showed remarkably low volume changes. There was a slight tendency for some water to go into the sample during the early stages (i.e. up to 100 minutes) of the test but later there was evidence of a slight volume of water leaving the sample. The phenomenon is readily understood when we realize that at the moment the pressures are applied, two secondary, transient processes commence. The air starts to diffuse through the water primarily from the top of the sample while the water tends to compress the occluded air bubbles from the bottom of the sample. The entrapped air bubbles appear to be compensated for fairly readily whereas with time the diffusion process reverts to a steady state process.

During January of 1972, a new triaxial apparatus was designed with more complete data acquisition capabilities. The null test program was used to simultaneously assess the performance of the apparatus and perform further precise null tests. Two new problems were encountered. First, there was a delay in the application of the cell pressure which allowed the upper load cap to be lifted from the

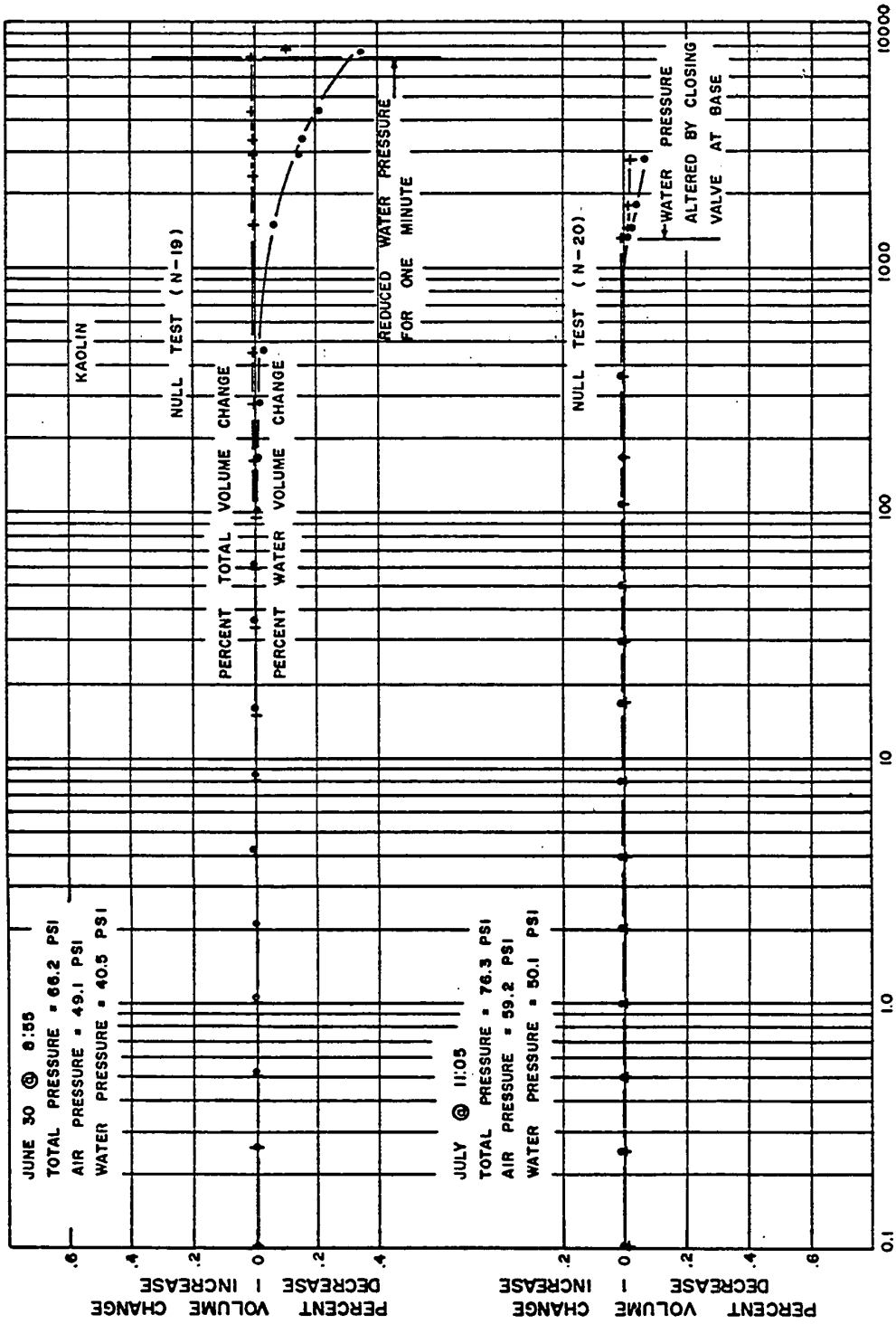


FIGURE 4.18 NULL TESTS (N-19) AND (N-20) ON SAMPLE NO. 6

sample at the start of the test. Second, there was a slow leakage of water through the rubber membranes surrounding the sample. The first problem was overcome by using a surge tank to rapidly increase the cell pressure. The second problem was overcome by means of a composite membrane consisting of two rubber membranes separated by slotted aluminum foil.

The last set of null tests (i.e. (N-35) to (N-41) were performed on Triaxial Apparatus No. 2 with the procedural problems solved. Figures 4.19 to 4.21 show the results of null tests N-35 to N-40. The results show essentially no volume change in either the total sample or the water phase. Expanding the volume change scale by 10 times (Figure 4.22) shows that the results are approaching the accuracy of the measuring systems. The volume changes after one day are within one part in ten thousand. The total volume changes were approximately 0.3 percent of the estimated volume change from a corresponding $(\sigma-u_w)$ increase. The water volume changes were approximately 2.5 percent of those estimated for a corresponding (u_a-u_w) decrease. Even when taking into account the increased stiffness of the samples, the two stress state variables for the unsaturated soils are verified at least as conclusively as the effective stress variable was for the saturated samples.

The means and standard deviations for all the loading and unloading null tests performed on sample #31 are presented in Figure 4.23. The standard deviations of the total volume changes completely mask any process that may be taking place over the entire set of null

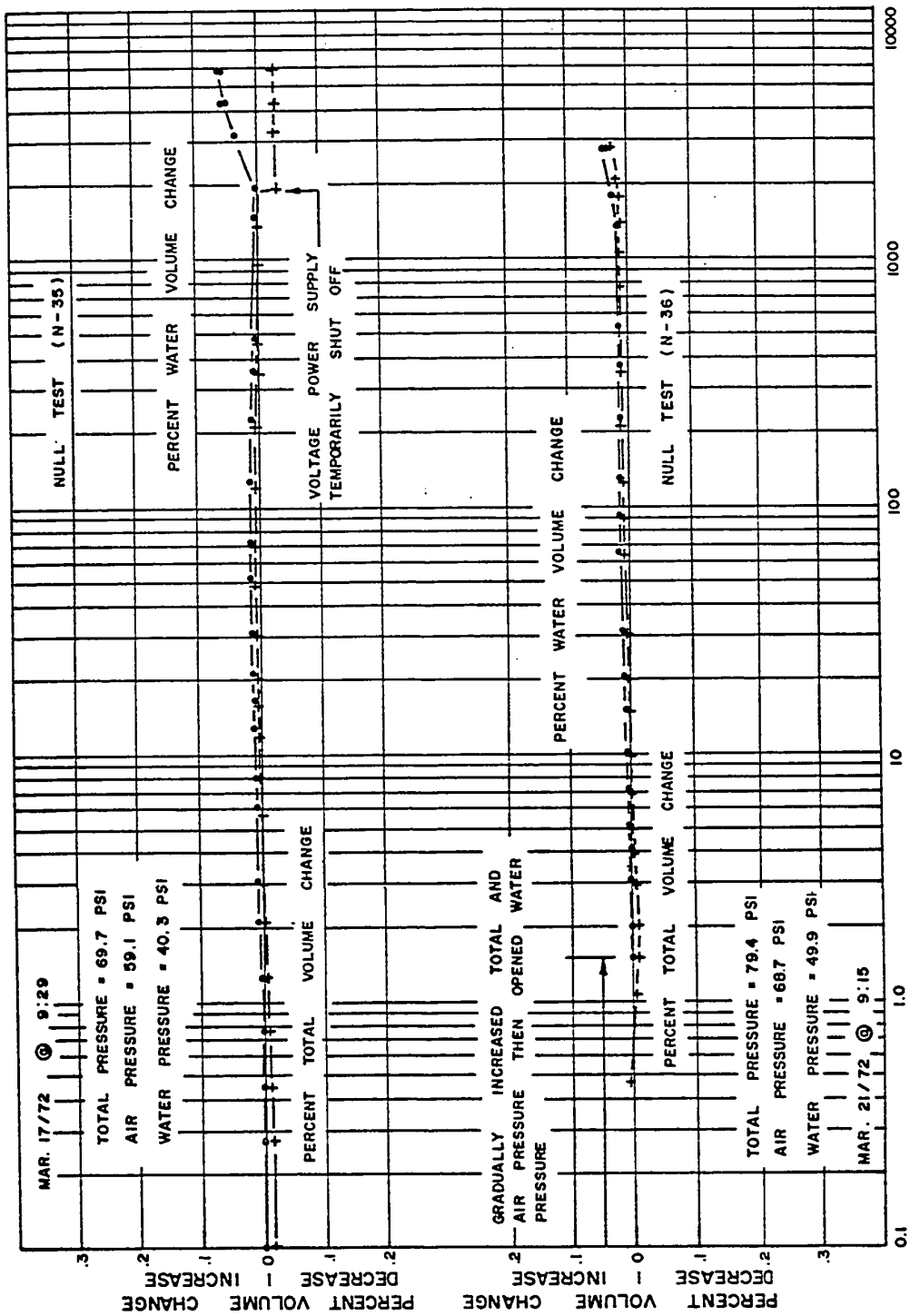


FIGURE 4.19 NULL TESTS (N-35) AND (N-36) ON SAMPLE NO. 31

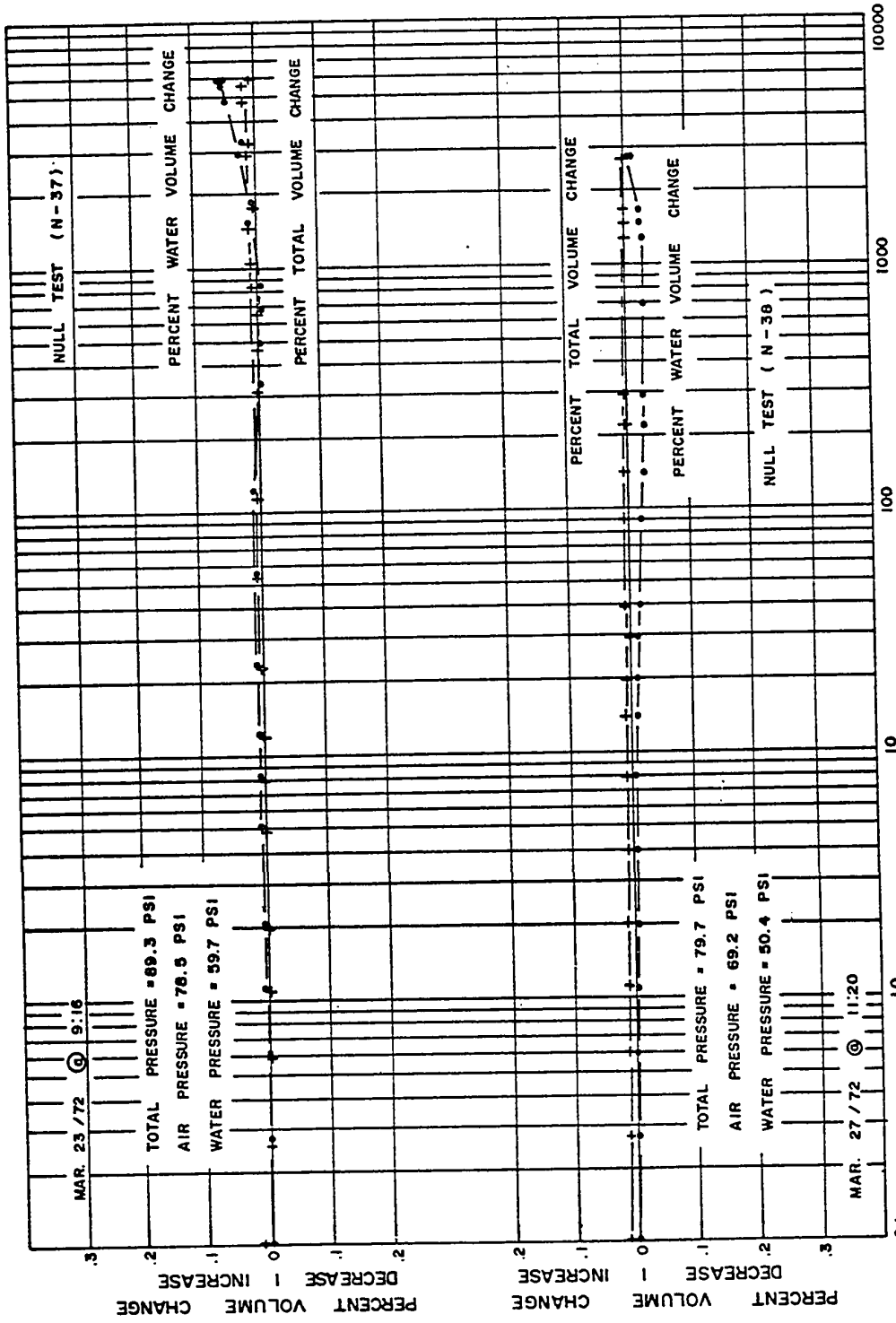


FIGURE 4.20 NULL TESTS (N-37) AND (N-38) ON SAMPLE NO. 31

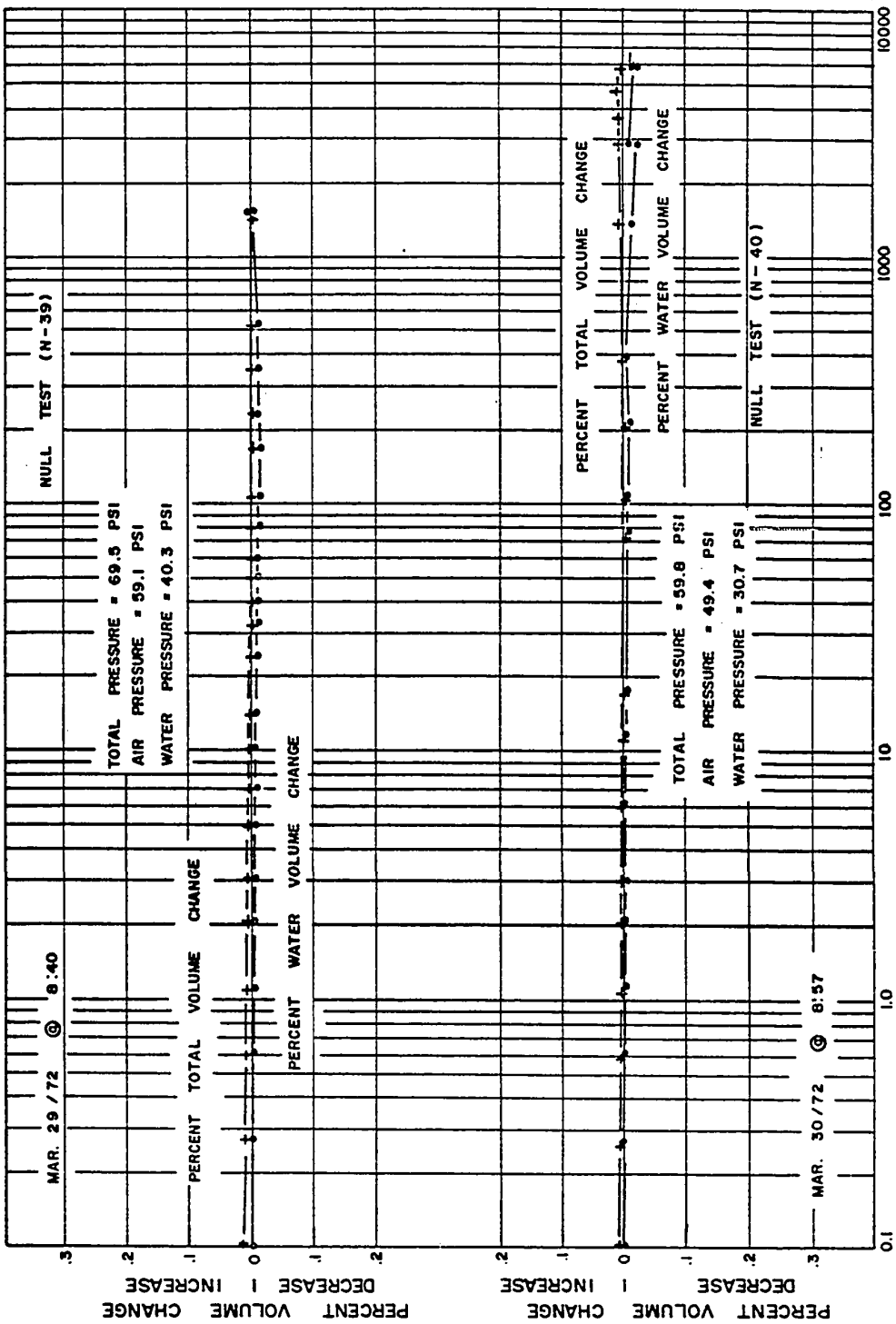


FIGURE 4.21 NULL TESTS (N-39) AND (N-40) ON SAMPLE NO. 31

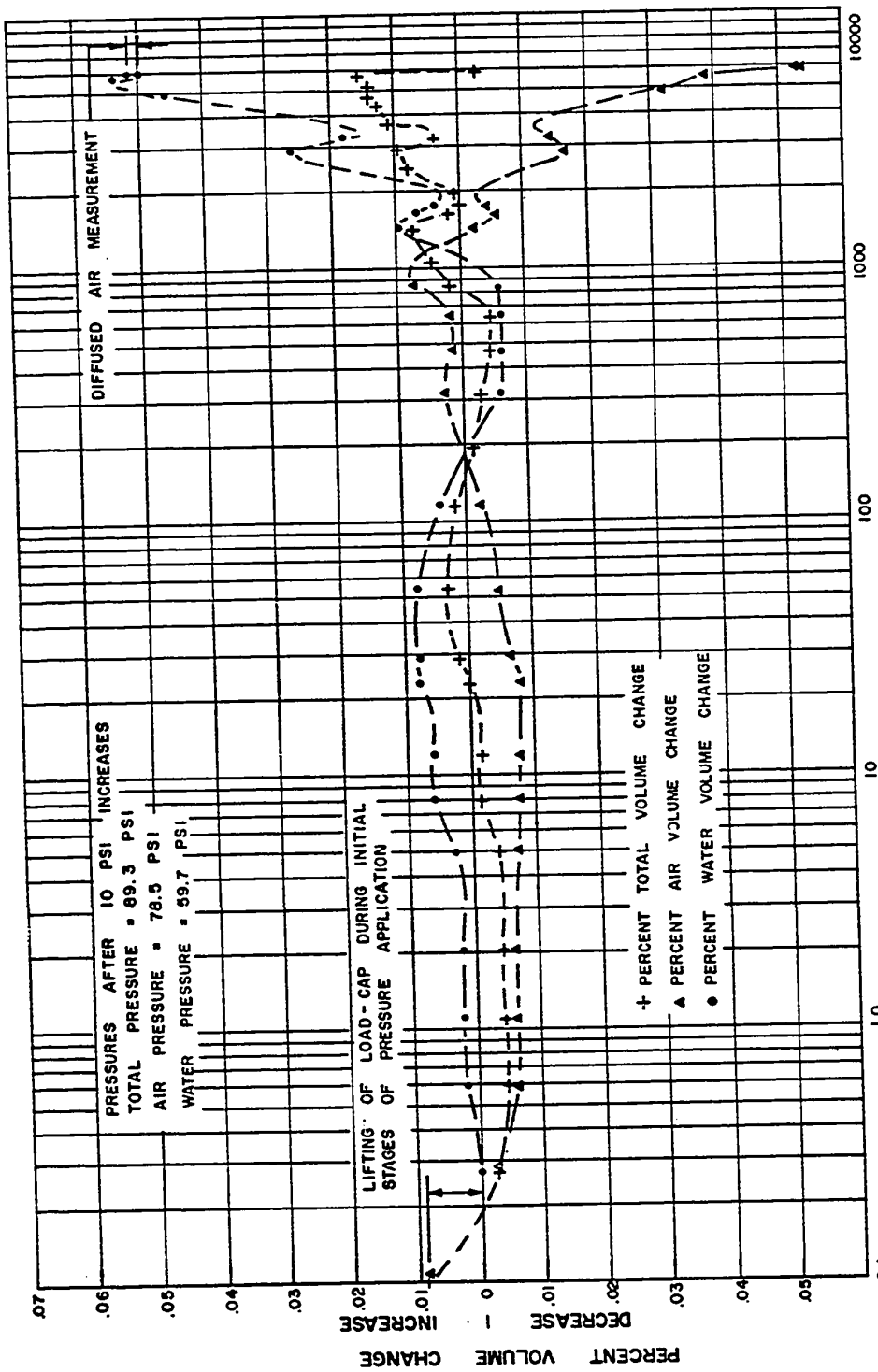


FIGURE 4.22 NULL TEST (N-37) ON SAMPLE NO. 31 (EXPANDED SCALE)
MARCH 23 @ 9:16

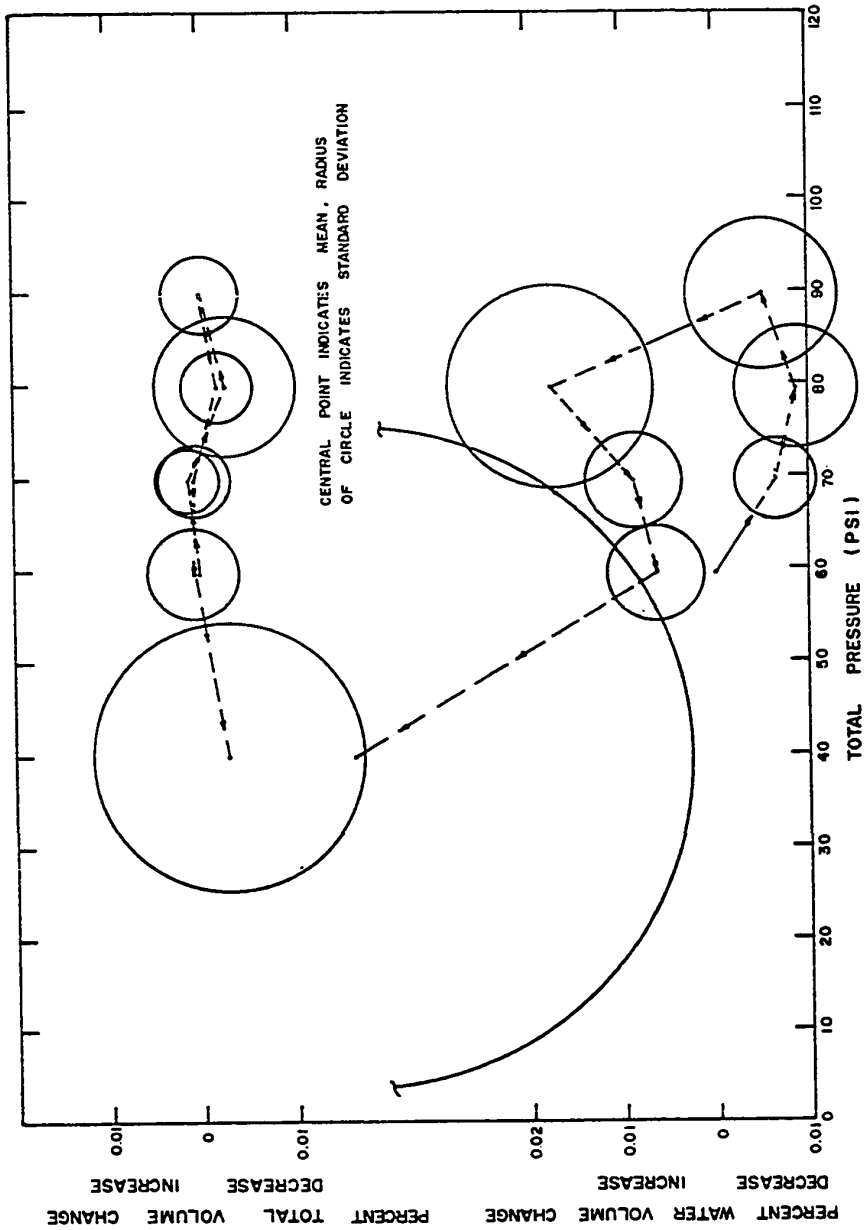


FIGURE 4.23 MEANS AND STANDARD DEVIATIONS FOR TOTAL AND WATER VOLUME CHANGES FROM ALL NULL TESTS ON SAMPLE NO. 31

tests. The water volume changes indicate a slight increase in the water volume but do not show any consistent evidence of a process.

These results are extremely encouraging and supply the necessary evidence to state with assurance that the proposed stress state variables can be used as the basis for formulating the volume change analysis in unsaturated soils. That is, any two of the following three stress component combinations,

(i) $\sigma - u_w$

(ii) $\sigma - u_a$

(iii) $u_a - u_w$,

can be considered as the stress state variables for an unsaturated soil.

CHAPTER V

DEFORMATION ANALYSIS OF MULTIPHASE SYSTEMS

5.1 General

Chapter IV presented the analysis of stress for an unsaturated soil. The soil was visualized as consisting of two solid phases (i.e. soil particles and contractile skin) and two fluid phases (i.e. water and air). There were eight unknown stress variables (σ_x, σ_y, σ_z, τ_{xy}, τ_{yz}, τ_{zx}, u_a and u_w) involved in the equilibrium equations for the soil structure and the contractile skin. However, in each case there are only three equations relating them. To completely describe the volume change behavior of an unsaturated soil element, both the soil structure and the contractile skin must be considered. Obviously, more information is required to formulate and solve problems. The additional information is supplied by the deformation-displacement equations and the constitutive relationships.

The deformation-displacement analysis involves the "mapping" of the movement (translation) of points or particles. In soil mechanics, the soil structure is often assumed to behave as a linearly elastic continuum and the deformation-displacement formulation is consistent with that employed in the elasticity of solids (Biot, 1941). In the case of the contractile skin, however, the author is unaware of any complete and satisfactory deformation-displacement analysis. Probably

this is due to the unusual nature of the contractile skin. In this chapter, an attempt is made to provide a complete deformation-displacement formulation applicable to unsaturated soils.

Basic to the study of the contractile skin is the assumption that it behaves as a solid (Fung, 1969; Goodrich, 1969). The justification for this assumption lies primarily in the fact that forces applied to solids cause deformations that come to equilibrium whereas forces applied to liquids cause continuous deformation or flow. Since the contractile skin in an unsaturated soil comes to equilibrium under the application of forces, it is assumed to behave as a solid with air and fluids on either side.

5.2 Deformation Analysis Literature Review

As early as 1941, Biot made commendable contributions to the deformation analysis of unsaturated soil systems. His presentation of three dimensional consolidation was based on the following assumptions of interest with respect to the deformation analysis.

(i) isotropy of the material

(ii) infinitesimal deformations

(iii) water in the pores is incompressible

(iv) the water may contain air bubbles.

The deformation of the soil structure was assumed to correspond to a linear elastic solid. Biot pointed out that this did not constitute a complete deformation description of the macroscopic unsaturated soil element. He suggested an additional deformation vari-

able to designate the amount of water in the pores. Theta, θ, was used to denote the increment of water as a ratio of the total volume. Since all deformations are assumed to be small, the relation between the soil structure and the water phase may be taken as linear in the first approximation.

In 1955, Biot considered the case of a porous anisotropic solid containing a compressible viscous fluid. He defines the deformation tensor for both the soil structure and the fluid phase. He states, "The solid skeleton is considered to have a compressibility and shearing rigidity, and the fluid may be compressible. The deformation of a unit cube is assumed to be completely reversible. By deformation is meant here that determined by both strain tensors in the solid and the fluid which will now be defined. The average displacement components of the solid is designated by u_x, u_y, u_z, and that of the fluid by U_x, U_z, and U_z".

The normal deformation component for the soil structure takes the form $e_x^s = \partial u_x/\partial x$ and the shear deformation component takes the form $\gamma_{xy}^s = \partial u_y/\partial x + \partial u_x/\partial y$. The normal deformation component for the viscous fluid takes the form $e_x^f = \partial U_x/\partial x$ and the shear component is $\gamma_{xy}^f = \partial U_y/\partial x + \partial U_x/\partial y$. The shear deformation in the fluid becomes irrelevant for the case of non viscous fluid (Biot, 1957). The non viscous fluid dilation is written as $e^f = \partial U_x/\partial x + \partial U_y/\partial y + \partial U_z/\partial z$. Biot points out that this "is not the actual deformation in the fluid but simply the divergence of the fluid displacement field...".

Bishop (1957) considered the compression of an unsaturated soil in an undrained test. The change in volume was due to the compression of the air and the dissolving of air in the water. The change

in volume of air was presented as a ratio of the total volume. Hilf used a similar approach in 1956. Coleman (1962) used two deformation variables to represent the volume change behavior in an unsaturated soil. These were the change in volume of water with respect to the total volume and the change in total volume with respect to the total volume.

Radhakrishna (1967) made a thorough analysis of the state of deformation in an unsaturated soil. He used the Eulerian deformation tensor for the soil structure. Due to the elastic-plastic nature of soil, he proposes an incremental deformation tensor which can be subdivided into a volumetric deformation increment and a deviatoric deformation increment. Since the volumetric and deviatoric deformations must be referenced to some initial soil properties, Radhakrishna proposes that volume-weight relationships be used to map the state of an element. The mapping of the movement of a "state point" under the influence of any or all of the "state parameters" produces a "state path". He uses void ratio, water content and degree of saturation for mapping and terms them "state point functions". If the "state point function" uniquely represents the changes in all "state parameters", the function is "path independent".

The author feels that the above concepts are useful when considering an unsaturated soil. The void ratio change can be viewed as a representation of the total volume change of the sample. Likewise, the water content change as a representation of the deformation in the water phase and the degree of saturation change as a represent-

ation of the deformation of the contractile skin.

5.3 Multiphase Element for the Deformation Analysis

In continuum mechanics, the analysis of deformation involves the mapping of movement with respect to a material phase. The change in the relative position of points or particles in a body forms the basis for evaluating the deformation state variables. The deformation state variables should be such that when integrated over the body under consideration, they produce the displacements of the body. This concept applies for a single or multi-phase system regardless of the physical properties of the materials.

The term "deformation" is used throughout the thesis instead of the word "strain" since strain is intuitively linked with a change in stress (Fung, 1965). Since the stress in the contractile skin is a constant (i.e., surface tension), it is best to sever the stress-strain link when considering the contractile skin. This is also true when mapping the deformation of the fluid phases in a multiphase system. The analysis of deformation is independent of the material properties involved and is equally applicable for solids, liquids and gases.

In the field of kinematics of continuum mechanics there are four types of descriptions of movement (i.e., material, referential, spatial and relative)(Malvern, 1969). However, only two of these (i.e. referential and spatial) are of interest in our problem (Li and Lam, 1964).

The referential description has the original position and time as the independent variables. A fixed element of mass is chosen and its motion is traced. When the reference configuration is the initial configuration, the description is generally called the Lagrangian description. The time variable disappears when equilibrium states are observed. In the elasticity of solids, the reference configuration is usually chosen as the initial unstressed state.

The spatial description has the present position and the present time as the independent variables. The spatial description fixes attention on a given region of space instead of a given body of matter. It is generally used in fluid mechanics and is commonly referred to as the Eulerian description (Frederick and Chang, 1965). Under steady state flow or equilibrium conditions, the time variable vanishes.

If we assume that the first derivatives of the displacements are small, then the squares and the products of the partial derivatives are negligible. This gives rise to the assumption of infinitesimal deformations under which the Lagrangian and Eulerian descriptions give the same results.

When considering multiphase systems, a large number of deformation and displacement terms become involved in the complete deformation analysis. In order to maintain proper differentiation of terms without creating new terms, superscripts are used to designate each phase. In the case of an unsaturated soil, the soil particle displacements and deformations have the superscript, p; the contractile

skin has the superscript, c; the air phase has the superscript, a; and the water phase has the superscript, w. The displacements and deformations of the overall element or soil structure has the superscript, s. Several volumetric designations are used in a synonymous manner for all phases. These are the percent volume change, the porosity change and the volumetric deformation.

5.4 Theoretical Deformation Analysis of Multiphase Systems

There is a direct analogy between stress and displacement gradients. The independent deformations are equal to the displacements divided by the total length of the element (Figure 5.1). Basic to the deformation analysis is the assumption that the deformations are continuous and the displacement functions are single-valued. In other words, discontinuities such as cracks are not permissible. In the deformation analysis of multiphase systems an independent referential element should not be used for each phase since the elements would not coincide after deformation. Two types of multiphase elements are functional. Either one consistent spatial element can be used for all phases (Lee, 1969) or a referential element can be used for one phase which becomes a spatial element with respect to the other phases. The latter procedure is used in most conventional soil mechanics analyses (e.g. theory of consolidation).

A basic consequence of the consistent element approach is that the sum of the deformations of the component phases must equal the deformation of the overall element. This is referred to as the "continuity requirement for multiphase systems". The continuity re-

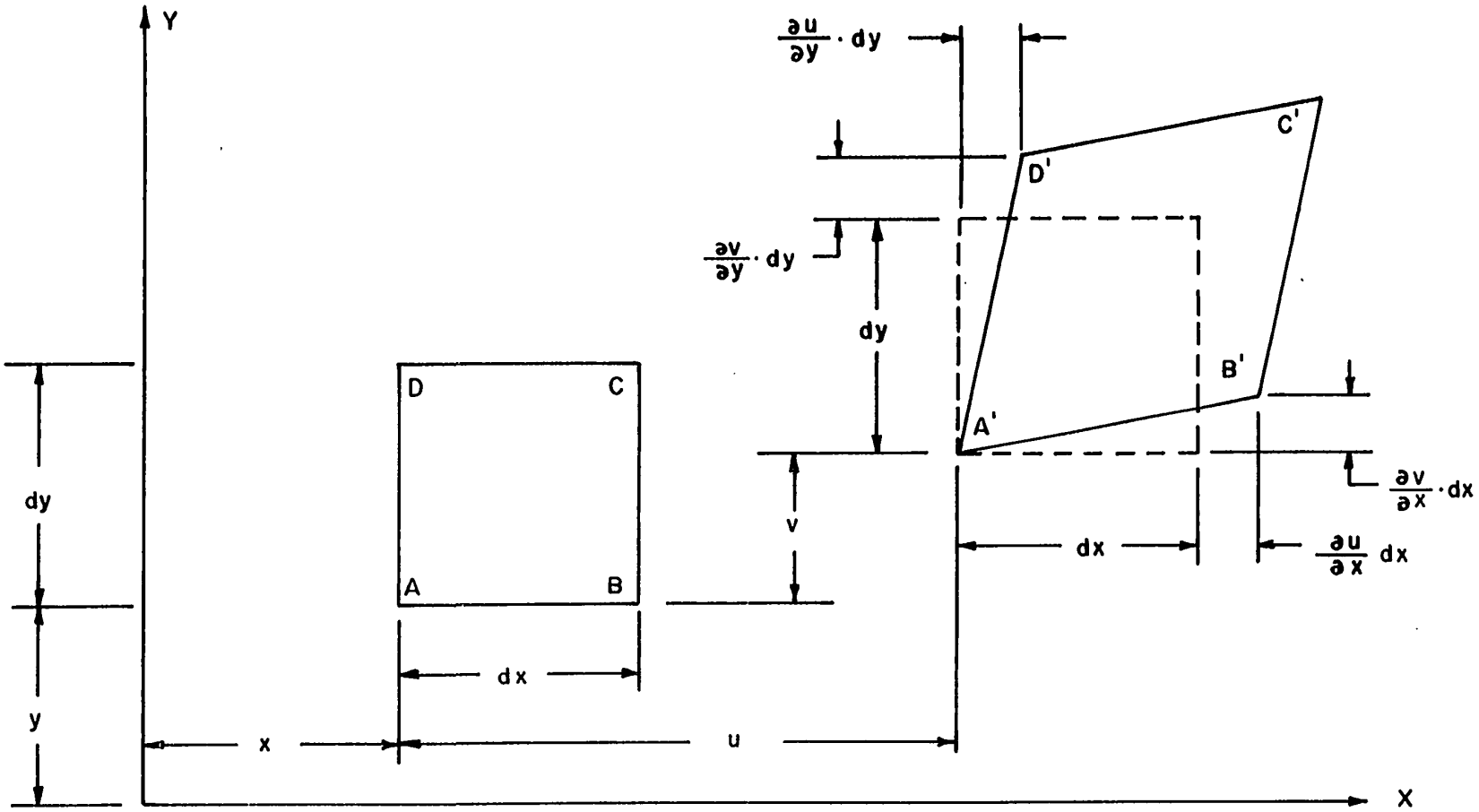


FIGURE 5.1 TRANSLATION AND DEFORMATION OF A TWO – DIMENSIONAL ELEMENT OF A ONE PHASE SOLID

quirement is a volumetric restriction that prevents "gaps" between the phases of a deformed multiphase system. On a volumetric basis, it is mathematically expressed as,

$$\frac{\Delta V}{V} = \sum_{i=1}^{N} \frac{\Delta V_i}{V} \quad \text{or}$$

$$e = \sum_{i=1}^{N} e_i$$

where ΔV = change in volume of the overall element

ΔV_i = change in volume of each phase

V = total volume of the element

e = deformation of the overall element

e_i = deformation of each phase

N = number of phases

The continuity requirement must also be maintained in each coordinate direction.

$$e_x = \sum_{i=1}^{N} e_{xi}$$

$$e_y = \sum_{i=1}^{N} e_{yi}$$

$$e_z = \sum_{i=1}^{N} e_{zi} \qquad 5.2$$

where e_x, e_y and e_z = overall deformation in the x,y and z directions, respectively

e_{xi}, e_{yi}, and e_{zi} = the deformations associated with each phase and the respective directions.

The deformations in each direction are a change in length referenced to the overall length of the element.

Let us now consider the application of the continuity requirement to the deformation analysis. Assume that each phase of a general two-phase multiphase is able to resist compression and shear (Figure 5.2). Phase I is used as a referential element while phase II is spatial with respect to phase I. For phase I, the displacements across the element are $\partial u^I/\partial x \cdot dx$ in the x-direction and $\partial v^I/\partial y \cdot dy$ in the y-direction. Dividing by the total length of the element, the normal deformations of phase I are $e_x^I = \partial u^I/\partial x$ in the x-direction and $e_y^I = \partial v^I/\partial y$ in the y-direction. Similarly, for phase II, the normal deformations are $e_x^{II} = \partial u^{II}/\partial x$ and $e_y^{II} = \partial u^{II}/\partial y$.

The shear deformation involved with phase I is $e_{xy}^I = \frac{1}{2}(\frac{\partial u^I}{\partial y} + \frac{\partial v^I}{\partial x})$. For phase II, it is $e_{xy}^{II} = \frac{1}{2}(\frac{\partial u^{II}}{\partial y} + \frac{\partial v^{II}}{\partial x})$. In the three-dimensional case, the independent deformation tensors for phase I and II are:

$$\begin{bmatrix} e_x^I & e_{yx}^I & e_{zx}^I \\ e_{xy}^I & e_y^I & e_{zy}^I \\ e_{xz}^I & e_{yz}^I & e_z^I \end{bmatrix}$$

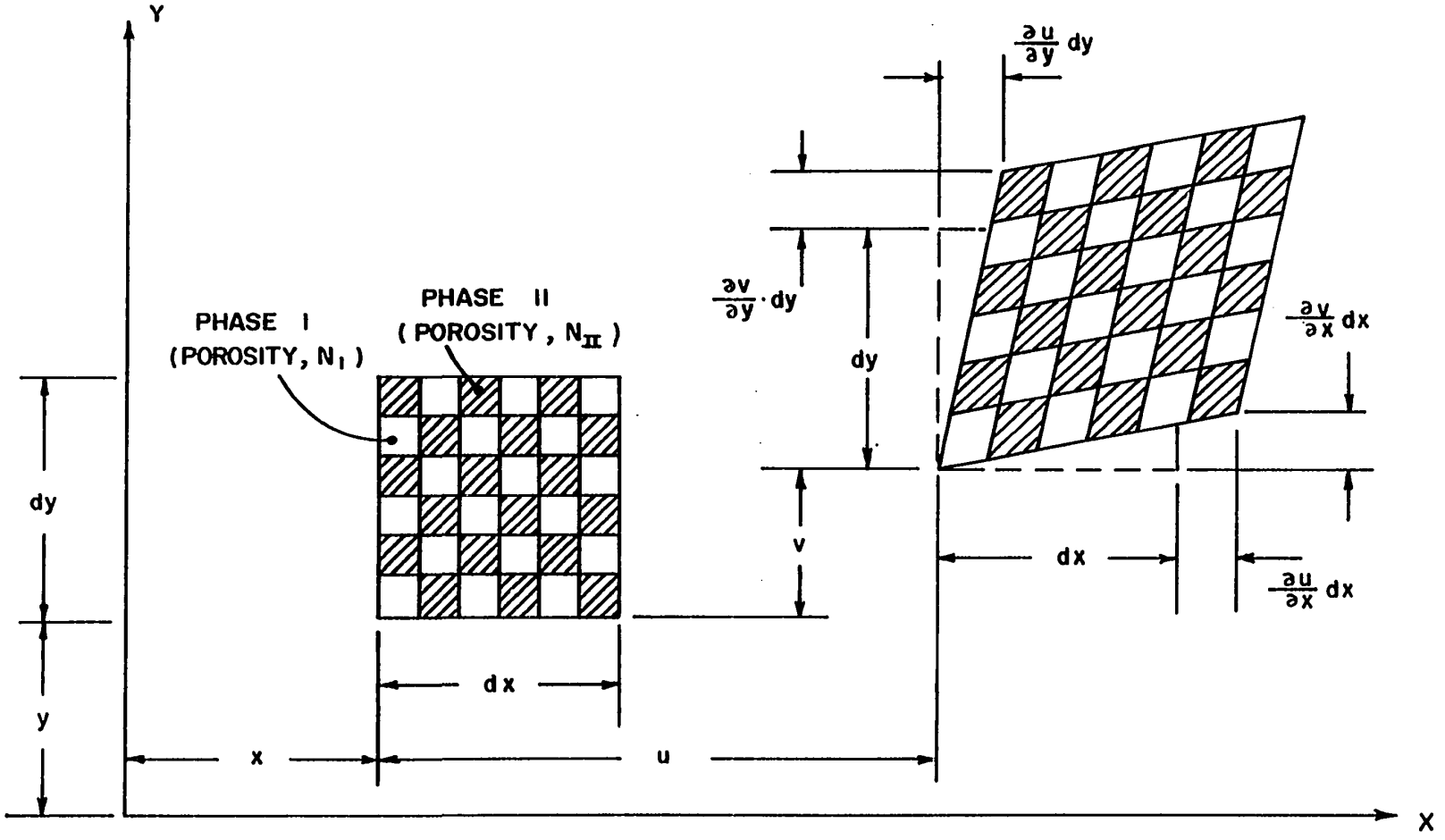


FIGURE 5.2 TRANSLATION AND DEFORMATION OF A TWO - DIMENSIONAL ELEMENT IN A TWO PHASE SYSTEM

and

$$\begin{bmatrix} e_x^{II} & e_{yx}^{II} & e_{zx}^{II} \\ e_{xy}^{II} & e_y^{II} & e_{zy}^{II} \\ e_{xz}^{II} & e_{yz}^{II} & e_z^{II} \end{bmatrix}$$

Since the deformation of each phase is described by a linear displacement field, it is possible to write a third set of deformation relationships that describe the overall element. However, only two of the three possible sets of deformation equations are independent for the two phase system. In general, the number of sets of independent deformation equations is equal to the number of phases in the multi-phase system.

The volumetric deformation of each phase depends only on the normal deformations. The volumetric deformation of phase I can be written,

$$e^I = e_x^I + e_y^I + e_z^I \qquad 5.6$$

In phase II, the volumetric deformation is,

$$e^{II} = e_x^{II} + e_y^{II} + e_z^{II} \qquad 5.7$$

Summing the volumetric deformations in each phase shows that the original volumetric continuity requirement has been maintained.

$$e = e^I + e^{II} \qquad 5.8$$

The sum of the shear deformations of all phases must also be equal to the overall shear deformation. If one phase cannot maintain shear it merely drops out.

5.5 Fluid-Solid Multiphase

The fluid-solid multiphase is visualized here as a particulate system of solids with interstitial spaces filled with water. This is not the only possible type of fluid-solid multiphase but it is the type given consideration at this point.

The soil particles can take compression and shear whereas the fluid can only take normal forces. A referential element of soil particles is chosen which becomes a spatial element with respect to the water phase.

The volumetric continuity requirement is,

$$\frac{\Delta V^s}{V} = \frac{\Delta V^p}{V} + \frac{\Delta V^w}{V} \quad \text{or}$$

$$e^s = e^p + e^w \qquad 5.9$$

where V^s = overall volume or soil structure volume

V^p = volume of soil particles

V^w = volume of water phase

e^s = deformation of soil structure

e^p = deformation of soil particle

e^w = deformation of water phase

The soil particles deformation tensor, written in terms of displacements is,

$$\begin{bmatrix} \frac{\partial u^p}{\partial x} & \frac{1}{2}\cdot\left(\frac{\partial u^p}{\partial y} + \frac{\partial v^p}{\partial x}\right) & \frac{1}{2}\cdot\left(\frac{\partial w^p}{\partial x} + \frac{\partial u^p}{\partial z}\right) \\ \frac{1}{2}\cdot\left(\frac{\partial u^p}{\partial y} + \frac{\partial v^p}{\partial x}\right) & \frac{\partial v^p}{\partial y} & \frac{1}{2}\cdot\left(\frac{\partial w^p}{\partial y} + \frac{\partial v^p}{\partial z}\right) \\ \frac{1}{2}\cdot\left(\frac{\partial u^p}{\partial z} + \frac{\partial w^p}{\partial x}\right) & \frac{1}{2}\cdot\left(\frac{\partial v^p}{\partial z} + \frac{\partial w^p}{\partial y}\right) & \frac{\partial w^p}{\partial z} \end{bmatrix}$$

The volumetric deformation of the soil particles is strictly due to the compression of the solids themselves. If we assume that the soil particles are incompressible, their volumetric deformation is zero (i.e. $\partial u^p/\partial x = \partial v^p/\partial y = \partial w^p/\partial z = 0$. However, the shear components do not disappear.

The water phase has an isotropic deformation tensor.

$$\begin{bmatrix} \frac{\partial u^w}{\partial x} & 0 & 0 \\ 0 & \frac{\partial v^w}{\partial y} & 0 \\ 0 & 0 & \frac{\partial w^w}{\partial z} \end{bmatrix}$$

The overall element or the soil structure has a deformation tensor composed of normal and shear components.

$$\begin{bmatrix} \frac{\partial u^s}{\partial x} & \frac{1}{2}\cdot\left(\frac{\partial u^s}{\partial y} + \frac{\partial v^s}{\partial x}\right) & \frac{1}{2}\cdot\left(\frac{\partial w^s}{\partial x} + \frac{\partial u^s}{\partial z}\right) \\ \frac{1}{2}\cdot\left(\frac{\partial u^s}{\partial y} + \frac{\partial v^s}{\partial x}\right) & \frac{\partial v^s}{\partial y} & \frac{1}{2}\cdot\left(\frac{\partial w^s}{\partial y} + \frac{\partial v^s}{\partial z}\right) \\ \frac{1}{2}\cdot\left(\frac{\partial u^s}{\partial z} + \frac{\partial w^s}{\partial x}\right) & \frac{1}{2}\cdot\left(\frac{\partial v^s}{\partial z} + \frac{\partial w^s}{\partial y}\right) & \frac{\partial w^s}{\partial z} \end{bmatrix}$$

The overall deformations reflect the volumetric effect of sliding and rolling between particles. The shear component deformations are equal to those of the soil particles deformation tensor.

The sum of the phase deformations is equal to the overall deformation both on a dimensional and volumetric basis. Since the soil particles volumetric deformation is zero, the water phase volumetric deformation is equal to the overall element deformation (i.e. $e^s = e^w$). In conventional soil mechanics testing, it is either the water volumetric deformation or the overall sample deformations that are measured.

The above analysis is equally applicable for a compressible pore fluid such as air. The analysis is also applicable for the case where the solid is an intact, porous rock, however, the physical interpretation is different. In this case, the volumetric deformation of the solids tends toward the overall volumetric deformation.

5.6 Air-Water Multiphase

The air-water multiphase is actually a three-phase system since it involves the contractile skin. Consider a spatial element involving air cavities and channels through a water matrix. The problem is somewhat fictitious since the contractile skin is unstable apart from the presence of another solid phase.

The volumetric continuity requirement can be stated,

$$\frac{\Delta V}{V} = \frac{\Delta V^w}{V} + \frac{\Delta V^a}{V} + \frac{\Delta V^c}{V} \quad \text{or}$$

$$e^o = e^w + e^a + e^c \qquad 5.10$$

where V = overall volume of the element

V^a = volume of air

V^c = volume of contractile skin

e^o = overall deformation

e^c = deformation of the contractile skin

The deformation tensors for each phase can be written directly. The air and water phases cannot withstand shear and therefore have an isotropic deformation tensor. The contractile skin is considered on a macroscopic scale and can have shear deformation components related to the stress components parallel to the surfaces of the element. The shear deformation exists for the same reason the shear stress components existed in Chapter IV.

$$\begin{bmatrix} \frac{\partial u^c}{\partial x} & \frac{1}{2}\cdot\left(\frac{\partial u^c}{\partial y} + \frac{\partial v^c}{\partial x}\right) & \frac{1}{2}\cdot\left(\frac{\partial w^c}{\partial x} + \frac{\partial u^c}{\partial z}\right) \\ \frac{1}{2}\cdot\left(\frac{\partial u^c}{\partial y} + \frac{\partial v^c}{\partial x}\right) & \frac{\partial v^c}{\partial y} & \frac{1}{2}\cdot\left(\frac{\partial w^c}{\partial y} + \frac{\partial v^c}{\partial z}\right. \\ \frac{1}{2}\cdot\left(\frac{\partial u^c}{\partial z} + \frac{\partial w^c}{\partial x}\right) & \frac{1}{2}\cdot\left(\frac{\partial v^c}{\partial z} + \frac{\partial w^c}{\partial y}\right) & \frac{\partial w^c}{\partial z} \end{bmatrix}$$

An overall deformation tensor can also be written. The volumetric deformation is equal to zero since we are considering a spatial element. The shear deformations are equal to those of the contractile skin tensor.

The phase deformations can be combined in accordance with the continuity requirement.

$$\frac{\Delta V}{V} = \frac{\Delta V^w}{V} + \frac{\Delta\Delta V^c}{V} + \frac{\Delta V^a}{V} \qquad 5.11$$

It is possible to have two physical interpretations of the continuity requirement. One approach is to assume that the volumetric deformation of the contractile skin is small and can be included in the volumetric deformation of the water phase. This is in fact what happens when attempting to measure the volume of water. Therefore, the continuity requirement can be written,

$$\frac{\Delta V}{y} = \frac{\Delta V^w}{V} + \frac{\Delta V^a}{y} \qquad 5.12$$

The volumetric deformation associated with the contractile skin can also be viewed as being equivalent to the volumetric deformation of the air phase. This approach towards the contractile skin is new and warrants a detailed presentation. Consider the special case of one bubble (i.e. soap bubble) in air (Figure 5.3). Remove an element of the bubble with dimensions dx, dy and dz. Suppose it

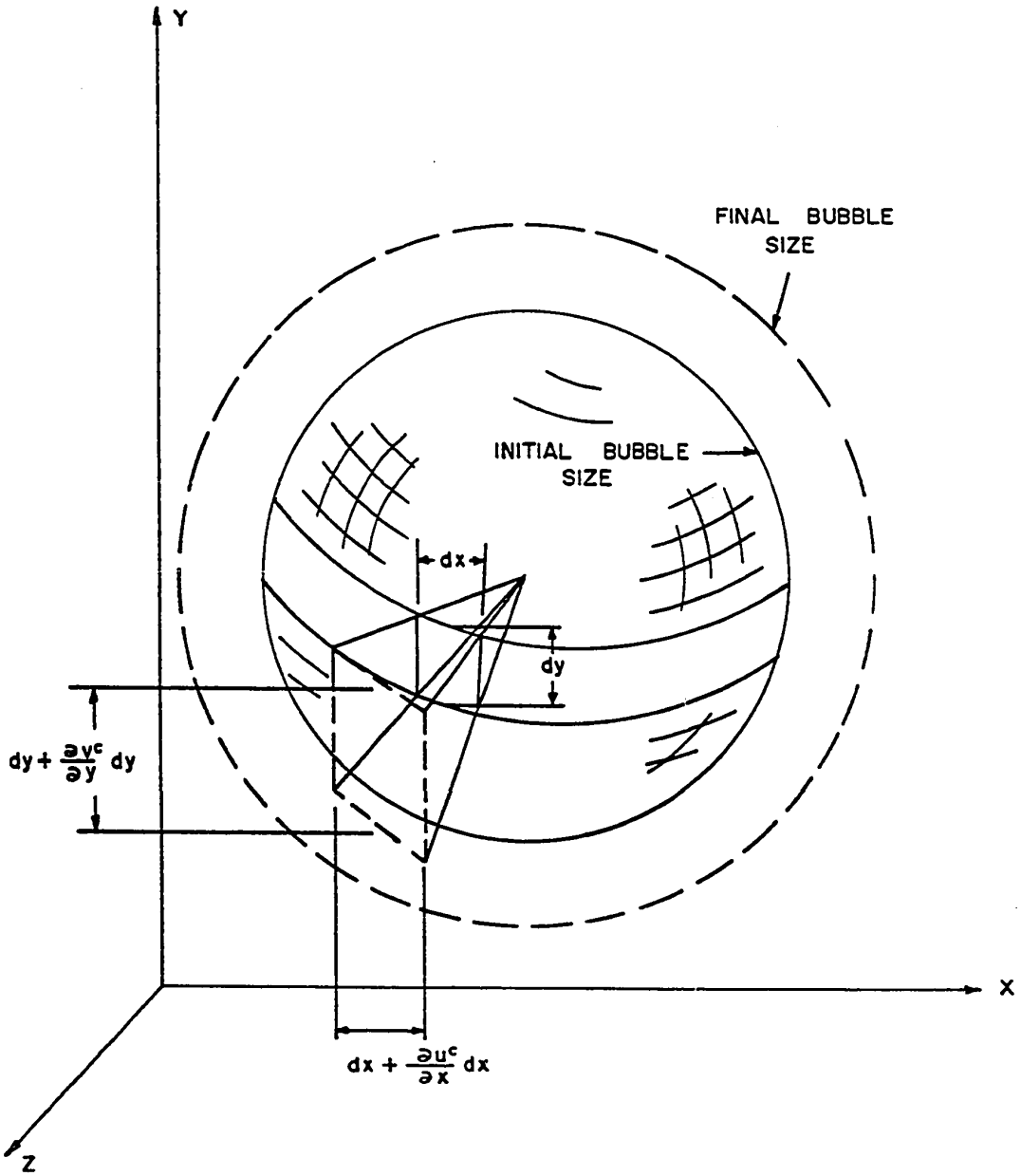


FIGURE 5.3 TRANSLATION AND DEFORMATION OF AN ELEMENT FROM A SOAP BUBBLE

were possible to insert a syringe needle into the bubble and inject more air. The bubble would increase in volume while it expanded. As the bubble expands, assume that sufficient fluid is added to keep the thickness of the contractile skin at a constant value. By choosing a sufficiently small element, the radius of curvature of the element does not introduce error into assuming that the tangential dimensions are planar. On the selected element, the deformation is $\partial u^c/\partial x$ in the x-direction and $\partial v^c/\partial y$ in the y-direction. No deformation has occurred in the z-direction since it is assumed that the contractile skin remains at a constant thickness, regardless of the radius of curvature.

When analysing a sphere, it is advantageous to express the deformations in terms of the radius, R(Figure 5.4). The translation and deformation of the element perpendicular to the z-axis maps two similar triangles. In the x-direction it can be expressed

$$\frac{(dx + \frac{\partial u^c}{\partial x} dx)}{R + \Delta R} = \frac{dx}{R} \qquad 5.13$$

Rearranging,

$$1 + \frac{\partial u^c}{\partial x} = 1 + \frac{\Delta R}{R} \quad \text{or}$$

$$e_x{}^c = \frac{\partial u^c}{\partial x} = \frac{\Delta R}{R} \qquad 5.14$$

In the y-direction,

$$e_y{}^c = \frac{\partial v^c}{\partial y} = \frac{\Delta R}{R} \qquad 5.15$$

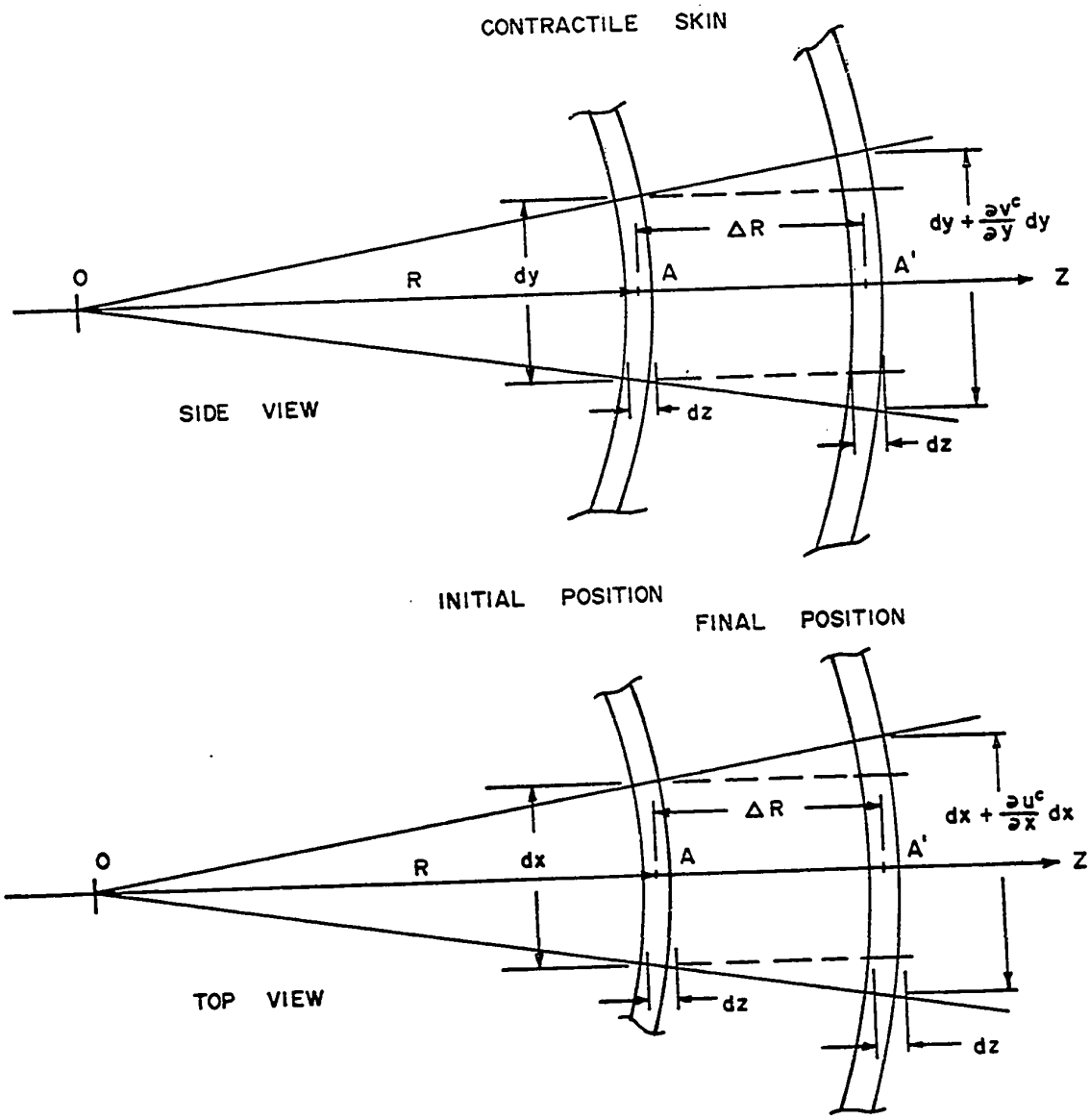


FIGURE 5.4 DIMENSIONS AND DISPLACEMENTS FOR AN ELEMENT OF THE BUBBLE ALONG THE Z-AXIS

The deformation in the z-direction is zero. The volumetric deformation of the bubble is therefore,

$$e^c = \frac{2 \cdot \Delta R}{R} \qquad 5.16$$

This relationship can also be obtained by differentiating the surface area equation and dividing by the original area. The surface area of a sphere is,

$$S^c = 4 \cdot \pi \cdot R^2 \qquad 5.17$$

A change in radius represents a change in surface area of

$$dS^c = 8 \cdot \pi \cdot R \cdot dR \qquad 5.18$$

The normalized increase in surface area is

$$\frac{dS^c}{S^c} = \frac{2 \cdot dR}{R} \qquad 5.19$$

The analysis shows that the volumetric deformation of the contractile skin is equivalent to the creation of surface area.

A similar analysis can be performed on an element with a contractile skin in the shape of a cylinder. An increase in internal

pressure results in a deformation in only one direction.

$$e_x^c = \frac{\partial u^c}{\partial x} \qquad e_y^c = 0 \qquad e_z^c = 0$$

By similar triangles, the deformation in the x-direction is $\Delta R/R$. This is also the volumetric deformation. For the general case of a contractile skin of irregular shape, the volumetric deformation is,

$$e^c = \int_{S^c} m \cdot \Delta R/R \qquad 5.20$$

where m = a variable depending on the shape of the contractile skin

R = radius associated with each element of the contractile skin

The above analysis shows that the deformation of the contractile skin can be envisaged as an increase in its surface area. When the contractile skin is combined with the air and water phase, its deformation is referenced to the overall dimensions of the element.

Let us first consider the increase in surface area with respect to the volume enclosed by the contractile skin. For example, the dimensionless volume change of a sphere is $3 \cdot dR/R$ whereas the surface area deformation is $2 \cdot dR/R$. This demonstrates that the volumetric deformation of a phase contained within the contractile skin

can be used as a measure of the deformation of the contractile skin. This simplifies the physical means of obtaining a measure of the deformation of the contractile skin. The above analysis demonstrates that the volumetric deformation of the contractile skin can also be viewed in terms of the volumetric deformation of the air phase.

5.7 Unsaturated Soil Case

In the case of an unsaturated soil, we are interested in mapping the movement of four phases (i.e. soil particles, contractile skin, air and water). The unsaturated soil can be visualized as a combination of the water-solid multiphase and the air-water multiphase. A referential element of soil particles is chosen and used as a spatial element with respect to the air, water and contractile skin phases.

Figure 5.5 shows the mapping of the displacements of the overall element. The displacements of each phase are written as continuous derivatives over the entire element. The consistent element and the linearity of the displacement fields allow the displacements of all phases to be superimposed.

The deformation tensors for all phases are the same as those previously outlined for the water-solid and air-water multiphases. The partial differential equations describing the volumetric deformation of each phase are as follows:

For the soil particles,

$$e^p = \frac{\partial u^p}{\partial x} + \frac{\partial v^p}{\partial y} + \frac{\partial w^p}{\partial z} \qquad 5.22$$

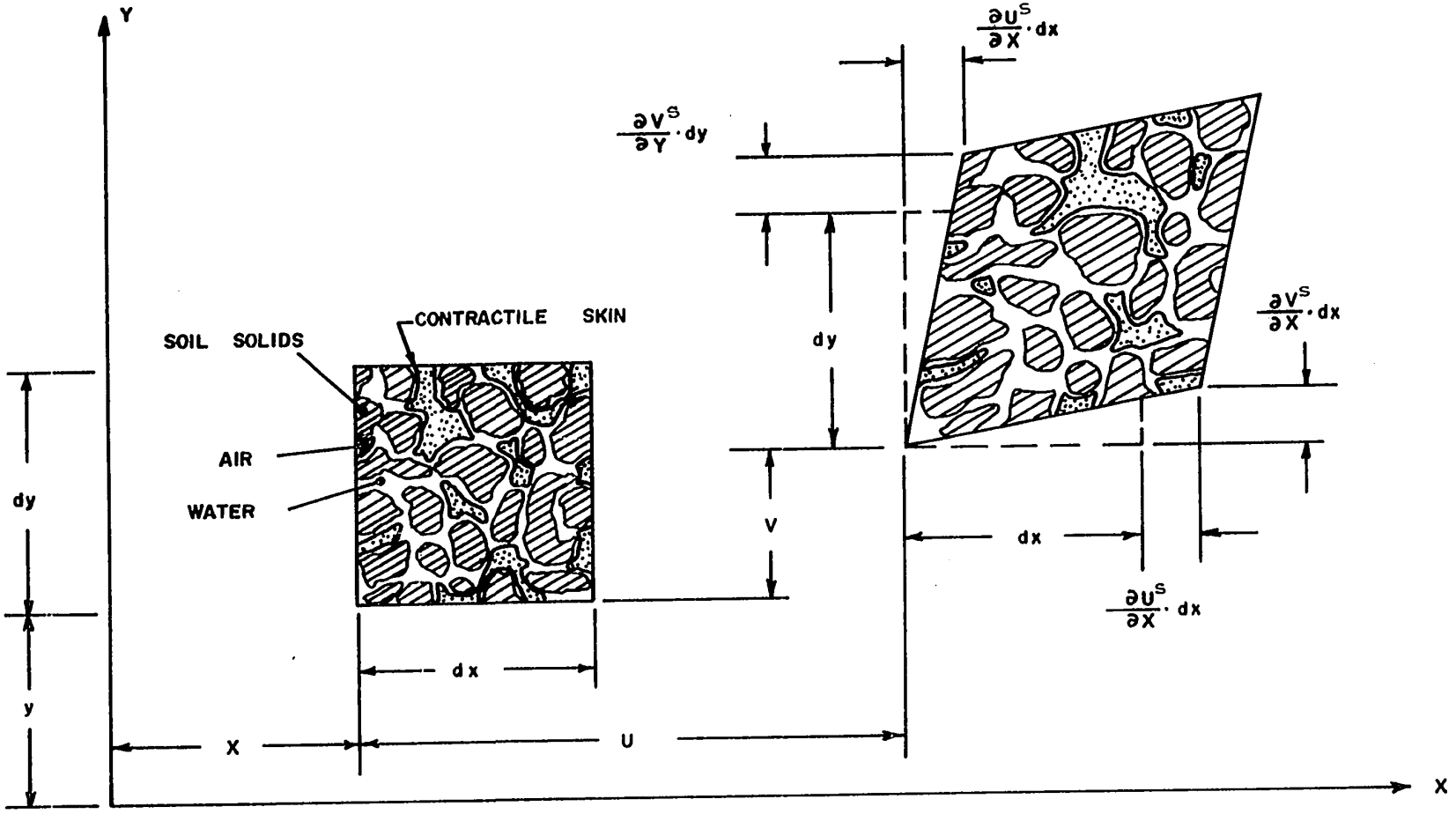


FIGURE 5.5 TRANSLATION AND DEFORMATION OF A TWO – DIMENSIONAL ELEMENT OF UNSATURATED SOIL

For the contractile skin,

$$e^c = \frac{\partial u^c}{\partial x} + \frac{\partial v^c}{\partial y} + \frac{\partial w^c}{\partial z} \qquad 5.23$$

For the air phase,

$$e^a = \frac{\partial u^a}{\partial x} + \frac{\partial v^a}{\partial y} + \frac{\partial w^a}{\partial z} \qquad 5.24$$

For the water phase,

$$e^w = \frac{\partial u^w}{\partial x} + \frac{\partial v^w}{\partial y} + \frac{\partial w^w}{\partial z} \qquad 5.25$$

The continuity requirement states that the sum of the deformation of each phase is equal to the overall deformation.

$$e^s = e^p + e^c + e^a + e^w \qquad 5.26$$

This equation can be physically interpreted in two ways. In the first case, the contractile skin is included with the water phase. Also, the volumetric deformation of the soil particles is assumed to be negligible. Therefore,

$$e^s = e^w + e^a \qquad 5.27$$

In the second case, the deformation of the air phase is used as a measure of the deformation of the contractile skin. Now,

$$e^S = e^W + e^C \qquad 5.28$$

It must be emphasized that there is only one continuity equation; however, there is the possibility of applying more than one physical restriction on the continuity requirement. The importance of this point becomes more obvious during the transient flow analysis (Chapter VII).

5.8 Other Volume-Weight Relationships

The deformations with respect to each phase can be presented in terms of conventional soil mechanics properties. The initial volume-weight properties must be known along with the deformations at any time. The void ratio can be written,

$$e = e_o + e^S \cdot V_T/V_S \qquad 5.29$$

where e = void ratio at any time

e_o = initial void ratio

e^S = volumetric deformation of the soil structure

V_T = total volume of the sample

V_S = volume of the soil solids

The water content is computed from the deformation of the water phase.

$$w = w_o + e^W \cdot V_T/W_S \qquad 5.30$$

where w = water content at any time

w_o = initial water content

e^w = deformation of the water phase

W_s = weight of soil solids

The change in the degree of saturation can be visualized as a deformation response of the contractile skin. It can be computed as,

$$S = S_o + e^a \cdot V_t/V_v \qquad 5.31$$

where S = degree of saturation at any time

S_o = initial degree of saturation

e^a = air volumetric deformation

V_v = volume of voids

The above equations show the relationship of the deformation mapping functions to the volume-weight properties commonly used in soil mechanics.

CHAPTER VI

CONSTITUTIVE RELATIONSHIPS FOR UNSATURATED SOILS

6.1 General

In Chapter IV the stress state variables were obtained by extraction from the independent equilibrium equations for each phase. In Chapter V the deformation state variables were developed based on the continuity requirement for a multiphase system. Since we have independently derived the stress and deformation state variables, the next logical step involves the development of constitutive relationships.

6.2 Constitutive Relationship Review

In 1940, Biot considered the three-dimensional consolidation of an unsaturated soil. His assumptions with regard to the material properties were that the stress-deformation relationship for the soil structure was reversible and linear. The soil was also assumed to be isotropic. Biot considers the case where the pore water may contain air bubbles. The effects of surface tension are ignored; however, the pore water pressure is considered as a second independent stress state variable. Using the terminology consistent with this thesis, the soil structure stress-deformation equations are,

$$e_x = \frac{(\sigma_x - u_w)}{E} - \frac{\nu}{E}(\sigma_y + \sigma_z - 2 \cdot u_w) + \frac{u_w}{3 \cdot H}$$

$$e_y = \frac{(\sigma_y - u_w)}{E} - \frac{\nu}{E}(\sigma_x + \sigma_z - 2 \cdot u_w) + \frac{u_w}{3 \cdot H}$$

$$e_z = \frac{(\sigma_z - u_w)}{E} - \frac{\nu}{E}(\sigma_x + \sigma_y - 2 \cdot u_w) + \frac{u_w}{3 \cdot H} \qquad 6.1$$

$$e_{xy} = \frac{1}{G} \cdot \tau_{xy}$$

$$e_{yz} = \frac{1}{G} \cdot \tau_{yz}$$

$$e_{zx} = \frac{1}{G} \cdot \tau_{zx} \qquad 6.2$$

where E = elastic modulus with respect to a change in total stress

G = shear modulus

ν = Poisson's ratio

H = an additional physical constant (Its physical significance is interpreted later)

The deformation of an unsaturated soil is therefore described in terms of the effective stress state variable and the pore fluid pressure. Biot realized that the above equations did not completely describe the deformation state of an unsaturated soil. Therefore, he proposed another constitutive relationship to describe the dependence of an increment of water content change on the above stress state variables.

$$\theta = a_1(\sigma_x - u_w) + a_2(\sigma_y - u_w) + a_3(\sigma_z - u_w) + a_4 \tau_{xy}$$

$$+ a_5 \cdot \tau_{yz} + a_6 \cdot \tau_{zx} + a_7 \cdot u_w \qquad 6.3$$

where θ increment of volumetric water content

a_1 to a_7 = soil parameters

If the soil is isotropic, $a_4 = a_5 = a_6 = 0$ and $a_1 = a_2 = a_3$. Therefore it is possible to write the constitutive equation in terms of two physical constants.

$$\theta = \frac{1}{3 \cdot H_1} (\sigma_x + \sigma_y + \sigma_z - 3 \cdot u_w) + \frac{u_w}{R} \qquad 6.4$$

By introducing the assumption of the existence of a potential energy of the soil, Biot proves that H_1 is equal to H. Thus there are four distinct physical constants (i.e. E, ν, H and R) that describe to a first approximation the behavior of the soil. Biot interprets the new physical constants as follows:

"To intrepret the constants H and R consider a sample of soil enclosed in a thin rubber bag so that the stresses applied to the soil be zero. Let us drain the water from this soil through a thin tube passing through the walls of the bag. If a negative pressure, $- u_w$, is applied to the tube a certain amount of water will be sucked out. This amount is given by,

$$\theta = - \frac{u_w}{R} \qquad 6.5$$

The corresponding volume change of the soil is given by

$$e = - \frac{u_w}{H} \qquad 6.6$$

The coefficient 1/H is a measure of the compressibility of the soil for a change in water pressure, while 1/R measures the change in water content for a given change in water pressure."

Biot's article has been reviewed in detail due to his profound comprehension of the physical behavior of unsaturated soils. Later it will be shown that with some modifications, Biot's constitutive relationships are consistent with those proposed in this thesis. In 1955, Biot extended his work to include an anisotropic solid and a viscous compressible pore fluid.

Biot's work appears to lack in a complete understanding of the behavior of the contractile skin. Although Lord Kelvin presented his constitutive relationship for the surface tension membrane in 1871, it had not been related to soil behavior at the time Biot did his research work. Kelvin's equation related the pressure difference across an air-water interface, (u_a-u_w), with its radius of curvature, r. Written in the form of a constitutive relationship, it is

$$d(u_a-u_w) = 2 \cdot T_s \cdot d(r^{-1}) \qquad 6.7$$

It was not until 1948 that Croney and Coleman brought the importance of the soil suction term (u_a-u_w), to the attention of soils

engineers. Croney (1952) proposed a constitutive relationship to account for a change in suction due to an applied external load. Their equation took the form,

$$\alpha \cdot P - S = u \qquad 6.8$$

where P = external or overburden pressure

S = negative pressure in the soil water as measured on an unloaded sample in the laboratory under atmospheric pressure.

If this equation is rewritten and interpreted within the context of this thesis, it takes the form,

$$\alpha \cdot d(\sigma_y - u_a) - (u_a - u_w)_o = (u_a - u_w)$$

or

$$(u_a - u_w) - (u_a - u_w)_o = \alpha \cdot d(\sigma_y - u_a) \qquad 6.9$$

Alpha, α, is a material property relating two stress state variables. Physically interpreted, it is the slope of the relationship between suction $(u_a - u_w)$ and the applied load $(\sigma_y - u_a)$. Croney's constitutive relationship says nothing about the total stress state variables in the x and y-directions. The uniqueness of the relationship and the constancy of α is doubtful except under specific test conditions.

Croney and Coleman plotted their measurements of pore water

tension using Schofield's (1935) pF scale or the logarithm of the water head in centimeters. The plot tends toward a straight line over a limited range of tensions.

The modifications to Terzaghi's effective stress equation can also be considered as constitutive relationships since they involve a soil property to link stress state variables. This applies for Bishop's equation, (1959); Aitchison's equation, (1956); Croney, Coleman and Black's equation, (1958); Jennings' equation, (1960) and Richards' equation (1966). Physically interpreted, they represent the relationship between stress state variables at a stress point in space.

Hilf (1956) and Bishop (1957) examined the relationship between volume change and air pressure change for a closed, unsaturated soil system. Bishop's equation was,

$$\frac{\Delta P}{P_o} = \frac{\frac{\Delta V}{V}}{\frac{\Delta V}{V} + (1-S_o+S_o \cdot h) \cdot n_o} \qquad 6.10$$

where P = air pressure

P_o = initial air pressure

$\Delta V/V$ = volumetric deformation

S_o = initial degree of saturation

n_o = initial porosity

h = Henry's coefficient of solubility

They assume that the soil solids and the water are incompressible (i.e. $e^S = e^W = 0$). Therefore, the overall or soil structure

deformation and the air phase deformation are equal. The difference between the air and water pressures is ignored. Written in terminology consistent with this thesis, the equation takes the form,

$$\frac{\Delta u_a}{u_{ao}} = \frac{-e^a}{e^a+(1-S_o+S_o \cdot h)\cdot n_o} \qquad 6.11$$

Rearranged in the form of a constitutive relationship, the equation is,

$$\Delta u_a = \frac{-u_{ao}}{1 + (1-S_o+S_o \cdot h)\cdot \frac{n_o}{e^a}} \; e^a \qquad 6.12$$

where

$$\frac{-u_{ao}}{1 + (1-S_o+S_o \cdot h) \cdot \frac{n_o}{e^a}} = \text{a stiffness coefficient}$$

Since the stiffness coefficient contains the deformation state variable, e^a, the constitutive relationship is non linear.

Jennings and Burland (1962) appear to be the first to question the uniqueness between void ratio and Bishop's effective stress equation. Bishop and Blight (1963) also recognized that there were problems and concluded that it was not the effective stress equations stress path that needed to be kept in mind but the paths of the two components (i.e. $(\sigma-u_a)$ and (u_a-u_w). They suggested plotting volume change data versus both state variables as a three-dimensional plot. In 1965, Burland re-iterated his dissatisfaction with Bishop's effective stress equation by explaining the independent roles of each component of Bishop's

equation. The author would also like to summarize his thoughts on the significance of Bishop's equation: First, Bishop's equation is a constitutive relationship and not a stress state variable, and secondly, it does not produce a unique relationship with deformation. This essentially eliminates its usefulness in the volume change analysis of unsaturated soils.

In 1962, Coleman uncoupled the components of Bishop's equation and proposed a set of constitutive relationships for the soil structure and water phase. He considered the volumetric deformations of a triaxial specimen. The mean stress is designated as $\sigma = \frac{1}{3} \cdot (\sigma_1 + 2 \cdot \sigma_3)$, where σ_1 is the vertical stress and σ_3 is the lateral stress. The water volumetric deformation with respect to the overall sample is

$$- \frac{dV_w}{V} = - C_{11} \cdot (du_w - du_a) + C_{12} \cdot (d\sigma - du_a) + C_{13} \cdot (d\sigma_1 - d\sigma_3) \qquad 6.13$$

where the compressibility parameters, C, depend solely upon the current values of the stresses and the stress history of the soil. The over- or total volume deformation is written as,

$$- \frac{dV}{V} = - C_{21} (du_w - du_a) + C_{22} \cdot (d\sigma - du_a) + C_{23} \cdot (d\sigma_1 - d\sigma_3) \qquad 6.14$$

The change in shear strain is written,

$$-(de_1 - de_3) = - C_{31} \cdot (du_w - du_a) + C_{32} \cdot (d\sigma - u_a) + C_{33} \cdot (d\sigma_1 - d\sigma_3) \qquad 6.15$$

Coleman states that "For elastic behavior of soil the only

coefficients needed are C_{22} and C_{33} which are then proportional to the reciprocal of the bulk and shear modulii respectively." "For drained, isotropic swelling and shrinking behavior of soil, the coefficients C_{11}, C_{12}, C_{21} and C_{22} are needed, all other terms being zero."

Coleman published these equations in a correspondence in Geotechnique and it appears they have gone unheeded. The similarity of these equations to those subsequently proposed by the author, should be noted.

Aitchison realized the importance of mapping volume change with respect to the independent state variables in 1967. In 1969 he presented typical volume change curves obtained by independently following the $(\sigma-u_a)$ and (u_a-u_w) stress paths.

In 1968, Matyas and Radhakrishna performed tests on a mixture of 80 percent flint powder and 20 percent kaolin in which they controlled the total, air and water pressures. The mixture formed had a meta-stable structure and their data demonstrates a collapse phenomena. They performed isotropic and Ko compression tests. The main purpose of the testing program was to predict the uniqueness of two surfaces. These were the surface traced out by void ratio versus $(\sigma-u_a)$ and (u_a-u_w), and the surface traced traced out by degree of saturation $(\sigma-u_a)$ and (u_a-u_w). Their technique involved preparing several samples under identical volume weight conditions and testing them over a variety of stress paths. When the (u_a-u_w) state variable was <u>decreased</u> or the $(\sigma-u_a)$ state variable was <u>increased</u> their void ratio results traced out a single warped surface. For the collapsing soil tested,

the degree of saturation was always an increasing variable and the soil structure always decreased in volume. In Radhakrishna's thesis (1967) a few tests were performed under constant water content conditions with an increasing degree of saturation. These tests are most significant from the standpoint of verifying uniqueness of the surface since they follow a stress path that is slightly skewed with respect to the previous paths. They appear to verify uniqueness for a meta-stable structured soil with respect to the stress paths considered.

Deviations from the above stipulated stress paths showed that the surface was not completely unique. They state that the "restrictions on the state paths arise from the fact that the hysteresis in the soil structure due to loading and unloading, wetting and drying, introduce certain non unique characteristics." The plots of degree of saturation versus $(\sigma-u_a)$ and (u_a-u_w) for the above stress paths show that "the wetting paths do not appear to lie wholly on this surface". They attribute the deviations to "incomplete saturation during the wetting process".

Barden, Madedor and Sides (1969) performed tests on low to high plasticity illite clay samples. The total, air and water pressures were controlled while investigating the effect of various stress paths. In all cases the applied stress $(\sigma-u_a)$ was <u>increased</u> subsequent to the initial conditions. In most cases the suction (u_a-u_w) was <u>increased</u> subsequent to the initial conditions, however, in a few cases it was decreased. Their results indicate that the soil structure volume change is dependent upon the direction of saturation. They conclude "that hysteresis between saturation and desaturation processes is the

major cause of stress path dependence". They suggest that there is also a strong similar stress path dependence of the degree of saturation surface upon the reversal of degree of saturation. They do not experimentally investigate the effect of a reversal in applied stress.

6.3 Approach to Constitutive Relationships for Multiphase Systems

Two approaches can be taken toward the establishment of stress-deformation relationships (Chou and Ragano, 1967). These are the "mathematical" approach and the "semi-empirical" approach. In the mathematical approach, each component of the deformation state variable tensor is expressed as a linear combination of the stress state variables. The "semi-empirical" approach is more commonly used to establish stress-deformation relationships and is the method used in this thesis. The constitutive equation must be checked experimentally to assure uniqueness. For an elastic solid with a positive definite strain energy function, the uniqueness theorem states that there exists a one-to-one correspondence between the elastic deformations and stresses (Fung, 1965).

In Chapter V it was shown that the mapping of the soil structure and the contractile skin can completely describe the deformation status of an unsaturated soil. Therefore, the constitutive relationships of primary interest should link the stress and deformation state variables for these two phases. The uniqueness of the constitutive relationships must be studied experimentally. If they are unique, the deformation of all phases can be evaluated from a

knowledge of the stress state variables and the soil parameters.

6.4 Constitutive Relationships for the Water-Solid and Air-Water Multiphases

First let us briefly consider the water-solid multiphase or a saturated soil. The assumptions are made that the soil is isotropic and behaves in a linearly elastic manner. The constitutive relationship for the soil structure, corresponding to the x-direction is,

$$e_x^s = \frac{(\sigma_x - u_w)}{E'} - \frac{\nu'}{E'}\cdot(\sigma_y + \sigma_z - 2\cdot u_w) \qquad 6.16$$

where E' = Youngs modulus for the soil structure corresponding to a change in effective stress

ν' = Poisson's ratio with respect to effective stress changes.

In the y and z-directions, the constitutive relationships are,

$$e_y^s = \frac{(\sigma_y - u_w)}{E'} - \frac{\nu'}{E'}\cdot(\sigma_x + \sigma_z - 2\cdot u_w)$$

$$e_z^s = \frac{(\sigma_z - u_w)}{E'} - \frac{\nu'}{E'}\cdot(\sigma_x + \sigma_y - 2\cdot u_w) \qquad 6.17$$

For the air-water multiphase, the contractile skin is assumed to behave as an elastic, isotropic solid that cannot withstand shear.

The deformation of the contractile skin in the x-direction is,

$$e_x^c = \frac{(u_a - u_w)}{H'} \qquad 6.18$$

where H' = elasticity parameter for the contractile skin.

In the y and z-directions, the equations are,

$$e_y^c = \frac{(u_a - u_w)}{H'}$$

$$e_z^c = \frac{(u_a - u_w)}{H'} \qquad 6.19$$

The above air-water multiphase is somewhat fictitious in the absence of a solid phase.

6.5 Soil Structure Constitutive Relationship for an Unsaturated Soil

An element of unsaturated soil can be considered as a combination of water-solid and air-water multiphase systems. In formulating the constitutive relationships, the assumptions of linearity, reversibility and infinitesimal deformations allow the effects of several stress state variables to be added with a negative or positive sign associated with each elasticity modulus. Thus, the constitutive relationships are developed within the context of a simple, linear elastic model.

Chapter IV showed that any two out of a possible three stress state variables describe the equilibrium of the soil structure and contractile skin. Let us first consider the use of the $(\sigma - u_w)$ and

(u_a-u_w) stress state variables. The deformation of the soil structure in the x-direction is,

$$e_x^s = \frac{(\sigma_x-u_w)}{E_t^s} - \frac{\nu_t^s}{E_t^s}\cdot(\sigma_y+\sigma_z-2\cdot u_w) + \frac{(u_a-u_w)}{H_a^s} \qquad 6.20$$

The superscript denotes the phase under consideration and the subscript denotes the phase pressure that must be changed in order to define the modulus. The modulus, E_t^s, denotes the elasticity modulus associated with the $(\sigma-u_w)$ stress state variable. The superscript, s, designates the soil <u>structure</u> while the subscript, t, signifies that the modulus is defined by changing the <u>total</u> pressure. The modulus, H_a^s, denotes the elasticity modulus for the soil structure, s, which is defined by changing the air pressure, a. The constitutive equations in the y and z-directions are,

$$e_y^s = \frac{(\sigma_y-u_w)}{E_t^s} - \frac{\nu_t^s}{E_t^s}\cdot(\sigma_x+\sigma_z-2\cdot u_w) + \frac{(u_a-u_w)}{H_a^s}$$

$$e_z^s = \frac{(\sigma_z-u_w)}{E_t^s} - \frac{\nu_t^s}{E_t^s}\cdot(\sigma_x+\sigma_y-2\cdot u_w) + \frac{(u_a-u_w)}{H_a^s} \qquad 6.21$$

The shear constitutive equations are

$$e_{xy}^s = \frac{1}{G^s}\cdot\tau_{xy}$$

$$e_{yz}^s = \frac{1}{G^s}\cdot\tau_{yz}$$

$$e_{zx}^s = \frac{1}{G^s}\cdot\tau_{zx} \qquad 6.22$$

The volumetric deformation of the soil structure is equal to the sum of the x, y and z-deformations. If in addition to the isotropic soil properties, we assume isotropic total stress conditions, the volumetric deformation is,

$$e^s = 3\left(\frac{1-2\cdot\nu_t^s}{E_t^s}\right)\cdot(\sigma-u_w) + \frac{3}{H_a^s}\cdot(u_a-u_w) \qquad 6.23$$

This equation can also be written in terms of compressibility modulii. Let $C_t^s = 3(1-2\nu_t^s)/E_t^s$ and $C_a^s = 3/H_a^s$.

$$e^s = C_t^s\cdot(\sigma-u_w) + C_a^s\cdot(u_a-u_w) \qquad 6.24$$

To put the equation in a more general form, the compressibility modulii are written in terms of partial differentials. The stress state variables should also be written as changes.

$$e^s = \frac{dv^s}{v} = \frac{\partial(v^s)}{\partial(\sigma-u_w)}\cdot d(\sigma-u_w) + \frac{\partial(v^s)}{\partial(u_a-u_w)}\cdot d(u_a-u_w) \qquad 6.25$$

where $\frac{\partial v^s}{\partial(\sigma-u_w)}$ = compressibility of the soil structure when $d(u_a-u_w)$ is zero and,

$\frac{\partial v^s}{\partial(u_a-u_w)}$ = compressibility of the soil structure when $d(\sigma-u_w)$ is zero.

A similar analysis can be conducted using the other two possible combinations of stress state variables. Using $(\sigma-u_a)$ and (u_a-u_w) as

stress state variables, the constitutive equation for the soil structure takes a similar form.

$$\frac{dv^s}{v} = \frac{\partial v^s}{\partial(\sigma-u_a)} \cdot d(\sigma-u_a) + \frac{\partial v^s}{\partial(u_a-u_w)} \cdot d(u_a-u_w) \qquad 6.26$$

where $\frac{\partial v^s}{\partial(\sigma-u_a)}$ = compressibility of the soil structure when $d(u_a-u_w)$ is zero and,

$\frac{\partial v^s}{\partial(u_a-u_w)}$ = compressibility of the soil structure when $d(\sigma-u_a)$ is zero.

Similarly using $(\sigma-u_a)$ and $(\sigma-u_w)$ as the independent stress state variables, the constitutive relationship for the soil structure

$$\frac{dv^s}{v} = \frac{\partial v^s}{\partial(\sigma-u_a)} \cdot d(\sigma-u_a) + \frac{\partial v^s}{\partial(\sigma-u_w)} \cdot d(\sigma-u_w) \qquad 6.27$$

Any one of the above three equations can be used to describe the volumetric deformation of the soil structure. However, only one equation is independent. Their uniqueness must be verified experimentally.

6.6 Contractile Skin Constitutive Relationship for an Unsaturated Soil

To the author's knowledge, no attempt has ever been made to develop a constitutive relationship for the contractile skin on a macroscopic basis. Commencing with the assumption that we are dealing with a linear, reversible model, the constitutive equation can be

written as a linear combination of stress state variables. This is essentially the same as the procedure used by Biot (1940) with respect to the water phase. Since the stress state variables associated with the contractile skin are the same as those for the soil structure, we know that the constitutive relationship for the contractile skin reduces to the same form as for the soil structure.

Let us first consider the relationship between deformation and the $(\sigma-u_w)$ and (u_a-u_w) stress state variables. The deformation of the contractile skin in the x-direction is,

$$e_x^c = \frac{(\sigma_x-u_w)}{E_t^c} - \frac{\nu_t^c}{E_t^c}\cdot(\sigma_y+\sigma_z-2\cdot u_w) + \frac{(u_a-u_w)}{H_a^c} \qquad 6.28$$

The E_t^c parameter is the modulus representing the relationship between a change in the $(\sigma-u_w)$ stress state variable and the deformation when the (u_a-u_w) stress state variable is held constant. The H_a^c parameter is the modulus representing the relationship between a change in the (u_a-u_w) stress and the deformation of the contractile skin when the $(\sigma-u_w)$ stress state variables are held constant. The stress-deformation equations for the y and z-directions are,

$$e_y^c = \frac{(\sigma_y-u_w)}{E_t^c} \frac{\nu_t^c}{E_t^c}\cdot(\sigma_x+\sigma_z-2\cdot u_w) + \frac{(u_a-u_w)}{H_a^c}$$

$$e_z^c = \frac{(\sigma_z-u_w)}{E_t^c} - \frac{\nu_t^c}{E_t^c}\cdot(\sigma_x+\sigma_y-2\cdot u_w) + \frac{(u_a-u_w)}{H_a^c} \qquad 6.29$$

There are also independent shear stress versus deformation equations for the contractile skin.

$$e^c_{xy} = \frac{1}{G^c} \cdot \tau_{xy}$$

$$e^c_{yz} = \frac{1}{G^c} \cdot \tau_{yz}$$

$$e^c_{zx} = \frac{1}{G^c} \cdot \tau_{zx} \qquad 6.30$$

The modulii associated with the contractile skin are independent of those for the soil structure. The modulii are soil properties or parameters relating state variables and should not be confused with being an elasticity modulii for the contractile skin itself.

In terms of compressibility modulii, the volumetric deformation of the contractile skin for an isotropic soil with an isotropic total stress is,

$$e^c = C_t{}^c \cdot d(\sigma - u_w) + C_a{}^c \cdot d(u_a - u_w) \qquad 6.31$$

where $$C_t{}^c = 3(1-2\nu_t{}^c)/E_t{}^c$$

$$C_a{}^c = 3/H_a{}^c$$

In the more general, partial differential form, the constitutive relationship is,

$$e^c = \frac{dv^c}{v} = \frac{\partial v^c}{\partial(\sigma-u_w)} \cdot d(\sigma-u_w) + \frac{\partial v^c}{\partial(u_a-u_w)} \cdot d(u_a-u_w) \qquad 6.32$$

where $\frac{\partial v^c}{\partial(\sigma-u_w)}$ = compressibility relationship of the contractile skin when $d(u_a-u_w)$ is zero,

$\frac{\partial v^c}{\partial(u_a-u_w)}$ = compressibility relationship of the contractile skin when $d(\sigma-u_w)$ is zero.

Similar equations can be developed using the other possible combinations of stress state variables. Only one of the three possible constitutive equations is independent and can be used to describe the deformation of the contractile skin. Their uniqueness must be verified experimentally.

The constitutive equations developed for the contractile skin are synonymous with those for the air phase. Therefore, the volumetric deformation of the air phase can be written,

$$\frac{dv^a}{v} = \frac{\partial v^a}{\partial(\sigma-u_w)} \cdot d(\sigma-u_w) + \frac{\partial v^a}{\partial(u_a-u_w)} \cdot d(u_a-u_w) \qquad 6.33$$

6.7 Water Phase Constitutive Relationship for an Unsaturated Soil

The constitutive relationship for the water phase can be written as a consequence of the continuity requirement and the constitutive relationships for the soil structure and the contractile skin. Using $(\sigma-u_w)$ and (u_a-u_w) as the stress state variables, the constitutive relationship is,

$$\frac{dv^w}{v} = \frac{\partial v^w}{\partial(\sigma-u_w)} \cdot d(\sigma-u_w) + \frac{\partial v^w}{\partial(u_a-u_w)} \cdot d(u_a-u_w) \qquad 6.34$$

where $\frac{\partial v^w}{\partial(\sigma-u_w)}$ and $\frac{\partial v^w}{\partial(u_a-u_w)}$ = compressibility modulii with respect to the water phase.

The continuity requirement states that the volumetric deformation in the water phase is equal to the difference between the soil structure and air volumetric deformations. Therefore, the compressibilities with respect to the water phase can be written as,

$$\frac{\partial v^w}{\partial(\sigma-u_w)} = \frac{\partial v^s}{\partial(\sigma-u_w)} - \frac{\partial v^c}{\partial(\sigma-u_w)}$$

and

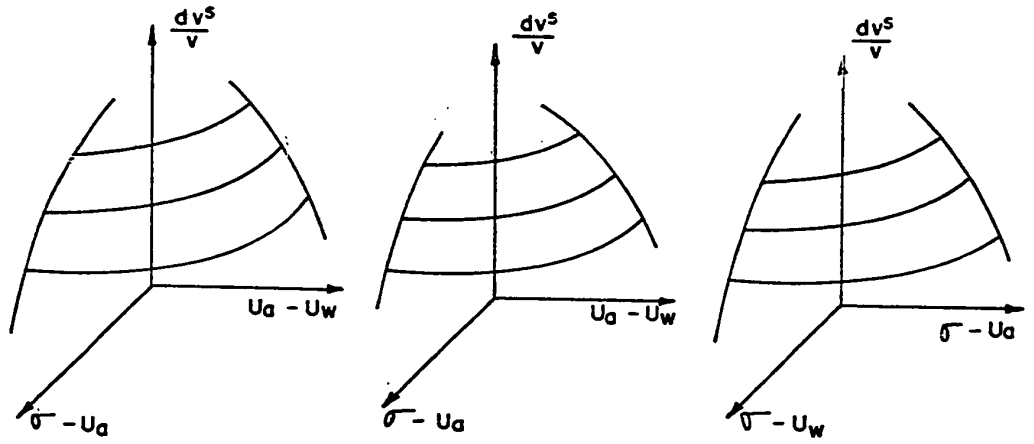
$$\frac{\partial v^w}{\partial(u_a-u_w)} = \frac{\partial v^s}{\partial(u_a-u_w)} - \frac{\partial v^c}{\partial(u_a-u_w)}$$

6.8 Graphical Presentation of Constitutive Relationships

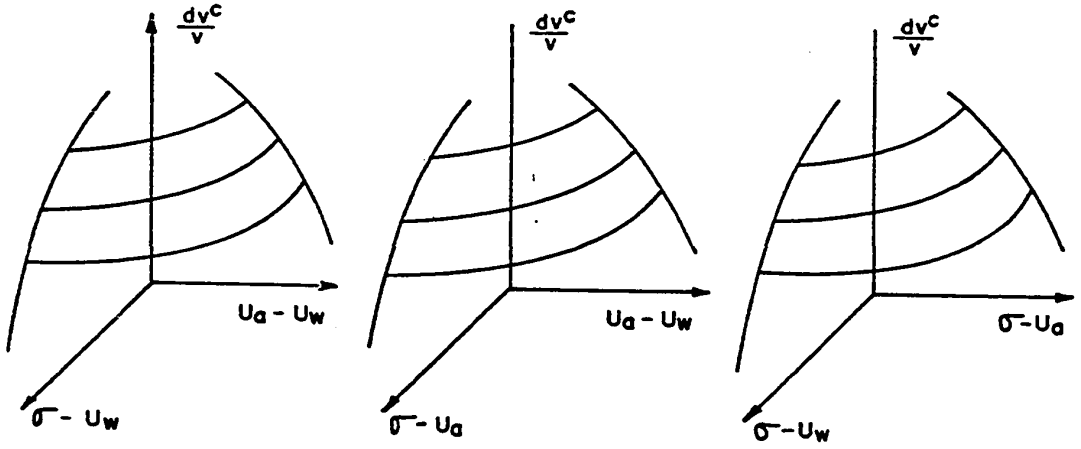
One of the unfortunate consequences of having two stress state variables to contend with is the fact that the constitutive relationships are three-dimensional. Difficulties arise in presenting them on plane paper. Expanded versions of the two types of plots proposed by Matyas and Radhakrishna (1968) are suggested for presenting constitutive surfaces.

The first type of plot is an isometric view of the constitutive surface. The two stress state variables are plotted along orthogonal axis in a plane surface. The deformation state variable is plotted along the ordinate. A separate diagram is required for each phase under consideration. For each phase there are three possible stress state variable combinations that can be used Figure 6.1.

The bisector of the angle formed by the axes of the two stress



CONSTITUTIVE SURFACE FOR THE SOIL STRUCTURE



CONSTITUTIVE SURFACE FOR THE CONTRACTILE SKIN

FIGURE 6.1 GRAPHICAL REPRESENTATION OF CONSTITUTIVE SURFACES FOR AN UNSATURATED SOIL

state variables (plotted to the same scale) produces an axis along which the two stress state variables are equal. When $(\sigma-u_w)$ and (u_a-u_w) are chosen as the independent stress state variables, the equation of the bisector is,

$$\sigma-u_w = u_a-u_w = \text{CONSTANT} \qquad 6.36$$

The constant is equal to $(\sigma-u_a)$. Thus, the bisector produces the axis of the third non independent stress state variable (Figure 5.2). Similarly, when $(\sigma-u_w)$ and $(\sigma-u_a)$ are chosen as the independent stress state variables, the bisector is equal to (u_a-u_w). The relationship assists in visualizing the behavior with respect to all stress state variables. Other axes originating from the origin represent constant ratios of the stress state variables.

The second type of plot uses contours to designate either one of the stress state variables or the volumetric deformation.

6.9 Sign Convention for Compressibility Modulii

A positive or negative sign must be associated with each compressibility modulus. This is not required in most volume change analysis since generally only one stress variable is of concern and the direction of deformation is well established. A sign convention becomes imperative in the analysis of unsaturated soils since an increase in the stress state variable does not always produce the same direction of volume change. Once the sign of the compressibility modulus is known, it could be incorporated into the differential equation. However, the sign need not be fixed and depends to some extent on the soil type under consideration.

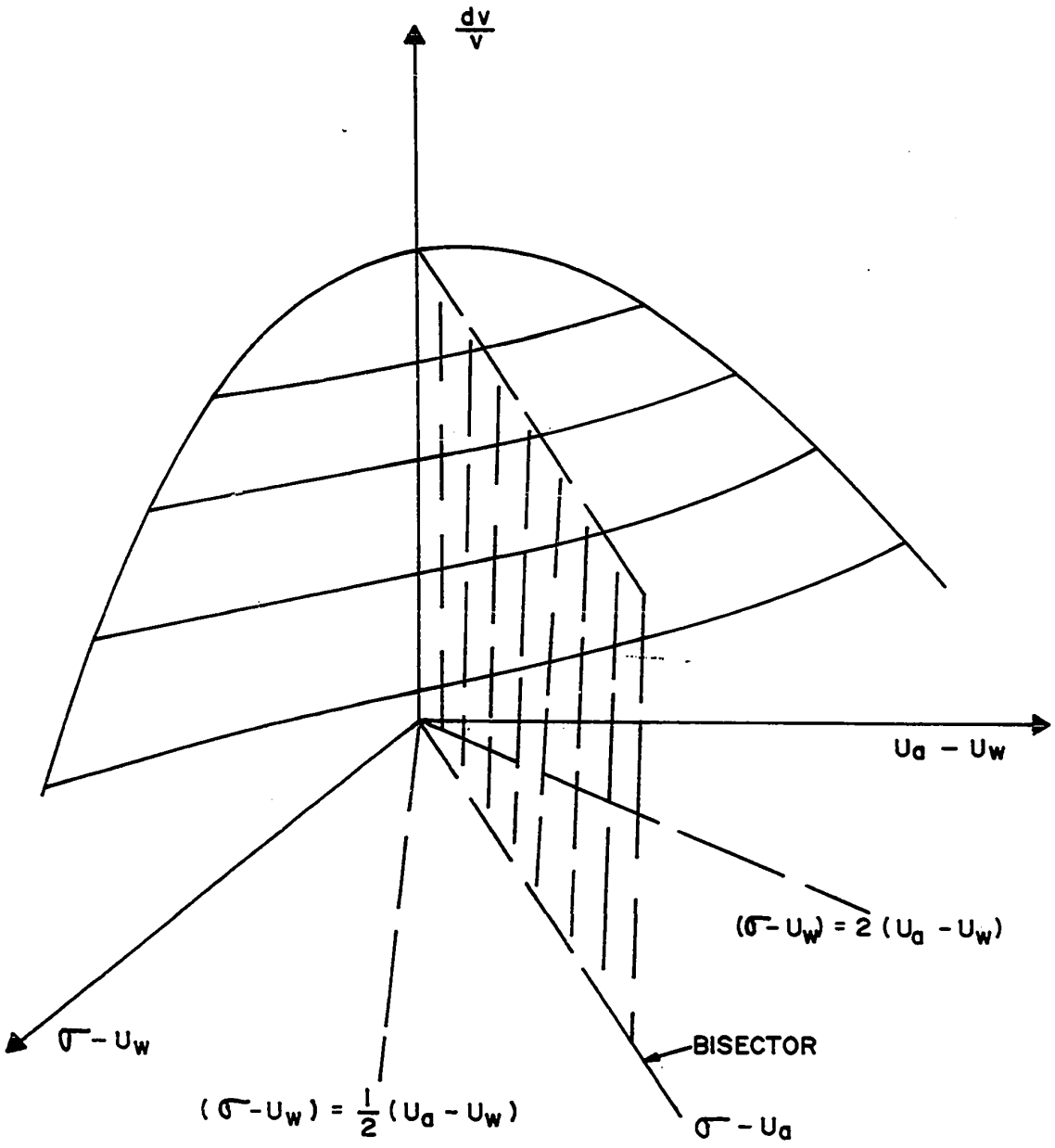


FIGURE 6.2 FEATURES OF THE CONSTITUTIVE SURFACE

The sign convention employed can be stated as follows: If an increase in the stress state variable produces a phase volume decrease, the compressibility modulus is POSITIVE. If the stress state variable increase produces a volume increase, the compressibility modulus is NEGATIVE. The convention is applicable to the soil structure, contractile skin (air phase) and the water phase.

Even for a particular soil, the sign for the compressibility modulus is not fixed with respect to the stress state variable. Rather, it can depend on which component of the stress state variable was changed. Consider, for example the (u_a-u_w) stress state variable and the deformation of the soil structure. The suction can be increased by either increasing the air pressure or decreasing the water pressure. If the air pressure is increased in an unsaturated soil, the soil structure generally expands making the compressibility modulus negative. If the water pressure is decreased, the soil structure generally compresses making the compressibility modulus positive.

Let us specify a normal soil as one with a stable, non collapsing soil structure. The directions of volume change can be anticipated for a stable structured soil by examining the effect of changing the components of the stress state variables. Let us first consider the effect of stress changes on the soil structure or overall element volume. The signs associated with each modulus are presented in Table VI.1. The signs associated with the soils tested are analysed in Section 6.10.

TABLE VI.1

SIGN OF THE SOIL STRUCTURE MODULII

Stress State Variable Change*	Component Change	Soil Structure Deformation	Sign
$(\sigma-u_w)$ Increasing	Increasing σ	Decrease	+
	Decreasing u_w	Decrease	+
$(\sigma-u_a)$ Increasing	Increasing σ	Decrease	+
	Decreasing u_a	Decrease	+
(u_a-u_w) Increasing	Increasing u_a	Increase	-
	Decreasing u_w	Decrease	+

*Reversing the direction of each stress state variable reverses the sign

Table VI.2 presents the sign associated with each of the modulii for the contractile skin or the air phase.

TABLE VI.2

SIGN OF THE CONTRACTILE SKIN (AIR PHASE) MODULII

Stress State Variable Change	Component Change	Soil Structure Deformation	Sign
$(\sigma-u_w)$ Increasing	Increasing σ	Decrease	+
	Decreasing u_w	Increase	-
$(\sigma-u_a)$ Increasing	Increasing σ	Decrease	+
	Decreasing u_a	Decrease	+
(u_a-u_w) Increasing	Increasing u_a	Increase	-
	Decreasing u_w	Increase	-

Similarly, the signs associated with the modulii for the water phase are presented in Table VI.3. It must be emphasized that each of the above signs are based on an intuitive knowledge of the behavior of a stable-structured soil. They need not be always correct; however, they provide a framework within which to order our thoughts.

TABLE VI.3

SIGN OF THE WATER PHASE MODULII

Stress State Variable Change	Component Change	Water Phase Deformation	Sign
$(\sigma-u_w)$ Increasing	Increasing σ	Decrease	+
	Decreasing u_w	Decrease	+
$(\sigma-u_a)$ Increasing	Increasing σ	Decrease	+
	Decreasing u_a	Increase	-
(u_a-u_w) Increasing	Increasing u_a	Decrease	+
	Decreasing u_w	Decrease	+

6.10 Observed Directions of Volumetric Deformation

The experimental data presented in sections I and II of Appendix F are analysed with respect to their direction and magnitude of volumetric deformation (Table VI.4).

Many variables are involved in a complete analysis of the direction of volumetric deformation. For example, a decrease in suction may produce a volume increase or decrease depending upon such factors as clay content and mineralogy, stress history and present

TABLE VI.4

EXPERIMENTAL DATA ON THE DIRECTIONS OF DEFORMATION

FOR VARIOUS STRESS COMPONENT CHANGES

Test No.	Pressure Change			Deformation (%)		
	Total (psi)	Air (psi)	Water (psi)	Soil Structure	Air	Water
D-1	-10	-10	0	+1.71	+ 7.81	-6.10
D-2	+13	0	0	+0.18	+ 0.02	+0.16
D-3	0	0	+10	-0.05	+ 0.24	-0.29
D-4	+14	0	0	+0.24	- 0.11	+0.35
D-5	0	0	+10	-0.06	+ 0.44	-0.50
D-6	0	0	+31	+0.05	+ 3.48	-3.43
D-7	0	0	+16	+1.12	+ 6.22	-5.10
D-8	0	0	-15	+0.35	- 1.09	+1.44
D-9	0	0	-30	+0.75	- 1.92	+2.67
D-10	0	-28	0	+5.80	+ 8.13	-2.33
D-11	0	-15	0	+8.30	+10.80	-2.50
D-12	0	+15	0	-0.02	- 0.96	+0.94
D-13	0	+27	0	-0.24	- 1.48	+1.24
D-14	0	0	+29	-0.74	+ 0.50	-1.24
C-1*	0	0	+11	-0.19	- 0.06	-0.13
C-2*	0	-10	0	+0.03	+ 0.33	-0.30
C-3*	-10	0	0	-0.18	+ 0.20	-0.38
C-4*	0	0	+10	-0.12	+ 0.40	-0.52
C-5*	0	-10	0	+0.05	+ 0.67	-0.62
C-6*	-10	0	0	-0.17	+ 0.33	-0.50
C-7	0	0	+10			
C-8	0	-10	0	+0.32	+ 0.41	-0.09
C-9	-10	0	0	-0.26	+ 0.09	-0.35
C-10	0	0	+10	-0.22	+ 0.20	-0.42
C-11	0	-10	0	-0.27	+ 0.40	-0.67
C-12	-10	0	0	-0 43	+ 0.16	-0.59
C-13	-10	0	0	-0.70	- 0.05	-0.65
C-14	0	0	+10	-0.24	+ 0.23	-0.47
C-15	0	-10	0	-0.01	+ 0.19	-0.20
C-16	-10	0	0	-0.26	+ 0.10	-0.36
C-17	0	0	+10	-0.21	+ 0.27	-0.48
C-18*	-10	0	0	-0.08	- 0.04	-0.04
C-19*	0	-10	0	-0.02	- 0.02	0.00

TABLE VI.4 (continued)

Test No.	Pressure Change			Deformation (%)		
	Total (psi)	Air (psi)	Water (psi)	Soil Structure	Air	Water
C-20*	0	0	+10	-0.04	+ 0.21	-0.25
C-21*	-10	0	0	-0.28	- 0.11	-0.17
C-22*	0	-10	0	-0.01	+ 0.08	-0.09
C-23*	0	0	+10	-0.15	+ 0.28	-0.43
C-24*	-10	0	0	-0.77	- 0.45	-0.32
C-25*	0	-10	0	+0.23	+ 0.94	-0.71
C-26*	0	0	+ 5	0.00	+ 0.86	-0.86
C-27*	-10	0	0	-0.71	+ 0.11	-0.82
C-28*	+ 9	0	0	+0.30	+ 0.24	+0.06
C-29*	0	0	- 5	+0.11	- 0.49	+0.60
C-30	+29	0	0	+2.14	+ 0.70	+1.44
C-31	0	+30	0	+0.05	- 0.89	+0.94
C-32	0	0	+30	-1.22	- 0.65	-0.57

*Deformations at an elapsed time of 3000 minutes.

stress state, degree of saturation, etc. However, the purpose of this section is simply to obtain a basic appreciation of directions of volumetric deformation.

Not every test performed can be assumed to be completely trustworthy. The long periods of time involved in each process may result in the secondary factors masking the primary process. For example, in some of the tests (C-series), the stress changes and the measured volume changes were small. Also, due to the extensive time required for complete equalization, some pressure changes were applied prior to the complete equalization under the previous pressure change.

Figure 6.3 shows the magnitude and direction of deformation in the soil structure, air and water phases for a total pressure change. Figures 6.4 and 6.5 show similar results for changes in the air and water pressures, respectively. The above results are graphically summarized in Figures 6.6, 6.8 and 6.11, respectively.

When the total pressure was increased, the soil structure always decreased in volume and vice versa. In other words, the soil structure deformation showed an inverse relationship with the total pressure increment. The water phase also showed an inverse relationship with total pressure. The air phase did not bear a definite directional relationship. Numerous tests performed on the oedometer showed an air volume decrease for a total pressure decrease. The volume changes involved are small and it is possible that the loss of moisture from the sample in the oedometer contributed to a fictitious decrease

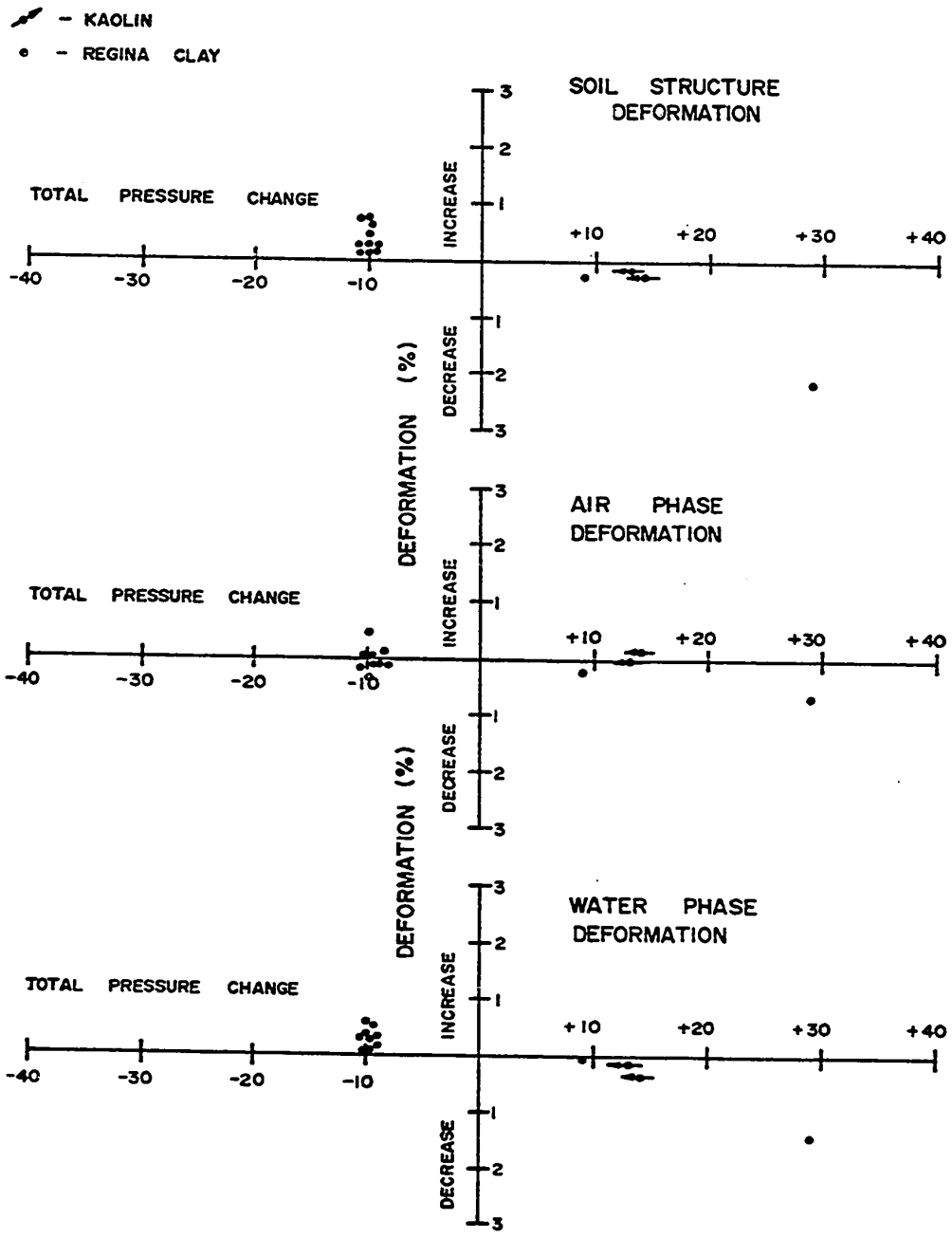


FIGURE 6.3 VOLUMETRIC DEFORMATIONS FOR A CHANGE IN TOTAL PRESSURE

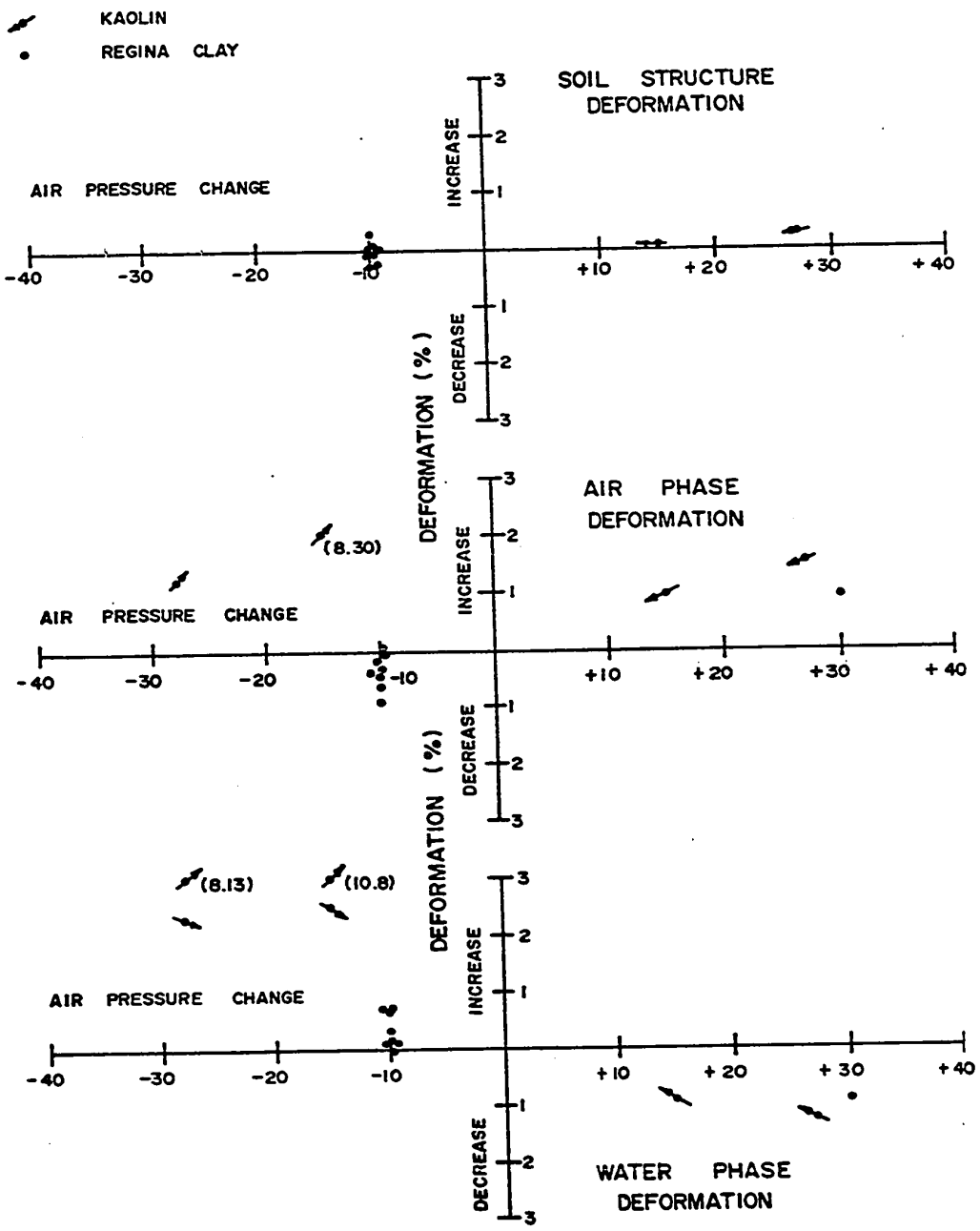


FIGURE 6.4 VOLUMETRIC DEFORMATIONS FOR A CHANGE IN AIR PRESSURE

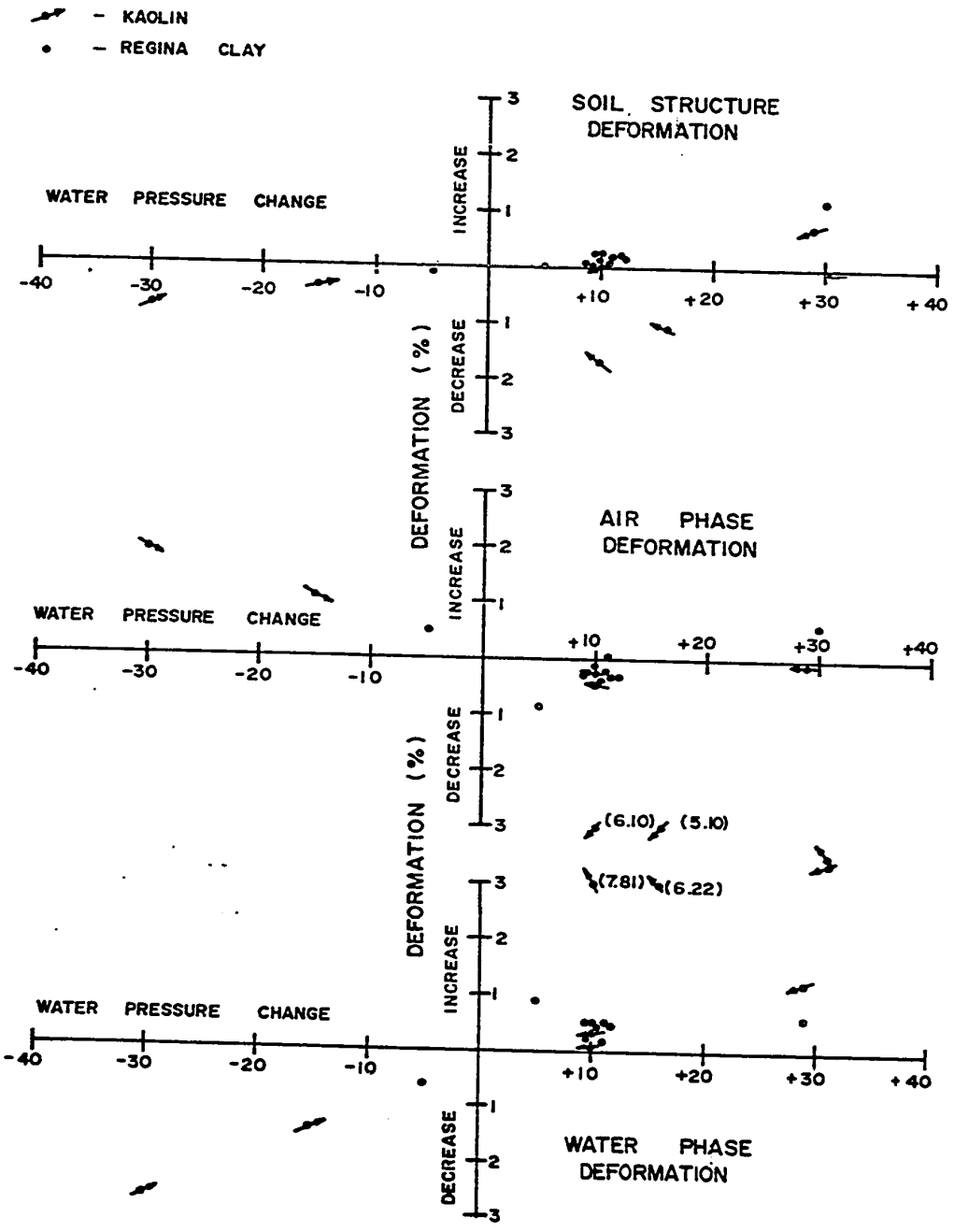


FIGURE 6.5 VOLUMETRIC DEFORMATIONS FOR A CHANGE IN WATER PRESSURE

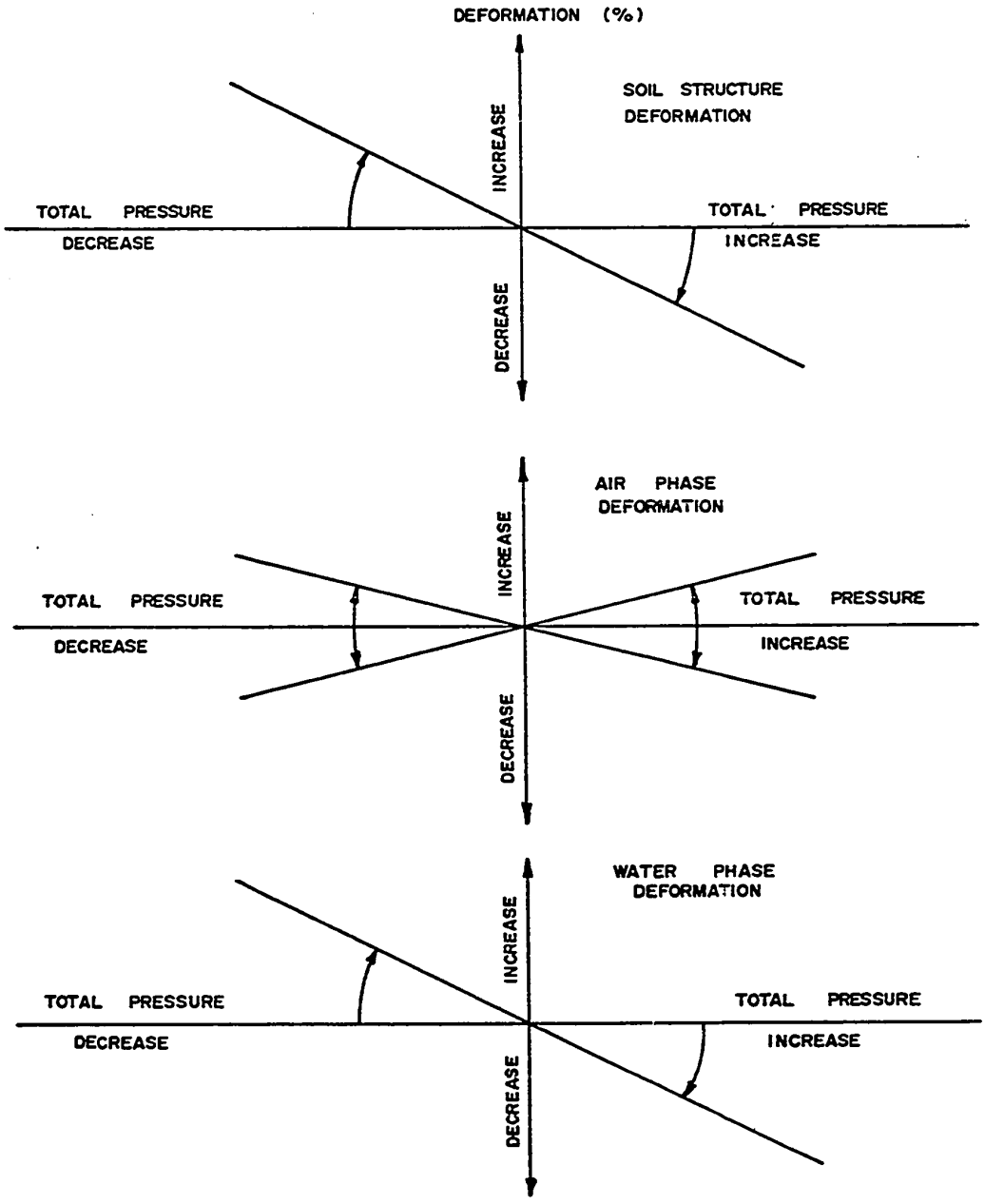


FIGURE 6.6 SUMMARY OF DIRECTIONS OF VOLUMETRIC DEFORMATIONS FOR A CHANGE IN TOTAL PRESSURE

in air volume. However, the dominant trend in the air phase volume change is towards an inverse function of total pressure.

Figure 6.7 shows a typical plot (Test C-30) of volumetric deformation versus logarithm of time for an increment in the total stress on a compacted kaolin. The soil structure, air and water phases show a decrease in volume during the process. The sample exhibited a relatively large instantaneous volume decrease at the time of the application of the total pressure. In this test, it is the large instantaneous compression that controls the direction of deformation of the air phase.

An increase in the air pressure acts on the inside of the unsaturated soil sample causing the soil structure to expand (Figure 6.8). However, this may be temporary and under equilibrium conditions, the volume may decrease. The net result appears to be related to the compressibility of the soil structure and the degree of saturation. For example, if the soil has a relatively high degree of saturation, the effect of the internal air pressure is minimal. However, the increase in air pressure produces an increase in soil suction which in turn can cause a decrease in the volume of the overall sample. It is possible for an overall volume increase to occur during the early stages of the test and a volume decrease to occur towards the time of complete equilization. Figure 6.9 shows the results of test C-31 which demonstrates the above phenomenon.

Although the soil structure showed either a direct or inverse relationship with the air pressure change, the air phase defor-

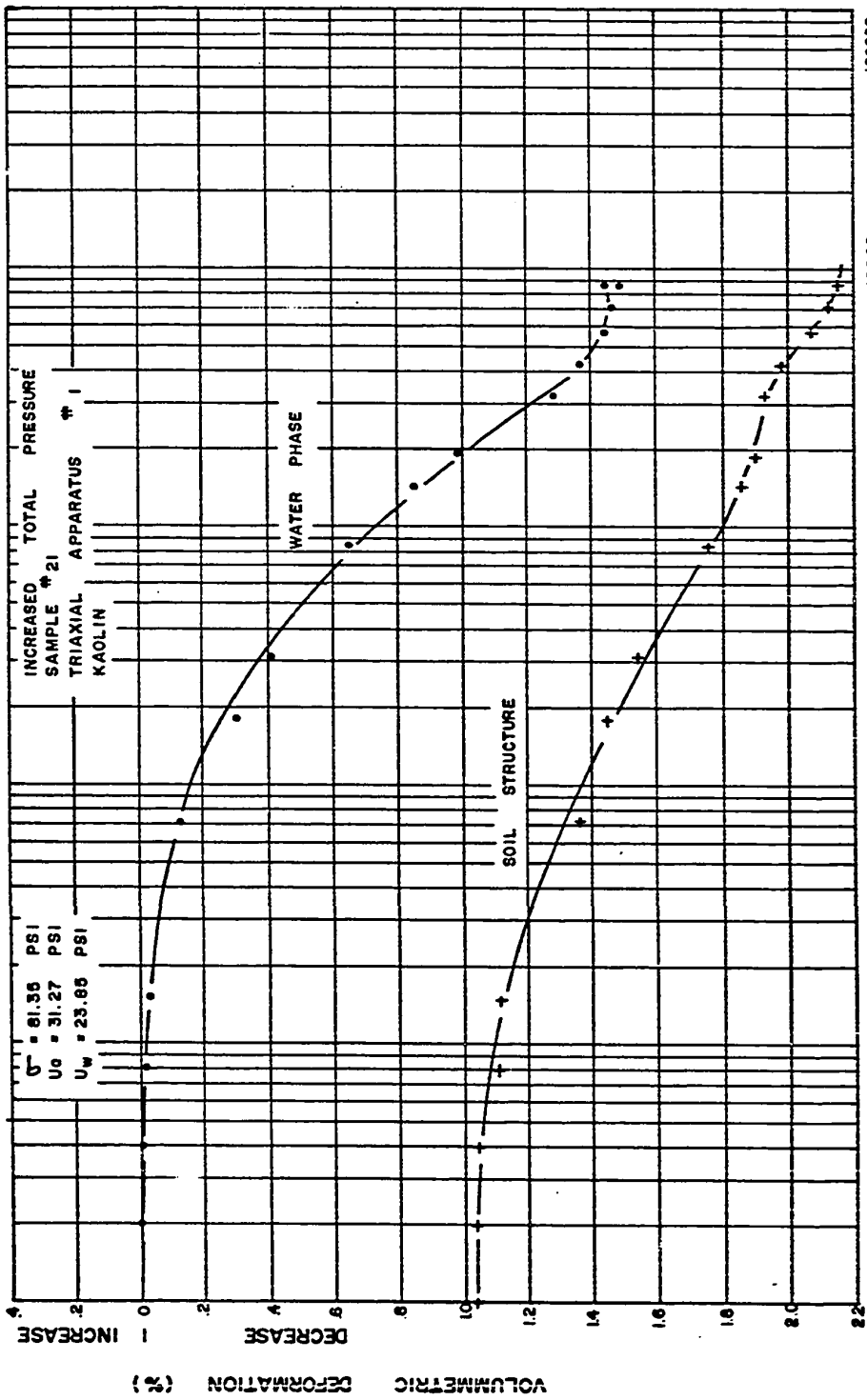


FIGURE 6.7 SOIL STRUCTURE AND WATER PHASE VOLUME CHANGES (C-30)

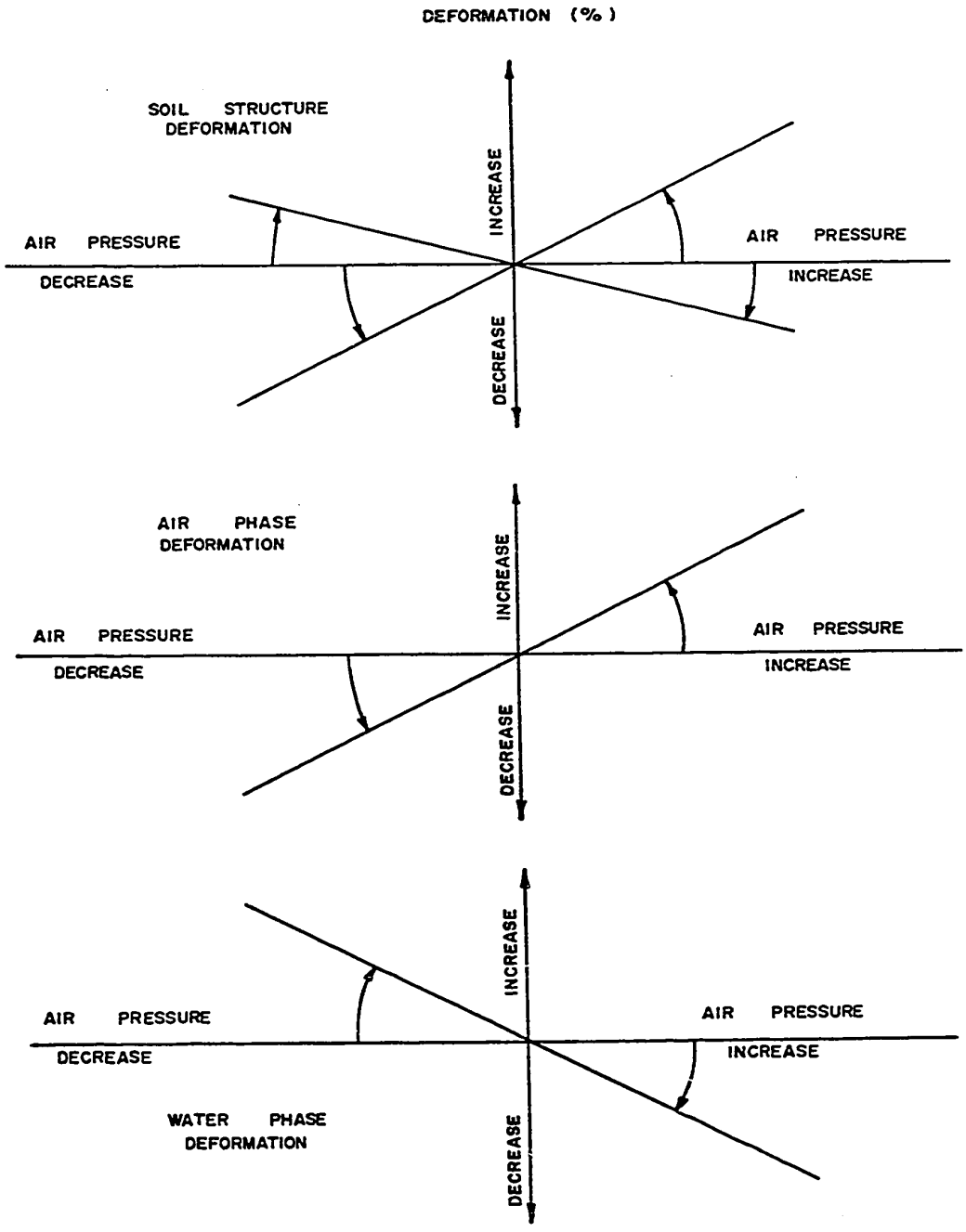


FIGURE 6.8 SUMMARY OF DIRECTIONS OF VOLUMETRIC DEFORMATIONS FOR A CHANGE IN AIR PRESSURE

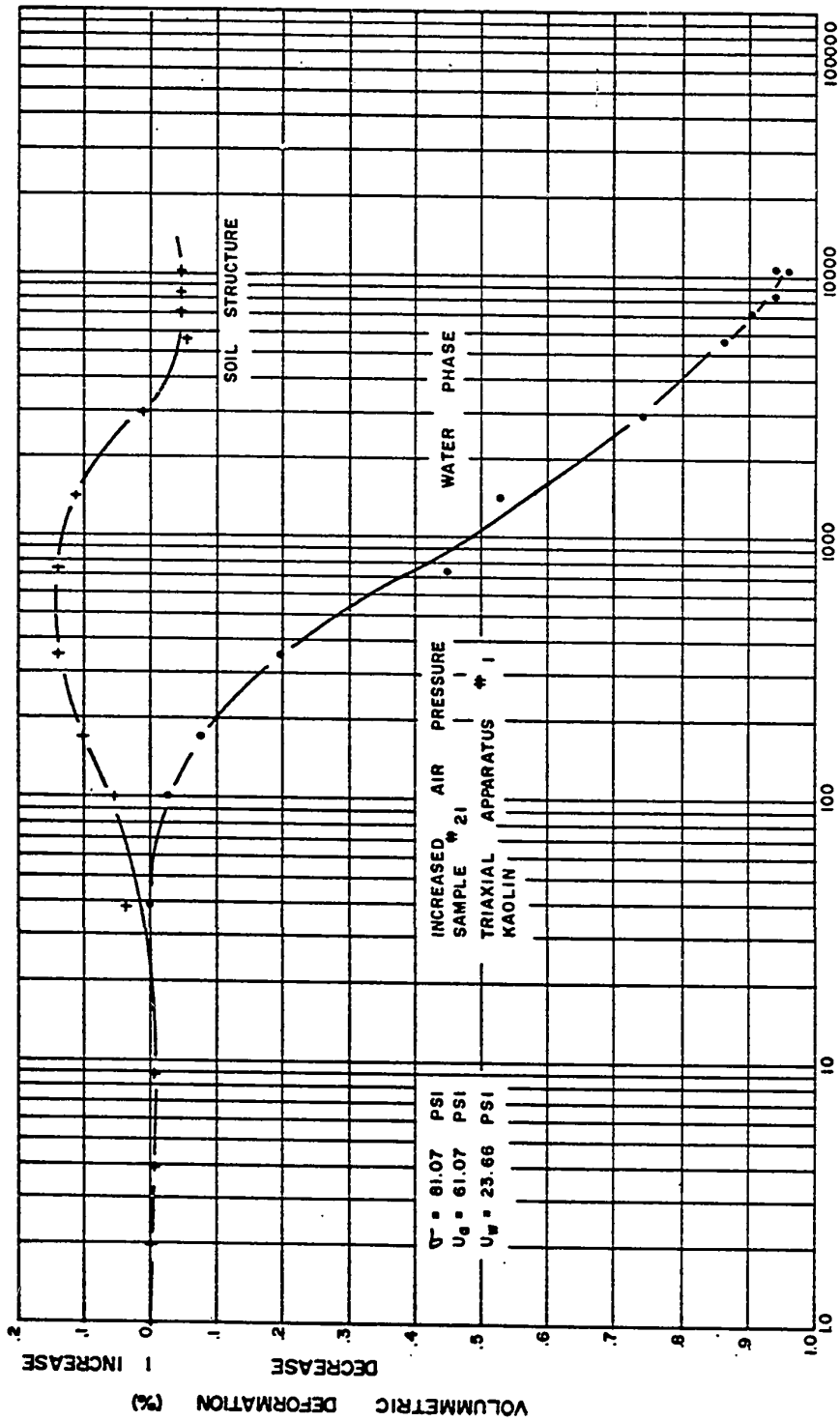


FIGURE 6.9 SOIL STRUCTURE AND WATER PHASE VOLUME CHANGES (C-31)

mation always showed a direct relationship with pressure. The water phase deformation always showed an inverse relationship with air pressure change.

Figure 6.10 shows a typical deformation versus logarithm of time curve for a decrease in air pressure (Test D-10). The soil structure underwent two distinct deformation decreases. The first volumetric decrease during the period up to 10 minutes was probably due to the decrease in internal air pressure. The second volume decrease proceeding to the end of the test appears related to the intake of water by the sample. The intake of water reduces the normal pressure and the volume decrease is likely indicative of a meta-stable structure. Stated in another way, the intrinsic shear stresses cause slip between the particles under conditions of reduced normal stress. This is in essence a collapse phenomenon. All processes appear to be smooth and continuous.

An increase in water pressure results in a swelling of the soil structure if the material has a stable structure (Figure 6.11). If the soil structure is meta-stable, the increased water pressure results in a collapse. It is interesting that there were no results which indicated a tendency for collapse when the water pressure was decreased. The air phase volume change, in general, showed an inverse relationship with water pressure. However, it is also probable that the air phase could show a direct relationship. The water phase volume changes always showed a direct relationship with water pressure.

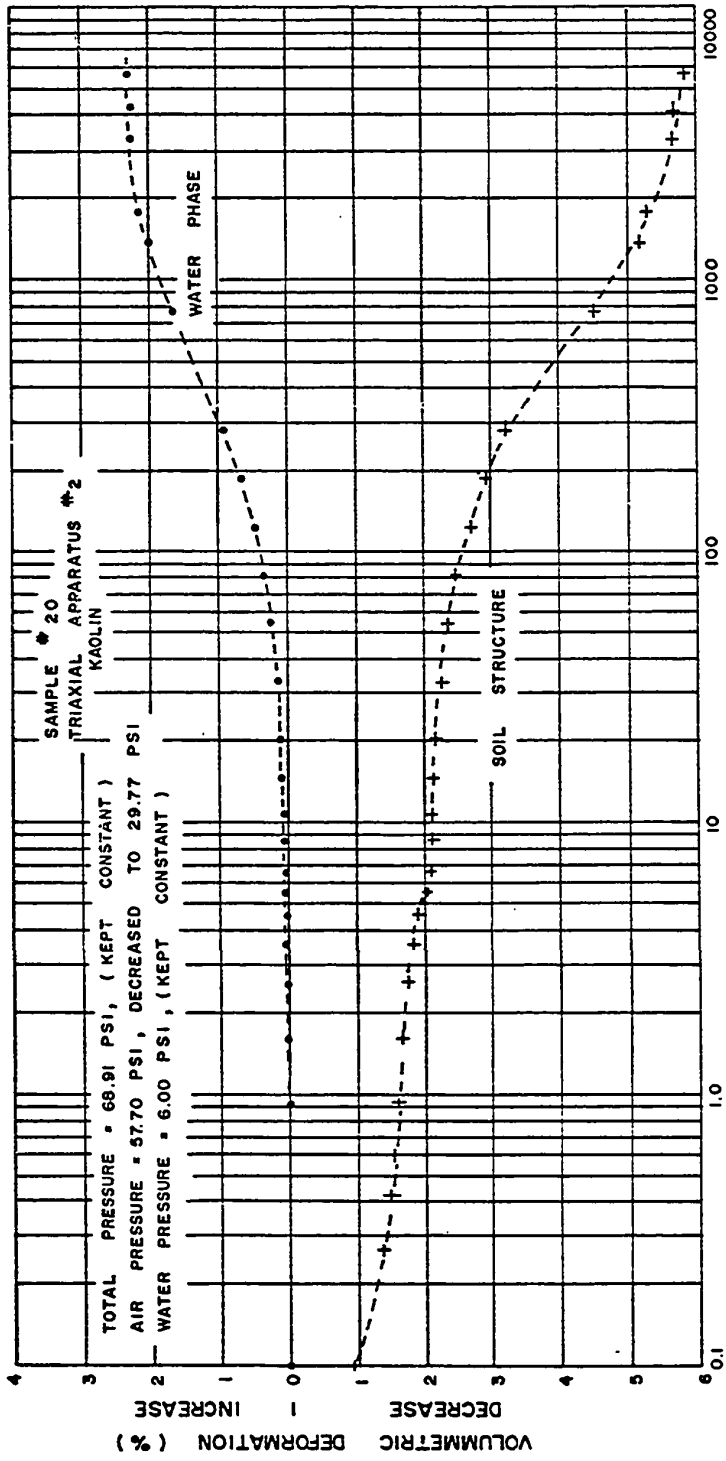


FIGURE 6.10 SOIL STRUCTURE AND WATER PHASE VOLUME CHANGES (D-10)

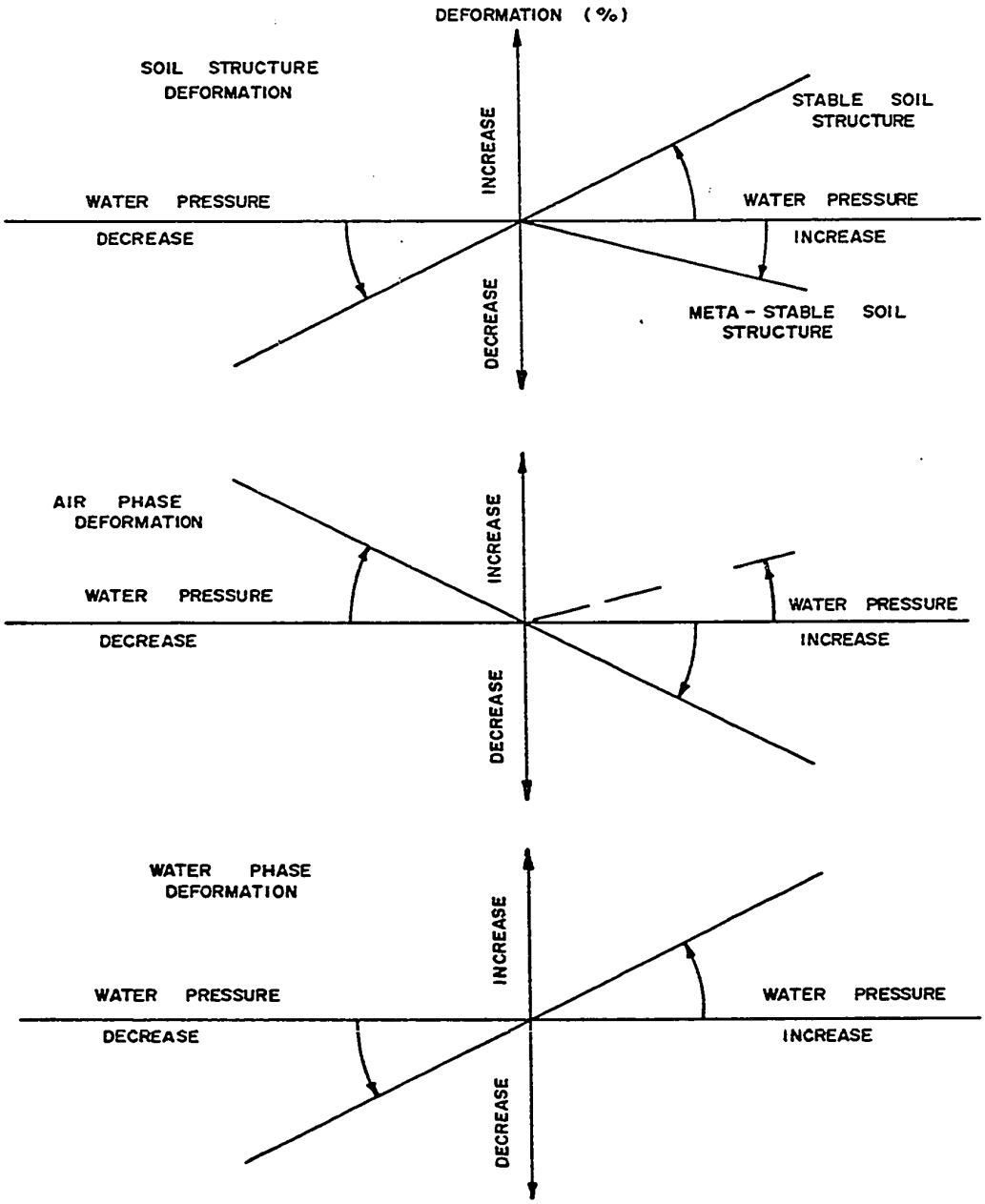


FIGURE 6.11 SUMMARY OF DIRECTIONS OF VOLUMETRIC DEFORMATIONS FOR A CHANGE IN WATER PRESSURE

Figure 6.12 shows a typical volumetric deformation versus logarithm of time curve for a stable-structured soil (D-14). The water pressure was increased by 29 psi. The soil structure expanded at a rate considerably slower than that of the water uptake by the sample. The air volume increased during the swelling process.

Figure 6.13 shows a deformation-time plot for a meta-stable structured soil (D-7). The water pressure was increased by 16 psi. The sample commenced its uptake of water almost immediately and the soil structure started to decrease (collapse) at approximately 50 minutes. The processes are smooth and continuous. A complete study of the collapse phenomenon is beyond the scope of this thesis. Suffice it to say that with the limited results available, collapse in unsaturated soils appears strongly related to an increase in water pressure. It was dominant only in the low swelling kaolin which was prepared at one-half standard compactive effort.

The laboratory test results indicate that the proposed directions of deformation appear reasonable for a soil with a stable structure. They must not, however, be taken as the only direction in which deformation can occur. The instability of the soil structure is the main factor causing deviations from the general case.

6.11 Procedure to Experimentally Verify the Uniqueness of the Constitutive Surface at a Point

The uniqueness of the proposed constitutive relationships must be verified experimentally prior to their use in an analysis. Unique-

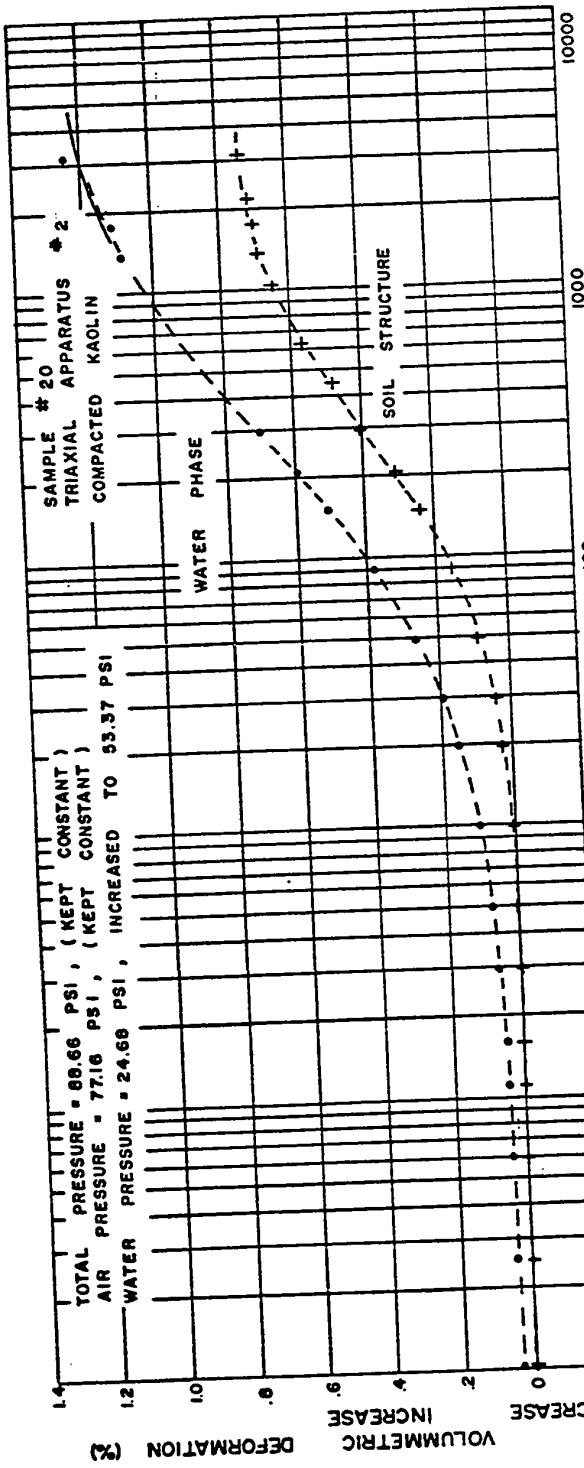


FIGURE 6.12 SOIL STRUCTURE AND WATER PHASE VOLUME CHANGES (D-14)

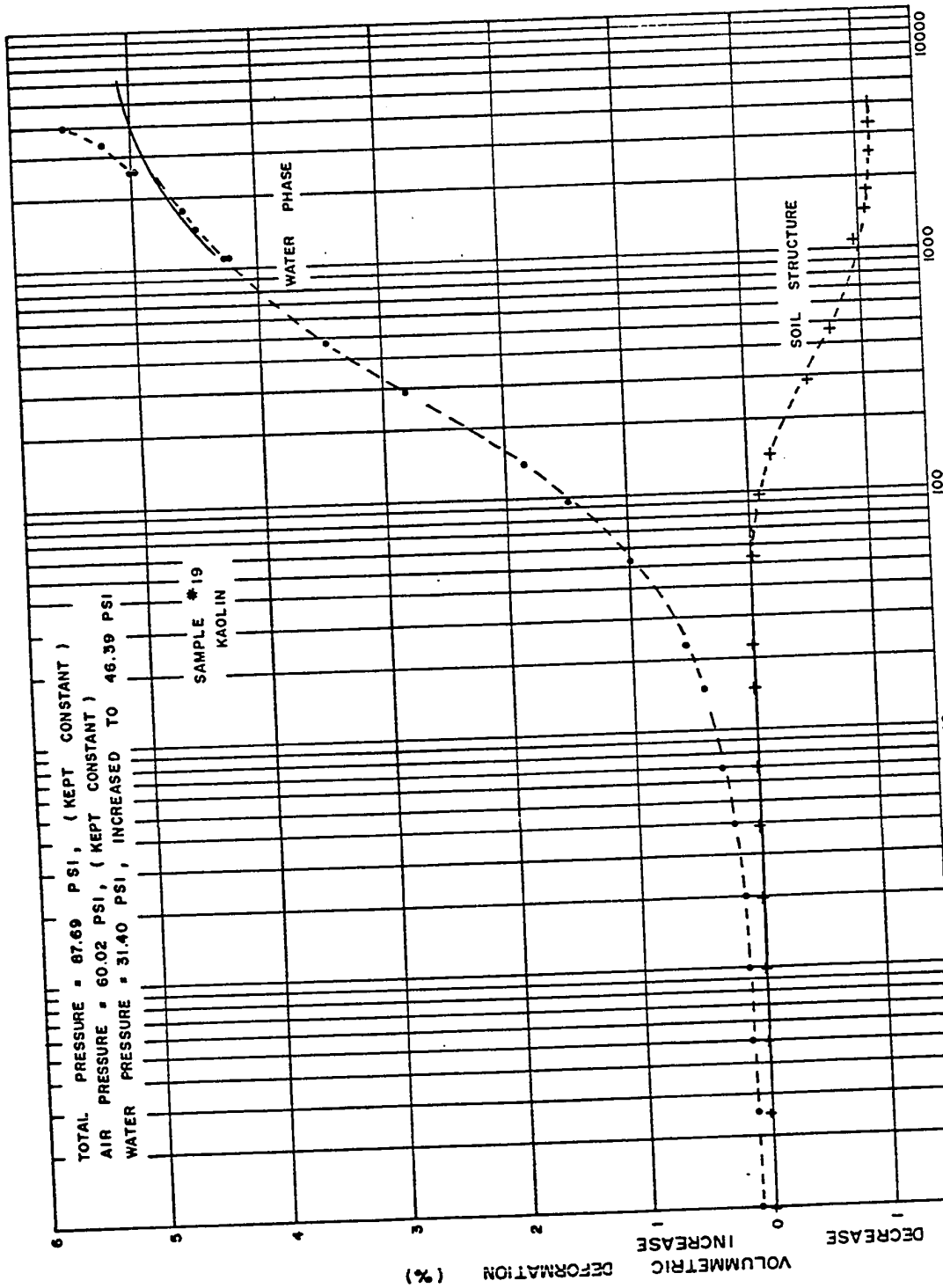


FIGURE 3.13 SOIL STRUCTURE AND WATER PHASE VOLUME CHANGES (D-7)

ness requires that there is one and only one relationship between the state variables. However, even if complete uniqueness does not exist, it is possible to place stress path restrictions on the constitutive relationship. This procedure is commonly used to account for hysteretic effects.

The uniqueness of the constitutive surfaces is analysed in two steps. First, the uniqueness of the constitutive surface is tested for small stress deviations from a stress point. Secondly, the constitutive surface is explored in terms of larger stress changes and reversals of stress.

Let us suppose that it is possible to prepare several identical unsaturated soil samples that are subjected to the same total, air and water pressures. Therefore all samples are at the same stress point in space and have the same initial volume-weight properties. Then let each sample be subjected to varying stress changes that would describe the spokes of a wheel (Figure 6.14). By monitoring the volume changes in each phase and the overall volume change, the corresponding constitutive surfaces can be mapped. The constitutive surface is unique if it is planar for 360 degrees around a point. If the constitutive surface at the point is unique, the compressibility modulii associated with any orthogonal directions can be used to describe the deformations produced by any combination of the stress state variables. The stress deviations are assumed to be small enough to produce compressibility modulii that are constants.

The above tests are somewhat fictitious since they would be

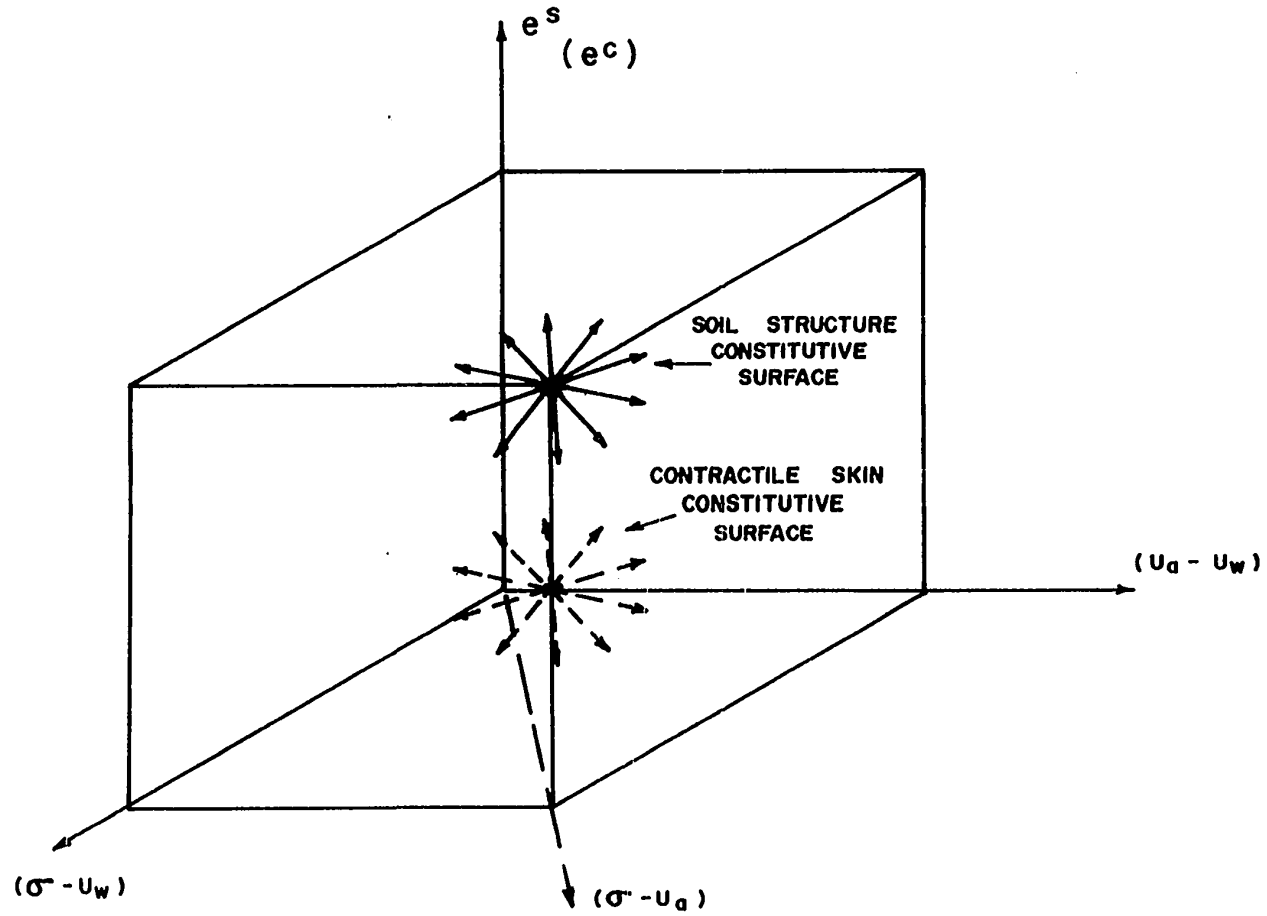


FIGURE 6.14 IDEAL TESTS TO PROVE UNIQUENESS OF THE CONSTITUTIVE SURFACE AT A POINT FOR THE SOIL STRUCTURE AND THE CONTRACTILE SKIN

difficult and extremely time consuming to conduct. Therefore, a simpler and more rapid procedure was adopted. One sample was subjected to small stress increments along three stress paths. Using the deformations from any two of the increments, it is possible to compute two corresponding compressibility modulii. Now the deformation equation can be used to compute the anticipated deformation along the third stress path. The computed deformation is compared with the measured deformation. The constitutive surface at a point is unique if the measured and predicted deformations are essentially equal. This procedure can be considered as a minimum check for uniqueness since it is impossible to prove uniqueness with less data (Figure 6.15).

Three stress paths of equal spacing can be obtained by changing the total, air and water pressure and allowing equalization after each pressure change (Figure 6.16). The uniqueness tests can be applied to any of the proposed constitutive equations (i.e. soil structure, contractile skin, air and water phases). As an example, let us consider the soil structure deformations for the above case. One form of the constitutive equation for the soil structure is,

$$\frac{dv^s}{v} = C_t{}^s \cdot d(\sigma - u_w) + C_a{}^s \cdot d(u_a - u_w) \qquad 6.37$$

Suppose the first pressure increment is a decrease in the total stress. Therefore,

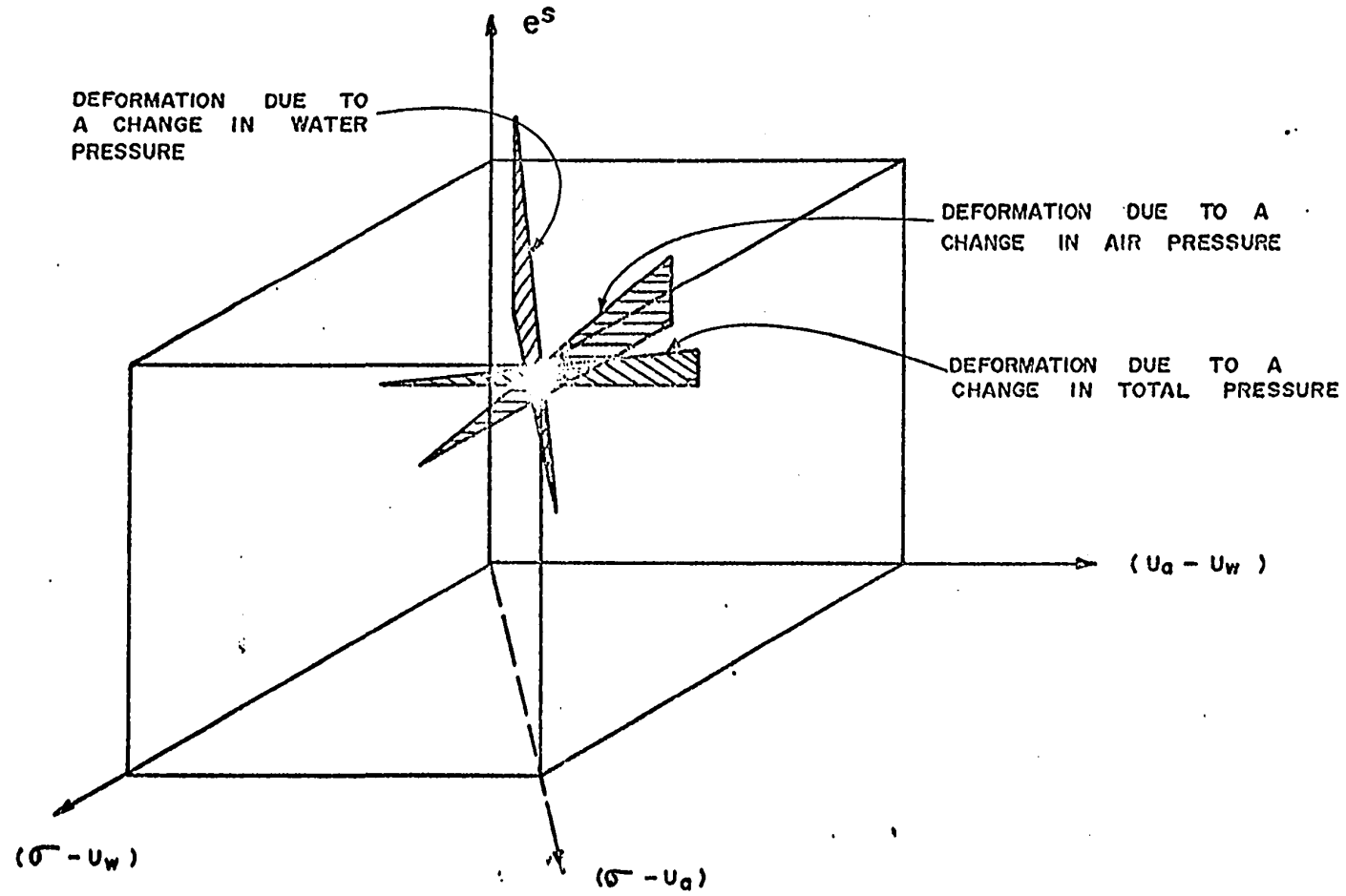


FIGURE 6.15 MINIMUM TEST REQUIREMENTS TO PROVE UNIQUENESS OF THE CONSTITUTIVE SURFACE AT A POINT

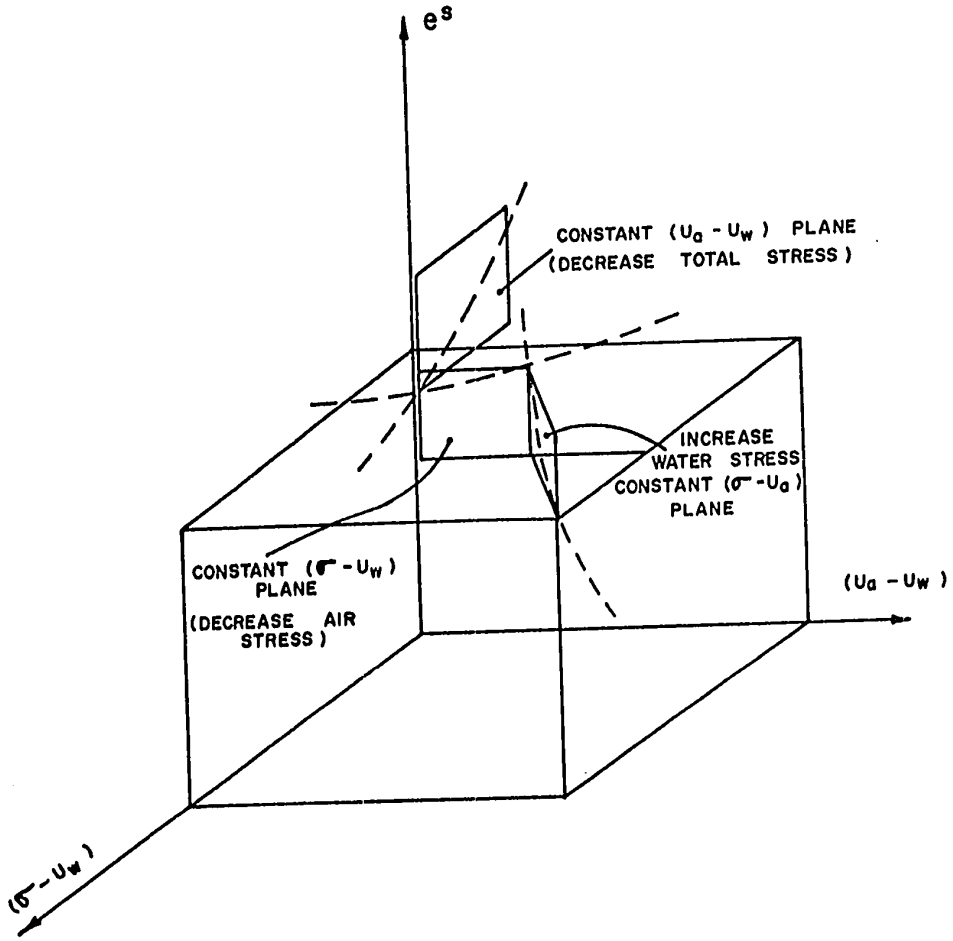


FIGURE 6.16 STRESS PATH ADHERED TO FOR THE SOIL STRUCTURE DURING THE UNIQUENESS TESTS AT A POINT

$$\frac{dv^s}{v} = C_t{}^s \cdot d(\sigma - u_w) \quad \text{or}$$

$$C_t{}^s = \frac{dv^s/v}{d(\sigma - u_w)} \qquad 6.38$$

Let the second pressure change be an increase in the air pressure. Therefore,

$$C_a{}^s = \frac{dv^s/v}{d(u_a - u_w)}$$

Now that the two compressibility modulii are known (i.e., $C_t{}^s$ and $C_a{}^s$), the volumetric deformation corresponding to a change in the pore water pressure can be computed. This value can be compared with the measured volumetric deformation. Similar values indicate uniqueness of the constitutive surface at a point. Some discrepancy is anticipated since all stress changes do not initiate from the same point.

The procedure used for most of the tests for the uniqueness analysis is as follows. The sample was allowed to come to equilibrium under an arbitrary set of stress conditions. An attempt was made to have a large initial suction. The water pressure was generally increased for the first pressure increment. After equalization, the air pressure was decreased. After equalization, the total pressure was decreased. The above procedure could be repeated through several cycles as long as the suction remained positive. Throughout these steps, the water phase volume was continually increasing. The soil structure and air

phase underwent a reversal in their direction of volume change (Figure 6.17). Other stress paths could also have been followed but this procedure lent itself to the operation of the equipment.

Mapping the equilibrium states of an unsaturated soil basically requires a knowledge of the soil structure and contractile skin constitutive surfaces. However, as a consequence of the continuity requirement for an unsaturated soil, the mapping of the water phase deformation also produces another constitutive surface. The soil structure and water phase constitutive surfaces are analysed in detail since they were independently measured in the laboratory.

6.12 Presentation of Uniqueness Test Data

The data used for the uniqueness analysis is presented in Appendix F. Four samples were tested for uniqueness at a point. The first three samples (#15A, #16 and #17) were Regina Clay while sample #21 was compacted kaolin. The volume changes observed as a result of the stress component changes are summarized in Table VI.5. The volume changes at two elapsed times are considered for each sample since it is difficult to determine the point of complete equalization. For example, the secondary volume change behavior of Regina clay results in volume changes that appear to continue almost indefinitely. These secondary effects may distort or warp the constitutive surface and actually decrease uniqueness with time.

As a result of changing one stress component, it is possible to compute six compressibility values. For example, the changing of the pore water pressure effects the overall volume, the air and water

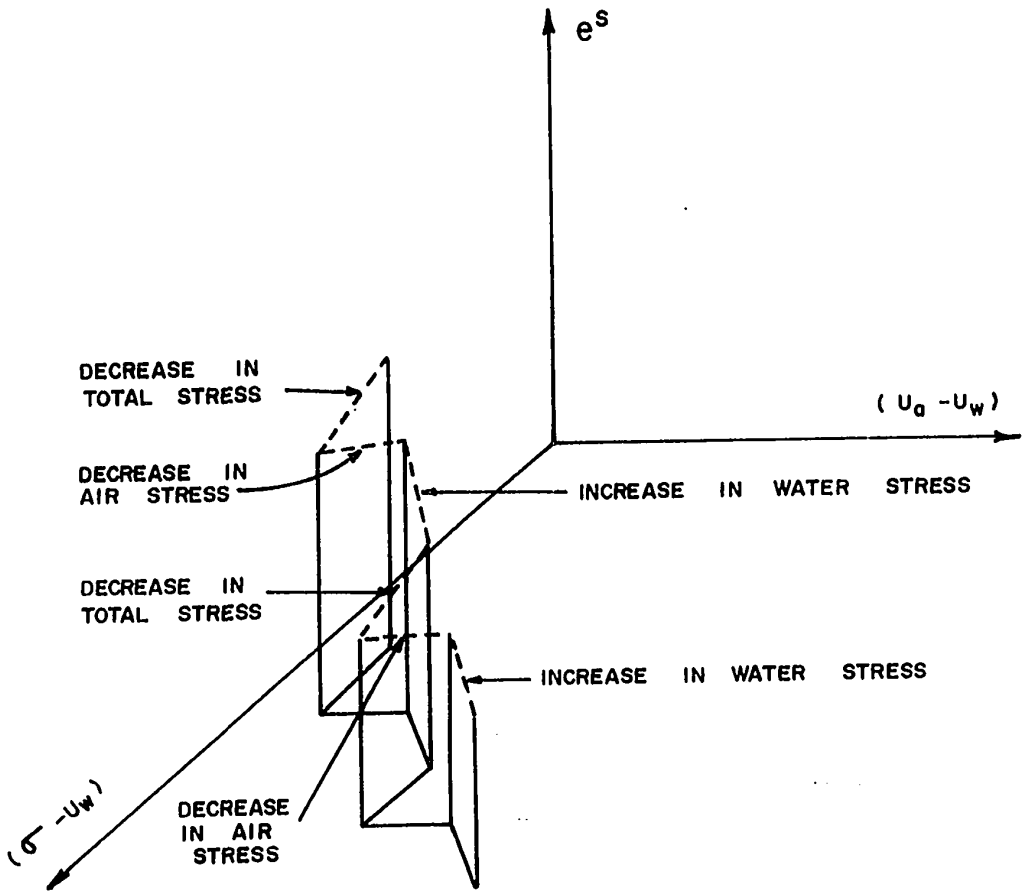


FIGURE 6.17 DEFORMATION OF THE SOIL STRUCTURE FOR SAMPLE # 15 A

TABLE VI.5

VOLUME-CHANGES CORRESPONDING TO STRESS COMPONENT CHANGES FOR TESTS TO EVALUATE UNIQUENESS OF THE CONSTITUTIVE SURFACE AT A POINT

Test No.	Elapsed Time (min)	Normalized Stress Component Changes			Percent Volume Change		
		$\Delta\sigma$ (psi)	Δu_a (psi)	Δu_w (psi)	Total or Soil Structure	Air	Water
Sample #15A							
C-1	1000	0	0	+10.54	-0.060	+0.080	-0.140
C-1	5000	0	0	+10.54	-0.188	+0.070	-0.258
C-2	1000	0	- 9.96	0	+0.030	+0.190	-0.160
C-2	5000*	0	- 9.96	-	+0.04	+0.44	-0.40
C-3	1000	-10.29	0	0	-0.110	-0.005	-0.105
C-3	5000	-10.29	0	0	-0.230	+0.280	-0.510
C-4	1000	0	0	+ 9.68	-0.050	+0.150	-0.200
C-4	5000	0	0	+ 9.68	-0.175	+0.565	-0.740
C-5	1000	0	-10.13	0	+0.045	+0.275	-0.230
C-5	5000	0	-10.13	0	+0.040	+0.860	-0.820
C-6	1000	-10.04	0	0	-0.110	+0.076	-0.185
C-6	5000	-10.04	0	0	-0.215	+0.385	-0.600
Sample #16							
C-7	2000	0	0	+ 9.95	+0.035	+0.163	-0.128
C-7	15000	0	0	+ 9.95	-0.090	+0.202	-0.292
C-8	2000	0	-10.03	0	+0.315	+0.375	-0.060
C-8	15000	0	-10.03	0	+0.290	+0.570	-0.280
C-9	2000	- 9.88	0	0	-0.160	-0.055	-0.105
C-9	15000	- 9.88	0	0	-0.255	+0.060	-0.315
C-10	2000	0	0	+ 9.88	-0.075	+0.040	-0.115
C-10	15000	0	0	+ 9.88	-0.220	+0.235	-0.455
C-11	2000	0	- 9.96	0	+0.225	+0.315	-0.090
C-11	15000	0	- 9.96	0	+0.265	+0.790	-0.525
C-12	2000	- 9.94	0	0	-0.210	-0.083	-0.127
C-12	15000	- 9.94	0	0	-0.430	+0.150	-0.580
C-13	2000	- 9.85	0	0	-0.335	-0.182	-0.153
C-13	15000	- 9.85	0	0	-0.705	-0.058	-0.647

*Deformations are very approximate

TABLE VI.5 (continued)

Test No.	Elapsed Time (min)	Normalized Stress Component Changes			Percent Volume Change		
		$\Delta\sigma$ (psi)	Δu_a (psi)	Δu_w (psi)	Total or Soil Structure	Air	Water
Sample #17							
C-14	1000	0	0	+10.00	-0.100	+0.090	0.190
C-14	5000	0	0	+10.00	-0.360	+0.230	-0.590
C-15	1000	0	-10.00	0	+0.018	+0.068	-0.050
C-15	5000	0	-10.00	0	-0.060	+0.230	-0.290
C-16	1000	-10.13	0	0	-0.140	-0.050	-0.090
C-16	5000	-10.13	0	0	-0.345	+0.135	-0.480
C-17	1000	0	0	+10.00	-0.095	+0.105	-0.200
C-17	5000	0	0	+10.00	-0.280	+0.320	-0.600
Sample #21							
C-18	2000	- 9.80	0	0	-0.110	-0.078	-0.032
C-18	10000**	- 9.80	0	0	-0.070	-0.080	+0.010
C-19	2000	0	- 9.95	0	-0.015	-0.015	0.000
C-19	10000**	0	- 9.95	0	-0.015*	-0.015	0.000*
C-20	2000	0	0	+10.04	-0.033	+0.167	-0.200
C-20	10000**	0	0	+10.04	-0.020*	+0.350	-0.370*
C-21	2000	- 9.75	0	0	-0.290	-0.120	-0.170
C-21	10000**	- 9.75	0	0	-0.320	-0.170	-0.150
C-22	2000	0	- 9.86	0	-0.037	+0.053	-0.090
C-22	10000**	0	- 9.86	0	-0.010*	+0.090	-0.100*
C-23	2000	0	0	+ 9.91	-0.127	+0.258	-0.385
C-23	10000**	0	0	+ 9.91	-0.180*	+0.310	-0.490*
C-24	2000	- 9.68	0	0	-0.700	-0.405	-0.295
C-24	10000	- 9.68	0	0	-0.820	-0.494	-0.326
C-25	2000	0	-10.03	0	+0.235	+0.805	-0.570
C-25	10000	0	-10.03	0	+0.180	+1.067	-0.887
C-26	2000	0	0	+ 4.87	-0.005	+0.655	-0.660
C-26	15000	0	0	+ 4.87	-0.010	+1.510	-1.520
C-27	2000	- 9.74	0	0	-0.595	-0.130	-0.465
C-27	15000	- 9.74	0	0	-0.730*	+0.120	-0.850*

**Estimated Equilibrium Conditions

TABLE VI.5 (continued)

Test No.	Elapsed Time (min)	Normalized Stress Component Changes			Percent Volume Change		
		$\Delta\sigma$ (psi)	Δu_a (psi)	Δu_w (psi)	Total or Soil Structure	Air	Water
C-28	2000	+ 9.30	0	0	+0.315	+9.260	+0.055
C-28	10000**	+ 9.30	0	0	+0.360*	+0.280	+0.080*
C-29	2000	0	0	- 4.83	+0.090	-0.390	+0.480
C-29	20000**	0	0	- 4.83	+0.260*	-0.670	+0.930*
C-30	2000	+29.20	0	0	+1.890	+0.870	+1.020
C-30	10000	+29.20	0	0	+2.160	+0.710	+1.450
C-31	2000	0	+30.03	0	-0.080	-0.730	+0.650
C-31	15000	0	+30.03	0	+0.045	-0.910	+0.955
C-32	2000	0	0	+29.86	-0.526	+0.456	-0.982
C-32	12000	0	0	+29.86	-0.567	+0.663	-1.230

volumes of the sample. However, the compressibilities are not computed with respect to the stress component changes but with respect to the stress state variable changes. The stress state variables affected by a change in pore water pressure are $(\sigma-u_w)$ and (u_a-u_w). The compressibilities that can be computed are:

Soil Structure

C_w^s -
- $C^s_{(\sigma-u_w)}$ - Compressibility of the soil structure with respect to a change in $(\sigma-u_w)$
- $C^s_{(u_a-u_w)}$ - Compressibility of the soil structure with respect to a change in (u_a-u_w)

Air Phase

C_w^a -
- $C^a_{(\sigma-u_w)}$ - Compressibility of the air phase with respect to a change in $(\sigma-u_w)$
- $C^a_{(u_a-u_w)}$ - Compressibility of the air phase with respect to a change in (u_a-u_w)

Water Phase

C_w^w -
- $C^w_{(\sigma-u_w)}$ - Compressibility of the water phase with respect to a change in $(\sigma-u_w)$
- $C^w_{(u_a-u_w)}$ - Compressibility of the water phase with respect to a change in (u_a-u_w)

When computing the compressibilities, the sign of the stress state variable must be taken into account. For example, a decrease in the air pressure produces a positive change in the $(\sigma-u_a)$ stress stress variable but a negative change in the (u_a-u_w) stress state variable

change. The sign designations for the stress state variable changes are summarized in Table VI.6.

TABLE VI.6

SIGN DESIGNATIONS FOR STRESS STATE VARIABLE CHANGES

Stress Component Change	Stress State Variable Change		
	$\sigma-u_w$	$\sigma-u_a$	u_a-u_w
$+\Delta\sigma$	(+)	(+)	-
$-\Delta\sigma$	(-)	(-)	-
$+\Delta u_a$	-	(-)	(+)
$-\Delta u_a$	-	(+)	(-)
$+\Delta u_w$	(-)	-	(-)
$+\Delta u_w$	(+)	-	(+)

Each compressibility value bears a sign that is a consequence of the sign of the volume change and the sign of the stress state variable changes. Table VI.7 summarizes the compressibility values with respect to the stress state variable changes for all tests.

6.13 Analysis of the Uniqueness Test Data

6.13.1 Possible Checks for Uniqueness

The object of the analysis is to compute two compressibility values and use them to predict volume change in the direction bisecting stress state variable axes. The predicted value can be compared with a laboratory measured value. The cyclic incrementing of the water, air

TABLE VI.7

SUMMARY OF COMPRESSIBILITIES WITH RESPECT TO SOIL STRUCTURE, AIR AND WATER PHASES

Test No.	Soil Structure Compressibility (sq.in/lb x 10^{-2})			Compressibility with Respect to Contractile Skin (Air Phase)*			Compressibility with Respect to Water Phase*		
	$\Delta(\sigma-u_w)$	$\Delta(\sigma-u_a)$	$\Delta(u_a-u_w)$	$\Delta(\sigma-u_w)$	$\Delta(\sigma-u_a)$	$\Delta(u_a-u_w)$	$\Delta(\sigma-u_w)$	$\Delta(\sigma-u_a)$	$\Delta(u_a-u_w)$
Sample #15A (1000 minutes)									
C-1	+0.0057	--	+0.0057	-0.0076	--	-0.0076	+0.0133	--	+0.0133
C-2	--	+0.0030	-0.0030	--	+0.0191	-0.0191	--	-0.0161	+0.0161
C-3	+0.0107	+0.0107	--	+0.0005	+0.0005	--	+0.0102	+0.0102	--
C-4	+0.0052	--	+0.0052	-0.0155	--	-0.0155	+0.0207	--	+0.0207
C-5	--	+0.0044	-0.0044	--	+0.0272	-0.0272	--	-0.0227	+0.0227
C-6	+0.0110	+0.0110	--	-0.0076	-0.0076	--	+0.0184	+0.0184	--
Sample #15A (5000 minutes)									
C-1	+0.0178	--	+0.0178	-0.0066	--	-0.0066	+0.0245	--	+0.0245
C-2	--	+0.004	-0.0040	--	+0.0442	-0.0442	--	-0.0402	+0.0402
C-3	+0.0224	+0.0224	--	-0.0272	-0.0272	--	+0.0496	+0.0496	--
C-4	+0.0181	--	+0.0181	-0.0485	--	-0.0584	+0.0765	--	+0.0765
C-5	--	+0.0039	-0.0039	--	+0.0849	-0.0849	--	-0.0810	+0.0810
C-6	+0.0214	+0.0214	--	-0.0384	-0.0384	--	+0.0598	+0.0598	--
Sample #16 (2000 minutes)									
C-7	-0.0035	--	-0.0035	-0.0164	--	-0.0164	+0.0129	--	+0.0129
C-8	--	+0.0314	-0.0314	--	+0.0374	-0.0374	--	-0.0060	+0.0060
C-9	+0.0162	+0.0162	--	+0.0056	+0.0056	--	+0.0106	+0.0106	--
C-10	+0.0076	--	+0.0076	-0.0040	--	-0.0040	+0.0116	--	+0.0116
C-11	--	+0.0226	-0.0226	--	+0.0316	-0.0316	--	-0.0090	+0.0090

*All compressibilities presented as sq.in. per pound x 10^{-2}

TABLE VI.7 (continued)

Test No.	Soil Structure Compressibility (sq.in/lb x 10^{-2})			Compressibility with Respect to Contractile Skin (Air Phase)*			Compressibility with Respect to Water Phase *		
	$\Delta(\sigma-u_w)$	$\Delta(\sigma-u_a)$	$\Delta(u_a-u_w)$	$\Delta(\sigma-u_w)$	$\Delta(\sigma-u_a)$	$\Delta(u_a-u_w)$	$\Delta(\sigma-u_w)$	$\Delta(\sigma-u_a)$	$\Delta(u_a-u_w)$
C-12	+0.0211	+0.0211	--	+0.0084	+0.0084	--	+0.0128	+0.0128	--
C-13	+0.0340	--	+0.0340	+0.0185	--	+0.0185	+0.0155	--	+0.0155
Sample #16 (15000 minutes)									
C-7	+0.0090	--	+0.0090	-0.0203	--	-0.0203	+0.0293	--	+0.0293
C-8	--	+0.0289	-0.0289	--	+0.0568	-0.0568	--	-0.0279	+0.0279
C-9	+0.0258	+0.0258	--	-0.0061	-0.0061	--	+0.0319	+0.0319	--
C-10	+0.0223	--	+0.0223	-0.0238	--	-0.0238	+0.0461	--	+0.0461
C-11	--	+0.0266	-0.266	--	+0.0793	-0.0793	--	-0.0527	+0.0527
C-12	+0.0433	+0.0433	--	-0.0151	-0.0151	--	+0.0584	+0.0584	--
C-13	+0.0716	+0.0716	--	+0.0059	+0.0059	--	+0.0657	+0.0657	--
Sample #17 (1000 minutes)									
C-14	+0.0100	--	+0.0100	-0.0090	--	-0.0090	+0.0190	--	+0.0190
C-15	--	+0.0018	-0.0018	--	+0.0068	-0.0068	--	-0.0050	+0.0050
C-16	+0.0138	+0.0138	--	+0.0049	+0.0049	--	+0.0089	+0.0089	--
C-17	+0.0095	--	+0.0095	-0.0105	--	-0.0105	+0.0200	--	+0.0200
Sample #17 (5000 minutes									
C-14	+0.0360	--	+0.0360	-0.0230	--	-0.0230	+0.0590	--	+0.0590
C-15	--	-0.0060	+0.0060	--	+0.0230	-0.0230	--	-0.0290	+0.0290
C-16	+0.0341	+0.0341	--	-0.0133	-0.0133	--	+0.0474	+0.0474	--
C-17	+0.0280	--	+0.0280	-0.0320	--	-0.0320	+0.0600	--	+0.0600

TABLE VI.7 (continued)

Test No.	Soil Structure Compressibility (sq.in/lb x 10^{-2})			Compressibility with Respect to Contractile Skin (Air Phase)*			Compressibility with Respect to Water Phase*		
	$\Delta(\sigma-u_w)$	$\Delta(\sigma-u_a)$	$\Delta(u_a-u_w)$	$\Delta(\sigma-u_w)$	$\Delta(\sigma-u_a)$	$\Delta(u_a-u_w)$	$\Delta(\sigma-u_w)$	$\Delta(\sigma-u_a)$	$\Delta(u_a-u_w)$
Sample #21 (2000 minutes)									
C-18	+0.0112	+0.0112	--	+0.0079	+0.0079	--	+0.0033	+0.0033	--
C-19	--	-0.0015	+0.0015	--	-0.0015	+0.0015	--	0.0000	0.0000
C-20	+0.0033	--	+0.0033	-0.0166	--	-0.0166	+0.0199	--	+0.0199
C-21	+0.0297	+0.0297	--	+0.0123	+0.0123	--	+0.0174	+0.0174	--
C-22	--	-0.0038	+0.0038	--	+0.0054	-0.0054	--	-0.0091	+0.0091
C-23	+0.0128	--	+0.0128	-0.0260	--	-0.0260	+0.0388	--	+0.0388
C-24	+0.0723	+0.0723	--	+0.0418	+0.0418	--	+0.0305	+0.0305	--
C-25	--	+0.0234	-0.0234	--	+0.0803	-0.0803	--	-0.0568	+0.0568
C-26	+0.0010	--	+0.0010	-0.1345	--	-0.1345	+0.1355	--	+0.1355
C-27	+0.0611	+0.0611	--	+0.0133	+0.0133	--	+0.0477	+0.0477	--
C-28	+0.0339	+0.0339	--	+0.0280	+0.0280	--	+0.0059	+0.0059	--
C-29	+0.0186	--	+0.0186	-0.0807	--	-0.0807	+0.0994	--	+0.0994
C-30	+0.0647	+0.0647	--	+0.0298	+0.0298	--	+0.0349	+0.0349	--
C-31	--	+0.0027	-0.0027	--	+0.0243	-0.0243	--	-0.0216	+0.0216
C-32	+0.0176	--	+0.0176	-0.0153	--	-0.0153	+0.0329	--	+0.0329
Sample #21 (Equilibrium Conditions)									
C-18	+0.0071	+0.0071	--	+0.0082	+0.0082	--	-0.0010	-0.0010	--
C-19	--	-0.0015	+0.0015	--	-0.0015	+0.0015	--	0.0000	0.0000
C-20	+0.0020	--	+0.0020	-0.0349	--	-0.0349	+0.0369	--	+0.0369
C-21	+0.0328	+0.0328	--	+0.0174	+0.0174	--	+0.0154	+0.0154	--
C-22	--	-0.0010	+0.0010	--	+0.0091	-0.0091	--	-0.0101	+0.0101
C-23	+0.0182	--	+0.0182	-0.0313	--	-0.0313	+0.0494	--	+0.0494
C-24	+0.0847	+0.0847	--	+0.0510	+0.0510	--	+0.0337	+0.0337	--

TABLE VI.7 (continued)

Test No.	Soil Structure Compressibility (sq.in/lb x 10^{-2})			Compressibility with Respect to Contractile Skin (Air Phase)*			Compressibility with Respect to Water Phase*		
	$\Delta(\sigma-u_w)$	$\Delta(\sigma-u_a)$	$\Delta(u_a-u_w)$	$\Delta(\sigma-u_w)$	$\Delta(\sigma-u_a)$	$\Delta(u_a-u_w)$	$\Delta(\sigma-u_w)$	$\Delta(\sigma-u_a)$	$\Delta(u_a-u_w)$
C-25	--	+0.0179	-0.0179	--	+0.1064	-0.1064	--	-0.0884	+0.0884
C-26	+0.0021	--	+0.0021	=0.3101	--	-0.3101	+0.3121	--	+0.3121
C-27	+0.0749	+0.0749	--	-0.0123	-0.0123	--	+0.0873	+0.0873	--
C-28	+0.0387	+0.0387	--	+0.0301	+0.0301	--	+0.0086	+0.0086	--
C-20	+0.0538	--	+0.0538	-0.1387	--	-0.1387	+0.1925	--	+0.1925
C-30	+0.0740	+0.0740	--	+0.0243	+0.0243	--	+0.0497	+0.0497	--
C-31	--	-0.0015	+0.0015	--	+0.0303	-0.0303	--	-0.0318	+0.0318
C-32	+0.0190	--	+0.0190	-0.0222	--	-0.0222	+0.0412	--	+0.0412

and total pressures gives rise to a number of possible uniqueness test combinations or "checks". Let each pressure increment be designated as U_i where i = 1, n and n is the total number of pressure increments.

For the prediction of volume change, the first combination of pressure increments involves tests,

$$U_i \text{ and } U_{i+1} \quad \text{for} \quad i = 1 \text{ to } n-1$$

A second combination of pressure increments involves tests,

$$U_i \text{ and } U_{i+2} \quad \text{for} \quad i = 1 \text{ to } n-2$$

Other combinations are also possible but they become unreasonable due to the non linearity of the constitutive surface.

The above predicted volume changes can be compared with the following measured volume changes. The first combination of pressure increments can be compared with the previous and subsequent volume changes measured.

$$U_{i-1} \text{ and } U_{i+2} \quad \text{for} \quad i > 1 \text{ and } i < n + 1$$

The second combination of pressure increments can be compared with the volume changes measured in test U_{i+1}. There are $[2\cdot(n-1)-2]$ "checks" for uniqueness performed from the first set of combinations and (n-2) "checks" performed from the second set of combinations. The total number of "checks" is $(3\cdot n-6)$.

6.13.2 Procedure for the Computation of Predicted Volume Changes

Let us consider an example problem and perform the calculations required to obtain the predicted volume change. Consider the soil structure volume changes obtained during tests C-2 and C-3 of Sample #15A (5000 minutes). During test C-2, the air pressure change was -9.96 psi and the measured soil structure volume change was +0.040 percent. During test C-3, the total pressure change was - 10.29 psi and the measured soil structure volume change was - 0.230 percent. The volume change equation to consider for this set of pressure changes is:

$$\frac{dv^s}{v} = C_t^s \cdot d\,(\sigma - u_w) + C_a^s \cdot d(u_a - u_w) \qquad 6.40$$

Substituting the values from test C-2 into the above equation gives

$$+\,0.040 = C_t^s \cdot (0) + C_a^s \cdot (-9.96)$$

Therefore, $C_a^s = -\,0.004$.

Substituting the values from test C-3 gives:

$$-\,0.230 = C_t^s \cdot (-\,10.29) + C_a^s \cdot (0)$$

Therefore, $C_t^s = +\,0.0224$.

With these two compressibility values known, it is possible

to move along the bisector of the two previous stress paths by changing the water pressure by +10 psi. The increase in water pressure by 10 psi decreases the $(\sigma-u_w)$ and (u_a-u_w) stress state variables by 10 psi. The predicted volume change is:

$$\frac{dv^s}{v} = - 0.004\cdot(-10.0) + 0.0224(-10.0)$$

or

$$\frac{dv^s}{v} = 0.184 \text{ percent.}$$

The predicted volume change can be compared with the measured volume changes from tests C-1 and C-4 which are -0.181 percent and -0.178 percent respectively.

A similar analysis can be performed with respect to the water phase volumetric deformations. Table VI.8 summarizes the predicted and measured volume changes on the four samples tested.

6.13.3 Comparison of Agreement Between Predicted and Measured Volume Changes

The comparison of the predicted and measured volume changes is referred to as the uniqueness analysis. The predicted and measured volume changes can be visually assessed by plotting the predicted volume changes versus the measured volume changes for each test. It is also desirable to have a quantatative measure of the degree of success of the correlation.

Three quantative measures are required to evaluate the success of the constitutive surface mathematical relationship. These

TABLE VI.8

COMPARISON OF PREDICTED AND MEASURED VOLUME CHANGES (UNIQUENESS AT A POINT)

Compressibilities Taken From Tests	Stress Change Considered	Soil Structure Volume Change (%)		Air Phase Volume Change (%)		Water Phase Volume Change (%)	
		Measured	Predicted	Measured	Predicted	Measured	Predicted
Sample #15A (1000 minutes)							
C-1 and C-2	$\Delta\sigma$ = - 10 psi	-0.110	-0.087	-0.005	-0.115	-0.105	+0.028
C-2 and C-3	Δu_w = + 10 psi	-0.060 -0.050	-0.077	-0.080 -0.150	+0.186	-0.140 -0.200	-0.263
C-3 and C-4	Δu_a = - 10 psi	+0.030 +0.045	+0.055	+0.190 +0.275	+0.160	-0.160 -0.230	-0.105
C-4 and C-5	$\Delta\sigma$ = - 10 psi	-0.107 -0.110	-0.096	-0.005 +0.076	-0.117	-0.102 -0.185	+0.020
C-5 and C-6	Δu_w = + 10 psi	-0.050	-0.066	+0.150	+0.348	-0.200	-0.411
C-1 and C-3	Δu_a = - 10 psi	+0.030	+0.050	+0.190	+0.081	-0.160	-0.031
C-2 and C-4	$\Delta\sigma$ = - 10 psi	-0.110	-0.082	-0.005	-0.036	-0.105	-0.046
C-3 and C-5	Δu_w = + 10 psi	-0.050	-0.063	+0.150	+0.267	-0.200	-0.329
C-4 and C-6	Δu_a = - 10 psi	+0.045	+0.058	+0.275	+0.079	-0.230	-0.023
Sample #15A (5000 minutes)							
C-1 and C-2	$\Delta\sigma$ = - 10 psi	-0.224	-0.218	+0.272	-0.376	-0.496	+0.157
C-2 and C-3	Δu_w = + 10 psi	-0.178 -0.181	-0.184	+0.066 +0.584	+0.714	-0.245 -0.765	-0.898
C-3 and C-4	Δu_a = - 10 psi	+0.04 +0.039	+0.043	+0.442 +0.849	+0.312	-0.402 -0.810	-0.269

TABLE VI.8 (continued)

Compressibilities Taken From Tests	Stress Change Considered	Soil Structure Volume Change (%)		Air Phase Volume Change (%)		Water Phase Volume Change (%)	
		Measured	Predicted	Measured	Predicted	Measured	Predicted
C-4 and C-5	$\Delta\sigma$ = - 10 psi	-0.224 -0.214	-0.220	+0.272 +0.384	-0.265	-0.496 -0.598	+0.045
C-5 and C-6	Δu_w = + 10 psi	-0.181	-0.175	+0.584	+1.233	-0.765	-1.408
C-1 and C-3	Δu_a = - 10 psi	+0.040	+0.046	+0.442	-0.206	-0.402	+0.251
C-2 and C-4	$\Delta\sigma$ = - 10 psi	-0.224	-0.221	+0.272	+0.142	-0.496	-0.363
C-3 and C-5	Δu_w = + 10 psi	-0.181	-0.185	+0.584	+1.121	-0.765	-1.306
C-4 and C-6	Δu_a = - 10 psi	+0.039	+0.033	+0.849	+0.200	-0.810	-0.167
Sample #16 (2000 minutes)							
C-7 and C-8	$\Delta\sigma$ = - 10 psi	-0.162	-0.279	-0.056	-0.210	-0.106	-0.069
C-8 and C-9	Δu_w = + 10 psi	+0.035 -0.075	+0.152	+0.164 +0.040	+0.318	-0.129 -0.116	-0.166
C-9 and C-10	Δu_a = - 10 psi	+0.314 +0.226	+0.086	+0.374 +0.315	+0.096	-0.060 -0.090	-0.010
C-10 and C-11	$\Delta\sigma$ = - 10 psi	-0.162 -0.211	-0.302	-0.056 -0.084	-0.276	-0.106 -0.128	-0.026
C-11 and C-12	Δu_w = + 10 psi	-0.076	+0.015	+0.040	+0.232	-0.116	-0.218
C-7 and C-9	Δu_a = - 10 psi	+0.314	+0.197	+0.374	+0.220	-0.060	-0.023
C-8 and C-10	$\Delta\sigma$ = - 10 psi	-0.162	-0.390	-0.056	-0.334	-0.106	-0.056
C-9 and C-11	Δu_w = + 10 psi	-0.076	+0.064	+0.040	+0.260	-0.116	-0.196
C-10 and C-12	Δu_a = - 10 psi	+0.226	+0.135	+0.316	+0.124	-0.090	+0.012

TABLE VI.8 (continued)

Compressibilities Taken From Tests	Stress Change Considered	Soil Structure Volume Change (%)		Air Phase Volume Change (%)		Water Phase Volume Change (%)	
		Measured	Predicted	Measured	Predicted	Measured	Predicted
Sample #16 (15000 minutes)							
C-7 and C-8	$\Delta\sigma$ = - 10 psi	-0.258	-0.379	+0.061	-0.365	-0.319	-0.014
C-8 and C-9	Δu_w = + 10 psi	-0.090 -0.223	+0.031	+0.203 +0.238	+0.629	-0.293 -0.461	-0.598
C-9 and C-10	Δu_a = - 10 psi	+0.289 +0.266	+0.035	+0.568 +0.793	+0.177	-0.279 -0.527	-0.142
C-10 and C-11	$\Delta\sigma$ = - 10 psi	-0.258 -0.430	-0.489	+0.061 +0.151	-0.555	-0.319 -0.584	+0.066
C-11 and C-12	Δu_w = + 10 psi	-0.223	-0.167	+0.238	+0.944	-0.461	-1.111
C-7 and C-9	Δu_a = - 10 psi	+0.289	+0.168	+0.568	+0.142	-0.279	+0.026
C-8 and C-10	$\Delta\sigma$ = - 10 psi	-0.258	-0.512	+0.061	-0.330	-0.319	-0.182
C-9 and C-11	Δu_w = + 10 psi	-0.223	+0.008	+0.238	+0.854	-0.461	-0.846
C-10 and C-12	Δu_a = - 10 psi	+0.266	+0.210	+0.793	+0.087	-0.527	+0.123
Samp e #17 (1000 minutes)							
C-14 and C-15	$\Delta\sigma$ = - 10 psi	-0.138	-0.118	-0.049	+0.022	-0.089	-0.140
C-15 and C-16	Δu_w = + 10 psi	-0.100 -0.095	-0.120	+0.090 +0.105	+0.019	-0.190 -0.200	-0.139
C-16 and C-17	Δu_a = - 10 psi	+0.018	+0.043	+0.068	+0.154	-0.050	-0.111
C-14 and C-16	Δu_a = - 10 psi	+0.018	+0.038	+0.068	+0.139	-0.050	-0.101
C-15 and C-17	$\Delta\sigma$ = - 10 psi	-0.138	-0.113	-0.049	+0.037	-0.089	-0.150

TABLE VI.8 (continued)

Compressibilities Taken From Tests	Stress Change Considered	Soil Structure Volume Change (%)		Air Phase Volume Change (%)		Water Phase Volume Change (%)	
		Measured	Predicted	Measured	Predicted	Measured	Predicted
Sample #17 (5000 minutes)							
C-14 and C-15	$\Delta\sigma$ = - 10 psi	-0.345	-0.300	+0.135	0.000	-0.480	-0.300
C-15 and C-16	Δu_w = + 10 psi	-0.360 -0.280	-0.401	+0.230 +0.320	+0.363	-0.590 -0.600	-0.764
C-16 and C-17	Δu_a = - 10 psi	-0.060	+0.061	+0.230	+0.187	-0.290	-0.126
C-14 and C-16	Δu_a = - 10 psi	-0.060	-0.019	+0.230	+0.097	-0.290	-0.116
C-15 and C-17	$\Delta\sigma$ = - 10 psi	-0.341	-0.220	+0.133	+0.090	-0.474	-0.310
Sample #21 (2000 minutes)							
C-18 and C-19	Δu_w = + 10.0 psi	-0.033	-0.127	+0.166	-0.094	-0.199	-0.033
C-19 and C-20	$\Delta\sigma$ = - 10.0 psi	-0.112 -0.297	-0.018	-0.079 -0.123	+0.181	-0.033 -0.174	-0.199
C-20 and C-21	Δu_a = - 10.0 psi	-0.015 -0.037	+0.264	-0.015 +0.053	+0.289	0.000 -0.090	-0.025
C-21 and C-22	Δu_w = + 10.0 psi	-0.033 -0.128	-0.335	+0.166 +0.260	-0.069	-0.199 -0.388	-0.265
C-22 and C-23	$\Delta\sigma$ = - 10.0 psi	-0.297 -0.723	-0.090	-0.123 -0.418	+0.206	-0.174 -0.305	-0.297
C-23 and C-24	Δu_a = - 10.0 psi	-0.038 +0.234	+0.595	+0.054 +0.803	+0.678	-0.091 -0.568	-0.083
C-24 and C-25	Δu_w = + 10.0 psi	-0.128 -0.010	-0.489	+0.260 +1.345	+0.385	-0.388 -1.355	-0.873
C-25 and C-26	$\Delta\sigma$ = - 10.0 psi	-0.723 -0.611	-0.244	-0.418 -0.133	+0.542	-0.305 -0.477	-0.787

TABLE VI.8 (continued)

Compressibilities Taken From Tests	Stress Change Considered	Soil Structure Volume Change (%)		Air Phase Volume Change (%)		Water Phase Volume Change (%)	
		Measured	Predicted	Measured	Predicted	Measured	Predicted
C-26 and C-27	Δu_a = - 10 psi	+0.234	+0.601	+0.803	+1.478	-0.568	-0.878
C-29 and C-30	Δu_a = + 10 psi	-0.027	+0.461	-0.243	+1.105	+0.216	-0.645
C-30 and C-31	Δu_w = + 10 psi	-0.186 -0.176	-0.620	+0.807 +0.153	-0.055	-0.994 -0.329	-0.565
C-31 and C-32	$\Delta\sigma$ = + 10 psi	+0.647	-0.203	+0.298	-0.090	+0.349	-0.113
C-18 and C-20	Δu_a = - 10 psi	-0.015	+0.079	-0.015	+0.245	0.000	-0.166
C-19 and C-21	Δu_w = + 10 psi	-0.033	-0.312	+0.166	-0.138	-0.199	-0.174
C-20 and C-22	$\Delta\sigma$ = - 10 psi	-0.297	+0.005	-0.123	+0.112	-0.174	-0.108
C-21 and C-23	Δu_a = - 10 psi	-0.038	+0.169	+0.054	+0.383	-0.091	-0.214
C-22 and C-24	Δu_w = + 10 psi	-0.128	-0.761	+0.260	-0.364	-0.388	-0.396
C-23 and C-25	$\Delta\sigma$ = - 10 psi	-0.723	-0.362	-0.418	-0.543	-0.305	+0.180
C-24 and C-26	Δu_a = - 10 psi	+0.234	+0.713	+0.803	+1.763	-0.568	-1.050
C-25 and C-27	Δu_w = + 10 psi	-0.010	-0.377	+1.345	+0.670	-1.355	-1.045
C-29 and C-31	$\Delta\sigma$ = + 10 psi	+0.647	-0.213	+0.298	+0.564	+0.349	-0.778
C-30 and C-32	Δu_a = + 10 psi	-0.027	+0.471	-0.243	+ .451	+0.216	+0.020
Sample #21 (Equilibrium Conditions							
C-18 and C-19	Δu_w = + 10 psi	-0.020	-0.086	+0.349	-0.097	-0.369	+0.010
C-19 and C-20	$\Delta\sigma$ = - 10 psi	-0.071 -0.328	-0.005	-0.082 -0.174	+0.364	+0.010 +0.154	-0.369

TABLE VI.8 (continued)

Compressibilities Taken From Tests	Stress Change Considered	Soil Structure Volume Change (%)		Air Phase Volume Change (%)		Water Phase Volume Change (%)	
		Measured	Predicted	Measured	Predicted	Measured	Predicted
C-21 and C-22	Δu_w = + 10 psi	-0.020 -0.182	-0.338	+0.349 +0.313	-0.083	-0.369 -0.494	-0.255
C-22 and C-23	$\Delta\sigma$ = - 10 psi	-0.328 -0.847	-0.172	-0.174 -0.510	+0.222	-0.154 -0.337	-0.393
C-23 and C-24	Δu_a = - 10 psi	-0.010 +0.179	+0.665	+0.090 +1.064	+0.823	-0.101 -0.884	-0.157
C-24 and C-25	Δu_w = + 10 psi	-0.182 -0.020	-0.668	+0.313 +3.101	+0.554	-0.494 -3.121	-1.221
C-25 and C-26	$\Delta\sigma$ = - 10 psi	-0.847 -0.749	-0.200	-0.510 -0.123	+2.037	-0.337 -0.873	-2.237
C-26 and C-27	Δu_a = - 10 psi	+0.179	+0.728	+1.064	+2.978	-0.884	-2.248
C-29 and C-30	Δu_a = + 10 psi	+0.015	-0.202	-0.303	-1.630	+0.318	+1.428
C-30 and C-31	Δu_w = + 10 psi	-0.538 -0.190	-0.755	+1.387 +0.222	+0.060	-1.925 -0.412	-0.815
C-31 and C-32	$\Delta\sigma$ = + 10 psi	-0.740	+0.175	+0.243	+0.081	+0.497	+0.094
C-18 and C-20	Δu_a = - 10 psi	-0.015	+0.051	-0.015	+0.431	0.000	-0.379
C-19 and C-21	Δu_w = + 10 psi	-0.020	-0.343	+0.349	-0.189	-0.369	-0.154
C-20 and C-22	$\Delta\sigma$ = - 10 psi	-0.328	-0.010	-0.174	+0.258	-0.154	-0.268
C-21 and C-23	Δu_a = - 10 psi	-0.010	+0.146	+0.091	+0.487	-0.101	-0.340
C-22 and C-24	Δu_w = + 10 psi	-0.182	-0.857	+0.313	-0.419	-0.494	-0.438
C-23 and C-25	$\Delta\sigma$ = - 10 psi	-0.847	-0.361	-0.510	-0.751	-0.337	+0.390
C-24 and C-26	Δu_a = - 10 psi	+0.179	+0.826	+1.064	+3.611	-0.884	-2.784
C-25 and C-27	Δu_w = + 10 psi	-0.021	-0.570	$\pm$3.101	+1.187	-3.121	-1.757
C-29 and C-31	$\Delta\sigma$ = + 10 psi	+0.740	+0.523	+0.243	-1.084	+0.497	+1.607
C-30 and C-32	Δu_a = + 10 psi	+0.015	-0.550	-0.303	-0.465	+0.318	-0.085

are the correlation coefficient, the slope and intercept of the best-fit line (Neville and Kennedy, 1966). In the problem under consideration, a perfect uniqueness analysis should show a slope of 1.00 and an intercept of 0.00. The correlation coefficient is a measure of the dispersion about the best-fit line. The correlation coefficient (r) is computed from the equation,

$$r = \frac{n\Sigma x \cdot y - \Sigma x \cdot \Sigma y}{\sqrt{[n \cdot \Sigma x^2 - (\Sigma x)^2]\,[n \cdot \Sigma y^2 - (\Sigma y)^2]}} \qquad 6.41$$

where x = predicted volume change values

y = measured volume change values.

When the correlation coefficient is zero, there is no correlation; and when it is unity, there is perfect correlation. The significance of the correlation coefficient can be evaluated by comparing the computed value with the value that can be expected at a given level of significance if the observations are drawn by chance (i.e. Critical Correlation Coefficient). Figure 6.18 shows the critical correlation coefficient plotted versus the degrees of freedom when the total number of variables involves is two. The number of degrees of freedom is equal to the number of observations minus two.

If the computed correlation coefficient exceeds the critical correlation coefficient, we conclude that a correlation exists. The level of significance corresponding to the measured correlation coefficient represents the probability of our having drawn the wrong conclusion. In other words, the correlation coefficient is an estimate

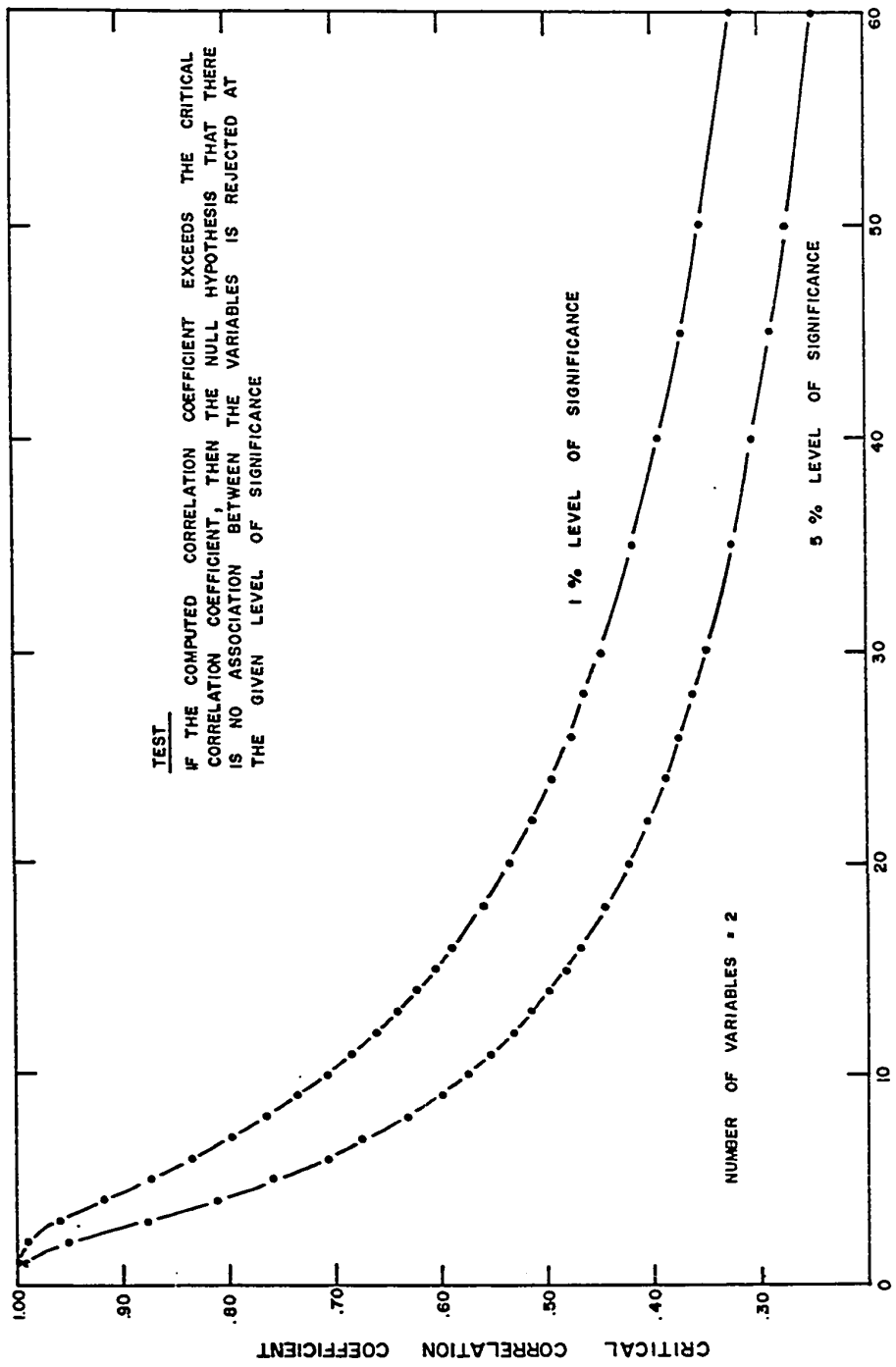


FIGURE 6.18 THEORETICAL CRITICAL CORRELATION COEFFICIENT

of the association between the predicted and measured variables. A high correlation coefficient implies causation and proves the existence of a reliable mathematical model of the constitutive surface.

The above three measures of the success of the mathematical constitutive model can check out as "perfect" only under the following conditions. First, there must be no technique or measurement errors in the data. Second, the constitutive surface of the soil structure and the contractile skin must be linear and not possess hysteresis upon a reversal of deformation.

6.13.4 Regression Analysis on Predicted and Measured Volume Changes for the Soil Structure, Air and Water Phases Assuming a Linear Constitutive Relationship

The statistical properties from the linear regression analysis between the predicted and measured volume changes are presented in Table VI.9.

The regression analysis between the predicted and measured soil structure volume changes for sample #15A show a virtually perfect correlation (Figure 6.19). The correlation coefficient is essentially 100 percent, the slope approaches 45 degrees and the intercept is less than the accuracy of the data. The correlation at 5000 minutes is slightly superior to that of 1000 minutes.

Sample #16 (Figure 6.20), tested under isotropic loading conditions, shows considerably more dispersion in the data. The results at 15,000 minutes are superior to those at 2000 minutes. The critical correlation coefficient for a one percent level of signifi-

TABLE VI.9

SUMMARY OF REGRESSION ANALYSIS USING

LINEAR CONSTITUTIVE SURFACES

Sample No.	Constitutive Surface	No. of Observations	Coef. of Correlation	Slope	Intercept
15A (1000 min)	Soil Structure	12	0.961	0.901	-0.009
	Air Phase	12	0.249	0.214	+0.069
	Water Phase	12	0.484	0.124	-0.153
15A (5000 min)	Soil Structure	12	0.999	0.993	-0.002
	Air Phase	12	0.341	0.118	+0.431
	Water Phase	12	0.514	0.116	-0.538
16 (2000 min)	Soil Structure	12	0.750	0.678	+0.038
	Air Phase	12	0.557	0.397	+0.099
	Water Phase	12	0.645	0.168	-0.089
16 (15000 min)	Soil Structure	12	0.779	0.763	+0.026
	Air Phase	12	0.209	0.107	+0.315
	Water Phase	12	0.153	0.027	-0.395
17 (1000 min)	Soil Structure	6	0.961	0.850	-0.017
	Air Phase	6	0.255	0.277	+0.021
	Water Phase	6	0.583	2.028	+0.152
17 (5000 min)	Soil Structure	6	0.904	0.650	-0.102
	Air Phase	6	0.875	0.373	+0.145
	Water Phase	6	0.931	0.433	-0.282
21 (2000 min)	Soil Structure	30	0.293	0.230	-0.082
	Air Phase	30	0.358	0.306	+0.091
	Water Phase	30	0.582	0.606	-0.052
21 (Equilibrium Conditions)	Soil Structure	30	0.458	0.358	-0.090
	Air Phase	30	0.320	0.229	+0.259
	Water Phase	30	0.612	0.475	-0.227

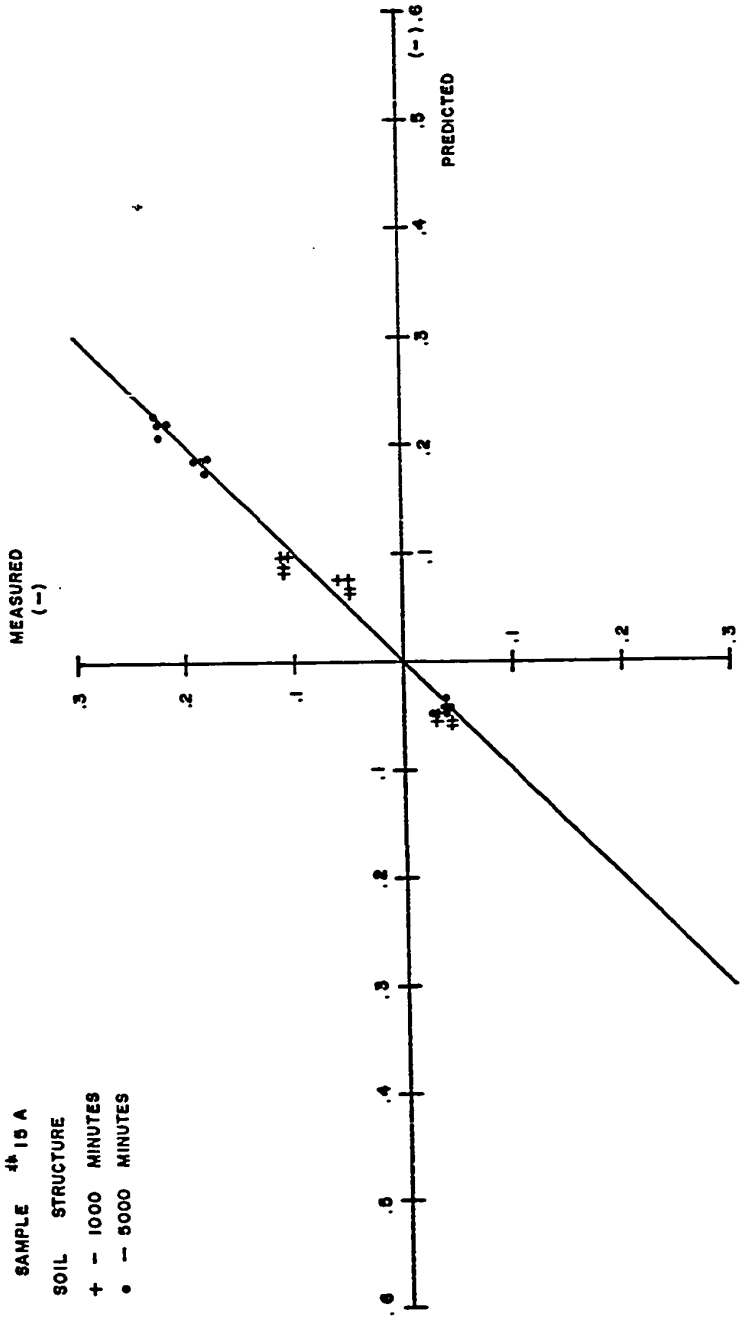


FIGURE 6.19 COMPARISON OF PREDICTED AND MEASURED SOIL STRUCTURE DEFORMATION FOR SAMPLE # 15 A

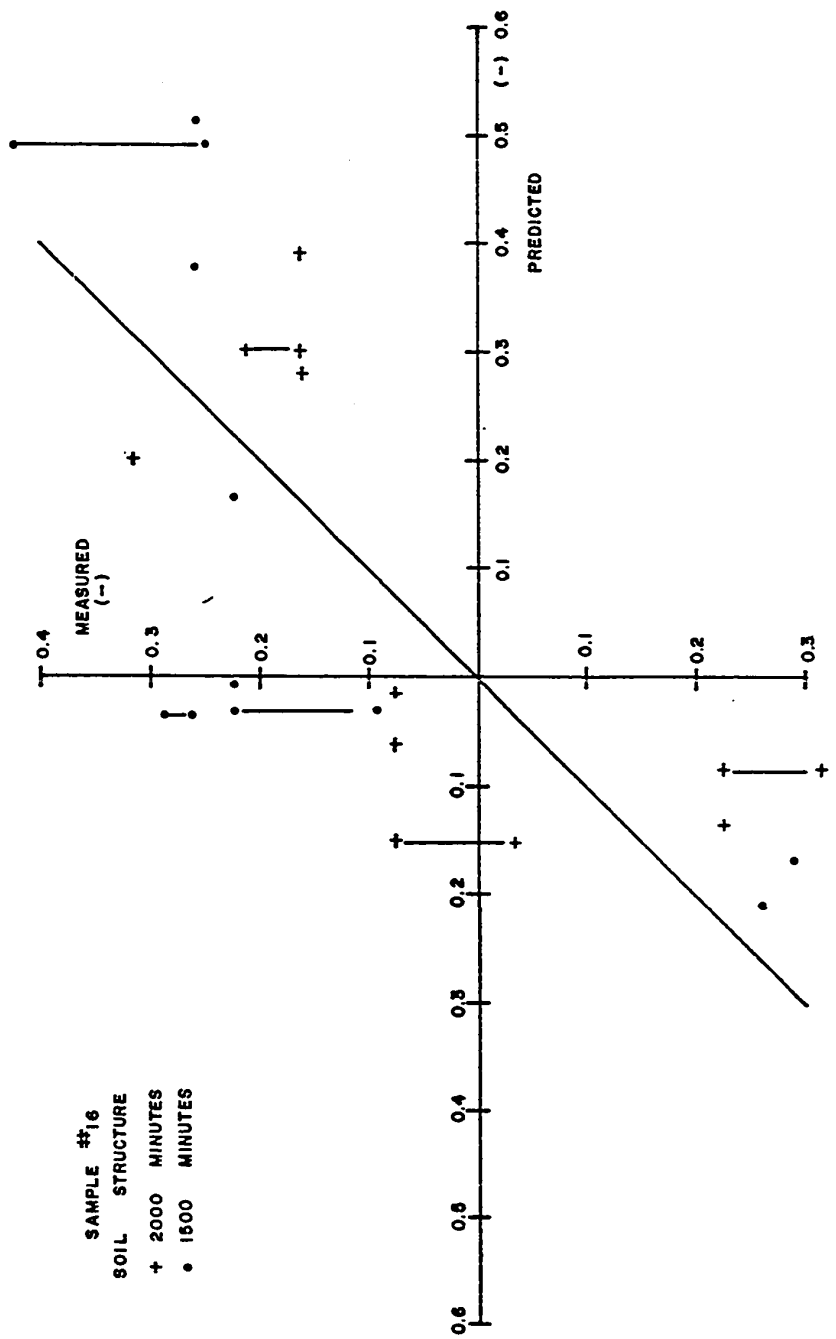


FIGURE 6.20 COMPARISON OF PREDICTED AND MEASURED SOIL STRUCTURE VOLUMETRIC DEFORMATIONS ON SAMPLE # 16

cance is 0.71 and since the computed correlation coefficient exceeds this value, a definite correlation exists. However, it is not nearly as convincing as the results from sample #15A. Further analysis are performed later on this data.

Sample #17 (Figure 6.21) shows a good correlation between the predicted and measured soil structure volume changes. However, the limited number of checks that can be performed, results in a high critical correlation coefficient. The critical correlation coefficient at a one percent level of significance is 0.915. The slope of the best-fit line is somewhat reduced from that of sample #15A. Due to the limited number of checks that could be performed, emphasis should not be placed on these statistical properties.

Sample #21 (Figures 6.22 and 6.23) was a kaolin sample tested under isotropic loading. It showed a low correlation coefficient. The correlation coefficient at equilibrium conditions was higher than the correlation coefficient at an elapsed time of 2000 minutes. The critical correlation coefficient is 0.46 for a one percent level of significance. The computed correlation coefficient at equilibrium conditions is approximately equal to the critical correlation coefficient at a one percent level of significance. The slope of the best-fit line is also far from 45°. Further analysis on Sample #21 is performed later with respect to Sample #21.

The statistical properties on the water phase volume changes deviate more from those of "perfect" conditions than do the soil structure volume changes. Sample #15A (Figure 6.24) shows a correlation coefficient

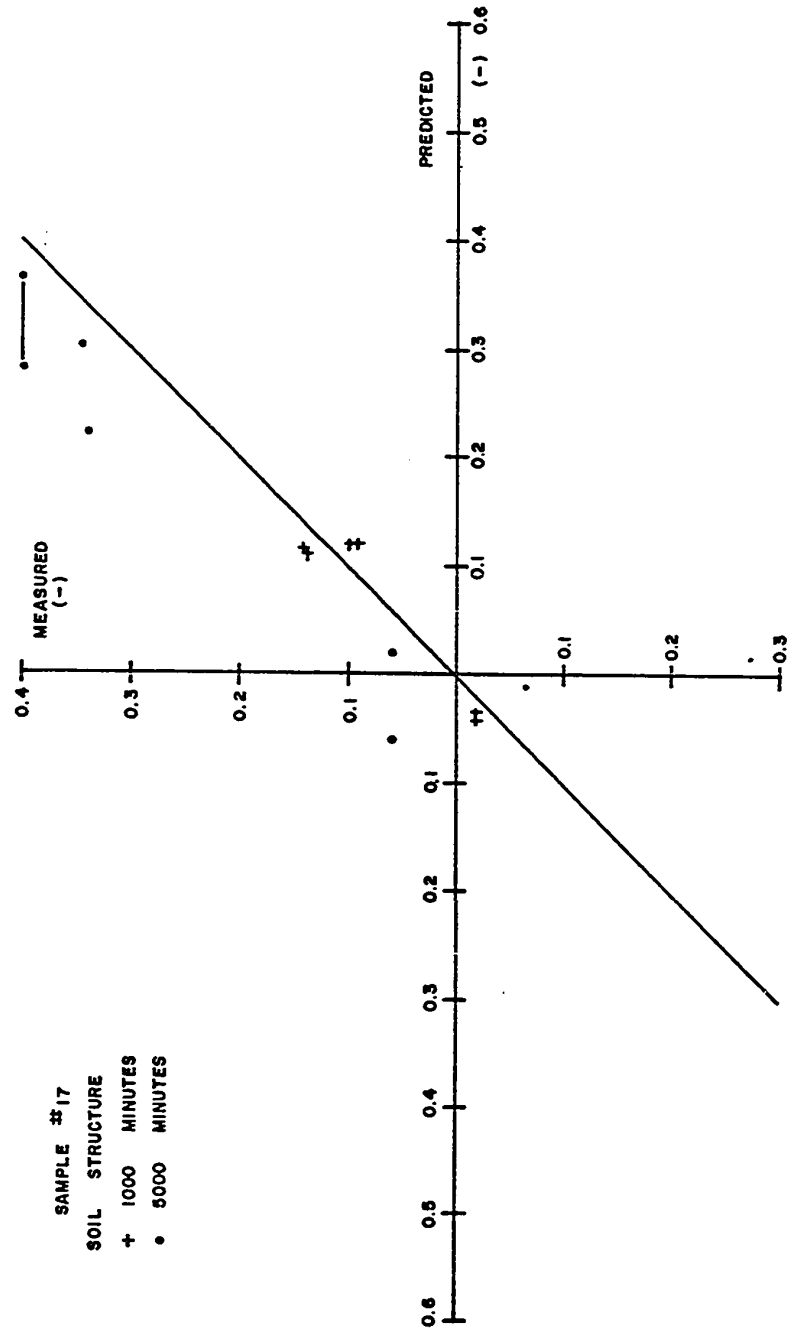


FIGURE 6.21 COMPARISON OF PREDICTED AND MEASURED SOIL STRUCTURE VOLUMETRIC DEFORMATION FOR SAMPLE # 17

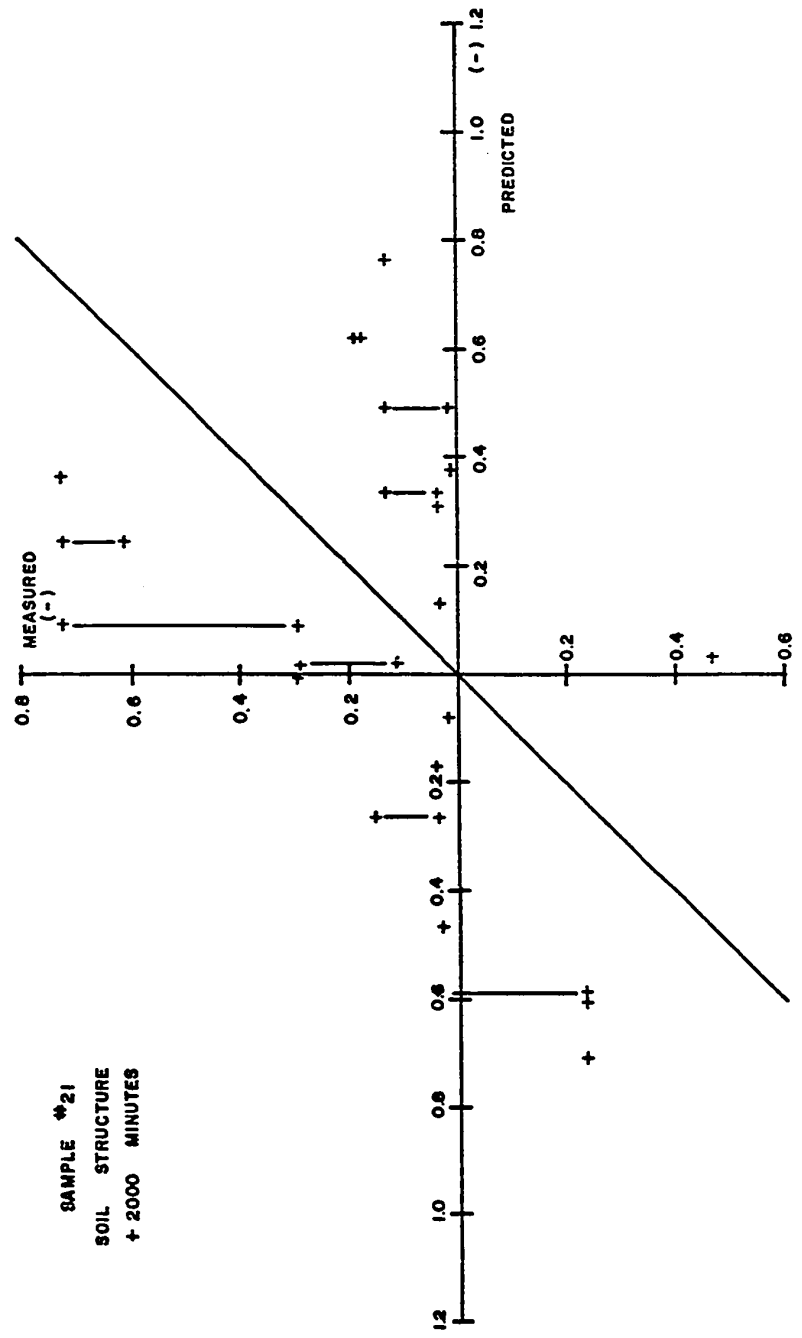


FIGURE 6.22 COMPARISON OF PREDICTED AND MEASURED SOIL STRUCTURE VOLUMETRIC DEFORMATION FOR SAMPLE #21 (AT 2000 MINUTES)

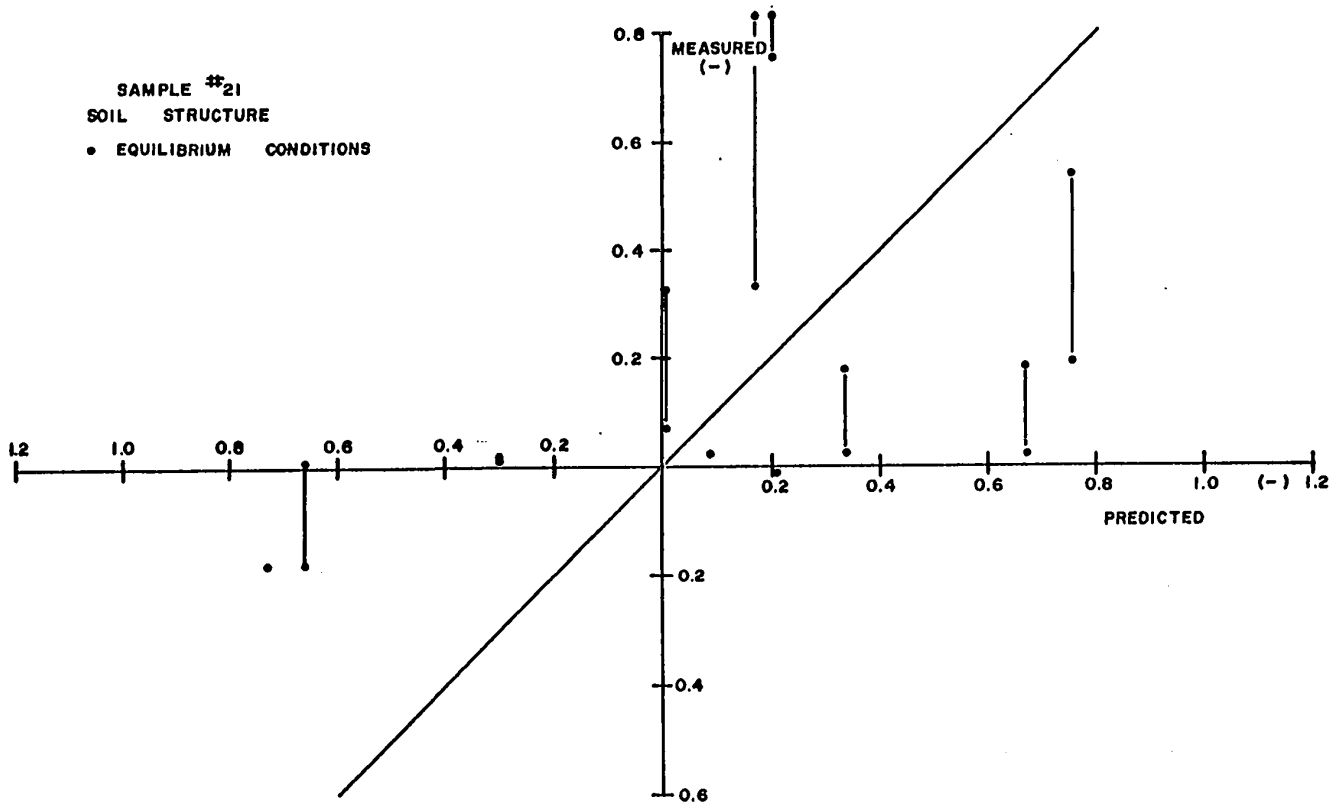


FIGURE 6.23 COMPARISON OF PREDICTED AND MEASURED SOIL STRUCTURE VOLUMETRIC DEFORMATION FOR SAMPLE #21 (EQUILIBRIUM CONDITIONS)

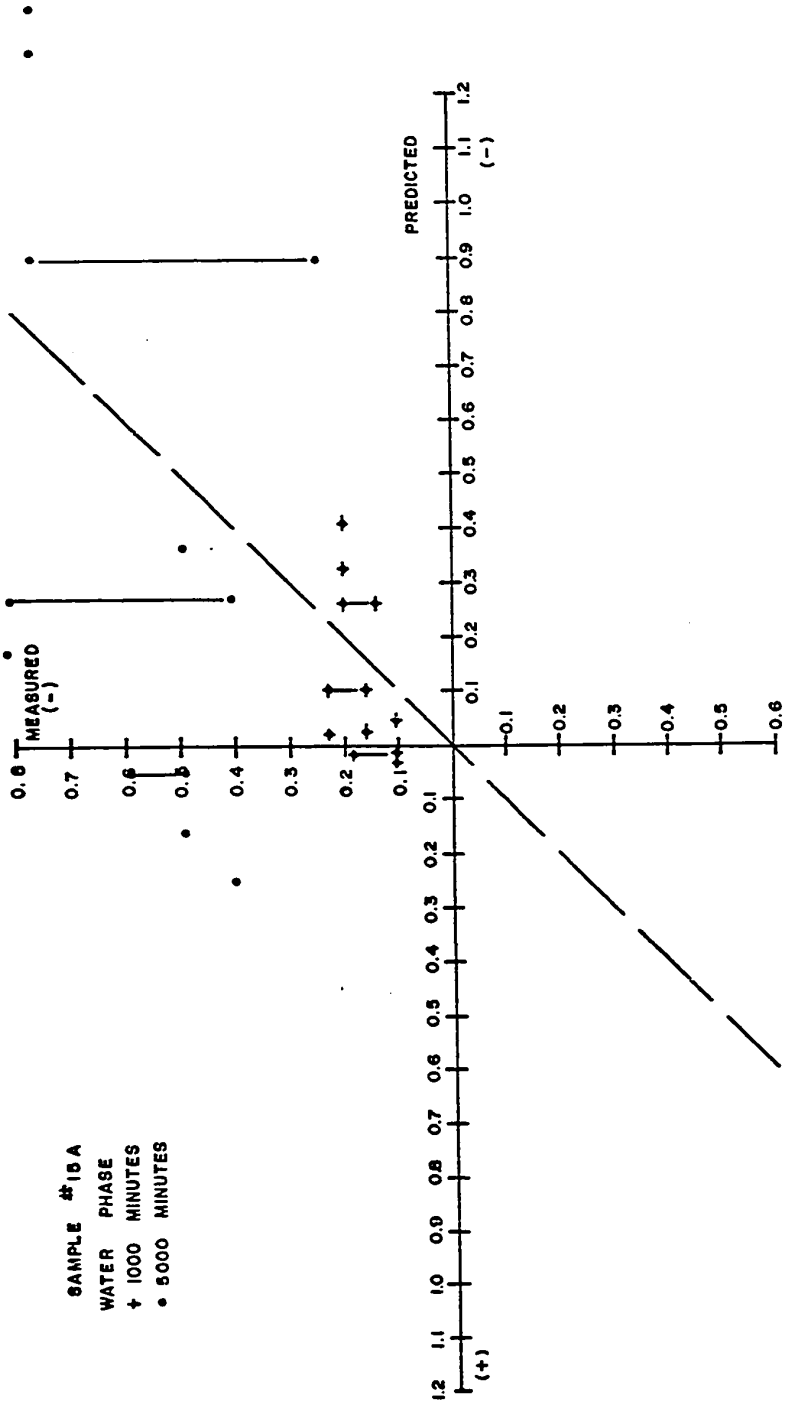


FIGURE 6.24 COMPARISON OF PREDICTED AND MEASURED WATER PHASE VOLUME CHANGES FOR SAMPLE #15 A

of approximately 0.5 which is slightly below the critical correlation coefficient for a 5 percent level of significance. The slope of the best-fit line is low (0.12) and the intercept is far from zero. This test was performed in the one-dimensional oedometer and it was later discovered that some moisture was lost from the sample by movement through the lucite walls of the chamber. The loss of even a small amount of moisture has a very pronounced affect on the uniqueness analysis. The excellent correlation from the uniqueness analysis on the soil structure (Sample #15A) showed that hysteresis cannot be considered as the factor causing the low correlation coefficient for the water phase. A further analysis is later performed to ascertain the cause of the discrepancies.

Sample #16 (Figure 6.25) shows a correlation coefficient greater than the critical correlation coefficient at a 5 percent level of significance, for an elapsed time of 2000 minutes. However, the results are poorer at 15000 minutes. The slopes were low while the intercepts were excessive.

Sample #17 (Figure 6.26) shows a high correlation coefficient, however, the critical correlation coefficient is also high due to the limited number of observations. The statistical properties indicate correlation; however, excessive emphasis should not be placed on this test.

Sample #21 (Figures 6.27 and 6.28) shows a correlation coefficient of approximately 0.60 for both elapsed times. The value is well above the critical correlation coefficient of 0.46 at a one percent level

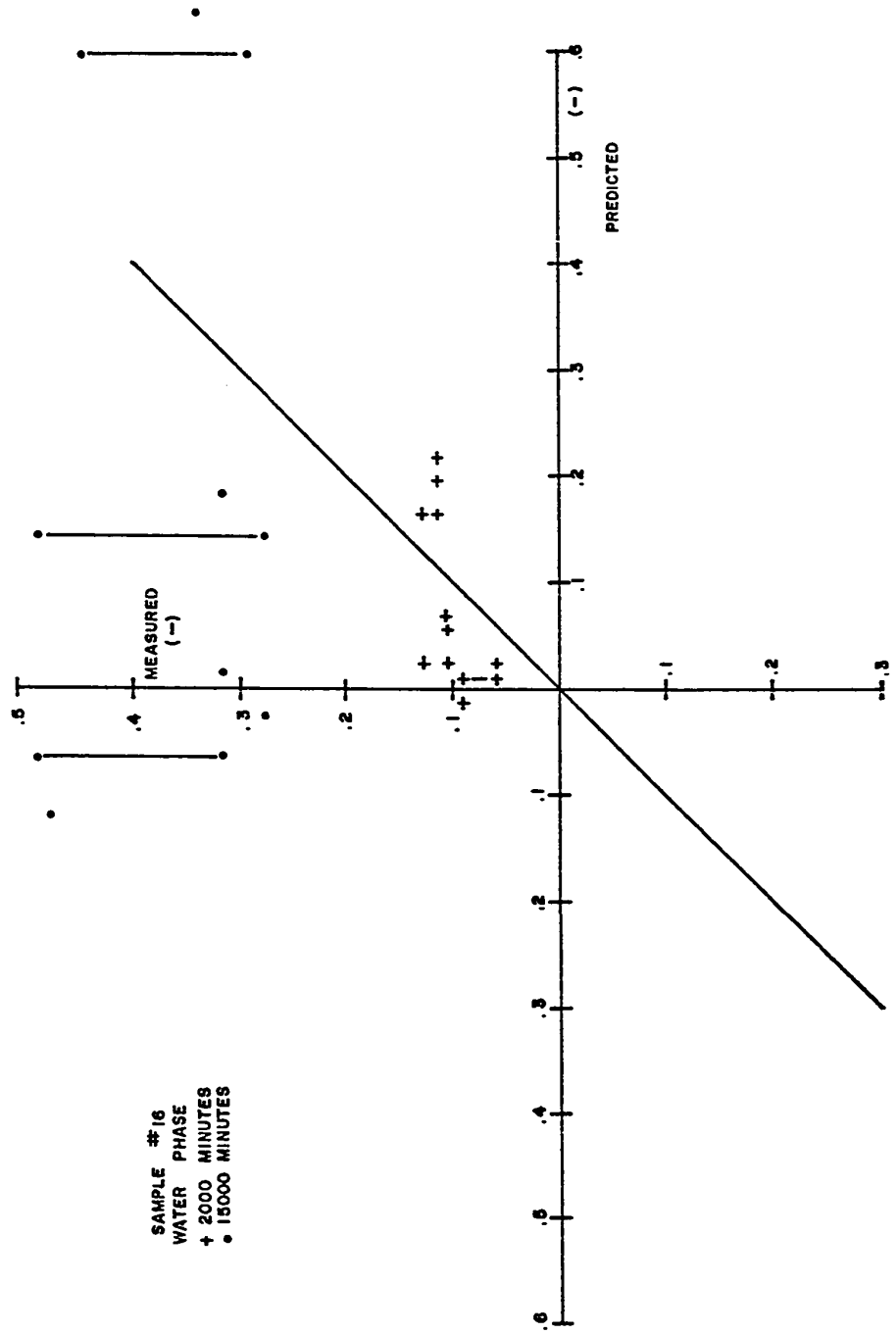


FIGURE 6.25 COMPARISON OF PREDICTED AND MEASURED WATER PHASE VOLUME CHANGES FOR SAMPLE # 16

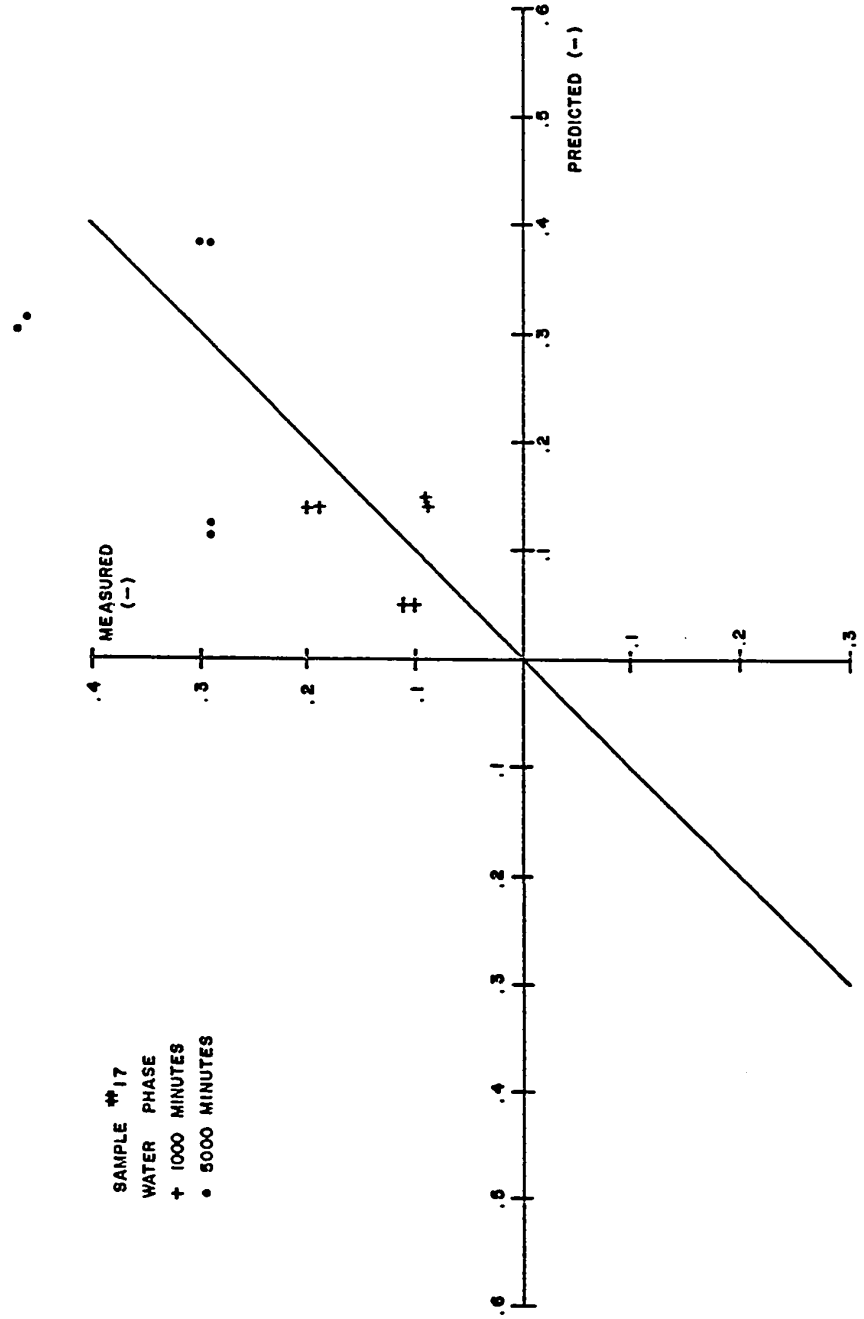


FIGURE 6.26 COMPARISON OF PREDICTED AND MEASURED WATER PHASE VOLUME CHANGES FOR SAMPLE #17

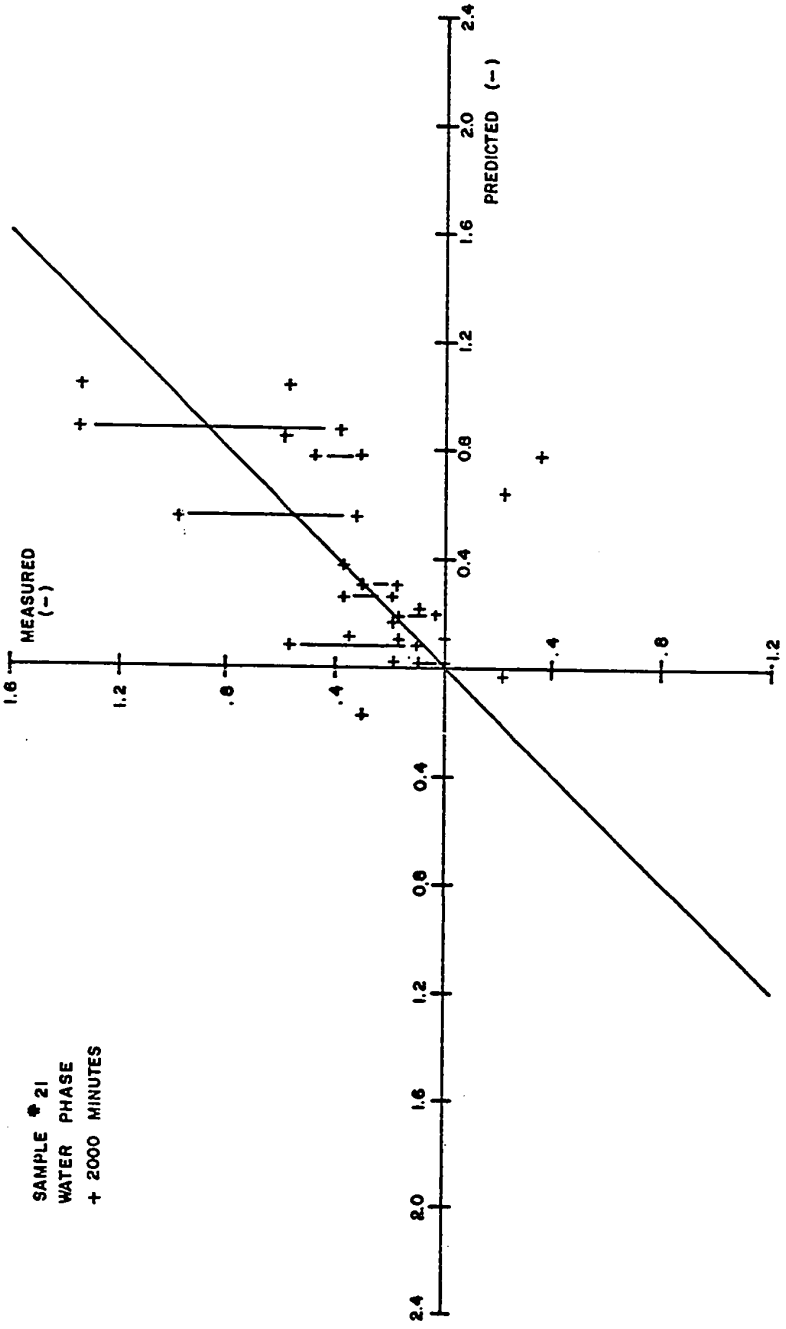


FIGURE 6.27 COMPARISON OF PREDICTED AND MEASURED WATER PHASE VOLUME CHANGES FOR SAMPLE # 21 (AT 2000 MINUTES)

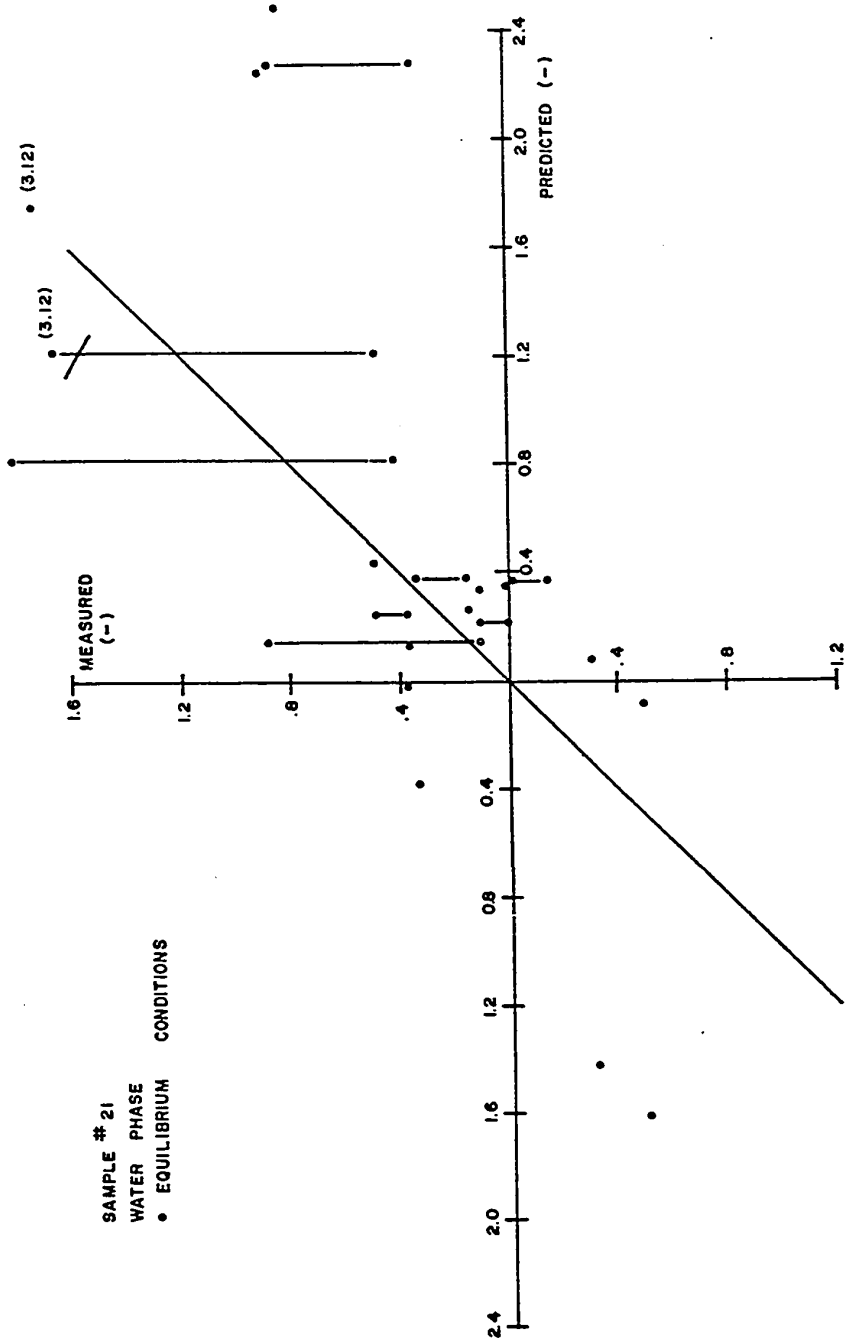


FIGURE 6.28 COMPARISON OF PREDICTED AND MEASURED WATER PHASE VOLUME CHANGES FOR SAMPLE #21 (EQUILIBRIUM CONDITIONS)

of significance. The slope and intercept is superior at an elapsed time of 2000 minutes than under equilibrium conditions.

The statistical properties for the air phase uniqueness analysis deviate more from those of "perfect" conditions than either the soil structure or the water phase. This is as anticipated since the air phase volumetric deformations are computed from the soil structure and water phase deformations. Any errors or limitations involved in either of the measured deformations are combined and in fact amplified in the uniqueness analysis of the air phase volume changes. Further detailed consideration is not given to the air phase volume change since its constitutive surface is not independently measured. On the other hand, if the soil structure and the water phase constitutive surfaces show uniqueness, then the air phase constitutive surface must automatically show uniqueness. This reasoning tends to be confirmed experimentally by all tests and in particular by Sample #17 (5000 minutes).

6.13.5 Sources of Deviation Between Predicted and Measured Soil Structure Volume Changes

The measurement of the volume change of the soil structure is estimated to be within $\pm$ 0.005 percent for samples #15A and #17 performed on the one-dimensional oedometer. Samples #16 and #21 were performed on Triaxial Apparatus No. 1 and the reliability of their volume change measurements is slightly less. Although this may have some effect on the uniqueness analysis, it is definitely not the primary factor producing deviations from a "perfect" uniqueness analysis.

The non linearity of the constitutive surface and the effect of hysteresis are factors that should be considered.

The effect of a non linear constitutive surface can be partly compensated for by correcting all slopes to the same stress point in space. The assumption is made that the slope of the constitutive surface is constant on a semi-log plot of any stress state variable versus volume change. Each compressibility is also assumed to correspond to the mean of the initial and final stress state variable points. All compressibility values are then corrected to the mean stress state point of the measured volume change used for comparison. Table VI.10 shows a typical set of calculations for Sample #16 (15000 minutes). Only the largest elapsed time results are analysed in this manner. The statistical properties are summarized in Table VI.11.

Sample #15A showed a virtually "perfect" correlation using the linear analysis and remains essentially the same for the non-linear analysis. The non-linear analysis on Sample #16 (Figure 6.29) shows a marked improvement over the linear analysis. The correlation coefficient is well above the critical correlation coefficient for a one percent level of significance. The slope of the best-fit line approaches one while the intercept remains essentially the same as before. The non-linear nature of the constitutive surface appears to have a significant effect on the analysis of uniqueness. Sample #17 showed a slight decrease in correlation coefficient when the compressibilities were corrected for non-linearity.

Sample #21 did not show any improvement in the statistical

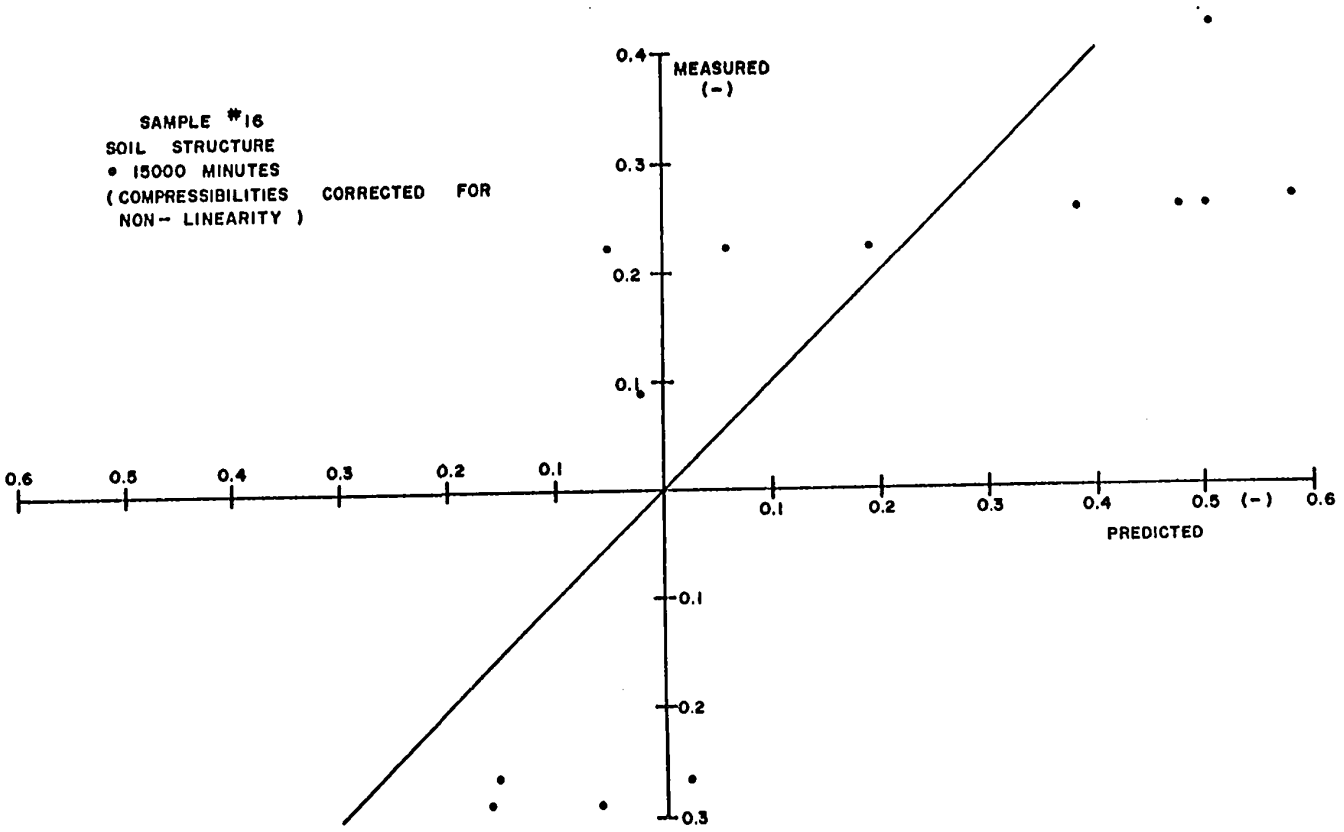


FIGURE 6.29 COMPARISON OF PREDICTED AND MEASURED OVERALL VOLUME CHANGES FOR SAMPLE #16 (COMPRESSIBILITES CORRECTED FOR NON LINEARITY)

TABLE VI.10

COMPARISON OF PREDICTED AND MEASURED VOLUME CHANGES (UNIQUENESS AT A POINT)

CORRECTION APPLIED FOR NON LINEAR CONSTITUTIVE SURFACE

Tests Considered	Stress Component Change	Final Stress State Variables			Soil Structure Volume Change	Stress State Variable	Magnitude	Modified Volume Change	Stress State Variable	Magnitude	Modified Volume Change	Total Volume Change (%)
		$\sigma-u_w$	$\sigma-u_a$	u_a-u_w								
Sample #16 (15000 minutes)												
C-7* and C-8*	$\Delta\sigma$=-10 psi	52.88	26.32	26.56	-0.258	$\sigma-u_w$	62.81	-0.094	$\sigma-u_a$	26.24	-0.289	-0.383
C-8* and C-9	Δu_w=+10	62.81	21.26	41.56	-0.090	u_a-u_w	31.58	+0.268	$\sigma-u_w$	52.88	-0.247	+0.021
C-8* and C-9	Δu_w=+10	43.00	21.38	21.61	-0.223	u_a-u_w	31.58	+0.325	$\sigma-u_w$	52.88	-0.272	+0.052
C-9 and C-10	Δu_a=-10	57.82	26.24	31.58	+0.289*	$\sigma-u_a$	26.32	+0.258	u_a-u_w	21.61	-0.198	+0.060
C-9 and C-10	Δu_a=-10	38.05	26.35	11.70	+0.266	$\sigma-u_a$	26.32	+0.258	u_a-u_w	21.61	-0.279	-0.021
C-10 and C-11	$\Delta\sigma$=-10	52.88	26.32	26.56	-0.258	$\sigma-u_w$	43.00	-0.211	$\sigma-u_a$	26.35	-0.266	-0.477
C-10 and C-11	$\Delta\sigma$=-10	33.09	26.34	6.75	-0.430	$\sigma-u_w$	43.00	-0.240	$\sigma-u_a$	26.35	-0.266	-0.506
C-10 and C-11	$\Delta\sigma$=-10	23.20	16.43	6.77	-0.716	$\sigma-u_w$	43.00	-0.267	$\sigma-u_a$	26.35	-0.311	-0.578
C-11 and C-12	Δu_w=+10	43.00	21.38	21.61	-0.223	u_a-u_w	11.71	+0.213	$\sigma-u_w$	33.09	-0.403	-0.190
C-7* and C-9	Δu_a=-10	57.82	26.24	31.58	+0.289	u_a-u_w	41.56	-0.097	$\sigma-u_a$	26.32	+0.258	+0.161
C-8* and C-10	$\Delta\sigma$=-10	52.88	26.32	26.56	-0.258	$\sigma-u_a$	26.24	-0.289	$\sigma-u_w$	43.00	-0.211	-0.500
C-9 and C-11	Δu_w=+10	43.00	21.38	21.61	-0.223	$\sigma-u_w$	52.88	-0.272	u_a-u_w	11.71	+0.213	-0.059
C-10 and C-12	Δu_a=-10	38.05	26.35	11.70	+0.266	u_a-u_w	21.61	-0.279	$\sigma-u_a$	26.34	+0.433	+0.154

TABLE VI.11

SUMMARY OF REGRESSION ANALYSIS USING A

NON-LINEAR CONSTITUTIVE SURFACE

Sample No.	Constitutive Surface	No. of Observations	Correlation Coefficient	Slope	Intercept
15A (5000 min)	Soil Structure	12	0.983	1.049	+0.014
16 (15000 min)	Soil Structure	12	0.820	0.928	+0.041
17 (5000 min)	Soil Structure	6	0.858	0.609	-0.111
21 (Equilibrium Conditions)	Soil Structure	30	0.410	0.339	-0.095
	Soil Structure omitting first 3 and last 4 tests	14	0.390	0.293	-0.242

properties as a result of the corrections for non-linearity. There appears to be some other factor affecting the data. Several regression analysis were performed on selected portions of the data to see if any particular set of data was introducing a large error. For example, the volume change data from the first three pressure increments on Sample #21 appear to be dominated by secondary compression effects and are therefore in question. However, their omission from the regression analysis did not improve the statistical properties. Also, the last four pressure increments were in an opposite direction from the remainder of the stress component changes. The omission of their results again did not improve the statistical properties.

The next factor considered was the effect of soil structure hysteresis due to a reversal in the direction of deformation when the air pressure was decreased. The direction of the air pressure change produces a consistent water deformation direction; however, the soil structure generally reverses direction. Table VI.12 shows a comparison of the measured and predicted soil structure volume changes when the air pressure was changed. The results are plotted on Figure 6.30. The one-dimensional test results on Regina clay indicate relatively close agreement between the predicted and measured values. The isotropic loading tests on Regina clay show the measured values greater than the predicted values. The isotropic loading of the compacted kaolin shows the measured values less than the predicted values. In this case, the reversal of stress produces essentially no volume change due to hysteresis.

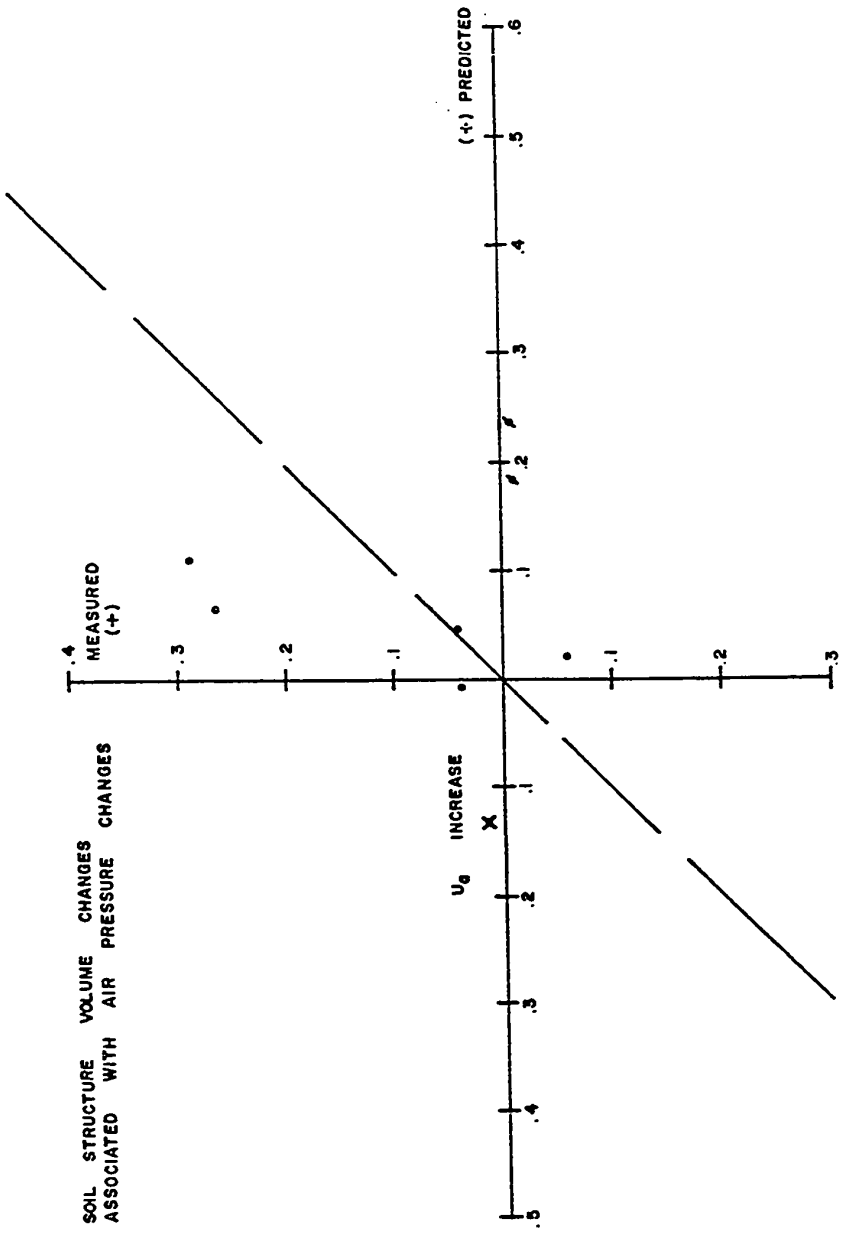


FIGURE 6.30 SOIL STRUCTURE VOLUMETRIC DEFORMATIONS ASSOCIATED WITH AIR PRESSURE CHANGES

TABLE VI.12

COMPARISON OF PREDICTED AND MEASURED SOIL STRUCTURE VOLUME CHANGES FOR A CHANGE IN AIR PRESSURE

Sample No.	Test No.	Soil Structure Volume Change (%)	
		Measured	Predicted
15A	C-2	+0.040	+0.046
	C-5	+0.039	-0.008
16	C-8	+0.289	+0.111
	C-11	+0.266	+0.067
17	C-15	-0.060	+0.020
21	C-19	-0.015	+0.181
	C-22	-0.010	+0.235
	C-25	+0.179	+0.679
	C-31*	+0.015	-0.131

*Air Pressure Increased

It would appear that hysteresis associated with the change in the air pressure may be the factor contributing to dispersion in the case of sample #21. The effect of hysteresis due to an air pressure change is investigated by assuming that the predicted volume change due to an air pressure change is equal to the measured volume change. The deformation due to a change in total and water pressures remain the same. Obviously, this will produce an improvement in the correlation coefficient. However, conclusions must be based on the magnitude of the improvement of the correlation coefficient.

Table VI.13 summarizes the statistical properties obtained when the above procedure is used to compensate for hysteresis. Table VI.14 shows a set of calculations for sample #16. The results of sample #16 are plotted on Figure 6.31. The correlation coefficient increased slightly to 0.87. By omitting the data from the check using tests C-10 and C-11, the correlation coefficient improves to 0.93. Although there is some improvement in the correlation coefficient, it is not dramatic and may indicate that the Regina clay behavior approaches that of an elastic material. The slope of the best-fit line approaches 45 degrees and the intercept is essentially zero.

TABLE VI.13

SUMMARY OF REGRESSION ANALYSIS USING A NON-LINEAR CONSTITUTIVE SURFACE AND APPLYING A CORRECTION FOR HYSTERESIS

Sample No.	Constitutive Surface	No. of Observations	Correlation Coefficient	Slope	Intercept
15A (5000 min)	Soil Structure	12	0.969	0.971	-0.005
16 (15000 min)	Soil Structure	13	0.868	1.145	-0.006
	Soil Structure (omission of C-10 and C-11)	12	0.934	0.953	-0.006
17 (5000 min)	Soil Structure	6	0.969	0.963	-0.008
21 (Equilibrium Conditions)	Soil Structure	30	0.831	0.829	+0.034
	Soil Structure (omission of first 3 and last 4 tests)	15	0.939	0.957	-0.056

TABLE VI.14

COMPARISON OF PREDICTED AND MEASURED VOLUME CHANGES (UNIQUENESS AT A POINT)

CORRECTIONS APPLIED FOR HYSTERESIS

Tests Considered	Stress Component Change	Final Stress State Variables			Soil Structure Volume Change	Stress State Variable	Magnitude	Modified Volume Change	Stress State Variable	Magnitude	Modified Volume Change	Total Volume Change (%)
		$\sigma-u_w$	$\sigma-u_a$	u_a-u_w								
Sample #16 (15000 minutes)												
C-7* and C-8*	$\Delta\sigma$=-10 psi	52.88	26.32	26.56	-0.258	$\sigma-u_w$	62.81	-0.094	$\sigma-u_a$	26.24	-0.111	-0.205
C-8* and C-9	Δu_w=+10	62.81	21.26	41.56	-0.090	u_a-u_w	31.58	+0.103	$\sigma-u_w$	52.88	-0.247	-0.144
C-8* and C-9	Δu_w=+10	43.00	21.38	21.61	-0.223	u_a-u_w	31.58	+0.125	$\sigma-u_w$	52.88	-0.272	-0.147
C-9 and C-10	Δu_a=-10	57.82	26.24	31.58	+0.111*	$\sigma-u_a$	26.32	+0.258	u_a-u_w	21.61	-0.198	+0.111
C-9 and C-10	Δu_a=-10	38.05	26.35	11.70	+0.067	$\sigma-u_a$	26.32	+0.258	u_a-u_w	21.61	-0.279	+0.067
C-10 and C-11	$\Delta\sigma$=-10	52.88	26.32	26.56	-0.258	$\sigma-u_w$	43.00	-0.211	$\sigma-u_a$	26.35	-0.067	-0.078
C-10 and C-11	$\Delta\sigma$=-10	33.09	26.34	6.75	-0.430	$\sigma-u_w$	43.00	-0.240	$\sigma-u_a$	26.35	-0.067	-0.307
C-10 and C-11	$\Delta\sigma$=-10	23.20	16.43	6.77	-0.716	$\sigma-u_w$	43.00	-0.267	$\sigma-u_a$	26.35	-0.078	-0.345
C-11 and C-12	Δu_w=+10	43.00	21.38	21.61	-0.223	u_a-u_w	11.71	+0.054	$\sigma-u_w$	33.09	-0.403	-0.349
C-7* and C-9	Δu_a=-10	57.82	26.24	31.58	+0.111	u_a-u_w	41.56	-0.097	$\sigma-u_a$	26.32	+0.258	+0.111
C-8* and C-10	$\Delta\sigma$=-10	52.88	26.32	26.56	-0.258	$\sigma-u_a$	26.24	-0.111	$\sigma-u_w$	43.00	-0.211	-0.322
C-9 and C-11	Δu_w=+10	43.00	21.38	21.61	-0.223	$\sigma-u_w$	52.88	-0.272	u_a-u_w	11.71	+0.054	-0.218
C-10 and C-12	Δu_a=-10	38.05	26.35	11.70	+0.067	u_a-u_w	21.61	+0.279	$\sigma-u_a$	26.34	+0.433	+0.067

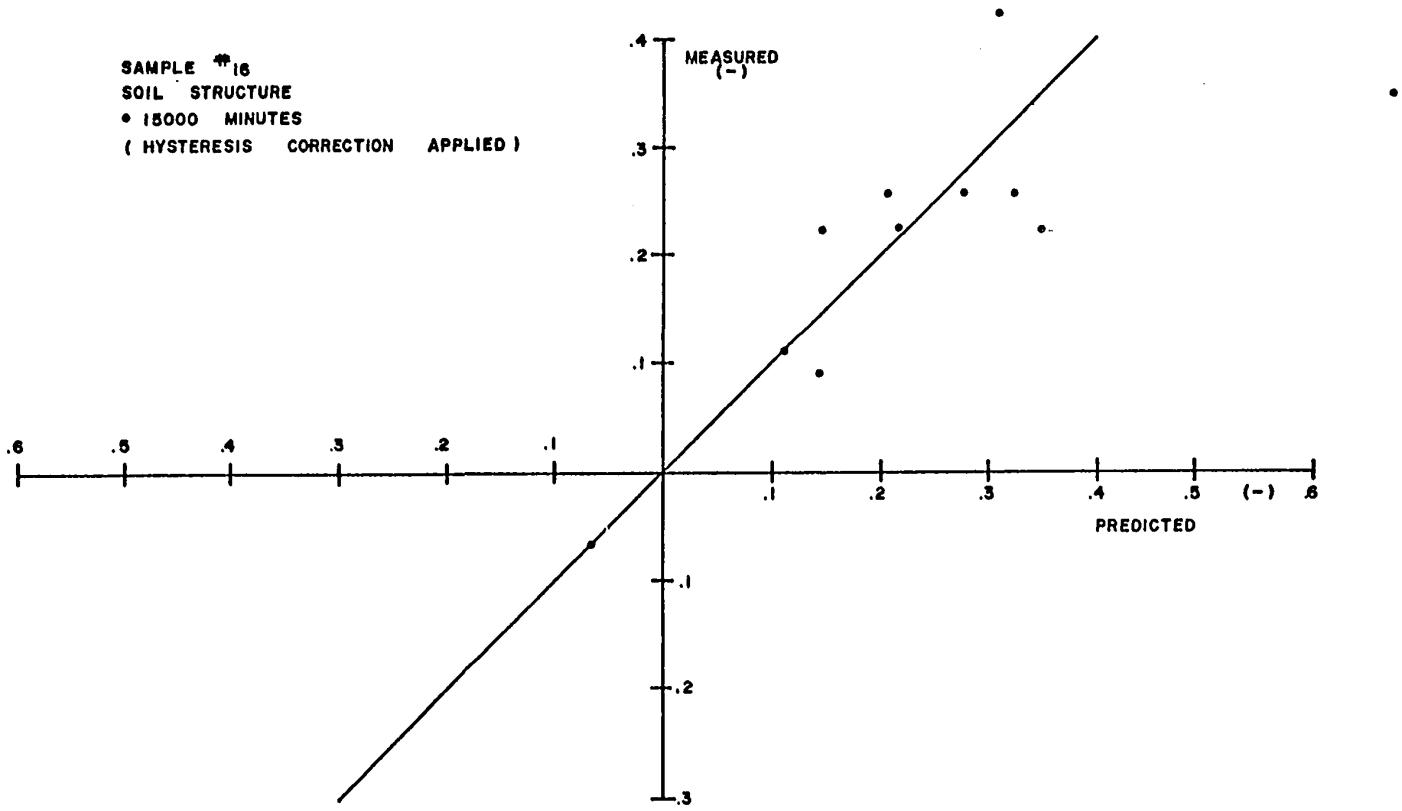


FIGURE 6.31 COMPARISON OF PREDICTED AND MEASURED OVERALL VOLUMETRIC DEFORMATIONS FOR SAMPLE # 16 (HYSTERESIS CORRECTION APPLIED)

The statistical properties of sample #21 show a dramatic improvement as a result of compensating for hysteresis. Considering all the data, the correlation coefficient improved from 0.41 to 0.83 (non-linear analysis). The slope of the best-fit line increased from 0.34 to 0.83 and the intercept changed from -0.09 to +0.03. Omitting the results from the first three and the last four pressure increments, the statistics are further improved (Figure 6.32). The correlation coefficient rose to 0.94, the slope to 0.96, while the intercept went to -0.06. The analysis isolates soil structure hysteresis as the prime cause of dispersion from a unique constitutive surface for the kaolin sample.

6.13.6 Sources of Deviation Between Predicted and Measured Water Phase Volume Changes

The laboratory testing technique associated with the water phase constitutive surface is considerably more difficult than for the soil structure constitutive surface. This factor is in addition to the effects of non linearity and hysteresis.

Sample #15A showed virtually perfect uniqueness for the soil structure constitutive surface. Therefore, non-linearity and hysteresis cannot be factors affecting the water phase constitutive surface. It is quite definite that sample #15A experienced some loss of moisture during the test and this factor was investigated. The water volume change for each load increment was plotted versus the elapsed time on an arithmetic scale (Figure 6.33). The plots show a gently curving section at the start, becoming asymptotic to a straight line portion

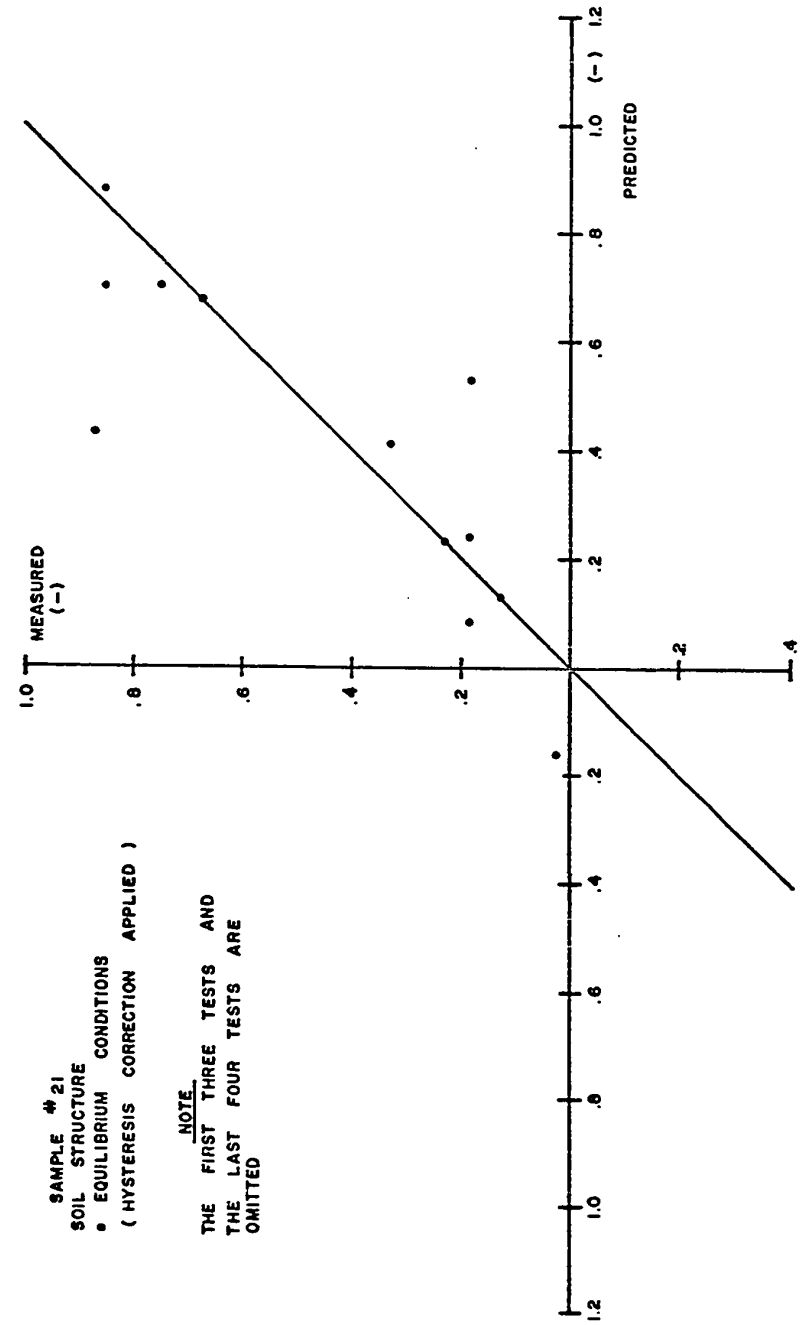


FIGURE 6.32 COMPARISON OF PREDICTED AND MEASURED OVERALL VOLUMETRIC DEFORMATIONS FOR SAMPLE #21 (HYSTERESIS CORRECTION APPLIED)

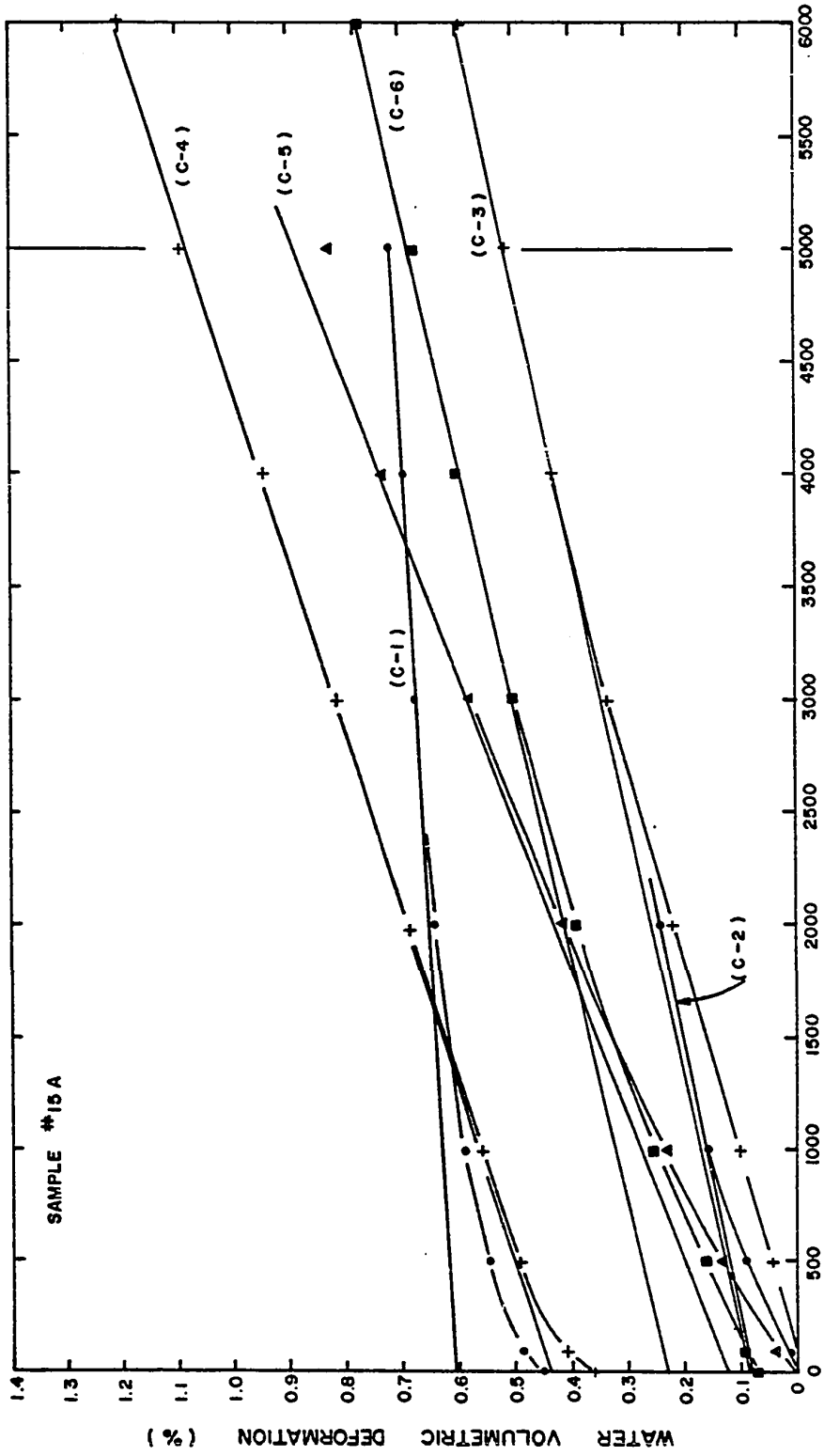


FIGURE 6.33 WATER VOLUMETRIC DEFORMATION VERSUS TIME FOR SAMPLE #15A

at approximately 3000 minutes. This time corresponds roughly to the completion of primary consolidation as measured in other tests. The straight line portion of the curves was extended back to zero time and the intercept was termed the excess of water entering or leaving the sample. The excess of water volume change was added to the soil structure volume change and used to check the uniqueness of the water phase constitutive surface. This method of analysis was used in an attempt to overcome the problem of the unknown amount of moisture lost from the sample. Although the procedure is not entirely satisfactory, it is probably the best estimate possible.

Table VI.15 summarizes the measured and predicted water volume changes for sample #15A (Figure 6.34). The correlation coefficient is 0.82 which is well above the critical correlation coefficient. However, the slope of the best-fit line is relatively low (0.55) and the intercept is quite far from zero (-0.12). Certainly the analysis is not as convincing as it was for the soil structure. From the above analysis it is possible to estimate the rate of water loss from each test. The mean rate is 0.349 percent per 5000 minutes. However, the rate appears to be quite variable. The standard deviation of the rates of water loss are $\pm$ 0.297 percent per 5000 minutes. All the factors involved in the rate of water loss are not completely understood.

If it is assumed that the water loss with respect to time is a constant, further comparisons can be made between the measured and predicted water volume changes. Table VI.16 shows the statistical

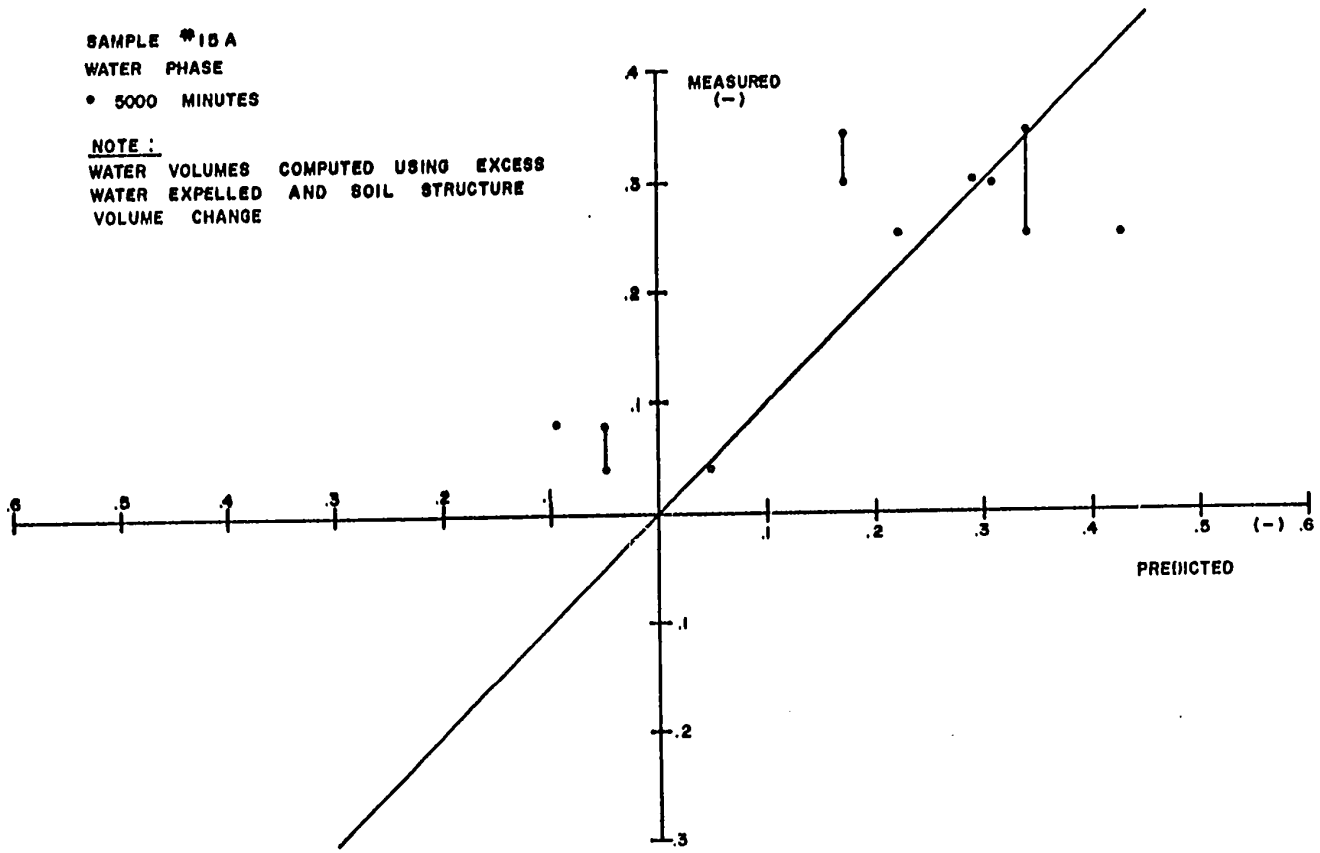


FIGURE 6.34 COMPARISON OF PREDICTED AND MEASURED WATER PHASE VOLUME CHANGES FOR SAMPLE #15A (WATER VOLUMES COMPUTED USING EXCESS WATER EXPELLED)

properties from the regression analysis after assuming rates of water loss from 0 to 0.6 percent per 5000 minutes.

TABLE VI.15

COMPARISON OF PREDICTED AND MEASURED WATER VOLUME CHANGES FOR SAMPLE #15A (5000 MINUTES) (WATER VOLUME = EXCESS WATER VOLUME + SOIL STRUCTURE DEFORMATION)

Compressibilities Taken From Tests	Stress Change Considered (psi)	Water Phase Volume Change (%)	
		Measured	Predicted
C-1 and C-2	$\Delta\sigma$ = - 10	-0.300	-0.308
C-2 and C-3	Δu_w = + 10	-0.299	-0.340
C-3 and C-4	Δu_a = - 10	-0.060	+0.050
C-4 and C-5	$\Delta\sigma$ = - 10	-0.323	-0.170
C-5 and C-6	Δu_w = + 10	-0.250	-0.425
C-1 and C-3	Δu_a = - 10	-0.040	-0.048
C-2 and C-4	$\Delta\sigma$ = - 10	-0.300	-0.290
C-3 and C-5	Δu_w = + 10	-0.250	-0.220
C-4 and C-6	Δu_a = - 10	-0.080	+0.095

Correlation Coefficient = 0.822

Slope = 0.548

Intercept = - 0.119

PHASE VI.16

SUMMARY OF REGRESSION ANALYSIS FOR THE WATER PHASE CONSTITUTIVE SURFACE ASSUMING VARIOUS RATES OF WATER LOSS (SAMPLE #15A, 5000 MIN)

Assumed Rate of Water Loss (% per 5000 minutes)	No. of Observations	Correlation Coefficient	Slope	Intercept
0	12	0.514	0.116	-0.538
0.2	12	0.605	0.196	-0.327
0.4	12	0.692	0.358	-0.129
0.6	12	0.546	0.294	+0.019

The best results are obtained at a rate of approximately 0.4 percent per 5000 minutes. This corresponds to the results from the previous analysis. The lower correlation coefficient indicates that the rate of water loss is not a constant. The continuing improvement in the intercept values with increasing assumed rates of water loss, indicates that water loss must be a factor involved in the deviations.

The water phase volume changes on Sample #16 (15000 minutes) were corrected for hysteresis due to a change in air pressure in order to examine the improvement in the statistical properties. The constitutive surface is assumed as linear. Table VI.17 and Figure 6.35 summarize the results.

TABLE VI.17

COMPARISON OF PREDICTED AND MEASURED WATER VOLUME CHANGES FOR SAMPLE #16 (15000 MINUTES) (COMPRESSIBILITIES CORRECTED FOR HYSTERESIS)

Compressibilities Taken From Tests	Stress Change Considered (psi)	Water Phase Volume Change (%)	
		Measured	Predicted
C-7 and C-8	$\Delta\sigma$ = - 10	-0.319	-0.235
C-8 and C-9	Δu_w = + 10	-0.377	-0.377
C-9 and C-10	Δu_a = - 10	-0.033	-0.142
C-10 and C-11	$\Delta\sigma$ = - 10	-0.451	-0.452
C-11 and C-12	Δu_w = + 10	-0.461	-0.593
C-7 and C-9	Δu_a = - 10	-0.058	+0.026
C-8 and C-10	$\Delta\sigma$ = - 10	-0.319	-0.403
C-9 and C-11	Δu_w = + 10	-0.461	-0.328
C-10 and C-12	Δu_a = - 10	-0.009	+0.123

Correlation Coefficient = 0.894

Slope = 0.798

Intercept = - 0.056

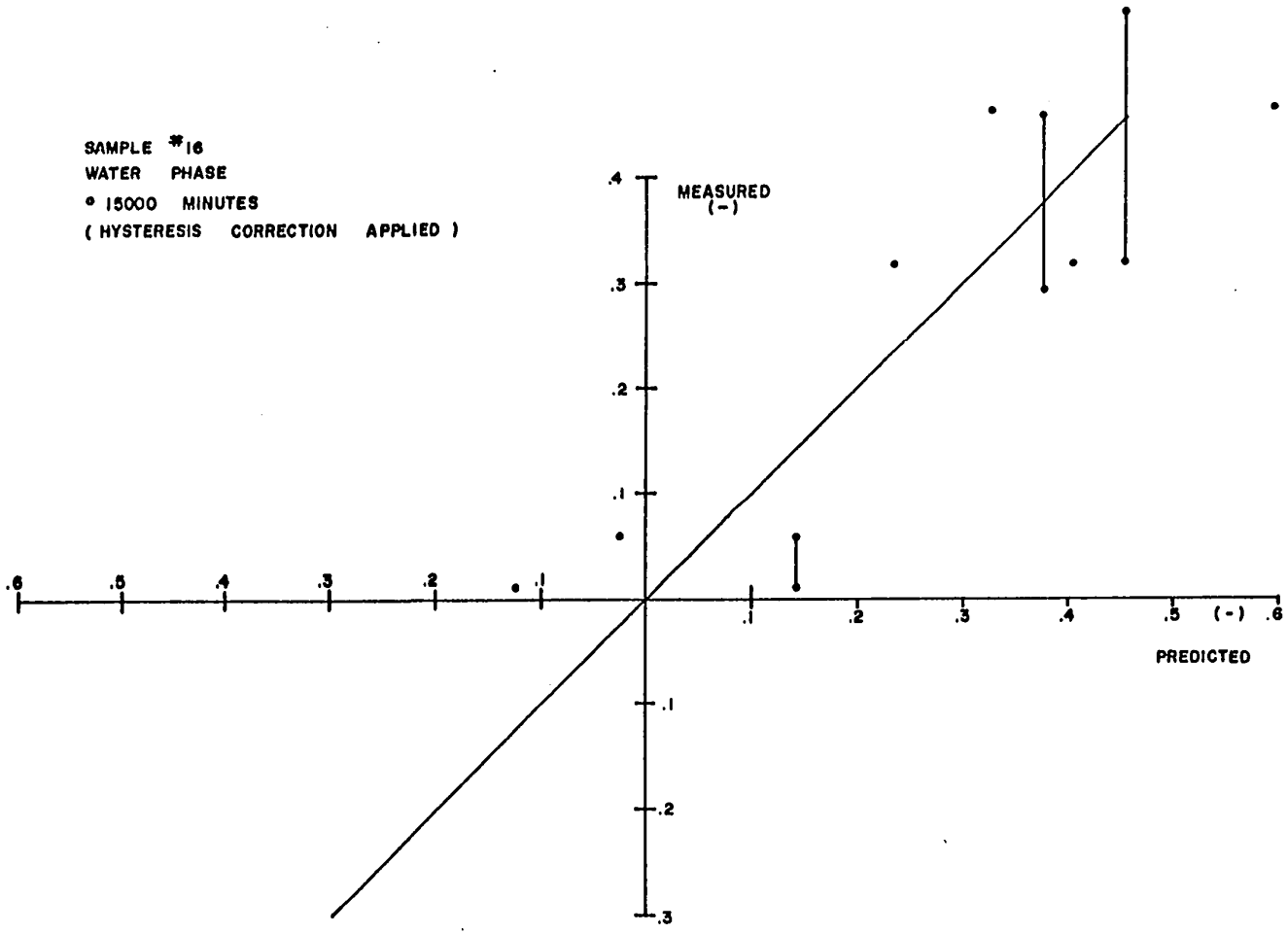


FIGURE 6.35 COMPARISON OF PREDICTED AND MEASURED WATER PHASE VOLUME CHANGES FOR SAMPLE #16 (HYSTERESIS CORRECTION APPLIED)

The correlation coefficient shows a dramatic increase from 0.15 to 0.89. This is well above the critical correlation coefficient of 0.71 for a one percent level of significance. The slope increases from 0.43 to 0.80. The marked improvement in statistical properties indicates that hysteresis in the soil structure produces dispersion in the uniqueness analysis of the water phase constitutive surface.

The original analysis on sample #17 showed a good correlation between the predicted and measured water volume changes. Therefore no further analyses were conducted.

The water volume changes for sample #21 were corrected for hysteretic effects due to a change in air pressure (Table VI.18 and Figure 6.36). Once again the first three and the last four pressure increment tests were ignored. The correlation coefficient increased to 0.82 which is well above the critical correlation coefficient of 0.46 for a one percent level of significance. The slope of the best-fit line increased to 0.54. The intercept was -0.63 which is higher than desirable but appears related to two "checks" showing a large discrepancy.

The data definitely confirms that the water phase constitutive surface is unique providing all testing technique limitations are overcome and there is no reversal in the direction of deformation of the soil structure. All tests were performed with a continuously increasing water volume and thus there should be no hysteretic effects associated with the contractile skin.

TABLE VI.18

COMPARISON OF PREDICTED AND MEASURED WATER VOLUME CHANGES FOR SAMPLE #21 (EQUILIBRIUM CONDITIONS) (COMPRESSIBILITIES CORRECTED FOR HYSTERESIS)

Compressibilities Taken From Tests	Stress Change Considered (psi)	Water Phase Volume Change (%)	
		Measured	Predicted
C-21 and C-22	Δu_w = + 10	-0.494	-0.397
C-22 and C-23	$\Delta\sigma$ = - 10	-0.246	-0.257
C-23 and C-24	Δu_a = - 10	-1.376	-0.157
C-24 and C-25	Δu_w = + 10	-1.808	-2.853
C-25 and C-26	$\Delta\sigma$ = - 10	-0.605	-0.605
C-26 and C-27	Δu_a = - 10	-2.516	-2.248
C-21 and C-23	Δu_a = - 10	-0.237	-0.340
C-22 and C-24	Δu_w = + 10	-0.494	-0.574
C-23 and C-25	$\Delta\sigma$ = - 10	-0.337	+2.022
C-24 and C-26	Δu_a = - 10	-2.516	-2.784
C-25 and C-27	Δu_w = + 10	-3.121	-3.389

Correlation Coefficient = 0.822

Slope = 0.542

Intercept = - 0.627

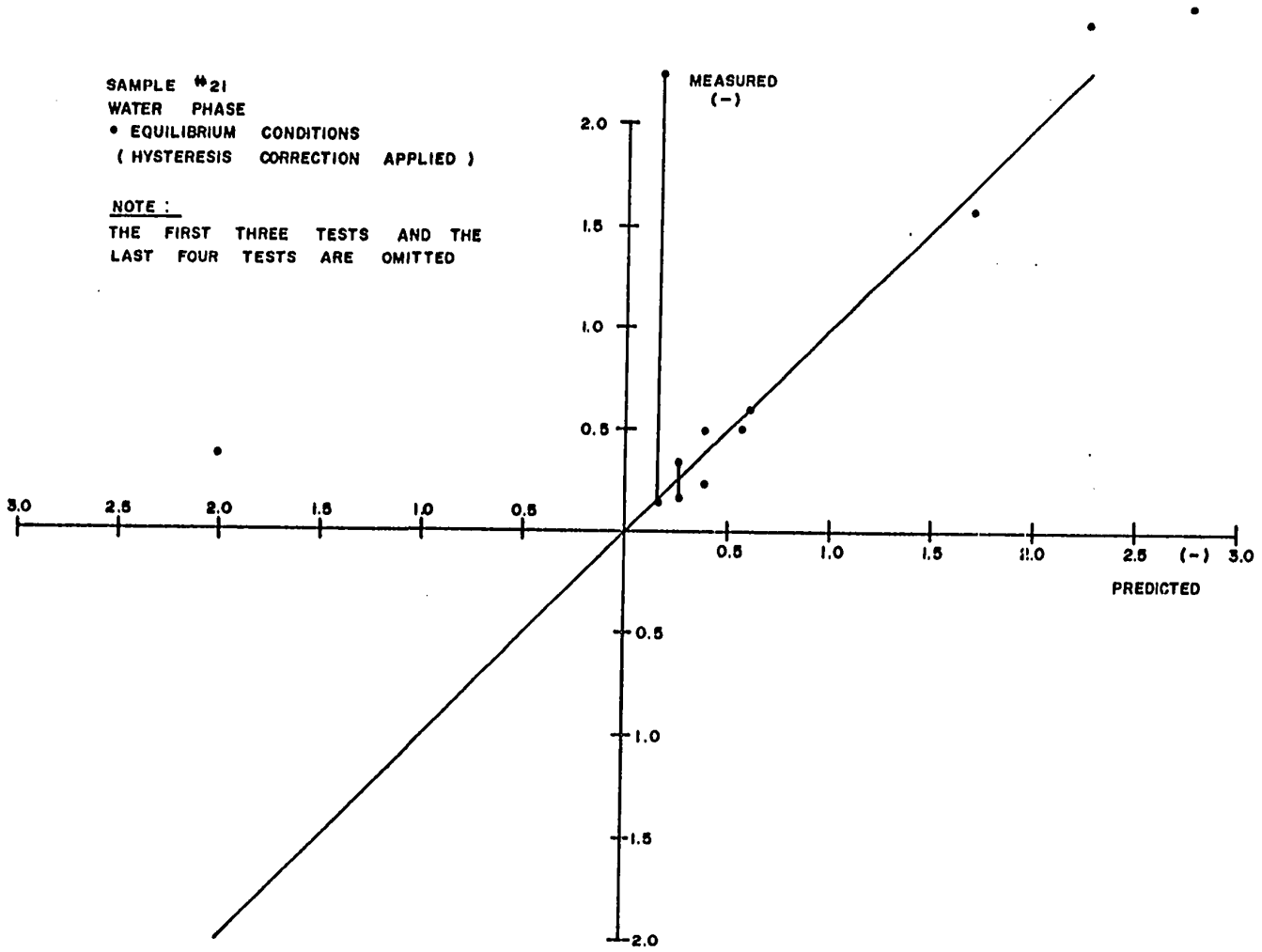


FIGURE 6.36 COMPARISON OF PREDICTED AND MEASURED WATER VOLUME CHANGES FOR SAMPLE #21 WITH THE HYSTERESIS CORRECTION APPLIED

6.14 Theoretical Exploration of the Constitutive Surface for Larger Stress Changes and Reversals of Stresses

In the previous section we used a reversible, linear model to consider small deviations from a state point. Now we wish to explore the possibilities of mapping an entire constitutive surface. This involves the consideration of large stress changes and the effect of a reversal in the direction of volume change.

Hysteresis is a measure of the shortcoming or deficiency of the "mathematical" model from the "real" model (Jaunzemis, 1967). Hysteresis is generally associated with any substance that can maintain equilibrium under an applied set of forces. In the case of unsaturated soils, it would be anticipated that both the soil structure and the contractile skin may exhibit hysteresis.

It is well known that increasing and decreasing the effective stress on a saturated soil results in a series of hysteresis loops. In fact, every reversal in the direction of the deformation of the soil structure produces hysteresis. Therefore, hysteresis destroys the overall uniqueness of a constitutive surface.

The contractile skin is also known to exhibit hysteresis. For example, the wetting and drying of an incompressible soil does not show complete reversibility with respect to the deformation of the contractile skin (Taylor, 1948; Childs, 1969). Since the soil structure and the contractile skin constitutive relationship independently exhibit hysteresis, the air and water constitutive surfaces will likewise show hysteretic effects.

The inter-dependence of the hysteretic effects can be demon-

strated either by examining the continuity equation or the differential form of the equation, $S \cdot e = w \cdot G_s$ That is,

$$dS = \frac{G_s}{e} \cdot dw - \frac{w \cdot G_s}{e^2} \cdot de$$

The equation shows that a change in the degree of saturation can result from either a change in water content or a change in void ratio. However, a change in the degree of saturation always corresponds to an opposite direction change in the air volume.

There are two methods whereby the hysteretic effects influence the constitutive surfaces. First, by reversing the directional change of one of the stress state variables and; second, by having one stress state variable producing deformation in one direction while the other stress state variable is causing deformation in the opposite direction (Figure 6.37). In the second case it is possible todefine a monotonic surface; however, it need not be unique. It can be stated that the monotonic surface is unique only with respect to the stress paths used to define it.

It is obvious that the constitutive surfaces are not completely unique for any unsaturated soil. However, an important question arises with respect to the second method of producing hysteresis. Will the constitutive surface be unique provided the deformations proceed in one direction? (Figure 6.37). This question could be explored on a purely experimental basis but it would be extremely time consuming. Therefore it is worth while to examine theoretically the effects of various stress

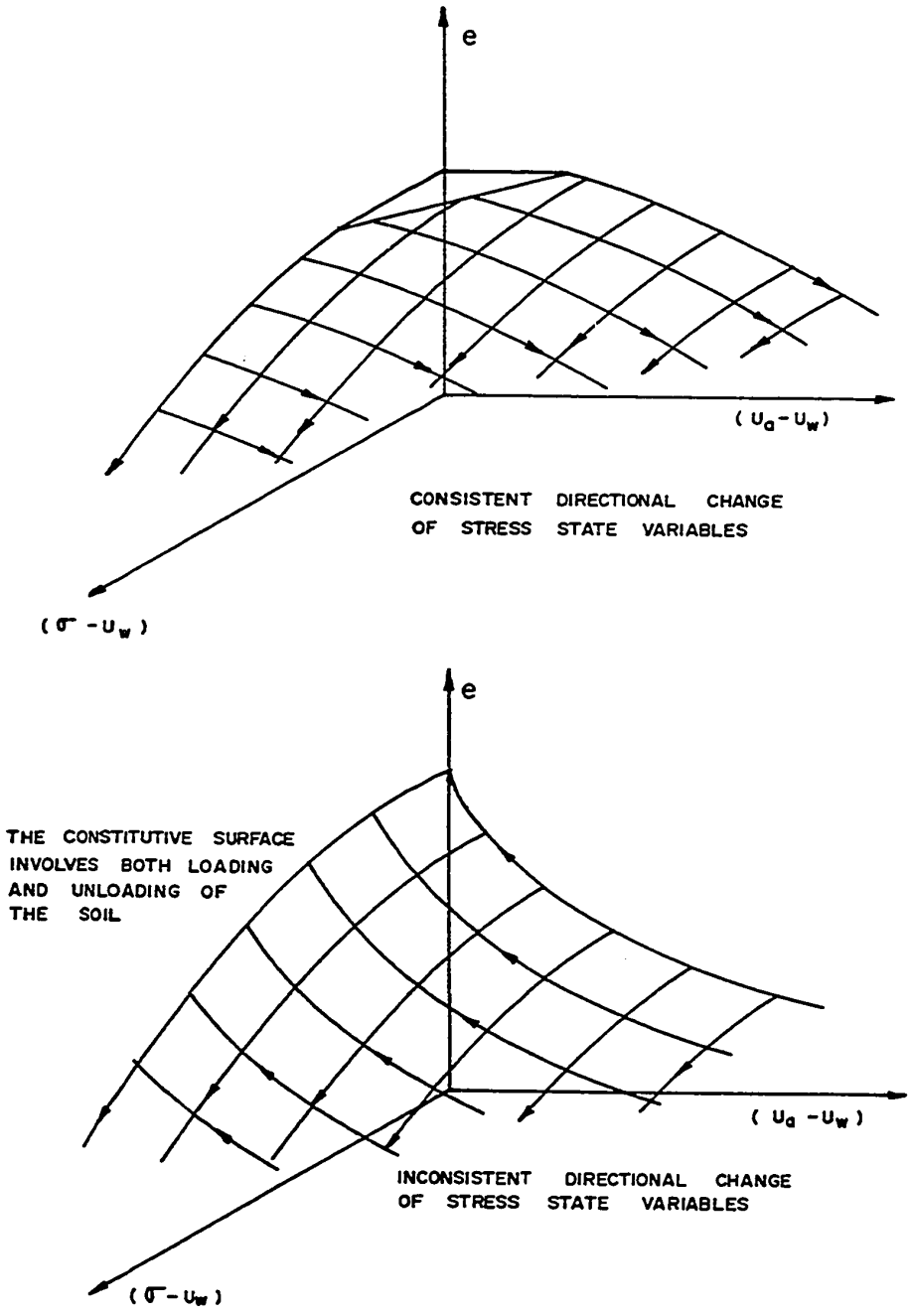


FIGURE 6.37 INCORPORATION OF HYSTERESIS INTO CONSTITUTIVE SURFACE BY INCONSISTENT DIRECTIONAL CHANGE OF STRESS STATE VARIABLES

changes on the direction of deformation of each phase.

From the information presented in section 6.13 it is possible to anticipate the direction of deformation associated with various stress changes applied to a stable-structured, unsaturated soil. First, assume that the total, air and water pressures are changed independently and we desire to prevent a reversal in the direction of deformation of the soil structure. Table VI.19 shows the only possible stress changes that satisfy this requirement.

TABLE VI.19

STRESS CHANGES THAT PRODUCE A CONSTANT

DIRECTION OF DEFORMATION OF THE SOIL STRUCTURE

Stress Changes	Soil Structure Deformation	Contractile Skin Deformation (Air Phase)	Water Phase Deformation
Case I			
Increase σ	Decrease	Decrease	Decrease
Decrease u_a	Decrease	Decrease	Increase
Decrease u_w	Decrease	Increase	Decrease
Case II			
Decrease σ	Increase	Increase	Increase
Increase u_a	Increase	Increase	Decrease
Increase u_w	Increase	Decrease	Increase

Case II is merely the reverse of Case I and either case produces uni-directional volume change of the soil structure. However, the contractile skin undergoes a deformation direction change during the change in water pressure. It is obvious that there is no possible

way to change all three stress components and maintain uni-directional deformations. The soil structure constitutive surface is likely to be affected by the reversal in deformation of the contractile skin. However, it may not be very significant if the water pressure changes are not extensive. In other words, it may be a secondary factor as far as deformation of the soil structure is concerned. Experimental research is necessary to verify the above reasoning.

Table VI.20 shows the stress change combinations that produce uni-directional deformation of the contractile skin.

TABLE VI.20

STRESS CHANGES THAT PRODUCE UNI-DIRECTIONAL DEFORMATION OF THE CONTRACTILE SKIN

Stress Changes*	Soil Structure Deformation	Contractile Skin Deformation (Air Phase)	Water Phase Deformation
Increase σ	Decrease	Decrease	Decrease
Decrease u_a	Decrease	Decrease	Increase
Increase u_w	Increase	Decrease	Increase

*Reversing all stress changes produces a second possible combination.

The deformations of the contractile skin are uni-directional but the soil structure undergoes a deformation reversal during the change in water pressure.

The above tables show that there is no way in which all three

stress components can be changed while assuring uni-directional volumetric deformation of both the soil structure and the contractile skin. Suppose, however, that the stress in one phase is kept constant while the other two stress components are changed. This supposition is realistic since most practical problems have at least one of the three stress components remaining constant. For example, in nature the air pressure tends toward atmospheric at equilibrium conditions. Let us examine the directions of deformation when the air pressure is kept constant (Table VI.21).

Table VI.21 shows that when the total and water pressures are changed in opposite directions, the soil structure exhibits uni-directional deformations. When the total and water pressures are changed in the same direction, the deformation of the contractile skin is uni-directional.

A similar analysis can be conducted for the cases when the total and water pressures are independently kept constant. Such an analysis shows that when the total pressure is kept constant, there is uni-directional deformation of the contractile skin when the air and water pressures are changed in opposite directions. There is uni-directional deformation of the soil structure when the air and water pressures are changed in the same direction. In the case where the water pressure is kept constant, there is uni-directional deformation of both the soil structure and contractile skin when the total and air pressures are changed in opposite directions. If the total and air pressures are changed in the same direction there are deformation reversals in both the soil structure and the contractile skin.

The only case of completely monotonic deformation appears related to the changing of the total and air pressure in opposite directions

TABLE VI.21

DIRECTIONS OF DEFORMATION WHEN AIR PRESSURE IS CONSTANT

Stress Change	Soil Structure Deformation	Contractile Skin Deformation (Air Phase)	Water Phase Deformation
Case I			
Increase σ	Decrease	Decrease	Decrease
Constant u_a	--	--	--
Decrease u_w	Decrease	Increase	Decrease
Case II			
Increase σ	Decrease	Decrease	Decrease
Constant u_a	--	--	--
Increase u_w	Increase	Decrease	Increase
Case III			
Decrease σ	Increase	Increase	Increase
Constant u_a	--	--	--
Decrease u_w	Decrease	Increase	Decrease
Case IV			
Decrease σ	Increase	Increase	Increase
Constant u_a	--	--	--
Increase u_w	Increase	Decrease	Increase

while the water pressure is kept constant. This case should produce a unique constitutive surface for a stable structured soil. Radhakrishna (1967) performed tests on a metastable soil that was susceptible to structural collapse. In most of his tests, the constitutive surface was mapped by <u>increasing</u> total pressure and <u>increasing</u> water pressure.

The increases in total and water pressure each resulted in a decrease in the volume of the overall sample. The test results showed a unique constitutive surface for the soil structure under these conditions. However, if the soil structure had been stable, the constitutive surface would likely have involved hysteresis. The degree of saturation constitutive surface did not appear to be completely unique in Radhakrishna's work.

In cases where only one stress component is changed in one direction, the constitutive relationship can always be assumed to be unique.

6.15 Presentation and Discussion of Data on Hysteresis

In the previous section, the author proposed that there were two hysteretic effects associated with the deformation of an unsaturated soil. To verify this point, a limited testing program was conducted. All tests were performed on compacted kaolin samples. The volume changes associated with the soil structure, the air and water phases are summarized in Table VI.22. All volume changes are normalized with respect to the total sample in order to compare the hysteretic effects with respect to a common base.

Sample #19 was subjected to two increases in water pressure and then two equal decreases in water pressure. Sample #21 was subjected to one water pressure increase and later a similar water pressure decrease. The results of the soil structure, water and air phase volume changes are plotted versus the $(\sigma-u_a)$ stress state variable in Figure 6.38.

TABLE VI.22

SUMMARY OF TESTS TO SHOW THE EFFECT OF HYSTERESIS*

Test No.	$\sigma-u_w$	$\sigma-u_a$	u_a-u_w	Soil Structure Volume Change(%)	Air Phase Volume Change(%)	Water Phase Volume Change(%)	Porosity (%)	Air Porosity (%)	Water Porosity (%)
Changing Water Pressure									
D-6	86.84	27.71	59.13	+0.05	+3.47	-3.42	52.98	21.44	31.54
	56.59	27.97	28.63				52.93	17.97	34.96
D-7	40.83	27.74	13.08	+1.12	+6.22	-5.10	51.81	11.75	40.06
D-8	56.44	27.74	28.70	+0.35	-1.09	+1.44	51.46	12.84	38.62
D-9	86.41	27.74	58.66	+0.75	-1.93	+2.68	50.71	14.77	35.94
Changing Air Pressure									
D-10	62.84	11.22	51.62	+5.80	+9.14	-2.34	60.84	28.34	32.49
	63.04	39.21	23.83				55.04	20.20	34.83
D-11	62.77	54.02	8.76	+8.30	+10.80	-2.50	46.74	9.40	37.33
D-12	63.01	39.38	23.62	-0.03	-0.97	+0.94	46.77	10.37	36.39
D-13	63.15	11.63	51.52	-0.24	-1.36	+1.12	47.01	11.73	35.27
Changing Total Pressure									
C-27	23.85	21.39	2.46	-0.73	+0.13	-0.86	50.92	8.20	42.72
	14.15	11.60	2.55				51.65	8.07	43.57
C-28	23.44	20.93	2.51	+0.33	+0.26	+0.07	51.32	7.81	43.50
Changing Water Pressure									
C-26	28.73	21.39	7.33	0.00	+1.52	-1.52	51.65	11.10	40.55
	23.85	21.39	2.46				51.65	9.58	42.07
C-29	28.26	20.93	7.33	+0.25	-0.68	+0.93	51.40	10.26	41.14

*All values are corrected for testing technique limitations

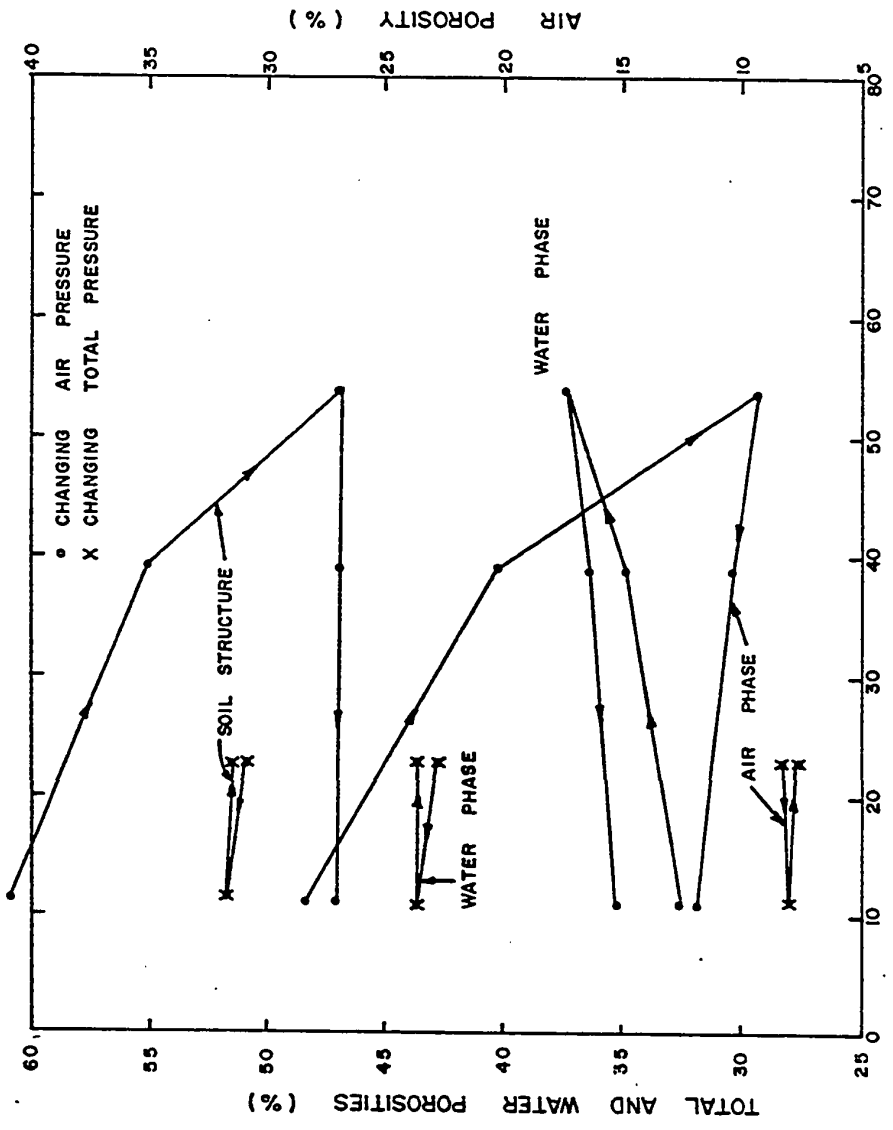


FIGURE 6.38 HYSTERESIS RESULTING FROM REVERSING THE TOTAL AND AIR PRESSURE COMPONENTS

Sample #20 was subjected to two air pressure decreases and then two corresponding air pressure increases. The results are shown in Figure 6.39. Also shown are the results of one total pressure loading and unloading increment on sample #21.

Sample #17 did not show any swelling of the soil structure during the reduction of the $(\sigma-u_w)$ stress state variable. Rather, the sample underwent a slight volume decrease and further decrease upon an increase in $(\sigma-u_w)$. There was some hysteresis in the soil structure but not nearly as much as experienced by the air phase. The air phase hysteresis loop indicates the hysteresis associated with the contractile skin. The water phase volume change reflects the combined response of soil structure and air phase.

Sample #20 produced a large soil structure hysteresis loop as a result of decreasing and increasing the air pressure. The volume changes were similar to those of the air phase. Therefore, the water phase underwent little volume change and hysteresis when compared with the soil structure and the air phase. Two hysteretic effects are occurring simultaneously and have almost the same magnitude.

The hysteresis loop associated with the soil structure, due to a change in total stress, has not been investigated in detail. However, the change in total stress should produce a primary soil structure hysteretic effect and a secondary or consequential contractile skin hysteretic effect.

The results verify that the hysteretic properties of a soil are not directly related to the stress component change or the stress state variable change. Rather, they are related to the direction of

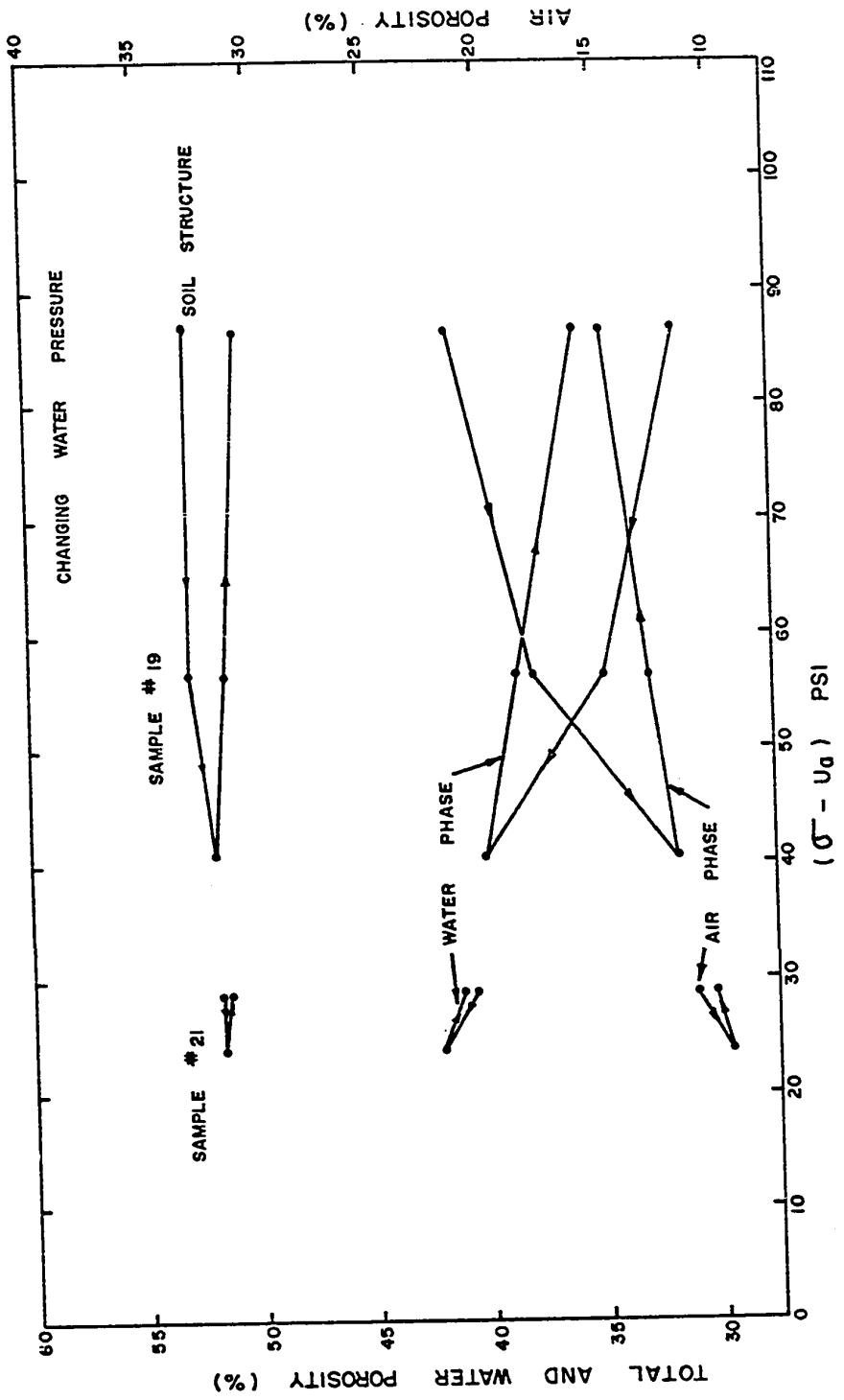


FIGURE 6.39 HYSTERESIS RESULTING FROM REVERSING THE WATER PRESSURE COMPONENT

deformation of the soil structure and/or the contractile skin.

6.16 The Prediction of Volume Change in Unsaturated Soils

The prediction of one-dimensional volume change has enjoyed a high degree of success when applied to saturated soils. The analysis is considerably simpler than the 2- and 3-dimensional analysis due to the constant total stress distribution.

One-dimensional problems can be analysed directly on the basis of the constitutive relationship. Let us consider an elastic, isotropic soil. The constitutive relationship applicable to the soil structure in the y-direction is,

$$e_y^s = \frac{(\sigma_y - u_w)}{E_t^s} - \frac{\nu_t^s}{E_t^s}\cdot(\sigma_x + \sigma_z - 2\cdot u_w) + \frac{(u_a - u_w)}{H_a^a} \qquad 6.42$$

The deformations in the x and z-directions are zero while their total stresses are equal. The constitutive relationship for the x or z-direction is,

$$\overset{0}{\not{e}_x^s} = \frac{(\sigma_x - u_w)}{E_t^s} - \frac{\nu_t^s}{E_t^s}\cdot(\sigma_y + \overset{\sigma_x}{\not{\sigma}_z} - 2\cdot u_w) + \frac{(u_a - u_w)}{H_a^a} \qquad 6.43$$

Rearranging and solving for $(\sigma_x - u_w)$

$$(\sigma_y - u_w) = \frac{\nu_t^s}{(1-\nu_t^s)}\cdot(\sigma_y - u_w) - \frac{E_t^s}{(1-\nu_t^s)\cdot H_a^a}\cdot(u_a - u_w) \qquad 6.44$$

Substituting into the deformation equation in the y-direction gives,

$$e_y^s = \frac{(\sigma_y - u_w)}{E_t^s} - \frac{2\nu_t^s}{E_t^s} \cdot \frac{\nu_t^s}{(1-\nu_t^s)} \cdot (\sigma_y - u_w)$$

$$+ \frac{2 \cdot \nu_t^s}{E_t^s} \cdot \frac{E_t^s}{(1-\nu_t^s) H_a^a} \cdot (u_a - u_w) + \frac{(u_a - u_w)}{H_a^a} \qquad 6.45$$

Collecting the terms gives,

$$e_y^s = (\sigma_y - u_w) \left[\frac{1}{E_t^s} \cdot \frac{(1+\nu_t^s)(1-2\nu_t^s)}{(1-\nu_t^s)} \right] + (u_a - u_w) \left[\frac{1}{H_a^a} \cdot \frac{(1-\nu_t^s)}{(1+\nu_t^s)} \right]$$

6.46

The combinations of elastic constants can be written in terms of compressibility modulii.

Let

$$m_t^s = \frac{1}{E_t^s} \cdot \frac{(1+\nu_t^s)(1-2\nu_t^s)}{(1-\nu_t^s)} \quad \text{and}$$

$$m_a^s = \frac{1}{H_a^a} \cdot \frac{(1-\nu_t^s)}{(1+\nu_t^s)} \qquad 6.47$$

The first compressibility value is identical with that for a saturated soil. The stress state variables should also be written in terms of changes in stress.

Integrating the volumetric deformations over the total height of the sample gives the total displacement in the y-direction.

$$v_y^s = H[m_t^s \cdot d(\sigma_y - u_w) + m_a^s \cdot d(u_a - u_w)] \qquad 6.48$$

where H = height of sample or layer under consideration.

If the total, pore air and pore water pressure boundary conditions and the compressibility soil parameters are known, the deformation of the soil structure can be computed. The soil parameters can be measured in a specially designed oedometer that can control the total, air and water pressures applied to a sample.

The m_t^s and m_a^s soil parameters are measured by independently changing the total and air pressures respectively and measuring the volume changes of the soil structure. Generally the problems of most practical interest involve changes in the total and/or water pressures. In this case it is advantageous to write the relationship in the following form.

$$v_y^s = H[m_t^s \cdot d(\sigma - u_a) + m_w^s \cdot d(u_a - u_w)] \qquad 6.49$$

where m_t^s = one-dimensional compressibility of the soil structure when the total stress is changed

m_w^s = one-dimensional compressibility of the soil structure when the water pressure is changed.

The soil structure or total sample volume changes can be predicted independently of changes in the degree of saturation. If the volume-weight soil properties are desired, the constitutive relationship for the contractile skin must be considered. It can be analysed

in the same manner as the equation for the soil structure. The final form of the equation is,

$$v_y^a = H[m_t^a \cdot d(\sigma - u_a) + m_w^a \cdot d(u_a - u_w)] \qquad 6.50$$

where m_t^a = one-dimensional compressibility value computed from the change in air volume due to a change in total pressure

m_a^a = one-dimensional compressibility value computed from the change in air volume due to a change in water pressure.

The above equations are primarily applicable to cases where the total stress increases or decreases and the water pressure increases. In the event that the water pressure decreases, the soil sample pulls away from the sides of the oedometer ring producing three-dimensional volume change.

In order to apply the above equations, it is necessary to know the initial and final air and water pressures. In many cases the final pressures are a function of the microclimatic conditions. This is an area that warrants further research.

6.16 Typical Constitutive Surfaces For Regina Clay

Four volume change tests were performed with the object of mapping the constitutive surface for natural Regina clay. Two of the samples were tested in the one-dimensional oedometer (sample #33 and #34). The other two samples were tested under isotropic loading conditions in the triaxial apparatus (sample #32 and #35). The volume-weight properties and the pressure change data are tabulated in Appendix F (Section III).

After the samples were placed in the apparatus, the total and/or air pressures were increased to prevent the swelling of the overall sample. An attempt was made to establish considerably different initial stress state variable conditions. However, this meant that the degrees of saturation at the initial equilibrium conditions could vary.

The constitutive surfaces were mapped by decreasing the total and air pressures until the suction was less than approximately 10 psi. Then the total pressure was further reduced. The load increment ratio with respect to the $(\sigma-u_a)$ and (u_a-u_w) stress state variables was always approximately one.

The purpose of this section is not to give a detailed analysis of constitutive surfaces but rather to present typical experimental data on a natural soil. The overall volumetric deformation data from the one-dimensional oedometer tests are presented in Figure 6.40. The isometric presentation is suitable for a qualatative view of the constitutive surface but it is generally unsuitable for engineering

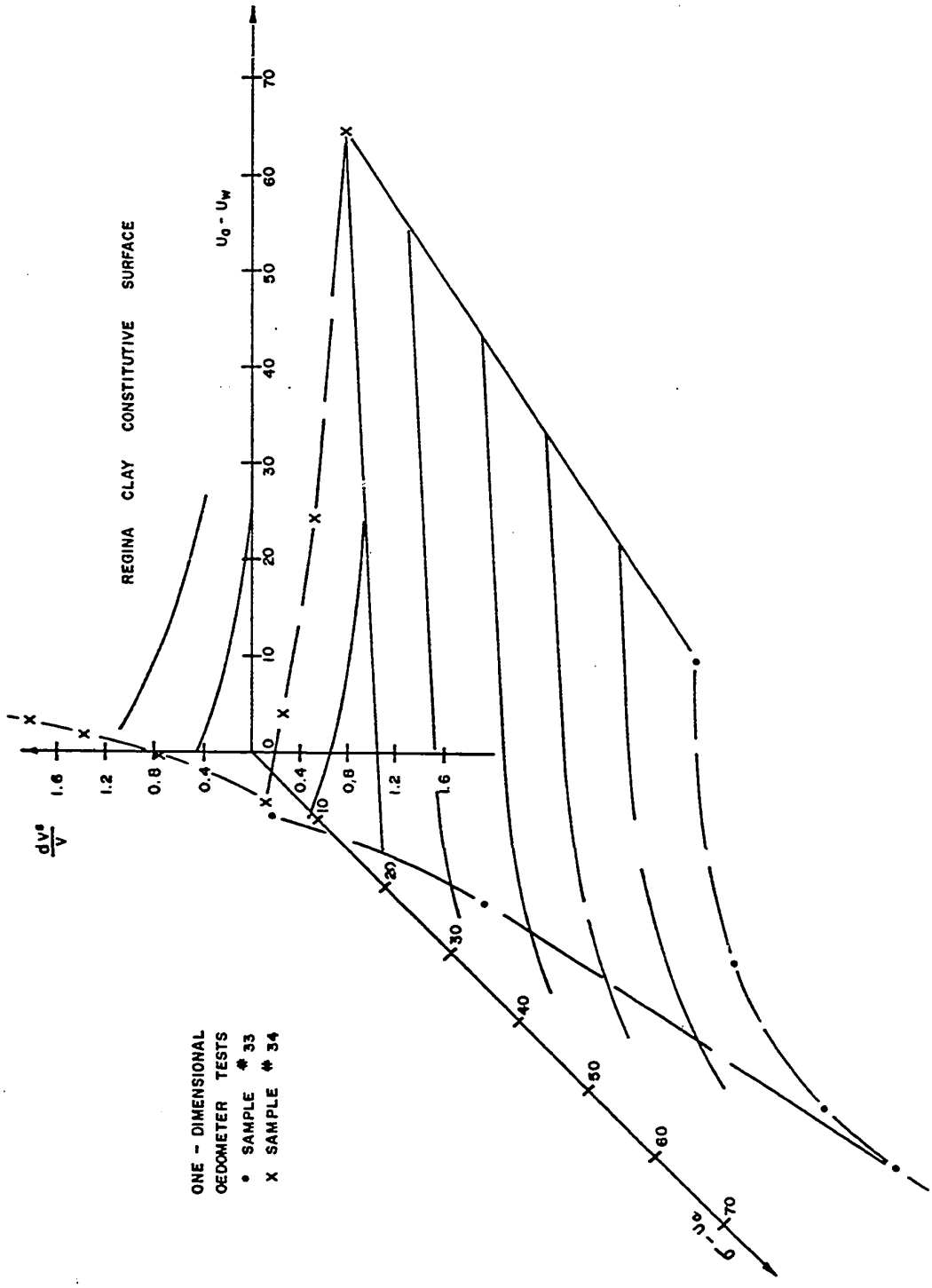


FIGURE 6.40 SOIL STRUCTURE VERSUS STRESS STATE VARIABLES FOR REGINA CLAY

analysis. The plot does, however, show that the constitutive surfaces from the two samples essentially matches even though there was a deformation reversal in the soil structure. The close agreement is likely related to the essentially elastic nature of the overconsolidated Regina clay. Figure 6.41 shows the same data plotted with the stress state variables on the axes and the volume changes as contours. Even with the limited amount of data from the two tests, it is easy to sketch the contours of volumetric deformation. The results indicate that there is a zone which is very insensitive to volume change. It originates from a value of approximately 20 psi on the $(\sigma-u_a)$ axis. (This value is commonly referred to as the swelling pressure). The zone forms a trumpet with one edge of the bell intercepting the (u_a-u_w) axis at approximately 77 psi. (This value would correspond to the initial suction under zero applied load. The plot is convenient for the assessment of volume change since the volumetric deformations corresponding to any two stress states can be quickly read from the plot. The isotropic loading of Regina clay produced a similar plot (Figure 6.42).

If the initial void ratios of the samples tested differ significantly, the volume change results should be plotted in terms of the actual void ratios or porosities. The void ratios from the tests performed on the oedometer are plotted in Figure 6.43. They show the same behavior as the volumetric deformation plot since the initial void ratios were essentially the same on the two samples tested.

Any of the volume weight soil properties can be plotted versus

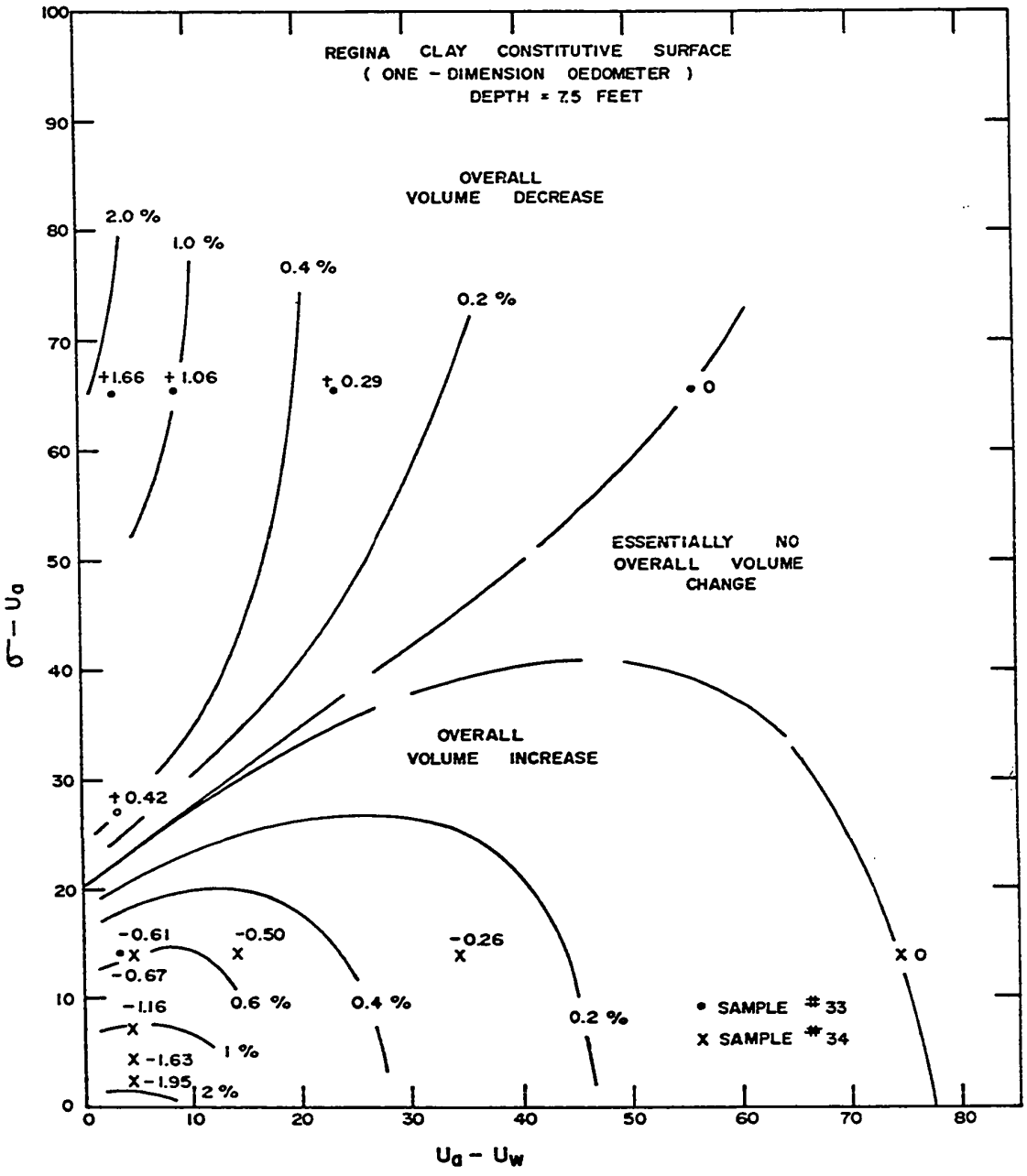


FIGURE 6.41 OVERALL VOLUMETRIC DEFORMATION VERSUS STRESS STATE VARIABLES FOR REGINA CLAY (ONE - DIMENSIONAL OEDOMETER)

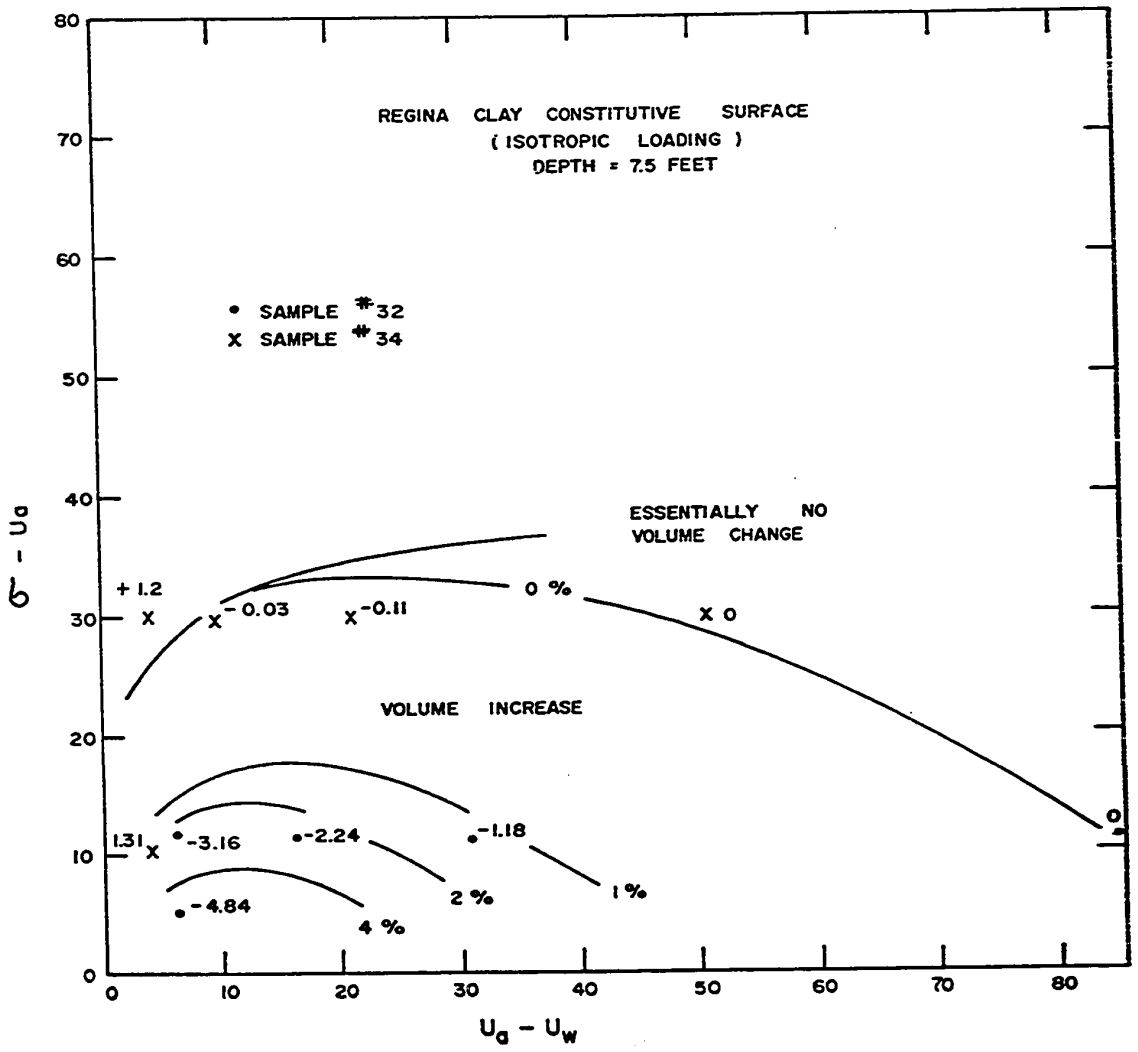


FIGURE 6.42 OVERALL VOLUMETRIC DEFORMATION VERSUS STRESS STATE VARIABLES FOR REGINA CLAY (ISOTROPIC LOADING)

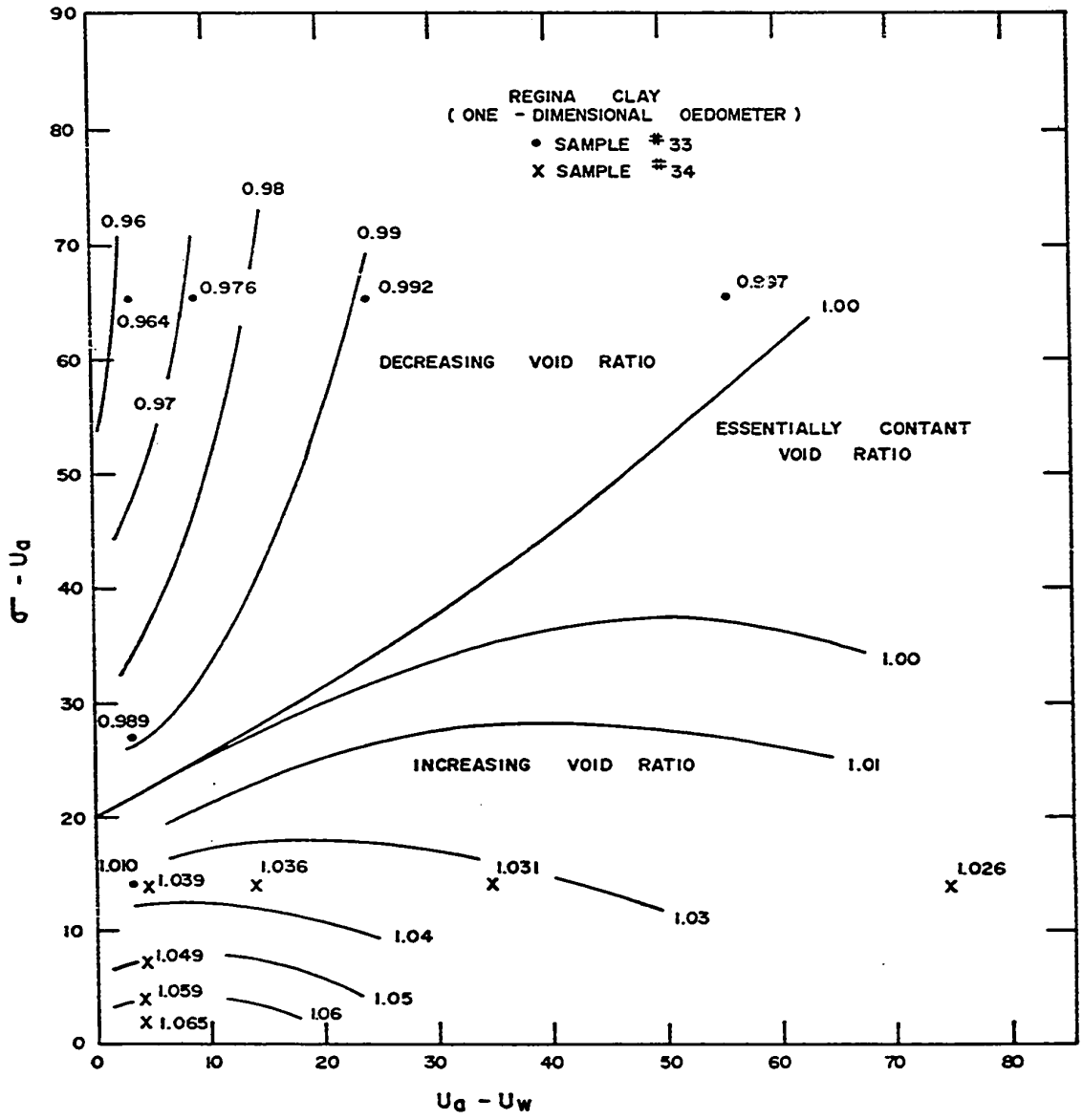


FIGURE 6.43 VOID RATIO VERSUS STRESS STATE VARIABLES FOR REGINA CLAY

any two of the stress state variables. Figure 6.44 shows the degrees of saturation versus the stress state variables for the oedometer tests.

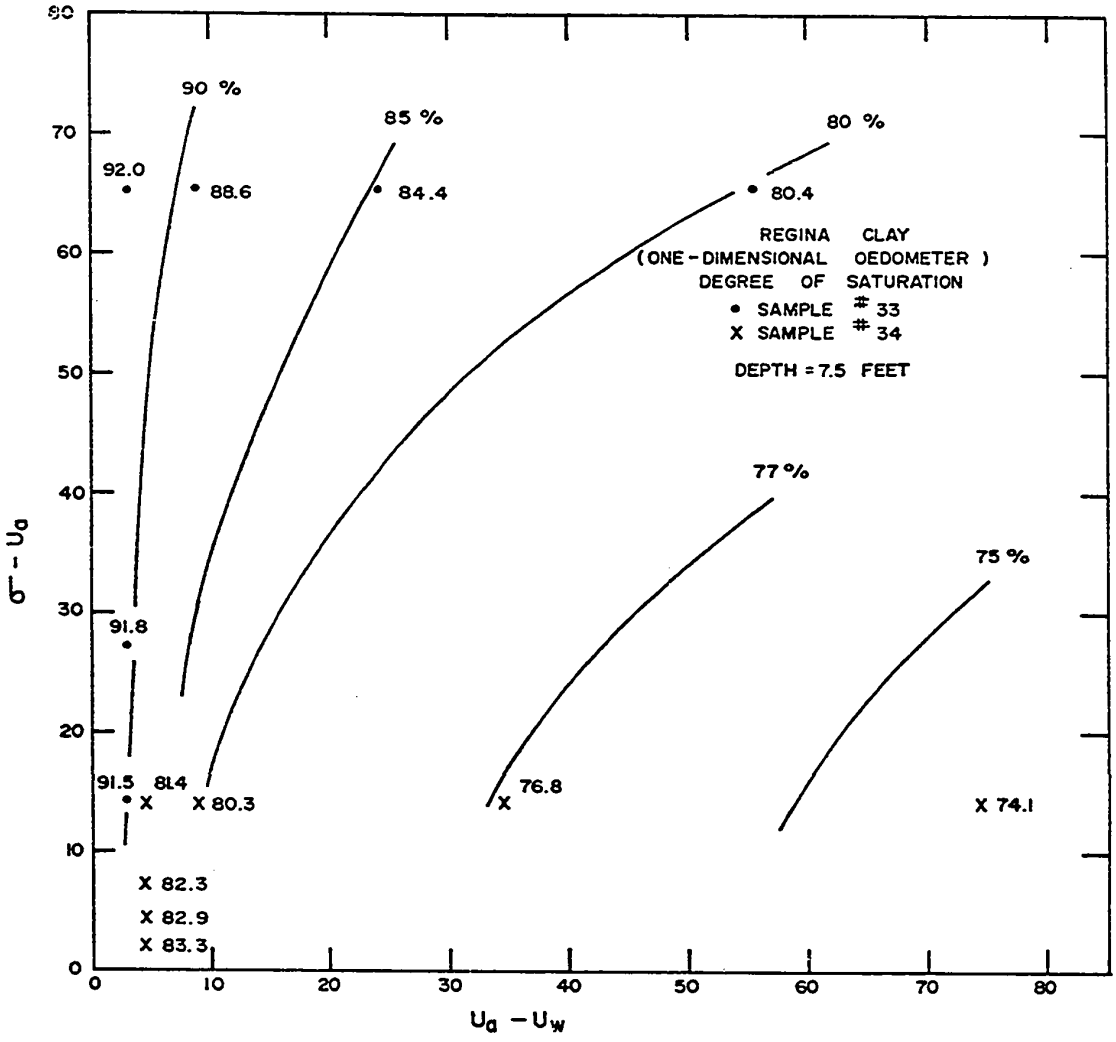


FIGURE 6.44 DEGREE OF SATURATION VERSUS STRESS STATE VARIABLES FOR REGINA CLAY

CHAPTER VII

TRANSIENT FLOW ANALYSIS

7.1 General

The transient flow analysis presented in Chapter VII is restricted to the one-dimensional case. The two and three dimensional cases can be readily formulated; however, there is little use in formulating them until the equations associated with the one-dimensional case have been experimentally verified.

The object of a transient flow analysis is the prediction of the pore pressure components and the volume change with time. The process can be initiated by a change in one or more of the pressure components. The total pressure variation with time is generally a known function. However, the air and water pressures must be computed. Since there are two unknown pressure components, two simultaneous equations with only these two unknownsmust be formulated and solved.

In order to formulate the transient flow problem for unsaturated soils, additional physical relationships must be incorporated. The first involves the flow laws for the air and water phases. The second area involves the conservation of mass for each phase of a multiphase system.

7.2 Literature Review on Transient Flow

Terzaghi (1943) stated that small amounts of air affected the rate of settlement but not the total amount of settlement. His comments were in keeping with Biot's (1940) research work. Biot's analysis of the transient flow problem is remarkable, keeping in mind the knowledge on unsaturated soil behavior at that time. Some of the characteristics of the analysis are as follows:

(i) The constitutive relationship for the soil structure has two stress state variables; however, the second one is, u_w, rather than (u_a-u_w).

(ii) The constitutive relationship for the water phase has two stress state variables. Again, u_w is used as the second stress state variable.

(iii) The compressibility of the soil structure and the fluid phase are used to evaluate the initial pore water pressure as a result of the application of a total stress increment.

(iv) A coefficient is derived to estimate the instantaneous compression.

(v) The flow of water from the soil is assumed to obey Darcy's Law. The air makes the pore fluid compressible but it was not assumed to flow from the soil in accordance with an independent flow law.

(vi) No account is taken of air going into or coming out of solution.

To the author's knowledge, Biot's analysis has never been put in contemporary terminology and solved.

Scott (1963) attempts to formulate the transient flow problem but is unable to satisfactorily complete the analysis. The main handicap relates to the lack of a constitutive relationship for the contractile skin. Also, no mention is made of a flow law for the air phase and the divergence of the air phase is not considered in the continuity requirements.

In 1965, Barden presented his analysis of the consolidation of an unsaturated compacted clay. Darcy's flow law is independently applied to the air and water phases. The derivation of the consolidation equation originates with the continuity of mass equations for the air and water phases. The change in overall porosity terms, occurring in the air and water continuity equations are linked with a soil structure constitutive relationship by means of Bishop's effective stress equation. The χ term becomes a non-unique, empirical parameter that must be evaluated experimentally. Barden lacks the constitutive relationship describing the contractile skin and is therefore unable to complete the analysis without making broad, simplifying assumptions.

Barden (loc cit) classifies the consolidation processes of compacted clays into the following categories.

(i) An extremely dry clay where the degree of saturation is less than 50 percent. The air voids are interconnected and only air will flow cut of the consolidating clay.

(ii) A clay dry of optimum with a degree of saturation ranging 50 to 90 percent. He states that "water still does not flow out from the clay".

(iii) Clays in the region of optimum water content when both air and water flow simultaneously.

(iv) Clays wet of optimum with a degree of saturation in excess of 90 percent. The air exists in an occluded state and cannot flow as a separate continuous fluid.

(v) Very wet clays with a degree of saturation greater than 95 percent. The fluid flowing from the clay is "fairly compressible".

De Wet (1965) presented a three-dimensional moisture movement formulation for an unsaturated soil. He commences the analysis with the conservation of mass, stating that the volume change is equal to the net loss of fluid and the mass transfer between the fluid and vapor. Biot's linear elastic model (1940) is criticized and in its place de Wet combines the conservation of energy and Gibb's equation of energy production to produce a relationship in terms of the product of "forces" and "fluxes". The forces are related to the fluxes by linear phenomenological equations in the neighborhood of the equilibrium state. The author cannot completely agree with this portion of the analysis since de Wet has not used proven stress state variables to formulate the constitutive relationships.

Aitchison (1965) presented the differential equation for water movement in unsaturated soils that is common to the soil science literature. The analysis considers water movement in response to a change in suction. It is based upon the conservation of mass of the water phase only and a flow law for the water phase.

It should be noted that the analysis fails to recognize that two stress state variables are operative rather than one. The formulation of flow is based on diffusivity rather than the coefficient of permeability. The use of diffusivity is common in the soil science literature and is incorporated as a consequence of a lack of understanding of the constitutive relationships involved. The continuity equation does not account for the solution of air in water, the movement in the air phase and volume change of the soil structure. In view of the above limitations the soil science analysis cannot be considered as a general and satisfactory analysis for soils engineering.

7.3 Flow Laws

Flow laws are the consequence of the fact that forces applied to liquids cause flow. Darcy's law is generally accepted as satisfactory for describing the flow of water through a saturated soil.

$$v = - k \cdot \frac{1}{\gamma_w} \cdot \frac{\partial u}{\partial z} \qquad 7.1$$

where k = coefficient of permeability (cm/sec)

v = superficial velocity (cm/sec)

u = pressure in the fluid (gms/cm^2)

γ_w = density of water which is used to convert any fluid pressure to an equivalent head of water (gms/cc)

The coefficient of permeability depends on the properties of the fluid and the medium through which flow is occurring.

$$k = K \cdot \gamma/\mu \qquad 7.2$$

where K = material coefficient of permeability which is a function of the porous medium alone (cc/sec^2).

γ = density of the pore fluid (gms/cc)

μ = viscosity of the pore fluid (gm/cm.sec)

This value should not be confused with the kinematic viscosity which is μ/γ.

Since the material coefficient of permeability is theoretically a constant, it is possible to compute the ratio of the coefficient of permeability with respect to air to the coefficient of permeability with respect to water.

$$\frac{k_a}{k_w} = \frac{\gamma_a \cdot \mu_w}{\mu_a \cdot \gamma_w} \qquad 7.3$$

Typical values of the k_a/k_w ratio for various temperatures are presented in Table VII.1.

TABLE VII.1

TYPICAL k_a/k_w RATIOS

Temperature °C	k_a/k_w
10	0.0927
20	0.0670
30	0.0501

The results indicate that the coefficient of permeability, (as defined by Darcy's law) with respect to the air is from 5 to 10 percent of the coefficient with respect to water. The above analysis assumes that the material coefficient of permeability remains the same, regardless of the pore fluid used for its measurement. This is not completely true and it has been shown that the material coefficient of permeability with respect to air is higher than the material coefficient of permeability obtained using water (Corey, 1937; Scheidegger, 1960).

The above results are contrary to Barden's statement (1965) that "the value of k_a is so high that despite the compressibility of air the transient process will in general not take long".

Fick's law is another flow law which is used in a number of mass transport processes such as thermal and osmotic migration of liquids through membranes and the molecular diffusion of gases and liquids (Crank, 1956; Poulos, 1964). Fick's law states that the velocity is proportional to a concentration gradient.

$$v = - D \cdot \frac{\partial c}{\partial z} \qquad 7.4$$

where D = diffusivity (cm^2/sec)

v = superficial velocity (cm/sec)

c = concentration (ratio by volumes)

$\frac{\partial c}{\partial z}$ = concentration gradient (per cm)

The decision as whether to use Fick's or Darcy's law must be

based on the physical phenomenon taking place. Fundamentally, a compressible or incompressible fluid does not flow through a porous medium in response to a concentration gradient but rather in response to a force gradient.

In order to better understand the independent roles of the two laws, let us consider a sample of sand which is subjected to differing gas compositions at the top and bottom. Let the gas at the top consist of 80 percent oxygen and 20 percent nitrogen, and be subjected to a pressure of 2 atmospheres. Let the gas at the bottom consist of 20 percent oxygen and 80 percent nitrogen, and be subjected to a pressure of 2 atmospheres. Darcy's law shows that there will not be an overall gas flow. However, Fick's law shows that the oxygen will diffuse from the top to the bottom and the nitrogen will diffuse from the bottom to the top until the concentrations are equal.

A change in the gas pressure at one end of the sample causes flow that is basically described by Darcy's law. However, there is an indirect sense in which Fick's law applies as a result of the general gas law which relates overall concentration and pressure.

Let us briefly review the research literature associated with the flow of air and water through an unsaturated soil. In 1950, Childs and Collis-George (Childs, 1969) conducted an experiment to directly verify the use of Darcy's law to describe the flow of water through an unsaturated soil. They devised a method whereby the water content and the suction were maintained constant throughout a column of unsaturated soil. Various magnitudes of gradient were applied and "the rate

of flow for a given degree of saturation was proportional to the potential gradient, as in the case of saturated materials".

Child's (1969) explanatory argument proceeds as follows: "The conductivity channels in the unsaturated material are those pores which are full of water at a particular suction corresponding to the chosen moisture content. The air-filled pores are ineffective since water can hardly pass through a pore without occupying it. It follows that the air-filled pores could be filled with solids, such as wax, without affecting the rate of flow of fluid through the remaining pores, and the porous material treated in this way must now be regarded as a new saturated material with the same properties as the original unsaturated material".

Olsen (1965,1966) has reported excellent conformity to Darcy's law for compacted kaolin. Darcy's law indeed appears essentially verified and certainly satisfactory for unsaturated soils.

The flow of air from an unsaturated soil has been ignored in most flow analysis. However, Barden (1965) applied Darcy's law to the air phase in his consolidation theory. Blight (1971) presented the results of laboratory tests where air was passed through dry soils. The steady state flow results were analysed with respect to Fick's and Darcy's law. The laboratory results indicate that either law adequately describes flow behavior. Yalin (1971) summarizes the results of a large number of tests that were performed using various pore fluids in differing porous mediums. The results indicate similar material coefficients of permeability regardless of whether oil, water or air was used as the

pore fluid.

7.4 Diffusivity Concept Applied to Flow in Unsaturated Soils

Common to most research literature on flow through unsaturated soils is the statement that Darcy's law must be modified prior to its application. Swartzendruber (1969) states that there must be a modification to Darcy's law that "involves the recognition that the air-filled pores will reduce the effective cross-section for liquid flow and will increase the tortuosity of the remaining liquid flow path". Therefore, the coefficient of permeability for unsaturated flow" becomes a function of water content". "Arguments of this type were first set forth by Buckingham (1907) ...".

Childs and Collis-George (1948) adopted Buckingham's postulate and developed the diffusivity approach to flow in unsaturated soils. Their approach has become widely accepted in the soil science field but has only recently been introduced to soil mechanics by Richards (1969).

Richards (loc cit) states, "It has now been clearly established that water flow in partially saturated soils closely obeys a modified form of Darcy's law for saturated sands". He writes the coefficient of permeability as either a function of water content or suction.

In view of the above statements, the question arises, Why is the non linearity of the coefficient of permeability with respect to water content so extremely important in transient flow analysis in unsaturated soils when it can be successfully assumed a constant in the transient flow analysis of saturated soils? It is well known that the coefficient of permeability for a saturated soil is a highly non-

linear function of void ratio or water content (Lambe and Whitman, 1969). Therefore, the necessity of making the coefficient of permeability a function of water content when analysing unsaturated soils suggests the omission of an element of physics from some aspect of the analysis.

Darcy's law is written as a function of water content by recognizing that suction is also a function of volumetric water content, θ. The slope of the constitutitive relationship between water content and suction, $\partial(u_a-u_w)/\partial\theta$, is multiplied by the coefficient of permeability to form the term generally referred to as soil-water diffusivity, D (Swartzendruber, 1969; Childs, 1969).

$$D(\theta) = k(\theta) \cdot \frac{-1}{\gamma_w} \quad \frac{\partial(u_a-u_w)}{\partial\theta} \qquad 7.5$$

where D = diffusivity (cm^2/sec).

The diffusivity term becomes a combination of two soil parameters. When the diffusivity term is inserted in the flow equation, flow becomes a response to a moisture content concentration gradient.

$$v = - D \cdot \frac{\partial\theta}{\partial x} \qquad 7.6$$

Childs (loc cit) points out that the equation shows "that the flow of water is directly proportional to the gradient of moisture content in the direction of the flow, a law which is obeyed by the molecular diffusion of solute through its solvent and which is known as Fick's law". Combining this equation with the continuity equation

for the water phase results in the common one-dimensional diffusion equation,

$$\frac{\partial \theta}{\partial t} = D \cdot \frac{\partial^2 \theta}{\partial x^2} \qquad 7.7$$

The diffusivity coefficient is comparable to the coefficient of consolidation, c_v, in the consolidation theory of a saturated soil (Richards, 1967).

Basically, their flow equation can be questioned since water does not flow in direct response to a concentration gradient. The form of the equation reminds us of Fick's law and Childs (1969) attempts to justify the equation by stating that the flow equation "is now commonly referred to as the diffusivity of water through the soil, and one may also, if somewhat loosely, refer to the diffusion of water through the body".

It appears that the soil science analysis improperly incorporates basic physics. First, the contractile skin has not been recognized as an independent phase that comes to equilibrium. Second, even if the slope of the moisture content characteristic is considered as a constitutive relationship, it only contains one of the two stress state variables involved.

The coefficient of permeability of air and water are actually functions of two volume-weight soil properties. It may be written as

$$k = k(e,w) \quad \text{or}$$

$$k = k(S,w), \text{ etc.} \qquad 7.8$$

During a transient flow analysis, the volume-weight properties can be considered as constants providing their changes are not large. The necessity of making the coefficient of permeability a function of water content (in the soil science literature), is the result of not properly incorporating the constitutive relationships for an unsaturated soil.

The research literature often contains statements to the effect that water flows in response to a suction gradient (de Wet, 1967; Richards, 1969). Basically, this is also false since the suction gradient is a gradient of one of the stress state variables controlling the behavior of the unsaturated soil. However, it is the components of suction that act on the fluid phases that produce flow. They can be acting in the same direction or opposite directions. In each case the suction is the same but the flow directions are different. This reinforces the findings of the equilibrium analysis that showed that the stress state variable describing the behavior of the water phase was u_w, and the air phase was u_a.

7.5 Continuity

In Chapter V the volumetric continuity requirement was given as the unifying relationship between the independent phases of a continuum.

In transient flow analysis the continuity requirement must be satisfied at all times and can be written as a partial differential with respect to time. The continuity requirement can be written in alternate forms by applying the principle of the conservation of mass to each phase of a multiphase system.

The formulation of the continuity equation, written in terms of the conservation of mass depends upon the type of element under consideration (i.e. referential or spatial element). Most of the soil mechanics literature uses a referential element for the soil structure and a spatial element for the water phase (Terzaghi, 1943). The consolidation theory has also been derived on the basis of a spatial element for both the soil structure and the water phase (Gibson, England and Hussey, 1967; Lee, 1968). Two compensating differences arise in these two formulations. When a spatial soil structure is used, Darcy's law must be written in terms of absolute velocities and the continuity equation takes a different form from the case of a referential element. The two differences compensate and the final equations are the same for conditions of infinitesimal deformations. The differences in the forms of the continuity equations follow.

7.6 Transformation Between the Referential and Spatial Descriptions of Motion

The motion of matter is generally defined either in terms of a referential or spatial element. This section formulates the transformation equation between the two systems.

In the referential description, the position of a "particle" and time, t, are the independent variables. In the real world, "particle" refers to a small identifiable mass of the substance under consideration. This system of designation is commonly referred to as the Lagrangian description and the coordinate designations used in this thesis will be x_1, x_2 and x_3. In the spatial description, the position of a "point" in space and time are the independent variables. The term "point" is a fixed position in space without respect to the material substance. This system of designation is commonly referred to as the Eulerian description and the coordinates will be designated as a_1, a_2 and a_3.

For clarity, let us consider motion in only one-dimension. The velocity of a "particle" in the referential (Lagrangian) description is written,

$$v_x|_r = \frac{\partial x}{\partial t}(x_1,t) \qquad 7.9$$

The velocity of a "point" in the spatial (Eulerian) description is,

$$v_x|_s = \frac{\partial x}{\partial t}(a_1,t) \qquad 7.10$$

If we know the spatial description and not the referential description, we can formulate a transformation between the two designations (Malvern, 1969). Let us assume that there exists a sufficiently differentiable and singled-valued function defining the motion of a

"particle". Therefore a relationship can be written between the velocities in the two systems of designation (Hodge, 1970)

$$v_x(x_1,t)|_r = v_x[x(x_1,t),t]|_s \qquad 7.11$$

The particle velocities can be differentiated with respect to time by means of the chain rule of calculus.

$$\frac{\partial v_x}{\partial t}\Big|_r = \frac{\partial v_x}{\partial t}\Big|_s + \frac{\partial v_x}{\partial x}\Big|_s \cdot \frac{\partial x}{\partial t} \qquad 7.12$$

Since x is a function of x_1 and time, t, the $\partial x/\partial t$ can be written as the velocity of the "particle", v_x. Therefore,

$$\frac{\partial v_x}{\partial t}\Big|_r = \frac{\partial v_x}{\partial t}\Big|_s + v_x \cdot \frac{\partial v_x}{\partial x}\Big|_s$$

or

$$\frac{\partial v_x}{\partial t}\Big|_s = \frac{\partial v_x}{\partial t}\Big|_r - v_x \cdot \frac{\partial v_x}{\partial x}\Big|_s \qquad 7.13$$

This equation allows the transformation from a spatial to a referential description of motion. The same type of transformation is used in other transport phenomena such as heat flow (Murray and Landis, 1959). In fact, this type of transformation can be used for any material property if its spatial description is known. For example, if the spatial description of density is given by a function,

$$\gamma = \gamma(x,t) \qquad 7.14$$

the rate of change of density in the neighborhood of the "particle" is given by

$$\left.\frac{\partial \gamma}{\partial t}\right|_r = \left.\frac{\partial \gamma}{\partial t}\right|_s + v_x \cdot \left.\frac{\partial \gamma}{\partial x}\right|_s \qquad 7.15$$

7.7 Continuity with Respect to a One Phase, Spatial and Referential System

The continuity of a one phase system is first derived for a spatial (Eulerian) element. Then the corresponding equation for a referential (Lagrangian) element is obtained by use of the transformation equation.

Consider an arbitrary volume, V, fixed in space which is filled with a continuous medium of density, γ, at time, t. (Malvern, 1969). The total mass, M, in the volume is,

$$M = \int_V \gamma \cdot dV \qquad 7.16$$

Let us assume the existence of a continuous density function. This is actually the definition of a continuum. Differentiating with respect to time gives the rate of change of total mass in the volume,

$$\frac{\partial M}{\partial t} = \int_V \frac{\partial \gamma}{\partial t} \cdot dV \qquad 7.17$$

This is the conservation of mass and can be physically interpreted as showing that the rate of change of mass in the volume is exactly equal to the amount of mass flowing into or out of the volume per unit of time. The flux through an element on the surface of the volume, V, is,

$$\gamma \cdot v \cdot ds \qquad 7.18$$

where v = the outward normal component of velocity

ds = an element on the surface of the volume.

The flux is integrated over the surface of the volume and by use of Gauss' theorem, the surface integral is converted to a volume integral.

$$\int_S \gamma \cdot v \cdot ds = \int_V \left[\frac{\partial(\gamma \cdot v_x)}{\partial x} + \frac{\partial(\gamma \cdot v_y)}{\partial y} + \frac{\partial(\gamma \cdot v_z)}{\partial z}\right] dV \qquad 7.19$$

Substituting into the $\partial M/\partial t$ equation gives,

$$\int_V \left[\frac{\partial \gamma}{\partial t} + \frac{\partial(\gamma \cdot v_x)}{\partial x} + \frac{\partial(\gamma \cdot v_y)}{\partial y} + \frac{\partial(\gamma \cdot v_z)}{\partial z}\right] \cdot dV = 0 \qquad 7.20$$

Only the integrand must vanish or be satisfied at all points in the region. Therefore,

$$\frac{\partial \gamma}{\partial t} + \mathrm{div}(\gamma \cdot v) = 0 \qquad 7.21$$

where div = divergence

The second term is the derivative of a product and can be expanded as,

$$\operatorname{div}(\gamma \cdot v) = \left[\frac{\partial \gamma}{\partial x} \cdot v_x + \frac{\partial \gamma}{\partial y} \cdot v_z \cdot \frac{\partial \gamma}{\partial z} \cdot v_z\right] + \left[\gamma \cdot \frac{\partial v_x}{\partial x} + \gamma \cdot \frac{\partial v_y}{\partial y} + \gamma \cdot \frac{\partial v_z}{\partial z}\right] \qquad 7.22$$

Reducing the equation to one-dimension, the final form is,

$$\frac{\partial \gamma}{\partial t} + \frac{\partial \gamma}{\partial x} \cdot v_x + \gamma \cdot \frac{\partial v_x}{\partial x} = 0 \qquad 7.23$$

The equation is a consequence of the conservation of mass and is known as the continuity equation of a one-phase system using a spatial element. The change in density with respect to time, $\partial\gamma/\partial t$ is with reference to a spatial element and must be transformed when considering a referential element.

$$\left.\frac{\partial \gamma}{\partial t}\right|_s = \left.\frac{\partial \gamma}{\partial t}\right|_r - v_x \cdot \left.\frac{\partial \gamma}{\partial x}\right|_s \qquad 7.24$$

Substituting $\partial\gamma/\partial t|_s$ into the previous continuity equation gives the continuity equation for a one-phase referential element.

$$\left.\frac{\partial \gamma}{\partial t}\right|_r + \gamma \cdot \frac{\partial v_x}{\partial x} = 0 \qquad 7.25$$

The equation shows that the divergence of the velocity field is equal to $-1/\gamma \cdot \partial\gamma/\partial t$.

7.8 Continuity with Respect to Multiphase Systems

The previous continuity equations apply to a one-phase system and can now be applied to multiphase systems in accordance with the overall volumetric continuity requirement. In other words, the conservation of mass requirements are incorporated into the analysis through a volume restriction.

For a saturated soil, the continuity requirement states that the deformation in the soil structure is equal to that of the water phase. This reasoning must apply at all times.

$$\frac{\partial e^s}{\partial t} = \frac{\partial e^w}{\partial t} \qquad 7.26$$

Consideration is herein given to the one-dimensional case only. The soil structure is of the referential type of element and has the following continuity relationship associated with it.

$$\frac{\partial \gamma_d}{\partial t} + \gamma_d \cdot \frac{\partial v_{sz}}{\partial z} = 0$$

or

$$\frac{\partial v_{sz}}{\partial y} = -\frac{1}{\gamma_d} \cdot \frac{\partial \gamma_d}{\partial t} \qquad 7.27$$

where v_{sz} = velocity of the soil structure in the z-direction

γ_d = dry density of the soil.

The velocity term can be written in terms of the soil structure displacement.

$$\frac{\partial v_{sz}}{\partial z} = \frac{\partial\left(\frac{\partial w_z^s}{\partial t}\right)}{\partial z} \qquad 7.28$$

where w_z^s = displacement of the soil structure in the z-direction.

Writing the velocity derivative in terms of deformation gives

$$\frac{\partial^2 w_z^s}{\partial z \cdot \partial t} = \frac{\partial e^s}{\partial t} \qquad 7.29$$

since $$\frac{\partial w_z^s}{\partial z} = e_z^s = e^s$$

The above analysis shows that the rate of deformation term in the continuity requirement can be written in terms of

(i) the divergence of the velocity,

(ii) the change in dry density or

(iii) simply left in terms of the rate of deformation.

All forms are acceptable; however, since the previously developed constitutive equations relate the deformation to the stress state variables, the continuity requirement is best left in its original form.

The water phase has a spatial type of element and the general continuity equation in one-dimensional is of the form,

$$\frac{\partial(n_w \cdot \gamma_w)}{\partial t} + \frac{\partial(\gamma_w \cdot v_z)}{\partial z} = 0 \qquad 7.30$$

The inclusion of the porosity term in the continuity equation warrants some explanation. The first density term in the above equation is defined with respect to the entire element. Therefore, the density can either be redefined as the weight of water with respect to the entire element or as the porosity times the actual density of the phase. The second alternative is selected. The second term, $(\gamma_w \cdot v_z)$, does not have a porosity term since the velocity is a superficial velocity defined with respect to the entire element.

When the above equation is expanded, the rate of change of the water density and the spatial derivative of water density drop out. Therefore,

$$\frac{\partial n_w}{\partial t} + \frac{\partial v_{wz}}{\partial z} = 0 \qquad 7.31$$

The change in porosity is equivalent to a change in volume. Therefore,

$$\frac{\partial e^w}{\partial t} = - \frac{\partial v_{wz}}{\partial z} \qquad 7.32$$

In this case, the divergence of the velocity term is the most useful designation since we have Darcy's law relating the velocity of flow to a pressure gradient. Substituting into the differentiated form of the continuity requirement gives,

$$\frac{\partial e^s}{\partial t} = \frac{\partial v_{wz}}{\partial z} \qquad 7.33$$

This is the commonly used continuity requirement for a saturated soil emement.

In the case of an unsaturated soil there is the addition of the air phase and the contractile skin. In writing the continuity requirement let us combine the volumetric deformation of the contractile skin with the volumetric deformation of the water phase. The differential form of the continuity requirement is,

$$\frac{\partial e^s}{\partial t} = \frac{\partial e^w}{\partial t} + \frac{\partial e^a}{\partial t} \qquad 7.34$$

The soil structure and water phase portions of the continuity equation remain the same as for the saturated soil case. The air phase has a spatial type of element and the principle of the conservation of mass allows it to be written

$$\frac{\partial (n_a \cdot \gamma_a)}{\partial t} + \frac{\partial (\gamma_a \cdot v_{az})}{\partial z} = 0 \qquad 7.35$$

Expanding gives,

$$n_a \frac{\partial \gamma_a}{\partial t} + \gamma_a \cdot \frac{\partial n_a}{\partial t} + \gamma_a \cdot \frac{\partial v_{az}}{\partial z} + v_{az} \cdot \frac{\partial \gamma_a}{\partial z} = 0 \qquad 7.36$$

Dividing by γ_a and solving for the rate of change of porosity

$$\frac{\partial n_a}{\partial t} = - \left[\frac{n_a}{\gamma_a} \frac{\partial \gamma_a}{\partial t} + \frac{\partial v_{az}}{\partial z} + \frac{v_{az}}{\gamma_a} + \frac{\partial \gamma_a}{\partial z} \right] \qquad 7.37$$

Substituting into the continuity requirement gives,

$$\frac{\partial e^s}{\partial t} = \frac{\partial v_{wz}}{\partial z} + \frac{\partial v_{az}}{\partial z} + \frac{n_a}{\gamma_a} \cdot \frac{\partial \gamma_a}{\partial t} + \frac{v_{az}}{\gamma_a} \cdot \frac{\partial \gamma_a}{\partial z} \qquad 7.38$$

The density of the air phase is written in terms of the pressure in the air phase by means of the gas law.

$$\gamma_a = u_a/(R \cdot T) \qquad 7.39$$

The solution of air in water does not enter into the density formulation but rather into the velocity term. The velocity term, v_{az}, involves two types of air flow from the space occupied by the free air. First, there is the flow of air past the boundaries of the element by way of the air voids. Second, there is the flow of air in and out of the water phase. Thus the velocity should be divided into two terms,

$$v_{az} = v_{az}^{f} + v_{az}^{d} \qquad 7.40$$

where v_{az}^{f} = velocity of the free air flow past the boundaries of the element

v_{az}^{d} = velocity of the free air flow through the contractile skin into the water phase.

Darcy's law describes the flow of air past the boundaries of the element. However, another independent flow law (Fick's law) is required to describe the velocity of air passage into and out of the water. In this second case, the boundary conditions are different and a correct analysis is indeed difficult. Therefore, various simplifying assumptions are made concerning the diffusion of air into the water. The simplest procedure is to assume that the quantity of air involved is negligible. As the degree of saturation decreases, this assumption becomes more reasonable. Another solution is to assume that the diffusion of air into the water is instantaneous and directly dependent upon the air pressure. No attempt is made to formulate the solution for this case.

In Chapter V it was shown that the volumetric deformation of the contractile skin could also be mapped in terms of the volumetric deformation of the air phase. It was emphasized that this did not constitute an independent continuity requirement but rather that it placed an independent physical restriction on the continuity requirement. In other words, the results from the continuity equation must also satisfy

the two representations of the air volume change.

The physical restriction on the continuity equation can be stated as follows. The air volume change can be written in terms of its compressibility and divergence of flow or in terms of a constitutive relationship for the contractile skin. This was the equation obtained when considering the continuity of the air phase in terms of the conservation of mass.

$$\frac{\partial e^c}{\partial t} = - \frac{n_a}{\gamma_a} \cdot \frac{\partial \gamma_a}{\partial t} - \frac{\partial v_{az}}{\partial z} - \frac{v_{az}}{\gamma_a} \cdot \frac{\partial \gamma_a}{\partial z} \qquad 7.41$$

where

$$\frac{\partial e^c}{\partial t} = \frac{\partial e^a}{\partial t}$$

7.9 Categorization of Processes

Barden (1965) categorized unsaturated soils into five types for transient flow analysis purposes. On the basis of our laboratory results and theoretical considerations, the author has subdivided the entire range of saturation into four categories.

(i) 100 percent saturation - All the voids are filled with water. This corresponds to the conventional theory of consolidation.

(ii) Greater than 90 percent saturation - The occluded air bubbles are trapped within the soil structure. The problem can be treated as a medium with a compressible pore fluid.

(iii) From approximately 90 percent saturation to a low degree of

saturation - This category is the largest and covers almost the entire range of unsaturation. It is the category that this thesis is most concerned with. The problem of rate of consolidation in response to a change in total pressure is given consideration.

(iv) Degree of saturation approaching zero percent - The pore space is completely filled with a compressible pore fluid.

7.10 Theory of Consolidation for Unsaturated Soils

The derivation of the theory of consolidation can be commenced from either of two independent conservation laws. These are the conservation of energy and the conservation of mass. The conservation of mass equation takes the form of a continuity requirement. A form of the conservation of energy is derived by combining the deformation - displacement relationship and the constitutive relationship with the equilibrium equations. The equation results in pressure and displacement unknowns in the same equation and cannot be solved directly.

The one-dimensional theory of consolidation is presented for an unsaturated soil that has continuous air and water phases.

The continuity equation is,

$$\frac{\partial e^s}{\partial t} = \frac{\partial v_{wz}}{\partial z} + \frac{\partial v_{az}}{\partial z} + \frac{n_a}{\gamma_a} \cdot \frac{\partial \gamma_a}{\partial t} + \frac{v_{az}}{\gamma_a} \cdot \frac{\partial \gamma_a}{\partial z} \qquad 7.42$$

where $\gamma_a = u_a/(R \cdot T)$.

Let us assume that negligible air is dissolved in the water.

Therefore, the entire velocity of the air phase is governed by Darcy's law. The above equation is written entirely in terms of pressures by substituting in

(i) the constitutive relationship for the soil structure,

(ii) Darcy's law for the flow of the air and water phases and

(iii) the general gas law for the density of air.

The resulting equation is,

$$m^s_t \cdot \frac{\partial(\sigma_z - u_w)}{\partial t} + m^s_a \cdot \frac{\partial(u_a - u_w)}{\partial t} = -\frac{k_w}{\gamma_w} \cdot \frac{\partial^2 u_w}{\partial z^2}$$

$$-\frac{k_a}{\gamma_w} \frac{\partial^2 u_a}{\partial z^2} - \frac{k_a}{\gamma_w \cdot u_a} \cdot \left(\frac{\partial u_a}{\partial z}\right)^2 + \frac{(1-S)n}{u_a} \cdot \frac{\partial u_a}{\partial t} \qquad 7.43$$

The equation contains three unknowns; σ_z, u_a and u_w. For the case where the change in total stress with respect to time is known, the equation has only two unknowns.

A second independent, restricting equation must also be satisfied. It is written entirely in terms of pressures by substituting in

(i) the constitutive relationship for the contractile skin,

(ii) Darcy's law for the flow of air and

(iii) the general gas law for the density of air.

$$m_t^c \cdot \frac{\partial(\sigma_z - u_w)}{\partial t} + m_a^c \cdot \frac{\partial(u_a - u_w)}{\partial t} = -\frac{(1-S)\,n}{u_a} \cdot \frac{\partial u_a}{\partial t}$$

$$+ \frac{k_a}{\gamma_w} \cdot \frac{\partial^2 u_a}{\partial z^2} + \frac{k_a}{\gamma_w \cdot u_a} \cdot \left(\frac{\partial u_a}{\partial z}\right)^2 \qquad 7.44$$

Both equations must be satisfied at all times. If these two equations are solved simultaneously, the pore air and pore water pressures are determined. With the excess pore pressures known, the displacements of the soil structure and contractile skin are evaluated directly from the constitutive relationships in the one-dimensional case. No attempt is made to solve the above equations or determine if some of the terms are insignificant and can be neglected.

If we consider the case where a total pressure increment is applied, the boundary conditions are:

$t = 0$ and $0 \leq z < H$	$u_w = u_{wo}$
	$u_a = u_{ao}$
$0 \leq t \leq \infty$ and $z = 0$	$\frac{\partial u_w}{\partial z} = 0$
	$\frac{\partial u_a}{\partial z} = 0$
$0 \leq t \leq \infty$ and $z = H$	$u_w = u_{we}$
	$u_a = u_{ae}$
$t = \infty$ and $0 \leq z \leq H$	$u_w = u_{we}$
	$u_a = u_{ae}$

where u_{wo} = the pore water pressure throughout the sample at the instant after the load is applied.

u_{ao} = the pore air pressure throughout the sample at the instant after the load is applied.

u_{we} = the water pressure immediately outside the sample. In other words, the water pressure to which the water phase will eventually come to equilibrium.

u_{ae} = the air pressure surrounding the sample.

The initial air and water pressures, (u_{ao} and u_{wo}) are dependent upon the relative compressibility characteristics of the phases involved. The buildup of the pore air and pore water pressure is assumed immediate. Therefore, the consolidation process starts the instant after the application of the total stress.

The displacements must be considered in two steps since some displacement has occurred at the instant after the application of the total pressure. The displacement is categorized as

(i) immediate settlement and

(ii) settlements associated with the consolidation process.

The immediate settlement is computed by substituting the immediate change in the stress state variables into the constitutive relationship for the soil structure. The immediate changes in degree of saturation and other volume-weight relationships can be computed after substituting the immediate change in the stress state variables into the constitutive relationship for the contractile skin. All pore pressures generated at the instant after loading are assumed constant throughout the sample.

7.11 Pore Pressure Boundary Conditions for the Consolidation Theories

When a total pressure is applied to a saturated soil, the pore water pressure is equal to the applied load. With a decrease in the degree of saturation, the induced pore pressure decreases. The consolidation process commences from the point of maximum response in the pore air and pore water pressures. The induced pore pressures are assumed to be immediate and related to the relative compressibilities involved. This, in essence, relates to Skempton's pore pressure parameters (1954); however, the equations are developed in a more general sense in keeping with the previous findings presented in this thesis.

The pore pressure responses can be visualized by means of a piston and spring analogy (Figure 7.1). The top loading cap is rigid and the amount of movement that occurs depends on the relative compressibilities of the phases and the stress change applied. The derivations are made by applying the continuity requirement to an isotropically loaded case.

Consider an unsaturated soil with continuous air voids and assume that at the instant of loading there is no time for the escape of air or water but there is time for the compression of the air phase. The continuity requirement is,

$$e^s = e^w + e^a \qquad 7.45$$

The left-hand side can be written in terms of pressures by using the soil structure constitutive equation.

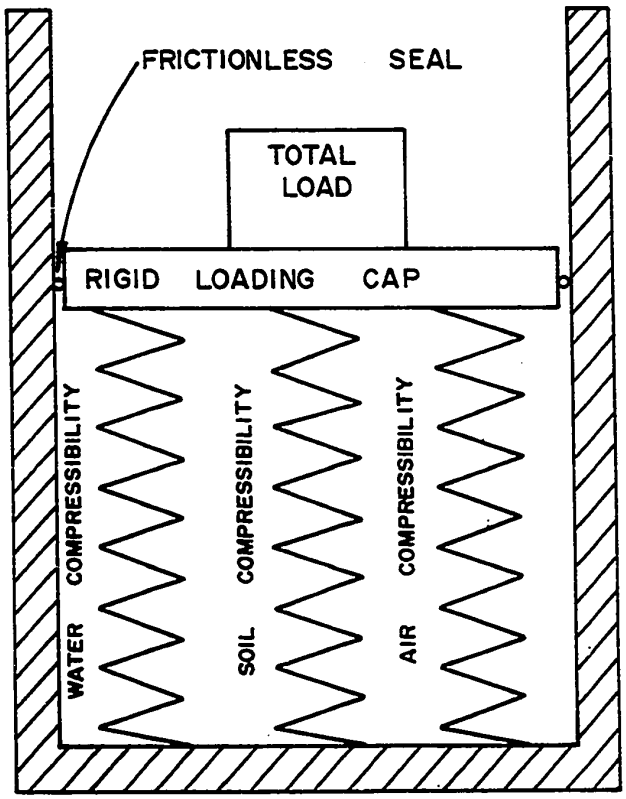


FIGURE 7.1 PISTON AND SPRING ANALOGY FOR THE GENERATION OF PORE PRESSURES

$$e^s = C_t^s \cdot d(\sigma - u_w) + C_a^s \cdot d(u_a - u_w) \qquad 7.46$$

where C_t^s = the bulk compressibility of the soil structure with respect to a change in total stress

C_a^s = the bulk compressibility of the soil structure with respect to a change in air pressure.

The water phase is essentially incompressible but its deformation can be written as

$$e^w = n \cdot S \cdot \beta_w \cdot du_w \qquad 7.47$$

where S = initial degree of saturation.

The volumetric deformation of the air phase can be written based on the general gas law,

$$e^a = \frac{n(1-S)}{u_a} \cdot du_a \qquad 7.48$$

A restriction that must also be satisfied arises from considering the volumetric deformation of the contractile skin as equal to the volumetric deformation of the air phase.

$$e^a = e^c = C_t^c \cdot d(\sigma - u_w) + C_a^c \cdot d(u_a - u_w) \qquad 7.49$$

where C_t^c = the bulk compressibility of the contractile skin with respect to a change in total pressure

C_a^c = the bulk compressibility of the contractile skin with respect to a change in air pressure.

In summary, the two equations that must be satisfied are:

$$C_t^s \cdot d(\sigma-u_w) + C_a^s \cdot d(u_a-u_w) = n \cdot S \cdot \beta_w \cdot du_w + \frac{n(1-S)}{u_a} \cdot du_a \qquad 7.50$$

and

$$C_t^c \cdot d(\sigma-u_w) + C_a^c \cdot d(u_a-u_w) = \frac{n\cdot(1-S)}{u_a} \cdot du_a \qquad 7.51$$

If the change in any one pressure component is known, the other two pressure components are obtained by solving the two simultaneous equations. The induced pore pressures for the one-dimensional case are obtained by using compressibility values obtained from an oedometer test.

The ratios of the induced pore pressures to the applied total pressure are the mathematical equivalent of the Ba and Bw parameters speculated by Bishop and Henkel (1957). The computed induced pore pressures are now used as the initial pressures for the theory of consolidation.

Numerous pore pressure reaction tests were performed during the testing program. They experimentally evaluate the induced pore

pressures due to changes in applied pressure. However, there was some problem with air diffusion through the high air entry disc. This meant that with time, the measured water pressure tended towards the applied air pressure. The solutions to this problem are at present not entirely satisfactory. Due to the lengthiness of the thesis and the incompleteness of this aspect, the data have been omitted from the thesis.

CHAPTER VIII

CONCLUSIONS AND SUGGESTIONS FOR FUTURE RESEARCH

8.1 Conclusions

The volume change behavior of unsaturated soils has been analysed within the context of continuum mechanics. This means that each phase of an unsaturated soil is an independent continuum that obeys the basic laws of physics and chemistry. The conclusions arrived at are based on the theoretical and experimental analyses conducted as part of this dissertation, as well as previous studies.

1. Previous experimental evidence substantiates the consideration of the surface tension membrane (i.e., contractile skin) as an independent phase. It qualifies as an independent phase due to its distinct physical properties. Therefore, an unsaturated soil is viewed as a four phase system rather than the conventional three phase system. In other words, the soil is composed of two solid phases (i.e. soil particles and the contractile skin) and two fluids (i.e. air and water phases. Force equilibrium equations for each phase of an unsaturated soil are written within the context of continuum mechanics. They are arranged in such a manner that the stresses associated with each phase are written in terms of the measurable stresses (i.e. σ, u_a and u_w). The equilibrium equations for the soil structure and the contractile skin are identical. In the x-direction, the equation is,

$$\frac{\partial(\sigma_x-u_w)}{\partial x}+\frac{\partial\tau_{yx}}{\partial y}+\frac{\partial\tau_{zx}}{\partial z}+\frac{n_c}{n_s}\cdot\frac{\partial(u_a-u_w)}{\partial x}+\gamma+F=0$$

The stress state variables governing the behavior of an unsaturated soil (i.e. soil particles and contractile skin) are extracted from the equilibrium equations to form independent stress tensors.

$$\begin{bmatrix}\sigma_x-u_w & \tau_{yx} & \tau_{zx}\\ \tau_{xy} & \sigma_y-u_w & \tau_{zy}\\ \tau_{xz} & \tau_{yz} & \sigma_z-u_w\end{bmatrix}$$

and

$$\begin{bmatrix}u_a-u_w & 0 & 0\\ 0 & u_a-u_w & 0\\ 0 & 0 & u_a-u_w\end{bmatrix}$$

Thus, two independent stress tensors control the equilibrium of an unsaturated soil. It is also possible to use other combinations of the stress state variables. These involve,

$$(\sigma-u_a) \quad \text{and} \quad (u_a-u_w)$$

or $(\sigma-u_a)$ and $(\sigma-u_w)$

Any two of the three stress state tensors are theoretically justifiable for describing unsaturated soil behavior.

3. Null tests were performed to experimentally verify the proposed stress state variables. The null tests consisted of changing the stress components in such a way as to leave unchanged the stress state variables (i.e. $\Delta\sigma = \Delta u_a = \Delta u_w$). The null criterion states that if no volume change occurs, the equilibrium of the soil has not been modified.

The experimental data from a large number of unsaturated soil samples indicated essentially no volume changes during the null tests. On the final set of tests, the overall and water volume changes were less than 1 part in 10,000 parts, even after several days duration. This corresponds to approximately two percent of the anticipated volume changes that would be associated with a change in either one of the stress state variables. The proposed stress state variables are well verified for both the soil structure and the contractile skin.

4. Independent displacement fields are written for each phase of an unsaturated soil within the context of continuum mechanics. The unifying continuity requirement states that the sum of the volumetric deformations of the phases must equal the volumetric deformation of the overall element.

5. Constitutive relationships are developed which link the

stress state variables and the deformation state variables for the soil structure and contractile skin. Two constitutive equations are required to completely describe the volumetric deformation of an unsaturated soil. Using $(\sigma-u_w)$ and (u_a-u_w) as the stress state variables, the constitutive relationship for the soil structure is,

$$\frac{dv^s}{v} = \frac{\partial v^s}{\partial(\sigma-u_w)} \cdot d(\sigma-u_w) + \frac{\partial v^s}{\partial(u_a-u_w)} \cdot d(u_a-u_w)$$

and for the contractile skin, it is

$$\frac{dv^c}{v} = \frac{\partial v^c}{\partial(\sigma-u_w)} \cdot d(\sigma-u_w) + \frac{\partial v^c}{\partial(u_a-u_w)} \cdot d(u_a-u_w)$$

As a consequence of the continuity requirement, similar constitutive equations are written for the air and water phases.

6. The uniqueness of the above constitutive equations were examined for two soil types by producing small stress changes from a stress point.

The Regina clay showed very close agreement between the soil structure volumetric deformations measured and those predicted by the constitutive equation. The kaolin samples showed some hysteresis as a result of a change in the direction of the overall volumetric deformation. Corrections for non linearity of the constitutive surfaces also improved the correlation. The results showed a correlation coefficient well in excess of the critical correlation for a 1% level of significance.

The comparison of the predicted and measured water volumetric deformations are not as convincing as the soil structure results. The loss of a small amount of water from the sample has an effect on the correlation coefficient in addition to the factors of hysteresis and non linearity. Although the correlation coefficients are lower than those for the soil structure, they are above the critical correlation for a 1% level of significance.

7. Larger stress changes from a stress point are significantly effected by hysteresis. On the basis of previous studies and the present research, there are hysteresis effects associated with both the soil structure and the contractile skin. Hysteresis results if the direction of deformation of the soil structure or the contractile skin is reversed. The limited data presented indicate that any surface defined by a uni-directional volume change of the soil structure and the contractile skin produces a unique constitutive surface.

8. The one-dimensional volume change in an unsaturated soil can be predicted by integrating the soil structure deformation over the height of the sample.

$$v_y^s = H \cdot [m_t^s \cdot d(\sigma_y - u_w) + m_a^s \cdot d(u_a - u_w)]$$

The changes in the volume-weight soil properties can be evaluated after integrating the contractile skin deformation over the height of the sample.

$$v_y^c = H \cdot [m_t^c \cdot d(\sigma_y - u_w) + m_a^c \cdot d(u_a - u_w)]$$

The anticipated directions of volumetric deformation for a stable structured soil can be obtained by considering the effect of the individual stress component changes.

9. The continuity requirement for an unsaturated soil states that the sum of the volumetric deformations of all phases is equal to the overall volumetric deformation, at all times.

$$\frac{\partial e^s}{\partial t} = \frac{\partial e^c}{\partial t} + \frac{\partial e^w}{\partial t} + \frac{\partial e^a}{\partial t}$$

The volumetric deformation of the contractile skin can be combined with the water volumetric deformation. An independent restricting equation can also be written which states that the volume change of the air phase can be used to represent the volumetric deformation of the contractile skin.

The conservation of mass equation can be applied to each phase independently. This allows each volumetric deformation to be also written as a divergence of the velocity or a change in density.

10. The one-dimensional theory of consolidation for unsaturated soils is derived on the basis of the continuity requirement. After incorporating the flow laws and constitutive equations, the partial differential equation is,

$$m_t^s \cdot \frac{\partial(\sigma_y - u_w)}{\partial t} + m_a^s \cdot \frac{\partial(u_a - u_w)}{\partial t} = - \frac{k_w}{\gamma_w} \frac{\partial^2 u_w}{\partial z^2} - \frac{k_a}{\gamma_w} \cdot \frac{\partial^2 u_a}{\partial z^2}$$

$$- \frac{k}{\gamma_w u_a} \cdot \left(\frac{\partial u_a}{\partial z}\right)^2 + \frac{(1-S) \cdot n}{u_a} \cdot \frac{\partial u_a}{\partial t}$$

The equation contains two unknowns (i.e. u_a and u_w). However, an additional independent equation can be written since there is a further restriction on the continuity equation.

$$m_t^c \cdot \frac{\partial(\sigma_y - u_w)}{\partial t} + m_a^c \cdot \frac{\partial(u_a - u_w)}{\partial t} = - \frac{(1-S) \cdot n}{u_a} \cdot \frac{u_a}{t}$$

$$+ \frac{k_a}{\gamma_w} \cdot \frac{\partial^2 u_a}{\partial z^2} + \frac{k_a}{\gamma_w \cdot u_a} \cdot \left(\frac{\partial u_a}{\partial z}\right)^2$$

The above equations must be solved simultaneously. At any time, the pore pressures can be substituted into the constitutive relationships to determine the volumetric deformation. No attempt has been made to solve the above equations.

11. The initial pore pressures for the theory of consolidation are theoretically derived on the basis of the compressibilities of the phases involved. Again there are two simultaneous equations.

$$m_t^s \cdot d(\sigma_y - u_w) + m_a^s \cdot d(u_a - u_w) = n \cdot S \cdot \beta_w \cdot du_w + \frac{n(1-S)}{u_a} \cdot du_a$$

and

$$m_t^c \cdot d(\sigma_y - u_w) + m_a^c \cdot d(u_a - u_w) = \frac{n(1-S)}{u_a} \cdot du_a$$

12. The density and compressibility of pure water is essentially unaffected by the solution of air in water. The dissolved air is believed to fit within the "holes" within the water structure. A piston and porous stone analogy is developed to explain the solution of air in water.

13. Diffusivity values for air passing through water in a high air entry, ceramic disc are almost one order of magnitude lower than the value for pure water. The reduction is believed partly related to increased tortuosity; however, the author is not certain whether this is the complete explanation.

14. Air and water mixtures interact in both a miscible and immiscible manner. The density relationship for a combined miscible and immiscible air-water mixture is,

$$\gamma_m = \gamma_w \cdot S + (1-S) \frac{u_{ai}}{u_a} + S \cdot h \cdot \frac{u_{ai}}{u_a}$$

The compressibility relationship is,

$$\beta_m = S \cdot \beta_w + \frac{(1-S)}{u_a} + \frac{S \cdot h}{u_a}$$

The above equations are discontinuous at the point when all the air is driven into solution. At this point, the density and compressibility equal that of pure water. The compressibility may increase by several orders of magnitude at the instant of complete solution. However, the increase depends upon the air pressure. The

compressibility equation demonstrates the pronounced effect of even a very small percentage of air. Experimental data obtained during the test program agrees with the compressibility equation.

The previous compressibility equation applies when the air and water pressures are equal. If they differ, the equation takes the form,

$$\beta_m = S \cdot \beta_w + B_{aw} \cdot \frac{(1-S)}{u_a} + B_{aw} \cdot \frac{S \cdot h}{u_a}$$

where B_{aw} = a pore pressure parameter equal to the ratio of B_a to B_w

The B_{aw} pore pressure parameter incorporates the compressibilities of the soil structure and the contractile skin with respect to the stress state variables.

15. Air diffuses through the water in the soil and the high air entry disc and collects below the ceramic disc. The diffused air volume must be collected and measured in order to correctly evaluate the water volume change. Failure to measure the diffused air volume causes significant errors in the test results after an elapsed time of a few days.

16. Water also diffuses through rubber and lucite at rates which are significant for a long duration test. In Triaxial Apparatus No. 2, a composite membrane consisting of two slotted aluminum foils between two rubber membranes was found to essentially eliminate moisture loss.

17. The four pieces of equipment developed for this thesis had the following basic design considerations.

(i) control of the total, air and water pressures and the undrained measurement of the water pressure.

(ii) measurement of the total and water volume changes. In addition, the diffused air volume was measured to ensure accurate water volume measurements.

A new diffused air volume indicator was built which uses a flushing technique to measure the diffused air volume by means of the displacement of water from a burret.

The checks of the measured initial volumes plus the changes in volume against the final volumes confirms the long term acceptability of all four pieces of equipment for testing unsaturated soils.

18. A pore pressure response theory is presented which predicts the equilization time for high air entry discs. The response curves are highly dependent upon the percentage of air in the compartment. Excellent agreement was obtained between the theory and the experimental results. A response test also yields the compressibility of the air-water mixture in the base plate compartment.

8.2 Suggestions for Future Research

1. With regard to the test equipment, it would be advantageous to secure a superior small valve that completely eliminated the loss of water over a long period of time.

A new type of base plate should be designed that would not

permit the entrance of diffused air. Research in this direction is essential prior to performing long term tests in which the pore water pressure is measured in an undrained system.

2. The values for the diffusivity of air through pure water are significantly higher than the values measured when the water is contained within a solid phase. Further research should be directed towards measuring diffusivity through various soils. A better understanding of the factors affecting diffusivity could prove useful in the design of equipment for testing unsaturated soils.

3. Further investigation should be conducted into the effects of hysteresis upon the constitutive surface. A general, theoretical approach was adopted towards the constitutive surface in this thesis; however, probably the types of problems encountered in practice should be categorized and the constitutive surface investigated for each case.

4. The one-dimensional volume change analysis should be checked against field case in order to obtain an indication of its reliability. Some consideration could then be given to two and three dimensional analysis. However, the priority should be placed on verifying the reliability of the one-dimensional analysis.

5. The partial differential equations associated with the one-dimensional theory of consolidation should be solved and experimentally verified. Also, the pore pressures induced as a result of the application of a total pressure should be experimentally verified. Then consideration could be extended to two and three-dimensional problems.

6. The stress state variables verified for the volume change problem should also be applied to the shear strength analysis of unsaturated soils.

LIST OF REFERENCES

Adam, N.K. (1938) "The Physics and Chemistry of Surfaces" Second Edition, Clarendon, Oxford.

Adamson, A.W. (1960) "Physical Chemistry of Surfaces" Interscience Publishers, Inc. New York.

Aitchison, G.D. (1956) "Some Preliminary Studies of Unsaturated Soils. a) The Circumstance of Unsaturation in Soils with Particular Reference to the Australian Environment". Proceedings of the Second Australia - New Zealand Conference on Soil Mechanics and Foundation Engineering, New Zealand Institution of Engineers.

Aitchison, G.D. (1960) "Relationship of Moisture Stress and Effective Stress Functions in Unsaturated Soils", Pore Pressure and Suction in Soils. Butterworth, London, 1961.

Aitchison, G.D. (1965) "Engineering Concepts of Moisture Equilibria and Moisture Changes in Soils", Statement of the Review Panel for the symposium in print. Moisture Equilibria and Moisture Changes in Soils Beneath Covered Areas, Butterworths, Australia.

Aitchison, G.D. (1967) "Separate Roles of Site Investigation, Quantification of Soil Properties, and Selection of Operational Environment in the Determination of Foundation Design on Expansive Soils", Proceedings of the Third Asian Regional Conference on Soil Mech. and Fdtn Eng., Haifa, Israel.

Aitchison, G.D. (1969) "Soil Suction in Foundation Design", Proceedings of the Seventh International Conference on Soil Mechanics and Foundation Engineering, Vol. 2, Mexico.

Balasubramanian, B.I. (1972) "Swelling of Compaction Shale", Ph.D. Thesis, University of Alberta.

Barden, L., A.O. Madedor and G.R. Sides (1969) "Volume Change Characteristics of Unsaturated Clay", Journ. of the Soil Mech. and Fdtn Div. ASCE (Jan.) .

Barden, L. and G.R. Sides (1967) "The Diffusion of Air Through the Pore Water of Soils", Proc. Third Asian Regional Conference, Vol. 1.

Barden, L. and G.R. Sides (1970) "Engineering Behavior and Structure of Compacted Clay", Journ. of Soil Mech. and Fdtn Eng. ASCE, July, pp. 1171-1200.

Bikerman, J.J. (1958) "Surface Chemistry, Theory and Applications" Second Edition, Academic Press Inc. New York.

Biot, M.A. (1941) "General Theory of Three-Dimensional Consolidation" Journal of Applied Physics, Volume 12, February.

Biot, M.A. (1955) "Theory of Elasticity and Consolidation for a Porous Anisotropic Solid", Journal of Applied Physics, Vol. 26, No. 2.

Biot M.A. (1957) "The Elastic Coefficients of the Theory of Consolidation", Journal of Applied Mechanics, Vol. 24.

Bishop, A.W. (1957) Some Factors Controlling the Pore Pressures Set Up During the Construction of Earth Dams. Fifth International Conf. on Soil Mech. and Fdtn. Eng. Vol. II.

Bishop, A.W. (1959) Lecture delivered in Oslo, Norway in 1955, "The Principle of Effective Stress", Printed in Tek. Ukeflad, No. 39.

Bishop, A.W. (1960a) "The Measurement of Pore Pressure in the Triaxial Test", Proc. Conf. on Pore Pressure and Suction in Soils, 38-46, London, Butterworth.

Bishop, A.W. (1960b) "Discussion on General Principles and Laboratory Measurements", Proc. Conf. on Pore Pressure and Suction in Soils, 63-66. London, Butterworth.

Bishop, A.W. (1969) "Pore Pressure Measurements in the Field and in the Laboratory", Specialty Sessions, Seventh Int. Conf. Soil Mech. and Fdtn Eng., Mexico.

Bishop, A.W., I. Alpan, G.E. Blight and I.B. Donald (1960) "Factors Controlling the Strength of Partly Saturated Cohesive Soils", Research Conference on Shear Strength of Cohesive Soils, American Society of Civil Engineers, Boulder, Colorado.

Bishop, A.W. and G.E. Blight (1963) "Some Aspects of Effective Stress in Saturated and Unsaturated Soils", Geotechnique, Vol. 13.

Bishop, A.W. and I.B. Donald (1961) "The Experimental Study of Partly Saturated Soil in the Triaxial Apparatus". Fifth International Conf. on Soil Mech. and Fdtn. Eng. 1:13-21.

Bishop, A.W. and A.K.G. Eldin (1950) Undrained Triaxial Tests on Saturated Sands and Their Significance in the General Theory of Shear Strength, Geotechnique, 2.

Bishop, A.W. and Henkel, D.J. (1962) "The Measurement of Soil Properties in the Triaxial Test". Edward Arnold (Publisher) Ltd., London, Second Edition.

Bishop, A.W., D.T. Webb and A.E. Skinner (1965) "Triaxial Tests on Soil at Elevated Cell Pressures", Sixth Int. Conf. on Soil Mech. and Fdtn Eng.

Blight, G.E. (1965) "A Study of Effective Stresses for Volume Change", Moisture Equilibrium and Moisture Changes in Soils Beneath Covered Areas. Butterworth, Australia.

Burland, J.B. (1965) "Some Aspects of the Mechanical Behavior of Partly Saturated Soils", Moisture Equilibrium and Moisture Changes in Soils Beneath Covered Areas. Butterworth, Australia.

Carslaw, H.S. and J.C. Jaeger (1959) "Conduction of Heat in Solids", 2nd Ed. Oxford, Clarendon Press.

Casagrande, A. and W.L. Shannon (1948) "Research on Stress-Deformation and Strength Characteristics of Soils and Soft Rocks Under Transient Loading", Soil Mechanics Series No. 31, Harvard University, Cambridge, Mass. (Appendix F).

Chattopadhyay, P.K. (1972) "Residual Shear Strength of Some Pure Clay Minerals", Ph.D. Thesis, University of Alberta.

Childs, E.C. (1969) "The Physical Basis of Soil Water Phenomena" Wiley-Interscience, John Wiley & Sons, London.

Christiansen, E.A. (1961) "Geology and Groundwater Resources of the Regina Area", Report No. 2, Saskatchewan Ressearch Council, Saskatoon.

Christie, T.F. (1965) "Secondary Compression Effects during One-Dimensional Consolidation Tests" Int. Conf. on Soil Mech. and Fdtn Eng., Montreal.

Chow, P.C. and N.J. Pagano (1967) "Elasticity" D.V. Nostrand Co. Inc., Toronto.

Coleman, J.D. (1962) Correspondence in Geotechnique "Stress/Strain Relations for Partly Saturated Soil", Vol. 12, No. 4, pp. 348 to 350.

Compton, P.V. (1970) "A Study of the Swelling Behavior of an Expansive Clay as Influenced by the Clay Microstructure, Soil Suction and External Loading" Technical Report No. AFWL-TR-70-26 Air Force Weapons Laboratory, New Mexico.

Corey, A.T. (1957) "Measurement of Air and Water Permeability in Unsaturated Soil" Soil Science Society of America Proceedings 21:7-10.

Crank, J. (1956) "The Mathematics of Diffusion" Oxford University Press.

Croney, D. (1952) "The Movement and Distribution of Water in Soils", Geotechnique, Vol. 3.

Croney, D., J.D. Coleman and W.P.M. Black (1958) "The Movement and Distribution of Water in Soil in Relation to Highway Design and Performance", Highway Research Board Special Report No. 40, Washington, D.C.

Davies, J.T. and E.K. Rideal (1963) "Interfacial Phenomena", Second Edition, Academic Press, New York.

Defay, R. and I. Prigogine (1966) "Surface Tension and Adsorption", Longmans, Great Britain.

Derjaguin, B.V. (1965) "Recent Research into the Properties of Water in Thin Films and in Micro-Capillaries", Society for Experimental Biology Symposia, XIX. The State and Movement of Water in Living Arganisms.

Donald, I.B. (1956) "Shear Strength Measurements in Unsaturated, Non-Cohesive Soils with Negative Pore Pressures", Proc. 2nd Austr. and New Zealand Conf. on Soil Mech. and Fdtn Eng. pp. 200-205.

Dorsey, N.E. (1940) "Properties of Ordinary Water-Substance", American Chemical Society, Monograph Series, Reinhold Publishing Corporation.

Dunn, C.S. (1965) "Developments in the Design of Triaxial Equipment for Testing Compacted Soils", Proc. of Symposium on the Economic Use of Soil Testing in Site Investigation pp. 3:19-25, Birmingham.

Ellis, J.G., D.F. Acton and J.S. Clayton (1965) "The Soils of the Regina Map Area" (72-1) University of Saskatchewan, Saskatoon.

Escario, V. (1969) "Swelling of Soils in Contact with Water at a Negative Pressure", Second International Conference on Expansive Soils, Texas A & M.

Faizullaev, D.F. (1969) "Laminar Motion of Multiphase Media in Conducts", Special Research Report, Translated from Russian by Consultants Bureau, New York.

Frederick, M.R. (1962) "The Significance of Particle Shape in Sand Behavior", Ph.D. Thesis, University of Birmingham.

Frederick, D. and T.S. Chang (1965) "Continuum Mechanics", Allyn and Bacon Series in Mechanical Engineering and Applied Mechanics.

Fredlund, D.G. (1972) "Manual of Volume Change Test Procedures for Unsaturated Soils", Internal Note: SM12, University of Alberta, Edmonton.

Fung, Y.C. (1965) "Foundations of Solid Mechanics" Prentice-Hall, Inc., Englewood Cliffs, N.J.

Fung, Y.C. (1969) "A First Course in Continuum Mechanics", Prentice-Hall, Inc., Englewood Cliffs, N.J.

Gibbs, H.J. (1963) "Pore Pressure Control and Evaluation for Triaxial Compression", ASMT Symposium on Laboratory Shear Testing of Soils, Special Technical Publication No. 361.

Gibbs, H.J. and C.T. Coffey (1969) "Techniques for Pore Pressure Measurements and Shear Testing of Soil", Proceedings of the Seventh Int. Conf. on Soil Mech. and Fdtn. Eng., Mexico.

Gibson, R.E. (1963) "An Analysis of System Flexibility and its Effect on Time-Lag in Pore-Water Pressure Measurements". Geotechnique, Vol. 13, pp. 1-11.

Gibson, R.E., G.L. England, and M.J.L. Hussey, (1967) "The Theory of One-Dimensional Consolidation of Saturated Clays", Geotechnique 17: 261-273.

Goodrich, F.C. (1969) "The Thermodynamics of Fluid Interfaces", Surface and Colloid Science, Volume I, Wiley-Interscience, Toronto.

Gove, P.B. (Editor) (1967) "Webster's Third New International Dictionary", G. & C. Merrian Co., Springfield, Mass.

Green, A.E. and P.M. Naghdi (1965) "A Dynamical Theory of Interacting Continua", Int. Journ. Eng. Science, Vol. 3, pp. 231-241, Pergamon Press, Great Britian.

Hamilton, J.J., (1963) Volume Changes in Undisturbed Clay Profiles in Western Canada". Canadian Geotechnical Journal, Vol. I, No. 1, pp. 27-42, Sept. NRC 7588.

Hamilton, J.J. (1965) "Shallow Foundations on Swelling Clays in Western Canada". Proceedings International Research and Engineering Conference on E pansive Clay Soils, Texas A & M University, Vol. II, p. 183-207, NRC 9872.

Hamilton, J.J. (1969) "Effects of Environment on the Performance of Shallow Foundations", Canadian Geotechnical Journal, Vol. VI, No. 1, February, NRC 10519.

Harr, M.E. (1966) "Foundations of Theoretical Soil Mechanics", McGraw-Hill Book Co.

Hilf, J.W. (1956) "An Investigation of Pore Water Pressures in Compacted Cohesive Soils", Technical Memorandum 654, U.S. Dept. of Interior, Bureau of Reclamation, Denver, Colorado.

Hodge, P.G., Jr. (1970) "Continuum Mechanics", McGraw-Hill Series in Advanced Engineering.

Hubbert, M.K. and W.W. Rubey (1959) "Role of Fluid Pressure in Mechanics of Overthrust Faulting", Bulletin of the Geol. Soc. of America, February, Vol. 70 pp. 115-166.

Jaunzemis, W. (1967) "Continuum Mechanics", Collier-MacMillan, Toronto, Canada.

Jennings, J.E.B. (1960) "A Revised Effective Stress Law for Use in the Prediction of the Behavior of Unsaturated Soils", Pore Pressure and Suction in Soils, Butterworth, London, 1961.

Jennings, J.E. and J.B. Burland (1962) "Limitations to the Use of Effective Stresses in Partly Saturated Soils", Geotechnique 12:2.

Kohn, P.G. (1965) "Tables of Some Physical and Chemical Properties of Water", S.E.B. Symposia, XIX, The State and Movement of Water in Living Organisms, Cambridge.

Koning, H.L. (1963) Some Observations on the Modulus of Compressibility of Water. Conf. Settlement and Compressibility of Soils, Wiesbaden.

Lambe, T.W. and R.V. Whitman (1969) "Soil Mechanics", John Wiley and Sons, Inc. New York.

Laughton, A.S. (1955) "The Compaction of Ocean Sediments", Ph.D. Thesis, University of Cambridge.

Lee, I.K. (1969) "Soil Mechanics Selected Topics", Butterworths, London.

Li, Wen-Hsiung and Sau-Hai Lam (1964) "Principles of Fluid Mechanics", Addison-Wesley Publishing Co. Inc., Reading, Massachusetts.

Lowe III, J. and T.C. Johnson (1960) "Use of Back Pressure to Increase Degree of Saturation of Triaxial Test Specimens", Research Conf. on Shear Strength of Cohesive Soils, ASCE, Boulder, Colorado.

Lowe III, J., P.F. Zaccheo and H.S. Feldman, (1964) "Consolidation Testing with Back Pressure", Journ. of the Soil Mech. & Fdtn Div., ASCE, Vol. 90, No. SM5, Paper #4058, Sept. pp. 69-86.

Malvern, L.E. (1969) "Introduction to the Mechanics of a Continuous Medium", Prentice-Hall, Series in Engineering of the Physical Sciences. New Jersey.

Matyas, E.L. and H.S. Radhakrishna (1968) "Volume Change Characteristics of Partially Saturated Soils", Geotechnique, Vol. XVIII, No. 4. Dec.

Matijevic, E. (1969) "Surface and Colloid Science", Volume I, Wiley-Interscience, Toronto.

Matveev, L.T. (1967) "Fundamentals of General Meteorology, Physics of the Atmosphere", Translated from Russian. Israel Program for Scientific Translations. Jerusalem.

Metsik, M.S. (1964) "Research in the Field of Surface Forces" II, p. 138, Moscow Nauka Press (In Russian).

M.I.T. (1963) "Engineering Behavior of Partially Saturated Soils", Soil Engineering Division, Massachusetts Institute of Technology, DA Project 1-T-0-21701-A-046-05 with U.S. Army Engineers Waterways Experiment Station, Vicksburg, Mississippi.

Murray. W.D. and F. Landis (1959) "Numerical and Machine Solutions of Transient Heat Conduction Problems Involving Melting and Freezing", Part I, Trans. of the ASME, May.

Neves, E.M.D. (1971) "Influencia das Tensoes Neutras Negativas Nas Caracteristicas Estruturais Dos Solos Compactados" Ministerio das Ofras Publicas, Laboratorio Nacional de Engenharia Civil, Memoria No. 386.

Neville, A.M. and J.B. Kennedy (1966) "Basic Statistical Methods for Engineers and Scientists", International Textbook Co., Scranton, Penn.

Northey, D. and F. Thomas (1965) "Consolidation Test Pore Pressures", Int. Conf. on Soil Mech. and Fdtn Eng., Montreal.

Nur, A. and J.D. Byerlee (1972) "An Exact Effective Stress Law for Elastic Deformation of Rock with Fluids", Journal of Geophysical Research, Sept. Vol. 76, No. 26, pp. 6414 to 6419.

Olson, R.E., and L.J. Langfelder (1959) "Pore Water Pressures in Unsaturated Soils", Proceedings, The American Society of Civil Engineers, Vol. 91, No. SM4, Part 1, pp. 127-150.

Padday, J.F. (1969) "Theory of Surface Tension", Surface and Colloid Science, Volume I, Wiley-Interscience, Toronto.Pa

Parker, H.W. and D.G. Miller (1970) "Operation Manual for Model A Anteus Back Pressure Consolidometers", Revised edition, Internal Report, Geotechnical Ocean Engineering Laboratory, Center for Marine & Environmental Studies, Lehigh University, Bethlehem, Pa.

Perloff, W.H., K. Nair and J.G. Smith (1965) "Effect of Measuring System on Pore Water Pressures in the Consolidation Test", Int. Conf. on Soil Mech. and Fdtn. Eng., Montreal.

Poulos, S.J. (1964) "Control of Leakage in the Triaxial Test", Soil Mechanics Series No. 71 Cambridge, Massachusetts.

Radhakrishna, H.S. (1967) "Compressibility of Partially Saturated Soils", Ph.D. Thesis, University of Waterloo, Canada.

Rendulic, L., (1936) "Relation Between Void Ratio and Effective Principle Stresses for a Remoulded Silty Clay", Proc. 1st. Int. Conf. Soil Mech., 3.

Richards, B.G. (1966) "The Significance of Moisture Flow and Equilibria in Unsaturated Soils in Relation to the Design of Engineering Structures Built on Shallow Foundations in Australia". Symposium on Permeability and Capillarity, American Society for Testing Materials, Atlantic City, New Jersey.

Rodebush, W.H. and A.M. Buswell (1958) Properties of Water Substance, Highway Research Board Spec. Report #40.

Rowe, P.W. and L. Barden (1966) "A New Consolidation Cell", Geotechnique, Vol. 16, No. 2.

Scheidegger, A.E. (1960) "The Physics of Flow Through Porous Media", the MacMillan Co.

Schiffman, R.L. (1970) "The Stress Components of a Porous Medium", Report No. 70-4 Computing Center, University of Colorado, Boulder.

Schofield, R.K. (1935) "The pF of the Water in Soil". Transactions of the Third International Congress of Soil Science, 2.

Schuurman, E. (1966) The Compressibility of an Air/Water Mixture and a Theoretical Relation Between the Air and Water Pressures. Geotechnique, Vol. 16, No. 4.

Scott, R.F. (1963) "Principles of Soil Mechanics", Addison-Wesley Publishing Co. Inc. London.

Scott, R. and Hon-Yim Ko (1969) "Stress-Deformation and Strength Characteristics", State of the Art Report, Seventh Int. Conf. on Soil Mech. and Fdtn Eng.

Shankland, R.S. (1962) (Editor) Handbook of Chemistry and Physics, Case Institute of Technology.

Shortley, G. and D. Williams (1955) "Elements of Physics" Second Edition, Prentice-Hall, Inc. N.J.

Sisler, H.H., C.A. Vander Werf and A.W. Davidson (1953) "General Chemistry - A Systematic Approach", MacMillan Co., New York.

Skempton, A.W. (1954) "The Pore-Pressure Coefficients A and B", Geotechnique 4, 143-147.

Skempton, A.W. (1961) "Effective Stress in Soils, Concrete and Rocks", Pore Pressure and Suction in Soils Conference, London, Butterworths.

Skempton, A.W. and A.W. Bishop (1954) Building Materials, Their Elasticity and Inelasticity. Soils.Chap. 10. North Holland Pub. Co., Amsterdam.

Sokolnikoff, I.S. and R.M. Redheffer (1966) "Mathematics of Physics and Modern Engineering". McGraw-Hill Book Co., Second Edition, London.

Spalding, D.B. and E.H. Cole (1958) "Engineering Thermodynamics", London, Edward Arnold (Publishers) Ltd.

Streeter, V.L. (1961) "Handbook of Fluid Mechanics", McGraw Hill Book Co., Toronto.

Taylor, D.W. (1948) "Fundamentals of Soil Mechanics", J. Wiley and Sons, New York.

Terzaghi, K. (1936) "The Shearing Resistance of Saturated Soils", Proc. First Int. Conf. Soil Mech., Vol. 1.

_____ (1933) "The International Critical Tables" by the National Research Council of U.S.A. Volumes I-VII McGraw-Hill Book Co. Inc., New York.

_____ (1961) "The International Dictionary of Physics and Electronics", D. Van Nostrand Co. Inc., Toronto, Second Edition.

Tiller, F.M. (1953) Chemical Engineering Progress 49, 467.

Truesdell, C. (1966a) The Elements of Continuum Mechanics", Springer-Verlag New York, Inc.

Truesdell, C. (1966b) "Continuum Mechanics I - The Mechanical Foundations of Elasticity and Fluid Dynamics" International Science Review Series #8, Gordon and Breach Science Publishers Inc., New York.

Truesdell, C. and R.A. Toupin (1960) "The Classical Field Theories", Handbuch der Physik, Vol. III/1 (Edited by S. Flugge), Springer-Verlag.

Tuwiner, S.B. (L.P. Miller and W.E. Brown) (1962) "Diffusion and Membrane Technology", American Chemical Society Monograph Series, Reinhold Publishing Corporation, New York.

Westergaard, H.M. (1952) "Theory of Elasticity and Plasticity", Dover Publications, New York.

Whitman, R.V., A.M. Richardson and K.A. Healy (1961) "Time-Lags in Pore Pressure Measurements", Int. Conf. on Soil Mech. and Fdtn Eng. Paris.

Williams, P.J. (1964) "Unfrozen Water Content of Frozen Soils and Soil Moisture Suction", Geotechnique, Volume 14, No. 3.

Wu, T.H. (1966) "Soil Mechanics", Allyn and Bacon, Inc. Boston.

Yalin, M.S. (1971) "Theory of Hydraulic Models", Butterworths.

APPENDIX A

SOIL AND TEST PROGRAM

CONTENTS OF APPENDIX A

		Page
A-1	General	A1
A-2	Field Test Plot	A1
A-3	Classification Data	A10
A-4	Laboratory Test Program	A15

SOIL AND TEST PROGRAM

A-1 General

Appendix A presents a summary of the soil properties and the history of each sample tested during the test program. Each sample generally had several types of tests performed on it. The majority of the data used in this thesis can be broadly categorized as null tests and tests to evaluate various types of processes. The process tests were also used for testing the uniqueness of the constitutive surface. A summary of the reaction test program is also presented; however, the data are not included in the thesis.

Three types of soil were used in the test program. These were a low plasticity soil referred to as Devon silt; the commercial clay mineral kaolin; and a highly plastic soil referred to as Regina clay. Two samples consisting of 80 percent Devon silt and 20 percent kaolin were also tested.

A-2 Field Test Plot

Three test holes were drilled in the northwest section of the City of Regina, Saskatchewan, during the summer of 1970. The test plot plan is shown in Figure A.1. The test logs for holes #10, #11, #12, and #13 are shown on Plates A.2, A.3, A.4 and A.5, respectively. The investigation obtained disturbed samples for a detailed classification of the soil and undisturbed, unsaturated samples for the labo-

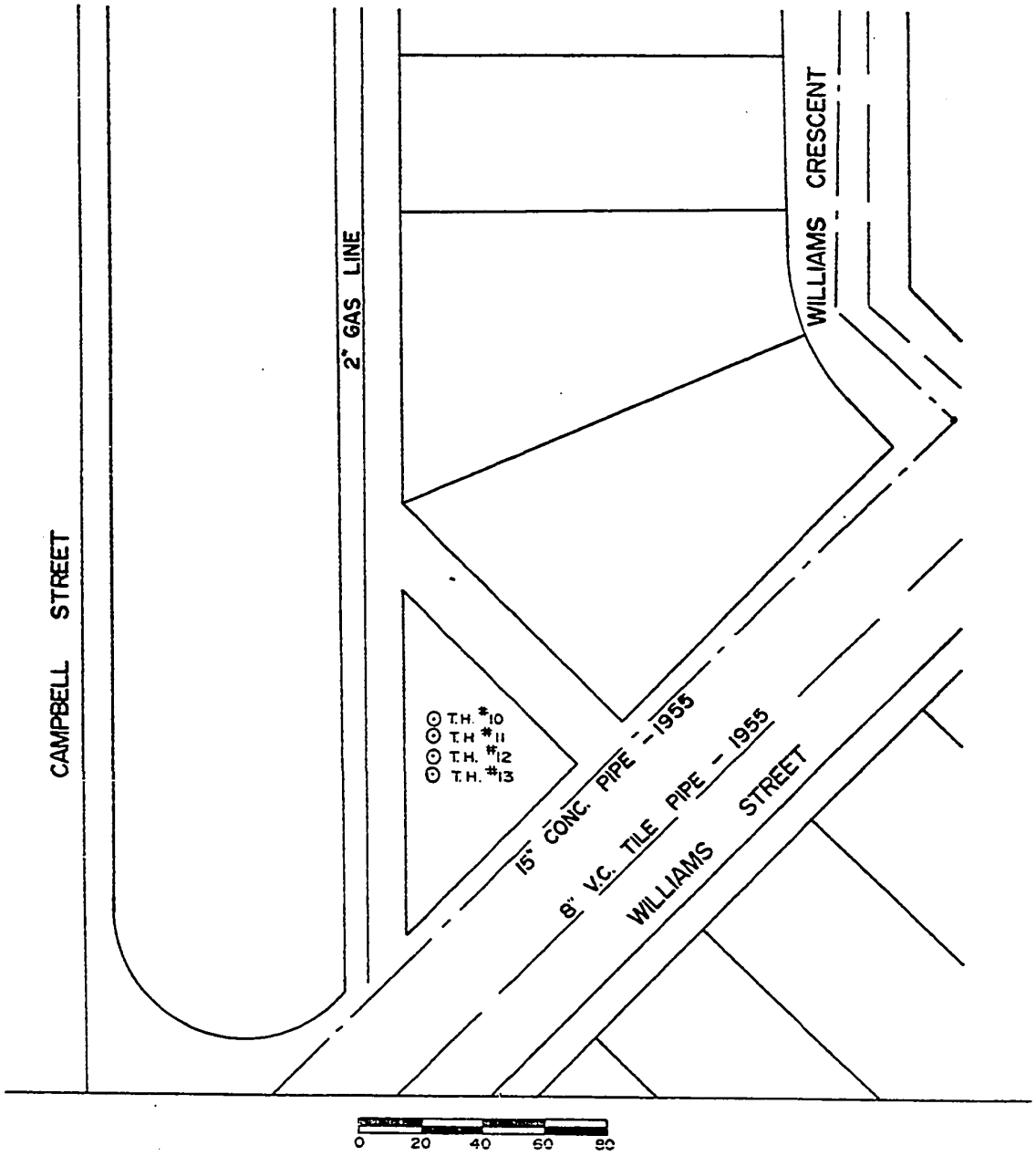
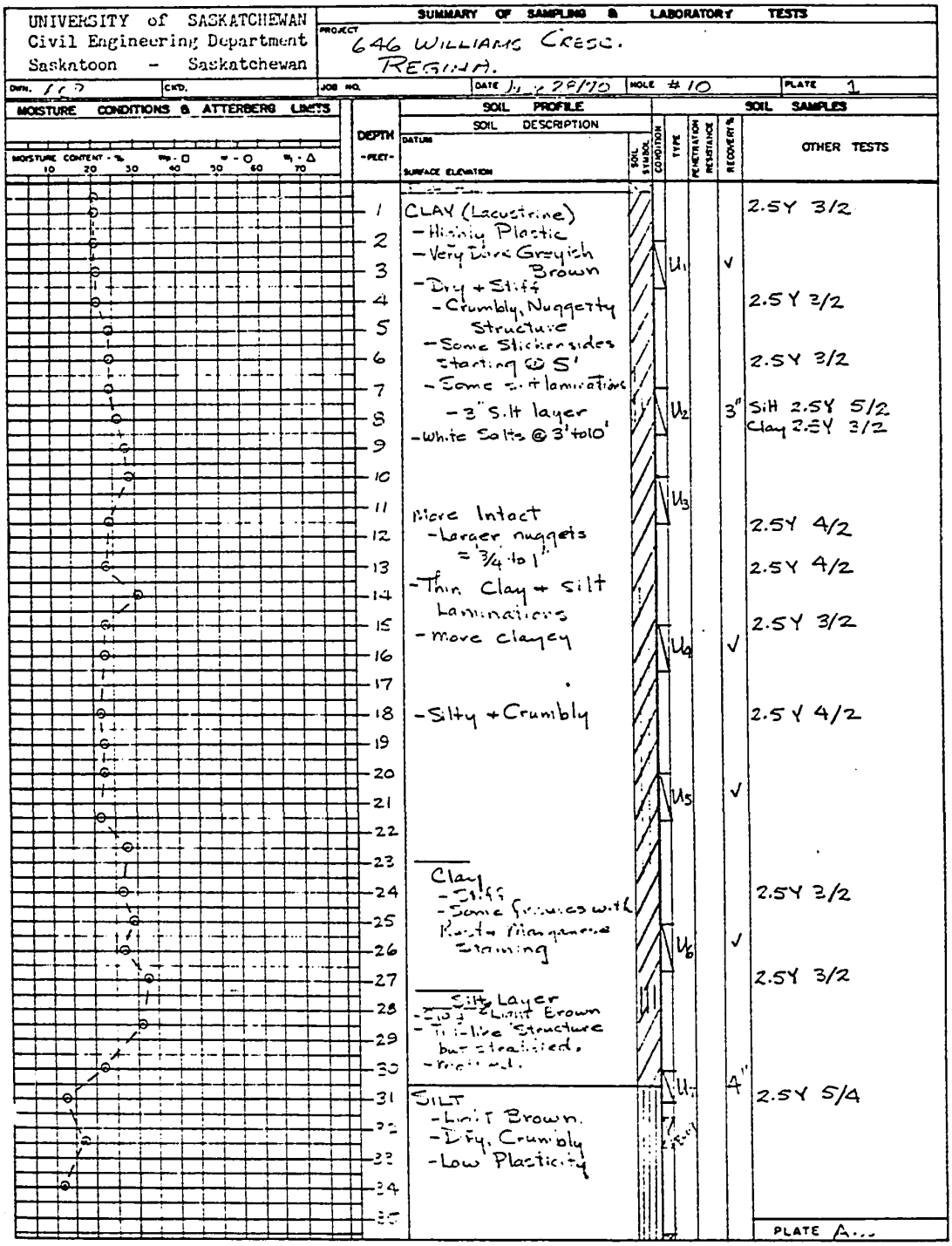


FIGURE A.1 LOCATION OF TEST HOLES AT REGINA TEST PLOT

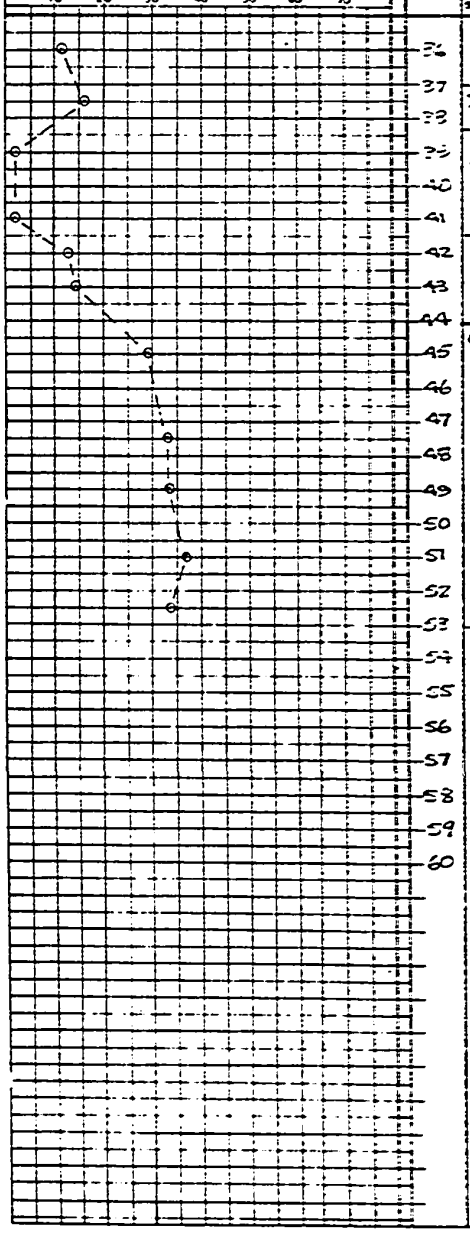

UNIVERSITY of SASKATCHEWAN
Civil Engineering Department
Saskatoon - Saskatchewan
SUMMARY OF SAMPLING & LABORATORY TESTS
PROJECT 646 WILLIAMS CRESC. REGINA.
DWN. I.C.D.
CK'D.
JOB NO.
DATE July 29/70
HOLE # 10
PLATE 1
MOISTURE CONDITIONS & ATTERBERG LIMITS
MOISTURE CONTENT - %
10 20 30 40 50 60 70
DEPTH - FEET -
SOIL PROFILE
SOIL DESCRIPTION
DATUM
SURFACE ELEVATION
SOIL SYMBOL
CONDITION
SOIL SAMPLES
TYPE
PENETRATION RESISTANCE
RECOVERY %
OTHER TESTS
CLAY (Lacustrine)
- Highly Plastic
- Very Dark Greyish Brown
- Dry + Stiff
- Crumbly, Nuggetty Structure
- Some Slickensides starting @ 5'
- Some silt laminations
- 3" Silt layer
- White Salts @ 3' to 10'
More Intact
- Larger nuggets = 3/4 to 1"
- Thin Clay + Silt laminations
- More clayey
- Silty + Crumbly
Clay
- Stiff
- Some fissures with Rusty Manganese staining
Silty Layer
- Light Brown
- Friable Structure but stratified.
SILT
- Light Brown.
- Dry, Crumbly
- Low Plasticity
U1
U2
U3
U4
U5
U6
U7
3"
4"
2.5Y 3/2
2.5Y 3/2
2.5Y 3/2
SiH 2.5Y 5/2
Clay 2.5Y 3/2
2.5Y 4/2
2.5Y 4/2
2.5Y 3/2
2.5Y 4/2
2.5Y 3/2
2.5Y 5/4
PLATE A...

UNIVERSITY of SASKATCHEWAN
Civil Engineering Department
Saskatoon - Saskatchewan

SUMMARY OF SAMPLING & LABORATORY TESTS

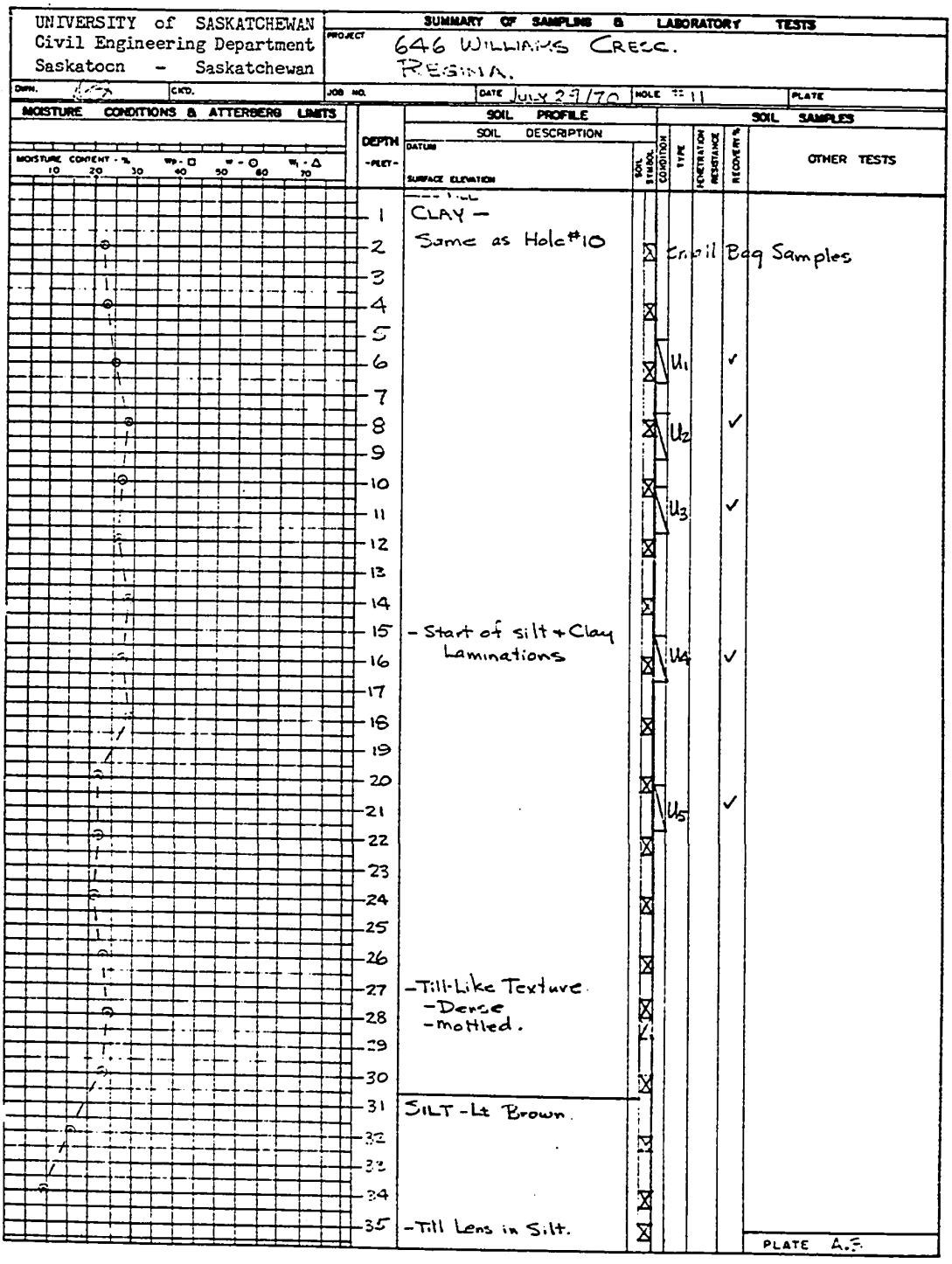
PROJECT: 646 WILLIAMS CRESC. REGINA

DWN. IT/ | CKD. | JOB NO. | DATE JULY 29/70 | HOLE NO. 3 (CONT'D) | PLATE 2



SOIL PROFILE — SOIL DESCRIPTION (DATUM / SURFACE ELEVATION)	SOIL SYMBOL	CONDITION	SOIL SAMPLES — TYPE	PENETRATION RESISTANCE	RECOVERY %	OTHER TESTS
SILT - Light Brown - Dusty						
SANDY CLAY (Till) - Gravel @ Contact - Rust Specks, Soft, Moist						2.5Y 4/2
SAND - Lt. Grey Brown - Med. Grained			Bag			
SANDY CLAY (Till) - Jointed, Rust Staining - Dense, Brown			Bag			2.5Y 3/2
CLAY (Shale) - Black, Highly Plastic. - Intact. - Few hard shale chips in softer matrix.			AM-9 Bag			5Y 2/2
Very Dark Grey			Piez. #1			5Y 3/1
End of Hole - Dry						

PLATE A.2


UNIVERSITY of SASKATCHEWAN
Civil Engineering Department
Saskatoon - Saskatchewan
SUMMARY OF SAMPLING & LABORATORY TESTS
PROJECT 646 WILLIAMS CRESC. REGINA.
DWN.
CKD.
JOB NO.
DATE July 29/70
HOLE # 11
PLATE
MOISTURE CONDITIONS & ATTERBERG LIMITS
MOISTURE CONTENT - %
10 20 30 40 50 60 70
DEPTH - FEET -
SOIL PROFILE
SOIL DESCRIPTION
DATUM
SURFACE ELEVATION
SOIL SYMBOL
CONDITION
SOIL SAMPLES
TYPE
PENETRATION RESISTANCE
RECOVERY %
OTHER TESTS
Fill
CLAY -
Same as Hole #10
Grab Samples
U1
U2
U3
U4
U5
- Start of silt + Clay Laminations
- Till-Like Texture
- Dense
- mottled.
SILT - Lt Brown.
- Till Lens in Silt.
PLATE A.5

UNIVERSITY of SASKATCHEWAN
Civil Engineering Department
Saskatoon - Saskatchewan

SUMMARY OF SAMPLING & LABORATORY TESTS

PROJECT 646 WILLIAMS CRESC. REGINA

DWN. [illegible] CKD. JOB NO. DATE JULY 29/70 HOLE #11 PLATE

MOISTURE CONDITIONS & ATTERBERG LIMITS

MOISTURE CONTENT - % 10 20 30 40 50 60 70 w_p - □ w - ○ w_l - △

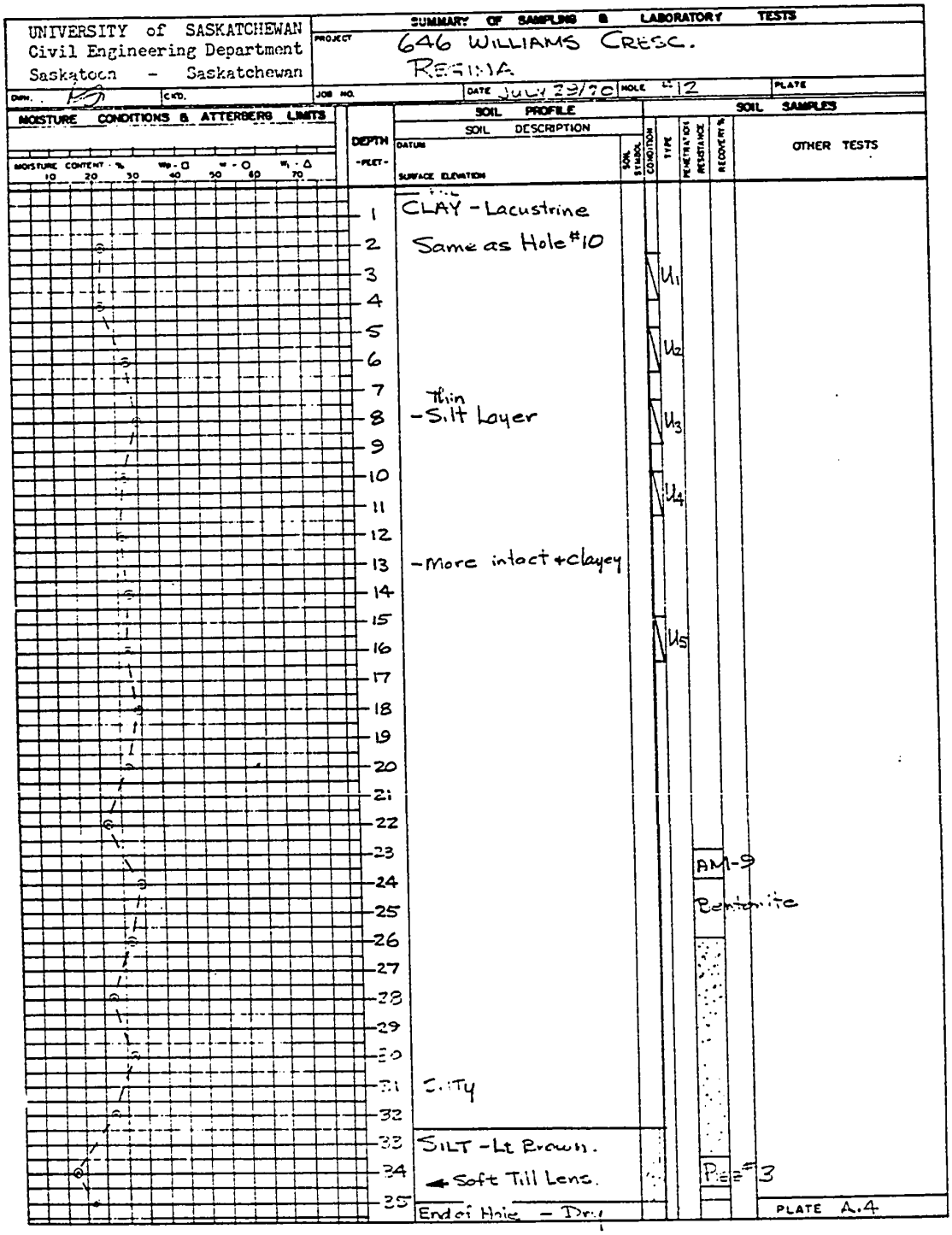
DEPTH - FEET -

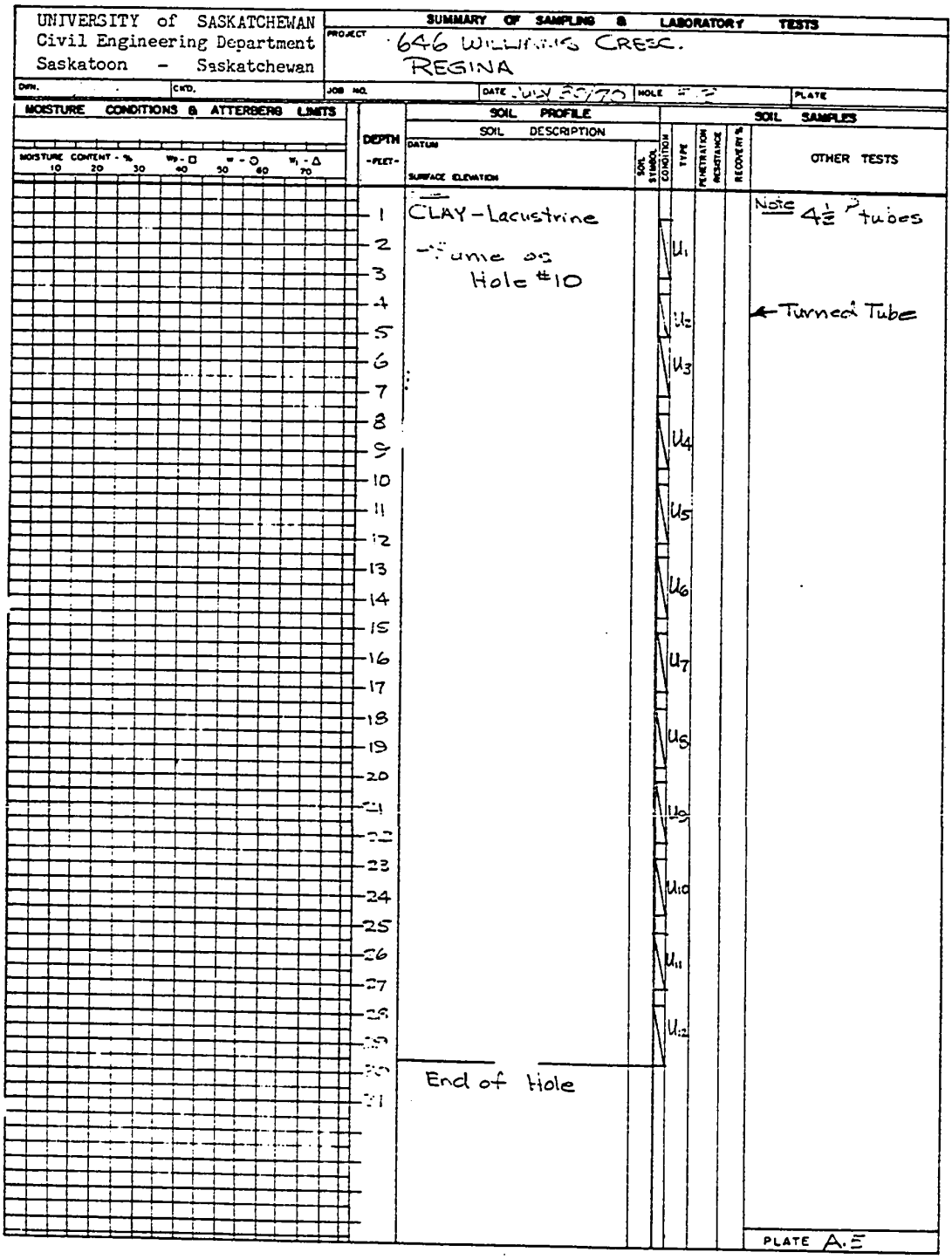
SOIL PROFILE
SOIL DESCRIPTION
DATUM
SURFACE ELEVATION

SOIL SAMPLES
SOIL SYMBOL
CONDITION
TYPE
PENETRATION RESISTANCE
RECOVERY %
OTHER TESTS

DEPTH	SOIL DESCRIPTION	OTHER TESTS
36	SILT - Lt. Brown	
37	Sandy Clay (T.11)	Bentonite
38	← Rock Lag	
39	- Dense	
40	- Jointed, Rust Staining	
41		
42		Piez #2
43	End of Hole	
44	Dry.	

PLATE [illegible]


UNIVERSITY of SASKATCHEWAN
Civil Engineering Department
Saskatoon - Saskatchewan
SUMMARY OF SAMPLING & LABORATORY TESTS
PROJECT 646 WILLIAMS CRESC. REGINA
DWN.
CKD.
JOB NO.
DATE JULY 29/70
HOLE # 12
PLATE
MOISTURE CONDITIONS & ATTERBERG LIMITS
MOISTURE CONTENT - %
10 20 30 40 50 60 70
DEPTH -FEET-
SOIL PROFILE
SOIL DESCRIPTION
DATUM
SURFACE ELEVATION
SOIL SYMBOL
CONDITION
SOIL SAMPLES
TYPE
PENETRATION RESISTANCE
RECOVERY %
OTHER TESTS
CLAY - Lacustrine
Same as Hole #10
Thin
-Silt Layer
-More intact + clayey
Silty
SILT - Lt Brown.
Soft Till Lens.
End of Hole - Dry
U1
U2
U3
U4
U5
AM-9
Bentonite
Pen = 3
PLATE A.4


UNIVERSITY of SASKATCHEWAN
Civil Engineering Department
Saskatoon - Saskatchewan
SUMMARY OF SAMPLING & LABORATORY TESTS
PROJECT 646 WILLIAMS CRESC. REGINA
DWN.
CK'D.
JOB NO.
DATE JULY 29/70
HOLE # 2
PLATE
MOISTURE CONDITIONS & ATTERBERG LIMITS
MOISTURE CONTENT - %
10 20 30 40 50 60 70
Wp - □ w - ○ Wl - △
DEPTH -FEET-
SOIL PROFILE
SOIL DESCRIPTION
DATUM
SURFACE ELEVATION
SOIL SYMBOL
CONDITION
SOIL SAMPLES
TYPE
PENETRATION RESISTANCE
RECOVERY %
OTHER TESTS
CLAY - Lacustrine
- Same as Hole #10
Note 4½" ϕ tubes
← Turned Tube
End of Hole
PLATE A.E

ratory program. Piezometers were installed in the test holes to observe the water conditions. Readings of the piezometers were made by National Research Council personnel on August 17, 1970; May 7, 1971 and June 14, 1971. There was difficulty in pushing the piezometer probe to the bottom of each piezometer. On August 17, 1970, the piezometer probe was stopped at the following depths.

Hole No.	Piezometer No.	Depth
10	1	45'0"
11	2	38'6"
12	3	28'10"

There was no evidence of water in any of the piezometers.

The location of the test plot is directly west of 646 Williams Crescent where the National Research Council has observed vertical ground movements for several years. Additional information on the area of interest can be found in the following research papers:

Hamilton, J.J., (1963) "Volume Changes in Undisturbed Clay Profiles in Western Canada". Can. Geot. Jour., Vol. I, No. 1, pp. 27-42, Sept., NRC 7588.

Hamilton, J.J., (1965) "Shallow Foundations on Swelling Clays in Western Canada", Proc. Int. Res. and Eng. Conf. on Expansive Clay Soils, Texas A & M University, Vol. II, pp. 183-207, NRC 9872.

Hamilton, J.J., (1969) "Effects of Environment on the Performance of Shallow Foundations", Can. Geot. Jour., Vol. VI, No. 1, Feb. NRC 10519.

Pedological soils information and the surficial geology are given in the following reports:

Ellis, J.G., D.F. Acton and J.S. Clayton, (1965) "The Soils of the Regina Map Area" (72-1), University of Saskatchewan, Saskatoon.

Christiansen, E.A. (1961) "Geology and Groundwater Resources of the Regina Area", Report #2, Saskatchewan Research Council, Saskatoon.

A-3 Classification Data

Soils data on the Devon silt are presented in Table A.1.

TABLE A.1

SOILS DATA ON DEVON SILT*

Specific Gravity	2.695
Atterberg Limits	
Liquid Limit	31.0
Plastic Limit	23.0
Shrinkage Limit	22.0
Plastic Index	8.0
Grain Size Analysis	
Percent Clay Sizes	13
Percent Silt Sizes	75
Percent Sand Sizes	12
Coefficient of Permeability	3.8×10^{-5} cm/sec

*The results are the average of 6 trials.

The data for the kaolin are presented in Table A.2

TABLE A.2

CLASSIFICATION DATA ON KAOLIN

Specific Gravity	2.616
Atterberg Limits	
Liquid Limit	64.2
Plastic Limit	34.7
Plastic Index	29.5
Grain Size Analysis	
Percent Clay Sizes	63
Percent Silt Sizes	36
Percent Sand Sizes	1

All the artificially prepared, unsaturated samples tested were kaolin compacted at either full or one-half Standard Proctor compactive effort. The initial water content versus dry density values are plotted in Figure A.6.

Table A.3 summarizes the classification tests performed on the Regina clay samples tested during the laboratory program.

Extensive classification testing was performed on the bag samples from test hole number 11. The results are summarized in Table A.4. The classification data shows consistent results with the highly plastic clay slowly decreasing in plasticity with depth. The natural water contents are presented on the test hole logs. The results show that the natural water contents in the upper zone are approximately five percent below the plastic limit. The soil is in a very dry and

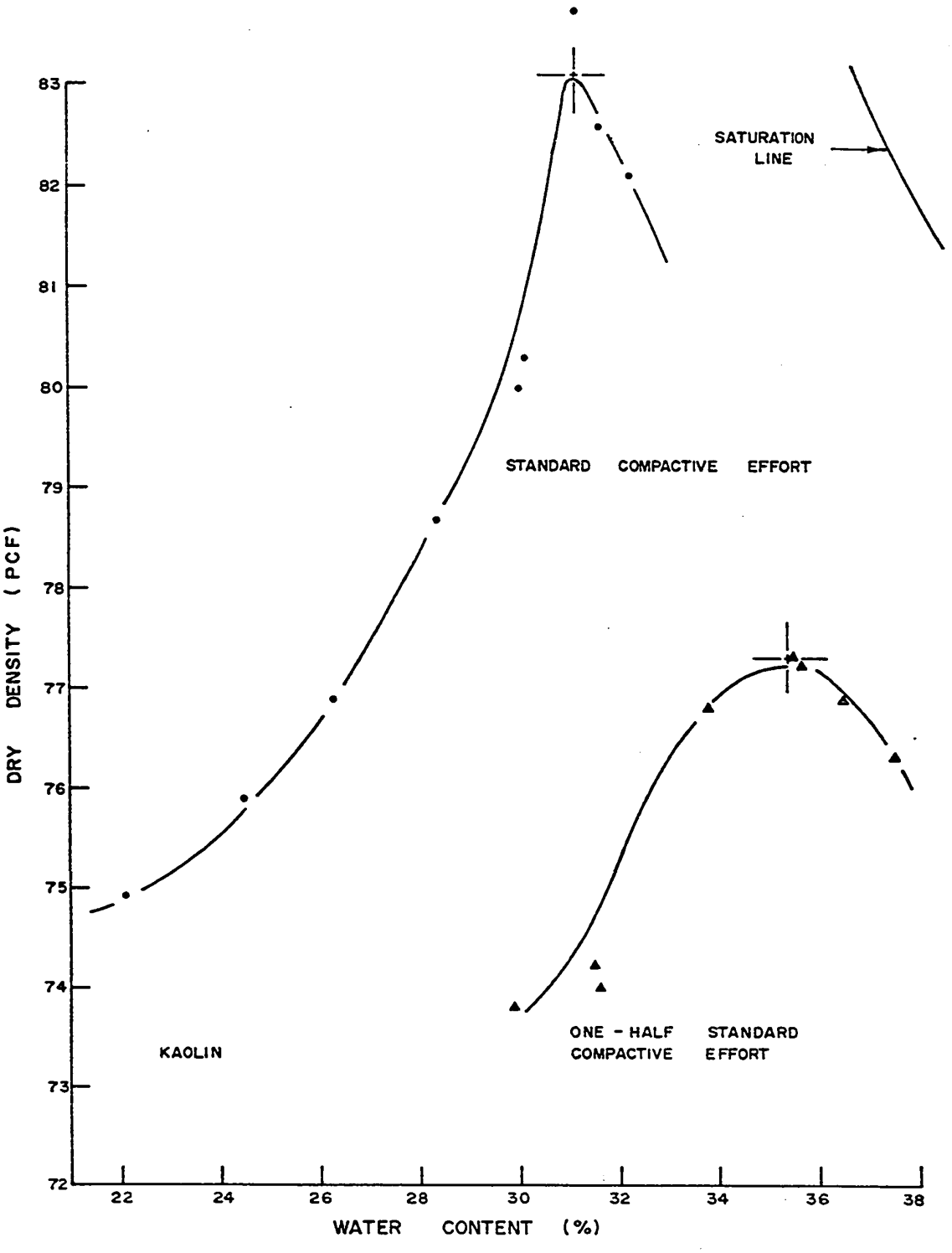


FIGURE A.6 COMPACTION CURVES ON KAOLIN

dense condition with an elaborate secondary structure. The fractures diminish with depth and the soil becomes more moist. The x-ray diffraction tests indicate that the clay is montmorillonite rich.

TABLE A.3

REGINA CLAY CLASSIFICATION DATA

Lab. Sample No.	Hole No.	Field Sample No.	Depth (Feet)	Grain Sizes %			Atterberg Limits	
				Clay	Silt	Sand	Liquid Limit %	Plastic Limit %
15	10	U_1	2.	65	30	5	75.0	26.0
16	13	middle U_6	15.3	55	45	0	77.0	26.8
17	10	U_1	2.	--	--	-	76.3	25.4
18	10	bottom U_1	2.	63	31	6	74.7	25.9
23	12	top U_4	10.11.5	--	--	-	76.4	27.2
24	12	bottom U_4	10-11.5	60	36	4	74.0	25.2
32	13	middle U_4	7.5	67	33	0	74.7	26.0
33	13	U_4	7.5	73	27	0	79.5	27.0
34	13	U_4	7.5	70	30	0	76.1	26.5
35	13	U_4	7.5	67	33	0	75.0	26.0

TABLE A.4

CLASSIFICATION TESTS ON BAG SAMPLES FROM HOLE NO. 11

Sample No.	Depth (Feet)	Grain Sizes (%)			Atterberg Limits			X-ray Diffraction Tests		
		Clay	Silt	Sand	Liquid Limit %	Plastic Limit %	Shrinkage Limit %	Montmorilonite %	Illite %	Kaolinite %
B1	2	62	29	9	80.8	32.3	15.3			
B2	4	62	35	3	77.2	27.0	14.5			
B3	6	76	17	7	88.7	28.0	14.5	55	35	10
B4	8	79	21	0	87.3	29.4	15.0			
B5	10	65	34	1	77.1	29.2	12.9			
B6	12	64	30	6	77.8	28.6	12.4	45	40	15
B7	14	68	32	0	82.6	26.6	11.9			
B8	16	64	36	0	77.4	24.0	11.6			
B9	18	59	39	2	76.2	25.0	11.5	45	40	15
B10	20	49	50	1	57.0	20.1	15.1			
B11	22	50	45	5	65.4	25.5	12.4			
B12	24	45	55	0	60.4	24.0	13.7	50	35	15
B13	26	51	46	3	65.0	22.6	12.3			
B14	27.5				69.8	23.2	10.8			
B15	28	52	47	1	62.0	24.2	12.7			
B16	30	44	49	7	55.2	22.1	13.3	45	45	10
B17	32	34	58	8	41.5	21.0	16.7			
B18	34	25	72	3	29.9	16.1	18.9			
B19	35				37.0	16.3	11.3	45	40	15
B20	39	39	37	24	40.3	17.0	11.1			
B21	40.5	39	38	23	40.6	16.5	11.4			
B22	42	37	36	27	38.7	16.3	10.6	35	45	20

A-4 Laboratory Test Program

Table A.5 summarizes the general data pertinent to each sample tested. The volume weight relations are presented on Table A.6 and the tests performed on each sample are outlined in Table A.7. The laboratory tests performed are subdivided into one of three types. These are:

(i) processes,

(ii) reaction tests and

(iii) null tests.

There is also a category designated "Allowed to Equilize" which means the sample was allowed to remain under prescribed pressures to equilize prior to the next test. The "Process" type of test involves either a volume increase or decrease due to a pressure component change. The volume changes can refer to the total sample and water phase which are measured independently. The "Reaction" tests are a measure of the pore water pressure change as a result of a total and/or air pressure change.

TABLE A.5

SUMMARY OF TEST PROGRAM

Sample No.	Apparatus No.	Soil Type	Starting Date	Date of Completion	Elapsed Time (Min.)	Preparation of the Sample
1	T-1	Devon Silt	Mar. 18/71	Apr. 2/71	21,890	Initially slurried, formed by consolidation to 8 psi.
2	T-1	80% Devon Silt + 20% Kaolin	May 8/71	June 3/71	37,110	Initially slurried, formed by consolidation to 4 psi.
3	OED-179	80% Devon Silt + 20% Kaolin	June 4/71	June 11/71	10,300	Initially slurried, formed by consolidation to 9.6 psi. Trimmed into ring.
4	T-1	Kaolin	June 9/71	June 21/71	17.090	Initially slurried, formed by consolidation to 9 psi.
5	OED-177	Kaolin	June 12/71	June 30/71	25,800	Initially slurried, formed by consolidation to approximately 9 psi. Trimmed from 4" dia. sample.
6	OED-179	Kaolin	June 17/71	July 10/71	23,060	Initially slurried, formed in ring by consolidation to approximately 8 psi.
7	T-1	Kaolin	June 21/71	July 10/71	27,090	Continuation of testing on Sample No. 4.
8	OED-179	Kaolin	---	---	---	Initially slurried, thin desiccated and trimmed. Test unsuccessful due to cavitation of the ceramic disc.
9	T-1	Kaolin	July 15/71	Aug. 9/71	35,900	Compacted sample, Mold #D of compaction test.

TABLE A.5 continued

Sample No.	Apparatus No.	Soil Type	Starting Date	Date of Completion	Elapsed Time (Min.)	Preparation of the Sample
10	OED-177	Kaolin	July 19/71	Aug. 4/71	23,340	Compacted sample, Mold #E of compaction test.
11	OED-179	Kaolin	July 19/71	Aug. 4/71	23,240	Sample was the remainder of Mold #E.
12	OED-177	Kaolin	Sept. 11/71	Sept. 20/71	12,710	Consolidated from a slurry.
13	T-1	Kaolin	Sept. 13/71	Sept. 28/71	21,200	Consolidated from a slurry. Carved a 6 cm dia. hole in center of sample.
14	OED-179	Kaolin	Sept. 14/71	Sept. 27/71	18,960	Consolidated from a slurry. Initially was simulating the sampling process.
15	OED-177	Regina Clay (Natural)	Sept. 21/71	Sept. 22/71	1,430	Hole #10, Depth 2 ft. middle section. (15 Bar-damaged base plate).
15A	OED-177	Regina Clay (Natural)	Sept. 24/71	Nov. 26/71	45,930	Same sample as #15 (15 Bar)
16	T-1	Regina Clay (Natural)	Sept. 28/71	Dec. 17/71	113,750	Four inch dia. Field sample #6 from 15 ft. Bottom of tube.
17	OED-179	Regina Clay (Natural)	Sept. 30/71	Oct. 21/71	30,070	Hole #10, Depth 2 ft. bottom section (15 Bar).
18	Bench-3	Regina Clay (Natural)	---	---	---	Hole #10 at 2 ft. Top portion, dry and crumbly.
19	OED-179	Kaolin	Nov. 18/71	Dec. 2/71	20,090	Mold #C, slightly loose in ring. Full compactive effort.
20	T-2	Kaolin	Nov. 20/71	Dec. 12/71	31,730	Remainder of Mold #C. Full compaction.
21	T-1	Kaolin	Jan. 4/72	Mar. 24/72	117,670	Mold #2H, half compactive effort.

TABLE A.5 continued

Sample No.	Apparatus No.	Soil Type	Starting Date	Date of Completion	Elapsed Time (Min.)	Preparation of the Source
22	T-2	Kaolin	Jan. 5/72	Feb. 3/72	41,890	Half compactive effort (small groove in base).
23	Bench-3	Regina Clay (Natural)	Jan. 14/72	Feb. 9/72	37,830	Bottom portion of tube U_4 at 10-11½ ft. from Hole #12.
24	OED-179	Regina Clay (Natural)	Jan. 25/72	Feb. 1/72	10,180	Sample #12. U_4 at 10-11½ ft. Middle section (cut tube) 15 Bar disc.
25	OED-177	Kaolin	Jan. 25/72	Feb. 3/72	13,090	Soft and wet of optimum (plastic O-ring).
26	OED-177	Kaolin	Feb. 5/72	Feb. 5/72	750	Mold #30F (Full compactive effort).
27	T-2	Kaolin	Feb. 29/72	Mar. 7/72	8,870	w/c approximately 35%, 1/2 compactive effort.
28	OED-177	Kaolin	Mar. 1/72	Mar. 6/72	7,470	1/2 compactive effort, w/c approximately 35%. Iso-octane below the disc.
29	T-2	Kaolin	Mar. 7/72	Mar. 14/72	9,790	Continuation of sample #27, installed a new membrane.
30	OED-177	Kaolin	Mar. 9/72	Mar. 21/72	17,070	Remaining half of mold used for sample #28.
31	T-2	Kaolin	Mar. 14/72	Apr. 5/72	31,600	Continuation of sample #29, installed a composite membrane.
32	T-1	Regina Clay (Natural)	Mar. 27/72	July 1/72	141,170	Four inch dia. sample #4 at 7-1/2 ft. (Top part)
33	OED-177	Regina Clay (Natural)	Mar. 28/72	June 23/72	126,680	Sample #4 at 7-1/2 ft., second sample from top.
34	OED-179	Regina Clay (Natural)	Mar. 29/72	June 23/72	125,280	Sample #4 at 7-1/2 ft., third sample from top.
35	T-2	Regina Clay (Natural)	Apr. 6/72	July 1/72	122,220	Sample #4 at 7-1/2 ft., fourth from the top.

TABLE A.6

SUMMARY OF VOLUME-WEIGHT RELATIONS

Sample No.	Initial Conditions					Final Conditions			Measured Changes		
	Water Content		Wt. of Dry Soil (Gms)	Height (cm)	Diameter (cm)	Water Content (%)	Height (cm)	Diameter (cm)	Water Vol. Change (cc)	Height Change (cm)	Diameter Change (cm)
	Trimmings	Whole Sample									
1	--	--	1120.40	--	--	16.86	9.380	9.548	+ 91.81	+ 0.226	+ 0.103
2	54.33	--	791.70	9.045	10.200	24.29	8.20	8.638	+ 31.15	+ 0.394	+ 0.141
3	--	--	119.48	--	6.350	27.50	2.445	6.350	+ 4.50	+ 0.142	0.000
4	59.46	--	506.00	6.026	10.160	--	--	--	+ 53.93	+ 0.397	+ 0.286
5	66.05	--	82.23	2.734	6.350	41.42	2.183	6.223	+ 19.65	+ 0.550	+ 0.104
6	64.04	--	76.03	2.633	6.350	48.86	2.114	6.292	+ 36.14	+ 0.522	0.000
7	--	--	506.00	--	--	43.81	5.866	9.538	+ 38.36	+ 0.263	+ 0.190
9	--	27.79	1198.10	11.733	10.169	36.28	12.200	10.060	-103.65	- 0.058	+ 0.105
10	32.04	31.74	112.29	2.515	6.346	31.90	2.569	6.346	+ 0.78	- 0.004	0.000
11	32.72	31.82	111.19	2.492	6.346	32.62	2.549	6.346	- 0.63	- 0.011	0.000
12	--	50.50	65.66	1.80	6.350	44.75	1.813	6.239	+ 0.82	+ 0.075	0.000
13	51.99	53.00	246.63	3.282	10.215	45.69	2.878	9.949	+ 14.63	+ 0.094	+ 0.205
14	--	61.38	79.26	2.470	6.350	46.32	2.194	6.248	+ 8.36	+ 0.357	0.000
15	--	18.05	128.98	1.905	6.350	--	--	6.350	- 0.013	0.000	0.000
15A	--	20.05	126.97	2.550	6.350	24.38	2.616	6.350	- 5.05	- 0.046	0.000
16	25.00	26.24	1245.76	10.043	10.288	28.09	10.131	10.281	- 28.11	- 0.088	+ 0.060
17	--	20.47	132.92	2.555	6.350	24.03	2.671	6.350	- 4.73	- 0.081	0.000
18	--	21.38	129.19	2.744	6.350	30.60	2.747	6.350	--	+ 0.022	0.000
19	--	25.40	89.00	2.273	6.350	31.00	2.231	6.350	- 10.13	+ 0.056	0.000
20	--	25.10	592.24	5.827	10.177	32.19	5.820	10.040	- 47.04	+ 0.081	+ 0.550
21	--	32.03	1174.38	11.740	10.160	33.40	11.672	9.874	- 8.69	- 0.001	+ 0.040
						Top=33.55 Middle=33.66 Bottom=33.60					
22	34.00	35.28	646.16	6.347	10.160	33.86	6.277	10.032	- 4.11	+ 0.097	+ 0.081
23	26.56	26.32	123.55	2.540	6.350	33.67	2.759	6.350	--	- 0.181	0.000
24	24.95	25.10	140.67	2.946	6.350	25.31	2.969	6.350	+ 0.311	- 0.012	0.000
25	36.12	36.14	130.34	3.172	6.350	36.12	3.205	6.350	- 0.50	+ 0.026	0.000
26	29.73	29.73	107.50	2.553	6.350	--	--	--	0.0	+ 0.020	0.000
27	35.19	35.15	643.99	6.374	10.160	--	--	--	- 8.54	+ 0.016	+ 0.024
28	35.04	34.98	76.14	1.921	6.350	32.78	1.901	6.350	0.0	+ 0.042	0.000
29	--	--	643.99	--	--	--	--	--	- 0.241	- 0.011	0.000
30	35.00	35.46	103.01	2.556	6.350	35.11	2.517	6.300	- 0.014	+ 0.033	+ 0.050
31	--	--	643.99	--	--	34.13	6.293	10.047	+ 0.021	- 0.009	+ 0.003
32	27.38	29.42	578.29	5.057	10.241	33.37	5.178	10.296	- 19.57	- 0.199	- 0.124
33	27.76	28.94	82.84	1.906	6.350	33.24	1.894	6.350	- 3.19	+ 0.026	0.000
34	26.87	26.54	95.75	2.216	6.350	31.89	2.235	6.350	- 6.32	- 0.040	0.000
35	27.50	--	567.78	5.089	10.218	32.55	5.118	10.226	- 23.32	- 0.057	+ 0.075

TABLE A.7

CHRONOLOGY OF TESTING

Sample No. 1 Apparatus No. T-1 Soil Type Devon Silt

Starting Date	Starting Time	Immediately Following A Pressure Change			Type of Test			
		Total Pressure (psi)	Air Pressure (psi)	Water Pressure (psi)	Process	Reaction	Null	Allowed to Equilize
Mar. 18/71	9:20	11.4	--	0.0				x
Mar. 18/71	9:37	20.6	--			x		
Mar. 18/71	10:35	11.4	--			x		
Mar. 18/71	13:35	11.4	--	7.2				x
Mar. 18/71	16:27	21.4	--					
Mar. 19/71	9:00	11.4	--			x		
Mar. 19/71	13:50	11.4	--	0.0				x
Mar. 20/71	11:05	12.5	--	4.5			x	
Mar. 20/71	11:20	13.4	--	5.6			x	
Mar. 20/71	11:30	14.4	--	6.7			x	
Mar. 20/71	11:40	15.5	--	7.8			x	
Mar. 20/71	11.50	16.4	--	8.8			x	
Mar. 20/71	13.30	17.4	--	9.9			x	
Mar. 20/71	13:40	18.4	--	11.0			x	
Mar. 20/71	13:50	19.4	--	12.0			x	
Mar. 20/71	14:00	20.5	--	13.1			x	
Mar. 20/71	14:14	21.4	--	14.2			x	
Mar. 21/71	15:35	31.4	--			x		
Mar. 21/71	15:44	21.5	--			x		
Mar. 21/71	16:00	21.5	--	14.3				x
Mar. 21/71	16:10	26.5	--	19.6			x	
Mar. 21/71	16:15	31.5	--	25.0			x	
Mar. 22/71	9:00	41.4	--			x		
Mar. 22/71	13:36	31.4	--			x		

TABLE A.7 continued

Starting Date	Starting Time	Immediately Following a Pressure Change			Type of Test			
		Total Pressure (psi)	Air Pressure (psi)	Water Pressure (psi)	Process	Reaction	Null	Allowed to Equilize
Mar. 22/71	15:40	51.5	--	46.5				x
Mar. 23/71	9:20	61.4	--			x		
Mar. 23/71	11:30	51.5	--	42.1				x
Mar. 23/71	19:10	61.6	--	41.7	x			
Mar. 24/71	9:16	71.5	--			x		
Mar. 24/71	13:30	61.5	--			x		
Mar. 24/71	15:47	61.5	--	41.9				x
Mar. 24/71	19:45	81.4	--	42.2	x			
Mar. 26/71	19:30	71.5	--	31.9			x	
Mar. 26/71	19:40	51.5	--	11.9			x	
Mar. 26/71	19:45	41.4	--	1.9			x	
Mar. 27/71	12:40	41.7	--	11.9		Permeability Test		
Mar. 29/71	9:00	61.4	--			x		
Mar. 29/71	14:05	41.4	--	1.9				x
Mar. 30/71	8:55	41.3	7.4	1.8				x
Mar. 31/71	8:45	41.4	12.8	1.9	x			
Mar. 31/71	12:33	41.5	18.1	1.9	x			
Apr. 2/71	9:00	41.3	23.5	2.2	x			
Apr. 2/71	14:00	41.3	0.3	1.9				x
Apr. 2/71	14:05	End of Test						
Sample No. 2		Apparatus No. T-1		Soil Type	80% Devon Silt & 20% Kaolin			
		9.5	--	1.7				x
May 8/71	14:00	14.5	--			x		
May 8/71	14:37	14.6	--	6.8				x
May 10/71	9:04	19.6	--			x		
May 10/71	11:05	19.6	--	11.8				x

TABLE A.7 continued

Starting Date	Starting Time	Immediately Following a Pressure Change			Type of Test			
		Total Pressure (psi)	Air Pressure (psi)	Water Pressure (psi)	Process	Reaction	Null	Allowed to Equilize
May 11/71	9:16	29.6	--			x		
May 11/71	11:45	29.6	--	21.8				x
May 14/71	9:00	39.6	--	31.8			x	
May 18/71	10:10	59.6	--			x		
May 18/71	13:00	59.6	--	51.8				x
May 19/71	8:30	69.6	--	51.8	x			
May 25/71	9:40	74.5	--				x	
May 25/71	10:40	79.6	--			x		
May 25/71	11:30	84.6	--			x		
May 25/71	12:30	89.6	--				x	
May 25/71	13:30	94.6	--				x	
May 25/71	14:35	99.7	--				x	
May 25/71	15:40	104.7	--				x	
May 25/71	16:00	99.7	--				x	
May 25/71	16:33	94.6	--				x	
May 25/71	20:00	89.6	--				x	
May 25/71	20:35	89.6	--	51.8	x			
June 1/71	13:30	69.6	--	31.8				x
June 2/71	20:00	44.5	--	6.8				x
June 2/71	End of Test							
Sample No. 3	Apparatus No. OED-179			Soil Type 80% Devon Silt + 20% Kaolin				
June 4/71	12:45	0.2	--	--				x
June 4/71	13:26	17.5	--	10.2				x
June 5/71	9:15	27.4	--	20.1			x	
June 5/71	10:15	37.2	--	29.9			x	
June 5/71	11:55	47.1	--	39.8			x	
June 5/71	11:57	57.3	--	50.0			x	

TABLE A.7 continued

Starting Date	Starting Time	Immediately Following a Pressure Change			Type of Test			
		Total Pressure (psi)	Air Pressure (psi)	Water Pressure (psi)	Process	Reaction	Null	Allowed to Equilize
June 5/71	13:45	63.9	--	50.0	x			
June 10/71	12:21	73.9	--	60.0			x	
June 10/71	15:30	83.7	--	69.8			x	
June 11/71	8:50	73.9	--	60.0			x	
June 11/71	9:20	63.9	--	50.0			x	
June 11/71	10:30	53.7	--	39.8			x	
June 11/71	11:35	43.9	--	29.9			x	
June 11/71	12:40	34.0	--	20.1				
June 11/71	14:30	24.1	--	10.2				
June 11/71	15:35	14.2	--	0.2				
June 11/71	16:20	End of Test						
Sample No. 4		Apparatus No. T-1		Soil Type Kaolin				
June 9/71	14:15	15.7	--	5.7				x
June 14/71	13:30	25.7	--	15.7			x	
June 15/71	13:00	35.8	--	25.7			x	
June 16/71	8:45	45.8	--	35.7			x	
June 17/71	9:25	55.8	--			x		
June 17/71	10:40	55.8	--	45.7				x
June 18/71	9:30	65.8	--	45.7	x			
June 21/71	11:00	End of Test						

TABLE A.7 continued

Starting Date	Starting Time	Immediately Following a Pressure Change: Total Pressure (psi)	Air Pressure (psi)	Water Pressure (psi)	Type of Test: Process	Reaction	Null	Allowed to Equilize
Sample No. 5	Apparatus No. OED-177	Soil Type Kaolin						
June 12/71	11:00	17.6	10.14	0.0				x
June 14/71	16:15	27.5	20.0	11.6				x
June 17/71	15:30	37.5	30.0	9.9	x			
June 21/71	11:00	47.5	40.0	9.9	x			
June 24/71	9:47	57.3	50.0	9.8	x			
June 25/71	9:10	67.4	59.9	9.7	x			
June 28/71	9:25	77.6	70.0	9.8	x			
June 28/71	16:40	Air started passing through the base						
June 30/71	9:05	End of Test.						
Sample No. 6	Apparatus No. OED-179	Soil Type Kaolin						
June 17/71	15:00	27.4	20.1	9.9				x
June 21/71	13:20	46.8	29.8	18.6	x			
June 24/71	9:30	56.4	39.3	30.1			x	
June 25/71	9:21	66.7	49.5	40.2			x	
June 28/71	10:51	56.5	39.3	30.3			x	
June 30/71	8:55	66.6	49.5	40.4			x	
July 5/71	11:05	76.3	59.2	50.2			x	
July 7/71	9:25	86.3	69.2			x		
July 7/71	14:10	76.5	59.2			x		
July 7/71	14:27	76.5	59.2	50.4				x
July 10.71	9:50	End of Test						

TABLE A.7 continued

Starting Date	Starting Time	Immediately Following a Pressure Change: Total Pressure (psi)	Air Pressure (psi)	Water Pressure (psi)	Type of Test: Process	Reaction	Null	Allowed to Equilize
Aug. 4/71	9:30	81.6	61.0	59.7				
Aug. 4/71	10:38	Flushed out the base						
Aug. 9/71	9:45	End of Test			x			
Sample No. 10		Apparatus No. OED-177		Soil Type Kaolin				
July 19/71	9:40	52.1	39.3	0.6				
July 21/71	9:15	72.0	59.1	22.4				x
		Mistake in calibration curve					x	
July 21/71	11:45	72.0	59.1	20.6				
July 22/71	10:25	81.9	69.0	30.8			x	
July 23/71	13:45	91.9	79.0				x	
July 23/71	15:45	81.9	69.0			x		
July 23/71	16:45	81.9	69.0	30.4		x		
July 26/71	9:20	91.9	79.0				x	
July 28/71	10:45	101.8	89.0			x		
July 29/71	10:40	101.8	89.0	72.6		x		
July 30.71	9:42	72.0	59.2	42.3				x
Aug. 2/71	10:24	85.6	59.3	42.6			x	
Aug. 3/71	10:00	85.5	59.3	52.5	x	x		

TABLE A.7 continued

Starting Date	Starting Time	Immediately Following a Pressure Change			Type of T st			
		Total Pressure (psi)	Air Pressure (psi)	Water Pressure (psi)	Process	Reaction	Null	Allowed to Equilize
Sample No. 11		Apparatus No. OED-179		Soil Type Kaolin				
July 19/71	11:08	47.1	39.8	0.5				x
		Attempting to Null in on the suction						
July 19/71	14:11	34.0	20.1	0.5				x
July 21/71	8:40	34.2	20.1	14.6	x			
July 26/71	9:39	44.0	30.0	26.2			x	
July 27/71	16:30	44.0	30.0			x		
		Check on stability of water pressure						
July 28/71	9:40	53.9	40.0			x		
July 29/71	9:33	53.8	39.9	26.2				x
July 30.71	9:25	34.0	20.0	5.9			x	
Aug. 2/71	10:15	47.8	20.1	6.3	x			
Aug. 3/71	9:08	47.8	20.1	16.0	x			
Sample No. 12		Apparatus No. OED-177		Soil Type Kaolin				
Sept. 11/71	15:22	17.5	10.0	1.0				x
Sept. 14/71	8:30	27.5	20.0			x		
Sept. 15/71	9:00	37.5	30.0			x		
Sept. 16/71	8:37	47.5	40.0			x		
Sept. 18/71	10:54	57.5	50.0			x		
Sept. 20/71	11:10	Test stopped						

TABLE A.7 continued

Starting Date	Starting Time	Immediately Following a Pressure Change			Type of Test			
		Total Pressure (psi)	Air Pressure (psi)	Water Pressure (psi)	Process	Reaction	Null	Allowed to Equilize
Sample No. 13		Apparatus No. T-1		Soil Type Kaolin				
Sept. 13/71	14:35	41.3	30.0	11.3				x
Sept. 16/71	9:30	51.6	40.4	21.7			x	
Sept. 17/71	9:21	61.3	50.2			x		
Sept. 18/71	9:23	71.1	60.1			x		
Sept. 20/71	10:54	81.3	60.4			x		
Sept. 21/71	8:45	81.3	70.4			x		
Sept. 22/71	10:35	91.1	70.3			x		
Sept. 24/71	9:00	90.8	80.1			x		
Sept. 25/71	9:45	100.9	80.1			x		
Sept. 27/71	9:24	100.9	90.3			x		
Sept. 28/71	8:00	End of Test						
Sample No. 14		Apparatus No. OED-179		Soil Type Kaolin				
Sept. 14/71	9:17	47.7	20.0	17.5				x
Sept. 14/71	9:23	39.1	20.0	17.5				x
Sept. 14/71	9:30	42.8	20.0	17.5				x
Sept. 16/71	9:05	52.9	30.0	27.7			x	
Sept. 17/71	8:45	62.9	40.0			x		
Sept. 18/71	9:02	72.9	50.0			x		
Sept. 20/71	9:45	73.4	60.0			x		
Sept. 22/71	11:11	82.8	60.0			x		
Sept. 24/71	9:23	92.6	60.0			x		
Sept. 25/71	10:02	92.7	70.0			x		
Sept. 27/71	8:30	102.7	70.0			x		
Sept. 27/71	13:15	End of Test						

TABLE A.7 continued

Starting Date	Starting Time	Immediately Following a Pressure Change			Type of Test			
		Total Pressure (psi)	Air Pressure (psi)	Water Pressure (psi)	Process	Reaction	Null	Allowed to Equilize
Sample No. 15		Apparatus No. OED-177		Soil Type Regina Clay				
Sept. 21/71	11:35	4.2	0.0	1.2				
Sept. 21/71	12:22	47.5	40.0	0.8				x
Sept. 21/71	13:31	114.2	100.0	0.8				x
Sept. 22/71	9:11	104.2	90.0	40.0				x
Sept. 22/71	10:53	104.2	90.0					x
Sept. 22/71	11:30	End of Test						x
		Removed sample to check base for contact						
		Broke the porous base plate						
Sample No. 15A		Apparatus No. OED-177		Soil Type Regina Clay				
Sept. 24/71	11:01	37.7	10.0	0.8				x
		Increased air pressure in increments						
Sept. 30/71	21:08	77.8	50.0	1.0				x
Oct. 4/71	9:35	77.7	50.0	11.8	x			
Oct. 7/71	9:00	78.0	40.2	12.2	x			
Oct. 8/71	8:40	67.9	40.2	12.1	x			
Oct. 12/71	8:54	67.7	40.2	22.1	x			
Oct. 19/71	8:37	67.9	30.2	22.0	x			
Oct. 22/71	9:42	57.9	30.2	22.2	x			
Oct. 26/71	8:30	End of Test						

TABLE A.7 continued

Starting Date	Starting Time	Immediately Following a Pressure Change			Type of Test			
		Total Pressure (psi)	Air Pressure (psi)	Water Pressure (psi)	Process	Reaction	Null	Allowed to Equilize
Sample No. 16		Apparatus No. T-1		Soil Type Regina Clay				
Sept. 28/71	11:35	71.5	50.2	3.7				x
Oct. 4/71	10:35	71.5	50.2	13.7	x			
Oct. 12/71	9:26	71.4	40.1	13.6	x			
Oct. 20/71	9:30	61.3	40.0	13.5	x			
Nov. 1/71	9:56	61.1	39.7	23.2	x			
Nov. 12/71	9:40	61.3	29.9	23.3	x			
Nov. 26/71	9:15	51.4	30.1	23.4	x			
Dec. 7/71	9:10	41.7	30.3	23.5	x			
Sample No. 17		Apparatus No. OED-179		Soil Type Regina Clay				
Sept. 30/71	11:45	27.7	0.0	1.4				x
		Increased the air pressure in increments						
Oct. 5/71	15.31	77.7	50.0	1.4				x
Oct. 8/71	8:22	77.7	50.0	11.5	x			
Oct. 12/71	8:35	77.8	40.0	11.5	x			
Oct. 14/71	9:40	67.8	40.0	11.5	x			
Oct. 18/71	9:30	67.8	40.0	21.4	x			
Oct. 21/71	8:50	End of Test						

TABLE A.7 continued

Starting Date	Starting Time	Immediately Following a Pressure Change			Type of Test			
		Total Pressure (psi)	Air Pressure (psi)	Water Pressure (psi)	Process	Reaction	Null	Allowed to Equilize
Sample No. 19		Apparatus No. OED-179		Soil Type Kaolin				
Nov. 18/71	10:56	87.7	59.9	0.8				x
Nov. 20/71	9:42	87.7	59.9	30.8	x			
Nov. 22/71	14:30	87.7	60.0	46.4	x			
Nov. 26/71	9:36	87.8	60.0	31.3	x			
Nov. 29/71	9:20	87.7	60.0	1.5	x			
Dec. 1/71	11:07	87.7	59.9	1.3				x
Dec. 2/71	9:45	End of Test						
Sample No. 20		Apparatus No. T-2		Soil Type Kaolin				
Nov. 20/71	14:12	78.9	57.8	6.1				x
Nov. 23/71	14:43	69.1	57.9	6.2	x			
Nov. 26/71	10:45	68.9	9.8	6.1	x			
Nov. 30/71	10:45	69.2	15.1	6.1	x			
Dec. 2/71	8:36	69.1	29.7	6.3	x			
Dec. 6/71	9:02	69.2	57.7	6.2	x			
Dec. 8/71	9:26	88.7	77.1	24.6			x	
Dec. 10/71	10:30	88.7	77.2	53.4	x			
Dec. 12/71	15:00	End of Test						

TABLE A.7 continued

Starting Date	Starting Time	Immediately Following a Pressure Change			Type of Test			
		Total Pressure (psi)	Air Pressure (psi)	Water Pressure (psi)	Process	Reaction	Null	Allowed to Equilize
Sample No. 21		Apparatus No. T-1		Soil Type Kaolin				
Jan. 4/72	16:24	82.0	61.2	4.4				x
Jan. 13/72	9:01	72.0	61.2	4.4	x			
Jan. 17/72	10:57	72.0	50.9	4.1	x			
Jan. 18/72	9:20	72.1	51.1	14.2	x			
Jan. 19/72	8:44	62.0	51.0	14.2	x			
Jan. 24/72	9:30	62.4	41.2	14.2	x			
Jan. 26/72	9:02	62.6	41.6	24.5	x			
Jan. 29/72	10:00	52.4	41.3	24.1	x			
Feb. 2/72	10:32	52.5	31.2	23.8	x			
Feb. 7/72	9:47	52.5	31.1	28.8	x			
Feb. 15/72	9:17	42.1	30.9	28.4	x			
Feb. 21/72	9:23	52.4	31.5	28.9	x			
Feb. 24/72	11:00	52.1	31.1	23.6	x			
Mar. 3/72	9:20	81.4	31.1	23.7	x			
Mar. 9/72	8:54	81.4	61.3	23.9	x			
Mar. 16/72	9:00	81.1	61.2	53.7	x			
Mar. 24/72	9:35	End of Test						

TABLE A.7 continued

Starting Date	Starting Time	Immediately Following a Pressure Change			Type of Test			
		Total Pressure (psi)	Air Pressure (psi)	Water Pressure (psi)	Process	Reaction	Null	Allowed to Equilize
Sample No. 22		Apparatus No. T-2		Soil Type Kaolin				
Jan. 5/72	13:50	39.8	29.3	3.3				x
Jan. 11/72	10:27	49.7	39.2	13.3			x	
Jan. 17/72	9:25	59.7	49.1	23.2			x	
		Leak on air connection on cap						
Jan. 18/72	8:52	59.7	48.8	23.3				x
Feb. 1/72	10:30	69.7	59.1	33.2			x	
Feb. 2/72	9:42	79.7	69.1	43.2			x	
Feb. 3/72	9:05	89.7	79.1	53.2			x	
Feb. 3/72	16:00	End of Test						
Sample No. 23		Apparatus No. Bench #3		Soil Type Regina Clay				
Sample No. 24		Apparatus No. OED-179		Soil Type Regina Clay				
Jan. 25/72	11:20	34.3	20.3	0.9				x
Jan. 25/72	11:27	Closed valves						
Feb. 1/72	13:05	End of Test						

TABLE A.7 continued

Starting Date	Starting Time	Immediately Following a Pressure Change			Type of Test			
		Total Pressure (psi)	Air Pressure (psi)	Water Pressure (psi)	Process	Reaction	Null	Allowed to Equilize
Sample No. 25	Apparatus No. OED-177			Soil Type Kaolin				
Jan. 25/72	13:36	17.9	10.4	1.8				x
Feb. 2/72	11:30	28.0	20.5	11.9			x	
Feb. 3/72	9:3]	38.1	30.6	22.0			x	
Feb. 3/72	15:45	End of Test						
Sample No. 26	Apparatus No. OED-177			Soil Type Kaolin				
Feb. 5/72	10:30	23.8	9.7	3.8				x
		Attempted to Null out the pore pressure at the base						
Feb. 5/72	23:00	End of Test						
Sample No. 27	Apparatus No. T-2			Soil Type Kaolin				
Feb. 29/72	9:40	39.6	29.3	10.6				x
Mar. 3/72	9:50	49.6	39.3	20.6			x	
Mar. 7/72	13:25	End of Test						
		Water was going through the membrane						

TABLE A.7 continued

Starting Date	Starting Time	Immediately Following a Pressure Change			Type of Test			
		Total Pressure (psi)	Air Pressure (psi)	Water Pressure (psi)	Process	Reaction	Null	Allowed to Equilize
Sample No. 28		Apparatus No. OED-177		Soil Type Kaolin				
Mar. 1/72	10:53	17.3	9.8	0.9				x
Mar. 3/72	10:53	27.2	19.7			x		
Mar. 4/72	9:33	37.1	29.6			x		
Mar. 4/72	9:56	Flushed out iso-octane and replaced with water						
Mar. 4/72	9:58	47.5	40.0					x
Mar. 4/72	10:00	57.7	50.2			x		
Mar. 4/72	10:03	68.6	61.1			x		
Mar. 6/72	9:25	77.9	70.4			x		
Mar. 6/72	15:23	End of Test						
Sample No. 29		Apparatus No. T-2		Soil Type Kaolin				
Mar. 7/72	13:50	49.7	39.3	20.5				x
Mar. 9/72	9:20	59.7	49.3	30.5			x	
Mar. 14/72	9:00	End of Test						
Sample No. 30		Apparatus No. OED-177		Soil Type Kaolin				
Mar. 9/72	13:58	57.1	49.6	23.7				x
Mar. 11/72	10:34	57.1	49.6	M		x		
Mar. 13/72	9:27	57.1	49.6	M		x		
Mar. 13/72	9:44	57.1	49.6	M		x		
Mar. 13/72	13:01	57.1	49.6	26.6				x
Mar. 15/72	15:34	67.5	60.0	26.7		x		
Mar. 15/72	16:03	57.1	49.6	26.4				x
Mar. 20/72	12:23	29.4	22.6	5.4				
Mar. 21/72	10:26	End of Test						

TABLE A.7 continued

Starting Date	Starting Time	Immediately Following a Pressure Change			Type of Test			
		Total Pressure (psi)	Air Pressure (psi)	Water Pressure (psi)	Process	Reaction	Null	Allowed to Equilize
Sample No. 31		Apparatus No. 31		Soil Type Kaolin				
Mar. 14/72	9:40	59.5	49.0	30.1				x
Mar. 17/72	9:29	69.6	59.1	40.2			x	
Mar. 21/72	9:15	79.7	69.2	50.3			x	
Mar. 23/72	9:16	89.4	78.7	59.9			x	
Mar. 27/72	11:20	79.7	69.2	50.3			x	
Mar. 29/72	8:40	69.7	59.2	40.4			x	
Mar. 30/72	8:57	59.5	49.1	30.3			x	
Apr. 4/72	8:33	39.9	29.4	10.7			x	
Apr. 5/72	8:15	End of Test						
Sample No. 32		Apparatus No. T-1		Soil Type Regina Clay				
Mar. 27/72	10:08	100.9	89.8	5.0				x
Apr. 6/72	9:13	50.9	39.8	9.4	x			
Apr. 18/72	9:05	36.8	25.5	9.7	x			
May 5/72	9:18	27.3	15.9	9.9	x			
June 5/72	9:45	20.5	15.8	9.6	x			
July 1/72	11:00	End of Test						

TABLE A.7 continued

Starting Date	Starting Time	Immediately Following a Pressure Change			Type of Test			
		Total Pressure (psi)	Air Pressure (psi)	Water Pressure (psi)	Process	Reaction	Null	Allowed to Equilize
Sample No. 33		Apparatus No. OED-177		Soil Type Regina Clay				
Mar. 28/72	11:10	124.8	59.4	3.9				x
Apr. 13/72	8:35	95.5	30.0	6.5	x			
Apr. 24/72	8:55	80.8	15.3	6.6	x			
May 5/72	10:40	75.1	9.8	6.8	x			
May 19/72	9:30	61.0	9.8	6.5	x			
May 26/72	9:30	37.1	9.5	6.3	x			
June 8/72	9:20	23.7	9.5	6.4	x			
June 23/72	10:30	End of Test Difficulty in flushing out the base						
Sample No. 34		Apparatus No. OED-179		Soil Type Regina Clay				
Mar. 29/72	11:02	95.0	81.0	6.6				x
Apr. 3/72	12:22	54.4	40.5	6.6	x			
Apr. 13/72	8:50	34.0	20.1	6.4	x			
Apr. 24/72	9:10	24.3	10.5	6.4	x			
May 5/72	10:45	18.2	11.0	6.5	x			
May 17/72	9:00	14.4	10.3	6.1	x			
June 2/72	9:30	12.8	10.5	6.3	x			
June 23/72	11:00	End of Test						

TABLE A.7 continued

Starting Date	Starting Time	Immediately Following a Pressure Change			Type of Test			
		Total Pressure (psi)	Air Pressure (psi)	Water Pressure (psi)	Process	Reaction	Null	Allowed to Equilize
Sample No. 35		Apparatus No. T-2		Soil Type Regina Clay				
Apr. 6/72	12:02	90.1	60.2	9.5				x
Apr. 18/72	8:50	60.2	30.4	9.5	x			
May 5/72	9:20	48.8	19.0	9.6	x			
May 24/72	15:30	42.9	13.0	9.3	x			
June 10/72	10:25	22.8	12.7	8.9	x			
July 1/72	9:00	End of Test						

APPENDIX B

CALIBRATIONS AND CHECKS TO ENSURE PROPER FUNCTIONING OF THE EQUIPMENT

CONTENTS OF APPENDIX B

		Page
B-1	General	B1
B-2	Temperature and Relative Humidity in the Laboratory	B1
B-3	Calibration of Pressure Transducers and Linear Voltage Displacement Transducers	B3
B-4	Compressibility of Test Equipment	B7
B-5	Properties of High Air Entry Ceramic Discs	B21
B-6	System Leaks	B28
B-7	The Permeability of Rubber and Lucite	B48
B-8	Check on Initial, Final and Change in Volume Relations	B59

CALIBRATIONS AND CHECKS TO ENSURE PROPER FUNCTIONING OF THE EQUIPMENT

B-1 General

The equipment used in the laboratory investigations was either of a new design or had been substantially modified from existing and proven designs. For this reason, Appendix B is used to explain the many calibrations and checks performed to ensure that the equipment was functioning properly. Time consuming meticulous tests were conducted to examine all possible sources of error, assess their significance and either eliminate or control them. Many of the difficulties were overcome by special procedural techniques and further modifications to the equipment.

B-2 Temperature and Relative Humidity in the Laboratory

All equipment was in the same well ventilated room. The temperature and relative humidity were continuously recorded on a strip chart recorder. The small fluctuations observed were not significant. Figure B.1 shows a typical temperature and relative humidity trace for the month of January, 1972. The means and standard deviations for each recorder strip are summarized in Table B.1.

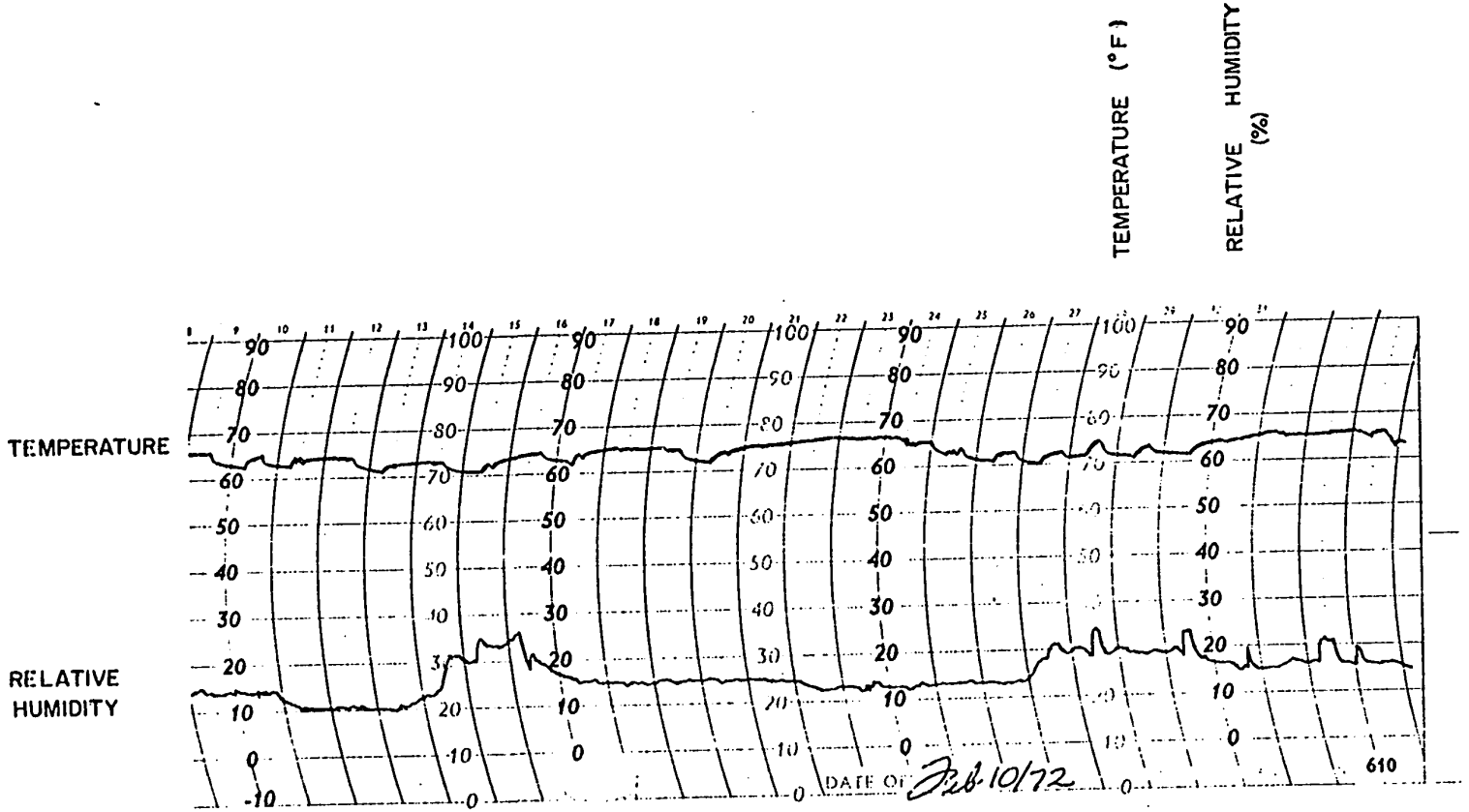


FIGURE B.1 TYPICAL TEMPERATURE AND RELATIVE HUMIDITY STRIP RECORDING

TABLE B.1

SUMMARY OF TEMPERATURE AND RELATIVE HUMIDITY IN THE LABORATORY

Time Period	Temperature °F		Relative Humidity %	
	Mean	Std. Dev.	Mean	Std. Dev.
Dec. 8/71 to Jan. 6/72	72.7	2.15	24.3	2.85
Jan. 6/72 to Feb. 10/72	73.8	1.48	25.1	3.24
Feb. 10/72 to Mar. 13/72	73.3	2.02	12.9	2.68
Mar. 13/72 to Apr. 17/72	74.5	1.56	23.6	3.08
Apr. 17/72 to June 1/72	73.7	1.63	27.3	4.33

The overall averate temperature was 73.6°F while the relative humidity was 22.6%. These values are later used in an analysis to assess the diffusion rates across various materials and the volume change in the air phase of a sample due to a change in temperature. In general, the air phase was operated as an open system and temperature effects were negligible.

B-3 Calibration of Pressure Transducers and Linear Voltage Displacement Transducers (LVDT)

The pore pressure transducers were manufactured by Dynisco and were of the range of 0-100 psi. Each transducer was calibrated on a CALIBRATOR manufactured by Barnet Instruments Ltd. The transducer was first loaded to 100 psi for at least one hour. The pressure was

reduced to 0.0 psi and the digital voltmeter was set to 0.00 mv. The transducer was then calibrated up to 100 psi in 10 psi increments for loading and unloading (Figure B.2). All transducers showed negligible hysteresis upon loading and unloading.

After calibration, the transducer was removed from the calibrator and torqued (40 inch pounds) into position on the test apparatus. A slight adjustment at zero pressure was made on the digital voltmeter in order to read 0.00 mv at 0.0 psi. After each soil test on the equipment, the 0.0 psi pressure reading was checked and corrected if necessary. This procedure assumes that the slope of the calibration curve remains constant and the slight creep in calibration was constant over the entire range. It should be mentioned that the greatest degree of accuracy is required in the pressure range approaching zero. Several checks of the entire calibration were made at later dates to ensure their constancy. Table B.2 summarizes the calibration factors for each transducer along with a designation of the manner of its usage. The calibration factors were obtained by performing a least square, best fit regression analysis between the dependent variable (pressure, psi) and the independent variable (digital output, mv). The equation of the best fit line had the form,

$$\underset{(psi)}{\text{Pressure}} = \underset{(psi/mv)}{\text{Slope}} * \underset{(mv)}{\text{Digital Output}} + \underset{(psi)}{\text{Intercept}}$$

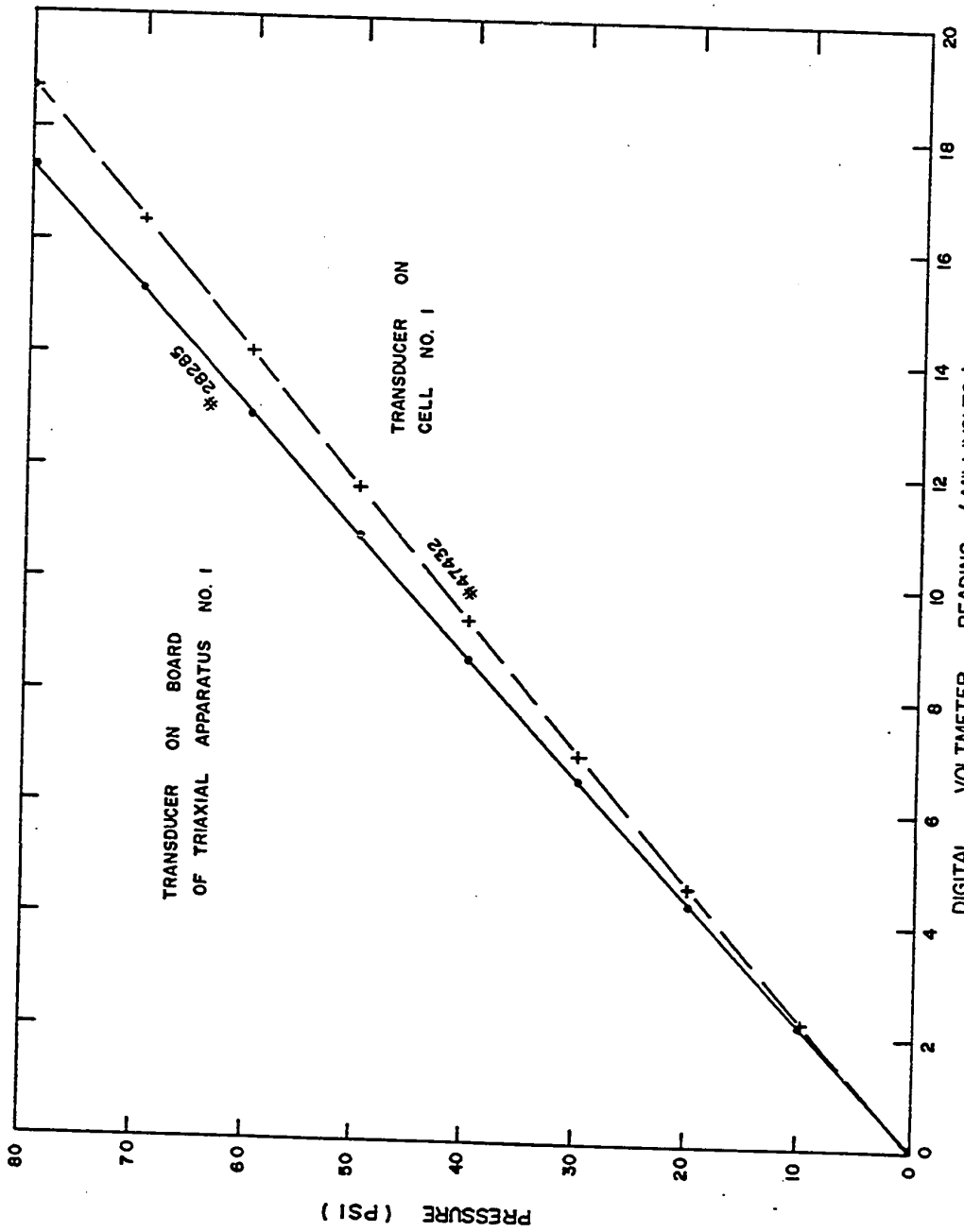


FIGURE B.2 TYPICAL CALIBRATION CURVES FOR PRESSURE TRANSDUCERS

TABLE B.2

SUMMARY OF CALIBRATION FACTORS FOR PRESSURE TRANSDUCERS

Date of Calibration	Transducer No.	Channel No.	Location on the Equipment	Range of Calibration (psi)	Slope (psi/mv)	Intercept (psi)
Feb. 20/71	28285	6	Board of T-1	0-100	+4.640	-0.004
Mar. 12/71	--	8	Cell of T-1	0-100	+4.307	+0.003
June 2/71	46511	7	Board of Oed-177 and Oed-179	0-70	+4.236	+0.010
June 2/71	22792	5	Base of Oed-177	0-100	+3.632	-0.017
June 2/71	SN39556	4	Base of Oed-179	0-100	+3.629	+0.051
Nov. 16/71	46511	7	Board of Oed-177 and Oed-179	0-100	+4.262	-0.031
Nov. 16/71	SN39556	4	Base of Oed-179	0-100	+3.781	+0.093
Nov. 15/71	50219	3	Base of T-2	0-100	+4.012	+0.106
				0-20	+4.053	+0.036
				20-100	+4.103	-0.718
Nov. 15/71	46254	1	Board of T-2	0-100	+3.489	+0.042
				0-20	+3.501	+0.016
				20-100	+3.488	+0.050
Feb. 1/72	42508*	4	Placed on base of Oed-179 on Feb. 1/72	0-50	+1.865	+0.071

*50 psi transducer

Twenty-four volt, LVDT's were used to measure the lateral and vertical displacement in Triaxial Apparatus No. 2. The LVDT's are a model 24DCDT manufactured by Hewlett Packard. The final LVDT's used had a range of one inch. The constant voltage power source was a model #6204B Hewlett Packard voltage regulator. The gauges were calibrated against a precise micrometer (0.001 inch divisions) mounted on a rigid base. (Manufactured by Mitutoya Co). The gauges showed negligible hysteresis and are essentially linear over the entire range (Figure B.3). The calibration factors are summarized in Table B.3.

The readings on the pore pressure and displacement transducers were recorded with a Hewlett Packard Data Acquisition System (Digital Voltmeter Model #3440A). There was only one problem with the equipment which involved slight fluctuations in the millivolt reading ($\pm$ 0.03 mv). This occurred in September, 1971 and was remedied in approximately two weeks.

B-4 Compressibility of Test Equipment

The measurements of vertical and lateral displacements of a soil sample must be corrected for the compressibility of the measuring systems. The compressibility is generally observed by placing an incompressible material (eg. Aluminum block) in the apparatus and changing the total pressure. This procedure is relatively common when testing saturated soils. However, the form of the compressibility curves become considerably more complicated when the air pressure can

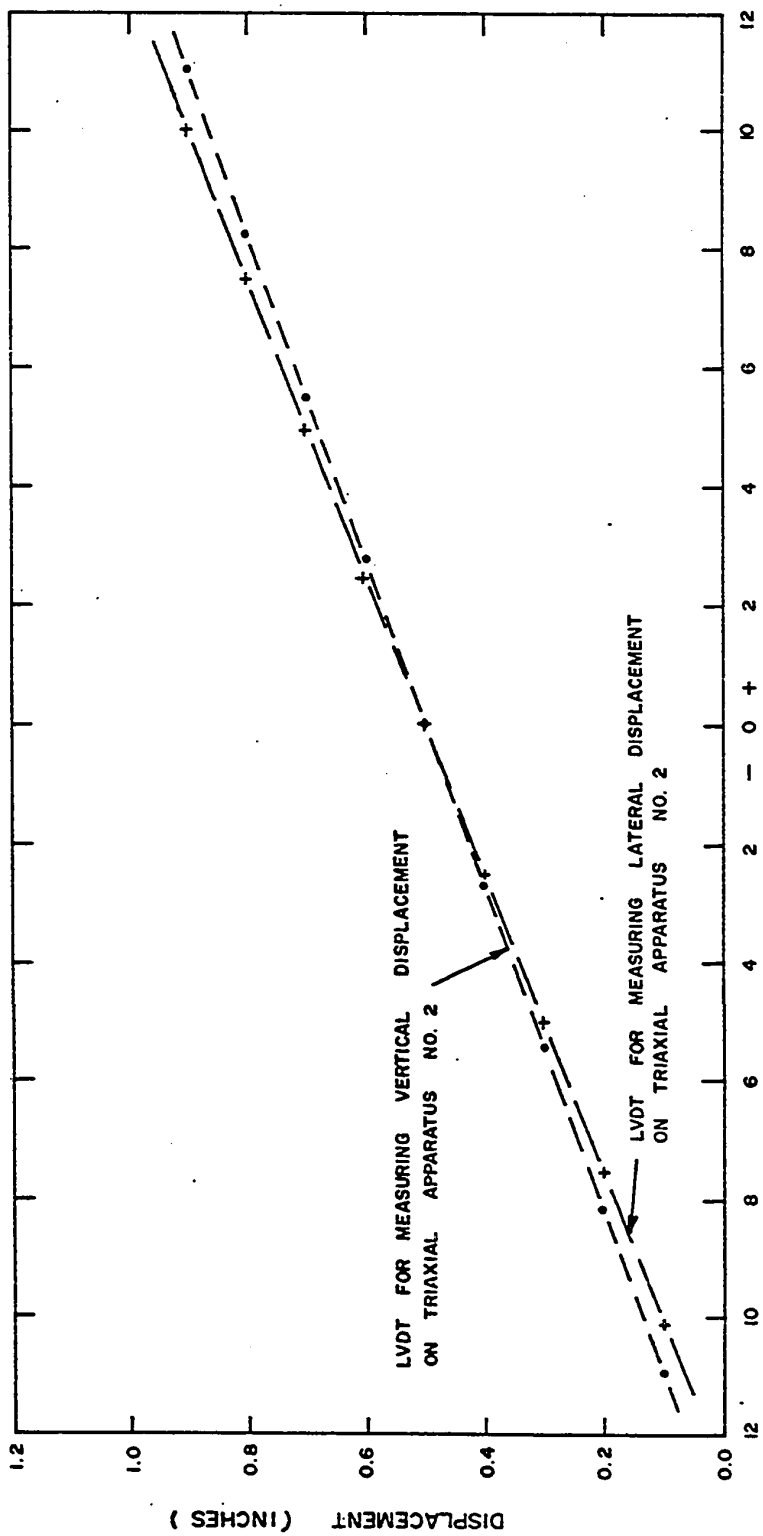


FIGURE B.3 TYPICAL CALIBRATION CURVES FOR LVDT'S

TABLE B.3

CALIBRATION FACTORS FOR LVDT GAUGES

Date of Calibration	Channel No.	Location of LVDT Gauge	Range of Calibration (inches)	Slide (inches/volt)	Intercept (inches)
Nov. 15/71	19	Lateral displacement indicator of T-2	±0.15	-0.009736	+0.14931
Nov. 15/71	20	Vertical displacement on T-2	±0.5	+0.036503	+0.49980
Jan. 3/72	19	Lateral displacement indicator of T-2	±0.5	+0.039766	+0.50189

can also be manipulated. Figure B.4 shows the hysteresis upon loading and unloading and the effect of the applied air pressure for Anteus Oedometer No. 177.

Figure B.5 shows the change in height of the loading cap and the mercury level due to a change in cell pressure for Triaxial Apparatus No. 1. The mercury level undergoes a considerable change in elevation in the low pressure range.

Triaxial Apparatus No. 2 required a constant voltage supply to activate the LVDT gauges. The manufacturers of the constant voltage supply (24 volts) guarantee a stability better than 0.1 percent plus 5 mv drift for an 8 hour period after a warm-up of 30 minutes. This corresponds to a vertical displacement of 0.0027 cm or 0.23 cc. Experience with the voltage supply over long periods of time, showed that the drift was approximately one order of magnitude less, provided the voltage supply was never turned off.

Table B.4 summarizes the lateral and vertical deformations monitored during the disassembling and adjusting of the lateral displacement indicator. The results indicate that the displacement readings are relatively insensitive to disturbance during set-up and disassembling.

Figure B.6 shows typical amounts of vertical and horizontal displacement upon changing the total and air pressure. Three more tests are shown in Figures B.7, B.8 and B.9. The vertical LVDT measurements showed extremely small deformations relative to the pressures applied. The lateral LVDT gauge underwent some creep

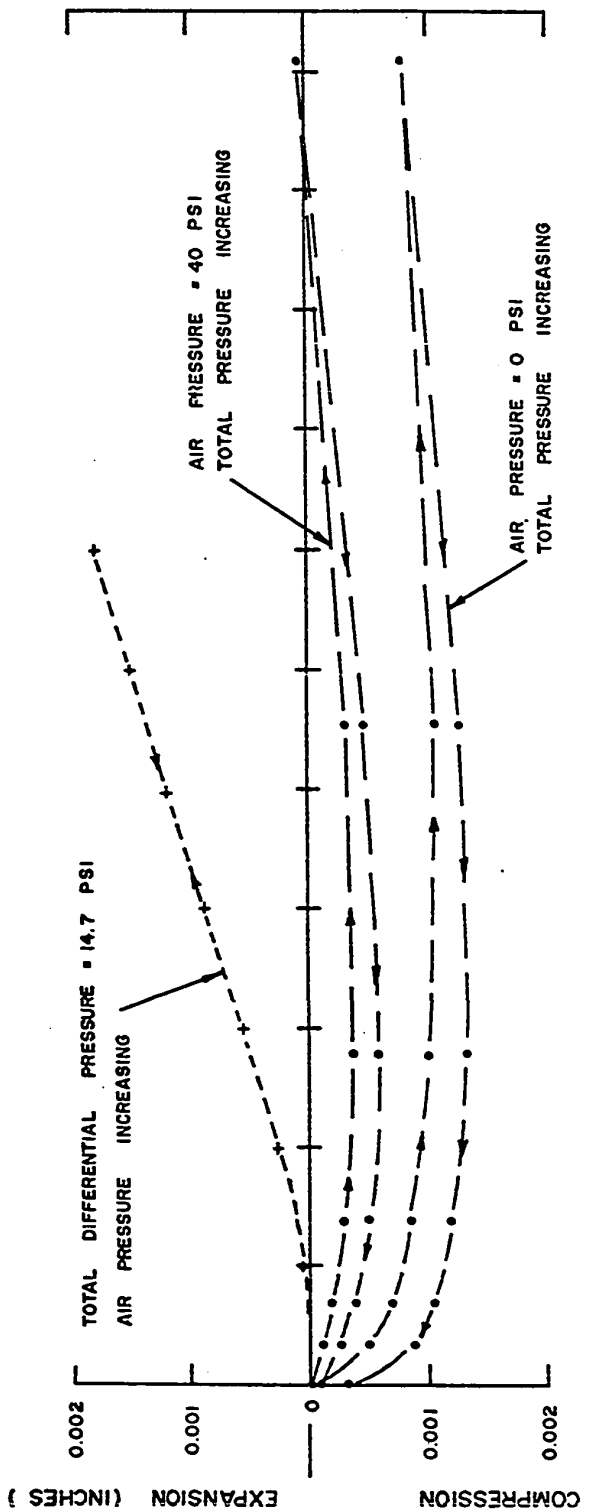


FIGURE B.4 COMPRESSIBILITY OF MODIFIED ANTEUS OEDOMETER NO. 177

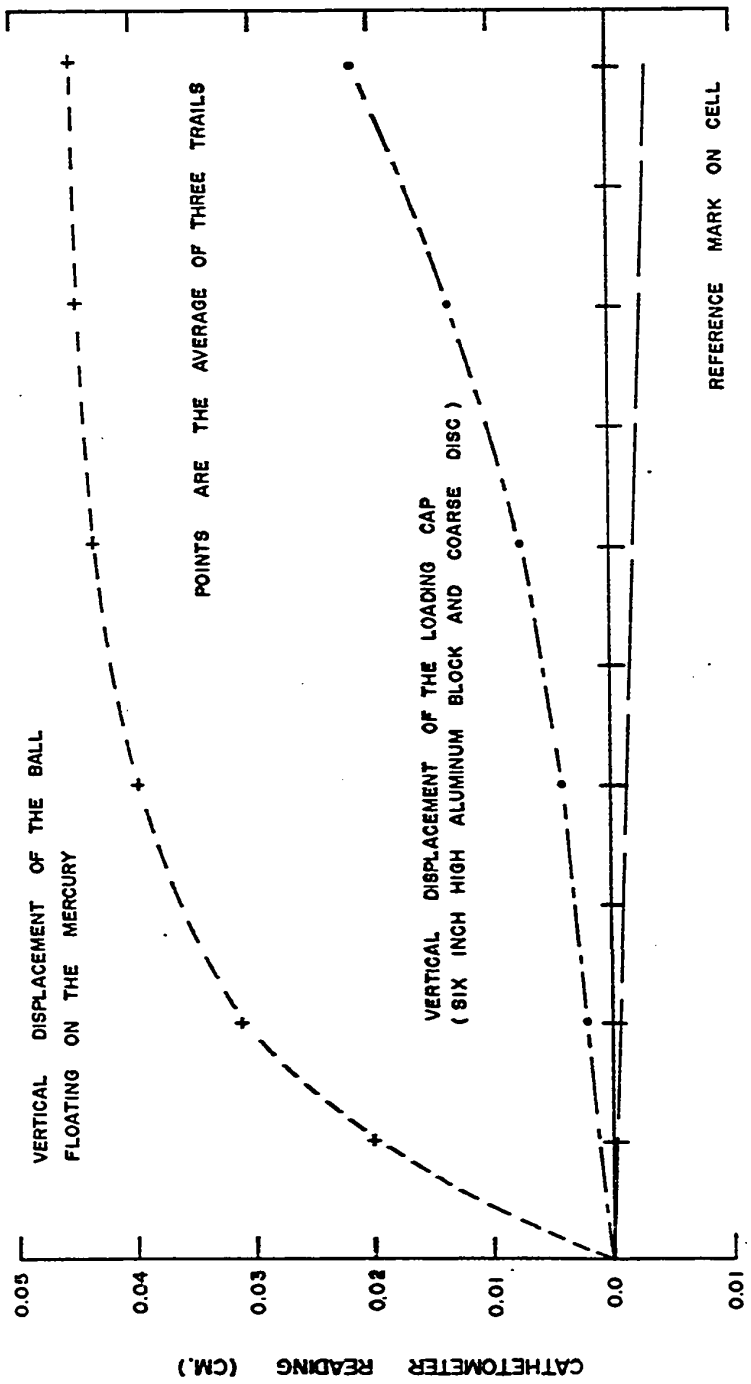


FIGURE B. 5 COMPRESSIBILITY IN THE VERTICAL AND LATERAL MEASURING SYSTEMS FOR TRIAXIAL APPARATUS NO. 1

TABLE B.4

LATERAL AND VERTICAL DEFORMATIONS WHILE DISASSEMBLING AND ADJUSTING THE LATERAL DEFORMATION INDICATOR ON TRIAXIAL APPARATUS #2

Adjustment Performed	Lateral* Deformation %	Vertical* Deformation %
Disconnected all pressure lines	0.0000	-0.0016
After loosening all bolts on the cell	0.0000	-0.0142
Removed the cell and bumped the lateral gauge	-0.0008	-0.0032
Twisted the lateral gauge upward on the sample	+0.0008	-0.0016
Twisted the lateral gauge downward on the sample	0.0000	0.0000
Moved the lateral gauge pivot to the right	-0.0097	-0.0158
Moved the lateral gauge pivot to the left	+0.0494	-0.0174
Reseated the lateral gauge in a central position	-0.0567	+0.0048
Moved the lateral gauge upward on the sample by 1/2 inch	-0.0520	-0.0048

*All deformations computed on the basis of a sample volume of 495 cc.

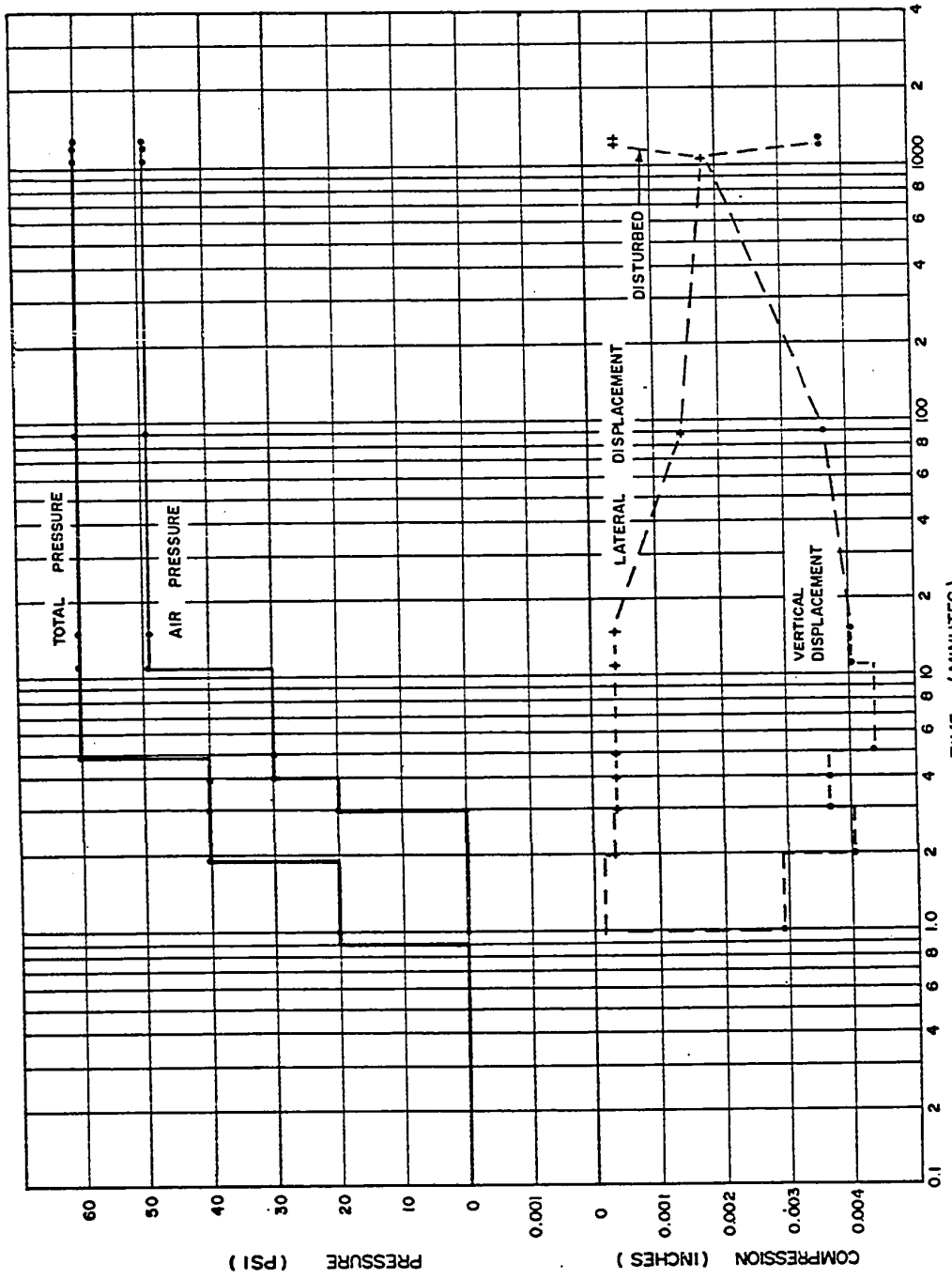


FIGURE B.6 VERTICAL AND LATERAL COMPRESSIBILITY OF TRIAXIAL APPARATUS NO. 2

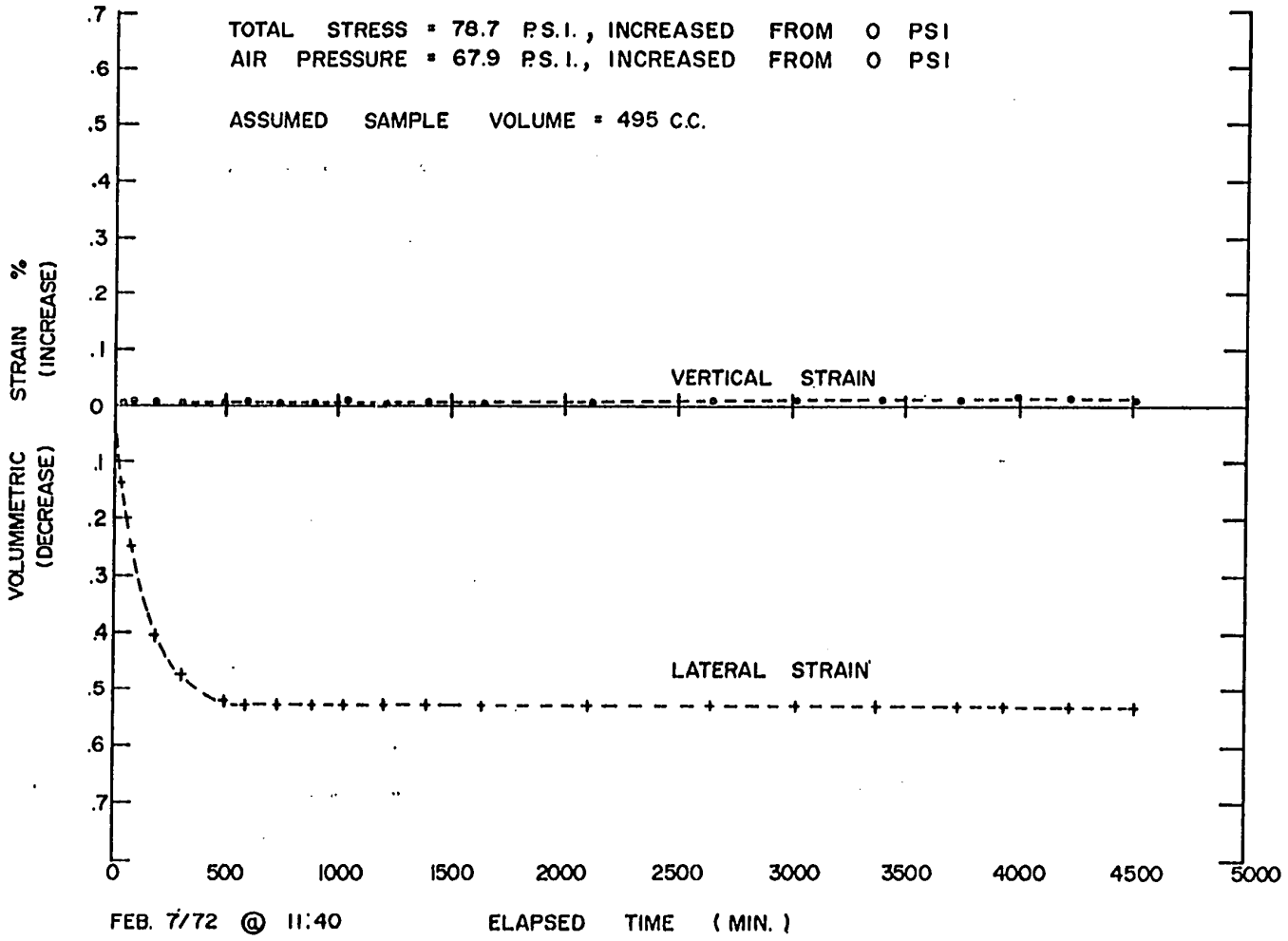


FIGURE B.7 STABILITY OF LVDT MEASUREMENTS WITH TIME AFTER THE APPLICATION OF A TOTAL AND AIR PRESSURE (PHASE I)

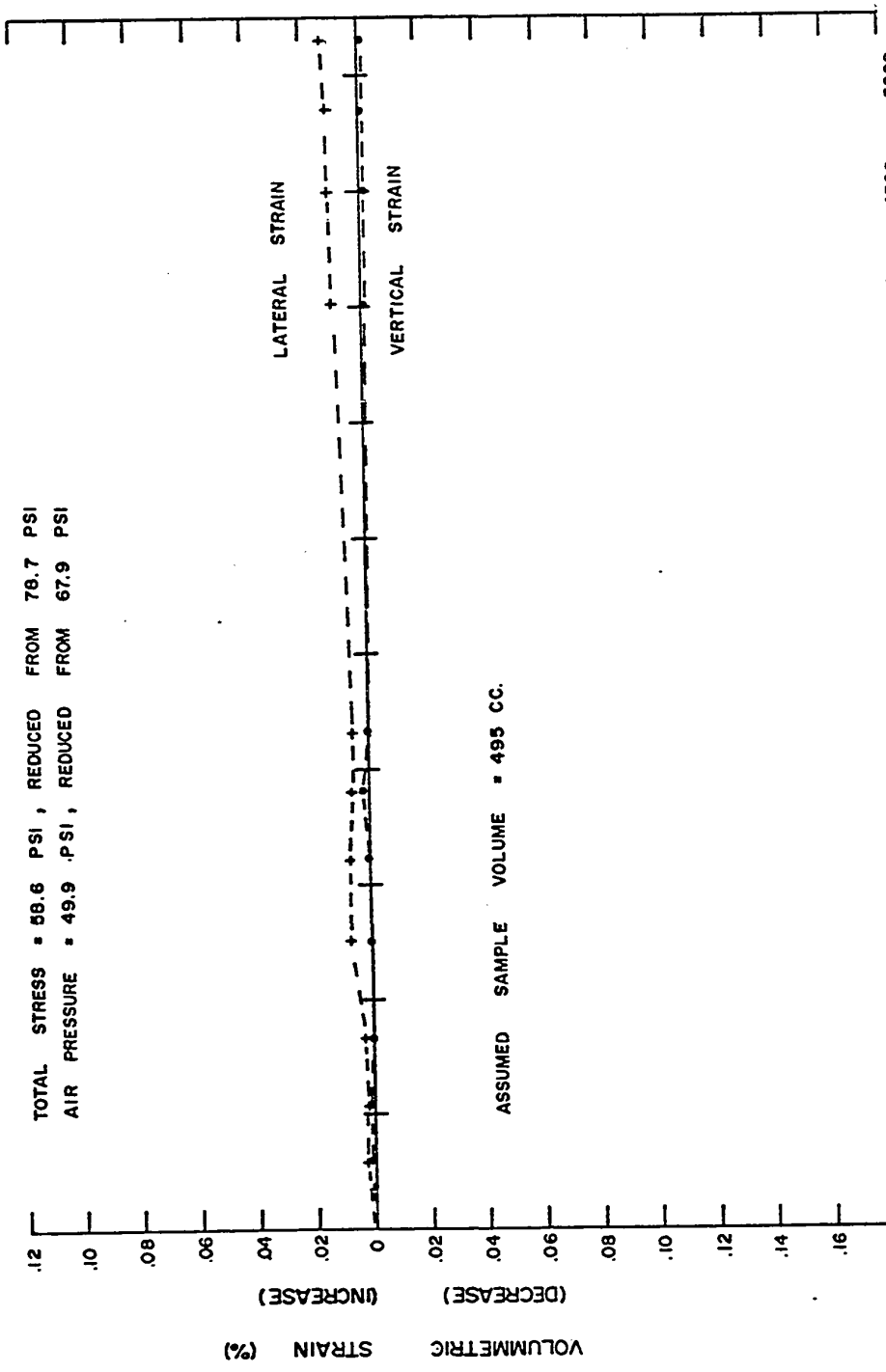


FIGURE B.8 STABILITY OF LVDT MEASUREMENTS WITH TIME AFTER A REDUCTION IN THE TOTAL AND AIR PRESSURE (PHASE II)

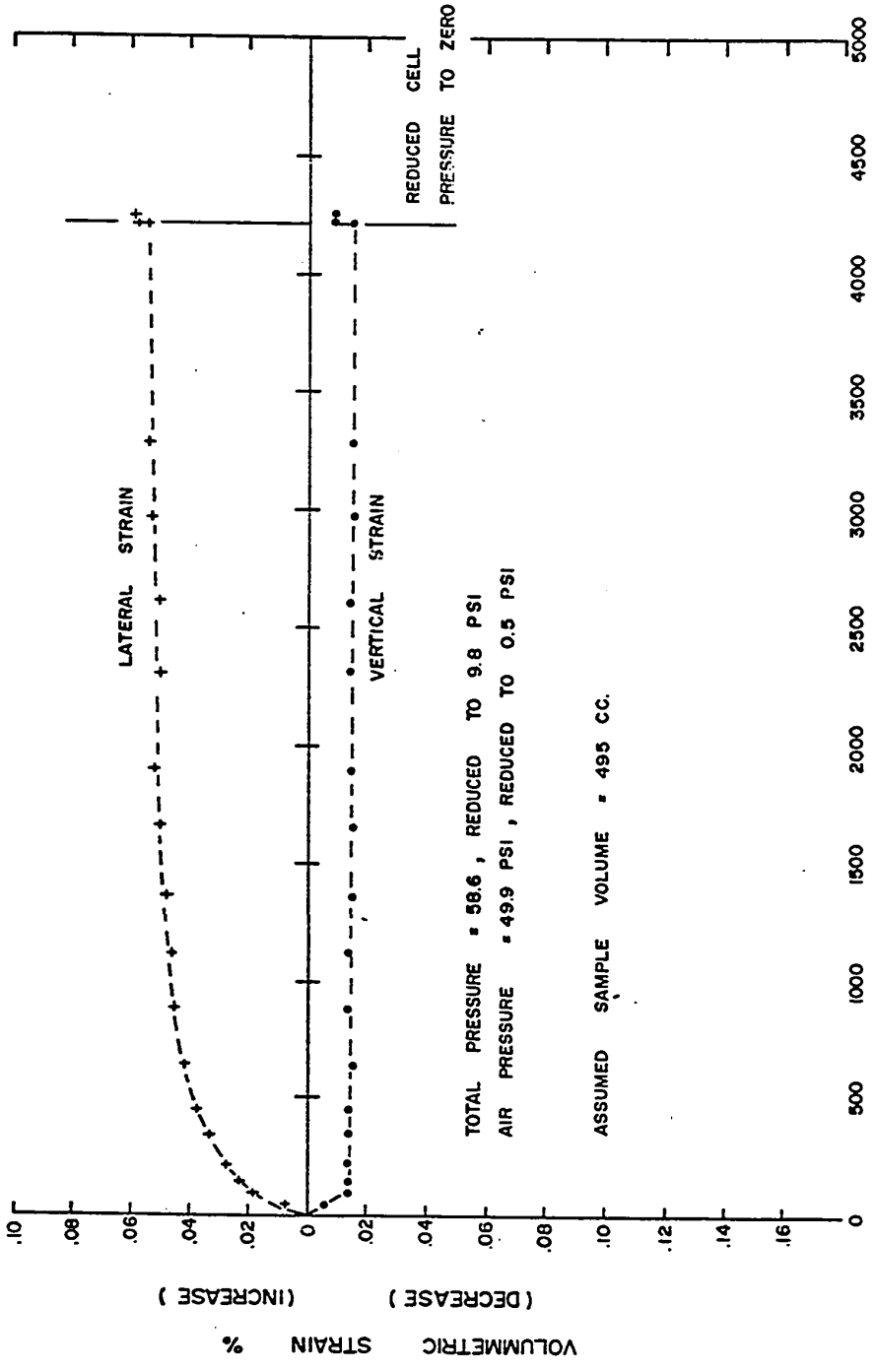


FIGURE B. 9 STABILITY OF LVDT MEASUREMENTS UPON COMPLETE REDUCTION IN APPLIED STRESSES (PHASE III)

during the first 500 minutes. Then the deformations remained constant over a period of several days. The creep during the first 500 minutes is likely related to creep between the rubber membrane and the aluminum dummy block.

The difficulty in predicting the nature of the compressibility plots encourages performing a duplicate dummy test for compressibility, for every soil sample tested. In this way, the same stress path used during each soil test can be simulated using a dummy. The displacements observed during the dummy test are subtracted from the displacements observed during the soil test.

If the surge tank is not used during the change in cell pressure on Triaxial Apparatus No. 2, a finite time is required to establish the new pressure in the cell. Figure B.10 shows the time required to build-up various applied cell pressures. If the surge tank is used, the equilization time is in the order of a couple of seconds.

A change in back pressure applied to the water volume change indicator registers a compression of the water and/or air in the lines between the volume change indicator and the soil sample. Figure B.11 shows the amount of compression recorded on two dates. The results are quite consistent when the measuring system is essentially deaired. However, a different method of evaluating the water volume change compressibility correction was incorporated due to its dependence on the amount of air in the system.

A change in the back pressure applied to the water volume change indicator results in an almost instantaneous volume change that precedes seepage through the fine ceramic disc. The volume change at

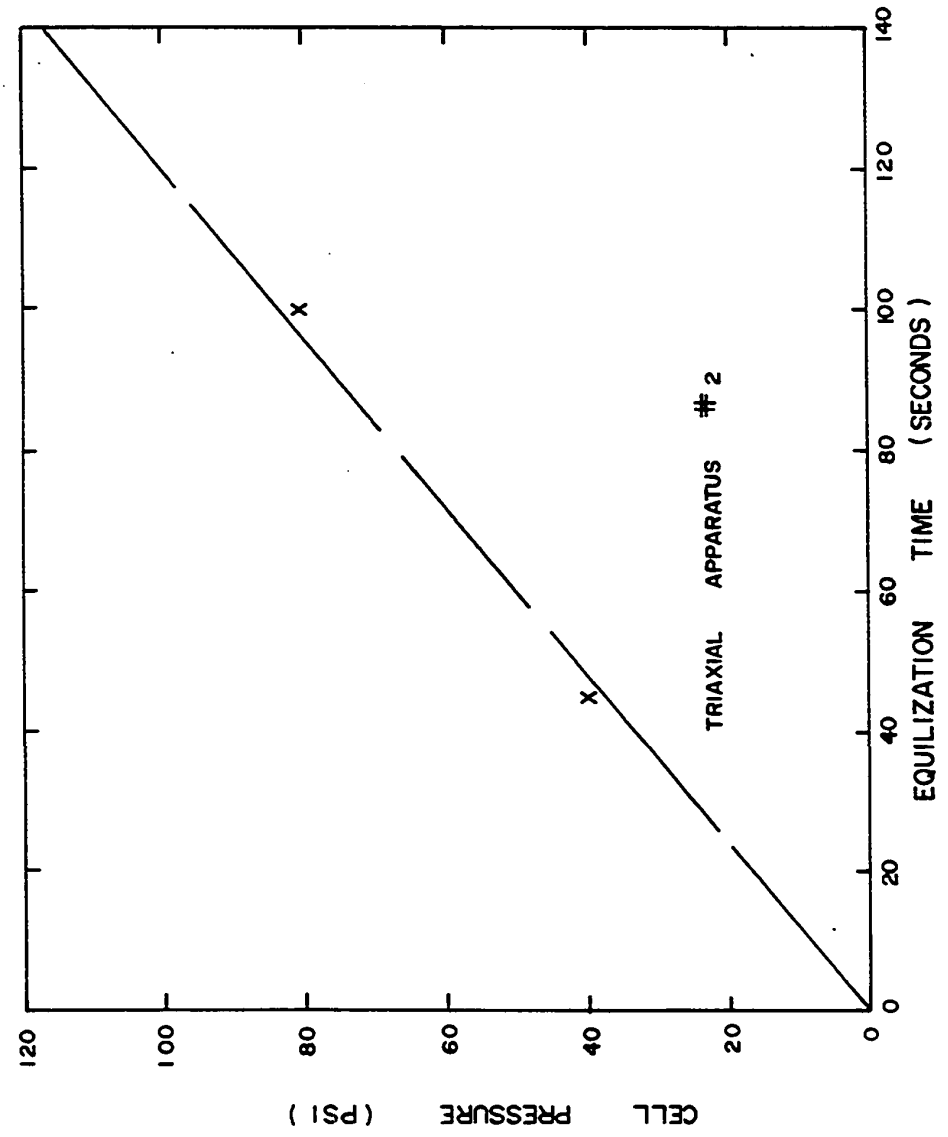


FIGURE B.10 RATE OF CELL PRESSURE BUILD - UP FROM ATMOSPHERIC PRESSURE CONDITIONS

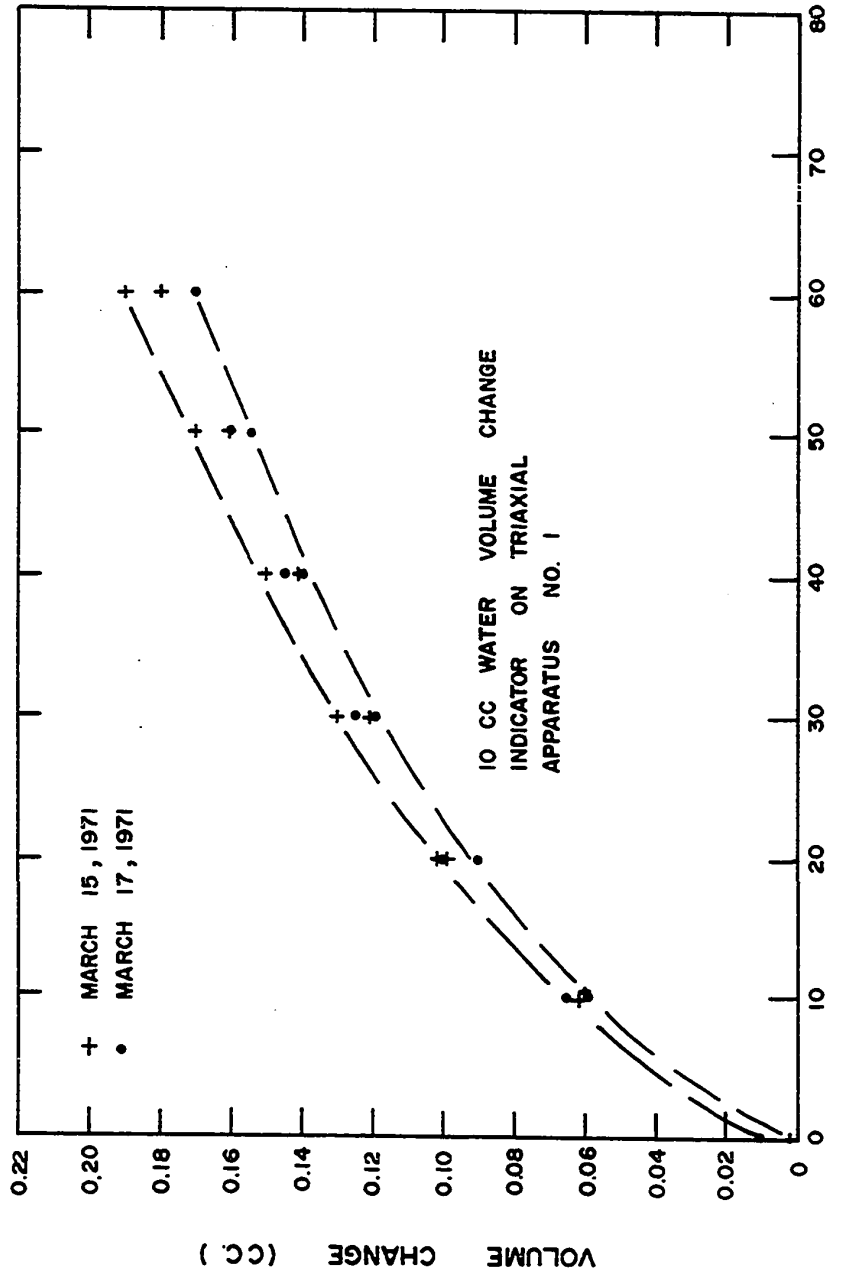


FIGURE B.11 COMPRESSIBILITY OF WATER VOLUME CHANGE INDICATOR WITH CHANGING BACKPRESSURE

the end of the first three seconds was noted on the data sheets and used as a compressibility correction. This procedure applies only when operating the equipment as an open system.

The compressibility corrections become imperative when testing stiff, unsaturated soils due to the small volume changes being monitored. Also, the desire during the NULL tests was to measure zero volume change in the water and soil structure while changing the stress components. Table B.5 shows the order of magnitude of the compressibility corrections associated with each test apparatus.

Considering the compressibility with respect to the volume of the soil sample, Triaxial Apparatus No. 2 is the most precise while the one dimensional oedometers are the least precise. However, long term tests showed some unpredictable creep associated with Triaxial Apparatus No. 2. Generally it was most dominant during the first few hours after changing the total stress.

B-5 Properties of High Air Entry Ceramic Discs

The high air entry discs on which the soil samples are placed act as a semi-permeable membrane to separate the air and water pressures. The ceramic disc must have an air entry value in excess of the maximum differential air-water pressure. At the same time, it is desirable to have the largest possible pore size in the disc to obtain rapid equilization or to prevent impeded drainage.

The air entry (or bubbling pressure) is defined by the capillary

TABLE B.5

APPROXIMATE MAGNITUDE OF COMPRESSIBILITY CORRECTION FOR A 10 PSI PRESSURE CHANGE
(Vertical and Lateral Displacement)

Test Apparatus	Approximate Volume of Soil Sample (cc)	Vertical of Displacement	Low Pressure Range		High Pressure Range	
			Changing u_a (cc)	Changing σ (cc)	Changing u_a (cc)	Changing σ (cc)
Anteus Oedometer	60	Vertical	-0.006	+0.040	-0.024	+0.009
#177 and #179	60	Lateral	0.0	0.0	0.0	0.0
Triaxial #1	820	Vertical	-0.080	+0.080	-0.265	+0.265
	820	Lateral	0.0	+1.60	0.0	+0.080
Triaxial #2	510	Vertical	-0.021	+0.103	-0.021	+0.082
	510	Lateral*	~0.0	+0.021	~0.0	+0.021

*The pads resting on the rubber membrane appear to undergo some creep with time.

model equation.

$$(u_a - u_w)_{max} = \frac{2 \cdot T_s}{r}$$

where T_s = surface tension of water with respect to air (72 dynes/cm)

r = radius of the maximum pore.

The unit generally used for measuring air entry value is the BAR. One bar is equal to 14.5 psi.

The high air entry ceramic discs used in this thesis were manufactured by Soilmoisture Equipment Corporation, Santa Barbara, California. The manufacturers properties of several discs are given in Table B.6.

TABLE B.6

SOILMOISTURE'S PROPERTIES ON HIGH AIR ENTRY DISCS

Air Entry Value (Bars)	Porosity (%)	Permeability (cm/sec)	Bubbling Pressure (psi)
3	36	1.73×10^{-7}	> 46
5	34	1.21×10^{-7}	> 80
15	32	2.60×10^{-9}	>220

The weights and volumes of fours high air entry discs were measured. It is difficult, however, to determine their porosity since the specific gravity of the material used in their construction is unknown. Table B.7 summarizes the results, tabulating the porosities based on an assumed specific gravity.

TABLE B.7

WEIGHT-VOLUME RELATIONSHIPS OF FOUR CERAMIC DISCS

Air Entry Value	No.	Diameter (cm)	Thickness (cm)	Density (Air-Dried) gm/cc	Density (Oven-Dried) gm/cc	Porosity G_S=2.62
5	1	6.362	0.9213	1.879	1.876	28.3
5	2	6.351	0.9204	1.891	1.887	27.9
15	3	6.218	0.6208	1.741	1.737	33.6
15	4	6.221	0.6353	1.753	1.747	33.2

The density of the 5 bar discs was unexpectedly greater than that of the 15 bar discs. However, Soilmoisture Co., report that 1 bar discs can be purchased that have a low flow rate and a porosity of 25 percent, or a high flow rate with a porosity of 42 percent. It appears that the sintering process is controlled to produce the desired air entry value rather than have the porosity controlling the air entry value.

The coefficient of permeability of the ceramic disc mounted

in the base plate can readily be measured by placing water above the disc, increasing the chamber pressure and measuring the flow in the water volume change indicator. Numerous permeability tests were performed and the results are summarized in Table B.8. A typical plot of flow versus time is shown in Figure B.12. The system for measuring permeability is precise and the data could be essentially duplicated on different dates. For example, the tests performed on Oedometer No. 177 on February 18, 1972 and February 22, 1972 are essentially the same.

The measured coefficients of permeability agree closely with those suggested by the manufacturer. Minute cracks in the discs caused an increase in the coefficient of permeability (eg. Oedometer #177, Jan. 5/72). However, the increase in permeability was generally small while the decrease in the air entry value was substantial (section B.6). In a couple of cases, the 15 bar discs appeared to be plugged since they essentially resisted all flow of water (eg. Triaxial No. 2, Nov. 17/71). New discs had to be substituted. It appears that the fine tolerance associated with manufacturing the 15 bar discs presents some difficulties in this regard.

The average coefficient of permeability of the 5 bar discs was 1.16×10^{-7} cm per second and 7.89×10^{-9} cm per sec for the 15 bar discs. The averages were computed using the data from tests on discs that were functioning properly. These values compare closely with the manufacturers results.

Contaminating the discs with n-Hexane and subsequently washing

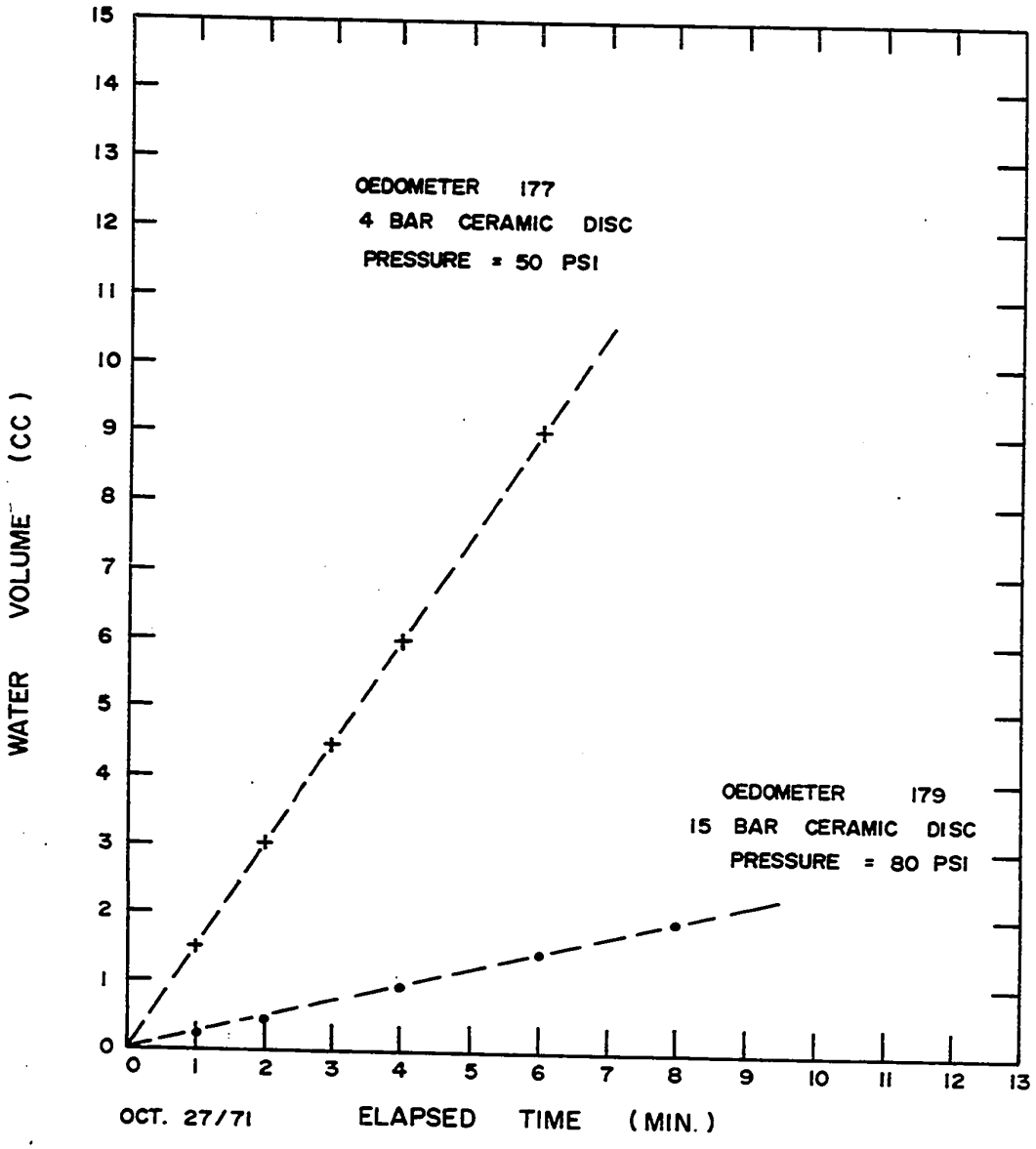


FIGURE B.12 . STEADY STATE SEEPAGE THROUGH HIGH AIR ENTRY CERAMIC DISCS

TABLE B.8

SUMMARY OF PERMEABILITY TESTS ON CERAMIC DISCS

	Date	Air Entry Value (Bars)	Diameter (cm)	Thickness (cm)	Pressure (psi)	Flow Per Unit Time (cc/min)	Permeability (cm/sec)
Low air entry disc on Triaxial #1 (from factory)	Feb. 21/71	?	6.33	0.955	10	7.50	5.39×10^{-6}
	Feb. 21/71		6.33	0.955	20	15.8	5.67×10^{-6}
	Feb. 21/71		6.33	0.955	40	29.9	5.28×10^{-6}
First disc installed on Anteus Oedometer #179	June 3/71	4	5.70	0.306	10	0.367	1.04×10^{-7}
Thin disc on Oedometer #179	Oct. 27/71	15	5.68	0.306	80	0.235	8.41×10^{-9}
Thin disc on Oedometer #177	Oct. 27/71	15	5.70	0.306	50	1.20	6.82×10^{-8}
Oedometer #179	Oct. 30/71	15	5.68	0.306	80	0.230	8.23×10^{-9}
Oedometer #177 (small crack along edge of disc)	Oct. 30/71	15	5.70	0.306	50	2.09	1.19×10^{-7}
Oedometer #177 (Added some glue to seal the crack)	Oct. 30/71	15	5.70	0.306	30	0.0433	4.10×10^{-9}
Oedometer #179	Nov. 17/71	15	5.63	0.306	78.8	0.197	7.29×10^{-9}
Thick disc on stainleas steel base, Oedometer #177	Dec. 1/71	5	5.68	0.622	78.8	1.76	1.30×10^{-7}
Triaxial #2	Nov. 17/71	15	6.35	0.306	46.8	0.0109	5.34×10^{-10}
New disc in Triaxial #2	Nov. 19/71	15	6.35	0.306	56.2	0.207	8.44×10^{-9}
Oedometer #177	Dec. 7/71	5	5.30	0.622	50.0	0.893	1.19×10^{-7}
Oedometer #179	Dec. 17/71	15	5.68	0.622	80.3	0.0968	7.02×10^{-9}
Oedometer #177 (crack in disc)	Jan. 5/72	5	5.68	0.622	79.4	1.388	1.02×10^{-7}
Oedometer #177 (new disc with new bevelled design)	Jan. 7/72	5	5.35	0.622	50.3	0.958	1.25×10^{-7}
Triaxial #2	Feb. 18/72	5	5.35	0.622	50.0	1.107	1.03×10^{-7}
Oedometer #177 (same disc as Jan. 7, after using h-Hexane in it	Feb. 18/72	5	5.35	0.622	50.0	0.898	1.18×10^{-7}
Oedometer #177 (cleaned with acetone)	Feb. 22/72 9:09	5	5.35	0.622	50.0	0.864	1.13×10^{-7}
	Feb. 22/72 9:57	5	5.35	0.622	5.0	0.0811	1.06×10^{-7}
	Feb. 22/72	5	5.35	0.622	12.0	0.205	1.12×10^{-7}
	Feb. 22/72 13:26	5	5.35	0.622	50.0	0.885	1.16×10^{-7}
Oedometer #179 (cleaned with ethyl alcohol)	Mar. 17/72	15	5.68	0.622	80.0	0.0788	5.73×10^{-9}

them with acetone does not appear to significantly affect the coefficient of permeability (eg. Oedometer #177, Jan. 7/72, Feb. 18/72 and Feb. 22/72). However, the response tests presented in Appendix E show that the response is far more rapid after washing the discs with acetone.

The results on Oedometer #177 (Feb. 22/72) indicate that the coefficient of permeability decreases slightly with a decreasing hydraulic gradient across the disc.

B-6 System Leaks

The portion of each apparatus associated with the measurement of water pressure and water volume change is highly susceptible to leakage. An attempt was made to eliminate leakage in all parts of the system, however, the water measuring portion must be very precise. The water measurement portion of the equipment can be visualized as consisting of the water volume change indicator and the base plate.

(a) Water Volume Change Indicator

The conventional double-acting Wykeham Farrance volume change indicator performs well when testing high water content soils over a short period of time. When testing low water content soils over long periods of time (i.e. one month or more) minute leaks accumulate to produce unacceptable errors in the analysis of the data. Table B.9 shows the order of magnitude of leakage associated with the conventional water volume change indicator. Leakage at a rate of 0.004 cc/min.

would accumulate to more than 150 cubic centimeters in one month. Most of the leakage is associated with the values. The standard values were replaced with Whitey valves.

TABLE B.9

LEAKAGE FROM WYKEHAM FARRANCE WATER VOLUME CHANGE INDICATOR WITH STANDARD VALVES (Nov. 18, 1971)

Trial No.	Applied Pressure (psi)	Elapsed Time (min)	Leakage (cc/min)	Comments
#1	50	50	0.004	Reading right burret
	50	50	0.0044	Reading left burret
Changed the O-rings in the valves				
#2	50	5	0.024	
	50	150	0.0089	
Reversed the direction of flow				
#3	50	7	0.0114	
Reversed the direction of flow				
#4	50	690	0.00042	

The amount of registered volume change when the lead from the indicator is plugged, is dependent upon the direction that the Whitney valves point. Figure B.13 shows the effect of reversing the direction of the valves while continuously reading the same burret. In one direction, there is very little volume change whereas a reversal of the

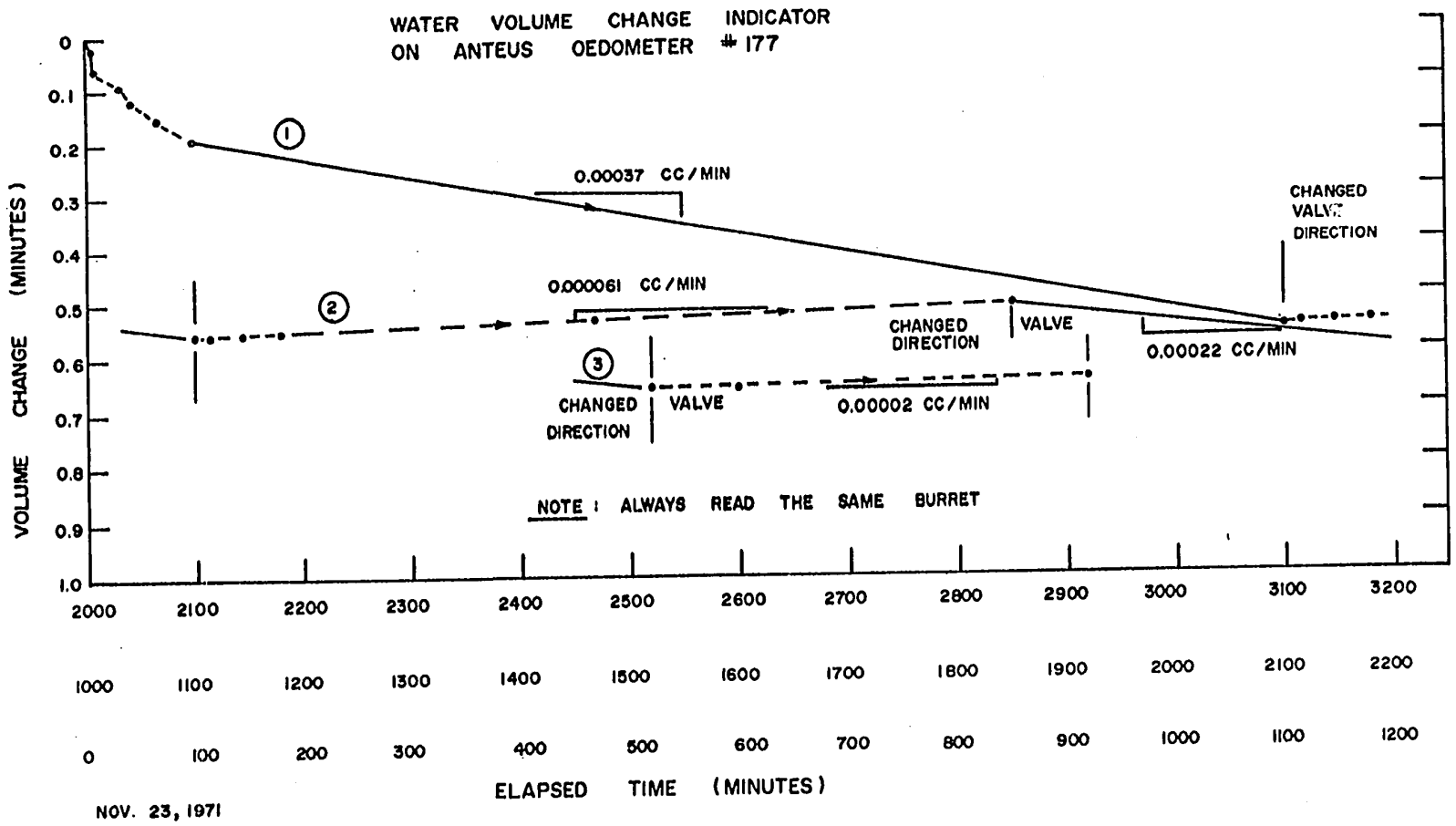


FIGURE B.13 EFFECT OF DIRECTION OF VALVES ON LEAKAGE FROM THE WATER VOLUME CHANGE INDICATOR

direction of the valves shows substantial leakage. The volume change indicators are designed such that all compression of the fluid in the indicator and leakage from the indicator is monitored on one burret while the other remains essentially constant. Air in the volume change indicator undergoes a volume change when the backpressure is changed or when the temperature is changed. This volume change is always monitored on the burret corresponding to the direction the valves point. The water between the burret and the outer lucite tube can also slowly diffuse through the outer lucite. This is registered on the same burret. It is essential that the burret opposite to the direction that the valves point, be monitored for accurate readings. It is interesting to observe that over long periods of time, (with the valves left in the same direction) the kerosene-water interface in one burret slowly rises until the burret is filled with water. Section B.7 discusses the rate of seepage of water through lucite.

On a couple of the volume change indicators it was observed that both burrets were undergoing a slow (but different) rate of volume change with time (Figure B.14). The volume change appeared to be the result of a slow leak past the rubber at the base of the burret. Attempts to tighten down the rubber seal simply forced the burrets up and out of the base. To overcome this difficulty, the volume change indicators were modified by inserting a small lucite washer below the rubber seal. The rubber seal could then be securely tightened and the volume change in one burret become negligible (Figure B.15). This modification was most necessary on the 5 cc burrets.

Both burrets were monitored for several days on the volume

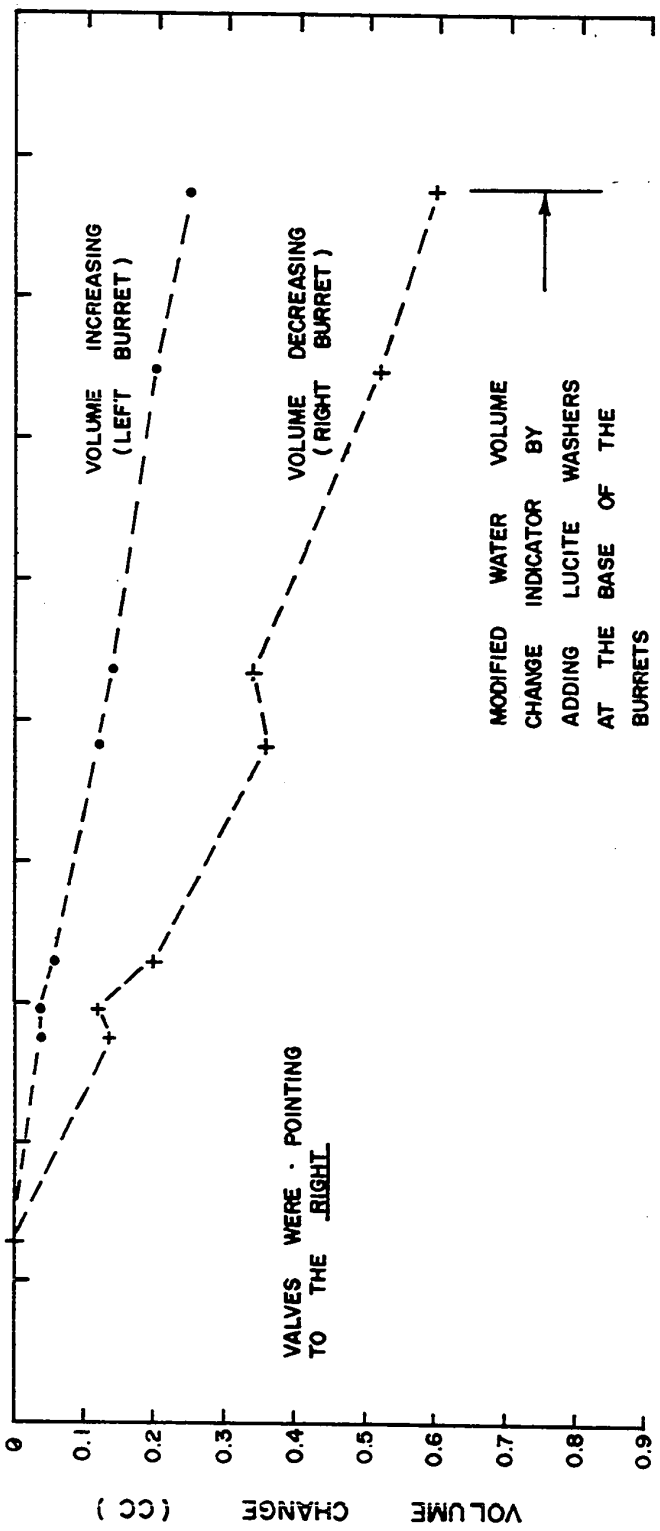
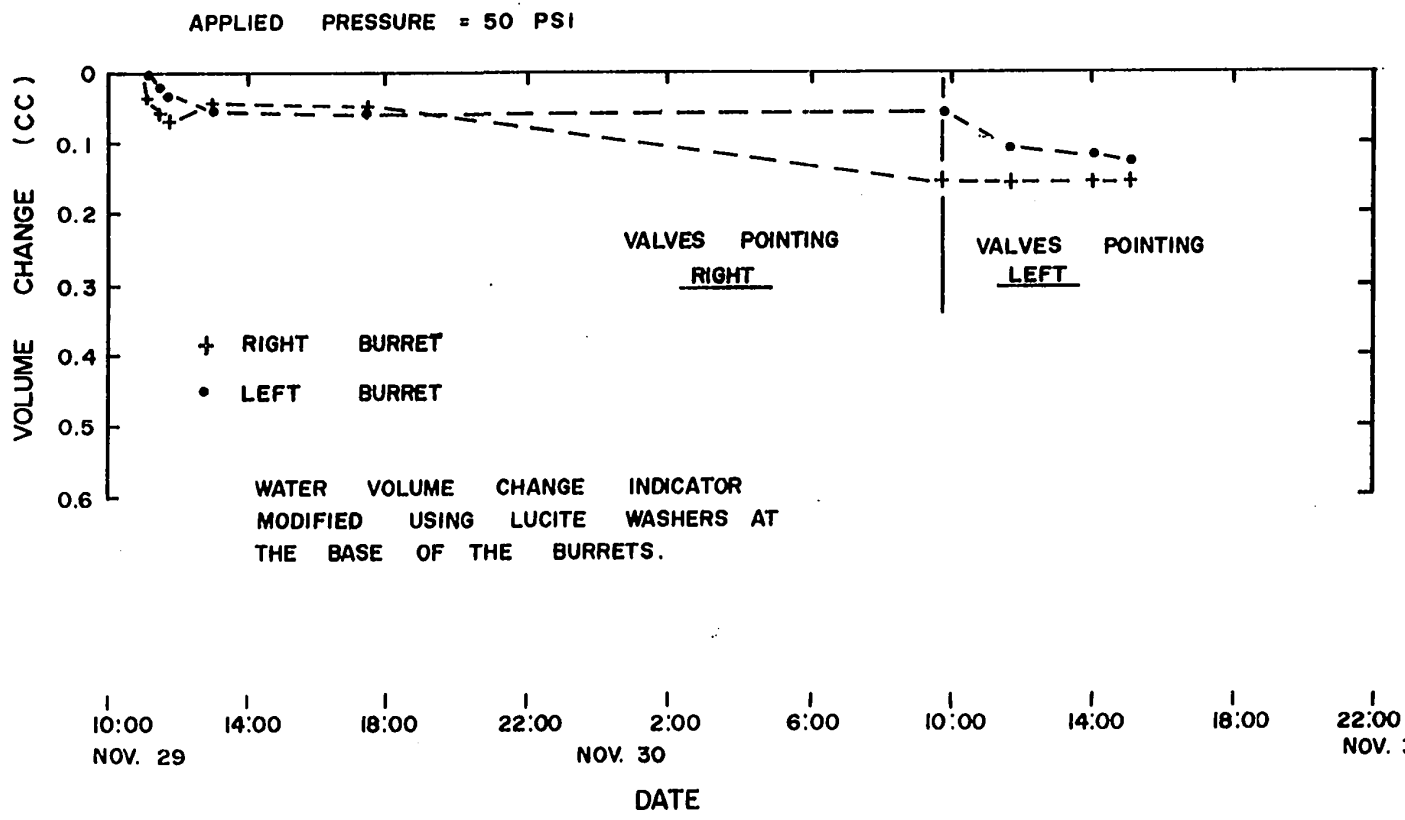


FIGURE B.14 LEAKAGE AROUND THE BASE OF THE BURRET



B33

FIGURE 9.15 LEAKAGE AFTER MODIFICATION TO THE WATER VOLUME CHANGE INDICATOR

change indicator used in conjunction with Oedometer #179 (Figure B.16). The pressure applied to the volume change indicator was 50 psi. Essentially zero volume change was recorded on the burret opposite to the direction the 3-way valves were pointing. A continuous volume change was recorded on the other burret. It should be noted that the pyrex glass burrets does not allow the diffusion of water.

To ensure the proper functioning of the water volume change indicator, it should be subjected to a back pressure of 50 psi with the valves pointing in one direction for several days. The observed volume change over a two day period should not exceed 1/10 th of a cc (Figure B.17). The direction of the valves should then be reversed and the check repeated.

The polyethylene lines on the volume change indicator and the line to the base plate also allow some leakage in response to a pressure gradient. The amount of leakage is generally insignificant but it can be reduced by using copper tubing rather than polyethylene tubing (Figure B.18).

The swedge-lock connectors do not appear to present any problems of leakage. In some instances, the Whitey valves had slow leaks. These were overcome by removing the plastic handle and tightening the valve packings.

(b) Base Plate

There are three possible sources of leakage from the base plate; namely, through the ceramic disc, past the O-ring seal between the base plate and the bottom of the chamber and through or around the valves connected to the base. Although water seeps through the

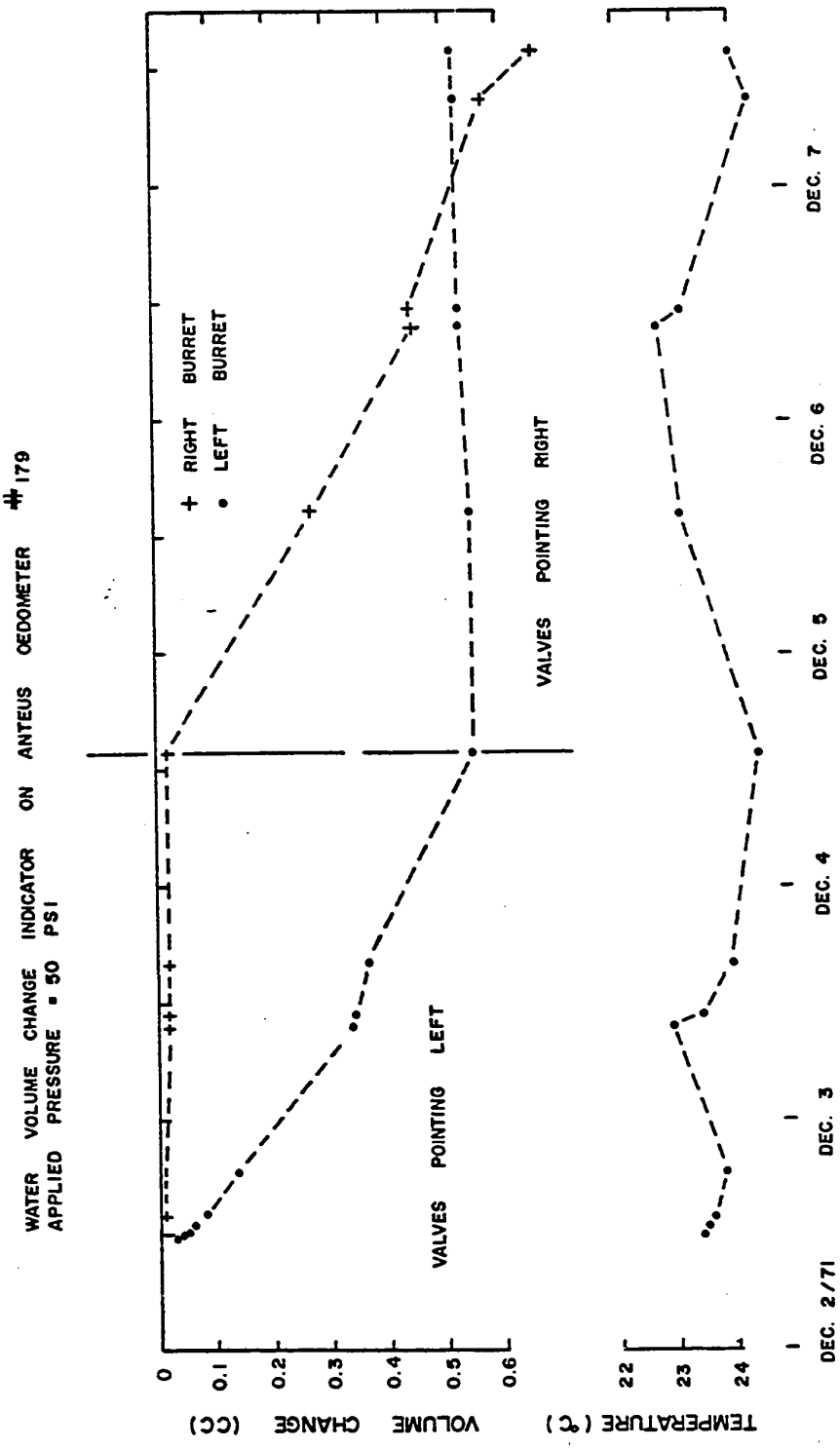


FIGURE B.16 EFFECT OF READING THE WRONG BURRET

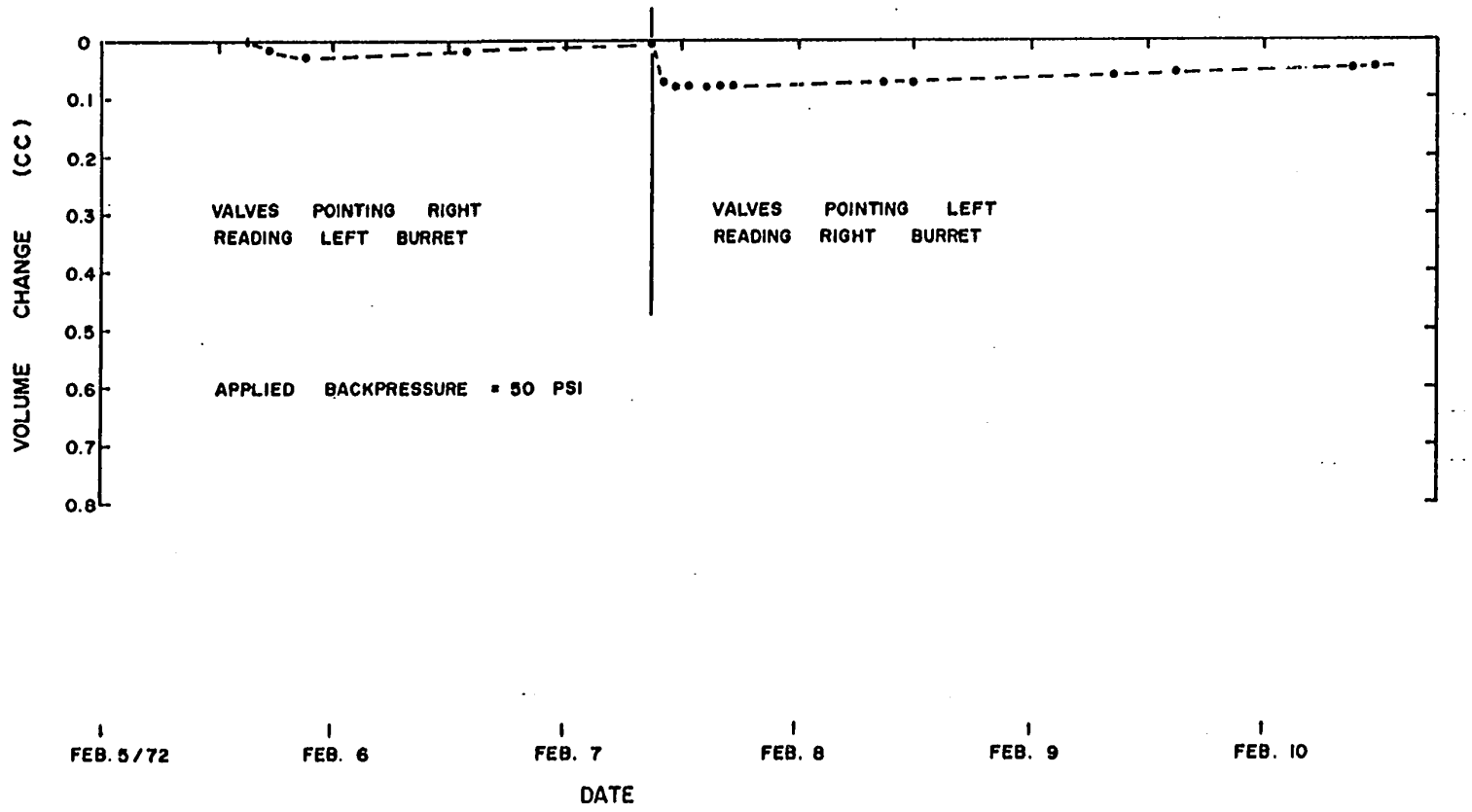


FIGURE B.17 CHECK TO ENSURE LEAKAGE FROM WATER VOLUME CHANGE INDICATOR

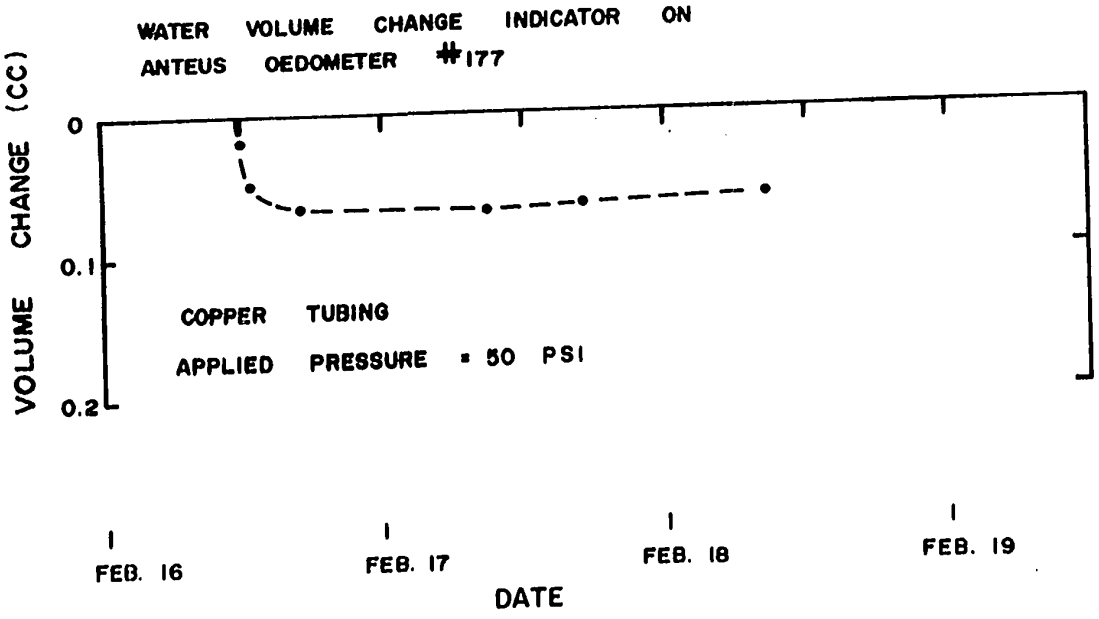


FIGURE B.18 CHECK AFTER USING COPPER TUBING FROM THE WATER VOLUME CHANGE INDICATOR

high air entry disc, it must not allow the passage of air at pressures below the air entry value. Air may diffuse through the water in the ceramic disc but this should not be considered as leakage. However, it becomes important to be able to differentiate between air diffusion and air leakage. The movement of air into the base plate compartment can readily be monitored by placing an air pressure directly on the saturated ceramic disc. Free air should not pass through the disc as long as it does not exceed the air entry value. Various attempts were made to stop the diffusion of air (Figure B.19) in order to check on air leakage past the O-ring between the base plate and the chamber base. For example, a rubber membrane (with silicone grease on top) was fastened over the disc. This merely changes the rate of diffusion but does not eliminate it. In Figure B.19, the rate of air diffusion through the disc without the rubber membrane is shown at an elapsed time of approximately 175 minutes. Diffusion through the rubber membrane and water is represented by the period from 200 to 260 minutes. The volume of air measured in the diffused air volume indicator checks closely with that measured on the water volume change indicator. Checks on the tightness of the valves and the alignment of the ports ensured they were not involved in the leakage. The rate of volume change is in keeping with that computed for the diffusion of air through water in the ceramic discs (see Chapter IV).

If free air is passing through the disc as a result of a rupture in the air-water meniscus, the rate of air flow increases by several orders of magnitude (Figure B.20). The rupture shown on the

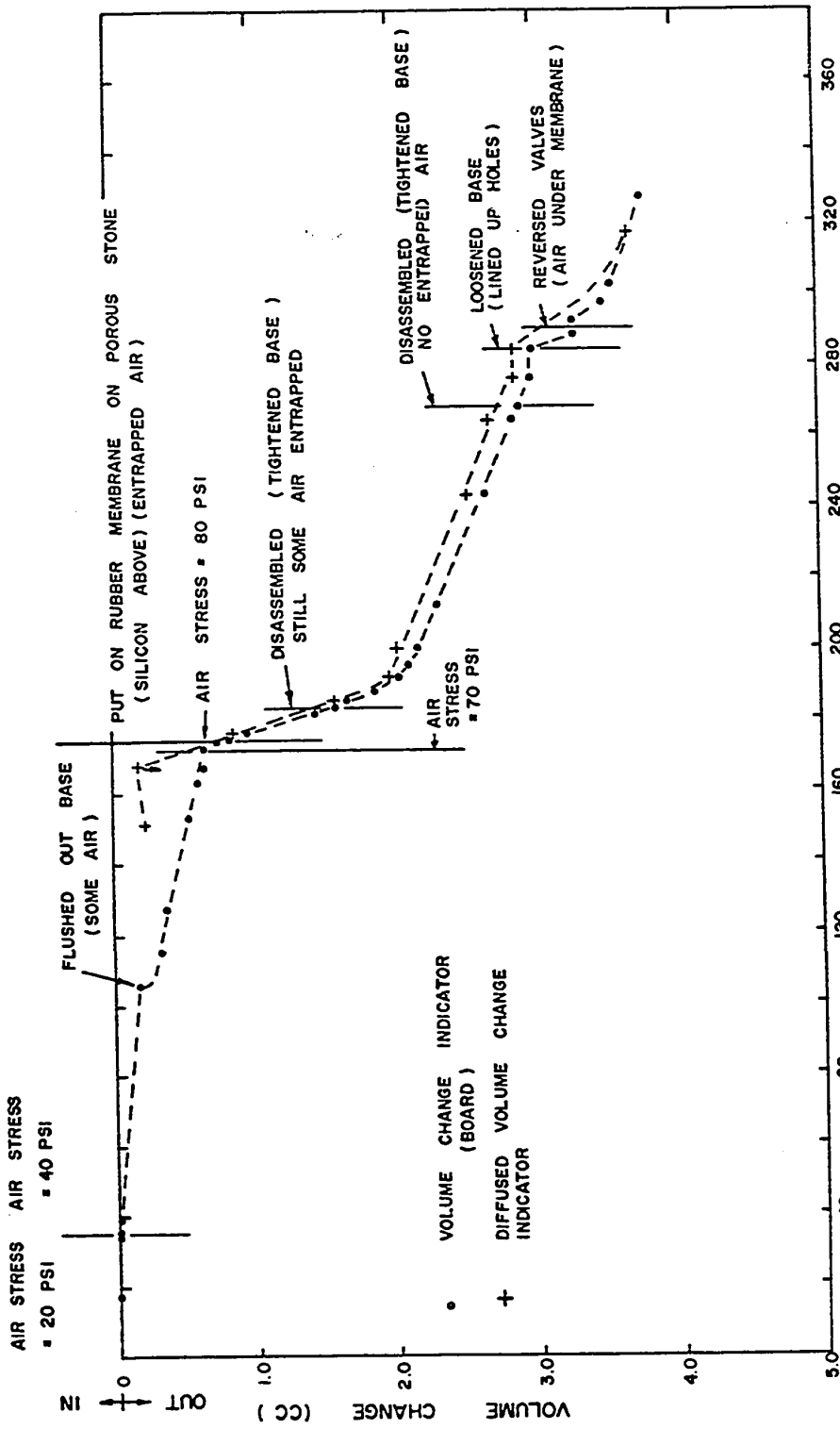


FIGURE B.19 LEAKAGE THROUGH HIGH AIR ENTRY DICS COVERED WITH A RUBBER MEMBRANE (OEDOMETER #179 ; 15 BAR, THIN CERAMIC DISC)

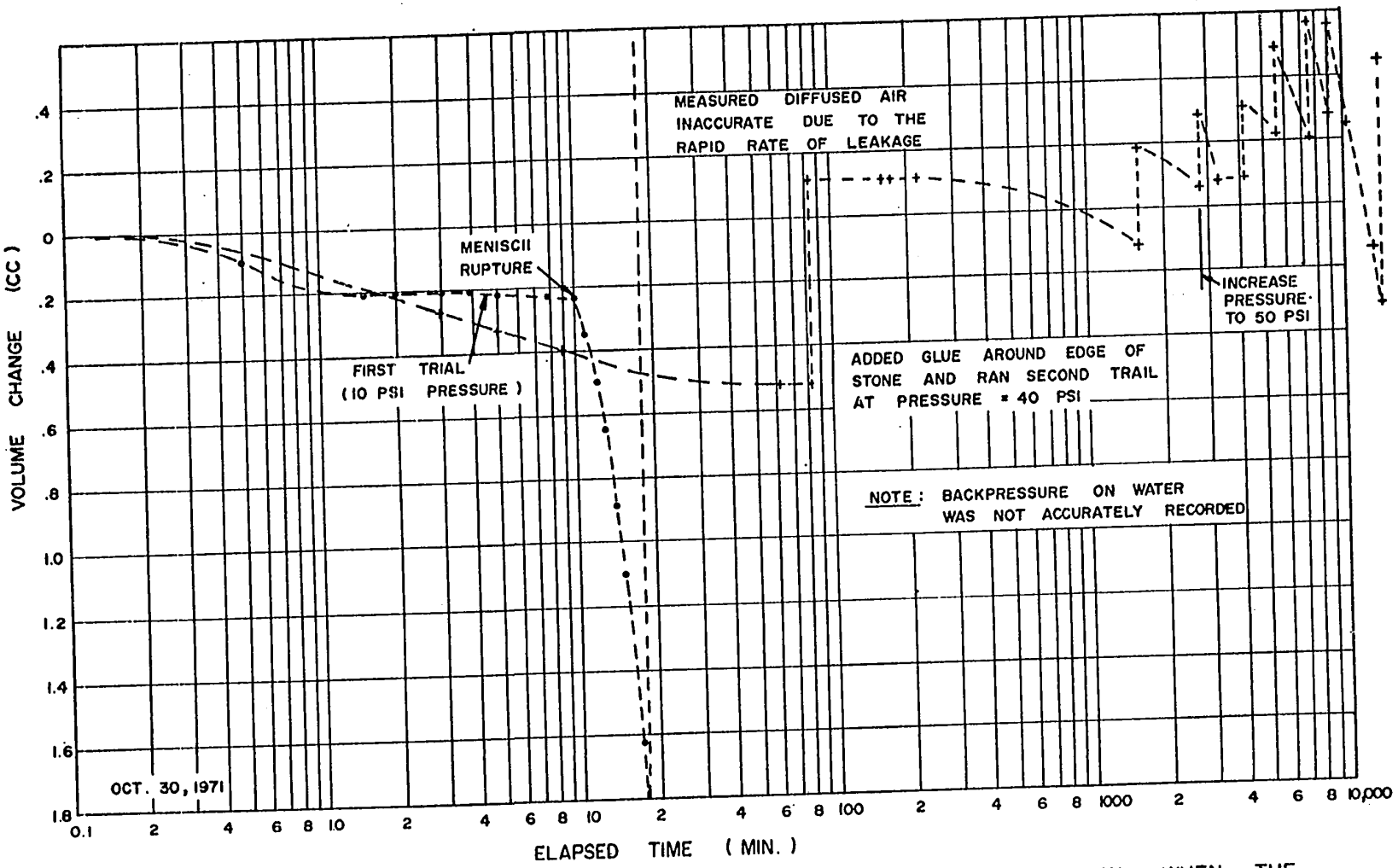


FIGURE B.20 MENISCUS RUPTURE ON A CRACKED DISC AND AIR DIFFUSION WHEN THE CRACK IS SEALED (OEDOMETER #177 ; 15 BAR , THIN CERAMIC DISC)

first trial was due to a fine crack in the ceramic disc. The crack in the disc was then sealed with Alpha Cyanoacrylate cement (VIGOR ARON ALPHA). The disc then withstood high air pressures with only a slow rate of air diffusion through the water. When the diffused air was monitored and subtracted from the water volume change indicator readings, the net result shows a cancelling effect. The two volume changes do not completely check due to an inaccuracy in the water back pressure reading. It was not realized at that time that the absolute pressure in the base plate must be accurately known. Also the flushing technique was not perfected at this time.

Another test (Figure B.21) was started with a small amount of water over the disc. The diffused air measured at the end of loading step #1 appears to have come out of solution due to the reduction in pressure. Loading steps #2 and #3 show that the water volume change indicator reading can be accounted for as diffused air.

The diffusion of air through the water in the disc is not considered as a leak. Only if the disc has a crack or does not withstand pressures up to the air entry value for some other reason, is the volume change termed a leak. Leakage and diffusion can generally be separated by observing the order of magnitude of the volume change. Leakage is generally considerable faster than diffusion. From Chapter II, diffusivity of air through water in a ceramic disc should always be less than 2×10^{-5} cm^2/sec. This is the diffusivity for pure water and the value when the water is in the high air entry, ceramic disc is approximately one order of magnitude less (i.e. 2×10^{-6} cm^2/sec).

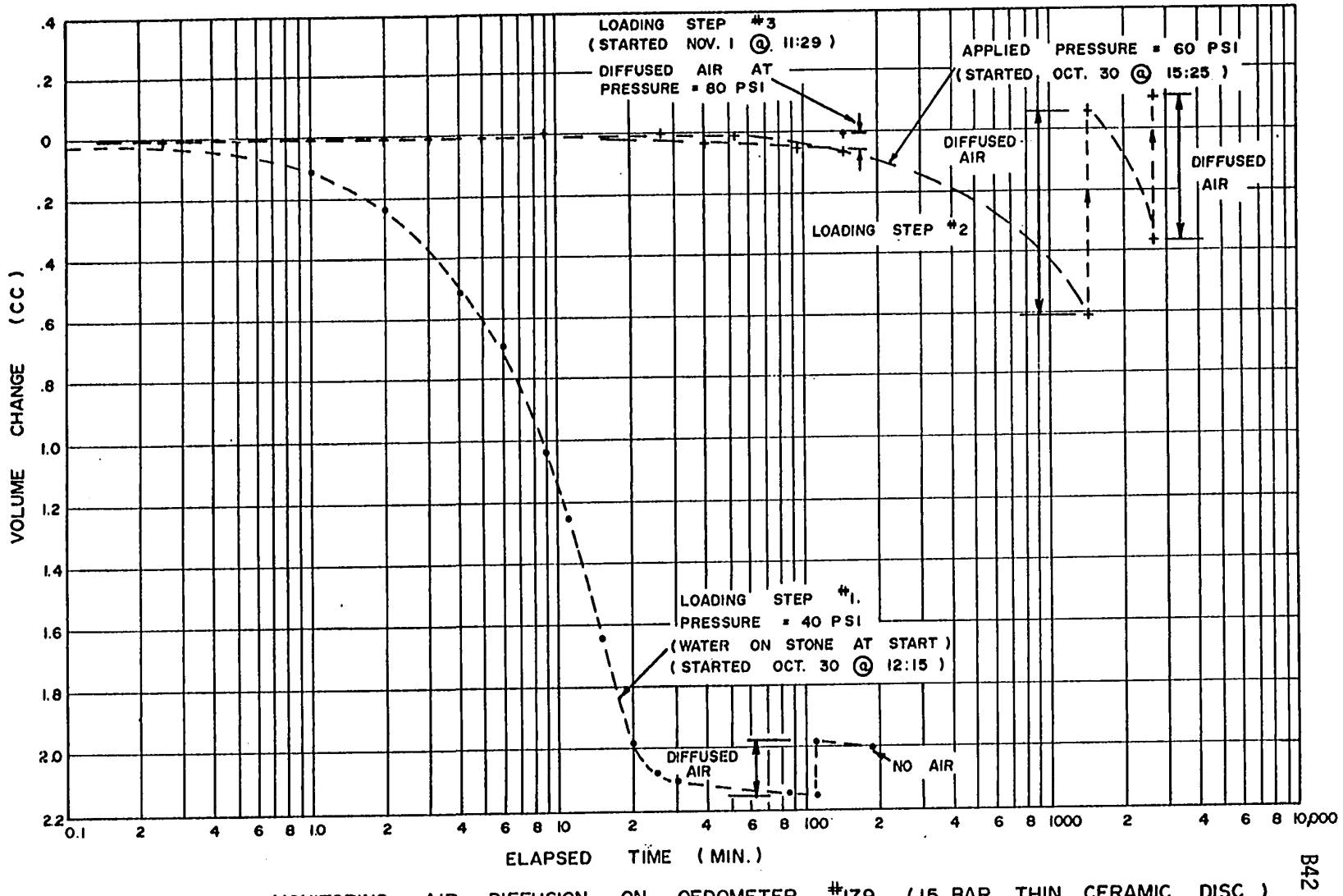


FIGURE B.21 MONITORING AIR DIFFUSION ON OEDOMETER #179 (15 BAR, THIN CERAMIC DISC)

B42

Leakage through the valves on the base plate can be observed by placing a high air pressure on the ceramic disc and a somewhat lower back pressure on the water. One part on the base is connected to the water volume change indicator and the other is closed. Water leakage from the closed or open valve is registered as a fictitious volume of water moving into the chamber (Figure B.22). There should be a few drops of water placed outside of the base plate (on the chamber base) during this test to assure 100 percent relative humidity in the chamber. To complete the check, the water volume change indicator should also be connected to the other port and the check repeated. Note that the diffusion of air through the base plate causes volume change opposite to that due to leakage of the valves. A correction is applied in agreement with the monitored diffused air.

Leakage from the valves can be checked more readily by performing a pore pressure response test. Any leakage from the compartment is reflected as a decrease in the slope of the response curve (from the theoretical value) or as a dramatic increase in the computed compressibility of the fluid in the measuring system (Figures B.23, B.24 and B.25). The pressure at which leakage occurs can be observed from the response curves (Figure B.24). This test can also be used to differentiate between a leak in the valves and a leak in the O-ring between the base plate and the chamber base. A leak in the O-ring would result in a response more rapid than that anticipated from the response theory.

A small nick in an O-ring in the Circle Seal valves on the

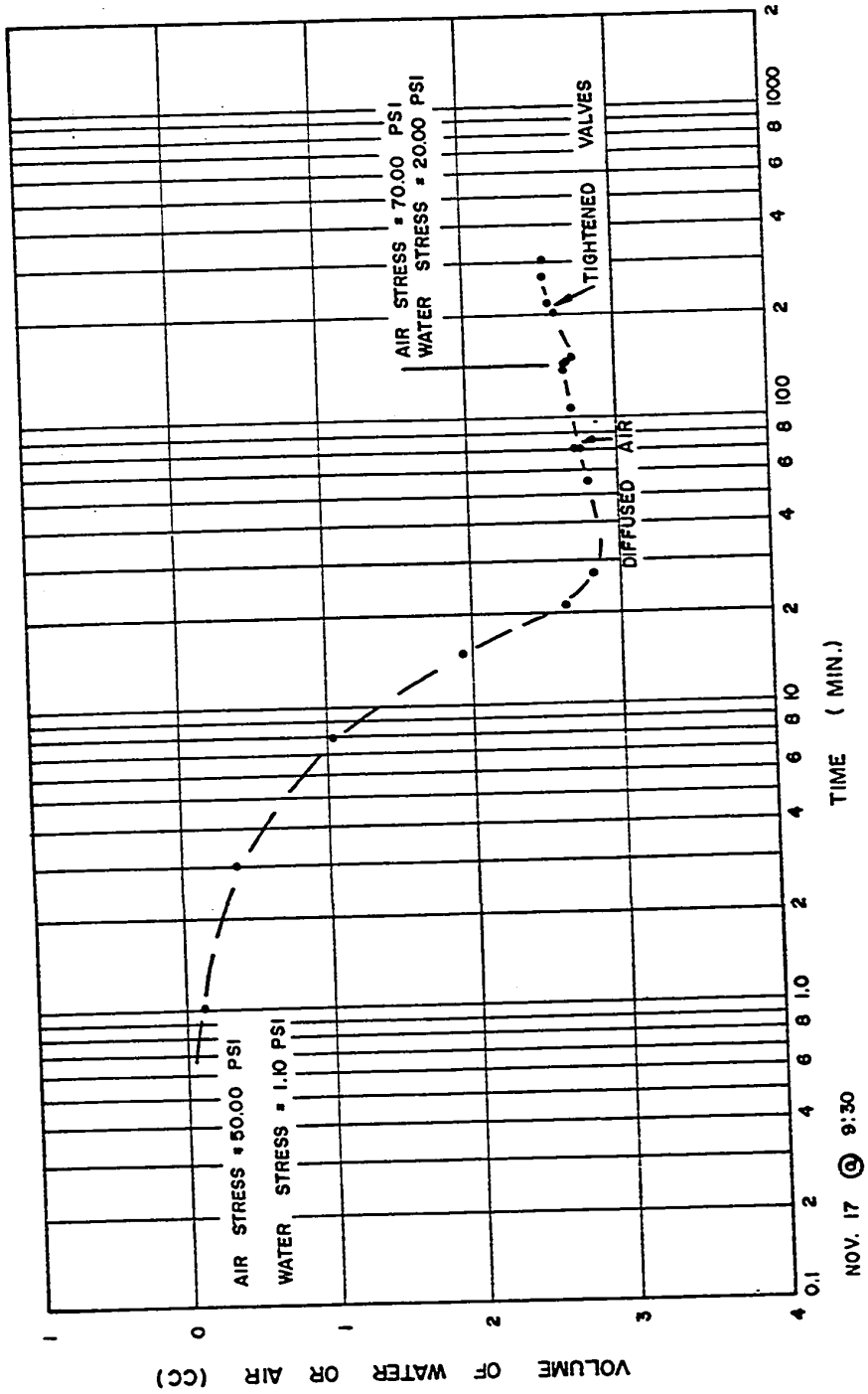


FIGURE B.22 EFFECT OF LEAKAGE FROM THE VALVES ON THE BASE PLATE
(OEDOMETER #179 ; 15 BAR , THIN CERAMIC DISC)

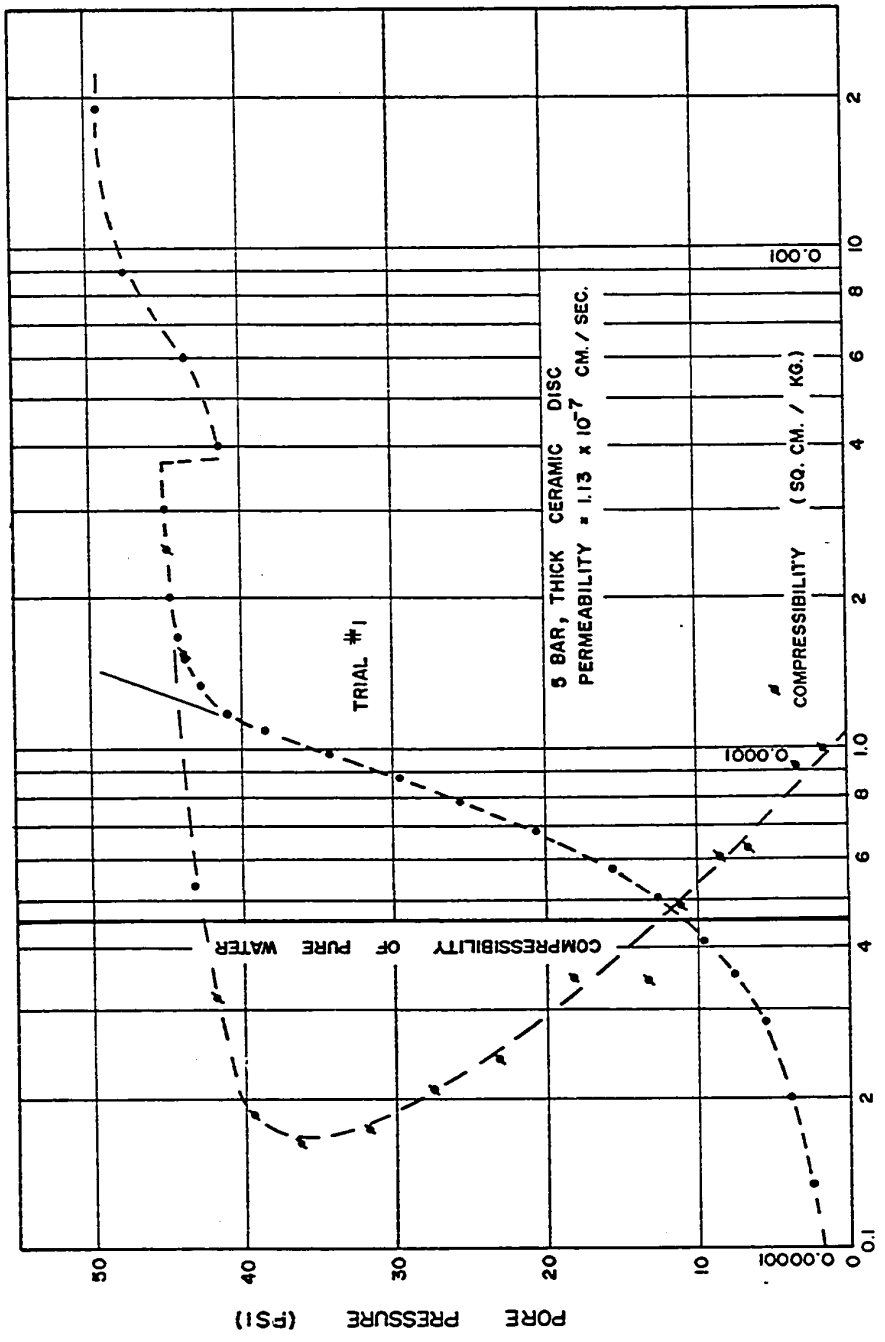


FIGURE B.23 PORE PRESSURE RESPONSE AND COMPRESSIBILITY FOR OEDOMETER #177 (FEB. 22, 1972)

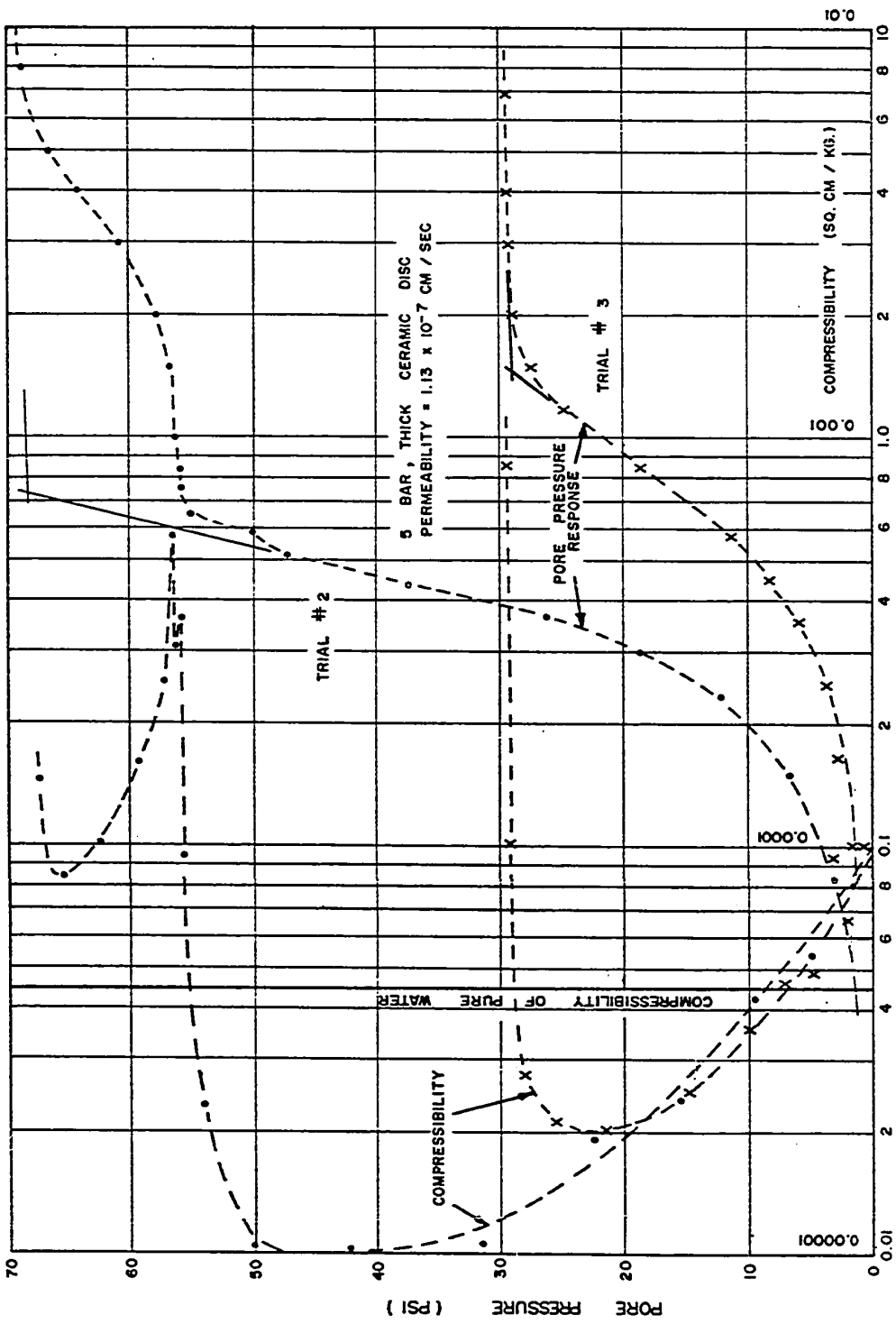


FIGURE B.24 PORE PRESSURE RESPONSE AND COMPRESSIBILITY FOR OEDOMETER # 177
(FEB. 22 , 1972)

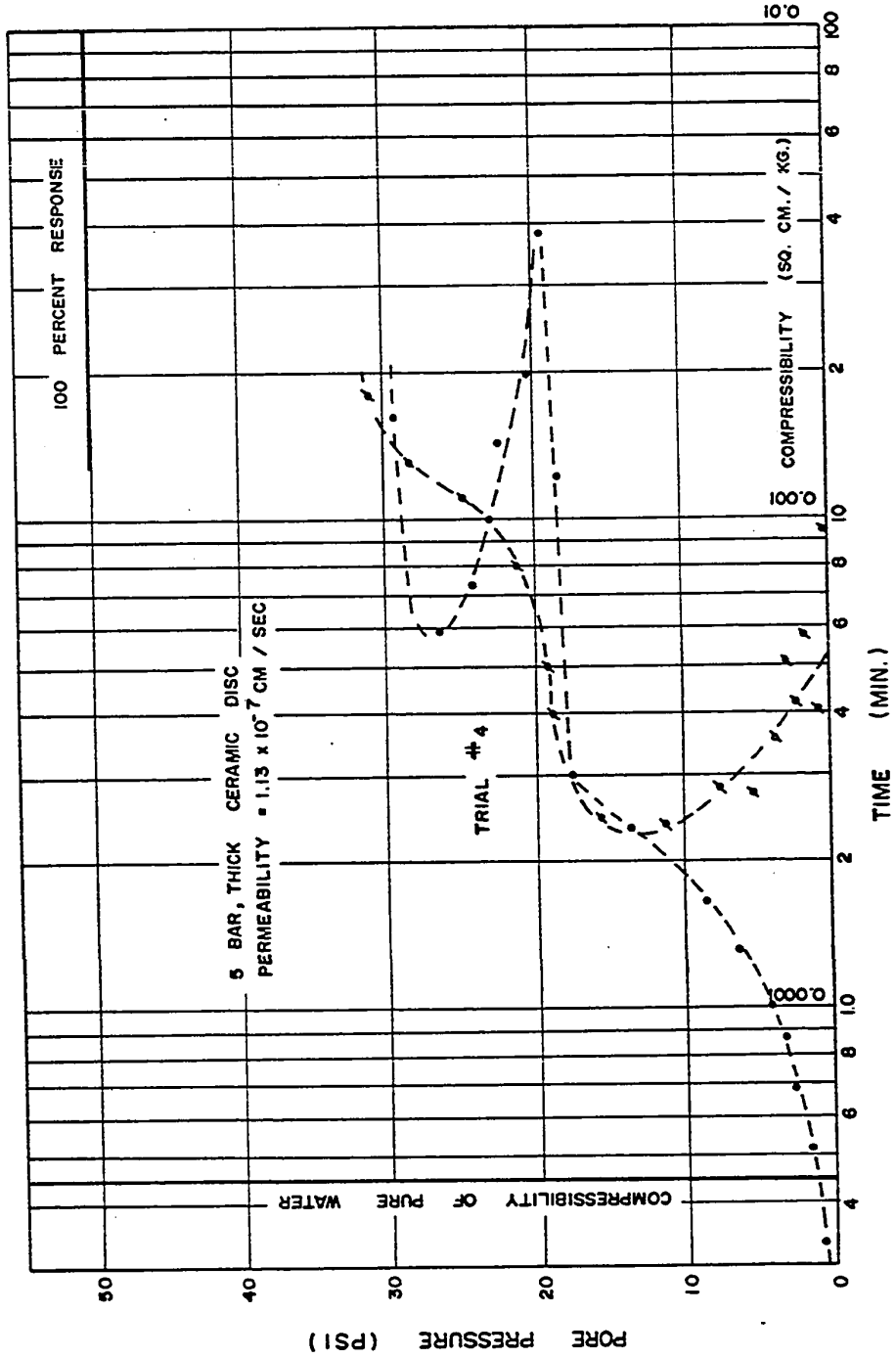


FIGURE B.25 PORE PRESSURE RESPONSE AND COMPRESSIBILITY FOR ŒDOMETER #177
(FEB. 22 , 1972)

base was the source of the leakages shown in the above Figures. The O-rings were made of neoprene rubber which reacted with the acetone used to wash out the ceramic disc. The reaction results in the swelling of the O-ring causing it to be squeezed out when the valve is turned. Attempts to close the valves pinched the O-ring, removing a nick. The old O-rings were substituted with Butyl rubber O-rings that do not react with acetone.

Water vapor is also lost or removed from the chamber if air leaks past the wall of the chamber. To ensure against air leakage from the chamber, the saturation vent valve is removed from the top of the dome and replaced with a pressure transducer. A pressure of 100 psi can be applied to the chamber and then the valve above the saturation water reservoir closed. The chamber pressure is monitored with time (Figure B.26). A leak shows up as a continuous and significant decrease in pressure. The monitored pressure change over a period of one day (Figure B.26) was less than 1 psi. The pressure change is believed primarily related to the air temperature change while leakage was insignificant.

B-7 The Permeability of Rubber and Lucite

A simple test was performed to observe the rate of movement of water through rubber and lucite (Figure B.27). Water was placed in several petri dishes that were then covered with a "latex" rubber membrane that was sealed against the dish with an O-ring. Pyrex glass does not allow any water loss over long periods of time and therefore

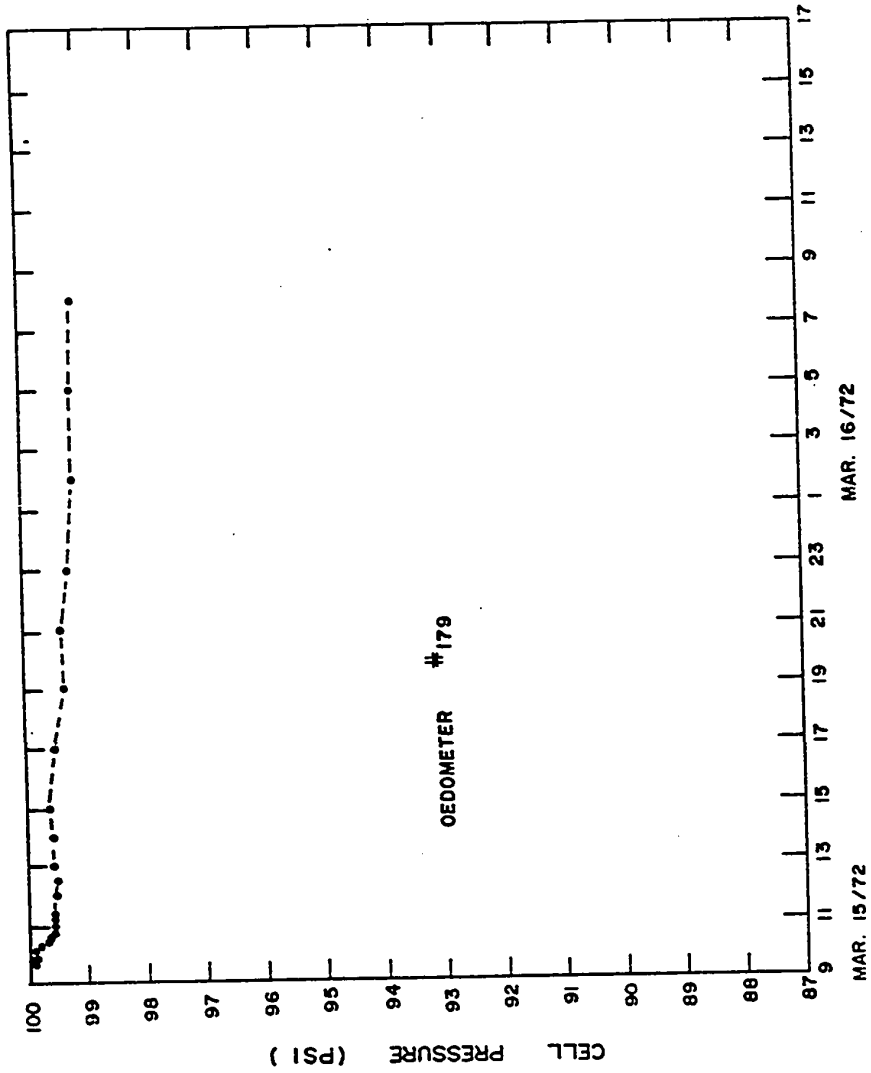
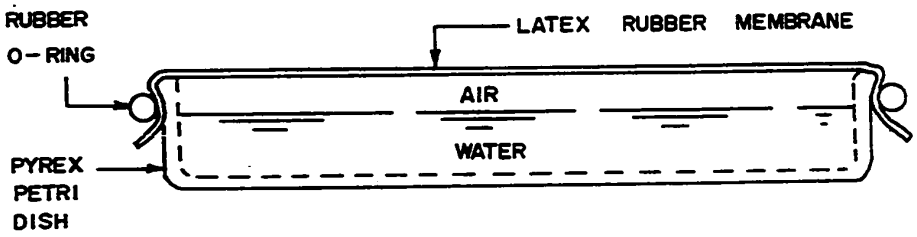
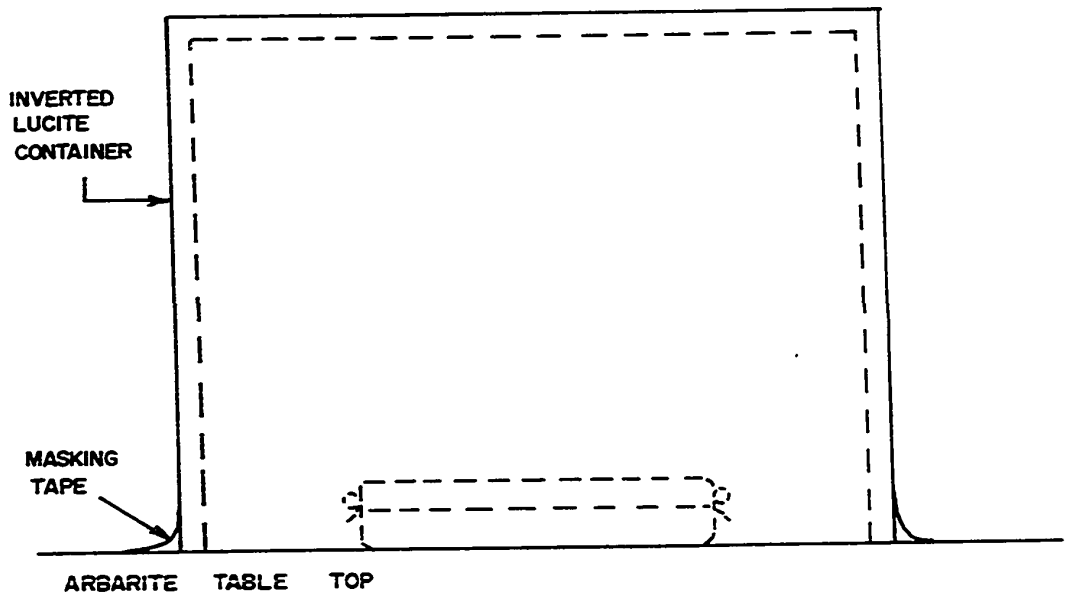


FIGURE B.26 CHECK ON AIR LEAKAGE FROM THE CHAMBER OF OEDOMETER #179



PETRI DISH COVERED WITH A LATEX RUBBER MEMBRANE



COVERED PETRI DISH PLACED BENEATH A LUCITE CONTAINER

FIGURE B.27 ASSEMBLAGE FOR MEASURING WATER AND WATER VAPOR LOSS THROUGH RUBBER AND LUCITE

any weight loss is due to the loss of water through the rubber. Water loss either in liquid or vapor form is of importance in assessing the performance of the laboratory equipment. The petri dishes were later placed under an enclosed lucite container to see if water vapor equilibrium could be established across the rubber membrane. The lucite container was taped to an arborite table top. Each three or four days, the tape was removed and the petri dish was carefully removed for weighing. An attempt was made to prevent any exchange of air under the lucite container.

Figures B.28 and B.29 show that steady state seepage through the latex membrane was established in approximately one day. The coefficient of permeability of rubber can be computed using Darcy's Law.

$$q = kiA \qquad \text{B.1}$$

where k = coefficient of permeability of rubber with respect to water

i = driving force designated as the change in vapor pressure across the membrane (i.e. $\Delta P_p/d$)

A = cross-sectional area of the membrane.

The rubber membranes in all three tests were 0.040 cm thick and the cross-sectional area of the petric dishes was 62.2 cm^2. Average environmental conditions in the laboratory were used to compute the vapor pressures above the rubber membrane. The relative humidity used was 25 percent and the temperature was 73°F (23°C). The air below the rubber membrane was assumed to have 100 percent relative humidity and

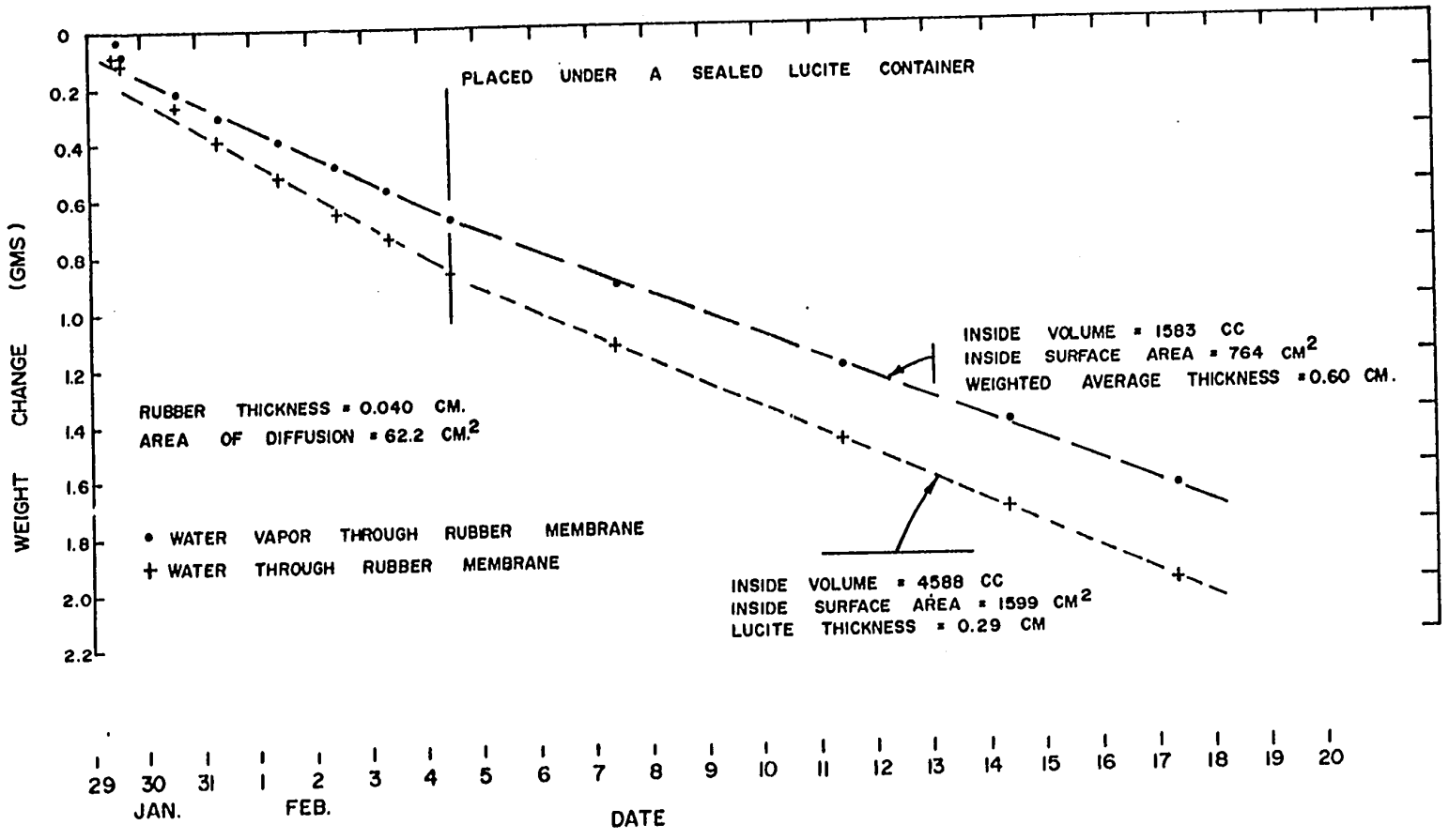


FIGURE B.28 DIFFUSION OF WATER AND WATER VAPOR THROUGH A RUBBER MEMBRANE

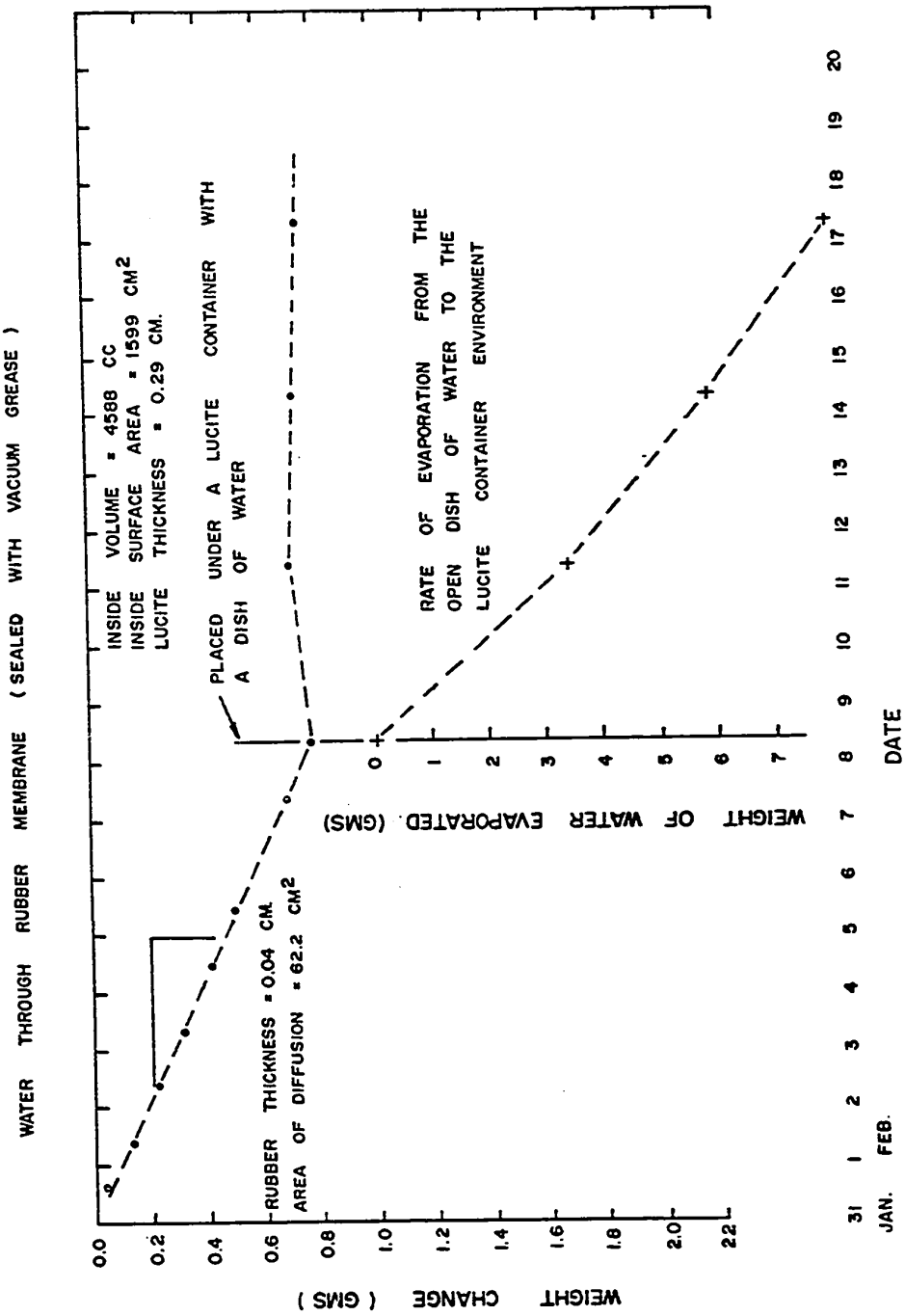


FIGURE B.29 DIFFUSION OF WATER THROUGH A RUBBER MEMBRANE SEALED WITH VACUUM GREASE

a temperature of 73°F. The vapor pressures corresponding to each relative humidity are computed from the general Gas Law. (see Chapter II). The vapor pressure at 100 percent relative humidity is 19.76 gms/cm^2 and 7.91 gms/cm^2 for 25 percent relative humidity. The coefficient of permeability is computed from

$$k = \frac{q(\text{cc/day}) \cdot d(\text{cm}) \cdot \gamma_w(\text{gms/cc})}{86{,}400(\text{sec/day}) \cdot A(\text{cm}^2) \cdot \Delta P_p(\text{gms/cm}^2)} \qquad \text{B.2}$$

The rates of flow and the coefficients of permeability are shown in Table B.10.

TABLE B.10

SUMMARY OF THE RATE OF WATER SEEPAGE THROUGH RUBBER

Test No.	Description	Rate of Flow(cc/day)	Permeability (cm/sec)
1	Water vapor below the rubber membrane (water at bottom of dish)*	0.093	5.84×10^{-11}
2	Water in contact with the membrane	0.113	7.10×10^{-11}
3	Water in contact with membrane (vacuum grease seal)	0.094	5.90×10^{-11}

*The membrane bowed up due to the vapor pressure increase.

The values are approximately one order of magnitude lower than those presented by Poulos (1964). Reporting on the work of Casagrande and Shannon (1948), Poulos showed "thin" latex membranes (0.005 cm) to have a permeability constant of 3.6×10^{-10} cm/sec.

It should be noted that latex rubber deteriorates with time when subjected to water or water vapor on one side and air on the other. By March 6, 1972 (elapsed time of 37 days) the rubber was completely cracked and rotten. The points of stress concentration deteriorated first. Deterioration was also noted in connection with soil tests that extended more than one month.

When the rubber covered petri dishes were placed under the lucite containers, the rate of water loss decreased (however, it was still substantial) but showed no sign of equilizing. In the case where open water containers were also placed under the lucite cover, the rate of water loss became essentially zero (Table B.11).

The lucite appears to impede the loss of water; however, it does not stop it. A test was performed placing some water in a small enclosed lucite container. The container was 234 cc with a surface area of 211 cm^2 and an average wall thickness of 0.66 cm (Figure B.30). The test was not continued long enough to accurately ensure the rate of water loss. The best-fit line through the data gives a value of 0.0162 cc per day corresponding to a permeability value of 4.95×10^{-11} cm/sec. This value is very similar to that of the rubber.

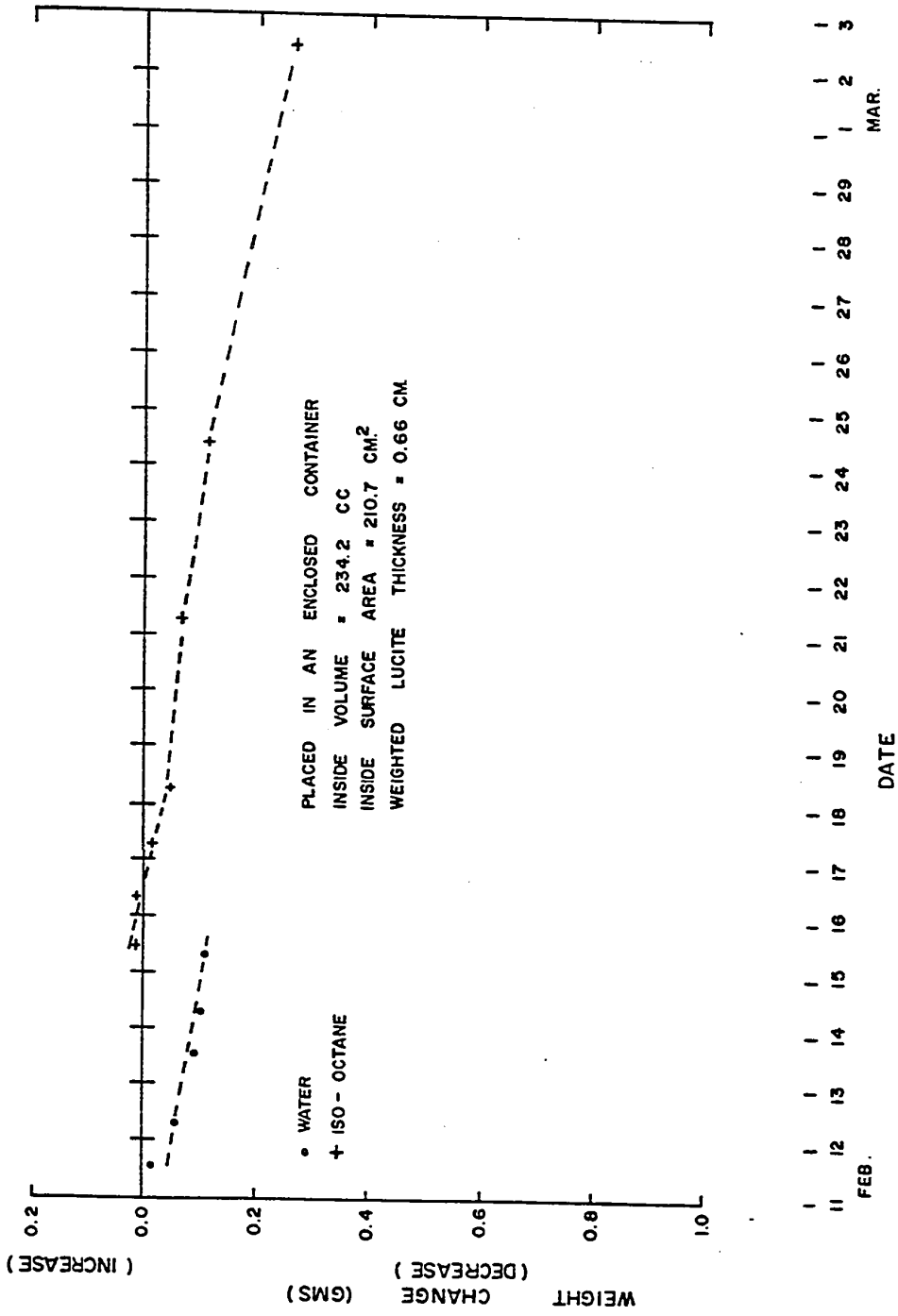


FIGURE B.30 DIFFUSION OF WATER AND ISO-OCTANE THROUGH A CLOSED LUCITE CONTAINER

TABLE B.11

RATE OF WATER LOSS FROM COVERED PETRI DISHES

PLACED BELOW LUCITE CONTAINERS

Test* No.	Rate of Water Loss (cc/day)	Volume of Lucite Container (cc)	Inside Surface Area (cm^2)	Average Lucite Thickness (cm)
1	0.077	1583	764	0.60
2	0.086	4588	1599	0.29
3	0.00**	4588	1599	0.29

*Test numbers correspond to those in Table B.10
**Rate of water loss from the open container was 0.170 cc/day

The International Critical Tables document three cases of measured transmission of moisture through Nitrocellulose ("Pyroxylin") plastics (Table B.12).

The values computed from the data in the International Critical Tables are in good agreement with those obtained in the laboratory. It would appear that lucite cannot be considered as impermeable to water transmission and must be kept in mind during equipment design.

Iso-Octane was also placed in the enclosed lucite container and the weight loss was approximately 0.016 cc/day (Figure B.30).

Two pieces of lucite were immersed in water and Figure B.31 shows their absorption of water with time. The small tube of lucite gained 0.43% by weight and the larger block gained 0.15% by weight after 6 days of immersion. The International Critical tables report

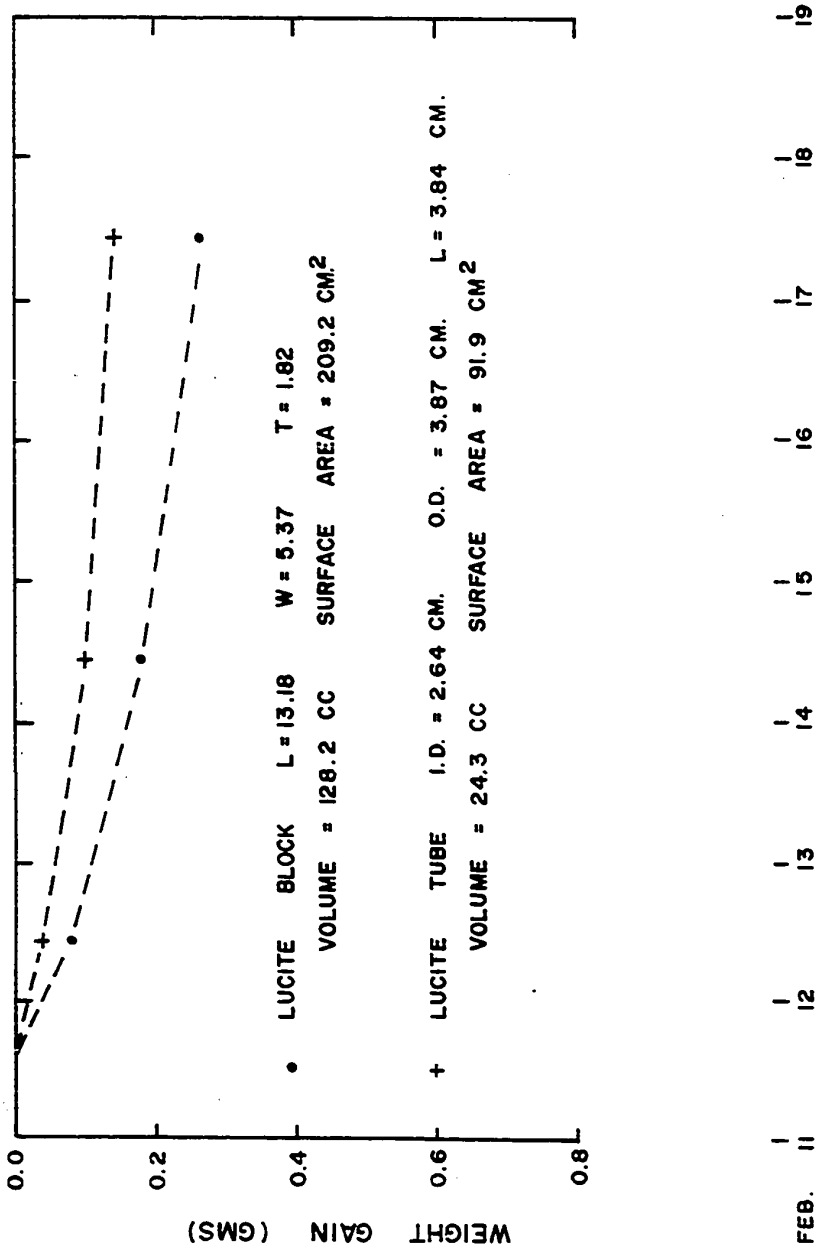


FIGURE B. 31 ABSORPTION OF WATER BY LUCITE

TABLE B.12

TRANSMISSION OF MOISTURE THROUGH NITROCELLULOSE PLASTICS

Case No.	Description	Thickness (cm)	Flow Rate ($cc/cm^2/day$)	Permeability** (cm/sec)
1 a.	One surface dried by $CaCl_2$ and the other exposed to the summer atmosphere	0.0762	0.000288	8.29×10^{-11}*
b.				1.38×10^{-10}*
2	Air dried by $CaCl_2$ on one side and saturated air on the other	0.160	0.00062	5.81×10^{-11}
3	Same as #2	0.0117	0.0117	3.08×10^{-11}

*Assumed a relative humidity of 100% for 1a) and 25% for 1b).
**A temperature of 63°F was assumed in all cases to compute the differential vapor pressure.

absorption values of 1.6% to 2.3% by weight. It appears that absorption in the tube and block was not complete.

B-8 Check on Initial, Final and Change in Volume Relations

The most significant check on the reliability of the volume change measurements relates to a comparison of the initial, final and change in volume measurements. For example, the measured initial conditions plus the change in volume conditions during the test should essentially equal the measured final conditions. If the results confirm this statement, it can be concluded that the equipment is functioning satisfactorily. The measurements related to the volume conditions, that are analysed are the height, diameter and water volume.

Tests #2 and #13 involved very soft specimens that underwent large deformations prior to the initial volume readings. Therefore they are ignored in the statistical evaluation of the volume measurements.

The height measurements are analysed primarily to emphasize the order of magnitude of the accuracy commonly associated with conventional consolidation testing. Table B.13 tabulates the height of sample measurements and compares the computed and measured final heights. The "deviation" of the computed and measured heights is designated as positive when the computed height is greater than the measured height.

On the one-dimensional oedometer tests, the mean of the "deviations" was -0.028 cm or a volume of 0.89 cc. Compared to an average height of the samples, the computed height was approximately 1.2 percent smaller than the measured height. The difference is probably related to the slight rebound in the sample between the time of the final vertical reading on the oedometer and the removal of the sample from the pedestal. The standard deviation between the computed and measured final heights is $\pm$ 0.03 or 0.96 cc.

On the triaxial specimens, the average difference between the computed and measured final heights is + 0.012 (0.96 cc) and the standard deviation is $\pm$ 0.058 (4.64cc). When compared to the average height of specimen used, the mean is approximately 0.2 percent and the standard deviation is approximately 1 percent of the total height. Thus, the reproducibility of the triaxial specimen heights are com-

TABLE B.13

ANALYSIS OF SAMPLE HEIGHT MEASUREMENTS

Test No.	Apparatus No.	Initial Height (cm)	Change in Height (cm)	Computed Final Height (cm)	Measured Final Height (cm)	Deviation (cm)
2	T-1	9.045	+0.394	8.651	8.20	+0.451
5	OED-177	2.734	+0.550	2.184	2.183	+0.001
6	OED-179	2.633	+0.522	2.111	2.114	-0.003
9	T-1	11.733	-0.058	11.791	12.200	-0.409
10	OED-177	2.515	-0.004	2.519	2.569	-0.050
11	OED-179	2.492	-0.011	2.503	2.549	-0.046
12	OED-177	1.80	+0.075	1.725	1.813	-0.088
13	T-1	3.282	+0.094	3.188	2.878	+0.310
14	OED-179	2.470	+0.357	2.113	2.194	-0.081
15A	OED-177	2.550	-0.046	2.596	2.616	-0.020
16	T-1	10.043	-0.088	10.131	10.131	0.000
17	OED-179	2.555	-0.081	2.636	2.671	-0.035
18	Bench-3	2.744	+0.022	2.722	2.747	-0.025
19	OED-179	2.273	+0.056	2.217	2.231	-0.014
20	T-2	5.827	+0.081	5.746	5.820	-0.074
21	T-1	11.740	-0.001	11.741	11.672	+0.069
22	T-2	6.347	+0.097	6.250	6.277	-0.027
23	Bench-3	2.540	-0.181	2.721	2.759	-0.038
24	OED-179	2.946	-0.012	2.958	2.969	-0.011
25	OED-177	3.172	+0.026	3.146	3.205	-0.059
28	OED-177	1.921	+0.042	1.879	1.901	-0.022
30	OED-177	2.556	+0.033	2.523	2.517	+0.006
32	T-1	5.057	-0.199	5.256	5.178	+0.078
33	OED-177	1.906	+0.026	1.880	1.894	-0.014
34	OED-179	2.216	-0.040	2.256	2.235	+0.021
35	T-2	5.089	-0.057	5.146	5.118	+0.028

parable to those of the one-dimensional oedometer tests.

The analysis of the diameter measurements on the triaxial specimens is presented in Table B.14. The mean final computed diameter is 0.008 cm (0.75 cc) larger than the final measured diameter. The standard deviation is $\pm$ 0.05 cm (4.72 cc). From the limited data available for analysis, it appears that the reliability of the diameter measurements is similar to those of the height measurements.

The most important volume analysis involves the water volume measurements. The results are presented in Table B.15. Samples tested prior to Test #15 did not have any flushing of diffused air capabilities. Tests #15A, #16 and #17 had the diffused air volume indicators installed after the first few days of testing. Therefore, the diffused air volume was accounted for during most of the test. The remainder of the tests had complete corrections applied for the diffused air volume.

The two triaxial tests performed with no flushing show a computed final water volume 2.0 cc greater than the measured final water volumes. Four oedometer tests show a computed water volume 1.5 cc greater than the measured final water volume. In the case of the oedometer tests, there are two factors involved in the loss of water from the specimen. First, some water may be lost from the sample via the lucite chamber. Second, the diffusion of air through the high air entry disc produces a fictitious water loss. The two factors produce compensating types of errors. The first factor (i.e., water loss from the chamber) appears to have been the most dominant. All

TABLE B.14

ANALYSIS OF SAMPLE DIAMETER MEASUREMENTS

Test No.	Apparatus No.	Initial Diameter (cm)	Change in Diameter (cm)	Computed Final Diameter (cm)	Measured Final Diameter (cm)	Deviation (cm)
2	T-1	10.200	+0.141	10.059	8.638	+1.421
9	T-1	10.169	+0.105	10.064	10.060	+0.004
13	T-1	10.215	+0.205	10.010	9.949	+0.061
16	T-1	10.288	+0.060	10.228	10.281	-0.053
20	T-2	10.177	+0.550	9.627	10.040	-0.413
21	T-1	10.160	+0.040	10.120	9.874	+0.246
22	T-2	10.160	+0.081	10.079	10.032	+0.047
32	T-1	10.241	-0.124	10.365	10.296	+0.069
35	T-2	10.218	+0.075	10.143	10.226	-0.083

the tests were of a relatively short average duration of 22,600 minutes.

In the triaxial tests where the diffused air volume was measured and accounted for, the mean computed final water volume is 1.73 cc less than the measured final water volumes. The standard deviation is $\pm$ 7.3 cc or 0.9 percent. This demonstrates a slightly greater reliability than that obtained for the total volume measurements.

The one-dimensional oedometer tests show a mean computed final water volume 0.76 cc greater than the measured final water volume and a standard deviation of $\pm$ 1.86 cc (3 percent). On a percentage basis, the water volume measurements in the oedometer samples

TABLE B.15

ANALYSIS OF WATER VOLUME MEASUREMENTS

Test No.	Apparatus No.	Duration of Test (min)	Initial Volume of Water (cc)	Change in Water Volume (cc)	Computed Final Water Volume (cc)	Measured Final Water Volume (cc)	Deviation (cc)
2	T-1	37,110	430.13	+31.15	398.98	192.30	+206.68
6	OED-179	23,060	48.69	+36.14	12.55	37.15	-24.60
9	T-1	35,900	332.95	-103.65	436.60	434.67	+ 1.93
10	OED-177	23.340	35.81	+ 0.78	35.03	35.82	- 0.79
11	OED-179	23,240	35.88	- 0.63	36.51	36.27	+ 0.24
12	OED-177	12,710	33.16	+ 0.82	32.34	29.38	+ 2.96
13	T-1	21,200	129.47	+14.63	114.84	112.69	+ 2.15
14	OED-179	18,960	48.65	+ 8.36	40.29	36.71	+ 3.58
15A	OED-177	45.930	25.46	- 5.05	30.51	30.96	- 0.45
16	T-1	113,750	319.16	-28.11	347.27	349.93	- 2.66
17	OED-179	30.070	27.21	- 4.73	31.94	31.94	0.00
19	OED-179	20,090	22.61	-10.13	32.74	27.59	+ 5.15
20	T-2	31,730	148.65	-47.04	195.69	190.64	+ 5.05
21	T-1	117,670	376.15	- 8.69	384.84	392.24	- 7.40
22	T-2	41.890	223.83	- 4.11	227.94	218.79	+ 9.15
24	OED-179	10.180	35.20	+ 0.31	34.89	35.60	- 0.71
25	OED-177	13,090	47.09	- 0.50	47.59	47.08	+ 0.51
28	OED-177	7,470	26.66	0.00	26.66	24.96	+ 1.70
30	OED-177	17,070	36.29	- 0.01	36.30	36.17	+ 0.14
32	T-1	141,170	164.23	-19.57	183.80	192.98	- 9.17
33	OED-177	126,680	23.49	- 3.19	26.68	27.54	- 0.86
34	OED-179	125,280	25.57	- 6.32	31.89	30.53	+ 1.36
35	T-2	122,220	156.14	-23.32	179.46	184.81	- 5.35

as reliable as the total volume measurements. However, the volumes of water involved are extremely small and the duration of the tests was relatively long. The average duration of the triaxial and one-dimensional tests was 64,300 minutes.

Table B.16 summarizes some of the accumulated diffused air volumes measured in the triaxial and oedometer tests. Obviously the omission of these volumes over the duration of a lengthy test produces a considerable error. The overall average rate of air diffusion in the samples tested is 0.12 cc of air per day. This value is merely a rough guide and is significantly affected by the air and water pressures involved during the test.

The foregoing discussions consider checking against the final measurements. Although the error involved in the diffusion of air may be relatively small over a period of a few days, it may significantly affect the results of the process under consideration. In other words, it is necessary to have a higher degree of accuracy on the measurements of volume change than on the initial and final measurements. Based on the measurements of total volume change recorded during a conventional one-dimensional consolidation test, the accuracy of the volume change measurement should be approximately one order of magnitude greater than the initial and final measurements. Applying this reasoning to the water phase, it becomes necessary to measure the volume of diffused air on essentially all tests involving the assessment of unsaturated soil processes. The modifications adopted in both the triaxial and the oedometer test

equipment appear to produce the desired reliability, even over extended periods of time.

TABLE B.16

SUMMARY OF DIFFUSED AIR VOLUMES

Test No.	Apparatus No.	Duration of Test (min)	Volume of Diffused Air at the Chamber Pressure
15A	OED-177	45,930	1.50*
16	T-1	113,750	2.21*
17	OED-179	30,070	1.88*
20	T-2	31,730	4.96
21	T-1	117,670	7.04
32	T-1	141,170	11.05
33	OED-177	126,680	4.81
34	OED-179	125,280	5.89
35	T-2	122,220	9.05

*Diffused air volume measured for only a part of the entire test.

APPENDIX C

ANALYSIS OF THE NULL TESTS

CONTENTS OF APPENDIX C

		Page
C-1	General	C1
C-2	Null Test Analysis on Saturated Samples (Section I)	C5
C-3	Null Test Analysis on Saturated Samples (Section II)	C25
C-4	Null Test Analysis on Unsaturated Samples	C39

ANALYSIS OF THE NULL TESTS

C-1 General

The null test program involved a series of tests on saturated samples and a series of tests on unsaturated samples. The program on the saturated samples can be divided into two sections. The tests in section I were performed by simultaneously changing the total and water pressures and measuring the overall volume change with time. These tests were performed to check the procedure and equipment for a known case, thereby establishing the degree of reliability and accuracy that could be anticipated. In the triaxial apparatus, the change in the total volume of the sample was monitored along with the change in the volume of water in the sample. In the one-dimensional apparatus, only the total volume change of the sample was monitored due to the design of the equipment.

The tests in section II have an air pressure applied to the top of the saturated samples. The null tests involved simultaneously changing the total, air and water pressures by equal amounts. In this case, the air pressure reaction time was instantaneous and it was desirable to ascertain whether or not equilibrium could be maintained with an air-water interphase (contractile skin) at the surface of the sample. The total and water volume changes were monitored for all tests.

The main part of the testing program involved null tests on

unsaturated samples with various degrees of saturation. The total and water volume changes were monitored with respect to time.

The basic data acquired and presented for all null tests, is the total and water volume changes with respect to time. In general, these volume changes are divided by the total volume of the sample. That is, the data is presented as a percent volume change or as a porosity change. The volume change is defined as positive (+) when the sample volume decreases or when water or air come out of the sample and vice versa. For most of the tests, the record of the pressure readings with time are also plotted. These indicate the accuracy of the constant pressure system.

The analysis of the experimental data is discussed with respect to the following general questions:

(i) What are the test procedural factors affecting the results?

(ii) What is the effect of air diffusion through the sample or water evaporation from the sample?

(iii) What is the effect of secondary consolidation?

(iv) Approximately what amount of volume change would be anticipated if the stress state variables were changed by the amount the stress components are changed?

(v) How much volume change occurred in the soil structure (total sample) and the water phase? Fundamentally, it is the stress state variables of the soil structure and the contractile skin that are being experimentally verified. The percent volume change in the contractile skin is

analogous to the percent air volume change. The test technique is such that the air porosity change is not directly measured. Rather, it is computed as the difference between the total volume change and the water volume change. Continuity assures that the contractile skin equilibrium is maintained when the total and water volume changes are maintained. Thus, the most basic data measured (i.e. total and water volume change) are plotted.

(vi) Is a PROCESS occurring? If so, why is it occurring? These questions are most important when assessing the validity of the proposed stress state variables. If a process is occurring that is related to factors other than a change in the stress components, it can be concluded that the null test has not produced a process. In other words, test procedural factors and secondary soil properties must be separated from any "real" process that may be taking place.

The null tests were performed on Devon silt, kaolin and a mixture of Devon silt and kaolin. The classification properties are presented in Table C.1.

TABLE C.1

SOIL PROPERTIES OF SAMPLES USED FOR NULL TESTS

Soil Type	Samples Tested	Specific Gravity	Liquid Limit %	Plastic Limit %	Silt Sizes %	Clay Sizes %
Devon silt	1	2.695	31	23	80	18
80% Devon silt plus 20% Kaolin	2,3	2.679	38	25	67	31
Kaolin	4,6,7,9,10, 11,20,22, 27,30,31	2.616	64	35	15	85

C-2 Null Test Analysis on Saturated Samples (Section I)

The null tests performed for Section I of the test program are summarized in Table C.2. The volume weight relationships for each sample are shown in Table C.3. The data represents the conditions at the start of each null test. The pressure changes associated with each null test are summarized in Table C.4. The "After Pressure Changes" tabulated are those at the end of the null test.

The results of three tests performed on Devon silt are shown in Figure C.1 to C.3 inclusive. The sample was initially mixed as a slurry; however, no attempt was made to remove entrapped air. The measured volume changes are primarily related to the entrapped air. The silt does not exhibit significant secondary consolidation characteristics but is very sensitive to disturbance. There was difficulty in obtaining accurate volume measurements on the soft, sensitive sample and as a result, the computed degrees of saturation may not be reliable.

On the first null test, (N-1) the total and water pressures were increased in one psi increments for a total of 10 psi. The first measurement of water pressure was somewhat inaccurate resulting in too large a water pressure change for the first increment. The effective stress dropped by two psi at the start and an additional 0.8 psi during the remainder of the test. Water went into the sample in response to the increase in the water pressure. The sample decreased slightly in volume; however, more readings of the total volume should have been recorded. For the first few null tests there was some difficulty in

TABLE C.2

SUMMARY OF NULL TESTS ON SATURATED SAMPLES

(Controlling Total and Water Pressures)

Test No.	Sample No.	Date	Starting Time	Apparatus No.	Soil Type	Change in Pressures (psi)	Comments
N-1	1	Mar. 20/71	11:05	T-1	Devon Silt	+ 10	Increased in 1 psi increments
N-2	1	Mar. 21/71	16:10	T-1	Devon Silt	+ 10	Increased in 5 psi increments
N-3	1	Mar. 26/71	19:30	T-1	Devon Silt	- 40	Decreased in 5 psi increments
N-4	2	May 14/71	9:00	T-1	80% Devon Silt + 20% Kaolin	+ 10	One increment
N-5	2	June 1/71	13:30	T-1	80% Devon Silt + 20% Kaolin	- 20	One increment
N-6	2	June 2/71	20:00	T-1	80% Devon Silt + 20% Kaolin	-25	One Increment
N-7	3	June 10/71	12:21	OED-179	80% Devon Silt + 20% Kaolin	+ 10	Measured total volume change
N-8	3	June 10/71	15:30	OED-179	80% Devon Silt + 20% Kaolin	+10	Measured total volume change
N-9	3	June 11/71	8:50	OED-179	80% Devon Silt + 20% Kaolin	- 10	Measured total volume change
N-10	3	June 11/71	9:20	OED-179	80% Devon Silt + 20% Kaolin	- 10	Measured total volume change
N-11	3	June 11/71	10:30	OED-179	80% Devon Silt + 20% Kaolin	-10	Measured total volume change
N-12	3	June 11/71	11:35	OED-179	80% Devon Silt + 20% Kaolin	- 10	Measured total volume change
N-13	4	June 14/71	13:30	T-1	Kaolin	+ 10	
N-14	4	June 15/71	13:00	T-1	Kaolin	+ 10	
N-15	4	June 16/71	8:45	T-1	Kaolin	+ 10	

TABLE C.3

VOLUME-WEIGHT RELATIONSHIPS FOR SATURATED SAMPLES

(Controlling Total and Water Pressures)

Test No.	Diameter (cm)	Height (cm)	Total Volume (cc)	Volume of Solids (cc)	Volume of Water (cc)	Volume of Air (cc)	Water Content %	Void Ratio	Dry Density (PCF)	Degree of Saturation (%)
N-1	9.618	9.565	694.96	415.73	271.56	7.67	24.24	0.6717	100.6	97.3
N-2	9.610	9.619	697.65	415.73	278.19	3.73	24.82	0.6781	100.2	98.8
N-3	9.552	9.399	673.49	415.73	257.76	0.00	24.02	0.6200	103.8	100.0
N-4	8.676	8.914	526.93	295.52	225.88	5.53	28.53	0.7831	93.8	97.6
N-5	8.542	8.532	488.92	295.52	192.53	0.88	24.32	0.6545	101.0	99.5
N-6	8.540	8.525	488.27	295.52	192.74	0.01	24.35	0.6522		100.0
N-7	6.350	2.448	77.51	44.60	32.91	--	27.55	0.7379	96.2	--
N-8	6.350	2.447	77.50	44.60	32.90	--	27.53	0.7376	96.2	--
N-9	6.350	2.447	77.48	44.60	32.88	--	27.52	0.7373	96.2	--
N-10	6.350	2.447	77.48	44.60	32.88	--	27.52	0.7373	96.2	--
N-11	6.350	2.447	77.48	44.60	32.88	--	27.52	0.7373	96.2	--
N-12	6.350	2.446	77.47	44.60	32.87	--	27.52	0.7371	96.2	--
N-13	9.854	6.280	478.96	193.43	279.66	5.87	55.27	1.4762	65.9	97.9
N-14	9.851	6.276	478.29	193.43	279.53	5.33	55.2	1.4727	66.0	98.1
N-15	9.846	6.275	477.77	193.43	279.41	4.93	55.22	1.4701	66.1	98.3

TABLE C.4

RECORD OF PRESSURE CHANGES FOR NULL TESTS ON SATURATED SAMPLES

(Controlling Total and Water Pressures)

Test No.	Prior to Pressure Changes			After Pressure Changes			Change in Total Pressure (psi)	Change in Water Pressure (psi)
	Total Pressure (psi)	Water Pressure (psi)	$\sigma-u_w$ (psi)	Total Pressure (psi)	Water Pressure (psi)	$\sigma-u_w$ (psi)		
N-1	11.55	1.86	9.69	21.48	14.34	7.14	+ 9.93	+12.48
N-2	21.48	14.11	77.38	31.41	24.87	6.54	+ 9.93	+10.76
N-3	81.25	41.56	39.69	41.72	1.47	40.25	-39.53	-40.09
N-4	29.49	21.69	7.80	40.11	32.23	7.89	+10.62	+10.54
N-5	89.58	51.85	37.73	69.51	31.76	37.75	-20.07	-20.09
N-6	69.51	31.76	37.75	44.66	6.93	37.73	-24.85	-24.83
N-7	63.99	50.06	13.93	74.11	60.18	13.93	+10.12	+10.12
N-8	74.11	60.18	13.93	83.71	69.78	13.93	+10.12	+10.12
N-9	83.71	69.78	13.93	73.92	59.99	13.93	+10.12	+10.12
N-10	73.92	59.99	13.93	63.92	49.99	13.93	-10.12	-10.12
N-11	63.92	49.99	13.93	53.50	39.57	13.93	-10.12	-10.12
N-12	53.50	39.57	13.93	43.85	29.92	13.93	-10.12	-10.12
N-13	15.73	5.66	10.07	25.73	15.62	10.11	+10.00	+ 9.96
N-14	25.73	15.62	10.11	35.80	25.84	9.96	+10.07	+10.22
N-15	35.80	25.84	9.96	45.89	35.80	10.09	+10.09	+ 9.96

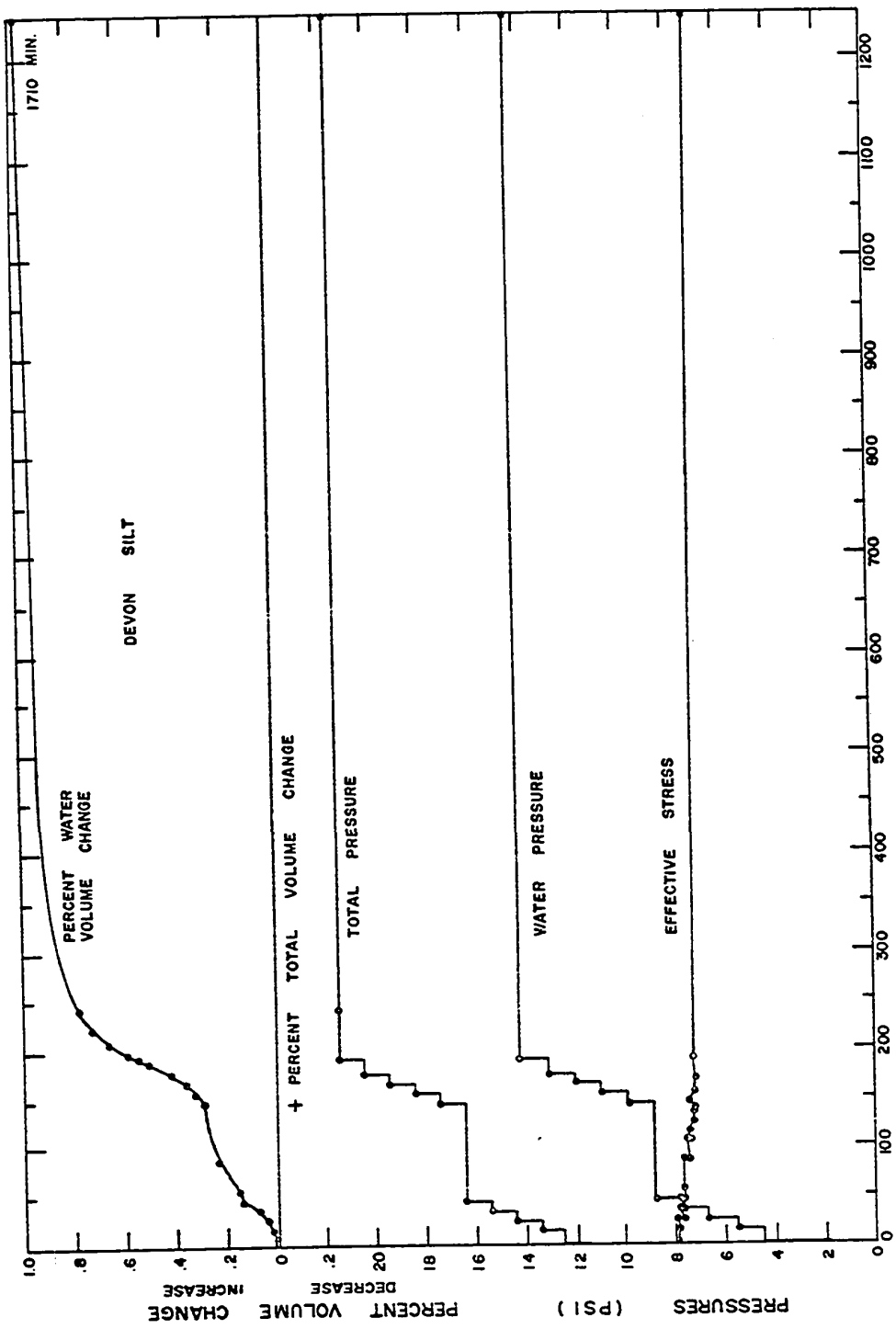


FIGURE C.1 NULL TEST (N-1) ON SAMPLE NO. 1

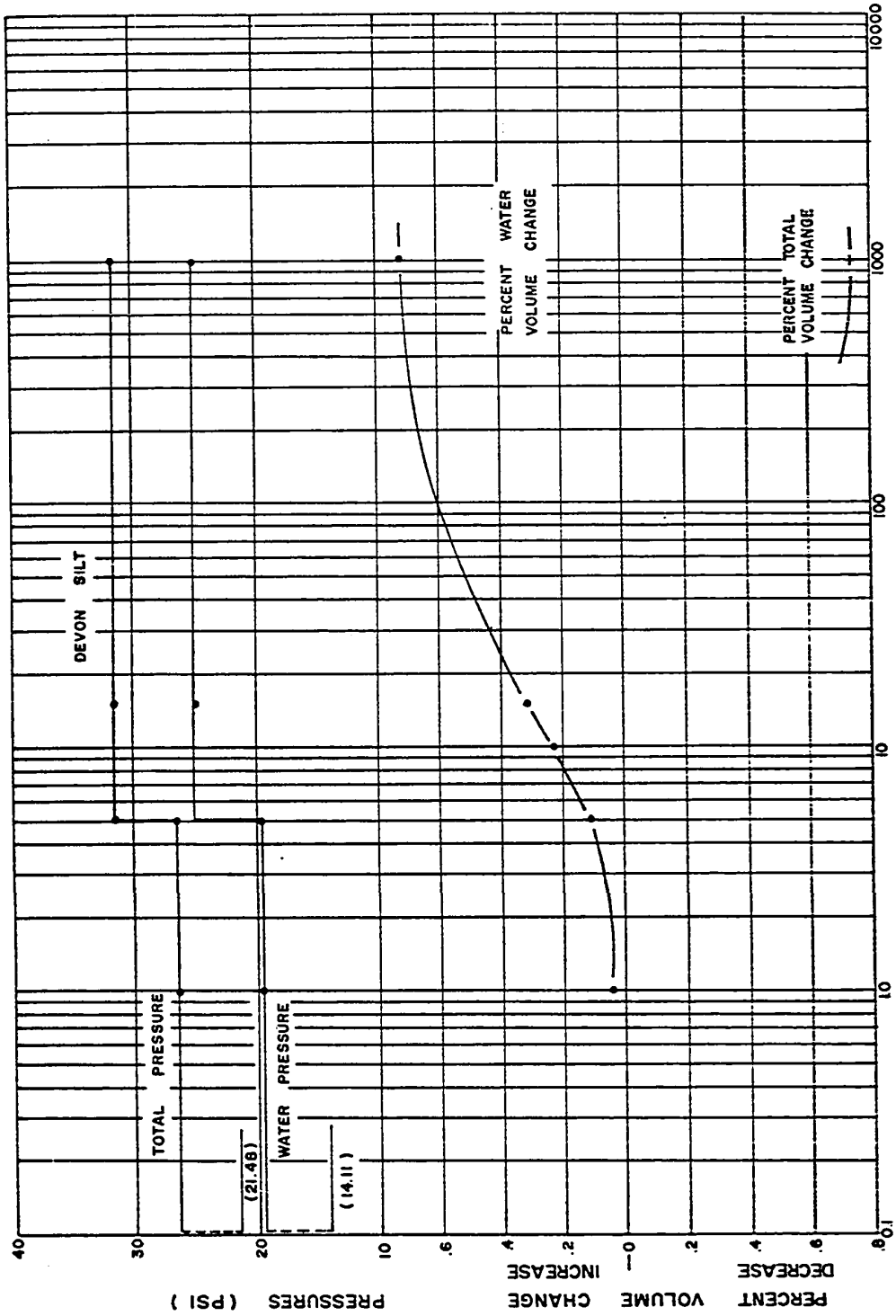


FIGURE C.2 NULL TEST (N-2) ON SAMPLE NO. 1

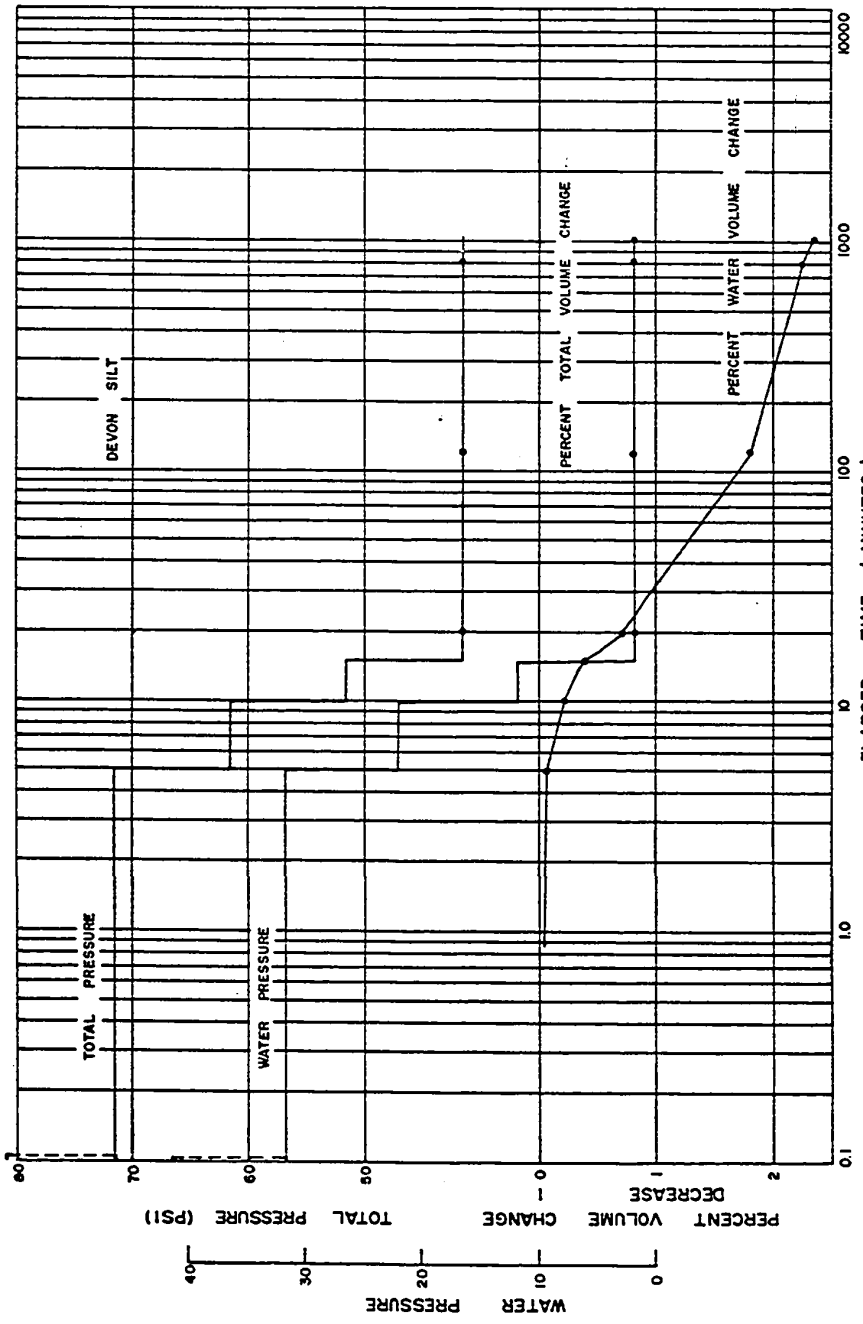


FIGURE C.3 NULL TEST (N-3) ON SAMPLE NO. 1

obtaining reproducable readings on the cathetometer.

For the N-2 test, the total and water pressures were increased in two, 5 psi increments. The total volume decreased and water went into the sample. For the N-3 test, the total and water pressures were decreased in four, 5 psi increments. There was a water volume decrease of almost 2-1/2 percent while the total volume remained essentially constant.

The amount of water going into the sample during the increase in water pressure, reflects the compressibility of the pore fluid. The calculated degrees of saturation approach 100 percent; however, the measured compressions indicate much lower values. Applying Boyle's law to the measured compression results in a degree of saturation as low as 85 percent.

Two points are obvious from the Null tests on sample #1. Attempts must be made to obtain a higher initial degree of saturation and a soil with a structure less sensitive to disturbance. The second set of tests (Figures C.4 and C.5) were performed on a sample consisting of 80 percent Devon silt and 20 percent kaolin. The slurried sample was tamped to remove entrapped air bubbles. Considerable amounts of air were observed as the sample was placed on a concrete vibrating table for several minutes. (All subsequent saturated sample were prepared in a similar manner). The sample was formed by one-dimensional consolidation to a pressure of 4 psi and tested in Triaxial Apparatus No. 1.

The changes in total and water pressure were applied simultaneously in one increment. The triaxial equipment functioned satisfactorily but the technique for operating the cathetometer was still

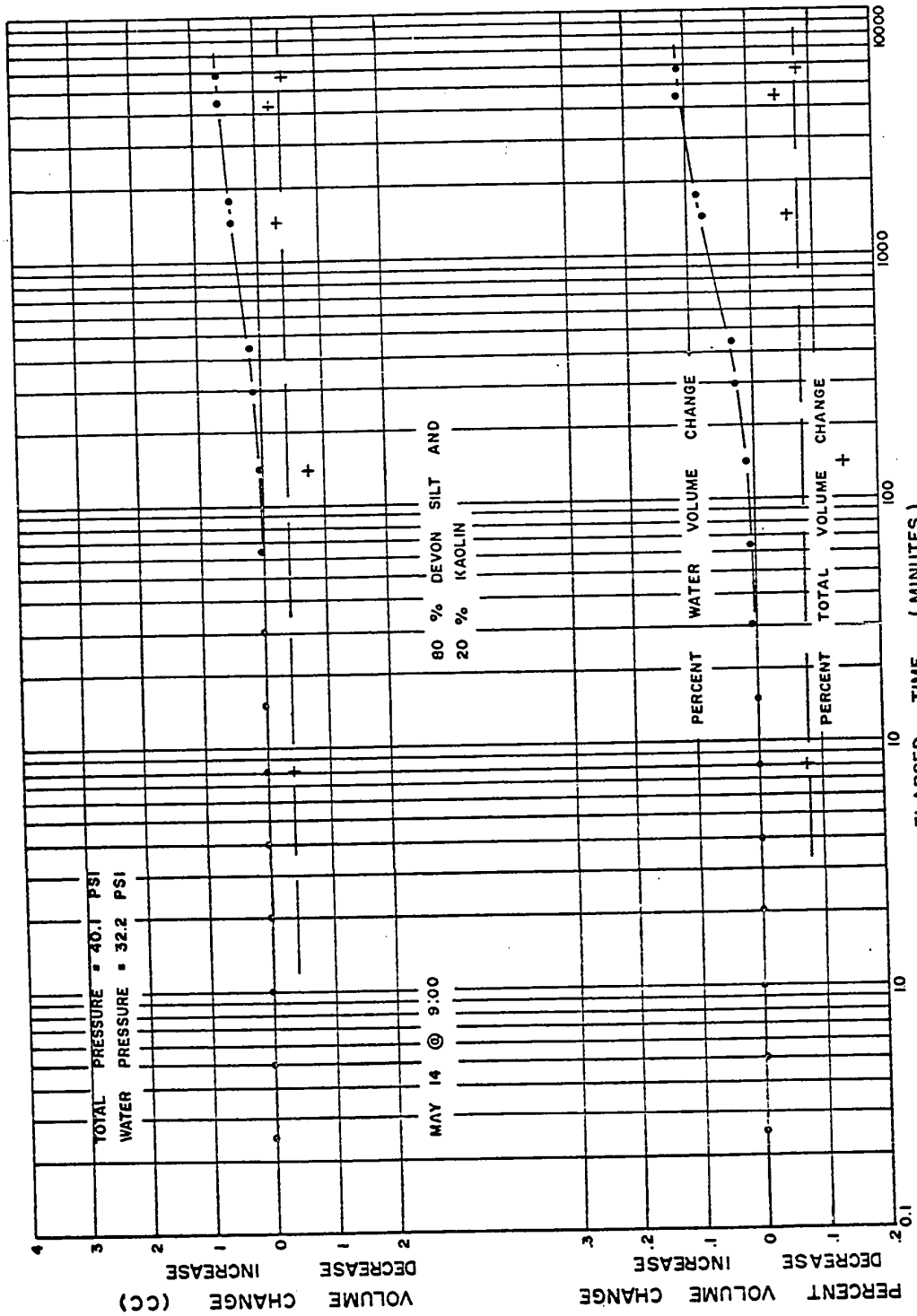


FIGURE C.4 NULL TEST (N-4) ON SAMPLE NO. 2

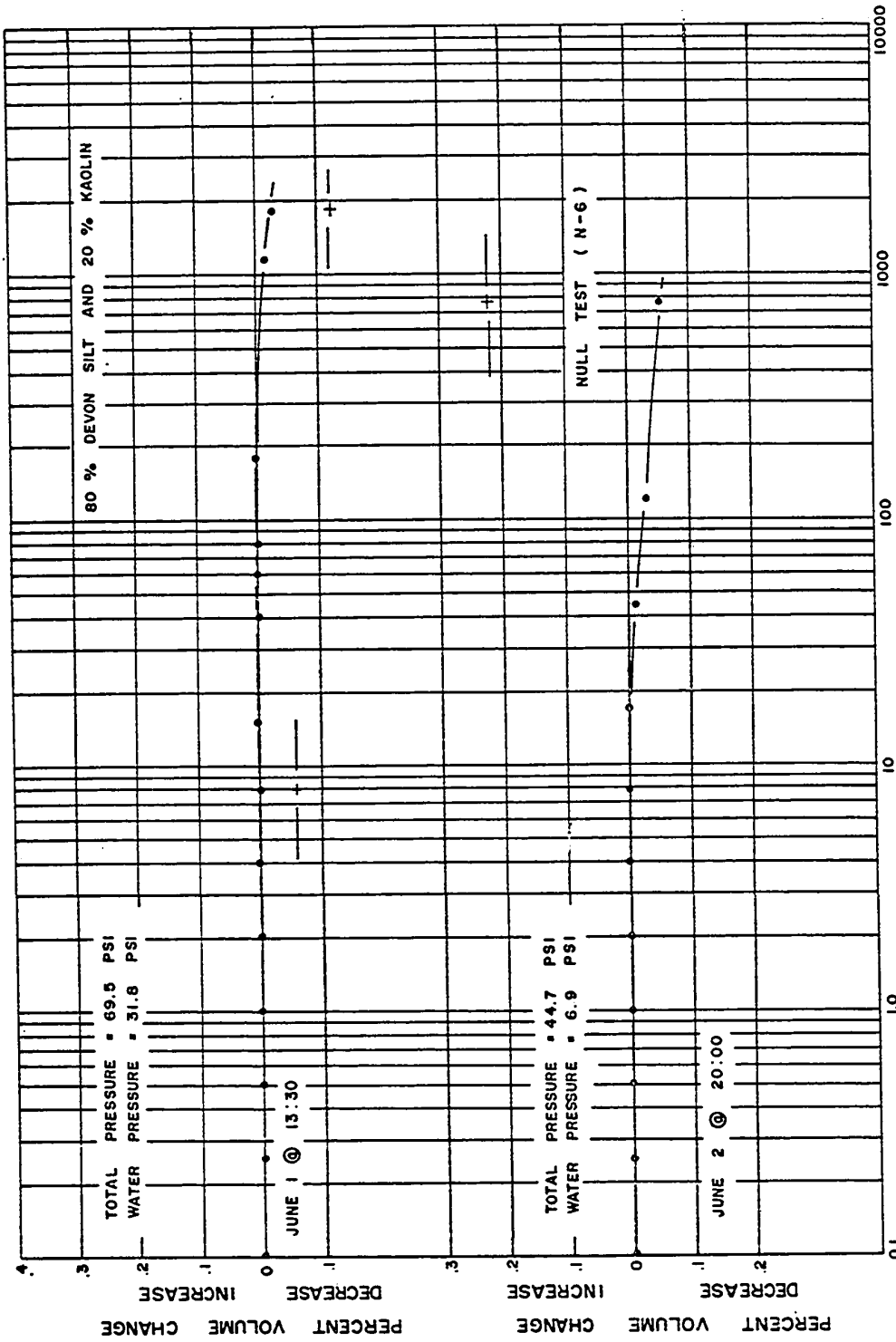


FIGURE C.5 NULL TESTS (N-5) AND (N-6) ON SAMPLE NO. 2

not perfected at this point. The scatter in the total volume change readings, (N-5), is indicative of the poor cathetometer technique. Also, more cathetometer readings should have been taken for tests (N-5) and (N-6).

Null test (N-4) showed a total volume change of 0.08 percent at the time of changing the pressures. No further volume change was evident during the elapsed time of 5760 minutes. There is some scatter in the cathetometer readings but there is no evidence of a continuous process. The water phase volume gradually increased with time. The process is due to the compressibility of the pore fluid. Only the entrapped air can account for the volume change since the soil solids and the water are essentially incompressible. Attributing all the volume change to the entrapped air, the degree of saturation is computed as 98.7 percent. The degree of saturation computed from the volume-weight measurements was 97.6 percent. The measured volume changes are small and consistent with those anticipated. The total volume change represents only 0.40 cc while the water volume change represents 0.58 cc. An effective stress increase of 10 psi would produce a volume change of approximately 5.0 percent or 26.5 cc.

Null test (N-5) was performed 14 days after test (N-4) when the sample was consolidated to an effective stress of 37.7 psi. The drop of 20 psi in the total and water pressures appear to have produced some disturbance to the soil structure since the total volume decreased. The limited number of cathetometer readings presents some handicap in interpreting the data.

The pressures were reduced by an additional 25 psi for the

(N-6) test. The total volume increased while the water volume decreased. Combining the effects of the (N-5) and (N-6) tests, the total volume increase was 0.095 percent and the water volume decrease was 0.08 percent. Applying Boyle's law to the volume changes indicates that the degree of saturation was approximately 99 percent.

A total of six null tests (Figures C.6 to C.8, inclusive) were performed in the oedometer on a sample composed of 80 percent Devon silt and 20 percent kaolin. Due to the construction of the oedometer, only the total volume change is monitored. The chamber is filled with water and the volume change in the water phase cannot be monitored. The tests are as much a check on the equipment as they are a study of null behavior. The tests involve increasing or decreasing the chamber pressure (water) by a designated amount. The total pressure (controlled by a differential pressure regulator) is automatically increased by an amount equal to the chamber pressure increase. If the water pressure change causes a change in volume of the sample, the dial gauge records it.

Performing the null test involves simultaneously opening the total and water pressure valves. The slight increase or decrease in the volume of the sample during the first six seconds of loading is the result of either the total or water pressure being applied first. Generally the water pressure lags slightly due to the volume of air above the water in the water saturation reservoir.

None of the tests showed any tendency for volume increase. Rather they show a slight volume decrease probably due to sample dis-

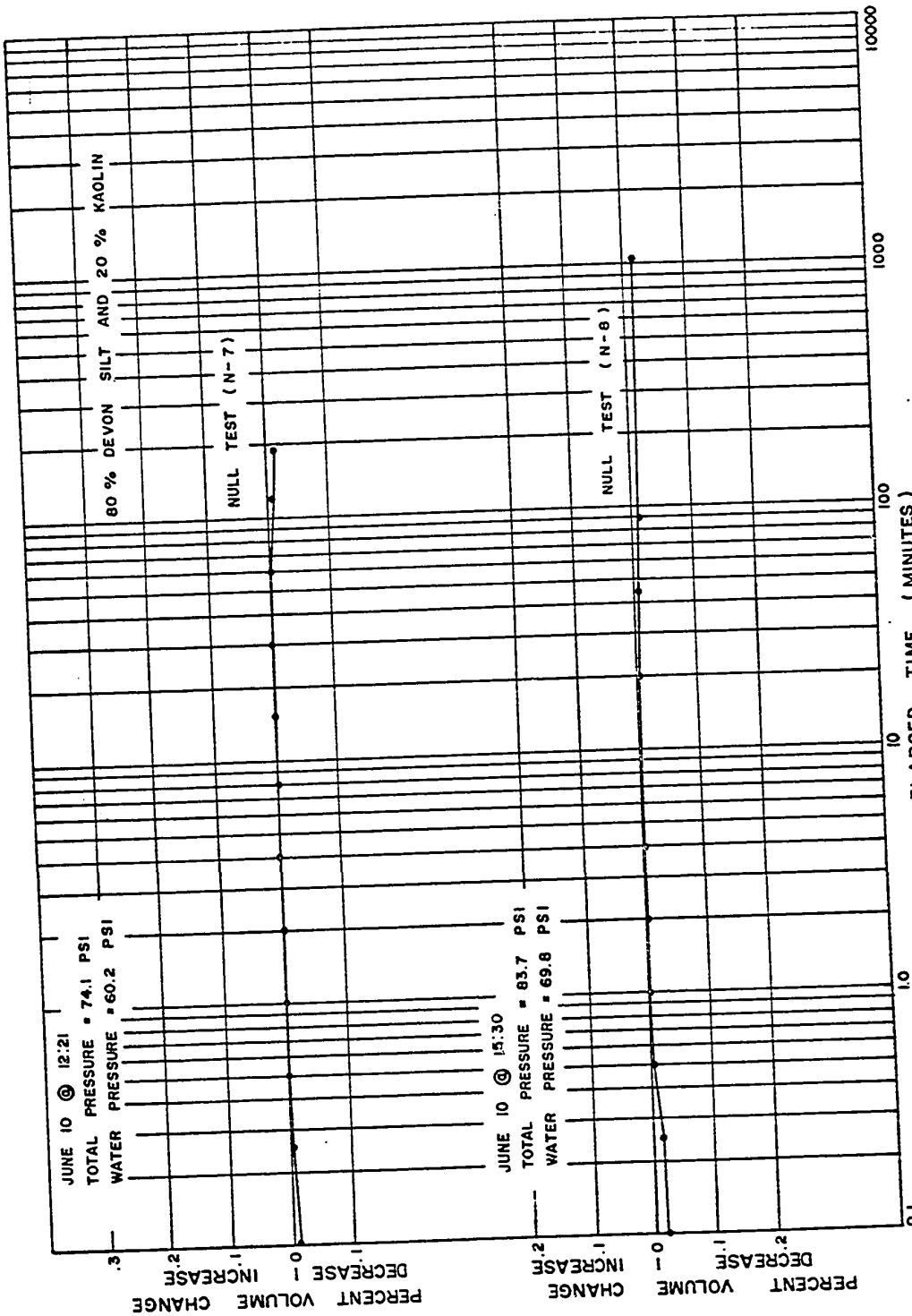


FIGURE C.6 NULL TESTS (N-7) AND (N-8) ON SAMPLE NO. 2

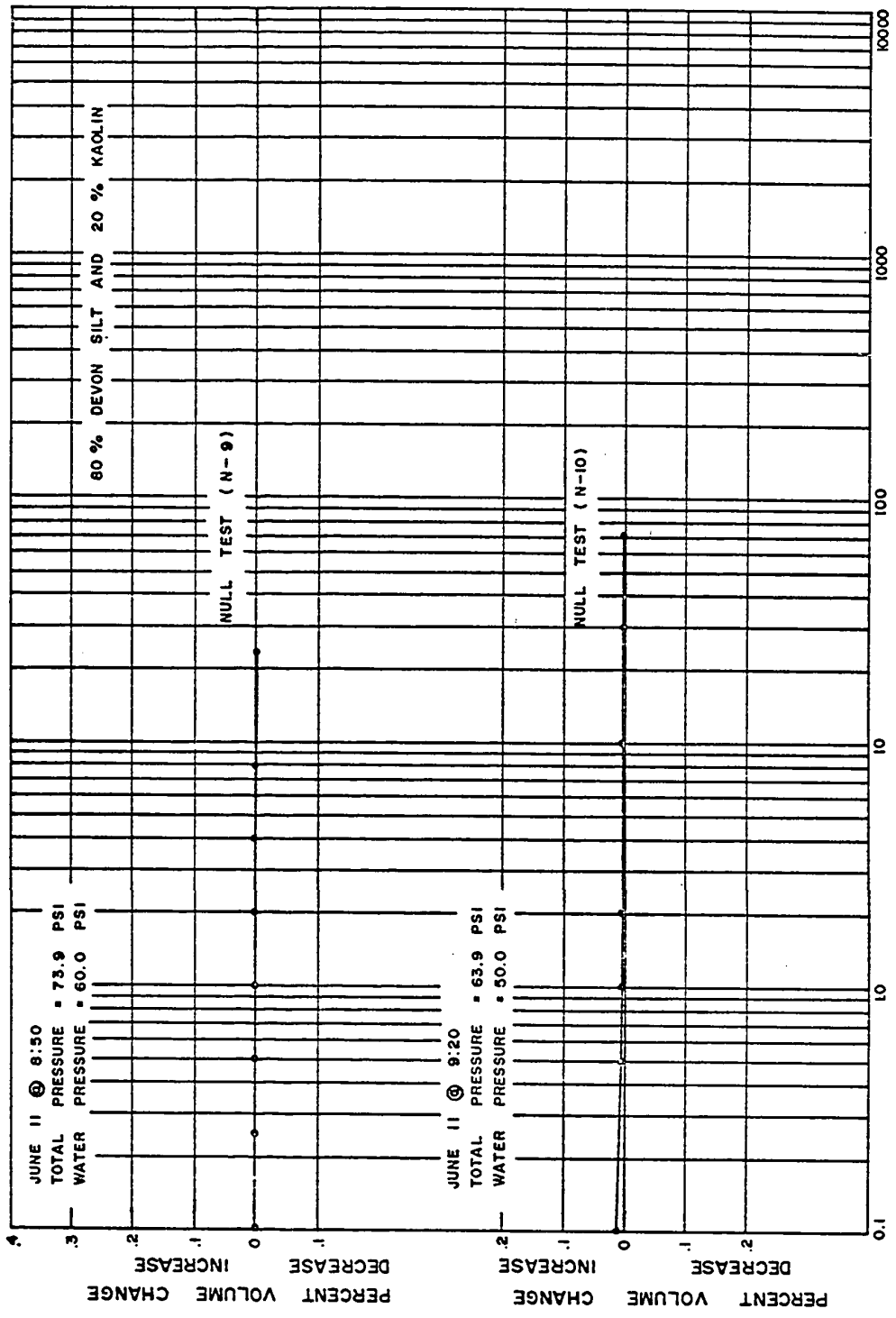


FIGURE C.7 NULL TESTS (N-9) AND (N-10) ON SAMPLE NO. 3

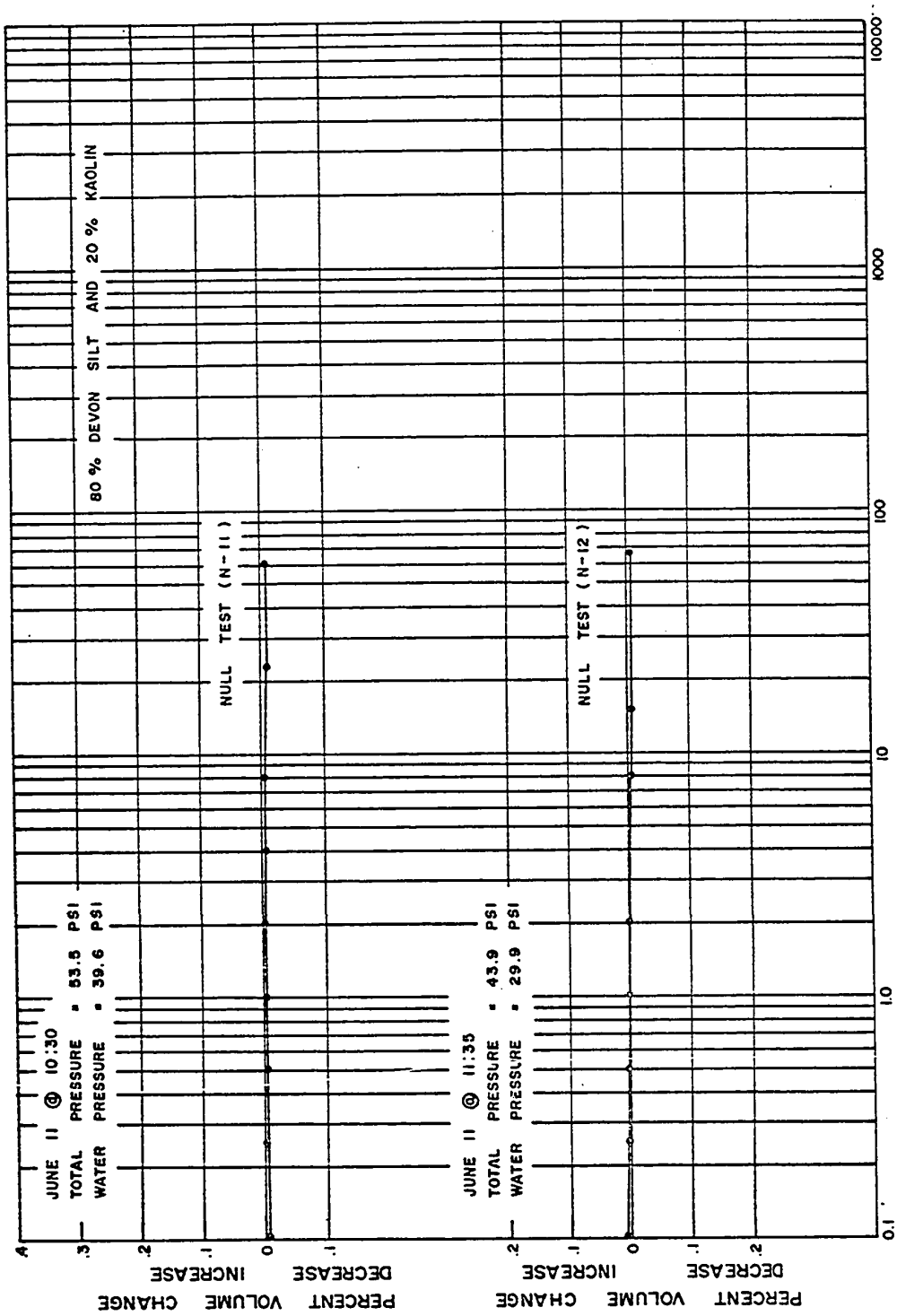


FIGURE C.8 NULL TESTS (N-11) AND (N-12) ON SAMPLE NO. 3

turbance and secondary consolidation.

Three null tests on a soft kaolin (Figure C.9 to C.11, inclusive) were performed on Triaxial Apparatus No. 1. In each case the applied pressures were increased in 10 psi increments. The technique for reading the cathetometer was perfected by this time and the results are consistent. The pressure regulators show a fluctuation of approximately 0.3 psi. The fluctuations are primarily due to variations in barometric pressure. In general, both the total and water pressures change by the same amount, leaving the effective stress constant.

The tests showed essentially no water going into the sample when the water pressure was increased. After periods of one day a slight amount of water had come out of each sample due to secondary consolidation. Tests (N-14) and (N-15) show some compression at the time and stresses were increased. With time, each test showed a decrease in volume approximately equal to the volume of water expelled. The immediate compressions may be due in part to the inability to completely correct for compression in the measuring system.

In each null test performed in Section I, only a small amount of total and water volume change was observed. The immediate volume change accounted for most of the total volume change. Entrapped air and compliance of the measuring system are believed responsible for the immediate volume changes. Slight volume changes over long periods of time are believed to be related to secondary consolidation. Table C.5 shows a summary of the volume changes monitored. Also tabulated

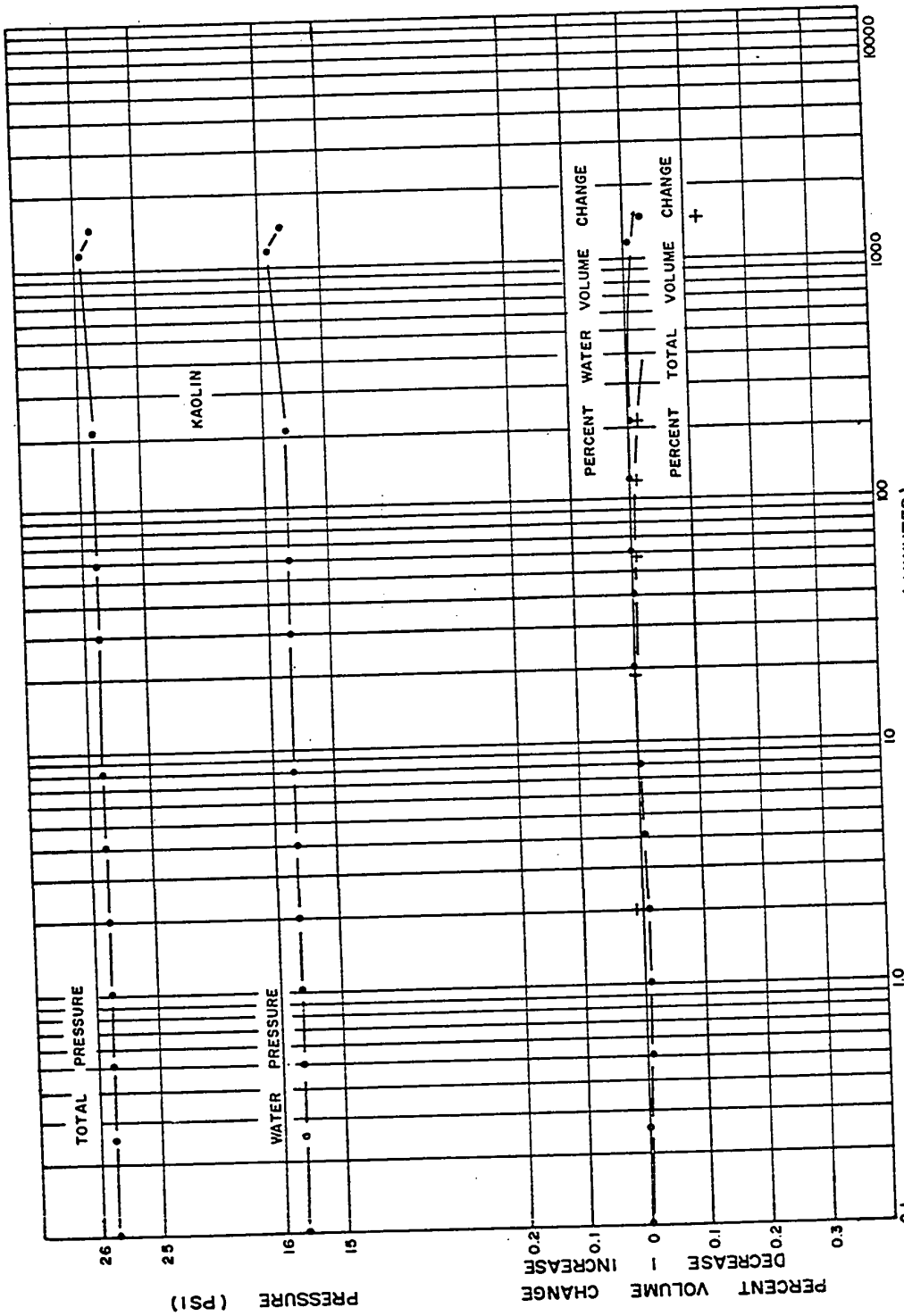


FIGURE C.9 NULL TEST (N-13) ON SAMPLE NO. 4

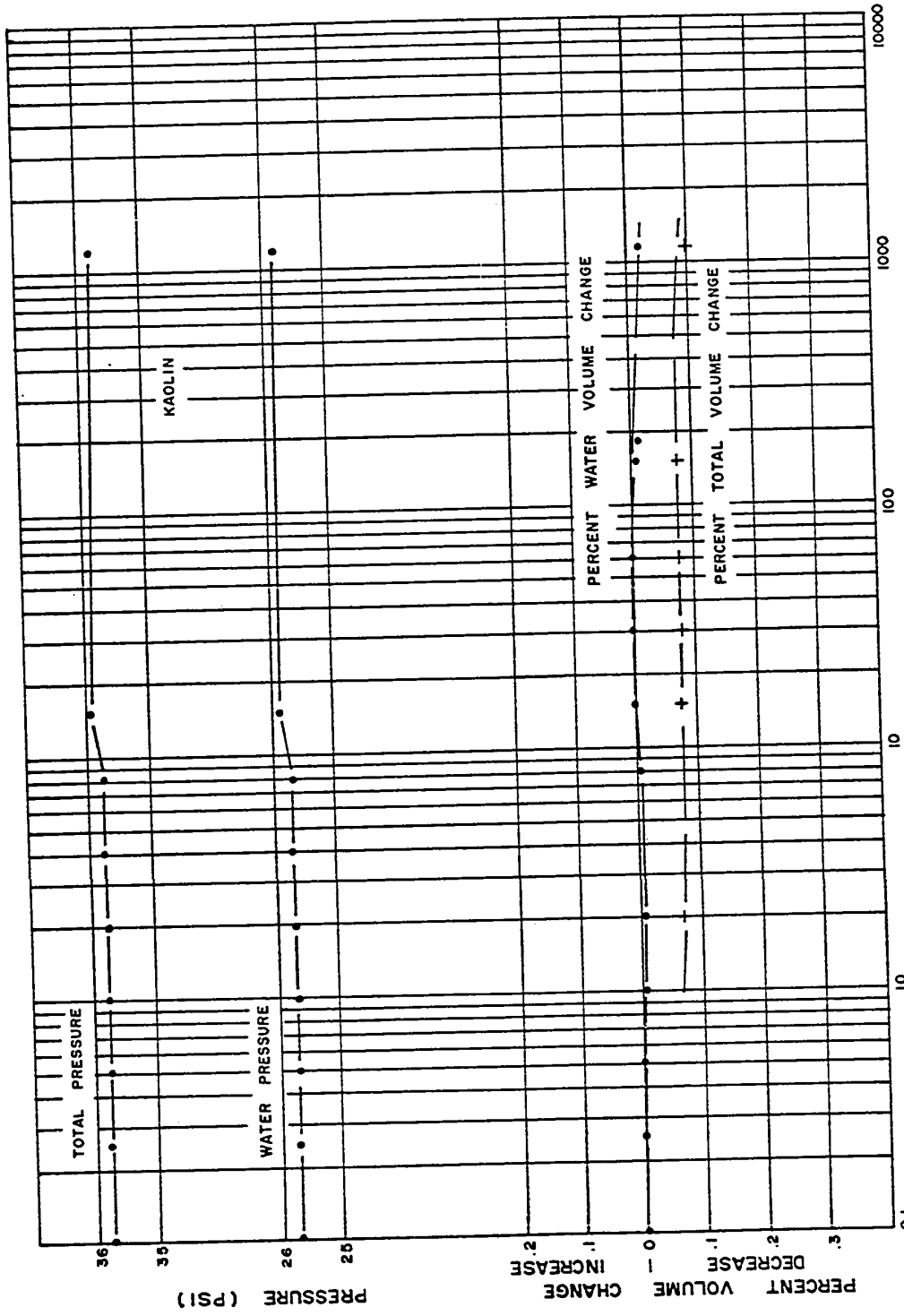


FIGURE C.10 NULL TEST (N-14) ON SAMPLE NO. 4

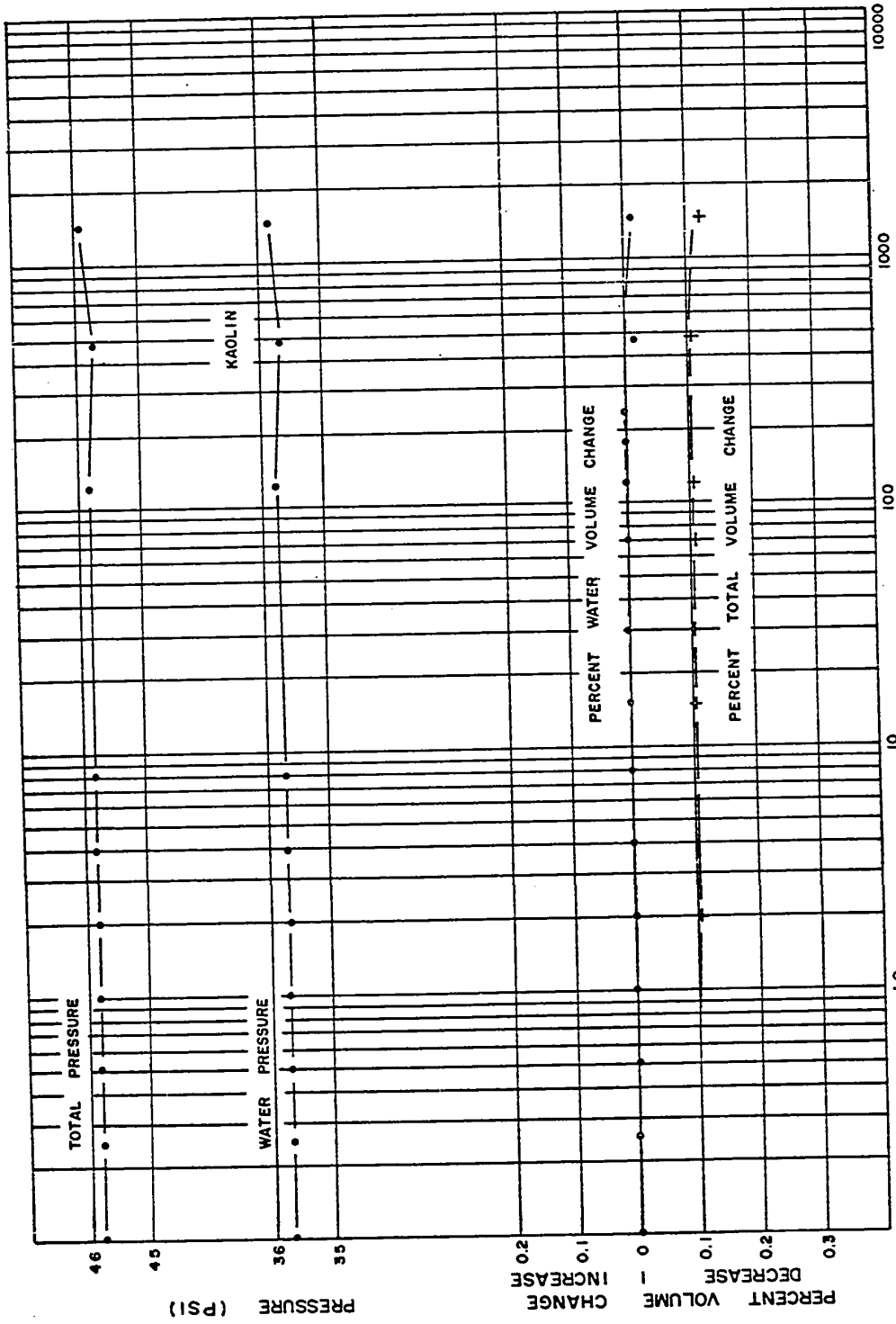


FIGURE C.11 NULL TEST (N-15) ON SAMPLE NO. 4

TABLE C.5

SAMPLE VOLUME CHANGE AND WATER VOLUME CHANGE

DURING NULL TESTS ON SATURATED SAMPLES

(Controlling Total and Water Pressures)

Test No.	Pressure Change (psi)	Sample, Volume Change		Water Volume Change (%)	Elapsed Time (min)	Volume Change For Corresponding Effective Stress Increase (%)
		Immediate (%)	At Elapsed Time (%)			
N-1	+10	--		-0.98	1710	4.28
N-2	+10	--	+0.72	-0.72	1010	4.54
N-3	-40	--	0.0	+2.37	1000	1.14
N-4	+10	+0.08	+0.08	-0.06	1000	5.02
		+0.08	+0.08	-0.11	6000	5.02
N-5	-20	--	+0.125	+0.02	2000	2.77
N-6	-25	--	-0.22	+0.06	800	3.31
N-7	+10	+0.011	+0.014	--	190	3.36
N-8	+10	+0.021	+0.020	--	1035	3.36
N-9	-10	-0.003	-0.010	--	23	3.36
N-10	-10	-0.010	-0.002	--	70	3.36
N-11	-10	+0.003	+0.011	--	60	3.36
N-12	-10	-0.003	+0.006	--	65	3.36
N-13	+10	-0.02	+0.10	+0.03	1400	5.92
N-14	+10	+0.07	+0.10	+0.025	1170	5.92
N-15	+10	+0.11	+0.11	0.0	120	--
		+0.11	+0.13	+0.012	1470	5.92

is an estimate of the volume change that would accompany an effective stress change equal to each stress component change. The volume changes are based on the initial effective stress and an estimate of the compressive index. The last set of null tests indicated a total volume change of approximately 1.8 percent of that for a corresponding effective stress increase. Similarly, the water volume change was approximately 0.4 percent. The volume changes observed bear no relation to the limitation of the effective stress state variable. Rather, they are an indication of the limitations of this testing technique. In any case, the results are sufficiently accurate to assess the stress state variables for engineering purposes.

C-3 Null Test Analysis on Saturated Samples (Section II)

In section II, the saturated samples had an air pressure applied to the top of the sample through a coarse corundum disc. The total and water volume changes were monitored in all tests. The testing technique is more difficult since three pressures must be applied simultaneously.

The test program (Section II) is summarized in Table C.6. The volume weight relationships at the start of each test are shown in Table C.7 and the pressure changes associated with each test are summarized in Table C.8. The changes in the three proposed stress state variables are also tabulated.

Five null tests (Figures C.12 to C.14, inclusive) were performed on a soft kaolin sample in the one-dimensional oedometer. The null test technique presented some problems on the oedometer. Although

TABLE C.6

SUMMARY OF NULL TESTS ON SATURATED SOILS

(Controlling Total, Air and Water Pressures)

Test No.	Sample No.	Date	Starting Time	Apparatus No.	Soil Type	Change in Pressures (psi)	Comments
N-16	6	June 24/71	9:30	OED-179	Kaolin	+10	
N-17	6	June 25/71	9:21	OED-179	Kaolin	+10	
N-18	6	June 28/71	10:51	OED-179	Kaolin	-10	
N-19	6	June 30/71	8:55	OED-179	Kaolin	+10	u_w altered at 7200 min.
N-20	6	July 5/71	11:05	OED-179	Kaolin	+10	u_w altered at 1330 min.
N-21	7	June 26/71	10:00	T-1	Kaolin	+ 8	Some water rose into air line
N-22	7	June 30/71	9:30	T-1	Kaolin	+10	

TABLE C.7

VOLUME-WEIGHT RELATIONSHIPS FOR SATURATED SAMPLES

(Controlling Total, Air and Water Pressures)

Test No.	Diameter (cm)	Height (cm)	Total Volume (cc)	Volume of Solids (cc)	Volume of Water (cc)	Volume of Air (cc)	Water Content (%)	Void Ratio	Dry Density (PCF)	Degree of Saturation (%)
N-16	6.350	2.119	67.11	29.06	37.95	0.10	49.91	1.309	70.69	99.7
N-17	6.350	2.118	67.06	29.06	37.87	0.13	49.81	1.307	70.75	99.7
N-18	6.350	2.119	67.10	29.06	37.42	0.62	49.21	1.309	70.71	98.4
N-19	6.350	2.118	67.08	29.06	37.19	0.83	48.91	1.308	70.72	97.8
N-20	6.350	2.115	66.98	29.06	36.92	1.00	48.56	1.305	70.83	97.4
N-21	9.685	6.062	446.54	193.43	253.1	0.00	50.37	1.309	70.71	100.0
N-22	9.575	5.917	426.06	193.43	227.47	5.17	44.95	1.203	74.11	97.8

TABLE C.8

RECORD OF PRESSURE CHANGES FOR NULL TESTS ON SATURATED SAMPLES

(CONTROLLING TOTAL, AIR AND WATER PRESSURES)

Test No.	Prior to Pressure Changes						After Pressure Changes						Change in Total Pressure (psi)	Change in Air Pressure (psi)	Change in Water Pressure (psi)
	Total Pressure (psi)	Air Pressure (psi)	Water Pressure (psi)	$\sigma-u_w$ (psi)	$\sigma-u_a$ (psi)	u_a-u_w (psi)	Total Pressure (psi)	Air Pressure (psi)	Water Pressure (psi)	$\sigma-u_w$ (psi)	$\sigma-u_a$ (psi)	u_a-u_w (psi)			
N-16	46.75	29.73	18.50	28.25	17.02	11.23	56.40	39.27	30.08	26.32	17.13	9.19	+ 9.65	+ 9.54	+11.58
N-17	56.40	39.27	30.08	26.32	17.13	9.19	66.53	49.36	40.33	26.20	17.17	9.03	+10.13	+10.09	+10.25
N-18	66.53	49.36	40.33	26.20	17.17	9.03	56.25	39.19	30.44	25.81	17.06	8.75	-10.28	-10.17	- 9.89
N-19	56.25	39.19	30.44	25.81	17.06	8.75	66.23	49.14	40.50	25.73	17.09	8.64	+ 9.98	+ 9.95	+10.06
N-20	66.23	49.14	40.50	25.73	17.09	8.64	76.28	59.19	50.08	26.20	17.19	9.11	+10.05	+10.05	+ 9.58
N-21	65.82	46.22	45.75	20.07	19.60	0.47	74.04	54.43	53.99	20.05	19.61	0.44	+ 8.22	+ 8.21	+ 8.24
N-22	74.01	54.36	34.15	39.86	19.65	20.21	83.90	64.22	44.06	39.84	19.68	20.16	+ 9.89	+ 9.86	+ 9.91

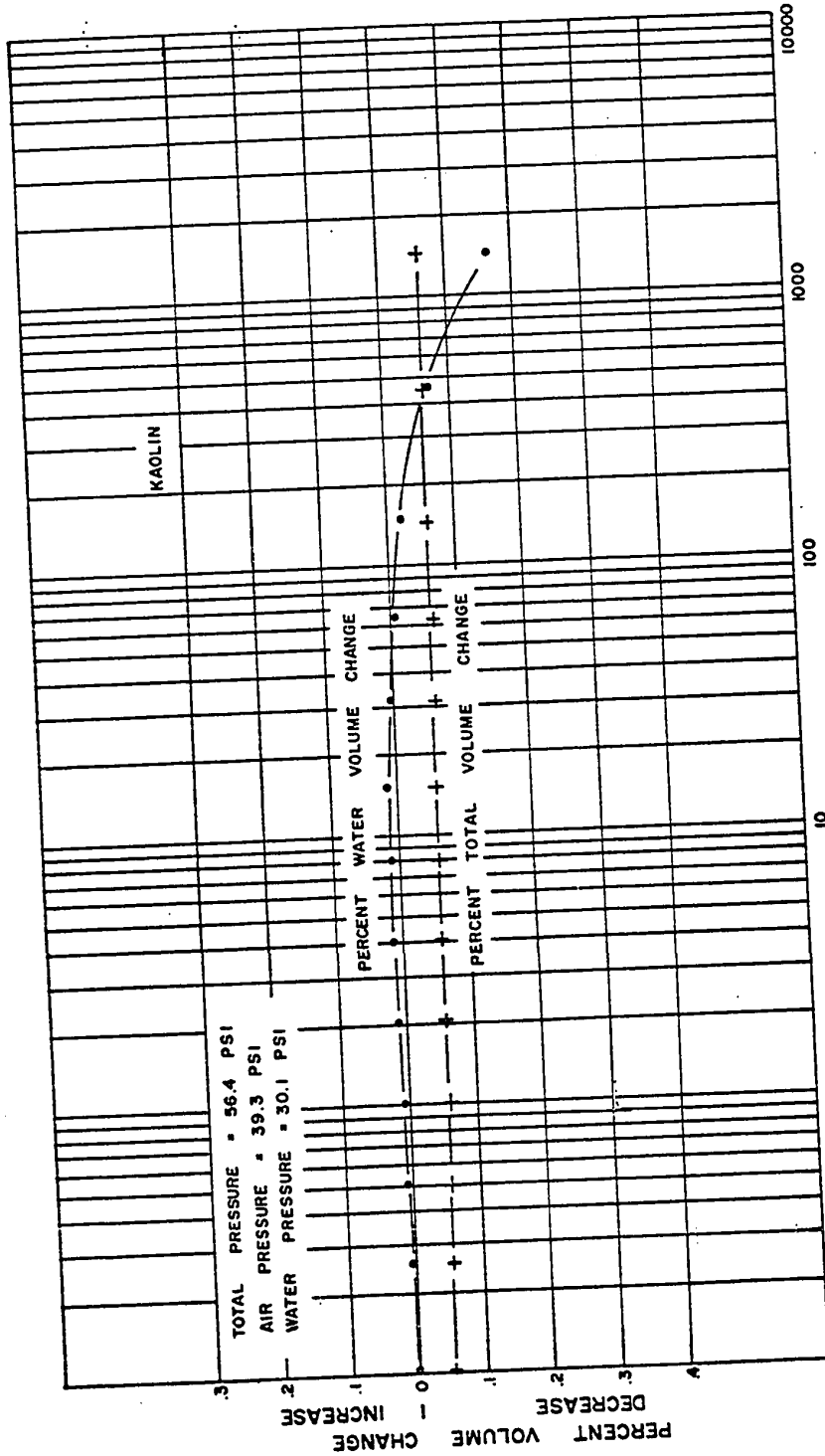


FIGURE C.12 NULL TEST (N-16) ON SAMPLE NO. 6

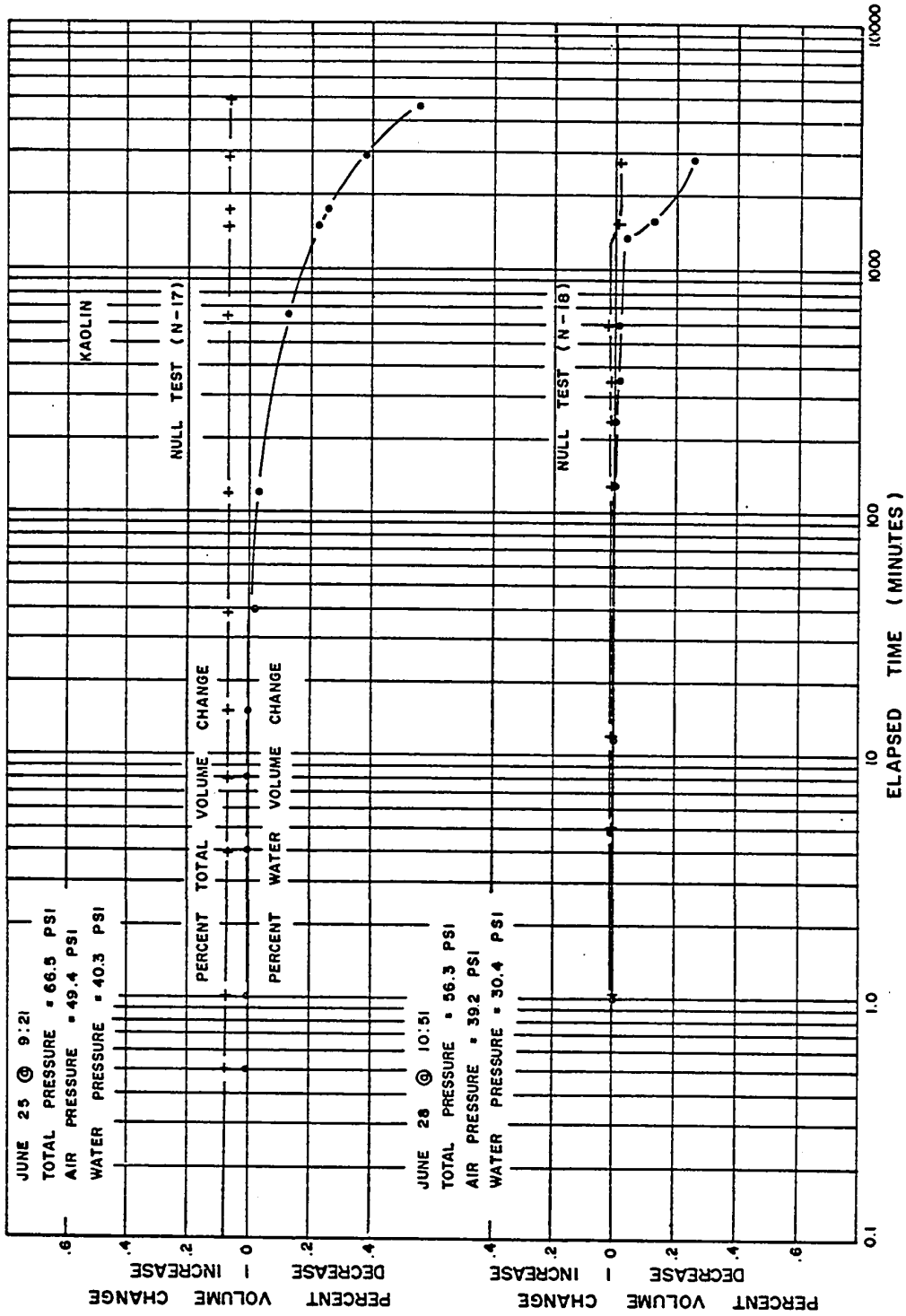


FIGURE C.13 NULL TESTS (N-17) AND (N-18) ON SAMPLE NO. 6

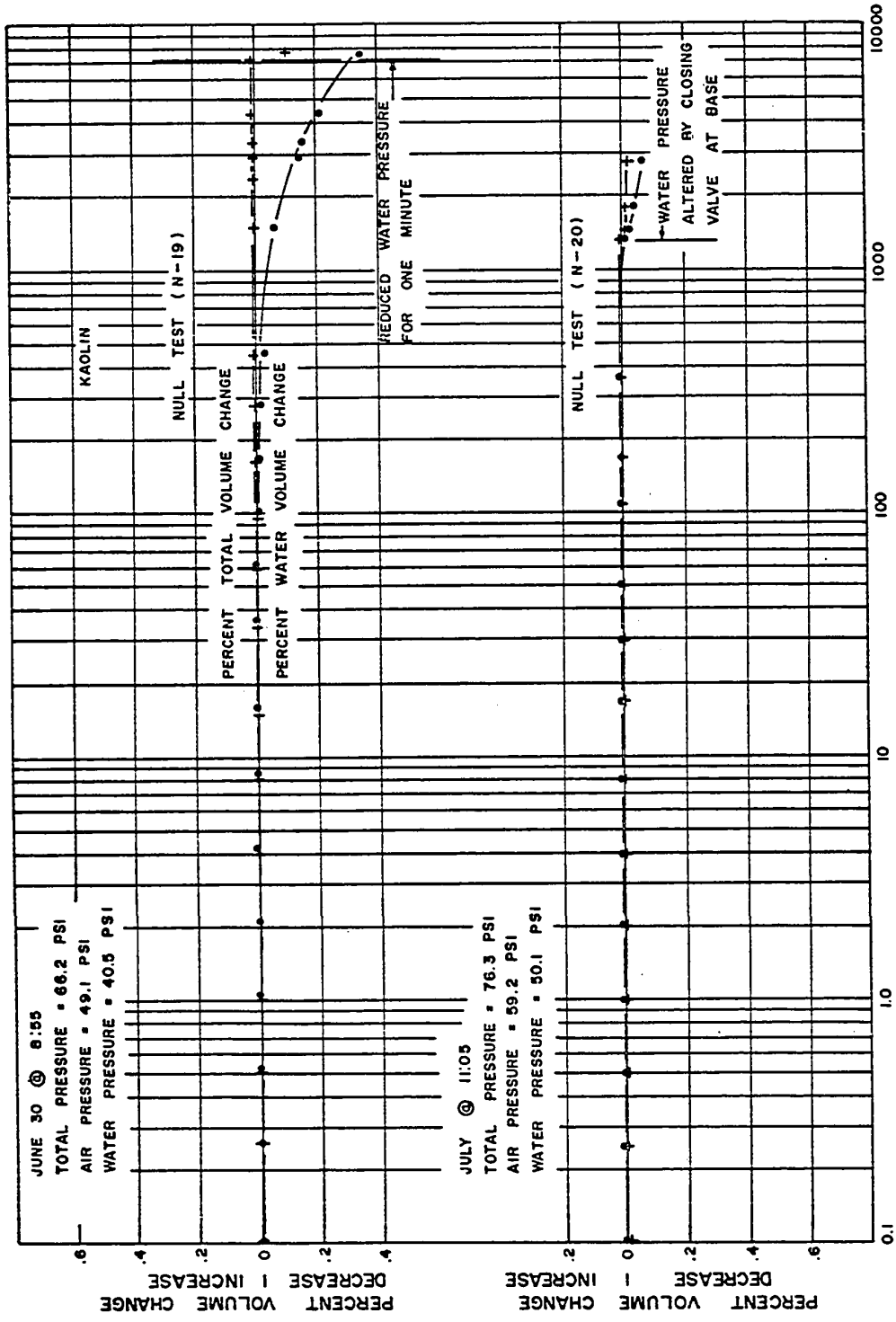


FIGURE C.14 NULL TESTS (N-19) AND (N-20) ON SAMPLE NO. 6

all three valves (i.e, total, air and water pressure valves) were opened at the same moment, the pressure changes may not reach the sample at the same time. In the case of the air pressure, a large air flow into the chamber is required to build up the pressure. The line leading to the apparatus was a 1/8 inch polyethylene tubing and several seconds are required for the air pressure change. On the other hand, the total stress on the cap is almost instantaneous. The net result is a slight compression of the sample (Figure C.12). If the air pressure valve is opened a couple seconds prior to the total pressure valve, essentially all the initial compression can be overcome (Figure C.14). The total pressure loading cap must be properly de-aired when using the second technique.

Null test (N-16) shows an immediate compression due to the total loading being applied before the air pressure was built up. The water volume change indicates that approximately 1/100 of a "cc" of water went into the sample in the first 20 minutes. Then water came out for the remainder of the test. After 1400 minutes, the apparent water volume change was 0.14 cc. A process is definitely occurring but the soil structure is unaffected. The apparent water volume decrease is due to the diffusion of air through the water in the sample and the high air entry disc. At this time, the apparatus did not have a diffused air volume indicator. This test and others verified the necessity of entrapping and measuring the volume of air diffusing through the sample.

At the start of null test (N-17), the load range selector was in the wrong position and the total pressure was reduced to zero

for the first 20 seconds. This explains the immediate volume increase 0.073 percent. With an elapsed time of 5000 minutes, there was no evidence of a process occurring in the total sample. On the other hand, the water volume change indicator shows a continuous, apparent movement of water out of the sample. Once again, air diffusion is the cause of the apparent water volume change. On a semi-log plot of time, the water volume change shows a gradual, increasing rate of volume change. The diffusion of air should be a linear relationship on an arithmetic plot of time if it is occurring as a steady state process. Figure C.15 shows that the apparent water volume change processes are essentially a straight line. The diffusivity of air through the sample can be computed provided the boundary conditions are known. The results show that the sample was not initially saturated with air. This is reasonable since on the previous day the sample was subjected to an air pressure 10 psi lower than on the day of testing. In order to compute the diffusivity, the sample must form a perfect seal against the sides of the ring. This is not a reasonable assumption since there was a small air gap between the ring and the sample at the end of the test. Therefore, it is impossible to accurately assess the length of diffusion path. However, assuming a diffusion path equal to the length of the sample gives a diffusivity value of 1.82×10^{-5} cm^2/sec. This value is higher than anticipated due to the use of a diffusion path that is too long.

The applied pressures were decreased by 10 psi for null test (N-18). There is essentially no evidence of a process in the

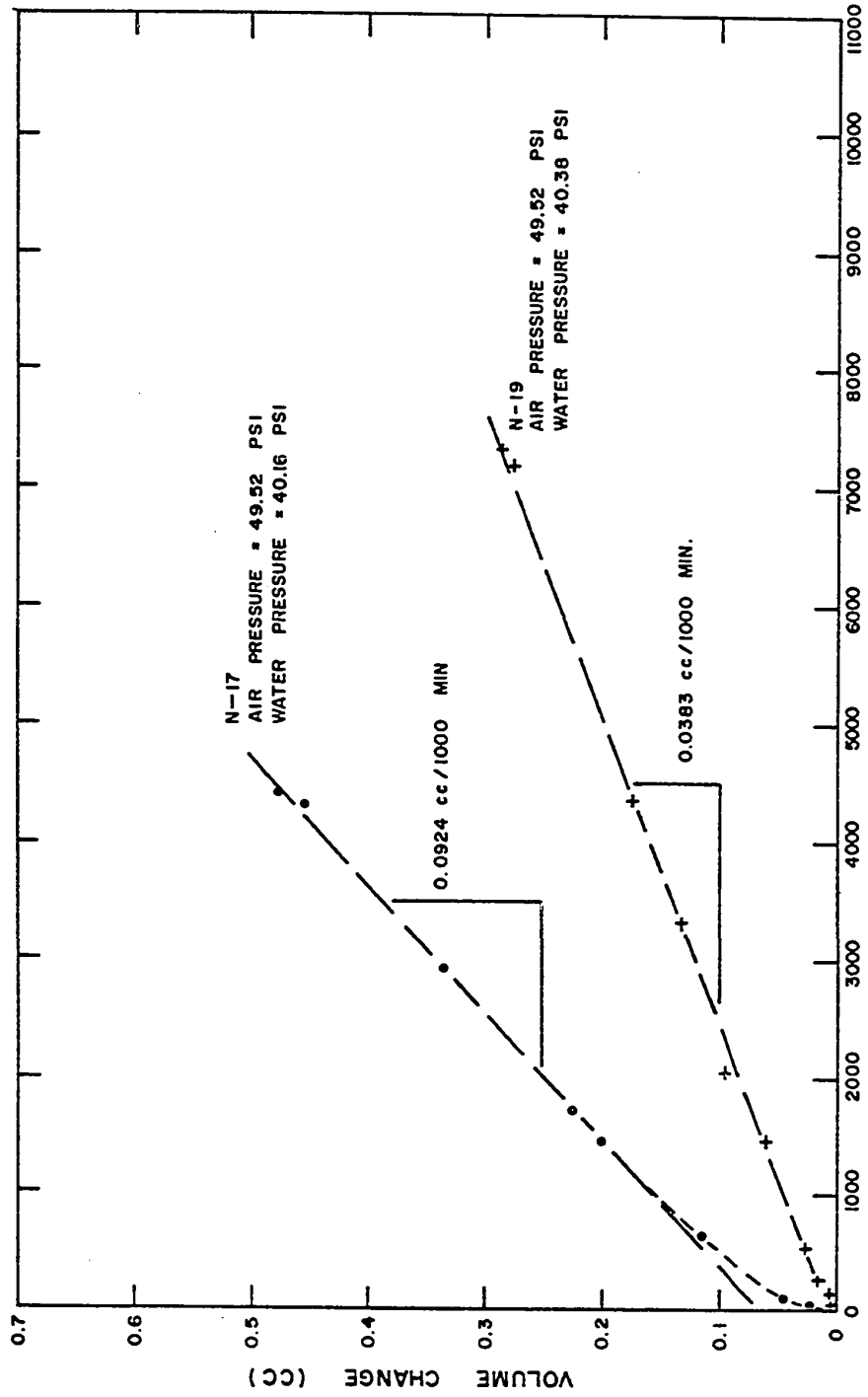


FIGURE C.15 REGISTERED WATER VOLUME CHANGE VERSUS TIME

soil structure or the water phase for the first 1000 minutes. At 1400 minutes there appears to have been some disturbance to the apparatus since the total and water volumes shows an abrupt decrease.

Null tests (N-19) and (N-20) show no indication of a process occurring to the soil structure. The only volume changes in the soil structure are the result of momentarily altering the water pressure. The water volume change curves show the effect of air diffusion. However, the rate is considerably lower than that previously measured under the same stress conditions. Using the same assumptions previously outlined, the diffusivity is 7.71×10^{-6} cm^2/sec. When the air and water pressures are increased for Null test (N-20), the rate of air diffusion shows a further decrease. These results show the difficulty in theoretically predicting air diffusion through the sample. Thus it becomes imperative to measure the volume of diffused air.

After applying corrections for immediate volume change, the net total volume change for the four times the pressures were increased is zero. A corresponding increase in effective stress should produce approximately 10 percent volume change. The water volume changes cannot be compared on a similar basis due to the effect of air diffusion.

Null tests (N-21) and (N-22) were performed on a kaolin sample in Triaxial Apparatus No. 1 (Figures C.16 and C.17). Sample #7 is a continuation of testing on sample #4. Some water appeared in the polyethylene air tube at the top of the sample by the end of

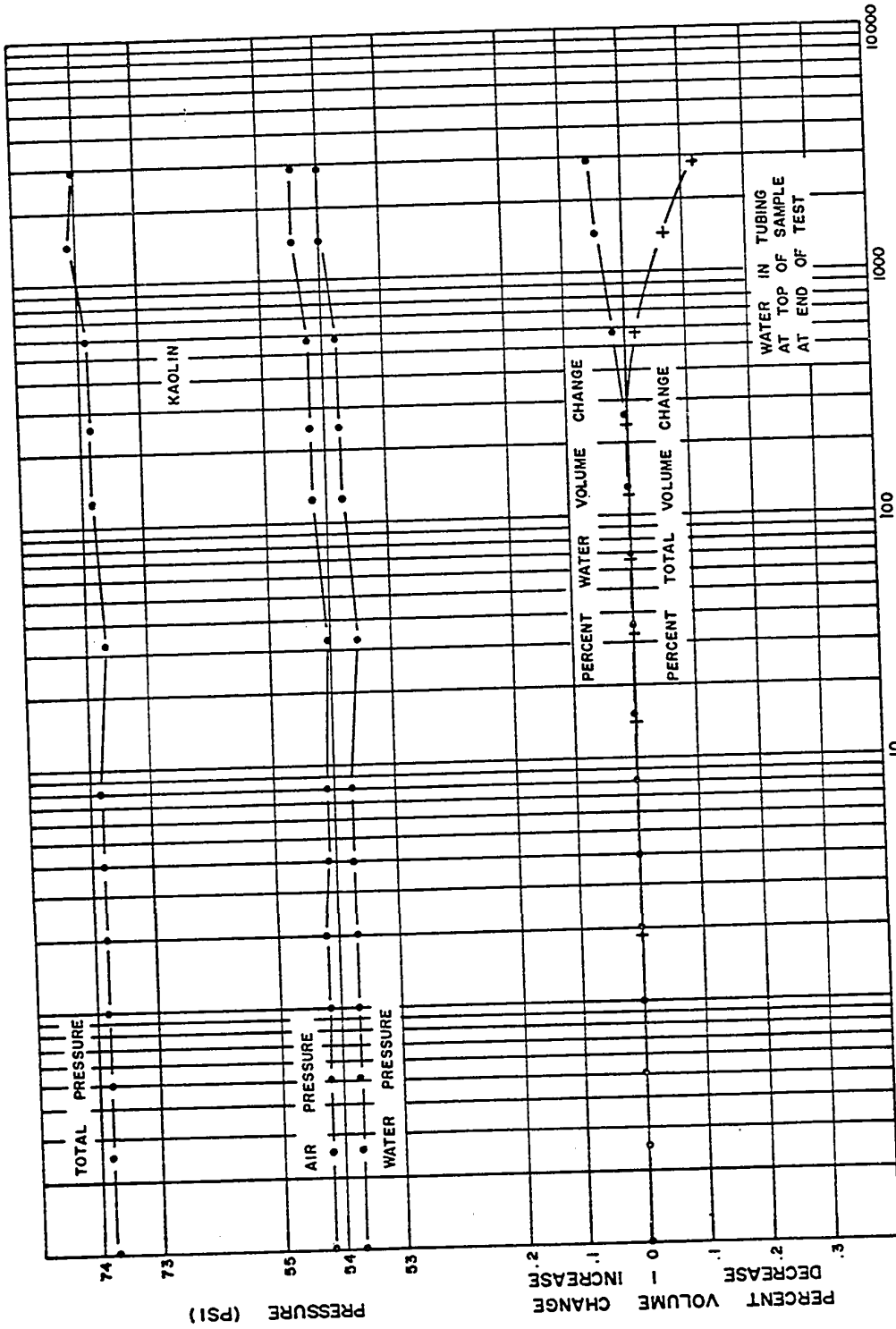
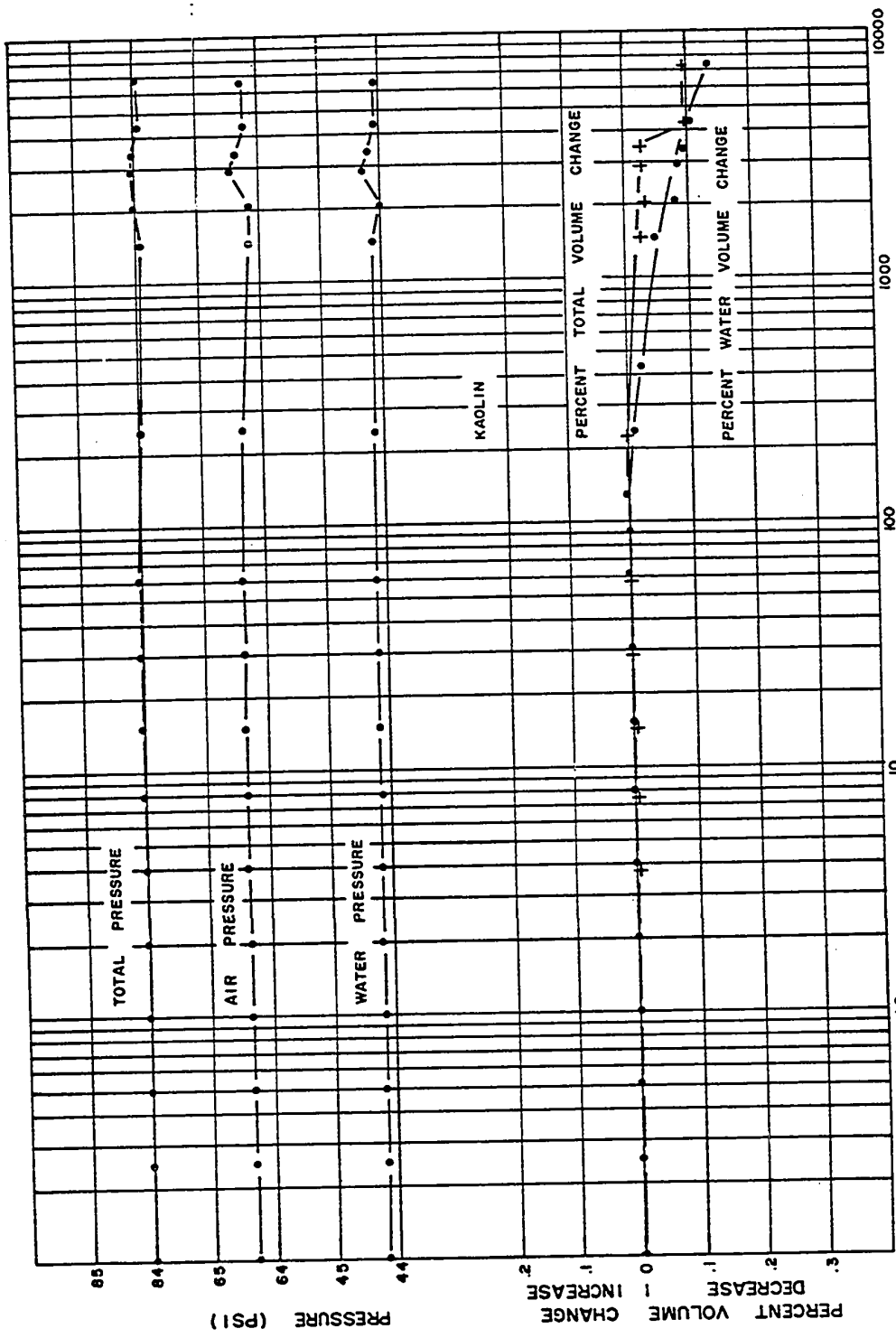


FIGURE C.16 NULL TEST (N-21) ON SAMPLE NO. 7



JUNE 30 @ 9:30

FIGURE C.17 NULL TEST (N-22) ON SAMPLE NO. 7

test (N-21). The difference between the air and water pressure was less than one psi. Therefore the surface tension effects in the coarse disc were significant. The water pressure was decreased and equilization allowed prior to null test (N-22).

In null test (N-21), the soil structure shows a slight decrease in volume after 500 minutes. Although the sample was allowed to equilize for 5 days, the volume change is likely the effect of secondary consolidation. The apparent increase in water volume in the sample is due to the uptake of water by the coarse corundum disc on top of the sample. The degree of saturation of the sample exceeded 100 percent for the same reason.

The sample was allowed to equilize for 2 days prior to performing null test (N-22). Once again, this may not be long enough to completely overcome secondary consolidation effects. The slight volume change after one day is likely due to secondary consolidation. The gradual apparent decrease in water volume is also primarily due to secondary consolidation of the sample. The slight difference between the total volume change and the water volume change could be due to some air diffusion. The increased length of diffusion path (i.e. height of sample) reduces the amount of diffused air.

The null test technique appears to be satisfactory for experimentally verifying the uniqueness of the stress state variables for a saturated soil. There is, however, a problem of air diffusion through the water in the soil and the high air entry disc. This results in an apparent water volume change. The water volume change should be

corrected for the diffused air volume.

Table C.9 summarizes the total and water volume changes that occurred during the null tests in section II. On carefully controlled tests, the volume change of the total sample and the water phase should be less than 0.1 percent for soft, saturated soils over a period of several days. This is approximately 2 percent of that anticipated for a corresponding effective stress change.

C-4 Null Test Analysis on Unsaturated Soils

The prime purpose of the entire null test program was to obtain experimental confirmation of stress state variables for unsaturated soils. A total of nineteen null tests were performed on unsaturated samples (Table C.10). The samples were allowed to equilize under a prescribed set of stress conditions and then the null tests were performed in the same manner as described for the saturated samples (Section II). The volume-weight relationships at the start of each null test are shown in Table C.11. The pressure changes associated with each null test are summarized in Table C.12.

The test data is examined primarily with the view to establishing whether or not any processes are occurring with respect to total volume change or water volume change. The test technique assumes that all air voids are continuous or inter-connected. Occluded air bubbles should tend to make the water phase behave as a compressible fluid.

One null test (N-23) was performed in Triaxial Apparatus

TABLE C.9

SAMPLE VOLUME CHANGE AND WATER VOLUME CHANGE

DURING NULL TESTS ON SATURATED SAMPLES

(Controlling Total, Air and Water Pressures)

Test No.	Pressure Change (psi)	Sample Volume Change		Water Volume Change (%)	Elapsed Time (min)	Volume Change For Corresponding Effective Stress Increase (%)
		Immediate (%)	At Elapsed Time (%)			
N-16	+10	+0.054	+0.063	+0.168	1410	2.93
N-17	+10	-0.073	-0.066	+0.054	100	--
		-0.073	-0.069	+0.19	1000	2.93
		-0.073	-0.062	+0.54	4300	2.93
N-18	-10	0.0	+0.019	+0.28	2760	2.93
N-19	+10	+0.006	0.00	+0.05	1000	2.93
		+0.006	-0.001	+0.33	7180	2.93
N-20	+10	+0.012	+0.027	+0.088	2770	2.93
N-21	+ 8	0.0	+0.129	-0.057	2870	3.07
N-22	+10	0.0	+0.110	+0.148	7170	2.14

TABLE C.10

SUMMARY OF NULL TESTS ON UNSATURATED SOILS

(CONTROLLING TOTAL, AIR AND WATER PRESSURES)

Test No.	Sample No.	Date	Starting Time	Apparatus No.	Soil Type	Change in Stresses (psi)	Compactive Effort	Comments
N-23	9	July 22/71	9:15	T-1	Kaolin	+10	Std	
N-24	10	July 21/71	9:15	OED-177	Kaolin	+20	Std	Corrected mistake in water stress after 150 min.
N-25	10	July 22/71	10:25	OED-177	Kaolin	+10	Std	
N-26	10	July 30/71	9:42	OED-177	Kaolin	-30	Std	Total stress momentarily dropped
N-27	11	July 26/71	9:37	OED-179	Kaolin	+10	Std	Water stress increased too much
N-28	20	Dec. 8/71	9:26	T-2	Kaolin	+20	Std	Mold #C
N-29	22	Jan. 11/72	10:27	T-2	Kaolin	+10	1/2 Std	Leak on air connection
N-20	22	Jan. 17/72	9:25	T-2	Kaolin			Mold #3H
N-31	22	Feb. 1/72	10:30	T-2	Kaolin	+10	1/2 Std	Mold #3H
N-32	22	Feb. 2/72	9:42	T-2	Kaolin	+10	1/2 Std	Mold #3H
N-33	22	Feb. 3/72	9:05	T-2	Kaolin	+10	1/2 Std	Mold #3H
N-34	27	Mar. 3/72	9:50	T-2	Kaolin	+10	1/2 Std	Holes in membrane
N-35	31	Mar. 17/72	9:29	T-2	Kaolin	+10	1/2 Std	Aluminum foil plus two membranes
N-36	31	Mar. 21/72	9:15	T-2	Kaolin	+10	1/2 Std	Aluminum foil plus two membranes,
N-37	31	Mar. 23/72	9:16	T-2	Kaolin	+10	1/2 Std	Aluminum foil plus two membranes
N-38	31	Mar. 27/72	11:20	T-2	Kaolin	-10	1/2 Std	Aluminum foil plus two membranes
N-39	31	Mar. 29/72	8:40	T-2	Kaolin	-10	1/2 Std	Aluminum foil plus two membranes
N-40	31	Mar. 30/72	8:57	T-2	Kaolin	-10	1/2 Std	Aluminum foil plus two membranes
N-41	31	Apr. 3/72	8:33	T-2	Kaolin	-20	1/2 Std	Aluminum foil plus two membranes

TABLE C.11

VOLUME-WEIGHT RELATIONSHIPS FOR UNSATURATED SOILS

(Controlling Total, Air and Water Pressures)

Test No.	Diameter (cm)	Height (cm)	Total Volume (cc)	Volume of Solids (cc)	Volume of Water (cc)	Volume of Air (cc)	Water Content (%)	Void Ratio	Dry Density (PCF)	Degree of Saturation (%)
N-23	10.160	11.791	955.87	457.99	378.12	119.75	31.56	1.087	78.21	75.9
N-24	6.346	2.538	80.27	52.92	34.99	2.36	31.16	0.8701	87.29	93.7
N-25	6.346	2.538	80.26	42.92	35.05	2.29	31.21	0.8698	87.30	93.9
N-26	6.346	2.542	80.41	42.92	35.63	1.86	31.73	0.8734	87.14	95.0
N-27	6.346	2.556	80.83	42.50	35.80	2.52	32.20	0.9017	85.84	93.4
N-28	9 827	5.755	436.50	226.39	189.72	20.39	32.03	0.9281	84.66	90.3
N-29	10.135	6.314	509.41	247.00	223.53	38.88	34.59	1.062	79.15	85.2
N-30	10.135	6.314	509.38	247.00	226.81	35.56	35.10	1.062	79.16	86.4
N-31	10.092	6.262	500.90	247.00	231.46	22.44	35.82	1.028	80.50	91.2
N-32	10.088	6.260	500.30	247.00	231.76	21.54	35.87	1.025	80.59	91.5
N-33	10.083	6.255	499.43	247.00	231.98	20.45	35.90	1.022	80.73	91.9
N-34	10.141	6.373	514.70	246.17	223.79	44.73	34.75	1.091	78.07	83.3
N-35	10.046	6.373	498.74	246.17	219.01	33.55	34.01	1.026	80.57	86.7
N-36	10.044	6.292	498.55	246.17	219.27	33.10	34.05	1.025	80.60	86.9
N-37	10.044	6.294	498.65	246.17	219.42	33.05	34.07	1.026	80.59	86.9
N-38	10.044	6.293	498.62	246.17	219.68	32.77	34.11	1.025	80.59	87.0
N-39	10.044	6.293	498.61	246.17	219.63	32.81	34.10	1.025	80.59	87.0
N-40	10.044	6.293	498.59	246.17	219.65	32.76	34.11	1.025	80.60	87.0
N-41	10.044	6.293	498.59	246.17	219.55	32.86	34.09	1.025	80.60	87.0

TABLE C.12

RECORD OF PRESSURE CHANGES FOR NULL TESTS ON UNSATURATED SAMPLES

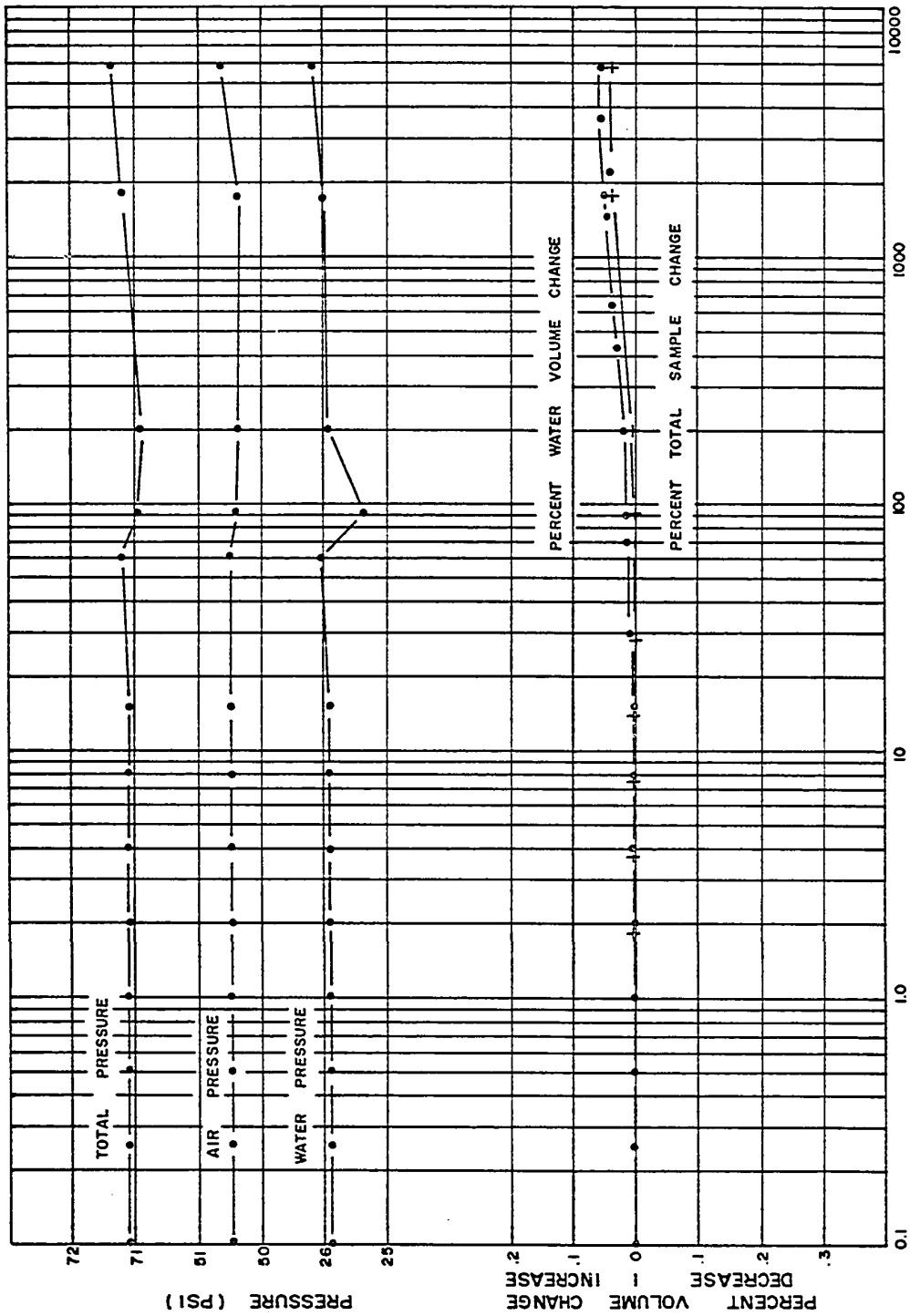
(CONTROLLING TOTAL, AIR AND WATER PRESSURES)

Test No.	Total Pressure (psi)	Air Pressure (psi)	Water Pressure (psi)	$\sigma-u_w$ (psi)	$\sigma-u_a$ (psi)	u_a-u_w (psi)	Total Pressure (psi)	Air Pressure (psi)	Water Pressure (psi)	$\sigma-u_w$ (psi)	$\sigma-u_a$ (psi)	u_a-u_w (psi)	Change in Total Pressure (psi)	Change in Air Pressure (psi)	Change in Water Pressure (psi)
N-23	61.02	40.42	15.89	45.13	20.61	24.52	71.37	50.62	26.15	45.22	20.74	24.48	+10.35	+10.20	+10.26
N-24	52.13	39.29	0.43	51.70	12.84	386.8	71.84	59.00	20.81	51.03	12.84	38.19	+19.71	+19.71	+20.38
N-25	71.84	59.00	20.81	51.03	12.84	38.19	81.78	68.90	30.51	51.27	12.88	38.39	+ 9.94	+ 9.90	+ 9.70
N-26	101.77	88.93	72.27	29.50	12.84	16.66	72.14	59.30	42.56	29.58	12.84	16.74	-29.63	-29.63	-29.71
N-27	33.97	20.06	14.54	19.43	13.91	5.52	43.95	30.00	26.27	17.68	13.95	3.73	+ 9.98	+ 9.94	+11.73
N-28	68.86	57.23	4.68	64.18	11.63	52.55	88.67	77.16	24.68	63.99	11.51	52.48	+19.81	+19.93	+20.00
N-29	39.82	29.32	3.25	36.57	10.50	26.07	49.76	39.23	13.23	36.53	10.54	25.99	+ 9.94	+ 9.91	+ 9.98
N-30	49.76	39.23	13.23	36.53	10.54	25.99	59.74	49.17	23.34	36.40	10.57	25.83	+ 9.98	+ 9.94	+10.11
N-31	59.67	49.06	23.24	36.43	10.61	25.82	69.54	58.93	33.00	36.54	10.61	25.93	+ 9.87	+ 9.87	+ 9.76
N-32	69.54	58.93	33.00	36.54	10.61	25.93	79.62	69.09	43.11	36.51	10.54	25.97	+10.08	+10.16	+10.11
N-33	79.62	69.09	43.11	36.51	10.54	25.97	89.63	78.96	53.02	36.61	10.67	25.94	+10.01	+ 9.87	+ 9.91
N-34	39.57	29.32	10.60	28.97	10.26	18.71	49.27	38.88	20.19	29.08	10.40	18.68	+ 9.70	+ 9.56	+ 9.59
N-35	59.60	49.10	30.21	29.39	10.50	18.89	69.68	59.14	40.32	29.36	10.54	18.82	+10.08	+10.04	+10.11
N-36	69.68	59.14	40.32	29.36	10.54	18.82	79.41	68.70	49.88	29.53	10.71	18.82	+ 9.73	+ 9.56	+ 9.56
N-37	79.41	68.70	49.88	29.53	10.71	18.82	89.25	78.50	59.65	29.60	10.74	18.86	+ 9.84	+ 9.80	+ 9.77
N-38	89.25	78.50	59.65	29.60	10.74	18.86	79.69	69.19	50.41	29.28	10.50	18.78	- 9.56	- 9.31	- 9.24
N-39	79.69	69.19	50.41	29.28	10.50	18.78	69.50	59.11	40.29	29.21	10.40	18.81	-10.10	-10.08	-10.12
N-40	69.50	59.11	40.29	29.21	10.40	18.81	59.84	49.41	30.66	29.18	10.43	18.75	- 9.66	- 9.70	- 9.63
N-41	59.84	49.41	30.66	29.18	10.43	18.75	39.47	29.07	10.39	29.08	10.40	18.68	-20.37	-20.34	-20.27

No. 1 on a compacted kaolin sample (Figure C.18). After 5720 minutes, the total sample showed a volume increase of 0.029 percent. This is approximately equal to the accuracy of the measuring system. The water volume change indicator showed some water moving into the sample. Presumably this is a reflection of the compression of occluded air bubbles. After 5720 minutes, the water volume increase (or compression) was 0.05 percent. Applying Boyle's law to the compression of the occluded air bubbles shows that the original volume of occluded air was approximately 3.62 cc. The air in the sample can theoretically be subdivided as 3% occluded air and 97% continuous air. No process is evident in the sample apart from the slight compression of occluded air.

Three null tests (N-24), (N-25), (N-26) were performed in the Oedometer on sample #10. (Figure C.19 to C.21, inclusive). In the first test (N-24), the water pressure was mistakingly increased by 21.94 psi rather than 20.00 psi. Water proceeded to enter the sample and some swelling of the total sample occurred. The error was noticed and corrected at an elapsed time of 150 minutes. Water then started to come out of the sample; however, the hysteretic effects prevented it from re-establishing its original conditions.

The water volume increase was 0.17 percent for an excess water pressure of 2.1 psi. Extrapolating to a excess water pressure of 20 psi gives an indication of the amount of water that could go into the sample under such a change. Although the results are not those of a satisfactory null test, they do show the type of process



JULY 22 @ 9:15

FIGURE C.18 NULL TEST (N-23) ON SAMPLE NO. 9

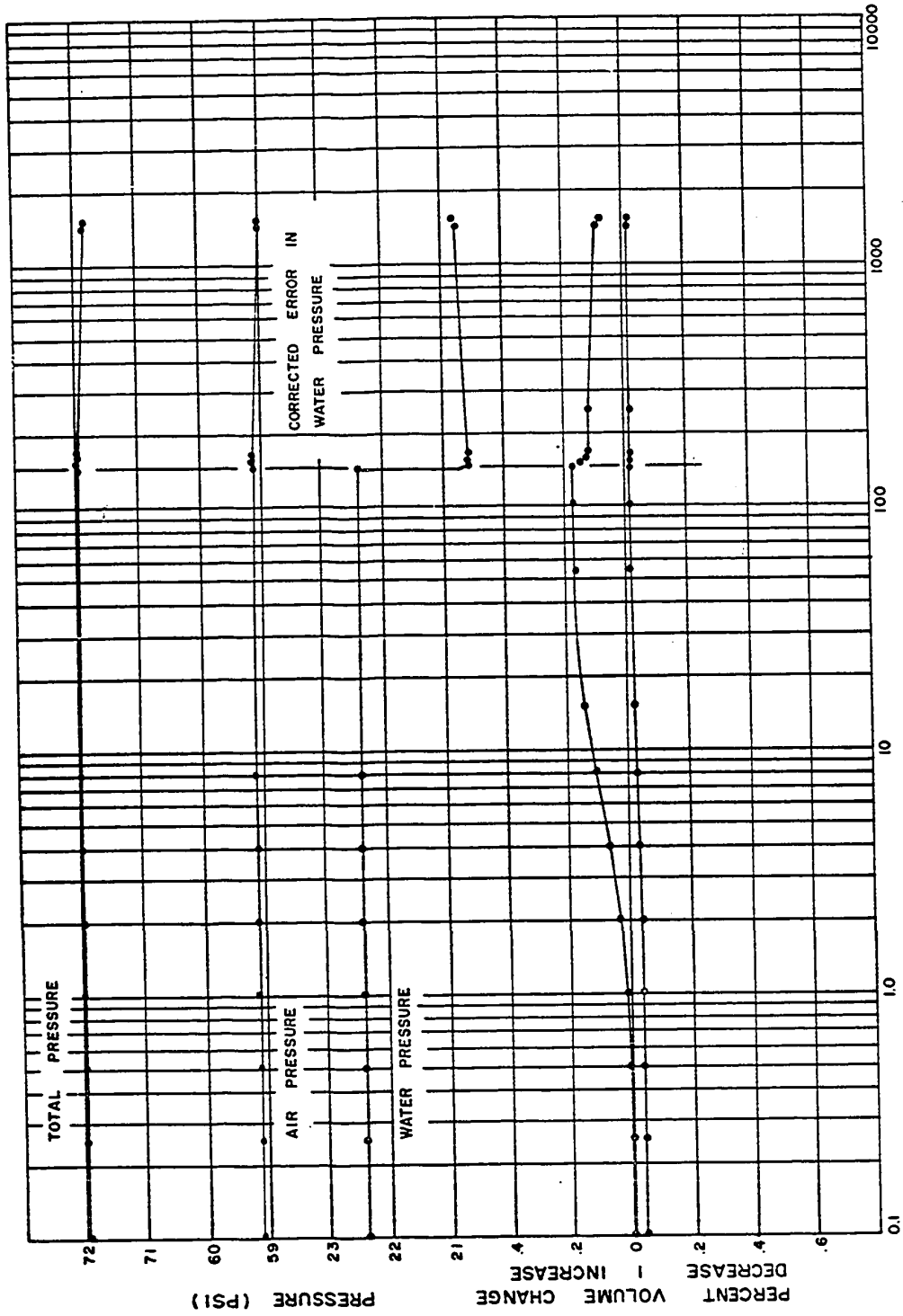
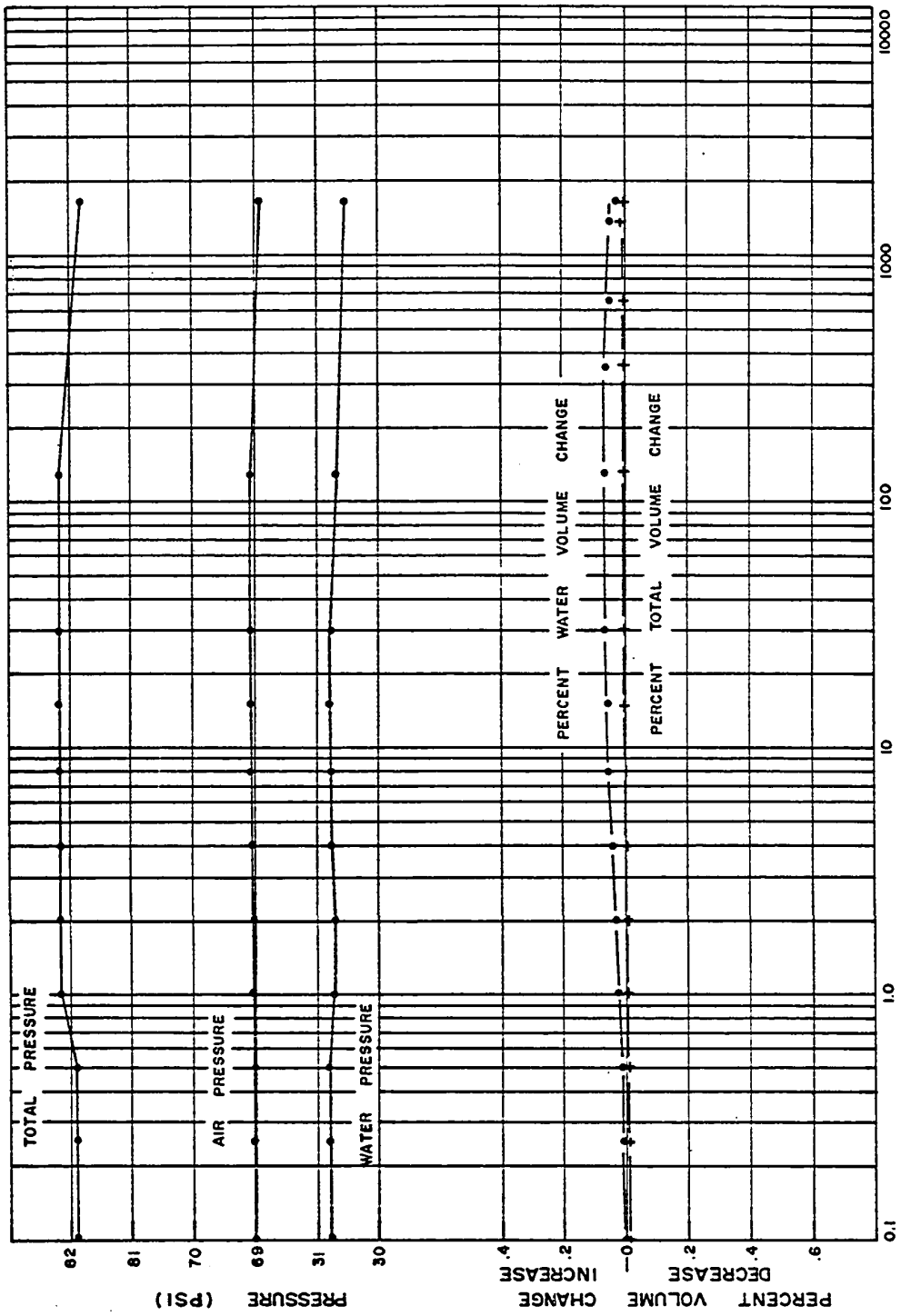


FIGURE C.19 NULL TEST (N-24) ON SAMPLE NO. 10



JULY 22 @ 10:25

FIGURE C.20 NULL TEST (N-25) ON SAMPLE NO. 10

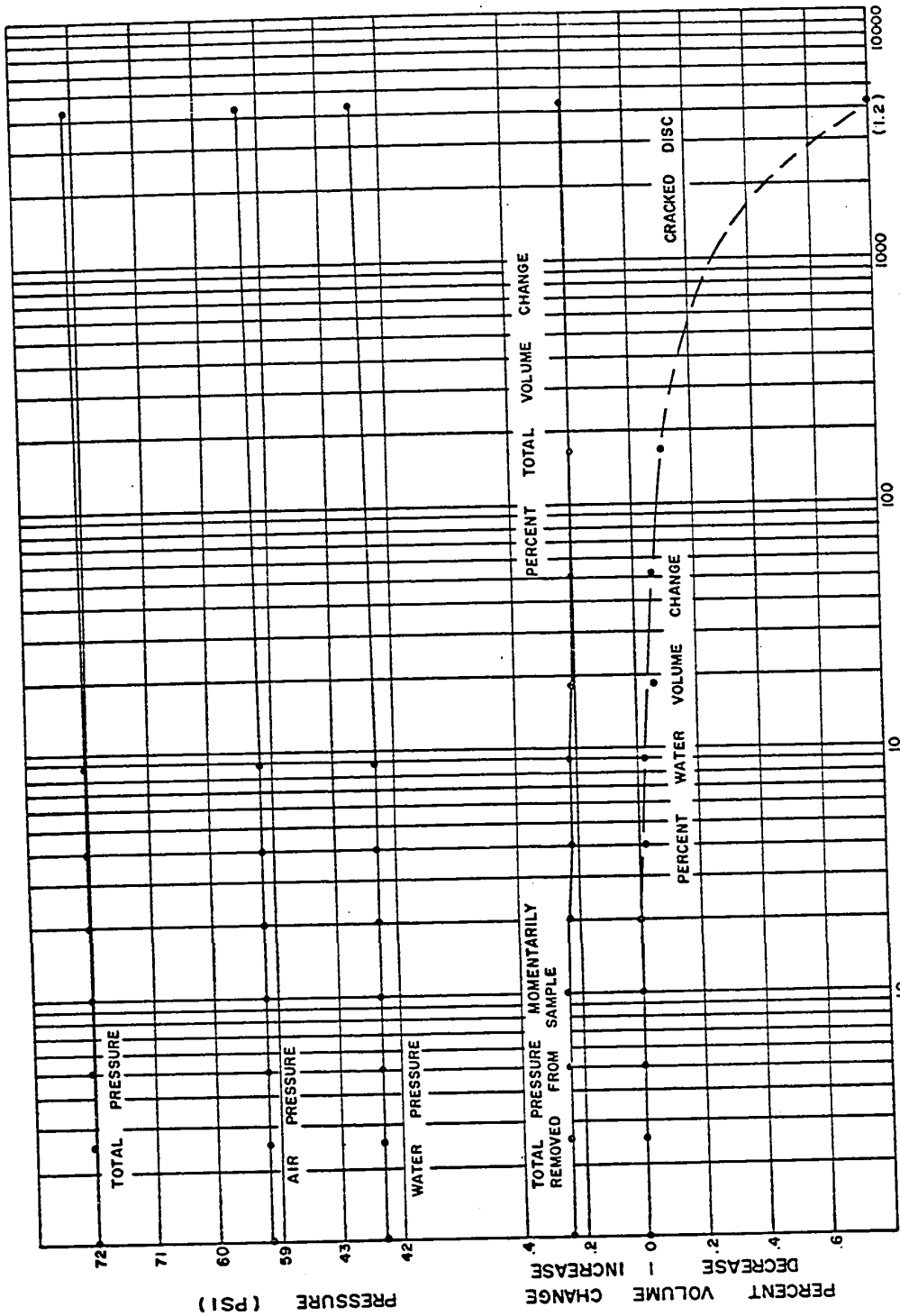


FIGURE C.21 NULL TEST (N-26) ON SAMPLE NO. 10

involved when the pressure changes are not precise.

Null test (N-25) show that no total volume change occurred following an increase in all pressures. Approximately 0.3 percent water had gone into the sample after 100 minutes. Again this is related to the compressibility of the water with the occluded air bubbles. The slight removal of water from the sample toward the end of the test is believed related to air diffusion through the sample.

At the start of null test (N-26), the load range selector was in the wrong position. This resulted in a momentary reduction of the total pressure to zero psi. Apparently the high water pressure during the rapid alteration of total and air pressures produced distress to the ceramic disc. It is believed a fine crack developed in the thin, 15 bar ceramic disc at this time. Although the total sample showed very little volume change with time, the water volume decrease was 1.2 percent after 3 days. Air was evident in the polyethylene line below the base of the oedometer.

Null test (N-27) was performed on kaolin sample #11 in the oedometer (Figure C.22). The water pressure was erroneously increased by 11.65 psi rather than 10.00 psi throughout the test. The test was unsuccessful as a null test but it does depict the magnitude of volume changes when there is a 12 percent error in the water pressure. The fact that a swelling process is occurring is definitely evident from the data.

The remaining null tests were performed in Triaxial Apparatus No. 2. The construction of the new triaxial apparatus was completed

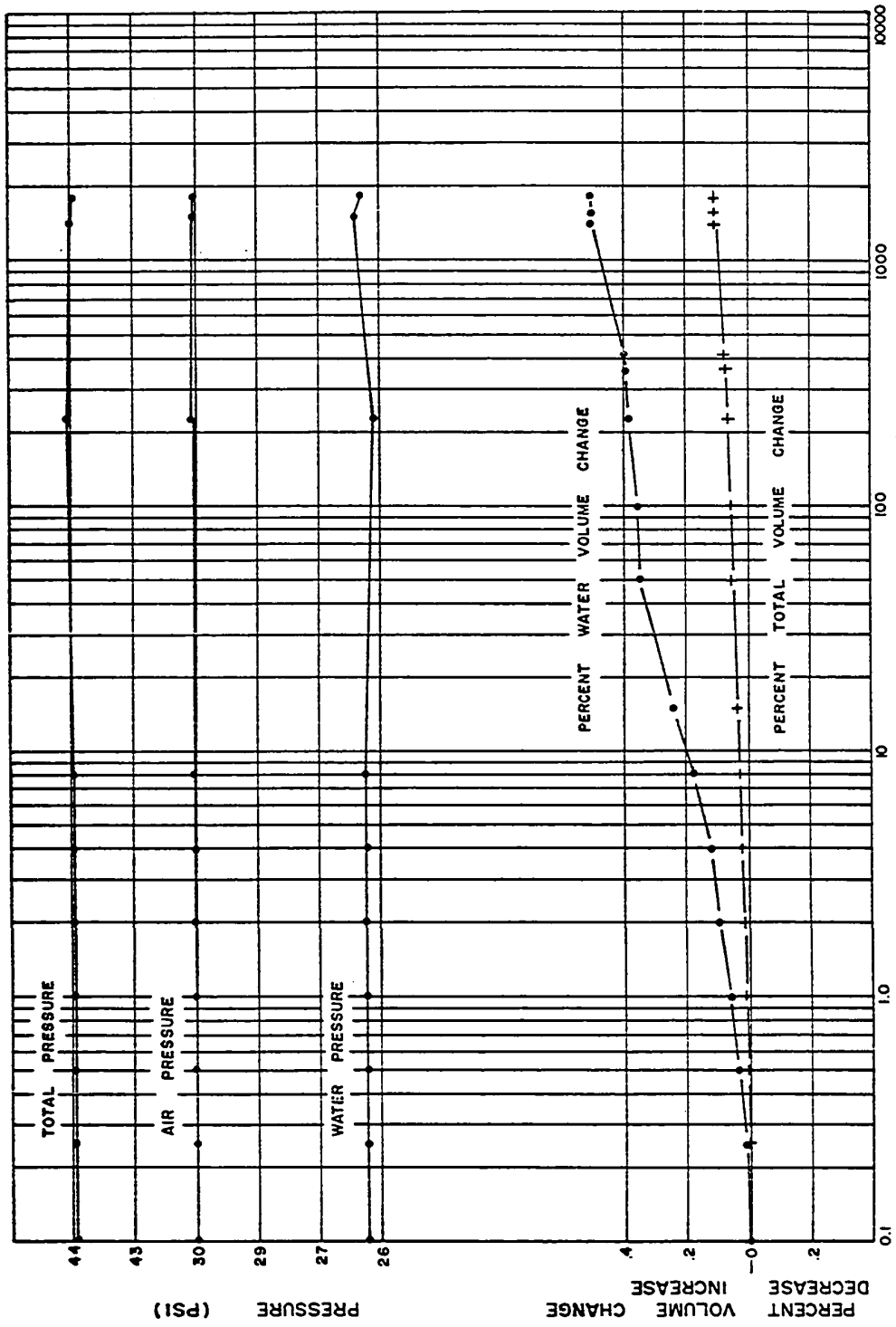


FIGURE C.22 NULL TEST (N-27) ON SAMPLE NO. 11

in January of 1972 and the null tests were used to obtain continuously monitored null tests and to check the performance of the equipment. Many features of the equipment were original and it was anticipated that they could present problems. There were two main problems; the time required to increase the cell pressure due to the large volume of air in the cell, and leakage of water through the membrane around the sample.

The effect of the above problems is clearly depicted in null test (N-28) (Figure C.23). Since the cell pressure does not increase as quickly as the air pressure in the top cap, the top cap lifts off the sample. This is reflected as a volume increase of approximately one percent during the early stages of loading. By one minute the total volume change was -0.15 percent and remains essentially constant for 2 days. There is no evidence of a process occurring in the total sample. The water volume change showed a slight amount of water entering the sample during the first 10 minutes. Then some water appears to be moving out of the sample. Flushing the base plate at 100 minutes showed that the apparent water volume decrease was due to diffused air. However, it should be noted that on this and subsequent flushings of the base, the water volume change indicated some water actually moving into the sample. This test and subsequent tests showed that water was evaporating through the rubber membrane. Initially it was anticipated that the water leakage would be insignificant. However, the water losses are substantial when dealing with dry, unsaturated soils.

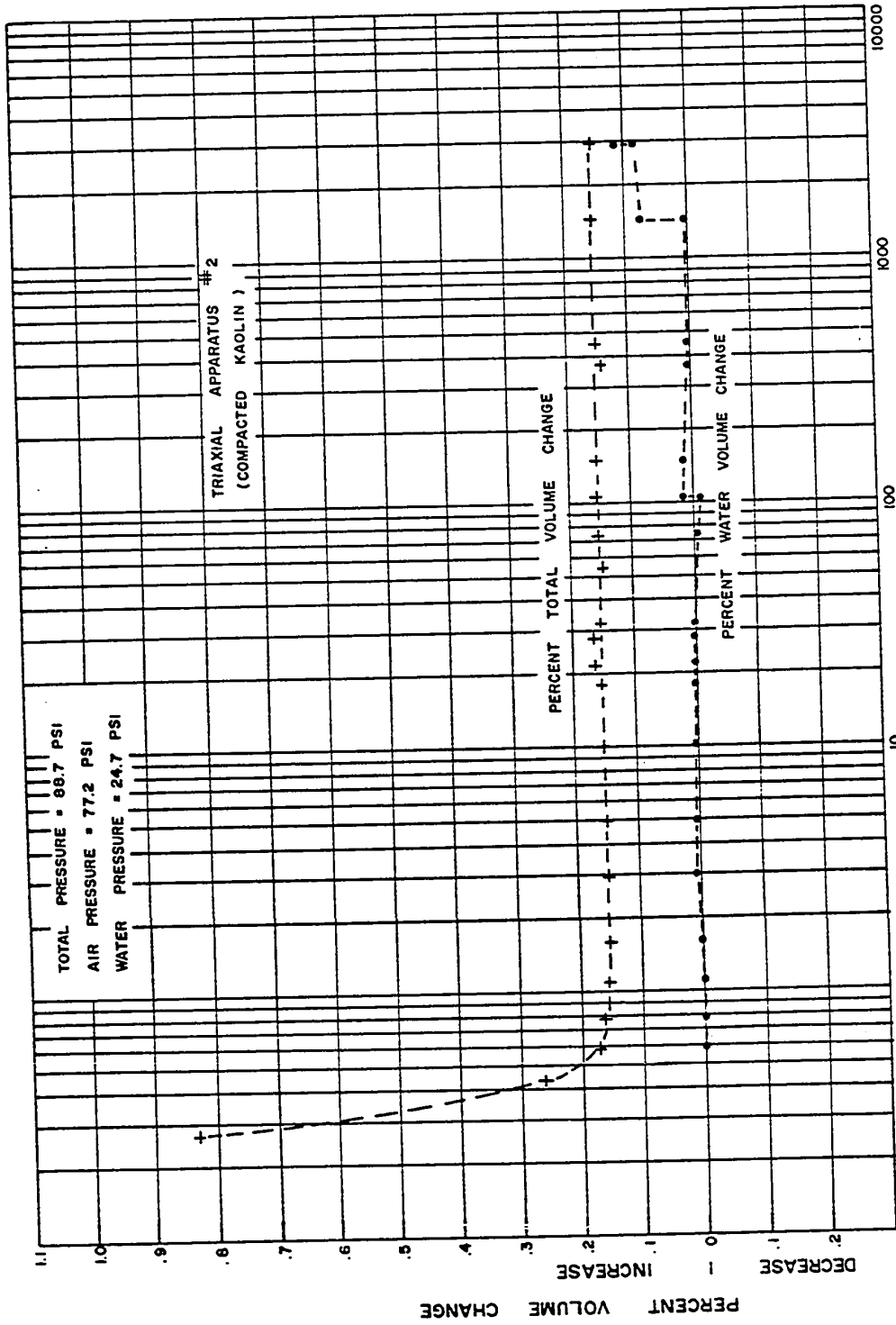


FIGURE C.23 NULL TEST (N-28) ON SAMPLE NO. 20

Null tests (N-29) and (N-30) did not have the air connection on the top of the cap properly secured (Figures C.24 and C.25). There was some leakage and it is assumed that the air pressure remained relatively constant at a pressure somewhere between the air and cell pressure. The connection was tightened on February 1, 1972. The cell pressure and the air pressure valves were opened simultaneously. In null test (N-29) there was some lifting of the load cap which returned to -0.01 percent after one minute. The test was continued for 6 days and the sample underwent a volume decrease of 0.03 percent. The water volume change curve shows a continuous inflow of water. After 6 days, 0.65 percent water had evaporated through the rubber membrane. If the moisture was kept in the triaxial cell, the air would approach 100 relative humidity and no further evaporation should take place. However, this does not appear to be the case. Independent tests on lucite have shown that a change in relative humidity can provide the driving force for moisture to move through lucite (Appendix B). The permeability of rubber and lucite to water are of a similar order of magnitude and it is doubtful if equilibrium could ever be established.

Null test (N-30) shows similar results to test (N-29). The test was only continued for one day. The total volume decreased slightly and the water volume depicted some evaporation of moisture through the membrane. Since the air pressure is always operated as an open system, some leakage of air does not affect the results.

Null tests (N-31), (N-32) and (N-33) show the results of an attempt to open the cell pressure at various times preceeding the

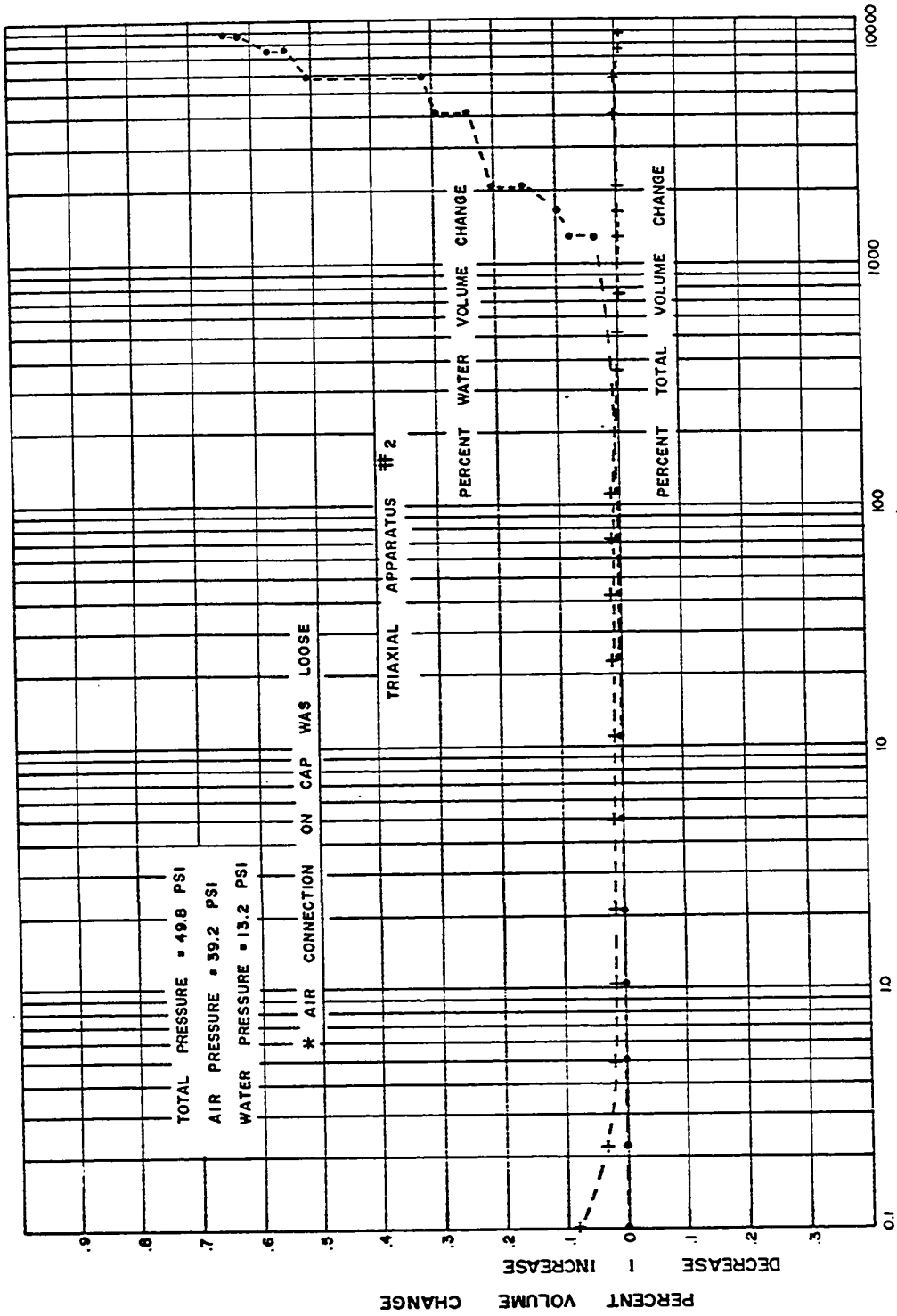


FIGURE C.24 NULL TEST (N-29) ON SAMPLE NO. 22

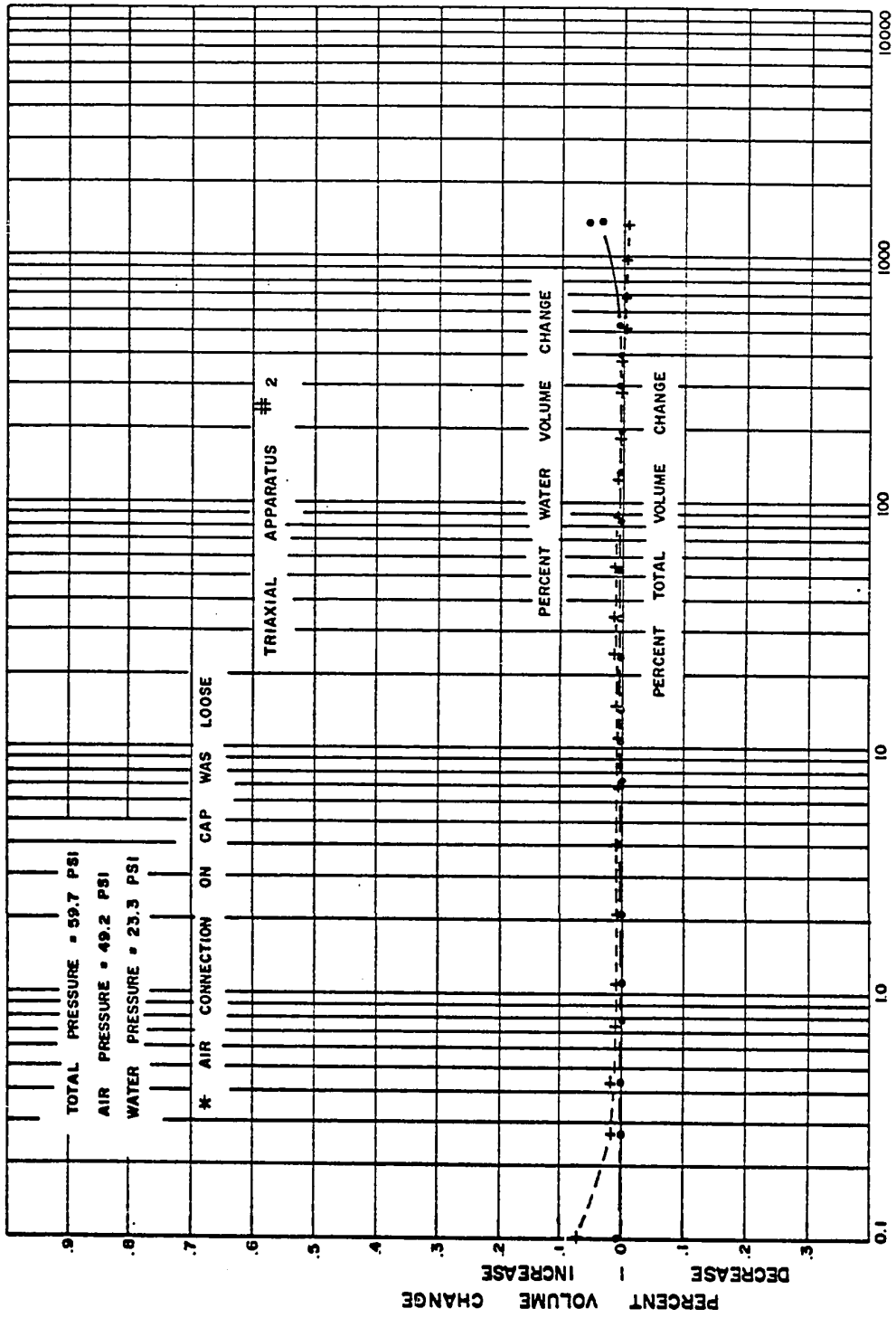


FIGURE C. 25 NULL TEST (N-30) ON SAMPLE NO. 22

opening of the air and water pressure (Figures C.26, C.27 and C.28). In all cases, the application of part of the total pressure produced an immediate compression of 0.2 to 0.3 percent. After approximately 10 minutes, the total volume became constant and remained so throughout the null test. All three tests showed a tendency for water loss through the rubber membrane.

Null test (N-34) showed similar behavior to the last three null tests (Figure C.29). This was the same latex membrane as was used for samples #22 and #27. After null test (N-34), the membrane was removed from the sample and carefully examined. The membrane was somewhat deteriorated and several small holes appeared after placing slight strain on the membrane. The latex membranes had been subjected to moisture on one side and air on the other for approximately two months.

The problem of leakage through the membrane was overcome by use of a composite membrane involving the latex membranes and a slotted aluminum foil. First, a rubber membrane is placed around the sample. It is covered with a film of vacuum grease. Then two layers of slotted aluminum foil (the same height as the sample) are wrapped around the sample. Vacuum grease is placed between the two layers of aluminum foil and on the outside of the aluminum foil. O-rings were used to seal the top and bottom of the sample. There was some concern that the compressibility of the composite membrane would affect the lateral displacement readings. This has proven to not be the case. It appears that the aluminum foil provides the prime cutoff for moisture migration.

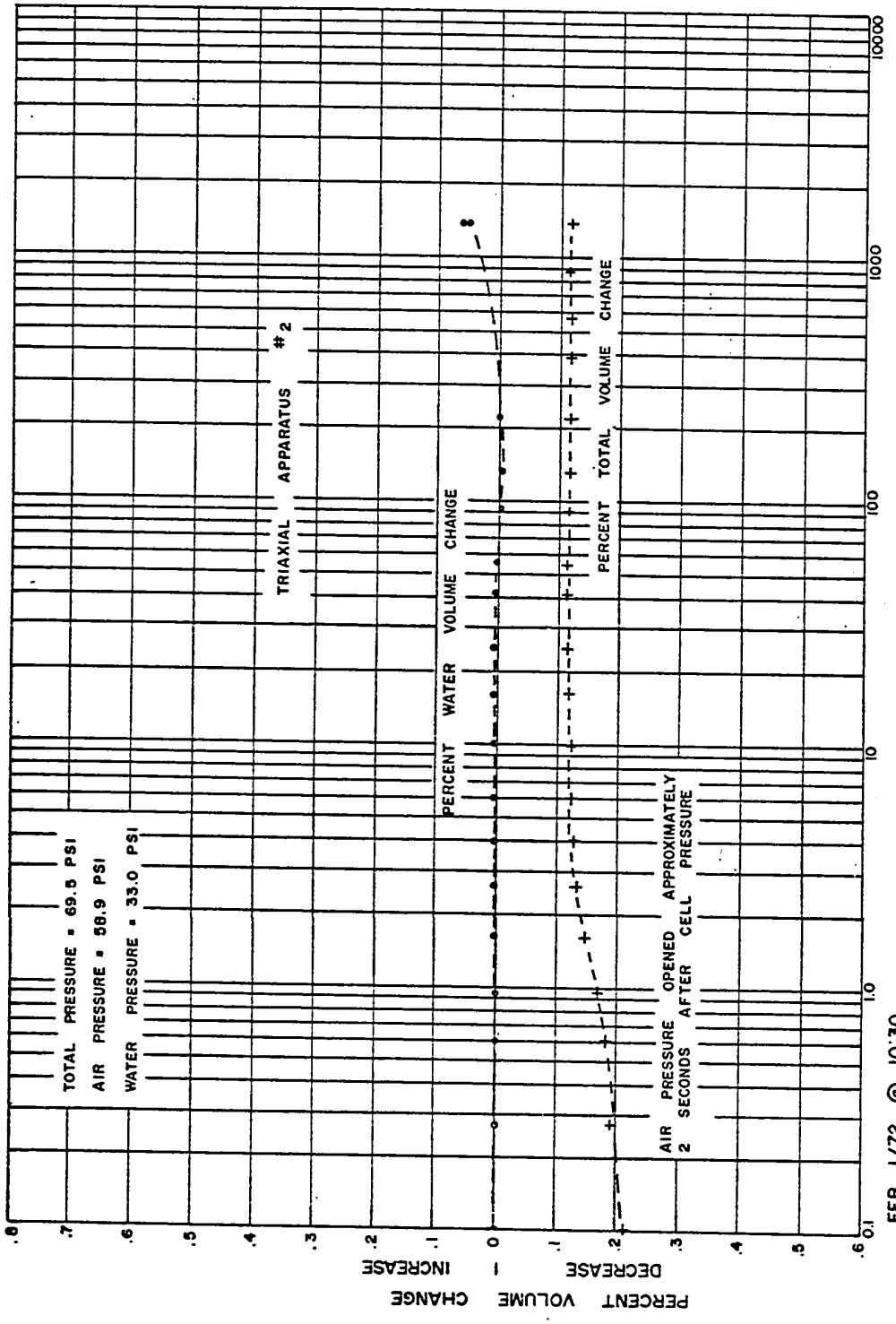


FIGURE C. 26 NULL TEST (N-31) ON SAMPLE NO. 22

FEB. 1/72 @ 10:30

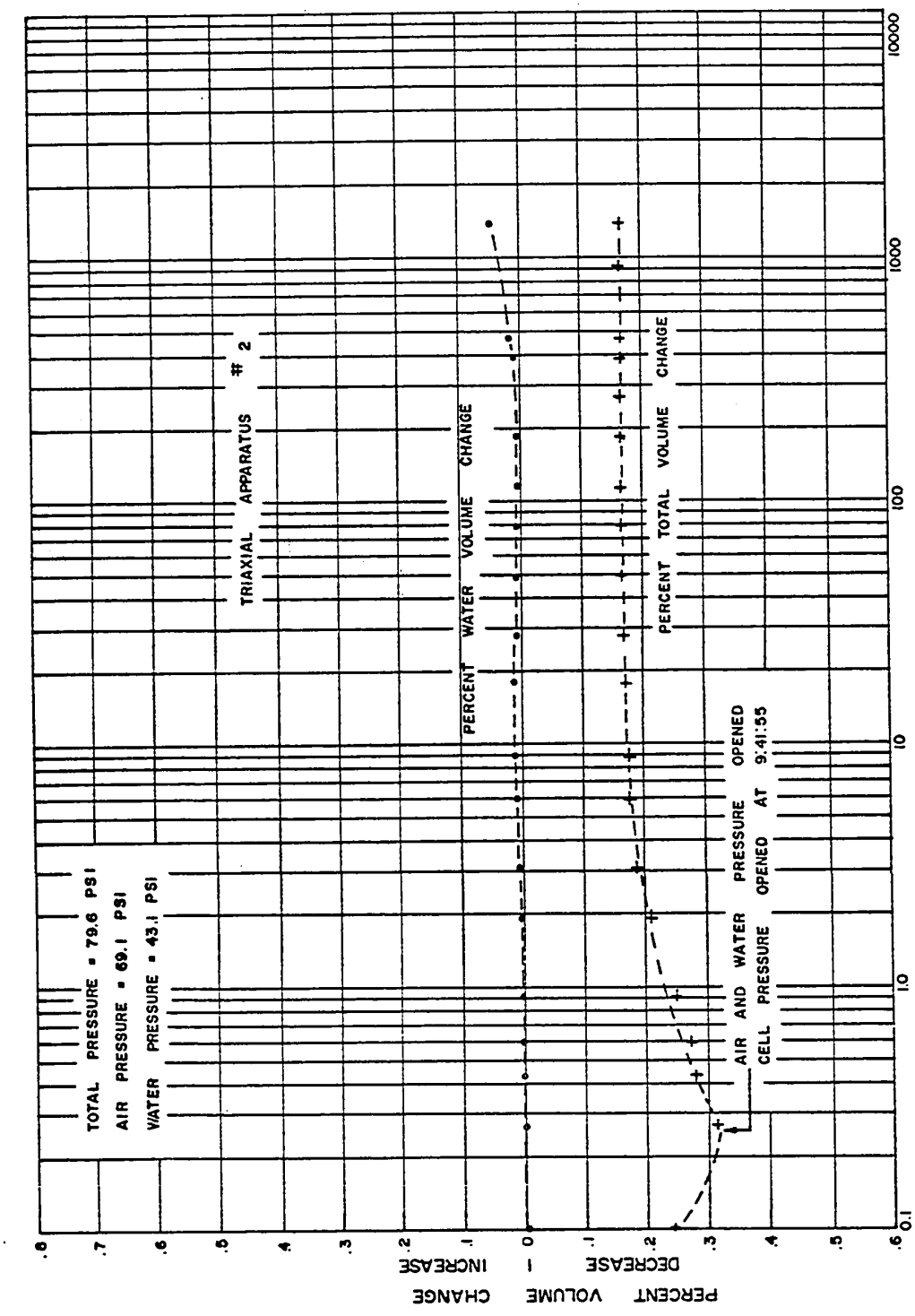


FIGURE C.27 NULL TEST (N-32) ON SAMPLE NO. 22

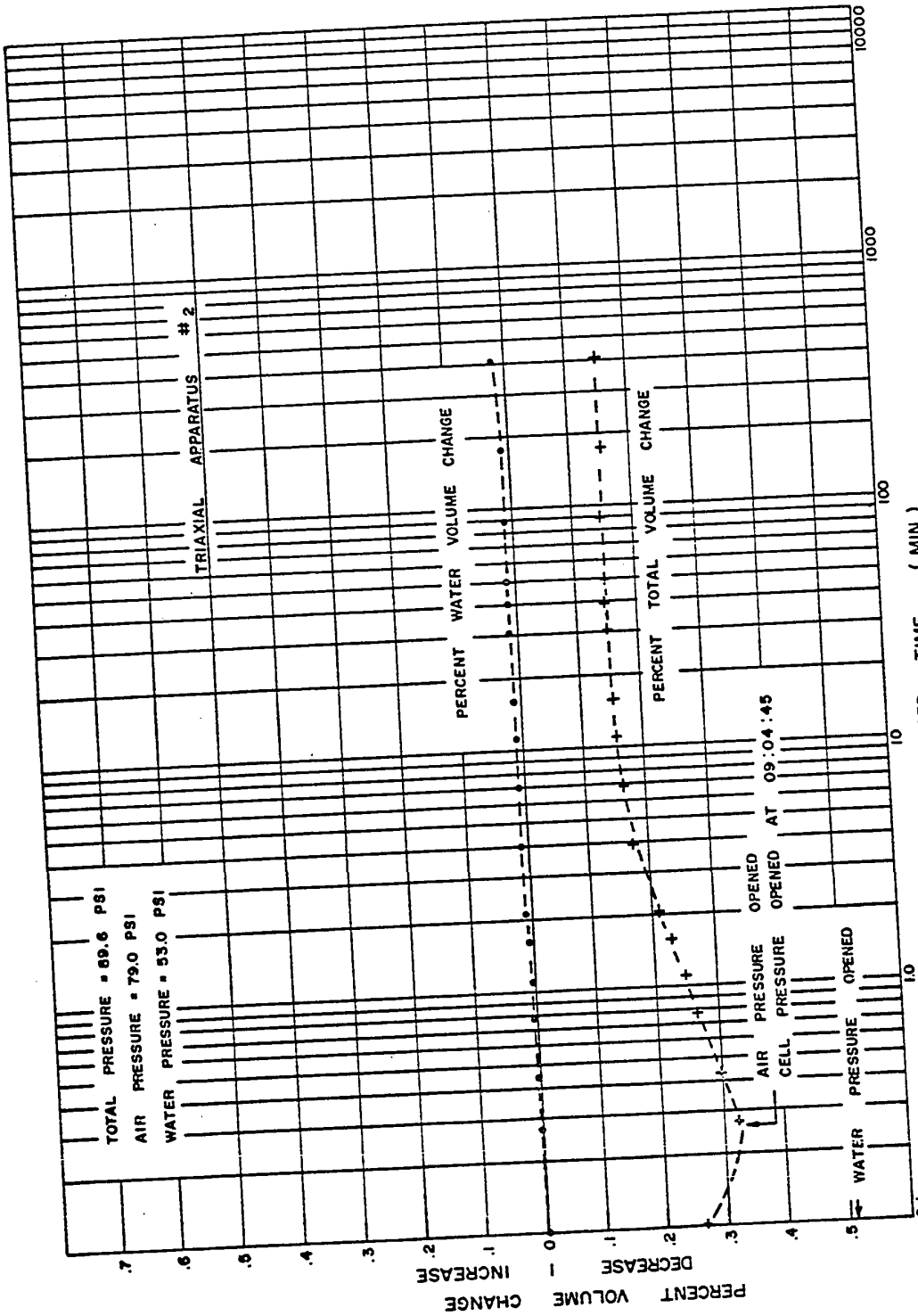


FIGURE C.28 NULL TEST (N-33) ON SAMPLE NO. 22
FEB. 3/72 @ 9:05

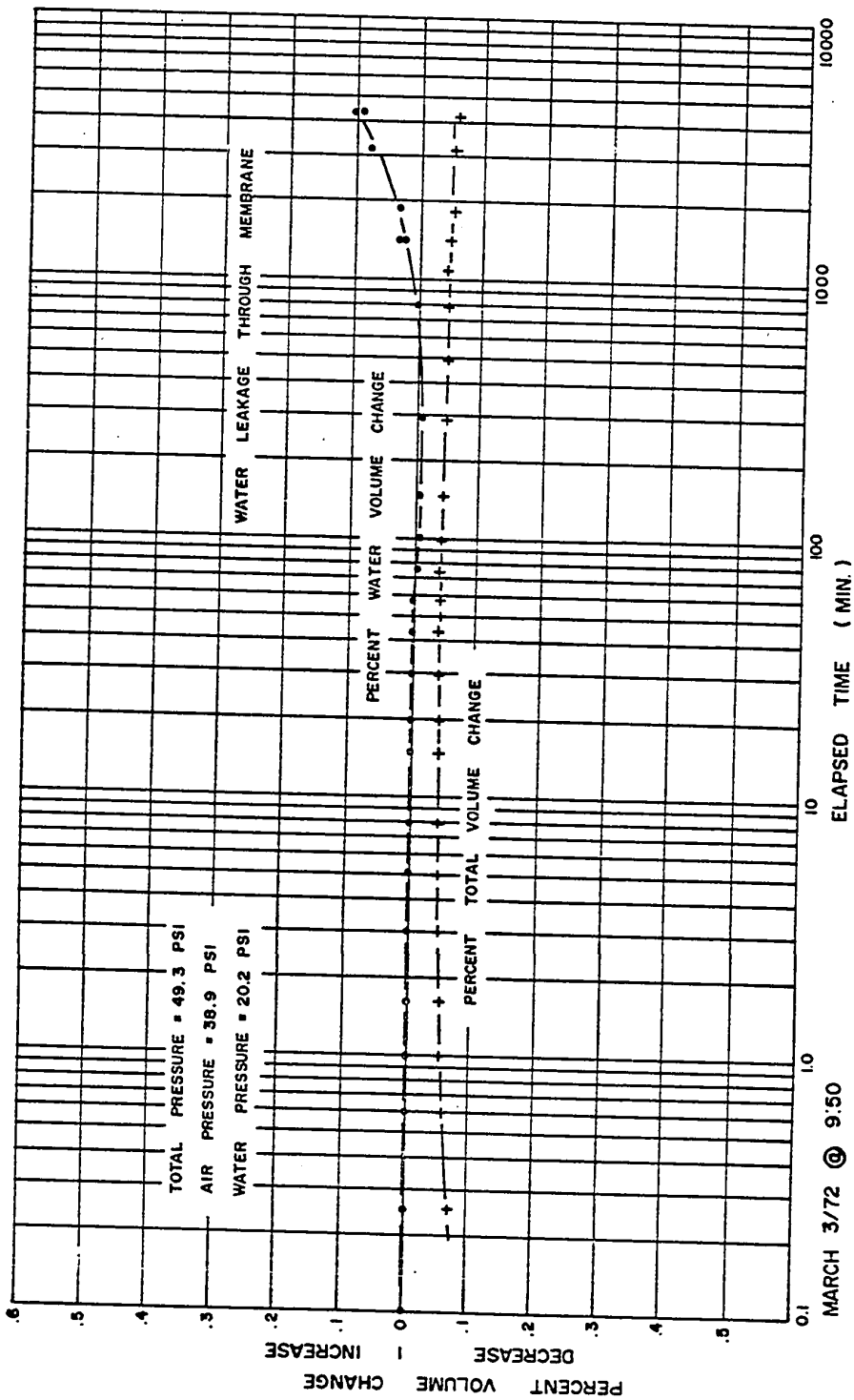


FIGURE C.29 NULL TEST (N-34) ON SAMPLE NO. 27

The problem of time for cell pressure equilization was overcome by using a surge tank with a volume approximately equal to the air volume in the triaxial cell. If the cell pressure is to be raised by 10 psi, the pressure in the surge tank is raised by 20 psi. Upon opening the valve from the surge tank to the triaxial cell, the cell pressure is increased by 10 psi in approximately one second. (The pipe from the cell to the surge tank is 3/8 inches in diameter).

The last set of null tests [(N-35) to (N-41), inclusive] were performed with the equipment problems essentially solved. The respective results are shown on Figures C.30 to C.33, inclusive.

The first three null tests (N-35), (N-36) and (N-37) were performed with all pressures being increased by 10 psi. In null test (N-35), the cell pressure increase was applied using the surge tank. The immediate total volume change was a volume decrease of approximately 0.015 percent. The volume then increased slightly and remained essentially constant until 1900 minutes when the voltage power supply for the LVDT's was shut off for a few minutes. Turning the voltage supply back on did not produce the same LVDT readings. The LVDT gauges are being used to a resolution beyond which the manufacturers guarantee. It is not definitely known whether the abrupt total volume change was due to disturbance of the triaxial cell or the limit of accuracy of the gauges. The increase in water volume at subsequent readings might indicate disturbance.

The total and air pressure were gradually increased by 10 psi over a period of 1-1/2 minutes at the start of null test (N-36).

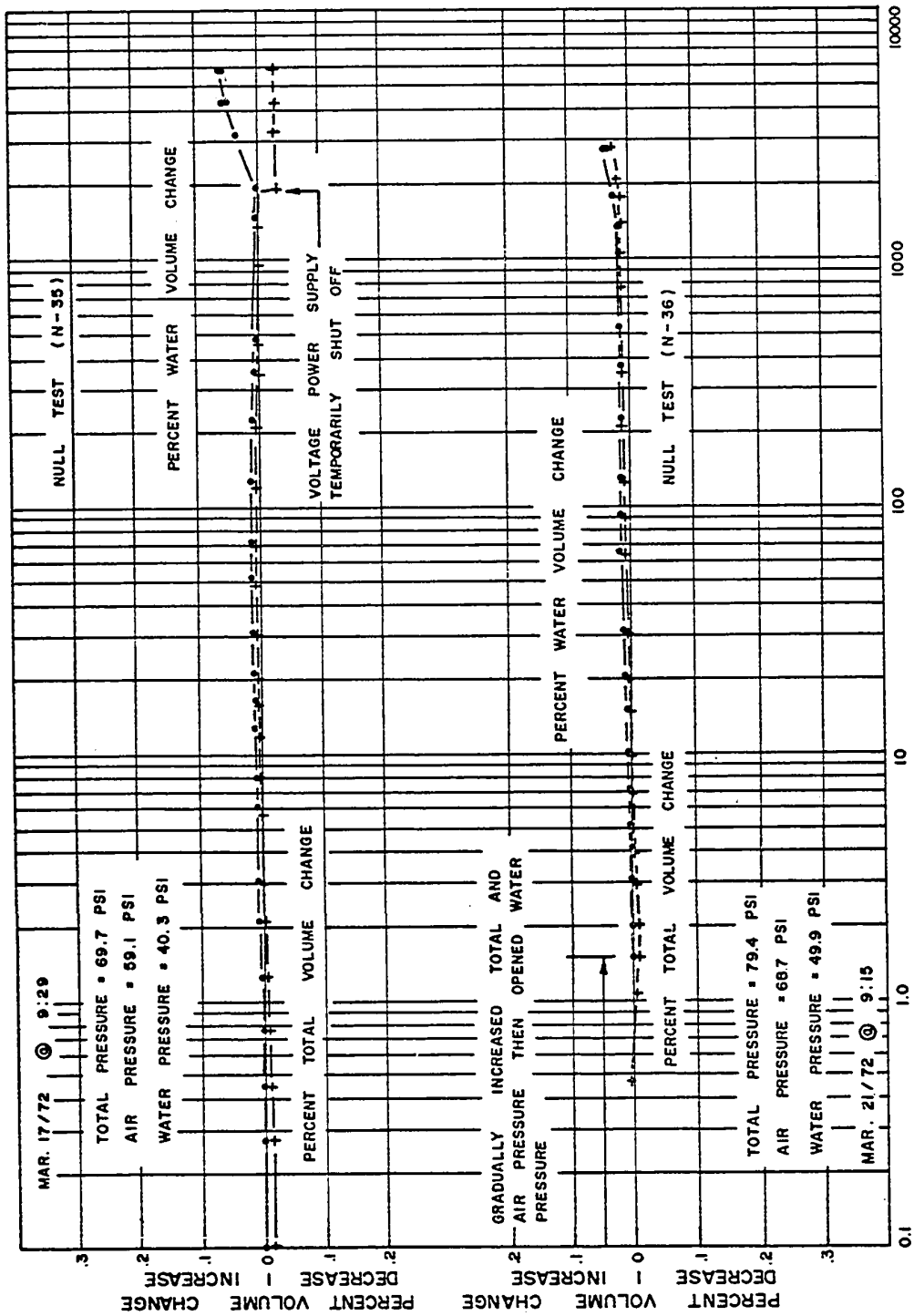


FIGURE C.30 NULL TESTS (N-35) AND (N-36) ON SAMPLE NO. 31

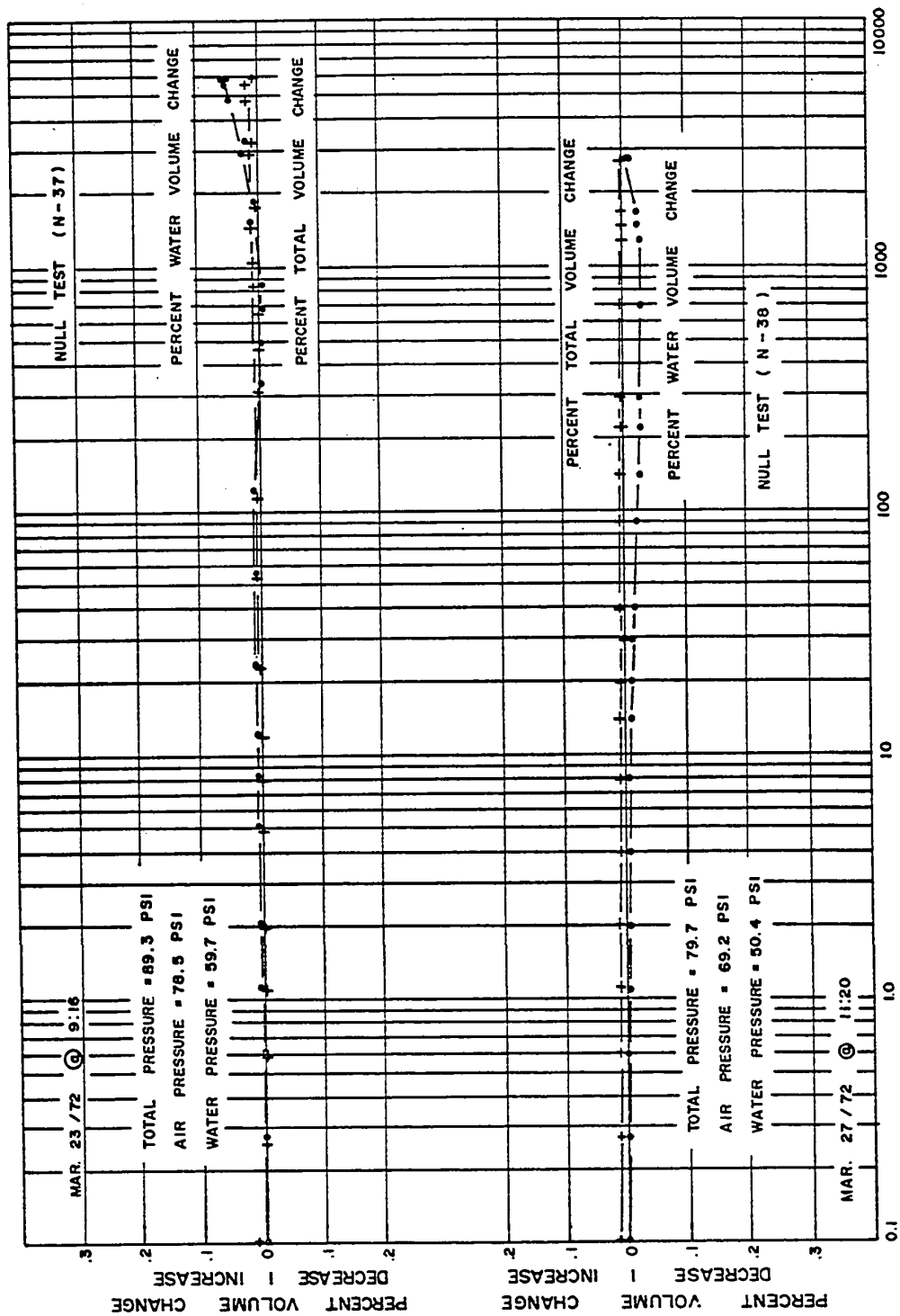


FIGURE C.31 NULL TESTS (N-37) AND (N-38) ON SAMPLE NO. 31

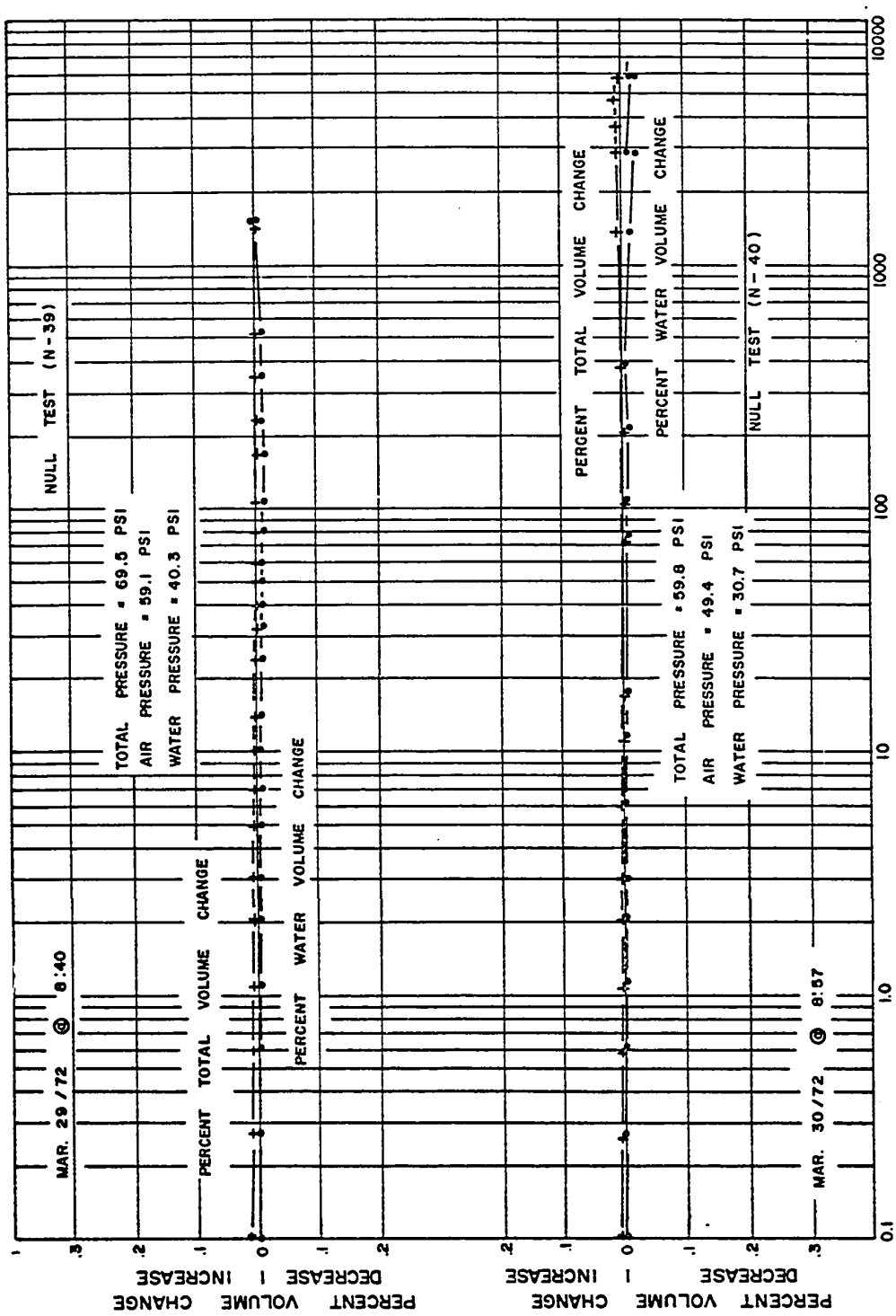


FIGURE C.32 NULL TESTS (N-39) AND (N-40) ON SAMPLE NO. 31

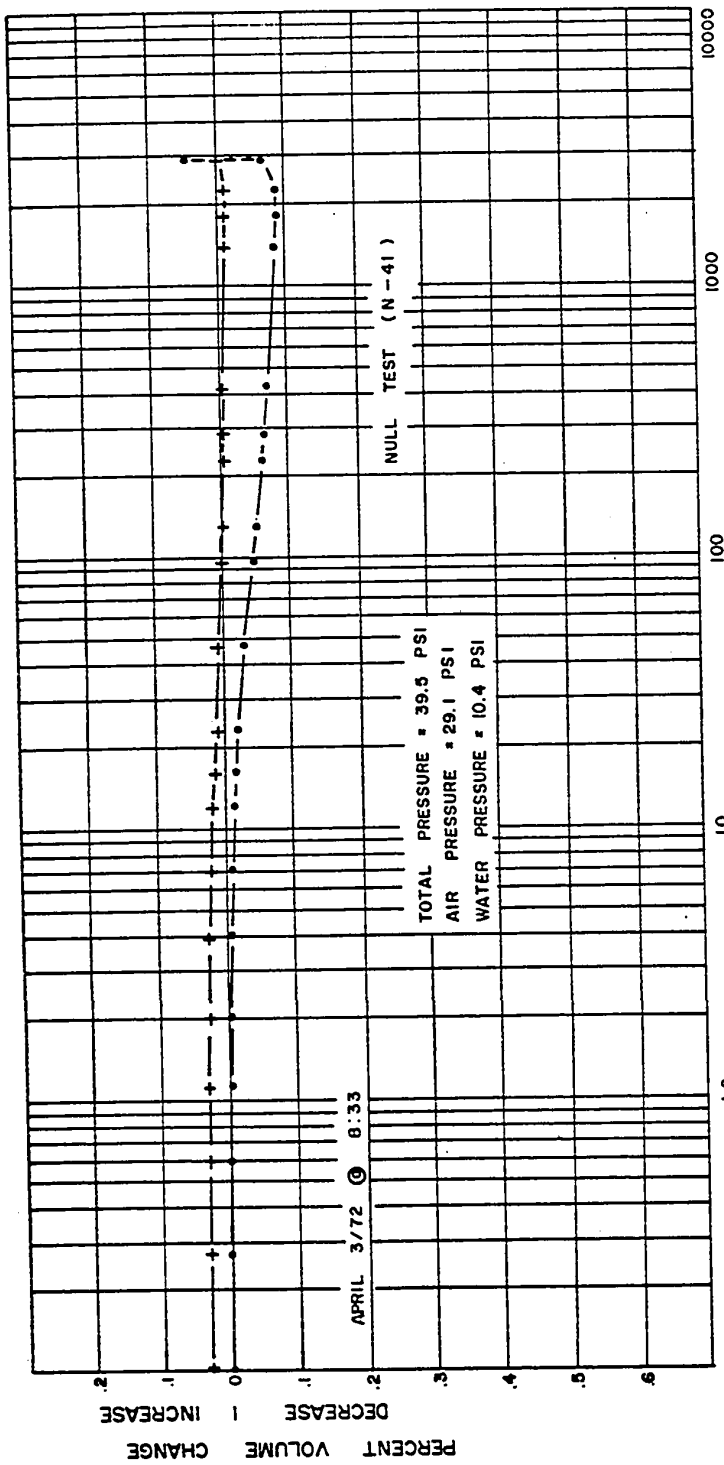


FIGURE C.33 NULL TEST (N-41) ON SAMPLE NO. 31

During this period the water pressure valve remained closed. The results show essentially no total volume change during the application of the pressures. This technique does not make use of the surge tank. Both the total and water volumes remained constant for an elapsed time of two days.

The surge tank was used for subsequent tests. Null test (N-37) shows the total sample remaining at a constant volume for six days. Some water appears to be coming out of the sample after one day. However, when combining the last seven null tests, there is a cancelling effect. It is doubtful if the apparent water volume change can be attributed to leakage through the membrane. Figure C.34 shows null test (N-37) with the volume changes amplified ten times. There is a correspondence between the total and water volume change with the volume changes magnified in the water phase. Although the results are approaching the resolution of all measuring systems, their similarity of behavior would indicate the effect of a "real" variable such as temperature. In any case, the volume changes are extremely small; in the order of one part in ten thousand.

The unloading null tests (N-38), (N-39), (N-40) and (N-41) also show essentially no tendency for total or water volume change with time. The largest volume changes were experienced in null test (N-41) when the pressures were reduced by 20 psi. The large pressure change increment appears to cause some disturbance to the soil structure. Null test (N-40) was replotted (Figure C.35) with the volume changes expanded ten times. The correspondence between the total and water

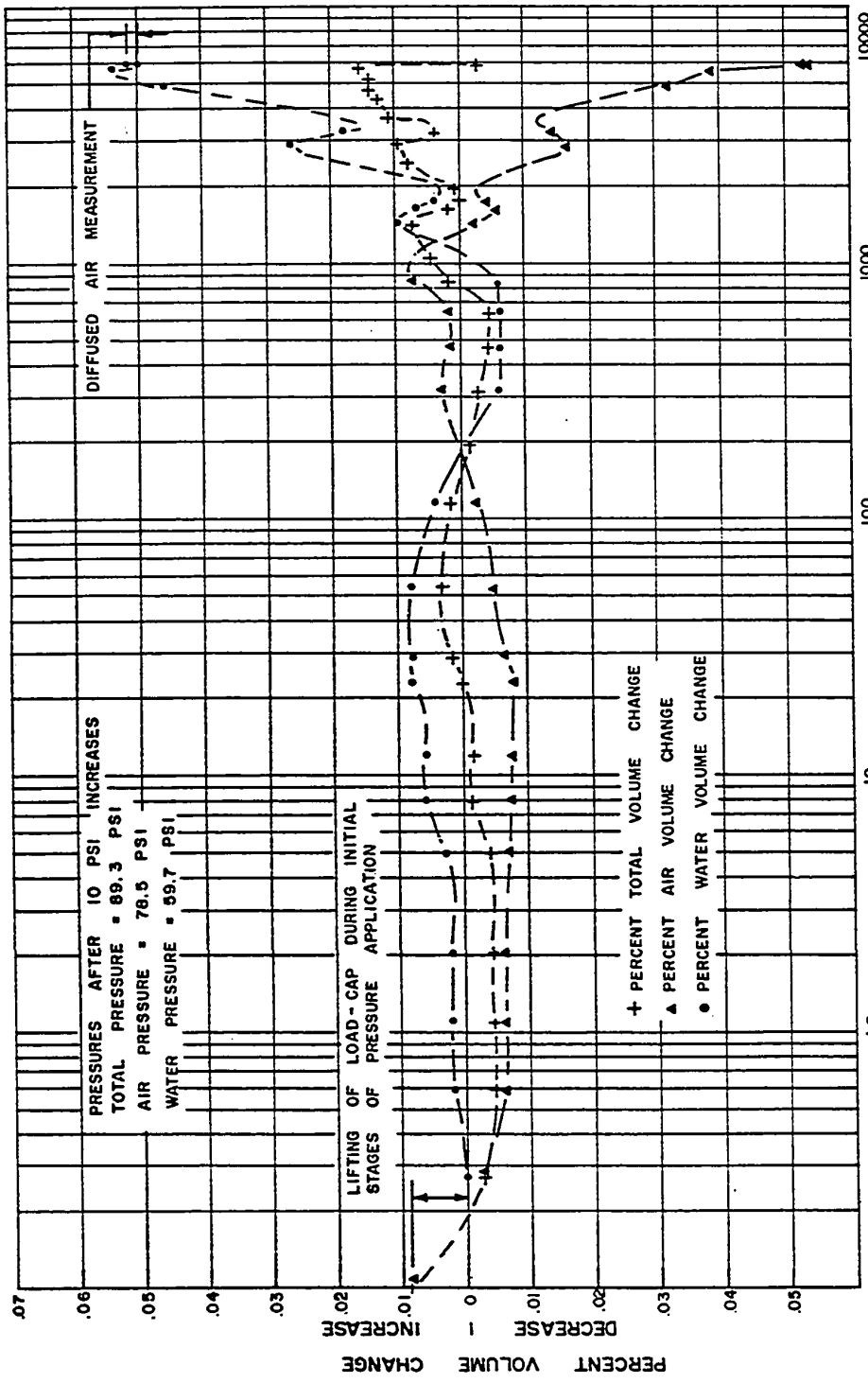


FIGURE C.34 NULL TEST (N-37) ON SAMPLE NO. 31 (EXPANDED SCALE)

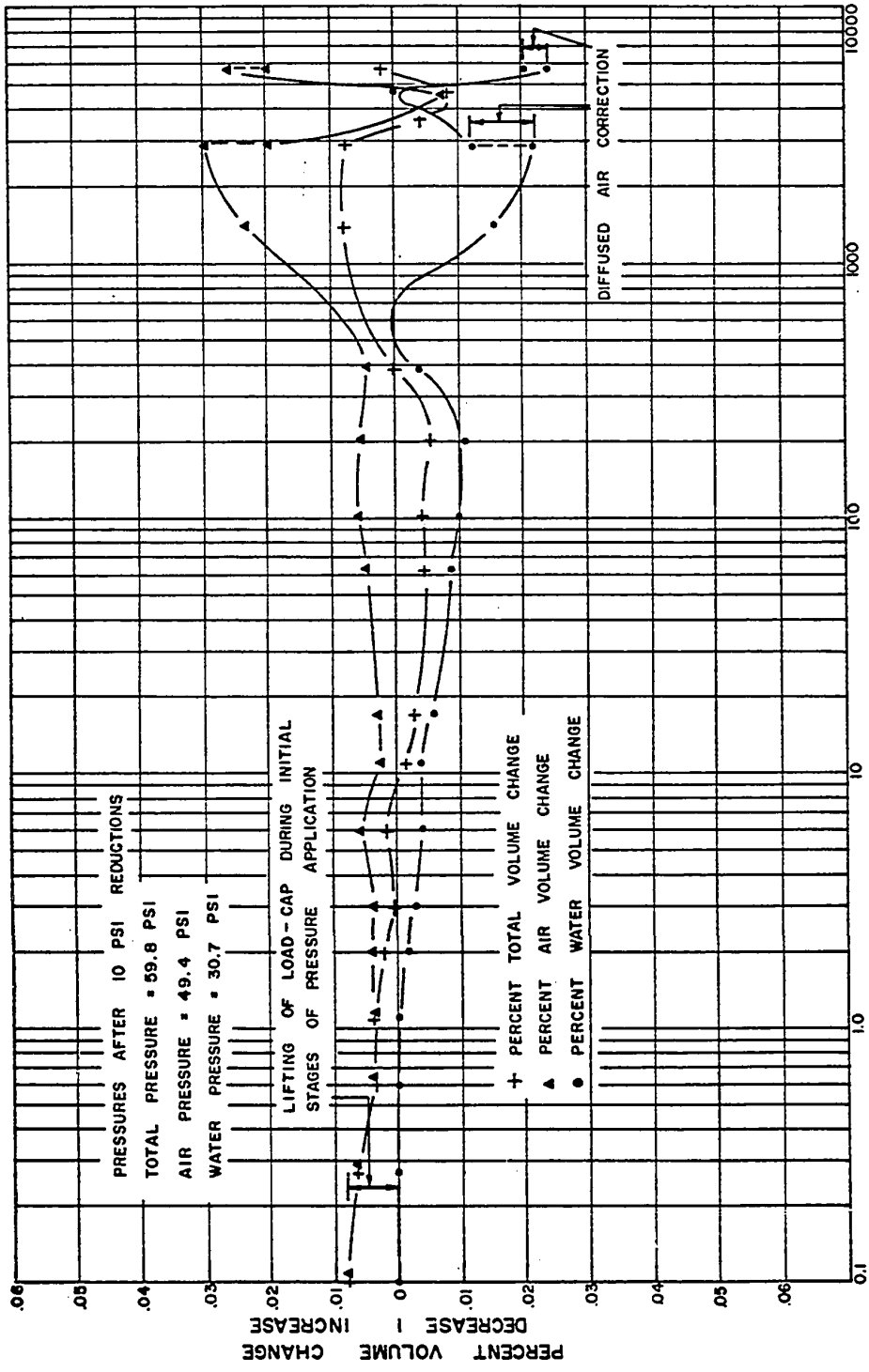


FIGURE C.35 NULL TEST (N-40) ON SAMPLE NO. 31 (EXPANDED SCALE)

volume change is evident for the first day. Then it appears to be more random. The results of the null tests show that no definite processes are occurring. The measured volume changes are essentially random.

It is difficult to compare the experimentally measured volume volume changes with those that would result if the stress state variables were changed by a corresponding amount. However, an attempt has been made in the summary of volume changes (Table C.13). The first estimated volume change is an approximation of the total volume change if the $(\sigma-u_w)$ stress state variable were increased by an amount equal to the stress component change. The estimate is based on the initial water content and volume changes measured on the kaolin samples. The second estimate is an approximation of the percent water volume change for a decrease in suction equal to the stress component change. The estimate is based on the degree of saturation and water volume changes measured on kaolin samples.

The net total volume change for null tests (N-35), (N-36) and (N-37) is -0.008 percent. This is only 0.3 percent of the estimated total volume change for a corresponding $(\sigma-u_w)$ increase. The water volume change is 0.145 percent or 2.5 percent of that anticipated from a corresponding suction decrease.

Since the volume changes on sample #31 appear to be random in nature, the mean and standard deviation for each null test were computed (Table C.14). The random nature of behavior is also discernible from amplified plots of water content, void ratio and degree of saturation (Figure C.36). The water volume change and the water

TABLE C.13

SAMPLE VOLUME CHANGE AND WATER VOLUME CHANGE

DURING NULL TESTS ON UNSATURATED SOILS

(Controlling Total, Air and Water Pressures)

Test No.	Pressure Change (psi)	Sample Volume Change		Water Volume Change (%)	Elapsed Time (min)	Estimated Volume Change for Corresponding Change in	
		Immediate (%)	At Elapsed Time (%)			$\sigma-u_w$ (%)	u_a-u_w (%)
N-23	+10	0.0	-0.03	-0.05	5800	0.6	2.3
N-24	+20	+0.04	+0.02	-0.07	1500	1.4	0.8
N-25	+10	+0.01	0.0	-0.02	1650	0.7	0.4
N-26	-30	-0.25	-0.20	--	4300	2.1	1.2
N-27	+10	0.0	-0.10	-0.50	1880	0.8	0.5
N-28	+20	≈-0.15	-0.15	-0.11	1900	1.6	1.8
N-29	+10	≈-0.015	+0.012	-0.642	8700	1.0	1.2
N-30	+10	≈-0.005	+0.012	-0.072	1350	1.0	1.2
N-31	+10	--	+0.12	-0.060	1380	1.1	0.8
N-32	+10	--	+0.17	-0.045	1390	1.1	0.8
N-33	+10	--	+0.15	-0.020	410	1.1	0.8
N-34	+10	≈+0.055	+0.060	-0.105	4350	1.0	2.5
N-35	+10	+0.015	+0.033	-0.060	5800	0.9	1.9
N-36	+10	+0.010	-0.020	-0.035	2800	0.9	1.9
N-37	+10	0.0	-0.005	-0.050	5800	0.9	1.9
N-38	-10	-0.015	+0.002	+0.010	2700	0.9	1.9
N-39	-10	-0.010	+0.005	-0.005	1500	0.9	1.9
N-40	-10	-0.007	-0.005	+0.015	5800	0.9	1.9
N-41	-20	-0.030	+0.007	-0.040	2900	1.8	3.8

TABLE C.14

MEANS AND STANDARD DEVIATIONS OF VOLUME-WEIGHT RELATIONSHIPS FOR SAMPLE N . 31

Test No.	Percent Volume Total Change		Percent Volume Water Change		Water Content		Void Ratio		Degree of Saturation	
	Mean	Standard Deviation	Mean	Standard Deviation	Mean	Standard Deviation	Mean	Standard Deviation	Mean	Standard Deviation
N-35	+0.0011	0.0037	-0.0066	0.0044	34.014	0.0034	1.0259	0.00008	86.73	0.006
N-36	-0.0029	0.0074	-0.0088	0.0067	34.057	0.0060	1.0252	0.00015	86.90	0.007
N-37	-0.0002	0.0040	-0.0050	0.0083	34.076	0.0064	1.0256	0.00008	86.92	0.013
N-38	-0.0020	0.0038	+0.0174	0.0110	34.098	0.0082	1.0255	0.00008	86.98	0.018
N-39	+0.0008	0.0039	+0.0088	0.0052	34.097	0.0040	1.0254	0.00008	86.99	0.010
N-40	+0.0005	0.0049	+0.0063	0.0050	34.102	0.0037	1.0253	0.00009	87.01	0.012
N-41	-0.0030	0.0148	+0.0385	0.0361	34.058	0.0237	1.0254	0.00030	86.89	0.036

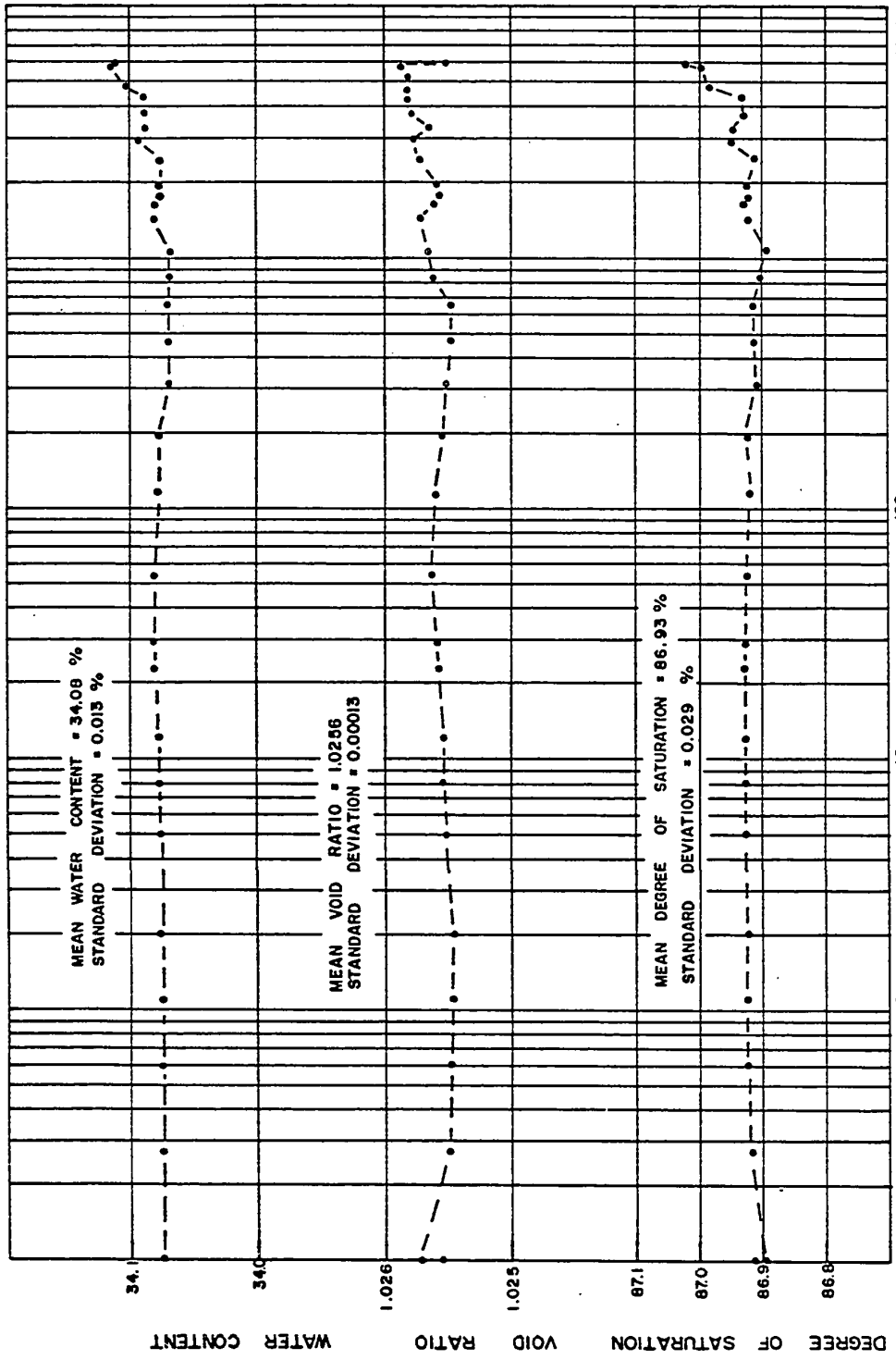


FIGURE C.36 WATER CONTENT, VOID RATIO AND DEGREE OF SATURATION VARIATIONS DURING NULL TEST (N-37)

content changes are not completely free of external influences since every measurement of water volume is not corrected for air diffusion. However, accurately applying the correction is impossible. The degree of saturation measurements are also affected. As well, any leakage of water through the membrane cannot be accounted for.

The total volume change measurements consistently show standard deviation values several times greater than the mean volume change. The indication is that a truly null behavior is being observed. The standard deviations are generally slightly less than the mean for the water volume change measurements. The increased standard deviation is related to the inability to correct all water volume change readings. The means and standard deviations are presented graphically for the null tests on sample #31 in Figure C.37. The standard deviations of the total volume changes completely masks any process that may be taking place. The water volume changes indicate a slight upward (increase) trend but definitely no consistent evidence of a process.

The average standard deviation for water content during a null test 0.006 percent. The void ratio, which corresponds to the total volume change measurements, has a standard deviation of 0.00009. The standard deviation for the degree of saturation measurements is in the order of 0.01. The results are graphically presented in Figure C.38.

The experimental verification of the proposed stress state variables is well within the accuracy of engineering practice. The

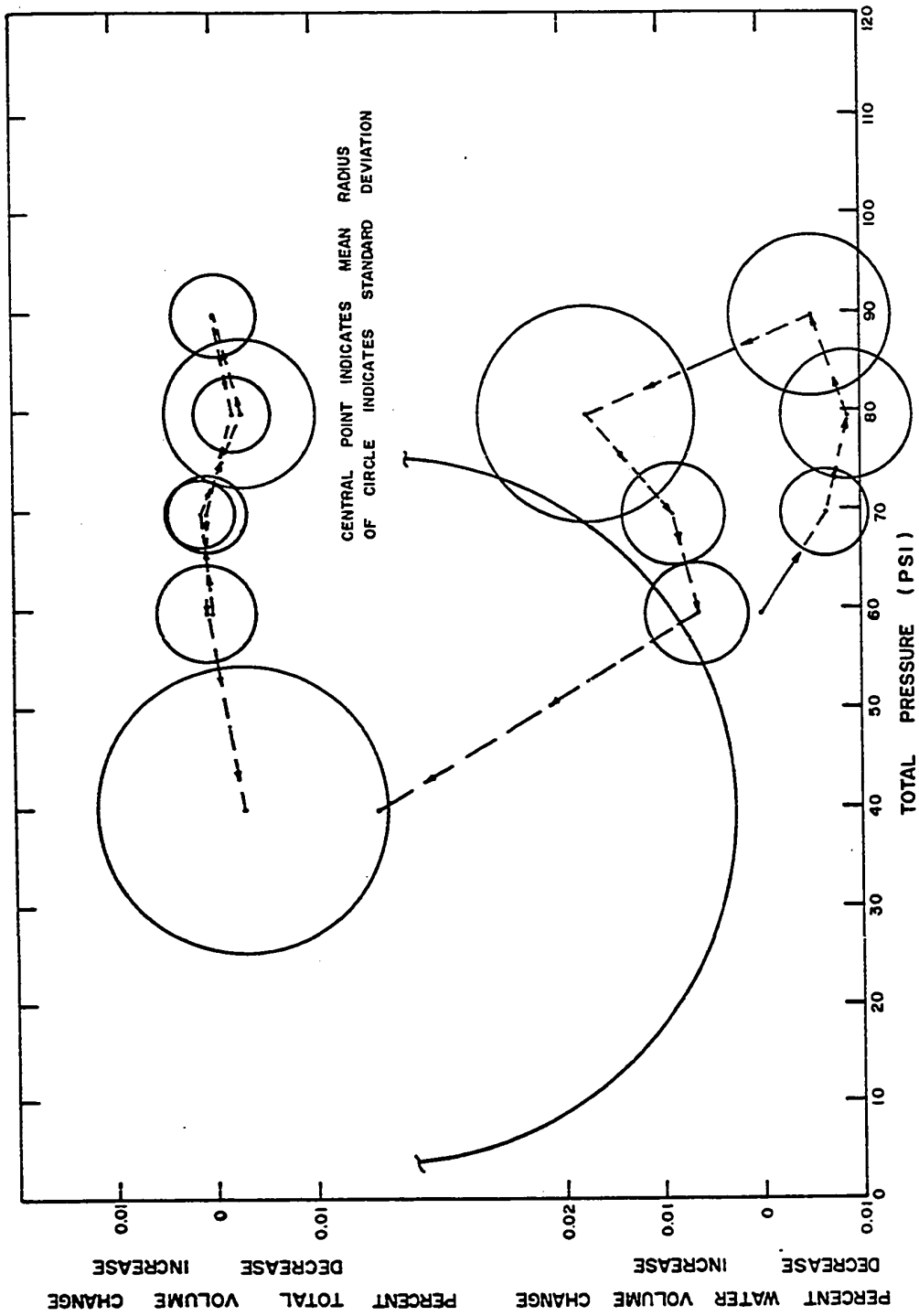


FIGURE C.37 MEANS AND STANDARD DEVIATIONS FOR TOTAL AND WATER VOLUME CHANGES FROM ALL NULL TESTS ON SAMPLE NO. 31

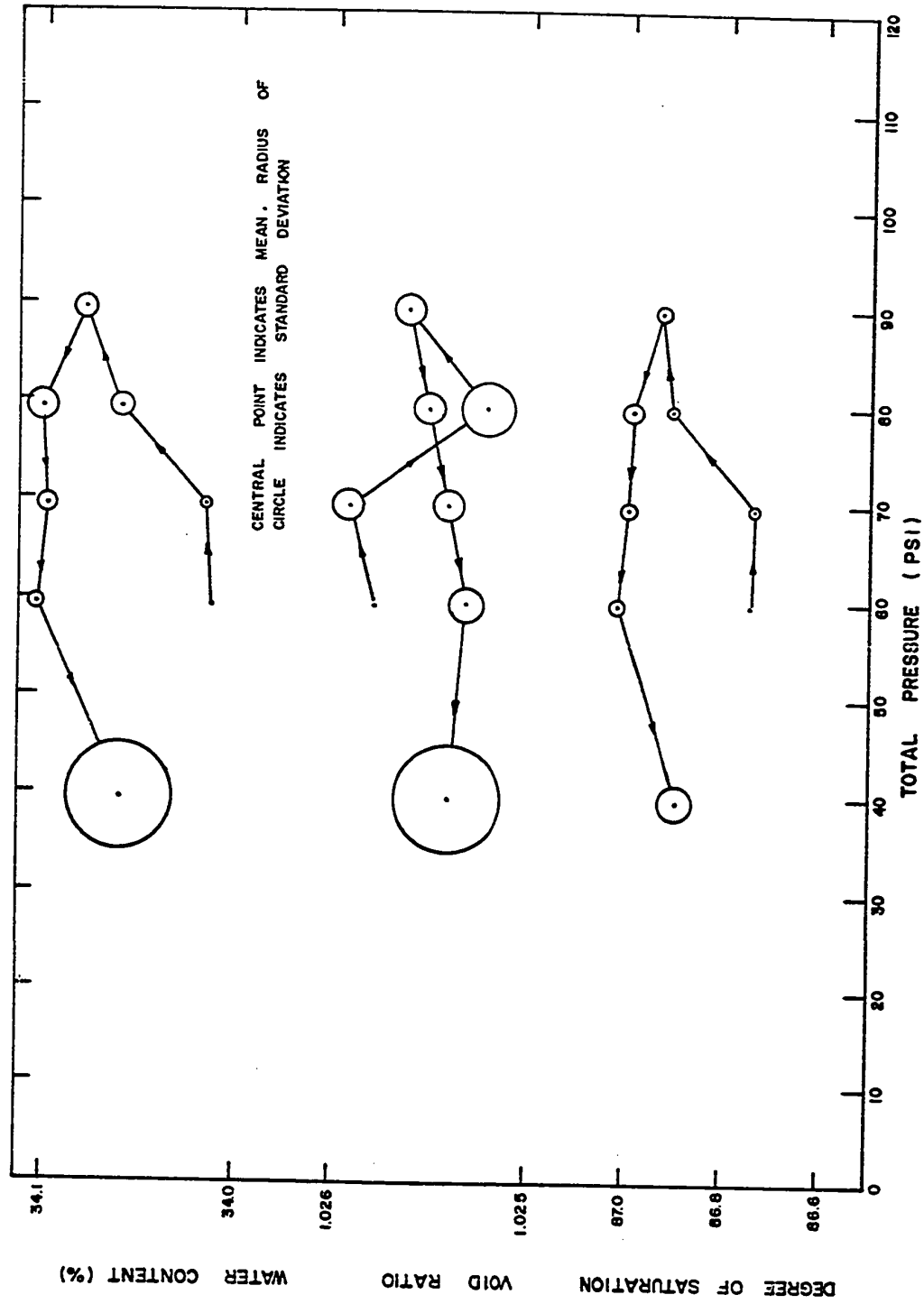


FIGURE C.38 MEANS AND STANDARD DEVIATIONS OF WATER CONTENT, VOID RATIO AND DEGREE OF SATURATION FOR ALL NULL TESTS ON SAMPLE NO. 31

accuracy of the more precise null tests show that the porposed stress state variables are verified tc within at least one part in ten thousand. This is well within the accuracy obtained for the null tests on saturated samples.

APPENDIX D

DATA REDUCTION

CONTENTS OF APPENDIX D

		Page
D-1	General	D1
D-2	Flow Charts	D1
D-3	Description of Variable Names	D4
D-4	Fortran Source Statement Listings	D11
D-5	Description of Input Data	D51
D-6	Description of Output	D62
D-7	Sample Calculations	D62

DATA REDUCTION

D-1 General

The amount of data accumulated when testing unsaturated soils is substantially more than when testing saturated soils. For example, in the triaxial tests there are 4 total volume change readings, 4 pressure transducer readings and the water and diffused air volume readings for every time under consideration. All volume-weight soil properties can be computed at each time. The voluminous data necessitates the use of a computer for a complete analysis.

Appendix D presents the computer programs written to analyse the data from the triaxial and oedometer tests. The program for Triaxial Apparatus No. 2 is presented in detail. The other programs are similar and can be understood with the assistance of a few comments on differing aspects. Similar variable names are used in all programs.

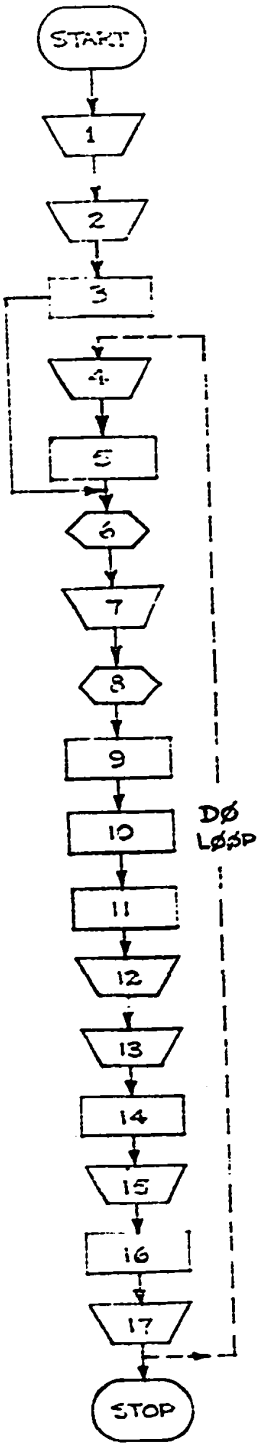
The coding form was designed to apply to various types of tests than can be performed on an unsaturated soil. The program contains a large number of decision statements in order to always execute only the available data. The write out is designed to be as complete as possible.

D-2 Flow Charts

The computer program for Triaxial Apparatus No. 2 consists

of a MAIN program and three subroutines. Subroutine PRESS calculates the total, water and air pressures, and the stress state variables. It also writes them out. The subroutine contains the calibrations for the pressure transducers. The subroutine ETIME calculates the elapsed time from the start of the test or from any other designated time. The later case is stipulated by putting a 1 in column 1 and the elapsed time is referred to as the LOCAL elapsed time. Generally this coincides with changes in pressure applied to the sample. Subroutine PAG checks the line count to ensure that the designated page length has not been exceeded. If it has, a new page is started with the appropriate heading and page number.

Figure D.1 shows a brief flow-chart of the MAIN program. All decision statements, checks for a new page and checks for comment cards have been omitted from the flow chart. The program is basically one DØ LØØP that reduces all the data on each card. The program first computes the elapsed time and pressures. Then the lateral and vertical volume changes of the total sample are calculated. If a reading was made on the amount of diffused air, the appropriate correction is applied to the water volume change reading. The volume changes in each phase from the last pressure change as well as from the start of the test are computed. Finally, the volume-weight soil properties are calculated.



1. READ HEADING CARD, COMMENT CARD, AND INITIAL VOLUME-WEIGHT CARD
2. READ FIRST DATA CARD
3. INITIALIZE VARIABLES
4. READ REMAINING DATA CARDS
5. COMPUTE LVDT DISPLACEMENT READINGS
6. CALL ETIME TO COMPUTE ELAPSED TIMES
7. WRITE INPUT DATA
8. CALL PRESS TO COMPUTE AND WRITE PRESSURES AND STRESS STATE VARIABLES
9. COMPUTE LATERAL AND VERTICAL VOLUME CHANGES ON TOTAL SAMPLE
10. COMPUTE WATER VOLUME CHANGES FROM BURRET READINGS
11. APPLY CORRECTION FOR DIFFUSED AIR IF READINGS ARE TAKEN
12. WRITE DIFFUSED AIR VOLUME AND CORRECTION
13. WRITE TOTAL SAMPLE VOLUME CHANGES
14. COMPUTE CHANGES IN AIR VOLUME
15. WRITE VOLUME CHANGES IN AIR AND WATER PHASES
16. COMPUTE VOLUME-WEIGHT SOIL PROPERTIES
17. WRITE THE VOLUMES OF EACH PHASE AND THE VOLUME-WEIGHT SOIL PROPERTIES

FIGURE D.1 DATA REDUCTION FLOW CHART FOR TRIAXIAL APPARATUS NO. 2

D-3 Description of Variable Names

The variable names used in the Fortran Source Program for Triaxial Apparatus No. 2 are listed below.

A - Project number (20 characters)

ADIF - Measured volume of diffused air at the back pressure in the diffused air volume indicator (cc)

ADIFF - Measured volume of diffused air at the pressure of the water in the base (cc)

AIR - Air pressure (psi)

AIRP - Air pressure (mv)

AIRSTR - Percent air volume change since the last pressure change (%)

AIRV - Air volume change from the start of the test (cc)

AIRVL - Air volume change since last pressure change (cc)

AO - Original cross-sectional area of sample (sq.cm.)

AREA1 - Cross-sectional area of the sample at any time (sq.cm.)

ATM - Total back pressure on the air in the diffused air volume indicator (psi)

B - Sample number (10 characters)

BACK - Back pressure on the water measured by the transducer on the board (psi)

BACKP - Water back pressure measured by the transducer on the board (mv)

BALCØR - Lateral LVDT correction reading (in both volts and centimeters)

BISH - Difference between the total and air pressures (psi)

C - Comments (80 characters)

CALIB - Conversion of the burret reading in the diffused air volume indicator to centimeters of water (i.e. cm of water per cc on burret)

CAPCØR - Vertical LVDT correction reading (in both volts and centimeters)

CATBAL - Lateral LVDT reading (in both volts and centimeters)

CATCAP - Vertical LVDT reading (in both volts and centimeters)

CELL - Cell or total pressure (psi)

CELLP - Cell or total pressure (mv)

CØM - Comments (80 characters)

CØNVER - Conversion factor to change centimeters of water to psi

DELDIA - Change in diameter of the sample from the start of the test (cm)

DIA1 - Diameter of the sample at any time (cm)

DIFA - Diffused air volume indicator reading at any time (cc)

DIFF - Diffused air volume indicator reading subsequent to flushing the base (cc)

DIFØ - Diffused air volume indicator reading prior to flushing the base (cc)

DIFPR - Back pressure applied to the diffused air volume change indicator by the air pressure regulator (psi)

DISSØL - Approximate volume of dissolved air (cc)

DØ - Original diameter of the sample (cm)

DØP - Diameter of the sample at the time of the last pressure change (cm)

DRYDEN - Dry density (PCF)

EFFECT - Difference between the total and water pressures (psi)

ELEX - Burret reading for the level of the exit tube in the diffused air volume change indicator (cc)

EØ - Original void ratio

EXHEAD - Distance from the top of the exit tube to the water level in the diffused air volume indicator

FPØRE - Pore water pressure at the time of the last pressure change (psi)

FSLAT - Percent lateral volume change at the time of the last pressure change (%)

FSTVØL - Percent total volume change at the time of the last pressure change (%)

FSVERT - Percent vertical volume change at the time of the last pressure change (%)

FTVØL - Total volume change at the time of the last pressure change (cc)

FVLAT - Lateral volume change at the time of the last pressure change (cc)

FVVERT - Vertical volume change at the time of the last pressure change (cc)

GS - Specific gravity of the soil solids

H - Height of the sample at any time (cm)

HØ - Original height of the sample (cm)

HØP - Height of the sample at the time of the last pressure change (cm)

IDAY1 - Day of the start of the test

IDAY2 - Day at the time of the last pressure change

IDAYX - Day at the time of any reading

IHØUR1 - Hour of the start of the test

IHØUR2 - Hour at the time of the last pressure change

IHØURX - Hour at the time of any reading

IL - Line number

IP - Page number

ISEC1 - Second of the start of the test

ISEC1 - Second at the time of the last pressure change

ISECX - Second at the time of any reading

IYEAR1 - Year of the start of the test

IYEARX - Year at the time of any reading

LA1 - Short lever arm (pivot to bearing pad) on the lateral strain indicator

LA2 - Long lever arm (pivot to LVDT wire) on the lateral strain indicator

LATCAL - Lateral strain indicator calibration factor (converts the LVDT displacement to a lateral displacement of the sample)

LSLAT - Percent lateral volume change from the time of the last pressure change (%)

LSTVØL - Percent total volume change from the time of the last pressure change (%)

LSVERT - Percent vertical volume change from the time of the last pressure change (%)

LSVWAT - Percent water volume change from the time of the last pressure change (%)

LTVØL - Total volume change from the time of the last pressure change (cc)

LVLAT - Lateral volume change from the time of the last pressure change (cc)

LVVERT - Vertical volume change from the time of the last pressure change (cc)

MIN1 - Minute of the start of the test

MIN2 - Minute at the time of the last pressure change

MINX - Minute at the time of any reading

MØNTH1 - Month of the start of the test

MØNTH2 - Month at the time of the last pressure change

MØNTHX - Month at the time of any reading

ØBALC - Original lateral LVDT correction reading (in both volts and centimeters)

ØCAPC - Original vertical LVDT correction reading (in both volts and centimeters)

PØRE - Pore water pressure measured at the base of the cell (psi)

PØRCEP - Pore water pressure measured at the base of the cell (mv)

PØRØS - Porosity (%)

PVØLCH - Water volume change at the time of the last pressure change (cc)

REG - Back pressure applied to the diffused air volume change indicator (mv)

RSAT - Degree of saturation at the time of the last pressure change (%)

RVV - Volume of voids at the time of the last pressure change (cc)

SAT - Degree of saturation (%)

SIGN - Designation for the direction of flow of water
- 1.0 signifies water flowing out of sample
1.0 signifies water flowing into sample

SLAT - Lateral deformation of the sample from the start of the test (%)

STP - Measured volume of diffused air at standard temperature and pressure (cc)

STVØL - Total deformation of the sample from the start of the test (%)

SUCT - Difference between the air and water pressures (psi)

SVERT - Vertical deformation of the sample from the start of the test (%)

SVØLW - Sum of the water volume changes between changes in direction of flow or resetting of the burret reading

SVWAT - Total water volume change since the last pressure change (cc)

SWAT - Total water volume change from the start of the test (cc)

TIME1 - Elapsed time from the start of the test (min)

TIME2 - Elapsed time from the last pressure change (min)

TØTDEN - Total unit weight (PCF)

TRIAX - Triaxial cell number (10 characters)

TVØL - Total volume change of the sample from the start of the test (cc)

V - Volume of the sample at any time (cc)

VAIR - Volume of air (free) at any time (cc)

VERT - Change in height from the start of the test (cm)

VØ - Original volume of the sample (cc)

VØLL - Lateral volume change of the sample from the start of the test (cc) (Same as VLAT)

VØLV - Vertical volume change of the sample from the start of the test (cc) (Same as VVERT)

VØP - Volume of the sample at the time of the last pressure change (cc)

VS - Volume of the soil solids (cc)

VV - Volume of voids at any time (cc)

VWAT - Volume of water at the start of the test (cc)

VWATER - Volume of water at any time (cc)

WC - Water content at any time (%)

WS - Dry weight of sample (gms)

D-4 Fortran Source Statement Listings

The following pages present the FORTRAN source statement listings for Triaxial Apparatus No. 2, Triaxial Apparatus No. 1 and the one-dimensional Oedometers, respectively.

```
C     ********************************************************************
C
C     PROGRAM TO REDUCE DATA FOR STRESS CHANGES ON UNSATURATED SOILS
C     -------- TESTS PERFORMED ON TRIAXIAL CELL NO. 2 ------------------
C
C     ********************************************************************
      DIMENSION  A(5),B(3),C(20),COM(20),SVOLW(10),TRIAX(3)
      REAL  LATCAL,LSVWAT,LTVOL,LSTVOL,LVLAT,LVVERT,LSLAT,LSVERT,LSWAT
      IP=0
      IL=40
      PI=3.14159
      LA2=12.12
      LA1=5.61
      LATCAL=2.54*LA1/LA2
C
C     ------------------------------------------------------------------
C     READ HEADING CARD
C     ------------------------------------------------------------------
C
C     A -      PROJECT NUMBER
C     B -      SAMPLE NUMBER
C     TRIAX - TRIAXIAL CELL NUMBER
      READ (5,1) A,B,TRIAX
C
C     ------------------------------------------------------------------
C     READ THE COMMENT CARD
C     ------------------------------------------------------------------
C
      READ (5,2) C
C
C     ------------------------------------------------------------------
C     READ THE INITIAL VOLUME WEIGHT DATA
C     ------------------------------------------------------------------
C
C     DO -    ORIGINAL DIAMETER OF THE SAMPLE (CM)
C     HO -    ORIGINAL HEIGHT OF THE SAMPLE (CM)
C     GS -    SPECIFIC GRAVITY OF THE SOIL SOLIDS
C     WS -    DRY WEIGHT OF THE TOTAL SAMPLE (GMS)
C     WC -    ORIGINAL WATER CONTENT (%)
C
      READ (5,3) DO,HO,GS,WS,WC
C
      AO=PI*DO*DO/4.
      VO=HO*AO
      VS=WS/GS
      VV=VO-VS
      EO=VV/VS
      POROS=EO/(1.+EO)*100.
      SAT=WC*GS/EO
      DRYDEN=GS*62.4/(1.+EO)
      TOTDEN=(GS+SAT*EO/100.)*62.4/(1.+EO)
      VWAT=SAT*VV/100.
      VAIR=VV-VWAT
      DISSOL=0.02*VWAT
      CALL PAG(IL,IP,A,B,TRIAX,C)
```

```
      WRITE(6,1022)
      WRITE(6,6314)
      IL=IL+19
      WRITE(6,1020)  GS,ES
      IL=IL+1
      ELEX=10.05
      CALIB=15.236/4.
      CONVER=62.4/(2.54*12.*12.*12.)
      H =HO
      HOP=H
      DIA1=DO
      DOP=DO
      AREA1=AO
      V=VO
      VOP=V
      CELL=0.0
      BACK=0.0
      AIR=0.0
      PORE=0.0
      IYEAR1=1972
      IYEARX=1972
      GO TO 113
C
C     ------------------------------------------------------------------
C     READ ADDITIONAL COMMENT CARDS
C     ------------------------------------------------------------------
C
  112 READ(5,10) CCM
      WRITE(6,11) CCM
      IL=IL+1
C
C     ------------------------------------------------------------------
C     READ THE FIRST DATA CARD
C     ------------------------------------------------------------------
C
  113 READ(5,7) IQ1,MONTH1,IDAY1,IHOUR1,MIN1,ISEC1,CELLP,BACKP,AIRP,
     1POREP,VOLCH,IQ2,IQ3,CATBAL,OBALC ,CATCAP,OCAPC,DIFA,REG
C       IQ1 - SHOULD ELAPSED TIME AND WATER VOLUME CHANGE OR PORE PRESSURE
C             REACTION BE COMPUTED FROM THIS TIME.
C             1  SIGNIFIES  YES
C             0  SIGNIFIES  NO
C             9  SIGNIFIES A COMMENT STATEMENT ON THE NEXT CARD
C             8  SIGNIFIES THAT THIS CARD CONTAINS THE FINAL DIFFUSED
C                AIR VOLUME.
C       QUESTIONS REGARDING THE BURRET.
C       IQ2 - IS WATER GOING INTO THE SAMPLE  (1)
C             OR COMING OUT OF THE SAMPLE  (2)
C       WILL RETAIN PREVIOUS (IQ2) IF ZERO OR BLANK IS RECORDED.
C       IQ3 - IS THERE A REVERSAL IN WATER FLOW, CORRECTION IN BURRET
C             READING OR A RESETTING OF THE BURRET?
C      MONTH1  - MONTH
C      IDAY1   - DAY
C      IHOUR1  - HOUR
C      MIN1    - MINUTE
C      ISEC1   - SECOND
```

```
C      CELLP   - CELL PRESSURE (MV)
C      BACKP   - WATER BACK PRESSURE MEASURED ON THE BOARD (MV)
C      AIRP    - AIR PRESSURE (MV)
C      PORSP   - PORE WATER PRESSURE MEASURED ON THE CELL (MV)
C      VOLCH   - WATER VOLUME CHANGE INDICATOR READING (CC)
C      CATBAL  - VERTICAL LVDT READING (VOLTS)
C      OBALC   - CORRECTION FOR VERTICAL LVDT READING (VOLTS)
C      CATCAP  - LATERAL LVDT READING (VOLTS)
C      OCAPC   - CORRECTION FOR  LATERAL LVDT READING (VOLTS)
C      DIFA    - DIFFUSED AIR VOLUME CHANGE INDICATOR READING (CC)
C      REG     - BACKPRESSURE ON DIFFUSED AIR VOLUME INDICATOR (MV)
       IF(IQ1.EQ.9) GO TO 112
       IF(DIFA.GT.0.0.AND.IQ1.NE.8) DIFO=DIFA
       IF(DIFA.GT.0.0.AND.IQ1.EQ.8) DIFF=DIFA
       IF(CATBAL.EQ.0.0) GO TO 6013
       CATBAL=(0.501894-0.0397657C*CATBAL)*LATCAL
       CATCAP=(0.499804+0.036503*CATCAP)*2.54
 6013  IF(OBALC.EQ.0.0) GO TO 6009
       OBALC =(0.501894-0.03976570*OBALC)*LATCAL
       OCAPC =(0.499804+0.036503*OCAPC )*2.54
C
C      ------------------------------------------------------------------
C      INITIALIZE VARIABLES
C      ------------------------------------------------------------------
C
 6009  IF(IQ1.EQ.1) FPORE=PORE
       IF(IQ1.EC.1) RVV=VV
       IF(IQ1.EC.1) RSAT=SAT
       MONTH2=MONTH1
       MONTHX=MONTH1
       IDAY2=IDAY1
       IDAYX=IDAY1
       IHOUR2=IHOUR1
       IHOURX=IHOUR1
       MIN2=MIN1
       MINX=MIN1
       ISEC2=ISEC1
       ISECX=ISEC1
       TIME1=0.0
       TIME2=0.0
       BALL1=CATBAL
       CAP1=CATCAP
       BALCOR=OBALC
       CAPCOR=OCAPC
       SLAT=0.0
       VOLL=0.0
       SVERT=0.0
       VOLV=0.0
       TVOL=0.0
       STVOL=0.0
       SSAT=0.0
       SVWAT=0.0
       LSVWAT=0.0
       LSWAT=0.0
       LSTVOL=0.0
```

```
      LTVOL=0.0
      LVLAT=0.0
      LVVERT=0.0
      LSLAT=0.0
      LSVERT=0.0
      FSVERT=0.0
      FSLAT=0.0
      FVVERT=0.0
      FVLAT=0.0
      FSTVOL=0.0
      FTVOL=0.0
      PVOLCH=VOLCH
      DO 201 IS=1,10
  201 SVOLW(IS)=0.0
      II=1
      GO TO 6010
C
C     ****************************************************************
C     DO LOOP TO READ ALL CARDS AND REDUCE DATA
C     ****************************************************************
C
  604 DO  105  I=1,1000
      READ(5,7) IQ1,MONTHX,IDAYX,IHOURX,MINX,ISECX,CELLP,BACKP,AIRP,
     1POREP,VOLCH,IQ2,IQ3,CATEAL,BALCOR,CATCAP,CAPCOR,DIFA,REG
      IF(IQ1.EQ.9) GO TO 109
      IF(DIFA.GT.0.0.AND.IQ1.NE.8) DIFO=DIFA
      IF(DIFA.GT.0.0.AND.IQ1.EQ.8) DIFF=DIFA
      IF(CATEAL.EQ.0.0) GO TO 6014
C
C     ----------------------------------------------------------------
C     COMPUTE LVDT DISPLACEMENT READINGS
C     ----------------------------------------------------------------
C
      CATEAL=(0.501894-0.0397657C*CATBAL)*LATCAL
      CATCAP=(0.499804+0.036503*CATCAP)*2.54
 6014 IF(BALCOR.EQ.0.0) GO TO 6010
      BALCOR=(0.501894-0.0397657C*BALCOR)*LATCAL
      CAPCOR=(0.499804+0.036503*CAPCOR )*2.54
 6010 IF(IQ1.EQ.1) HOP=H
      IF(IQ1.EQ.1) VOP=V
      IF(IQ1.EQ.1) COP=DIA1
      IF(IHOURX.EQ.0.AND.MINX.EQ.0) GO TO 106
      CALL PAG(IL,IP,A,B,TRIAX,C)
C
C     ----------------------------------------------------------------
C     CALL SUBROUTINE TO COMPUTE ELAPSED TIME
C     ----------------------------------------------------------------
C
      CALL ETIME(IYEAR1,MONTH1,IDAY1,IHOUR1,MIN1,ISEC1,IYEARX,MONTHX,
     1IDAYX,IHOURX,MINX,ISECX,TIME1)
      IF(IQ1.EQ.0.OR.IQ1.EQ.8) GO TO 100
      MONTH2=MONTHX
      IDAY2=IDAYX
      IHOUR2=IHOURX
      MIN2=MINX
```

```
C
      IF(IQ2.EQ.0) GO TO 605
C
C     WATER GOING INTO SAMPLE.
      IF(IQ2.EQ.1) SIGN=-1.0
C
C     WATER COMING OUT OF SAMPLE.
      IF(IQ2.EQ.2) SIGN= 1.0
  605 IF(IQ1.EQ.0.OR.IQ1.EQ.8) GO TO 104
      II=1
      SVWAT=0.0
      PVOLCH=VOLCH
      GO TO 203
  104 SVWAT=SVWAT-SVOLW(II)
      SWAT=SWAT-SVOLW(II)
      IF(IQ3.EQ.0) GO TO 203
      SVWAT=SVWAT+SVOLW(II)
      SWAT=SWAT+SVOLW(II)
      PVOLCH=VOLCH
      II=II+1
  203 SVOLW(II)=ABS(PVOLCH-VOLCH)*SIGN
      SWAT=SWAT+SVOLW(II)
      SVWAT=SVWAT+SVOLW(II)
      LSVWAT=SVWAT/VOP*100.
C     ------------------------------------------------------------
C     COMPUTE AND APPLY AIR DIFFUSION CORRECTION
C     ------------------------------------------------------------
C
      IF(IQ1.NE.8) GO TO 103
      EXHEAD=(ELEX-(DIFO+DIFF)/2.)*CALIB
      ADIF=DIFO-DIFF
      DIFPR=3.4864*REG+0.05
      ATM=DIFPR+14.7+EXHEAD*CONVER
      IF(PORE.LE.0.0) PORE=BACK
      ADIFF= ADIF*(                    ATM)/(PORE+14.7)
      STP=ADIF*(                      ATM)/14.7
      IF(SIGN.GT.0.0) GO TO 856
      SWAT=SWAT-ADIFF
      SVWAT=SVWAT-ADIFF
      GO TO 857
  856 SWAT=SWAT-ADIFF
      SVWAT=SVWAT-ADIFF
  857 LSVWAT=SVWAT/VOP*100.
C     ------------------------------------------------------------
C     WRITE AIR DIFFUSION VOLUME AND CORRECTION
C     ------------------------------------------------------------
C
      WRITE(6,864) DIFC,DIFF,ADIF,ATM  ,STP
      IL=IL+1
      CALL PAG(IL,IP,A,B,TRIAX,C)
      WRITE(6,421) ADIFF
      IL=IL+3
  103 CONTINUE
```

```
      IF(CATBAL.EQ.0.0) GO TO 9997
      IF(IG1.EQ.0.OR.IG1.GT.1) GO TO 2711
C
C     ------------------------------------------------------------------
C     COMPUTE OVERALL AND LOCAL SAMPLE VOLUME CHANGES
C     ------------------------------------------------------------------
C
      FTVOL=TVOL
      FSTVOL=STVOL
      FVLAT=VLAT
      FVVERT=VVERT
      FSLAT=SLAT
      FSVERT=SVERT
 2711 LTVOL=TVOL-FTVOL
      LSTVOL=STVOL-FSTVOL
      LVLAT=VLAT-FVLAT
      LVVERT=VVERT-FVVERT
      LSLAT=SLAT-FSLAT
      LSVERT=SVERT-FSVERT
C
C     ------------------------------------------------------------------
C     WRITE TOTAL SAMPLE VOLUME CHANGES
C     ------------------------------------------------------------------
C
      WRITE(6,41) VLAT,VVERT,TVOL,LVLAT,LVVERT,LTVOL
      WRITE(6,51) SLAT,SVERT,STVOL,LSLAT,LSVERT,LSTVOL
      IL=IL+2
      CALL PAG(IL,IP,A,B,TRIAX,C)
 9997 IF(VOLCH.EQ.0.0) GO TO 175
C
C     ------------------------------------------------------------------
C     COMPUTE CHANGES IN AIR VOLUME
C     ------------------------------------------------------------------
C
      AIRV=TVOL-SWAT
      AIRVL=LTVOL-SVWAT
      AIRSTR=LSTVOL-LSVWAT
C
C     ------------------------------------------------------------------
C     WRITE VOLUME CHANGES IN AIR AND WATER PHASES
C     ------------------------------------------------------------------
C
      WRITE(6,629) AIRV,AIRVL,AIRSTR
      WRITE(6,19) SWAT,SVWAT,LSVWAT
      IL=IL+2
      CALL PAG(IL,IP,A,B,TRIAX,C)
      IF(CATBAL.EQ.0.0) GO TO 105
C
C     ------------------------------------------------------------------
C     COMPUTATION OF VOLUME-WEIGHT SOIL PROPERTIES BASED ON THE TOTAL
C     AND WATER VOLUME MEASUREMENTS.
C     ------------------------------------------------------------------
C
  175 VV=V-VS
      E=VV/VS
```

```
      POROS=E/(1.+E)*100.
      VWATER=VWAT-SWAT
      VAIR=VV-VWATER
      DISSOL=0.02*VWATER
      WC=VWATER/WS*100.
      SAT=WC*GS/E
      DRYDEN=GS*62.4/(1.+E)
      TOTDEN=(GS+SAT*E/100.)*62.4/(1.+E)
C
C     ------------------------------------------------------------------
C     WRITE THE VOLUME OF EACH PHASE AND THE VOLUME-WEIGHT SOIL PROPERTIES
C     ------------------------------------------------------------------
C
      WRITE(6,5) DIA1,H,AREA1,V,VS,VV,VWATER,VAIR,DISSOL
      IL=IL+3
      WRITE(6,6) WC,E,POROS,SAT,DRYDEN,TOTDEN
      IL=IL+1
      CALL PAG(IL,IP,A,B,TRIAX,C)
      GO TO 105
C
C     ------------------------------------------------------------------
C     READ AND WRITE COMMENT CARDS
C     ------------------------------------------------------------------
C
  109 READ(5,10) COM
      WRITE(6,11) COM
      IL=IL+1
      CALL PAG(IL,IP,A,B,TRIAX,C)
  105 CONTINUE
  106 WRITE(6,1021)  B
      STOP
C
C     ******************************************************************
C     F O R M A T   S T A T E M E N T S
C     ******************************************************************
C
    1 FORMAT(5A4,2A4,A2,2A4,A2)
    2 FORMAT(20A4)
    3 FORMAT(5F10.0)
 1022 FORMAT(3X,'-------------------------------------------------'/3X,
     1'I01 - SHOULD ELAPSED TIME AND WATER VOLUME CHANGE OR PORE PRESSUR
     2E'/3X,'   REACTION BE COMPUTED FROM THIS TIME.               '/3X,
     3'       1  SIGNIFIES  YES              '/3X,
     4'       0  SIGNIFIES  NO                '/3X,
     5'       9  SIGNIFIES A COMMENT STATEMENT ON THE NEXT CARD.  '/3X,
     5'       8  SIGNIFIES THAT THIS CARD CONTAINS THE FINAL DIFFUSED AIR
     5 VOLUME READING'/3X,
     6'QUESTIONS REGARDING THE BURRET.          '/3X,
     7'I02 - IS WATER GOING INTO THE SAMPLE  (1)       '/3X,
     8'      OR COMING OUT OF THE SAMPLE  (2)          '/3X,
     9'WILL RETAIN PREVIOUS (I02) IF ZERO OR BLANK IS RECORDED.'/3X,
     1'I03 - IS THERE A REVERSAL IN WATER FLOW. CORRECTION IN BURRET'/3X
     2,'     READING OR A RESETTING OF THE BURRET?      '/3X,
     3'-------------------------------------------------'/)
 1020 FORMAT(5X,' THE SPECIFIC GRAVITY USED IN THE COMPUTATIONS IS  '
```

```
     1 ,F8.3,/5X,' THE WEIGHT OF THE DRY SOIL SAMPLE IS ',F9.3/)
    5 FORMAT(1X,' SAMPLE DIMENSIONS AND VOLUME WEIGHT RELATICNSHIPS'
     1                                /1X,'DIAMETER = ',F10.4,' CM    HEIG
     1HT = ',F10.4,' CM     AREA = ',F10.4,' SQ. CM     VOLUME = ',
     2F10.3,' CU. CM.'/1X,'VOL. SOLIDS = ',F8.2,4X,'VOL. VOIDS = ',F8.2,
     3  4X,'VOL. WATER = ',F8.2,4X,'VOL. AIR (FREE) = ',F8.2,' (DISSOLVE
     1D) = ',F8.2,' (CC)')
 6314 FORMAT( 5X,'DEFORMATICNS AND VOLUME CHANGES ARE (+) WHEN THE TOTAL
     1 VOLUME DECREASES OR WHEN WATER OR AIR COME OUT OF THE SAMPLE'/ 5X
     2,'LATERAL AND VERTICAL LVDT READINGS ARE PRINTED OUT IN CENTIMETER
     3S'/)
    6 FORMAT(1X,'W/C = ',F8.3,' %     E = ',F8.5,4X,'N = ',F7.3,
     1' %     SATURATION = ',F7.3,' %     DRY DEN. = ',F7.2,' PCF    TOTA
     2L DEN. = ',F7.2,' PCF')
    7 FORMAT(I1,5I2,5F6.2,2I1,6F6.3)
   18 FORMAT(1X,'-------------------------------------------',  /
     1         1X,  5I6,F8.0,4F8.3,F8.2,F8.3,2X,3I1,4F8.5)
   41 FORMAT(1X,'VOL. CH. (CC) LAT.=',
     1F7.3,' VERT.=',F7.3,' TOTAL=',F7.3,6X,'LOC. LAT. =',F7.3,
     2 '   LOC. VERT=',F7.3,'   LOC. TOT.=',F9.3)
   51 FORMAT(1X,  'STRAIN (%)    LAT.=',
     1F7.4,' VERT.=',F7.4,' TOTAL=',F7.4,6X,'LOC. LAT. =',F7.4,
     2 '   LOC. VERT=',F7.4,'   LOC. TOT.=',F9.4)
  864 FORMAT(1X,'ORIG. DIF. AIR =',F7.3,'   FINAL DIF. AIR = ',F7.3,
     1'     DIF. VOL. =',F7.3,  '   DIF. PRES.=',F7.3,'   STP VOL.=',
     4  F7.3)
  421 FORMAT(1X,'CCCCCCCCCCCCCCCCCCCCCCCCCCCCCC',/
     1  1X,'C  WATER VOLUME CORRECTION  C',/
     2  1X,'CCCCCCCCCCCCCCCCCCCCCCCCCCCCCC          (',F6.3,')')
  629 FORMAT(1X,'TOT. AIR VOL. CH. =',F8.3,9X,'LOC. AIR VOL. CH. =',F8.3
     1,'   LOC. AIR STR.=',F10.4)
   19 FORMAT(1X,'TOT. WAT. VOL. CH.=',F8.3,9X,'LOC. WAT. VOL. CH.=',F8.3
     1 ,'   LOC. WAT. STR.=',F10.4)
   10 FORMAT(20A4)
   11 FORMAT(10X,'-------------------------------------------------------
     1-----------------------------------',/10X,20A4)
 1021 FORMAT(1X,'-------------------------------------------------------',/
     13X,' END OF TEST ',2A4,A2,/1X,'-------------------------------------
     2----------')
      END
```

```
      SUBROUTINE PRESS(CELLP,BACKP,AIRP,POREP,CELL,BACK,AIR,PORE,IL)
C
C     ****************************************************************
C     SUBROUTINE TO COMPUTE PRESSURES FOR THE TRIAXIAL EQUIPMENT.
C     ****************************************************************
C
      CELL=3.4884*CELLP+0.05
      IF(CELLP.LT.6.5) CELL=3.501*CELLP+0.0163
      IF(CELLP.EQ.0.0) CELL=0.0
      BACK=3.4884*BACKP+0.05+1.517
      IF(BACKP.LT.6.5) BACK=3.501*BACKP+0.05+1.517
      IF(BACKP.EQ.0.0) BACK=0.0
      AIR=3.4884*AIRP+0.05
      IF(AIRP.LT.6.5) AIR=3.5010*AIRP+0.05
      IF(AIRP.EQ.0.0) AIR=0.0
      PORE=4.10259*POREP-0.718
      IF(POREP.LT.5.5) PORE=4.05297*POREP+0.036
      IF(POREP.EQ.0.0) PORE=0.0
      IF(CELL.EQ.0.0.AND.BACK.EQ.0.0.AND.AIR.EQ.0.0.AND.PORE.EQ.0.0) GO
     1       TO 116
      WRITE(6,14) CELL,BACK,AIR,PORE
   14 FORMAT(19X,'PRESSURES IN PSI     ',4F8.3)
      IL=IL+1
      IF(CELL.EQ.0.0.AND.BACK.EQ.0.0.AND.AIR.EQ.0.0) GO TO 116
      IF(AIR.EQ.0.0) GO TO 1118
      BISH=CELL-AIR
      GO TO 1117
 1118 BISH=0.0
 1117 IF(BACK.EQ.0.0.AND.PORE.EQ.0.0) GO TO 116
      EFFECT=CELL-BACK
      IF(BACK.EQ.0.0.AND.PORE.GT.0.0) EFFECT=CELL-PORE
      IF(AIR.LT.BACK) AIR=BACK
      SUCT=AIR-BACK
      IF(BACK.EQ.0.0.AND.PORE.GT.0.0) SUCT=AIR-PORE
      IF(EFFECT.LT.0.0) EFFECT=0.0
      IF(SUCT.LT.0.0) SUCT=0.0
      IF(BISH.LT.0.0) BISH=0.0
      WRITE(6,603) EFFECT,        SUCT,        BISH
  603 FORMAT(1X,'(SIGMA-UW)=',F8.3,' PSI'                    ,19X'(UA-UW)='
     1,F8.3,' PSI'                  ,19X,'(SIGMA-UA)=',F8.3,' PSI')
      IL=IL+1
  116 RETURN
      END
```

```
      SUBROUTINE ETIME(IYEAR1,MONTH1,IDAY1,IHOUR1,MIN1,ISEC1,IYEARX,
     1    MONTHX,IDAYX,IHOURX,MINX,ISECX,TIME)
C
C     ***************************************************************
C     SUBROUTINE TO COMPUTE THE ELAPSED TIME
C     ***************************************************************
C
      GO TO (4,3,4,5,4,5,4,4,5,4,5,4),MONTH1
    3 K=IYEAR1/4*4-IYEAR1
      IF(K)7,8,7
    7 TIME=FLOAT(ISECX-ISEC1)/60.+FLOAT(MINX-MIN1)+
     1FLOAT(IHOURX-IHOUR1)*60.+FLOAT(28*(MONTHX-MONTH1)-IDAY1+IDAYX)
     2  *1440.
      GO TO 11
    8 TIME=FLOAT(ISECX-ISEC1)/60.+FLOAT(MINX-MIN1)+
     1FLOAT(IHOURX-IHOUR1)*60.+FLOAT(29*(MONTHX-MONTH1)-IDAY1+IDAYX)
     2  *1440.
      GO TO 11
    4 TIME=FLOAT(ISECX-ISEC1)/60.+FLOAT(MINX-MIN1)+
     1FLOAT(IHOURX-IHOUR1)*60.+FLOAT(31*(MONTHX-MONTH1)-IDAY1+IDAYX)
     2  *1440.
      GO TO 11
    5 TIME=FLOAT(ISECX-ISEC1)/60.+FLOAT(MINX-MIN1)+
     1FLOAT(IHOURX-IHOUR1)*60.+FLOAT(30*(MONTHX-MONTH1)-IDAY1+IDAYX)
     2  *1440.
   11 RETURN
      END
```

```
      SUBROUTINE PAG(IL,IP,A,B,TRIAX,C)
C
C     ****************************************************************
C     SUBROUTINE TO WRITE THE HEADING FOR A NEW PAGE
C     ****************************************************************
C
      DIMENSION A(5),B(3),TRIAX(3),C(20)
      IF(IL.LT.40)  GO TO 111
      IL=0
      IP=IP+1
      WRITE(6,8) IP,A,B,TRIAX,C
      WRITE(6,9)
    8 FORMAT(1H1,                                    9X,'*********************
     1**************'              , 65X,'PAGE NO. __________'/1H+,118X,I6
     2/10X,'*',34X,'*',/10X,'*  ISOTROPIC VOLUME CHANGE TEST     *'
     2  ,/10X,'*',34X,'*',/10X,'*************************************'
     3     ,//3X,      'PROJECT _____________________',10X,'SAMPLE _____
     4_____________',5X,'TRIAXIAL CELL _____________'
     4                 ,/ 1H+,12X,5A4,18X,2A4,A2,28X,2A4,A2/
     7                                    /3X,'REMARKS _____________
     8_____________________________________________________________
     9_____________________________'/1H+,11X,20A4)
    9 FORMAT(1X,'_____________________________________________________
     1_____________________________________________________________
     1___'/ 13X,'TIME',15X,'|ELAPSED|   BOARD TRANSDUCER     '
     1                                          ,'|  CELL | LOCAL |
     1BURRET| IQ| LVDT READINGS                    |'
     1                          ,/    1X,'-------------------------------
     2-|  TIME |  CELL | WATER |  AIR  |  PORE |ELAPSED| READ-G|    ', '|
     3-------------------------------|'              /5X,'MON|DATE | HRS
     5| MIN | SEC | (MIN) | PRESS | PRESS | PRESS | PRESS | TIME  | (CC)
     6  |123|  LAT. |CORR-N | VERT. |CORR-N |'     /
     7  1X,'_____________________________________________________________
     8_____________________________________________________________
     9___')
  111 RETURN
      END
```

```
C     ***********************************************************************
C
C     PROGRAM TO REDUCE DATA FOR STRESS CHANGES ON UNSATURATED SOILS
C     -------- TESTS PERFORMED ON TRIAXIAL CELL NO. 1 ----------------
C
C     ***********************************************************************
C
      DIMENSION  A(5),B(3),C(20),CDM(20),SVOLW(10)
      REAL  LATCAL,LSVWAT,LTVOL,LSTVOL,LVLAT,LVVERT,LSLAT,LSVERT,LSWAT
C
C      PROGRAM TO REDUCE DATA FROM TRIAXIAL TEST ON UNSATURATED SOILS.
C
      ELEX=10.05
      CONVER=62.4/(2.54*12.*12.*12.)
      CALIB=15.235/4.
C      ------------------  TEMP  ------------------
      REG=0.0
      IP=1
      IL=0
C
C     ---------------------------------------------------------------------
C     READ HEADING CARD
C     ---------------------------------------------------------------------
C
C     A -      PROJECT NUMBER
C     B -      SAMPLE NUMBER
C     LATCAL  - CALIBRATION FOR LATERAL DISPLACEMENT
C     VERCAL  - CALIBRATION FOR VERTICAL DISPLACEMENT
      READ (5,1) A,B,              LATCAL,VERCAL
    1 FORMAT(5A4,2A4,A2,20X,2F10.0)
C
C     ---------------------------------------------------------------------
C     READ THE COMMENT CARD
C     ---------------------------------------------------------------------
C
      READ (5,2) C
    2 FORMAT(20A4)
C
C     ---------------------------------------------------------------------
C     READ THE INITIAL VOLUME WEIGHT DATA
C     ---------------------------------------------------------------------
C
C     DO -    ORIGINAL DIAMETER OF THE SAMPLE (CM)
C     HO -    ORIGINAL HEIGHT OF THE SAMPLE (CM)
C     GS -    SPECIFIC GRAVITY OF THE SOIL SOLIDS
C     WS -    DRY WEIGHT OF THE TOTAL SAMPLE (GMS)
C     WC -    ORIGINAL WATER CONTENT (%)
C
      READ (5,3) DO,HO,GS,WS,WC
    3 FORMAT(5F10.0)
C
      LATCAL=87.4088
      VERCAL=80.9515
      PI=3.14159
      AO=PI*DO*DO/4.
```

```
      VO=HO*AO
      VS=WS/GS
      VV=VO-VS
      EO=VV/VS
      POROS=EO/(1.+EO)*100.
      SAT=WC*GS/EO
      DRYDEN=GS*62.4/(1.+EO)
      TOTDEN=(GS+SAT*EO/100.)*62.4/(1.+EO)
      VWAT=SAT*VV/100.
      VAIR=VV-VWAT
      DISSOL=0.02*VWAT
      WRITE(6,8) IP,A,B,                LATCAL,VERCAL,C
    8 FORMAT(1H1,                                9X,'**********************
     1**************', 65X,'PAGE NO. __________'/1H+,118X,I6
     2                /10X,'*',34X,'*',/10X,'*    T R I A X I A L    T E
     2 S T    *',/10X,'*',34X,'*',/10X,'*********************************
     3****',//3X,      'PROJECT _____________________',10X,'SAMPLE _____
     4_____',/ 1H+,12X,5A4,18X,2A4,A2,/
     63X,'LATERAL CALIB. FACTOR (BALL) _____ CC/CM',10X,'VERTICAL
     7 CALIB. FACTOR (CAP) _____ CC/CM',/1H+,32X,F10.5,45X,F10.5,
     7                                .//3X,'REMARKS _____________
     8_____
     9_____'/1H+,11X,20A4)
      WRITE(6,9)
    9 FORMAT(1X,'_____
     1_____
     1___'/ 13X,'TIME',15X,'|ELAPSED|   BOARD TRANSDUCER    '
     1                                        ,'|  CELL | LOCAL |
     1BURRET| IQ|  CATHETOMETER',/    1X,'-------------------------------
     2-|  TIME |  CELL | WATER |  AIR  |  PORE |ELAPSED| READ-G|    ', '|
     3-----------------------------',/         5X,'MCN|DATE | HRS
     5| MIN | SEC | (MIN) | PRESS | PRESS | PRESS | PRESS | TIME  | (CC)
     6  |123|  REF. |  BALL |CORR-N |  CAP  |CORR-N'/
     7  1X,'_____
     8_____
     9___')
      WRITE(6,1022)
 1022 FORMAT(3X,'-------------------------------------------------------'/3X,
     1'IQ1 - SHOULD ELAPSED TIME AND WATER VOLUME CHANGE OR PORE PRESSUR
     2E'/3X,'   REACTION BE COMPUTED FROM THIS TIME.                '/3X,
     3'       1  SIGNIFIES  YES              '/3X,
     4'       0  SIGNIFIES  NO                '/3X,
     5'       9  SIGNIFIES A COMMENT STATEMENT ON THE NEXT CARD.  ',/3X,
     6'QUESTIONS REGARDING THE BURRET.            '/3X,
     7'IQ2 - IS WATER GOING INTO THE SAMPLE  (1)        ',/3X,
     8'       OR COMING OUT OF THE SAMPLE  (2)          ',/3X,
     9'WILL RETAIN PREVIOUS (IQ2) IF ZERO OR BLANK IS RECORDED.',/3X,
     1'IQ3 - IS THERE A REVERSAL IN WATER FLOW, CORRECTION IN BURRET'/3X
     2,'     READING OR A RESETTING OF THE BURRET?       ',/3X,
     3'-------------------------------------------------------'/)
      WRITE(6,6936)
 6936 FORMAT(20X,'WATER AND AIR MOVEMENT OUT OF THE SAMPLE IS DESIGNATED
     1 AS  P O S I T I V E',/ 20X,'WATER AND AIR MOVEMENT INTO THE SAMPL
     2E IS DESIGNATED AS   N E G A T I V E')
      WRITE(6,1020) GS,WS
```

```
1020 FORMAT(5X,' THE SPECIFIC GRAVITY USED IN THE COMPUTATIONS IS  '
     1 ,F8.3,/5X,' THE WEIGHT OF THE DRY SOIL SAMPLE IS ',F9.3)
      IL=IL+18
      WRITE(6,5) DO,HO,AO,VC,VS,VV,VWAT,VAIR ,DISSOL
    5 FORMAT(1X,' SAMPLE DIMENSIONS AND VOLUME WEIGHT RELATIONSHIPS'
     1                              /1X,'DIAMETER = ',F10.4,' CM    HEIG
     1HT = ',F10.4,' CM     AREA = ',F10.4,' SQ. CM    VOLUME = ',
     2F10.3,' CU. CM.'/1X,'VOL. SOLIDS = ',F8.2,4X,'VOL. VOIDS = ',F8.2,
     3  4X,'VOL. WATER = ',F8.2,4X,'VOL. AIR (FREE) = ',F8.2,' (DISSOLVE
     1D) = ',F8.2,' (CC)')
      IL=IL+3
      WRITE(6,6) WC,EO,PORCS,SAT,DRYDEN,TOTDEN
    6 FORMAT(1X,'W/C = ',F8.3,' %     E = ',F8.5,4X,'N = ',F7.3,
     1' %     SATURATION = ',F7.3,' %     DRY DEN. = ',F7.2,' PCF    TOTA
     2L DEN. = ',F7.2,' PCF')
      IL=IL+1
      H =HO
      DIA1=DO
      AREA1=AO
      V=VO
      CELL=0.0
      BACK=0.0
      AIR=0.0
      PORE=0.0
      IYEAR1=1971
      IYEARX=1971
      GO TO 113
C
C     ------------------------------------------------------------------
C     READ ADDITIONAL COMMENT CARDS
C     ------------------------------------------------------------------
C
  112 READ(5,10) COM
      WRITE(6,11) COM
      IL=IL+2
C
C     ------------------------------------------------------------------
C     READ THE FIRST DATA CARD
C     ------------------------------------------------------------------
C
  113 READ(5,7) IQ1,MONTH1,IDAY1,IHOUR1,MIN1,ISEC1,CELLP,BACKP,AIRP,
     1POREP,VOLCH,IQ2,IQ3,CATREF,CATBAL,OBALC ,CATCAP,OCAPC,DIFA
    7 FORMAT(I1,5I2,5F6.2,2I1,2F6.3,F6.3,F6.3,F6.3,2F6.3)
C       IQ1 - SHOULD ELAPSED TIME AND WATER VOLUME CHANGE OR PORE PRESSURE
C             REACTION BE COMPUTED FROM THIS TIME.
C             1  SIGNIFIES  YES
C             0  SIGNIFIES  NO
C             9  SIGNIFIES A COMMENT STATEMENT IS TO FOLLOW.
C       QUESTIONS REGARDING THE BURRET.
C       IQ2 - IS WATER GOING INTO THE SAMPLE  (1)
C             OR COMING OUT OF THE SAMPLE  (2)
C       WILL RETAIN PREVIOUS (IQ2) IF ZERO OR BLANK IS RECORDED.
C       IQ3 - IS THERE A REVERSAL IN WATER FLOW, CORRECTION IN BURRET
C             READING OR A RESETTING OF THE BURRET?
C      MONTH1  - MONTH
```

```
C      IDAY1    - DAY
C      IHOUR1   - HOUR
C      MIN1     - MINUTE
C      ISEC1    - SECOND
C      CELLP    - CELL PRESSURE (MV)
C      BACKP    - WATER BACK PRESSURE MEASURED ON THE BOARD (MV)
C      AIRP     - AIR PRESSURE (MV)
C      POREP    - PORE WATER PRESSURE MEASURED ON THE CELL (MV)
C      VOLCH    - WATER VOLUME CHANGE INDICATOR READING (CC)
C      CATREF   - CATHETOMETER REFERENCE POINT READING
C      CATBAL   - CATHETOMETER READING ON THE BALL
C      OBALC    - CORRECTION READING ON THE BALL
C      CATCAP   - CATHETOMETER READING ON THE CAP
C      OCAPC    - CORRECTION READING ON THE CAP
C      DIFA     - DIFFUSED AIR VOLUME CHANGE INDICATOR READING (CC)
       IF(IQ1.EQ.9) GO TO 112
C
C      ------------------------------------------------------------------
C      CALL SUBROUTINE TO COMPUTE PRESSURES
C      ------------------------------------------------------------------
C
       CALL PRESS(CELLP,BACKP,AIRP,POREP,                CELL,BACK,
     1     AIR,PORE,CELLM,BACKM,AIRM,POREM)
C
C      ------------------------------------------------------------------
C      INITIALIZE VARIABLES
C      ------------------------------------------------------------------
C
       IF(IQ1.EQ.1) FPORE=PORE
       IF(IQ1.EQ.1) RVV=VV
       IF(IQ1.EQ.1) RSAT=SAT
       MONTH2=MONTH1
       IDAY2=IDAY1
       MIN2=MIN1
       IHOUR2=IHOUR1
       ISEC2=ISEC1
       TIME1=0.0
       TIME2=0.0
       BALL1=(CATREF-CATBAL)
       CAP1=(CATREF-CATCAP)
       SLAT=0.0
       VOLL=0.0
       SVERT=0.0
       VOLV=0.0
       TVOL=0.0
       STVOL=0.0
       SWAT=0.0
       SVWAT=0.0
       LSWAT=0.0
       LSVWAT=0.0
       LSTVOL=0.0
       LTVOL=0.0
       LVLAT=0.0
       LVVERT=0.0
       LSLAT=0.0
```

```
      LSVERT=0.0
      FSVERT=0.0
      FSLAT=0.0
      FVVERT=0.0
      FVLAT=0.0
      FSTVOL=0.0
      FTVOL=0.0
      AIRV=0.0
      AIRVL=0.0
      AIRSTR=0.0
      PVOLCH=VOLCH
      DO 201 IS=1,10
  201 SVOLW(IS)=0.0
      II=1
      WRITE(6,18)MONTH1,IDAY1,IHCUR1,MIN1,ISEC1,TIME1,CELLP,BACKP,AIRP,
     1POREP,TIME2,VOLCH,IQ1,IQ2,IQ3,CATREF,CATBAL,GBALC ,CATCAP,OCAPC
   18 FORMAT(1X,'-----------------------------------------',  /
     1         1X,  5I6,F8.0,4F8.3,F8.2,F8.3,2X,3I1,5F8.3)
      WRITE(6,14) CELL,BACK,AIR,PORE
   14 FORMAT(19X,'PRESSURES IN PSI     ',4F8.3)
      WRITE(6,15) CELLM,BACKM,AIRM,POREM
   15 FORMAT(15X,'PRESSURES IN KG/SQ.CM.   ',4F8.4)
      IF(BACK.EQ.0.0.AND.PORE.EQ.0.0) GO TO 604
      EFFECT=CELL-BACK
      IF(BACK.EQ.0.0.AND.PORE.GT.0.0) EFFECT=CELL-PORE
      EFFECM=CELLM-BACKM
      IF(BACKM.EQ.0.0.AND.POREM.GT.0.0) EFFECM=CELLM-BACKM
      IF(AIR.LT.BACK) AIR=BACK
      SUCT=AIR-BACK
      IF(AIRM.LT.BACKM) AIRM=BACKM
      SUCTM=AIRM-BACKM
      BISH=CELL-AIR
      BISHM=CELLM-AIRM
      IF(EFFECT.LT.0.0) EFFECT=0.0
      IF(EFFECM.LT.0.0) EFFECM=0.0
      IF(SUCT.LT.0.0) SUCT=0.0
      IF(SUCTM.LT.0.0) SUCTM=0.0
      IF(BISH.LT.0.0) BISH=0.0
      IF(BISHM.LT.0.0) BISHM=0.0
      WRITE(6,603) EFFECT,EFFECM,SUCT,SUCTM,BISH,BISHM
  603 FORMAT(1X,'(SIGMA-UW)=',F8.3,' PSI OR',F8.4,' K/CM', 3X,'(UA-UW)='
     1,F8.3,' PSI OR',F8.4,' K/CM', 3X,'(SIGMA-UA)=',F8.3,' PSI OR',F8.4
     2,' K/CM')
      WRITE(6,41) VOLL,VOLV,TVOL,LVLAT,LVVERT,LTVOL
   41 FORMAT(1X,'VOL. CH. (CC) LAT.=',
     1F7.3,' VERT.=',F7.3,' TOTAL=',F7.3,6X,'LOC. LAT. =',F7.3,
     2 '   LOC. VERT=',F7.3,'   LOC. TOT.=',F9.3)
      WRITE(6,51) SLAT,SVERT,STVOL,LSLAT,LSVERT,LSTVOL
   51 FORMAT(1X,  'STRAIN (%)    LAT.=' ,
     1F7.4,' VERT.=',F7.4,' TOTAL=',F7.4,6X,'LOC. LAT. =',F7.4,
     2 '   LOC. VERT=',F7.4,'   LOC. TOT.=',F9.4)
      WRITE(6,629) AIRV,AIRVL,AIRSTR
      WRITE(6,19) SWAT,SVWAT,LSVWAT
      IL=IL+5
C
```

```
C     ****************************************************************
C
C     DO LOOP TO READ AND REDUCE ALL DATA CARDS
C
C     ****************************************************************
C
  604 DO  105  I=1,1000
      READ(5,7) IQ1,MONTHX,IDAYX,IHOURX,MINX,ISECX,CELLP,BACKP,AIRP,
     1POREP,VOLCH,IQ2,IQ3,CATREF,CATBAL,BALCOR,CATCAP,CAPCOR,DIFA
      IF(DIFA.GT.0.0.AND.IQ1.NE.8) DIFO=DIFA
      IF(DIFA.GT.0.0.AND.IQ1.EQ.8) DIFF=DIFA
      IF(IQ1.EQ.1) HOP=H
      IF(IQ1.EQ.1) VOP=V
      IF(IQ1.EQ.1) DOP=DIA1
      IF(IQ1.EQ.9) GO TO 109
      IF(IHOURX.EQ.0.AND.MINX.EQ.0) GO TO 106
      IF(IL.LT.39)  GO TO 111
      IL=0
      IP=IP+1
      WRITE(6,8) IP,A,B,              LATCAL,VERCAL,C
      WRITE(6,9)
C
C     ------------------------------------------------------------------
C     CALL SUBROUTINE TO COMPUTE ELAPSED TIME
C     ------------------------------------------------------------------
C
  111 CALL ETIME(IYEAR1,MONTH1,IDAY1,IHOUR1,MIN1,ISEC1,IYEARX,MONTHX,
     1IDAYX,IHOURX,MINX,ISECX,TIME1)
      IF(IQ1.EQ.0.OR.IQ1.EQ.8) GO TO 100
      MONTH2=MONTHX
      IDAY2=IDAYX
      IHOUR2=IHOURX
      MIN2=MINX
      ISEC2=ISECX
  100 CALL ETIME(IYEAR1,MONTH2,IDAY2,IHOUR2,MIN2,ISEC2,IYEARX,MONTHX,
     1 IDAYX,IHOURX,MINX,ISECX,TIME2)
C
C     ------------------------------------------------------------------
C     CALL SUBROUTINE TO COMPUTE PRESSURES
C     ------------------------------------------------------------------
C
      CALL PRESS(CELLP,BACKP,AIRP,POREP,              CELL,BACK,
     1  AIR,PORE,CELLM,BACKM,AIRM, POREM)
      IF(IQ1.EQ.1) FPORE=PORE
      IF(IQ1.EQ.1) RSAT=SAT
      IF(IQ1.EQ.1) RVV=VV
C
C     ------------------------------------------------------------------
C     WRITE INPUT DATA
C     ------------------------------------------------------------------
C
      WRITE(6,18)MONTHX,IDAYX,IHOURX,MINX,ISECX,TIME1,CELLP,BACKP,AIRP,
     1POREP,TIME2,VOLCH,IQ1,IQ2,IQ3,CATREF,CATBAL,BALCOR,CATCAP,CAPCOR
      IL=IL+2
      IF(CATBAL.EQ.0.0) GO TO 101
```

```
C
C     ------------------------------------------------------------------
C     COMPUTE LATERAL AND VERTICAL VOLUME CHANGES OF THE TOTAL SAMPLE
C     ------------------------------------------------------------------
C
      VOLL =(((CATREF-CATBAL)-BALL1)-(BALCOR-OBALC))*LATCAL
      VERT=((CATREF-CATCAP)-CAP1)-(CAPCOR-OCAPC)
      VOLV=VERT*VERCAL
      TVOL=VOLL+VOLV
      V=VO-TVOL
      H=HO-VERT
      DIA1=SQRT(4.0*V/(PI*H))
      SLAT=VOLL*100./VOP
      AREA1=PI*DIA1*DIA1/4.
      VVERT=VERT*AREA1
      SVERT=VVERT*100./VOP
      VLAT=TVOL-VVERT
      STVOL=TVOL*100. /VOP
      GO TO 102
  101 SLAT=0.0
      VOLL=0.0
      SVERT=0.0
      VOLV=0.0
      TVOL=0.0
      STVOL=0.0
  102 IF(VOLCH.EQ.0.0) GO TO 103
      IF(IQ2.EQ.0) GO TO 605
C
C     ------------------------------------------------------------------
C     COMPUTE WATER VOLUME CHANGES FROM BURRET READINGS
C     ------------------------------------------------------------------
C
C
C     WATER GOING INTO SAMPLE.
      IF(IQ2.EQ.1) SIGN=-1.0
C
C     WATER COMING OUT OF SAMPLE.
      IF(IQ2.EQ.2) SIGN= 1.0
  605 IF(IQ1.EQ.0.OR.IQ1.EQ.8) GO TO 104
      II=1
      SVWAT=0.0
      PVOLCH=VOLCH
      GO TO 203
  104 SVWAT=SVWAT-SVOLW(II)
      SWAT=SWAT-SVOLW(II)
      IF(IQ3.EQ.0) GO TO 203
      SVWAT=SVWAT+SVOLW(II)
      SWAT=SWAT+SVOLW(II)
      PVOLCH=VOLCH
      II=II+1
  203 SVOLW(II)=ABS(PVOLCH-VOLCH)*SIGN
      SWAT=SWAT+SVOLW(II)
      SVWAT=SVWAT+SVOLW(II)
      LSVWAT=SVWAT/VOP*100.
      IL=IL+1
```

```
      IF(IQ1.NE.8) GO TO  103
C
C     ------------------------------------------------------------------
C     COMPUTE AND APPLY AIR DIFFUSION CORRECTION
C     ------------------------------------------------------------------
C
      EXHEAD=(ELEX-(DIFO+DIFF)/2.)*CALIB
      ADIF=DIFO-DIFF
      DIFPR=3.4884*REG+0.05
      ATM=DIFPR+14.7+EXHEAD*CONVER
      IF(PORE.LE.0.0) PORE=BACK
      ADIFF= ADIF*(               ATM)/(PORE+14.7)
      STP=ADIF*(              ATM)/14.7
      IF(SIGN.GT.0.0) GO TO 856
      SWAT=SWAT-ADIFF
      SVWAT=SVWAT-ADIFF
      GO TO 857
  856 SWAT=SWAT-ADIFF
      SVWAT=SVWAT-ADIFF
  857 LSVWAT=SVWAT/VOP*100.
C
C     ------------------------------------------------------------------
C     WRITE AIR-DIFFUSION VOLUME AND CORRECTION
C     ------------------------------------------------------------------
C
      WRITE(6,864) DIFO,DIFF,ADIF,ATM   ,STP
  864 FORMAT(1X,'ORIG. DIF. AIR  =',F7.3,'   FINAL DIF. AIR =',F7.3,
     1'     DIF. VOL. =',F7.3,'   DIF. PRES.=',F7.3,'   STP VOL.='
     2 ,F7.3)
      IL=IL+1
      WRITE(6,421) ADIFF
  421 FORMAT(1X,'CCCCCCCCCCCCCCCCCCCCCCCCCCCCCC',/
     1  1X,'C  WATER VOLUME CORRECTION  C',/
     2  1X,'CCCCCCCCCCCCCCCCCCCCCCCCCCCCCC          (',F7.3,')')
      IL=IL+3
      IF(IL.LT.38) GO TO 103
      IL=0
      IP=IP+1
      WRITE(6,8) IP,A,B,              LATCAL,VERCAL,C
      WRITE(6,9)
  103 CONTINUE
      GO TO 4568
 4567 WRITE(6,19) SWAT,SVWAT,LSVWAT
      GO TO 4569
 4568 IF(CATBAL.EQ.0.0.AND.VOLCH.GT.0.0) GO TO 4567
 4569 IF(CATBAL.EQ.0.0.OR.VOLCH.EQ.0.0) GO TO 6027
      IF(IQ1.EQ.0.OR.IQ1.GT.1) GO TO 2711
C
C     ------------------------------------------------------------------
C     COMPUTE OVERALL AND LOCAL SAMPLE VOLUME CHANGES
C     ------------------------------------------------------------------
C
      FTVOL=TVOL
      FSTVOL=STVOL
      FVLAT=VLAT
```

```
      FVVERT=VVERT
      FSLAT=SLAT
      FSVERT=SVERT
 2711 LTVOL=TVOL-FTVOL
      LSTVOL=STVOL-FSTVOL
      LVLAT=VLAT-FVLAT
      LVVERT=VVERT-FVVERT
      LSLAT=SLAT-FSLAT
      LSVERT=SVERT-FSVERT
C
C     ------------------------------------------------------------------
C     WRITE TOTAL SAMPLE VOLUME CHANGES
C     ------------------------------------------------------------------
C
      WRITE(6,4) VLAT,VVERT,TVOL,LVLAT,LVVERT,LTVOL
      WRITE(6,5) SLAT,SVERT,STVOL,LSLAT,LSVERT,LSTVOL
      IL=IL+2
      IF(IL.LT.38) GO TO 6934
      IL=0
      IP=IP+1
      WRITE(6,8) IP,A,B,                    LATCAL,VERCAL,C
      WRITE(6,9)
C
C     ------------------------------------------------------------------
C     COMPUTE CHANGES IN AIR VOLUME
C     ------------------------------------------------------------------
C
 6934 AIRV=TVOL-SWAT
      AIRVL=LTVOL-SVWAT
      AIRSTR=LSTVOL-LSVWAT
C
C     ------------------------------------------------------------------
C     WRITE VOLUME CHANGES IN AIR AND WATER PHASES
C     ------------------------------------------------------------------
C
      WRITE(6,629) AIRV,AIRVL,AIRSTR
  629 FORMAT(1X,'TOT. AIR VOL. CH. =',F8.3,9X,'LOC. AIR VOL. CH. =',F8.3
     1,'   LOC. AIR STR.=',F10.4)
      WRITE(6,19) SWAT,SVWAT,LSVWAT
   19 FORMAT(1X,'TOT. WAT. VOL. CH.=',F8.3,9X,'LOC. WAT. VOL. CH.=',F8.3
     1 ,'   LOC. WAT. STR.=',F10.4)
      IL=IL+2
 6027 IF(CELL.EQ.0.0.AND.BACK.EQ.0.0.AND.AIR.EQ.0.0.AND.PORE.EQ.0.0) GO
     1       TO 116
      IF(IL.LT.38) GO TO 6935
      IL=0
      IP=IP+1
      WRITE(6,8) IP,A,B,                    LATCAL,VERCAL,C
      WRITE(6,9)
 6935 WRITE(6,14) CELL,BACK,AIR,PORE
      WRITE(6,15) CELLM,BACKM,AIRM,POREM
      IL=IL+2
      IF(CELL.EQ.0.0.AND.BACK.EQ.0.0.AND.AIR.EQ.0.0) GO TO 116
      IF(AIR.EQ.0.0) GO TO 1118
      BISH=CELL-AIR
```

```
      BISHM=CELLM-AIRM
      GO TO 1117
 1118 BISH=0.0
      BISHM=0.0
 1117 IF(BACK.EQ.0.0.AND.PORE.EQ.0.0) GO TO 116
      EFFECT=CELL-BACK
      IF(BACK.EQ.0.0.AND.PORE.GT.0.0) EFFECT=CELL-PORE
      EFFECM=CELLM-BACKM
      IF(BACKM.EQ.0.0.AND.POREM.GT.0.0) EFFECM=CELLM-POREM
      IF(AIR.LT.BACK) AIR=BACK
      SUCT=AIR-BACK
      IF(AIRM.LT.BACKM) AIRM=BACKM
      SUCTM=AIRM-BACKM
      IF(EFFECT.LT.0.0) EFFECT=0.0
      IF(EFFECM.LT.0.0) EFFECM=0.0
      IF(SUCT.LT.0.0) SUCT=0.0
      IF(SUCTM.LT.0.0) SUCTM=0.0
      IF(BISH.LT.0.0) BISH=0.0
      IF(BISHM.LT.0.0) BISHM=0.0
      WRITE(6,603) EFFECT,EFFECM,SUCT,SUCTM,BISH,BISHM
      IL=IL+1
  116 IF(IL.LT.38) GO TO 175
      IL=0
      IP=IP+1
      WRITE(6,8) IP,A,B,              LATCAL,VERCAL,C
      WRITE(6,9)
C
C     ------------------------------------------------------------
C     COMPUTATION OF VOLUME-WEIGHT SOIL PROPERTIES
C     ------------------------------------------------------------
C     COMPUTATIONS BASED ON THE TOTAL VOLUME AND WATER VOLUME MEASUREMENTS.
C
  175 V=VO-TVOL
      VV=V-VS
      E=VV/VS
      POROS=E/(1.+E)*100.
      VWATER=VWAT-SWAT
      VAIR=VV-VWATER
      DISSOL=0.02*VWATER
      WC=VWATER/WS*100.
      SAT=WC*GS/E
      DRYDEN=GS*62.4/(1.+E)
      TOTDEN=(GS+SAT*E/100.)*62.4/(1.+E)
C
C     ------------------------------------------------------------
C     WRITE THE VOLUME OF EACH PHASE AND THE VOLUME-WEIGHT SOIL PROPERTIES
C     ------------------------------------------------------------
C
      WRITE(6,5) DIA1,H,AREA1,V,VS,VV,VWATER,VAIR,DISSOL
      IL=IL+3
      IF(IL.LT.38) GO TO 9021
      IL=0
      IP=IP+1
      WRITE(6,8) IP,A,B,LATCAL,VERCAL,C
      WRITE(6,9)
```

```
 9021 WRITE(6,6) WC,E,POROS,SAT,DRYDEN,TOTDEN
      IL=IL+1
      GO TO 105
C
C     ------------------------------------------------------------------
C     READ AND WRITE COMMENT CARDS
C     ------------------------------------------------------------------
C
  109 READ(5,10) CCM
   10 FORMAT(20A4)
      WRITE(6,11) CCM
   11 FORMAT(10X,'-------------------------------------------------------
     1-------------------------------------',/10X,20A4)
      IL=IL+2
  105 CONTINUE
  106 WRITE(6,1021)  B
 1021 FORMAT(1X,'-------------------------------------------------------',/
     13X,' END OF TEST ',2A4,A2,/1X,'-------------------------------------
     2-------------')
      STOP
      END
```

```
      SUBROUTINE PRESS(CELLP,BACKP,AIRP,POREP,                CELL,BACK,
     1  AIR,PORE,CELLM,BACKM,AIRM,POREM)
C
C     ------------------------------------------------------------------
C SUBROUTINE TO COMPUTE PRESSURES FOR THE TRIAXIAL EQUIPMENT.
C     ------------------------------------------------------------------
C
      CELL=4.6405*CELLP-0.00377+1.30
      IF(CELLP.EQ.0.0) CELL=0.0
      CELLM=CELL*0.070307
      BACK=4.6405*BACKP-0.00377+1.30
      IF(BACKP.EQ.0.0) BACK=0.0
      BACKM=BACK*0.070307
      AIR=4.6405*AIRP-0.00377
      IF(AIRP.EQ.0.0) AIR=0.0
      AIRM=AIR*0.070307
      PORE=4.3067*POREP+0.00315
      IF(POREP.EQ.0.0) PORE=0.0
      POREM=PORE*0.070307
      RETURN
      END
```

```
      SUBROUTINE ETIME(IYEAR1,MONTH1,IDAY1,IHOUR1,MIN1,ISEC1,IYEARX,
     1    MONTHX,IDAYX,IHOURX,MINX,ISECX,TIME)
C
C     ***************************************************************
C     SUBROUTINE TO COMPUTE THE ELAPSED TIME
C     ***************************************************************
C
      GO TO (4,3,4,5,4,5,4,4,5,4,5,4),MONTH1
    3 K=IYEAR1/4*4-IYEAR1
      IF(K)7,8,7
    7 TIME=FLOAT(ISECX-ISEC1)/60.+FLOAT(MINX-MIN1)+
     1FLOAT(IHOURX-IHOUR1)*60.+FLOAT(28*(MONTHX-MONTH1)-IDAY1+IDAYX)
     2  *1440.
      GO TO 11
    8 TIME=FLOAT(ISECX-ISEC1)/60.+FLOAT(MINX-MIN1)+
     1FLOAT(IHOURX-IHOUR1)*60.+FLOAT(29*(MONTHX-MONTH1)-IDAY1+IDAYX)
     2  *1440.
      GO TO 11
    4 TIME=FLOAT(ISECX-ISEC1)/60.+FLOAT(MINX-MIN1)+
     1FLOAT(IHOURX-IHOUR1)*60.+FLOAT(31*(MONTHX-MONTH1)-IDAY1+IDAYX)
     2  *1440.
      GO TO 11
    5 TIME=FLOAT(ISECX-ISEC1)/60.+FLOAT(MINX-MIN1)+
     1FLOAT(IHOURX-IHOUR1)*60.+FLOAT(30*(MONTHX-MONTH1)-IDAY1+IDAYX)
     2  *1440.
   11 RETURN
      END
```

```
C     ****************************************************************
C
C     PROGRAM TO REDUCE DATA FOR STRESS CHANGES ON UNSATURATED SOILS
C     -------- TESTS PERFORMED ON ONE-DIMENSIONAL OEDOMETER ----------
C
C     ****************************************************************
C
      DIMENSION  A(5),B(3),C(20),COM(20),SVOLW(10),ANTEUS(3)
      REAL LSVWAT,LTVOL,LSTVOL,LVLAT,LVVERT,LSLAT,LSVERT,LSWAT
      IP=1
      IL=0
C
C     ----------------------------------------------------------------
C     READ HEADING CARD
C     ----------------------------------------------------------------
C
C     A -      PROJECT NUMBER
C     B -      SAMPLE NUMBER
C     ANTEUS  - OEDOMETER NUMBER
      READ (5,1) A,B,ANTEUS
    1 FORMAT(5A4,2A4,A2,        2A4,A2)
C
C     ----------------------------------------------------------------
C     READ THE COMMENT CARD
C     ----------------------------------------------------------------
C
      READ (5,2) C
    2 FORMAT(20A4)
C
C     ----------------------------------------------------------------
C     READ THE INITIAL VOLUME WEIGHT DATA
C     ----------------------------------------------------------------
C
C     DO -     ORIGINAL DIAMETER OF THE SAMPLE (CM)
C     HO -     ORIGINAL HEIGHT OF THE SAMPLE (CM)
C     GS -     SPECIFIC GRAVITY OF THE SOIL SOLIDS
C     WS -     DRY WEIGHT OF THE TOTAL SAMPLE (GMS)
C     WC -     ORIGINAL WATER CONTENT (%)
C
      READ (5,3) DO,HO,GS,WS,WC
    3 FORMAT(5F10.0)
C
      PI=3.14159
      ELEX=10.05
      CALIB=15.235/4.
      CONVER=62.4/(2.54*12.*12.*12.)
      AO=PI*DO*DO/4.
      VO=HO*AO
      VS=WS/GS
      VV=VO-VS
      EO=VV/VS
      POROS=EO/(1.+EO)*100.
      SAT=WC*GS/EO
      DRYDEN=GS*62.4/(1.+EO)
      TOTDEN=(GS+SAT*EO/100.)*62.4/(1.+EO)
```

```
      VWAT=SAT*VV/100.
      VAIR=VV-VWAT
      DISSOL=0.02*VWAT
      WRITE(6,8) IP,A,B,ANTEUS,C
    8 FORMAT(1H1,                                    9X,'**********************
     1**************', 65X,'PAGE NO. __________'/1H+,118X,I6
     2                /10X,'*',34X,'*',/10X,'*        ONE-DIMENSIONAL
     2TEST    *',/10X,'*',34X,'*',/10X,'*******************************
     3****',//3X,      'PROJECT  _____________________',10X,'SAMPLE  _____
     4_____________',/ 1H+,12X,5A4,18X,2A4,A2,/
     6 3X,'ANTEUS CONSOLIDOMETER NO. __________ '/1H+,29X,2A4,A2,
     7                                  //3X,'REMARKS _______________
     8_____________________________________________________________________
     9_____________________________'/1H+,11X,20A4)
      WRITE(6,9)
    9 FORMAT(1X,'_____________________________________________________________
     1_____________________________________________________________________
     1___'/ 13X,'TIME',15X,'|ELAPSED|   BOARD TRANSDUCER     '
     1                                              ,'|  CELL | LOCAL |
     1BURRET| IQ| DIAL GAUGE     | TOTAL | LOCAL |LOCAL',/
     1                                  1X,'-------------------------------
     2-|  TIME |  CELL |  BACK |  AIR  |  PORE |ELAPSED| READ-G|    ', '|
     3-------<---------| VOLUME| VOLUME| VOL.',/        5X,'MON|DATE | HRS
     5| MIN | SEC | (MIN) | PRESS | PRESS | PRESS | PRESS | TIME  | (CC)
     6  |123|  CAP  |CORR-N | WATER | WATER |STRAIN'/
     7  1X,'_____________________________________________________________
     8_____________________________________________________________________
     9___')
      WRITE(6,1022)
1022 FORMAT(3X,'-------------------------------------------------------'/3X,
     1'IQ1 - SHOULD ELAPSED TIME AND WATER VOLUME CHANGE OR PORE PRESSUR
     2E'/3X,'   REACTION BE COMPUTED FROM THIS TIME.                '/3X,
     3'       1  SIGNIFIES  YES            '/3X,
     4'       0  SIGNIFIES  NO               '/3X,
     5'       9  SIGNIFIES A COMMENT STATEMENT ON THE NEXT CARD.  ',/3X,
     6'QUESTIONS REGARDING THE BURRET.            '/3X,
     7'IQ2 - IS WATER GOING INTO THE SAMPLE  (1)        ',/3X,
     8'       OR COMING OUT OF THE SAMPLE  (2)           ',/3X,
     9'WILL RETAIN PREVIOUS (IQ2) IF ZERO OR BLANK IS RECORDED.',/3X,
     1'IQ3 - IS THERE A REVERSAL IN WATER FLOW, CORRECTION IN BURRET'/3X
     2,'      READING OR A RESETTING OF THE BURRET?       ',/3X,
     3'-------------------------------------------------------'/)
      WRITE(6,1020)  GS,WS
1020 FORMAT(5X,' THE SPECIFIC GRAVITY USED IN THE COMPUTATIONS IS  '
     1 ,F8.3,/5X,' THE WEIGHT OF THE DRY SOIL SAMPLE IS ',F9.3)
      IL=IL+16
      WRITE(6,5) DO,HO,AO,VC,VS,VV,VWAT,VAIR ,DISSOL
    5 FORMAT(1X,' SAMPLE DIMENSIONS AND VOLUME WEIGHT RELATIONSHIPS'
     1                              /1X,'DIAMETER = ',F10.4,' CM    HEIG
     1HT = ',F10.4,' CM     AREA = ',F10.4,' SQ. CM     VOLUME = ',
     2F10.3,' CU. CM.'/1X,'VOL. SOLIDS = ',F8.2,4X,'VOL. VOIDS = ',F8.2,
     3  4X,'VOL. WATER = ',F8.2,4X,'VOL. AIR (FREE) = ',F8.2,' (DISSOLVE
     1D) = ',F8.2,' (CC)')
      IL=IL+3
      WRITE(6,6) WC,EO,POROS,SAT,DRYDEN,TOTDEN
```

```
    6 FORMAT(1X,'W/C = ',F8.3,' %     E = ',F8.5,4X,'N = ',F7.3,
     1' %     SATURATION = ',F7.3,' %     DRY DEN. = ',F7.2,' PCF     TOTA
     2L DEN. = ',F7.2,' PCF')
      IL=IL+1
      H =HO
      DIA1=DO
      AREA1=AO
      V=VO
      HOP=H
      VOP=V
      ISIDE=2
      ITYPE=2
      IYEAR1=1971
      IYEARX=1971
      TIME1=0.0
      TIME2=0.0
      GO TO 113
C
C     ------------------------------------------------------------------
C     READ ADDITIONAL COMMENT CARDS
C     ------------------------------------------------------------------
C
  112 READ(5,10) COM
      WRITE(6,11) COM
      IL=IL+1
C
C     ------------------------------------------------------------------
C     READ THE FIRST DATA CARD
C     ------------------------------------------------------------------
C
  113 READ(5,7) IQ1,MONTH1,IDAY1,IHOUR1,MIN1,ISEC1,CELLP,BACKP,AIRP,
     1POREP,VOLCH,IQ2,IQ3,CAP,OCAPC,DIFO,DIFF,TEMP,IQ4,IQ5
    7 FORMAT(I1,5I2,5F6.2,2I1,F6.3,F6.3,F5.2,F6.2,F5.2,7X,2I1)
C       IQ1 - SHOULD ELAPSED TIME AND WATER VOLUME CHANGE OR PORE PRESSURE
C             REACTION BE COMPUTED FROM THIS TIME.
C                1  SIGNIFIES  YES
C                0  SIGNIFIES  NO
C                9  SIGNIFIES A COMMENT STATEMENT IS TO FOLLOW.
C                8  SIGNIFIES THAT THIS CARD CONTAINS THE FINAL DIFFUSED
C                   AIR VOLUME.
C       QUESTIONS REGARDING THE BURRET.
C       IQ2 - IS WATER GOING INTO THE SAMPLE  (1)
C             OR COMING OUT OF THE SAMPLE  (2)
C       WILL RETAIN PREVIOUS (IQ2) IF ZERO OR BLANK IS RECORDED.
C       IQ3 - IS THERE A REVERSAL IN WATER FLOW, CORRECTION IN BURRET
C             READING OR A RESETTING OF THE BURRET?
C       QUESTIONS REGARDING THE PROCEDURE OF COMPUTATIONS.
C       IQ4 - DOES THE SAMPLE PULL AWAY FROM THE SIDES OF THE RING.
C             0 SIGNIFIES TO TAKE THE PREVIOUS VALUE.
C             1 SIGNIFIES  YES.
C             2 SIGNIFIES  NO.
C       IQ5 - WHAT TYPE OF ANALYSIS IS DESIRED?
C             0 SIGNIFIES THAT THE PREVIOUS TYPE NUMBER BE RETAINED.
C             1 - ASSUMES THAT THE VOLUME OF AIR REMAINS EQUAL TO ITS
C                 PREVIOUS VALUE.
```

```
C            2 - ASSUMES THAT THE VOLUME OF VOIDS IS EQUAL TO THE DIFFEREN
C                BETWEEN THE MEASURED TOTAL VOLUME AND THE COMPUTED VOLUME
C                OF SOLIDS.
C            3 - BASED ON THE APPLICATION OF BOYLES AND HENRY'S LAW.
C                THE VOLUME OF WATER "GENERALLY" REMAINS CONSTANT AND
C                THE VOLUME OF AIR IS COMPRESSED.
      IF(IQ4.GT.0) ISIDE=IQ4
      IF(IQ5.GT.0) ITYPE=IQ5
C     MONTH1  - MONTH
C     IDAY1   - DAY
C     IHOUR1  - HOUR
C     MIN1    - MINUTE
C     ISEC1   - SECOND
C     CELLP   - CELL PRESSURE (MV)
C     BACKP   - WATER BACK PRESSURE MEASURED ON THE BOARD (MV)
C     AIRP    - AIR PRESSURE (MV)
C     POREP   - PORE WATER PRESSURE MEASURED ON THE CELL (MV)
C     VOLCH   - WATER VOLUME CHANGE INDICATOR READING (CC)
C     CAP     - DIAL GAUGE READING ON THE CAP
C     DCAPC   - DIAL GAUGE CORRECTION ON THE CAP
C     DIFO    - DIFFUSED AIR VOLUME READING PRIOR TO FLUSHING
C     DIFF    - DIFFUSED AIR VOLUME READING SUBSEQUENT TO FLUSHING
C     TEMP    - TEMPERATURE OF THE CEDOMETER (CENTIGRADE)
      IF(IQ1.EQ.9) GO TO 112
C
C     ------------------------------------------------------------------
C     INITIALIZE VARIABLES
C     ------------------------------------------------------------------
C
      IF(IQ1.EQ.1) RSAT=SAT
      IF(IQ1.EQ.1) RVV=VV
      MONTH2=MONTH1
      IDAY2=IDAY1
      IHOUR2=IHOUR1
      MIN2=MIN1
      ISEC2=ISEC1
      PCAP=CAP
      SLAT=0.0
      VCLL=0.0
      VLAT=0.0
      VVERT=0.0
      SVERT=0.0
      VOLV=0.0
      TVOL=0.0
      STVOL=0.0
      SWAT=0.0
      SVWAT=0.0
      LSVWAT=0.0
      LSWAT=0.0
      LSTVOL=0.0
      LTVOL=0.0
      LVLAT=0.0
      LVVERT=0.0
      LSLAT=0.0
      LSVERT=0.0
```

```
      AIRV=0.0
      AIRVL=0.0
      AIRSTR=0.0
      PVOLCH=VOLCH
      DO 201 IS=1,10
  201 SVOLA(IS)=0.0
      II=1
      RESVOL=0.0
      WRITE(6,18)MONTH1,IDAY1,IHOUR1,MIN1,ISEC1,TIME1,CELLP,BACKP,AIRP,
     1POREP,TIME2,VOLCH,IQ1,IQ2,IQ3,CAP,OCAPC
   18 FORMAT(1X,'----------------------------------------',/
     1        1X,  5I6,F8.0,4F8.3,F8.2,F8.3,2X,3I1,2F8.5)
      WRITE(6,19) SWAT,SVWAT,LSWAT
      CALL PRESS(CELLP,BACKP,AIRP,POREP,PORE,BACK,AO,IL)
      IF(IQ1.EQ.1) FPORE=PORE
      WRITE(6,41) VLAT,VVERT,TVOL,LVLAT,LVVERT,LTVOL
      WRITE(6,51) SLAT,SVERT,STVOL,LSLAT,LSVERT,LSTVOL
   41 FORMAT(1X,'VOL. CH. (CC) LAT.=',
     1F7.3,' VERT.=',F7.3,' TOTAL=',F7.3,6X,'LOC. LAT. =',F7.3,
     2 '   LOC. VERT=',F7.3,'   LOC. TOT.=',F9.3)
   51 FORMAT(1X,  'STRAIN (%)    LAT.=',
     1F7.4,' VERT.=',F7.4,' TOTAL=',F7.4,6X,'LOC. LAT. =',F7.4,
     2 '   LOC. VERT=',F7.4,'   LOC. TOT.=',F9.4)
      IL=IL+2
C
C     ****************************************************************
C
C     DO LOOP TO READ AND REDUCE ALL DATA CARDS
C
C     ****************************************************************
C
  604 DO  501  I=1,1000
      READ(5,7) IQ1,MONTHX,IDAYX,IHOURX,MINX,ISECX,CELLP,BACKP,AIRP,
     1POREP,VOLCH,IQ2,IQ3,CAP,CAPCOR,DIFO,DIFF,TEMP,IQ4,IQ5
      IF(IQ4.GT.0) ISIDE=IQ4
      IF(IQ5.GT.0) ITYPE=IQ5
      IF(IQ1.EQ.1) VOP=V
      IF(IQ1.EQ.1) HOP=H
      IF(IQ1.EQ.9) GO TO 109
      IF(IQ1.EQ.8) GO TO 914
C   THE CELL PRESSURE COLUMN 12 CONTAINS A VOLUME CHANGE CORRECTION.
      IF(IHOURX.EQ.0.AND.MINX.EQ.0) GO TO 106
      IF(IL.LT.38)  GO TO 111
      IL=0
      IP=IP+1
      WRITE(6,8) IP,A,B,ANTEUS,C
      WRITE(6,9)
C
C     ----------------------------------------------------------------
C     CALL SUBROUTINE TO COMPUTE ELAPSED TIME
C     ----------------------------------------------------------------
C
  111 CALL ETIME(IYEAR1,MONTH1,IDAY1,IHOUR1,MIN1,ISEC1,IYEARX,MONTHX,
     1IDAYX,IHOURX,MINX,ISECX,TIME1)
      IF(IQ1.EQ.0) GO TO 100
```

```
      MONTH2=MONTHX
      IDAY2=IDAYX
      IHOUR2=IHOURX
      MIN2=MINX
      ISEC2=ISECX
  100 CALL ETIME(IYEAR1,MONTH2,IDAY2,IHOUR2,MIN2,ISEC2,IYEARX,MONTHX,
     1 IDAYX,IHOURX,MINX,ISECX,TIME2)
C
C     ------------------------------------------------------------------
C     WRITE INPUT DATA
C     ------------------------------------------------------------------
C
      WRITE(6,18)MONTHX,IDAYX,IHOURX,MINX,ISECX,TIME1,CELLP,BACKP,AIRP,
     1POREP,TIME2,VOLCH,IQ1,IQ2,IQ3,CAP,CAPCOR
      IL=IL+2
C
C     ------------------------------------------------------------------
C     CALL SUBROUTINE TO COMPUTE AND WRITE PRESSURES AND STRESS STATE
C     VARIABLES.
C     ------------------------------------------------------------------
C
      CALL PRESS(CELLP,BACKP,AIRP,POREP,PORE,BACK,AREA1,IL)
      IF(IL.LT.38)  GO TO 1209
      IL=0
      IP=IP+1
      WRITE(6,8) IP,A,B,                ANTEUS,C
      WRITE(6,9)
 1209 IF(VOLCH.EQ.0.0) GO TO 103
      IF(IQ2.EQ.0) GO TO 605
C
C     ------------------------------------------------------------------
C     COMPUTE WATER VOLUME CHANGES FROM BURRET READINGS
C     ------------------------------------------------------------------
C
C
C     WATER GOING INTO SAMPLE.
      IF(IQ2.EQ.1) SIGN=-1.0
C
C     WATER COMING OUT OF SAMPLE.
      IF(IQ2.EQ.2) SIGN= 1.0
  605 IF(IQ1.EQ.0) GO TO 104
      II=1
      SVWAT=0.0
      PVOLCH=VOLCH
      GO TO 203
  104 SVWAT=SVWAT-SVOLW(II)
      SWAT=SWAT-SVOLW(II)
      IF(IQ3.EQ.0) GO TO 203
      SVWAT=SVWAT+SVOLW(II)
      SWAT=SWAT+SVOLW(II)
      PVOLCH=VOLCH
      II=II+1
  203 SVOLW(II)=ABS(PVCLCH-VOLCH)*SIGN
      SWAT=SWAT+SVOLW(II)
      SVWAT=SVWAT+SVOLW(II)
```

```
      LSVWAT=SVWAT/VOP*100.
      IF(DIFF.EQ.0.0) GO TO  914
      WRITE(6,19) SWAT,SVWAT,LSVWAT
      IL=IL+1
C
C     ------------------------------------------------------------------
C     COMPUTE AND APPLY AIR DIFFUSION CORRECTION
C     ------------------------------------------------------------------
C
      EXHEAD=(ELEX-(DIFO+DIFF)/2.)*CALIB
      ADIF=DIFO-DIFF
      DIFPR=4.23566*REG+0.00997
      IF(REG.EQ.0.0) DIFPR=0.0
      ATM=DIFPR+14.7+EXHEAD*CONVER
      IF(PORE.EQ.0.0) PORE=BACK
      ADIFF= ADIF*(ATM)/(PORE+14.7)
      STP=ADIF*(ATM)/14.7
      IF(IL.LT.38)  GO TO 8433
      IL=0
      IP=IP+1
      WRITE(6,8) IP,A,B,ANTELS,C
      WRITE(6,9)
C
C     ------------------------------------------------------------------
C     WRITE AIR DIFFUSION VOLUME AND CORRECTION
C     ------------------------------------------------------------------
C
 8433 WRITE(6,864) DIFO,DIFF,ADIF ,ATM  ,STP
  864 FORMAT(1X,'ORIG. DIF. AIR =',F7.3,'   FINAL DIF. AIR = ',F7.3,
     1'     DIF. VOL. =',F7.3,  '   DIF. PRES.=',F7.3,'   STP VOL.=',
     4  F7.3)
      IL=IL+1
      GO TO 8856
  914 IF(IQ1.NE.8) GO TO 915
      ADIFF=CELLP
 8856 IF(SIGN.GT.0.0) GO TO 856
  842 SWAT=SWAT-ADIFF
      SVWAT=SVWAT-ADIFF
      GO TO 857
  856 SWAT=SWAT-ADIFF
      SVWAT=SVWAT-ADIFF
  857 LSVWAT=SVWAT/VOP*100.
      WRITE(6,421)  ADIFF
  421 FORMAT(1X,'CCCCCCCCCCCCCCCCCCCCCCCCCCCCCC'/
     1  1X,'C  WATER VOLUME CORRECTION  C'/
     2       1X,'CCCCCCCCCCCCCCCCCCCCCCCCCCCCCC          (',F6.3,')')
      IL=IL+3
  915 IF(IL.LT.38)  GO TO 423
      IL=0
      IP=IP+1
      WRITE(6,8) IP,A,B,                ANTEUS,C
      WRITE(6,9)
  423 IF(IQ1.EQ.8) GO TO 6934
  103 CONTINUE
      IF(CAP   .EQ.0.0) GO TO 101
```

```
C
C     ------------------------------------------------------------------
C
      VERT=((CAP-PCAP)-(CAPCOR-OCAPC))*2.54
      VOLV=VERT*AREA1
      H=HO-VERT
      GO TO 102
  101 SLAT=0.0
      VLAT=0.0
      VVERT=0.0
      TVOL=0.0
      SVERT=0.0
      STVOL=0.0
      GO TO 501
  102 GO TO(115,2011),ISIDE
C
C     //////////////////////////////////////////////////////////////////
C
C     ASSUMES THAT THE SAMPLE PULLS AWAY FROM THE SIDES OF THE RING.
C     ALSO ASSUMES THAT THE VOLUME OF AIR REMAINS CONSTANT.
C     ------------------------------------------------------------------
C
  115 IF(CAP.EQ.0.0) GO TO 501
      VWATER=VWAT-SWAT
      VV=VWATER+VAIR
      V=VV+VS
      AREA1=V/H
      DIA1=SQRT(4.*AREA1/PI)
      SLAT=(DO-DIA1)*100./DO
      TVOL=VO-V
      VVERT=VERT*AREA1
      VLAT=TVOL-VVERT
      SLAT=(DO-DIA1)*100./DO
      SVERT=VERT*100./HCP
      STVOL=TVOL*100. /VCP
      IF(IQ1.EQ.0) GO TO 2711
      FTVOL=TVOL
      FSTVOL=STVOL
 2711 LTVOL=TVOL-FTVOL
      LSTVOL= STVOL-FSTVOL
      WRITE(6,41) VLAT,VVERT,TVOL,LVLAT,LVVERT,LTVOL
      WRITE(6,51) SLAT,SVERT,STVOL,LSLAT,LSVERT,LSTVOL
      IL=IL+2
      GO TO 209
C
C     ------------------------------------------------------------------
C     ASSUME THAT THE SAMPLE REMAINS FIXED TO THE SIDES OF THE RING.
C     ------------------------------------------------------------------
C
 2011 VOLL=0.0
      TVOL=VOLL+VOLV
      V=VO-TVOL
      VLAT=0.0
      SLAT=0.0
      VVERT=VOLV
```

```
      SVERT=VERT*100./HOP
      STVOL=TVOL*100. /VOP
      LVLAT=0.0
      LSLAT=0.0
      SVERT=STVOL
      LSVERT=LSTVOL
      LVVERT=LTVOL
      IF(IQ1.EQ.0.OR.IQ1.GT.1) GO TO 2712
      FTVOL=TVOL
      FSTVOL=STVOL
      FVLAT=VLAT
      FVVERT=VVERT
      FSLAT=SLAT
      FSVERT=SVERT
 2712 LTVOL=TVOL-FTVOL
      LSTVOL=STVOL-FSTVOL
      LVLAT=VLAT-FVLAT
      LVVERT=VVERT-FVVERT
      LSLAT=SLAT-FSLAT
      LSVERT=SVERT-FSVERT
      WRITE(6,41) VLAT,VVERT,TVOL,LVLAT,LVVERT,LTVOL
      WRITE(6,51) SLAT,SVERT,STVOL,LSLAT,LSVERT,LSTVOL
      IL=IL+2
      IF(IL.LT.38)  GO TO 6934
      IL=0
      IP=IP+1
      WRITE(6,8) IP,A,B,ANTEUS,C
      WRITE(6,9)
C
C     ------------------------------------------------------------------
C     COMPUTE CHANGES IN AIR VOLUME
C     ------------------------------------------------------------------
C
 6934 AIRV=TVOL-SWAT
      AIRVL=LTVOL-SVWAT
      AIRSTR=LSTVOL-LSVWAT
C
C     ------------------------------------------------------------------
C     WRITE VOLUME CHANGES IN AIR AND WATER PHASES
C     ------------------------------------------------------------------
C
      WRITE(6,629) AIRV,AIRVL,AIRSTR
  629 FORMAT(1X,'TOT. AIR VOL. CH. =',F8.3,9X,'LOC. AIR VOL. CH. =',F8.3
     1,'   LOC. AIR STR.=',F10.4)
      WRITE(6,19) SWAT,SVWAT,LSVWAT
   19 FORMAT(1X,'TOT. WAT. VOL. CH.=',F8.3,9X,'LOC. WAT. VOL. CH.=',F8.3
     1 ,'   LOC. WAT. STR.=',F10.4)
      IL=IL+2
  209 GO TO (2001,175,2002),ITYPE
C
C     ------------------------------------------------------------------
C     COMPUTATION OF VOLUME-WEIGHT SOIL PROPERTIES
C     ------------------------------------------------------------------
C
C     ||||||||||||||||||||||||||||||||||||||||||||||||||||||||||||||||||
```

```
C     COMPUTATIONS BASED ON THE ASSUMPTION THAT THE VOLUME OF AIR
C     REMAINS CONSTANT.
C
 2001 VWATER=VWAT-SWAT
      VV=VWATER+VAIR
      E=VV/VS
      V=VV+VS
      POROS=E/(1.+E)*100.
      DISSOL=0.02*VWATER
      WC=VWATER/WS*100.
      SAT=WC*GS/E
      DRYDEN=GS*62.4/(1.+E)
      TOTDEN=(GS+SAT*E/100.)*62.4/(1.+E)
C
C     ------------------------------------------------------------------
C     WRITE THE VOLUME OF EACH PHASE AND THE VOLUME-WEIGHT SOIL PROPERTIES
C     ------------------------------------------------------------------
C
      WRITE(6,5) DIA1,H,AREA1,V,VS,VV,VWATER,VAIR,DISSOL
      IL=IL+3
      WRITE(6,6) WC,E,POROS,SAT,DRYDEN,TOTDEN
      IL=IL+1
      GO TO 501
C
C     ||||||||||||||||||||||||||||||||||||||||||||||||||||||||||||||||||
C     BASED ON THE ASSUMPTION THAT THE VOLUME OF VOIDS IS EQUAL TO THE
C     DIFFERENCE BETWEEN THE MEASURED TOTAL VOLUME AND THE COMPUTED
C     VOLUME OF SOLIDS.
C
  175 VV=V-VS
      E=VV/VS
      POROS=E/(1.+E)*100.
      VWATER=VWAT-SWAT
      VAIR=VV-VWATER
      DISSOL=0.02*VWATER
      WC=VWATER/WS*100.
      SAT=WC*GS/E
      DRYDEN=GS*62.4/(1.+E)
      TOTDEN=(GS+SAT*E/100.)*62.4/(1.+E)
C
C     ------------------------------------------------------------------
C     WRITE THE VOLUME OF EACH PHASE AND THE VOLUME-WEIGHT SOIL PROPERTIES
C     ------------------------------------------------------------------
C
      WRITE(6,5) DIA1,H,AREA1,V,VS,VV,VWATER,VAIR,DISSOL
      IL=IL+3
      WRITE(6,6) WC,E,POROS,SAT,DRYDEN,TOTDEN
      IL=IL+1
      GO TO 501
C
C     ||||||||||||||||||||||||||||||||||||||||||||||||||||||||||||||||||
C     COMPUTATIONS BASED ON HENRY'S LAW AND BOYLES LAW.
C     THE VOLUME OF WATER "GENERALLY" REMAINS CONSTANT AND THE VOLUME
C     OF AIR IS COMPRESSED.
C
```

```
 2002 DELTAV=-1.*((FPORE+14.7)/(PORE+14.7)-1.)*(1.-RSAT/100.+RSAT/100.*0
     1.02)*RVV
      VOAIR=VAIR-DELTAV
      IF (VOAIR.LT.0.0) VOAIR=0.0
      VWATER=V-VS-VCAIR
      VV=VWATER+VOAIR
      E=VV/VS
      POROS=E/(1.+E)*100.
      DISSOL=0.02*VWATER
      WC=VWATER/WS*100.
      SAT=WC*GS/E
      DRYDEN=GS*62.4/(1.+E)
      TOTDEN=(GS+SAT*E/100.)*62.4/(1.+E)
C
C     ------------------------------------------------------------------
C     WRITE THE VOLUME OF EACH PHASE AND THE VOLUME-WEIGHT SOIL PROPERTIES
C     ------------------------------------------------------------------
C
      WRITE(6,5) DIA1,H,AREA1,V,VS,VV,VWATER,VOAIR,DISSOL
      IL=IL+3
      WRITE(6,6) WC,E,POROS,SAT,DRYDEN,TOTDEN
      IL=IL+1
      GO TO 501
C
C     ------------------------------------------------------------------
C     READ AND WRITE COMMENT CARDS
C     ------------------------------------------------------------------
C
  109 READ(5,10) COM
   10 FORMAT(20A4)
      WRITE(6,9034)
 9034 FORMAT (1X,'------------------------------------------------------
     1----------')
      IL=IL+1
      WRITE(6,11) COM
   11 FORMAT(10X,20A4)
      IL=IL+1
  501 CONTINUE
  106 WRITE(6,1021)  B
 1021 FORMAT(1X,'------------------------------------------------------',/
     13X,' END OF TEST ',2A4,A2,/1X,'-------------------------------
     2----------')
      STOP
      END
```

```
      SUBROUTINE PRESS(CELLP,BACKP,AIRP,POREP,PORE,BACK,AREA1,IL)
      AREA2=AREA1/2.54/2.54
C
C     ------------------------------------------------------------------
C     SUBROUTINE FOR ANTEUS CONSOLIDOMETER #177
C     ------------------------------------------------------------------
C
      CELL=((0.130966*CELLP-64.7979)/AREA2)*13.889
      IF(CELLP.EQ.0.0) CELL=0.0
      CELLM=CELL*0.070307
      AIR =4.23566*AIRP +0.00997
      IF(AIRP.EQ.0.0) AIR=0.0
      AIRM=AIR*0.070307
      CELL=CELL+AIR
      CELLM=CELLM+AIRM
      BACK=4.23566*BACKP+0.00997
      IF(BACKP.EQ.0.0) BACK=0.0
      BACKM=BACK*0.070307
      PORE=3.63158*POREP-0.01695
      IF(POREP.EQ.0.0) PORE=0.0
      POREM=PORE*0.070307
      IF(POREP.EQ.0.0) PORE=0.0
      POREM=PORE*0.070307
      IF(CELL.EQ.0.0.AND.BACK.EQ.0.0.AND.AIR.EQ.0.0.AND.PORE.EQ.0.0) GO
     1       TO 116
      WRITE(6,16) CELL,BACK,AIR,PORE
   16 FORMAT(19X,'PRESSURES IN PSI     ',4F8.3)
      WRITE(6,17) CELLM,BACKM,AIRM,POREM
   17 FORMAT(15X,'PRESSURES IN KG/SQ.CM.  ',4F8.3)
      IL=IL+2
      IF(CELL.EQ.0.0.AND.BACK.EQ.0.0.AND.AIR.EQ.0.0) GO TO 116
      IF(AIR.EQ.0.0) GO TO 1118
      BISH=CELL-AIR
      BISHM=CELLM-AIRM
      GO TO 1117
 1118 BISH=0.0
      BISHM=0.0
 1117 IF(BACK.EQ.0.0.AND.PORE.EQ.0.0) GO TO 116
      EFFECT=CELL-BACK
      IF(BACK.EQ.0.0.AND.PORE.GT.0.0) EFFECT=CELL-PORE
      EFFECM=CELLM-BACKM
      IF(BACKM.EQ.0.0.AND.POREM.GT.0.0) EFFECM=CELLM-POREM
      IF(AIR.LT.BACK) AIR=BACK
      SUCT=AIR-BACK
      IF(AIRM.LT.BACKM) AIRM=BACKM
      SUCTM=AIRM-BACKM
      IF(EFFECT.LT.0.0) EFFECT=0.0
      IF(EFFECM.LT.0.0) EFFECM=0.0
      IF(SUCT.LT.0.0) SUCT=0.0
      IF(SUCTM.LT.0.0) SUCTM=0.0
      IF(BISH.LT.0.0) BISH=0.0
      IF(BISHM.LT.0.0) BISHM=0.0
      WRITE(6,603) EFFECT,EFFECM,SUCT,SUCTM,BISH,BISHM
  603 FORMAT(1X,'(SIGMA-UW)=',F8.3,' PSI OR',F8.4,' K/CM', 3X,'(UA-UW)='
     1,F8.3,' PSI OR',F8.4,' K/CM', 3X,'(SIGMA-UA)=',F8.3,' PSI OR',F8.4
```

```
     2,' K/CM')
      IL=IL+1
116  RETURN
     END
```

D-5 Description of Input Data

The input data cards have the same format apart from the first three cards of the test. The data for the first three cards is derived from the "SETUP AND DISMANTLING OF SAMPLE" form. The remaining data is tabulated on large, versatile data sheets prepared on the computer. Keypunch operators punch the data onto cards.

The first card of any test is called the HEADING card and is filled in as follows:

COLUMNS	ITEM	FORMAT
1-20	Project Number	A
21-30	Sample Number	A
31-40	Apparatus Number	A

The second card of any test is called the DESCRIPTION OF SAMPLE CARD. The entire 80 columns can be filled with information about the sample (A-Format).

The third card of any test is called the INITIAL VOLUME-WEIGHT DATA card and is filled in as follows:

COLUMNS	ITEM	FORMAT
1-10	Initial Sample Diameter (cm)	F10.0
11-20	Initial Sample Height (cm)	F10.0
21-30	Specific Gravity of Solids	F10.0
31-40	Weight of Soil Solids (gms)	F10.0
41-50	Initial Water Content (%)	F10.0

Figure D.2 shows a typical "Setup and Dismantling of Sample" data sheet from which the information for the first three cards is extracted.

The remaining cards are considered as GENERAL DATA cards. However, a comment card can be inserted anywhere in the deck by first inserting a card with a nine in column 1. Also, a blank card will STØP the execution of the program.

The GENERAL DATA cards are essentially the same for all test apparatus. The only portions of the card that differ relate to the measurement of the total sample volume change and the diffused air volume readings. The GENERAL DATA cards for Triaxial Apparatus No. 2 are filled out as follows:

COLUMN	ITEM	FORMAT
1	IQ1	I1
2-3	MØNTH	I2
4-5	DAY	I2
6-7	HØUR	I2
8-9	MINUTE	I2
10-11	SECOND	I2
12-17	CELL Pressure (mv)	F6.2
18-23	Water Back Pressure on Board (mv)	F6.2
24-29	Air Pressure (mv)	F6.2
30-35	Water Pressure on cell (mv)	F6.2

VOLUME CHANGE TEST

(UNSATURATED SOIL)

☐ ONE-DIMENSIONAL ☐ FIXED RING ☑ TRIAXIAL
☐ FLOATING RING

SET UP AND DISMANTLING OF SAMPLE

PROJECT Null Test (20) SAMPLE #27 (30) APPARATUS NO. 2 (40)

DESCRIPTION OF SAMPLE Pure Kaolin prepared at ½ compactive effort (80)

DATE Feb. 29/72

AIR-ENTRY VALUE 5 Bar

INITIAL DIAMETER 10.16, _____, _____, _____ AVE. 10.16

INITIAL HEIGHT 6.370, 6.376, 6.375, _____ AVE. 6.374

SPECIFIC GRAVITY 2.616 ☐ FROM TEST ☑ ASSUMED

WATER CONTENTS

	START		END	
	TRIMMINGS	SAMPLE	SAMPLE	
CONTAINER NO.				
WT. CONTAINER + WET SOIL				
WT. CONTAINER + DRY SOIL				
WT. CONTAINER				
WEIGHT OF WATER				
WEIGHT OF DRY SOIL				
WATER CONTENT	35.19	35.15	34.13	

DIA_o 10.16 (10) HT_o 6.374 (20) G_s 2.616 (30) W_s 634.99 (40) W/C 35.15 (50)

FINAL DIAMETER 10.085, 10.020, 10.035, _____ AVE. 10.047

FINAL HEIGHT 6.291, 6.296, 6.297, _____ AVE. 6.293

REMARKS Sample #27 taken down on Mar. 7/72. New Membrane Installed and tested as Sample #29. Later tested as sample #31 with a composite membrane. Test ended on April 5/72

FIGURE D.2 TYPICAL "SETUP AND DISMANTLING OF SAMPLE" DATA SHEET

COLUMN	ITEM	FORMAT
36-41	Water Volume Change Indicator (cc)	F6.2
42	IQ2	I2
43	IQ3	I2
44-49	Lateral Strain Indicator (volts)	F6.3
50-55	Lateral Indicator Correction (volts)	F6.3
56-61	Vertical Strain Indicator (volts)	F6.3
62-67	Vertical Indicator Correction (volts)	F6.3
68-73	Diffused Air Volume Indicator (cc)	F6.3
74-79	Back Pressure Applied to Air Indicator (mv)	F6.3

The coding forms (Figures D.3, D.4 and D.5) also show the input data format for Triaxial Apparatus No. 2, Triaxial Apparatus No. 1 and the Oedometer Apparatus, respectively. Figure D.6 shows the listing for the program that writes out the data sheets for Triaxial Apparatus No. 2. The decimal points for each real number are generally keypunched. Therefore, the number in each "box" is started in the column designated at the top of the coding sheets.

Figure D.7 shows the manner in which the data was filled in at the start of testing Sample No. 27. The manner of completing the data sheet for several special cases is shown in Figure D.8. In the first case, the line with the final diffused air volume reading must

PAGE NO. _____

TRIAXIAL TEST

PROJECT _____(20) SAMPLE _____(30) APPARATUS _____(40)

10 11	TIME				BOARD TRANSDUCER			CELL	BURET	1	1	LVDT READINGS				DIFFUSE	REG.
	MON	DATE	HRS	MIN	SEC	CELL PRESS	WATER PRESS	AIR PRESS	PORE PRESS	READ-G (CC)	0 2	0 3	LAT.	CORR-N	CAP	CORR-N	AIR VOL.	PRESS.
1 2	4	6	8	10	12	18	24	30	36	42 43	44	50	56	62	68	74		

FIGURE D.3 CODING FORM FOR TRIAXIAL APPARATUS NO. 2

PAGE NO. _____

TRIAXIAL TEST

PROJECT _____(20) SAMPLE _____(30) APPARATUS _____(40)

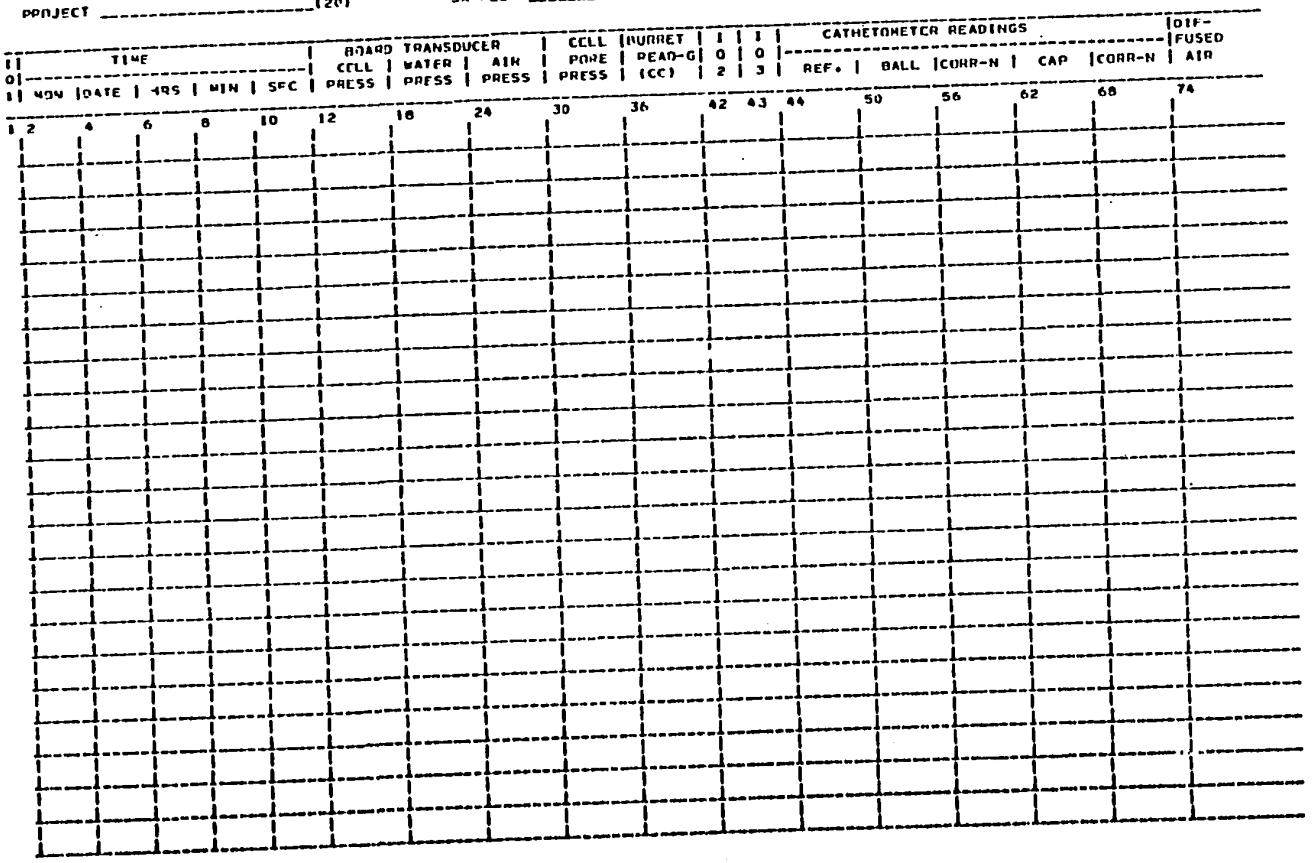


FIGURE D.4 CODING FORM FOR TRIAXIAL APPARATUS NO. 1

PAGE NO. _____

ONE-DIMENSIONAL TEST

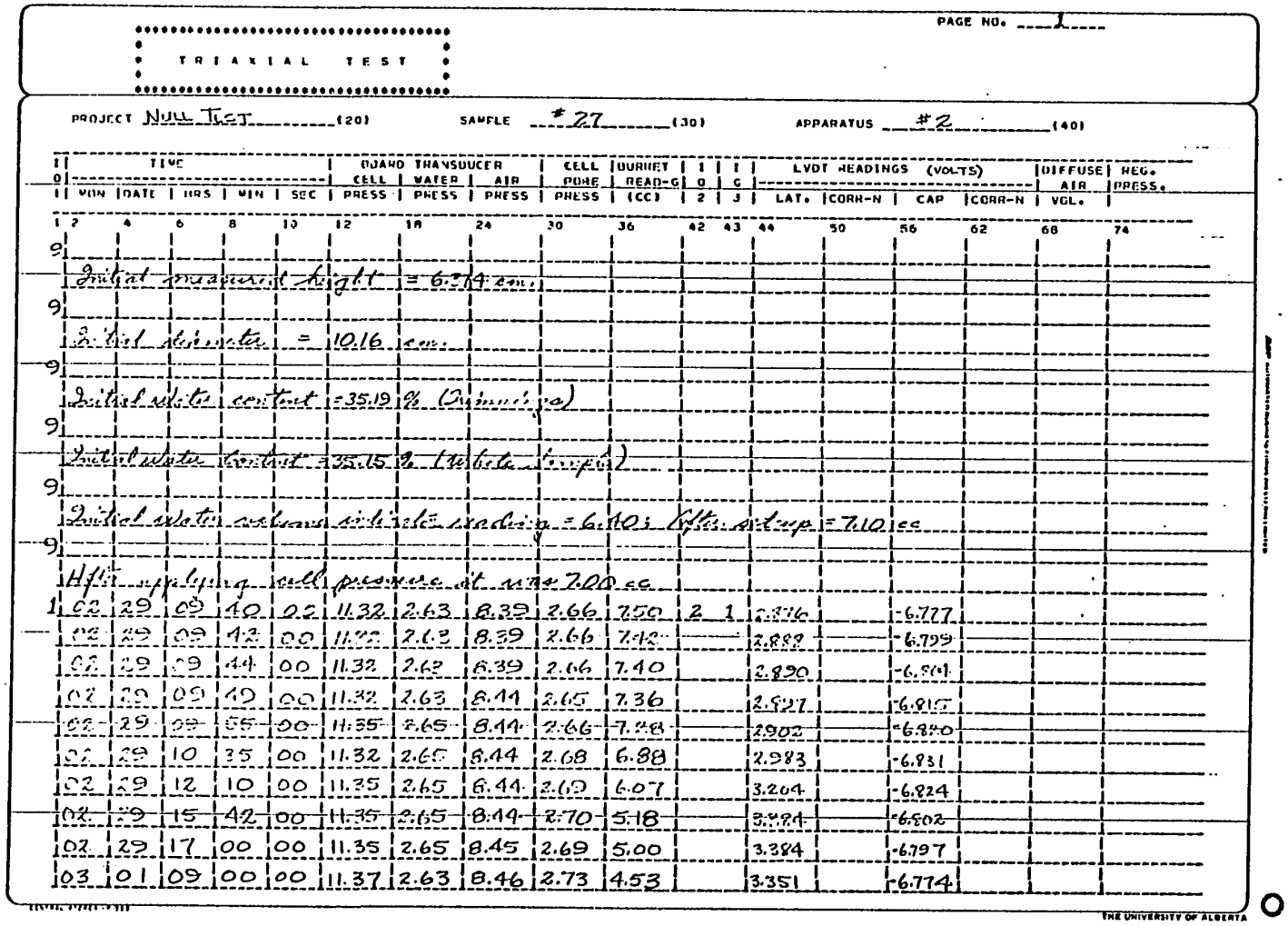
PROJECT _____(20) SAMPLE _____(30) CONSOLIDOMETER _____(40)

I O	TIME				BOARD TRANSDUCER			CELL PORE PRESS	BURRET PEAD-G (CC)	I O 2	I O 3	DIAL GAUGE		DIFFUSED AIR		
	MON	DATE	HRS	MIN	SEC	CELL PRESS	WATER PRESS	AIR PRESS				CAP	CORR-N	DIF-O	DIF-F	PRESS
1	2	4	6	8	10	12	18	24	30	36	42	43	44	50	56	61	67	74

FIGURE D.5 CODING FORM FOR MODIFIED ANTEUS OEDOMETER

```
C
C     ************************************************************************
C     PROGRAM TO WRITE DATA SHEETS FOR TRIAXIAL APPARATUS NO. 2
C     ************************************************************************
C
      DO 100 N=1,3
      WRITE(6,1)
    1 FORMAT(1H1,100X,'PAGE NO. _____',/10X,'**********************
     1**************',/10X,'*',34X,'*',/10X,'*    T R I A X I A L    T E
     2 S T    *',/10X,'*',34X,'*',/10X,'*********************************
     3****',//3X,'PROJECT _____(20)',10X,'SAMPLE  _____
     4_____(30)', 10X,'APPARATUS _____(40)',/)
      WRITE(6,2)
    2 FORMAT (1X,'_____
     1_____
     3_____')
      WRITE(6,3)
    3 FORMAT(1X,'I|',9X,'TIME',16X,'|   BOARD TRANSDUCER     '
     1,'|  CELL |BURRET | I | I |    LVDT READINGS                |DIFFUSE
     2| REG.'/
     1  'Q|-----------------------------|  CELL | WATER |  AIR  |  PORE
     3| READ-G| Q | Q |-------------------------------|  AIR  |PRESS.'/
     41X,'I| MON |DATE | HRS | MIN | SEC | PRESS | PRESS | PRESS | PRESS
     5 | (CC)  | 2 | 3 |  LAT. |CORR-N |  CAP  |CORR-N | VOL.  | '/
     7  1X,'_____
     8_____
     9___')
      WRITE(6,67)
   67 FORMAT(1X,'1 2      4      6      8      10     12       18       24
     1 30       36       42  43  44       50       56       62       68       7
     24')
      DO 200 I=1,22
      DO 206 NN=1,2
  206 WRITE(6,4)
    4 FORMAT(2X,'|',5X,'|',5X,'|',5X,'|',5X,'|',5X,'|',5X,'|',11('       |'))
  200 WRITE(6,26)
   26 FORMAT (1H+,1X,'_____
     1_____
     3_____')
  100 CONTINUE
      STOP
      END
```

FIGURE D.6 LISTING FOR PROGRAM TO WRITE OUT DATA SHEETS FOR TRIAXIAL APPARATUS NO. 2



TRIAXIAL TEST

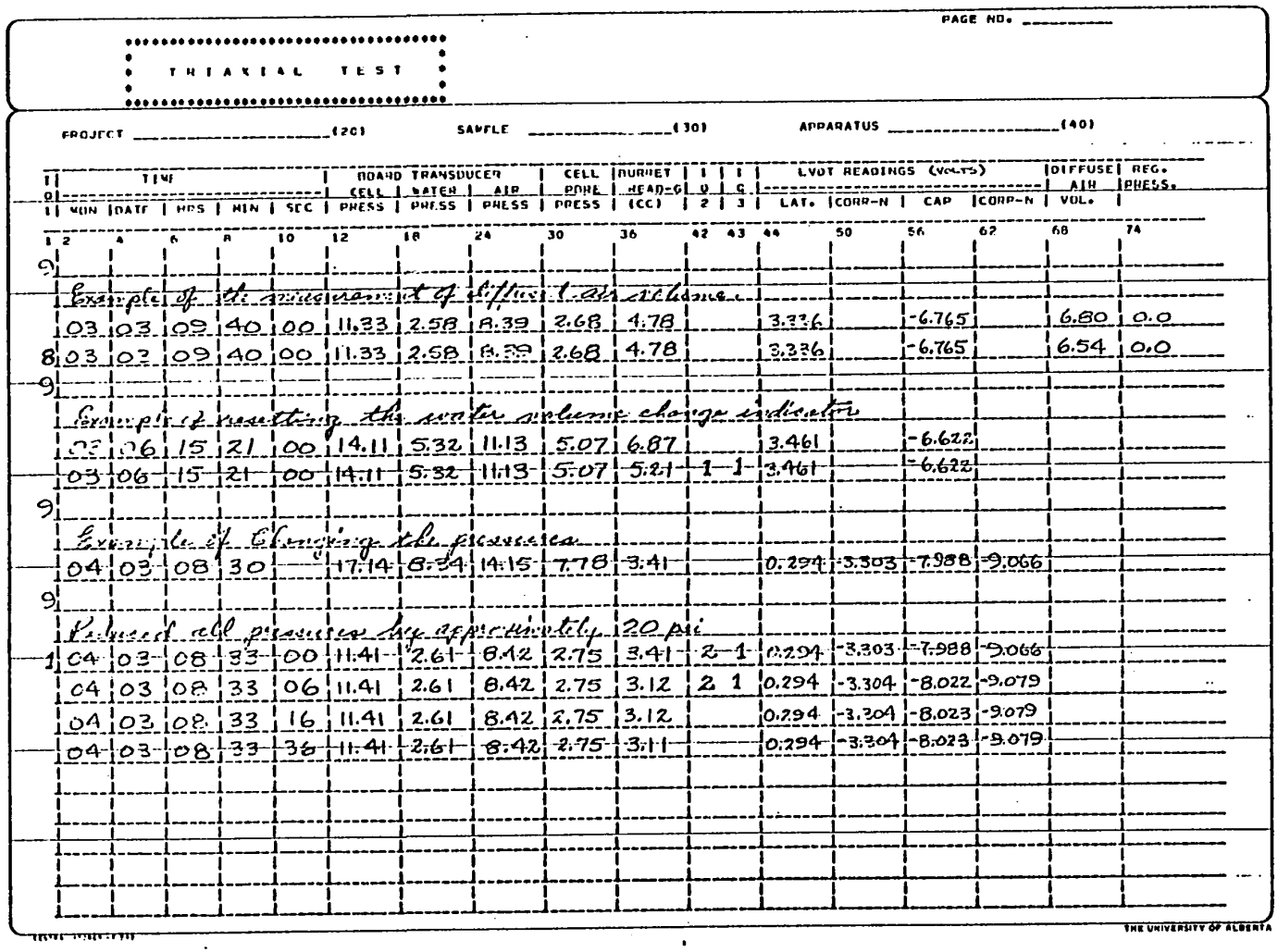
PAGE NO. 1

PROJECT Null Test (20) SAMPLE #27 (30) APPARATUS #2 (40)

IO	TIME					GUARD TRANSDUCER			CELL	BURRET	I	I	LVDT HEADINGS (VOLTS)				DIFFUSE	REG.
	MON	DATE	HRS	MIN	SEC	CELL PRESS	WATER PRESS	AIR PRESS	PORE PRESS	READ-G (CC)	Q 2	G 3	LAT.	CORR-N	CAP	CORR-N	AIR VOL.	PRESS.
1	2	4	6	8	10	12	18	24	30	36	42	43	44	50	56	62	68	74
9	Initial mean specimen height = 6.314 cm.																	
9	Initial diameter = 10.16 cm.																	
9	Initial water content = 35.19 % (Quinn's no)																	
9	Initial water content = 35.15 % (Roberts Temp.)																	
9	Initial water volume burette reading = 6.403 Lytic Actuator = 7.10 cc																	
9	Hydraulic applying cell pressure at min = 200 cc																	
1	02	29	09	40	02	11.32	2.63	8.39	2.66	7.50	2	1	2.876		-6.777			
	02	29	09	42	00	11.32	2.63	8.39	2.66	7.42			2.889		-6.799			
	02	29	09	44	00	11.32	2.62	8.39	2.66	7.40			2.890		-6.801			
	02	29	09	49	00	11.32	2.63	8.41	2.65	7.36			2.927		-6.815			
	02	29	09	55	00	11.35	2.65	8.44	2.66	7.28			2.902		-6.820			
	02	29	10	35	00	11.32	2.65	8.44	2.68	6.88			2.983		-6.931			
	02	29	12	10	00	11.35	2.65	8.44	2.69	6.07			3.204		-6.824			
	02	29	15	42	00	11.35	2.65	8.44	2.70	5.18			3.384		-6.802			
	02	29	17	00	00	11.35	2.65	8.45	2.69	5.00			3.384		-6.797			
	03	01	09	00	00	11.37	2.63	8.46	2.73	4.53			3.351		-6.774			

THE UNIVERSITY OF ALBERTA

FIGURE D.7 DATA AT THE START OF SAMPLE NO. 27



PAGE NO. _____

TRIAXIAL TEST

PROJECT _____ (20) SAMPLE _____ (30) APPARATUS _____ (40)

ID	TIME				BOARD TRANSDUCER			CELL PORE	BURRET HEAD-G	I	I	LVDT READINGS (VOLTS)				DIFFUSE	REG.
	MON	DATE	HRS	MIN	SEC	CELL PRESS	WATER PRESS	AIR PRESS	PRESS	(CC)	2	3	LAT.	CORR-N	CAP	CORR-N	AIR VOL.	PRESS.
1 2		4	6	8	10	12	18	24	30	36	42	43	44	50	56	62	68	74
9																		
	Example of the measurement of effective cell volume.																	
	03	03	09	40	00	11.33	2.58	8.39	2.68	4.78			3.336		-6.765		6.80	0.0
8	03	03	09	40	00	11.33	2.58	8.39	2.68	4.78			3.336		-6.765		6.54	0.0
9																		
	Example of reading the water volume change indicator																	
	03	06	15	21	00	14.11	5.32	11.13	5.07	6.87			3.461		-6.622			
	03	06	15	21	00	14.11	5.32	11.13	5.07	5.21	1	1	3.461		-6.622			
9																		
	Example of changing the pressures																	
	04	03	08	30	00	17.14	8.34	14.15	7.78	3.41			0.294	-3.303	-7.988	-9.066		
9																		
	Reduced all pressures by approximately 20 psi																	
1	04	03	08	33	00	11.41	2.61	8.42	2.75	3.41	2	1	0.294	-3.303	-7.988	-9.066		
	04	03	08	33	06	11.41	2.61	8.42	2.75	3.12	2	1	0.294	-3.304	-8.022	-9.079		
	04	03	08	33	16	11.41	2.61	8.42	2.75	3.12			0.294	-3.304	-8.023	-9.079		
	04	03	08	33	36	11.41	2.61	8.42	2.75	3.11			0.294	-3.304	-8.023	-9.079		

THE UNIVERSITY OF ALBERTA

FIGURE D.8 MANNER OF COMPLETING DATA SHEET FOR SPECIAL CASES

be preceeded by the integer 8. The remaining data on the card is the same as the previous card containing the initial diffused air volume reading. The use of two data cards to record the diffused air volumes, is not necessary for the Oedometer tests.

In the second case, the level of the water-kerosene interface is changed and a new zero reading is established. Column 42 designates the direction of water flow with respect to the sample. Column 43 informs the computer to use the burret reading as the new starting value for water volume change computations. The remainder of the data card remains the same as the previous card.

In the third case, the starting values for a new set of applied pressures are put equal to the last set of readings from the previous set of pressures. A 1 is placed in column 1 and the IQ2 and IQ3 questions are answered appropriately. The sample volume corrections for the zero elapsed time (local) are the same as for the final readings at the previous pressures. The new corrections are applied for the 6 second reading. Also, the effect of instantaneous compression of the fluid in the base can be compensated for by repeating the IQ2 and IQ3 values at the 6 second burret reading.

Every data card must have a time associated with each set of readings. The absence of time values sends the execution to STØP. Essentially all other variables on the card can be considered as optional.

D-6 Description of Output

A detailed analysis and printout is performed on each data card. In most cases, the detailed information is not required. However, for research purposes the complete analysis proved useful.

The first sheet of output for each test (Figure D.9) contains the interpretation of the questions (i.e. IQ1, IQ2, and IQ3), the sign convention for deformations and the input initial volume-weight properties. Comment cards are written out whenever encountered in the data.

Figure D.10 shows a typical sheet of output where a correction for volume of diffused air has been applied.

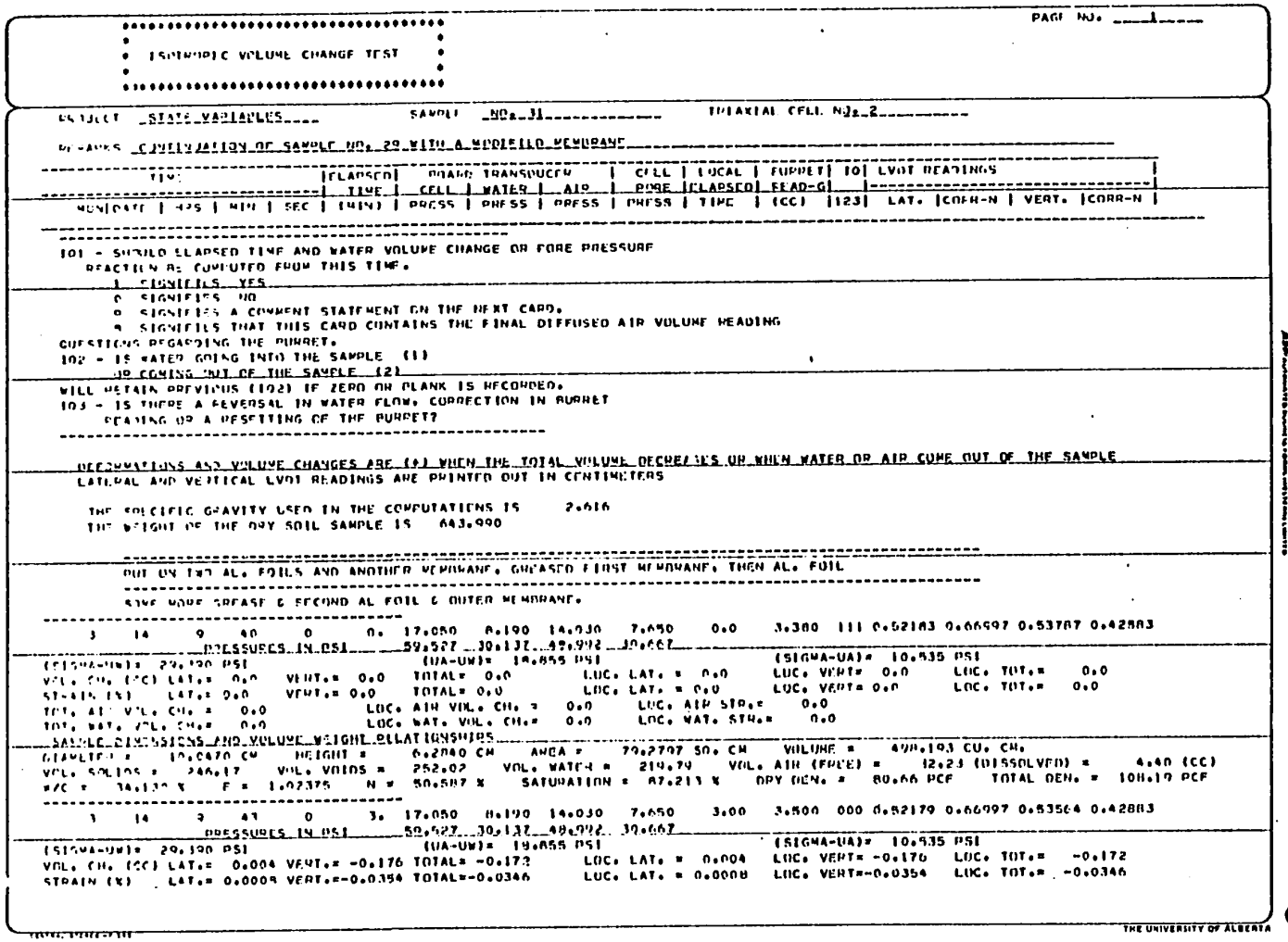
On the final sheet of output, (Figure D.11) the final water content and volume measurements along with the transducer calibrations are inserted as comment cards.

D-7 Sample Calculations

The format for calculations can generally be deciphered by examining the computer program. This section contains some amplification of the total volume computations and the water volume computations.

The total volume of the sample is computed from the initial volume and the measured volume changes. On Triaxial Apparatus No. 2, the lateral LVDT measures a change in diameter and the vertical LVDT measures the change in height. Corrections for compressibility are applied to both readings.

The lateral displacement reading at any time (volts) is first



```
                                                                    PAGE NO. ____1_____

        ISOTROPIC VOLUME CHANGE TEST

PROJECT _STATE VARIABLES____        SAMPLE _NO.31_____        TRIAXIAL CELL NO.2_____

REMARKS CONSOLIDATION OF SAMPLE NO. 29 WITH A MODIFIED MEMBRANE

          TIME          |ELAPSED|   BOARD TRANSDUCER    | CELL | LOCAL | PUPPET| IO| LVDT READINGS
                        |  TIME | CELL | WATER |  AIR  | PORE |ELAPSED| READ-G|   |-----------------------|
 RUN|DATE | HRS | MIN | SEC | (MIN) | PRESS | PRESS | PRESS | PRESS | TIME  | (CC)  |123| LAT. |CORR-N | VERT. |CORR-N |

 101 - SHOULD ELAPSED TIME AND WATER VOLUME CHANGE OR PORE PRESSURE
    REACTION BE COMPUTED FROM THIS TIME.
       1  SIGNIFIES YES
       0  SIGNIFIES NO
       0  SIGNIFIES A COMMENT STATEMENT ON THE NEXT CARD.
       0  SIGNIFIES THAT THIS CARD CONTAINS THE FINAL DIFFUSED AIR VOLUME READING
 QUESTIONS REGARDING THE BURRET.
 102 - IS WATER GOING INTO THE SAMPLE  (1)
       OR COMING OUT OF THE SAMPLE  (2)
 WILL RETAIN PREVIOUS (102) IF ZERO OR BLANK IS RECORDED.
 103 - IS THERE A REVERSAL IN WATER FLOW, CORRECTION IN BURRET
       READING OR A RESETTING OF THE BURRET?

 DEFORMATIONS AND VOLUME CHANGES ARE (+) WHEN THE TOTAL VOLUME DECREASES OR WHEN WATER OR AIR COME OUT OF THE SAMPLE
 LATERAL AND VERTICAL LVDT READINGS ARE PRINTED OUT IN CENTIMETERS

   THE SPECIFIC GRAVITY USED IN THE COMPUTATIONS IS      2.616
   THE WEIGHT OF THE DRY SOIL SAMPLE IS    643.990

        PUT ON TWO AL. FOILS AND ANOTHER MEMBRANE, GREASED FIRST MEMBRANE, THEN AL. FOIL

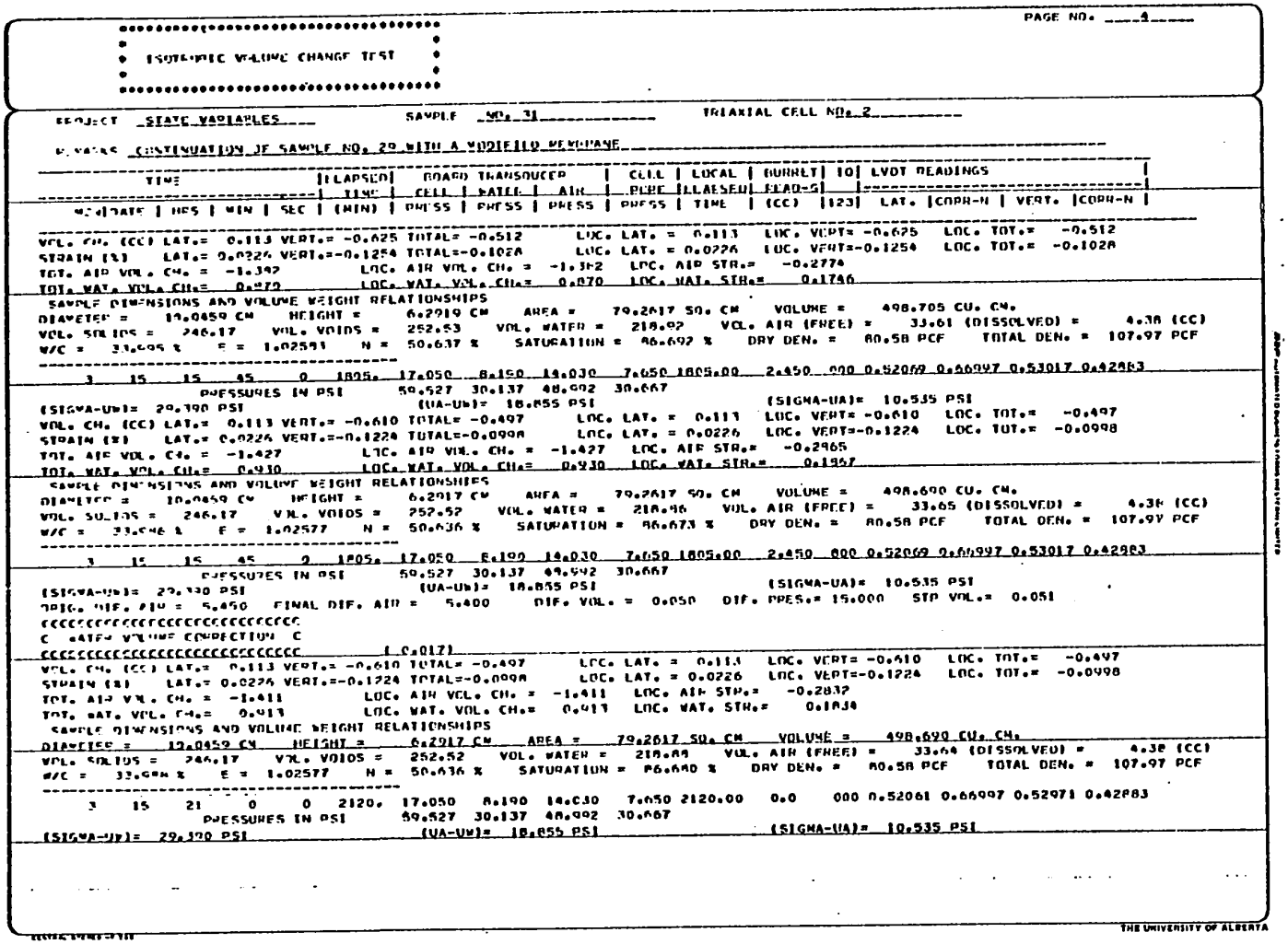
        GIVE MORE GREASE & SECOND AL FOIL & OUTER MEMBRANE.

   3    14     9     40     0      0.   17.050   8.190  14.030   7.650    0.0    3.380  111 0.62183 0.66997 0.53787 0.42883
                  PRESSURES IN PSI       59.527  30.137  49.092  30.667
 (SIGMA-UW)= 29.390 PSI                (UA-UW)= 19.855 PSI                (SIGMA-UA)= 10.535 PSI
 VOL. CH. (CC) LAT.=  0.0   VERT.=  0.0   TOTAL=  0.0      LOC. LAT. =  0.0    LOC. VERT=  0.0    LOC. TOT.=   0.0
 STRAIN (%)    LAT.= 0.0     VERT.= 0.0    TOTAL= 0.0      LOC. LAT. = 0.0     LOC. VERT= 0.0     LOC. TOT.=   0.0
 TOT. AIR VOL. CH. =   0.0          LOC. AIR VOL. CH. =   0.0     LOC. AIR STR.=    0.0
 TOT. WAT. VOL. CH.=   0.0          LOC. WAT. VOL. CH.=   0.0     LOC. WAT. STR.=   0.0
 SAMPLE DIMENSIONS AND VOLUME WEIGHT RELATIONSHIPS
 DIAMETER =   10.0470 CM    HEIGHT =    6.2040 CM    AREA =   79.2707 SQ. CM    VOLUME =   491.793 CU. CM.
 VOL. SOLIDS =   246.17    VOL. VOIDS =   252.02    VOL. WATER =   219.79    VOL. AIR (FREE) =    12.23 (DISSOLVED) =    4.40 (CC)
 W/C =  34.130 %    F =  1.02375    N =  50.587 %    SATURATION =  87.213 %    DRY DEN. =   80.66 PCF    TOTAL DEN. =  108.19 PCF

   3    14     9     43     0      3.   17.050   8.190  14.030   7.650   3.00    3.500  000 0.62179 0.66997 0.53564 0.42883
                  PRESSURES IN PSI       59.527  30.137  49.092  30.667
 (SIGMA-UW)= 29.390 PSI                (UA-UW)= 19.855 PSI                (SIGMA-UA)= 10.535 PSI
 VOL. CH. (CC) LAT.=  0.004 VERT.= -0.176 TOTAL= -0.172     LOC. LAT. =  0.004   LOC. VERT= -0.170   LOC. TOT.=  -0.172
 STRAIN (%)    LAT.= 0.0009 VERT.=-0.0354 TOTAL=-0.0346     LOC. LAT. = 0.0008   LOC. VERT=-0.0354   LOC. TOT.= -0.0346

                                                                    THE UNIVERSITY OF ALBERTA
```

FIGURE D.9 FIRST SHEET OF COMPUTER OUTPUT FOR SAMPLE NO. 31



```
                                                                    PAGE NO. ____4_____

        ISOTROPIC VOLUME CHANGE TEST

PROJECT  STATE VARIABLES          SAMPLE  NO. 3              TRIAXIAL CELL NO. 2

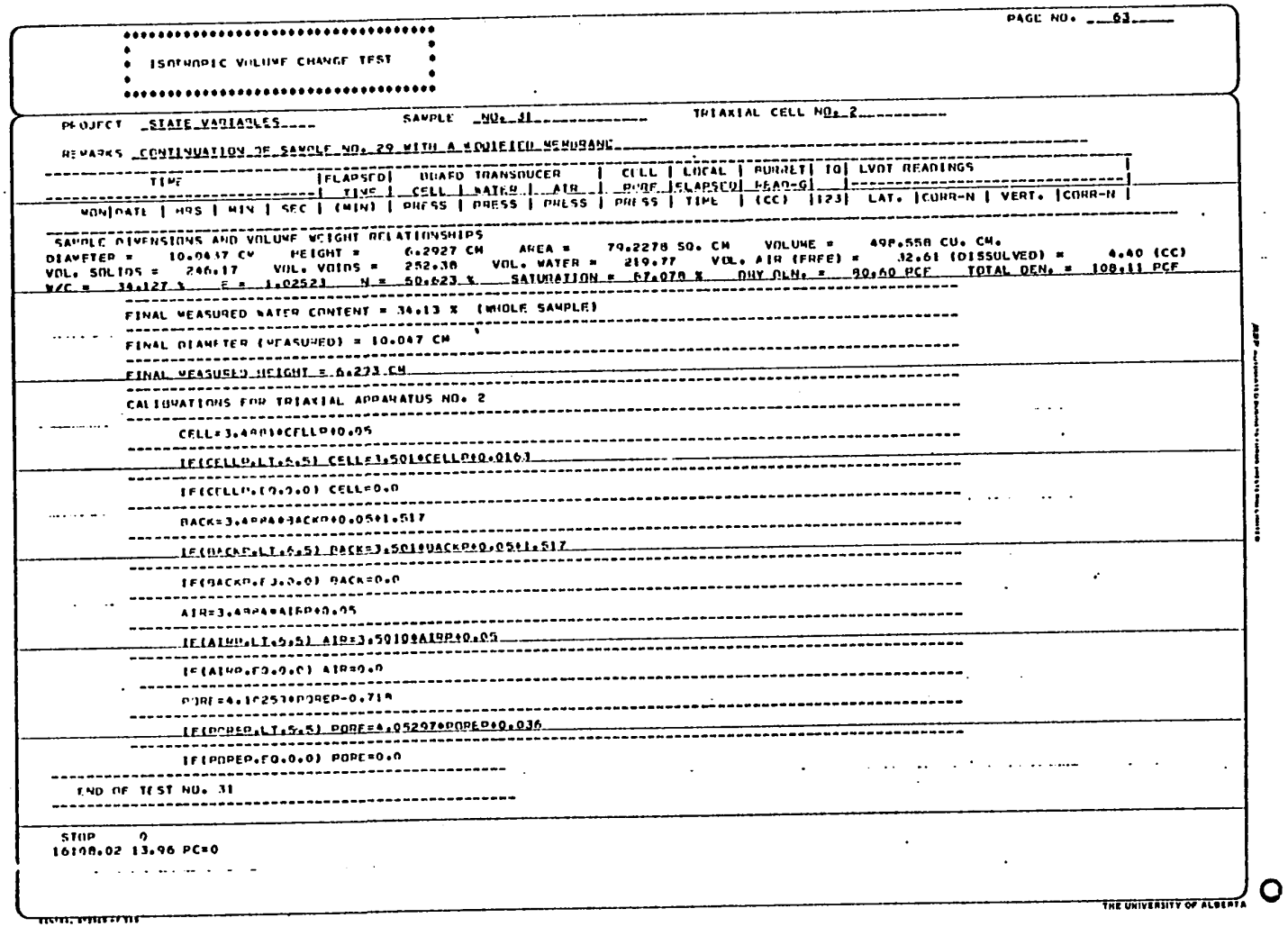
REMARKS  CONTINUATION OF SAMPLE NO. 29 WITH A MODIFIED MEMBRANE

|          TIME                |ELAPSED|   BOARD TRANSDUCER    |  CELL | LOCAL | BURRET| IO| LVDT READINGS                  |
|------------------------------| TIME  | CELL | WATER |  AIR  | PORE |ELAPSED| READ-G|   |--------------------------------|
| MO|DATE | HRS | MIN | SEC | (MIN) | PRESS | PRESS | PRESS | PRESS | TIME  | (CC)  |123| LAT. |CORR-N | VERT. |CORR-N |

VOL. CH. (CC) LAT.=  0.113 VERT.= -0.625 TOTAL= -0.512      LOC. LAT. =  0.113   LOC. VERT= -0.625   LOC. TOT.=   -0.512
STRAIN (%)    LAT.= 0.0226 VERT.=-0.1254 TOTAL=-0.1028      LOC. LAT. = 0.0226   LOC. VERT=-0.1254   LOC. TOT.=  -0.1028
TOT. AIR VOL. CH. =  -1.342          LOC. AIR VOL. CH. =  -1.342   LOC. AIR STR.=    -0.2774
TOT. WAT. VOL. CH.=   0.870          LOC. WAT. VOL. CH.=   0.870   LOC. WAT. STR.=    0.1796
 SAMPLE DIMENSIONS AND VOLUME WEIGHT RELATIONSHIPS
DIAMETER =   10.0459 CM    HEIGHT =    6.2919 CM    AREA =   79.2617 SQ. CM    VOLUME =   498.705 CU. CM.
VOL. SOLIDS =   246.17    VOL. VOIDS =   252.53    VOL. WATER =   218.92    VOL. AIR (FREE) =    33.61 (DISSOLVED) =    4.38 (CC)
W/C =   33.695 %    E =  1.02591    N =  50.637 %    SATURATION =  86.692 %    DRY DEN. =   80.58 PCF    TOTAL DEN. =  107.97 PCF
-----------------------------------
    3   15   15   45    0  1805.  17.050   8.190  14.030   7.650 1805.00   2.450   000 0.52069 0.66997 0.53017 0.42883
              PRESSURES IN PSI      59.527  30.137  48.992  30.667
(SIGMA-UW)=  29.390 PSI                (UA-UW)=  18.855 PSI                (SIGMA-UA)=  10.535 PSI
VOL. CH. (CC) LAT.=  0.113 VERT.= -0.610 TOTAL= -0.497      LOC. LAT. =  0.113   LOC. VERT= -0.610   LOC. TOT.=   -0.497
STRAIN (%)    LAT.= 0.0226 VERT.=-0.1220 TOTAL=-0.0998      LOC. LAT. = 0.0226   LOC. VERT=-0.1220   LOC. TOT.=  -0.0998
TOT. AIR VOL. CH. =  -1.427          LOC. AIR VOL. CH. =  -1.427   LOC. AIR STR.=    -0.2965
TOT. WAT. VOL. CH.=   0.930          LOC. WAT. VOL. CH.=   0.930   LOC. WAT. STR.=    0.1967
 SAMPLE DIMENSIONS AND VOLUME WEIGHT RELATIONSHIPS
DIAMETER =   10.0459 CM    HEIGHT =    6.2917 CM    AREA =   79.2617 SQ. CM    VOLUME =   498.690 CU. CM.
VOL. SOLIDS =   246.17    VOL. VOIDS =   252.52    VOL. WATER =   218.98    VOL. AIR (FREE) =    33.65 (DISSOLVED) =    4.38 (CC)
W/C =   33.696 %    E =  1.02577    N =  50.636 %    SATURATION =  86.673 %    DRY DEN. =   80.58 PCF    TOTAL DEN. =  107.97 PCF
-----------------------------------
    3   15   15   45    0  1805.  17.050   8.190  14.030   7.650 1805.00   2.450   000 0.52069 0.66997 0.53017 0.42883
              PRESSURES IN PSI      59.527  30.137  48.992  30.667
(SIGMA-UW)=  29.390 PSI                (UA-UW)=  18.855 PSI                (SIGMA-UA)=  10.535 PSI
TRIG. DIF. AIR =   5.450   FINAL DIF. AIR =   5.400    DIF. VOL. =  0.050   DIF. PRES.=  15.000   STP VOL.=   0.051
CCCCCCCCCCCCCCCCCCCCCCCCCCCCCC
C  WATER VOLUME CORRECTION  C
CCCCCCCCCCCCCCCCCCCCCCCCCCCCCC          ( 0.017)
VOL. CH. (CC) LAT.=  0.113 VERT.= -0.610 TOTAL= -0.497      LOC. LAT. =  0.113   LOC. VERT= -0.610   LOC. TOT.=   -0.497
STRAIN (%)    LAT.= 0.0226 VERT.=-0.1224 TOTAL=-0.0998      LOC. LAT. = 0.0226   LOC. VERT=-0.1224   LOC. TOT.=  -0.0998
TOT. AIR VOL. CH. =  -1.411          LOC. AIR VOL. CH. =  -1.411   LOC. AIR STR.=    -0.2832
TOT. WAT. VOL. CH.=   0.913          LOC. WAT. VOL. CH.=   0.913   LOC. WAT. STR.=    0.1830
 SAMPLE DIMENSIONS AND VOLUME WEIGHT RELATIONSHIPS
DIAMETER =   10.0459 CM    HEIGHT =    6.2917 CM    AREA =   79.2617 SQ. CM    VOLUME =   498.690 CU. CM.
VOL. SOLIDS =   246.17    VOL. VOIDS =   252.52    VOL. WATER =   218.98    VOL. AIR (FREE) =    33.64 (DISSOLVED) =    4.38 (CC)
W/C =   33.696 %    E =  1.02577    N =  50.636 %    SATURATION =  86.680 %    DRY DEN. =   80.58 PCF    TOTAL DEN. =  107.97 PCF
-----------------------------------
    3   15   21    0    0  2120.  17.050   8.190  14.030   7.650 2120.00   0.0     000 0.52061 0.66997 0.52971 0.42883
              PRESSURES IN PSI      59.527  30.137  48.992  30.667
(SIGMA-UW)=  29.390 PSI                (UA-UW)=  18.855 PSI                (SIGMA-UA)=  10.535 PSI

THE UNIVERSITY OF ALBERTA
```

FIGURE D.10 TYPICAL COMPUTER OUTPUT SHOWING DIFFUSED AIR VOLUME CORRECTIONS



PAGE NO. 63

ISOTROPIC VOLUME CHANGE TEST

PROJECT STATE VARIABLES SAMPLE NO. 31 TRIAXIAL CELL NO. 2

REMARKS CONTINUATION OF SAMPLE NO. 29 WITH A MODIFIED MEMBRANE

TIME			ELAPSED	BOARD TRANSDUCER			CELL	LOCAL	BURRET	IQ	LVDT READINGS			
MON	DATE	HRS	MIN	SEC	TIME (MIN)	CELL PRESS	WATER PRESS	AIR PRESS	PORE PRESS	ELAPSED TIME	HEAD-G (CC)	123	LAT.	CORR-N	VERT.	CORR-N

SAMPLE DIMENSIONS AND VOLUME WEIGHT RELATIONSHIPS

DIAMETER = 10.0047 CM HEIGHT = 6.2927 CM AREA = 79.2278 SQ. CM VOLUME = 498.558 CU. CM.

VOL. SOLIDS = 246.17 VOL. VOIDS = 252.38 VOL. WATER = 219.77 VOL. AIR (FREE) = 32.61 (DISSOLVED) = 4.40 (CC)

W/C = 34.127 % E = 1.02523 N = 50.623 % SATURATION = 87.070 % DRY DEN. = 90.60 PCF TOTAL DEN. = 108.11 PCF

FINAL MEASURED WATER CONTENT = 34.13 % (WHOLE SAMPLE)

FINAL DIAMETER (MEASURED) = 10.047 CM

FINAL MEASURED HEIGHT = 6.273 CM

CALIBRATIONS FOR TRIAXIAL APPARATUS NO. 2

```
      CELL=3.4881*CELLP+0.05
      IF(CELLP.LT.6.5) CELL=3.501*CELLP+0.0163
      IF(CELLP.EQ.0.0) CELL=0.0
      BACK=3.4884*BACKP+0.05+1.517
      IF(BACKP.LT.6.5) BACK=3.501*BACKP+0.05+1.517
      IF(BACKP.EQ.0.0) BACK=0.0
      AIR=3.4884*AIRP+0.05
      IF(AIRP.LT.6.5) AIR=3.5019*AIRP+0.05
      IF(AIRP.EQ.0.0) AIR=0.0
      PORE=4.1C253*POREP-0.718
      IF(POREP.LT.6.5) PORE=4.05297*POREP+0.036
      IF(POREP.EQ.0.0) PORE=0.0
```

END OF TEST NO. 31

```
STOP     0
16:08.02 13.96 PC=0
```

THE UNIVERSITY OF ALBERTA

FIGURE D.11 FINAL SHEET OF COMPUTER OUTPUT FOR SAMPLE NO. 31

converted to cm and then multiplied by the mechanical lever arm advantage (LATCAL). The change in diameter (DELDIA) is equal to:

(Original Lateral Displacement - Present Lateral Displacement) -
(Original Lateral Correction - Present Lateral Correction)

The present diameter (DIA1) is equal to the original diameter minus the change in diameter (DELDIA).

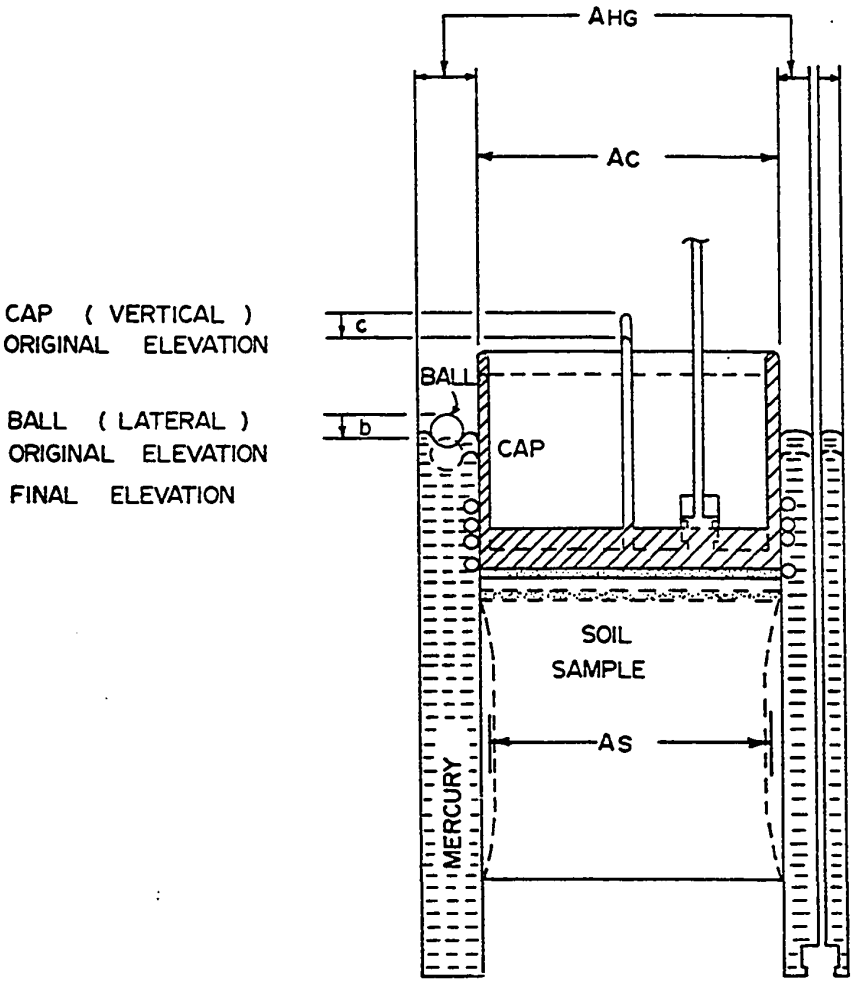
The change in height (VERT) is equal to:

((Original Vertical Displacement - Present Vertical Displacement)
(Original Vertical Correction - Present Vertical Correction))*(-1)

The present height (H) is equal to the original height (HO) minus the change in height (VERT).

On Triaxial Apparatus No. 1, the calculations of the total volume are more complex (Figure D.12). The change in volume of the sample can be envisaged as the total of the lateral and vertical volume changes. However, the cross sectional area at any time (A_s) is unknown. Therefore, the vertical movement of the mercury (b) can be considered as a net volume change with reference to the cross-sectional area of the mercury. Two calibration factors are required. The calibration factor relating the volume change to the vertical movement of the cap is 80.958 cc per cm. The calibration factor relating the vertical movement of the mercury surface to the volume change described by the mercury surface is 87.409 cc per cm.

$$A_{HG} \cdot b = A_C \cdot c - \text{Change in Sample Volume (TVOL)} \qquad D.1$$



A_s – AVERAGE CROSS – SECTIONAL AREA OF SOIL SAMPLE

A_c – CROSS – SECTIONAL AREA OF LOADING CAP

A_{HG} – CROSS – SECTIONAL AREA OF THE MERCURY

FIGURE D. 12 VERTICAL AND LATERAL VOLUME CHANGE COMPUTATIONS FOR TRIAXIAL APPARATUS NO. 1

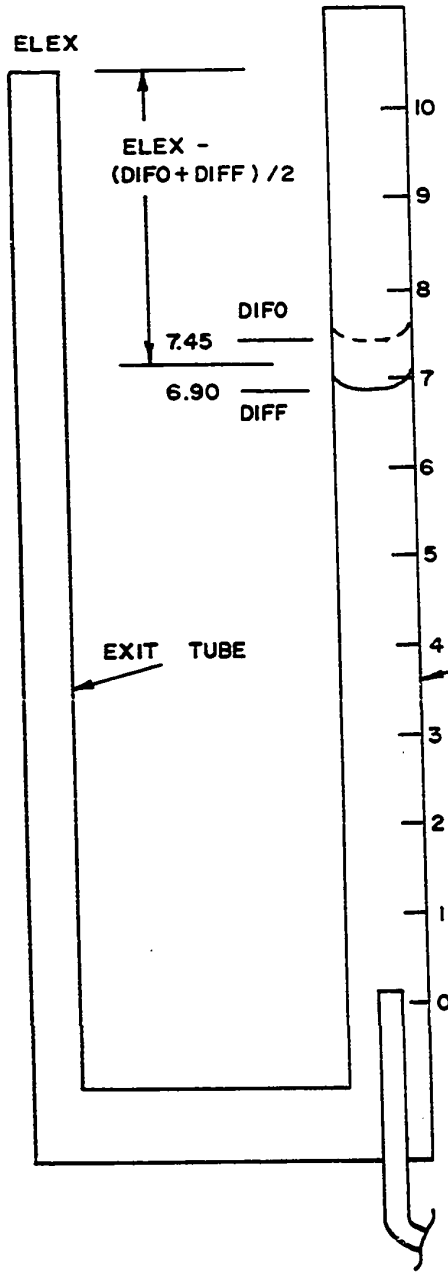
or $$TV\emptyset L = A_C \cdot c - A_{HG} \cdot b \qquad D.2$$

The present volume of the sample (V) is equal to the original volume (VØ) minus the change in volume (TVØL). The present height (H) is equal to the original height (HØ) minus the change in height (VERT). The present cross-sectional area (AREA1) is equal to the volume divided by the height. Now the present diameter can also be computed.

In the oedometer test, the lateral volume change is zero and the total volume change is computed from the vertical movement of the load cap.

The water volume change was computed in the same manner for all apparatus. In the program, water flowing into the sample is designated as negative and vice versa. On the data sheet, water flowing into the sample was designated as a 1 for IQ2. A 1 in answer to IQ3 designates a new starting point for computing the water volume change. The volume changes from the intermediate starting points are added together and designated as the subscripted variable SVØLW. The sum of the water volume changes from the last pressure change is SVWAT and from the start of the test is SWAT.

The determination of the correction for the diffused air depends on a precise evaluation of pressure. The pressure on the diffused air in the indicator is equal to the applied back pressure plus the head difference between the exit tube and the air-water interface. Figure D.13 shows the detailed calculation of the air pressure



$$\text{CALIB} = \frac{\text{LENGTH OF BURRET}}{\text{NUMBER OF CC'S}}$$

AIR BACKPRESSURE TO INDICATOR

ATM = DIFRR + 14.7

HEAD ON AIR IN TUBE IN CM OF WATER

EXHEAD = (ELEX-(DIFO + DIFF) /2)* CALIB

THE AIR VOLUME CHANGE IN INDICATOR

ADIF = DIFO − DIFF

THE CORRESPONDING CHANGE IN THE BASE OF THE CELL

ADIFF = (ADIF * EXHEAD * CONVER + ATM) / (PORE + 14.7)

WHERE CONVER = CONVERSION OF CM OF WATER TO PSI

FIGURE D.13 COMPUTATIONS FOR THE DIFFUSED AIR VOLUME CORRECTION

and volume. The volume of diffused air (ADIF) is reduced to an equivalent volume in the base of the cell (ADIFF) by means of the gas law.

The diffused air can always be visualized as a fictitious volume of water flowing out of the sample (Figure D.14). The water volume change indicator has recorded it as such and therefore the correction for diffused air must always be subtracted from the recorded water flow.

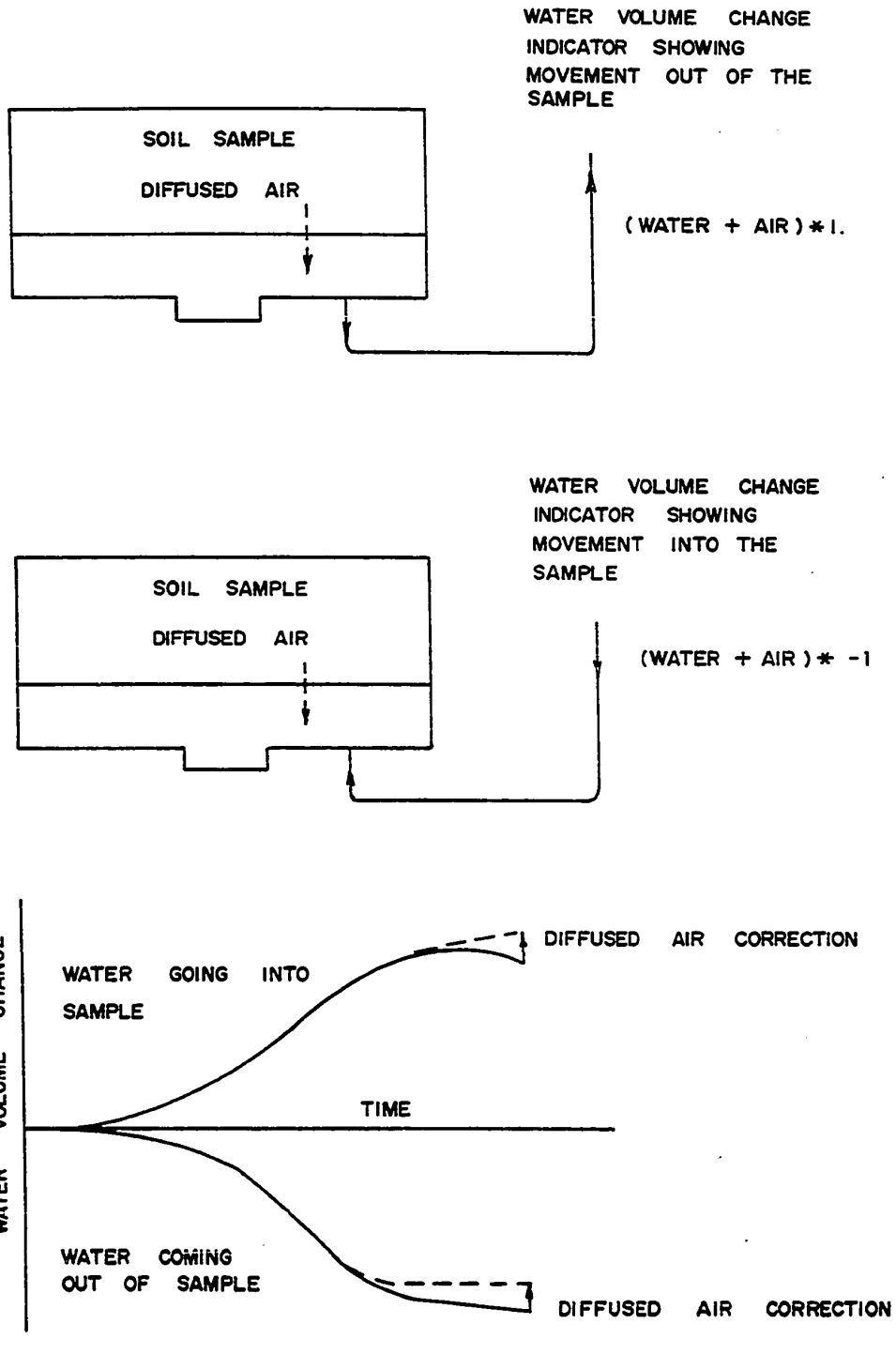


FIGURE D.14 APPLICATION OF DIFFUSED AIR VOLUME CORRECTION

APPENDIX E

PORE PRESSURE RESPONSE TESTS ON HIGH AIR ENTRY DISCS

CONTENTS OF APPENDIX E

		Page
E-1	General	E1
E-2	Literature Review	E1
E-3	Pore Pressure Response Theory	E3
E-4	Effect of Change in Volume of the Compartment	E8
E-5	Theoretical Response Relationships	E9
E-6	Experimental Pore Pressure Response Tests	E23
E-7	Comparison of Experimental Data with the Theory	E44
E-8	Relationship Between Stiffness Ratio and Compliance Factor	E48
E-9	Effect of Acetone on Pressure Response	E51

PORE PRESSURE RESPONSE TESTS ON HIGH AIR ENTRY DISCS

E-1 General

The low permeability of the high air entry ceramic disc and the compressibility of the fluid in the base plate result in a finite time being required to measure a pressure response on the base plate transducer. Appendix E develops a theory to predict the pore pressure response and develops theoretical curves relating the dominant variables. Test data are presented to verify the proposed theory.

E-2 Literature Review

Numerous research workers have attempted to incorporate the flexibility of the measuring system (compliance) into the analysis of pore pressure measurements. The research has been directed mainly toward the analysis of pore pressure measurements at the base of the sample in one-dimensional oedometers.

Whitman, Richardson and Healy (1961) used an electrical analog model to simulate the flexibility of pore pressure measuring systems. They assume that the soil is saturated and there is no side friction. The flexibility of the measuring compartment is designated as lamda (λ), with units of in^3 per psi. The flexibility is combined with other factors affecting pore pressure response to form a stiffness ratio

$$B = \frac{\lambda}{H \cdot m_v \cdot A}$$

where H = height of the sample

m_v = compressibility of the soil

A = cross-sectional area of the sample

Earlier results obtained at MIT were reviewed but the correlations are not very convincing.

Gibson (1963) examined the time lag in pore pressure response in an open standpipe and a closed system pore pressure measurement at the base of a clay layer. The time lag is related to permeability (k), compressibility of the soil (m_v) and the flexibility of the measuring system (λ). Their stiffness ratio can be written

$$\eta = \frac{A \cdot k \cdot H}{\gamma_w \cdot c_v \cdot \lambda} = \frac{A \cdot H \cdot m_v}{\lambda}$$

which is the inverse of that used by Whitman et al (1961). The formulation and solution of the problem are analytical.

Later research workers (Perloff, Nair and Smith, 1965; Northey and Thomas, 1965; and Christie, 1965) used the same definition of stiffness ratio and expanded the analytical solution to describe the distribution of pore pressure in a specimen during consolidation. Attempts to correlate the theory with laboratory tests have met with limited success.

Previous studies (Christie, 1965) have assumed that the flexibility of the measuring system was comprised of such factors as

(i) the compressibility of the fluid used to transmit the pore pressure,

(ii) expansibility of the pipes and valves containing the fluid,

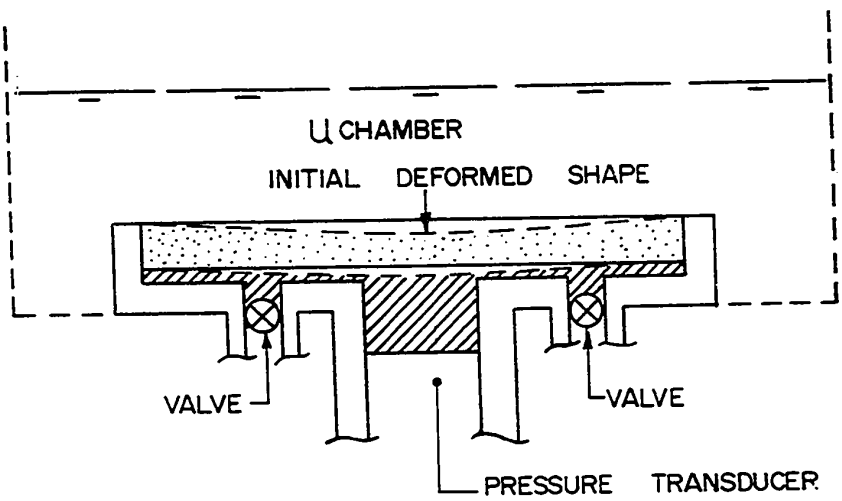
(iii) expansibility of the system due to the deflection of the transducer diaphragm.

All these factors have been combined linearly into one factor, λ. The affect of the non linear behavior of entrapped air has not been considered. Whitman et al (1961) reported that they felt "even a modest amount of air in the measuring system will not introduce great error". Christie (1965) states that entrapped air "has the effect of increasing the flexibility of the measuring system by an unknown amount".

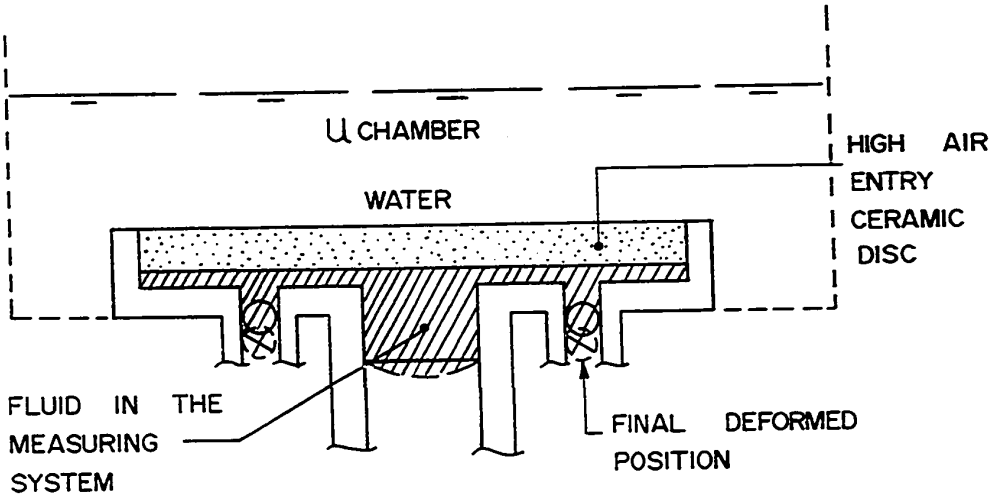
In the present study, the compliance factor of the measuring system is kept separate from the effects due to the soil sample. The effect of entrapped air is given primary consideration. The porous discs under consideration in this investigation have a high air entry value and a low coefficient of permeability whereas previous investigators considered coarse, high permeability discs.

E-3 Pore Pressure Response Theory

The model used to characterize the reaction of the pressure transducer is shown in Figure E.1. Initially one valve on the base plate is left open and water seeps from the chamber through the high air entry disc under steady state conditions. When the valve is closed, the flow of water into the base plate causes a compression of the fluid, resulting in a build-up of pressure (as measured on the transducer). The increase in pore pressure reduces the hydraulic gradient across the disc and lessens the inflow of water. Equilibrium is reached when the pressure in the base plate is equal to the pressure applied



(a) INSTANT AFTER CLOSING VALVES AT THE END OF STEADY STATE SEEPAGE



(b) AT EQUILIBRIUM

FIGURE E.1 CHARACTERIZATION OF THE PORE WATER PRESSURE MEASURING SYSTEM COMPLIANCE

to the water in the chamber.

There are two possible sources of compressibility; namely, the air-water mixture in the base plate and the base plate compartment housing the mixture. The significance of the second factor depends on the rigidity of the base plate construction, thickness and method of mounting the ceramic disc, the deflection of the transducer membrane and volume change in the two base plate valves during the pressure build-up. All these factors tend to produce a final compartment in the base plate that is larger under pressure than its initial size. Compressibility resulting from an increase in the compartment size is initially assumed insignificant, meaning that the measured compressibility is due to the air-water mixture. The theory also assumes that no leakage occurs from the compartment. Leakage would be reflected as an increase in compressibility.

Flow across the high air entry disc occurs as a result of a pressure head and is assumed to obey Darcy's Law.

$$\Delta Q = kiAt \qquad \text{E.1}$$

where A = cross-sectional area of the disc (cm^2)

i = hydraulic gradient across the disc

k = coefficient of permeability (cm/sec)

t = elapsed time (sec)

Since the gradient is continuously changing, equation E.1 can be written in a finite difference form.

$$\Delta Q = k \cdot i_{ave} \cdot A \cdot (t_j - t_i) \qquad E.2$$

In this way, an average hydraulic gradient is assumed to apply for a short period of time. The hydraulic gradient is then recomputed for the next time period. The pressures involved are defined as follows:

u_c = pressure applied to the water in the chamber

u_o = initial pressure registered on the transducer prior to closing the valve on the base

u_i = compartment pressure registered at time, t_i

u_j = compartment pressure registered at a later time, t_j

The hydraulic gradient during the time period t_i to t_j is defined as the difference between the chamber pressure and the average compartment pressure, divided by the thickness of the disc, d.

$$i_{ave} = \frac{1}{\gamma_w}\left[\frac{\frac{(u_c - u_i)}{d} + \frac{(u_c - u_j)}{d}}{2}\right] \qquad E.3$$

Rearranging

$$i_{ave} = \frac{1}{\gamma_w}\left[u_c - \frac{(u_i + u_j)}{2}\right]\frac{1}{d} \qquad E.4$$

Substituting into equation E.2

$$\Delta Q = \frac{k \cdot A}{\gamma_w \cdot d}\left[u_c - \frac{(u_i + u_j)}{2}\right] \cdot (t_j - t_i) \qquad E.5$$

The compressibility of the air-water mixture in the compartment is defined as

$$\beta = \frac{1}{V} \cdot \frac{\Delta V}{\Delta u} \qquad \text{E.6}$$

where ΔV = the change in volume due to a pressure change (assumed equal to ΔQ)

V = volume of the compartment in the base plate (i.e. volume of air and water)

Δu = the change in pressure over the time period that compressibility is being computed.

In coupling the compressibility equation with Darcy's equation, the change in pressure corresponds to the time period t_i to t_j. Therefore, Δu is equal to $(u_j - u_i)$. Rewriting the compressibility equation and solving for the change in volume gives

$$\Delta V = \beta \cdot V \cdot (u_j - u_i) \qquad \text{E.7}$$

Equating equations E.5 and E.7 gives

$$\beta = \frac{k \cdot A}{d \cdot V \cdot \gamma_w} \left[\frac{u_c - \frac{(u_i + u_j)}{2}}{(u_j - u_i)} \right] \cdot (t_j - t_i) \qquad \text{E.8}$$

Let the Compliance Factor of the system, η, be defined as

$$\frac{\gamma_w \cdot V \cdot d}{k \cdot A}$$

The units of the compliance factor, η, are (cm^2/kg/sec). Therefore,

$$\beta = \frac{1}{\eta}\left[\frac{u_c - \frac{(u_i+u_j)}{2}}{(u_j-u_i)}\right](t_j-t_i) \qquad \text{E.9}$$

In the laboratory, it is possible to measure accurately the pressure development with time by means of the data acquisition system. By marching forward in time and substituting the values of pressure into equation E.9, it is possible to compute the compressibility of the mixture in the base plate compartment.

E-4 Effect of Change in Volume of the Compartment

If the compartment increases in size during the pressure build-up, part of the water flowing into the compartment is due to this increase in size.

ΔV_c = Final Compartment Volume - Initial Compartment Volume

The total volume of water flowing into the compartment, ΔV, now has two components. One part, ΔV_m, represents the compression of the air-water mixture while the other part, ΔV_c, compensates for the increase in compartment size. The increased size is related linearly to the change in pressure.

$$\Delta V_c = \beta_c \cdot (u_j-u_i) \cdot V \qquad \text{E.10}$$

where β_c = an average compressibility for the components of compressibility in the compartment.

The volume change in the air-water mixture is the same as equation E.7. The total volume, ΔV, can be equated to the water flow, ΔQ, to form the equation,

$$\frac{k \cdot A}{\gamma_w \cdot d}\left[u_c - \frac{(u_i+u_j)}{2}\right]\cdot(t_j-t_i) = (\beta_m+\beta_c)\cdot V\cdot(u_j-u_i) \qquad E.11$$

Rearranging and solving for β, gives

$$\beta = \frac{k \cdot A}{d \cdot V \cdot \gamma_w}\left[\frac{u_c - \frac{(u_i+u_j)}{2}}{(u_j+u_i)}\right]\cdot(t_j-t_i) - \beta_c \qquad E.12$$

The difficulty in applying equation E.12 arises from the complex nature of β_c. The compressibility is a combination of effects of several materials (i.e. stainless steel, rubber, ceramic) and may be non linear and time dependent in behavior. Due to the difficulty in evaluating the compressibility of the compartment, the laboratory data is first analysed by assuming that the compressibility is controlled by the air-water mixture. Then the effect and significance of the compartment compressibility is discussed.

E-5 Theoretical Response Relationships

The compressibility of the air-water mixture can be evaluated from laboratory data since the compressibility is the only unknown in the equation. However, in attempting to predict the theoretical pore pressure response curve, the compressibility and time constitute two unknowns. Therefore, an additional physical relationship is required in the form of a constitutive relationship for the air-water mixture.

In this way, the compressibility is written in terms of the pore pressure and the percentage air in the compartment.

Assume that initially the compartment contains a mixture of air and water, and with time pure water flows through the high entry disc, compressing the mixture. In other words, the amount of air in the compartment (by volume) decreases as the pore pressure builds up (Figure E.2). It is also assumed that no further air comes out of solution in the compartment and that the time involved is insufficient for the dissolving of free air. Computations based on a diffusivity of 2×10^{-5} cm^2/sec show that the above assumption is certainly reasonable for elapsed times less than 10 minutes. This is later verified in section E-6 (Figure E.25).

The compressibility is continuously changing as described for an immiscible air-water mixture (Chapter II).

$$\beta = \beta_w \cdot S + \frac{(1-S)}{u_a} \qquad \text{E.13}$$

The percent air is (1-S) and u_a is the absolute compartment pressure. The assumption is made that the air pressure is equal to the water pressure. When compared with equation E.9 the pressure is equivalent to $(u_i+u_j)/2$.

Equation E.3 is the proposed constitutive relationship for the air-water mixture in the compartment and is plotted in Figure E.13 for various percentages of air. The initial pressure in the air is taken as equal to atmospheric.

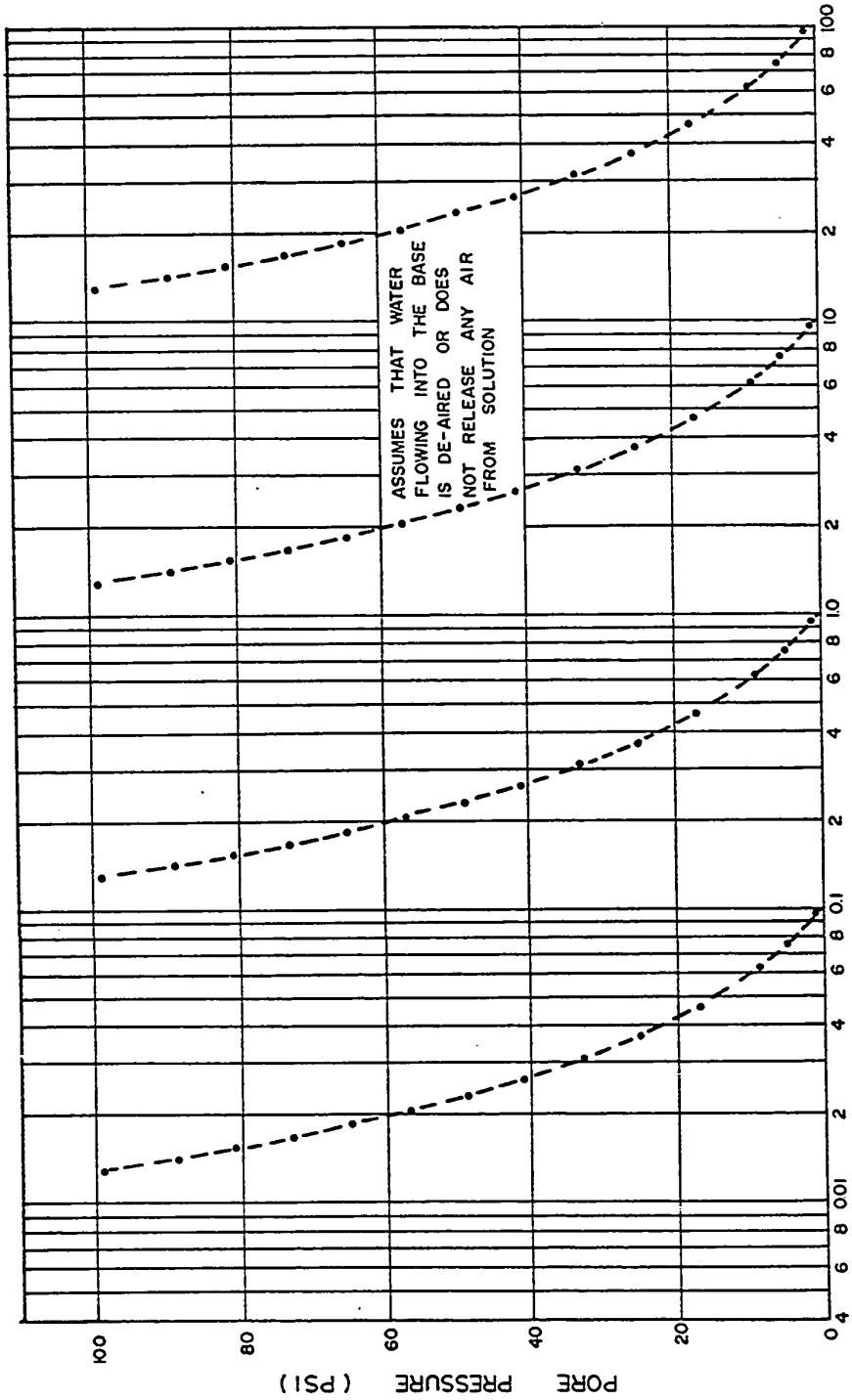


FIGURE E.2 CHANGE IN VOLUME OF THE AIR IN THE MEASURING SYSTEM WITH AN INCREASE IN PRESSURE

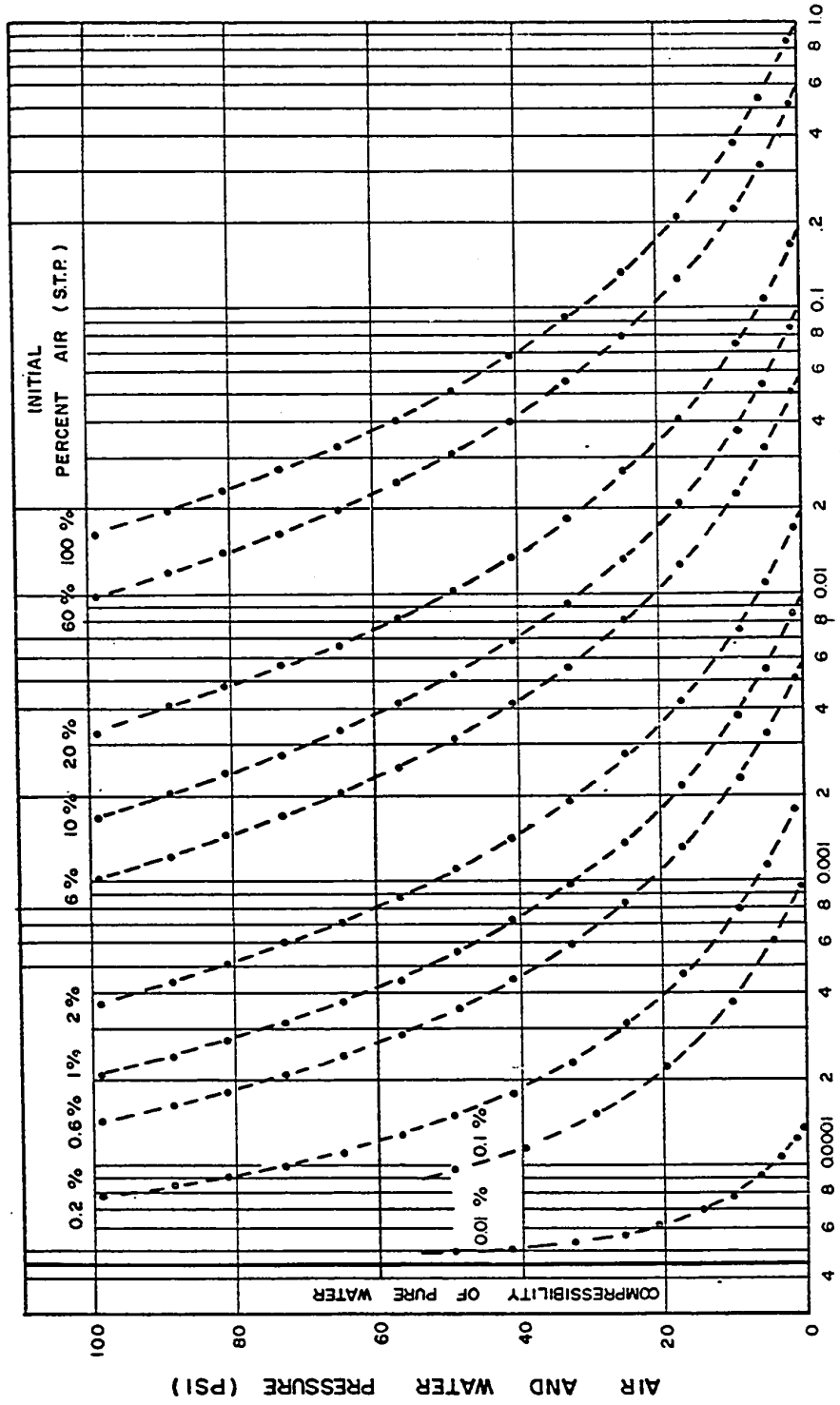


FIGURE E.3 COMPRESSIBILITY VERSUS PRESSURE OF AN IMMISCIBLE AIR - WATER MIXTURE

Starting with an assumed percentage of air in the compartment, the compressibility of the mixture at any other pressure, can be computed. To develop theoretical response curves, equation E.9 is rearranged to solve for a change in time.

$$t_j - t_i = \Delta t = \frac{\beta \cdot \eta \cdot (u_j - u_i)}{\left[u_c - \frac{(u_i + u_j)}{2}\right]} \qquad \text{E.14}$$

Choosing various compliance factors and a pressure increment, the increment of time is computed. The elapsed time is equal to

$$t = t_i + \frac{t_j - t_i}{2} = \frac{t_i + t_j}{2} \qquad \text{E.15}$$

Similarly, the average pressure response is

$$u = (u_i + u_j)/2 \qquad \text{E.16}$$

Figure E.4 is a listing of a program written to compute the pore pressure response curves. Definitions of the variables used are as follows:

C - compliance factor ($cm^2/kg/sec$)

DELU - pressure increment (psi)

DELUM - pressure increment (kg/cm^2)

PAIR - initial percentage of air (%)

AIR - ratio of the volume of air to the volume of the compartment (dimensionless)

```
C      ************************************************************************
C      COMPLIANCE OF MEASURING SYSTEMS
C      ************************************************************************
       C=10.
       DELU=1.0
       DELUM=DELU*0.0703
C      DO LOOP TO INCREMENT 'COMPLIANCE'
       DO 101 J=1,4
       PAIR=0.02
       C=C*10.
C      DO LOOP TO INCREMENT 'PERCENT AIR'
       DO 102 K=1,3
       UC=50.
       TI=0.0
       UI=2.0
       PAIR=PAIR*10.
       AIR=(PAIR/100.)*14.7/(14.7+UI+DELU/2.)
       WRITE(6,3)
     3 FORMAT(1H1,' THEORETICAL RESPONSE AND COMPRESSIBILITY RELATIONSHIP
      1S FOR FINE DISC MEASURING SYSTEMS')
       WRITE(6,2) UC,DELU,C,PAIR
     2 FORMAT(1X,'CHAMBER PRESSURE =',F10.3,'     PRESSURE INCREMENT =',
      1F10.3,'     COMPLIANCE FACTOR =',F10.1,'     PERCENT AIR =',F10.4/
      21X,'**********************************************************
      2************************************************************')
       WRITE(6,4)
     4 FORMAT(5X,'TI',10X,'TJ',10X,'TAVE',8X,'UI',10X,'UJ',10X,'UAVE',8X,
      1'AIR',9X,'BETA1')
C      DO LOOP TC INCREMENT 'PRESSURE'
       DO 100 I=1,48
       UJ=UI+DELU
       UAVE=(UI+UJ)/2.
       UIM=UI*0.0703
       UJM=UJ*0.0703
       UAVEM=UAVE*0.0703
       BETA1=0.00004S*(1.-AIR)+AIR/(UAVEM+1.033)
       DELT=BETA1*C*DELU/(UC-(UI+DELU/2.))
       TJ=TI+DELT
       TAVE=(TI+TJ)/2./60.
       WRITE(6,1) TI,TJ,TAVE,UI,UJ,UAVE,AIR,BETA1
     1 FORMAT(1X,6F12.6,2E14.6)
       AIR=(PAIR/100.)*(1.033)/(UJM+1.033+DELUM/2.)
       UI=UJ
       TI=TJ
   100 CONTINUE
   102 CONTINUE
   101 CONTINUE
       STOP
       END
```

FIGURE E.4 PROGRAM TO COMPUTE THEORETICAL PORE PRESSURE RESPONSE CURVES ON MEASURING SYSTEMS USING HIGH AIR ENTRY POROUS DISCS

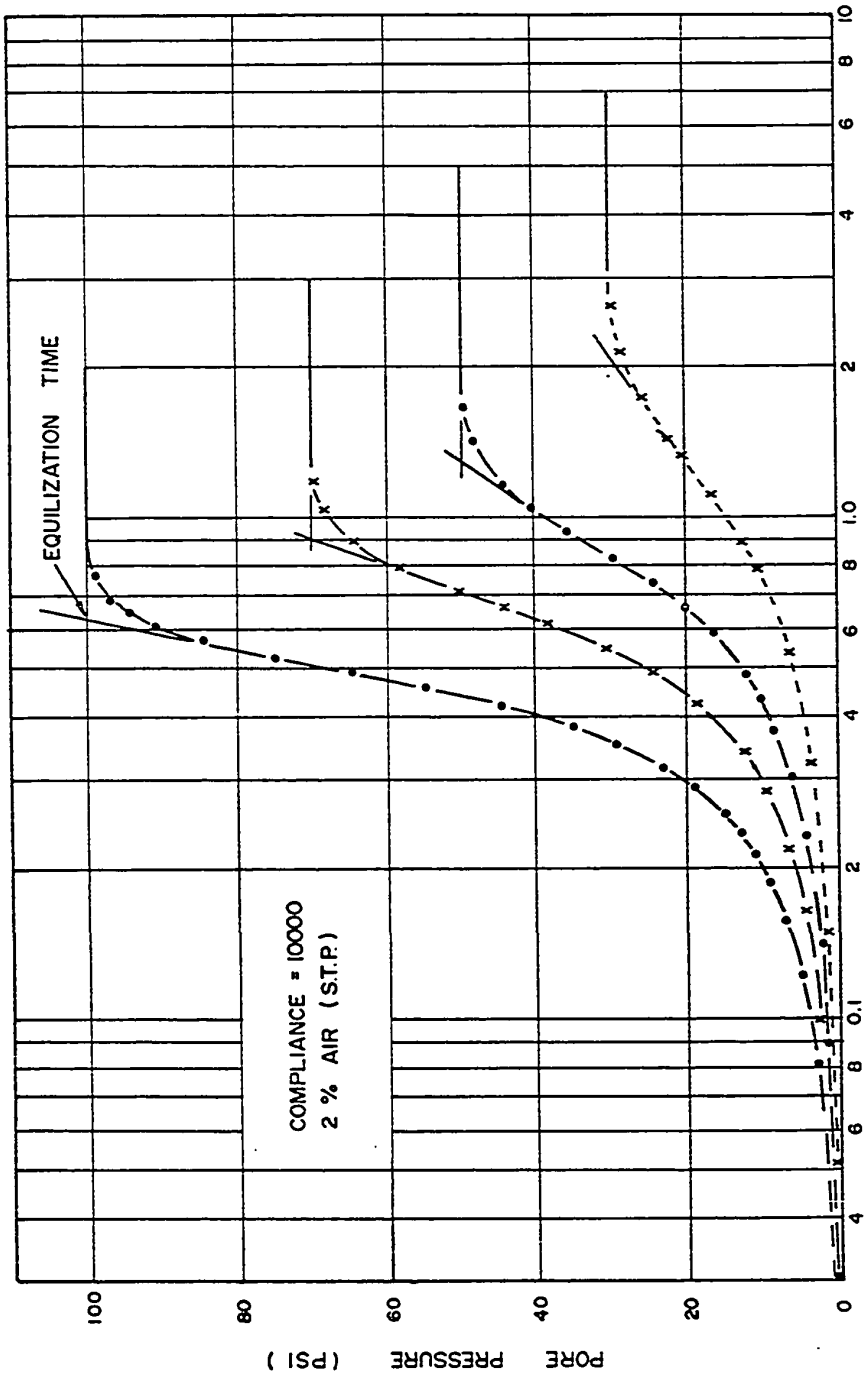


FIGURE E.7 PORE PRESSURE RESPONSE CURVES FOR VARIOUS APPLIED PRESSURES

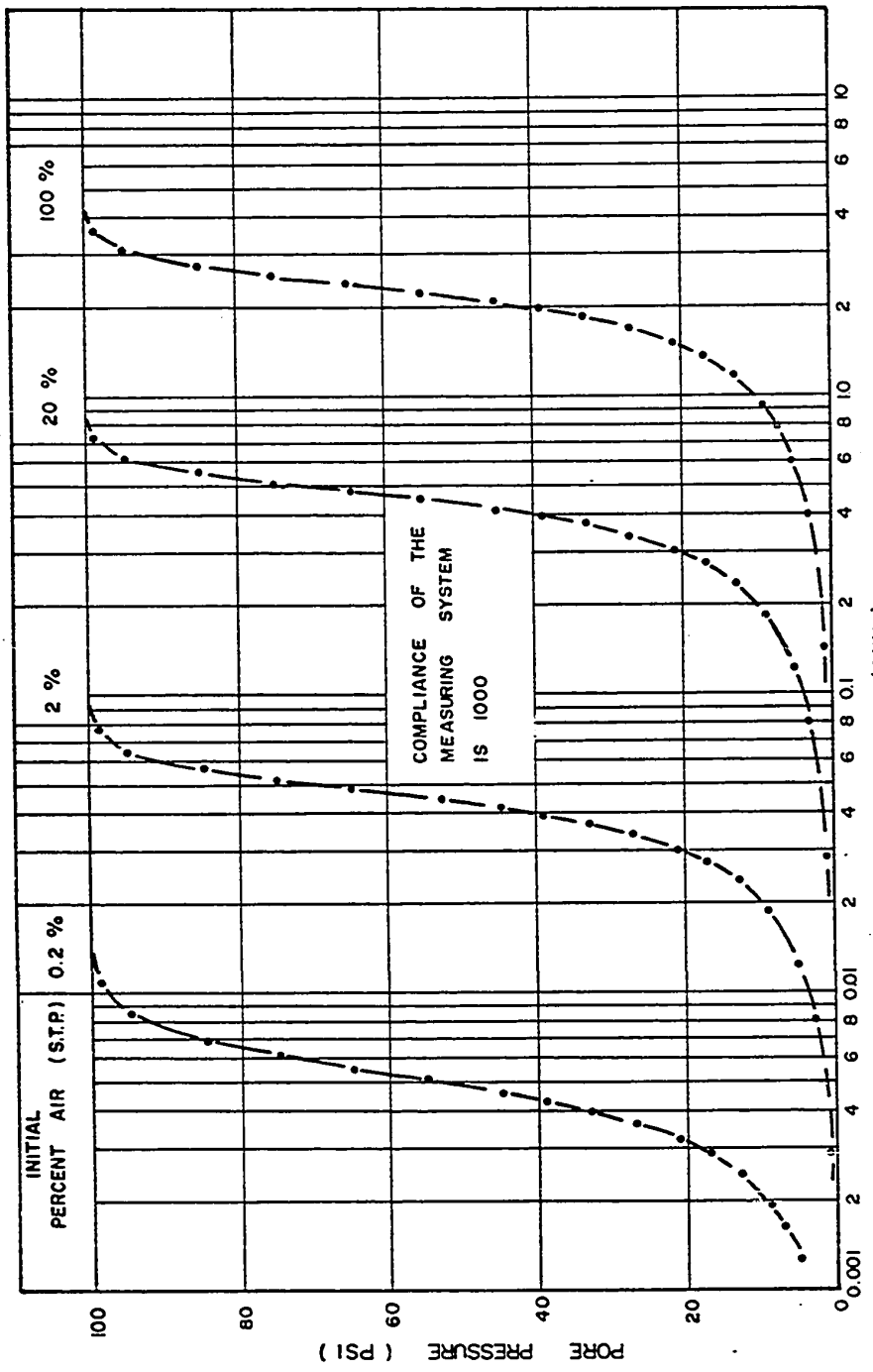


FIGURE E.6 PORE PRESSURE RESPONSE CURVES FOR VARIOUS PERCENTAGES OF AIR IN THE BASE PLATE (COMPLIANCE = 1000)

causes a lateral shift in the response curve (Figure E.6). The "slope of the response curve" remains essentially constant as long as the initial percent air is greater than approximately one percent. Below one percent, the compressibility of the water becomes significant.

The effect of the applied chamber pressure is examined by choosing a compliance of 10,000 and an initial air content of two percent (Figure E.7). The slope of the response curve decreases and the time required for pressure equilization across the ceramic disc increases as the applied chamber pressure decreases.

The theoretical increase in compressibility with time is presented on a double logarithm plot of time and compressibility (Figure E.8). The curves exhibit a straight line portion, however, there is no new information gleaned from this plot.

From the previous theoretical plots it appears that only two variables are required to describe the response curves.

(i) The slope of the straight line portion of the response curve on a semi-logarithm plot and

(ii) One point that can represent the lateral shift of the response curve. Any point between 40 and 80 percent could be used for correlation purposes; however, a more meaningful value is obtained by using the point of intersection of the extended straight line portion of the response curve and the horizontal line of 100 percent response. This point is termed the "equilization time". Actually it represents approximately 94 percent response.

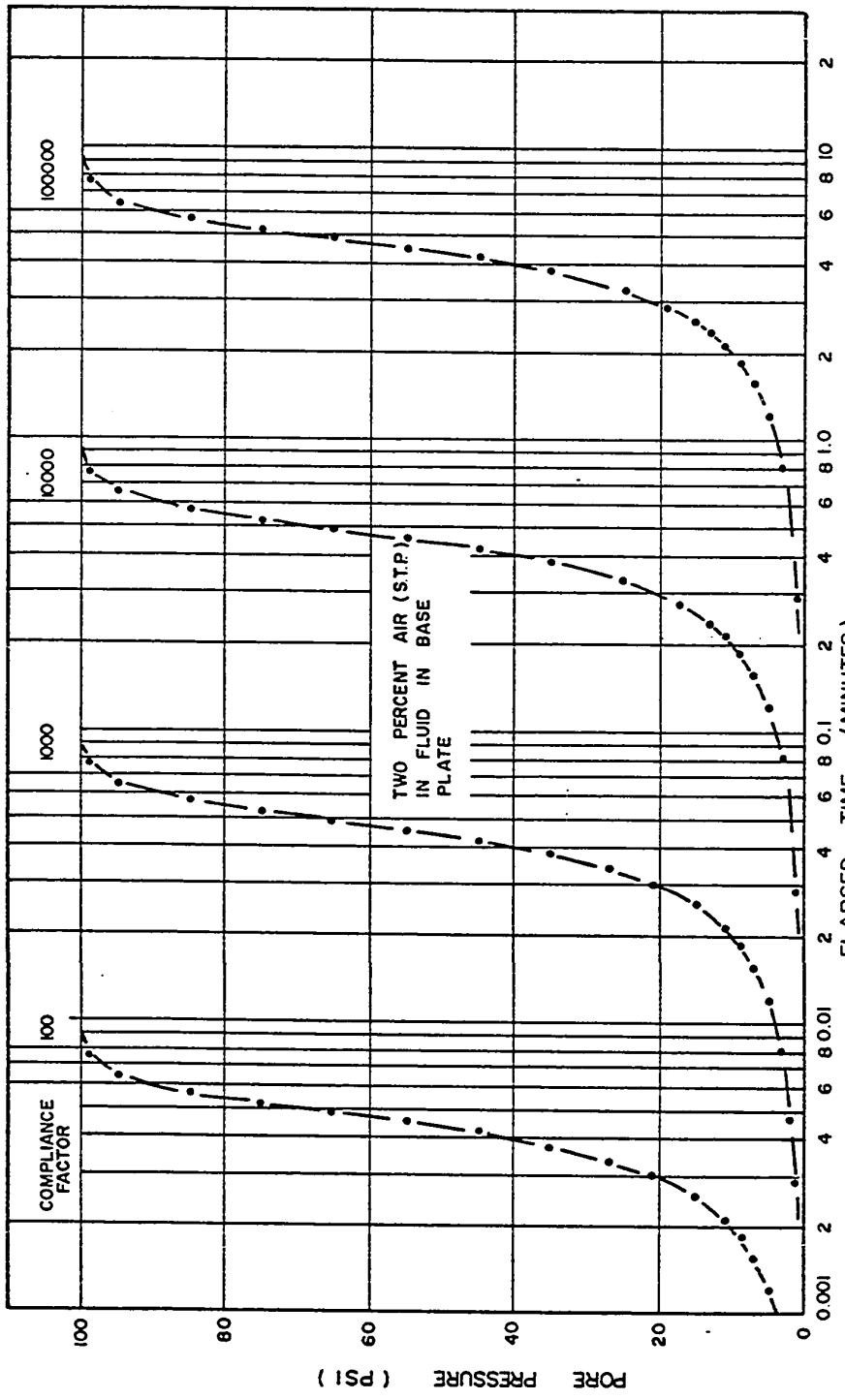


FIGURE E.5 PORE PRESSURE RESPONSE CURVES FOR VARIOUS COMPLIANCE FACTORS (TWO PERCENT AIR S.T.P.)

UC - applied chamber pressure (psi)

TI - elapsed time at point i (seconds)

TJ - elapsed time at point j (seconds)

TAVE - average elapsed time (minutes)

UI - pressure response at time T_i (psi)

UJ - pressure response at time T_j (psi)

UAVE - average pressure response at time t_{ave} (psi)

UIM - pressure response at time T_i (kg/cm^2)

UJM - pressure response at time T_j (kg/cm^2)

UAVEM - average response at time T_{ave}(kg/cm^2)

BETA1 - compressibility of air water mixture in the compartment (cm^2/kg)

DELT - time increment from T_i to T_j (seconds)

Figure E.5 shows typical pressure response curves for compliance factors ranging from 100 to 100,000 for an initial air content of 2 percent. The wide range of compliance factors arises from the variation in coefficient of permeability associated with 3 to 15 bar air entry ceramic discs. The curves are plotted on a semi-log plot with respect to time and are S-shaped. The straight line portion starts at approximately 40 percent response and continues up to approximately 80 percent. The slope of the straight portion (on the semi-log plot) is the same for all compliance factors. A changing compliance factor merely shifts the response curves laterally.

Changing the initial percent air in the compartment changes the constitutive relationship for the air-water mixture. The change

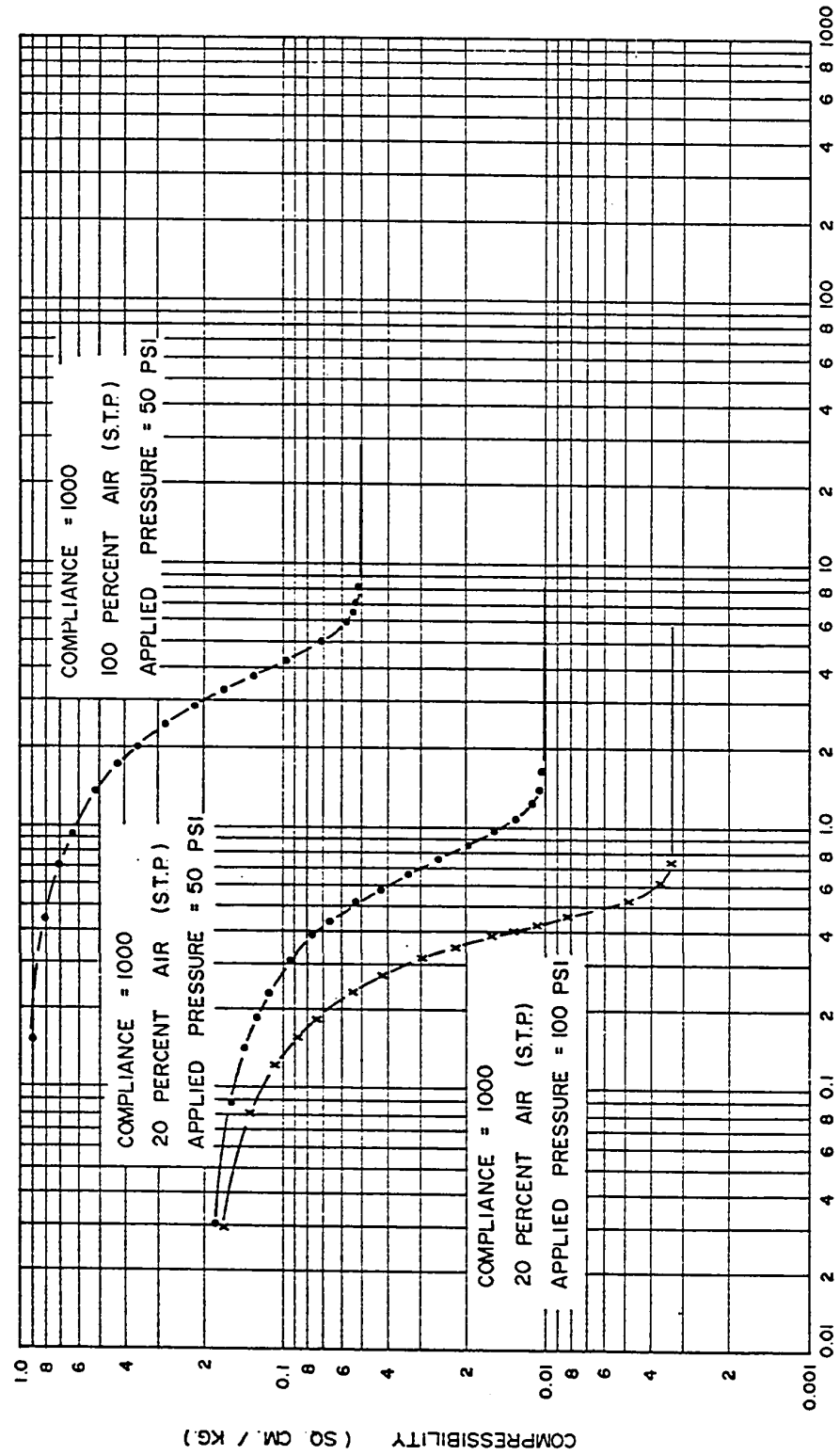


FIGURE E.8 THEORETICAL DEVELOPMENT OF COMPRESSIBILITY WITH ELAPSED TIME

The equilization time is dependent upon

(i) the initial percentage of air

(ii) the compliance factor of the system and

(iii) the applied chamber pressure.

Figure E.9 shows a plot of the logarithm of equilization time versus logarithm of compliance factor for an applied chamber pressure of 100 psi. Lines of equal initial air content are linear on this plot and are spaced at a constant logarithmic scale except at the low percent air range (less than one percent). Similar theoretical plots can be developed for other chamber pressures. From these plots it is possible to estimate the equilization time for various percentages of air if the compliance factor is known. Later, this plot is used to compare the experimental results with the theoretical analysis.

Attempts were made to put the variables involved in a dimensionelss form. However, this appears to be of little advantage. The constitutive relationship can be put in dimensionless form by dividing the absolute pressures by the standard atmospheric pressure and dividing the compressibility by that of pure water. Plotting both variables gives a straight line on a double logarithm plot for initial air contents greater than one percent. The compressibility due to air content alone can be linearized over its entire range on the above plot. The pressure variable on the response curves can be made dimensionless by plotting the response as a percentage of the initially applied differential head. However, a family of curves is still obtained for various applied pressures.

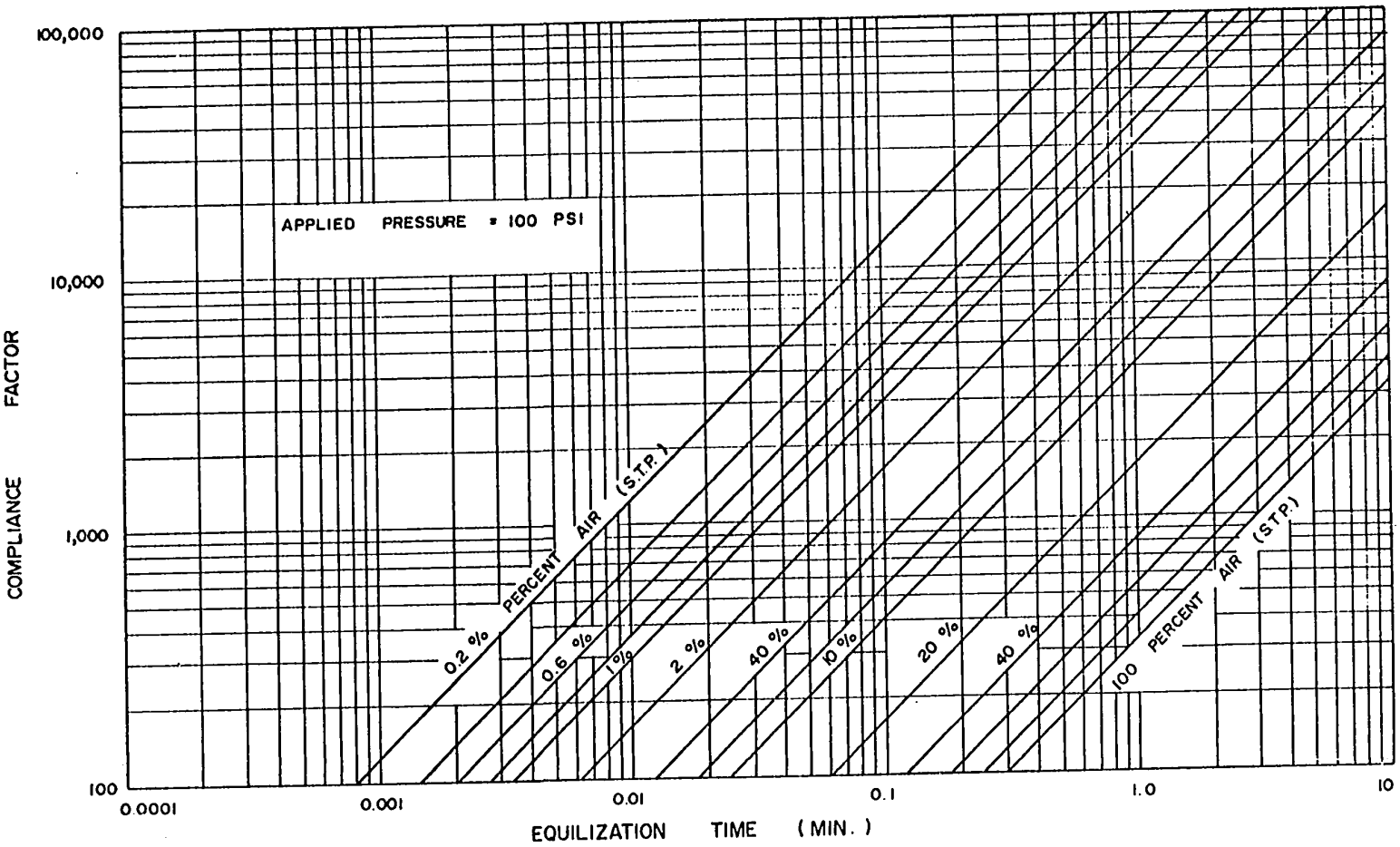


FIGURE E.9 TIME FOR PORE PRESSURE EQUILIZATION FOR AN APPLIED PRESSURE OF 100 PSI

E-6 Experimental Pore Pressure Response Tests

Approximately twenty four pore pressure response tests were performed with a range of

(i) ceramic disc thicknesses,

(ii) air entry and permeability values,

(iii) applied chamber pressures and

(iv) air contents.

The base plates were constructed for both aluminum and stainless steel. The data was reduced using the computer program on Figure E.10. The definition of the variables involved are as follows:

HEAD - heading card used for identification (20A4)

WDEN - density of water (kg/cm^3)

PERM - permeability of the ceramic disc (cm/sec)

THICK - thickness of the ceramic disc (cm)

UCAAM - applied chamber pressure (psi)

VOLC - volume of the compartment (cc)

HOURO - starting hour

HOURJ - hour at any elapsed time

MINO - starting minute

MINJ - minute at any elapsed time

SECO - starting second

SECJ - second at any elapsed time

POREI - starting compartment pressure (mv)

POREJ - compartment pressure at any elapsed time (mv)

UI - compartment pressure at point i (psi)

```
      DOUBLE PRECISION PERM
      REAL MINO,MINJ,MIN
      DIMENSION HEAD(20)
      WDEN=0.001
      READ(5,15) HEAD
   15 FORMAT(20A4)
      WRITE (6,23) HEAD
   23 FORMAT(5X,20A4)
      READ(5,1) PERM,THICK,AREA,UCHAM,VOLC
    1 FORMAT(F20.12,4F10.0)
      WRITE(6,20)
   20 FORMAT(1X,'      PERMEABILITY           THICKNESS     AREA         U CH
     1AMBER    VOL. CH.')
      WRITE(6,10)PERM,THICK,AREA,UCHAM,VOLC
   10 FORMAT(10X,E15.6,4F12.5)
      READ(5,2) HOURO,MINO,SECO,POREI
    2 FORMAT(3F2.0,F10.0)
      WRITE(6,21)
   21 FORMAT(1X,' T ELAPSED      T AVE.         UI            UJ            U
     1AVE.      BETA')
      WRITE(6,22)
   22 FORMAT(1X,'_____________________________________________________________
     1_____')
      WRITE(6,11)HOURO,MINO,SECO,POREI
   11 FORMAT(10X,3F5.0,F12.5)
      TIMEI=0.0
      UI=3.63158*POREI-0.017
      CONST=PERM*AREA/THICK/VOLC
      DO 100 I=1,100
      READ(5,2) HOURJ,MINJ,SECJ,POREJ
      IF(HOURJ.EQ.0.0) GO TO 101
      WRITE(6,11)HOURJ,MINJ,SECJ,POREJ
      UJ=3.63158*POREJ-0.017
      UAVE=(UI+UJ)/2.
      HOUR=(HOURJ-HOURO)*60.
      MIN=MINJ-MINO
      SEC=(SECJ-SECO)/60.
      TIMEJ=HOUR+MIN+SEC
      TAVE=(TIMEI+TIMEJ)/2.
      BETA=CONST*(UCHAM-(UI+UJ)/2.)*(TIMEJ-TIMEI)*60./(UJ-UI)/WDEN
      WRITE(6,3) TIMEJ,TAVE,UI,UJ,UAVE,BETA
    3 FORMAT(5F12.4,E14.6)
      UI=UJ
  100 TIMEI=TIMEJ
  101 STOP
      END
```

FIGURE E.10 PROGRAM TO REDUCE DATA FROM PORE PRESSURE RESPONSE TESTS

UJ - compartment pressure at point j (psi)

UAVE - average compartment pressure between points i and j (psi)

TIMEI - elapsed time to point i (minutes)

TIMEJ - elapsed time to point j (minutes)

TAVE - average time between points i and j (minutes)

BETA - compressibility of the air water mixture in the compartment (cm^2/kg)

In order to compute the compliance factor of the measuring system it is necessary to measure the volume of the compartment in the base plate. Estimate of this value were obtained by saturating the compartment with water and opening the valves and blowing out the water with an air pressure. (Table E.1)

TABLE E.1

VOLUME OF COMPARTMENT IN PRESSURE MEASURING SYSTEMS

Apparatus No.	Volume (cc)
Triaxial #2	6.79
Anteus Oedometer #177	4.20
Anteus Oedometer #179	3.90

Table E.2 summarized chronologically the classification details for the response tests on the high air entry discs. The pressure response with time curves and the compressibility versus pressure curves

TABLE E.2

SUMMARY OF RESPONSE TESTS ON CERAMIC DISCS

Apparatus No.	Date	Air Entry Value (Bars)	Thickness (cm)	Permeability (cm/sec)	Applied Pressure (psi)	Equalization Time (min)	Final Vol. of Air (cc)
Oed. #179	Oct. 27/71	15	0.306	8.41×10^{-9}	77	5.4	--
Oed. #177	Oct. 27/71	15	0.306	6.82×10^{-8}	50	1.0	--
Oed. #179	Oct. 30/71	15	0.306	8.23×10^{-9}	76	6.6	-- *
Oed. #177	Oct. 30/71	15	0.306	1.19×10^{-7}	51	0.55	--
Oed. #179	Nov. 17/71	15	0.306	7.16×10^{-9}	76	3.0	--
Triaxial #2	Nov. 19/71	15	0.306	8.44×10^{-9}	56.2	13.9	--
Oed. #177	Dec. 1/71	5	0.622	1.30×10^{-7}	80	0.80	-- *
Oed. #179	Dec. 17/71	15	0.622	7.02×10^{-9}	76	12.6	--
Oed. #177	Jan. 5/72	5	0.622	1.02×10^{-7}	76	0.12	-- *
Oed. #177	Jan. 7/72	5	0.622	1.25×10^{-7}	50	1.35	--
Oed. #179	Jan. 24/72 (15:34)	15	0.622	7.02×10^{-9}	50	32.5	0.77
Oed. #179	Jan. 24/72 (16:19)	15	0.622	7.02×10^{-9}	50	11.8	0.10
Triaxial #2	Feb. 18/72 (10:55)	5	0.622	1.03×10^{-7}	52	1.41	0.15
Triaxial #2	Feb. 18/72 (11:03)	5	0.622	1.03×10^{-7}	52	1.33	0.10
Oed. #177	Feb. 18/72 (9:15)	5	0.622	8.36×10^{-8}	50	3.9	0.19
Oed. #177	Feb. 18/72 (9:28)	5	0.622	8.36×10^{-8}	50	2.75	0.16
Oed. #177	Feb. 22/72 (9:15)	5	0.622	1.13×10^{-7}	50	1.40	0.11
Oed. #177	Feb. 22/72 (9:42)	5	0.622	1.13×10^{-7}	70	0.73	0.02
Oed. #177	Feb. 22/72 (10:44)	5	0.622	1.13×10^{-7}	30	1.5	0.03
Oed. #177	Feb. 22/72 (11:17)	5	0.622	1.13×10^{-7}	50	--	--
Oed. #177	Feb. 22/72 (13:10)	5	0.622	1.16×10^{-7}	50	0.46	0.13
Oed. #177	Feb. 22/72 (13:19)	5	0.622	1.16×10^{-7}	50	0.42	0.01
Oed. #177	Feb. 22/72 (13:35)	5	0.622	1.16×10^{-7}	50	4.60	4.20

*Disc was cracked

for many of the tests are presented in Figures E.11 to E.24. In a few cases, insufficient data were recorded and these have been omitted. Tests performed on the system with leaks are presented in Appendix B. Tests on discs treated with acetone are presented later in this Appendix.

The pore pressure response curves show the characteristic shape predicted by the theory. All curves form continuous, smooth functions. The upper portion, approaching 100 percent response, is slightly slower in reaching 100 percent than the theory predicts. The pore pressure response curves could be reproduced with only a slight horizontal translation due to differing air contents (Figure E.23).

The compressibility versus pressure plots have the same shape as the theoretical curves up to a response of approximately 80 percent. At this point the curves tend to bend to the right, indicating an increase in compressibility. Several factors may be involved in this phenomenon. With the increasing elapsed time, some air may be dissolved in the water. This is reflected as an increase in compressibility. Assuming a one-dimensional diffusion model with air overlying water, an estimate was made of the significance of diffusion (Figure E.25). Although diffusion shows the correct trend, it does not appear to completely account for the observed behavior. It is probable that a better agreement between the theoretical and measured compressibilities could be obtained if the actual geometric configuration of the air and water mixture in the compartment were known and

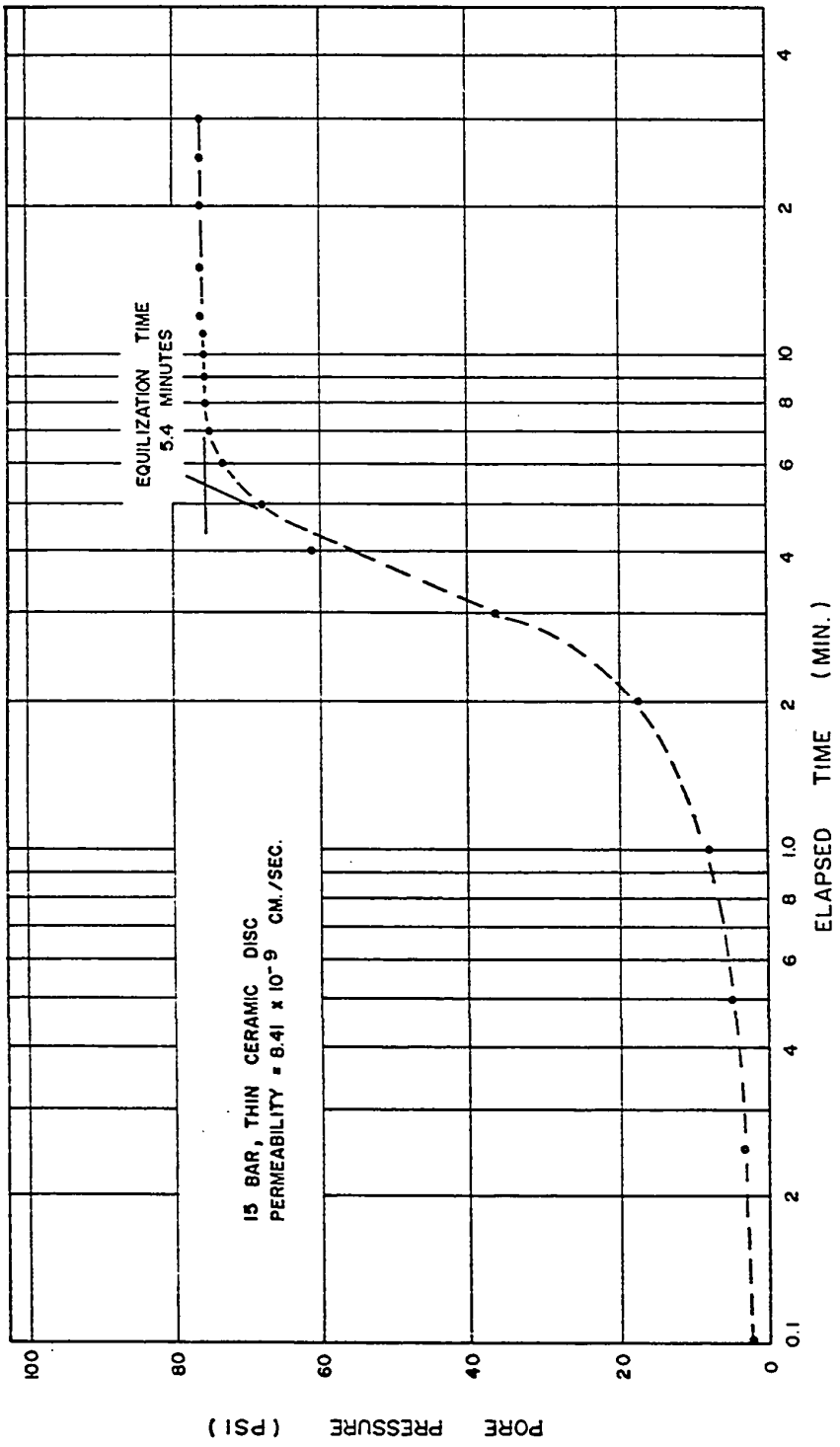


FIGURE E.11 PORE WATER PRESSURE RESPONSE ON ANTEUS OEDOMETER + 179
(OCT. 27, 1971)

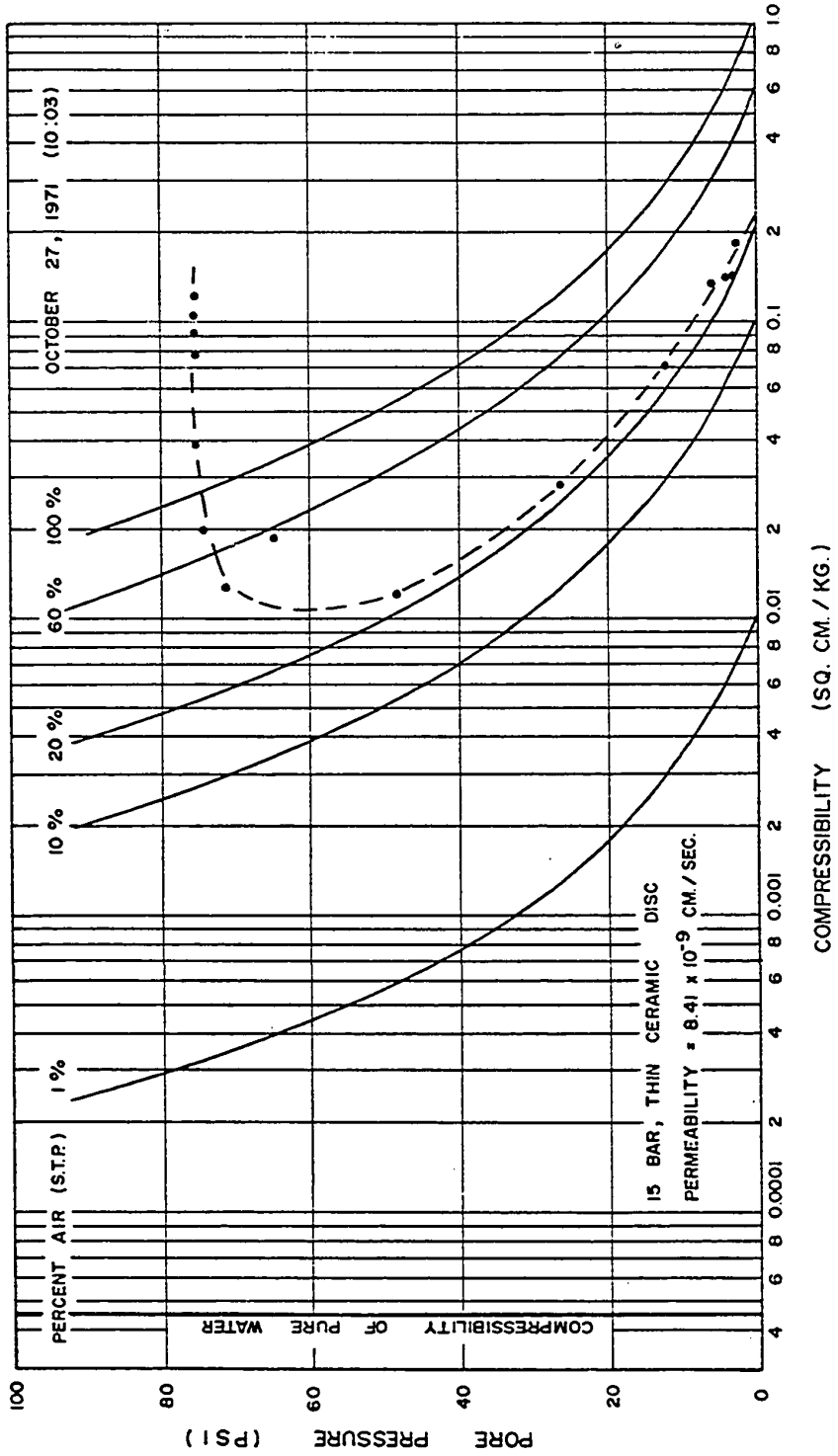


FIGURE E.12 COMPRESSIBILITY OF FLUID IN MEASURING SYSTEM ON ANTEUS OEDOMETER # 179

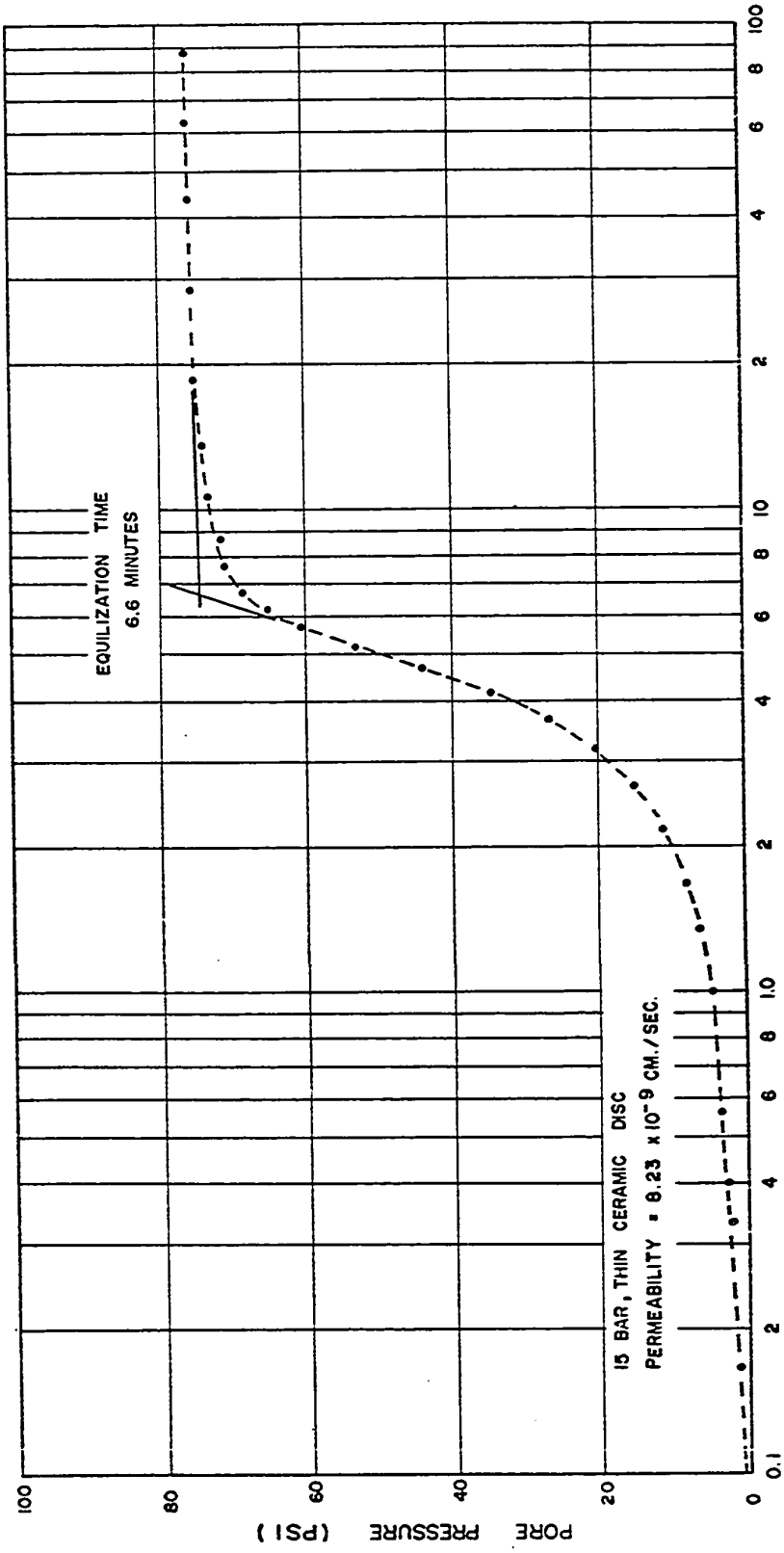


FIGURE E.13 PORE WATER PRESSURE RESPONSE ON ANTEUS OEDOMETER # 179 (OCT. 30, 1971)

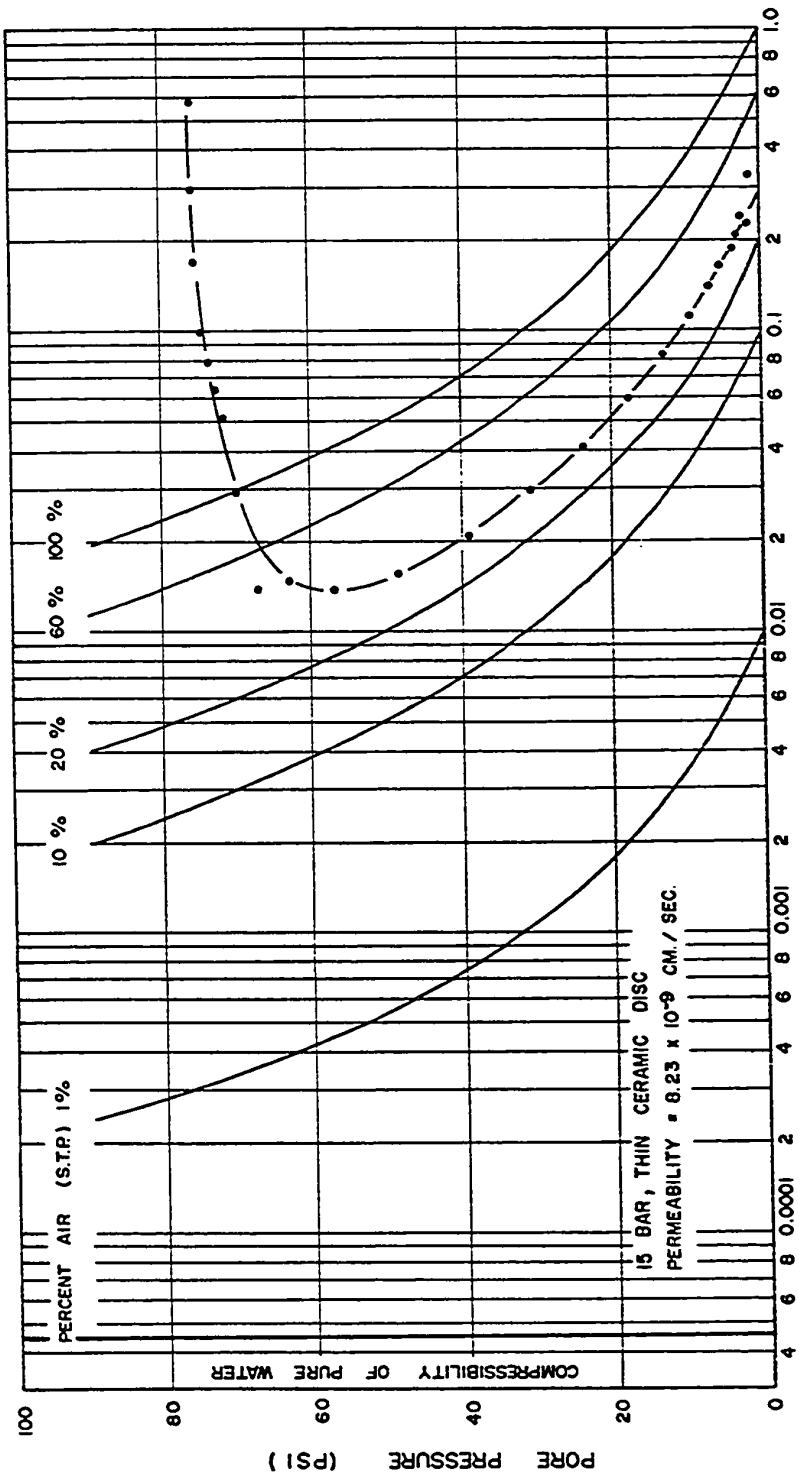


FIGURE E.14 COMPRESSIBILITY OF THE FLUID IN THE PORE PRESSURE MEASURING SYSTEM ON ANTEUS OEDOMETER #179 (DECEMBER 30, 1971)

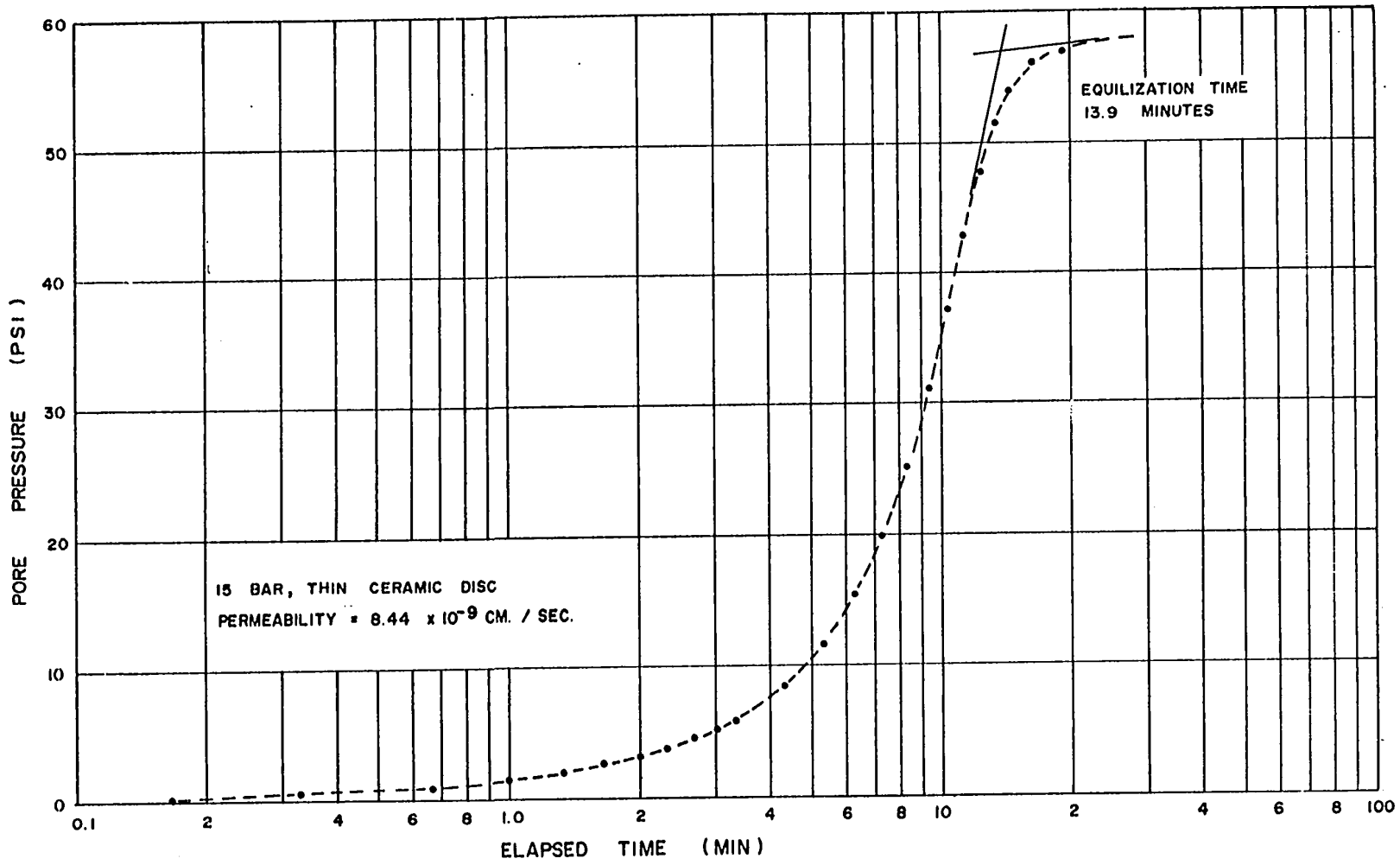


FIGURE E.15 PORE WATER PRESSURE RESPONSE ON TRIAXIAL # 2 (NOVEMBER 19, 1971)

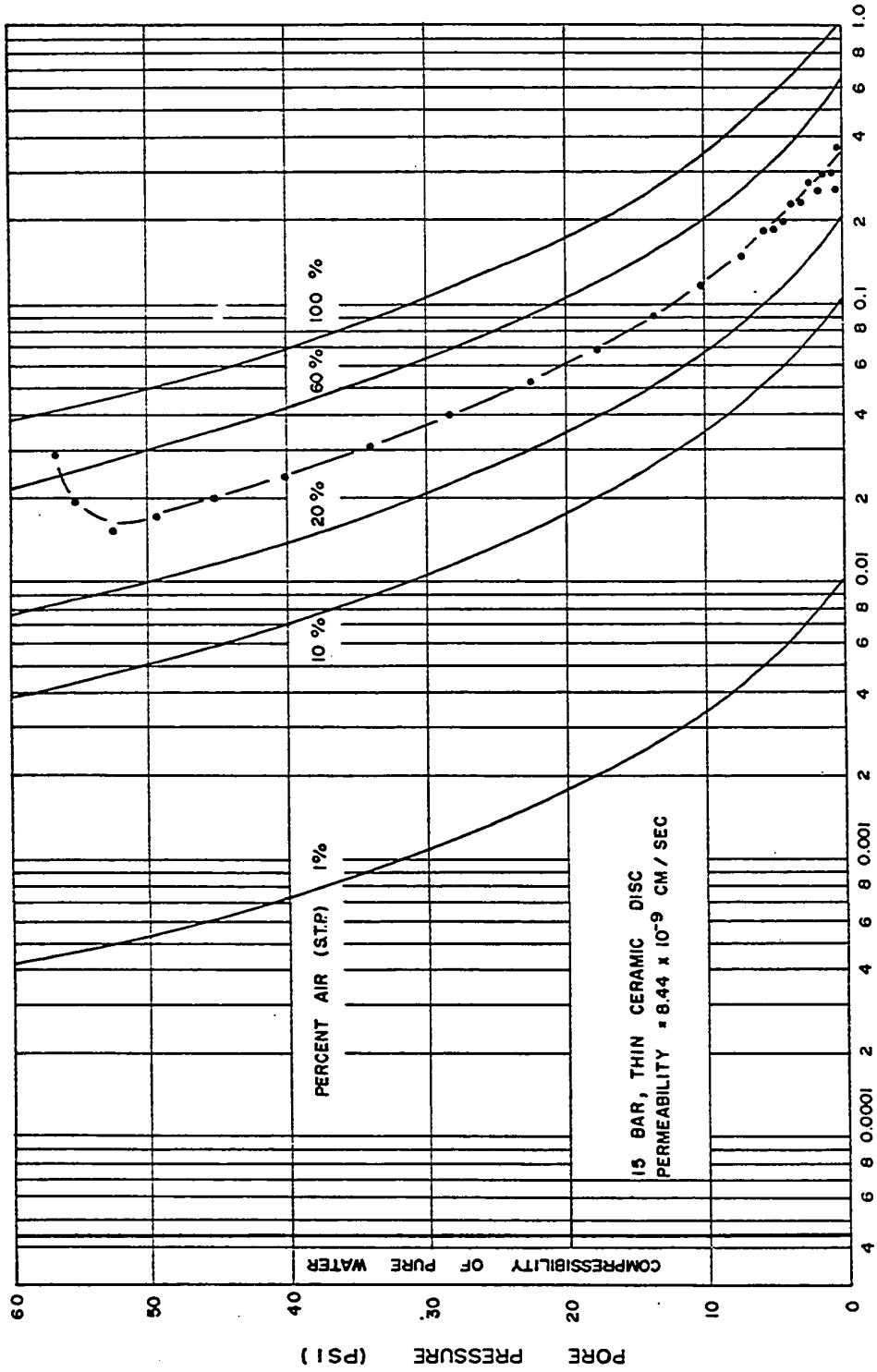


FIGURE E.16 COMPRESSIBILITY OF THE FLUID IN THE PORE PRESSURE MEASURING SYSTEM ON TRIAXIAL # 2 (NOVEMBER 19, 1971)

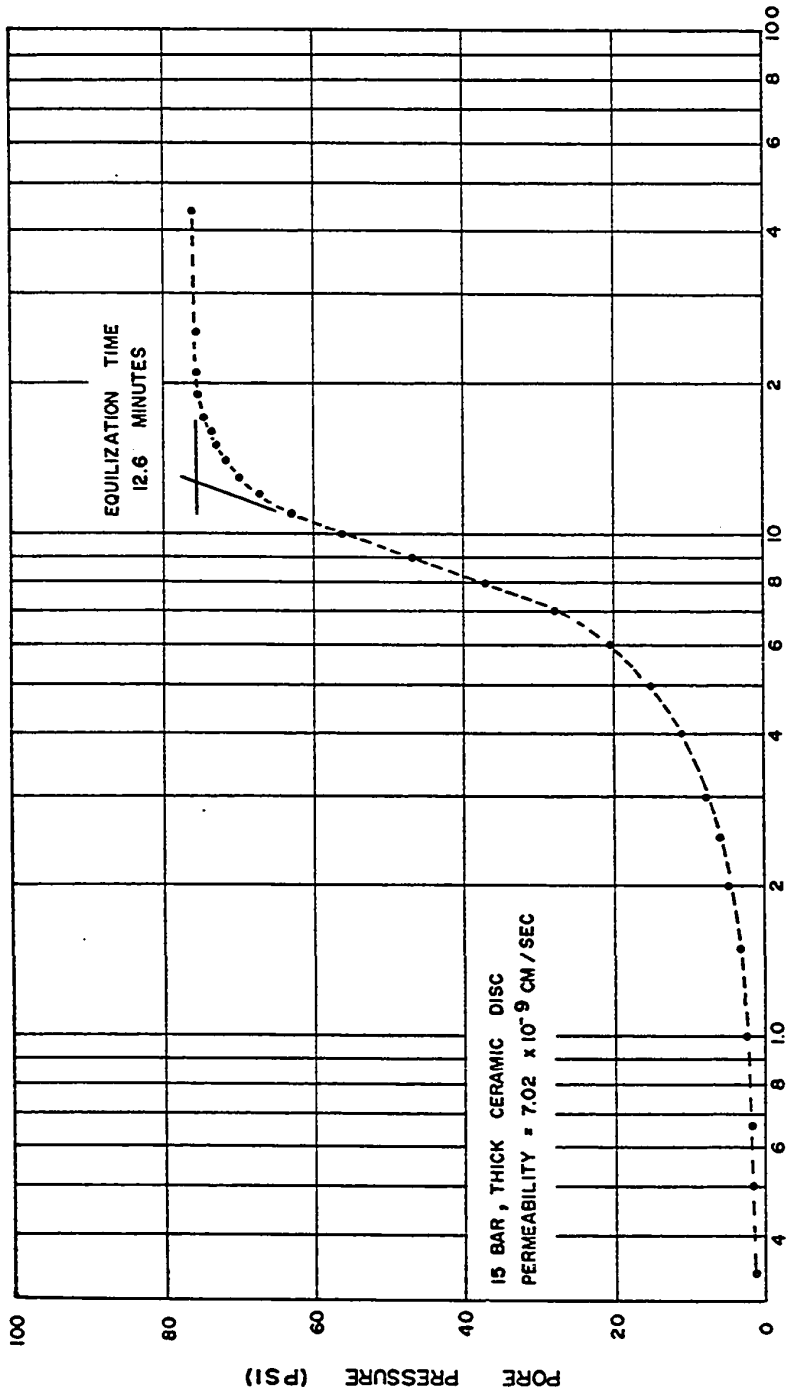


FIGURE E.17 PORE PRESSURE RESPONSE ON ANTEUS OEDOMETER #179
(DECEMBER 17, 1971)

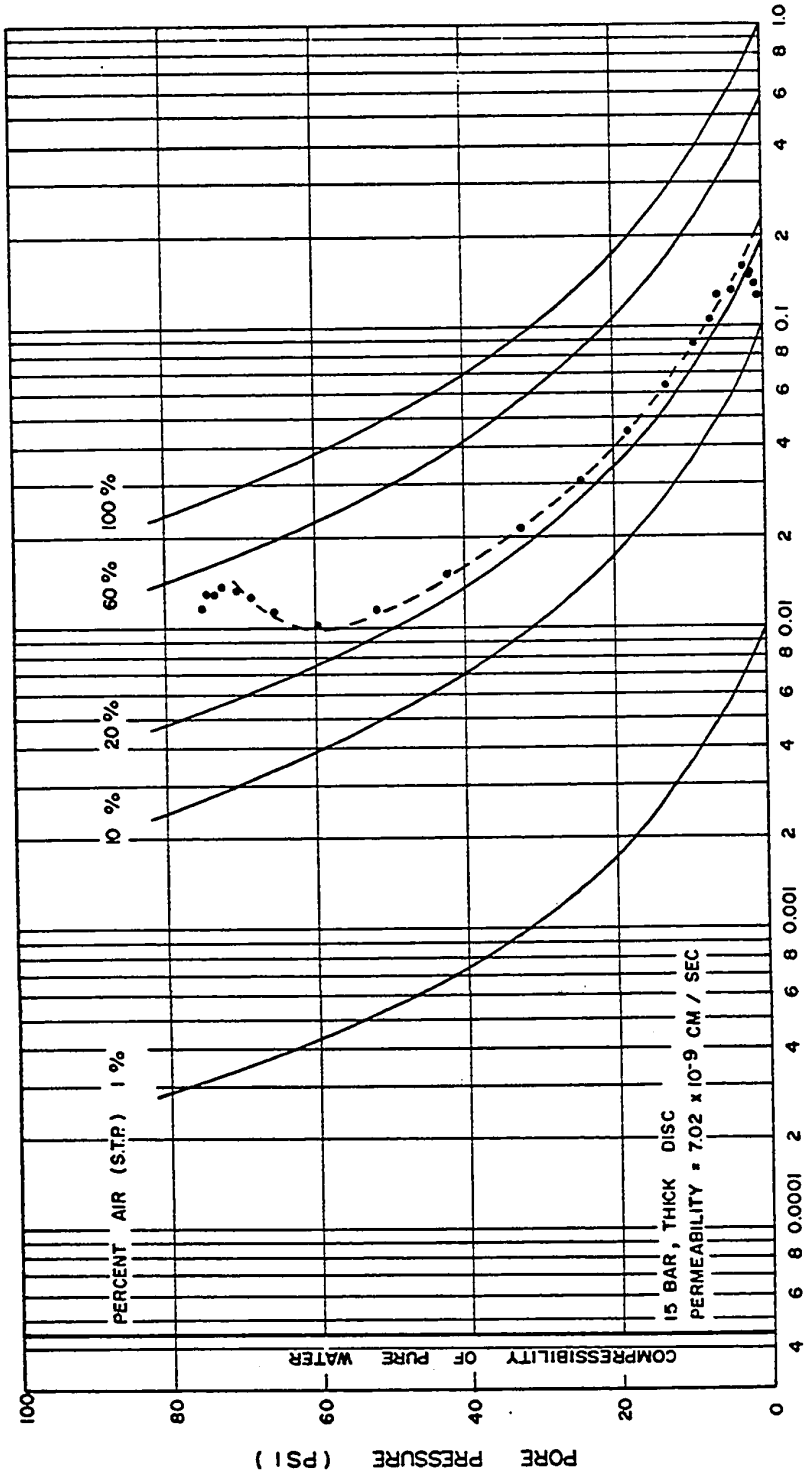


FIGURE E.18 COMPRESSIBILITY OF THE FLUID IN THE PORE PRESSURE MEASURING SYSTEM ON ANTEUS OEDOMETER # 179 (DECEMBER 17 , 1971)

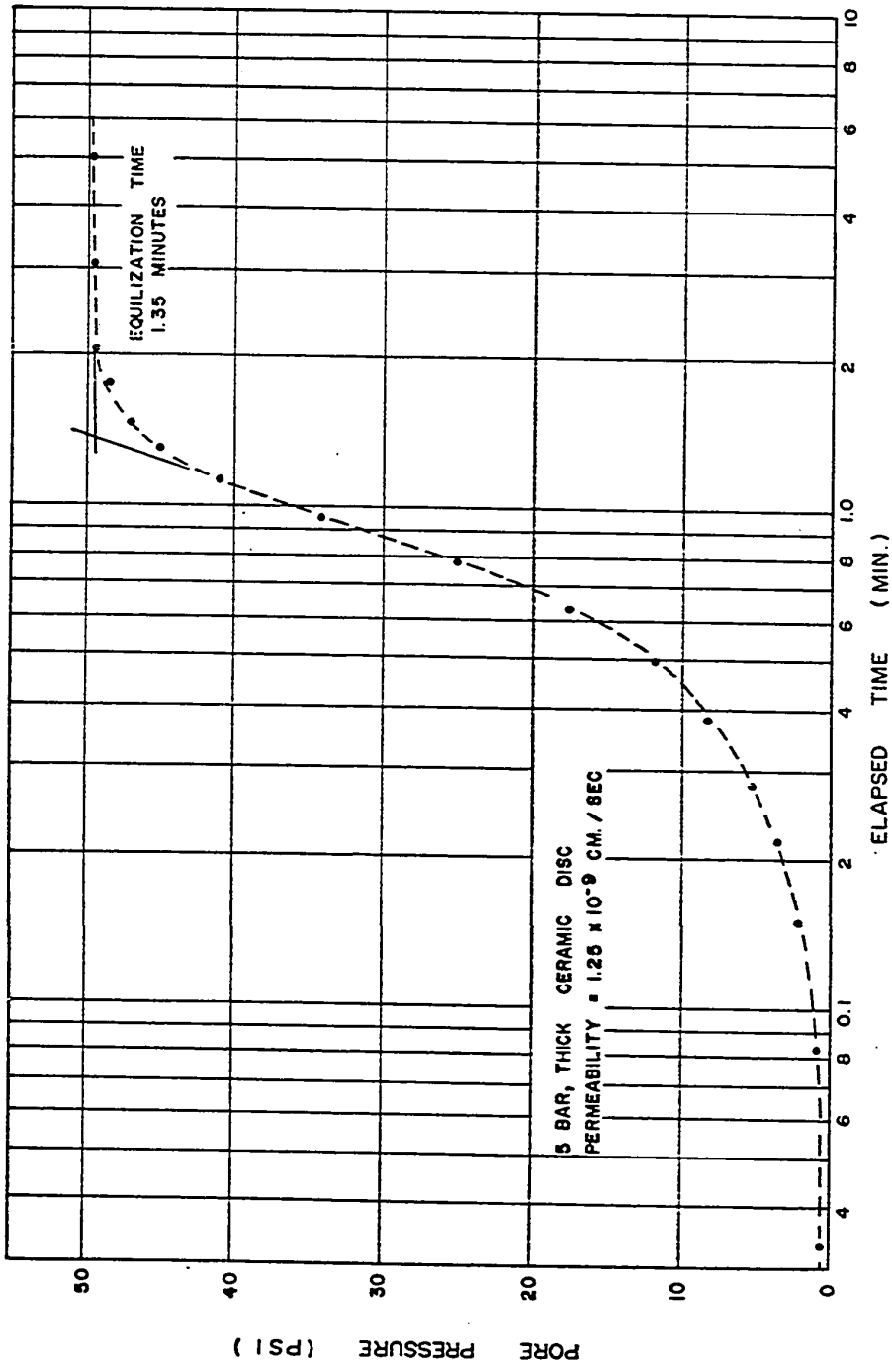


FIGURE E.19 PORE PRESSURE RESPONSE ON ANTEUS OEDOMETER #177 (JAN. 7, 1972)

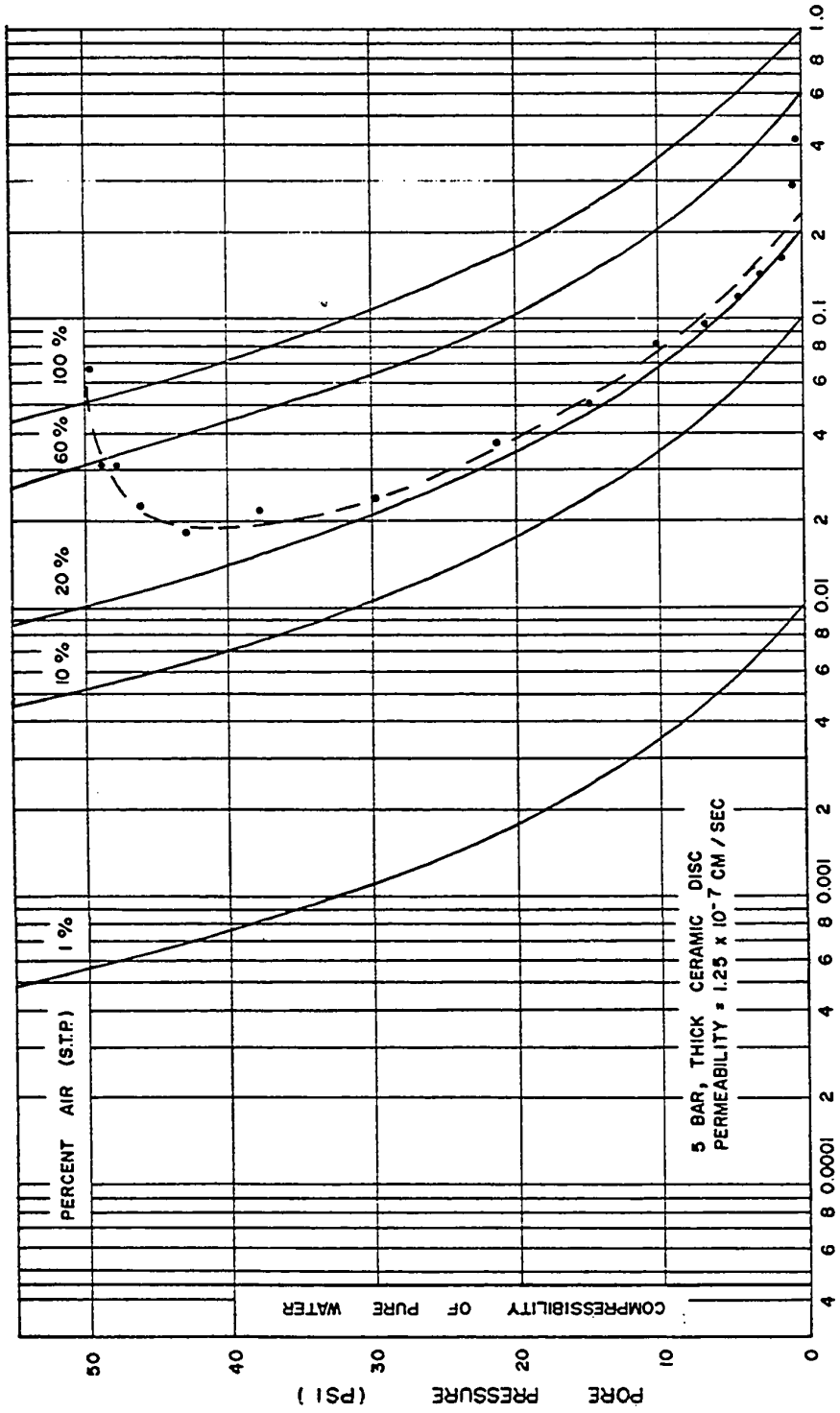


FIGURE E.20 COMPRESSIBILITY OF THE FLUID IN THE PORE PRESSURE MEASURING SYSTEM OF ANTEUS OEDOMETER #177 (JAN. 7, 1972)

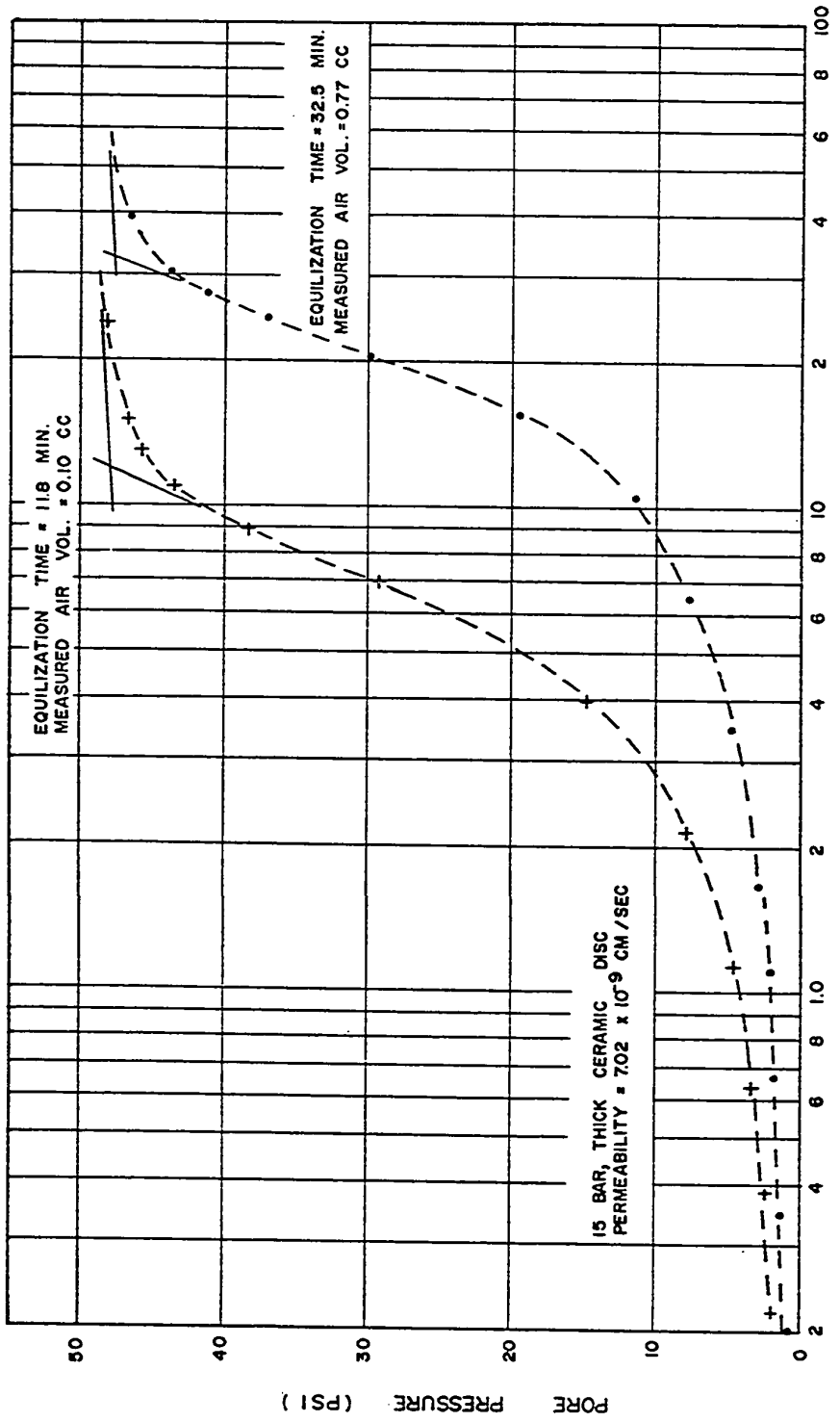


FIGURE E.21 PORE PRESSURE RESPONSE ON OEDOMETER #179 (JAN. 24, 1972)

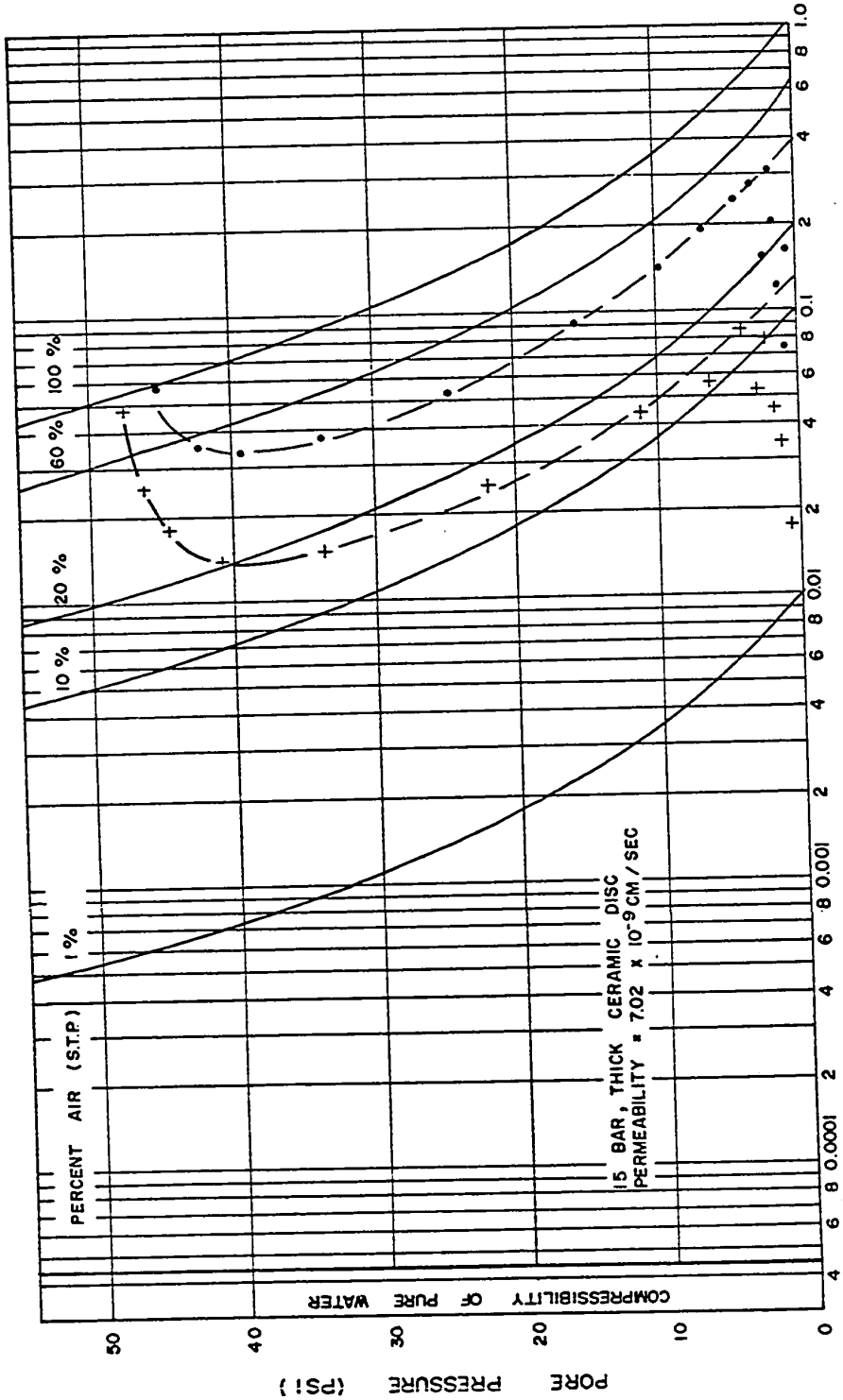


FIGURE E.22 COMPRESSIBILITY OF THE FLUID IN THE PORE PRESSURE MEASURING SYSTEM ON OEDOMETER # 179 (JAN. 24, 1971)

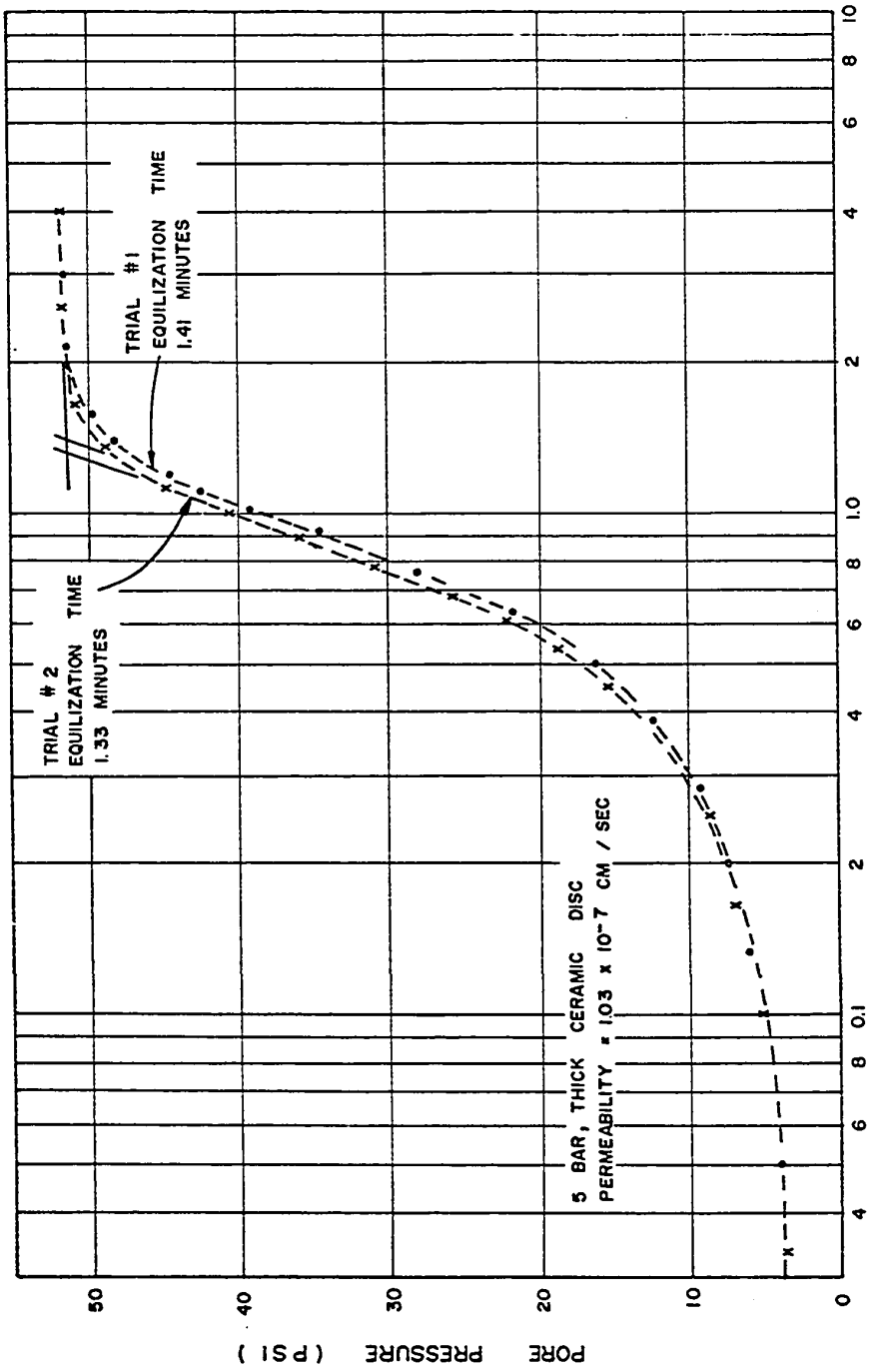


FIGURE E.23 PORE PRESSURE RESPONSE FOR TRIAXIAL #2 (FEB. 18, 1972)

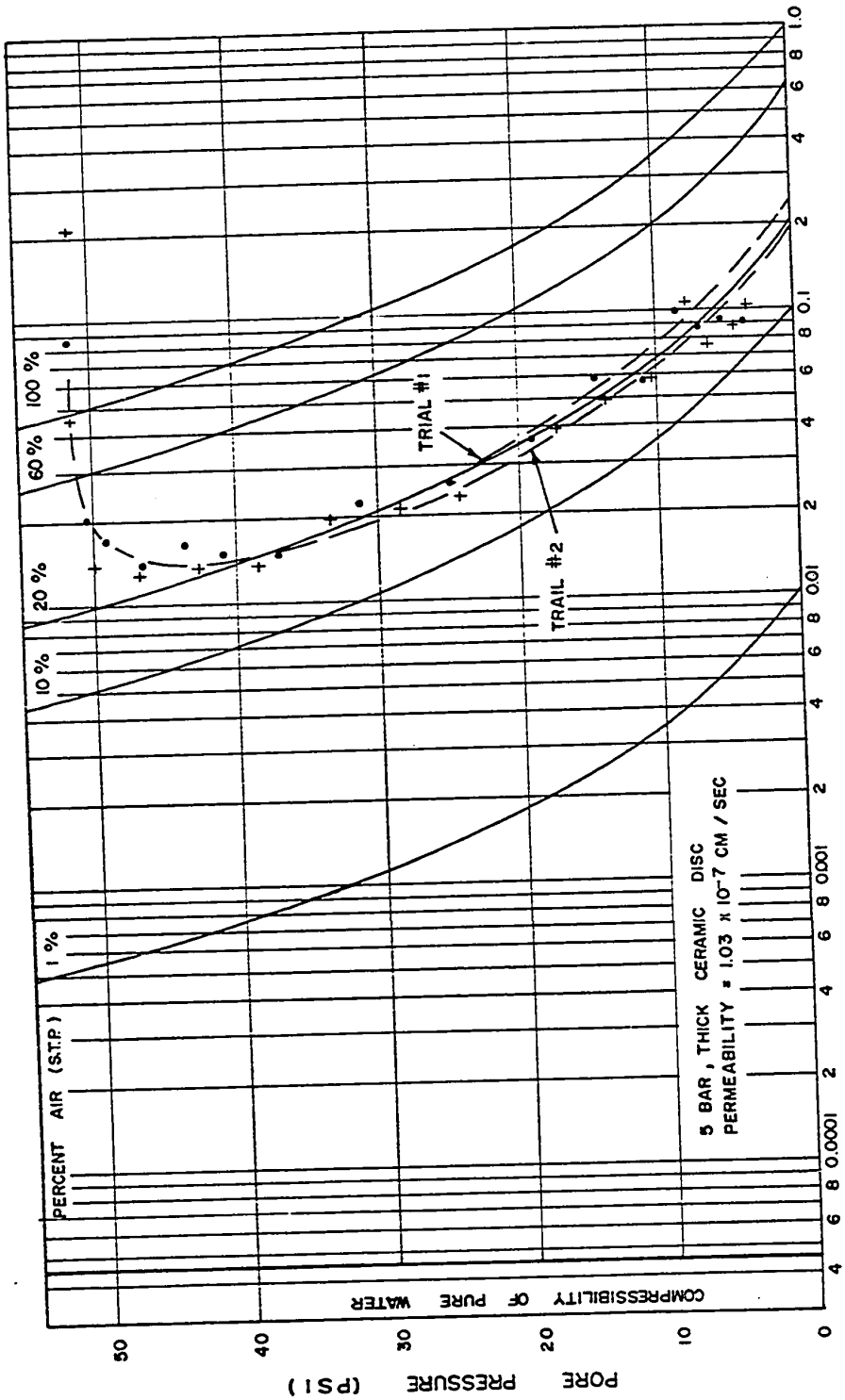


FIGURE E.24 COMPRESSIBILITY OF THE FLUID IN THE PORE PRESSURE MEASURING SYSTEM ON TRIAXIAL #2 (FEB. 18, 1972)

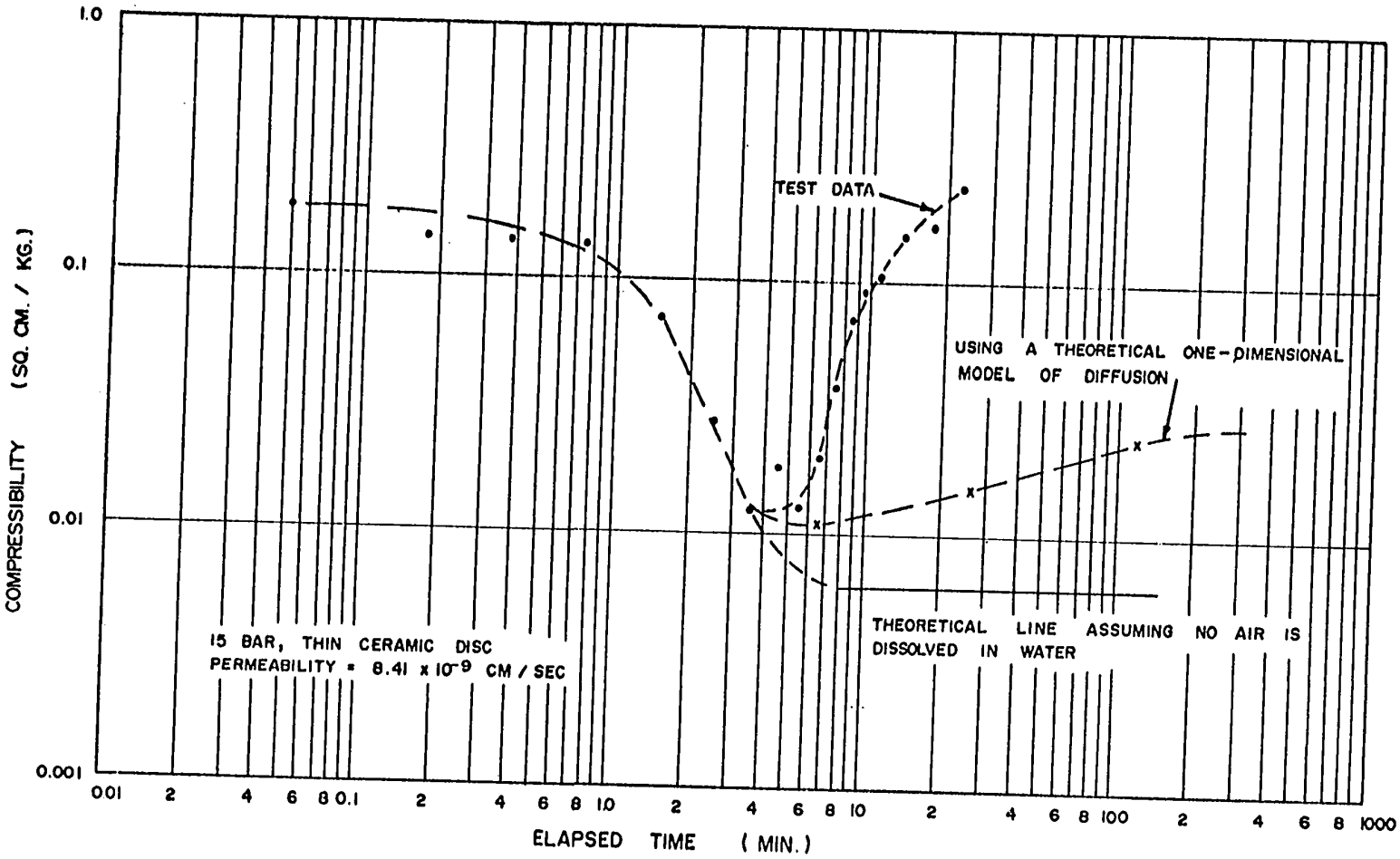


FIGURE E.25 DEVELOPMENT OF COMPRESSIBILITY WITH TIME FOR OEDOMETER #179 (OCT. 27, 1971)

amenable to analysis. Minute volume changes associated with the seating of the components of the compartment (i.e. O-rings in the valves) may also be significant during the final stages of equilibrium. Any leakage from the compartment would also be expressed as a dramatic increase in compressibility.

The equation used to compute the compressibility is sensitive to the initial, absolute, compartment pressure measurement (Figure E.23) and the applied pressure in the chamber. For example, a fictitious alteration of the applied chamber pressure can cause the upper portion of the compressibility curve to shift from the extreme right to a vertical position or even to the left (Figure E.18).

If the coefficient of permeability were reduced at low hydraulic gradients, the described shift to the right can be explained. The only known reason for a decrease in the apparent coefficient of permeability is the presence of impurities in the ceramic disc. During the research program it was noted that the presence of n-Hexane in the disc produced a relatively high threshold gradient with respect to the passage of water. The interfacial tension between the n-Hexane and water appeared to cause a closure of the pores. It is possible that this type of effect could be produced on a much smaller scale as a result of impurities in the pore fluid. One set of permeability tests presented in Appendix B showed that the coefficient of permeability decreased slightly with a decrease in hydraulic gradient.

E-7 Comparison of Experimental Data with the Theory

As previously stated, two variables are necessary to describe the response curves (i.e. slope of the response curve and equilization time). Since the slope of the response curve is dependent on only the applied chamber pressure, there is a unique relationship between these two variables (Figure E.26). The experimental results all lie close to the theoretical line, indicating good agreement. The moderate scatter is partly related to the difficulty in accurately measuring the slope of the response curve. However, other factors are likely involved. It should be noted that a couple of the tests were performed on discs with cracks. Also, the discs treated with acetone have similar slopes. Leaks from the compartment would tend to produce a shifting to the left; however this is not believed to be a factor in the results (Appendix A).

The experimental and theoretical times for equilization (for an applied pressure of 50 psi) are compared on Figure E.27. The equilization time is assumed fixed and can be plotted versus the measurement of either the initial amount of air or the compliance factor. The percent air is estimated either by flushing out the base plate and measuring the amount of air or from the computed compressibility versus pressure plot. The results indicate close agreement between the compliance factor and the percent air computed from the data. In three cases, the measured air content is too low. This indicates that all the air is not removed during the flushing process. Probably higher flushing pressures would have proven more satisfactory.

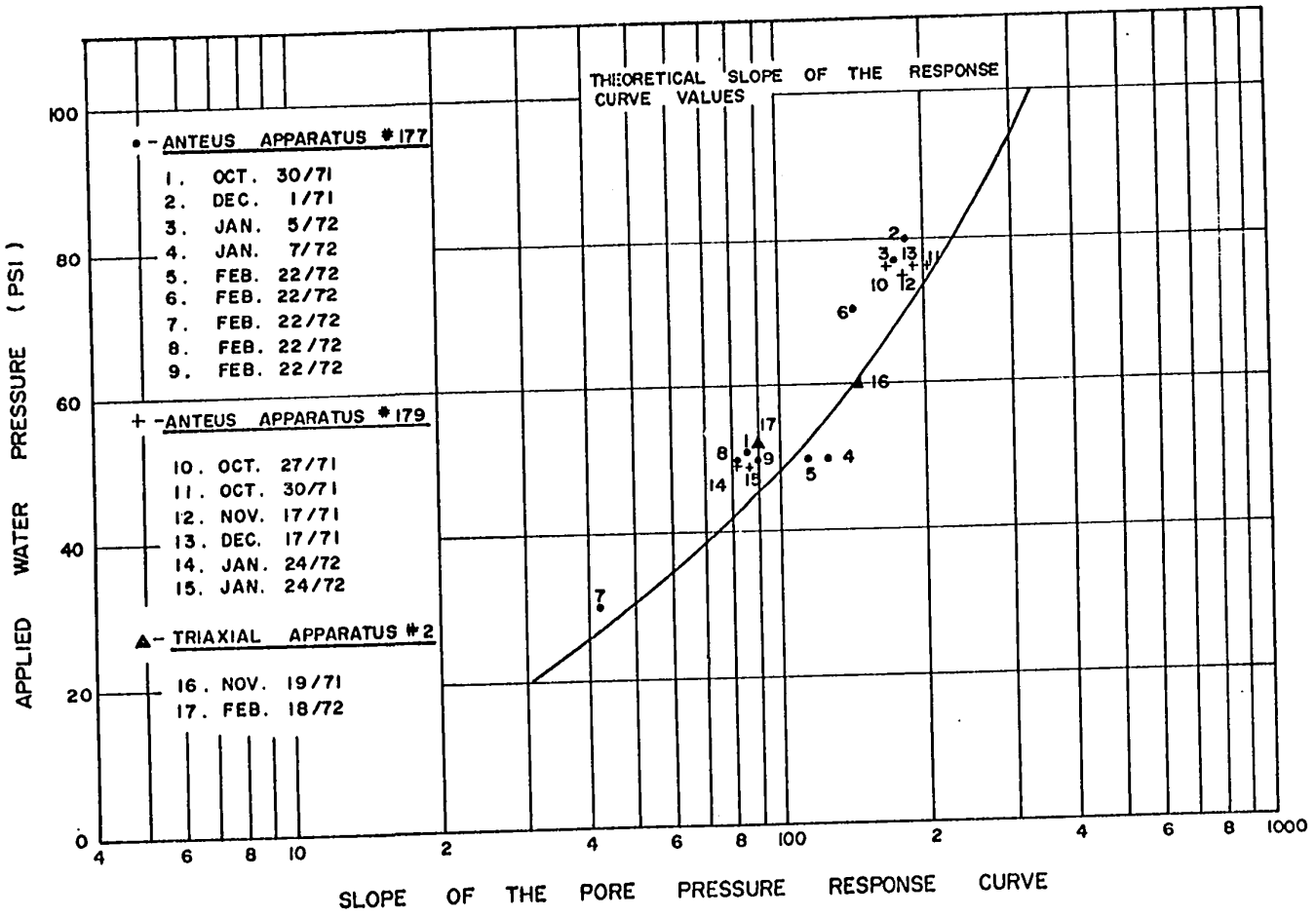


FIGURE E.26 COMPARISON OF THE EXPERIMENTAL 'SLOPE OF THE RESPONSE CURVE' WITH THEORETICAL VALUES

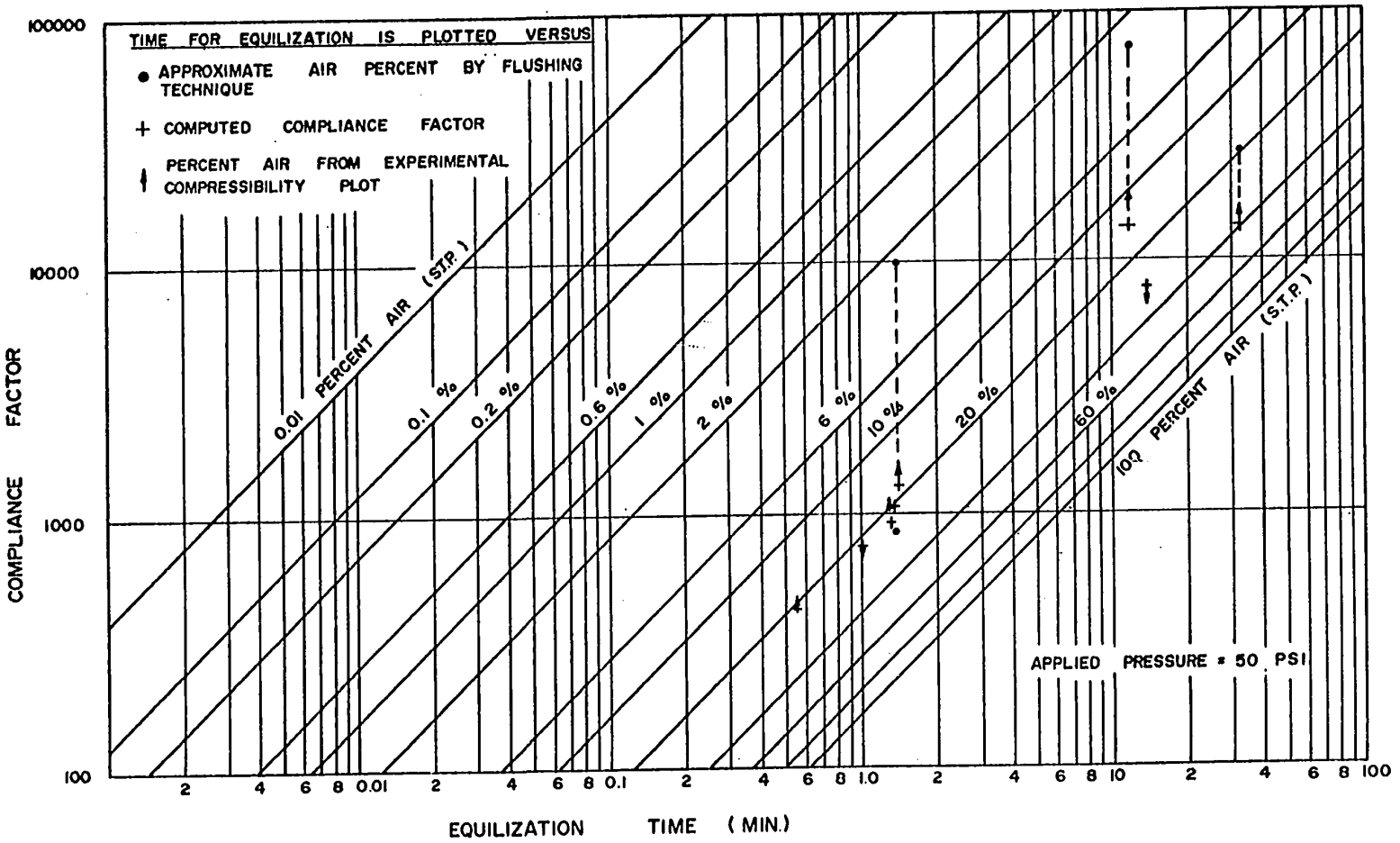


FIGURE E.27 COMPARISON OF EXPERIMENTAL AND THEORETICAL TIMES FOR PORE PRESSURE EQUILIZATION

This observation does not limit the effectiveness of the flushing technique since it is the relative change in diffused air volume that is of importance. When performing tests on unsaturated soils it was observed that the amount of air flushed out depended to some extent on the pressure differential used for flushing. The present results indicate that the increased pressure was producing more thorough flushing.

There also is the possibility that there was not as much air in the compartment as the theoretical computations insinuate. However, even if this is the case, the compressibility due to the volume change of the compartment must also be non linear and behave as an air-water mixture. In other words, either interpretation verifies that the assumed constitutive relationship is correct. Further verification of this point is presented in the direct compressibility measurements in Chapter V.

The experimental data shows reasonable agreement with the theory for both the slope of the response curve and the equilization time. This lends credence to the assumed constitutive relationship for the air-water mixture. The effect of air and the difficulty of obtaining a completely saturated measuring system are clearly depicted. An assumption that the compressibility of the fluid in the measuring system is equal to that of pure water could not produce results similar to those presented.

E.8 Relationship Between Stiffness Ratio and Compliance Factor

The volumetric compliance of the pore water measuring system was defined as λ (the system volume change per unit pressure change) by Gibson (1963), Perloff, Nair and Smith (1965), Northey and Thomas (1965) and Christie (1965). The units used for the present comparison are metric (i.e. cc per kg/cm^2). The volumetric compliance includes both the volume change of the fluid and the chamber; however, the present research indicated that the compressibility of the fluid is of prime importance. At least, the constitutive relationship to describe the total volumetric compliance is identical to that of an air-water mixture. The compressibility is defined as

$$\beta = \frac{1}{V} \cdot \frac{\Delta V}{\Delta u} \qquad \text{E.17}$$

but $\Delta V/\Delta u$ is equal to λ. Therefore

$$\lambda = \beta \cdot V \qquad \text{E.18}$$

The stiffness ratio used by previous research workers is defined as

$$\eta = \frac{A \cdot H \cdot m_v}{\lambda} = \frac{A \cdot H \cdot k_{soil}}{\lambda \cdot c_v \cdot \gamma_w} \qquad \text{E.19}$$

The compliance factor defined in the present research is

$$C = \frac{d \cdot V \cdot \gamma_w}{k_{disc} \cdot A} \qquad E.20$$

or by rearranging

$$\frac{A}{V \cdot \gamma_w} = \frac{d}{C\ k_{disc}} \qquad E.21$$

Substituting equations E.18 and E.21 into A.19 and rearranging gives

$$\eta = \frac{H \cdot k_{soil}}{c_v} \cdot \frac{d}{\beta \cdot C \cdot k_{disc}} \qquad E.22$$

Define C_1 as $H \cdot k_{soil}/c_v$ and C_2 as $d/(\beta \cdot C \cdot k_{disc})$.

The stiffness ratio is therefore composed of two parts; the compliance of the soil (C_1) and the compliance of the measuring system (C_2).

Using this modified definition of stiffness ratio it is possible to again examine the pore pressure response at the base and the distribution throughout a sample in the oedometer (single-drainage). The pore pressure for a saturated soil is governed by the differential equation

$$c_v \frac{\partial^2 u}{\partial x^2} = \frac{\partial u}{\partial t} \qquad E.23$$

for $0 \leq x \leq H$ and

$t > 0$

The compliance of the measuring system necessitates the flow of some water into the system in order to register a response. The quantity per unit time is

$$\dot{q} = \beta \cdot V \cdot \frac{\partial u}{\partial t} \qquad \text{E.24}$$

where $\partial u/\partial t$ is the rate of pressure change in the system. The flow out of the soil sample at the base is in accordance with Darcy's Law.

$$q = k_i A = \frac{k \cdot A}{\gamma_w} \left(\frac{\partial u}{\partial x}\right)_{x=H} \qquad \text{E.25}$$

The solution to equation E.26 is the same at that presented by Carslaw and Jaeger (1956) for heat conduction through a flat plate in contact with a well-stirred liquid.

$$u = 2u_o \sum_{n=1}^{\infty} \frac{(A_n + \eta^2/A_n)\sin A_n - \eta}{(A_n^2 + \eta^2 + \eta)\sin A_n} \cdot \sin\left(\frac{A_n x}{H}\right) e^{-A_n^2 T} \qquad \text{E.26}$$

where u_o = initial uniform pore pressure

$\eta = \dfrac{H \cdot k_{soil}}{c_v} \cdot \dfrac{d}{\beta \cdot C \cdot k_{disc}}$; the stiffness ratio

A_n = positive roots of $A_n \tan A_n = \eta$

e = base of natural logarithm

$T = \dfrac{c_v t}{H^2}$; dimensionless time factor.

Equation E.26 must be solved by an iterative process since η involves a pore pressure term in the compressibility variable, β.

$$\beta = \beta_w \cdot S + \frac{(1-S)}{u_a} \qquad \text{E.27}$$

Time will not be expended at present to solve equation E.27.

E-9 Effect of Acetone on Pressure Response

The 5 bar, ceramic disc on the Anteus Oedometer #177 was cleaned by flushing with acetone for approximately one day. Then the disc was rinsed with distilled, de-aired water for about one day. Several response tests were then performed (Figures E.28 and E.29). The results indicate that the slopes of the response curves were approximately what the theory would predict. However, the equilization time is several times faster than that predicted by the theory. Using the previously proposed theory, the compressibility of the measuring system fluid must be in the order of magnitude of that of pure water. Even in the case where all the water was removed from the measuring system, (Figure E.29) the computed compressibility corresponds to an initial air content of 0.08 percent.

The plot of equilization time versus compliance factor shows the extreme scatter in the data (Figure E.30). It should also be noted that no changing of the various constants involved in the computations can produce curves that fit the theory. This shows that the previous theory does not explain the observed phenomena.

The reason for the rapid response is believed related to the high vapor pressure of the acetone (approximately 7 psi) and the reaction that occurs when acetone and water are mixed. The acetone in

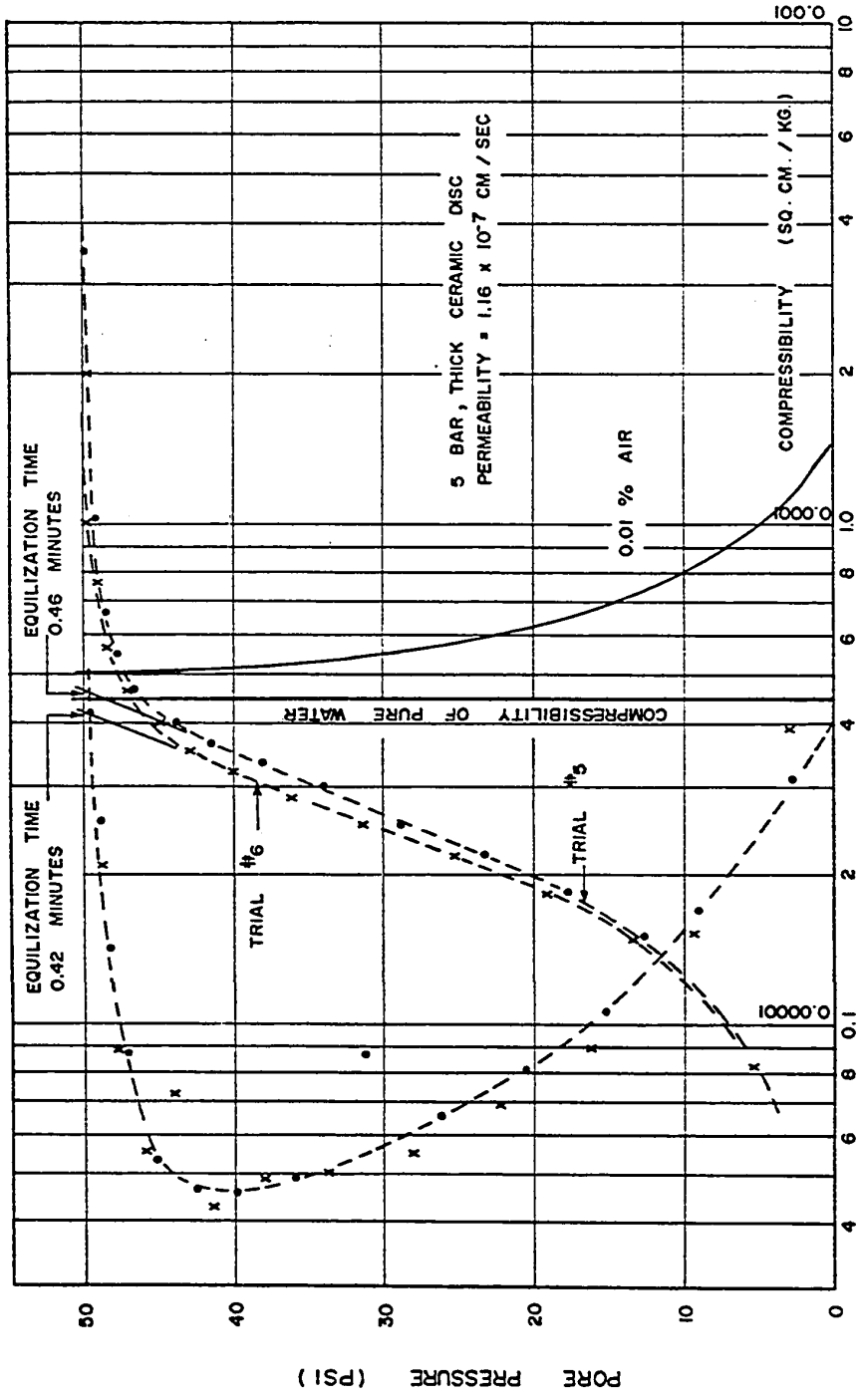


FIGURE E.28 PORE PRESSURE RESPONSE AND COMPRESSIBILITY CURVES FOR OEDOMETER #177 (FEB. 22, 1972)

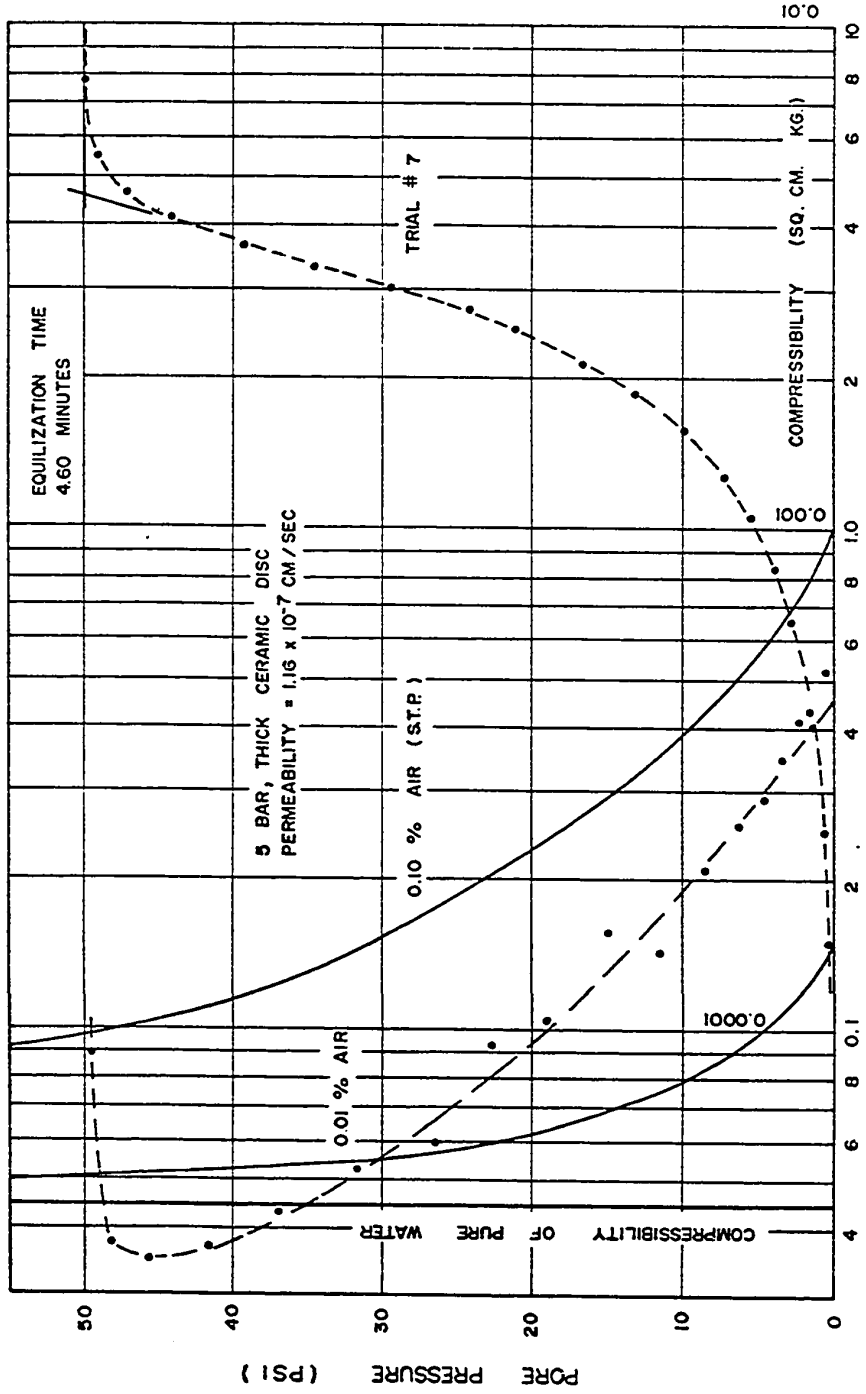


FIGURE E.29 PORE PRESSURE RESPONSE AND COMPRESSIBILITY CURVES FOR OEDOMETER #177 (FEB. 22, 1972)

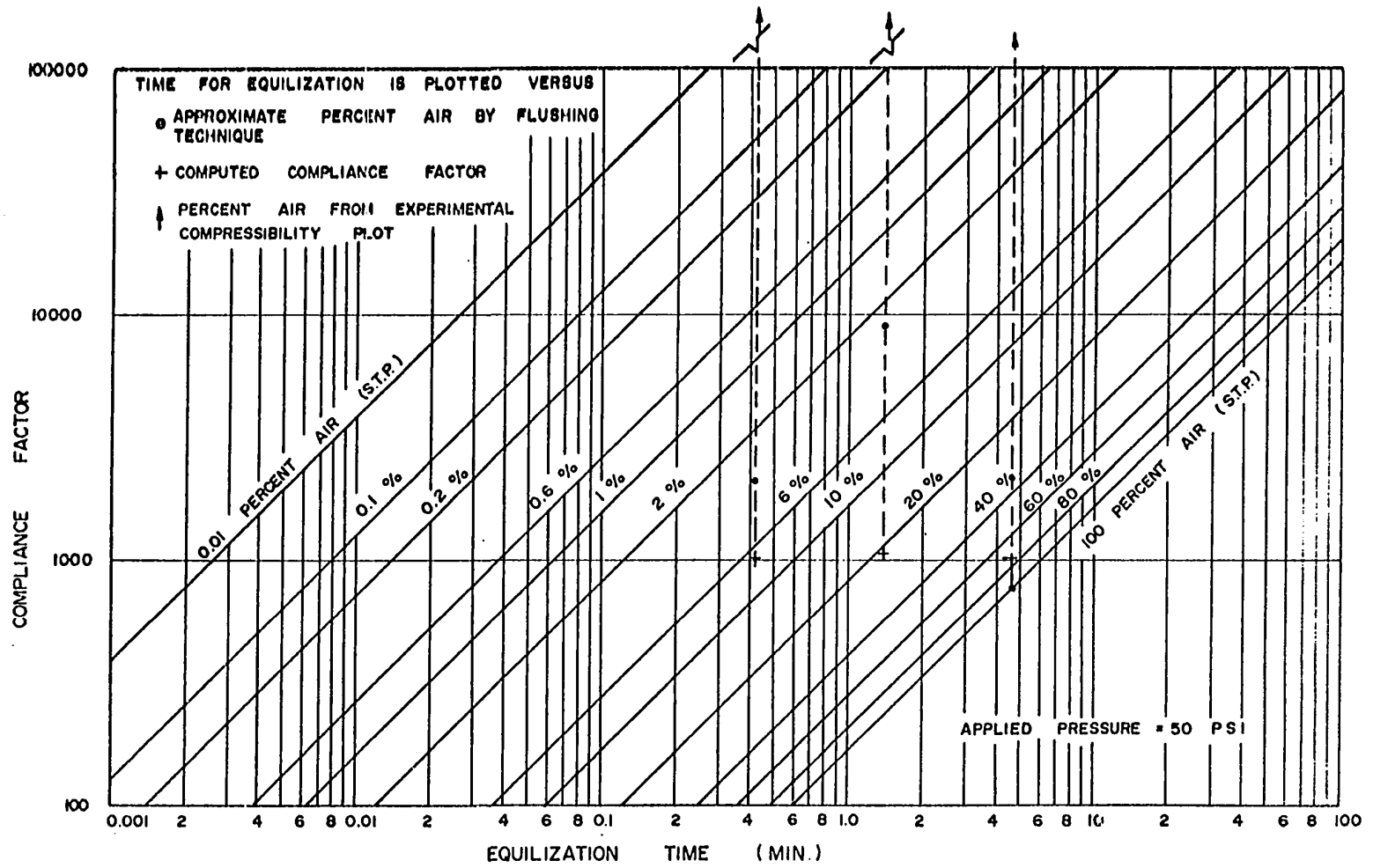


FIGURE E.30 COMPARISON OF EXPERIMENTAL AND THEORETICAL TIME TO EQUILIZATION AFTER WASHING CERAMIC DISC WITH ACETONE

the acetone-water mixture vaporizes almost immediately when subjected to a drop in pressure. The result is a rapid buildup of pressure. The rapid response (eg. 0.44 minutes as compared to 1.5 minutes) suggests interesting possibilities for measuring the pore pressure response of a soil sample.

APPENDIX F

VOLUME CHANGE DATA ON UNSATURATED SOILS

CONTENTS OF APPENDIX F

		Page
F-1	General	F1
F-2	Section I - Direction of Deformations and Hysteresis	F3
F-3	Section II - Uniqueness of Constitutive Surface at a Point	F24
F-4	Section III - Exploration of the Constitutive Surface	F71

VOLUME CHANGE DATA ON UNSATURATED SOILS

F-1 General

Volume change tests were performed on two principle soil types; a highly plastic clay and commercial kaolin. The highly plastic clay was natural, undisturbed samples from Lake Regina (Appendix A). The kaolin samples were prepared by wetting to various water contents and artifically compacting the samples.

The volume change program was not laid down as a fixed set of tests since the object of much of the testing was to ensure the proper functioning of the equipment. The assurance of the proper and accurate performance of the equipment was felt to be of utmost importance. As a result of the flexible testing program, the data in Appendix F are used for several purposes throughout the thesis. Some examples are;

(i) the direction of volumetric deformation analysis

(ii) the analysis of hysteresis

(iii) the evaluation of the uniqueness of the constitutive surface at a point

(iv) the exploration of the entire constitutive surface

(v) the analysis of the performance of the equipment

(vi) the analysis of rate processes.

The test results are presented in three sections.

Section I (Directions of Deformation and Hysteresis)

The first five tests (D-1 to D-5) show typical volumetric deformations resulting from changing various stress components. Four tests (D-6 to D-9) show the volumetric deformation hysteresis resulting from increasing and decreasing the water pressure. Tests D-9 to D-14 show the volumetric deformation hysteresis resulting from increasing and decreasing air pressure.

Section II (Uniqueness of the Constitutive Surface at a Point)

Four samples were tested by alternately varying the total, air and water pressures. A total of 32 tests or increments were performed (C-1 to C-32).

Section III (Exploration of the Constitutive Surface)

Four tests were performed to explore uniqueness of the constitutive surface. A large number of tests would be required to check various stress state variable change combinations. The time-consuming nature of the tests prohibited such a program. Two additional tests were performed on a conventional one-dimensional oedometer.

The main problems associated with the tests revolve about the accurate measurement of the water volume change. The water volume change can be in error due to a lack of or a faulty measurement of diffused air. Over periods of time greater than a few days, the diffused air volume measurements are imperative. The diffused air volume indicators were installed on all apparatus about the first of October 1971. Tests prior to this date do not have corrections applied for

the diffusion of air.

The water volume change measurements were later found to also be appreciably affected by water loss from the samples. In the case of Triaxial Apparatus #2, there was a water loss due to moisture migration through the rubber membrane. This was not remedied until March 10, 1972. Triaxial Apparatus #1 die not appear to undergo losses of moisture even over long time periods. Modified Oedometers #177 and #179 had a problem of moisture loss from the chamber. It was originally anticipated that the chambers would quickly attain a relative humidity equal to that of the sample and remain constant. However, it appeared that moisture was lost by leakage from the chamber. To overcome this loss, the lucite-walled cells were replaced with stainless steel sleeves, and water was placed at the bottom of the reservoir saturation chamber. Checks were also made to ensure against air loss from the chamber. These remedies were put into affect in approximately March, 1972 and have essentially eliminated losses.

SECTION I

F-2 Directions of Deformation and Hysteresis

F-2.1 General

The tables at the start of Section I summarize data pertinent to the interpretation of the test results. The tables are as follows :

Table F.1 Summary of Soil Properties on Samples Tested to Assess the Directions of Deformation and Hysteresis

Table F.2 Summary of Tests to Evaluate the Directions of Deformation and Hysteresis

Table F.3 Volume-Weight Relationship of Samples Tested to Evaluate the Directions of Deformation and Hysteresis

Table F.4 Summary of Pressure Changes for Tests to Evaluate the Directions of Deformation and Hysteresis.

F-2.2 Discussion of the Test Data

The test results are presented in the form of volumetric deformations of the soil structure and water phase versus the logarithm of time. The data are interpreted when used in the body of the thesis and the discussion in the Appendix primarily draws attention to limitations in the testing techniques.

Test D-1 - Apparently there was initially a lack of continuity of the water phase through the ceramic disc. This was either due to cavitation or simply an excess of free air in the base plate. The base plate had not been flushed at the start of the test. The deformation processes appear to start at the time of flushing.

Test D-2 - The upward bend near the end of the water phase deformation curve is related to the loss of water from the sample.

Test D-3 - The discontinuous upward jump in the water phase deformation curve is related to a loss of water from the sample. The moisture moves from the chamber either by leakage of air or diffusion of water through the lucite chamber wall.

Test D-4 - Again moisture is lost from the sample after approximately 400 minutes. The increased degree of saturation beyond 400 minutes is fictitious.

Test D-5 - Moisture lost from the sample after approximately 200 minutes becomes dominant with respect to the water phase deformation curve.

Test D-6 - There appears to be a small amount of moisture loss from the sample after one day. The apparatus appears to have been slightly disturbed at 2900 minutes.

Test D-7 - The moisture loss from the sample after one day is now becoming of significance. The moisture loss has increased from Test D-6, although the air pressure has remained the same.

Test D-8 - The moisture loss has continued to increase with time. It becomes the dominent feature of the water deformation curve after 500 minutes. After 4500 minutes it appears that approximately 0.61 cc of water has been lost.

Test D-9 - There was a faulty measurement of diffused air at an elapsed time of 110 minutes. Once again the moisture losses from the sample are excessive.

Test D-10 - No known testing technique limitations.

Test D-11 - No known testing technique limitations.

Test D-12 - The triaxial cell was heavily jarred at 38 minutes. Apart from that the data is satisfactory.

Test D-13 - There was a substantial diffused air correction at 1400 minutes. This may have been somewhat excessive. Also, there is evidence of some loss of moisture through the triaxial membrane.

Test D-14 - The final water volume reading indicates some loss of water through the rubber membrane.

TABLE F.1

SUMMARY OF SOIL PROPERTIES ON SAMPLES TESTED TO ASSESS

THE DIRECTION OF DEFORMATION AND HYSTERESIS

Lab. Sample No.	Field Test Hole No.	Field Sample No.	Depth	Liquid Limit (%)	Plastic Limit (%)	Plastic Index (%)	Grain Sizes			Soil Description
							Clay (%)	Silt (%)	Sand (%)	
9				64.2	34.7	29.5	63	35	2	Compacted Kaolin (Mold #D)
10				64.2	34.7	29.5	63	35	2	Compacted Kaolin (Mold #E)
11				64.2	34.7	29.5	63	35	2	Compacted Kaolin (Mold #E)
19				64.2	34.7	29.5	63	35	2	Compacted Kaolin
20				64.2	34.7	29.5	63	35	2	Compacted Kaolin

TABLE F.2

SUMMARY OF TESTS TO EVALUATE THE DIRECTION OF DEFORMATION AND HYSTERESIS

Test No.	Sample No.	Date	Starting Time	Total Elapsed Time (Min.)	Apparatus No.	Pressure Change			Comments
						Total (psi)	Air (psi)	Water (psi)	
D-1	9	Aug. 4/71	9:30	7215	T-1	-10.07	- 9.65	- 0.23	Cavitation at the base plate at the start
D-2	10	Aug. 2/71	10:24	1356	OED #177	+13.35	- 0.05	- 0.09	
D-3	10	Aug. 3/71	10:00	1720	OED #177	+ 0.13	+ 0.10	+10.06	
D-4	11	Aug. 2/71	10:15	1365	OED #179	+13.95	0.00	- 0.02	Air not monitored
D-5	11	Aug. 3/71	9:08	1757	OED #179	- 0.14	+ 0.04	+10.12	
D-6	19	Nov.20.71	9:42	3166	OED #179	+ 0.34	+ 0.08	+30.58	Considerable moist air loss from the chamber during this test
D-7	19	Nov.22/71	14:30	5455	OED #179	- 0.22	0.00	+15.54	
D-8	19	Nov.26/71	9:36	4299	OED #179	- 0.07	- 0.06	-15.68	
D-9	19	Nov.29/71	9:20	2900	OED #179	- 0.01	- 0.02	-29.98	
D-10	20	Nov.26/71	10:45	5756	T-2	+ 0.25	-27.75	+ 0.04	
D-11	20	Nov.30/71	10:45	2741	T-2	- 0.11	-14.92	+ 0.16	
D-12	20	Dec. 2/71	8:36	5784	T-2	+ 0.19	+14.94	- 0.04	
D-13	20	Dec. 6/71	9:02	2878	T-2	- 0.38	+27.37	- 0.53	
D-14	20	Dec.10/71	10:30	3150	T-2	- 0.19	- 0.16	+29.28	

TABLE F.3

VOLUME-WEIGHT RELATIONSHIPS OF SAMPLES TESTED

TO EVALUATE THE DIRECTION OF DEFORMATION AND HYSTERESIS

Test No.	Diameter (cm)	Height (cm)	Total Volume (cc)	Volume of Water (cc)	Volume of Air (cc)	Water Content (%)	Void Ratio	Dry Density (PCF)	Degree of Saturation (%)
D-1	10.155	11.784	954.34	379.23	117.12	31.65	1.0838	78.34	76.40
D-2	6.346	2.547	80.57	34.60	3.05	30.81	0.8769	86.97	91.91
D-3	6.346	2.543	80.43	34.50	3.00	30.73	0.8737	87.12	92.01
D-4	6.346	2.555	80.82	35.66	2.66	32.07	0.9015	85.85	93.05
D-5	6.346	2.549	80.63	35.48	2.65	31.91	0.8970	86.05	93.05
D-6	6.350	2.283	72.29	25.27	12.99	28.39	1.1247	76.83	66.04
D-7	6.350	2.283	72.29	31.18	10.52	31.18	1.1247	76.83	72.51
D-8	6.350	2.257	71.47	32.24	5.21	36.22	1.1008	77.70	86.08
D-9	6.350	2.249	71.22	31.82	5.38	35.76	1.0934	77.98	85.54
D-10	10.453	5.867	503.53	175.40	101.73	29.62	1.2242	73.39	63.29
D-11	10.191	5.821	474.80	186.61	61.79	31.51	1.0972	77.83	75.12
D-12	9.834	5.747	436.46	197.31	12.76	33.32	0.9279	84.67	93.93
D-13	9.822	5.747	435.46	194.25	14.82	32.80	0.9235	84.87	92.91
D-14	9.832	5.758	437.16	190.22	20.54	32.12	0.9310	84.54	90.25

TABLE F.4

SUMMARY OF PRESSURE CHANGES FOR TESTS TO EVALUATE

THE DIRECTION OF DEFORMATION AND HYSTERESIS

Test No.	Initial Conditions						Final Conditions					
	σ (psi)	u_a (psi)	u_w (psi)	$\sigma-u_w$ (psi)	$\sigma-u_a$ (psi)	u_a-u_w (psi)	σ (psi)	u_a (psi)	u_w (psi)	$\sigma-u_w$ (psi)	$\sigma-u_a$ (psi)	u_a-u_w (psi)
D-1	101.30	80.74	59.74	--	--	--	81.88	61.39	59.79	22.09	20.49	1.60
D-2	72.14	59.30	42.56	29.59	12.84	16.74	85.49	59.25	42.47	43.01	26.23	16.78
D-3	85.49	59.25	42.47	43.01	26.23	16.78	85.62	59.35	52.53	33.09	26.27	6.81
D-4	33.99	20.05	6.07	27.93	13.95	13.98	47.94	20.05	6.05	41.89	27.89	14.00
D-5	47.94	20.05	6.05	41.89	27.89	14.00	47.80	20.09	16.17	31.63	27.71	3.93
D-6	87.65	59.94	0.82	86.84	27.71	59.13	87.99	60.02	31.40	56.59	27.97	28.63
D-7	87.99	60.02	31.40	56.59	27.97	28.63	87.77	60.02	46.94	40.83	27.74	13.08
D-8	87.77	60.02	46.94	40.83	27.74	13.08	87.70	59.96	31.26	56.44	27.74	28.70
D-9	87.70	59.96	31.26	56.44	27.74	28.70	87.69	59.94	1.28	86.41	27.74	58.66
D-10	68.91	57.70	6.08	62.84	11.22	51.62	69.16	29.95	6.12	63.04	39.21	23.82
D-11	69.16	29.95	6.12	63.04	39.21	23.83	69.05	15.03	6.28	62.77	54.02	8.76
D-12	69.05	15.03	6.28	62.77	54.02	8.76	69.24	29.86	6.24	63.01	39.38	23.62
D-13	69.24	29.86	6.24	63.01	39.38	23.62	68.86	57.23	5.71	63.15	11.63	51.52
D-14	88.67	77.16	25.72	62.95	11.51	51.44	88.48	77.00	55.00	33.48	11.48	22.00

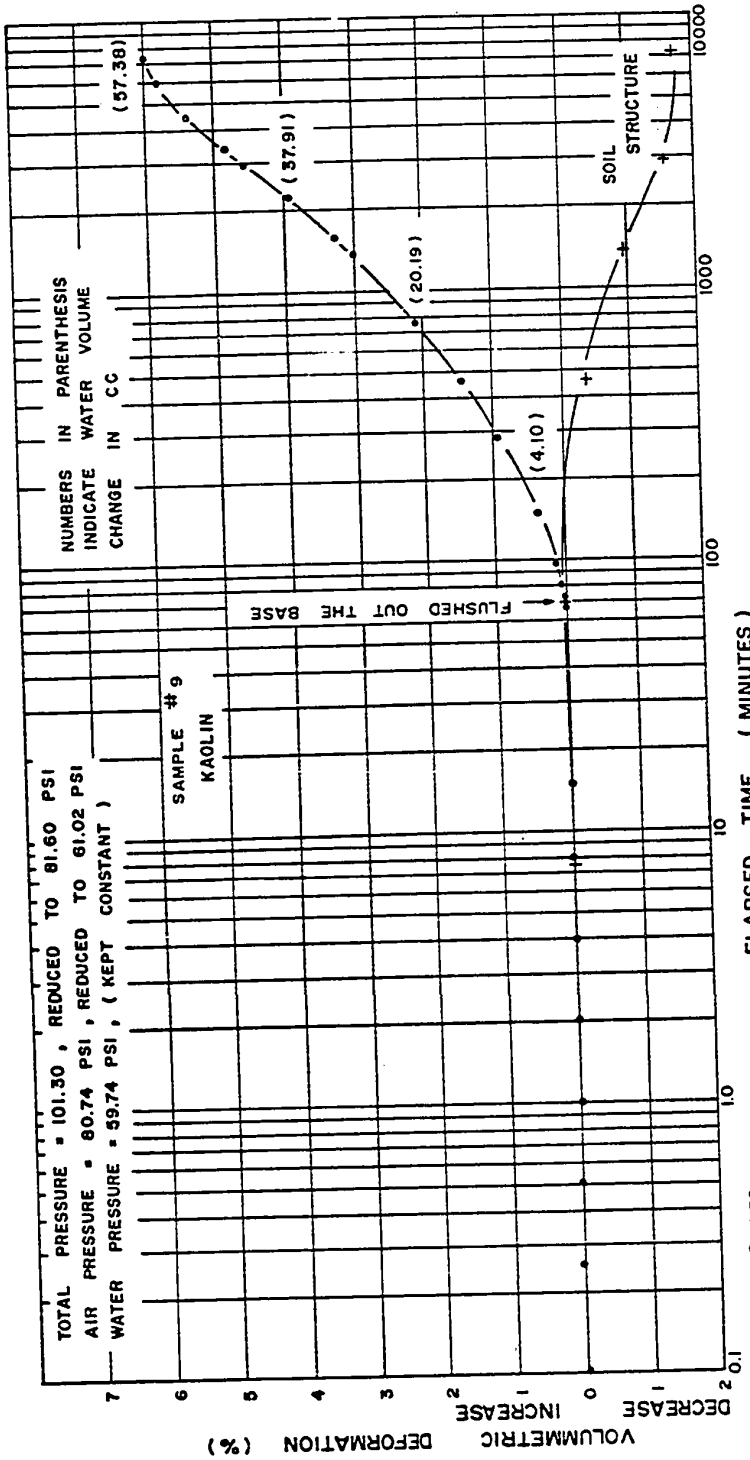


FIGURE F.1 SOIL STRUCTURE AND WATER PHASE VOLUME CHANGES (D-1)

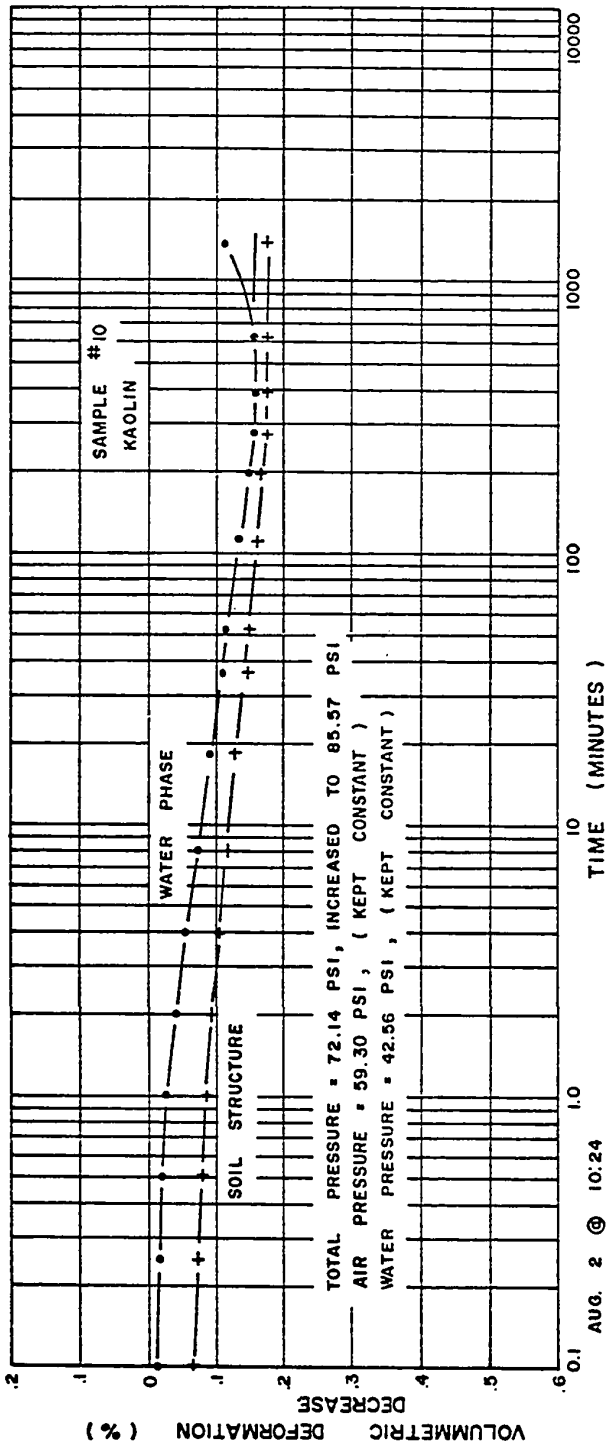


FIGURE F. 2 SOIL STRUCTURE AND WATER PHASE VOLUME CHANGE (D - 2)

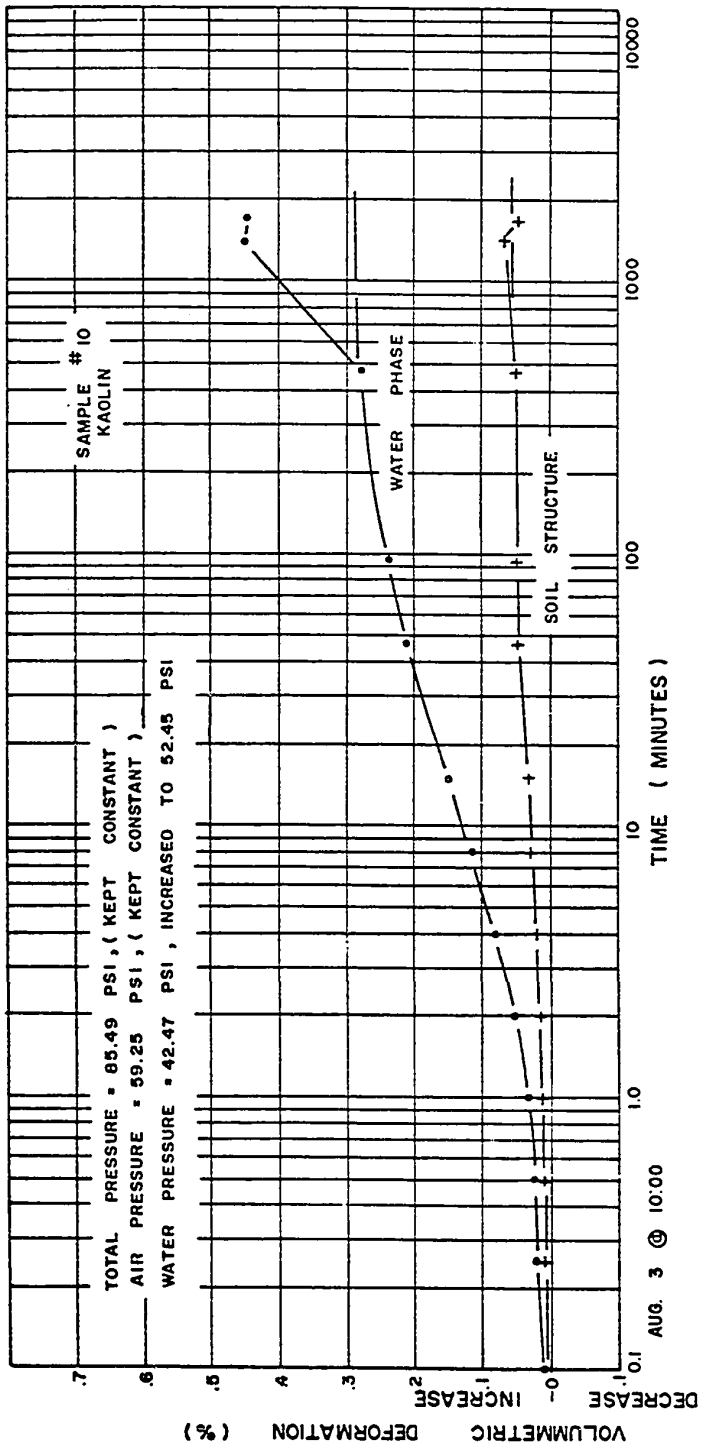


FIGURE F.3 SOIL STRUCTURE AND WATER PHASE VOLUME CHANGES (D-3)

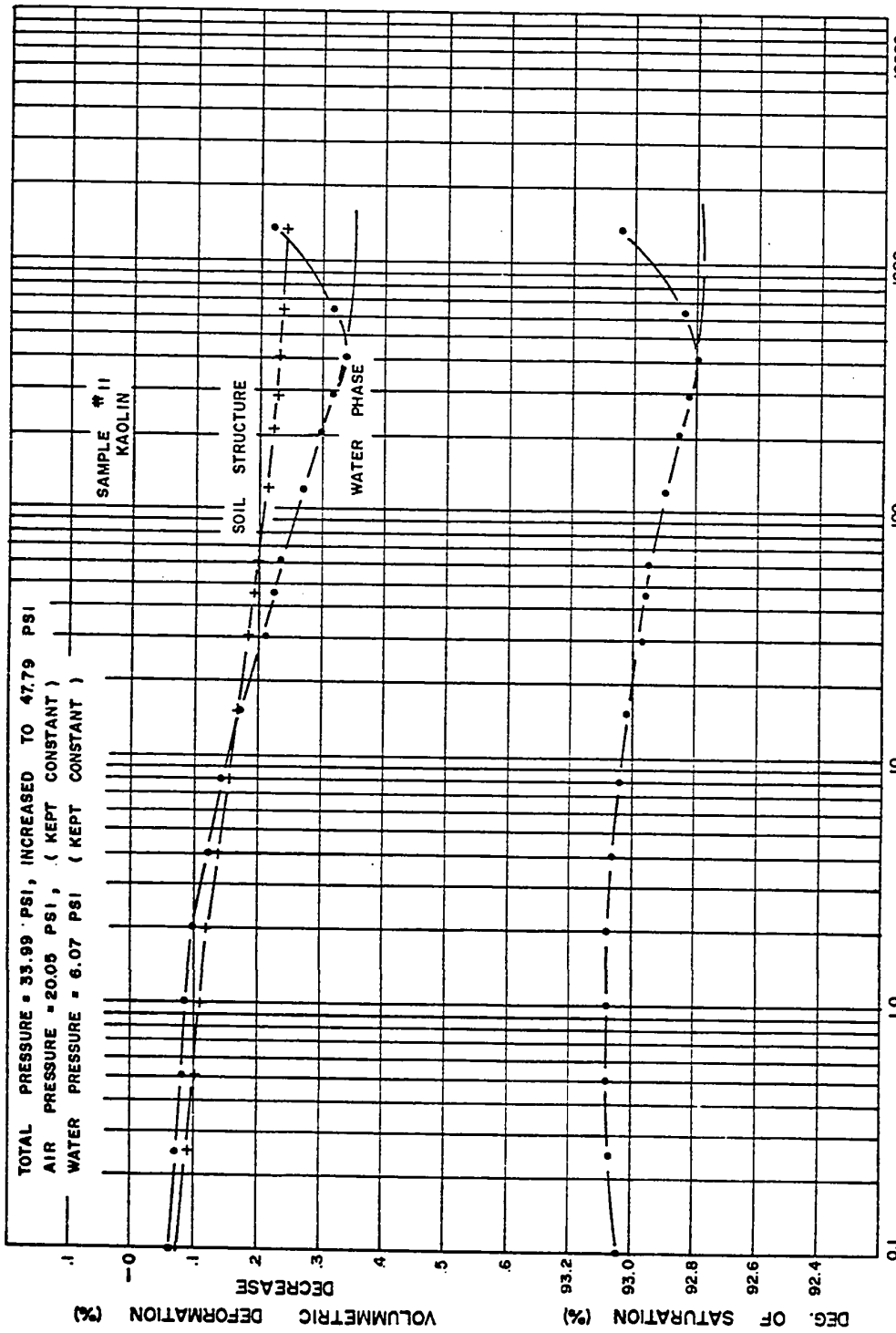


FIGURE F. 4 SOIL STRUCTURE AND WATER PHASE VOLUME CHANGES (D-4)

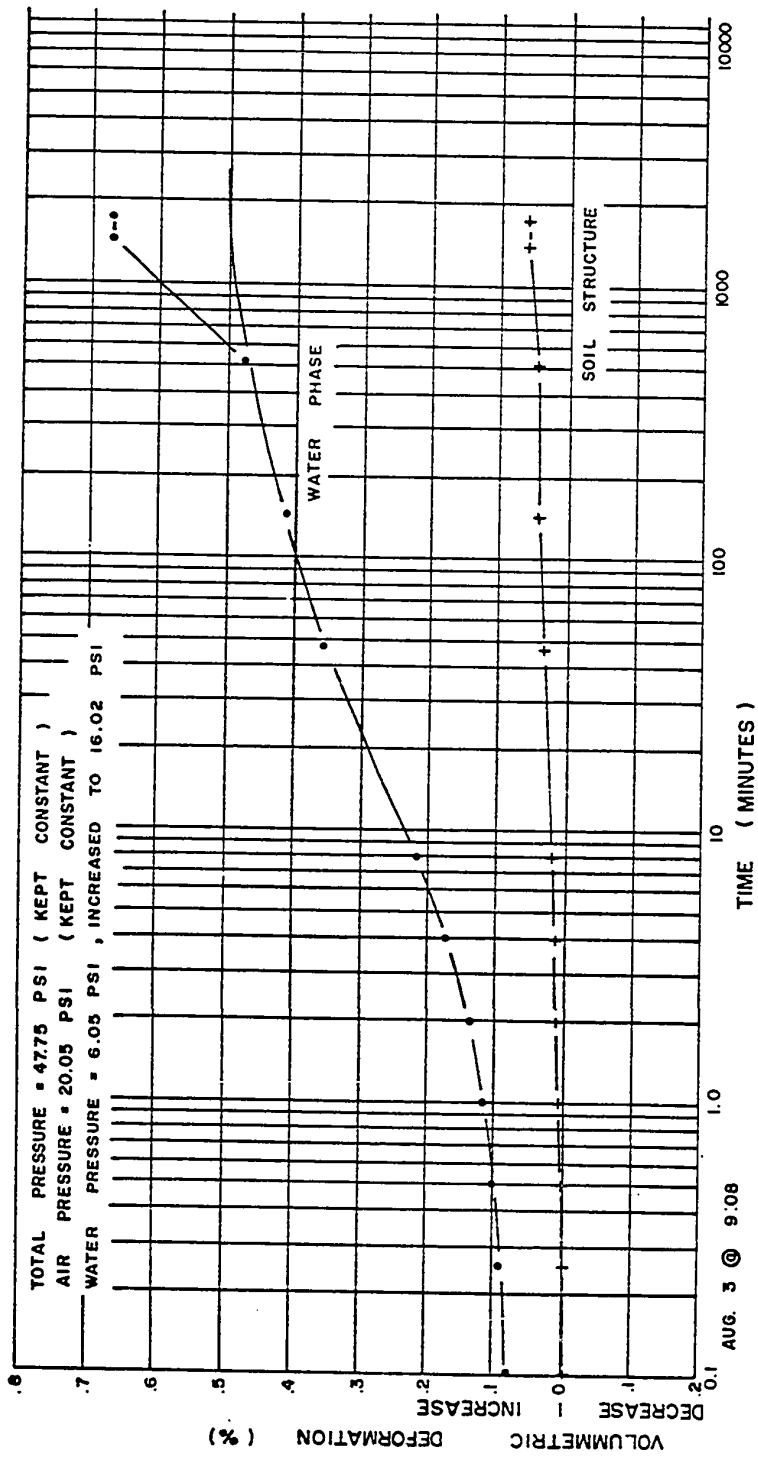


FIGURE F.5 SOIL STRUCTURE AND WATER PHASE VOLUME CHANGES (D-5)

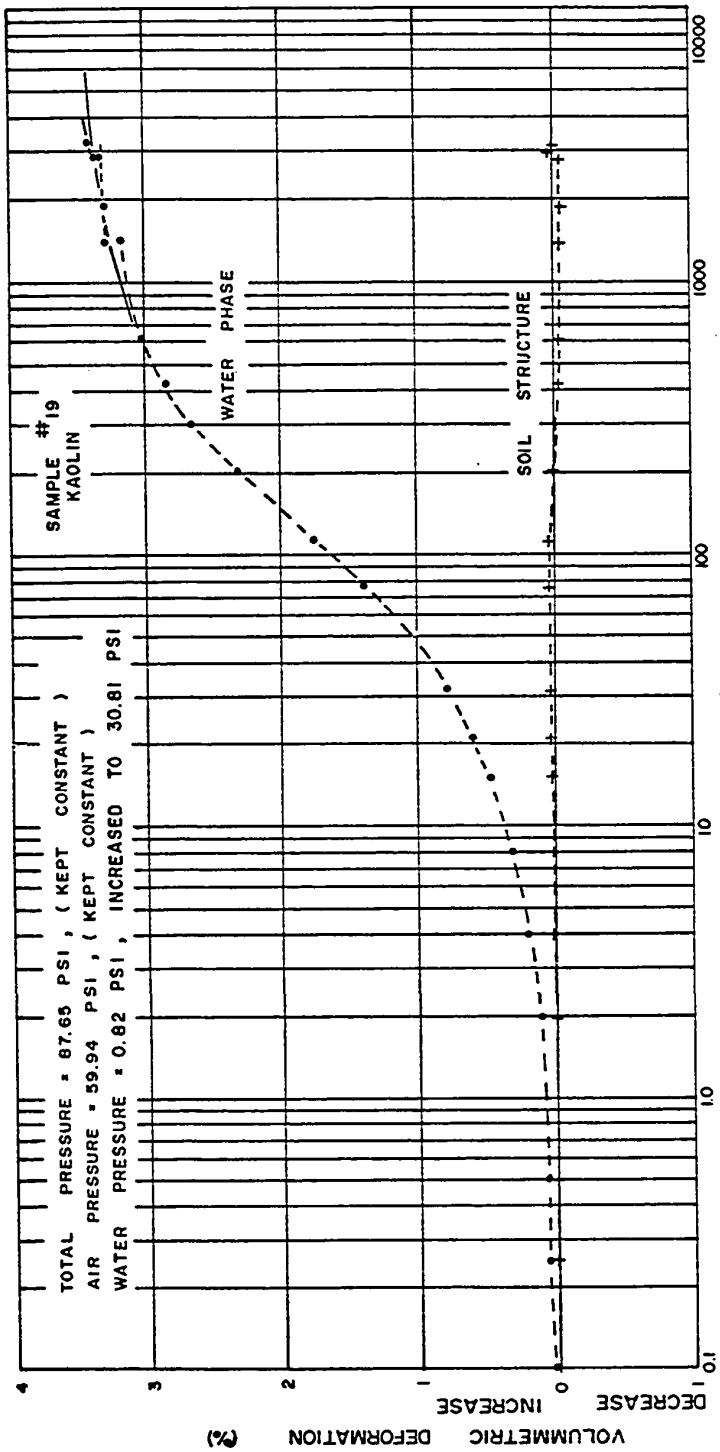


FIGURE F. 6 SOIL STRUCTURE AND WATER PHASE VOLUME CHANGES (D-6)

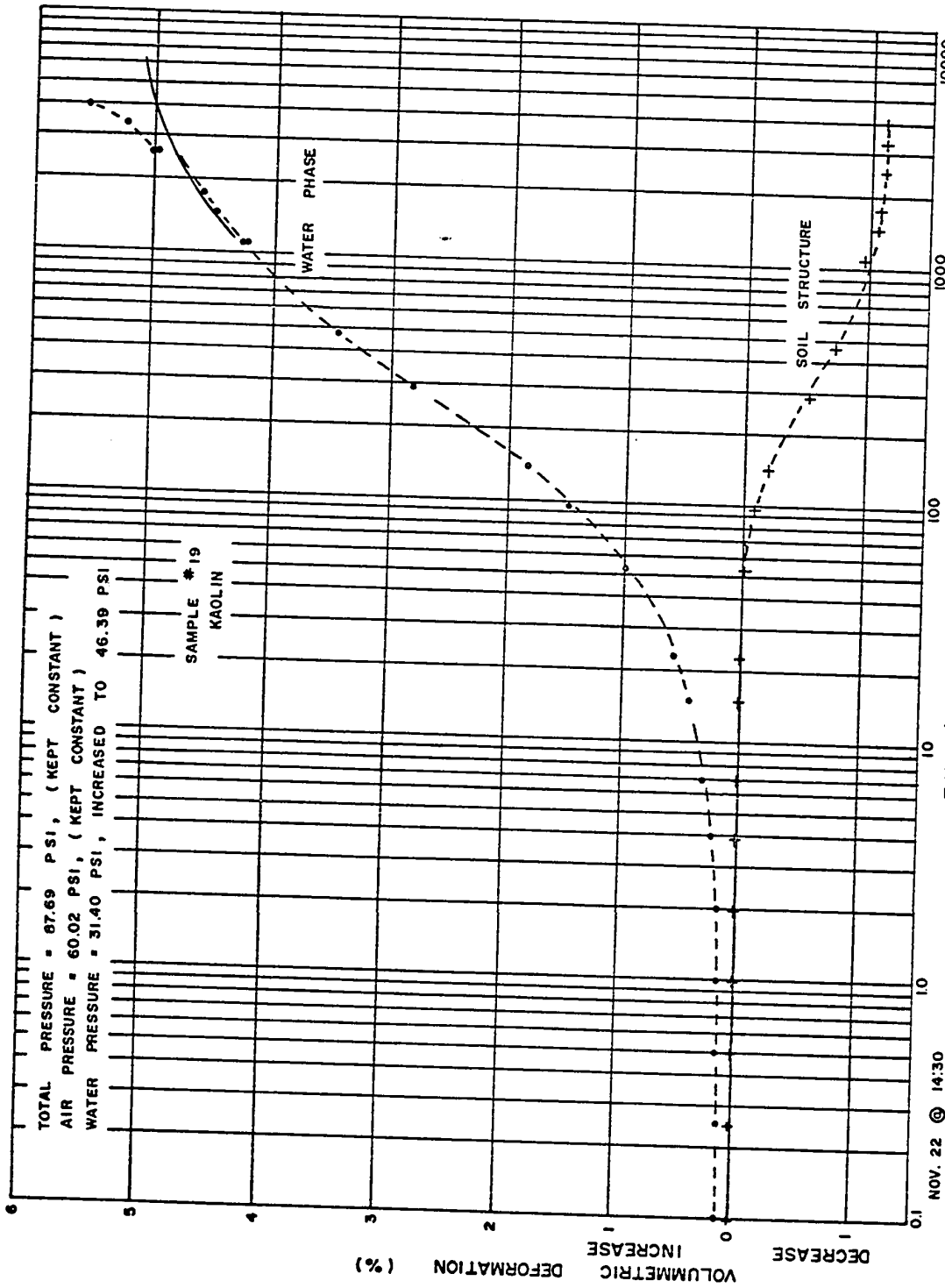


FIGURE F.7 SOIL STRUCTURE AND WATER PHASE VOLUME CHANGES (D-7)

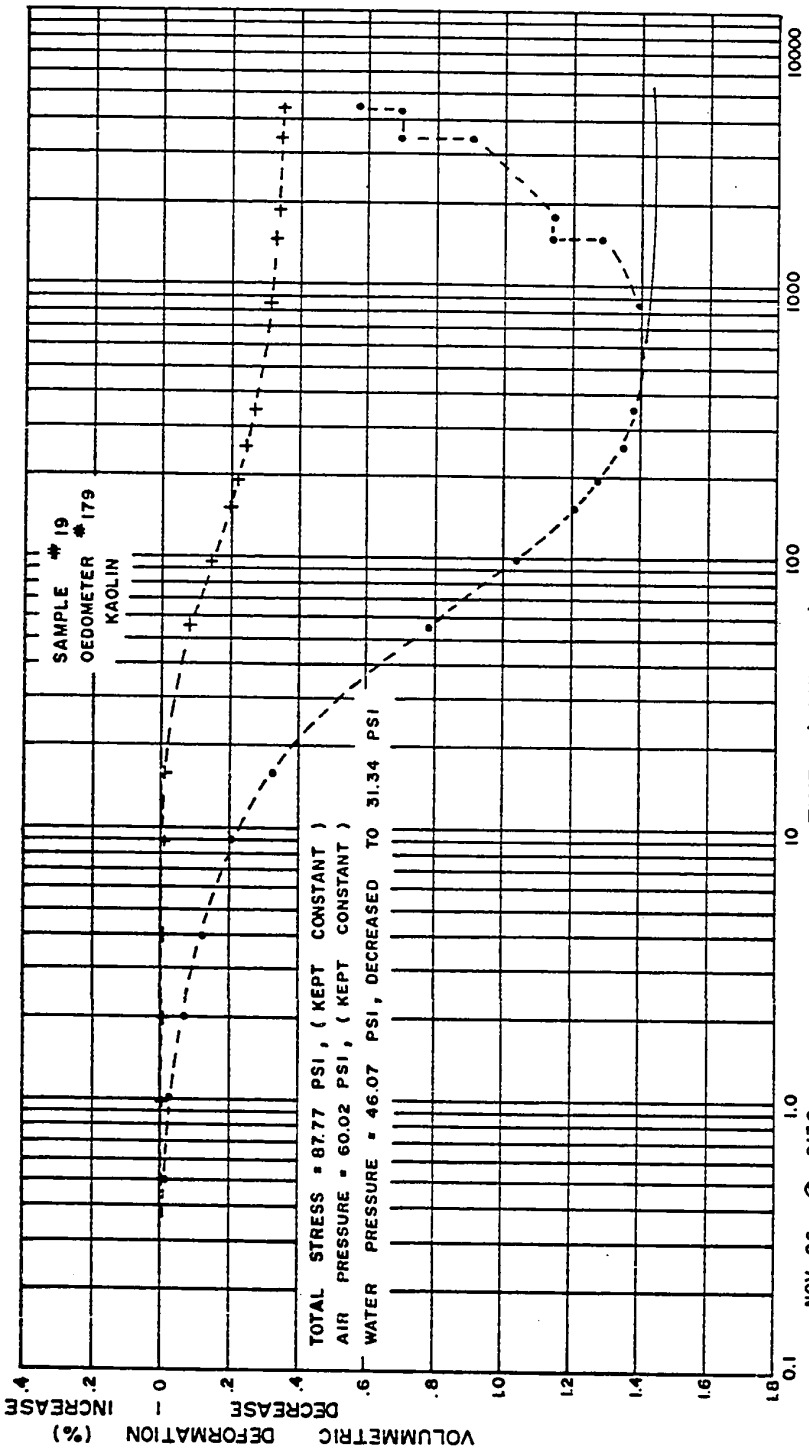


FIGURE F.8 SOIL STRUCTURE AND WATER PHASE VOLUME CHANGES (D-8)

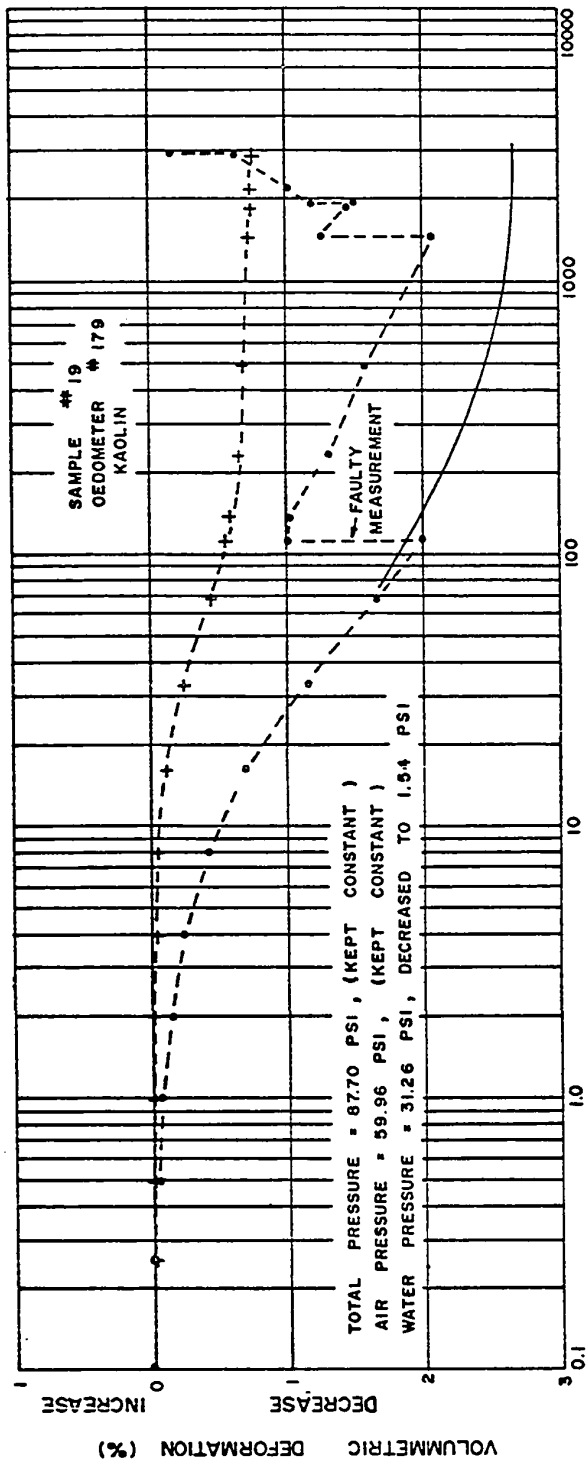


FIGURE F.9 SOIL STRUCTURE AND WATER PHASE VOLUME CHANGES (D-9)

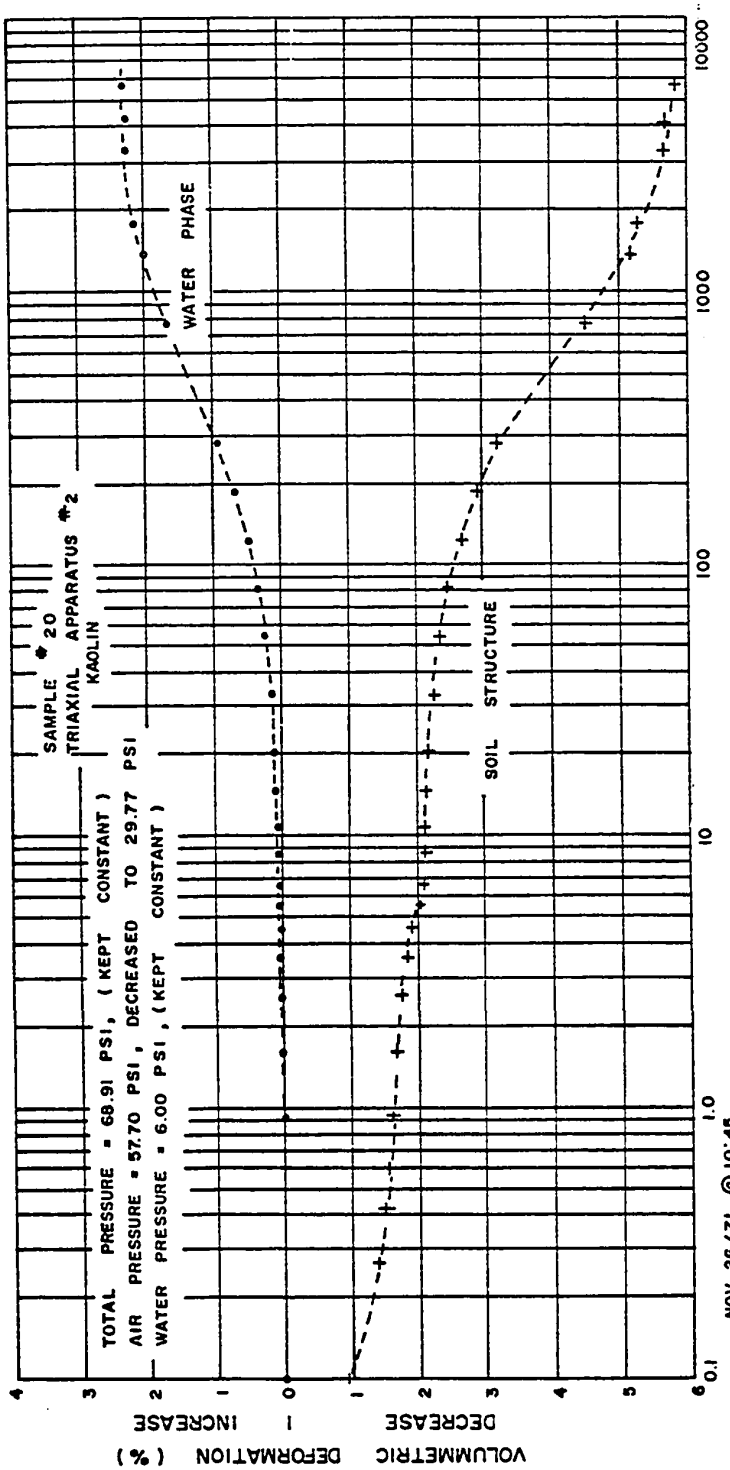


FIGURE F.10 SOIL STRUCTURE AND WATER PHASE VOLUME CHANGES (D-10)

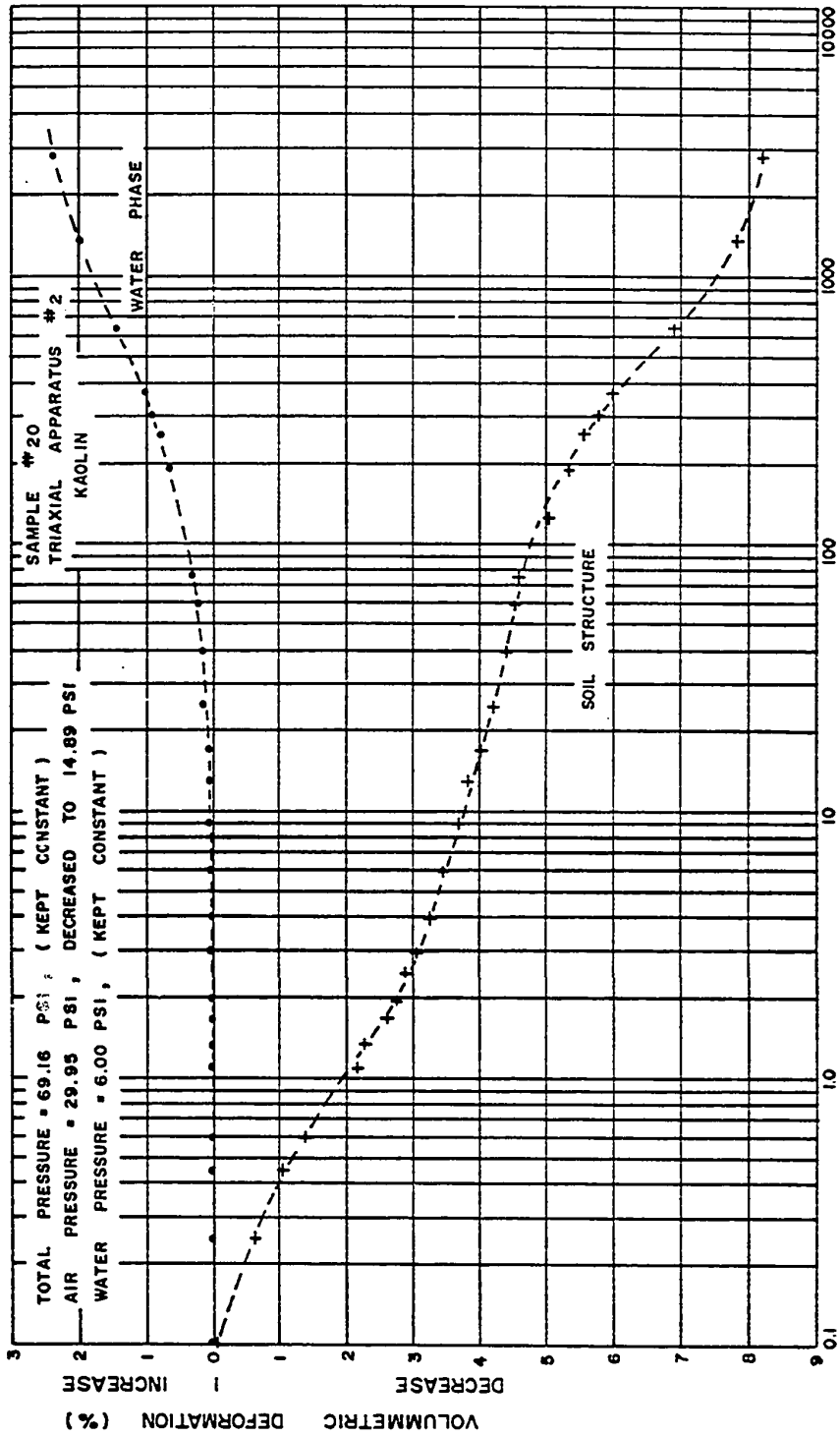


FIGURE F. 11 SOIL STRUCTURE AND WATER PHASE VOLUME CHANGES (D-11)

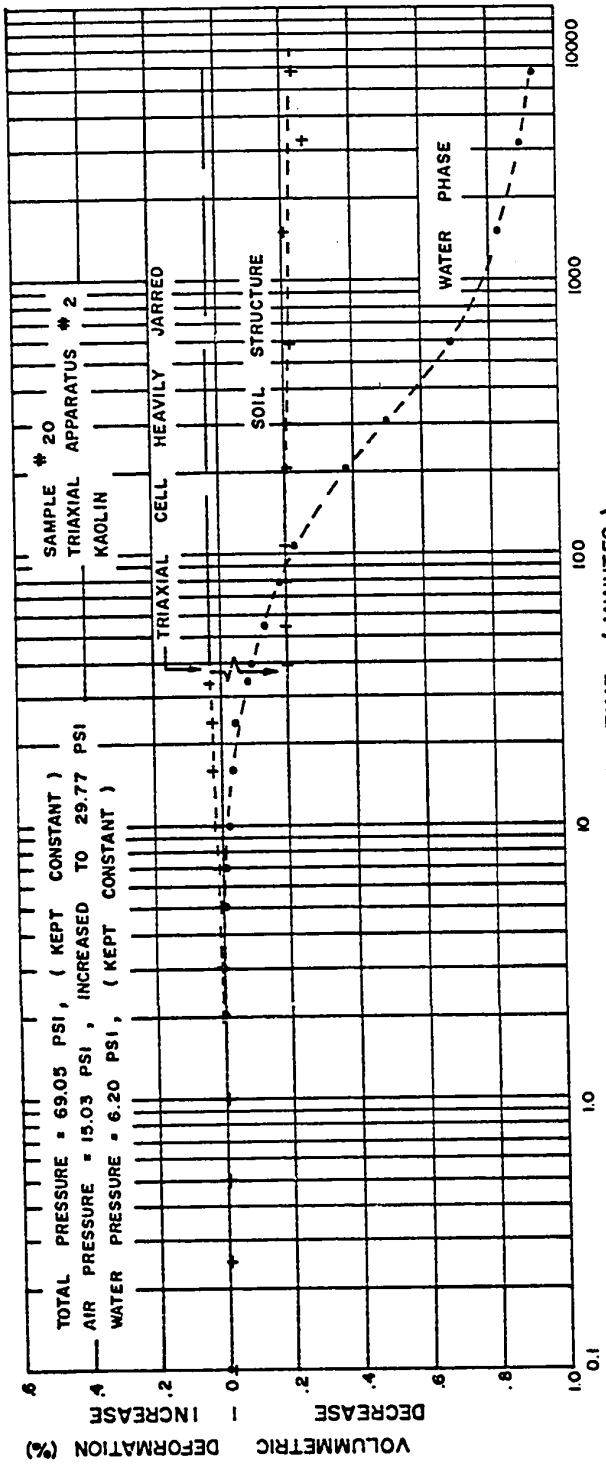


FIGURE F. 12 SOIL STRUCTURE AND WATER PHASE VOLUME CHANGES (D-12)

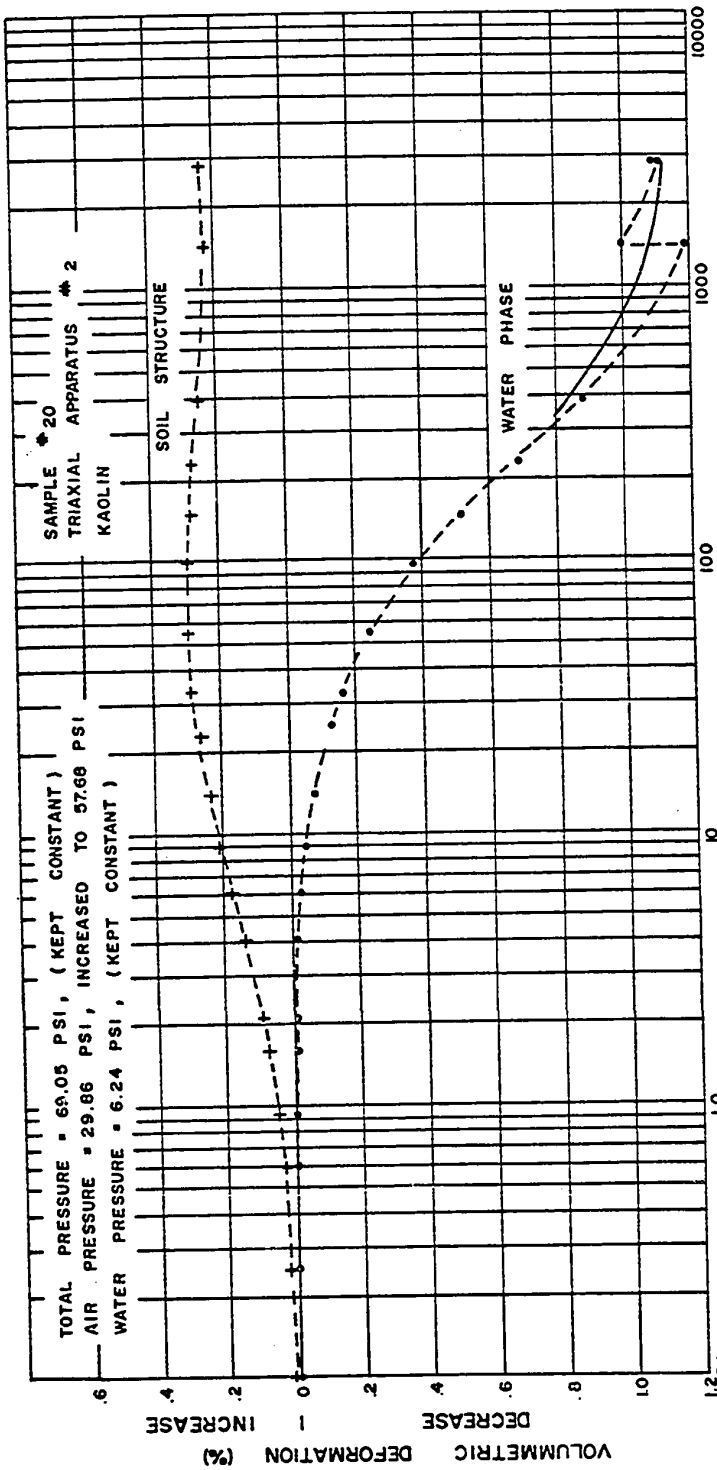


FIGURE F.13 SOIL STRUCTURE AND WATER PHASE VOLUME CHANGES (D-13)

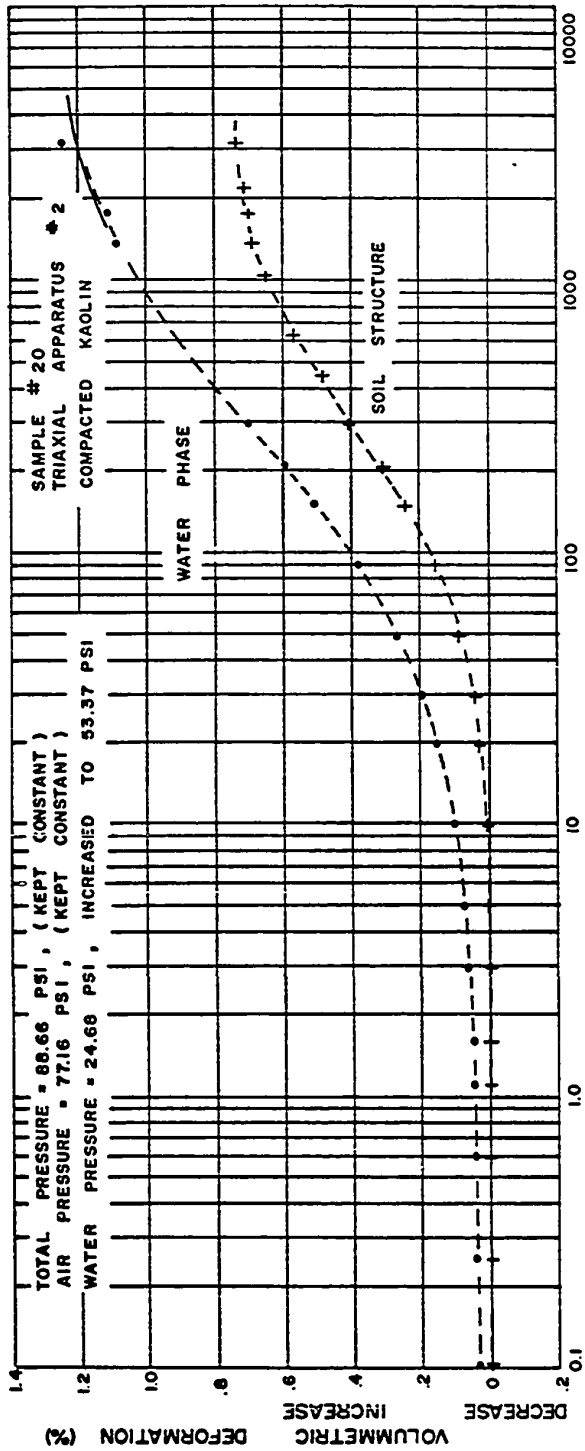


FIGURE F. 14 SOIL STRUCTURE AND WATER PHASE VOLUME CHANGES (D-14)

SECTION II

F-3 Uniqueness of the Constitutive Surface at a Point

F-3.1 Discussion of the Test Data

The tests to verify the uniqueness of the constitutive surface at a point involved small stress changes (10 psi) independently applied to the total, air and water components. The small stress changes were necessary to keep the deviations from the original stress state to a minimum. However, the small stress changes do not produce the conventionally-shaped deformation versus logarithm of time plots. Three of the four samples tested were on Regina clay which has extreme secondary swelling and compression characteristics. In most cases, it was impossible to wait until complete equilibrium had occurred. Therefore, a practical time limit was chosen for the length of each process.

The data pertinent to each deformation process is presented in a manner similar to Section I. Table F.5 summarizes the tests performed; Table F.7 summarizes the volume-weight relationships and Table F.8 summarizes the pressure changes applied to the sample. The test technique limitations associated with each test are as follows:

SAMPLE #15A

Test C-1 - No correction was applied for the initial compression of the water phase. The starting point of the water phase deformation should be approximately 0.45 percent. There is the possibility of some water loss from the sample with time but the amount is difficult to assess. It would appear to be small for this pressure increment.

Test C-2 - The air pressure decrement was applied for only one day and it is difficult to evaluate the water phase deformation for longer periods.

Test C-3 - There may be some loss of water from the sample after one day but the amount is difficult to quantify.

Test C-4 - The correction for the initial compression of the water in the base plate was not applied but should be approximately 0.36 percent. Some water appears to be lost from the sample over the long periods of time.

Test C-5 - Some water may be lost from the sample after one day.

Test C-6 - The diffused air was not flushed from the base plate prior to starting the test. Therefore the correction at 8 minutes applies primarily to test C-5. Some moisture may be lost from the sample after one day.

SAMPLE #16

No moisture should be lost from the sample due to the surrounding mercury. These tests give a better indication of the water phase deformation behavior than the tests performed in the oedometers.

Test C-7 - There are no known test technique limitations.

Test C-8 - The total sample volume decrease reading at 4300 minutes may be slightly excessive. However, there appears to be some secondary swelling at times beyond 5000 minutes.

Test C-9 - There are no known test technique limitations.

Test C-10 - There are no known test technique limitations. However, it is obvious that the water intake of the sample is not complete even

after 15,000 minutes.

Test C-11 - The water intake is incomplete even after 20,000 minutes. The first volume change readings on the overall sample at times less than 15 minutes may be too high.

Test C-12 - There are no known testing technique limitations.

Test C-13 - There was a total volume increase of 0.1 percent. The reliability of this value is uncertain. The process in both the soil structure and the water phase is incomplete after 15,000 minutes.

SAMPLE #17

Sample #17 was tested in Oedometer #179. The amount of moisture lost from the sample during each process is somewhat uncertain.

Test C-14 - Apart from possible losses of moisture from the sample, there are no known testing technique limitations.

Test C-15 - The upward trend near the end of the test indicates a dominant secondary swelling effect.

Test C-16 - There appears to be some loss of moisture from the sample.

Test C-17 - There is no known testing technique limitations.

SAMPLE #21

Sample #21 was tested in Triaxial Apparatus #2. The loss of moisture from the sample appears to be insignificant.

Test C-18 - The sample may not have been completely at equilibrium prior to the start of the test. This is revealed in terms of slight secondary compression effects after 3000 minutes.

Test C-19 - There is some doubt as to the reliability of this test.

The slight total volume increase may not be indicative of any measurable volume change. The slight water volume decrease after one day appears to be in the wrong direction and is probably not of significance. There may have been cavitation of the water at the base stone.

Test C-20 - The test results are reasonable but the process should have continued for a longer period of time.

Test C-21 - There are no known testing technique limitations. The shapes of the deformation curves after one day indicate that the rupture of meniscii in the sample may have produced an overall sample increase and the expulsion of some water.

Test C-22 - The total sample deformation result at 75 minutes is in doubt.

Test C-23 - There are no known testing technique limitations.

Test C-24 - There are no known testing technique limitations.

Test C-25 - The final total sample volumetric deformation may be too large.

Test C-26 - There are no known testing technique limitations.

Test C-27 - There are no known testing technique limitations.

Test C-28 - The processes are not quite complete.

Test C-29 - There are no known testing technique limitations.

Test C-30 - There are no known testing technique limitations.

Test C-31 - There are no known testing technique limitations.

Test C-32 - There are no known testing technique limitations.

TABLE F.5

SUMMARY OF SOIL PROPERTIES ON SAMPLES TESTED

TO EVALUATE UNIQUENESS OF THE CONSTITUTIVE SURFACE AT A POINT

Lab. Sample No.	Field Test Hole No.	Field Sample No.	Depth (ft.)	Liquid Limit (%)	Plastic Limit (%)	Plastic Index (%)	Grain Sizes			Soil Description
							Clay (%)	Silt (%)	Sand (%)	
15A	10	U_1	2	75.0	26.0	49.0	65	31	4	Dark brown, dry and crumbly, Regina Clay (Middle portion of 3"ϕ tube)
16	13	U_6	15	77.0	26.8	50.2	55	45	0	Dry, desiccated, highly fractured, some silt and sandy lenses, Regina Clay (Bottom portion of 4-1/2"ϕ tube)
17	10	U_1	2	76.3	25.4	50.9	--	--	--	Dark brown, dry Regina Clay (Bottom portion of 3"ϕ tube)
21	--	--	--	64.2	34.7	29.5	63	35	2	Compacted Kaolin Mold #2H (4"ϕ)

TABLE F.6

SUMMARY OF TESTS TO EVALUATE UNIQUENESS OF

CONSTITUTIVE SURFACE AROUND A POINT

Test No.	Sample No.	Date	Starting Time	Total Elapsed Time (Min.)	Apparatus No.	Pressure Change			Comments
						Total (psi)	Air (psi)	Water (psi)	
C-1	15A	Oct. 4/71	9:35	4270	OED #177	+ 0.20	+ 0.13	+10.72	Installed diffused air indicator
C-2	15A	Oct. 7/71	9:00	1413	OED #177	+ 0.01	- 9.99	- 0.08	
C-3	15A	Oct. 8/71	8:40	5762	OED #177	-10.29	+ 0.01	0.00	
C-4	15A	Oct.12/71	8:54	10041	OED #177	+ 0.26	0.00	+ 9.81	By-passed burret, end of test
C-5	15A	Oct.19/71	8:37	4355	OED #177	+ 0.03	- 9.97	+ 0.29	
C-6	15A	Oct.22/71	9:42	5688	OED #177	-10.00	0.00	+ 0.09	
C-7	16	Oct. 4/71	10:35	11440	T-1	- 0.07	- 0.02	+ 9.91	By-passed burret for 1 time interval
C-8	16	Oct.12/71	9:26	11509	T-1	- 0.09	-10.12	- 0.09	Difficult to read ball and cap
C-9	16	Oct.20/71	9:30	17290	T-1	-10.19	- 0.32	- 0.30	Removed air by surging
C-10	16	Nov. 1/71	9:56	15814	T-1	+ 0.18	+ 0.21	+10.07	Missed some water volume readings
C-11	16	Nov.12/71	9:40	20120	T-1	+ 0.15	- 9.82	+ 0.14	
C-12	16	Nov.26/71	9:15	15825	T-1	- 9.79	+ 0.18	+ 0.13	
C-13	16	Dec. 7/71	9:10	14530	T-1	-10.07	- 0.22	- 0.23	

TABLE F.6 (continued)

Test No.	Sample No.	Date	Starting Time	Total Elapsed Time (Min.)	Apparatus No.	Pressure Change			Comments
						Total (psi)	Air (psi)	Water (psi)	
C-14	17	Oct. 8/71	8:22	5763	OED #179	+ 0.04	- 0.03	+10.00	
C-15	17	Oct.12/71	8:35	2930	OED #179	+ 0.08	- 9.99	- 0.05	
C-16	17	Oct.14/71	9:40	5712	OED #179	-10.17	0.00	- 0.08	
C-17	17	Oct.18/71	9:30	4280	OED #179	+ 0.05	- 0.01	+10.02	
C-18	21	Jan.13/72	9:01	5864	T-1	-10.07	- 0.27	- 0.28	
C-19	21	Jan.17/72	10:57	1333	T-1	+ 0.09	- 9.84	+ 0.14	
C-20	21	Jan.18/72	9:20	1395	T-1	- 0.04	- 0.09	+ 9.98	
C-21	21	Jan.19/72	8:44	7231	T-1	- 9.61	+ 0.23	+ 0.04	
C-22	21	Jan.24/72	9:30	2840	T-1	+ 0.23	- 9.65	+ 0.19	
C-23	21	Jan.26/72	9:02	4358	T-1	- 0.18	- 0.24	+ 9.70	
C-24	21	Jan.29/72	10:00	5760	T-1	- 9.93	- 0.18	- 0.33	
C-25	21	Feb. 2/72	10:32	7148	T-1	0.00	-10.03	0.00	Valve to diffused air indicator open 1 night
C-26	21	Feb. 7/72	9:47	11483	T-1	- 0.28	- 0.27	+ 4.60	
C-26	21	Feb. 7/72	9:47	11483	T-1	- 0.28	- 0.27	+ 4.60	
C-27	21	Feb.15/72	9:17	8623	T-1	- 9.19	+ 0.60	+ 0.51	
C-28	21	Feb.21/72	9:23	4402	T-1	+ 9.00	- 0.33	- 0.28	
C-29	21	Feb.24/72	11:00	9970	T-1	- 0.04	- 0.04	- 4.87	
C-30	21	Mar. 3/72	9:20	8605	T-1	+29.33	+ 0.18	+ 0.09	
C-31	21	Mar. 9/72	8:54	10066	T-1	- 0.28	+29.80	- 0.19	
C-32	21	Mar.16/72	9:00	11555	T-1	0.00	- 0.05	+29.84	

TABLE F.7

VOLUME-WEIGHT RELATIONSHIPS OF SAMPLES USED TO

EVALUATE UNIQUENESS OF THE CONSTITUTIVE SURFACE AROUND A POINT

Test No.	Diameter (cm)	Height (cm)	Total Volume (cc)	Volume of Water (cc)	Volume of Air (cc)	Water Content (%)	Void Ratio	Dry Density (PCF)	Degree of Saturation (%)
C-1	6.350	2.594	81.16	23.43	13.06	18.46	0.7990	96.43	64.21
C-2	6.350	2.599	82.30	27.37	9.26	21.56	0.8020	96.27	74.73
C-3	6.350	2.598	82.27	27.55	9.05	21.70	0.8014	96.30	75.28
C-4	6.350	2.604	82.47	28.04	8.76	22.09	0.8058	96.07	76.20
C-5	6.350	2.611	82.69	29.25	7.77	23.04	0.8106	95.81	79.02
C-6	6.350	2.610	82.66	29.88	7.10	23.54	0.8099	95.85	80.80
C-7	10.227	10.013	822.47	327.35	47.01	26.28	0.8354	94.51	87.44
C-8	10.226	10.025	823.35	330.23	45.00	26.51	0.8374	94.41	88.01
C-9	10.213	10.022	821.01	332.54	40.36	26.69	0.8321	94.68	89.18
C-10	10.215	10.041	822.90	335.32	39.47	26.92	0.8364	94.47	89.47
C-11	10.218	10.058	824.71	339.25	37.35	27.23	0.8404	94.26	90.08
C-12	10.204	10.058	822.53	344.82	29.60	27.68	0.8355	94.51	92.09
C-13	10.213	10.085	826.11	349.75	28.25	28.08	0.8435	94.10	92.53
C-14	6.350	2.644	83.72	29.92	5.99	22.51	0.7510	99.07	83.31
C-15	6.350	2.654	84.04	30.61	5.62	23.03	0.7577	98.69	84.48
C-16	6.350	2.654	84.06	30.84	5.41	23.20	0.7582	98.67	85.07
C-17	6.350	2.664	84.37	31.45	5.10	23.66	0.7646	98.31	86.04

TABLE F.7 (continued)

Test No.	Diameter (cm)	Height (cm)	Total Volume (cc)	Vo ume of Water (cc)	Volume of Air (cc)	Water Content (%)	Void Ratio	Dry Density (PCF)	Degree of Saturation (%)
C-18	9.974	11.736	916.93	371.11	96.89	31.60	1.0425	79.30	79.92
C-19	9.974	11.745	917.65	371.18	97.55	31.61	1.0441	79.19	79.86
C-20	9.976	11.743	917.84	370.66	98.25	31.56	1.0445	79.05	79.84
C-21	9.975	11.748	918.16	372.36	96.87	31.71	1.0453	79.36	79.81
C-22	9.981	11.768	920.65	373.82	97.91	31.83	1.0508	79.25	79.60
C-23	9.982	11.765	920.76	374.69	97.15	31.91	1.0510	79.41	79.59
C-24	9.988	11.770	922.21	379.15	94.14	32.29	1.0543	80.11	79.46
C-25	10.016	11.804	930.03	382.31	98.80	32.56	1.0717	79.47	78.79
C-26	10.010	11.798	928.41	390.55	88.94	33.26	1.0681	81.45	78.93
C-27	10.006	11.807	928.44	404.55	74.97	34.45	1.0682	84.37	78.94
C-28	10.024	11.848	935.08	412.15	74.01	35.10	1.0830	84.78	78.37
C-29	10.015	11.825	931.47	411.54	71.01	35.04	1.0749	85.28	78.67
C-30	10.006	11.815	929.09	403.00	77.16	34.32	1.0696	83.93	78.87
C-31	9.945	11.703	909.10	389.54	70.63	33.17	1.0251	84.65	80.61
C-32	9.946	11.706	909.51	380.99	79.60	32.44	1.0260	82.72	80.57

TABLE F.8

SUMMARY OF PRESSURE CHANGES FOR TESTS TO EVALUATE

UNIQUENESS OF THE CONSTITUTIVE SURFACE AROUND A POINT

Test No.	Initial Conditions						Final Conditions					
	σ (psi)	u_a (psi)	u_w (psi)	$\sigma-u_w$ (psi)	$\sigma-u_a$ (psi)	u_a-u_w (psi)	σ (psi)	u_a (psi)	u_w (psi)	$\sigma-u_w$ (psi)	$\sigma-u_a$ (psi)	u_a-u_w (psi)
C-1	77.71	50.01	1.47	76.24	27.69	48.54	77.91	50.14	12.19	65.72	27.77	37.95
C-2	77.91	50.14	12.19	65.72	27.77	37.95	77.92	40.15	12.11	65.81	37.77	28.04
C-3	77.92	40.15	12.11	65.81	37.77	28.04	67.63	40.16	12.11	55.52	27.47	28.05
C-4	67.63	40.16	12.11	55.52	27.47	28.05	67.89	40.16	21.92	45.98	27.73	18.24
C-5	67.89	40.16	21.92	45.98	27.73	18.24	67.92	30.19	22.21	45.71	37.74	7.98
C-6	67.92	30.19	22.21	45.71	37.74	7.98	57.92	30.19	22.30	35.62	27.73	7.89
C-7	71.46	50.18	3.66	67.80	21.28	46.52	71.39	50.16	13.57	57.82	21.23	36.59
C-8	71.39	50.16	13.57	57.82	21.23	36.59	71.30	40.04	13.48	57.82	31.25	26.57
C-9	71.30	40.04	13.48	57.82	31.25	26.57	61.11	39.72	13.18	47.94	21.39	26.54
C-10	61.11	39.72	13.18	47.94	21.39	26.54	61.29	39.93	23.25	38.05	21.37	16.68
C-11	61.29	39.93	23.25	38.05	21.37	16.68	61.44	30.11	23.39	38.05	31.32	6.73
C-12	61.44	30.11	23.39	38.05	31.32	6.73	51.65	30.29	23.52	28.12	21.35	6.77
C-13	51.65	30.29	23.52	28.12	21.35	6.77	41.58	30.07	23.29	18.28	11.51	6.77
C-14	77.72	50.01	1.50	76.21	27.71	48.50	77.76	49.98	11.50	66.26	27.78	34.48
C-15	77.76	49.98	11.50	66.26	27.78	38.48	77.84	39.99	11.45	66.40	37.85	28.55
C-16	77.84	39.99	11.45	66.40	37.85	28.55	67.67	39.99	11.37	56.29	27.67	28.62
C-17	67.67	39.99	11.37	56.29	27.67	28.62	67.72	39.98	21.39	46.33	27.74	18.59

TABLE F.8 (continued)

Test No.	Initial Conditions						Final Conditions					
	σ (psi)	u_a (psi)	u_w (psi)	$\sigma-u_w$ (psi)	$\sigma-u_a$ (psi)	u_a-u_w (psi)	σ (psi)	u_a (psi)	u_w (psi)	$\sigma-u_w$ (psi)	$\sigma-u_a$ (psi)	u_a-u_w (psi)
C-18	82.04	61.20	4.36	77.68	20.84	56.85	71.97	60.93	4.08	67.89	11.05	56.85
C-19	71.97	60.93	4.08	67.89	11.05	56.85	72.06	51.09	4.22	67.84	20.98	46.87
C-20	72.06	51.09	4.22	67.84	20.98	46.87	72.02	51.00	14.20	57.82	21.02	36.80
C-21	72.02	51.00	14.20	57.82	21.02	36.80	62.41	51.23	14.24	48.17	11.18	36.98
C-22	62.41	51.23	14.24	48.17	11.18	36.98	62.64	41.58	14.43	48.22	21.07	27.15
C-23	62.64	41.58	14.43	48.22	21.07	27.15	62.46	41.34	24.13	38.33	21.11	17.22
C-24	62.46	41.34	24.13	38.33	21.11	17.22	52.53	41.16	23.80	28.73	11.37	17.36
C-25	52.53	41.16	23.80	28.73	11.37	17.36	52.53	31.13	23.80	28.73	21.39	7.33
C-26	52.53	31.13	23.80	28.73	21.39	7.33	52.25	30.86	28.40	23.85	21.39	2.46
C-27	52.25	30.86	28.40	23.85	21.39	2.46	43.06	31.46	28.91	14.15	11.60	2.55
C-28	43.06	31.46	28.91	14.15	11.60	2.55	52.06	31.13	28.63	23.44	20.93	2.51
C-29	52.06	31.13	28.63	23.44	20.93	2.51	52.02	31.09	23.76	28.26	20.93	7.33
C-30	52.02	31.09	23.76	28.26	20.93	7.33	81.35	31.27	23.85	57.50	50.07	7.42
C-31	81.35	31.27	23.85	57.50	50.07	7.42	81.07	61.07	23.66	57.40	20.00	37.40
C-32	81.07	61.07	23.66	57.40	20.00	37.40	81.07	61.02	53.50	27.56	20.05	7.52

SAMPLE NO. 15A

(REGINA CLAY)

C-1	Oct. 4/71	u_w	Increased
C-2	Oct. 7/71	u_a	Decreased
C-3	Oct. 8/71	σ	Increased
C-4	Oct. 12/71	u_w	Decreased
C-5	Oct. 19/71	u_a	Decreased
C-6	Oct. 22/71	σ	Decreased

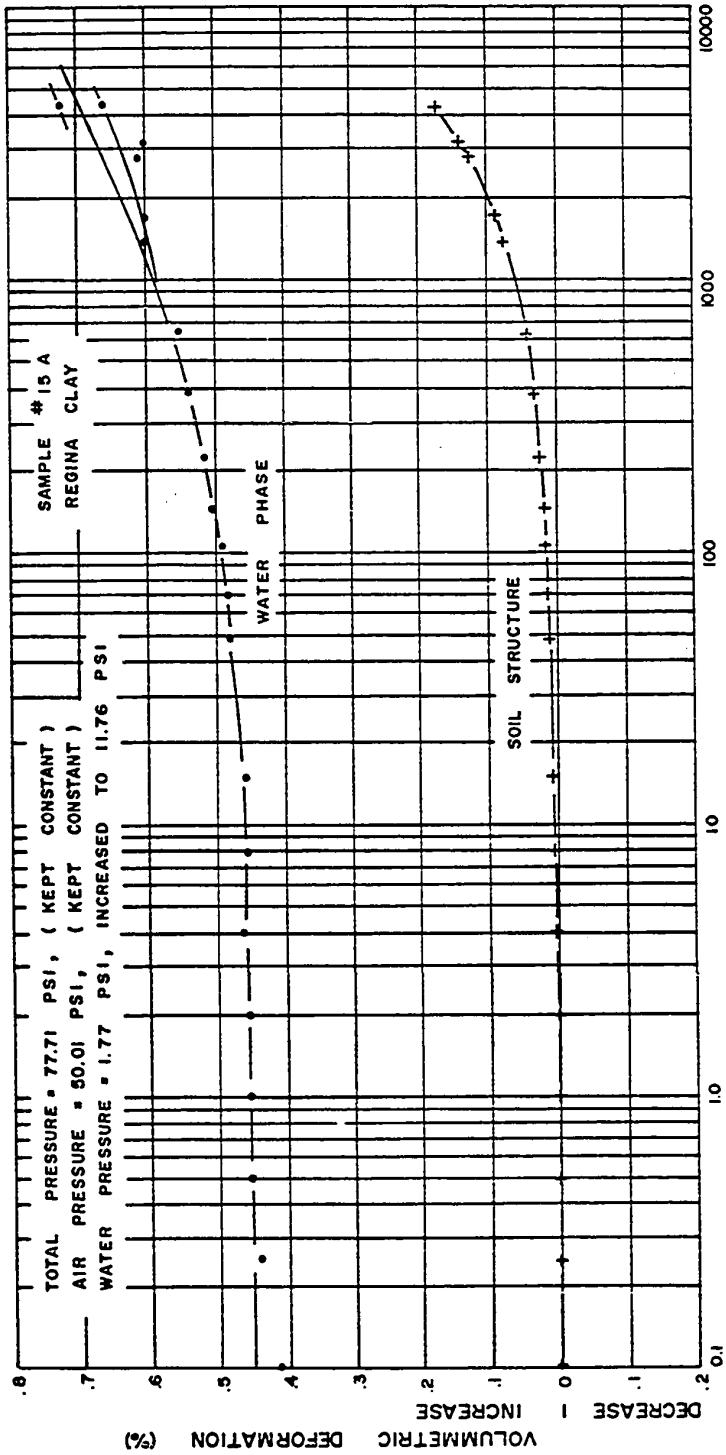


FIGURE F. 15 SOIL STRUCTURE AND WATER PHASE VOLUME CHANGES (C-1)

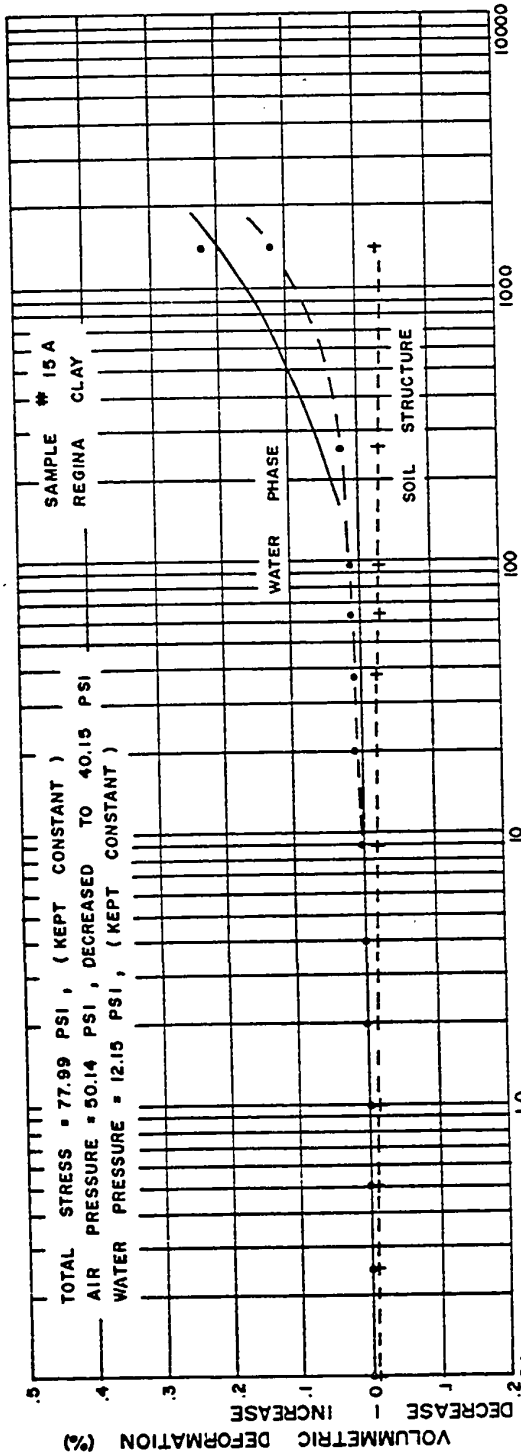


FIGURE F.16 SOIL STRUCTURE AND WATER PHASE VOLUME CHANGES (C-2)

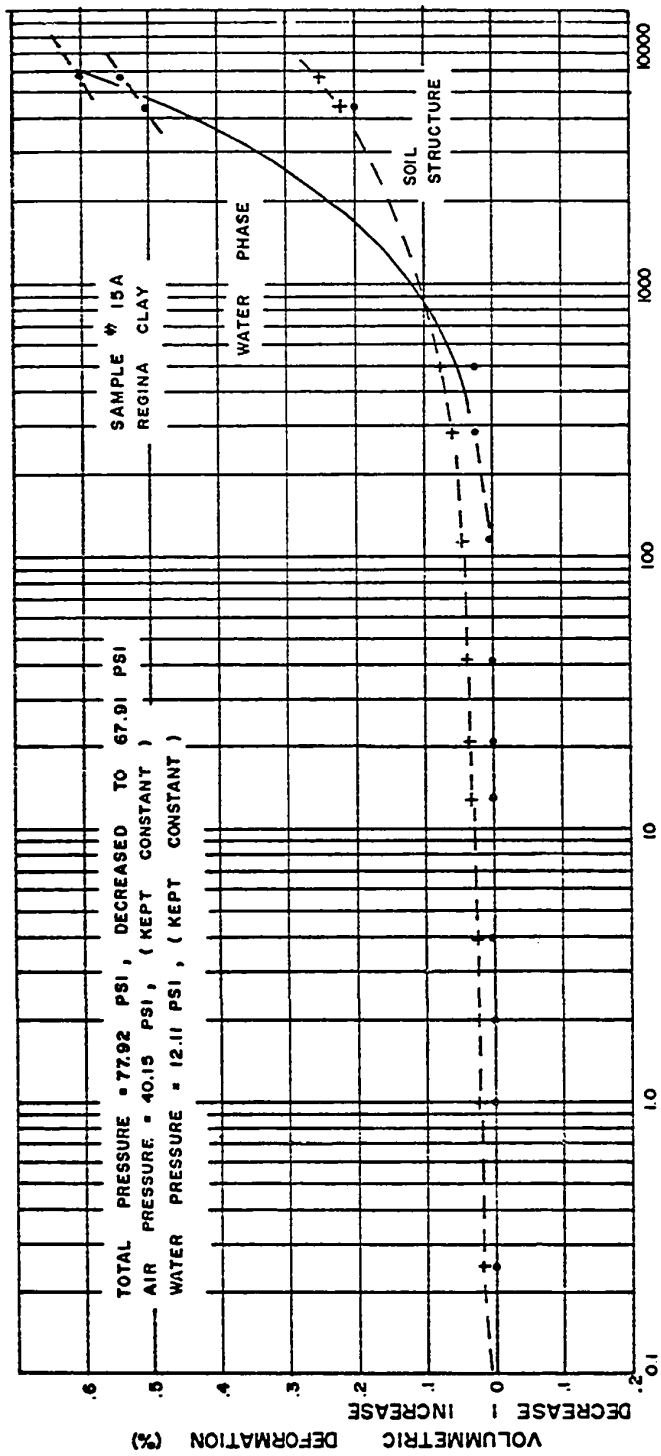


FIGURE F. 17 SOIL STRUCTURE AND WATER PHASE VOLUME CHANGES (C-3)

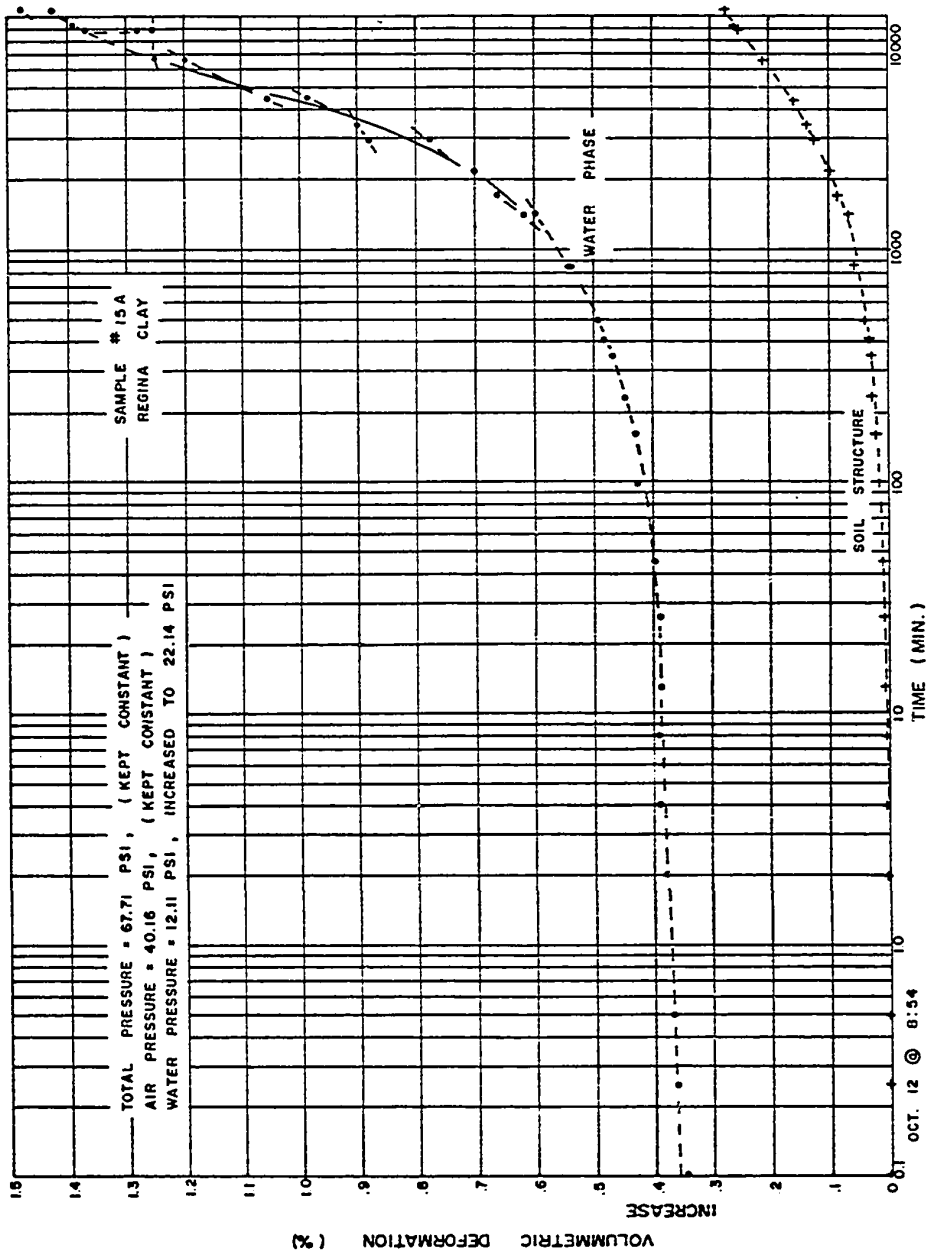


FIGURE F. 18 SOIL STRUCTURE AND WATER PHASE VOLUME CHANGES (C-4)

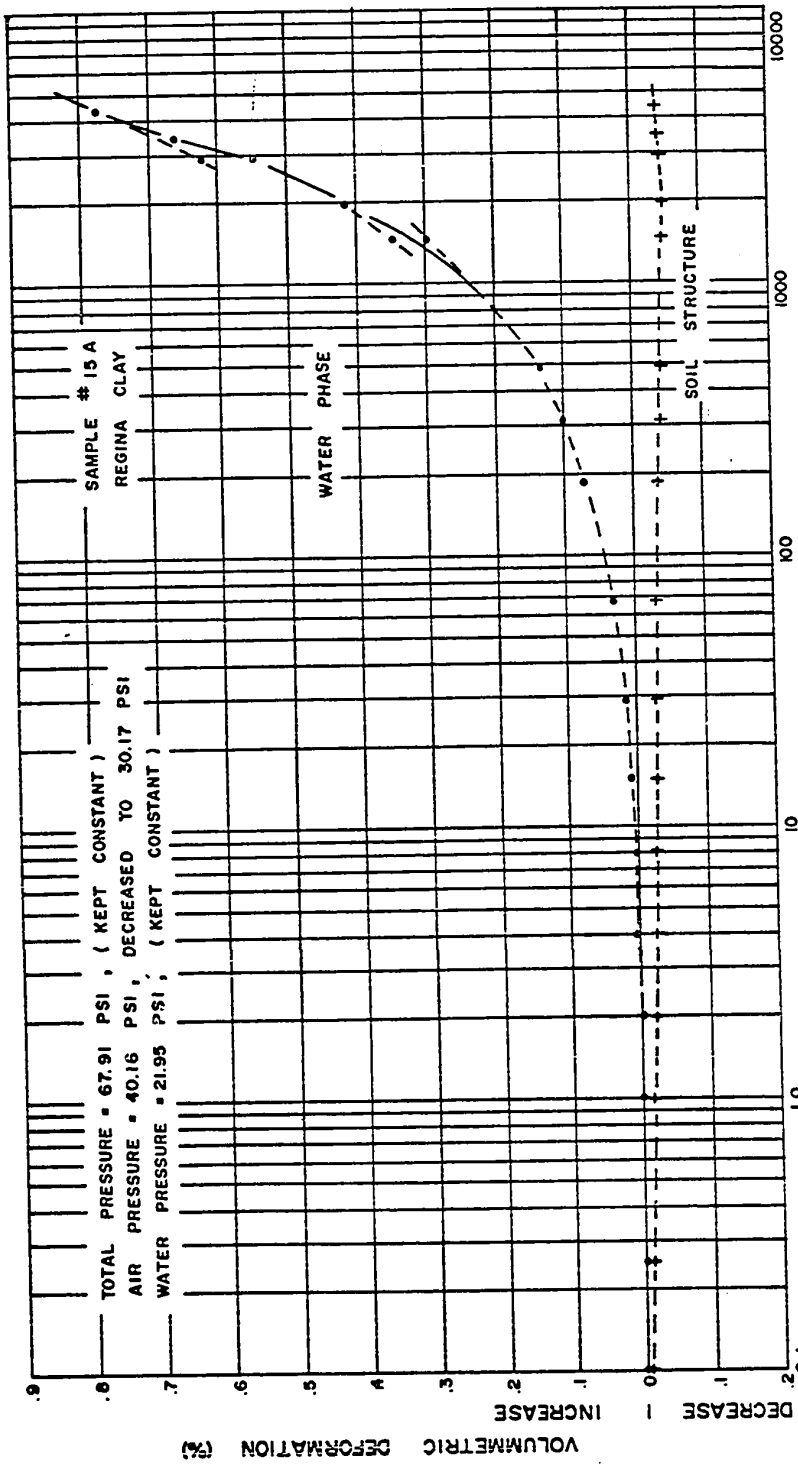


FIGURE F. 19 SOIL STRUCTURE AND WATER PHASE VOLUME CHANGES (C-5)

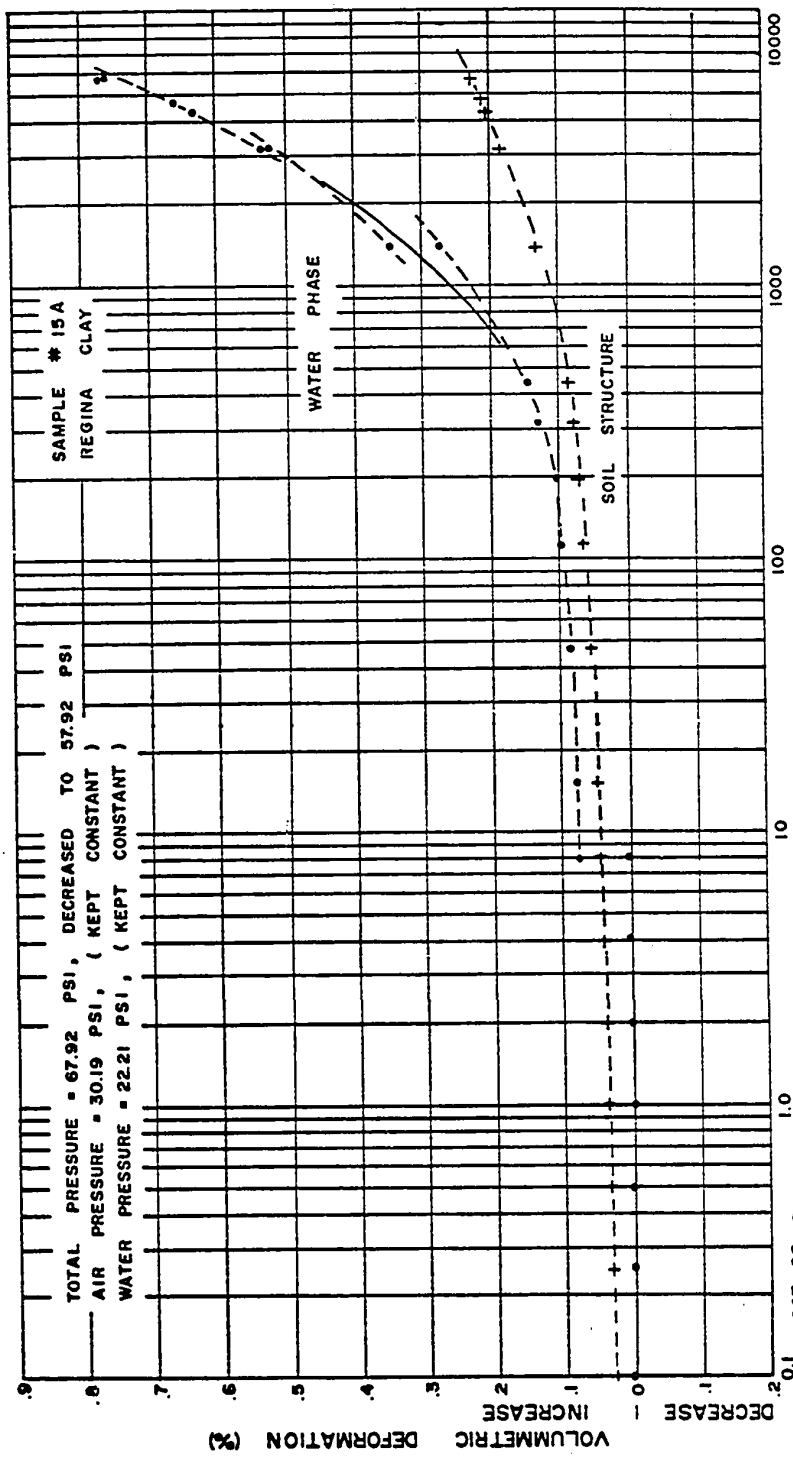


FIGURE F. 20 SOIL STRUCTURE AND WATER PHASE VOLUME CHANGE (C-6)

SAMPLE NO. 16

(REGINA CLAY)

C-7	Oct. 4/71	u_w	Increased
C-8	Oct. 12/71	u_a	Decreased
C-9	Oct. 20/71	σ	Decreased
C-10	Nov. 1/71	u_w	Increased
C-11	Nov. 12/71	u_a	Decreased
C-12	Nov. 26/71	σ	Decreased
C-13	Dec. 7/71	σ	Decreased

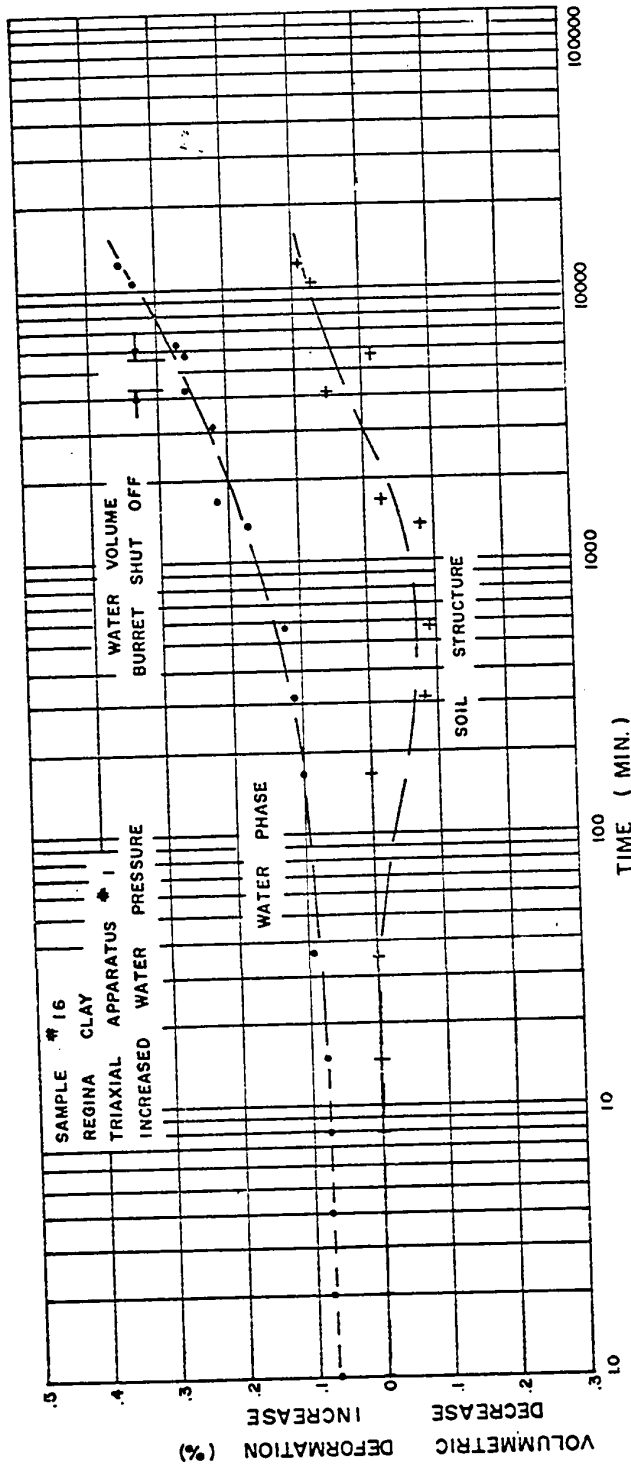


FIGURE F. 21 SOIL STRUCTURE AND WATER PHASE VOLUME CHANGES (C-7)

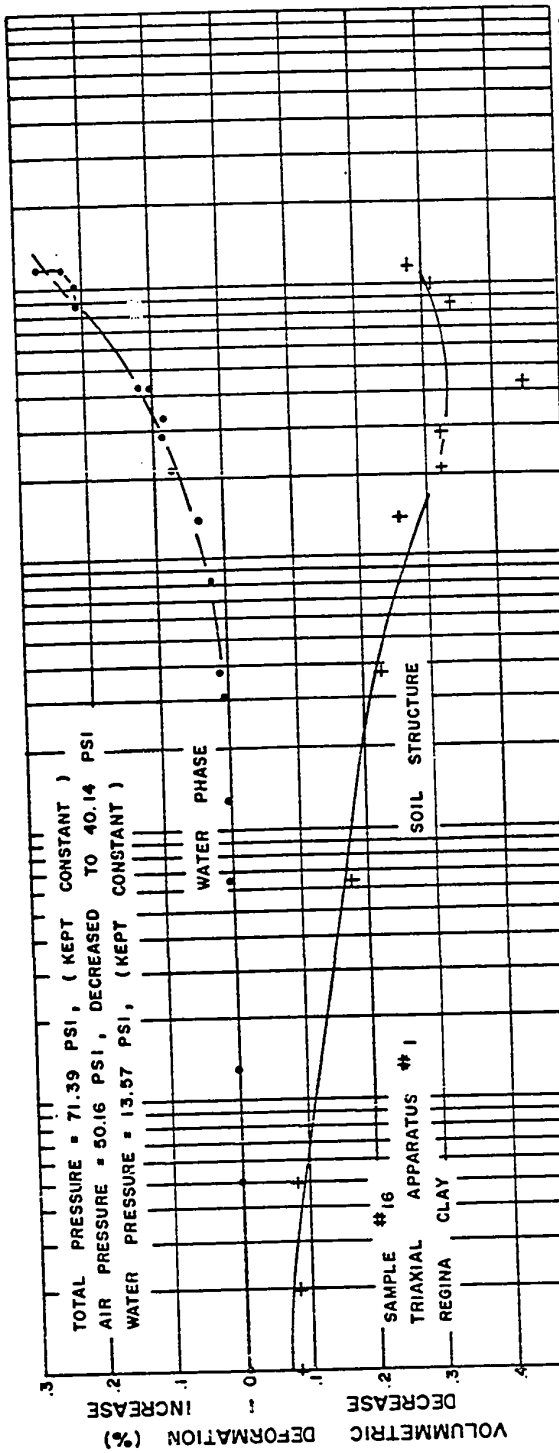


FIGURE F.22 SOIL STRUCTURE AND WATER PHASE VOLUME CHANGES (C-8)

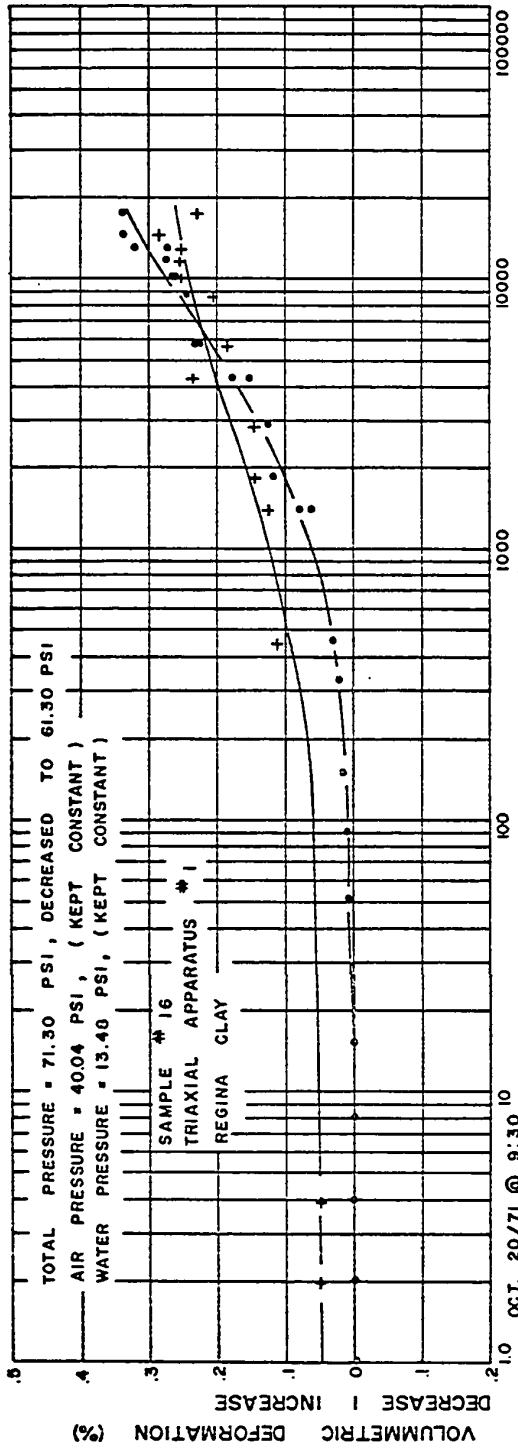


FIGURE F. 23 SOIL STRUCTURE AND WATER PHASE VOLUME CHANGES (C-9)

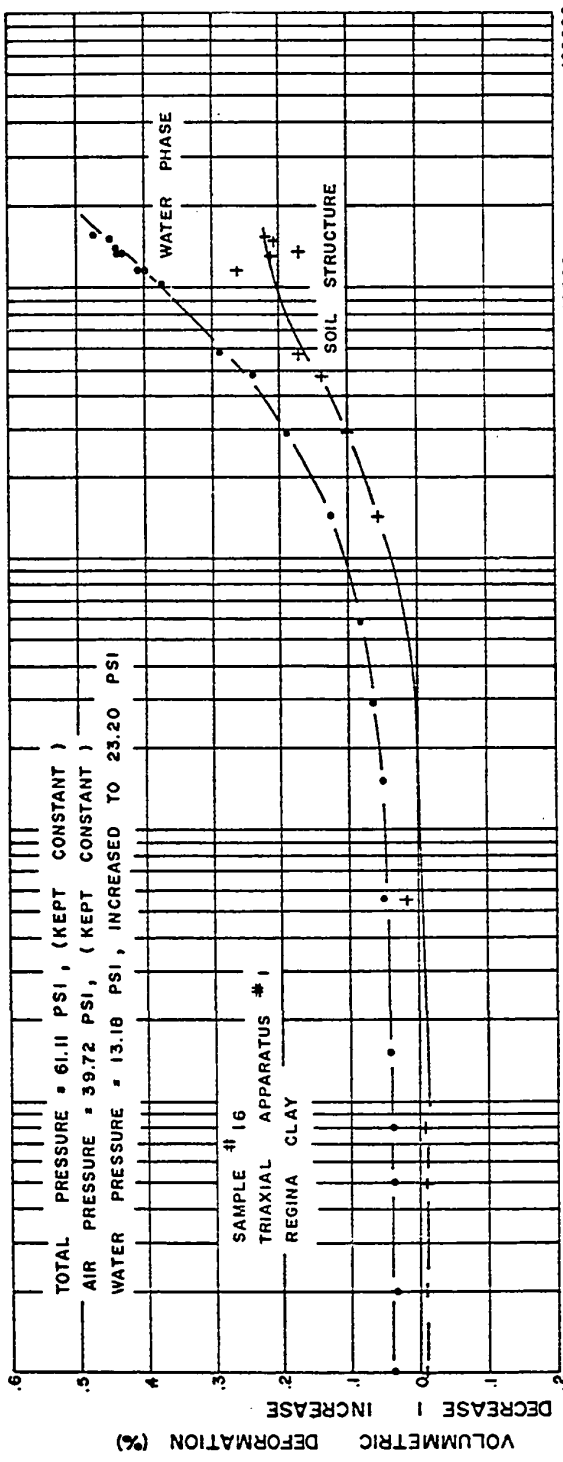


FIGURE F.24 SOIL STRUCTURE AND WATER PHASE VOLUME CHANGES (C-10)

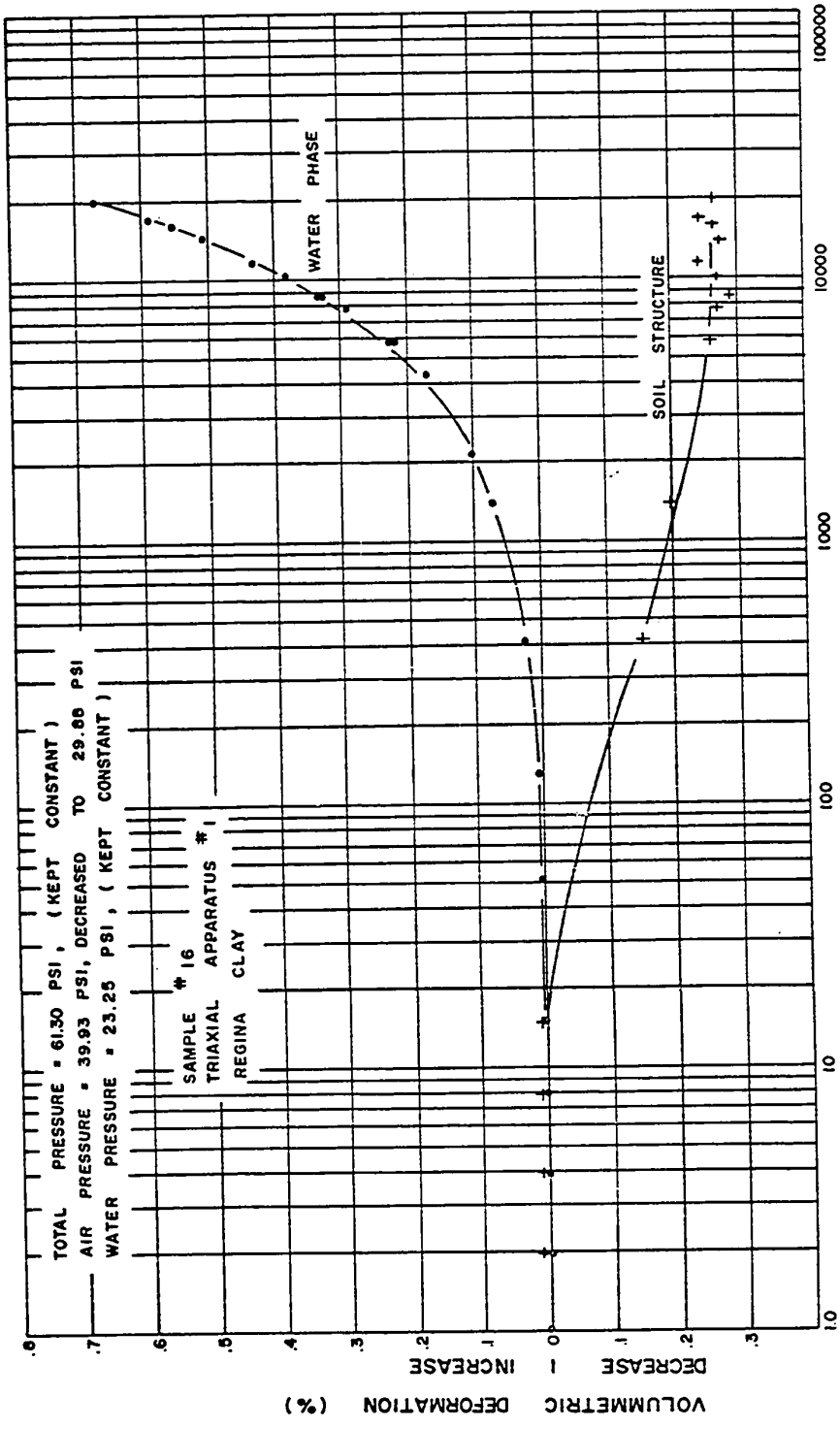


FIGURE F. 25 SOIL STRUCTURE AND WATER PHASE VOLUME CHANGES (C-11)

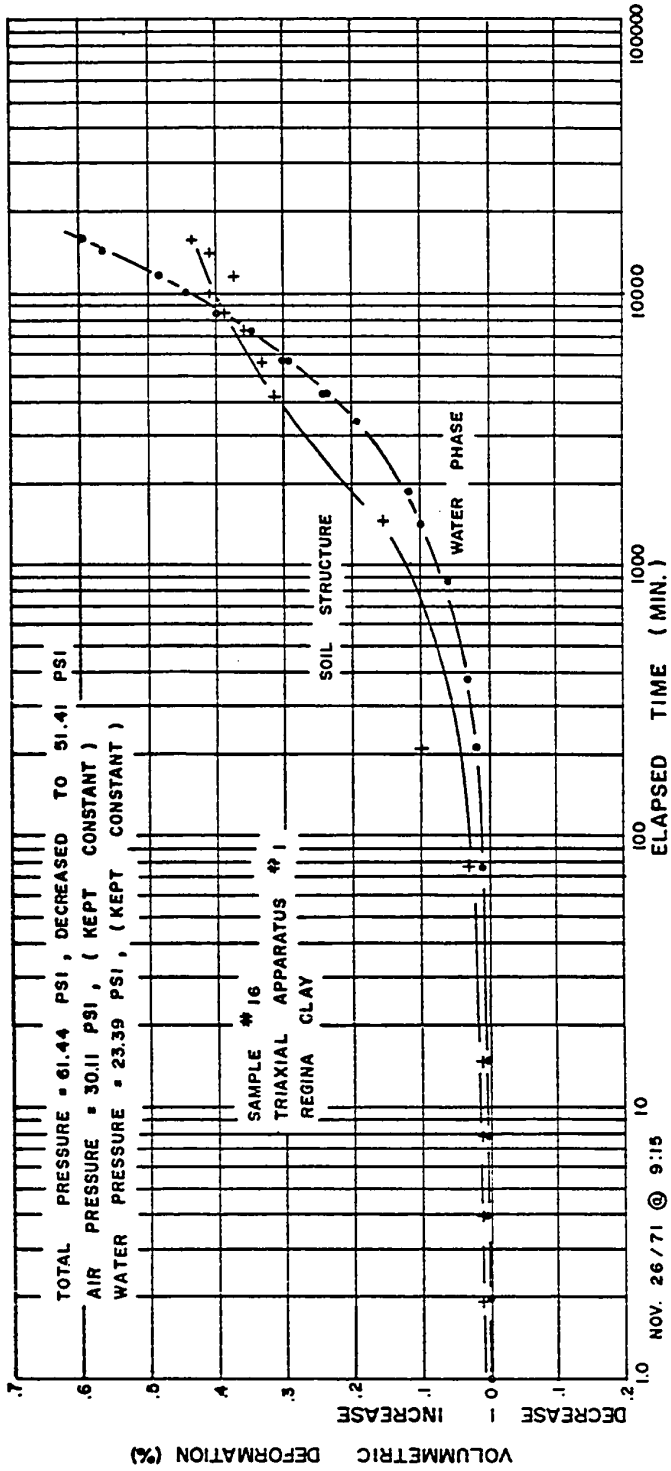


FIGURE F.26 SOIL STRUCTURE AND WATER PHASE VOLUME CHANGES (C-12)

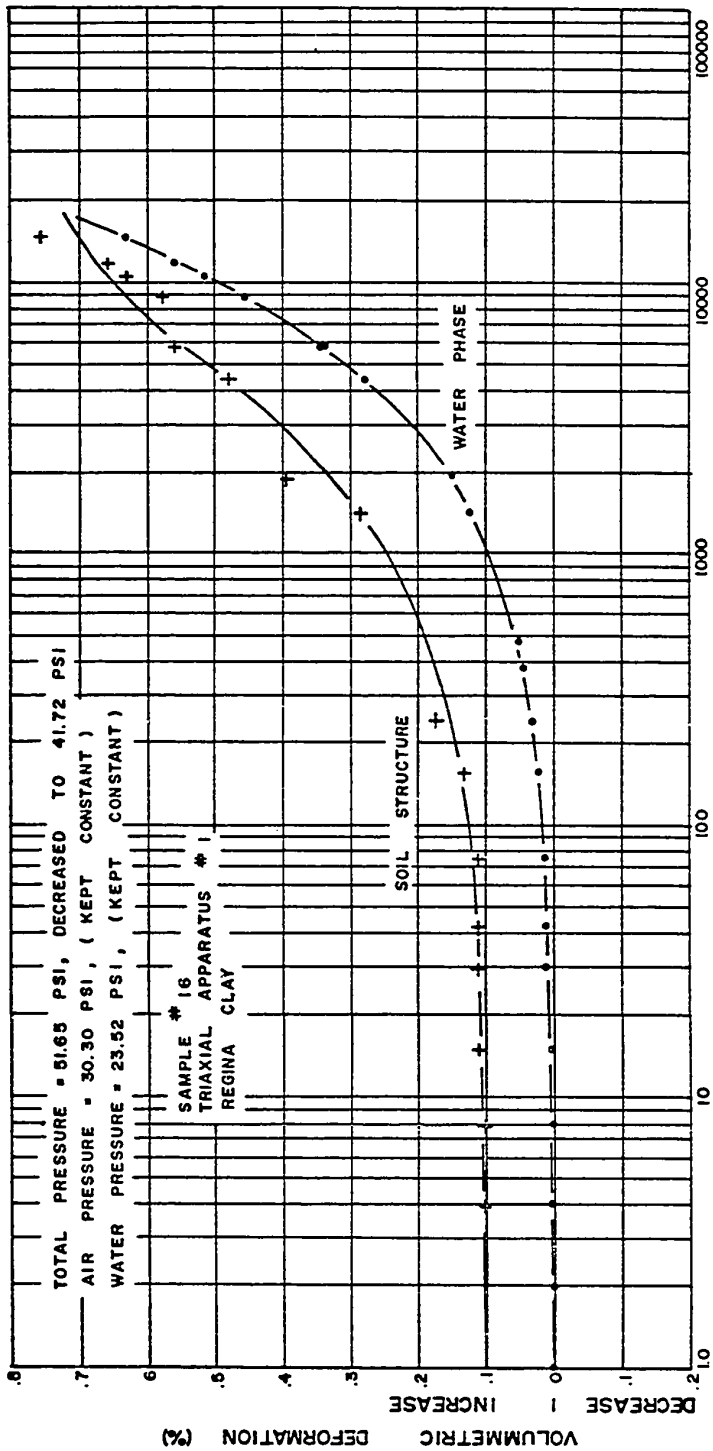


FIGURE F. 27 SOIL STRUCTURE AND WATER PHASE VOLUME CHANGES (C-13)

SAMPLE NO. 17

(REGINA CLAY)

C-14	Oct. 8/71	u_w	Increased
C-15	Oct. 12/71	u_a	Decreased
C-16	Oct. 14/71	σ	Decreased
C-17	Oct. 18/71	u_w	Increased

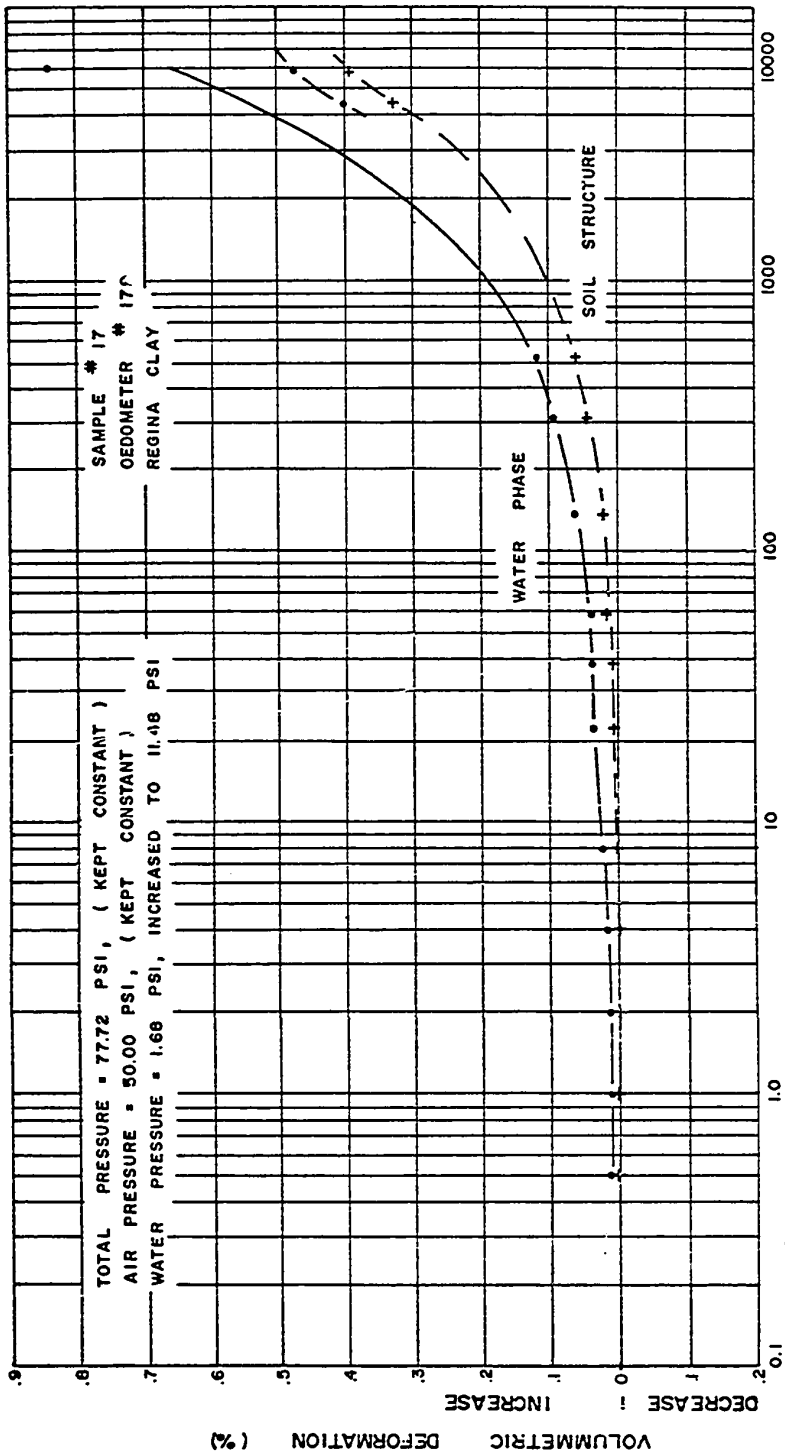


FIGURE F. 28 SOIL STRUCTURE AND WATER PHASE VOLUME CHANGES (C-14)

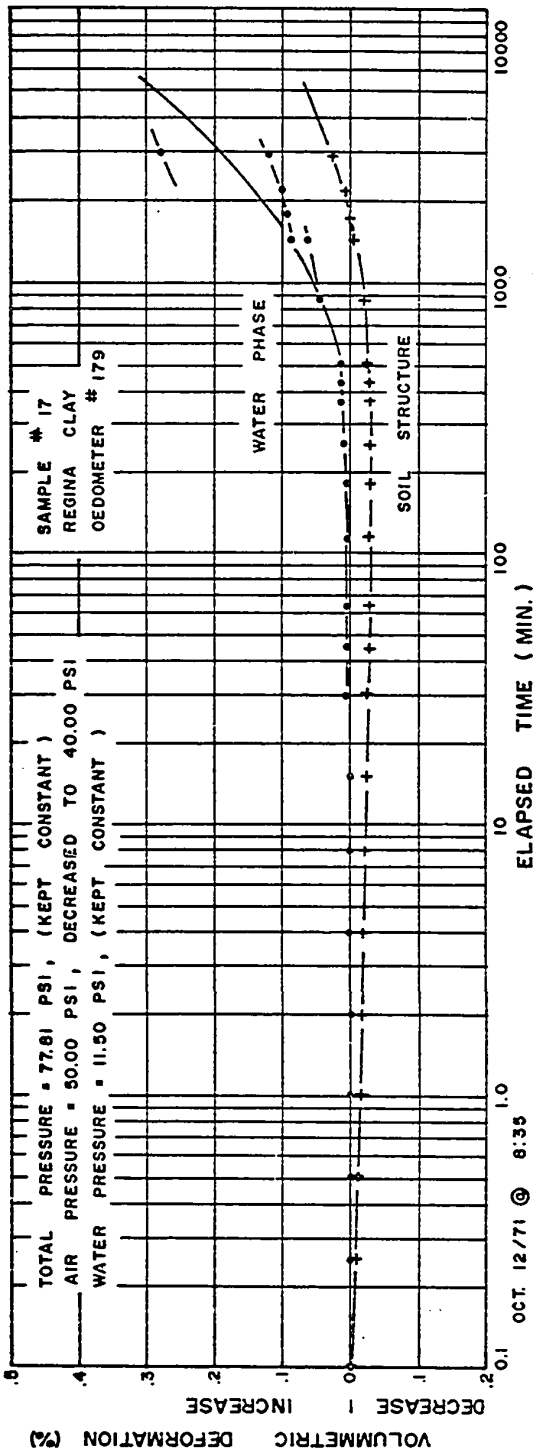


FIGURE F. 29 SOIL STRUCTURE AND WATER PHASE VOLUME CHANGES (C-15)

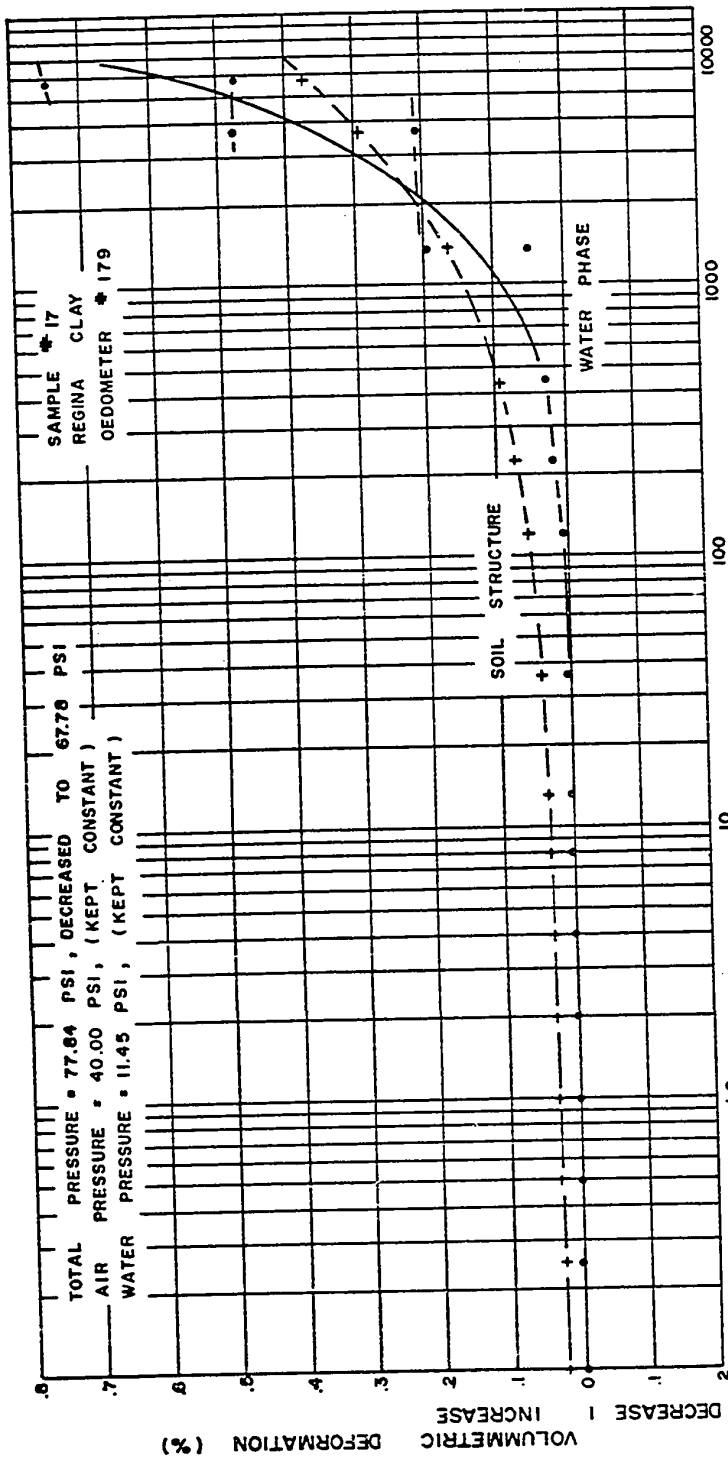


FIGURE F. 30 SOIL STRUCTURE AND WATER PHASE VOLUME CHANGES (C-16)

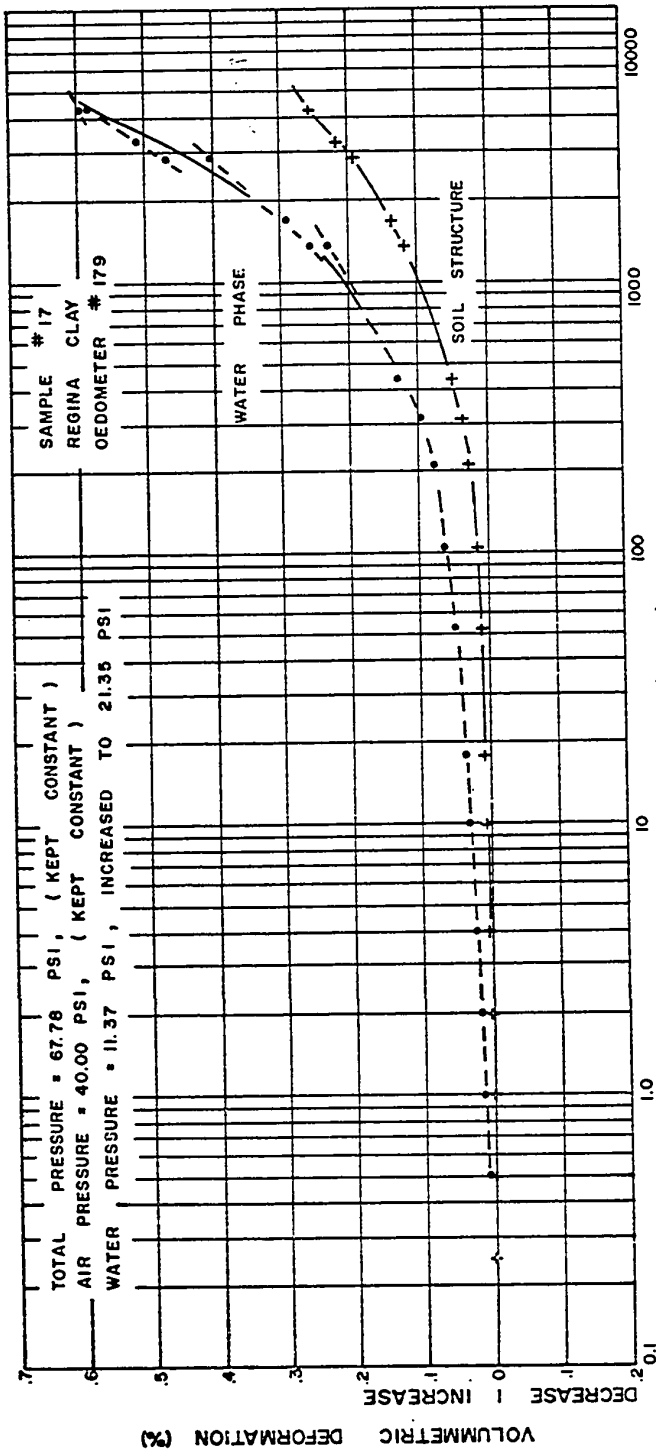


FIGURE F 31 SOIL STRUCTURE AND WATER PHASE VOLUME CHANGES (C-17)

SAMPLE NO. 21

(KAOLIN)

C-18	Jan. 13/72	σ	Decreased
C-19	Jan. 17/72	u_a	Decreased
C-20	Jan. 18/72	u_w	Increased
C-21	Jan. 19/72	σ	Decreased
C-22	Jan. 24/72	u_a	Decreased
C-23	Jan. 26/72	u_w	Increased
C-24	Jan. 29/72	σ	Decreased
C-25	Feb. 2/72	u_a	Decreased
C-26	Feb. 7/72	u_w	Increased
C-27	Feb. 15/72	σ	Decreased
C-28	Feb. 21/72	σ	Increased
C-29	Feb. 24/72	u_w	Decreased
C-30	Mar. 3/72	σ	Increased
C-31	Mar. 9/72	u_a	Increased
C-32	Mar. 16/72	u_w	Increased

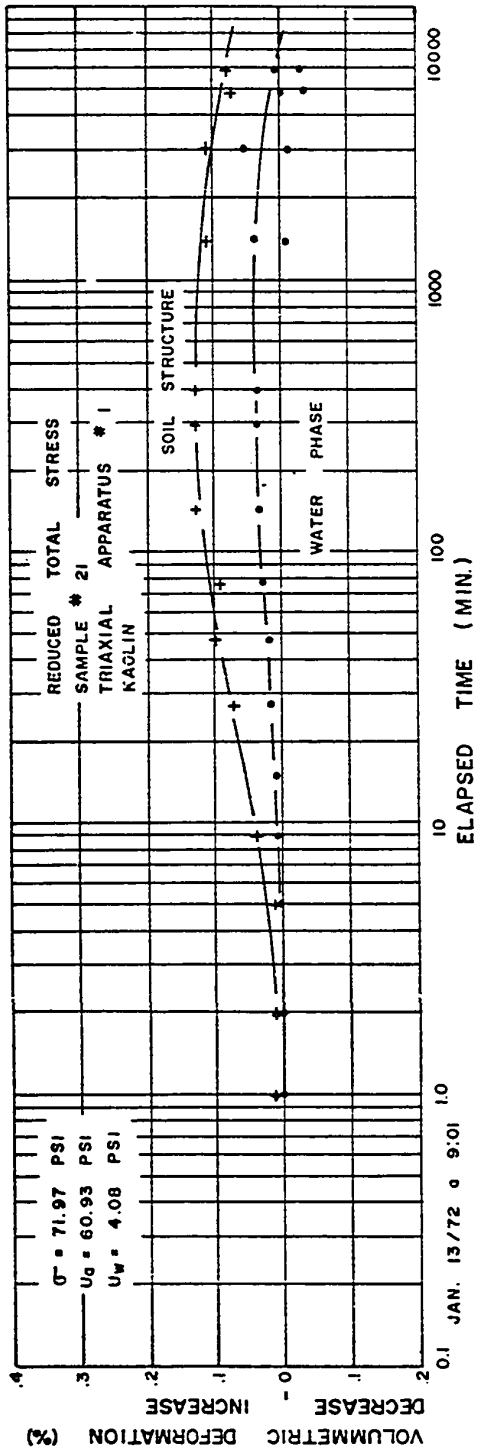


FIGURE F. 32 SOIL STRUCTURE AND WATER PHASE VOLUME CHANGES (C-18)

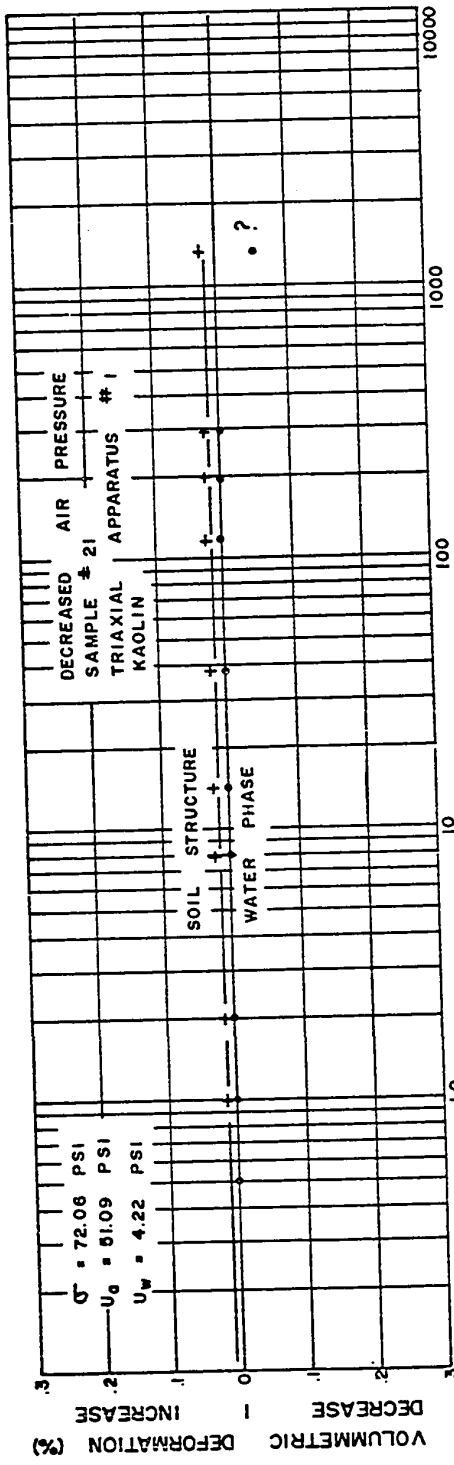


FIGURE F. 33 SOIL STRUCTURE AND WATER PHASE VOLUME CHANGES (C-19)

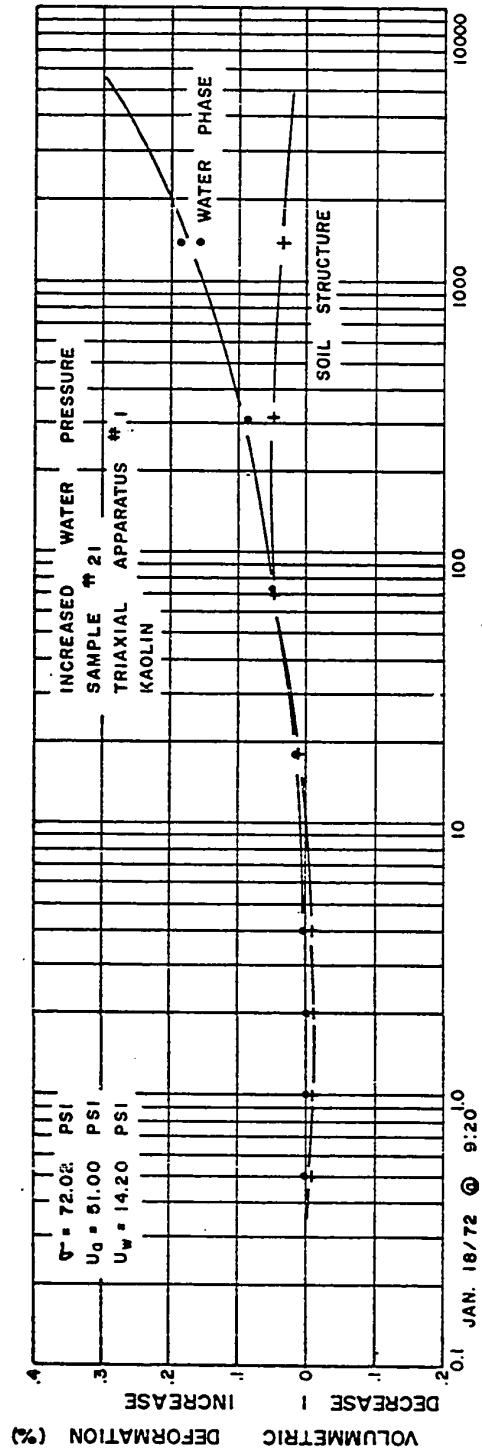


FIGURE F. 34 SOIL STRUCTURE AND WATER PHASE VOLUME CHANGES (C-20)

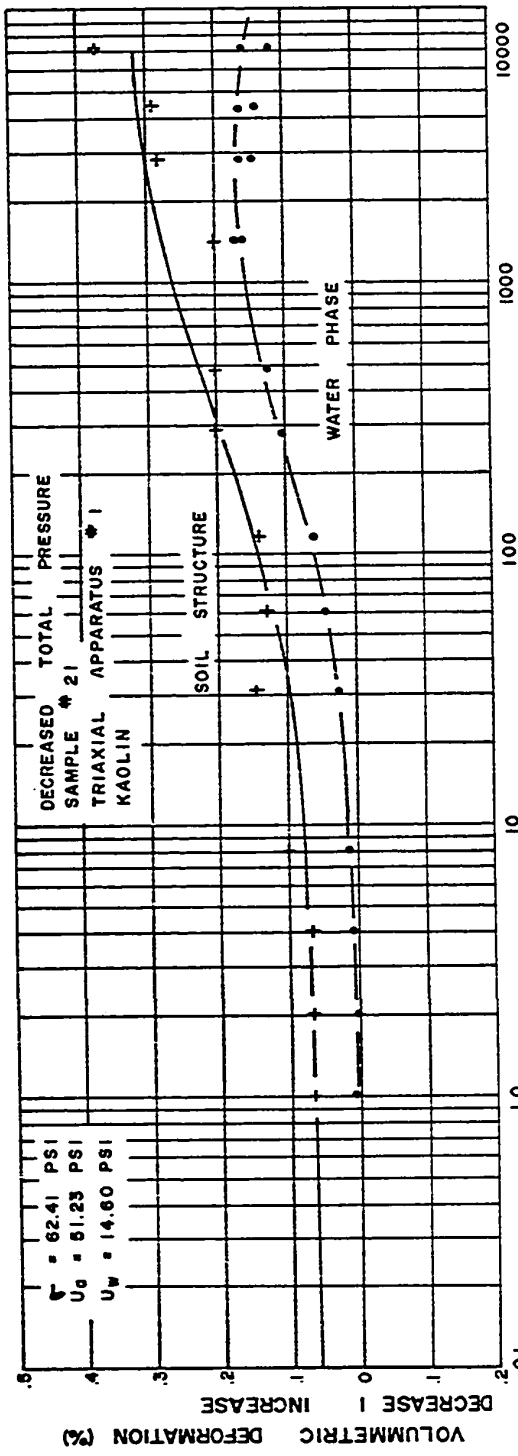


FIGURE F. 35 SOIL STRUCTURE AND WATER PHASE VOLUME CHANGES (C-21)

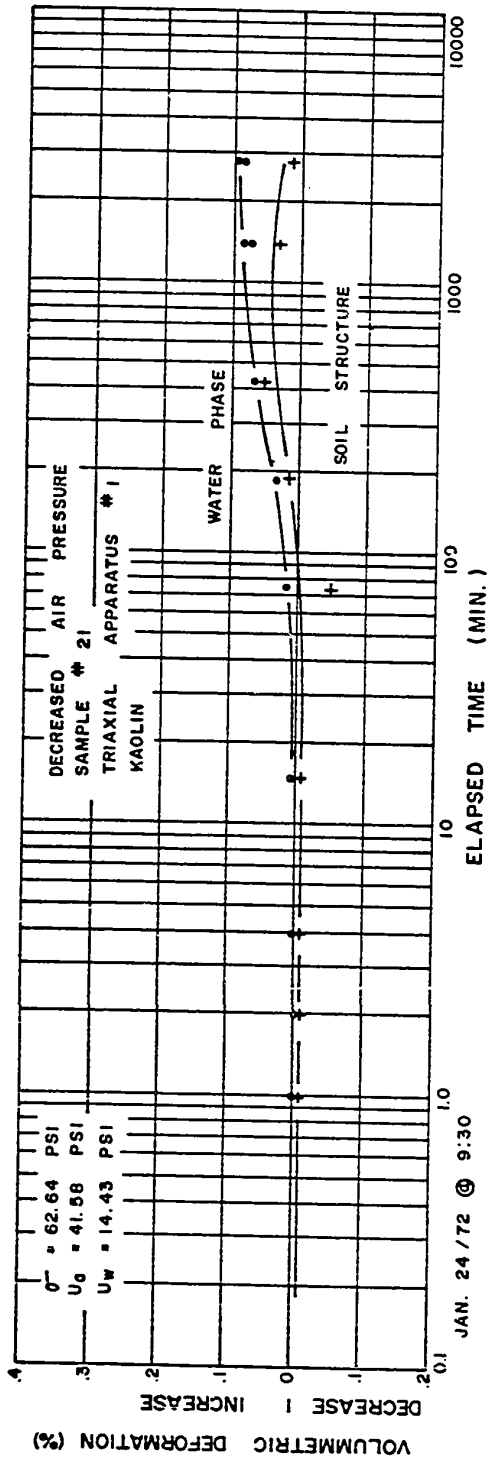


FIGURE F. 36 SOIL STRUCTURE AND WATER PHASE VOLUME CHANGES (C-36)

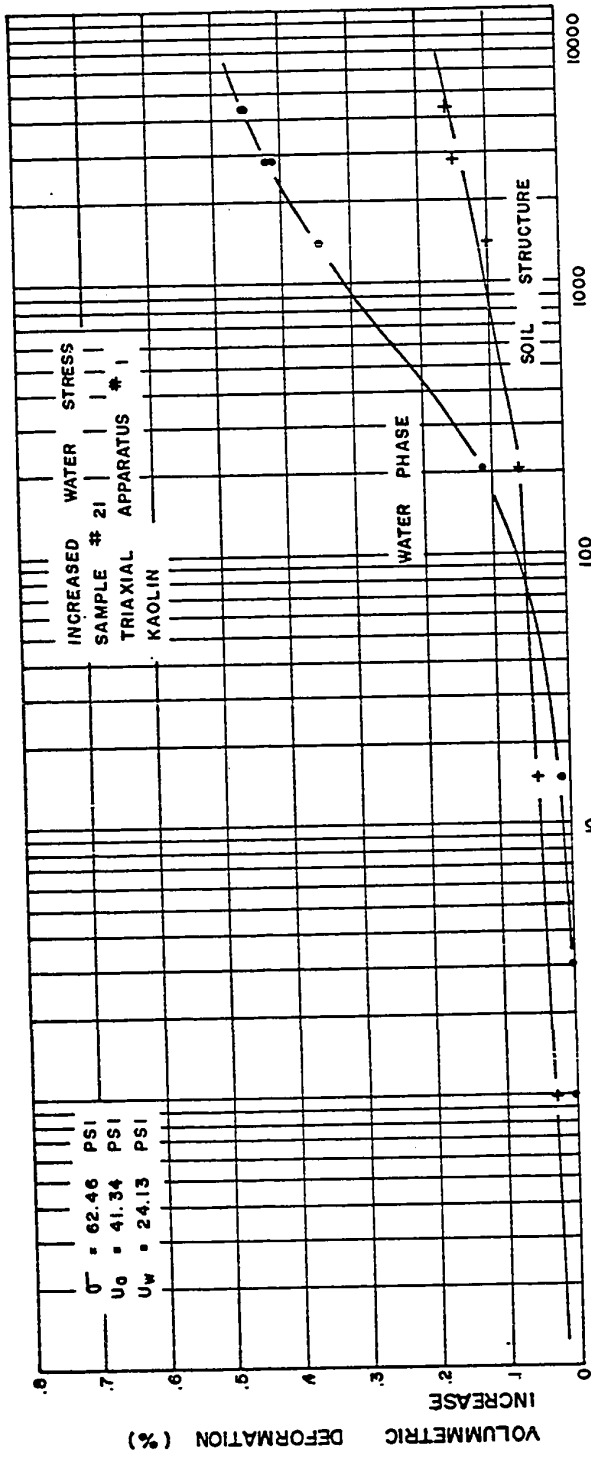


FIGURE F. 37 SOIL STRUCTURE AND WATER PHASE VOLUME CHANGES (C-23)

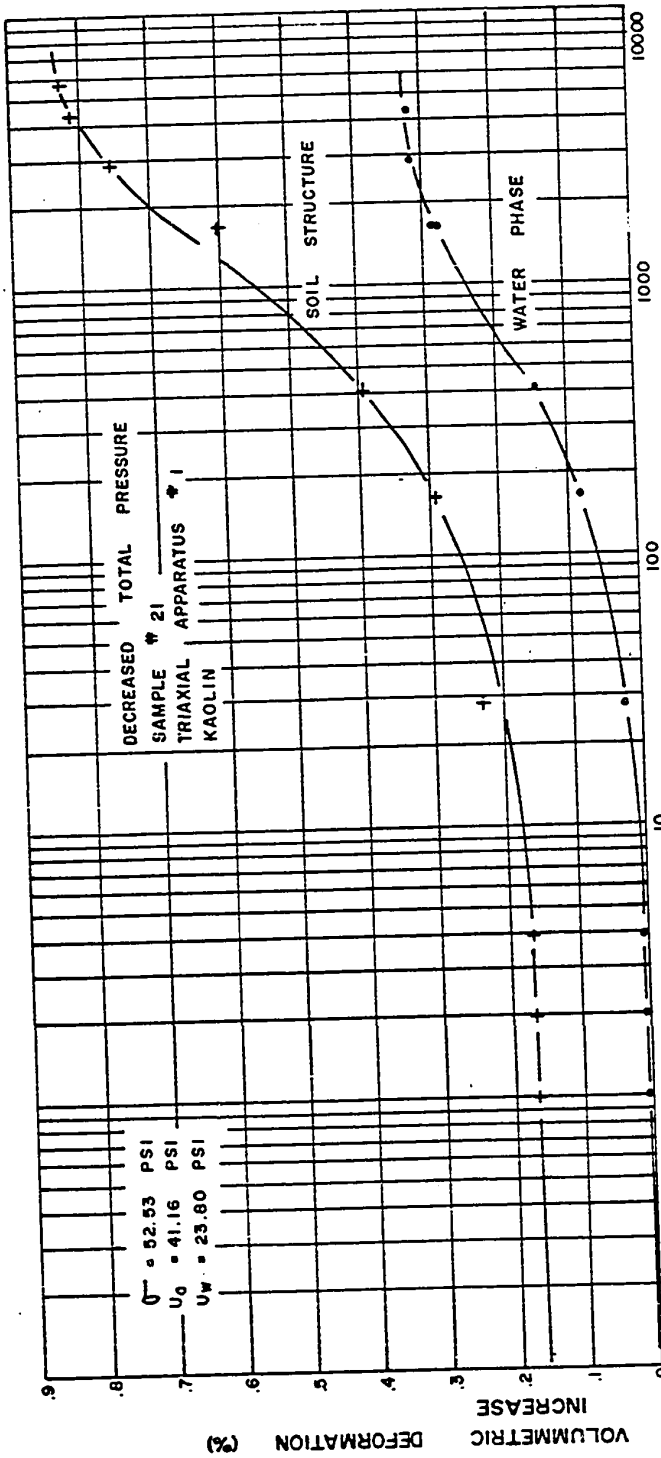


FIGURE F. 38 SOIL STRUCTURE AND WATER PHASE VOLUME CHANGES (C-24)

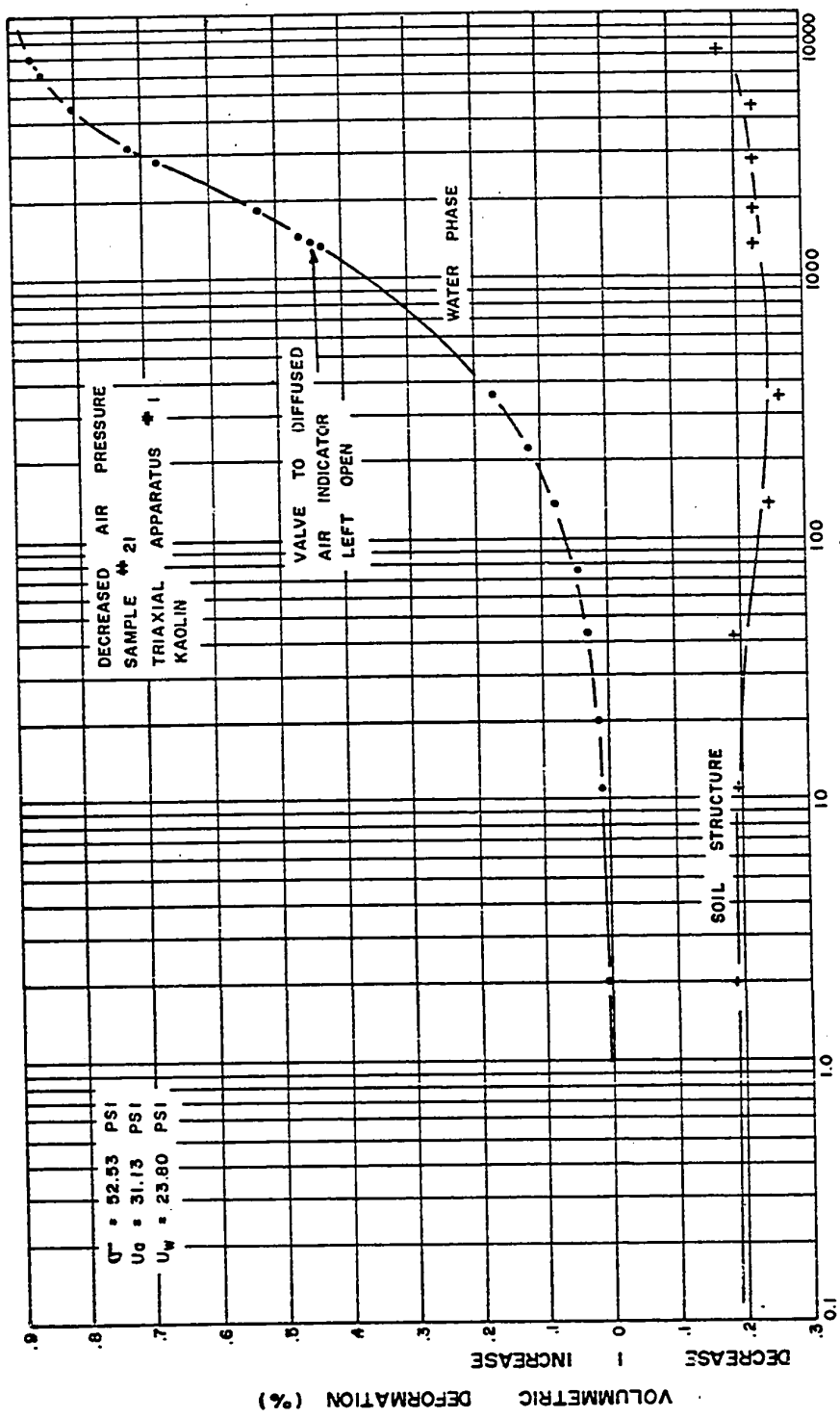


FIGURE F. 39 SOIL STRUCTURE AND WATER PHASE VOLUME CHANGES (C-25)

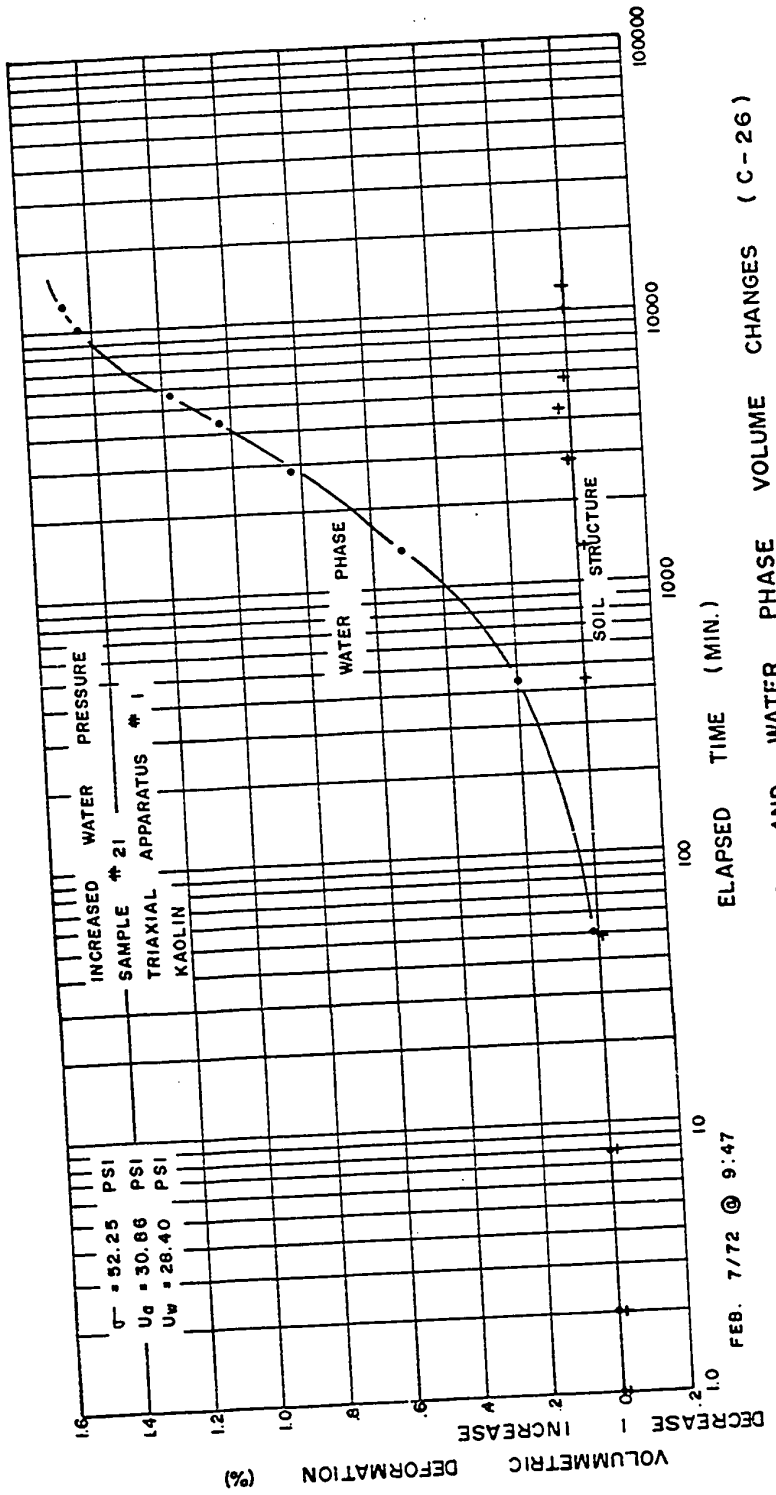


FIGURE F. 40 SOIL STRUCTURE AND WATER PHASE VOLUME CHANGES (C-26)

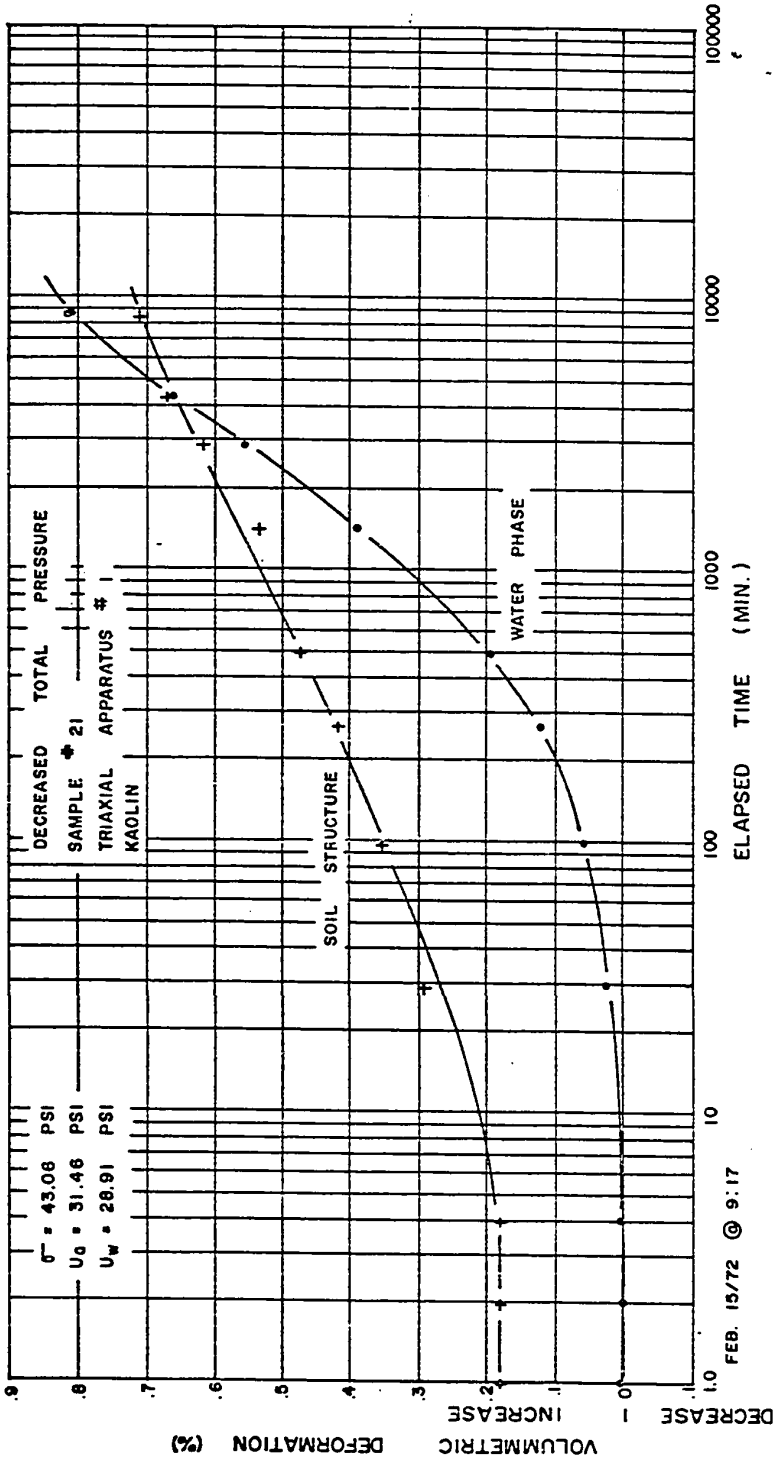


FIGURE F. 41 SOIL STRUCTURE AND WATER PHASE VOLUME CHANGES (C-27)

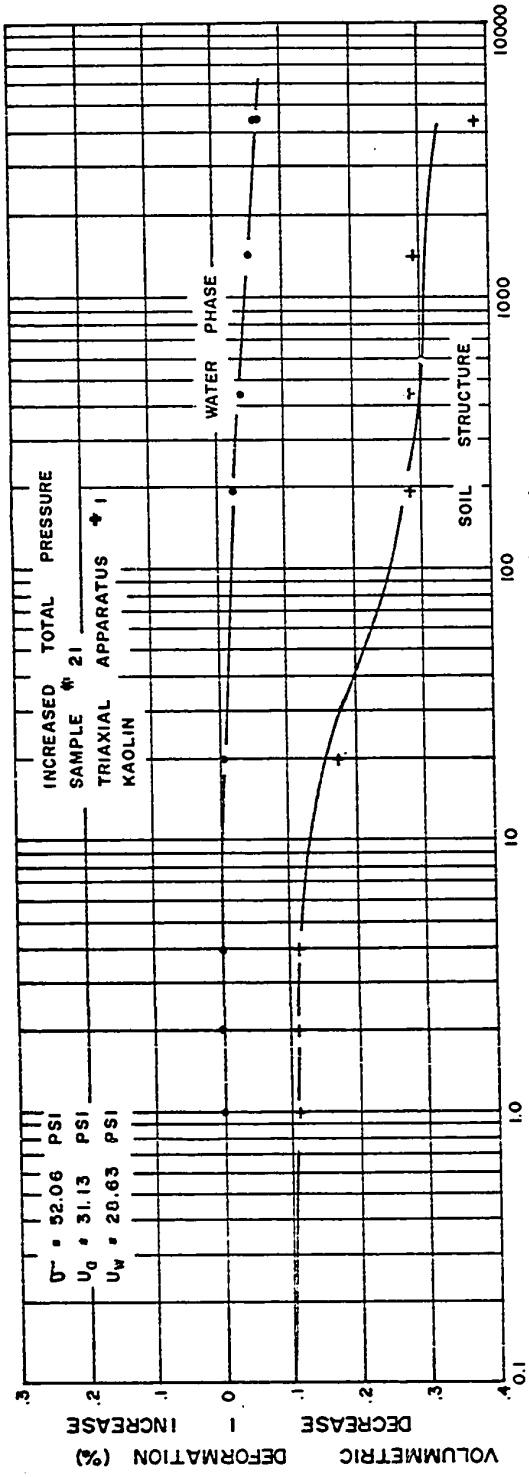


FIGURE F. 42 SOIL STRUCTURE AND WATER PHASE VOLUME CHANGES (C-28)

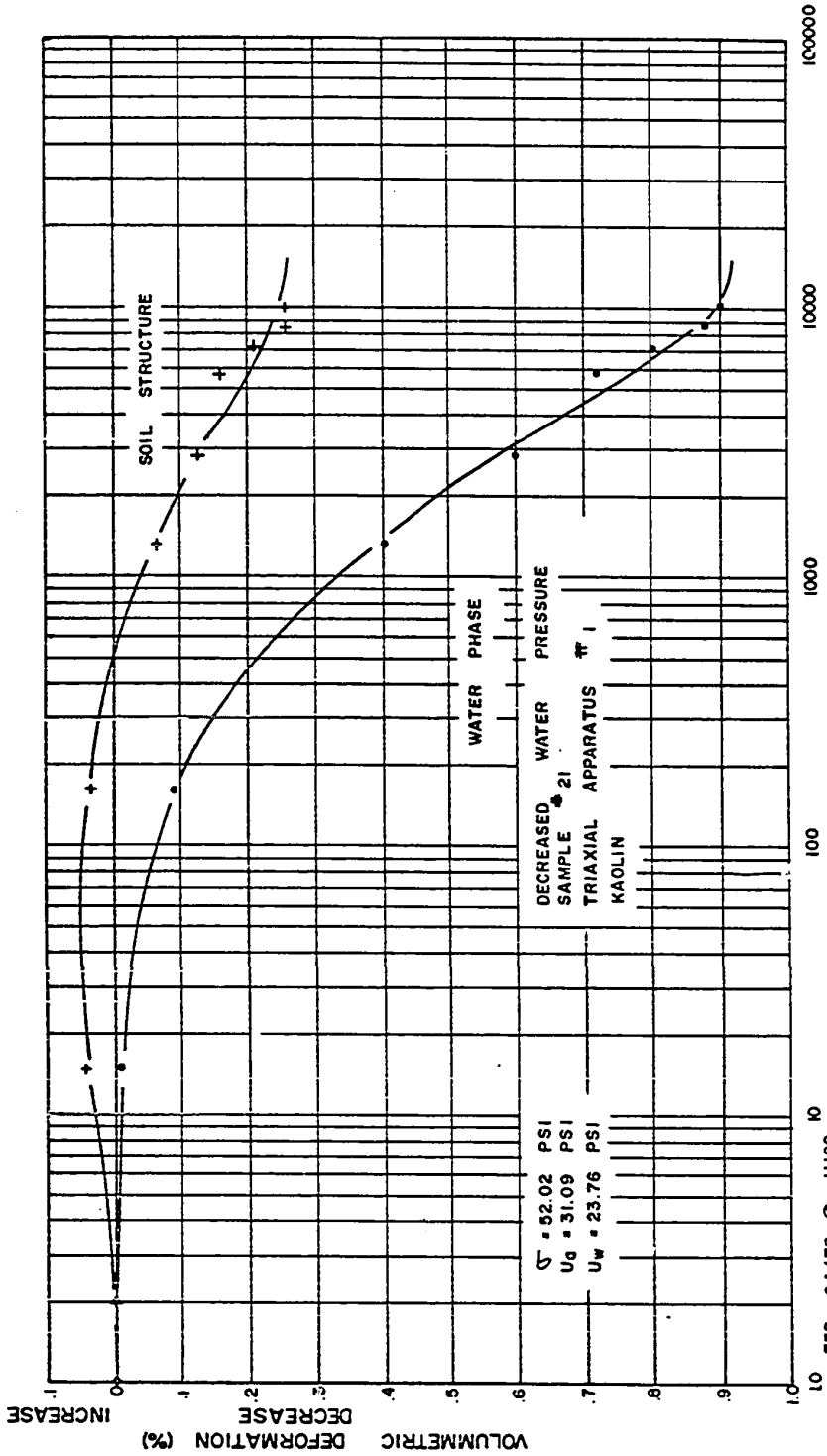


FIGURE F. 43 SOIL STRUCTURE AND WATER PHASE VOLUME CHANGES (C-29)

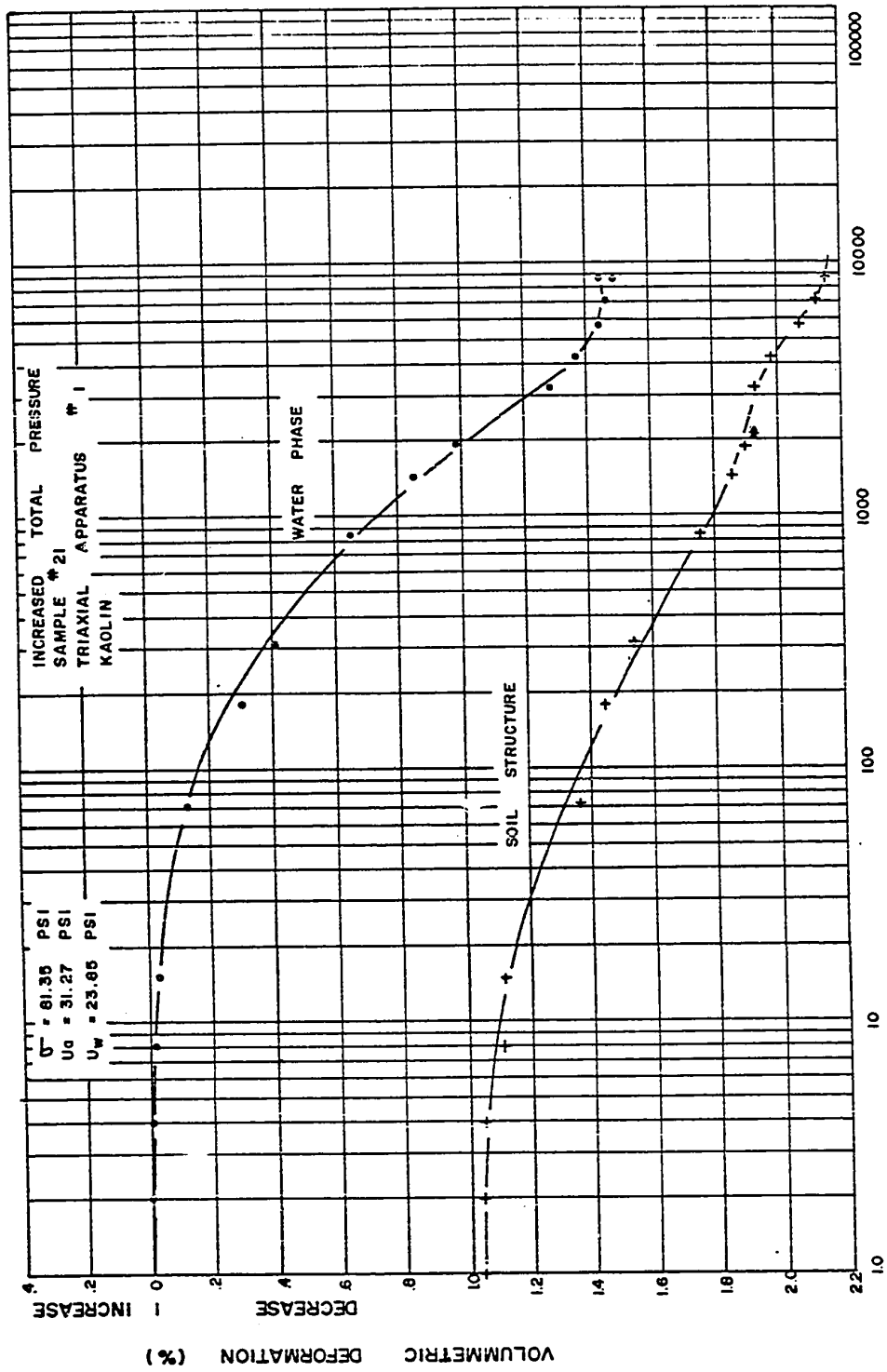


FIGURE F. 44 SOIL STRUCTURE AND WATER PHASE VOLUME CHANGES (C-30)

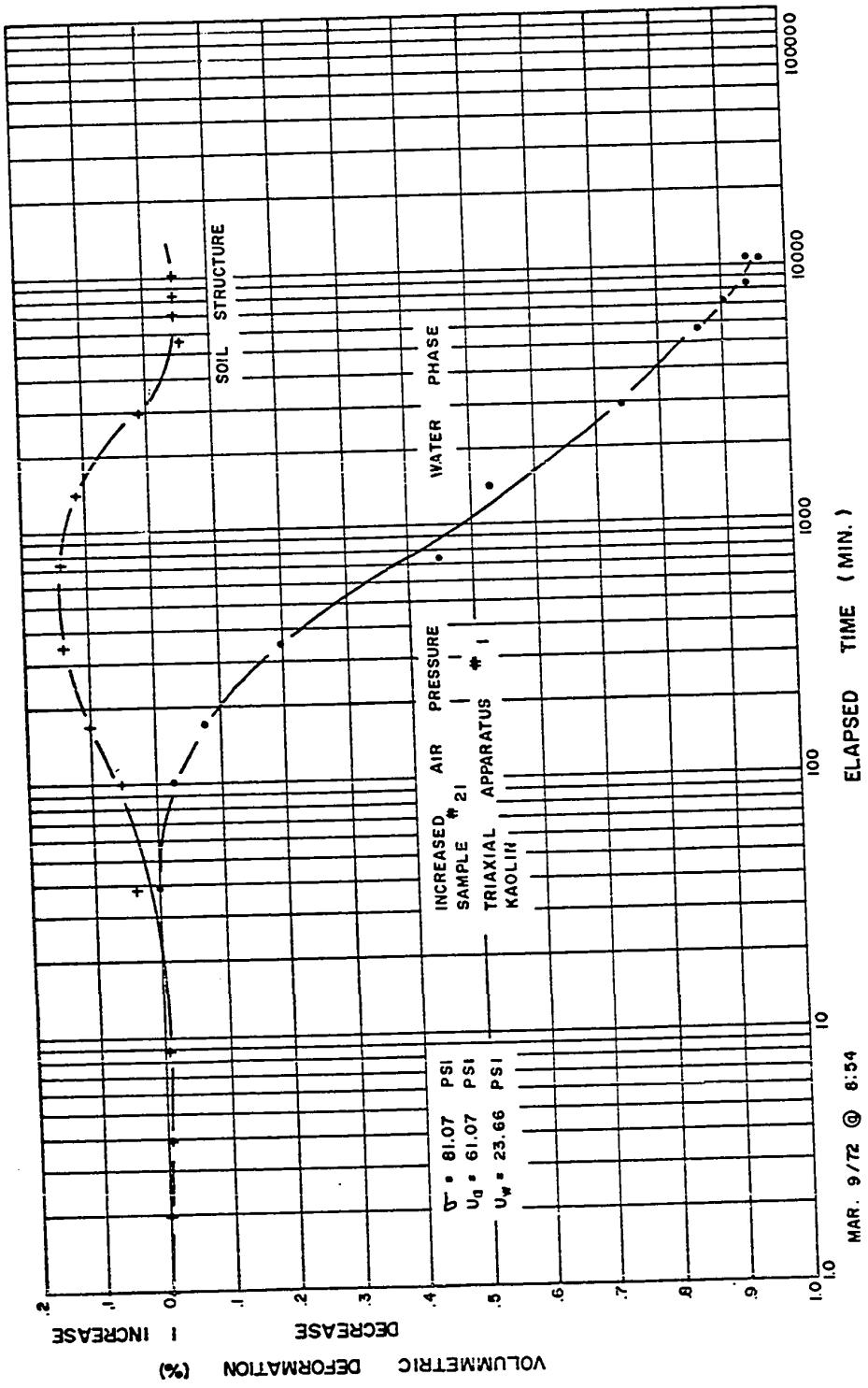


FIGURE F. 45 SOIL STRUCTURE AND WATER PHASE VOLUME CHANGES (C-31)

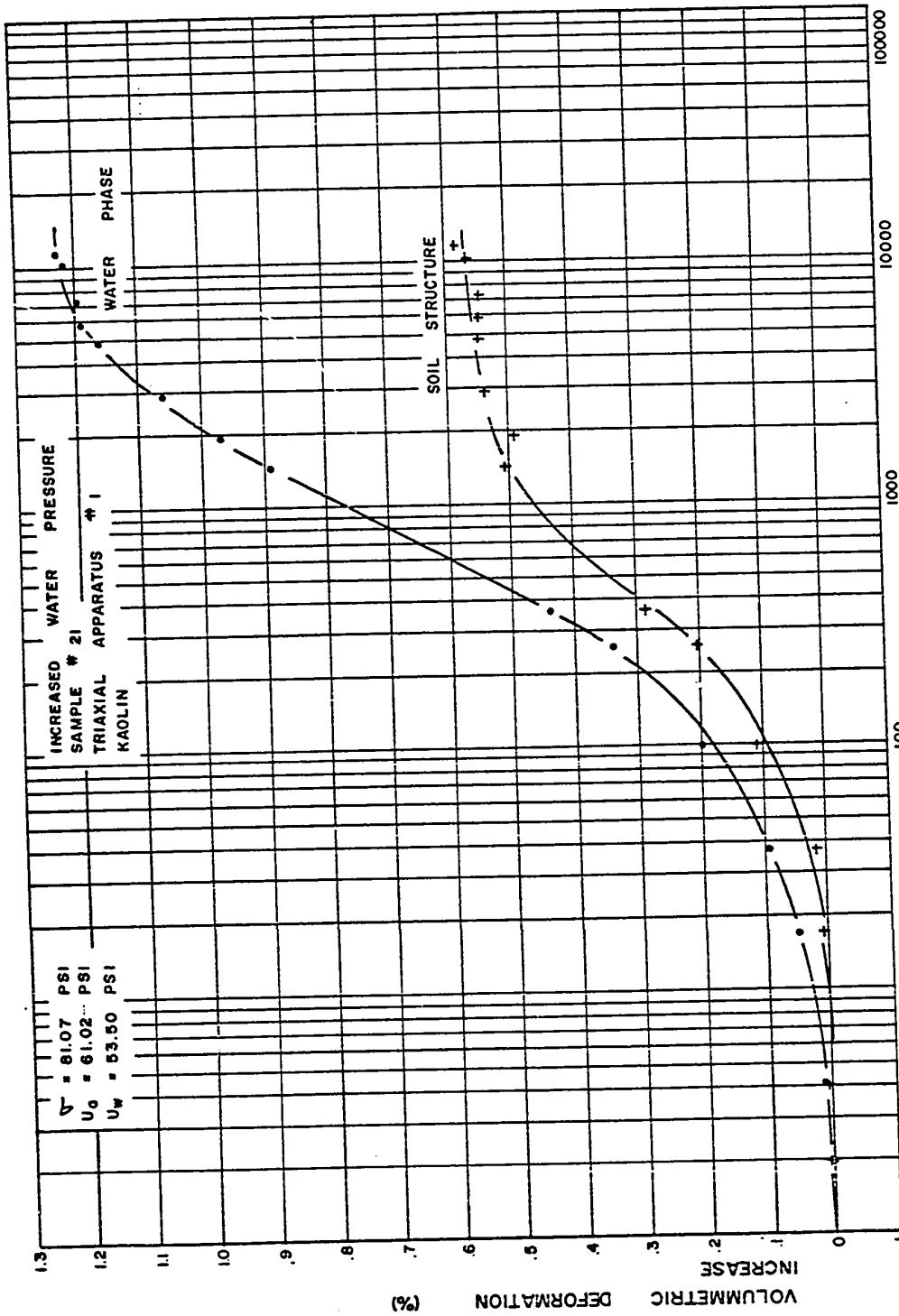


FIGURE F. 46 SOIL STRUCTURE AND WATER PHASE VOLUME CHANGE (C-32)

SECTION III

F-4 Exploration of the Constitutive Surface

F-4.1 Discussion of the Test Results

The tests that explore the constitutive surface adopt larger stress changes and are concerned only with equilibrium conditions. The constitutive surface is mapped by changing one of the stress state variables by an amount corresponding to a load increment ratio of approximately one. All tests were performed on Regina Clay.

Two tests (#33 and #34) were performed under Ko conditions in the modified Anteus oedometers. All known precautions were taken to ensure against water loss. The samples were first allowed to come to equilibrium and then the suction was reduced in increments. When the suction became small, the total stress was reduced. Similar isotropic loading tests (#32 and #35) were performed in the triaxial cells.

Two conventional constant volume swell pressure tests (#18 and #23) were performed in one-dimensional oedometers where only the total stress was controlled. The results are summarized in the following tables. Table F.9 summarizes the soil properties; Table F.10 summarizes the tests performed; Table F.11 summarizes the volume-weight relationships and Table F.12 summarizes the pressure changes. Table F.13 summarizes the pressure changes and volume-weight relationships for sample #18 and #23. The void ratio versus effective stress plot for sample #18 as well as several typical volumetric deformation plots are also shown.

TABLE F.9

SUMMARY OF SOIL PROPERTIES ON SAMPLES TESTED TO

EXPLORE THE ENTIRE CONSTITUTIVE SURFACE

Lab. Sample No.	Field Test Hole No.	Field Sample No.	Depth (ft)	Liquid Limit (%)	Plastic Limit (%)	Plastic Index (%)	Grain Sizes			Soil Description
							Clay (%)	Silt (%)	Sand (%)	
32	13	4	$7\frac{1}{2}$	74.7	26.0	48.7	67.0	33.0	0	Regina clay, med. to dark brown (top portion)
33	13	4	$7\frac{1}{2}$	79.5	27.0	52.5	73.0	32.0	0	Regina clay, (second from the top)
34	13	4	$7\frac{1}{2}$	76.1	26.5	49.6	70.0	30.0	0	Regina clay, (third from the top)
35	13	4	$7\frac{1}{2}$	75.0	26.1	48.9	67.5	32.5	0	Regina clay, (fourth from the top)
18	10	1	2	--	--	--	--	--	-	Regina clay, very dry and crumbly, difficult to trim. Some cracks.
23	12	4	$10\text{-}11\frac{1}{2}$	--	--	--	--	--	-	Regina clay, bottom portion of sample.

TABLE F.10

SUMMARY OF CONSTITUTIVE SURFACE TESTS

Sample No.	Load Increment No.	Date	Starting Time	Total Elapsed Time (Min.)	Apparatus No.	Pressure Change			Comments
						Total (psi)	Air (psi)	Water (psi)	
32	0	Mar.27/72	10:08	14330	T-1				Applied cell pressure, then air pressure
32	1	Apr. 6/72	9:13	17260	T-1				
32	2	Apr.18/72	9:05	24490	T-1				
32	3	May 5/72	9:15	44650	T-1				
32	4	June 5/72	9:45	37515	T-1				
32	End	July 1/72	11:00	--	T-1				
33	0	Mar.28/72	11:10	22880	OED-177				Jagged edges on sample crumbly
33	1	Apr.13/72	8:35	15860	OED-177				
33	2	Apr.24/72	8:55	15940	OED-177				
33	3	May 5/72	10:40	20090	OED-177				
33	4	May19/72	9:30	28780	OED-177				
33	5	June 8/72	9:20	21670	OED-177				Couldn't flush water through the base plate
33	End	June23/72	10:30	--	OED-177				
34	0	Mar.29/72	11:02	7270	OED-179				
34	1	Apr. 3/72	12:22	14180	OED-179				
34	2	Apr.13/72	8:50	15860	OED-179				
34	3	Apr.24/72	9:10	15930	OED-179				
34	4	May 5/72	10:45	17180	OED-179				
34	5	May17/72	9:00	23070	OED-179				
34	6	June 2/72	9:30	30330	OED-179				
34	End	June23/72	11:00	--	OED-179				

TABLE F.10 (continued)

Sample No.	Load Increment No.	Date	Starting Time	Total Elapsed Time (Min.)	Apparatus No.	Pressure Change			Comments
						Total (psi)	Air (psi)	Water (psi)	
35	0	Apr. 6/72	12:02	17080	T-2				
35	1	Apr.18/72	8:50	24510	T-2				
35	2	May 5/72	9:20	27730	T-2				
35	3	May24/72	15:30	24170	T-2				
35	4	June10/72	10:25	30160	T-2				
35	End	July 1/72	9:00	--	T-2				

TABLE F.11

VOLUME-WEIGHT RELATIONSHIPS OF SAMPLES USED TO MAP CONSTITUTIVE SURFACE

Sample No.	Load Increment	Diameter (cm)	Height (cm)	Total Volume (cc)	Volume of Water (cc)	Volume of Air (cc)	Water Content (%)	Void Ratio	Dry Density (PCF)	Degree of Saturation (%)
32	Initial	10.241	5.057	416.55	173.37	35.16	29.98	1.0025	86.63	83.14
32	0	10.282	5.095	423.04	170.33	44.69	29.45	1.0336	85.30	79.22
32	1	10.306	5.131	428.05	174.66	45.37	30.20	1.0577	84.30	79.38
32	2	10.318	5.173	432.50	179.65	44.83	31.07	1.0791	83.44	80.03
32	3	10.333	5.204	436.40	187.59	40.79	32.44	1.0979	82.69	82.14
32	4	10.365	5.256	443.50	192.94	42.53	33.37	1.1320	81.37	81.94
33	Initial	6.350	1.920	60.81	24.35	6.65	29.40	1.0405	85.01	78.55
33	0	6.350	1.879	59.52	23.88	5.84	28.83	0.9973	86.85	80.36
33	1	6.350	1.874	59.35	24.94	4.61	30.11	0.9917	87.10	84.40
33	2	6.350	1.860	58.89	25.76	3.33	31.10	0.9764	87 77	88.55
33	3	6.350	1.848	58.53	26.43	2.30	31.90	0.9641	88.32	91.99
33	4	6.350	1.871	59.27	27.06	2.41	32.66	0.9889	87.22	91.82
33	5	6.350	1.891	59.88	27.54	2.55	33.24	1.0096	86.32	91.54
34	Initial	6.350	2.206	69.86	24.22	11.19	25.30	1.0284	85.52	68.39
34	0	6.350	2.203	69.77	26.18	9.15	27.34	1.0257	85.63	74.09
34	1	6.350	2.209	69.95	27.26	8.25	28.47	1.0309	85.42	76.77
34	2	6.350	2.214	70.12	28.64	7.04	29.91	1.0359	85.21	80.27
34	3	6.350	2.218	70.24	29.12	6.68	30.41	1.0394	85.06	81.35
34	4	6.350	2.229	70.58	29.74	6.39	31.06	1.0492	84.66	82.31
34	5	6.350	2.239	70.91	30.23	6.24	31.57	1.0589	84.26	82.88
34	6	6.350	2.246	71.13	30.54	6.14	31.90	1.0651	84.00	83.25

TABLE F.11 (continued)

Sample No.	Load Increment	Diameter (cm)	Height (cm)	Total Volume (cc)	Volume of Water (cc)	Volume of Air (cc)	Water Content (%)	Void Ratio	Dry Density (PCF)	Degree of Saturation (%)
35	Initial	10.310	5.089	424.85	161.48	59.14	28.44	1.0802	83.39	73.19
35	0	10.246	5.069	417.93	165.07	48.62	29.07	1.0463	84.77	77.25
35	1	10.238	5.082	418.39	170.50	43.65	30.03	1.0486	84.68	79.62
35	2	10.226	50.91	418.05	175.08	38.74	30.84	1.0469	84.75	81.88
35	3	10.214	5.095	417.41	178.59	34.58	31.46	1.0438	84.88	83.77
35	4	10.235	5.146	423.40	184.80	34.36	32.55	1.0731	83.68	84.32

TABLE F.12

SUMMARY OF PRESSURE CHANGES FOR TESTS TO MAP CONSTITUTIVE SURFACE

Sample No.	Increment No.	Initial Conditions						Final Conditions					
		σ (psi)	u_a (psi)	u_w (psi)	$\sigma-u_w$ (psi)	$\sigma-u_a$ (psi)	u_a-u_w (psi)	σ (psi)	u_a (psi)	u_w (psi)	$\sigma-u_w$ (psi)	$\sigma-u_a$ (psi)	u_a-u_w (psi)
32	0	101.35	90.07	4.92	96.43	11.28	85.15	100.93	89.84	5.01	95.92	11.09	84.83
32	1	100.93	89.84	5.01	95.92	11.09	84.83	51.88	40.55	9.74	42.14	11.32	30.81
32	2	51.88	40.55	9.74	42.14	11.32	30.81	37.35	25.94	9.88	27.47	11.42	16.06
32	3	37.35	25.94	9.88	27.47	11.42	16.06	27.47	15.82	9.56	17.91	11.65	6.26
32	4	27.47	15.82	9.56	17.91	11.65	6.26	21.07	16.01	9.74	11.32	5.06	6.26
33	0	125.08	59.78	0.73	124.35	65.30	59.05	124.81	59.39	3.91	120.90	65.41	55.49
33	1	124.81	59.39	3.91	120.90	65.41	55.49	95.75	30.34	6.60	89.16	65.41	23.74
33	2	95.75	30.34	6.60	89.16	65.41	23.74	80.99	15.77	6.83	74.17	65.23	8.94
33	3	80.99	15.77	6.83	74.17	65.23	8.94	74.83	9.75	6.53	68.30	65.08	3.22
33	4	74.83	9.75	6.53	68.30	65.08	3.22	36.45	9.54	6.36	30.09	26.91	3.18
33	5	36.45	9.54	6.36	30.09	26.91	3.18	23.68	9.58	6.28	17.40	14.09	3.30
34	0	94.73	80.87	6.07	88.66	13.86	74.80	94.97	81.04	6.62	88.35	13.93	74.42
34	1	94.97	81.04	6.62	88.35	13.93	74.42	54.70	40.84	6.36	48.34	13.86	34.48
34	2	54.70	40.84	6.36	48.34	13.86	34.48	34.29	20.47	6.45	27.84	13.82	14.02
34	3	34.29	20.47	6.45	27.84	13.82	14.02	24.50	10.90	6.53	17.96	13.60	4.36
34	4	24.50	10.90	6.53	17.96	13.60	4.36	17.55	10.35	6.07	11.48	7.21	4.28
34	5	17.55	10.35	6.07	11.48	7.21	4.28	14.44	10.47	6.28	8.17	3.97	4.19
34	6	14.44	10.47	6.28	8.17	3.97	4.19	12.55	10.30	6.15	6.40	2.25	4.15

TABLE F.12 (continued)

Sample No.	Increment No.	Initial Conditions						Final Conditions					
		σ (psi)	u_a (psi)	u_w (psi)	$\sigma-u_w$ (psi)	$\sigma-u_a$ (psi)	u_a-u_w (psi)	σ (psi)	u_a (psi)	u_w (psi)	$\sigma-u_w$ (psi)	$\sigma-u_a$ (psi)	u_a-u_w (psi)
35	0	89.91	59.91	9.23	80.68	30.00	50.68	90.05	60.23	9.55	80.50	29.83	50.68
35	1	90.05	60.23	9.55	80.50	29.83	50.68	60.64	30.71	9.58	50.06	29.93	21.13
35	2	60.64	30.71	9.58	50.06	29.93	21.13	48.89	18.99	9.34	39.55	29.90	9.65
35	3	48.89	18.99	9.34	39.55	29.90	9.65	42.64	12.72	8.88	33.76	29.92	3.84
35	4	42.64	12.72	8.88	33.76	29.92	3.84	23.53	13.14	9.27	14.26	10.38	3.88

TABLE F.13

SUMMARY OF PRESSURE AND VOLUME-WEIGHT RELATIONSHIPS FOR SAMPLES TESTED ON CONVENTIONAL OEDOMETERS TO EXPLORE THE CONSTITUTIVE RELATIONSHIP OF THE SOIL STRUCTURE

Sample No.	Load Increment	Date	Starting Time	Total Elapsed Time (Min.)	Apparatus No.	Total Pressure (psi)	Height at Equilibrium (cm)	Equilibrium Void Ratio	Equilibrium % Volume Change	Comments
18	0	Oct.13/71	10:30	--	Bench	0	2.744	0.8698	0.0	Dia.=6.350cm
	1	Oct.13/71	10:30	7100	Model	31.72	2.750	0.8739	-0.218	W/C_o=30.05%
		Swelling Pressure			#3	36.00				S_o%=96.04%
	2	Oct.18/71	8:50	2867		59.51	2.706	0.8440	+1.378	
	3	Oct.20/71	9:00	2900		115.08	2.601	0.7728	+5.261	
	4	Oct.22/71	9:30	4303		59.51	2.613	0.7807	+5.026	Unloading
	5	Oct.25/71	9:15	2834		31.72	2.628	0.7912	+4.418	
	6	Oct.27/71	8:30	2970		17.83	2.645	0.8028	+3.743	
	7	Oct.29/71	10:27	4364		14.34	2.654	0.8084	+3.409	
	8	Nov. 1/71	11:15	2850		7.41	2.669	0.8189	+2.815	W/Cf=30.60%
	9	Nov. 3/71	10:50	18910		2.47	2.722	0.8549	+0.819	S_f=99.51%
23	0	Jan.14/72	10:15	--	Bench	0	2.540	0.8100	0.0	Dia.=6.350cm
	1	Jan.14/72	10:15	5695	Model	59.05	2.541	0.8109	-0.056	W/C_o=26.34%
		Swelling Pressure			#3					S_o%=90.40%
	2	Jan.18/72	9:35	2835		114.62	2.516	0.7931	+0.935	
	3	Jan.20/72	9:00	5798		35.52	2.557	0.8223	-0.687	Unloading
	4	Jan.24/72	9:38	5722		13.86	2.609	0.8594	-2.715	
	5	Jan.28/72	9:00	7300		6.86	2.659	0.8950	-4.570	W/Cf=33.67%
	6	Feb. 2/72	10:53	10427		2.23	2.721	0.9391	-6.816	S_f=99.67%

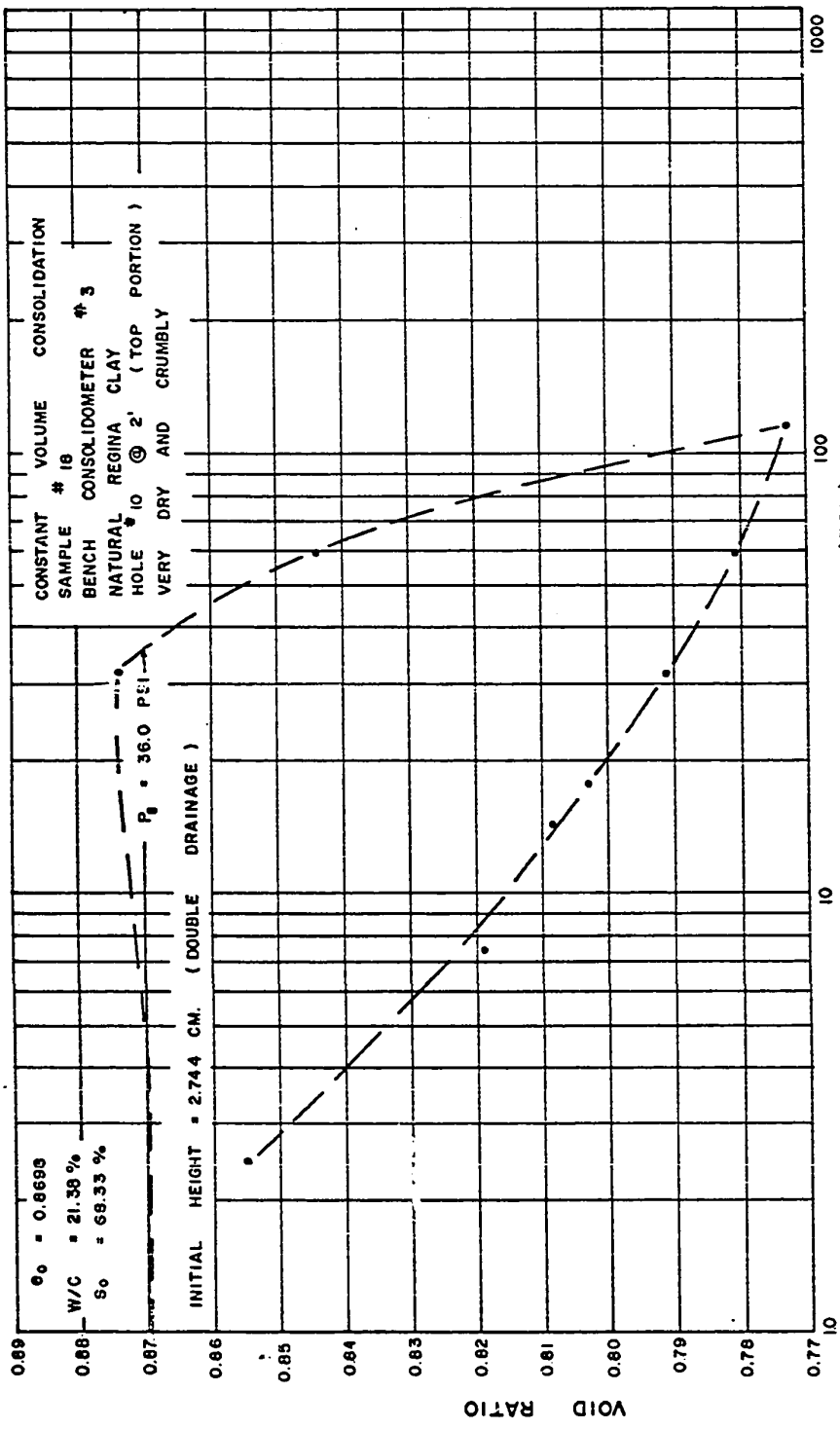


FIGURE F.47 CONSTANT VOLUME CONSOLIDATION, SAMPLE #18

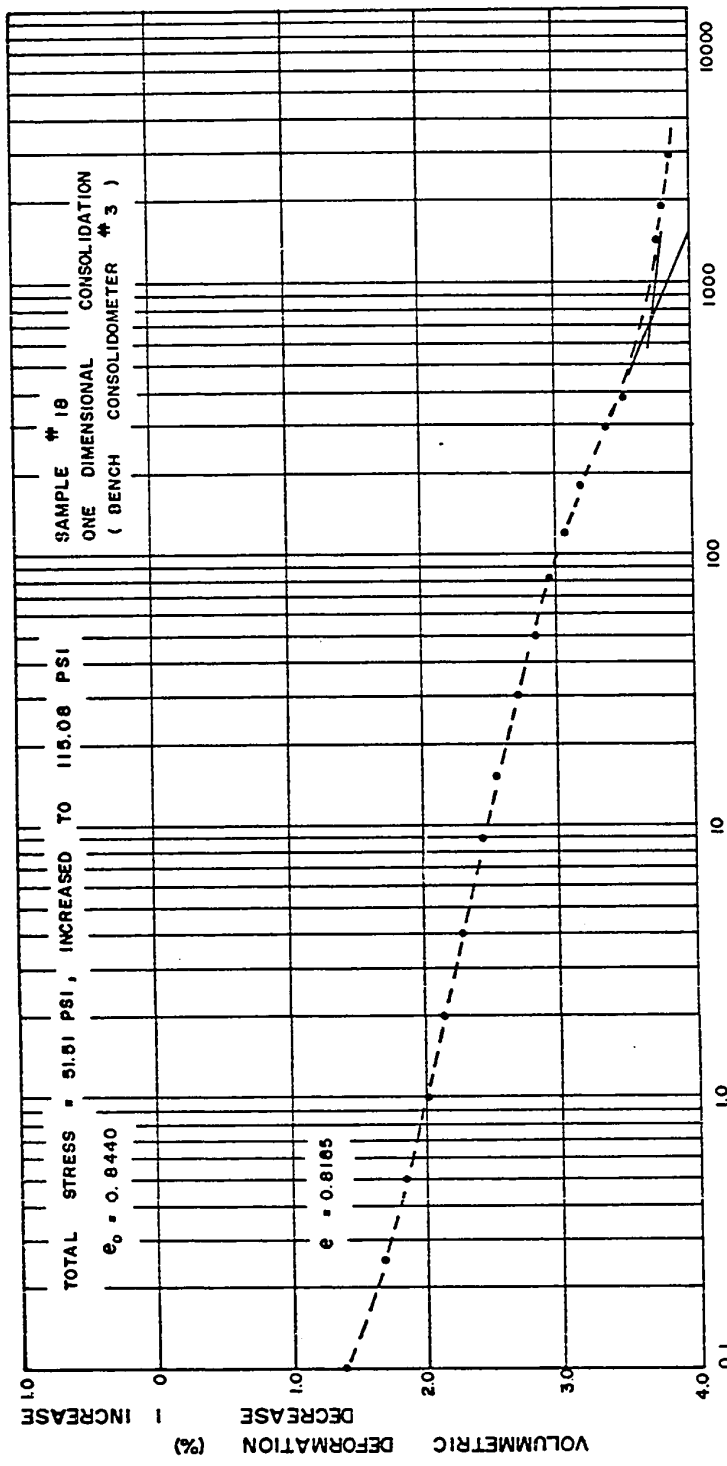


FIGURE F. 48 SOIL STRUCTURE VOLUMMETRIC DEFORMATION VERSUS LOG TIME
(LOAD INCREMENT # 3)

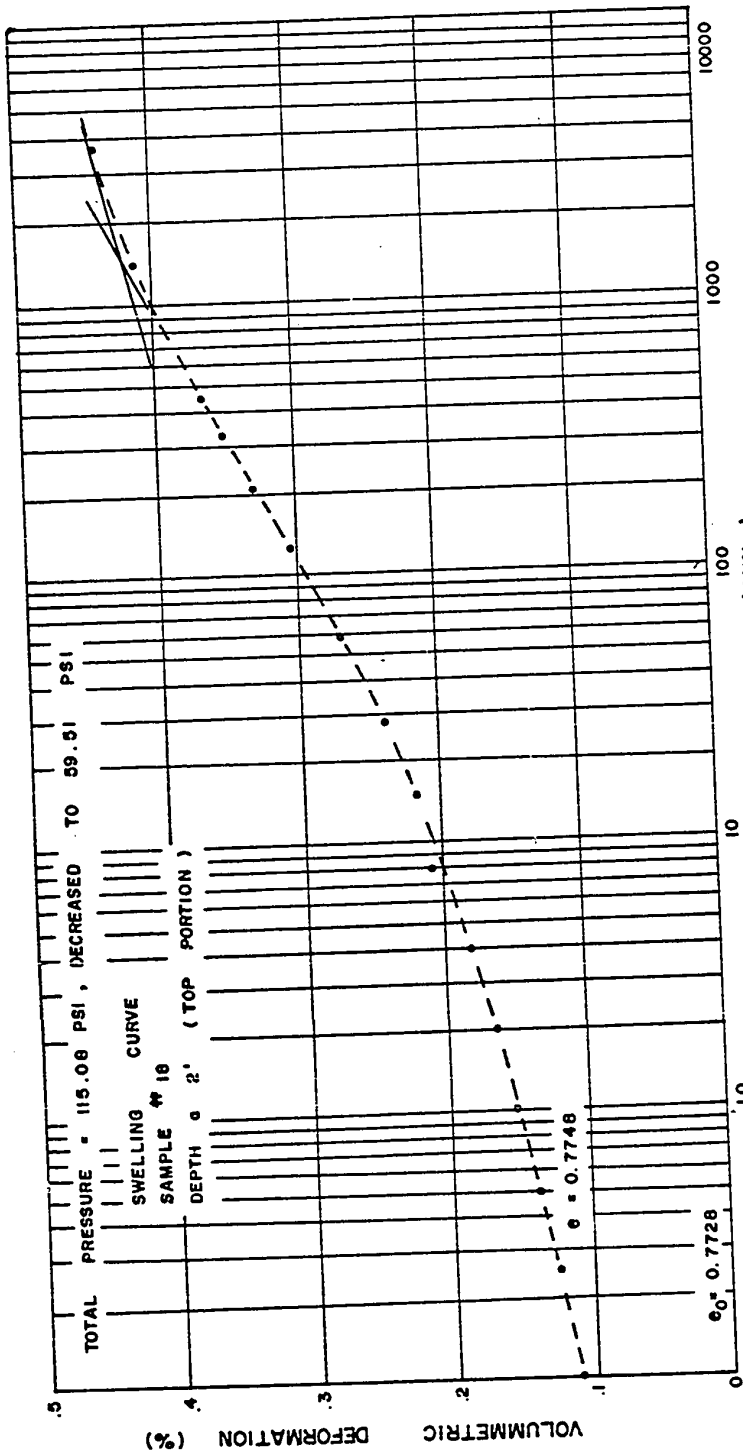


FIGURE F. 49 SOIL STRUCTURE VOLUMMETRIC DEFORMATION VERSUS LOG TIME (LOAD INCREMENT # 4)

END OF REEL